

Environmental Challenges and Solutions

Series Editor: Robert J. Cabin

Pravat Kumar Shit

Partha Pratim Adhikary

Debashish Sengupta *Editors*

Spatial Modeling and Assessment of Environmental Contaminants

Risk Assessment and Remediation

 Springer

Environmental Challenges and Solutions

Series Editor

Robert J. Cabin, Brevard College, Brevard, NC, USA

The Environmental Challenges and Solutions series aims to improve our understanding of the Earth's most important environmental challenges, and how we might more effectively solve or at least mitigate these challenges. Books in this series focus on environmental challenges and solutions in particular geographic regions ranging from small to large spatial scales. These books provide multidisciplinary (technical, socioeconomic, political, etc.) analyses of their environmental challenges and the effectiveness of past and present efforts to address them. They conclude by offering holistic recommendations for more effectively solving these challenges now and into the future. All books are written in a concise and readable style, making them suitable for both specialists and non-specialists starting at first year graduate level. Proposals for the book series can be sent to the Series Editor, Robert J. Cabin, at cabinrj@brevard.edu.

More information about this series at <http://www.springer.com/series/11763>

Pravat Kumar Shit • Partha Pratim Adhikary •
Debashish Sengupta
Editors

Spatial Modeling and Assessment of Environmental Contaminants

Risk Assessment and Remediation

 Springer

Editors

Pravat Kumar Shit
PG Department of Geography
Raja N. L. Khan Women's College
(Autonomous)
Vidyasagar University
Midnapore, West Bengal, India

Partha Pratim Adhikary
ICAR-Indian Institute of Water Management
Bhubaneswar, Odisha, India

Debashish Sengupta
Department of Geology and Geophysics
Indian Institute of Technology (IIT)
Kharagpur, West Bengal, India

ISSN 2214-2827

ISSN 2214-2835 (electronic)

Environmental Challenges and Solutions

ISBN 978-3-030-63421-6

ISBN 978-3-030-63422-3 (eBook)

<https://doi.org/10.1007/978-3-030-63422-3>

© Springer Nature Switzerland AG 2021

This work is subject to copyright. All rights are reserved by the Publisher, whether the whole or part of the material is concerned, specifically the rights of translation, reprinting, reuse of illustrations, recitation, broadcasting, reproduction on microfilms or in any other physical way, and transmission or information storage and retrieval, electronic adaptation, computer software, or by similar or dissimilar methodology now known or hereafter developed.

The use of general descriptive names, registered names, trademarks, service marks, etc. in this publication does not imply, even in the absence of a specific statement, that such names are exempt from the relevant protective laws and regulations and therefore free for general use.

The publisher, the authors, and the editors are safe to assume that the advice and information in this book are believed to be true and accurate at the date of publication. Neither the publisher nor the authors or the editors give a warranty, expressed or implied, with respect to the material contained herein or for any errors or omissions that may have been made. The publisher remains neutral with regard to jurisdictional claims in published maps and institutional affiliations.

This Springer imprint is published by the registered company Springer Nature Switzerland AG.
The registered company address is: Gewerbestrasse 11, 6330 Cham, Switzerland

Dedicated to beloved teachers and parents

Foreword by Dr. V Balaram



Human activities such as mining, smelting, refining, energy production, industrial and vehicular emissions, faulty agricultural operations, and improper sewage discharge and waste disposal lead to the rapid accumulation of toxic metals as well as harmful organic compounds in the environment which poses a continuous threat to mankind. When we look forward, the global drivers such as climate change, contamination of the air, soils, sediments, and groundwater, the energy requirements, population growth and longevity, and the resource challenges will drive the need for new technologies which can lead to more sustainable products, such as low carbon operations, clean air, clean energy, sustainable agricultural operations, and improved health and medical care.

Contamination of farmlands is a major problem as our country mainly depends on agriculture for food security. The contamination of agricultural soil by toxic metals and harmful organic substances, soil erosion and depletion of micronutrients, faulty agricultural practices, and several other anthropogenic activities are affecting our agricultural practices in a big way, as the quality of the soil determines the yield and quality of the crops.

Arsenic-contaminated sediments, soils, and groundwater are a global environmental and health concern due to the toxic and carcinogenic nature of As and its

species. The lower Indo-Gangetic plain is a hot spot of arsenic contamination. Phytoremediation, the process of removal or degradation of contaminants such as As from the soil, is one of the very effective ways of dealing with this problem. Understanding the spatial and temporal variation of leachate contamination from sanitary landfill sites of suburban areas of megacities such as Kolkata is extremely important for taking up necessary remedial measures.

Delineation of beach sands enriched with heavy minerals situated along the Eastern coastal areas of India is extremely important as these sands are enriched with rare earth elements (REE). These metals are being consumed at an unprecedented rate for a variety of industrial applications. Unfortunately, we are currently dependent on imports for these elements. This book written and edited by country's leading experts in these areas highlights these important aspects apart from others in the various chapters and provides suitable remediation measures and benchmark/baselines for future studies. This book can serve as a text for an introductory course in environmental sciences for undergraduate/graduate students with at least an elementary-level background in earth sciences, chemistry, and mathematics. The reader gets updated knowledge on these aspects and an overall idea of the studies undertaken worldwide apart from the study areas selected by the respective authors. It is therefore hoped that this book will prove to be a useful and valuable source of teaching material, both for individual students and for teachers of science courses.



CSIR-NGRI, Hyderabad, India

V. Balaram

Foreword by Prof. N. Janardhana Raju



I am happy to learn that Springer is bringing out a book on *Spatial Modeling and Assessment of Environmental Contaminants: Risk Assessment and Remediation* under the book series *Environmental Challenges and Solutions*. The book is jointly edited by Pravat Kumar Shit, Partha Pratim Adhikary, and Debashish Sengupta who are eminent scholars and researchers in the field of environmental sciences and advanced geospatial technology.

Nowadays, rapid urbanization, industrialization, associated environmental contaminants, and pollutants pose serious health risks and increase the magnitude of challenge. Our human society needs to establish policies that will considerably reduce the real and potential contaminants and pollution using geospatial modeling and low-cost bioremediation technologies through eco-friendly approaches.

This book illustrates the measurement, monitoring, and risk mapping and remediation of environmental contaminants in soil and sediment, air, and water. It also presents modifications of and improvements to existing control technologies for remediation of environmental contaminants. This book also demonstrated bioremediation technologies as a tool for environmental protection and management.

The present compilation is an outcome of selected papers from a wide spectrum of disciplines. The editors have undertaken painstaking efforts and have carried out a

wonderful task to edit and compile the papers. The essence of this interdisciplinary fusion can be realized by going through the chapters of this enriching volume. I do believe that this book will be very beneficial for the research scientists employed in the field of environmental sciences, soil sciences, and agricultural sciences along with learners, scientists, ecologists, and policymakers.

I extend my warm greetings to all those associated with the publication and congratulate Springer for launching this book.



School of Environmental Sciences,
Jawaharlal Nehru University [JNU],
New Delhi, India

N. Janardhana Raju

Preface

In the twenty-first century, population explosion and anthropogenic pressure are vital problems in the world and have significant effects on the land, soil, surface water, groundwater, and environment. Major factors such as industrialization, rapid urbanization, and land use patterns enhance the negative impacts associated with environmental contaminants and pollution. Sustainable development is possible when the environment is healthy.

The sustainable development goal of the United Nations will be very difficult to achieve without properly addressing the environmental concerns. Environment is the surroundings or conditions in which a person, animal, or plant lives or operates. It is the sum total of all surroundings of a living organism, including natural forces and other living things. Both biotic and abiotic components form the environment. These two components interact with each other and are interdependent. This interdependency to each other is the key reason for the human urge either to keep the environment safe and free from contamination or to invent gadgets for making humans isolated from the environment. Whatever the case may be, a proper assessment of environmental contaminants not to a point scale but to a wide spatial scale is required.

This book has 32 chapters associated with the measurement, monitoring, and mapping of environmental contaminants in soil and sediment, surface and groundwater, and the atmosphere. The book has been organized into three parts: (I) Soil and Sediment Contaminants, Risk Assessment and Remediation; (II) Water Contaminants, Risk Assessment and Remediation; and (III) Environmental contaminants, Impacts, and Sustainable Management. This book explores state-of-the-art techniques based on methodology and modeling in modern geospatial techniques specifically focusing on the recent trends in data mining techniques and robust modeling. It also presents modifications of and improvements to existing control technologies for remediation of environmental contaminants. In addition, it includes four separate sections on contaminants, risk assessment, and remediation of different

existing and emerging pollutants. It covers major topics such as radioactive wastes, solid and hazardous waste, heavy metal contaminants, modeling radon behavior, arsenic contaminants, microplastic pollution, microbiology of soil and sediments, soil salinity and sodicity, aquatic ecotoxicity assessment, fluoride contamination, hydrochemistry, geochemistry, indoor pollution, and human health aspects. The content of this book will be of interest to researchers, professionals, and policymakers whose work involves environmental contaminants and related solutions.

We are very much thankful to all the authors who have meticulously completed their documents on short notice and made this a very edifying and beneficial publication. We do believe that this will be a very convenient book for the geographers, ecologists, those interested in environmental sciences, geochemistry, geology, geophysics, hydrology, sedimentology, geospatial sciences, remote sensing and GIS, agriculture, crop science, horticulture, soil science, and agronomy, and others working in the field of environmental contaminants and management including the research scholars, environmentalists, and policymakers.

Midnapore, West Bengal, India
Bhubaneswar, Odisha, India
Kharagpur, West Bengal, India

Pravat Kumar Shit
Partha Pratim Adhikary
Debashish Sengupta

Acknowledgments

We are obliged to the experts for their kind support and valuable time to evaluate the chapters included in this book. We are very much thankful to our respected teachers, Prof. Malay Mukhopadhyaya, Prof. Sunando Bandyopadhyay, Prof. L.N. Satpati, Prof. Ashis Kumar Paul, Prof. Ramkrishna Maiti, Prof. Soumendu Chatterjee, Prof. Nilanjana Das Chatterjee, Prof. Dilip Kr. Pal, Prof. Sanat Kumar Guchait, Prof. N.C. Jana, Dr. Jatishankar Bandopadhyay, and Dr. Ratan Kumar Samanta, for sharing their experiences, useful suggestions, continuous encouragement, and immense support throughout the work.

We would like to thank the anonymous reviewers, acting as independent referees. Their inputs were consistently constructive and have substantially improved the quality of the final product.

We would also like to thank Éva Lörinczi and Prof. Robert J. Cabin, whose love, encouragement, and support kept us motivated to make this book a reality. Finally, the book has been several years in the making, and we therefore want to thank family and friends for their continuous support.

Dr. Pravat Kumar Shit thanks Dr. Jayasree Laha, Principal, Raja N.L. Khan Women's College (Autonomous), Midnapore, for her administrative support to carry on this project. We also acknowledge the Department of Geography, Raja N.L. Khan Women's College (Autonomous), for providing the logistic support and infrastructure facilities.

This work would not have been possible without constant inspiration from my students, lessons from my teachers, enthusiasm from my colleagues and collaborators, and support from my family.

Disclaimer The authors of individual chapters are solely responsible for the ideas, views, data, figures, and geographical boundaries presented in the respective chapters in this book, and these have not been endorsed, in any form, by the publisher, the editor, and the authors of forewords or other chapters.

Contents

Part I Soil and Sediment Contaminants, Risk Assessment and Remediation

- 1 Introduction to Part I: Soil and Sediment Contaminants, Risk Assessment, and Remediation 3**
Partha Pratim Adhikary
- 2 Combating Arsenic Pollution in Soil Environment via Alternate Agricultural Land Use 7**
A. K. Sahoo and Abhijit Halder
- 3 Temporal and Seasonal Variation in Leachate Pollution Index (LPI) in Sanitary Landfill Sites: A Case Study of Baidyabati Landfill, West Bengal, India 29**
Rachna Jain, Dipanjali Majumdar, and Rita Mondal
- 4 Quantification of Landfill Gas Emission and Energy Recovery Potential: A Comparative Assessment of LandGEM and MTM Model for Kolkata 55**
Babul Das and Tumpa Hazra
- 5 Assessment of Natural Enrichment of Heavy Minerals along Coastal Placers of India: Role of Lake and River Mouth Embayment and Its Implications 69**
Shayantani Ghosal, Sudha Agrahari, Debashish Banerjee, and Debashish Sengupta
- 6 Assessment on the Impact of Plastic-Contaminated Fertilizers on Agricultural Soil Health: A Case Study in Memari II C.D. Block, Purba Bardhaman, West Bengal, India 83**
Piyush Maji and Biswaranjan Mistri

7	Determining the Role of Leaf Relative Water Content and Soil Cation Exchange Capacity in Phytoextraction Process: Using Regression Modelling	107
	Akash Mishra and Bindhu Lal	
8	Phytoremediation of Arsenic Using <i>Allium sativum</i> L. as a Model System	121
	Soumik Chatterjee and Sabyasachi Chatterjee	
9	Spatio-temporal Analysis of Open Waste Dumping Sites Using Google Earth: A Case Study of Kharagpur City, India	137
	Abhishek Singhal and Sudha Goel	
Part II Water Contaminants, Risk Assessment and Remediation		
10	Introduction to Part II: Water Contaminants, Risk Assessment, and Remediation	155
	Pravat Kumar Shit	
11	Groundwater Arsenic Contamination Zone Based on Geospatial Modeling, Risk, and Remediation	159
	Merina Ghosh	
12	Geospatial Assessment of Surface Water Pollution and Industrial Activities in Ibadan, Nigeria	189
	Olutoyin Adeola Fashae and Rotimi Oluseyi Obateru	
13	Aquaculture-Based Water Quality Assessment and Risk Remediation along the Rasulpur River Belt, West Bengal	213
	Suraj Kumar Mallick, Biswajit Maity, and Somnath Rudra	
14	Heavy Metal Contamination in Groundwater and Impact on Plant and Human	233
	A. Nivetha, C. Sakthivel, and I. Prabha	
15	Emerging Threats of Microplastic Contaminant in Freshwater Environment	247
	Pratik Ghosh, Ritwik Patra, Prasanta Patra, Nabarun Chandra Das, Suprabhat Mukherjee, Bidhan Chandra Patra, Bhaskar Behera, and Manojit Bhattacharya	
16	Exploring Particle Size Transport Variability of Suspended Sediments in Two Alpine Catchments Over the Lesser Himalayan Region, India	259
	Omvir Singh	
17	Salinity and Corrosion Potential of Groundwater in Mewat District of Haryana, India	277
	Gaurav Verma, Smita Sood, Priyanka Sharma, and Shakir Ali	

18 Threats to Quality in the Coasts of the Black Sea: Heavy Metal Pollution of Seawater, Sediment, Macro-Algae and Seagrass 289
 Levent Bat, Elif Arici, and Aysah Öztekin

19 Geospatial Assessment of Groundwater Quality for Drinking through Water Quality Index and Human Health Risk Index in an Upland Area of Chota Nagpur Plateau of West Bengal, India 327
 Baisakhi Chakraborty, Sambhunath Roy, Amit Bera, Partha Pratim Adhikary, Biswajit Bera, Debashish Sengupta, Gouri Sankar Bhunia, and Pravat Kumar Shit

20 Existence of Pharmaceuticals and Personal Care Products (PPCPs) in the Conventional Water Treatment Process 359
 Noor A. Khan, Kavita N. Gandhi, Vidyasagar Devtade, Kirti Nandanwar, Deep Chand, S. Kashyap, and N. P. Thacker

21 Arsenic-Rich Surface and Groundwater around Eastern Parts of Rupnagar District, Punjab, India 379
 Navjot Kaur and Susanta Paikaray

Part III Environmental Contaminants, Impacts and Sustainable Management

22 Introduction to Part III: Environmental Contaminants, Risk Assessment and Remediation 397
 Debashish Sengupta

23 Dynamics of Ultrafine Particles in Indoor and Outdoor Environments: A Modelling Approach to Study the Evolution of Particle Characteristics 401
 S. Anand, Jayant Krishan, and Y. S. Mayya

24 Environmental Impacts of Coal-Mining and Coal-Fired Power-Plant Activities in a Developing Country with Global Context 421
 Md. Ahasan Habib and Rahat Khan

25 Overview of Indoor Air Pollution: A Human Health Perspective . . . 495
 Ambikapathi Ramya, Ambikapathi Nivetha, and Periyasamy Dhevagi

26 Mineralogy and Morphological Characterization of Technogenic Magnetic Particles (TMP) from Industrial Dust: Insights into Environmental Implications 515
 Supriya Mondal, Saurodeep Chatterjee, and Debesh Gain

27 Pesticides: Types, Toxicity and Recent Updates on Bioremediation Strategies 531
 Rujul Deollikar, Soumya Pandit, Jyoti Jadhav, Govind Vyavahare, Ranjit Gurav, Neetin Desai, and Ravishankar Patil

28	Commonly Available Plant Neem (<i>Azadirachta indica</i> A. Juss) Ameliorates Dimethoate Induced Toxicity in Climbing Perch <i>Anabas testudineus</i>	569
	Santosh Kumar Giri, Sanjib Gorain, Monoj Patra, Dinesh Gope, Nimai Chandra Saha, and Surjyo Jyoti Biswas	
29	Estimating Particulate Matter Concentrations from MODIS AOD Considering Meteorological Parameters Using Random Forest Algorithm	591
	Eeshan Basu and Chalantika Laha Salui	
30	Biomonitoring and Bioremediation of a Transboundary River in India: Functional Roles of Benthic Mollusks and Fungi	611
	Susanta Kumar Chakraborty, Hirulal Pakhira, and Kishalay Paria	
31	Assessing the Maximum Aerobic Biodegradation Potential of Leaf Litter, an Organic Fraction of Municipal Solid Waste, Under Optimum Nutrient Conditions	663
	Basavaraj R. Hiremath and Sudha Goel	
32	Rising Trend of Air Pollution and Its Decadal Consequences on Meteorology and Thermal Comfort Over Gangetic West Bengal, India	689
	Debjani Dutta and Srimanta Gupta	

About the Editors



Pravat Kumar Shit is an Assistant Professor at the PG Department of Geography, Raja N. L. Khan Women's College (Autonomous), West Bengal, India. He received his M.Sc & Ph.D. degrees in Geography from Vidyasagar University and PG Diploma in Remote Sensing & GIS from Sambalpur University. His research interests include applied geomorphology, soil erosion, groundwater, forest resources, wetland ecosystem, environmental contaminants & pollution and natural resources mapping & modeling. He has published seven books (five books in Springer) and more than 50 papers in peer-reviewed journals. He is currently the editor of the GIScience, and Geo-environmental Modelling (GGM) Book Series, Springer-Nature.



Partha Pratim Adhikary is a Senior Scientist at ICAR-Indian Institute of Water Management, Bhubaneswar, India. He obtained his Ph.D. in Agricultural Physics from ICAR-Indian Agricultural Research Institute, New Delhi, India. His research interests include solute transport, soil and water conservation and management, pedotransfer functions, and geospatial modeling of natural resources. Dr. Adhikary has published more than 60 research papers in peer-reviewed journals and three books. His other publications include book chapters, popular articles, technology brochures, technical bulletins, and scientific reports. He is the associate editor of Indian Journal of Soil

Conservation. Currently, he is the editor of Springer-Nature book series “GIScience and Geo-environmental Modelling”.



Debashish Sengupta is working as Professor, Higher Administrative Grade and Former Head of the Department of Geology and Geophysics in Indian Institute of Technology (IIT) Kharagpur, West Bengal, India. Prof. Sengupta has more than 30 years of teaching and research experience. He has completed his PhD in 1987 in Applied Geophysics. His areas of interests are nuclear geophysics including petroleum logging using subsurface nuclear data, radioactive methods and geochronology, radon emanometry and its applications, applications of isotopes and radionuclides in earth and environmental geosciences, heat flow, and geothermics. Prof. Sengupta has 100 research publications in international journals and more than 60 papers in Conference Proceedings apart from a large number of Invited Talks delivered both in India and abroad. The research work has been seminal and resulted in the formulation of Environmental Regulation policies in various countries both in India and countries like USA, South America and the European Union. Prof. Sengupta had also been a Visiting Professor at the University of Sao Paulo, Brazil and as Senior Visiting Professor at the University of Salamanca, Spain, earlier, while on a sabbatical leave from the institute. He has received Society of Geoscientists and Allied Technologists (SGAT's) Award of Excellence in Earth Sciences for the year 2003. Prof. Sengupta has published four books.

Part I
Soil and Sediment Contaminants, Risk
Assessment and Remediation

Chapter 1

Introduction to Part I: Soil and Sediment Contaminants, Risk Assessment, and Remediation



Partha Pratim Adhikary

Abstract Contaminants in soil and sediment are posing a threat to the environment. As the contaminants can change the health of any system over time, periodic revisit on the topic of soil and sediment contamination is necessary. Mostly the soil and sediment contaminants are external in origin; therefore, the ill effects of this are linked to the mismanagement of natural resources by human beings. Faulty agricultural practices induce accelerated soil erosion and nonpoint sources of contamination. Point sources of contamination are mainly linked to waste and garbage disposal, leakage, and indiscriminate use of natural resources. The risk arising from the contamination of soil and sediments needs to be assessed, and remediation of the risk needs to be explored. The risk assessment and remediation is not an easy task and becomes more complicated when we talk about soil and land resources as these resources are considered personal property. The first section of this book highlights different issues related to soil and sediment contaminants, how one can assess different geogenic and anthropogenic contaminants, and how the risk of contamination can be remediated.

Keywords Anthropogenic contamination · Geogenic contamination · Land and society · Point and nonpoint source contamination · Risk assessment

1.1 Introduction

Soil and sediment contamination is a highly discussed topic, and periodic revisiting is necessary for a better understanding of the consequences arising out of contamination of soils and sediment. Soil being the universal sink ultimately bears the furies of nature as well as the mismanagement of human beings. Contaminants are undesirable substances that alter the physical, chemical, and biological health of

P. P. Adhikary (✉)

ICAR-Indian Institute of Water Management, Bhubaneswar, Odisha, India
e-mail: partha.adhikary@icar.gov.in

© Springer Nature Switzerland AG 2021

P. K. Shit et al. (eds.), *Spatial Modeling and Assessment of Environmental Contaminants*, Environmental Challenges and Solutions,
https://doi.org/10.1007/978-3-030-63422-3_1

any system. In the case of soil contaminants, most of the contaminants are external in origin and are being dumped into the soil by municipal garbage disposal, industrial waste disposal, leakage from septic tanks and sewage water pipes, open defecation, indiscriminate use of pesticides and fertilizers to grow agricultural crops, etc. (Adhikary et al. 2010). The geogenic contaminants are arsenic and fluoride, but anthropogenic activities are responsible for these geogenic contaminants to show their harmful effect.

Soil is the basis of our existence because agricultural activity is only possible on soil. However, due to faulty agricultural practices and related other anthropogenic activities, accelerated soil erosion has become a normal phenomenon. Eroded sediments from the agricultural fields flow with the runoff water and are being deposited in the depressions such as ponds, lakes, and upstream parts of dams. The sediments are rich in nutrients, so the source soils become nutrient poor gradually and the sink reservoirs become gradually nutrient rich (Adhikary et al. 2018). On the one hand, in the source soil, because of low soil fertility, the crop yield will decrease, but on the other hand, in the sink reservoir, because of high nutrient content, eutrophication will result. Both these cases are harmful and cause social, ecological, and economic loss. Therefore, a proper risk assessment of soil and sediment contamination is necessary to address this twin problem.

The risk assessment of soil and sediment contamination is not an easy task, not only because of its complicated nutrient cycle and numerous links but also because of its social consequences (Shirani et al. 2020). The exposure to hazardous chemicals from different anthropogenic sources and its future implications are really very challenging to assess. Another challenge lies in the fact that irrespective of other natural resources such as air and water, which are considered free for all, soil or land is often considered private property and traded as real estate. Therefore, the divergence between different stakeholders such as scientists, academicians, engineers, managers, farmers, businessmen, administrators, lawyers, politicians, and nongovernment organizations starts to happen. Even if we neglect these aspects, there will be a number of other unresolved problems in assessing the risk of soil and sediment contamination.

The first section of the book deals with these problems and how we can get first-hand information about soil and sediment contaminants, their risks to the environment and society, and how to cope up with these contaminants.

1.2 Individual Chapters

There are eight chapters in this section to address soil and sediment contaminants. Chap. 2 deals with arsenic pollution in soil and how to combat it by alternate land-use practices. The lower Indo Gangetic plain is a hot spot for arsenic contamination, and in this chapter, the importance of alternate land-use systems involving jute, wheat, sesame, groundnut, and rapeseed/mustard crops having less irrigation water requirement has been described. The spatial and temporal variation of leachate

contamination from sanitary landfill sites of the suburban area of Kolkata municipality has been described in chap. 3. The leachate pollution index and its three variations such as organic, inorganic, and heavy metal indices seem to be very effective to describe the temporal and spatial trends of leachate contamination. The chapter concludes that the leachate sample shows seasonwise variation, and therefore a suitable strategy should be followed for its treatment as per requirement. Primary treatment alone is not sufficient, and hence some other suitable technologies, either microbial or physicochemical, are required to reduce the leachate contamination to an acceptable level before it could be released into the environment. The gases emitted from the landfill sites are being lost to nature. These gases have a very high climate change impact. On the other hand, these gases can be used for producing energy. Chap. 4 deals with this aspect with the objective to estimate and compare the emission of landfill gas from an uncontrolled landfill site located in Dhapa, Kolkata, India using LandGEM (3.02) and the modified triangular method (MTM) model. The energy generation potential of the generated landfill gas is also assessed. The use of the model to address this type of issue is really innovative and needs extensive calibration and validation. Chap. 5 deals with the delineation of heavy mineral enrichment of beach sands situated along the eastern coastal areas of India. The results obtained are discussed in terms of radioactive elements and rare earth element concentration in the study area. Certain radiological attributes such as radium equivalent, absorbed dose rate, and annual effective dose rate values have been presented. The study discusses the effect of the lacustrine and estuarine environment on the heavy mineral deposition, enhancement along the beach placers, and its implications. The effect of consistent mining along the beach area on the elevated radioelement concentration as well as the beach geomorphology has been discussed. Additionally, the chapter also highlights the disruption caused by the dredging activities to the marine species dwelling along the beach areas. Plastic contamination in marine and lake systems has been studied extensively, but plastic pollution in the terrestrial environment, especially in agricultural lands, has largely been overlooked. Therefore, chap. 6 deals with the application of plastic-enriched biofertilizers and sewage sludge water in farmlands. The chapter concludes with some possible and indigenous ways to minimize this hazardous pollution in soils. Chap. 7 deals with the role of leaf relative water content and soil cation exchange capacity in the phytoextraction process. They have used a regression model to conclude that the coarser fraction of soil has a direct effect on the phytoextraction process of contaminants. Phytoremediation is the process by which removal or degradation of contaminants from the soil by using green plants takes place. The aim of chap. 8 is to study the phytoremediation capacity of arsenic (As) from soil by the use of *Allium sativum* crop. It was found that *Allium sativum* has the ability to accumulate arsenic in its root tissues and thus made it an effective phytoaccumulator of arsenic. The last chapter of the section describes the effectiveness of open-source software and images such as google earth to analyze the dynamics of open waste dumping sites. The areal cover, size of the dumps, and seasonal behavior of the dumps are analyzed in this chapter. The chapter gives a very good solution for proper

monitoring of the dumping sites in an urban area and gives a clue to the policymakers for better governance.

References

- Adhikary PP, Chandrasekharan H, Chakraborty D, Kamble K (2010) Assessment of groundwater pollution in West Delhi, India using geostatistical approach. *Environ Monit Assess* 167:599–615
- Adhikary PP, Hombegowda HC, Barman D, Madhu M (2018) Soil and onsite nutrient conservation potential of aromatic grasses at field scale under a shifting cultivated, degraded catchment in eastern Ghats, India. *Int J Sediment Res* 33(3):340–350
- Shirani M, Afzali KN, Jahan S et al (2020) Pollution and contamination assessment of heavy metals in the sediments of Jazmurian playa in Southeast Iran. *Sci Rep* 10:4775. <https://doi.org/10.1038/s41598-020-61838-x>

Chapter 2

Combating Arsenic Pollution in Soil Environment via Alternate Agricultural Land Use



A. K. Sahoo and Abhijit Haldar

Abstract This chapter highlights the severity of arsenic contamination in Nadia district (3927 sq. km), West Bengal, India (22°52'30" and 24°05'40" N; 88°08'10" and 88°48'15" E) comprising 17 blocks belonging to the alluvial tract of the highly productive Gangetic plain under the rice-based cropping system. Groundwater in all the blocks of the district is reported to be arsenic contaminated (0.01–>0.05 mg l⁻¹). Arsenic in soils ranging from 1.34 mgkg⁻¹ to 14.09 mgkg⁻¹, considerably influencing its accumulation in crops, is also reported. The methodology for mitigation of arsenic pollution in the soil environment through alternate agricultural land use, avoiding large-scale withdrawal of groundwater for irrigation, is vividly outlined. Land resource information for the district was generated on the 1:50000 scale, and nine land management units were identified. Land suitability for cultivation of crops viz. jute, wheat, sesame, groundnut, and rapeseed/mustard having less irrigation water requirement was assessed in the identified land management units. Data revealed high (S1) to moderate suitability (S2) for cultivation of jute, rapeseed/mustard, and groundnut in 95%, 88.2%, and 34.8% area, moderate suitability (S2) for wheat and sesame in 19.3% and 41.8% area, and marginal suitability (S3) for wheat, rapeseed/mustard, sesame, and groundnut in 75.7%, 6.8%, 53.2%, and 60.2% area, respectively. Introduction of these crops as alternate land-use options, along with prevailing rainfed rice crops, is advocated for reducing arsenic loading in the soil. An appropriate cropping system for the district is also proposed.

Keywords Arsenic · Soil environment · Land management units · Land suitability · Alternate agricultural land use

A. K. Sahoo (✉) · A. Haldar
ICAR, National Bureau of Soil Survey and Land Use Planning, Kolkata, West Bengal, India

2.1 Introduction

Arsenic, a toxic metalloid, is ubiquitous in the natural environment viz. land, air, water, plants, and animals and therefore is of utmost concern. Over 200 million people across 70 countries, including India, are affected by As-contaminated groundwater (Sun et al. 2010; Takahashi et al. 2004). Continuous use of As-contaminated groundwater for drinking and irrigation resulted in adverse health effects (Singh et al. 2014, 2015; Smedley and Kinniburgh 2002), even causing death (Hopenhayn 2006).

Arsenic in groundwater and soil environment is usually present as arsenites ($\text{As}^{\text{III}}\text{O}_3^{3-}$), arsenates ($\text{As}^{\text{V}}\text{O}_4^{3-}$), or both apart from the less toxic or nontoxic organic forms. The arsenites are much more soluble, mobile, and toxic than the arsenates (Sanyal 2005). The magnitude of groundwater arsenic contamination (believed to be of geogenic origin) in West Bengal, India is alarming where arsenic concentration is reported to be above 0.05 mg l^{-1} , far exceeding the World Health Organization permissible limit for drinking water (WHO 1993, 1996).

Extensive use of arsenic-contaminated groundwater for irrigation (85–90%) results in the build-up of arsenic concentration in agricultural soils, possibly due to oxidation of arsenic-rich pyrites during large-scale withdrawal of groundwater (Sanyal 2005). Soil arsenic is the major source for the arsenic uptake of crops (Huang et al. 2006). Furthermore, soil acts as a major sink of arsenic inflow to agroecosystems and acts as a medium for the passage of the toxin to human population via the food web (Carey et al. 1996; Ghosh et al. 2002; Majumdar and Sanyal 2003). Undoubtedly, the scale of the problem is grave and unprecedented, exposing millions of people in the Bengal delta basin to risk and therefore urgently warrants effective mitigation measures to combat the deadly menace.

Arsenic toxicity in humans is due to the inactivation of the enzyme system as a result of binding through various biological ligands (Abhyankar et al. 2012). Several health effects due to arsenic poisoning are well documented (Guha Mazumder et al. 2000; Guha Majumdar 2008; Saha 1983).

Several mitigation measures reported *hitherto* over the past two decades include a number of arsenic removal technologies involving physicochemical and biological treatment of drinking water (Santra et al. 2013) using technologies comprising oxidation, co-precipitation, lime treatment, etc.; *phytoremediation* of arsenic-contaminated agricultural soils (Kramer 2005; Ma et al. 2003; Chen et al. 2006; Ma et al. 2001; Visoottiviset et al. 2002; Zhao et al. 2002); microbial alleviation of arsenic-contaminated soils (Cheng and Focht 1979; Johnson et al. 2003; Gihring and Banfield 2001; Maity et al. 2011); and lessening of soil arsenic contamination using organic amendments (Ghosh and Bhattacharyya 2004; Mukhopadhyay and Sanyal 2004; Jones 2007; Mukhopadhyay et al. 2002). Bioremediation proves to be comparatively superior to the physical and chemical methods, which are often very expensive and produce toxic sludge that again becomes a matter of concern.

Notwithstanding the development of various mitigation measures as briefed above, studies involving agricultural management strategies are limited (Samal

et al. 2009; Ross et al. 2005). Some effective remedial options in this regard were outlined (Sanyal 2016). Undeniably, exploring the suitability of crops requiring low irrigation with a view to promoting such crops/cropping sequence without the large-scale abstraction of groundwater for agricultural irrigation in arsenic-contaminated areas certainly assumes mammoth importance.

This chapter has made an attempt to address the issue of arsenic contamination in Nadia district, West Bengal – an arsenic hotspot (<http://www.cgwb.gov.in>), belonging to the alluvial tract of the highly productive Gangetic plain under the rice-based cropping system and suggests a knowledge-based alternate agricultural land-use option toward combating arsenic loading in the soil environment.

2.2 Materials and Methods

2.2.1 Study Location: An Overview

Nadia district (22°52'30" and 24°05'40"N; 88°08'10" and 88°48'15"E), West Bengal, predominantly a rural district in the Gangetic alluvial plain, comprises four major physiography viz. (a) flood plain, (b) meander plain, (c) low-lying or marshy area, and (d) river valley. The climate is sub-humid subtropical with annual rainfall ranging from 940 to 1612 mm and annual temperature varying from 25.3 °C to 26.9 °C.

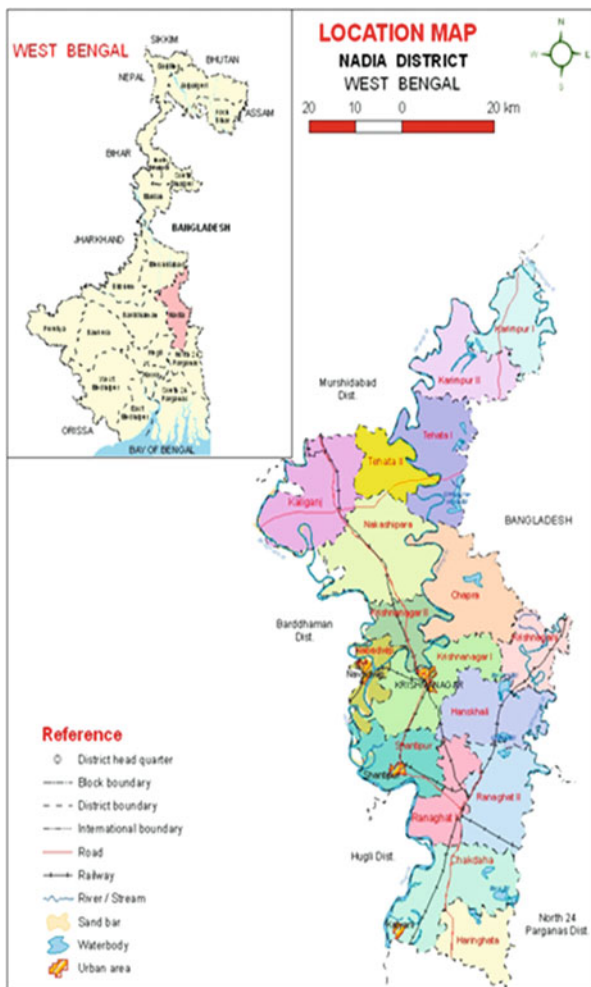
The district is composed of four subdivisions Krishnagar Sadar, Ranaghat, Kalyani, and Tehatta subdivided into 17 community development blocks with a total area of 3927 sq.km. The community development blocks are Karimpur I, Karimpur II, Tehatta I, Tehatta II, Kaliganj, Nakashipara, Chapra, Krishnaganj, Krishnanagar I, Krishnanagar II, Nabadwip, Santipur, Hanskhali, Ranaghat I, Ranaghat II, Chakdaha, and Haringhata (Fig. 2.1).

The land utilization pattern of Nadia district reveals that the net sown area is 292,940 ha, covering 74.98% area followed by areas under non agricultural use (22.64%), current fallow (1.09%), land under miscellaneous trees (0.66%), forest land (0.31%), and others (0.32%) (Census 2011). Around 58% area in the district is irrigated by various sources (predominant source being shallow tube well), and the remaining 42% area is rainfed.

Agriculture is the mainstay of the district, and its economy is intricately interwoven with the development of agriculture. More than three-fourths of the total workers of the district are engaged in agricultural pursuits either as a cultivator or as an agricultural laborer. The total number of holdings in the district is 424,206 ha with a total area of 349,988 ha with an average size of 0.82 ha. The size of holdings is predominantly marginal (<1 ha; 79.8% of the total holdings), followed by small farmers (1–2 ha; 17.3%).

The cropping intensity in the different blocks of the district varies from 224% to 267%. There are three seasons in the district viz., *kharif*, *rabi*, and summer (*pre-kharif*). *Kharif* is the predominant season, which extends from the beginning of June

Fig. 2.1 Location map of Nadia district



to mid of November. The climate and soil types of the district render it possible to grow various types of crops and tree plants. *Aman* rice, maize, arhar, and black gram are the main *kharif* crops. *Boro* rice, wheat, gram, lentil, oilseeds (mustard and groundnut), chilli, and potato are the main *rabi* crops. *Aus* rice and sesame are the main summer crops. Jute, the dominant cash crop in the district, is grown during March to September. Sugarcane is planted throughout the year. However, the crops in the district are classified according to their respective harvesting seasons into three broad categories, namely, *bhadoi* or *aus* (the autumn crops), *aghrani* or *aman* (the winter crop), and *rabi* (the late winter crop). Cereals, pulses, and oilseed crops are grown in an area of 295.0, 52.7, and 102.3 thousand ha with the production of 875.2, 49.3, and 104.9 thousand tonnes, respectively. Jute is grown in about 126.8 thousand

ha. while sugarcane occupies an area of 1.8 thousand ha. These apart, horticulture, animal husbandry, fisheries, and sericulture also hold great promise in the district.

2.2.2 Arsenic Contamination Status Appraisal

The arsenic contamination status in the district was ascertained by a review of several reports as well as authentic internet source (Mukherjee et al. 2009; Santra et al. 2013; Chakraborti et al. 2009; Ghosh et al. 2002; Sanyal 2005; <http://www.cgwb.gov.in>).

2.2.3 Combating Arsenic Pollution via Alternate Agricultural Land Use

Alternate agricultural land use avoiding excessive withdrawal of arsenic-contaminated groundwater and, for that matter, exploring the suitability of crops requiring less irrigation is certainly the way forward toward decreasing arsenic loading in the soil environment.

The suitability of different crops having less irrigation water requirement was explored as per the exhaustive methodology (Sahoo et al. 2017), which is briefly outlined below.

2.2.4 Soil Resource Mapping, Land-Use Mapping, and Climatic Data Analysis

Soil resource mapping of Nadia district was carried out on the 1:50,000 scale by standard procedures using remote sensing techniques following a 3-tier approach viz. image interpretation, soil survey and laboratory investigation, and GIS and printing. The soil map generated was further generalized on the basis of physiography and the most significant variable of soil properties (soil texture, drainage, and calcareousness) for delineating meaningful soil units. The land-use map was generated from the interpretation of multiseasonal satellite data IRS P6 LISS III. Analysis of climatic data obtained from IMD stations from different places of the district was used for delineation of agro-ecological units in the district.

2.2.5 *Spatial Integration of Generalized Soil and Land-Use Map for Identifying Land Units*

Generalized soil and land-use maps were integrated through the overlay process for obtaining different land units. The vector overlay resulted in a large number of slivers (spurious polygons), which were eliminated through careful editing and merging to adjoining units by specifying the tolerance limit. The attribute data set generated contained information on soil characteristics and land use.

2.2.6 *Identification of Major Production Systems and Delineation of Land Management Units (LMUs)*

Four major production systems were identified in the district (Sahoo et al. 2017). Land units having similar production system, soils, and land use were further re-grouped for delineating the land management units (LMUs) for the district.

2.2.7 *Evaluation of Land Management Units for Exploring the Crop Suitability for Alternate Land Use*

The soil and land resource of all the LMUs of Nadia district were assessed and evaluated for their suitability for growing crops viz. jute (*Corchorus olitorius*), wheat (*Triticum aestivum*), sesame (*Sesamum indicum*), groundnut (*Arachis hypogaea*), and rapeseed/mustard (*Brassica* spp.) having less irrigation water requirement to the tune of about 500 mm, 550 mm, 300 mm, 550 mm, and 250 mm, respectively, as alternate land-use options by matching the crop requirements and soil-site characteristics (FAO 1976; Sys et al. 1993; Naidu et al. 2006). Subsequently, the crop suitability maps were generated in the geographic information system.

2.3 Results and Discussion

2.3.1 *Arsenic Contamination Status Scenario*

The status of groundwater arsenic contamination in West Bengal is shown in Fig. 2.2. A total of 38, 861 km² area is highly arsenic affected, including Nadia and adjoining districts of Malda and Murshidabad (Santra et al. 2013; Chakraborti et al. 2009; <http://www.cgwb.gov.in>).

Several workers have reported about arsenic contamination status in groundwater and its adverse effect on health in Nadia district (Chakraborti et al. 2009; Das et al.

Fig. 2.2 Arsenic contamination status in groundwater of West Bengal, India. Source: Mukherjee et al. (2009)



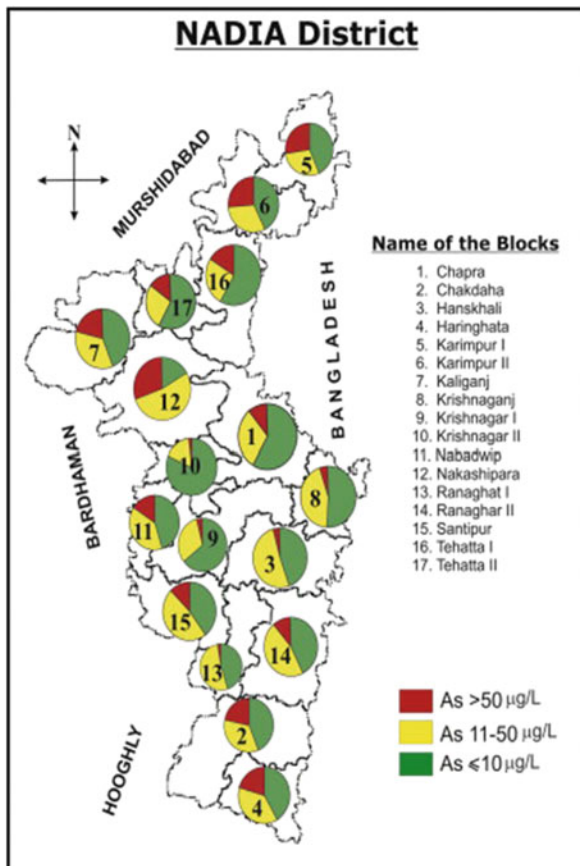
1994; Das 2007; Guha Mazumder et al. 1998; <http://www.cgwb.gov.in>; Santra et al. 2013; Bhattacharya et al. 2010). Alarming, groundwater of all the blocks of Nadia district is arsenic contaminated (Fig. 2.3; Table.2.1).

Arsenic contamination in soils to the tune of 1.34–14.09 mg kg⁻¹ in Haringhata, Chakdaha, Shantipur, Krishnanagar, and Ranaghat I is reported by several authors (Bhattacharya et al. 2010; Sanyal 1999). Furthermore, arsenic accumulation in the crops grown in the district is also reported (Das 2007; Biswas et al. 2012; Samal et al. 2011). However, accumulation depends on the types of crop and follows the trend viz. Root > Stem > Leaf > Grains.

2.3.2 Combating Arsenic Pollution Via Alternate Agricultural Land Use

(a) Delineation of land management units via soil resource mapping and related activities.

Fig. 2.3 Arsenic contamination in groundwater of different blocks, Nadia. Source: Mukherjee et al. (2009)



Soil resource mapping (1:50,000 scale) of Nadia district resulted in identification of 22 soil series, mapped into 43 soil mapping units as soil series association (Fig. 2.4).

Soils of the district belong to three soil orders viz. Inceptisols (66.1%), Alfisols (21.4%), and Entisols (7.5%). Coarse texture in active flood plain areas, imperfect to poor soil drainage, flooding, stagnation of water in low-lying areas, and arsenic contamination in groundwater are the major constraints threatening the production system.

The soil map of the district was generalized on the basis of physiography and the most significant variable soil properties (soil texture, drainage, and calcareousness), and 12 soil units were identified in 3 major physiographic regions (Fig. 2.5). Satellite image (temporal data of IRS P6 LISS III) interpretation revealed that about 3591 sq. km area was agricultural land, which was either under double crop or under triple crop. Double crop area covered about 1598 sq. km area, and triple crop area covered nearly 1993 sq. km area (Fig. 2.6). Spatial integration of land features, soils (generalized), current land use, and administrative divisions through overlay technique in

Table 2.1 Arsenic in groundwater in different blocks of Nadia district, West Bengal

S. No.	Block	Location	Arsenic (0.01– 0.05mg l ⁻¹)	Block	Location	Arsenic (>0.05mg l ⁻¹)
1.	Krishnaganj	Bhajanghat, Bijoypur, Gede, Gobindopur, Krishnaganj Matari, Mazda, Nalapur	0.01–0.02	Krishnaganj	–	–
2.	Ranaghat I	Birnagar, Kamgachi, Taherpur		Ranaghat I	–	–
3.	Chakdaha	Palpara, Rabindranagar, Silinda, Nartipara	0.01–0.03	Chakdaha	^a Ghentugachi Bagpara ^a Gotera	^a 0.131 0.40 ^a 0.133
4.	Chapra	Andulia, Chapra, Gongra, Hridaypur, Maharajpur, Mahatpur, Patia, Dakshin Bangalghi		Chapra	–	–
5.	Krishnannagar II	Babaipukur, Chowgachia, Gournagar, Jahangirpur		Krishnannagar II	Shakdahmore Chowgachia	0.123 0.148
6.	Santipur	Babla, Kulia, Santipur, Baganchra		Santipur	–	–
7.	Kaliganj	Chandanpur, Debgram, Juranpur, Kaliganj, Katwaghat, Laldighi, Plassey, Panchkhala, Chanpur	0.01–0.04	Kaliganj	Asachia, Basarkhol, Dangapara	0.07
8.	Karimpur II	Nandanpur, Narayanpur, Wazidpur, Pipulberia, Sardarpara, Berramchandrapur, Babakpur		Karimpur II	Debagram Kaliganj Mahishkhola Mahishbathan Kathalia Jhanpara Nandanpur	0.078 0.082 0.059 0.061 0.063 0.102 0.184
9.	Nakashipara	Bheladanga, Nakashipara, Sontala, Burpur, Gachha, Uttar Bahingachi, Shaligram, Kalabangra, Brahmanitala		Nakashipara	Nakashipara Chichuria	0.063 0.119

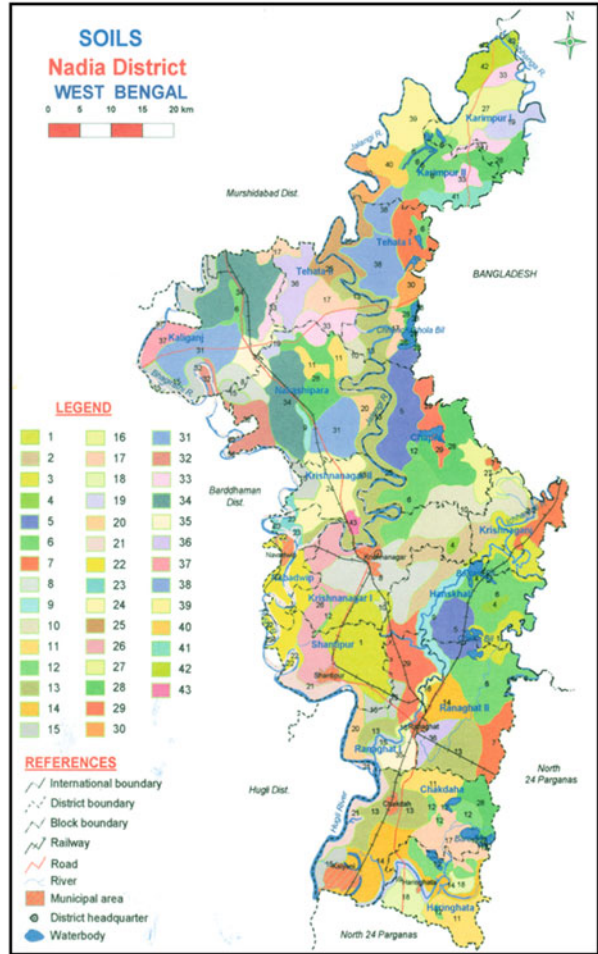
(continued)

Table 2.1 (continued)

S. No.	Block	Location	Arsenic (0.01– 0.05mg l ⁻¹)	Block	Location	Arsenic (>0.05mg l ⁻¹)
10.	Tehatta II	Betai, Debnathpur, Kharuigachi, Nazipur, Baliara, Garibpur, Haripur, Shyamnagar		Tehatta II	–	–
11.	Ranaghat II	Hijula, Patuli, Kuparscamp, Astala Garebagan		Ranaghat II	Patuli	0.065
12.	Hanskhali	Badkulla, Bagula, Chitrashali, Hanskhali, Khamarsimulia, Ulas	0.01–0.05	Hanskhali	–	–
13.	Karimpur I	Madhya Gopalpur, Sikarpur, Bagehijamshepur, Marutia, Fulberi, Kechuadanga, Kumari 55 mile, Mahishbathan, Natna, Prabpur		Karimpur I	UTR Kechuadanga Natna Natundangamore Madhya Gopalpur Arabpur Karimpur Hanspukuria	0.093 0.097 0.097 0.123 0.149 0.332 0.076
14.	Tehatta II	Palashipara, Arbetia				
15.	Haringhata	Barajagulia, Bilandi, Birohi, Subarnapur	0.02–0.04	Haringhata	^b Nonaghata ^b Mollabelia	^b 0.06– ^b .53 ^b 0.16
16.	Krishnanagar I	Bhaluka, Bhatjangla, Bishmupur, Dignagar, Kalinagar, Krishnanagar, Maheshganj, Panimala	0.02–0.05	Krishnanagar I	–	–
17.	Nabadwip	Mukundapur	0.04	Nabadwip	Tiorkhali Jamtala	0.063

Source: <http://www.egwb.gov.in>^aGhosh et al. (2002)^bSanyal (2005)

Fig. 2.4 Soil map of Nadia district



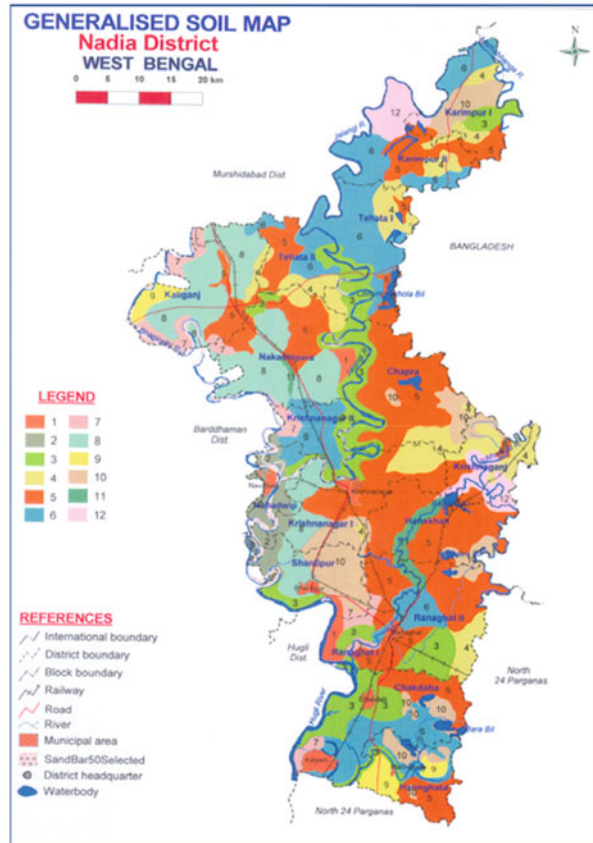
GIS generated land unit map with 20 mapping units (Fig. 2.7). Land units having similar production system, soils, and land use were further re-grouped for delineating the land management units (LMUs) for the district. In Nadia district, 9 LMUs were delineated (Fig. 2.8) having arsenic concentration in the groundwater ranging from 0.01–>0.05 mg l⁻¹ (Table 2.1), and all the LMUs were associated with four prevailing production systems.

The delineation of land management units is schematically represented in Fig. 2.9.

The salient features of the nine identified land management units are presented in Table 2.2.

(b) Land evaluation for identification of potential areas for different crops toward alternate land use.

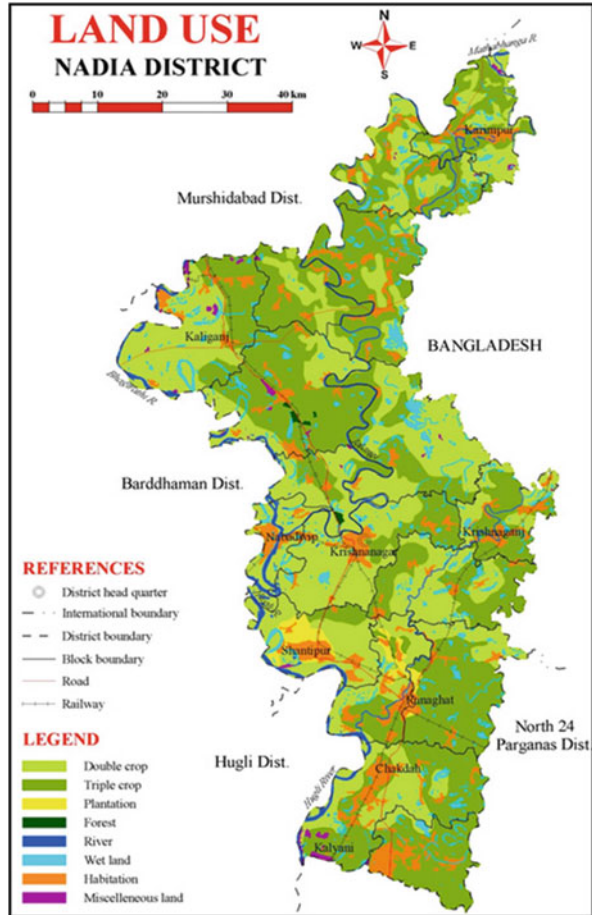
Fig. 2.5 Generalized soil map



The groundwater in Nadia district, West Bengal is highly arsenic contaminated and therefore warrants its careful use for irrigation purpose. Furthermore, it is presumed that use of a large volume of arsenic-contaminated irrigation water as in the case of summer (*boro*) paddy cultivation would certainly increase the arsenic content in soils. With a view to combating and reducing the arsenic contamination, it would be imperative to lift as minimum water as possible for the purpose of irrigation and therefore more emphasis should be given on rainfed agriculture and use of minimum water during non-rainy season as a remedial measure particularly by replacement of *boro* paddy cultivation as per water requirement. It is in such background that an attempt was made to assess the soil-site suitability of some selected crops viz. jute, wheat, rapeseed/mustard, sesame, and groundnut, which are characterized by overlapping growing period (in some cases partial) with summer (*boro*) paddy but with much less irrigation water requirement.

Cropwise land suitability for the selected crops in the different LMUs is presented in Table 2.3.

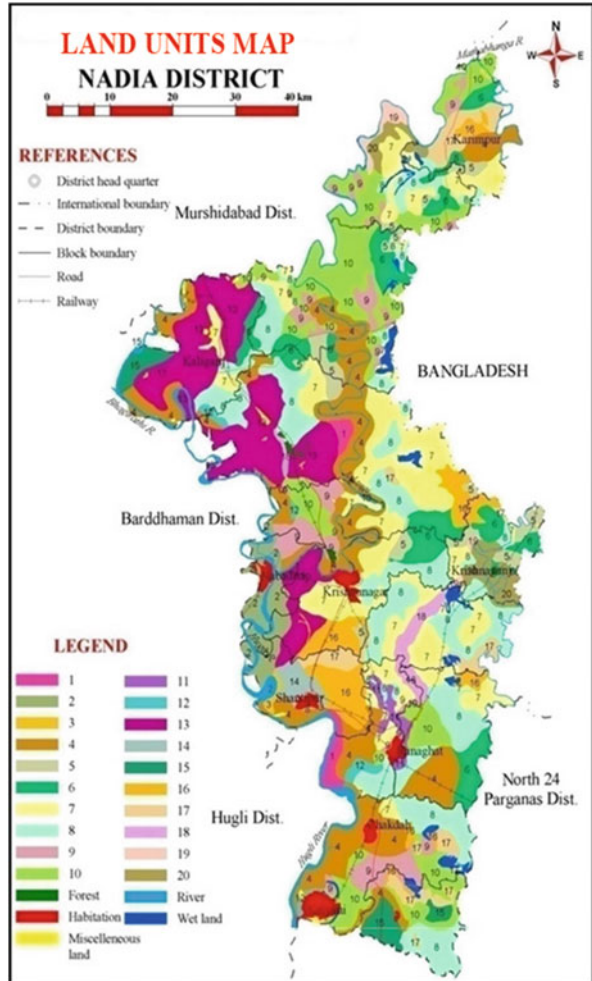
Fig. 2.6 Land-use/land cover map



A scan through the data (Table 2.3) reveals cultivation of jute, rapeseed/mustard, and groundnut to be highly suitable (S1) in LMU (13.4% area). Moderate suitability (S2) was registered by wheat (19.3% area) comprising LMUs 1 and 5, jute (91.6% area) comprising LMUs 2, 3, 4, 5, 6, 7, 8, and 9, rapeseed/mustard (84.8% area) comprising LMUs 2, 3, 4, 5, 6, 7, and 9, sesame (41.8% area) comprising LMUs 1, 2, 3, 6, and 9, and groundnut (31.4% area) comprising LMUs 2, 6, 7, and 9. Marginal suitability (S3) was exhibited by wheat (75.7% area) comprising LMUs 2, 3, 4, 6, 7, 8, and 9, rapeseed/mustard (6.8% area) in LMU 3, sesame (53.2% area) comprising LMUs 4, 5, 7, and 8, and groundnut (60.2% area) comprising LMUs 3, 4, 5, and 8. In general, moderate-to-marginal suitability for different crops were due to different classes of drainage limitations and calcareousness prevalent in soils pertaining to the different LMUs (Table 2.2).

Overall high-to-moderate suitability registered by jute in the entire district followed by rapeseed/mustard in 88.2% area and groundnut in 34.8% indicates

Fig. 2.7 Land unit map

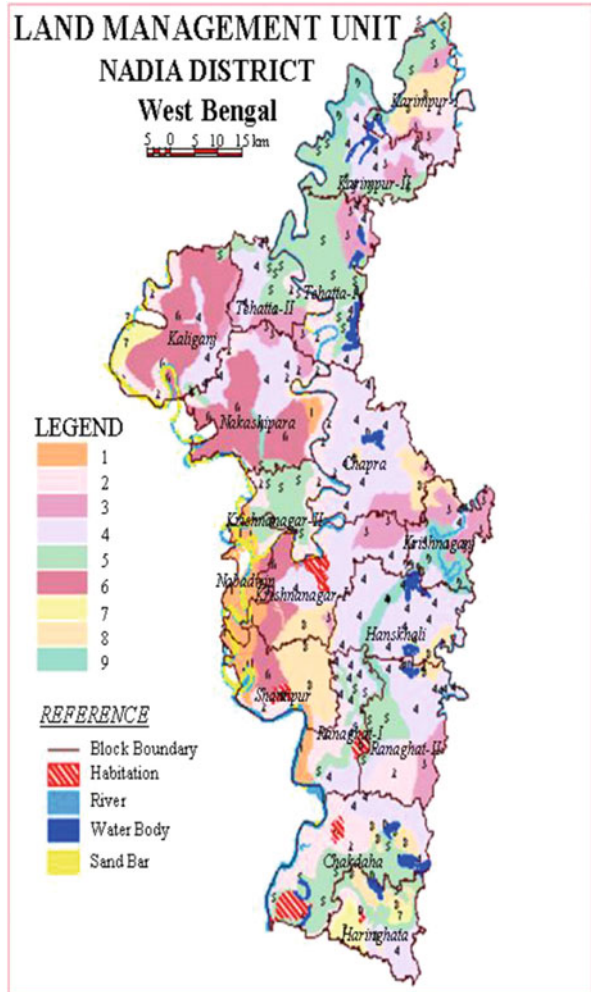


high potential for cultivation of the same. However, marginal suitability exhibited by wheat, groundnut, and sesame in the majority area of the district does not preclude their importance as choice toward alternate land use and also holds great promise with adequate soil management. Consequently, an appropriate cropping system in the district may be adopted as jute–kharif paddy–mustard/rapeseed/wheat/sesame/groundnut.

Some crop suitability maps generated by matching the crop requirements and soil-site characteristics are shown in Figs. 2.10a-c.

The results of crop suitability evaluation are certainly promising for promoting alternate land use with a view to reducing arsenic contamination in the district.

Fig. 2.8 Land management units



2.4 Risk Assessment and Remediation

Nadia district of West Bengal lying in the Gangetic alluvial plain supported by huge groundwater reserve and fine textured fertile soils being suitable for raising summer (*boro*) paddy is extensively used by the farmers for cultivation of the same, which consumes huge amount of groundwater, obviously ignoring the quality of groundwater resources used for irrigation that is highly arsenic contaminated and the consequent contamination of the soil/crop system with the toxin. During irrigation, higher withdrawal of arsenic-contaminated groundwater is responsible for creation of vacuum in the underground, which draws oxygen in the aquifers resulting in oxygenated decomposition of arsenopyrite, thereby creating pollution plume of

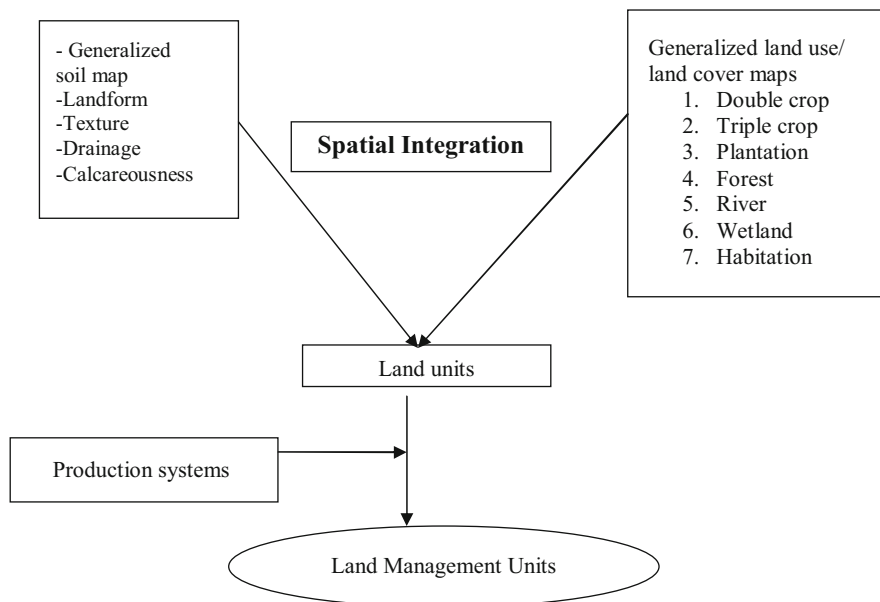


Fig. 2.9 Identification of land management units – Schematic

arsenic in the underground aquifer (Roy 1997). Evidently, practice of using arsenic-contaminated groundwater over the years resulted in accumulation of arsenic in the soil environment that acts as an excellent sink for this toxin (Majumdar and Sanyal 2003). In spite of having immense potential, the district is severely threatened by groundwater arsenic contamination.

Therefore, with a view to combating and reducing the arsenic contamination, it would be imperative to lift as minimum water as possible for the purpose of irrigation. More emphasis should be given on rainfed agriculture and use of minimum water during non-rainy season as a remedial measure particularly by replacement of *boro* paddy cultivation with alternate crops viz. jute, wheat, rapeseed/mustard, sesame, and groundnut which are characterized by overlapping growing period (in some cases partial) with summer (*boro*) paddy but with much less irrigation water requirement.

2.5 Conclusion

The entire Nadia district, West Bengal suffers from arsenic contamination in groundwater, causing arsenic pollution in the soil–crop environment. In view of such alarming crisis, excessive utilization of groundwater and its overexploitation need to be checked on priority for which adoption of alternate land-use option is perhaps the way forward toward mitigation from agricultural perspective.

Table 2.2 Salient features of the land management units

LMU (area in ha.)	Blocks covered	Cropping system	Landform and soil characteristics
LMU-1 (13476)	Nabadwip, Shantipur, Ranaghat I, Nakasipara, Krishnanagar I and II	I. Rice/jute/rice–rice/ mustard/vegetables/ses- ame/potato/lentil II. Rice–rice/wheat/mus- tard/rapeseed/vegetables– sesame III. Sugarcane	Well to moderately well- drained calcareous fine silty soils with silt loam surface occurring on nearly level to very gently sloping flood plain
LMU-2 (52463)	Chakdah, Ranaghat I and II, Chapra, Krishnanagar I and II, Kaliganj, Nakasipara, Tehatta I and II, Shantipur, Karimpur I, Haringhata, Nabadwip	I. Rice/jute–rice/mustard/ rapeseed/lentil/gram/ peas/vegetables/marigold II. Rice–rice/black gram/ mustard/rapeseed/lentil/ potato/gram/vegetables– sesamum III. Sugarcane	Imperfectly drained cal- careous coarse silty soils with silt loam surface occurring on nearly level flood plain and river valley
LMU-3 (33939)	Krishnaganj, Tehatta I and II, Krishnanagar I, Ranaghat II, Chapra, Karimpur I and II, Nakasipara, Kaliganj, Hanskhali	I. Rice/jute–rice–rice II. Jute–rice–mustard/ses- ame/lentil III. Rice–rice/mustard/ sesame	Moderately well-drained calcareous fine soils with silty clay loam to silty clay surface occurring on nearly level to very gently sloping meander plain
LMU-4 (113478)	Chapra, Hanskhali, Krishnanagar I, Ranaghat I and II, Nakasipara, Karimpur I and II, Chakdah, Tehatta I and II, Haringhata, Kaliganj, Krishnaganj, Shantipur, Nabadwip	I. Jute–rice–rice II. Rice/jute–rice–rice/ mustard/linseed/lentil III. Rice–rice/mustard/ rapeseed–sesame	Poor to imperfectly drained fine soil with silty clay surface occurring on very gently sloping mean- der plain
LMU-5 (62238)	Tehatta I, Chakdah, Karimpur II, Krishnanagar II, Tehatta II, Ranaghat II, Haringhata, Karimpur I, Ranaghat I, Nabadwip, Nakasipara, Kaliganj	I. Rice/jute–rice–rice/ vegetables/mustard/ses- ame/potato//tuberose/ marigold/sugarcane/ banana II. Rice–rice/mustard– sesame	Poorly drained calcareous fine loamy soils with silt loam surface on very gently sloping meander plain
LMU-6 (46844)	Kaliganj, Nakasipara, Krishnanagar I, Shantipur, Nabadwip, Krishnanagar II, Tehatta II	I. Jute–rice–rice II. Jute–rice–vegetables/ sesame III. Rice–rice–rice/vege- tables/potato IV. Rice–rice/mustard/ rapeseed/sesame V. Sugarcane/banana	Poorly drained fine silty soils with silty loam to loam surface on nearly level to very gently slop- ing meander plain
LMU-7 (6356)	Haringhata, Kaliganj	I. Rice/jute–rice–rice/ mustard/vegetables/ses- ame/marigold/tuberose/	Poorly drained calcareous fine silty soils with silt loam surface occurring on

(continued)

Table 2.2 (continued)

LMU (area in ha.)	Blocks covered	Cropping system	Landform and soil characteristics
		potato/lentil II. Rice–rice/mustard/sesame III. Sugarcane/banana	very gently sloping meander plain
LMU-8 (26624)	Shantipur, Karimpur I, Haringhata, Hanskhali, Chakdah, Krishnaganj, Ranaghat I and II	I. Rice/jute–rice/mustard/rapeseed/lentil II. Rice–rice/mustard/rapeseed/sesame	Poorly drained fine to very fine soils with severe flooding with silty clay surface on nearly level to very gently sloping low-lying/marshy land
LMU-9 (17482)	Krishnaganj, Karimpur II, Chapra, Hanskhali, Ranaghat II, Ranaghat I, Nakasipara, Karimpur I, Krishnanagar I	I. Jute/rice–rice–rice/wheat/mustard/rapeseed/lentil/gram/vegetables/marigold/black gram/tuberoses–sesamum II. Rice–rice/mustard–sesame	Imperfect to poorly drained, calcareous, fine loamy soils with silt loam to silty clay loam surface on very gently sloping river valley/low-lying land

Table 2.3 Land suitability for various crops

Crops	Suitability classes	Area (ha)	% TGA	LMU(s) covered
Wheat	S2	75,714	19.3	1,5
	S3	297,186	75.7	2,3,4,6,7,8,9
Jute	S1	13,476	3.4	1
	S2	359,432	91.6	2,3,4,5,6,7,8,9
Rapeseed/mustard	S1	13,476	3.4	1
	S2	332,800	84.8	2,3,4,5,6,7,9
	S3	26,624	6.8	8
Sesame	S2	164,204	41.8	1,2,3,6,9
	S3	208,696	53.2	4,5,7,8
Groundnut	S1	13,476	3.4	1
	S2	123,145	31.4	2,6, 7,9
	S3	236,279	60.2	3,4,5,8

S1 – highly suitable; S2 – moderately suitable; S3 – marginally suitable

Introduction of the field crops having less irrigation water requirement compared to the rice crop viz. jute, wheat, rapeseed/mustard, sesame, and groundnut as alternate crops along with prevailing rainfed rice crop certainly would lessen lifting of the quantum of arsenic-contaminated groundwater and thus may be instrumental in reducing arsenic pollution in the soil environment.

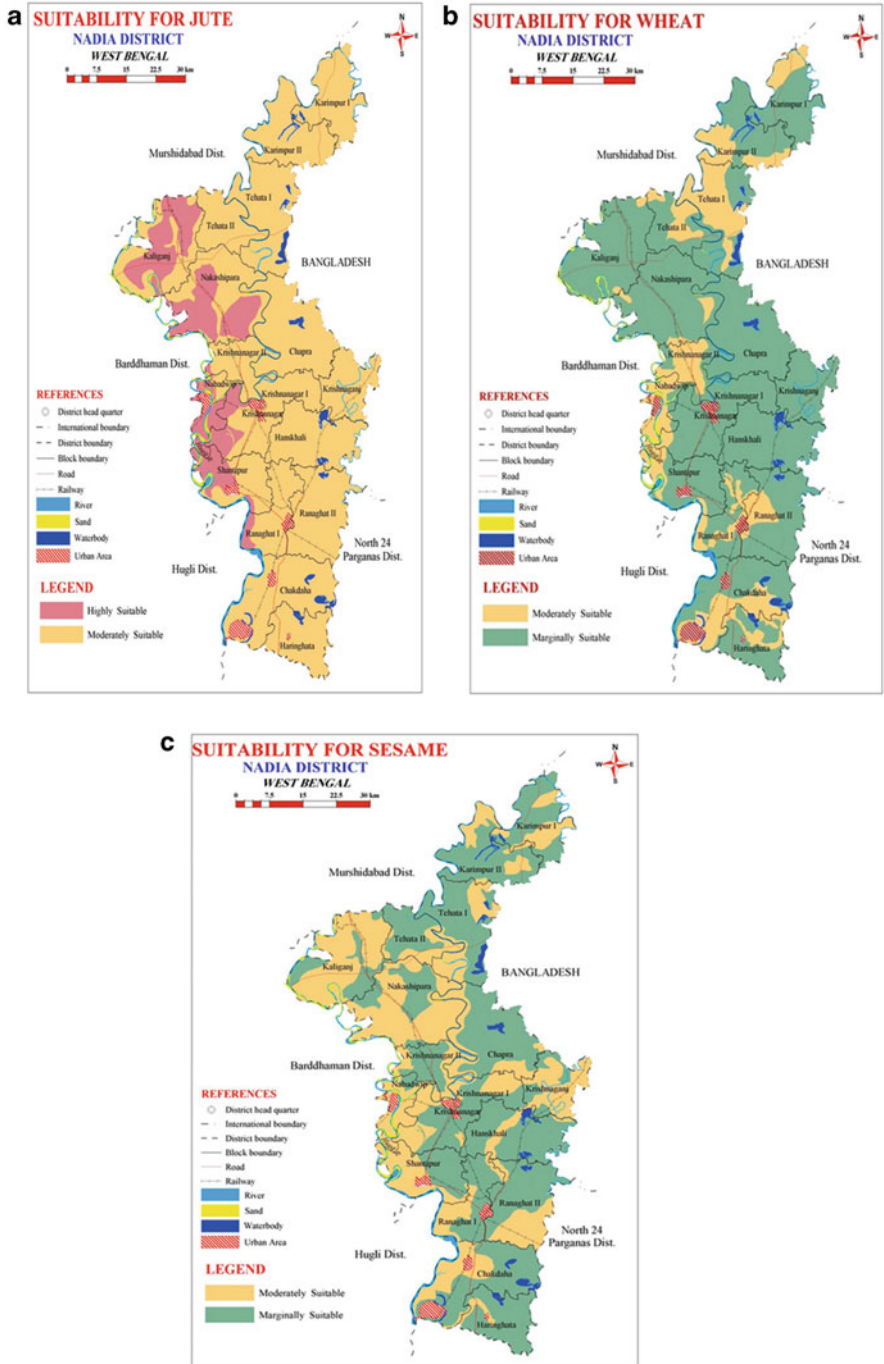


Fig. 2.10 (a) Suitability for jute. (b) Suitability for wheat. (c) Suitability for sesame

References

- Abhyankar LN, Jones MR, Guallar E, Navas-Acien A (2012) Arsenic exposure and hypertension: a systematic review. *Environ Health Perspectives* 120:494–500
- Bhattacharya P, Samal AC, Majumdar J, Santra SC (2010) Arsenic contamination in rice, wheat, pulses, and vegetables: a study in an arsenic affected area of West Bengal, India. *Water Air Soil Pollut* 213:3–13
- Biswas A, Samal AC, Santra SC (2012) Arsenic in relation to protein content of rice and vegetables. *Res J Agricultural Sci* 3(1):80–83
- Carey PL, McLaren RG, Adams JA (1996) Sorption of cupric, dichromate and arsenate ions in some New Zealand soils. *Water Air Soil Pollut* 87:189–203
- Census (2011). <http://www.census2011.co.in>
- Chakraborti D, Das B, Rahman MM, Chowdhury UK, Biswas B, Goswami AB, Nayak B, Pal A, Sengupta MK, Ahmed S, Hossain A, Basu G, Roychowdhury T, Das D (2009) Status of groundwater arsenic contamination in the state of West Bengal, India: a 20-year study report. *Molecular Nutrition Food Res* 53(5):542–551
- Chen BD, Zhu YG, Smith FA (2006) Effect of arbuscular mycorrhizal inoculation on uranium and arsenic accumulation by Chinese brake fern (*Pteris vittata*) from uranium mining- impacted soil. *Chemosphere* 62(9):1464–1473
- Cheng CN, Focht DD (1979) Production of arsine and methylarsines in soil and in culture. *Appl Environ Microbiol* 38:494–498
- Das D (2007) Arsenic in soil and groundwater environment. In: Bhattacharya P, Mukherjee AB, Bundschuh J, Zevenhoven R, Loepper RH (eds) Trace metals and other contaminants in the environment. Elsevier, Amsterdam, The Netherlands, pp 339–362
- Das D, Chatterjee A, Samanta G, Mandal B, Chowdhury TR (1994) Arsenic contamination in groundwater in six districts of West Bengal, India, the biggest arsenic calamity in the world. *Analyst* 119:168–170
- FAO (1976) A framework for land evaluation. *Soils bull.* FAO, Rome, p 32
- Ghosh AK, Bhattacharyya P (2004) Arsenate sorption by reduced and reoxidized rice soils under the influence of organic matter amendments. *Environ Geol* 45(7):1010–1016
- Ghosh AK, Sarkar D, Sanyal SK, Nayak DC (2002) Status and distribution of arsenic in alluvium derived soils of West Bengal and their interrelationship with some soil properties. *J Indian Soc Soil Sci* 50:51–56
- Gihring TM, Banfield JF (2001) Arsenite oxidation and arsenate respiration by a new *Thermus* isolate. *FEMS Microbiol Lett* 204:335–340
- Guha Majumdar DN (2008) Chronic arsenic toxicity & human health. *Indian J Med Res* 128:436–447
- Guha Mazumder DN, Haque R, Ghose N, De BK, Santra A, Chakraborti D (2000) Arsenic in drinking water and the prevalence of respiratory effects in West Bengal, India. *Int J Epidemiol* 29:1047–1052
- Guha Mazumder DN, Haque R, Ghosh N, De BK, Santra A, Chakraborti D, Smith AH (1998) Arsenic levels in drinking water and the prevalence of skin lesions in West Bengal, India. *Int J Epidemiol* 27:871–877
- Hopenhayn C (2006) Arsenic in drinking water: impact on human health. *Elements* 2:103–107. <https://doi.org/10.2113/gselements.2.2.103>
- Huang RQ, Gao SF, Wang W, Staunton S, Wang G (2006) Soil arsenic availability and the transfer of soil arsenic to crops in suburban areas in Fujian Province, Southeast China. *Sci Total Environ* 368:531–541
- Johnson DB, Okibe N, Roberto FF (2003) Novel thermo-acidophilic bacteria isolated from geothermal sites in Yellowstone National Park: physiological and phylogenetic characteristics. *Arch Microbiol* 180:60–68
- Jones FT (2007) A broad view of arsenic. *Poult Sci* 86:2–14

- Kramer U (2005) Phytoremediation: novel approaches to cleaning up polluted soils. *Curr Opin Biotechnol* 16:133–141
- Ma LQ, Komar KM, Tu C, Zhang WH, Cai Y, Kennelley ED (2001) A fern that hyperaccumulates arsenic: a hardly, versatile, fast growing plant helps to remove arsenic from contaminated soils. *Nature* 409:579
- Ma LQ, Tu MS, Fayiga AO, Stamps RH, Zillioux EJ (2003) Phytoremediation of arsenic contaminated groundwater using an arsenic hyperaccumulating fern *Pteris vittata* L. the 19th annual international conference on soils, sediments and water. University of Massachusetts, Amherst
- Maity JP, Kar S, Liu JH, Jean JS, Chen CY, Bundschuh J, Santra SC, Liu CC (2011) The potential for reductive mobilization of arsenic [as(V) to as(III)] by OSBH 2 (*Pseudomonas stutzeri*) and OSBH 5 (*Bacillus cereus*) in an oil-contaminated site. *J Environ Sci Health* 46(11):1239–1246
- Majumdar K, Sanyal SK (2003) pH-dependent arsenic sorption in an Alfisol and an Entisol of West Bengal. *Agropedology* 13:25–29
- Mukherjee SC, Pati S, Dutta RN, Saha KC (2009) Groundwater arsenic contamination situation in West-Bengal. A nineteen year study *Bhujal News Quarterly Journal*, April-Sept, 2009, India
- Mukhopadhyay D, Mani PK, Sanyal SK (2002) Effect of phosphorus, arsenic and farmyard manure on arsenic availability in some soils of West Bengal. *J Indian Soc Soil Sci* 50(1):56–61
- Mukhopadhyay D, Sanyal SK (2004) Complexation and release isotherm of arsenic in arsenic-humic/fulvic equilibrium study. *Aust J Soil Res* 42:815–824
- Naidu LGK, Ramamurthy V, Challa O, Hegde R, Krishnan P (2006) Manual soil-site suitability criteria for major crops. *Tech. Bull. No. 129*. NBSSLUP, Nagpur (India), p 118
- Ross Z, Duxbury JM, Paul DNR, DeGloria SD (2005) Potential for arsenic contamination of rice in Bangladesh: spatial analysis and mapping of high risk areas. In: *Behavior of arsenic in aquifers, soils and plants (Conference Proceedings)*, Dhaka
- Roy AK (1997) In *Desh*, A fortnightly periodical in vernacular language, Ananda Bazar Publicationm 26th July, 1997 pp: 113–119
- Saha KC (1983) Docket No. S/158/33/83 relating to outdoor patient from Ramnagar, Baruipara PS, South 24 Parganas, West Bengal. Department of dermatology, School of Tropical Medicine, Calcutta, West Bengal, India
- Sahoo AK, Banerjee T, Nayak DC, Sarkar D, Chaturvedi A, Singh SK (2017) District land use planning Nadia, West Bengal. NBSS publ no. 1104, NBSS&LUP, Nagpur, pp. 114
- Samal AC, Kar S, Bhattacharya P, Santra SC (2009) Assessment of potential health risk through arsenic flow in food chain – a study in Gangetic delta of West Bengal. In: Ramanathan AL, Bhattacharya P, Nepunae B, Dittmar T, Prasad MBK (eds) *Management and sustainable development of coastal zone environment*. Springer, Germany). Jointly published with Capital Publishing Company, pp 259–269
- Samal AC, Kar S, Bhattacharya P, Santra SC (2011) Human exposure to arsenic through food stuffs cultivated using arsenic contaminated groundwater in areas of West Bengal, India. *J Environ Sci Health* 46(11):1259–1265
- Santra SC, Samal AC, Bhattacharya P, Banerjee S, Biswas A, Majumdar J (2013) Arsenic in food chain and community health risk: a study in Gangetic West Bengal international symposium on environmental science and technology. *Procedia Environ Sci* 18:2–13
- Sanyal SK (1999) Chemodynamics of Geogenic contaminants in the soil environment – Arsenic. 2nd International Conference on Contaminants in Soil Environment in the Australasia Pacific Region held during 12–17 Dec, New Delhi, pp 389–390
- Sanyal SK (2005) Arsenic contamination in agriculture: a threat to water-soil-crop-animal human continuum. Presidential Address, Section of Agriculture & Forestry Sciences, 92nd Session of the Indian Science Congress Association (ISCA), Ahmedabad, January 3–7, 2005; Indian Science Congress Association, Kolkata
- Sanyal SK (2016) Arsenic toxicity in plants, animals and humans and its alleviation strategies. Invited article. *Indian J Fertilizers* 12:74–83

- Singh S, Barla A, Shrivastava A, Bose S (2014) Interplay of arsenic alteration in plant, soil and water: distribution, contamination and remediation. *Global Journal of Multidisciplinary Studies* 3: 11. ISSN –2348–0459
- Singh S, Barla A, Shrivastava A, Bose S (2015) Isolation of arsenic resistant bacteria from Bengal Delta sediments and their efficiency in arsenic removal from soil in association with *Pteris vittata*. *Geomicrobiology*. <https://doi.org/10.1080/01490451.2015.1004141>
- Smedley PL, Kinniburgh DG (2002) A review of the source, behavior and distribution of arsenic in natural waters. *Appl Geochem* 17:517–568
- Sun WJ, Sierra-Alvarez R, Milner L, Field JA (2010) Anoxic oxidation of arsenite linked to chlorate reduction. *Appl Environ Microbiol* 76:6804–6811. <https://doi.org/10.1128/AEM.00734-10>
- Sys C, Van Ranst E, Debaveye J (1993) Land Evaluation. Part 3: crop requirements, *Agricultural Publications* 7, 3. General Administration of Development Cooperation of Belgium, Brussels. 199p
- Takahashi Y, Minamikawa R, Hattori KH, Kurishima K, Kihou N, Yuita K (2004) Arsenic behavior in paddy fields during the cycle of flooded and non-flooded periods. *Environ Sci Technol* 38:1038–1044
- Visoottiviset P, Francesconi K, Sridokchan W (2002) The potential of Thai indigenous plant species for the phytoremediation of arsenic contaminated land. *Environ Pollut* 118:453–461
- WHO (1993) Guidelines for drinking water quality, vol 1, 2nd edn. WHO, Geneva
- WHO (1996) Anon., World Health Organization guidelines for drinking water quality, vol II, 2nd edn. WHO, Geneva
- Zhao FJ, Dunham SJ, McGrath SP (2002) Arsenic hyper accumulation by different fern species. *New Phytol* 156:27–31

Chapter 3

Temporal and Seasonal Variation in Leachate Pollution Index (LPI) in Sanitary Landfill Sites: A Case Study of Baidyabati Landfill, West Bengal, India



Rachna Jain, Dipanjali Majumdar, and Rita Mondal

Abstract Landfill leachate poses a massive threat to the environment as well as human beings. Leachate Pollution Index (LPI) is a new tool to quantify the contamination potential of leachate. LPI constitutes three parts, termed as $LPI_{organic}$, $LPI_{inorganic}$, and $LPI_{heavy\ metals}$. The organic component of LPI constitutes biological oxygen demand (BOD), chemical oxygen demand (COD), phenols, and total coliforms (Tc). All of them are susceptible to seasonal and temporal variations. The present study aims to characterize the difference of LPI_{or} in different seasons and hence observes the temporal variations among them. Leachate samples were collected before and after primary treatment (aeration) from the sanitary landfill site at Baidyabati, Hoogly, West Bengal in three seasons: monsoon, winter, and summer. LPI_{or} index was calculated based on the Delphi technique. Results showed that LPI for both raw as well as treated leachate follows the order $LPI_{Summer} > LPI_{Winter} > LPI_{Monsoon}$. The LPI varied from 32.4 to 39.2 for sanitary landfill leachate and 31.4 to 32.6 for aerated leachate. LPI decreased after primary treatment in each season (3.1%, 13.6%, and 17.0% in monsoon, winter, and summer, respectively). A steep rise of 16.4% in the LPI for leachate from monsoon to winter was observed, whereas, after primary treatment, it was only 3.8%. From winter to summer, the rise was observed to be 4.1% in raw, whereas after treatment, LPI in both seasons was the same. Overall there is an increment of 21.2% in LPI from monsoon to summer, whereas after primary treatment, the difference of LPI was found to be only 3.8%. Overall the study concludes that the leachate sample showed season-wise variation, and therefore suitable strategy should be followed for their treatment as per requirement. It was also observed that primary treatment alone is not sufficient, and hence some other suitable technology, either microbial or physico-chemical, is required to reduce the LPI to an acceptable level before it could be released into the environment.

R. Jain (✉) · D. Majumdar · R. Mondal
CSIR-National Environmental Engineering Research Institute (NEERI), Kolkata, India
e-mail: ra_jain@neeri.res.in

© Springer Nature Switzerland AG 2021

P. K. Shit et al. (eds.), *Spatial Modeling and Assessment of Environmental Contaminants*, Environmental Challenges and Solutions,
https://doi.org/10.1007/978-3-030-63422-3_3

29

Keywords Landfill · Leachate · Contamination · Physicochemical parameters

3.1 Introduction

Waste generation is continuously increasing at an exponential rate due to the increasing population as well as changing lifestyles. An effective and efficient waste management technique is the need of the hour (Rathod et al. 2013; Salami et al. 2014). Landfilling is one of the widely used waste management techniques followed by most of the developing as well as developed countries (Mor et al. 2006; Motling et al. 2013). It has been defined as the process of collecting all the unwanted material and dumping it at a specified site, wherein by the natural process, it decomposes into smaller and non-hazardous particles (Patil et al. 2013). A landfill has to be sustainable so that the essential elements of waste materials cycles in the ecosystem seamlessly, and also it has to be cost-effective to be easily adapted without much stress to the national economy (Kjeldsen and Christophersen 2001; Burton and Watson-Craik 1999).

The chief environmental concern of the landfilling process is the generation of various harmful gaseous pollutants and liquid generated by the natural metabolic process (Venkata Ramaiah and Krishnaiah 2014). The percolating liquid generated during the metabolism of waste is termed leachate. It is the concentrated liquid containing the metabolic by-products of all the waste being dumped at the site (Burrows et al. 1997; Brune et al. 1991). It is highly toxic in its characteristics and much more polluting than typical wastewater. Organic matter comprises the major part of leachate contamination, which is mainly represented in terms of biological oxygen demand (BOD) and chemical oxygen demand (COD). Their concentration ranges in high multiples of standard values as described by various regulatory authorities such as EPA and CPCB (Deng and Englehardt 2006). This high concentration of complex organic contaminants, i.e., BOD, COD, ammonia, inorganic salts, etc., make landfill leachate a potential source of ground and surface water contamination, which further leads the authorities to prioritize its treatment before discharging it to local water bodies (Bashir et al. 2010). Once released, landfill leachate tends to mix with the underground water table and contaminates it (Hazra and Goel 2009). It is thus essential to treat this highly toxic liquid at the source to prevent water table contamination for both ecological and human health point of view (Yaquout Al and Hamoda 2003). Leachate Management is, therefore, the foremost factor to be considered during the planning and designing of a long-term operational MSW landfill (Halim et al. 2010).

According to amended hazardous waste management rules, 2016, in India, open dumpsites were disregarded, and it has been made compulsory to make lined landfill sites according to space availability at the earliest possible. At these landfills, leachate is required to be collected and treated up to the prevailing environmental standards before discharge. It has also been specified to segregate the waste before

dumping so that it can be treated easily. Lined landfill sites prevent the mixing of leachate into groundwater and protect it from environmental damages.

Life of a landfill majorly depends on the waste composition being dumped in there, which is less in the case of domestic waste, which is organic in nature but varies widely with complex waste composition, being produced and released by modern industrial society. The methods adopted for landfilling are based on the assumption that waste should be stabilized and mineralized in the least possible time by different metabolic reactions (Bogner and Lagerkvist 1997). It is also to be considered that the landfill can be safely abandoned after a period of 30–50 years, depending on the area and waste dissolution rate (Binner et al. 1997; Odukoya and Abimbola 2010).

The disposal strategy should be designed in view of leachate characteristics and their changes during the metabolic reaction so that it will reach the final disposal standards in least possible time. The designed strategy should be applicable to a wide range of wastes (Blakey et al. 1997; Bogner and Lagerkvist 1997). The following disposal/waste management strategies are being employed in single or in combination in various countries across the globe, i.e., Encapsulation or total containment (dry tomb), Containment and collection of leachate, Controlled contaminant release, and Unrestricted contaminant release.

Encapsulation and containment are based on the input of energy and hence are referred to as a part of an active environmental protection system, whereas controlled release of contaminants and unrestricted release does not require any kind of maintenance or energy input and hence comprise a passive environmental protection system.

Active environmental protection systems are being employed in the first stages of landfill development, and only the passive systems have long-term sustainability.

3.1.1 Encapsulation/Total Containment

Encapsulation of waste is the formations of a preventive layer on the trash so that percolation of water and hence leachate emission are entirely restricted. In this process, the moisture present in the waste remains intact under controlled conditions, and thus there is no leakage. But the major drawback of this process is that along with the restriction of leachate emission; it also restricts the metabolism of waste. In such containment, if the system fails, then uncontrolled leachate may outburst and creates potential environmental risk (Assmuth et al. 1991). The process does not facilitate waste for final storage quality and hence becomes an indefinite responsibility and a risk for the future generation.

3.1.2 Containment and Collection of Leachate

It is one of the most common traditionally designed landfill strategy, also termed sanitary landfills. It is adapted by many of the developed as well as developing countries. It consists of a liner system in which the percolating leachate is being collected in drainage and treated to surface water body standards and then discharged into the environment. In order to regularize the inflow and outflow and to reach the final storage quality in minimum possible time, leaching rate should be increased by either ways infiltrating the waste matrix, or by addition of microbes (i.e., wastewater having high BOD) or by recirculating the leachate (Butler et al. 1999; Capodaglio et al. 1999).

This process is a part of an active environmental system and hence required input energy and is not sustainable for the long term. It is applicable only in the initial years of landfill development; once the landfill is stabilized, a new strategy has to be adopted for sustainable management of waste. This method is both space and cost-intensive (Clement 1995).

3.1.3 Controlled Contaminant Release

In this type of strategy, an environmentally acceptable amount of generated leachate is released as effluent from the site by following the appropriate quantity- and quality-check measures. Therefore the leachate is not stored but released into the environment as it is formed in the landfill (Ehrig 1991). But there is a requirement of the constant monitoring process to ensure that there is the least possible impact of effluent on the environment. The process can be made more efficient and ecofriendly by initial treatment of waste at source. During this process, the contaminants are continually being released out, and thence there will be a steady decrease in its contamination potential. It is the best suitable option for inorganic waste management. For the other diverse kinds of garbage, an entirely controlled contaminant release strategy has to be adopted, which should be having a more efficient operating system for management of leachate in a more sustainable manner so that it cannot cause any harsh environmental impact and treat the waste in less time (Armstrong and Rowe 1999).

3.1.4 Unrestricted Contaminant Release

It can be explained as a scenario in which the waste is dumped into a place, and there is a natural generation of leachate without any restriction. It is the most dangerous situation from an environmental point of view, as there is no quality/quantity check on the generated leachate (Genon et al. 1995). It solely depends on the waste

characteristics, prevailing climate conditions susceptibility of the contiguous environment. As discussed, there is a total lack of control in this type of strategy, and hence it cannot be used as the management strategy of waste. Most of the developing and under-developed countries around the world are still practicing open dumping of waste widely around the globe (Driessen et al. 1995).

Categories of Landfills

Leachate characteristics are grossly dependent on the type of landfill. Landfills are majorly categorized on the type of waste being dumped there, environment protection measures like the thickness of the liner, leachate collection, and treatment system, etc (Dharmarathne and Gunatilake, 2013; Christensen et al. 2001). Waste categorization depends on the assumption of generated leachate, which is defined from waste characteristics such as pure biodegradable waste, utter inorganic waste or combination of both (Demirekler et al. 1999). The landfill classification system is based on the hazard quotient of dumped waste ranging from inert, hazardous, and nonhazardous waste. These criteria vary with different countries and are often supplemented with other restrictions based on the prevailing conditions and environmental vulnerability (Gómez Martín et al. 1995a, b).

Leachate Generation

Leachate generation is always considered a potential source of water pollution. Therefore, minimization of leachate generation is regarded as a possible solution for efficient landfill management. But nowadays, it is being considered that the leachate generation process can minimize the potential hazardousness of waste (Bendz et al. 1997b). Therefore, it is prudent to control the leaching process to decrease the hazard quotient of waste (Bendz et al. 1997a). The controlled leaching process does not affect the rate of leachate generation, but the generated leachate is collected and treated and then recycled into the immediate environment. It will be important to interpret and control the leachate volumes for efficient landfill management.

Water balance equations are used to calculate leachate volume before building new landfill sites to efficiently manage landfills and interpret the levels for existing landfill sites (D'Antonio and Porozzi 1991; ENVPROT 3C 1995). These equations are also very useful in determining the landfill area keeping in view the management strategies. However, they are not suitable for predicting the leakage rates. Also, these equations should be re-evaluated from time to time due to climatic and other environmental changes for efficient management (Robinson et al. 1999).

These equations calculate the incoming and outgoing liquids from the landfills, and any difference is defined as absorbed or leaked leachate. Ups and downs in quantity depends upon the storage conditions of the waste, which are complex and uncertain.

Rainfall is the major input factor, and treated effluent is the major output at containment landfills (Matravers and Robinson 1991). Leachate volumes depend on the following factors:

1. The absorption capacity of waste during the operational phase.

2. Runoff rate of low permeability top cover areas.

Consumption of moisture during anaerobic digestion and in landfill gas is almost considered negligible, except for landfills located in dry arid regions where the degradation is subject to limited moisture content. In some of the landfills, non-hazardous waste is added into the MSW landfills to increase the moisture content and hence the rate of degradation. These strategies are required to increase the waste degradation rate to reach the final storage quantity in fewer time frames.

Following measures are applied for controlling the quantity and quality of leachate:

Appropriate Site Location

Landfill site is selected so that the leachate generation rate, as well as a potential risk of groundwater pollution, can be reduced.

- Sites are engineered with liners of appropriate thickness, cut-off barriers are implemented to control water flow, surface diversion of water, and low permeability top cover are also necessary measures.
- Landfills are made at the highest possible height from the groundwater level so that intrusion of surface water into the landfill can be avoided, which in turn helps to control the leachate volume. They are made in order to reduce rainfall exposure, which is also a control measure.
- In some cases, the landfill is placed below the water surface so that a hydraulic gradient can be created for efficient management (Joseph and Mather 1993; Smart 1993; Lee and Jones-Lee 1993).

The best available technology (BAT) to minimize the leachate quantity depends upon the strategy of operation. In the encapsulation scheme, the leachate generation is minimum, whereas, in bioreactor or inorganic landfills, the leaching rate is quite high, which is further increased by feeding the seed water or by increasing the percolation rate as and when required (Matsuto et al. 1991; Blakey et al. 1995).

Concept of Leachate Pollution Index

Kumar and Alappat (2005) have termed a new terminology for the calculation of contamination potential of a landfill known as the Leachate Pollution Index (LPI). Identification and quantification of contaminants in landfill leachate are the major limitations for its successful treatment (Trankler et al. 2005). Therefore LPI is a measure to determine the contamination potential of a landfill, which will further decide landfill condition and assess its remediation potential. On the basis of their status, landfills can be prioritized for management and remediation measures.

Leachate Pollution Index (LPI) is a measure to estimate the potential contamination efficiency of a particular landfill site. The basic concept of LPI is an attempt to make an efficient system to compare the contamination potential of different landfills present in a given geographical area (Umar et al. 2010). For this, a panel of various academic institutes, environmentalists, persons from different regulatory authorities, consultants, engineers, and of International Solid Waste Association (ISWA) from

around the world was made to conduct a survey using variable questionnaires to develop and consolidated index for the evaluation of leachate contaminant potential.

Therefore LPI can be defined as a mathematical means for the calculation of a composite value from overall physicochemical parameters of the concerned landfill leachate.

This single LPI value ranks the landfill on the basis of its contamination potential calculated from the overall physicochemical parameters of a landfill. About 18 different physicochemical parameters were used for the calculation of LPI, and their weight factors were ranked on a scale of 1 to 5 by the panelists. Based on these LPI pollutant variables, a curve was drawn with respect to leachate pollution ranging from 5 (the best) to 100 (the worst). The leachate pollution level was indicated as ordinate value 0 to 100 on each graph, whereas abscissa contains the maximum reported value of any particular pollutant variable. An average subindex curve was drawn by using the average of curves made by the panelists for each pollutant variable, as reported in the literature (Deng and Englehardt 2006).

Aggregation is an important function for accuracy and efficiency in making different environmental indices. There are mainly three different forms of aggregation:

1. Additive aggregation: In which individual pollutant variables are summated.
2. Multiplicative aggregation: In which pollutant variables are multiplied.
3. Maximum or minimum operator from aggregation: In which either maximum or minimum sub-index value of individual pollutant variable is directly accepted.

On the basis of their LPI index, the leachate can be categorized into different risk zones.

Parameters Affecting LPI

Leachate Pollution Index is a measure of contaminants present in the landfill. On the basis of types of waste, LPI is sub-categorized into three main parts:

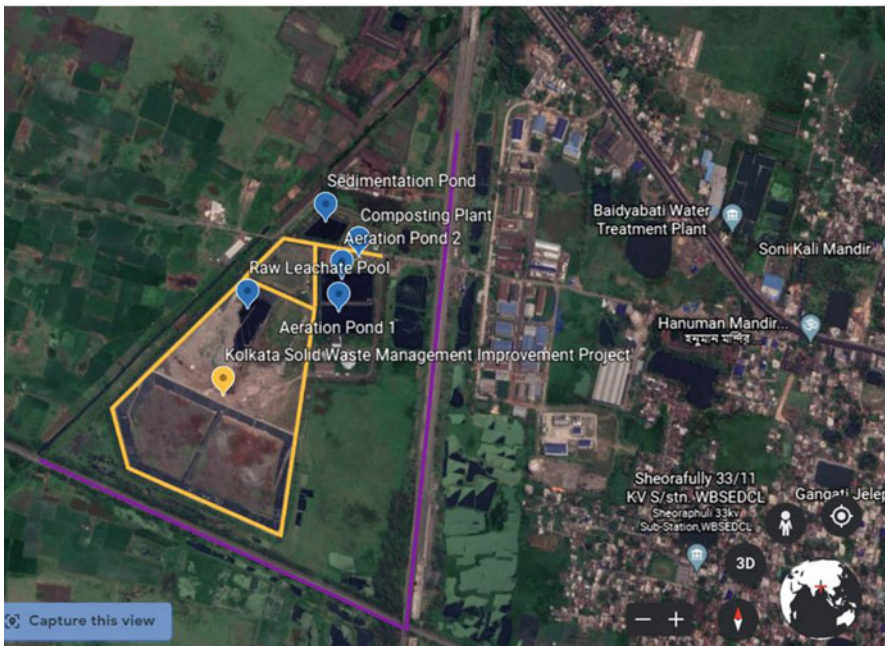
- A. *Organic LPI*: It comprises all the organic parameters of the waste like BOD, COD, TOC, and total phenols, etc.
- B. *Inorganic LPI*: It comprises all the inorganic parameters of waste like alkalinity, TDS, TSS, Phosphate, sulfate, chloride, nitrogen, etc.
- C. *Heavy metals*: It comprises all the heavy metals present in the leachate. Heavy metals are released due to environmental pressure and microbial metabolism in free form, which is more potent in nature and causes serious environmental and health hazards.

Among all these parameters, organic LPI is subjected to variations due to environmental and operational changes (Belevi et al. 1993; Belevi and Baccini 1989). Therefore these are very sensitive, and utmost care is required.

Vahabian et al. 2019, show a wide variation in the physicochemical characteristics of leachate collected from different sanitary landfills across the globe. The age of landfills and stability, along with the degree of solid waste, have a significant effect on leachate characteristics. Different environmental factors like temperature, pH,



(a)



(b)

Fig. 3.1 (a) GIS-based open Street map (Credit: QGIS Software); (b) satellite view of the sampling site (Credit: Google Earth), Kolkata Solid-Waste Improvement Project. Both figures show the location of raw (R), aeration ponds (A1 & A2), and sedimentation ponds (S) at the landfill site. Roads are mapped in orange and gray color in GIS map. Inside and main roads are mapped in yellow and magenta color, respectively, in the satellite map. Samples for the present study were taken from raw (R) and sedimentation pond (S), respectively

humidity, and seasonal variations also create an impact on leachate characteristics. These factors play an essential role in the organic content of leachate (Statom et al. 2004). Therefore, the study of seasonal variation in the organic LPI content is a measure of finding the overall LPI index of the concerned landfill, which will further help in finding the contamination index of various landfill sites and thus, based on that exhaustive list of landfills, remedial actions can be prioritized.

It will also help in understanding the leachate characteristics in different seasons, and hence better remedial technology can be devised based on the requirement. The present case study deals with organic LPI variation in three very distinct seasons and determines the difference in the LPI_{org} index of leachate from a typical landfill in the Indian scenario.

3.2 Materials and Methods

3.2.1 Sampling Site

The samples were collected from the Baidyabati Landfill site, also known as the Kolkata Solid Waste Improvement Project (Fig. 3.1). It is the only sanitary landfill site in West Bengal, India, to date. It is situated at Latitude 22.78' North and Longitude 88.31' East. It is maintained by the Baidyabati municipality. It collects and dumps waste from six different municipalities of Hooghly district, i.e., Baidyabati, Konnagar, Rishra, Serampore, Champdani, and Uttarpara-Kotrung. The site is 35 km far from Kolkata city. It is spread into the total area of this 51 acre. It has the capacity to sustain 200 tonnes of waste per day. The landfill site is lined, and the leachate percolating from the waste is being collected in a raw water pool. The raw leachate after collection is transferred to an open tank for primary treatment. In the open tank, the raw leachate is subjected to aeration treatment in two consecutive aeration ponds and then allowed to settle in the sedimentation pond. After this primary treatment process, the water is discharged into the environment (Shabhimaan & Dikshit, 2011).

3.2.2 Sampling Process and Physicochemical Analysis

Figure 3.1 a & b shows the GIS location map and satellite view of the sampling site. For the study of seasonal variation and geochemistry of the leachate sample, two leachate samples were collected each from the leachate pit (raw) and sedimentation pond (primary treated) in different seasons (Summer, Monsoon, and Winter) from the landfill site. After collection, the samples were transported to the laboratory in cooler boxes to maintain the temperature below 5⁰ C. After reaching the laboratory, leachate samples were stored in a refrigerator at 4 °C before proceeding for analysis.

3.2.3 LPI Index

LPI index was measured as described in the steps below.

3.2.3.1 Laboratory Analysis

Various physicochemical parameters pertaining to organic constituents of leachate, before and after treatment were analyzed by standard methods (APHA 2012) as given below.

BOD

Biochemical Oxygen Demand (BOD) was assessed by the bioassay method. 1% dilution was used for sample analysis. For dilution of the samples, we used 24 h aerated double distilled water (DDW). In 300 mL capacity BOD bottles, we poured an adequate amount of sample required as per dilution; after dilution, we measured the initial Dissolved Oxygen (DO) (Winkler Method with Azide Modification) of the sample after that the samples were incubated in BOD incubator at 27 °C for 3 days. After 3 days, the final DO of the sample was measured as the same process of DO measured mentioned in above. DO is the measure of oxygen present in the sample at the given time. BOD is calculated as the difference in dissolved oxygen content of leachate for three consecutive days under controlled incubation conditions due to microbial usage.

COD

Chemical Oxygen Demand (COD) of leachate samples had been analyzed by the reflux method. The organic matter present in the leachate sample gets oxidized by $K_2Cr_2O_7$ and in the presence of silver sulfate in acidic medium and reduces to CO_2 and H_2O . Afterward, excess $K_2Cr_2O_7$ is titrated with $Fe(NH_4)_2(SO_4)_2$. The difference in the amount of $Fe(NH_4)_2(SO_4)_2$ used for control and test sample is used for the calculation of COD. The amount of consumed dichromate is inversely proportional to the COD of the sample.

Total Phenols

Total phenol content of the leachate sample was calculated by the colorimetric method. The phenols present in the sample react with 4-aminoantipyrine in the presence of potassium ferricyanide in alkaline conditions to form a stable reddish-brown colored antipyrine dye. The concentration of the dye can be determined at 460 nm.

Total Coliform (Tc)

Total coliform present in the leachate sample was estimated by the standard APHA method. M-Endo agar medium was used for the detection of microbes in the samples. The collected leachate sample was filtered with a 47-mm membrane filter using the membrane filtration technique and incubated at 37 °C for 24 h. The

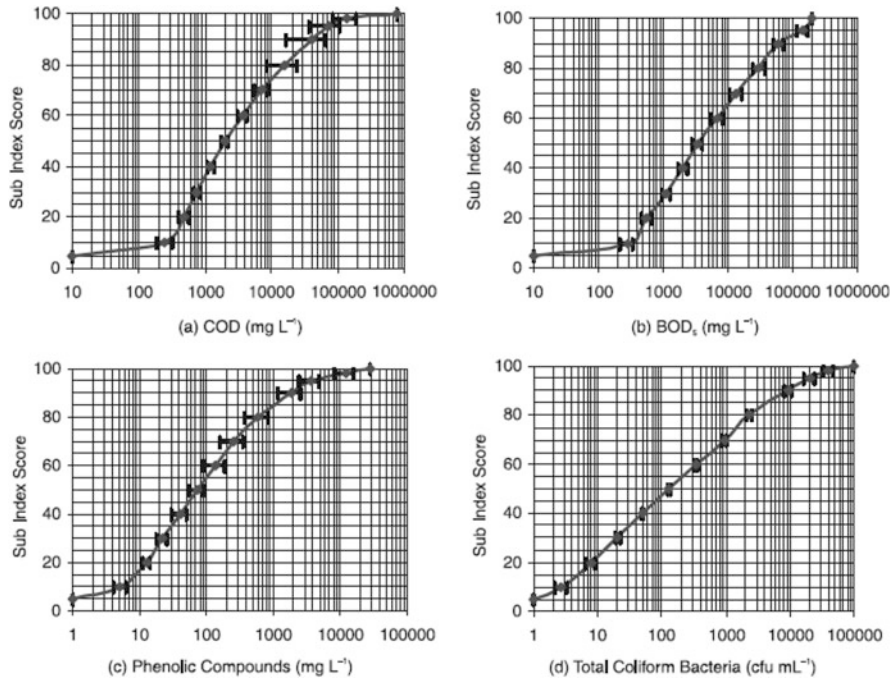


Fig. 3.2 Subindex average curves with 90% confidence limit for LPI_{or}: (a) COD; (b) BOD; (c) total phenols or phenolics; (d) total coliforms. (Kumar and Alappat 2005)

Table 3.1 Leachate pollution index parameters with subindex weight factors

Index	Parameters	Weight factor
LPI organic (LPI _{or})	COD	0.267
	BOD	0.263
	Phenolic compounds	0.246
	Total coliform bacteria	0.224

colonies with golden sheen were counted and recorded as the total coliform content of the sample.

3.2.3.2 Calculation of Sub-index Value and Pollutant Weight Factor

Sub-Index value of individual parameter was calculated by placing the observed value into the standard charts as given by. The observed concentration of individual parameter was located on the horizontal axis, and the sub-index value (*p*) was determined where it intersects the standard curve. It is also represented as *p_i*, *i*-represents the different variables (Fig. 3.2).

3.2.3.3 Pollutant Weights

Weight factors are a measure of the significance of individual pollutant variables. Therefore, different pollutant variables have different weight factors depending on their contribution to overall leachate pollution. Weight factors are derived by calculating the arithmetic sum of the significance ratings of all the selected pollutant variables, and each one of them is given significance in proportion to its weight on the scale of 1, so as to make the total weight of all the pollutant variables 1.

The weight calculated for each pollutant variable based on the significance values are shown in Table 3.1 (Kumar and Alappat 2005).

3.2.3.4 Aggregation of Sub-index Values

The determined sub-index values were then aggregated by multiplying it with their respective weight factors (w_i). It is also called as a cumulative pollution rating ($w_i * p_i$).

After following these steps, the LPI was calculated according to.

$$LPI = \frac{\sum_{i=1}^m w_i p_i}{\sum_{i=1}^m w_i}, \tag{3.1}$$

m —number of leachate pollutant parameters.

w_i —weight for i^{th} pollutant variable.

p_i —sub-index score of the i^{th} leachate pollutant variable.

**It is to be noted that when all the leachate parameters are unknown, $m < 18$.*

$$\sum_{i=1}^m w_i < 1. \tag{3.2}$$

Table 3.2 Sub-index value (p_i) of individual leachate parameter before and after primary treatment

Physicochemical parameters	Leachate			Primary treated leachate		
	Monsoon	Winter	Summer	Monsoon	Winter	Summer
BOD	8	10	10	6	7	7
COD	40	55	65	43	43	43
Total coliform	80	80	75	72	75	75
Total phenols	10	10	10	10	10	10

3.2.3.5 LPI_{or} Calculation

Overall LPI of the concerned landfill site is the sum aggregation of all the three subindices of constituent parts and can be calculated by the following equation:

$$\text{LPI} = 0.232 \text{LPI}_{\text{or}} + 0.257 \text{LPI}_{\text{in}} + 0.511 \text{LPI}_{\text{hm}} \quad (3.3)$$

LPI- combined or overall LPI of the concerned site.

LPI_{or}- Sub-indices for the organic fraction of leachate.

LPI_{in}- Sub-indices for the inorganic fraction of leachate.

LPI_{hm}- Sub-indices for the heavy metal fraction.

The above Eq. (3.3) has been derived on the basis of the weight factors of selected parameters and their contribution to overall LPI.

As for the present study, we are only discussing the organic fraction; therefore, we can say that the contribution of the organic fraction is a factor of 0.232 of the combined LPI.

Therefore for the comparative analysis and risk assessment, we will only consider 0.232 fractions of the standard LPI limit (7.4) for accuracy and efficient presentation of observed results.

3.3 Results

3.3.1 Sub-index Value

The sub-index value of the individual pollutant parameter is given in Table 3.2.

The sub-index value of individual parameters ranges between 6–10, 43–65, and 72–80 for BOD, COD, and total coliforms, respectively. Total phenol concentration does not show any deviation with seasons, and hence the sub-index value was found to be constant at 10. The values for BOD and COD were found lowest in monsoon in leachate samples, whereas summers showed the highest, which is most likely due to the rain-dilution effect. Sub-indices for all the parameters decrease after treatment except COD value, which increases by 7.5% during monsoon. This may be due to the reason that the open aeration tank is also receiving rainwater surface runoff during monsoon, which may add to the existing COD load of the raw leachate. Sub-index value for COD decreases by 22 and 34% in winter and summer, respectively, after primary treatment. Sub-index value for BOD decreases by 25, 30, and 30% in monsoon, winter, and summer, respectively, after primary treatment. For total coliforms, the value decreased by 10 and 6.25% for monsoon and winter, whereas in summer, the value remained constant.

Table 3.3 Cumulative pollution rating of individual leachate parameter

Physicochemical parameters	Sub-index value (p_i)			Individual weight factor (w_i)	Cumulative pollution rating ($p_i^*w_i$)		
	Monsoon	Winter	Summer		Monsoon	Winter	Summer
BOD	8	10	10	0.26	2.10	2.63	2.63
COD	40	55	65	0.27	10.68	14.69	17.36
Total coliforms	80	80	75	0.22	17.92	17.92	16.80
Total phenols	10	10	10	0.25	2.46	2.46	2.46
Total					33.2	37.7	39.2

Table 3.4 Cumulative pollution rating of individual leachate parameter after primary treatment

Physicochemical parameters	Sub-index value (p_i)			Individual weight factor (w_i)			Cumulative pollution rating ($p_i * w_i$)		
	Monsoon	Winter	Summer	Monsoon	Winter	Summer	Monsoon	Winter	Summer
BOD	6	7	7	0.26			1.58	1.84	1.84
COD	43	43	43	0.27			11.48	11.48	11.48
Total coliform	72	75	75	0.22			16.13	16.80	16.80
Total phenols	10	10	10	0.25			2.46	2.46	2.46
Total							31.6	32.6	32.58

Table 3.5 Correlation matrix for inter-seasonal variation in cumulative pollution ratings of leachate samples

		Monsoon	Winter	Summer
BOD	Monsoon	1		
	Winter	0.46	1	
	Summer	0.99	0.5	1
COD	Monsoon	1		
	Winter	-1	1	
	Summer	1	-1	1
Total coliforms (TC)	Monsoon	1		
	Winter	-0.65	1	
	Summer	-0.5	0.98	1
Total phenols (TP)	Monsoon	1		
	Winter	1	1	
	Summer	1	1	1

Table 3.6 Correlation matrix for inter-seasonal variation in cumulative pollution ratings of leachate samples after aeration treatment

		Monsoon	Winter	Summer
BOD	Monsoon	1		
	Winter	-0.40	1	
	Summer	-0.35	0.99	1
COD	Monsoon	1		
	Winter	0.99	1	
	Summer	0.99	1	1
Total coliforms (TC)	Monsoon	1		
	Winter	-0.5	1	
	Summer	-1	0.5	1
Total phenols (TP)	Monsoon	1		
	Winter	0.99	1	
	Summer	1	0.99	1

3.3.2 Cumulative Pollution Rating

It is a multiplicative factor of subindex value (p_i), and weight factor (w_i) for the individual- tested parameter. The individual weight factor of tested parameters is a standard, as mentioned by Kumar & Alappat 2005. The following tables show the cumulative pollution rating (p_i) for leachate before and after primary treatment (Table 3.3).

In leachate samples, the ratings ranged 2.1–2.63, 10.68–17.36, and 16.8–17.92 for BOD, COD, and total coliforms, respectively. For phenols, the ratings remained constant to 2.46 for all the seasons. After primary aeration treatment, the pollution ratings decreased by 25–30% and 6.5–10% for BOD and total coliforms,

Table 3.7 Correlation matrix for intra-seasonal variation in cumulative pollution ratings of leachate samples after aeration treatment

Monsoon									
Leachate					Aerated leachate				
	BOD	COD	TC	TP		BOD	COD	TC	TP
BOD	1				BOD	1			
COD	-1	1			COD	-1	1		
TC	-1	1	1		TC	-1	1	1	
TP	0.46	-0.5	0.5	1	TP	-1	1	1	1
Winter									
Leachate					Aerated leachate				
	BOD	COD	TC	TP		BOD	COD	TC	TP
BOD	1				BOD	1			
COD	0.5	1			COD	0.5	1		
TC	0.98	0.7	1		TC	-1	-0.5	1	
TP	1	0.5	1	1	TP	0.44	1	0	1
Summer									
Leachate					Aerated leachate				
	BOD	COD	TC	TP		BOD	COD	TC	TP
BOD	1				BOD	1			
COD	-1	1			COD	0.45	1		
TC	0.5	-0.5	1		TC	-0.5	-1	1	
TP	0.5	-0.5	1	1	TP	0.45	1	-1	1

respectively. The seasonal variation of COD showed a completely different pattern. From monsoon to winter, the COD rating increased by 7.5%, whereas after treatment, the rating decreased by 22–34% for winter and summer, respectively. Interseasonal comparison of BOD ratings shows that it increased by 25% from monsoon to summer and winter, respectively, as shown in Tables 3.3 and 3.4. COD ratings showed a wide variation and increased by 37.5, 62.5, and 18.2% from monsoon to winter; monsoon to summer, and winter to summer, respectively. After aeration, the ratings became static. For total coliforms, the leachate ratings were the same for monsoon and winter but decreased by 6.25 in the summer season, whereas after aeration, the rating increased by 4.17% from monsoon to winter and then remains static.

Phenols showed a static behavior for all the seasons before and after treatment as the values showed a minor variation, and hence it places within the same sub-index slot.

The total pollution ratings ranged from 31.6–39.2 for leachate both before and after treatment, as shown in Tables 3.3 and 3.4. For leachate samples, the pollution ratings were found to be 33.2, 37.7, and 39.2 for monsoon, winter, and summer, respectively. After primary aeration treatment, the values reduced by 4.57, 13.56, and 16.98 percent for monsoon, winter, and summer, respectively. The inter-seasonal variation shows that pollution ratings increase by 13.66, 18.34, and 4.12 from

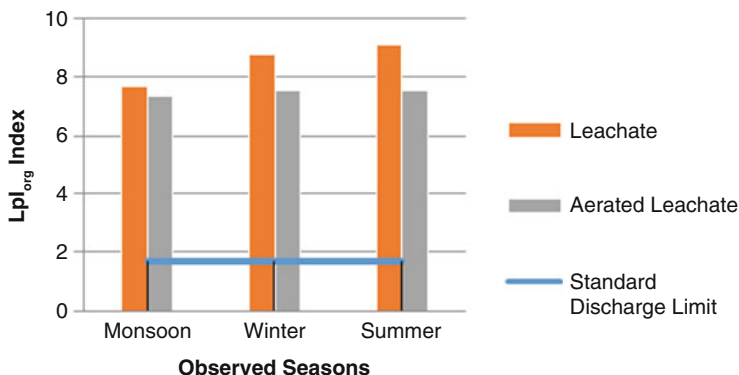


Fig. 3.3 Inter- and intra-seasonal variation of LPI_{or} of leachate samples before and after treatment with respect to the standard discharge limit

monsoon to winter, monsoon to summer, and winter to monsoon, respectively for leachate samples. After treatment, the increase was not very significant and showed an increase of 2.95 percent for both monsoons to winter and monsoon to summers, whereas for winter to summer, the value decreases by 0.06 percent.

Cumulative pollution ratings were correlated for intra- as well as inter-seasonal variations, and the obtained results are shown in the below Tables 3.5, 3.6, and 3.7. It is clearly evident from the table that all the analyzed parameters are in good correlation.

Positive correlation means that variables 1 and 2 are having a synchronized association whereas negative correlation shows a non-synchronized association between the variables. Value 0 represents a non-predictable relationship among them. Correlation coefficient (r) from 0.5 to 1 and from -1 to -0.5 are regarded as strong relation (DeCoursey 2003; Soong 2004).

In both treated and non-treated samples, there is a good correlation among all the analyzed parameters, as revealed by the correlation coefficient (r) mentioned in Tables 3.5 and 3.6 below. Total phenols showed a perfect correlation factor $r = 1$ in leachate samples, whereas after aeration also, the r -value is nearly perfect $r = 0.99$. Only in the intra-seasonal analysis of winter season, total phenols and total coliforms showed nil correlation with an $r = 0$.

In intra-seasonal statistics (Table 3.7), aerated monsoon samples showed a strong correlation with all the tested parameters with r ranging from -1 to 1. Summer aerated samples also showed a strong correlation for all the parameters except BOD.

3.3.3 Calculation of LPI_{or}

As discussed in the introduction and material method section, LPI constitutes three parts: organic, inorganic, and heavy metals. In the present study, we are only dealing

with the organic fraction, and hence the obtained value is only a 0.232 fraction of the total LPI value as given in the equation below:

$$\text{LPI} = 0.232\text{LPI}_{\text{or}} + 0.257\text{LPI}_{\text{in}} + 0.511\text{LPI}_{\text{hm}}$$

Hence LPI_{or} represents only a 0.232 fraction of overall LPI index, i.e., 0.232 fractions of combined cumulative pollution ratings of all the organic factors, i.e., BOD, COD, total coliforms, and total phenols in a particular landfill site.

LPI_{or} for different seasons ranged from 7.6–9.1 for leachate, and after aeration the values were found to be in the range of 7.3–7.56. As can be seen by the Fig. 3.3, LPI_{or} was highest in summer followed by winter and monsoon.

The standard discharge limit for overall LPI was found to be 7.4 as per MOEF 2000. And hence as per the equation given above standard discharge limit for LPI_{or} will be 1.71 (0.232 fractions of overall LPI, i.e., 7.4).

It is evident from Fig. 3.3 that LPI_{or} is far beyond the standard limit. Primary aeration treatment decreases the organic LPI by 4.55, 13.7, and 16.9 percent for monsoon, winter, and summer, but they were found still far higher than the standard limit in all seasons. And hence it is recommended to apply other treatment strategies to bring the LPI down and reach the standard limit so that the water can be safely returned into the environment.

3.4 Discussion

In India, leachate characterization studies have been carried out mostly in the states of Kerala, Delhi, and Punjab by Afsar et al. 2015; Anil et al. 2015; Kumar and Alappat 2005 and Bhalla et al. 2012 & 2014. They have observed very high BOD, COD, and TOC values, which may cause harm to the environment and cause groundwater contamination. Some other researchers have done toxicological studies to find the effect of leachate on groundwater quality and their genotoxic and cytotoxic effects (Rana et al. 2018; Alimba et al. 2016; Ghosh et al. 2015; Kale et al. 2010; Sivanesan et al. 2004). All these studies have reported the toxic effect of leachate contaminants (heavy metals, industrial chemicals) on the groundwater table as well as the human beings and marine ecosystem that come in their contact (Aulin and Neretnicks, 1995). The basic characteristics of leachate depend mostly upon the type of waste received by the landfill. Age of landfill, season, geographical, and meteorological condition of the area also play a role in determining the characteristics of landfill leachate.

Seasonal variation data of the leachate samples indicate variability in values (Bhalla et al. 2013). The physicochemical parameters analyzed in the present study showed a hike in summer and a decrease in monsoon. It can be because of the high evaporation rate in summer, which concentrates the sample, and as a result, the parameters hike and also the risk of contamination.

Esakku et al. 2007, have also reported that the pollutant concentration of leachate was found maximum in the summer season, and eventually, by mixing of rainwater, it gets diluted. Precipitation rate is highest in monsoon, which percolates downwards, but due to rain-dilution effects, the concentration decreases (El-Fadel et al. 2002; Maity et al. 2016). On the contrary, Aluko et al. 2003 have reported higher pollutant concentrations in the wet season as compared to dry ones.

Ganiyu et al. 2018 conducted a study to find the seasonal variation in physico-chemical parameters of groundwater from nearby hand-dug wells located within the Ajakanga solid- waste disposal site. They have also reported that the different physico-chemical parameters were high in the dry season as compared to the wet season. Badmus et al. 2015 also reported a wide range of variations in physico-chemical parameters in the wet season than in dry season.

Vahabian et al. 2019 in their study reported that BOD and COD of a semi-arid landfill site were found to be higher in the wet season than the dry season. Galarpea and Parmilla 2012 revealed that organic as well as inorganic parameters of leachate were higher in the wet season due to rain-dilution effect. It is a process by which the waste contaminants (organic, inorganic, and heavy metals) present in the dump are percolated downwards after mixing with rainwater, and hence the concentration of particular physicochemical parameter increases (Sullivan et al. 2005). But in the present study, we are dealing with inert waste leachate; hence the probability of an increase in the organic matter content due to rain- dilution is the least possible. And hence the parameter does not increase, but due to the mixing of rainwater, the organic matter already present in the leachate dilutes, and hence the value decreases.

Some other studies particularly focused on seasonal variations of heavy metals also state that metal concentrations were 10 to 40 times higher in the rainy season (Mavakala et al. 2016; Tsarpali et al. 2012).

Further, the LPI values in all the observed seasons were found significantly higher in all the seasons as compared with the standard discharge limit, as shown in Fig. 3.3; i.e., 1.71 (MOEF 2000; Esakku et al. 2007; Ugbebor and Ntesat 2019). Also, it is to keep in mind that this is only the value of organic LPI index except that two other parts of LPI, i.e., inorganic and heavy metals, are not considered in the present study, and hence the overall LPI will be much higher than the standard limit. It signifies that the sampled landfill site is a potential threat to the environment.

Hence further treatment of leachate at source is the need of the hour, and only after proper treatment, the water should be discharged into the environment so that it cannot create any kind of pollution out there (Abbas et al. 2009).

3.5 Risk Assessment and Remediation

The above discussion clearly states that landfill site poses a major threat to the environment in every season observed, the LPI value of the landfill site was found quite high from the standard discharge limit. Primary aeration treatment is being done at the landfill site prior to its discharge into the environment. But it is clear from

the Fig. 3.3 that primary treatment is not effective and the LPI value is still very high. Hence, some other secondary treatment is required.

Furthermore, some physicochemical and microbial treatment strategies are required to deal with the issue. If the contaminated water is discharged without proper treatment, it will create a huge environmental impact (Martinen et al. 2003). Also, it will be very difficult to remove the contaminants if mixed with groundwater. Treatment at source is the best way to deal with the problem; hence, we have to apply some specific treatment strategies at the site to decrease LPI value.

Ahead of this study, we are planning to do some strategical experiments like combination of physico-chemical and microbial treatment methods to treat the leachate and decrease the LPI to safe environmental standards and recycle the water to fulfill our basic requirements.

3.6 Conclusion

From the above study, it can be concluded that the leachate pollution index is found to be a potential measure for computing the contamination potential of the landfill sites. Also, it was observed that organic waste plays a major role in the overall polluting potential of a landfill site.

It is also revealed that aeration treatment alone is not sufficient to reduce the pollutant level of leachate up to the standard discharge limit. Hence, along with this, some other treatment process is required. Therefore, we can say that a cumulative treatment strategy is the need of the hour for safe recycling of leachate water into the environment. Organic matter content is dependent on the prevailing environmental conditions, and hence LPI changes with seasonal variations. Therefore, seasonal computation of LPI should be done in every landfill as a necessary measure for efficient landfill management so that an appropriate treatment strategy can be decided.

Acknowledgments The authors gratefully acknowledge the support of *Department of Biotechnology, Government of India under grant no. BT/PR2730S/BCE/8/1432/2018*. The guidance and support of *Director, CSIR-NEERI* is highly appreciated. We also thank our associates *Ms Anoushka and Ms Prateeti* for their support in sampling. The KRC (Knowledge Resource Center of CSIR-National Environmental Engineering Research Institute) number for the manuscript is *CSIR-NEERI/KRC/2020/JUNE/KZC/1*.

References

- Abbas G, Jingsong LZ, Ping PY, Al-Rekabi WS (2009) Review on landfill leachate treatments. *J Appl Sci Res* 5(5):534–545
- Afsar SS, Kumar S, Alam P (2015) Characterization of leachate at various landfill site of Delhi, India. *Int J Advan Tech Eng Sci* 3(1):552–558

- Alimba CG, Gandhi D, Sivanesan S, Bhanarkar MD, Naoghare PK, Bakare AA, Krishnamurthi K (2016) Chemical characterization of simulated landfill soil leachates from Nigeria and India and their cytotoxicity and DNA damage inductions on three human cell lines. *Chemosphere* 164:469–479
- Aluko OO, Sridhar MKC, Oluwande PA (2003) Characterization of leachates from a municipal solid waste landfill site in Ibadan. *Nigeria J Environ Health Res* 2(1):32–37
- Anil KA, Dipu S, Thanga VSG (2015) Effect of municipal solid waste leachate on ground water quality of Thiruvananthapuram District, Kerala, India. *Appl Ecol Environ Sci* 3(5):151–157
- APHA, AWWA, WEF (2012) Standard methods for examination of water and wastewater, 22nd edn. American Public Health Association, Washington
- Armstrong MD, Rowe RK (1999) Effect of landfill operations on the quality of municipal solid waste leachate. In: Christensen TH, Cossu R, Stegmann R (eds) *Sardinia 99*, proceedings of the seventh international landfill symposium, vol II. CISA, Cagliari, Italy, pp 81–88
- Assmuth T, Poutanen H, Strandberg T, Melanen M (1991) Occurrence, attenuation and toxicological significance of hazardous chemicals in uncontrolled landfills – codisposal risks reconsidered. In: Christensen TH, Cossu R, Stegmann R (eds) *Sardinia 91*, proceedings of the third international landfill symposium, vol II. CISA, Cagliari, Italy, pp 1489–1505
- Aulin C, Neretnieks I (1995) Material balance for an industrial landfill. In: Christensen TH, Cossu R, Stegmann R (eds) *Sardinia 95*, proceedings of the fifth international landfill symposium, vol III. CISA, Cagliari, Italy, pp 173–180
- Badmus BS, Ozebo VC, Idowu OA, Ganiyu SA, Olurin OT (2015) Seasonal variations of Physico chemical properties and quality index of groundwater of hand-dug Wells around Ajakanga dump site in southwestern Nigeria. *Res J Phys* 9:1–10
- Bashir MJK, Aziz HA, Yusoff MS, Adlan MN (2010) Application of response surfacemethodology (RSM) for optimization of ammoniacal nitrogen removal from semi-aerobic landfill leachate using ion exchange resin. *Desalination* 254(1–3):154–161
- Belevi H, Baccini P (1989) Long-term behaviour of municipal solid waste landfills. *Waste Manag Res* 7:43–56
- Belevi H, Agustoni-Phan N, Baccini P (1993) Influence of organic carbon on the long-term behaviour of bottom ash monofills. In: Christensen TH, Cossu R, Stegmann R (eds) *Sardinia 93*, proceedings of the fourth international landfill symposium, vol II. CISA, Cagliari, Italy, pp 2165–2173
- Bendz D, Singh VP, Åkeson M (1997b) Accumulation of water and generation of leachate in a young landfill. *J Hydrol* 203:1–10
- Bendz D, Singh VP, Berndtsson R (1997a) The flow regime in landfills – implications for modelling. In: Christensen TH, Cossu R, Stegmann R (eds) *Sardinia 97*, proceedings of the sixth international landfill symposium, vol II. CISA, Cagliari, Italy, pp 97–108
- Bhalla B, Saini MS, Jha MK (2012) Characterization of leachate from municipal solid waste (Msw) landfilling sites of Ludhiana, India: a comparative study. *Int J Eng Res Appl (Ijera)* 2(6):732–745
- Bhalla B, Saini MS, Jha MK (2013) Effect of age and seasonal variations on leachate characteristics of municipal solid waste landfill. *Int J Res Eng Tech* 02(08):223–232
- Barjinder B, Saini MS, Jha MK (2014) Assessment of municipal solid waste landfill leachate treatment efficiency by leachate pollution index. *Int J Innov Res Sci Eng Technol* 3(1):8447–8454
- Binner E, Lechner P, Ziegler C, Riehl-Herwirsch G (1997) Breitenau landfill – water balance, emissions and a look into the landfill body. In: Christensen TH, Cossu R, Stegmann R (eds) *Sardinia 97*, proceedings of the sixth international landfill symposium, vol I. CISA, Cagliari, Italy, pp 301–310
- Blakey N, Archer D, Reynolds P (1995) Bioreactor landfill: a microbiological review. In: Christensen TH, Cossu R, Stegmann R (eds) *Sardinia 95*, proceedings of the fifth international landfill symposium, vol I. CISA, Cagliari, Italy, pp 97–116

- Blakey N, Bradshaw K, Reynolds P, Know K (1997) Bio-reactor landfill – a field trial of accelerated waste stabilisation. In: Christensen TH, Cossu R, Stegmann R (eds) Sardinia 97, proceedings of the sixth international landfill symposium, vol I. CISA, Cagliari, Italy, pp 375–385
- Bogner J, Lagerkvist A (1997) Organic carbon cycling in landfills: model for a continuum approach. In: Christensen TH, Cossu R, Stegmann R (eds) Sardinia 97, proceedings of the sixth international landfill symposium, vol I. CISA, Cagliari, Italy, pp 45–56
- Brune M, Ramke HG, Collins HJ, Hanert HH (1991) Incrustation processes in drainage systems of sanitary landfills. In: Christensen TH, Cossu R, Stegmann R (eds) Sardinia 91, proceedings of the third international landfill symposium, vol I. CISA, Cagliari, Italy, pp 999–1035
- Burrows MR, Joseph JB, Mather JD (1997) The hydraulic properties of in-situ landfilled waste. In: Christensen TH, Cossu R, Stegmann R (eds) Sardinia 97, proceedings of the sixth international landfill symposium, vol II. CISA, Cagliari, Italy, pp 73–83
- Burton SAQ, Watson-Craik A (1999) Accelerated landfill refuse decomposition by recirculation of nitrified leachate. In: Christensen TH, Cossu R, Stegmann R (eds) Sardinia 99, proceedings of the seventh international landfill symposium, vol I. CISA, Cagliari, Italy, pp 119–126
- Butler AP, Zacharof AI, Sollars CJ (1999) A stochastic flow and transport model for landfill leachate production. In: Christensen TH, Cossu R, Stegmann R (eds) Sardinia 99, proceedings of the seventh international landfill symposium, vol II. CISA, Cagliari, Italy, pp 25–32
- Capodaglio AG, Bacchi P, Claus E, Olmo M, Nettuno L (1999) Leachate generation in landfills: model sensitivity and case studies. In: Christensen TH, Cossu R, Stegmann R (eds) Sardinia 99, proceedings of the seventh international landfill symposium, vol II. CISA, Cagliari, Italy, pp 11–16
- Christensen TH, Kjeldsen P, Bjerg PL et al (2001) Biogeochemistry of landfill leachate plumes. *Appl Geochem* 16(7–8):659–718
- Clement B (1995) Physico-chemical characterization of 25 French landfill leachates. In: Christensen TH, Cossu R, Stegmann R (eds) Sardinia 95, proceedings of the fifth international landfill symposium, vol I. CISA, Cagliari, Italy, pp 315–325
- D’Antonio G, Porozzi F (1991) Hydraulic behaviour of leachate at the bottom of sanitary landfills. In: Christensen TH, Cossu R, Stegmann R (eds) Sardinia 91, proceedings of the third international landfill symposium, vol I. CISA, Cagliari, Italy, pp 989–997
- DeCoursey WJ (2003) *Statistics and Probability for Engineering Applications With Microsoft® Excel*. Elsevier Science (USA). Library of Congress Cataloging-in-Publication Data, ISBN: 0-7506-7618-3
- Demirekler E, Rowe RK, Unlu K (1999) Modeling leachate production from municipal solid waste landfills. In: Christensen TH, Cossu R, Stegmann R (eds) Sardinia 99, proceedings of the seventh international landfill symposium, vol II. CISA, Cagliari, Italy, pp 17–24
- Deng Y, Englehardt JD (2006) Treatment of landfill leachate by the Fenton process. *Water Res* 40 (20):3683–3694
- Dharmarathne N, Gunatilake J (2013) Leachate characterization and surface groundwater pollution at municipal solid waste landfill of Gohagoda, Sri Lanka. *Int J Sci Res Publ* 3(11)
- Driessen JHA, Moura ML, Korzilius EPE, van der Sloot HA (1995) The sustainable landfill. In: Christensen TH, Cossu R, Stegmann R (eds) Sardinia 95, proceedings of the fifth international landfill symposium, vol I. CISA, Cagliari, Italy, pp 15–24
- Ehrig HJ (1991) Control and treatment of landfill leachate. A review. In: Harwell 1991 symposium: challenges in waste management. AEA Harwell, UK
- El-Fadel M, Bou-Zeid E, Chahine W, Alayli B (2002) Temporal variation of leachate quality from pre-sorted and baled municipal solid waste with high organic and moisture content. *Waste Mgt* 22:269–282
- ENVPROT 3C (1995) Water balance and pollution flows in secure industrial waste landfill sites. EUproject, record Control number 12184. Prime contractor: Agence pour la Récupération et l’Élimination des Déchets
- Esakku S, Karthikeyan Obuli P, Joseph Kurian, Nagendran R, Palanivelu K, Pathirana KPMN, Karunarathna AK and Basnayake BFA (2007) Seasonal variations in leachate characteristics

- from municipal solid waste dumpsites in India and Srilanka. *Proceedings of the International Conference on Sustainable Solid Waste Management*: 341–347
- Galarpea VRK, Parillaa RB (2012) Influence of seasonal variation on the bio-physicochemical properties of leachate and groundwater in Cebu City Sanitary Landfill, Philippines. *Int J Chem Environ Eng* 3(3)
- Ganiyu SA, Badmus BS, Olurin OT, Ojekunle ZO (2018) Evaluation of seasonal variation of water quality using multivariate statistical analysis and irrigation parameter indices in Ajakanga area. *Ibadan, Nigeria Appl Water Sci* 8:35
- Genon G, Marchese F, Pacitti M, Canistro C (1995) Quality of industrial landfill leachate at Barricalla site Italy. In: Christensen TH, Cossu R, Stegmann R (eds) *Sardinia 95, proceedings of the fifth international landfill symposium, vol III*. CISA, Cagliari, Italy, pp 235–246
- Pooja G, Asmita G, Shekhar TI (2015) Combined chemical and toxicological evaluation of leachate from municipal solid waste landfill sites of Delhi, India. *Environ Sci Pollut Res Int* 22 (12):9148–9158
- Gómez Martín MA, Antigüedad Auzmendi I, Pérez Olozaga C (1995a) Landfill leachate: variation of quality with quantity. In: Christensen TH, Cossu R, Stegmann R (eds) *Sardinia 95, proceedings of the fifth international landfill symposium, vol I*. CISA, Cagliari, Italy, pp 345–354
- Gómez Martín MA, Antigüedad Auzmendi I, Pérez Olozaga C (1995b) Multivariate analysis of leachate analytical data from different landfills in the same area. In: Christensen TH, Cossu R, Stegmann R (eds) *Sardinia 95, proceedings of the fifth international landfill symposium, vol I*. CISA, Cagliari, Italy, pp 365–376
- Halim AA, Aziz HA, Johari MAM, Ariffin KS, Adlan MN (2010) Ammoniacal nitrogen and COD removal from semi-aerobic landfill leachate using a composite adsorbent: fixed bed column adsorption performance. *J Hazard Mater* 175(1–3):960–964
- Hazra T, Goel S (2009) *Solid waste management in Kolkata, India: Practices and challenges*. Waste Manag 29:470–478
- Ugbebor JN, Ntesat B (2019) A comparative study on the effects of leachate on groundwater in selected dumpsites in rivers state, Nigeria. *Asian J Environ Ecol* 11(1):1–13
- Joseph JB, Mather JD (1993) Landfill – does current containment practice represent the best option? In: Christensen TH, Cossu R, Stegmann R (eds) *Sardinia 93, proceedings of the fourth international landfill symposium, vol I*. CISA, Cagliari, pp 99–107
- Kale SS, Kadam AK, Kumar S, Pawar NJ (2010) Evaluating pollution potential of leachate from landfill site, from the Pune metropolitan city and its impact on shallow basaltic aquifers. *Environ Monit Assess* 162:327–346
- Kjeldsen P, Christophersen M (2001) Composition of leachate from old landfills in Denmark. *Waste Manag Res* 19(3):249–256
- Kumar D, Alappat BJ (2005) Evaluating leachate contamination potential of landfill sites using leachate pollution index. *Clean Techn Environ Policy* 7(3):190–197
- Lee GF, Jones-Lee A (1993) “Dry tomb” vs. wet-cell landfills. In: Christensen TH, Cossu R, Stegmann R (eds) *Sardinia 93, proceedings of the fourth international landfill symposium II*. CISA, Cagliari, Italy, pp 1787–1796
- Maity SK, Dea S, Hazrab T, Debsarkarb A, Duttab A (2016a) Characterization of leachate and its impact on surface and groundwater quality of a closed dumpsite - a case study at Dhapa, Kolkata, India. *Procedia Environ Sci* 35:391–399
- Marttinen SK, Kettunen RH, Rintala JA (2003) Occurrence and removal of organic pollutants in sewages and landfill leachates. *Sci Total Environ* 301(1–3):1–12
- Matsuto T, Tanaka N, Koyama K (1991) Stabilization mechanism of leachate from semiaerobic sanitary landfills of organics-rich waste. In: Christensen TH, Cossu R, Stegmann R (eds) *Sardinia 91, proceedings of the third international landfill symposium, vol I*. CISA, Cagliari, Italy, pp 875–888
- Mattravers N, Robinson H (1991) Infiltration of rainfall into landfill sites. In: Christensen TH, Cossu R, Stegmann R (eds) *Sardinia 91, proceedings of the third international landfill symposium, vol I*. CISA, Cagliari, Italy, pp 889–903
- Mavakala BK, le Faucheur S, Mulaji CK, Laffite A, Devarajan N, Biey EM, Giuliani G, Otamonga JP, Kabatusuila P, Mpiana PT, Poté J (2016) Leachates draining from controlled municipal solid

- waste landfill: detailed geochemical characterization and toxicity tests. *Waste Manag* 55:238–248
- MoEF (2000) ‘Municipal solid waste management and handling rules’, Ministry of environment and forests, Govt. of India
- Mor S, Ravindra K, Dahiya RP, Chandra A (2006) Leachate characterization and assessment of groundwater pollution near municipal solid waste landfill site. *Environ Monit Assess* 118:435–456
- Motling S, Mukherjee SN, Dutta A (2013) Leachate characteristics of municipal solid waste landfill site in Kolkata” Published in *Indian Journal of Public Health Engineering*, 2013–14(3)
- Umar M, Aziz HA, Yusoff MS (2010) Variability of parameters involved in leachate pollution index and determination of LPI from four landfills in Malaysia. *Int J Chem Eng* 2010:747953. <https://doi.org/10.1155/2010/747953>
- Odukoya AM, Abimbola AF (2010) Contamination assessment of surface and groundwater within and around the two dumpsites. *Environ Sci Technol* 7(2):367–376
- Patil C, Narayanakar S, Virupakshi A (2013) Assessment of groundwater quality around solid waste landfill area - a case study. *Int J Innovative Res Sci, Eng Tech* 2(7)
- Rana R, Ganguly R, Gupta AK (2018) Indexing method for assessment of pollution potential of leachate from non-engineered landfill sites and its effect on ground water quality. *Environ Monit Assess* 190:46
- Rathod M, Mishra H, Karmakar S (2013) Leachate characterization and assessment of water pollution near municipal solid waste landfill site. *Int J Chem Phy Sci IJCPS* 2(Special Issue)
- Robinson H, Carey M, Watson G, Gronow J (1999) In-situ monitoring of the unsaturatedbzone beneath Stangate east landfill site: sixteen years of detailed data. In: Christensen TH, Cossu R, Stegmann R (eds) *Sardinia 99*, proceedings of the seventh international landfill symposium, vol IV. CISA, Cagliari, Italy, pp 117–124
- Salami L, Fadayini MO, Madu C (2014) Assessment of a closed dumpsite and its impact on surface and groundwater integrity: a case of okeafa dumpsite, Lagos, Nigeria. *IJRRAS* 18(3)
- Shabhimaan MA, Dikshit AK (2011) Treatment of landfill leachate using coagulation. 2nd International Conference On Environmental Science and Technology 6: VI 119-VI 122
- Sivanesan SD, Krishnamurthi K, Wachasunder SD, Chakrabarti T (2004) Genotoxicity of pesticide waste contaminated soil and its leachate. *Biomed Environ Sci* 17:257–265
- Smart P (1993) The principles and advantages of landfilling below the water table. In: Christensen TH, Cossu R, Stegmann R (eds) *Sardinia 93*, proceedings of the fourth international landfill symposium, vol II. CISA, Cagliari, Italy, pp 1807–1812
- Soong TT (2004) *Fundamentals of probability and statistics for engineers*. John Wiley & Sons Ltd, The Atrium, Southern Gate, Chichester, West Sussex PO19 8SQ, England
- Statom RA, Thyne GD, McCray JE (2004) Temporal changes in leachate chemistry of a municipal solid waste landfill cell in Florida. *USA Environmental Geology* 45(7):982–991
- Sullivan PJ, Clark JJJ, Agardy FJ (2005) *The environmental science of drinking water*. Elsevier Inc., UK
- Trankler J, Visvanathan C, Kuruparan P, Tubtimthai O (2005) Influence of tropical seasonal variations on landfill leachate characteristics—results from lysimeter studies. *Waste Manag* 25 (10):1013–1020
- Tsarpali V, Kamilari M, Dailianis S (2012) Seasonal alterations of landfill leachate composition and toxic potency in semi-arid regions. *J Hazard Mater* 233–234:163–171
- Vahabian M, Hassanzadeh Y, Marofi S (2019) Assessment of landfill leachate in semi-arid climate and its impact on the groundwater quality case study: Hamedan. *Iran Environ Monit Assess* 191:109
- Venkata Ramaiah G, Krishnaiah S (2014) Characterization of contaminated soil and surface water/ground water surrounding waste dump sites in Bangalore. *Int J Environ Res Develop* 4 (2):99–104
- Yaqout Al F, Hamoda MF (2003) Evaluation of landfill leachate in arid climate-a case study. *Environ Int* 29(5):593–600

Chapter 4

Quantification of Landfill Gas Emission and Energy Recovery Potential: A Comparative Assessment of LandGEM and MTM Model for Kolkata



Babul Das and Tumpa Hazra

Abstract Solid waste management (SWM) and disposal is a major environmental concern in recent times and is getting rapidly complicated day by day. In developing countries, municipal solid waste (MSW) is generally disposed of through open dumping and landfilling in semiengineered landfills resulting in the generation of a huge amount of greenhouse gases like CO₂ and CH₄. Methane has the highest climate change impact (5.94 kg CO₂eq/KWhe). Again, methane can be used as a renewable energy source since its energy generation potentiality is 37.2 MJ/m³.

The objective of this study is to estimate and compare the emission of landfill gas (LFG) from an uncontrolled landfill site, located in Dhapa, Kolkata, India using LandGEM (3.02) and the modified triangular method (MTM) model. The energy generation potential of the generated landfill gas is also assessed. It is estimated that methane emission varies from 10.87 to 24.01 Mm³/year and 28.36 to 44.23 Mm³/year using LandGEM and the MTM model, respectively, for the period of 2010–2030. It is also estimated that the annual power generation from LFG emissions varies from 18.045 to 39.858 MWh and 47.079 to 73.424 MWh using the estimates of LandGEM and the MTM model, respectively, for the same period.

Keywords Municipal solid waste disposal · Landfill gas emission · Greenhouse gas · Methane emission estimation · LandGEM · MTM · Energy recovery potential

4.1 Introduction

Solid wastes (SWs) are the discarded solid materials generated through the use of resources of the earth by humans and animals to support their life. It may be generated through residential activities, commercial activities, industrial activities,

B. Das · T. Hazra (✉)
Jadavpur University, Kolkata, India

institutional works, construction and demolition works, and agricultural activities (Tchobanoglous et al. 1993). Development of a sustainable management plan for solid waste (SW) is a serious challenge to policy makers now a days, mainly for developing countries, since total solid waste generation escalates with the growth in the total population of the area. Again, with the rapid industrialization, level of urbanization, economic development, and changing consumption patterns, per capita municipal solid waste (MSW) generation increases rapidly. About 2.01×10^9 tons of MSW was generated globally in 2016 and expected to become 3.4×10^9 tons in 2050 (Kaza et al. 2018). About 19.86 million tons of MSW is generated in urban India per year (Annual Report 2018–19, MoEFCC). Major parts of the MSW (>70%) of the developing countries are organic in nature, which is readily degradable (Ramachandra et al. 2018). In spite of the growing practice of resource conservation and recycling of waste and stringent rules against waste disposal, the landfilling method is still widely used for final waste disposal due to process simplicity and low economic investment worldwide. In India, about 51% of 83% collected MSW are dumped in landfill sites without any treatment and with a negligible amount of daily cover (Annual Report 2018–19, MoEFCC). One of the consequences of solid waste disposal in landfills is the generation of landfill gas (LFG), a serious environmental threat since it is composed of 45–60% (V/V) methane and 40–55% (V/V) carbon dioxide (USEPA 2014). Methane emission from solid waste disposal sites is computed as 3–19% of the total anthropogenic methane generation, and it is the third major anthropogenic source of CH_4 (IPCC 1996). In the year 2014, India emitted 16 Mg CO_2 eq of methane, which is expected to reach 20 Mg CO_2 eq by the year 2020 (Kumar and Sharma 2014). Methane generation from India contributes about 29% of the total greenhouse gas (GHG) emission of the country (Ghosh et al. 2019; Kumar and Sharma 2014; Siddiqui et al. 2006). The increase in GHG emissions can lead to an increase in global temperature and threaten human life and the environment (Hughes 2000). As LFG is one of the major sources of GHGs, proper management of LFG can reduce GHG emission into the atmosphere. Collection and flaring or oxidizing in biofilters is one of the possible management options of LFG. Since energy generation potential of CH_4 is 37.2 MJ/ m^3 (Cudjoe and Su 2020), another possible management option is LFG collection and using it as a renewable waste to energy source. For implementation of these management systems, it is essential to quantify the LFG emission from the landfill site.

The literature revealed very little work on the estimation of landfill gas emission in Kolkata region. Again, whatever works have been done so far considered the default model parameters. Locality-specific parameters like rate constant of methane generation (k) and potential of methane yield (L_0) from waste are required to be calculated for the Kolkata region since these parameters are very important for accurate determination of landfill gas emission. Again, estimation of global warming potential and energy generation potential from landfill gas emission are also required to make decision about developing any sustainable management plan. So, estimation and comparison of landfill gas (LFG) emission and energy recovery potential of the Dhapa landfill site located at Kolkata using LandGEM (3.02) and the modified triangular method (MTM) is the main aim of this paper.

4.2 Materials and Methods

4.2.1 Study Area

This study was conducted in Kolkata (latitude 22°34' N and longitude 88°24' E), the largest metropolitan city in eastern India. It is located on the east bank of River Hooghly and is 30 km away from the Bay of Bengal with an average elevation of 17 feet above the mean sea level. The rate of generation of municipal solid waste in Kolkata is about 470 gcpd (gram per capita per day) for the 4.5 million resident population and 250 gcpd for the six million floating population resulting about 3520 tons of municipal solid waste generation daily (Ali 2016). The waste is mainly biodegradable in nature (50.56%) with high moisture content (46%) and low calorific value (1201Kcal/kg) (Chattopadhyay et al. 2009; KMC, 2019). Presently in Kolkata, these wastes are directly disposed of at different disposal sites located around the city without any segregation and prior treatment. The Kolkata Municipal Corporation (KMC) runs three disposal sites located at Dhapa, Garden Reach, and Naopara. The Dhapa disposal site is located at eastern Kolkata on an average 20 km away from all the collection points and accepts about 95% of the total solid waste generated in the KMC area (Hazra and Goel 2009). Presently, 24.47 ha area is used at Dhapa for MSW disposal. The total area of the Dhapa MSW disposal site is 24.47 ha. It is an open dumpsite without any liner or leachate or gas collection and management system. The landfill is overexploited since the height of disposed waste (more than 20 m from ground level) exceeds the designed slope and life. However, this landfill site is still under operation and receives about 3000–3200 T of solid waste per day from both KMC's public waste haulers and private haulers. The present study deals with the LFG emission potential of the Dhapa disposal site. LandGEM (3.02) and the modified triangular method (MTM) were applied to estimate and compare the quantity of LFG generated from the Dhapa disposal site. The energy generation potential of LFG has also been calculated. Salient features of the Dhapa disposal site are presented in Table 4.1.

4.2.2 Prediction of Disposed MSW in Dhapa

Estimation of GHG generation from landfill requires accurate prediction of SW disposed in the landfill, considering that the 100% generated SW is disposed in landfill. For estimation of landfill gas emission, historical data on MSW disposed to the landfill site from the starting year to the year of closure of disposal site are required. The starting year of the Dhapa disposal site was 1981, and the closure year is 2020. The available waste disposal data for 2001 to 2012, obtained from the paper of SCS Engineers 2010, were used to predict waste disposal in the Dhapa landfill site for the year 2013–2020 using the geometric increase method. From Table 4.2, it is obtained that the annual average increases in solid waste disposal rate of 13.44%. By

Table 4.1 Salient features of the Dhapa open dumpsite, Kolkata, India (SCS Engineers 2010)

Characteristics	Dhapa landfill site
Starting year	1980
Year of closure	2020
Waste management facility	Daily spreading and compaction
Area (ha)	34.2
Climate	Tropical and rainy
Humidity	52%–82%
Average height (m)	30
Dumping quantity (TPD)	3500
Annual precipitation (mm/year)	1770
Temperature(°C)	26.1
LFG collection system	No gas collection system
Soil cover	Little or no

Table 4.2 Waste disposal data used for prediction of the waste disposal rate

Year	Annual waste disposal (Mg)	% annual increase rate	Average annual increase rate (%)
2000	256,200	–	13.44
2001	294,600	14.98	
2002	338,800	15.00	
2003	389,600	14.99	
2004	448,000	14.98	
2005	515,200	15.00	
2006	592,500	15.00	
2007	681,400	15.00	
2008	912,000	33.8	
2009	1,277,500	40.10	
2010	1,303,100	2.0	
2011	1,329,200	2.0	
2012	1,042,100	–21.6	

using this rate, the solid waste disposal data between the years 2013–2020 are predicted and used for GHG emission estimation.

4.2.3 Selection of LFG Emission Models

The rate of gas production in landfills can be estimated by modeling. The gas production in the disposal site relies on the decomposition rate of the organic matter. The decomposition of the organic materials depends on the order of the reaction that takes place in the landfill. Based on the order of reaction, different models are developed viz. zero-order models, first-order models, and second-order models. As most of the biological reactions are first order, first-order models are extensively

used for estimating LFG emission. The available models for estimation of LFG emission are IPCC DM, IPCC FOD models, LandGEM, TNO model, TM, MTM, EPER Germany model, SWANA model, Multiphase model, etc. Many Indian researchers used different models to calculate the LFG production from MSW disposal sites, and it is concluded that LandGEM gives more realistic results in Indian conditions than other models. LandGEM (3.02) is a first-order model, and the most important parameters for the model are the rate constant of CH_4 generation (k) and methane yield (L_0). To determine the value of model parameters such as rate constant of methane production (k), methane yield (L_0), etc. accurately, information like historical waste quantities, composition, characteristics, waste disposal practices, temperature variation, rainfall variation, distribution of waste, moisture content, compaction and density of waste, etc. are required.

Since the historical data on waste composition, characteristics, quantities, disposal, and management practices are not available for Indian conditions, the LandGEM model may not give an accurate estimation of methane emissions. In the absence of detailed information about the waste components, distribution, characteristics, disposal procedures and statistical data on temperature, rainfall, waste generation, and information about landfill management practice, the MTM method of gas estimation can be adopted (Kumar et al. 2004). Hence, in the present work, the MTM model is also adopted along with the LandGEM (3.02) model for the assessment of LFG emissions from the MSW dumping site at Dhapa.

4.2.4 LandGEM (3.02)

The Landfill Gas Emission Model (LandGEM) developed by USEPA (2005) is widely used for estimating the generation of methane from the degradation of MSW in landfills over time. The LandGEM (3.02) model uses the first-order decay rate equation for the assessment of LFG generation from the degradation of MSW in disposal sites. The methane production rate attains its maximum value very rapidly after the MSW is disposed to the disposal site and decreases slowly during the next period of degradation. Eq. (1) shows the decomposition rate equation used to quantify the rate of methane generation (Q , m^3/year).

$$Q_{\text{CH}_4} = \sum_{i=1}^n \sum_{j=0.1}^1 kL_0 \left(\frac{M_i}{10} \right) e^{-kt_{ij}} \quad (4.1)$$

L_0 = methane yield (m^3/Mg).

i = increment of time (1 year).

n = (year of estimation) - (year of first waste disposal).

j = increment of time (0.1 year).

k = first order rate constant of methane generation (year^{-1}).

M_i = mass of MSW deposited in the i^{th} year (Mg).

t_{ij} = age of the j^{th} section of waste mass M_i accepted in the i^{th} year.

The model assumes that total LFG consists of 50% of methane and 50% of carbon dioxide with the presence of nonmethanogen organic carbons and other pollutants. Furthermore, one can use a specified value of methane content within the value of 40–60%. In the present study, it is assumed that LFG consists of CH₄ by 55% and CO₂ by 45% along with trace constituents of nonmethanogenic compounds and other pollutants. The carbon dioxide generation (Q_{CO_2}) is quantified from the production of methane (Q_{CH_4}) and the percentage of methane content (P_{CH_4}) using Eq. (2).

$$Q_{CO_2} = Q_{CH_4} \left[\left\{ \frac{1}{\frac{P_{CH_4}}{100}} \right\} - 1 \right] \quad (4.2)$$

To estimate landfill gas generation from a disposal site using LandGEM, it is required to input different parameters like rate constant of methane generation, opening year of landfill, closing year of landfill, CH₄ yield, and waste disposal rates (Mg/year) (USEPA 2005).

4.2.5 Evaluation of Rate Constant for Methane Generation (K)

The rate constant for methane generation (k) represents CH₄ production rate and decay of solid waste in the disposal site. The prediction of time over which methane is produced from a particular waste stream is controlled by the value of the rate constant of the decomposition (Amini et al. 2012). The rate constant is primarily a function of four factors: available moisture content, pH, nutrients availability for degrading microorganisms, and temperature of the waste mass.

There are different methods for evaluation of k value. The laboratory simulation method (De la Cruz and Barlaz 2010; Wang and Barlaz 2016) is used for computation of k value in the present study.

4.2.6 Laboratory Simulation Method

Each waste component has different decay rates. First k values of individual waste component are determined in laboratory condition (k_{lab}) by experiment, and after that, the k value of MSW ($k_{lab,MSW}$) is computed by taking weighted average of k values of individual waste component. Laboratory k values are generally higher in magnitude than field conditions since laboratory situations are more perfect. Karanjekar et al. (2015) presented a correction factor (f) on the basis of annual average precipitation and average temperature to convert the laboratory k values of MSW component into field k values ($k_{field, i}$).

Table 4.3 Different waste composition in Kolkata and corresponding k value

Composition	% waste ^a	k _{lab} (y ⁻¹) ^b	f value ^c	k _{field} (y ⁻¹) ^d
Food waste	45.5	15.02	0.0046	0.07
Branches/wood	1.2	1.56	0.0046	0.007
Green waste (leaves+grass)	5	24.5	0.0046	0.11
Textiles	4	3.08	0.0046	0.014
Paper	4	3.27	0.0046	0.015
Other organics	3.4	13.68	0.0046	0.06

(a) Engineers 2010 (b) De la Cruz and Barlaz 2010 (c) Eq. 4.5 (d) Eq. 4.4.

$$k_{\text{fieldMSW}} = f \left\{ \sum k_{\text{lab},i} \times (\text{wt. fraction})_i \right\} \quad (4.3)$$

$$k_{\text{field},i} = f \times k_{\text{lab},i} \quad (4.4)$$

$$f = -0.00758 T + 0.0135 R + 0.137 \quad (4.5)$$

where i is the i^{th} waste component, T is the ambient temperature ($^{\circ}\text{C}$), and R is the average annual precipitation (mm/day).

Table 4.3 shows the fraction of different waste components present in MSW of Kolkata and their corresponding k value.

It is estimated that the k value of MSW in the field for Kolkata is 0.04 y^{-1} using Eq. 4.3. Kumar and Sharma (2014) used k value as 0.07 y^{-1} for the assessment of CH_4 emission from the MSW landfill site.

4.2.7 Evaluation of Methane Generation Potential (L_0)

L_0 is the quantity of methane (m^3) produced per megagram of MSW decomposition under idealized conditions for methane generation. The composition and type of waste disposed in the disposal site controls the value of methane yield. L_0 value is calculated based on per megagram of dry waste. So, dry waste should be considered for calculation of methane yield. In our study, we use the data of moisture content reported in IPCC (2006) for the computation of methane yield. For calculation of L_0 value of a landfill, it is assumed that the L_0 value of a waste mix is equal to the weighted average L_0 value of individual waste component. Ultimate methane yield and moisture content of various waste components are shown in Table 4.4. It is calculated that Kolkata has an L_0 value of $46.51 \text{ m}^3/\text{Mg}$.

4.2.8 Modified Triangular Method (MTM)

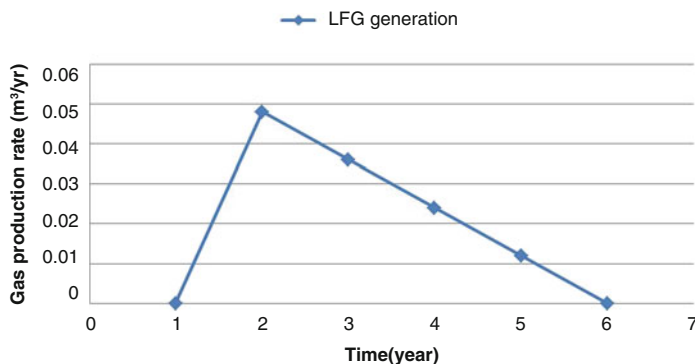
Triangular method is based on the first-order decomposition methodology with modification of the total amount of landfill gases generated from the waste

Table 4.4 Moisture content and ultimate CH₄ yield of different waste components (Staley and Barlaz 2009)

Waste categories	Moisture content (%) [8]	Ultimate CH ₄ yield (L ₀) (m ³ /Mg)
Compostable matter ^a	45	145.1
Paper ^a	10	132.8
Textile	20	14.8

^aAverage of newspaper, office paper, glossy paper, and old corrugated containers (OCC)/Kraft bags

^bAverage of food waste, green waste, and wood waste

**Fig. 4.1** Triangular gas production for RBW of Kolkata

represented by the area of triangle for a particular period of time; i.e., the rate of gas emission is linear rather than exponential (Tchobanoglous et al. 1993). Modified triangular method (MTM) is slight modification to the triangular method. In this method, it was assumed that the total LFG production is equal to the gas estimated by the default methodology. The peak rate of gas generation is calculated by equating the landfill gas estimate obtained from IPCC default methodology and the area of triangle. In this model, the biodegradable organic materials present in MSW are separated into two parts: (1) rapidly biodegradable waste (RBW) and (2) slowly biodegradable waste (SBW) (Tchobanoglous et al. 1993). The rapidly degradable wastes of MSW consist of food waste, paper, and a portion of yard wastes and the slowly degradable wastes of MSW consisting of rubber, leather, woody portions of yard waste, and wood (Tchobanoglous et al. 1993). It is assumed that the MSW starts gas production after 1 year of deposition. Gas emission from the RBW reaches a maximum in the second year after waste deposition and gradually decreases to zero at the end of the sixth year; i.e., gas emission from RBW takes place over a period of 5 years. For the SBW, gas generation starts at the end of the first year and reaches the peak after 6 years of waste deposition and then gradually decreases to zero after the sixteenth year; i.e., gas emission for SBW takes place over a period of 15 years. The rate and amount of gas generated at the end of each year from 1 kg rapidly biodegradable and slowly biodegradable organic matter are shown in Figs. 4.1 and 4.2.

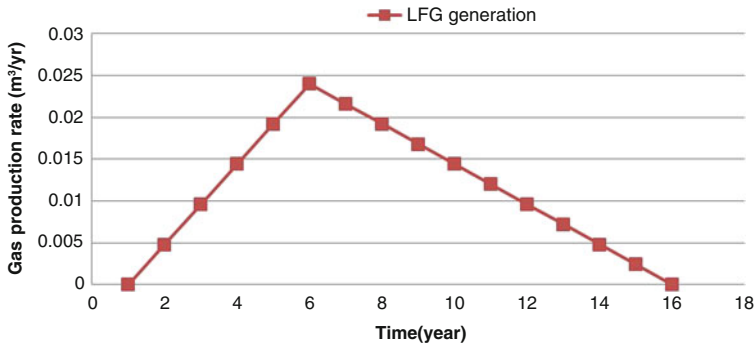


Fig. 4.2 Triangular gas production for SBW of Kolkata

Table 4.5 Parameters used for evaluating energy generation potential from landfill gas

Parameter	Value considered
Low calorific value of CH ₄ (MJ/m ³)	37.2 (Cudjoe and Su 2020)
Oxidation factor in landfill	0.9 (IPCC 2006)
Energy generation efficiency of gas engine	30% (Ghosh et al. 2019)
Capacity factor	0.85 (Cudjoe and Su 2020)
Landfill gas collection efficiency	70% (Ghosh et al. 2019)

The total rate of gas generation from a landfill in which wastes were placed is obtained graphically by summing the amount of gas generation from RBW and SBW portions of MSW deposited each year.

4.2.9 Evaluation of Energy Generation Potential of Landfill Gas

The amount of methane generation as predicted for 2010 to 2030 using both LandGEM (3.02) method and MTM method was used to evaluate the energy generation potential using Eq. 4.6 (Cudjoe and Su 2020).

$$\begin{aligned}
 &\text{Energy Generation Potential of Methane from Landfill Site (MJ/yr)} \\
 &= \text{Generated CH}_4 \text{ (m}^3\text{/yr)} / \times \text{Low calorific value of CH}_4 \text{ (MJ/m}^3\text{)} \\
 &\quad \times \text{Oxidation factor in the landfill} \\
 &\quad \times \text{Energy generation efficiency of the gas engine} \times \text{Capacity factor} \\
 &\quad \times \text{Landfill gas collection efficiency} \tag{4.6}
 \end{aligned}$$

After the estimation of the energy generation potential of methane in MJ, it was multiplied by 0.2778 to convert it into MWh.

To calculate the amount of energy generation potential of LFG from the Dhapa landfill site, the data which were assumed are presented in Table 4.5.

4.3 Results and Discussion

The predicted solid waste disposed at the Dhapa landfill site for 2013–2020 was used for landfill gas estimation. Using the LandGEM (3.02) method, it is found that the total LFG, CH₄, and CO₂ emission during the period 2010–2030 are 716.35 Mm³, 393.99 Mm³, and 322.33 Mm³, respectively. Fig. 4.3 shows the LFG emission over the period of 1981–2100 from the Dhapa open dumpsite. It is also shown that maximum emission takes place in the closure year, i.e., in the year 2020. Using the MTM method, it is found that the total LFG, CH₄, and CO₂ emission during the period 2010–2030 are 1160.73 Mm³, 638.40 Mm³, and 522.32 Mm³, respectively. Fig. 4.4 shows the LFG emission over the period of 1981–2035 from the Dhapa open dumpsite. It is also shown that maximum emission takes place 2 years after the closure year, i.e., in the year 2022.

It is seen that methane emission obtained using the MTM model is 62.1% greater than the methane emission using the LandGEM version 3.02 model. In the MTM method, it is assumed that the total LFG emission occurs from MSW, disposed in a year, within a base period of 16 years from the time of disposal. Again, this method assumes linear variation of LFG emission, but actually, the variation of landfill gas emission follows an exponential distribution due to first-order biological reaction. These assumptions may lead to a higher result.

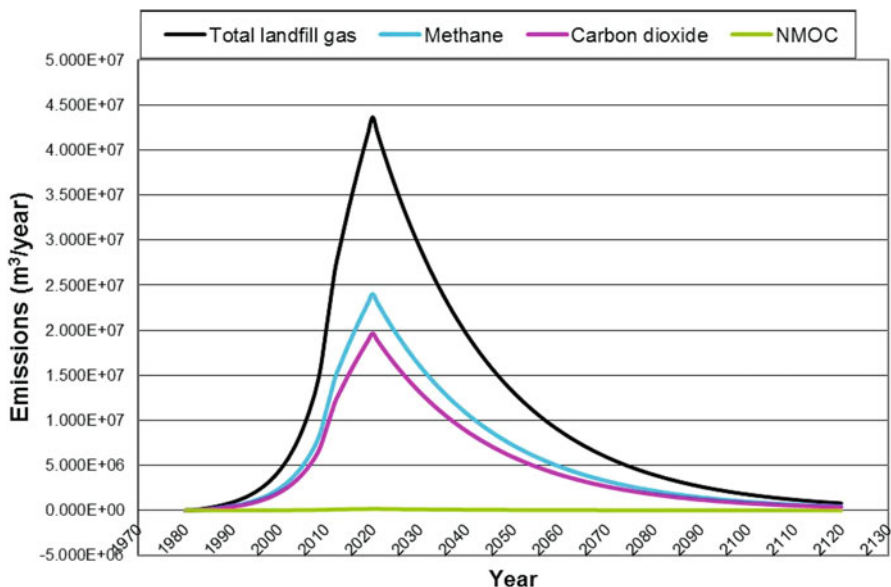


Fig. 4.3 LFG emissions from the Dhapa open dumpsite by LandGEM

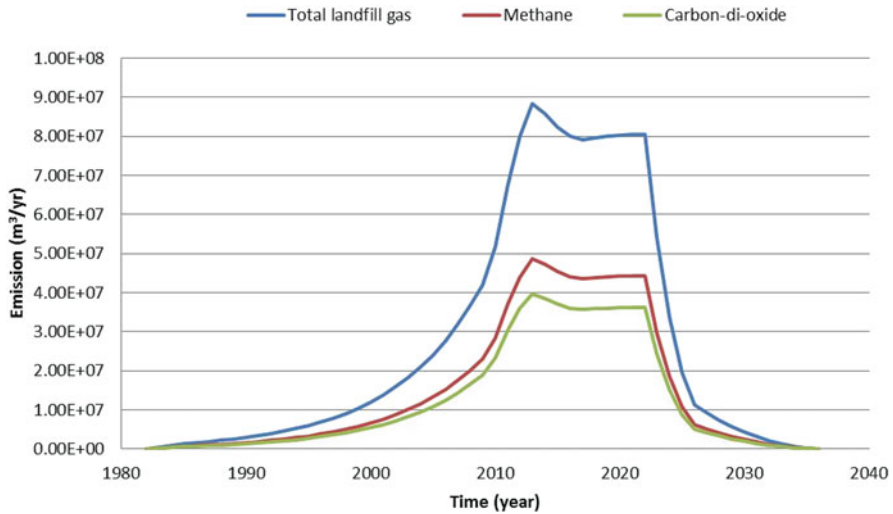


Fig. 4.4 LFG emissions from the Dhapa open dumpsite by MTM

It is also estimated that methane emission varies from 10.87 to 24.01 Mm^3/year and 28.36 to 44.23 Mm^3/year using LandGEM (3.02) and the MTM method, respectively, for the period of 2010–2030 from the Dhapa landfill site in Kolkata.

From the LFG emission curves, it is shown that the highest rate of gas emission occurs between the period 2010 to 2030. So, the present study shows the value of LFG emission between the periods of 2010–2030. But, gas emission also takes place beyond this time period, although the emission rate is less. After the closure year, the LFG emission rate decreases faster than the LFG emission rate before the closure year. From the LFG emission graphs, it is also obtained that considerable LFG emission takes place during the period of 10–15 years after the closure year.

From the CH_4 emission calculated by the LandGEM (3.02) method, it is estimated that annual energy generation varies from 64.961 TJ to 143.488 TJ ($1 \text{ TJ} = 10^{12} \text{ J}$) and power generation varies from 18.045 MWh to 39.858 MWh, which is about 1–2% of the power demand of Kolkata city. By using CH_4 emission from the MTM method, it is seen that annual energy generation varies from 169.484 TJ to 264.326 TJ ($1 \text{ TJ} = 10^{12} \text{ J}$) and power generation varies from 47.079 MWh to 73.424 MWh, which is about 2.2–3.5% of the power demand of Kolkata city. Presently, the electric supply of Kolkata city is fully dependent on coal-based thermal power plants. Generation of electricity from LFG reduces the dependency on using non-renewable energy sources. Furthermore, the emission of GHG and other air pollutants due to combustion of fossil fuel and direct emission from landfills can be decreased. The reduction of GHG also helps Kolkata Municipal Corporation to earn revenue by trading the certified emission reduction (CER) credits under the clean development mechanism (CDM) project.

4.4 Conclusion

MSW disposal sites are major sources of GHG emission to the atmosphere. The present investigation revealed that methane emission from the Dhapa open dumpsite of Kolkata varies from 10.87 to 24.01 Mm³/year by using LandGEM (3.02) and 28.36 to 44.23 Mm³/year estimated by using the MTM model for the period of 2010–2030. Presently, this huge amount of GHGs is directly emitted to the atmosphere and causes the greenhouse effect, which leads to global warming and different undesirable effects on the environment. Again, LFG has high energy potential and can be used as fuel for power generation. Generated electricity can be used in landfill itself for operating electric equipment, lighting, etc. The budget savings for electricity can be considered as revenue. The generated electricity can be used as a revenue generator by supplying electricity in the national grid. The revenue obtained from the energy project can be used for developing the solid waste management system, which supports environmental sustainability. This management process also supports the economy of the country and gives a renewable energy source. Environmental benefits can also be claimed through reducing GHG emission.

However, there are certain limitations in the present study. Most of the data used in this study were secondary data, collected from different published papers. For realistic estimation in Indian conditions, a detailed investigation is required to determine the congenial factors affecting LFG generation and their variations. A detailed environmental and economic assessment is required to be done before implementation of landfill gas to energy project for the Dhapa landfill area.

References

- Ali SKA (2016) Status of solid waste generation and management practice in Kolkata municipal corporation, West Bengal. *Int J Environ Sci* 6(6)
- Amini HR, Reinhart DR, Mackie KR (2012) Determination of first-order landfill gas modelling parameters and uncertainties. *Waste Manag* 32:305–316
- Annual Report (2018–19) MoEFCC obtained from https://www.google.com/url?sa=t&rct=j&q=&esrc=s&source=web&cd=&cad=rja&uact=8&ved=2ahUKewjPxsDppY3rAhW_wzgGHRsNCB4QFjAFegQICBAB&url=http%3A%2F%2Fmoef.gov.in%2Fwp-content%2Fuploads%2F2019%2F08%2FAnnual-Report-2018-19-English.pdf&usg=AOvVaw1VWtc7aWZ3Mtqr_qsjqI_X. Accessed 9th August, 2020
- Chattopadhyay S, Dutta A, Ray S (2009) Municipal solid waste management in Kolkata, India- a review. *Waste Manag* 29:449–458
- Cudjoe D, Su HM (2020) Economic and environmental assessment of landfill gas electricity generation in urban districts of Beijing municipality. *Sustainable Production and Consumption* 23:128–137
- De la Cruz FB, Barlaz MA (2010) Estimation of waste component specific landfill decay rates using laboratory-scale decomposition data. *Environ Sci Technol* 44:4722–4728

- Ghosh P, Shah G, Chandra R, Sahota S, Kumara H, Vijaya VK, Thakur IS (2019) Assessment of methane emissions and energy recovery potential from the municipal solid waste landfills of Delhi, India. *Bioresour Technol* 272:611–615
- Hazra T, Goel S (2009) Solid waste management in Kolkata, India: practices and challenges. *Waste Manag* 29:470–478
- Hughes L (2000) Biological consequences of global warming: is the signal already apparent? *Trends Ecol Evol* 15(2):56–61
- IPCC (1996) Report of the twelfth session of the intergovernmental panel on climate change, intergovernmental panel on climate change (IPCC). Mexico City:11–13
- IPCC (2006) IPCC guidelines for national greenhouse gas inventories. In: Task force on national greenhouse gas inventories Cambridge, vol. 5 U.K. and New York, NY, USA
- Karanjekar RV, Bhatt A, Altouqui S et al (2015) Estimating methane emissions from landfills based on rainfall, ambient temperature, and waste composition: the CLEEN model. *Waste Manag* 46:389–398
- Kolkata Municipal Corporation (2019) Solid waste management activities in Kolkata City. https://www.google.com/url?sa=t&rct=j&q=&esrc=s&source=web&cd=&cad=rja&uact=8&ved=2ahUKewjK2rOxtYnrAhXN7XMBHSBLAhQQFjADegQIAhAB&url=https%3A%2F%2Fwww.kmccgov.in%2FKMCCPortal%2Fdownloads%2FPublic_domain_Statis_report_SWM_28_10_2019.pdf&usg=AOvVaw00ooM0ItMHZ6zcOuuPykvl. Accessed on 7.8.2020
- Kumar A, Sharma MP (2014) GHG emission and carbon sequestration potential from MSW of Indian metro cities. *Urban Clim* 8:30–41
- Kumar, S., Mondal, A.N., Gaikwad, SA Devotta, S., (2004) Qualitative assessment of methane emission inventory from municipal solid waste disposal sites: a case study. *Atmospheric Environ* (38):4921–4929
- Ramachandra TV, Bharath HA, Kulkarni G, Han SS (2018) Municipal solid waste: generation, composition and GHG emissions in Bangalore, India. *Renew Sust Energ Rev* 82:1122
- Engineers SCS (2010) Methane to markets assessment report, Dhapa disposal site Kolkata. Kolkata Municipal Corporation, Kolkata
- Siddiqui TZ, Siddiqui FZ, Khan E (2006) Sustainable development through integrated municipal solid waste management (MSWM) approach – a case study of Aligarh District. In: Proceedings of National Conference of advanced in mechanical engineering (AIME-2006). Jamia Millia Islamia, New Delhi, India, pp 1168–1175
- Staley BF, Barlaz MA (2009) Composition of municipal solid waste in the United States and implications for carbon sequestration and methane yield. *J Environ Eng* 135:901–909
- Tchobanoglous G, Theisen H, Vigil SA (1993) Integrated solid waste management: engineering principles and management issues. McGraw Hill, International editions
- USEPA (United States Environmental Protection Agency) (2005) Landfill Gas Emissions Model (LandGEM version 3.02): Version 3.02, User's Guide, EPA-600/R-05/047, <http://www.epa.gov/ttn/catc/dir1/LandGEMversion3.02-v302-guide.pdf>, USA
- USEPA (2014) U.S Energy Information Administration. Monthly energy review. Washington DC 2015
- Wang X, Barlaz MA (2016) Decomposition and carbon storage of hardwood and softwood branches in laboratory-scale landfills. *Sci Total Environ* 557–558:355–362
- Kaza S, Yao L, Bhada-Tata P, Van Woerden F (2018) What a waste 2.0: a global snapshot of solid waste management to 2050. Overview booklet. World Bank, Washington, DC

Chapter 5

Assessment of Natural Enrichment of Heavy Minerals along Coastal Placers of India: Role of Lake and River Mouth Embayment and Its Implications



Shyantani Ghosal, Sudha Agrahari, Debashish Banerjee, and Debashish Sengupta

Abstract The study delineates the heavy mineral enrichment of beach sands situated along the eastern coastal areas of India, which has been extensively studied for its economic resources. The results obtained are discussed in terms of radioactive element and rare earth element (REE) concentration in the study area. Certain radiological attributes like radium equivalent, absorbed dose rate, and annual effective dose rate values have been presented. In the study area, the average Th/U ratio is found to be about 22. The absorbed dose rate and the thorium concentration show a positive correlation. The average TREE concentration varies between 774 and 1066 ppm with an average of about 6749 ppm. The TREE and thorium concentrations show a good concordance, which is indicative of the fact that these are sourced primarily from the radioactive mineral monazite. This is important as the strategic and critical minerals, specifically the rare earths, are primarily extracted from naturally occurring radioactive minerals like bastnaesite, monazite, and loparite, all of which are primarily radioactive in nature. The study discusses the effect of lacustrine and estuarine environment on the heavy mineral deposition, enhancement along the beach placers, and its implications. The effect of consistent mining along the beach area on the elevated radioelement concentration as well as the beach geomorphology has been discussed. Additionally, the chapter also highlights the disruption caused by the dredging activities to the marine species dwelling along the beach areas.

Keywords Estuarine environment · Heavy minerals · Radioelement analysis · Rare earth elements

S. Ghosal (✉) · S. Agrahari · D. Sengupta
Department of Geology and Geophysics, Indian Institute of Technology (IIT), Kharagpur,
West Bengal, India

D. Banerjee
Radiochemistry Division, Variable Energy Cyclotron Centre, BARC, Kolkata, India

© Springer Nature Switzerland AG 2021

P. K. Shit et al. (eds.), *Spatial Modeling and Assessment of Environmental Contaminants*, Environmental Challenges and Solutions,
https://doi.org/10.1007/978-3-030-63422-3_5

5.1 Introduction

The Indian subcontinent has a long coastal stretch of approximately 7516 km. It extends from the beach areas of Gujarat in the west to West Bengal in the east. The coastal area is surrounded by the Arabian Sea in the west, the Indian Ocean in the south, and the Bay of Bengal in the east. With such an extensive coastal region, there exist a number of beaches that are noted to report a high concentration of heavy minerals that includes zircon, garnet, monazite, ilmenite, and rutile. The mineral concentration of this vast coastal region differs with the differing lithology of its adjacent areas. The beach area along the south-western part of peninsular India, in the state of Kerala, is highly enriched with heavy minerals; the minerals typically found are monazite, zircon, magnetite, and garnet (Ramamamy et al. 2014). Beach areas along the eastern part of the country, particularly along the states of Odisha and Andhra Pradesh, are also enriched with heavy minerals. High concentration of ilmenite, garnet, sphene, rutile, monazite, and zircon is present along these areas (Mohanty et al. 2004; Ghosal et al. 2017; Palaparthi et al. 2017).

Placer deposits along river and beach regions show an enrichment of heavy minerals caused by mechanical concentration and gravity separation. The effect of the sorting action of the adjacent water body results in the formation of heavy mineral concentrates. Throughout the world, there are a number of beach areas that have a high concentration of heavy minerals. Certain beach areas along the coast of Brazil, Madagascar, and India are economically explored for the heavy mineral deposit. Apart from the economically profitable minerals, placer deposits are also known to contain minerals of high strategic value. The presence of the mineral monazite and zircon in a deposit indicates the presence of radioactive minerals and rare earth elements (REEs). The mineral zircon is a zirconium oxide that contains uranium in its crystal lattice, and the mineral monazite is a rare earth phosphate that consists of thorium and REE in its crystal lattice. There are a number of beach areas around the world, as discussed in Table 5.1, that are highly enriched with heavy minerals including radioactive minerals, containing thorium and uranium.

Beach areas alongside the eastern fringes of India are considered as a high background radiation area (HBRA) (Mohanty et al. 2004; Rao et al. 2009; Ghosal et al. 2017). Between monazite and zircon, the higher concentration of monazite along these beach areas results in an elevated assemblage of thorium and REEs (Behera 2003; Ghosal et al. 2020a, b). China is the largest supplier of rare earths around the world, but with the recent developments, it is of utmost importance that every country should look for native resources of REEs. The importance of REEs are multifold, it is used in the electronic industries, smartphones, batteries, wind turbines, and electronic vehicles, and it is also of importance in the field of medical science (Balaram 2019). The nuclear program of India is designed based on the fact that India has one of the largest thorium reserves in the world. ^{232}Th is required as a nuclear fuel in the second and third stage of the three-stage program, and right now, the country is at the second stage (Sarangi 2017). Considering these factors, it can be understood that these placer deposits are of immense economic and strategic

Table 5.1 Beach areas from around the world consisting of a high concentration of heavy mineral deposits

S. No.	Name of the beach	Minerals present	Country	Source
1.	São Paulo, Rio de Janeiro, and Espírito Santo	Monazite	Brazil	Anjos et al. (2006)
2.	Guangdong and Guangxi, Hainan	Monazite	China	Orris and Grauch (2002)
4.	Namakwa	Zircon and gemstones	South Africa	Philander and Rozendaal (2015); Rozendaal and Philander (2000)
5.	Mozambique	Ilmenite, rutile, and zircon	Africa	Van Gosen et al. (2014)
6.	Taolagnaro and Toliara, Madagascar	Ilmenite and zircon	Africa	Van Gosen et al. (2014)
7.	Senegal	Ilmenite and zircon	Africa	Van Gosen et al. (2014)
8.	Pulmoddai and Verugal	Titanium and zircon	Sri Lanka	Udarika et al. (2016)
9.	Tra Co, Ha Tinh, Qui Nhon, and Ham Tan regions	Ilmenite, monazite, and zircon	Vietnam	Van Duong et al. (1996)
10.	Trail Ridge, Florida	Titanium, zircon, and staurolite	USA	Force and Rich (1989)
11.	Lakehurst, New Jersey	Ilmenite and zircon	USA	Van Gosen et al. (2014)
12.	Murray	Ilmenite, rutile, leucoxene, and zircon	Australia	Roy et al. (2000)
13.	Sithonia	Zircon, monazite, apatite, garnet, epidote, and allanite	Greece	Papadopoulus et al. (2015)
14.	Rosetta beach	Monazite and zircon	Egypt	Mubarak et al. (2017)

importance. The Indian Rare Earth Limited already has a dredging plant in Ganjam district, Odisha, which primarily deals with the separation of minerals like ilmenite, rutile, zircon, sillimanite, and garnet.

The heavy mineral enrichment of the coastal placer deposits along the eastern coastal region of India is primarily dependent upon the adjacent hinterland geology. The Eastern Ghat Mobile Belt (EGMB) lying alongside these placer deposits is a high-grade metamorphic terrain consisting of various rock types like charnockite, granite, khondalite, anorthosite, and migmatite. The minerals present in these rocks are the main source of the heavy mineral deposits. The various rivers flowing through these highlands carry the weathered detritus from these rocks and deposits along the river mouth and then by the action of tides and waves the sediment gets distributed along the length of the beach. The eastern coast of India is very much

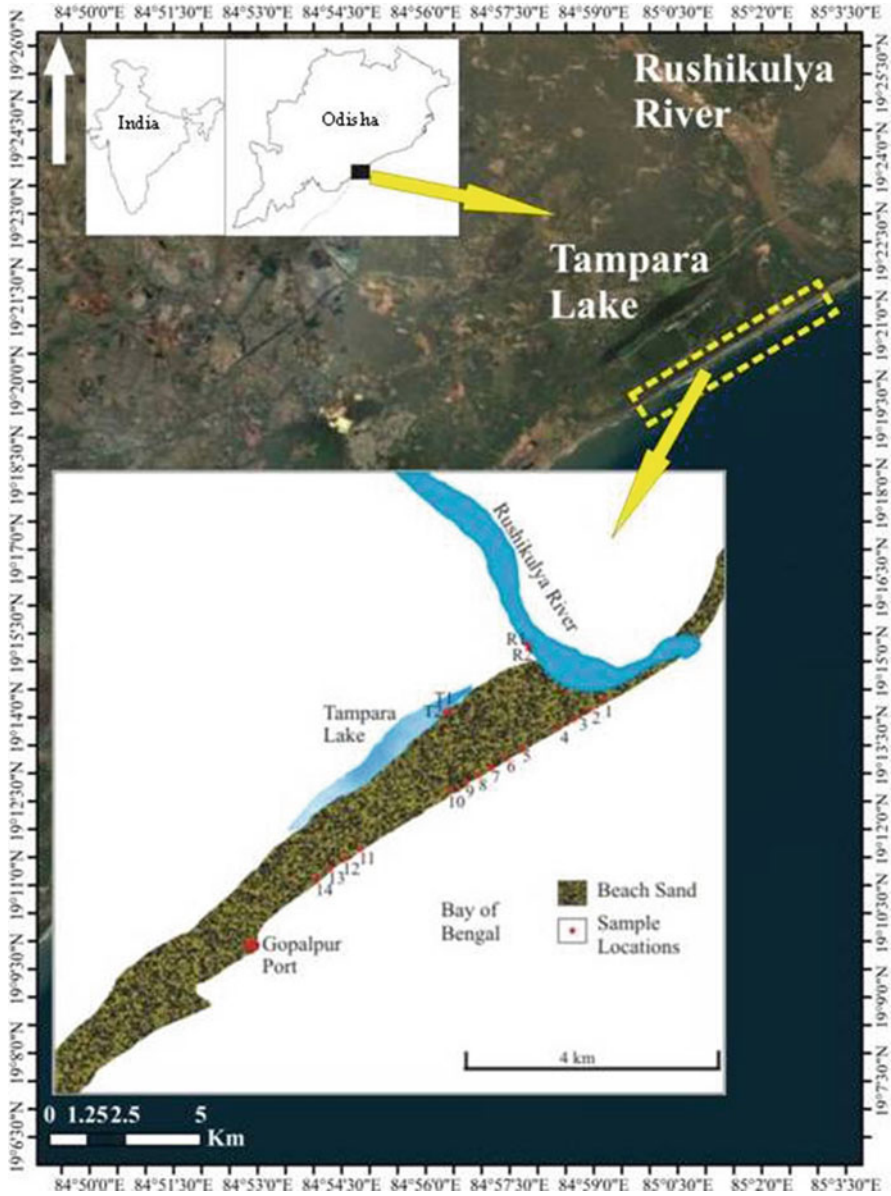


Fig. 5.1 Location of the study area. The locations of the beach and river placer samples are presented

prone to storm surges, and hence, they have an impact on the distribution of the heavy minerals (Sundar 2015; Ghosal et al. 2020a, b).

The discussed study area in this chapter lies along the southern coastal areas of Odisha, India. The area lies toward the southwest of the Rushikulya river mouth (Fig. 5.1) and adjacent to the Tampara Lake, which is a freshwater lake. The beach area in question is wide and has distinct dune, berm, and swash zone. The swash zone shows a moderate slope, and the wave current is quite strong. The berm area of the beach shows a very high concentration of dark fragments, which denotes the presence of heavy minerals (Fig. 5.1). The present study analyzes the heavy mineral concentration of the beach placer deposits in terms of radioelement and REE concentration.

5.2 Methodology

The beach sand samples were collected along the berm region of the beach. The total length of the studied beach area is approximately 10 km. The samples were collected from a shallow depth (not more than 15 cm) after removing the impurities like rootlets or anthropological wastes. Sand samples were also collected along the banks of the Rushikulya river, close to its mouth. Representative sand samples were also collected along the areas adjacent to the Tampara Lake. The sand samples were then kept in an oven at 80 °C for 3 hours followed by sieving through a 0.355 mm sieve. Both the radioelement activity concentration measurement and the REE analysis were done to bulk sand samples.

5.2.1 Radioelement Analysis

After sieving, the beach sand samples were packed in a glass vial, and then they are sealed and preserved for 28 days to attain secular equilibrium. It is then analyzed based on the absolute method to measure the activity concentration of thorium, uranium, and potassium (Fig. 5.2). The investigation has been conducted in a GEM series High Purity Germanium (HPGe) coaxial detector, ORTEC, USA with 50% efficiency and 1.8 keV energy resolution at 1332 keV of ^{60}Co at the Radiochemistry Division (BARC), Variable Energy Cyclotron Centre (VECC), Kolkata, India. Natural radioactivity of an area is a consequence of the joint effect of the radioelements ^{238}U , ^{232}Th , and ^{40}K . Uranium and thorium cannot be measured directly, and hence, their daughter products are measured to get an estimate of these radioelements. Potassium is measured by analyzing its respective peak. Uranium is measured by analyzing the following daughter products ^{214}Pb (295 keV and 352 keV) and ^{214}Bi (609 keV). The following daughter products of thorium have been analyzed to get an idea about its activity concentration: ^{228}Ac (338 keV, 911 keV), ^{212}Pb (239 keV), ^{212}Bi (727 keV), and ^{208}Tl (583 keV). The calibration of the instrument

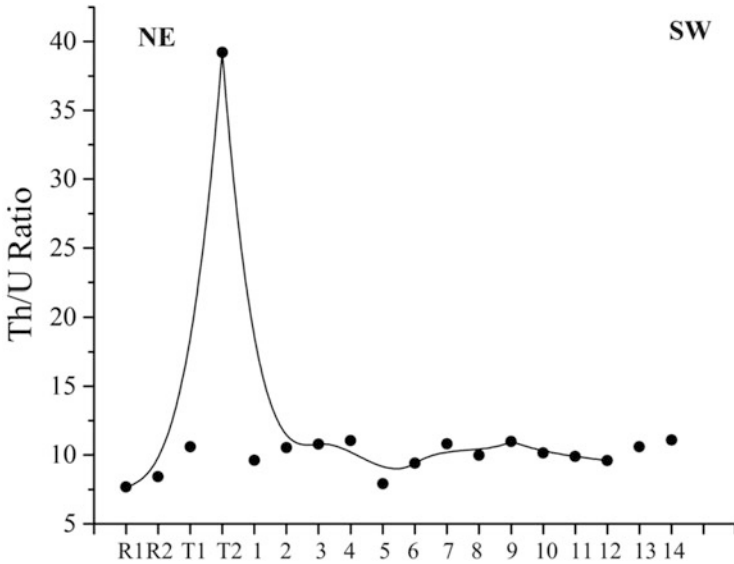


Fig. 5.2 The variation of the Th/U ratio following a northeast–southwest trend along the study area

and the respective peak efficiencies, as calculated from eq. 5.1, have been based on ^{152}Eu , with a known half life. The measurement for each sample was done for 40,000 seconds; this allows us to get an appropriate gamma-ray peak area. The peak areas were measured by a multichannel analyzer, Canberra DSA 1000, connected to Genie 2 K software.

$$\epsilon_i = \frac{CPS_i \times 100}{A_{ti} \times I_i} \quad (5.1)$$

where, A_t = activity of ^{152}Eu , ϵ = efficiency, CPS = counts per second, I = intensity of ^{152}Eu , and i = individual peak.

Following the measurement of the activity concentration of respective radioelements, certain radiological parameters like radium equivalent, annual effective dose rate, and absorbed dose rate are calculated.

5.2.2 Absorbed Dose Rate

Absorbed dose rate quantifies radiation received by an individual per kilogram of their mass. For dose rate calculation above 1 m from the surface, by the consistent dispersion of gamma radiations from ^{238}U , ^{232}Th , and ^{40}K , the following conversion factor as proposed by UNSCEAR 2000 was used.

$$D \text{ (nGyh)} = 0.461A_U + 0.623A_{Th} + 0.0414A_K \quad (5.2)$$

where A_U , A_{Th} , and A_K are specific activity of ^{238}U , ^{232}Th , and ^{40}K in Bq kg^{-1} , respectively.

5.2.3 Annual Effective Dose Rate

The idea for the internal and external radiation exposure is provided by the annual effective dose rate. It is calculated with 0.2 as the outdoor occupancy factor and using the conversion coefficients (0.7 SvGy^{-1}), as proposed by UNSCEAR 2000.

$$\text{AED (mSvy}^{-1}\text{)} = D \text{ (nGyh}^{-1}\text{)} \times 8760 \text{ (hy}^{-1}\text{)} \times 0.2 \times 0.7\text{Sv Gy}^{-1} \times 10^{-6} \quad (5.3)$$

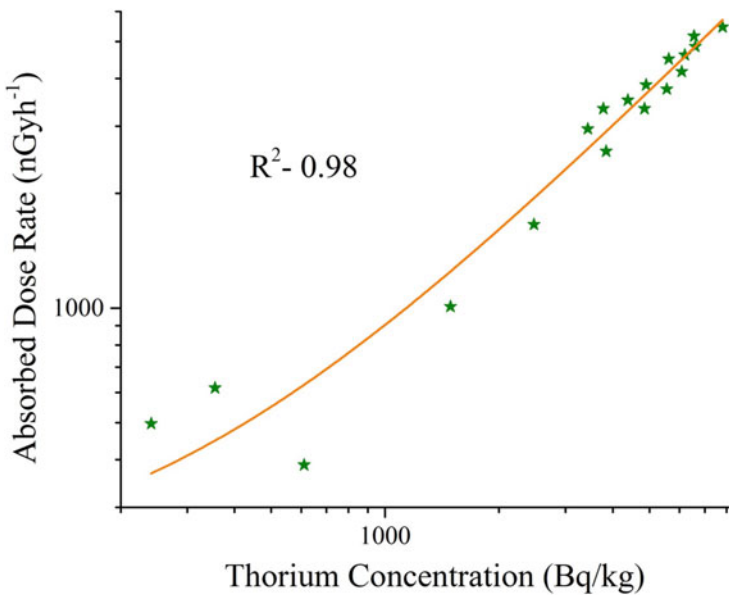


Fig. 5.3 Correlation analysis between absorbed dose rate and thorium concentration along the study area

5.2.4 Radium Equivalent

The gamma output from a varietal mix of uranium, thorium, and potassium activity concentration in a sample is defined by the radium equivalent (Fig. 5.3). The radiation exposure caused by different radioisotopes is compared by the respective radium equivalent values obtained.

$$(Ra_{eq}) = A_U + 1.43 A_{Th} + 0.077 A_K \quad (5.4)$$

The above-mentioned equation is based on the assumption that the contributions received from the other radionuclides are insignificant.

5.2.5 Rare Earth Element Analysis

The coastal placer deposits have been analyzed to estimate their REE concentration with the help of a quadrupole inductively coupled plasma mass spectrometer (ICP-MS, Thermo Scientific X-Series II) at the Centre for Earth Sciences, IISc, Bangalore. For calibration, the USGS standards AGV-2, BHVO-2, and BCR-2 were used. HF, HCl, and HNO₃ acid solution is processed with 25 mg of the sand sample in a Teflon beaker, and then the acid solution is evaporated. This is followed by dilution of the remnants in 2% HNO₃ solution to 100 ml solution by diluting it with 18.2 mega-ohm water. Monitoring of instrumental drift is accomplished by using an internal standard of 10 ppb solution of Be, In, Cs, and Bi; it is applied for all the samples, standards, and blanks, following the lab protocols (Banerjee et al. 2016). Data precision based on the analysis of USGS standard AGV-1 is better than 2%.

5.3 Results

High concentrations of dark colored particles signifying the presence of heavy minerals along the berm were observed along the study area. The sand samples collected along the beach were done so maintaining a northeast–southwest trend. The radioelement concentration of the sand samples was estimated with HPGe, and the subsequent results have been listed in Table 5.2. The collected samples from the study area show a high Th/U ratio, varying between 7.7 and 39.2 with an average of 21.9, which exceeds the crustal average of 3.8. The Th/K ratio of the study area ranges between 0.3 and 134.3 with an average of 17.1. The average absorbed dose rate of the study area is 3126 nGyh⁻¹, and it varies between 387.8 and 5462.5 nGyh⁻¹. The annual effective dose rate and the radium equivalent of the area vary between 0.5 and 6.7 mSvy⁻¹ (average 3.8 mSvy⁻¹) and 437.6 and 11918.8 (average 6411.5), respectively. The REE concentration of the sand samples is also listed in

Table 5.2 Radioelement and rare earth element concentrations of the study area

Sample name	Th/U	Th/K	Absorbed dose rate (nGy ^h ⁻¹)	AED (mSvy ⁻¹)	Radium equivalent	TREE
R1	7.7	0.3	497.5	0.6	437.6	3605.0
R2	8.4	BDL	1009.2	1.2	2306.1	3952.8
T1	10.6	134.3	1658.0	2.0	3776.0	–
T2	39.2	BDL	387.8	0.5	889.3	–
1	9.6	BDL	2578.3	3.2	5894.9	774.4
2	10.5	21.8	4174.2	5.1	9303.9	7114.2
3	10.8	40.9	3755.8	4.6	8472.2	9318.3
4	11.0	11.8	5462.5	6.7	11918.8	9928.2
5	7.9	2.3	2953.1	3.6	5460.6	7480.6
6	9.4	3.2	3512.2	4.3	6839.2	9127.9
7	10.8	18.8	3337.1	4.1	7408.3	7871.2
8	10.0	3.2	4501.0	5.5	8745.1	8284.8
9	11.0	5.3	4613.5	5.7	9525.5	10656.7
10	10.1	3.5	5169.0	6.3	10169.0	2868.2
11	9.9	0.4	617.5	0.8	614.5	–
12	9.6	1.9	3335.0	4.1	5941.4	–
13	10.6	3.5	3847.6	4.7	7573.0	–
14	11.1	5.9	4857.8	6.0	10131.9	–

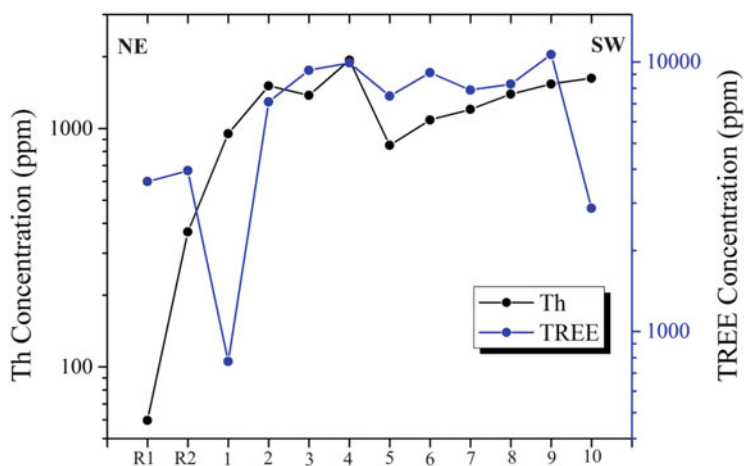
**Fig. 5.4** Comparison of the total rare earth element (TREE) and thorium concentration following a northeast–southwest trend along the study area

Table 5.2. The total rare earth element (TREE) concentration of the area varies between 774.4 and 10656.7 ppm with an average of 6748.5 ppm, which is almost 45 times higher than the crustal average (Fig. 5.4).

5.4 Discussion

The Th/U ratio variation along the study area from northeast to southwest shows an overall regular pattern apart from sample T2, which has been collected from adjacent Tampara lake (Fig. 5.2). Compared to the river placers, the beach sand samples show a higher variation of the Th/U ratio (Table 5.2). The area under study shows a conspicuous high concentration of ^{232}Th as compared to uranium. In nature, the occurrence of uranium usually happens in two states: U^{+4} and U^{+6} ; out of these two, the U^{+6} state is more sensitive and susceptible to leaching than the U^{+4} state. For thorium, it occurs in nature in only Th^{+4} state and it is not prone to leaching. Considering that the study area lies in close proximity to water bodies, it can be expected that the concentration of uranium will be low. The high Th/U ratio also entails a high concentration of the mineral monazite compared to zircon.

The beach area shows a high absorbed dose rate as evident from the values observed in Table 5.2. A correlation of the absorbed dose rate of the study area and the activity concentration of ^{232}Th shows a value close to unity, which indicates a positive correlation. This entails that the absorbed dose rate of the study area is mostly dependent upon the thorium concentration. Keeping this factor, along with the high Th/U and Th/K ratio in mind, it can be said that the placer deposit along the study area can be considered as thorium placers.

The TREE concentration along the study area as observed in Fig. 5.4 shows a lower value along the banks of the Rushikulya river. A comparatively high TREE concentration is observed along the beach areas (Fig. 5.4). A comparison between the TREE and ^{232}Th concentration of the study area as presented in Fig. 5.4 shows a good correlation. A high thorium concentration along the area indicates a high TREE concentration; this particular aspect can be utilized for on-field REE prospectivity studies based on thorium concentration. A good correlation between thorium and TREE also indicates that the REE concentration along the study area has been mostly derived from the mineral monazite (Palaparathi et al. 2017).

Based on the Th/U ratio and the TREE concentration, it can be said that the beach area shows an almost regular and homogeneous distribution of heavy minerals, which is a peculiarity along these beach areas on this part of the Indian subcontinent. Studies conducted in close vicinity of the study area exhibit a heterogeneous and patchy distribution of heavy minerals as indicated by their radioelement and REE concentration (Ghosal et al. 2017; Ghosal et al. 2020a, b). This peculiarity can be accredited to the almost confining presence of the various water bodies along the study area. The presence of the Rushikulya river mouth and the Tampara lake might be an important contributing factor behind the heavy mineral enrichment along the beach area. The presence of the mouth of the Rushikulya river ensures a constant supply of the heavy minerals, which, by the action of the longitudinal and transverse current, results in the deposition along the length of the beach. The presence of the Tampara lake acts as a natural barrier and mostly helps in arresting the heavy minerals along the beach profile. Hence, it can be said that by the joint effect of

the lacustrine environment and river mouth, the study area exhibits a high enrichment along with a regular and almost homogeneous distribution of heavy minerals.

5.5 Risk and Remediation

The consistent placer mining occurring toward the south-western part of the study area involves extensive dredging activities that disrupt the typical beach morphology. The mining activities disturb the natural berm-dune sequences, which act as a natural barrier preventing beach erosion. Additionally, the study area faces frequent storm surges (Sundar 2015); a disturbed beach area along the mine site will result in carrying of the heavy minerals toward inland. Considering the high thorium concentration and the high dose rate of the beach sand, this inland transportation is not a feasible outcome. These released heavy minerals when coming in contact with the natural water system can contaminate the said surface water, which can percolate and reach the subsurface water table, thereby contaminating the groundwater as well. Hence, it can be said that consistent mining activity can be detrimental and appears to be a risk to the environment. The threat is not only to the beach morphology but also to the local population and biota owing to the health hazard that is associated with radioelements. Moreover, mining along beach areas also has an immense impact on the habitat of marine organisms. The southern beach areas of Odisha, India are noted as a nesting ground for the Oliver ridley turtles (Pandav et al. 2006) and horseshoe crab habitation zone. Dredging activities along the beach areas affect the natural habitat of these organisms, which are sensitive to even minute changes within the biota. The Oliver ridley turtles prefer a specific grain size as their nesting ground similar to the horseshoe crabs, which usually dwell on sediment sizes ranging between 2.8 and 2.46 Φ (Chatterji and Abidi 1993). A minor deviation from these specific living conditions will result in the subsequent removal of these organisms elsewhere and consequently a decrease in the number of these rare marine species. Following the process of mobile mining can be a possible remediation to the problems faced by consistent dredging and mining (Sengupta and Ghosal 2017). Along with this, the plantation of local vegetation along the beach areas also helps in maintaining the beach morphology.

5.6 Conclusion

The radioelement and REE concentration of the study area shows a heavy mineral enrichment along the beach. The placer deposit shows a high Th/U ratio as compared to the crustal ratio. A positive correlation between the activity concentration of ^{232}Th and the absorbed dose rate indicates that thorium has the most dominant effect on the dose rate compared to uranium and potassium along the beach area. The beach area shows that a high thorium concentration is almost always accompanied by a high

TREE concentration, indicating that the thorium and TREE enrichment is an effect of the enrichment of the mineral monazite. The enrichment of heavy minerals along the study area and its almost regular and homogeneous distribution along the beach is indicative of an impact of the lacustrine environment and river mouth in close vicinity of the beach. The effects of consistent mining along the beach areas both on its morphology and biota have been discussed, and possible methods of remediation have also been listed.

Acknowledgments The authors thank the Science and Engineering Research Board (SERB), DST, Govt. of India, for the financial assistance received under the project Code: YSS/2015/000979.

References

- Anjos RM, Veiga R, Macario K, Carvalho C, Sanches N, Bastos J, Gomes PRS (2006) Radiometric analysis of quaternary deposits from the southeastern Brazilian coast. *Mar Geol* 229(1-2):29–43
- Balaram V (2019) Rare earth elements: a review of applications, occurrence, exploration, analysis, recycling, and environmental impact. *Geosci Front* 10:1285–1303
- Banerjee A, Chakrabarti R, Mandal S (2016) Geochemical anatomy of a Spheroidally weathered Diabase. *Chem Geol* 440:124–138
- Behera P (2003) Heavy minerals in Beach Sands of Gopalpur and Paradeep along Orissa coastline, East Coast of India. *Indian J Marine Sci* 32:172–174
- Chatterji A, Abidi SAH (1993) The Indian horse shoe crab- a living fossil. *J Indian Ocean Stud* 1:43–48
- Force ER, Rich FJ (1989) Geologic evolution of trail ridge Eolian heavy-mineral sand and underlying peat, northern Florida. US Geological Survey Professional Paper 1499:16
- Ghosal S, Agrahari S, Banerjee S, Chakrabarti R, Sengupta D (2020a) Geochemistry of the heavy Mineral Sands from the Garampeta to the Markandi beach, southern coast of Odisha, India: implications of high contents of REE and Radioelement's, attributed to placer monazite. *J Earth System Sci* 129:152
- Ghosal S, Agrahari S, Guin R, Sengupta D (2017) Implications of Modelled radioactivity measurements along coastal Odisha, eastern India for heavy mineral resources. *Estuar Coast Shelf Sci* 184:83–89
- Ghosal S, Singh A, Agrahari S, Sengupta D (2020b) Delineation of heavy mineral placer deposits by electrical resistivity and radiometric techniques along coastal Odisha, India. *Pure Appl Geophys*
- Mohanty AK, Sengupta D, Das SK, Saha SK, Van KV (2004) Natural radioactivity and radiation exposure in the high background area at Chhatrapur Beach placer deposit of Orissa, India. *J Environ Radioact* 75:15–33
- Mubarak F, Fayez-Hassan M, Mansour NA, Salah Ahmed T, Ali A (2017) Radiological investigation of high background radiation areas. *Sci Rep* 7:15223
- Orris GJ, Grauch RI (2002) Rare earth element mines, deposits, and occurrences: U.S. Geological Survey Open-File Report 02-189, version 1. Available at <http://pubs.usgs.gov/of/2002/of02-189/>
- Palaparthi J, Chakrabarti R, Banerjee S, Guin R, Ghosal S, Agrahari S, Sengupta D (2017) Economically viable rare earth element deposits along beach placers of Andhra Pradesh, eastern coast of India. *Arab J Geosci* 10:201
- Pandav B, Choudhury BC, Kar CS (2006) Sea turtle nesting habitats on the coast of Orissa. *Marine turtles of the Indian subcontinent* 1:88

- Papadopoulus A, Christofides G, Koroneos A, Hauzenberger C (2015) U, Th and REE content of heavy minerals from beach sand samples of Sithonia peninsula (northern Greece). *NeuesJahrbuchfürMineralogie-Abhandlungen (Journal Mineral Geochemistry)* 192(2):107–116
- Philander C, Rozendaal A (2015) Detrital zircon geochemistry and U–Pb geochronology as an indicator of provenance of the Namakwa Sands heavy mineral deposit, west coast of South Africa. *Sediment Geol* 328:1–16
- Ramasamy V, Sundarrajan M, Suresh G, Paramasivam K, Meenakshisundaram V (2014) Role of light and heavy minerals on natural radioactivity level of high background radiation area, Kerala, India. *Appl Radiat Isot* 85:1–10
- Rao NS, Sengupta D, Guin R, Saha SK (2009) Natural radioactivity measurements in beach sand along southern coast of Orissa. *Environ Earth Sci* 59(3):593–601
- Roy PS, Whitehouse J, Cowell PJ, Oakes G (2000) Mineral Sands occurrences in the Murray Basin, south-eastern Australia. *Econ Geol*:1107–1128
- Rozendaal A, Philander C (2000) Mineralogy of heavy mineral placers along the west coast of South Africa. In: Rammlmar D, Mederer J, Oberthür T, Heiman RB, Pentinghaus H (eds) *Applied mineralogy in research, economy, technology, ecology and culture. Proceedings of ICAM 2000, Göttingen*, pp 417–421
- Sarangi AK (2017) Uranium resource development and sustainability-Indian case study. In: Sengupta D, Agrahari S (eds) *Modelling Trends in Solid and Hazardous Waste Management*. Springer Nature, Singapore, pp 105–126
- Sengupta D, Ghosal S (2017) Environmental implications of Mining of Beach Placers for heavy minerals. *Fish & Ocean Opj* 2(3):OFOAJ.MS.ID.555588
- Sundar V (2015) *Ocean wave mechanics: applications in marine structures*. Wiley, New York
- Udarika RML, Udayakumara EPN, Amalan K, Ratnayake NP, Premasiri HMR (2016) Comparison of heavy mineral composition along Mahaweli River with placer deposits at North East Coast of Sri Lanka. In: *International symposium on agriculture and environment 2016*. University of Ruhuna, Sri Lanka
- UNSCEAR (2000) *Sources and effects of ionizing radiation*. United Nations Scientific Committee on the Effects of Atomic Radiation, New York
- Van Duong P, Tschurlovits M, Buchtela K, Quang Dien P (1996) Enrichment of radioactive materials in sand deposits of Vietnam as a result of mineral processing. *Environ Int* 22(1): S271–S274
- Van Gosen BS, Fey DL, Shah AK, Verplanck PL, Hoefen TM (2014) Deposit model for heavy-mineral sands in coastal environments. U.S. Geological Survey Scientific Investigations Report 2010–5070–L, 51 p. doi:<https://doi.org/10.3133/sir20105070L>

Chapter 6

Assessment on the Impact of Plastic-Contaminated Fertilizers on Agricultural Soil Health: A Case Study in Memari II C.D. Block, Purba Bardhaman, West Bengal, India



Piyush Maji and Biswaranjan Mistri

Abstract From the last few decades, many studies have focused on plastic pollution in the marine or lake environment, but pollution in the terrestrial environment, especially in agricultural lands, has largely been overlooked. In Memari II Block, Purba Bardhaman, West Bengal, it has been observed that farmers have applied plastic-enriched biofertilizers and sewage sludge water in their farmlands. The major objectives of the present work are quantifying the plastic additives in agricultural lands, identifying the amount of detected plastics with description, observing the possible sources of plastics, and its impact on agricultural soil health. Two different treatments have been observed for this analysis: plastic control clusters (28 grids) and contaminated clusters (28 grids). Averagely 4500 mg/Kg^{-1} soil has been quantified as macroplastic, while in the case of microplastic, averagely 430 mg/Kg^{-1} soil has been found. Low-density polyethylene (44.50%) is predominately higher in the fields. A total of 98 (61.25%) fields are mainly plastic-contaminated compost-based fields and the remaining 62 fields (38.75%) are sewage sludge-based fields. From the results, it is confirmed that plastic control fields are much more healthy than contaminated. Higher bulk density ($\text{pb} = 1.58 \text{ g/cm}^3$), low porosity (40.26%), comparably lower soil aggregation (36%), and declining microbial activities and respiration have been reported in contaminated clusters. In comparison with control clusters, the result shows ideal bulk density ($\text{pb} = 1.04$, as per USDA-NRCS), healthy soil porosity (60.61%), higher aggregation (48%), improving respiration, and active microbial activities. The work is concluded with some possible and indigenous ways to minimize this hazardous pollution in soils.

Keywords Agricultural soil health · Plastics · Control clusters · Contaminated clusters · Bulk density

P. Maji · B. Mistri (✉)

Department of Geography, The University of Burdwan, Burdwan., West Bengal, India

© Springer Nature Switzerland AG 2021

P. K. Shit et al. (eds.), *Spatial Modeling and Assessment of Environmental Contaminants*, Environmental Challenges and Solutions,

https://doi.org/10.1007/978-3-030-63422-3_6

6.1 Introduction

“Soil Health refers to the ecological equilibrium and the functionality of soil and its capacity to maintain a well-balanced ecosystem with high biodiversity above and below surface and productivity” (Cardoso et al. 2013a, b). According to the United States Department of Agriculture (USDA), soil health assessment is not only assessing the way soils function now but it also predicts how functions will be active in the future. Soil functions are ingrained capabilities of soil, include balancing of soil biota, transpiration of water and air within soil, cycling of necessary nutrients, productive soil health, etc. (Giannakis et al. 2017). In their book, Bhupinder Pal Singh et al. (2019) define soil health as a good combination of key properties of soils and mentioned that the major key components of soil are properties, process, and synergistic cooperation among them. Basically, soil health is determined through three major indicators of soil, viz. physical, chemical, and biological (Cardoso et al. 2013a, b). Soil health is quite similar to human health as well (Magdoff 2001). So, excessive practices and application of any kind of external materials into soil are harmful to agricultural soil and its functions (Kibblewhite et al. 2008; Rjaesh Aggarwal 2017). In recent times, plastic particles in agricultural soils are one of those kinds of external application intentionally or unintentionally. Nowadays, it is hard to find a place without plastic. Before the World War I (early 1920s), Bakelite was the first plastic material, although it was restricted within the military purposes only. However, after the World War II (after 1945), the growing of production was gigantic. After 1950s, the production was 2Mt and it jumped its rate at around 8.4% annually and eventually reached 380Mt. in 2015 (Geyer et al. 2017). In the year 2018, a fascinating study by the University of California and Santa Barbara and others has estimated that since 1950s nearly about 8.3bmt. of plastics have been produced in the world. Among which, 6.3bmt (76%) of plastic left as waste, nearly about 9% of it has been recycled, 12% of waste has been incinerated, and rest 79% of plastics have been gathered in landfills, which affect the terrestrial environment, ocean, and water bodies (Narain 2018). In case of India, an estimated study was conducted by the Central Pollution Control Board (CPCB). Based on 60 major cities of India, data have been confirmed that averagely 4059.18 tonnes of plastic waste have been generated per day, almost 6.92% of its share in municipal solid waste. On average, daily 11 kg of plastic has been consumption by an Indian (Venkatesh et al. 2018) and estimating to almost double to 44 pounds (20 kg) by 2022 (Agarwal, director of New Delhi based environmental group, 2018). The term plastic was derived from the Greek word *plastikos*, which means “capable of being shaped or molded” (<https://en.wikipedia.org/wiki/Plastic>, retrieved on 15th May, 2020). Plastic products are usually made of with various hazardous chemical bonding such as ethylene, propylene, polymer or hydrocarbon, etc. (Geyer et al. 2017). From the last some decades, many studies have focused on how plastic pollutes the marine (He et al. 2018; Duckett and Repaci 2015), lake environment (Sruthy and Ramasamy 2017), or other freshwater (Wagner et al. 2014), but its impact on terrestrial environment, especially in agricultural lands, has largely been overlooked.

Similarly, a handful of studies have been reported in the problem and management of plastic in the rural environment. According to previous studies, major sources of plastics in agricultural soils are plastic-contaminated organic fertilizers (Weithmann et al. 2018), sludge water (Corradini et al. 2019), surface water (Sighicelli et al. 2018), plastic mulching (Qi et al. 2018), and other various immeasurable sources. In the study area, Memari II Block, consisting of nine Gram Panchayats, villagers have mostly been using plastic bags as a carrier of grocery products from local shop or nearby market. Averagely the daily wastes of plastics per household have been recorded at about 5 gm. The major source of plastic wastes came from local shops (52%). Various ways of utilization of plastic products had never been a problem, but the wastes were generated after it is used, considering as harmful and hazardous for the environment and human health as well. Here, most of the garbage is plastic-contaminated and eventually all are lasted in agricultural lands, because, according to cultivators, garbages are enriched with organic fertilizers, which are helpful for good soil health and productivity as well. But after observation and detection, it has been recorded that a pile of plastics are mixing with agricultural soils; eventually, all are stuck on the plow layer (soil depth up to 7 inch) and the lower surface of soil. Some studies have revealed that plastic in soils is a major problem because it changes the various soil properties internally (Dhayagode et al. 2011; Wang et al. 2019), which are invisible until one tests it. Soil bulk density is one of the physical properties of soil, which indicates the compaction of soil (USDA-NRCS), meaning how far or close the particles are accumulated in soil and it also correlated with many physical, chemical, and biological properties of soil (Al-Shammary et al. 2018). These synthetic particles have influences on soil properties and eventually declination of soil fertility. For long-term perspective, if this issue has not been stopped now, then it will also be a reason for decreasing of crop production.

The present study mainly emphasizes quantifying plastic particles, divides the counted plastic categorically, identifies the potential pathways of plastic additives in agricultural farmlands and, most importantly, the impact of plastic additives on biophysical properties of soil, and also addresses the soil health condition in plastic-contaminated fields.

6.2 Materials and Methods

To understand the impact of plastics on soil bulk density and other properties of soil, there are some important methods, which need to be known and applied. Adaptive cluster sampling (after Thompson 1996) method has been applied to identify the plastics-contaminated agricultural lands properly. In this method, at first, a total of 110 edge grids have been selected randomly. After randomly selected initial units (grids have plastics), the surrounding grids have been checked to observe the problems, and this process has been stopped until the particular grid has found plastic-free. Edge unit means the grids which have the problem but surrounding grids are free from plastics. In that way, finally 58 grids with 10 clusters (Fig. 6.1),

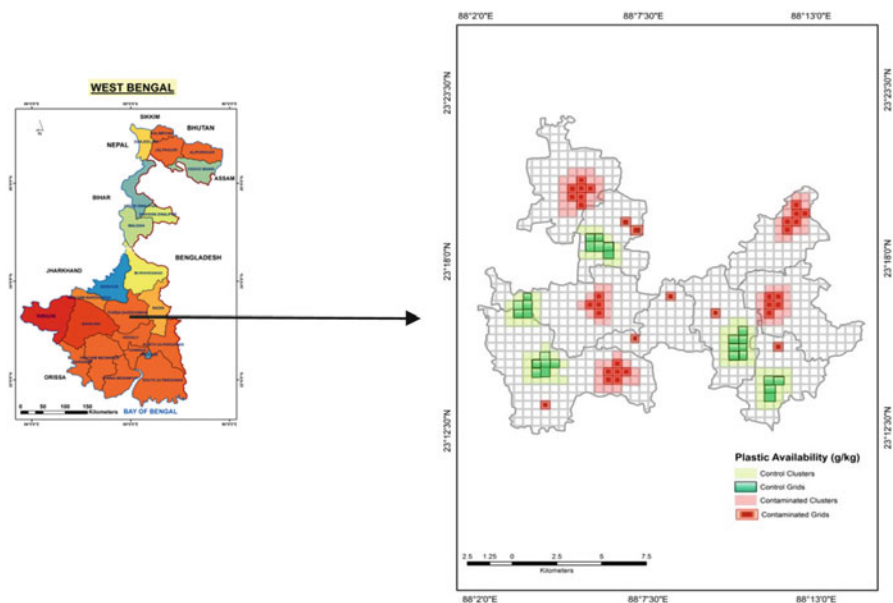


Fig. 6.1 Selected plastic control grids (green) and contamination grids (red) followed by adaptive clusters sampling

including five controls (do not have any plastics) and five contaminated (have problems of plastics) clusters, have been selected to proceed for further analytical part.

All the clusters in green color are control grids, meaning there is no problem of plastics. The purple clusters are representing contaminated lands; there have been found various plastics particles. It is not so easy to measure or quantify the amount of plastics particles in agricultural soils, as very few are visible on the upper surface of the land, and most of the plastics remain within plow (upto 7 inch) and compact layer (7-10 inch) of the soil. On the basis of the size of the plastic, it is divided into four, macro (>25 mm), meso (5-25 mm), micro (1-5 mm), and nano plastic (<1 mm) (Imhof et al. 2017). Microplastics are the smallest plastic pieces with a size of less than 5 mm (Seijo et al. 2019), while in the case of macroplastic, the sizes increase to >25 mm (Imhof et al. 2017). Micro or macroplastic could be differed in shape and length wise. To detect the macroplastics (>25 mm), visual detection and separation and multi-tier sieving (25 mm) methods have been used. To quantify the microplastic, first of all multi-tier sieving (1-5 mm) has been applied to separate the microplastic from other sizes of plastic, and then the density separation method has been applied. To complete the method, saturated NaCl 1.2 g/cm^{-3} density solution (Crawford and Quinn 2017) has been applied. NaCl 1.2 g/cm^{-3} has been selected because most of the plastic materials (polypropylene, polystyrene, polypropylene, polyethylene terephthalate, and polystyrene, etc.) are less dense than the

Fig. 6.2 Density separation method (source: Crawford and Quinn 2017)

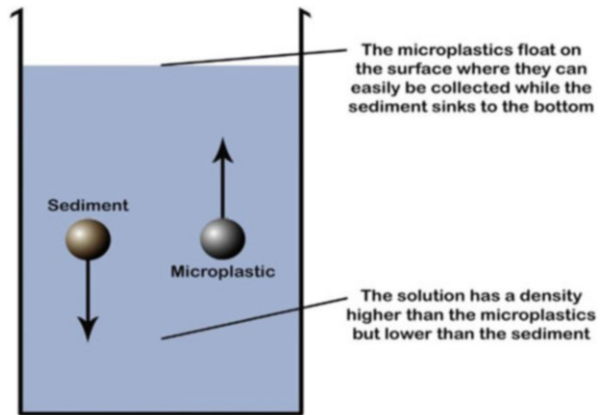
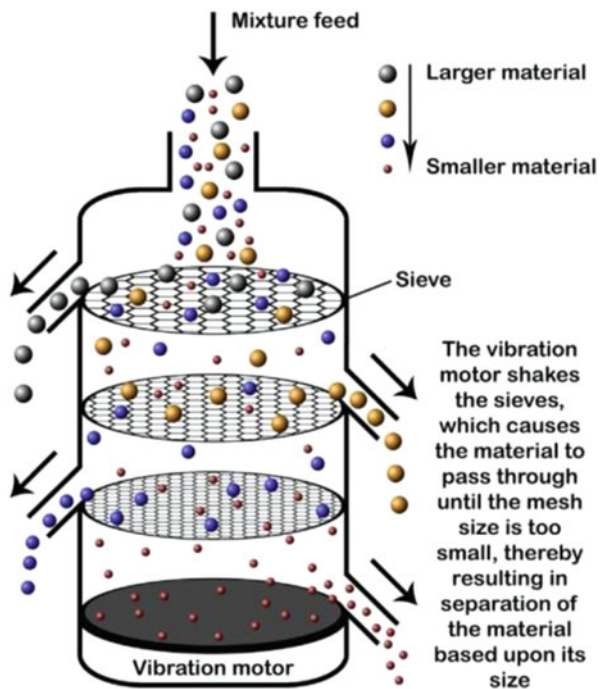


Fig. 6.3 Multi-tier sieving method (source: Crawford and Quinn 2017)



solution apart from polyvinyl chloride (PVC) and PVC is hardly found in soil. So this solution is suitable for separation of microplastics. Core cutter method has been employed to quantify soil dry bulk density. The width and height of the cutter ring were 4.50 cm and 7.80 cm, respectively. The calculation has been followed by the procedure given by USDA-NRCS. The pore spaces filled with water, water content of soil, soil porosity, and soil aggregate stability, all are determined through the procedure of USDA-NRCS (Figs. 6.2 and 6.3).

6.3 Results and Discussion

The correlation with soil texture, bulk density gets fluctuated with major textural classes of soil (Tanveera et al. 2016). Apart from soil texture, plant root growth (USDA-NRCS), water (Yang and Jong 1971), or air holding capacities are also dependent on soil bulk density. To determine the bulk density, one must to know about the textural classes of the soil because after USDA-NRCS, each and every textural group has some ideal bulk density value. If the bulk density (pb) value becomes exceed with its corresponding textural class extremely, then there must be some problem. USDA defines agricultural system as a scientific phenomenon. Nowadays, agro-scientists are more talking and spreading about the information of sustainable agriculture. Sustainable agriculture includes not only increasing production but also it is more focusing on maintaining or balancing the soil health condition (Tuğrul 2019). Various unscientific agricultural practices cause declination of soil health, which means unawareness about the practices acting as a reason for modification of various soil properties in a negative way. (Chakraborty and Mistri 2015).

6.3.1 *Measurement of the Amount of Plastic Additives in Agricultural Lands*

It has been observed that among the total 28 grids, averagely 4500 mg/kg^{-1} soil quantified as macroplastics with highest plastics grid of 6400 mg/kg^{-1} in Bohar-I GP. After quantification of microplastics, it has been identified that microplastics averagely 430 mg/kg^{-1} soil are found. Among the total nine GPs, Bohar II stands at first in the case of microplastics with 840 mg/kg^{-1} . These fields have been considered as contaminated sites. However, there are some fields with plastic-free and leveled as control sites. For example, GPs like Barapalashan II, Satgachia I, Satgachia II, and Northern and middle portion of Kuchut are in control sites. So counted plastics particles are so diversified in shape, size, and nature. Apart from high-density polyethylene (HDPE), all the other type of plastic particles are majorly distributed.

6.3.2 *Categorically Description of Detected Plastic Additives*

In the year 1988, the Society of Plastic Industry (PSI) standardized the plastic products and its associated products with some code to understand about it is recyclable or not. On the basis of that standard products and their density are interlinked to observe and identify the plastic items. There are so many plastic items have been identified, maximum are household- used plastic products. After laboratory separation and detection, it has been confirmed that 44.50% items are

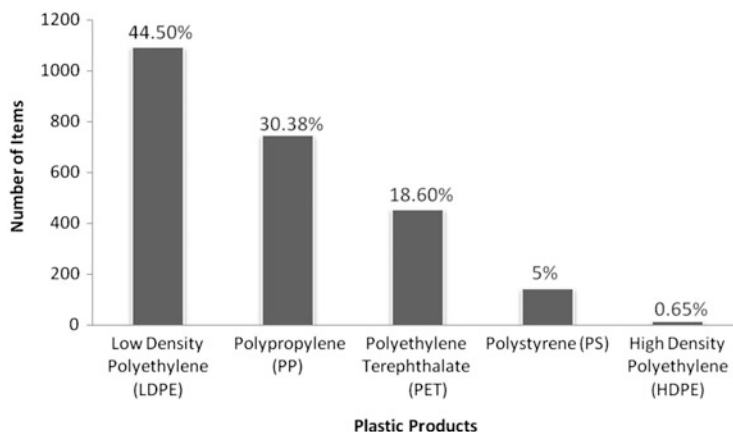


Fig. 6.4 Major plastics items with their particular names and amount in percent

low-density polyethylene (LDPE). These kinds of plastic items are mostly daily and single used, for example, plastic carry bags or plastic bottles. A total of 1095 items have been found throughout the block, which are tremendously high. LDPE is followed by polypropylene (PP) with 748 items (30.38%). These plastic products are being used as wrapper for the food, and all are single-used like chocolate wrapper, chips packets, etc. These products are relatively a little denser than LDPE. Polyethylene terephthalate (PET) is the product of plastics, and it has been seen that with 458 (18.60%) items, it stands third position (Fig. 6.4).

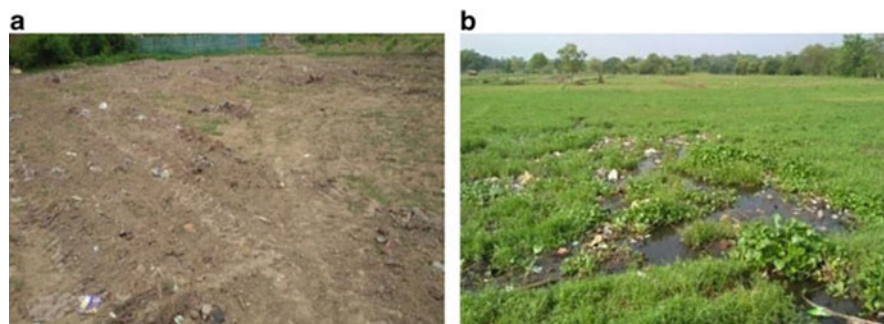
Last but not the least polystyrene (PS) comes forth position among four major plastics with 145 (5%) items. These plastics are rarely used in rural area but still some items like micro parts of coffee cups, plastic boxes have been found. In the rural environment, hardly we can find hard plastics, though a total of 16 (0.65%) items have been found to be high-density polyethylene (HDPE). Items are hard plastics, and all are detected visually. Items are compost, broken, and remaining parts mostly found below the plow layer of soil. Among all plastic materials, low-density polyethylene (LDPE) is most dangerous one, LDPE acts as carrier of various chemical including hazardous pesticides (Seijo et al. 2019) and it also takes much time to degrade fully in soil (Das and Kumar 2015) (Table 6.1 and Fig. 6.5).

6.3.3 Major Sources of Plastics in Agricultural Lands

If averagely at about 5 gm daily plastics have generated, then it becomes monthly 150 gm, which is huge in mass. After conversation with the villagers especially who are farmers, it came to know that this huge amount of plastics usually remained as pile of plastics in the dumping ground which mainly used as compost site. Farmers apply this compost as biofertilizer in the lands for betterment of the soil health, but

Table 6.1 Sources and description of major types of plastic additives

Major Plastic Products	Sources	Number of Items	Household Uses
1. Low-density polyethylene (LDPE).	Carry bags, squeezable bottles, etc.	1095	Primarily low-density plastics, mostly used to carry items, all are single-use plastics.
2. Polypropylene (PP).	Chips packets, biscuits wrappers, straw, fabric, etc.	748	Denser than LDPE plastics, mostly used to carry items, all are single-use plastics.
3. Polyethylene terephthalate (PET).	Clothing fibers, rope, fibers, jar, etc.	458	Used as a container of beverage or other goods.
4. Polystyrene (PS).	Coffee cup, food boxes, etc.	145	All are medium dense plastics, used as food keeper.
5. High-density polyethylene (HDPE).	Compost containers, bin, pipes, etc.	16	All are hard in density, various kind of use, but less

**Fig. 6.5** (a) Residues of plastics in agricultural lands biofertilizers act; (b) Sewage sludge water, carrier of plastic in agricultural soil

plastics-mixed fertilizers are equally harmful for soil. It is a way to drag the plastic into the agricultural lands. Apart from compost, organic-enriched, sewage sludge water is useful for crop production but sewage sludge water is equally responsible for dragging the plastics into the farmlands. (Bläsing and Amelung 2018).

Many studies have been shown that one of the major sources of macro to microplastics in agricultural fields are biofertilizer (Anikwe and Nwobodo 2002; Atuanya et al. 2012) and sewage sludge water (Mikola et al. 2016; Piehl et al. 2018). After detail questioning with 160 farmers and observation of their fields all along the nine GPs, it is reported (Fig. 6.6) that 98 (61.25%) fields are mainly plastics-contaminated compost-based. The major conveyer of plastic materials in these 98 fields is biofertilizer, while remaining 62 fields (38.75%) are mainly sewage sludge-based fields. Major conveyers of these fields are sludge water. Due to lack of proper techniques, some other sources are remained immeasurable, for example

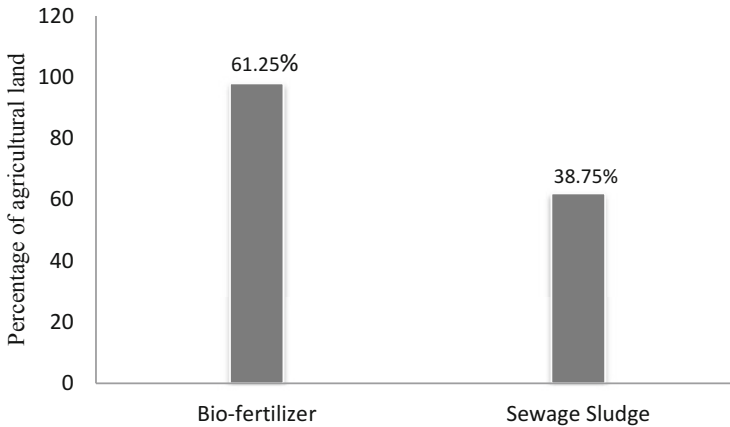


Fig. 6.6 Major conveyers of plastics in agricultural lands in Memari II Block

wind conveys micro to macroplastic in everywhere. Some canals are also dragged the plastics into the agricultural lands but these are limitation in the case of measuring the sources of plastics in agricultural fields. It has been observed that seasonally, numbers of plastics items have been fluctuated. According to the cultivators, during rainy season, it is always being a problem of plastics, as the drains are fully packed with plastics and food items. But the plastics- contaminated fertilizers are always being used in lands, so the major source of plastics is bio fertilizer.

6.3.4 Soil Properties

Total 58 grids (including 10 clusters) are showing the textual class of clay loam (Sand 20-45%, Silt 15-53%, Clay 27-40%). From the data it is confirmed that the major particles of soils are more or less equally distributed. Clay loam is good for agriculture especially for those crops which are grown on wet soil, because water holding capacity is much higher in this textual class. In the case of dry bulk density, average density has been recorded in contaminated clusters is 1.58 g/cm^3 . While in the case of control clusters, it is 1.04 g/cm^3 . So there is 0.54 g/cm^3 gap between two zones.

Bulk density has pretty much influenced on porosity of soil, after calculating the soil porosity it is confirmed that there is also a gap between two zones, contaminated and control, recorded as 40.26% and 60.61%, respectively. Pore space filled with water condition is also varying from contaminated (38.77%) and control clusters (56.10%). In the case of soil respiration and microbial activities, the result shows that it is highly fluctuated in two different treatments. After comparison between two sites with an ideal graph, in contaminated clusters, it has been seen that respiration

and microbial activities are lower in compare to control cluster. Soil aggregate stability is another most important physical property to determine the soil internal health. To understand the impact of plastic on Soil aggregate Stability (SAS), three different treatments fields have been selected, viz. bare fields, control fields, and contaminated fields. The results have revealed a clear difference among three treatments, bare soil (32%), control fields (48%), and contaminated fields (36%). So, control fields are more aggregated compare to others two fields.

6.4 Risk Assessment and Remediation

USDA-NRCS has given a list, which shows the standard relationship between soil texture and soil bulk density. The results have been compared with that standard chart and observed some significant differences between two zones, i.e., control and contaminated.

The Table 6.2 shows that each and every textual class have particular bulk density, which is treated as ideal for root growth, and which also indicates the

Table 6.2 General relationship of soil bulk density to root growth and soil health based on soil texture

Soil texture	Ideal bulk density for plant growth (grams/cm ³)/ Good Soil Health	Bulk density that affects root growth (grams/cm ³)/affects Soil Health	Bulk density that restricts root growth (grams/cm ³)/Indicated Pollution and Highly Affects Soil Health
Sand, loamy sand	<1.60	1.69	>1.80
Sandy loam, loam	<1.40	1.63	>1.80
Sandy clay loam, clay loam	<1.40	1.60	>1.75
Silt, silt loam	<1.40	1.60	>1.75
Silt loam, silty clay loam	<1.40	1.55	>1.65
Sandy clay, silty clay, clay loam	<1.10	1.49	>1.58
Clay (>45 percent clay)	<1.10	1.39	>1.47

USDA-NRCS, 2020

good soil health condition. In the case of clay loam textual class, the ideal bulk density of soil should be $<1.10 \text{ g/cm}^3$, the bulk density of soil is 1.49 g/cm^3 , indicating affected growth of plant root and if it is exceeding the value 1.58 g/cm^3 that is mean highly affecting the root growth and polluted soil or some problems are there in the soils. Good soil health means balanced infiltration and air transpiration, productive in nature, and others properties should be maintained in a balance way.

6.4.1 Assessing the Correlation between Plastic Additives and Bulk Density

The result of coefficient of correlation (Fig. 6.7) shows that the relation of plastic additives in soils and dry bulk density (BD) is highly positive and it is also confirmed that in control clusters all the values of bulk density have been analyzed under the ideal line which is 1.10, where all the values of bulk density in contaminated clusters are beyond the ideal value. That is mean pollution is there and soil is not indicating as good as in control clusters. The highest plastic-concentrated grid has been found in Bohar I GP (6200 mg/kg^{-1} soil). Through the questionnaire survey, it is confirmed that farmers like to apply a lot of compost in their farms, according to the farmers they do not want to waste their time to separate the piles of plastic because it is hard to separate plastic additives from compost, these are always there in the dumping sites. These kinds of neglected attitudes are reflected on this graph. On the others side, GPs like Barapalashan II, Satgachia I, Satgachia II, and some parts of Kuchhut have been observed on less number of plastics in soil. According to a farmer in Kucchut, “we apply compost fertilizer, which we made in separate place but we do not apply the compost fertilizers in dumping site because dumping site consists of a lot of hazadous materials sometimes glasses as well, so we avoid that site.” Whatever the reason they mentioned, but the real thing is that they have applied totally pure biological fertilizer, it consists of only cow dung and animals’ excreta. From the graph (Fig. 6.7), it helps to confirm their opinion or attitude, excessive plastics in soil affect the soil health internally, it is mostly long-term, so we

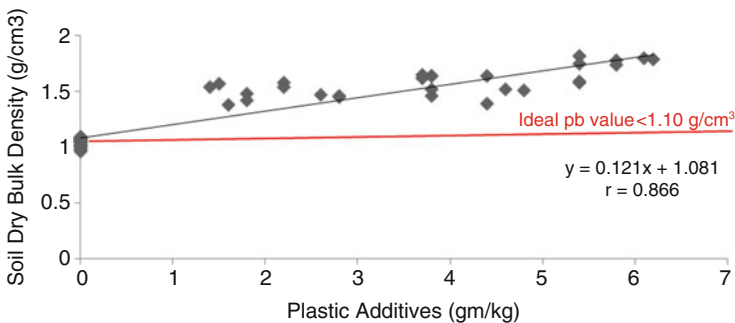


Fig. 6.7 Correlation between plastic additives and soil bulk density

hardly can be aware about this problem but in future it will definitely a problem for farm and farmers as well.

6.4.2 Plastic Additives and Soil Porosity

Soil porosity is the pore spaces between the soil particles; it mostly depends on bulk density of soil. Because highly compacted soil generally showing low porosity. Two different clusters, plastics-free clusters and plastic-contaminated clusters, have been surveyed. After collecting the soil samples and determining the dry BD, soil porosity has been calculated for both the clusters and some surprising facts have come out. The average soil porosity in control clusters is 60.61%, while in the case of contaminated clusters it is 40.26%. So, averagely more than 20% gap between control and contaminated clusters. Due to low porosity, it is hard to penetrate the water or even for air, it is going to be tough to circulate. From the graph (Fig. 6.8), it is clearly showed that if there are plastic additives in soil that means it makes soil more compacted. Because macroplastics break into thousands of microplastics, which easily get stuck on the pore spaces of soil and decline the soil health. The broken particles act as a barrier for water and air transpiration. From the diagram (Fig. 6.9), it is confirmed that plastics decline the soil pore spaces and create a major problem within soil. To know this fact deeply, soil water content and pore spaces filled with water condition for both the clusters have been quantify and understand that how plastic in soil differs in soil health. Plastic-contaminated clusters are only taken in this graph to know the relationship between soil porosity and plastic additives in agricultural lands. The results revealed that the relation is negative. Thus it can state that, plastic additives, present in soil, reduce the soil porosity.

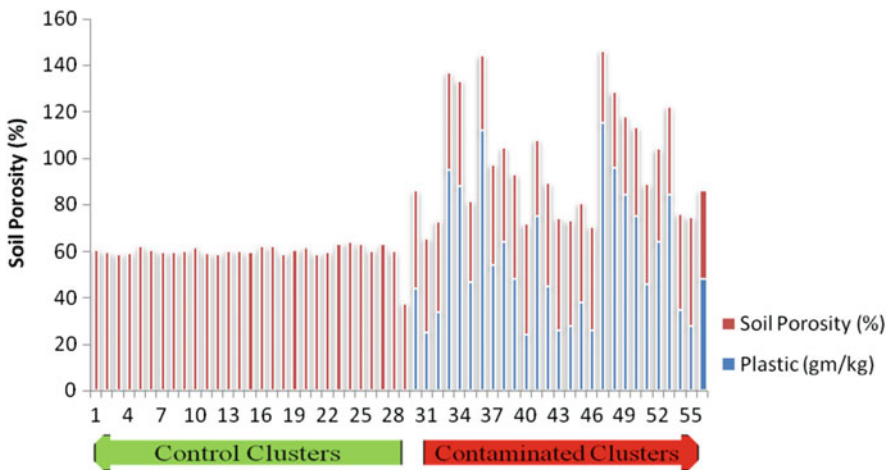


Fig. 6.8 Comparison of soil porosity (%) between control and contaminated clusters

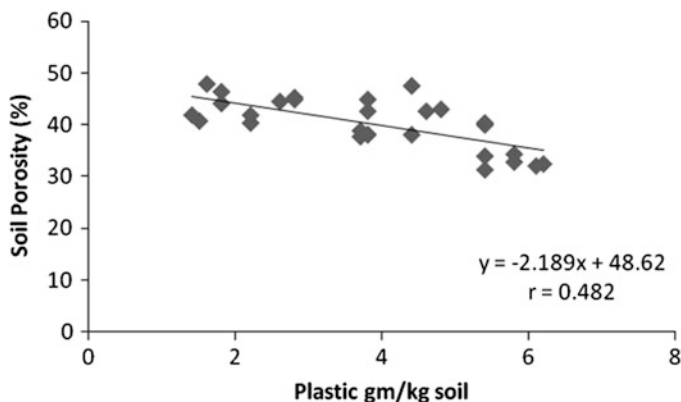


Fig. 6.9 Relation between plastic additives and soil porosity in plastic-contaminated clusters

6.4.3 Impact of Plastic on Soil Water Content and Pore Spaces Filled with Water of Agricultural Soils

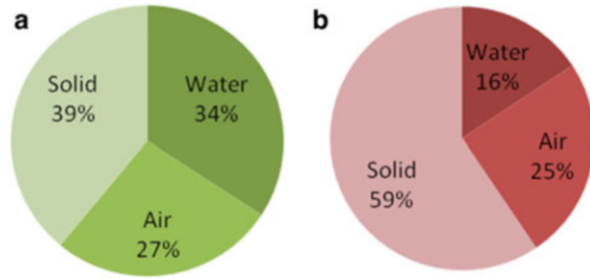
USDA-NRCS procedure has been applied to calculate the water content in soil. Where, soil water content means the difference of the weight between wet soil and oven dry soil. While this value has been used to calculate the pore spaces filled with water percentage, which shows the water condition within the soil pore spaces (Table 6.3), which is also indicating the condition for soil health is going to tough or not. The procedure has been applied for both the clusters, i.e., control and contaminated. And the average results have been reported that in the case of control clusters, the average water content value is $0.34 \text{ (g/cm}^3\text{)}$. After applying the value to calculate the percentage of pore spaces filled water, it shows 56.10%, which is inciting a good water holding and water infiltrated condition.

In the case of contaminated clusters, the average value for water content is $0.34 \text{ (g/cm}^3\text{)}$ and pore spaces filled with water percentage are 38.77% which is indicating hard condition for water transpiration. The difference between the two is almost 20%, so from this value it is again proved that plastic additives reduce the percentage of pore space filled with water condition.

Table 6.3 Calculation table for pore space filled with water condition for both the clusters

Sample site	Water content (grams/cm ³)	Soil porosity	Calculation: (water content ÷ soil porosity) x 100	Percent of pore space filled with water
Control	0.342	0.61	$(0.342 \text{ g/cm}^3 \div 0.610) \times 100$	56.10
Contaminated	0.157	0.40	$(0.157 \text{ g/cm}^3 \div 0.405) \times 100$	38.77

Fig. 6.10 (a and b)
Distribution of major soil ingredients for control fields (left) and contaminated fields (right)



The two circles (Fig. 6.10 a and b) show that in the case of contaminated clusters total pore spaces are 40% and among which 38.77% spaces water filled and remaining 61.23% spaces filled with air. The soil is composed of solid, water, and air. After converting the value within 100%, the following values have been calculated as solid (59.5%), water (15.7%), and air (24.8%). In control clusters, the total pore spaces is 61% among which 56.10% spaces filled with water and the remaining 43.9% spaces filled with air. After converting the values into 100%, it has been shown that the total solid percentage in the control cluster is 39%, water has 34.2%, and 26.9% distribution of air.

6.4.4 Impact of Plastic on Soil Aggregate Stability

Aggregate stability of soil measures the aggregation power of soil against flowing water (USDA-NRCS). It determines how the accumulated soil particles attached with one another. Higher proportion of organic matter in soil indicates fine soil aggregate stability (SAS); because organic microparticles are biological ingredients and it help to stick the soil properly. The organic matter is easily degradable as it easily mixes with the soil. But in soil, some artificial or synthetic materials are equally hazardous. The artificial materials like plastic additives are not degraded with soil. It just stuck on soil for a long time. In the case of aggregate stability, the plastics particles disintegrate the soil easily and when water is flowing over the soil, it gets break due to this disintegration. To compare the aggregate stability of plastic-contaminated fields, total three different zones have been selected, i.e., bare fields, plastic-free compost-based fields, plastic-contaminated compost-based fields. After Bronick and Lal (2005), there are various factors are responsible for modification of soil aggregation and one of the important factors is anthropogenic perturbation. Anthropogenic factors are mostly external factors; here the very important one is application like application of fertilizers, water or tillage system. Sometimes people do not become aware or even think before applying. Like everything, soil has its limitation to take external aspects, excessive application of fertilizers, tillage, or water affecting the soil biophysical properties. Likewise, applications of the hazardous materials are equally effective for changes of various soil properties. SAS is one

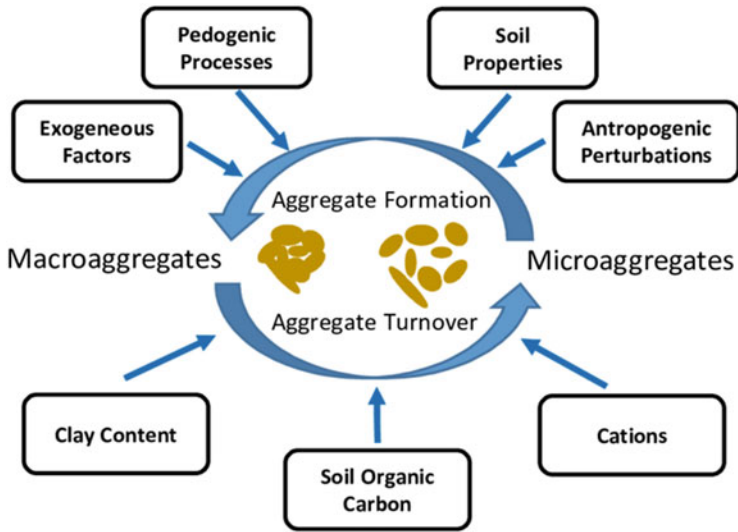


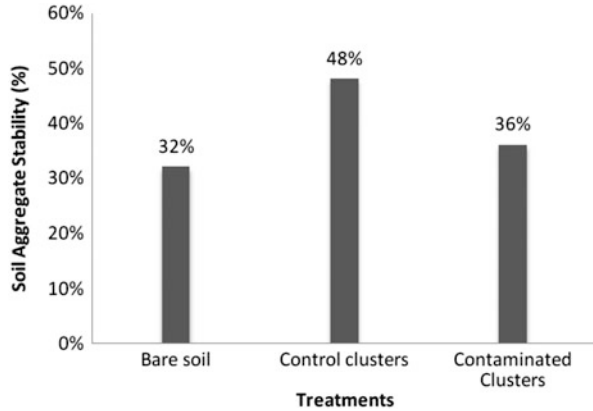
Fig. 6.11 Comparison of soil aggregate stability between three different fields

of the major physical properties, which actually depends on the ingredients materials of soil. To know the actuality of aggregate stability in contaminated clusters, three different treatment fields have been selected, i.e., (i) bare soil, (ii) control clusters, and (iii) Contaminated clusters. The first one is nonagricultural fellow lands, where agricultural activities have been inactive for a long time and it just remain as fellow lands. So the percentage of organic matter is low (32%) in the case of bare soil. The control clusters are compost-based agricultural fields, and most importantly, these all are plastic-free compost fertilizers. So it is purely natural and organic enriched. The last one is plastic-enriched biofertilizers fields, where farmers apply compost fertilizers but it enriched with plastic additives. After observation, detection and questionnaire survey, total 150 fields have been identified as bare fields (50 fields), control fields (50 fields), and contaminated fields (50 fields) (Fig. 6.11).

To quantify the aggregate stability of soil, USDA-NRCS procedure has been applied. After applying the method on three different treatment fields, average data have been put on the diagram (Fig. 6.12). From the diagram, it is clearly showed that the average SAS differs from each treatments, it was 32% in bare soil, 36% in contaminated clusters, and 48% in control clusters.

From the data, it has been confirmed that organic-based fertilizers have better SAS, while in the case of farms cultivated with plastic-enriched fertilizers, the average SAS has been reported below the control clusters. The conclusion is that plastics do impact on SAS. It reduces the aggregates so that soil easily breaks down and declines soil health.

Fig. 6.12 Comparison of soil aggregate stability between three different fields



6.4.5 Compare the Result with Soil Respiration and Microbial Activities

Soil pore spaces control the various properties of soil, among which soil respiration is one of the major one. Soil respiration defines as the releasing of CO₂ percentage from the soil. Various technologies have been used to quantify the respiration. But this portion is just comparing the result of pore spaces of soil with soil respiration. Soil respiration is a biological indicator of soil that is why a lot of biological activities are totally depending on it. Microbial activities are one of the most important one. Basically low pore spaces indicating low transpiration and decline of microbial activities. A diagram (Fig. 6.13) was prepared by Linn and Doran (1984). This diagram is showing some standard relations with water-filled pore spaces. This standard diagram shows that soil respiration is being considered as good, if the pore spaces filled with water condition lie nearly about 60%. In the case of microbial activities, it stands at top when water-filled pore spaces value is 60%. Before and after the 60%, the values are going to decline in the case of soil respiration and microbial activities. So, from the acquired data, it has been observed that in control clusters, the water-filled pore spaces 56.10%, which is indicating good soil respiration and relative microbial activities. It also means the air gets space to transpire and microbial activities are running so comfortably. It is indicating healthy soil. While, in the case of contaminated clusters, the water-filled pore spaces value is 38.77%, which is very low, the respiration line showing problem in soil and the value of microbial activities is below 0.6, which is not good for microbes in soil.

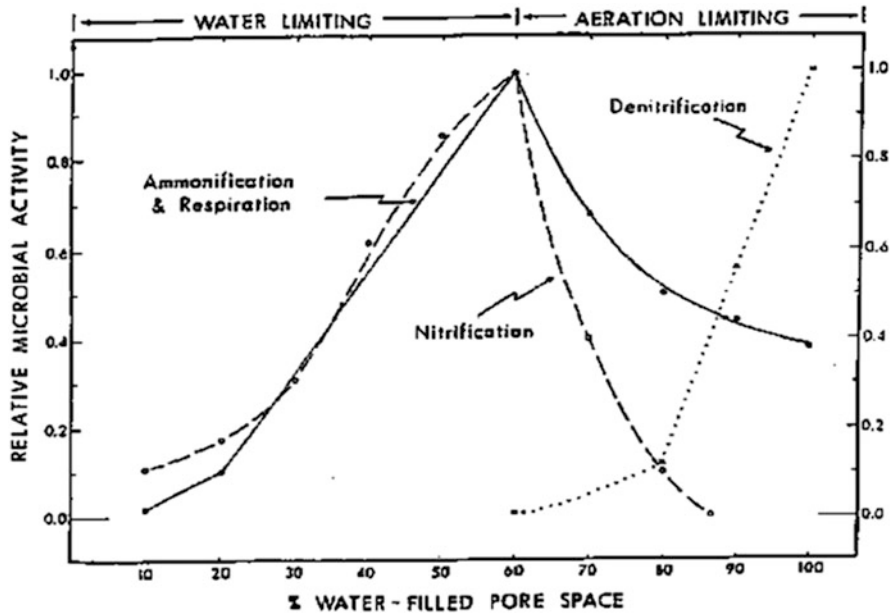


Fig. 6.13 Soil respiration and microbial activity as related to soil water-filled pore space. The diagram was prepared by Linn and Doran (1984)

6.4.6 *Plastics and pH*

In the case of control clusters, average pH value has measured as 6.05, while in contaminated clusters it is 6.50. Therefore, there is no significant difference in pH values of both. Both the sites represent slightly acidic soil. So the study has concluded that plastic hardly influences the soil pH.

6.4.7 *Consciousness of the Farmers about the Influences of Plastics on Soil Health*

After conversation among the people, it has been revealed that people do not care about the plastic, as they throw the plastics to anywhere. Apart from some hard plastic products (Plastic bottle, jar, pipe, etc.), more of the plastics (82%) are single-used like plastic carry bags. So, maximum mass of the plastic products last as waste. In villages, farmers like to use the waste materials as a biofertilizer and eventually plastic-enriched fertilizer remains within the agricultural soil. With the passage of time, it breaks its biochemical bonds and releases various hazardous materials like hydrocarbon, benzene, etc. (Hahladakis et al. 2018). All are harmful for the agricultural soil health. Questionnaire survey (Fig. 6.14) has revealed that only 22.44%

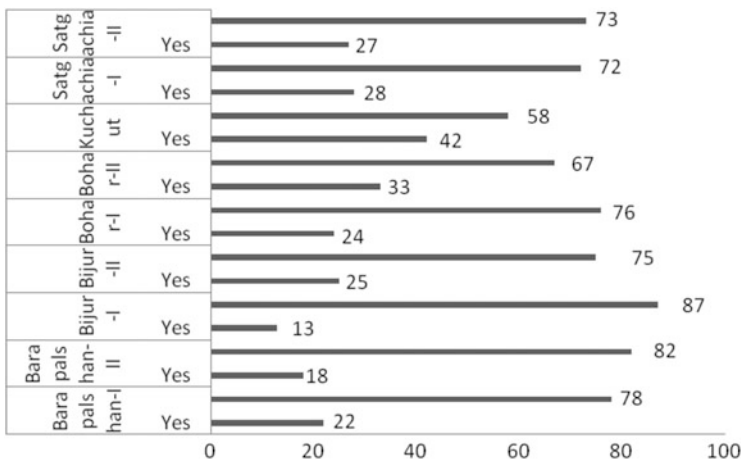


Fig. 6.14 Gram Panchayat-wise responses of awareness about influences of plastic on soil health

farmers are truly aware about plastic pollution and its hazardous effects on soil health, so a huge mass of people (77.56%) of the block even do not know is it harmful or not. Some farmers are thought plastics act as fertilizers stating that chemicals are mixed through these products. They do not think about separation of plastics particles from compost. Some farmers told that it is hard to separate the microplastics, these are always there in the compost. So they just avoid that, while in the case of macro, they like to separate by hand which are visual to them. So, the overall awareness about plastics and its harmful impact on soil are miserable here.

6.5 Remediation

Separation of plastic films from soil needs hard work, numurous labors, specific skills, tools, and technology as well, but there are some inidgenous management procedureds which are possible way to avoid plastic additives in soil. Nowadays with the hands of various countries, India has taken this problem very seriously and find a way to manage it, but the problem of unawareness and unwillingness disrupts this purposive solution. People, especially in rural areas, are mostly uneducated and unawareness about the impact of this hazardous materials. Some remediation procedureds have been suggested here referencing with numurous analysis and process.

6.5.1 Biodegradable Plastics

Biodegradable plastics are basically made with natural materials which all are easily degraded in soil. There are many countries and even some states of India already have taken this initiative to develop and use of biodegradable plastic bags and other products. Hrenovic et al. 2004 have conducted an experiment on weight loss of two synthetic and one natural plastic with a time period. After heat experiment, high-density polyethylene (HDPE) and low-density polyethylene (LDPE) particles had lost their 1.3% and 2.1% weight within 4 weeks, respectively. In the case of Naturegrad Plus (NP), a biodegradable plastic, it had lost almost 16% weight within same time period (Fig. 6.14). So, the experiment has indicated that biodegradable plastics are more ecofriendly than nondegradable synthetic plastics. The central government has to work on it, like some states are trying to made biodegradable plastics (Fig. 6.15).

6.5.2 Alternative Materials

Biodegradable bags or materials must be used as an alternative of nonbiodegradable plastic. So, the government should be more focused on making the process of biodegradable materials like jute bags, paper bags, degradable fibers, etc. This initiative must be developed if the government concentrates on jute, paper, and other plastic alternative industries. And, along with these, the government should take a strict law or totally ban plastic production.

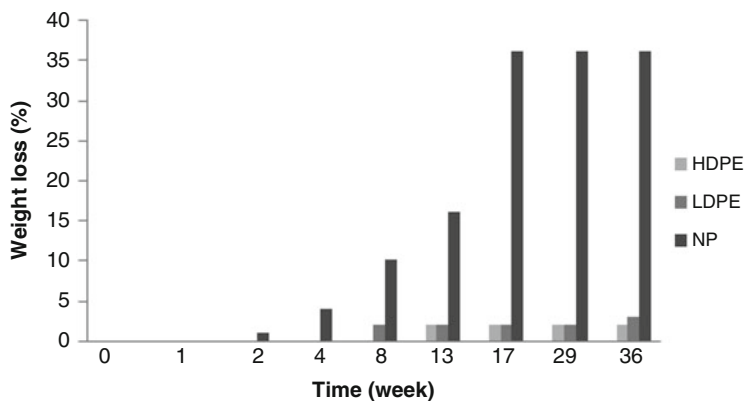


Fig. 6.15 Weight loss (%) of high-density polyethylene (HDPE), low-density polyethylene (LDPE), and degradable polyethylene (NP) films during soil burial. (Source: Hrenovic et al. 2004)

6.5.3 *Separate Compost Pit*

Separate compost pit means a pit which is totally separated from dump site and it usually built in farmers' house. Most of the farmers like to apply the compost of dumping site, but these sites are mostly combined with piles of plastic. In the study area, some farmers are aware about the fact that mixes with any inorganic content in compost; it will ultimately last in soil and eventually decline soil condition. So especially they avoid the plastics particles in their pit. It seems to be very nice initiative but only 13% farmers have taken. So, still a lot of awareness needs to be spread in the block.

6.5.4 *Tillage Separation*

During tillage, practice farmers must separate the plastic particles. Because during tillage, indisposed plastic in inner surface of soil is easily up through and visible. So in that time, it is easy to separate the plastic particles. At the same time, plastics make problem in tillage system also.

6.5.5 *Spreading Awareness*

Spreading awareness about plastic problems and management is the ultimate and the most important method to decrease the plastic particles in soil. Farmers are mostly uneducated and unaware of the impact of plastic on soil health. So, local government, like Panchayat or Krishi Daptar, must take this responsibility to make farmers aware of this hazardous problem and how to deal with the problem.

6.6 Conclusion

The study has concluded that plastic particles in agricultural soils are always harmful to soil health. Plastics decline soil physical properties like dry bulk density, soil porosity, pore spaces filled with water, soil aggregation, and biological properties like soil respiration and microbial activities, and all are reasons for making the soil unfertile in future. Biofertilizer (61.25%) and sludge water (38.75%) are identified as two major sources of plastic in agricultural soils. So farmers must be aware about the material that they have applied in their lands; although using more fertilizers helps one to get more production, it also declines the soil health internally. The government should take responsibility for not only banning or managing the plastic products but also for organizing some awareness programs, especially in rural

areas, so that people can understand this hazardous impact on soil and the environment. Plastic enters our body through the food chain and causes several dangerous diseases like autophagy, fibrosis, and even DNA mutations. Apart from that, several symptoms, such as irritation of eyes, breathing or vision problems, birth effect, skin diseases, etc., have been identified due to the intake of toxic plastics. Measurement of the influences of plastic additives on crop productivity is a temporal study; it takes several years to reach a logical conclusion. However, based on the data, several studies have proved that short-term plastic mulching can be helpful for productivity as mulching assists in holding the water and keeping the soil warm, but from the long-term point of view, it affects productivity as particles are stuck on root and reduce its growth, leading to decreasing of nutrient intake and creating a harmful environment for respiration and consequently declining microbial activities. The study mostly included the pollution of plastics, meaning how plastics impact soil health. Thus, it has opened new possibilities for management of this pollution through scientific way.

References

- Aggarwal R (2017) To address declining soil fertility, Indian agriculture needs renewed focus on soil health. Retrieved 16 January 2019, from <https://ruralmarketing.in/industry/agriculture/to-address-declining-soil-fertility-indian-agriculture-needs-renewed-focus-on-soil-health>
- Al-Shammary AAG, Kouzani AZ, Kaynak A, Khoo SY, Norton M, Gates W (2018) Soil bulk density estimation methods: a review. *Pedosphere* 28(4):581–596
- Anikwe MAN, Nwobodo KCA (2002) Long-term effect of municipal waste disposal on soil properties and productivity of sites used for urban agriculture in Abakaliki, Nigeria. *Bioresour Technol* 83(3):241–250
- Atuanya EI, Aborisade WT, Nwogu NA (2012) Impact of plastic-enriched composting
- Bläsing M, Amelung W (2018) Plastics in soil: analytical methods and possible sources. *Sci Total Environ* 612:422–435
- Bronick CJ, Lal R (2005) Manuring and rotation effects on soil organic carbon concentration for different aggregate size fractions on two soils in northeastern Ohio, USA. *Soil Tillage Res* 81(2):239–252
- Cardoso EJBN, Vasconcellos RLF, Bini D, Miyauchi MYH, Santos CAD, Alves PRL et al (2013a) Soil health: looking for suitable indicators. What should be considered to assess the effects of use and management on soil health? *Sci Agric* 70(4):274–289
- Cardoso E, Vasconcellos R, Bini D, Miyauchi M, Santos C, Alves P et al (2013b) Soil health: looking for suitable indicators. What should be considered to assess the effects of use and management on soil health? *Sci Agric* 70(4):274–289. <https://doi.org/10.1590/s0103-90162013000400009>
- Chakraborty K, Mistri D (2015) Declining of soil health through agricultural practices: a case study in Sagar Mouza. Burdwan-I, West Bengal
- Corradini F, Meza P, Eguiluz R, Casado F, Huerta-Lwanga E, Geissen V (2019) Evidence of microplastic accumulation in agricultural soils from sewage sludge disposal. *Sci Total Environ* 671:411–420
- Crawford CB, Quinn B (2017) Plastic production, waste and legislation. *Microplast Pollut* 30:39–56
- Das MP, Kumar S (2015) An approach to low-density polyethylene biodegradation by *Bacillus amyloliquefaciens*. *3 Biotech* 5(1):81–86

- Dhayagode NI, Shinde NG, Pardeshi RS (2011) Dispersal of municipal solid waste and its impact on the agriculture soil property in Shelgi village of Solarpur District. *Geosci Res* 2(2):61–69
- Duckett PE, Repaci V (2015) Marine plastic pollution: using community science to address a global problem. *Mar Freshw Res* 66(8):665–673
- Geyer R, Jambeck JR, Law KL (2017) Production, use, and fate of all plastics ever made. *Sci Adv* 3(7):e1700782
- Giannakis GV, Nikolaidis NP, Valstar J, Rowe EC, Moirogiorgou K, Kotronakis M et al (2017) Integrated critical zone model (1D-ICZ): a tool for dynamic simulation of soil functions and soil structure. In: *Advances in agronomy*, vol 142. Academic Press, pp 277–314
- Hahladakis JN, Velis CA, Weber R, Iacovidou E, Purnell P (2018) An overview of chemical additives present in plastics: migration, release, fate and environmental impact during their use, disposal and recycling. *J Hazard Mater* 344:179–199
- He D, Luo Y, Lu S, Liu M, Song Y, Lei L (2018) Microplastics in soils: analytical methods, pollution characteristics and ecological risks. *TrAC Trends Anal Chem* 109:163–172
- Home NRCSSoils (2019) Retrieved 17 January 2020, from <https://www.nrcs.usda.gov/wps/portal/nrcs/site/soils/home/>
- Hrenovic J, Orhan Y, Buyukgungor H (2004) Biodegradation of plastic compost bags under controlled soil conditions. *Acta Chim Slov* 51(3):579–588
- Imhof HK, Sigl R, Brauer E, Feyl S, Giesemann P, Klink S, Muszynski S (2017) Spatial and temporal variation of macro-, meso- and microplastic abundance on a remote coral island of the Maldives, Indian Ocean. *Mar Pollut Bull* 116(1-2):340–347
- Kibblewhite MG, Ritz K, Swift MJ (2008) Soil health in agricultural systems. *Philosophical Transactions of the Royal Society B: Biological Sciences* 363(1492):685–701
- Linn DM, Doran JW (1984) Effect of water-filled pore space on carbon dioxide and nitrous oxide production in tilled and nontilled soils. *Soil Sci Soc Am J* 48(6):1267–1272
- Magdoff F (2001) Concept, components, and strategies of soil health in agro ecosystems. *J Nematol* 33(4):169
- Narain S (2018) What are we doing to stop plastic menace?. Retrieved 5 June 2019, from <https://www.downtoearth.org.in/blog/environment/what-are-we-doing-to-stop-plastic-menace> 60678 (2020). Retrieved 9 June 2020, from https://www.ryedale.gov.uk/attachments/article/690/Different_plastic_polymer_types.pdf
- Piehl S, Leibner A, Löder MG, Dris R, Bogner C, Laforsch C (2018) Identification and quantification of macro- and microplastics on an agricultural farmland. *Scientific reports*, 8(1), 1-9. On soil structure, fertility and growth of maize plants. *European J App Sci* 4(3):105–109
- Qi Y, Yang X, Pelaez AM, Lwanga EH, Beriot N, Gertsen H et al (2018) Macro- and micro-plastics in soil-plant system: effects of plastic mulch film residues on wheat (*Triticum aestivum*) growth. *Sci Total Environ* 645:1048–1056
- Seijo A, Santos B, da Silva EF, Cachada A, Pereira R (2019) Low-density polyethylene microplastics as a source and carriers of agrochemicals to soil anearthworms. *Environ Chem* 16(1):8–17
- Sighicelli M, Pietrelli L, Lecce F, Iannilli V, Falconieri M, Coscia L, Zampetti G (2018) Microplastic pollution in the surface waters of Italian Subalpine Lakes. *Environ Pollut* 236:645–651
- Sruthy S, Ramasamy EV (2017) Microplastic pollution in Vembanad Lake, Kerala, India: the first report of microplastics in lake and estuarine sediments in India. *Environ Pollut* 222:315–322
- Tanveera A, Kanth TA, Tali PA, Naikoo M (2016) Relation of soil bulk density with texture, total organic matter content and porosity in the soils of Kandi Area of Kashmir valley. *India Int Res J Earth Sci* 4(1):1–6
- Thompson SK (1996) Adaptive cluster sampling based on order statistics. *Environmetrics* 7(2):123–133
- Tuğrul KM (2019) Soil management in sustainable agriculture. In *Soil Management and Plant Nutrition for Sustainable Crop Production*. IntechOpen

- Venkatesh Set al (2018) India's plastic consumption increases at over 10 per cent year-on-year. Retrieved 8 June 2018, from <https://www.downtoearth.org.in/news/waste/breaching-the-threshold-60748>
- Wagner M, Scherer C, Alvarez-Muñoz D, Brennholt N, Bourrain X, Buchinger S et al (2014) Microplastics in freshwater ecosystems: what we know and what we need to know. *Environ Sci Eur* 26(1):1–9
- Wang J, Liu X, Li Y, Powell T, Wang X, Wang G, Zhang P (2019) Microplastics as contaminants in the soil environment: a mini-review. *Sci Total Environ* 691:848–857
- Weithmann N, Möller JN, Löder MG, Piehl S, Laforsch C, Freitag R (2018) Organic fertilizer as a vehicle for the entry of microplastic into the environment. *Sci Adv* 4(4):eaap8060
- Yang SJ, Jong ED (1971) Effect of soil water potential and bulk density on water uptake patterns and resistance to flow of water in wheat plants. *Can J Soil Sci* 51(2):211–220

Chapter 7

Determining the Role of Leaf Relative Water Content and Soil Cation Exchange Capacity in Phytoextraction Process: Using Regression Modelling



Akash Mishra and Bindhu Lal

Abstract Cation exchange capacity (CEC) is defined as the total capacity of soil to hold exchangeable cations. Some of the major nutrients that plants uptake from soil are transported from soil to plants in the form of cations only, such as Ca^{2+} , Mg^{2+} , K^+ , Na^+ , H^+ , Al^{3+} , Fe^{2+} , Mn^{2+} , Zn^{2+} , and Cu^{2+} . Therefore, it is very important to study the interlinking factors responsible for nutrient transport in plants. Our study here aims at establishing a correlation between soil CEC and leaf RWC of the mining area. For this purpose, soil samples were collected from six different sites in and around Rajrappa mines with each site having two replicate samples to determine the CEC of the soil, soil texture, and soil pH. Leaf samples were also collected from all the sites subject to their availability in each site to determine relative water content (RWC) and pH of the plant leaves. The soil samples range from sandy soil to sandy clay loam in texture, and soil pH ranges from slightly acidic to neutral. The CEC values were found to be below 15 meq/100 g of soil samples for all the sites except for two samples taken from forest stand beside the mine where it was observed to be 26 meq/100 g. The RWC values range from 29% in lowest seam mining surface plants to 87% in reclaimed OB dumpsite. Using Minitab software, a correlation was drawn between soil CEC and leaf RWC in purview of soil texture. It was observed that there is a significant positive correlation between soil CEC and leaf RWC. A high value of CEC clearly suggests a value of leaf RWC. Moreover, in contrast to soil texture, it was clear that the presence of coarser soil particles reduces the soil CEC values and thus also reduces the leaf RWC values. However, no significant correlation was observed between plant leaf pH values and other factors.

Keywords Cation exchange capacity (CEC) · Relative water content (RWC) · Soil texture · Correlation analysis · Minitab software

A. Mishra (✉) · B. Lal
Department of Civil and Environmental Engineering, Birla Institute of Technology Mesra,
Ranchi, Jharkhand, India
e-mail: bindhu@bitmesra.ac.in

© Springer Nature Switzerland AG 2021

P. K. Shit et al. (eds.), *Spatial Modeling and Assessment of Environmental Contaminants*, Environmental Challenges and Solutions,
https://doi.org/10.1007/978-3-030-63422-3_7

107

7.1 Introduction

Cation exchange capacity (CEC) is defined as the total capacity of soil to hold exchangeable cations (Soil Nutrient Management for Maui County 2019). Almost all of the major nutrients that plants uptake from soil are transported from soil to plants in the form of cations only, such as calcium (Ca^{2+}), magnesium (Mg^{2+}), potassium (K^+), sodium (Na^+), hydrogen (H^+), aluminum (Al^{3+}), iron (Fe^{2+}), manganese (Mn^{2+}), zinc (Zn^{2+}), and copper (Cu^{2+}) (Robertson et al. 1999). This transportation process occurs by three methods: root interception (Ca, Mg, Zn, and Mn), mass flow (N, Ca, Mg, S, Cu, B, Mn, and Mo), and diffusion (P, K, Zn, and Fe) through xylem and phloem (Ugwu and Igbokwe 2019; Wuana and Okieimen 2011; Cailliatte et al. 2009; Barber et al. 1963; Epstein 1956). The flow pathway is shown in Fig. 7.1.

The soil pH is a measure of the hydrogen ions (H^+) in soil. Soil pH controls the uptake of macro- and micronutrients in plants (Gentili et al. 2018). Thus, together with cation exchange capacity, soil pH becomes one of the most important factors for determining the transport of nutrients. The soil texture class is the classification of grain size, i.e., amount of sand, silt, and clay particles present in the soil. It has been noted under previous studies that most of the exchangeable cations present in the soil are in the form of clay particles (Khorshidi and Lu 2016).

Plants maintain internal temperature and water equilibrium by continuous transpiration process. The transpiration process also regulates the flow of nutrients within plants through xylem and phloem by fostering a water deficit condition within plants leading to suction of nutrient dissolved water from soil (Jensen et al. 2000; Tanner and Beevers 2001; Morgan and Connolly 2013). Therefore, it is very important to study the interrelation between the nutrient exchange between soil and plants in contrast to water concentration in plant leaves. Our study aims at establishing a correlation between soil pH, CEC, leaf pH, and leaf relative water content (RWC) in purview of soil texture and thus formulating a regression model between different soil factors studied and the leaf RWC.

In today's world, plants are not only sought as a tool for reducing pollutant load in a degraded site and land reclamation of degraded site but also as an environmentally friendly method for extraction of minerals through phytoextraction processes—a phytoremediation technique (Ghosh and Singh 2005; Ahmadpour et al. 2012; Mahar et al. 2016; Chandra and Kumar 2017). The study conducted here is based on an abandoned mining site, which would enable us in understanding the flow of nutrients in the form of cations from soil to plants through mathematical equations. Many of these cationic nutrients are heavy metals (a major polluting substance for the mining activities), and their presence in excess quantity is a nuisance, but their presence in a limited amount is necessary (Ghosh and Singh 2005). Hence, this study might add a

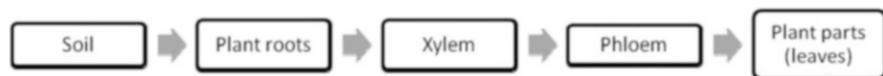


Fig. 7.1 The flow pathway of nutrients from soil into plant

new aspect for selection of tree species used for phytoremediation and phytoextraction processes to not only bring down the level of such pollutants from contaminating level back to essential levels but also extract those excess concentrations for other uses.

7.2 Materials and Methods

7.2.1 Study Area

The current study was conducted over an abandoned mining site of Chitarpur block in Ramgarh district of Jharkhand state, India, as shown in Fig. 7.2. Mining has been abandoned in the selected area since 2017 due to slope instability. The soil and plant samples were collected from six different places in and around the mining site during the monsoon season of 2019. The site was distinguished into six regions, which are as follows:

- A. Core mining region at the bottom of mine.
- B. Reclaimed OB dump with fully grown vegetation.
- C. Nonreclaimed fresh OB dump.
- D. Undisturbed site near mine with human settlement.
- E. Undisturbed site with tree stand near mine.

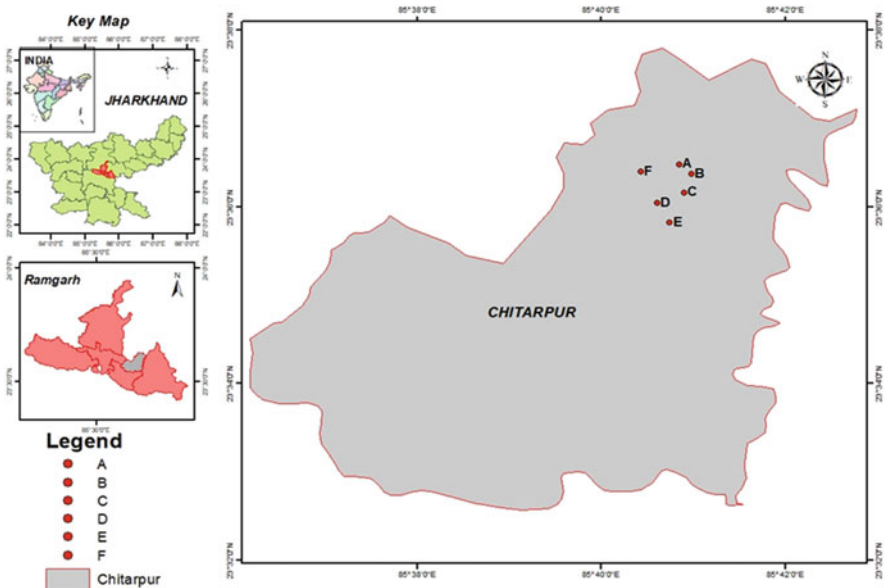


Fig. 7.2 GIS-based map of sampling site in Chitarpur block of Ramgarh district, Jharkhand state, India

F. Undisturbed site beside mine at the uppermost surface.

In total, 14 plant species were found in the region distributed in sites A, B, E, and F. Sites C and D did not have any vegetation. The plant species found in the region are listed below:

<i>Ziziphus mauritiana</i>	<i>Terminalia catappa</i>	<i>Neolamarckia cadamba</i>
<i>Lantana camara</i>	<i>Dalbergia sissoo</i>	<i>Cassia fistula</i>
<i>Sterculia urens</i>	<i>Melia azedarach</i>	<i>Bombax ceiba</i>
<i>Ficus benghalensis</i>	<i>Azadirachta indica</i>	<i>Anogeissus latifolia</i>
<i>Madhuca latifolia</i>	<i>Diospyros melanoxylon</i>	

7.2.2 Methodology

Soil Analysis

The soil samples from each site were collected and analyzed for soil pH, texture, and cation exchange capacity (CEC). The detailed methodology of the analysis is discussed below.

Soil pH

A 10 g of the soil sample was taken in a 100-ml beaker, and 20 ml of deionized water was added to it. The suspension of the soil and water was then stirred using a glass rod, the beaker was then covered with a cover glass, then it was allowed to stand for about an hour, with occasional intermittent stirring, and then the pH of the suspension was measured using pH electrode to the nearest 0.1 pH units.

Soil Texture

Soil grain size was analyzed as per IS code 2720 (part 4, 1985). Sodium oxalate (0.8 g) was added to 50 g of pre-weighed soil sample and left for saturation in a container submerged in water for 24 h. Wet sieving was done, and the sample was passed through 75 μm sieve. The sample retained on the sieve was dried and then passed through 4.75 mm, 4.00 mm, 3.35 mm, 2.80 mm, 2.00 mm, 1.40 mm, 1.00 mm, 0.60 mm, 0.30 mm, 0.212 mm, and 0.1063 mm mesh size sieve. The soil samples that passed through 75 μm sieve were analyzed using the hydrometer method, and by using nomographic chart, the silt, sand, and clay percentage (%) were recorded. The gravel, silt, sand, and clay percentage (%) gave the textural class of soil sample.

Soil CEC

Soil CEC was analyzed as per IS code 2720 (part 24, 1967). About 5 g of soil was taken in a 100-ml centrifuge tube and stirred in 50 ml of 1 N CH_3COONa of pH 5.0 to obtain the soil suspension, which was then digested in a boiling water bath (about 90 °C) for approximately 30 minutes, with intermittent stirring. The supernatant liquid obtained during the digestion process was then removed by decantation after

centrifugation of the suspension. Subsequently, the soil sample was given at least 5 washings with 1 N CaCl₂ solution to exchange all the exchangeable sites with calcium ions. Excess calcium salt was removed by washing each time with 80% acetone. The above aliquot was then titrated against standard Versene solution by the addition of 10 ml (pH 10.0) of buffer and 10 drops of the EBT indicator and 1 ml of NaCN. The cation exchange capacity is calculated from the expression given below and is expressed in milli equivalents (meq)/100 g soil:

$$\text{CEC (meq)} = \frac{\text{ml of versene} \times \text{Normality of versene} \times 100}{\text{Weight of soil (gm)} \times \text{Volume of washing}}$$

Plant Analysis

Plant leaf samples were collected from all the sites, subjected to the availability of flora in the region. In total, 20 plants' leaf samples were collected, and they were analyzed for plant pH and leaf relative water content (RWC).

Plant pH

Fresh green leaves (5 g) collected from the site were chopped into small pieces and taken in a 50-ml beaker. Deionized water (20 ml) was added in the beaker. The sample was then shaken for total time duration of 15 minutes in a mechanical shaker, and the aliquot was collected after filtering the sample using Whatman No.42 filter paper. The pH readings of aliquot collected were then recorded.

Plant RWC

Plant RWC analysis was done by following the methodologies used by González and González-Vilar 2001. Four samples (replications) of a plant species were taken and cut down into discs of a size large enough (around 1.5 cm in diameter) and weighed to obtain the fresh leaf sample weight (W), and then the samples were immediately hydrated to full turgidity by floating it on deionized water in a closed Petri dish for 8 h under normal room light conditions and temperature. The leaf discs were then taken out and soaked with tissue paper and immediately weighed to obtain fully turgid weight (TW). The samples were then oven dried at 80 °C for a time duration of 24 h and weighed again (after being cooled down in desiccators) to determine dry weight (DW).

$$\text{RWC (\%)} = \frac{W - DW}{TW - DW} \times 100$$

where W—Sample fresh weight.

TW—Sample turgid weight.

DW—Sample dry weight.

Statistical Analysis

Minitab software was used to draw a correlation between the factors and to establish a regression equation.

7.3 Results and Discussion

7.3.1 Soil

The results of soil analysis are shown in Table 7.1. Soil pH of all the regions was observed to be ranging from slightly acidic in sites A, C, D, and F to neutral in sites B and E. The average value of pH was observed to be slightly acidic in nature. The soil textural class ranges from sandy soil in site A to loamy sand in sites B, C, and D and sandy loam in site F with an exception of sandy clay loam in site E. However, % sand values remained highest in all of the sites showing the grain structure to be coarser. The CEC values were observed in the following order: site A (7.57) < site C (8.03) < site D (9.05) < site B (9.55) < site F (15.01) < site E (26.00).

Among all the variables studied, soil pH and % sand show negative correlation with a correlation value (corr.) of -0.587 , whereas the soil pH and % clay show positive correlation with a correlation value of 0.604 . CEC is found to be significantly negatively correlated with % sand, with a corr. value of -0.864 and significantly positively correlated with % clay with a corr. value of 0.892 . The three variable correlation values (corr. for pH, sand %, and CEC = 0.947 and corr. for pH, silt %, and CEC = 0.816) suggest that soil pH, % sand & CEC and soil pH, % silt & CEC are significantly positively correlated. However, no correlation was observed among soil pH, % sand, CEC, and % silt & CEC.

The simple linear regression fit model was drawn among all the variables as shown in Fig. 7.2. The normal probability plot in the Fig. 7.3 shows that observational values are clustered in close proximity of trend line, which suggests that the regression model is a very good predictor of our assumption; i.e., the soil pH, CEC, and soil texture are significantly interrelated.

The regression equation of the predictive model is as follows:

$$\text{Regression Equation : CEC} = 58.8 + 1.58 \text{ pH} - 0.653\% \text{ sand} - 0.376\% \text{ silt}$$

Table 7.1 Soil pH, texture, CEC, and correlation values among various soil factors

Sample	Soil pH	Soil texture				Soil CEC
		% sand	% silt	% clay	Textural class	
A	6.27	93.64	6.36	0.00	Sandy soil	7.57 ± 1.2*
B	6.56	82.00	13.00	5.00	Loamy sand	9.55 ± 1.1*
C	5.85	78.00	19.00	3.00	Loamy sand	8.03 ± 1.8*
D	6.27	77.5	22.00	0.50	Loamy sand	9.05 ± 1.4*
E	6.63	55.00	21.00	24.00	Sandy clay loam	26.00 ± 1.4*
F	5.71	60.00	39.50	0.50	Sandy loam	15.01 ± 2.2*
Average	6.22	74.36	20.14	5.5	–	12.54 ± 1.5*

Note: *represents standard deviation

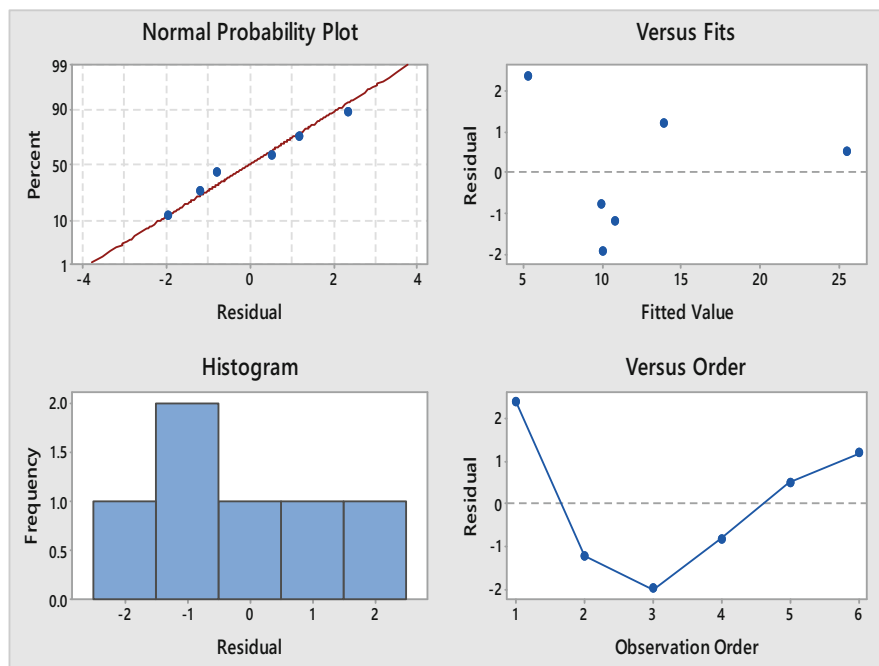


Fig. 7.3 Residual plots for CEC against soil pH, % sand, % silt, and % clay by fitting regression model

The above equation shows that soil CEC is positively affected by soil pH while negatively affected by % sand and % silt. Thus, an increase in soil pH will increase soil CEC, whereas increase in % sand and % silt will decrease soil CEC values.

7.3.2 Plant

Correlation study of two variables leaf pH and leaf RWC was done. No significant correlation was observed among the variables. A fitted line plot of leaf RWC v/s leaf pH shows a scattered plot with R-sq value only 10.2%. Even the regression equation of leaf pH on leaf RWC shows a very low slope value (0.029) as shown in Fig. 7.4. Thus, no correlation can be established between the leaf pH and RWC (Table 7.2).

7.3.3 Interaction between Soil and Plant

The intercorrelation studies between soil pH, % sand, % silt, % clay, CEC, leaf pH, and RWC are presented in Fig. 7.5. The correlation analysis for soil CEC & leaf

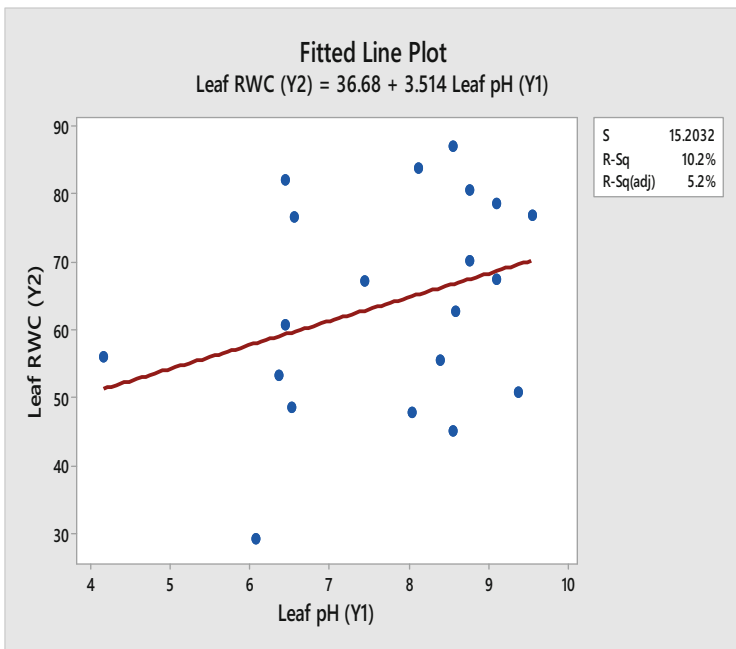


Fig. 7.4 Fitted line plot between leaf RWC and leaf pH. Regression equation: Leaf pH (Y1) = 5.88 + 0.0290 Leaf RWC (Y2)

RWC and % sand & leaf RWC gives values 0.70 and -0.60 , respectively. This shows that the soil CEC and leaf RWC show a significant positive correlation and leaf RWC was found to be negatively correlated with % sand. The three-factor correlation among soil % sand concentration, CEC, and leaf RWC shows a significant positive correlation with a corr. value of 0.83. Similarly, results were observed for three-factor correlation among % silt, CEC, leaf RWC and % clay, CEC, leaf RWC with corr. values of 0.74 and 0.93, respectively. A significant positive correlation was observed among the soil pH, CEC, and leaf RWC as well with soil pH, CEC, and leaf RWC as well with corr. values of 0.75. No significant correlation was observed among leaf pH and any of the factors.

Regression equation for the residual plot of Fig. 7.5 is as follows:

$$\text{Leaf RWC} = 66.6 - 2.72 \text{ Soil CEC} + 25.7 \text{ Soil pH} - 1.701\% \text{ sand}$$

The residual plot in Fig. 7.5 shows a linear alignment of observational values clustered around the trend line. Thus, the above regression model is an efficient regression model. The other plots also suggest that the regression model drawn for leaf RWC is significantly efficient. From the regression equation, it can be seen that soil CEC, pH, and % sand are the best fit for predicting leaf RWC values.

Table 7.2 Leaf pH, leaf RWC, and correlation among leaf pH and leaf RWC (Fig. 7.4)

Sample	Leaf pH (Y_1)	Leaf RWC (Y_2)	Corr. (Y_1, Y_2)
A2	6.06	29.07	0.319 ($P = 0.17$)
A3	4.15	55.84	
A4	8.54	44.94	
A5	6.52	48.37	
A7	8.38	55.30	
A11	6.35	53.06	
B1	8.03	47.61	
B4	9.10	67.34	
B5	8.54	86.86	
B6	9.54	76.67	
E7	6.43	82.02	
E8	6.44	60.67	
E9	7.43	66.97	
E10	8.75	80.49	
F2	9.36	50.68	
F4	8.57	62.72	
F5	8.11	83.63	
F7	6.55	76.41	
F13	8.75	70.10	
F14	9.10	78.44	

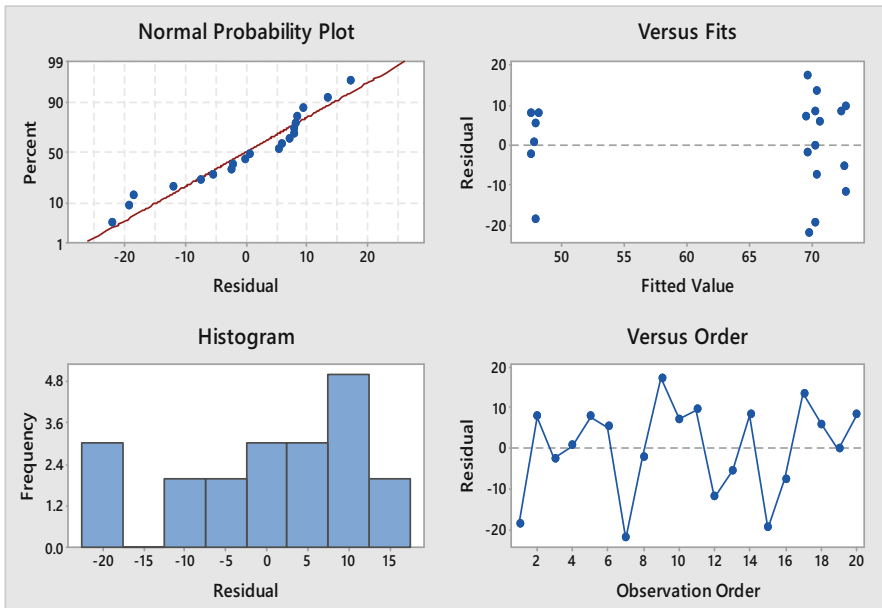


Fig. 7.5 Residual plots for leaf RWC vs soil pH, CEC, % sand, % silt, and % clay regression equation model

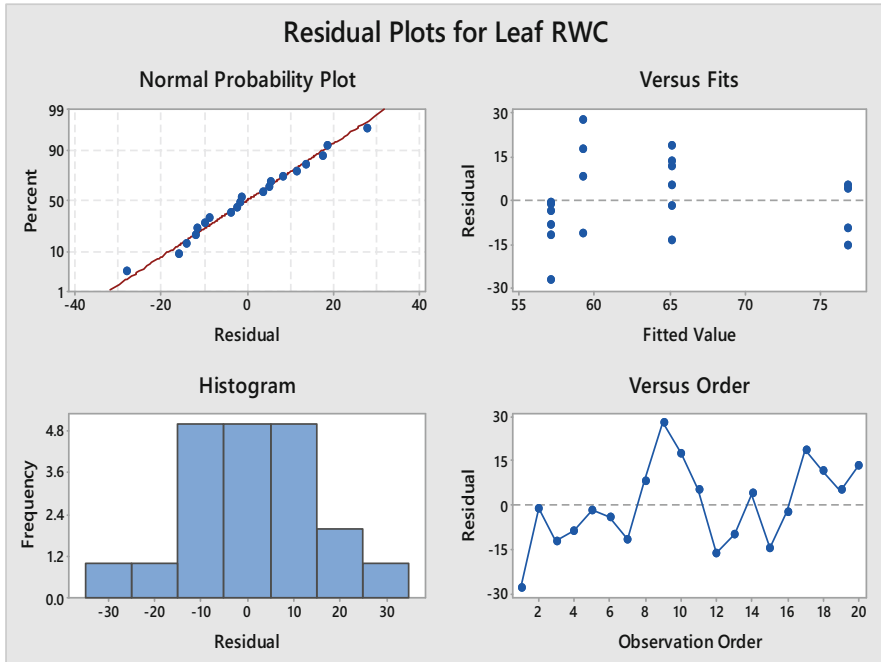


Fig. 7.6 Residual plots for leaf RWC vs soil CEC

The leaf RWC vs soil CEC plot as shown in Fig. 7.6 also suggests an efficient regression model for the two variables. The normal probability plot is collinear and clustered around the trend line. The frequency plot for RWC is highest near 0. Thus, it can be inferred that almost all values fit in the model.

The regression equation of the model is as follows:

$$\text{Leaf RWC} = 48.98 + 1.072 \text{ soil CEC}$$

It is clear from the equation as well that soil CEC is linearly correlated with leaf RWC. This means that an increase in soil CEC will result in an increase in leaf RWC values and vice versa.

7.4 Discussion

The study here suggests that soil pH alone is not correlated with soil CEC or leaf RWC, but soil texture class greatly affects its correlation coefficient for both the factors. Soil textural class has a great impact on soil CEC values. The presence of finer particles in soil (clay) positively affects the soil CEC, while coarser particles negatively affect the soil CEC values. For leaf pH, no significant correlation was

observed in any of the factors. Leaf RWC is observed to be significantly dependent on combined soil factors (pH, texture, and CEC). However, when single-factor correlation was studied between leaf RWC and soil CEC, it was observed that soil CEC significantly affects the leaf RWC. Leaf RWC is significantly dependent on soil CEC alone as well as when combined with soil pH, CEC, and texture. Thus, the transport of nutrients in plants is greatly dependent on interrelationship between leaf RWC and soil CEC. Soil pH, grain size, and texture determine the flow of nutrients in the form of cations from soil to plant leaf, which is governed by leaf RWC.

The plant species with the highest leaf RWC values (above 80%) in the present study are observed in *D. sissoo* in reclaimed OB dump with fully grown vegetation and undisturbed site beside mine at the uppermost surface and in *S. urens* and *F. benghalensis* in undisturbed site with tree stand near mine. The undisturbed site with tree stand near mine is constantly facing loading of pollutants due to transportation of coal and vehicular emissions, whereas the reclaimed OB dump site with full fledged vegetation beside mine and the undisturbed sites near mine do not face such loading of pollutants due to the coal transportation and vehicular emissions. The core mining region at the bottom was not seen to have any plant species with leaf RWC values above 56%. This may be attributed to the greater % sand quantity in the soil of the region. The undisturbed site with tree stand near mine has the highest clay % and thus the highest soil CEC and leaf RWC of most of the plant species values, whereas the other sites have considerably less amount of % sand but more than the undisturbed tree stand, hence an intermediate values of soil CEC, and thus, leaf RWC was inferred in the site.

The analysis of the regression equation further suggests that if there is an increase in soil CEC, then the uptake of nutrients may increase due to higher values of leaf RWC. Hence, plants growing in degraded lands (degradation in this case caused due to coal mining), which are primarily used for land reclamation and restoration purposes (Sinha et al. 2007), with higher leaf RWC values shall be considered as a better option for phytoremediation, phytoextraction, and land reclamation and management. Phytoextraction, an environmentally friendly method, which is used for extraction of minerals, may be applied in places that are abandoned after conventional mineral extraction processes.

7.5 Risk Assessment and Remediation

Soil contamination is a major problem in today's industrialized world, and coal is the powerhouse for running this world, which adds up to the soil contamination. Coal mining leads to the release of a large number of nutrients (some of which are also termed as heavy metals) apart from land inundation such as Al, Si, K, Mg, Fe, As, Cd, Co, Hg, Ni, Sb, Mn, Tl, V, Cu, and Se (Pandey et al. 2014; Nalbandian 2012; and Schweinfurth 2009). The minerals of these elements serve as a nuisance and pollutant, but if extracted in reasonable concentration and used, then serve as an important economic asset. The coal mining processes leave behind completely

destructured land with an excess of heavy metals and its compounds and other nutrient minerals. The abandoned mining lands cannot be used for other purposes for quite a long time; instead, it adds up more problems (such as leaching) (Dutta et al. 2009), and hence, it takes a quite long time for restoration. During this restoration phase, it serves no economical uses and its uses may be seen to be only aesthetic (Dittrich et al. 2019; and Kuter 2013).

The restoration of abandoned mines is primarily done by afforestation processes (Gentcheva-Kostadinova and Haigh 1988). However, fast-growing tree species are sought to be the most efficient technique after mining for eco-restoration. The abandoned mining land is left after a restoration phase of a few years. The land serves of no economic values during restoration and after it. But, if phytoextraction technique along with phytoremediation and phytorestoration is applied, then this will enhance the economic value of the land, the views of which coincide with the outputs of Cutright et al. 2012 & RoyChowdhury et al. 2019. The minerals and heavy metals, once being seen as pollutants, can be mined using plants by using their natural ability to extract minerals from the soil. This will serve as an economic value in addition to the aesthetic values during the ecological restoration processes, and thus, the plants with higher leaf RWC values would serve as an optimal suit for the purpose.

7.6 Conclusions

From the study, it can be concluded that leaf RWC is significantly dependent in both terms with soil CEC alone as well as combined soil factors, soil pH, CEC, and texture. Thus, the transport of nutrients in plants is greatly dependent on interrelationship between leaf RWC and soil CEC. Soil pH, grain size, and texture determine the flow of nutrients in the form of cations from soil to plant leaf, which is governed by leaf RWC. Thus, the plant species with higher leaf RWC values shall be able to extract nutrients more efficiently from abandoned degraded land with higher soil CEC values. Plants with greater leaf RWC values serve as an efficient tool for phytoextraction of minerals from abandoned mining sites.

References

- Ahmadpour P, Ahmadpour F, Mahmud TMM, Abdu A, Soleimani M, Tayefeh FH (2012) Phytoremediation of heavy metals: a green technology. *Afr J Biotechnol* 11(76):14036–14043
- Barber SA, Walker JM, Vasey EH (1963) Mechanisms for movement of plant nutrients from soil and fertilizer to plant root. *J Agric Food Chem* 11(3):204–207
- Cailliatte R, Lapeyre B, Briat JF, Mari S, Curie C (2009) The NRAMP6 metal transporter contributes to cadmium toxicity. *Biochem J* 422(2):217–228

- Chandra R, Kumar V (2017) Phytoextraction of heavy metals by potential native plants and their microscopic observation of root growing on stabilised distillery sludge as a prospective tool for in situ phytoremediation of industrial waste. *Environ Sci Pollut Res* 24(3):2605–2619
- Cutright TJ, Senko J, Sivaram S, York M (2012) Evaluation of the phytoextraction potential at an acid-mine-drainage-impacted site. *Soil Sediment Contam Int J* 21(8):970–984
- Dittrich R, Ball T, Wreford A, Moran D, Spray CJ (2019) A cost-benefit analysis of afforestation as a climate change adaptation measure to reduce flood risk. *Journal of Flood Risk Management* 12 (4):e12482
- Dutta BK, Khanra S, Mallick D (2009) Leaching of elements from coal fly ash: assessment of its potential for use in filling abandoned coal mines. *Fuel* 88(7):1314–1323
- Epstein E (1956) Mineral nutrition of plants: mechanisms of uptake and transport. *Annu Rev Plant Physiol* 7(1):1–24
- Gentcheva-Kostadinova S, Haigh MJ (1988) Land reclamation and afforestation research on the coal-mine-disturbed lands of Bulgaria. *Land Use Policy* 5(1):94–102
- Gentili R, Ambrosini R, Montagnani C, Caronni S, Citterio S (2018) Effect of soil pH on the growth, reproductive investment and pollen allergenicity of *Ambrosia artemisiifolia* L. *Front Plant Sci* 9:1335
- Ghosh M, Singh SP (2005) A review on phytoremediation of heavy metals and utilization of its by products. *Asian J Energy Environ* 6(4):18
- González L, González-Vilar M (2001) Determination of relative water content. In: *Handbook of plant ecophysiology techniques*. Springer, Dordrecht, pp 207–212
- IS: 2720-Part 24 (1967) Methods of test for soils– determination of base exchange capacity
- IS: 2720-Part 4 (1985) Methods of test for soils–Grain size analysis
- Jensen CR, Jacobsen SE, Andersen MN, Nunez N, Andersen SD, Rasmussen L, Mogensen VO (2000) Leaf gas exchange and water relation characteristics of field quinoa (*Chenopodium quinoa* Willd.) during soil drying. *Eur J Agron* 13(1):11–25
- Khorshidi M, Lu N (2016) Intrinsic relation between soil water retention and cation exchange capacity. *J Geotech Geoenviron* 143(4):04016119
- Kuter N (2013) Reclamation of degraded landscapes due to opencast mining. In *Advances in landscape architecture*, IntechOpen
- Mahar A, Wang P, Ali A, Awasthi MK, Lahori AH, Wang Q, Zhang Z (2016) Challenges and opportunities in the phytoremediation of heavy metals contaminated soils: a review. *Ecotoxicol Environ Saf* 126:111–121
- Morgan JB, Connolly EL (2013) Plant-soil interactions: nutrient uptake. *Nature Education Knowledge* 4(8):2
- Nalbandian H (2012) Trace element emissions from coal. IEA Clean Coal Centre 601
- Pandey B, Agrawal M, Singh S (2014) Coal mining activities change plant community structure due to air pollution and soil degradation. *Ecotoxicology* 23(8):1474–1483
- Robertson GP, Sollins P, Ellis BG, Lajtha K (1999) Exchangeable ions, pH, and cation exchange capacity. In: *Standard soil methods for long-term ecological research*. Oxford University Press, New York, pp 106–114
- RoyChowdhury A, Sarkar D, Datta R (2019) A combined chemical and phytoremediation method for reclamation of acid mine drainage-impacted soils. *Environ Sci Pollut Res* 26 (14):14414–14425
- Schweinfurth SP (2009) An introduction to coal quality. US Geological Survey Professional Paper, The National Coal Resource Assessment Overview
- Sinha RK, Herat S, Tandon PK (2007) Phytoremediation: role of plants in contaminated site management. In: *Environmental bioremediation technologies*. Springer, Berlin, Heidelberg, pp 315–330
- Soil Nutrient Management for Maui County (2019) Soil-Nutrient Relationships. College of Tropical Agriculture and Human Resources (CTAHR). University of Hawai'i at Manoa soilquality.org.au. (2019). Fact Sheets. <http://soilquality.org.au/factsheets>

- Tanner W, Beevers H (2001) Transpiration, a prerequisite for long-distance transport of minerals in plants. *Proc Natl Acad Sci* 98(16):9443–9447
- Ugwu IM, Igbokwe OA (2019) Sorption of heavy metals on clay minerals and oxides: a review. In: *Advanced sorption process applications*. IntechOpen
- Wuana RA, Okieimen FE (2011) Heavy metals in contaminated soils: a review of sources, chemistry, risks and best available strategies for remediation. *Isrn Ecology* 2011

Chapter 8

Phytoremediation of Arsenic Using *Allium sativum* L. as a Model System



Soumik Chatterjee and Sabyasachi Chatterjee

Abstract Heavy metals are toxic for the environment and are harmful to humans and animals and also affect plants and bacteria. Phytoremediation is the process by which removal or transformation of contaminants from the soil by the use of green plants takes place. The aim of this research is to study the phytoremediation capacity of arsenic (As) from soil by the use of *Allium sativum* L., which belongs to the family Liliaceae. These plants have heavy metals uptake mechanism in a particular part of a plant. The study was designed to examine the effect of arsenic (As) on germination and growth and also effects on cell divisions in the root meristems of germinated *Allium sativum* L. The *Allium sativum* L. blubs were germinated within the three different concentrations of arsenic (As) solution. Roots lengths, numbers, and growth of *Allium sativum* L. gradually decreased up to 100 ppm arsenic concentrations. The mitotic index and chromosomal abnormalities were used to evaluate genotoxicity and cytotoxicity to verify the effect of arsenic. The FESEM-EDAX was done to study the structural modifications and to identify concentration and distribution of As in roots of *Allium sativum* L. The results showed that *Allium sativum* L. plants have the ability to accumulate arsenic in their root tissue. Atomic % of As in control, 20 ppm, 50 ppm, and 100 ppm treated *Allium sativum* L. roots (scale area 50 and 100 μm) was found to be 0.00%, 0.05%, 0.16%, and 0.04%, respectively. Arsenic accumulated in the root tissue and adversely affected the growth and productivity of the plants. The results showed that germinated *Allium sativum* L. had the ability to accumulate As in their tissue. *Allium sativum* L. can uptake arsenic up to the root portion. In this study, it has been revealed that gradually increasing the concentration of As in *Allium sativum* L. showed higher accumulation capacities of arsenic, which may be a better remediation option in the near future.

Keywords Soil treatment with arsenic · *Allium sativum* L. blubs · Phytoremediation · Genotoxicity · Cytotoxicity · Arsenic detection

S. Chatterjee · S. Chatterjee (✉)
PG Department of Botany, Ramananda College, Bishnupur, Bankura, West Bengal, India

8.1 Introduction

Humanity is facing many horrible ecological crises because environmental problems like environmental pollution are growing rapidly. Heavy metals contaminating the sediments is the major environmental problem all over the world. Heavy metals are generated through industrial processes and are released by effluents generated from various industries (metals finishing industries, metallurgy, tannery, battery manufacturing industries, glass factories, plastic industries, etc.), and the released heavy metals pollute the environment (Chandran and Niranjana 2012). There has been a gradual increase in the accumulation of heavy metals in the environment, which are very harmful and affect both human health and the natural environment. Accumulation of higher concentrations of heavy metals in the environment results in their incorporation in food chains and their subsequent biomagnifications in higher trophic levels of the nutritional pyramid (Chopra et al. 2009). These biomagnifications of heavy metals adversely affect the behavioural, structural, and functional activities of living organisms. Many studies have been done to determine the toxic effects of heavy metals on edible plants. According to different studies, it was indicated that plants usually uptake Cd, Cr, Mn, Zn, and As corresponding to the increasing level of soil contamination (Fargasova and Listiakova 2009). A gradual increase of As concentration in the soil results in increased accumulation of As in the plant tissues. When exposed to high concentrations of As, it affects some physiological processes and ultimately reduces the growth of plants, showing many toxic symptoms. Plants that have the ability to uptake and tolerate higher levels of metals in their biomass are termed as hyperaccumulator plants (Fiskesjo 1985). Although heavy metals are not harmful to those plants, due to biomagnifications of metals in the food chains, they are consequently found to be poisonous for human or animal health (Fiskesjo 1997). In this research, the ability of *Allium sativum* L. as a metal accumulator and effects of arsenic accumulation in different parts were investigated. The finding showed that the lower concentration of As stimulated the root and shoot elongation of *Allium sativum* whereas at higher concentrations, significant reduction in germination (%) and plant growth, especially root and shoot elongation, was observed. The plant root system accumulated the highest As concentrations in most plant species (Kwankua et al. 2012), which was corroborated with the present study. Phytoremediation technology uses green plants to reduce, remove, or immobilize environmental toxins from the soil. Phytoremediation technology depends on the selection of appropriate plants species because all plants do not show phytoremediation. Exposures of high concentrations of arsenic have carcinogenic and mutagenic effects on a large number of plant species (Kumar and Tripathi 2003). The visual symptoms of heavy metal toxicity due to arsenic are inhibition of root growth and stunted growth of plant. *Allium sativum* L. showed rapid growth in a wide range of soil types and had the ability to tolerate heavy metal pollution.

8.2 Materials and Methods

8.2.1 *In Vivo Culture and Treatment of Arsenic on Allium sativum L. (Garlic)*

Arsenic trioxide (As_2O_3) salt was used for arsenic source for this study. Stock solution (500 ml) of arsenic trioxide (concentration 200 ppm) was prepared, and from the stock solution, three different concentrations (20 ppm, 50 ppm, and 100 ppm) of arsenic trioxide solution were prepared (Marin et al. 1992). Soil was collected from local garden and placed in four different pots (Soil 200gm) for planting of *Allium sativum* L. blubs, and different concentrations of arsenic trioxide solution (20 ppm, 50 ppm, 100 ppm) were added (20 ml) in three different pots except the pot marked as control (Carbonell-Barrachina et al. 1995). Healthy garlic blubs were grown in different pots for study.

8.2.2 *Cytological Studies*

The root tips of cultivated *Allium sativum* L. were collected after 7 days and used for cytological studies. The root tips were collected between 9 am and 9.45 am from different concentrations of arsenic-treated *Allium sativum* L. for cytological investigation (Panda and Patra 1997). Root tips of *Allium sativum* L. squashes were made by using an iron alum hematoxylin squash technique (Marimuthu and Subramaniam 1960). This technique was found to be suitable for the cytological investigation and observed under a microscope for chromosomal abnormalities. The number of cells at the division phase, abnormal cells, and chromosomal aberrations were noted in each concentration, and the mitotic index was calculated.

$$\text{Mitotic index} = (\text{Number of dividing cells} / \text{Total number of cells}) \times 100$$

8.2.3 *Field Emission Scanning Electron Microscope (FESEM) and Energy-Dispersive X-Ray Spectroscopy (EDAX)*

Primary fixation of roots, blubs, and leaves was done. The sections of *Allium sativum* L. with and without As treatment were done for each part by immersing in 4% glutaraldehyde and in 0.2 M phosphate buffer (pH 7.2) at room temperature. After that, samples were rinsed 4 times for 15–20 min with above buffer without aldehyde fixatives (Nagpal and Grover 1994). Then, all samples were dehydrated with ethanol series. Samples were mounted, and gold coating was done by IB2 ion coater machine

for FESEM investigations. Internal roots stem and leaf structures were examined by FESEM photographs. FESEM model Hitachi-SU attached with energy-dispersive x-ray spectroscopy provides supplementary information and is used for As and other element detections in different plant parts.

8.3 Results and Discussions

In this study, *Allium sativum* L. blubs were germinated in control as well as different arsenic concentrations treated soil. Arsenic did not inhibit the germination of *Allium sativum* L. up to 100 ppm concentrations, but it was reported that the germination rate of some plants like *Oryza sativa* was inhibited by 100 ppm concentration of arsenic (Table 8.1) (Abedin and Meharg 2002). The growth of *Allium sativum* L. was gradually decreased with increasing arsenic concentrations. In 20 ppm, 50 ppm, and 100 ppm arsenic concentration, height of *Allium sativum* L. was recorded at 22 cm, 18 cm, and 14 cm, respectively, and in control condition, *Allium sativum* L. height was 24 cm because arsenic inhibited the growth (Figs. 8.1, 8.2, 8.3, and 8.4) (Singh and Keefer 1989). The number of roots and root length of *Allium sativum* L. were gradually decreased with the increasing arsenic concentrations (Figs. 8.3, 8.5, and 8.6 and Table 8.2). In 100 ppm arsenic concentrations, root length of *Allium sativum* L. was decreased. It is thought that germination and seedling establishment are critical stages in the life cycle of plants and can be affected in the presence of a high level of arsenic in the immediate environment. It was observed that among the

Table 8.1 Germination rate of *Allium sativum* L. with different arsenic concentrations

S. No.	Heavy metal concentration (ppm) As_2O_3	Number of seeds	Day	Number of seeds germinated	Germination rate
1	Control	2	10	2	100%
2	20 ppm	2	10	2	100%
3	50 ppm	2	10	2	100%
4	100 ppm	2	10	2	100%

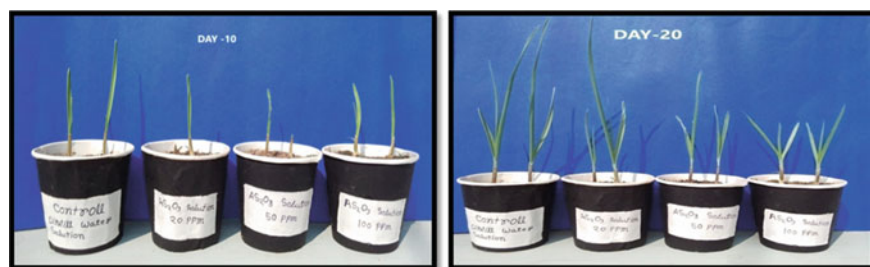


Fig. 8.1 Cultivation of *Allium sativum* L. blubs in different pots with different concentrations of arsenic



Fig. 8.2 *Allium sativum* L. growth rate was gradually decreased with the increasing arsenic concentrations after 20 and 40 days



Fig. 8.3 Number of roots and length of *A. sativum* L. in different concentrations of arsenic

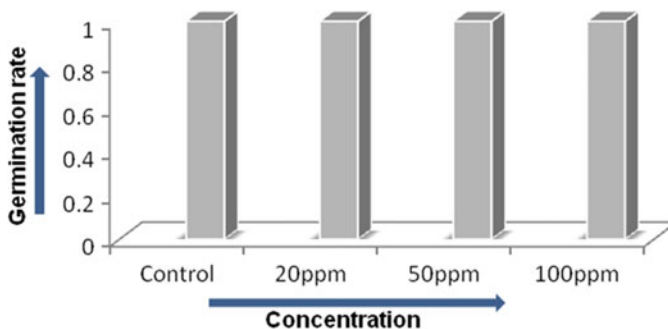


Fig. 8.4 Germination rate of *Allium sativum* L. with different arsenic concentrations

other heavy metals, arsenic was found toxic at a higher level (Singh and Sharma 2007). The present investigation confirmed that the growth of *Allium sativum* L. was affected under different concentrations of arsenic.

To study the effect of arsenic on meristematic cells of *Allium sativum* L., roots were analyzed to record the mitotic index (Fiskesjo 1995). Germinated roots, which were exposed to without arsenic condition, did not show significant mitotic

Fig. 8.5 Root numbers of *Allium sativum* L

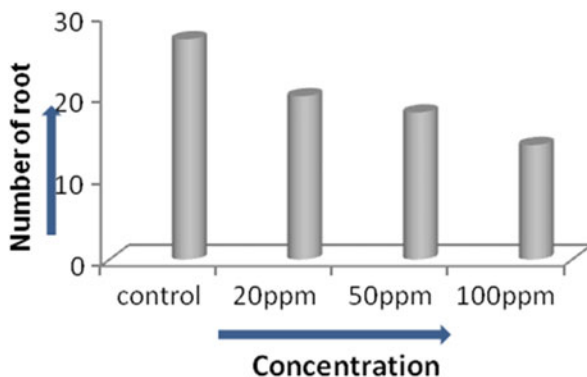


Fig. 8.6 Root lengths of *Allium sativum* L

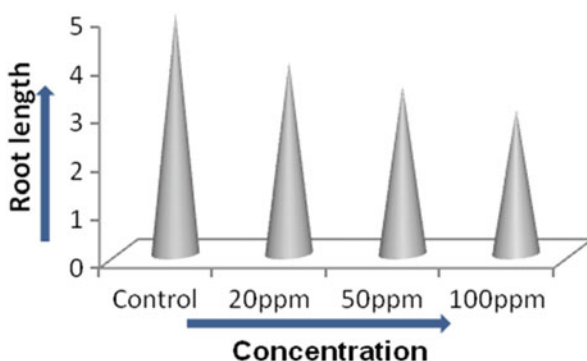


Table 8.2 Root numbers and lengths of *Allium sativum* L. at different arsenic concentrations

S. No.	Heavy metal concentration	Number of roots	Root length (cm)
1	Control	27	5 cm
2	20 ppm	20	4 cm
3	50 ppm	18	3.5 cm
4	100 ppm	14	3 cm

Table 8.3 Cytological effects of cells of *Allium sativum* L. at different concentrations of arsenic

No. of dividing cells	Mitotic index %
(Control) 168	16.8
(20 ppm) 154	15.4
(50 ppm) 115	11.5
(100 ppm) 97	9.7

inhibition. The different concentrations of arsenic (20 ppm, 50 ppm, 100 ppm) treatment reduced the mitotic activity of roots of *Allium sativum* L. (Table 8.3). Mitotic anomalies like anaphase bridges and laggards were recorded (Table 8.4). Additionally, the primary action of arsenic on the mitotic spindle-promoted spindle-related abnormalities such as laggard chromosome and bridges during cell division was observed (Bushra et al. 2002). Heavy metal-induced genotoxicity effects on

Table 8.4 Chromosomal aberration of cells of *Allium sativum* L. at different concentrations of arsenic

Concentration	No. of dividing cells	Laggard	Vagrant	Sticky chromosome	Chromosomal bridge	Total aberration ratio %
Control	209	2	1	0	0	1.43
20 ppm	172	0	0	2	1	1.71
50 ppm	167	1	0	0	2	2.43
100 ppm	152	0	1	0	3	2.22

plants and other biological systems depend on the oxidation state of those metals and their concentration and duration of the exposure (Srivastava and Jain 2010). In general, effects of arsenic are more pronounced at higher concentrations and at longer duration of exposures. Considering cyto/genotoxic studies, arsenic showed a strong phytotoxic effect on *Allium sativum* L. chromosome at the concentration of 100 ppm. Reduction in cell division due to arsenic is reported in many plants. The result of this investigation showed a significant reduction of mitotic index in *Allium sativum* L. roots meristematic cells in the presence of arsenic. This might be due to inhibition of mitosis or extension of cell cycles (Fiskesjo 1985). Arsenic may contribute by blocking the cell division at the end of the prophase. In this case, arsenic may be considered a premetaphase inhibitor. Chromosomal aberrations were induced at all the tested concentrations. The most frequent abnormalities were bridges and sticky chromosomes. Sticky chromosomes represent poisoned chromosomes with a sticky surface, probably leading to cell death (Chauhan et al. 2001). Sticky chromosomes at metaphase and anaphase were abundant in the *Allium sativum* L. roots at higher concentrations, indicating arsenic toxicity (Fig. 8.7). It was also found that a significant increase in the frequency of abnormal cells with chromosomal abnormality in *Allium sativum* L. root meristematic cells corresponds to the addition of various concentrations of arsenic (Chakraborty et al. 2008).

Arsenic-treated *Allium sativum* L. plants were showed significant changes in the internal structures of leaves, stems, and roots as compared to the control set. Structures of leaf stomata and epicuticular wax of *Allium sativum* L. were unchanged with the increasing arsenic concentrations (Figs. 8.8 and 8.9). The FESEM micrographs of As-treated leaf samples of *Allium sativum* L. showed reduction in epidermal and palisade cell size and a decrease in the amount of epicuticular wax on epidermis as compared to the control set, which supports the theory of Han et al. 2004. The microscopic study of arsenic-treated *Allium sativum* L. blub cross sections showed no structural changes in xylem vessels with the increasing As concentrations (Fig. 8.10). The root surface of *Allium sativum* L. changes gradually with increasing arsenic concentrations (Fig. 8.11). In this study, FESEM allowed examination of the topography of the internal structure of roots, stems, and leaves and internal accumulation of As, which is similar to the study done by Han et al. 2003. The arsenic-treated leaf surface of *Allium sativum* L. showed no significant structural changes as compared to the control. It was found from the FESEM micrographs that the

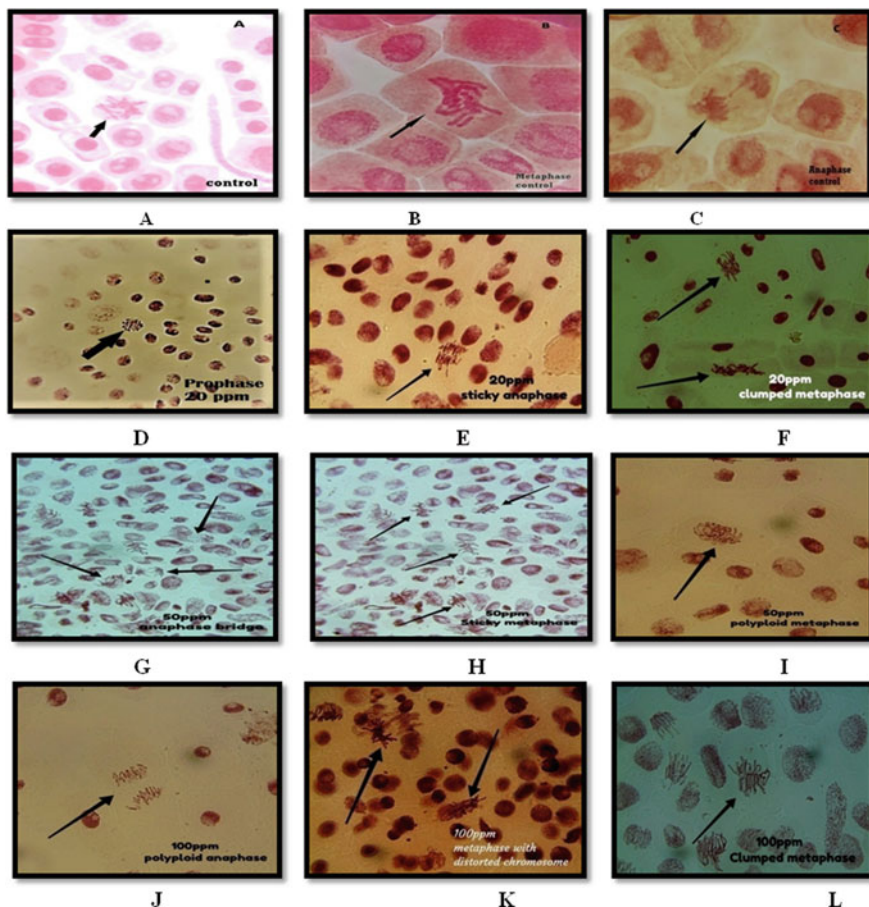


Fig. 8.7 (a) Metaphase, (b) metaphase, (c) anaphase, (d) prophase, (e) sticky anaphase, (f) clumped metaphase, (g) anaphase bridge, (h) sticky metaphase, (i) polyploid metaphase, (j) polyploid anaphase, (k) metaphase with distorted chromosome, and (l) clumped metaphase of *Allium sativum* L

100 ppm As-treated *Allium sativum* L. leaf surface did not show any arsenic deposit, which is similar to the finding of Losi et al. 1994. The root surface of *Allium sativum* L. showed significant morphological changes in 20, 50 and 100 ppm of arsenic, and arsenic was detected in root portion only (Fig. 8.11 and 8.14). The EDAX analyzer produced a spectrum of the elements present in targeted areas of the samples allowing detectable elements to be quantified or mapped, which corroborated with findings of Lytle et al. 1998. The FESEM micrographs of 20, 50, and 100 ppm of arsenic-treated roots showed arsenic depositions (Fig. 8.11). The elemental composition of the root surfaces was simultaneously measured by EDAX. The FESEM-EDAX spectra of the control and metal-loaded root surfaces were shown (Fig. 8.12). In FESEM study, external characteristics of leaves of *Allium sativum* L. were not

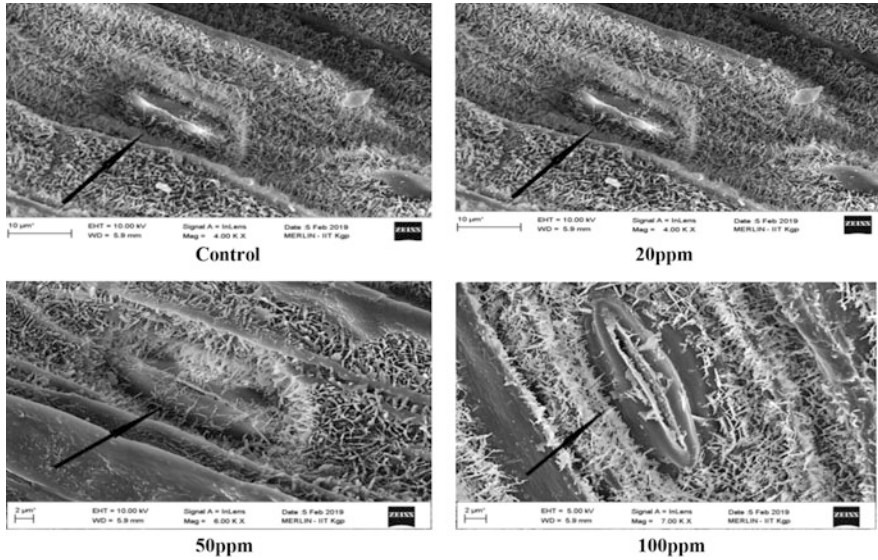


Fig. 8.8 FESEM of *Allium sativum* L. leaf stomata in control plant and arsenic treated (20 ppm, 50 ppm, 100 ppm)

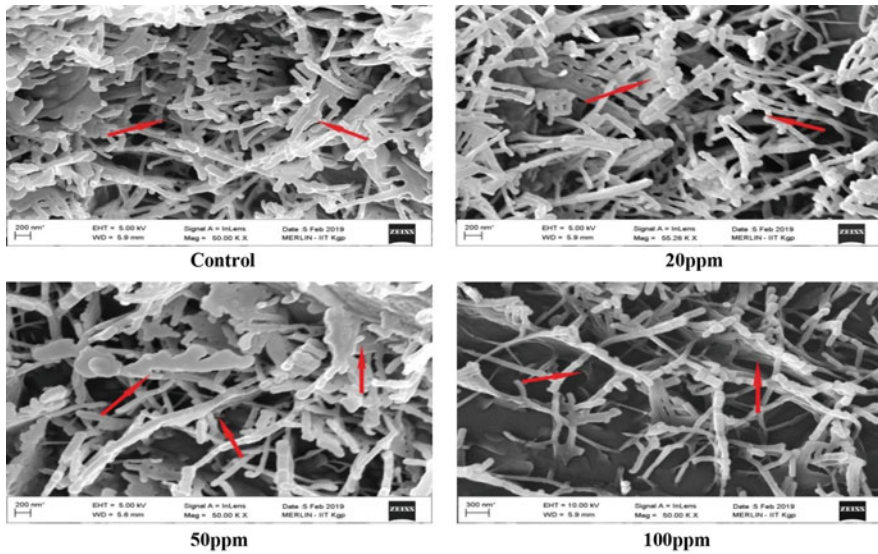


Fig. 8.9 FESEM of leaf epidermal epicuticular wax in control as well as arsenic-treated (20 ppm, 50 ppm, 100 ppm) *Allium sativum* L.

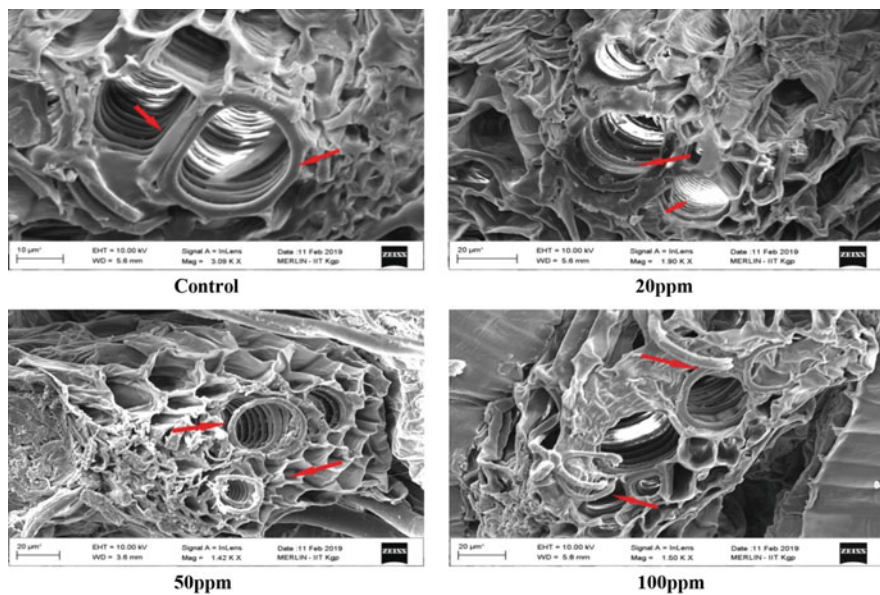


Fig. 8.10 FESEM of blub in control as well as arsenic-treated (20 ppm, 50 ppm, 100 ppm) *Allium sativum* L.

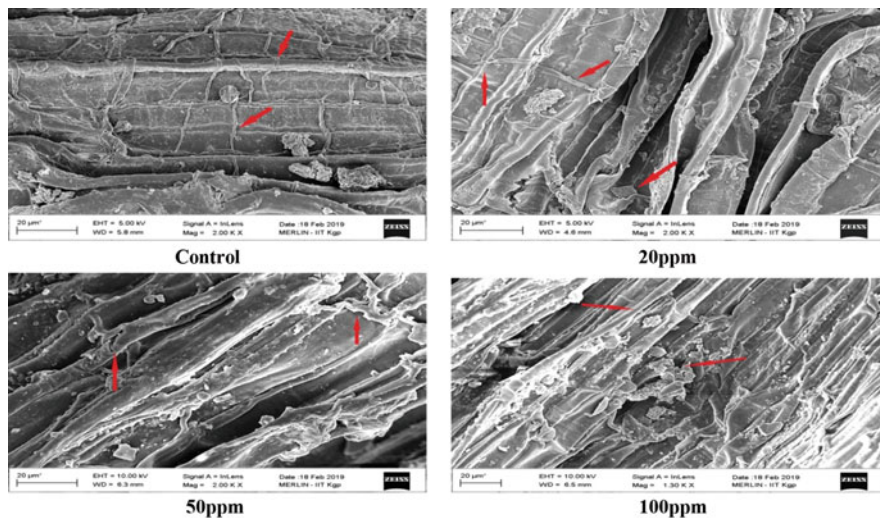


Fig. 8.11 FESEM of root external surface in control as well as arsenic-treated (20 ppm, 50 ppm, 100 ppm) *Allium sativum* L.

strongly affected by the treatment with arsenic at different concentrations (Fig. 8.8), but the epicuticular wax on the epidermal cell of *Allium sativum* L. leaves gradually decreased with an increase in Arsenic concentration and the thickness increased

(Fig. 8.9), which supports the findings of Komar et al. 2001. Leaf stomata structures were unchanged after treating with arsenic (Fig. 8.8). Indeed, no major cell shrinkage or tissue necrosis was observed in leaves of these *Allium sativum* L. after the treatment. Internal structure of garlic bulbs under FESEM shows that xylem lumens were unchanged. The external structure of roots gradually changed with increasing Arsenic concentration (Fig. 8.11), which is very close to the findings of Puryear and Newton 2002.

The EDAX analyzer produced a spectrum of the elements present in targeted areas of the samples allowing detectable elements to be quantified or mapped (Fig. 8.12, 8.13 and 8.14), which is similar to the findings of Wagner 1993. The

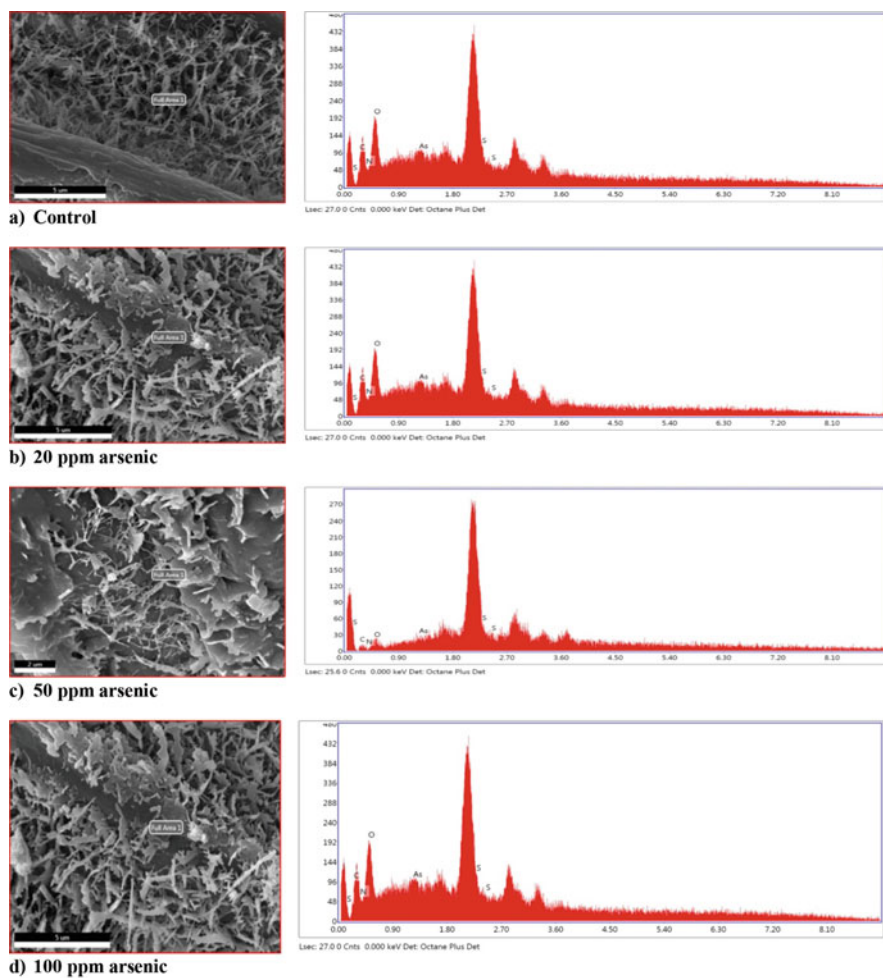


Fig. 8.12 FESEM micrographs of leaves of *Allium sativum* L. with respect to (a) control, (b) 20 ppm, (c) 50 ppm, and (d) 100 ppm of arsenic and corresponding (EDAX) analysis

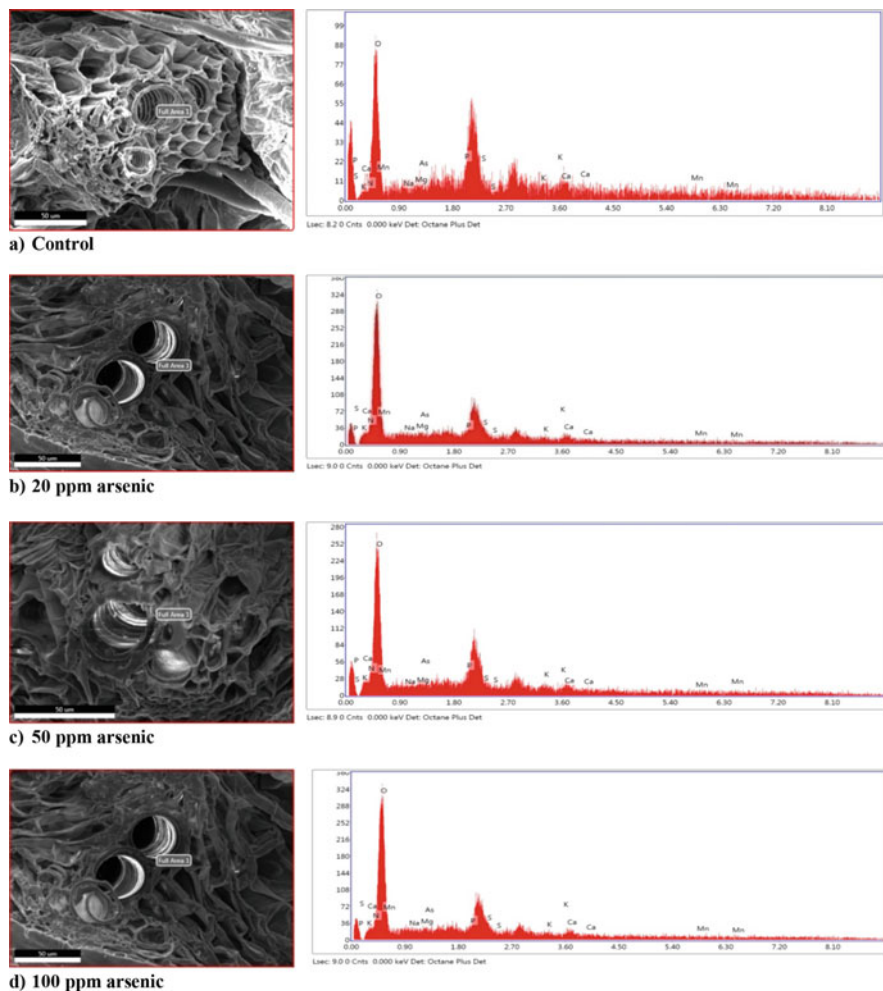


Fig. 8.13 FESEM micrographs of bulbs of *Allium sativum* L. with respect to (a) control, (b) 20 ppm, (c) 50 ppm, and (d) 100 ppm of arsenic and corresponding (EDAX) analysis

FESEM micrographs of 20, 50, and 100 ppm of As-treated roots of *Allium sativum* L. showed arsenic deposits (Fig. 8.11). Atomic % of As in control, 20 ppm, 50 ppm, and 100 ppm arsenic-treated *Allium sativum* L. roots (Scale area 50 and 100 μm) was found to be 0.00%, 0.05%, 0.16%, and 0.04%, respectively (Table 8.5). So, it was confirmed from the study that *Allium sativum* L. uptake arsenic up to the roots but not to the bulb and leaf portions, which corroborated with the study of Walker et al. (1977).

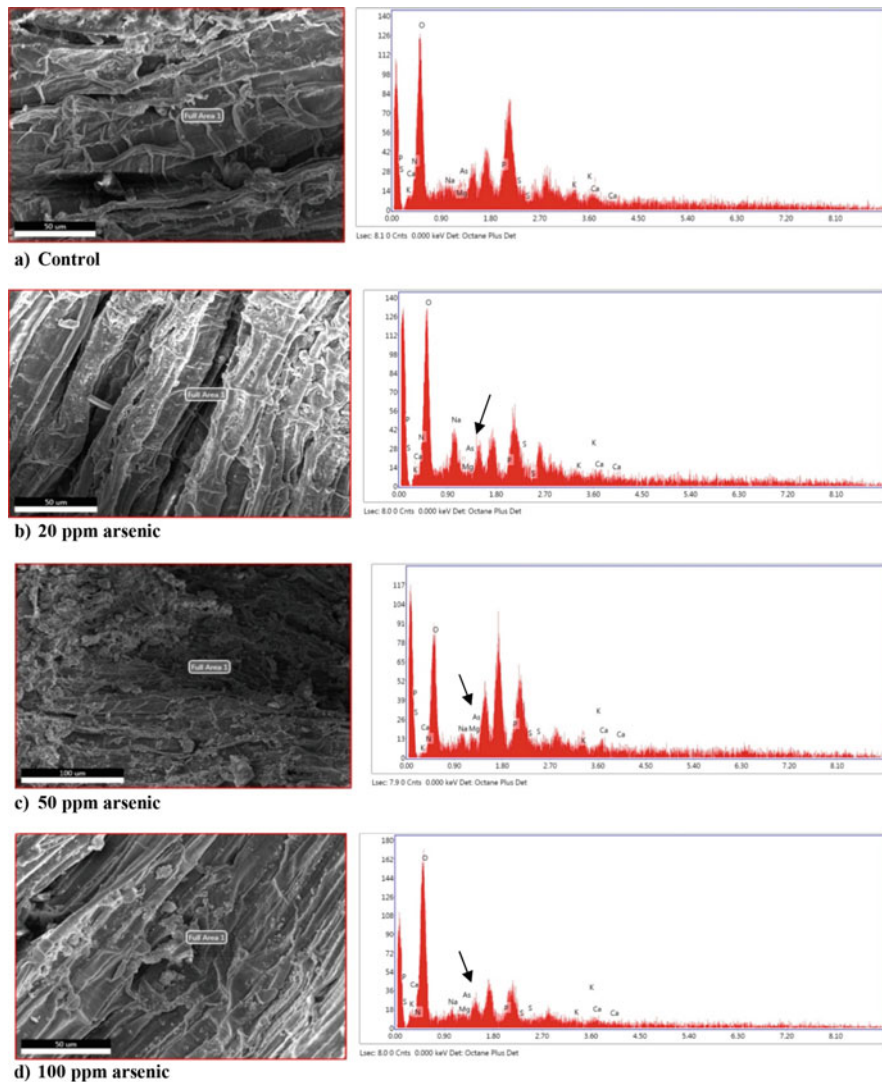


Fig. 8.14 FESEM micrographs of roots of *Allium sativum* L. with respect to (a) control, (b) 20 ppm, (c) 50 ppm, and (d) 100 ppm of arsenic and corresponding (EDAX) analysis

Table 8.5 Energy-dispersive X-ray spectroscopy (EDAX) of *Allium Sativum* L.

Plants parts of <i>Allium sativum</i> L.	Atomic % of As in control	Atomic % of As in 20 ppm	Atomic % of As in 50 ppm	Atomic % of As in 100 ppm
Leaves	0.00	0.00	0.00	0.00
Blubs	0.00	0.00	0.00	0.00
Roots	0.00	0.05	0.16	0.04

8.4 Risk Assessment and Remediation

The term “phytoremediation” is used to describe the cleanup of heavy metals from contaminated sites by plants. Phytoremediation, which signifies the use of plants to clean pollutants, represents a green and environmentally friendly tool for cleaning the heavy metal-polluted soil and water (Wallace et al. 1992). The conventional chemical and physical remediation technologies are generally too costly and often harmful to soil characteristics. The premise of this method is to find out the hyper accumulator of heavy metals, which has greater power to accumulate the heavy metals (Weigel and Jäger 1980). Arsenic is more toxic and widely distributed in the earth’s surface and present in four oxidation states: +5, +3, 0, and -3 (Wójcik et al. 2005). However, the high amount of these states of arsenic is in the pentavalent and the trivalent forms. In this study, we see that *Allium sativum* L. were easily grown in arsenic-contaminated soil. *Allium sativum* L. uptake arsenic up to root portions and consequently stored in roots (Fig. 8.14), which agrees with the findings by Zhang et al. 2000. Only roots of *Allium sativum* L. were affected, and other parts of plants were not affected. The other parts like blubs and leaves did not contain arsenic, so such parts of plants may be used for edible purpose. *Allium sativum* L. were capable of uptaking arsenic easily (Zornoza et al. 2002). If we select this plant for arsenic remediation from any contamination area, we may get a less contaminant zone by a cost-effective approach.

8.5 Conclusion

Arsenic was known for its toxicity in plants and animals. This study concluded that arsenic adversely affects the growth of all plant parts and yield of the *Allium sativum* L. In this study, arsenic effects on *Allium sativum* L. growth and chromosomal structures are observed. Accumulation of arsenic was detected only up to the root system of *Allium sativum* L. In many of the arsenic-affected countries like Bangladesh, India (some Districts of West Bengal), Nepal, Vietnam, and Southern China, *Allium sativum* L. was a much cultivated crop. The contamination level is low in these arsenic-affected areas and the contamination occurs at the rooting level of *Allium sativum* L., so this plant can be used as an agriculturally viable and efficient phytoaccumulator. In such a case, only root parts of *Allium sativum* L. accumulated arsenic, whereas the leaf and bulb system did not, which would encourage the farmers to harvest *Allium sativum* L. (garlic).

Acknowledgement The authors acknowledge the Ramananda College, Bishnupur, Bankura for providing financial assistance to carry out this research work. The authors also acknowledge the Ph. D. scholar Sutapa Deb, Department of Civil Engineering, Indian institute of Technology Kharagpur (IIT) for helping with the FESEM-EDAX study.

References

- Abedin MJ, Meharg AA (2002) Relative toxicity of arsenite and arsenate on germination and early seedling growth of rice (*Oryza sativa* L.). *Plant Soil* 24(3):57–66
- Bushra A, Abdul FM, Naimat AM, Ahmad M (2002) Clastogenecity of pentachlorophenol 2,4-D and Butachlor evaluated by *Allium sativum* root tip test. *Mutat Res* 514:105–113
- Carbonell-Barrachina AA, Burlo-Carbonell F, Mataix-Beneyto J (1995) Arsenic uptake distribution and accumulation in tomato plants and effect of arsenic on plant growth and yield. *Plant Nutri* 18:1237–1250
- Chakraborty R, Mukherjee AK, Mukherjee A (2008) Evaluation of genotoxicity of coal fly ash in *Allium cepa* L. *Environment Moniterring Assessment* 15(3):351–357
- Chandran S, Niranjana V (2012) Accumulation of heavy metals in waste water irrigated crops in Mudurai India. *J Environ Res Develop* 6(3):432–438
- Chauhan LK, Saxena PN, Gupta SK (2001) Evaluation of cytogenetic effects of Isoproturon on the root meristem cells of *Allium sativum* L. *Biomed Environ Sci* 14(3):214–219
- Chopra AK, Pathak C, Prasad G (2009) Scenario of heavy metal contamination in agricultural soil and its management. *J Appl Nat Sci* 1(1):99–108
- Fargasova A, Listiakova J (2009) Cr and Ni simultaneous phytotoxicity and mutagenicity assay. *Nova Biotech* 9(2):107–112
- Fiskesjo G (1985) The allium test as a standard in environmental monitoring. *Hereditas* 10 (2):99–112
- Fiskesjo G (1995) Allium test *In vitro* toxicity testing protocols. *Methods Mol Biol* 43:119–127
- Fiskesjo G (1997) Allium test for screening chemicals evaluation of cytologic parameters in plants for environmental studies. 33:308–333
- Han FX, Di M, Plodinec MJ, Banin A, Triplett GB (2003) Assessment of global industrial-age anthropogenic arsenic contamination. *Natur wissenschaften* 90:395–401
- Han FX, sridhar BBM, Di M (2004) Phytoavailability and toxicity of trivalent and hexavalent chromium to *Brassica juncea*. *New Phytol* 16(9):489–499
- Komar KM, Zhang W, Kenelley ED (2001) A fern that hyper accumulates arsenic. *Nature* 40 (9):579
- Kumar G, Tripathi A (2003) Comparative mitotoxicity and mutagenicity of two heavy metals in *Allium cepa* L. *Cytol Genet* 4:169–173
- Kwankua W, Sengsai S, Muangphra P, Euawong N (2012) Screening of plants sensitive to heavy metals using cytotoxic and genotoxic biomarkers. *Nat Sci* 46:10–23
- Losi ME, Amrhein C, Frankenberger W (1994) Factors affecting chemical and biological reduction of cr (vi) in soil. *Environ Toxicol Chem* 13:1727–1735
- Lytle CM, Lytle FW, Yang N, Qian J, hansen D, Zayed A, Terry N (1998) Reduction of cr (vi) to cr (iii) by wetland plants potential for *in situ* heavy metal detoxification. *Environ Sci Technol* 32:3087–3097
- Marimuthu KM, Subramaniam MK (1960) A haematoxylin squash method for the root tips of *Dolichos lablab* L. *Curr Sci* 29:482–493
- Marin AR, Masscheleyn PH, Patrick WH (1992) The influence of chemical form and concentration of arsenic on rice growth and tissue arsenic concentration. *Plant Soil* 13(9):175–183
- Nagpal A, Grover IS (1994) Genotoxic evaluation of systemic pesticides in *Allium cepa* L. mitotic effects. *Nucleus* 37:99–105
- Panda SK, Patra HK (1997) Physiology of Cr toxicity in plants-a review. *Plant Physiol Biochem* 24 (1):10–17
- Puryear JD, Newton RJ (2002) Assessment of cr tolerance and accumulation in selected plant species. *Plant Soil* 24(7):223–231
- Singh RN, Keefer RF (1989) Uptake of nickel and cadmium by vegetables grown on soil amended with different sewage sludges. *Agric Ecol Environ* 25:27–38

- Singh DK, Sharma YK (2007) Response of wheat seed germination and seedling growth under copper stress. *Environ Biol* 28:409–414
- Srivastava S, Jain R (2010) Effect of distillery spent wash on Cytomorphological behavior of sugarcane settlings. *J Environ Biol* 3(5):809–812
- Wagner GJ (1993) Accumulation of cadmium in crop plants and its consequences to human health. *Adv Agron* 51:173–212
- Walker WM, Miller JE, Hassett JJ (1977) Effect of lead and cadmium upon the calcium, magnesium, potassium, and phosphorus concentration in young corn plants. *Soil Sci* 12(4):145–151
- Wallace A, Wallace GA, Cha JW (1992) Some modifications in trace metal toxicities and deficiencies in plants resulting from interactions with other elements and chelating agents—the special case of iron. *J Plant Nutr* 15:1589–1598
- Weigel HJ, Jäger HJ (1980) Subcellular distribution and chemical form of cadmium in bean plants. *Plant Physiol* 65:480–482
- Wójcik M, Vangronsveld J, D’Haen J, Tukiendorf A (2005) Cadmium tolerance in *Thlaspi caerulescens* and localization of cadmium in *Thlaspi caerulescens*. *Environ Exp Bot* 53:163–171
- Zhang G, Fukami M, Sekimoto H (2000) Genotypic differences in effects of cadmium on growth and nutrient compositions in wheat. *J Plant Nutr* 23:1337–1350
- Zornoza P, Vázquez S, Esteban E, Fernández M, Carpena R (2002) Cadmium-stress in nodulated white lupin strategies to avoid toxicity. *Plant Physiol Biochem* 40:1003–1009

Chapter 9

Spatio-temporal Analysis of Open Waste Dumping Sites Using Google Earth: A Case Study of Kharagpur City, India



Abhishek Singhal and Sudha Goel

Abstract Google Earth provides high resolution satellite images over a long period of historical time period which can be used to study land use/land cover (LULC) changes in any area over an extended period of time. In this study, Google Earth Pro was used to identify problems with current locations of solid waste dumping sites and conduct a time-series analysis of the areas occupied by waste dumping sites in Kharagpur city. Five dumping locations were studied of which three are official dumping sites, one is an illegal dumping site and the last one is an official dumping site which was cleaned in 2015. Satellite images of the same dumping locations were taken to evaluate changes in the areas of the dumping sites from 2010 to 2017. The results of the study show that most of the sites are situated very close to an airbase runway, railway line, residential area or highway/road which is in contravention of regulations. Time-series analysis shows that the sizes of all dumps have varied significantly with respect to time except for the unauthorized dumping site. The reasons behind the fluctuations in area are frequent burning of garbage and partial clean-up of the site due to local complaints. The methodology used in this study can be extended to an entire city or even several cities to find problems related to the existing illegal or official waste dumping site within a specific time period.

Keywords Municipal solid waste · Open dumps · Satellite images · Google Earth · Time-series analysis

9.1 Introduction

According to the latest Census of India, the population of India in 2011 was 1.21 billion, which makes India the second most populated nation in the world. The urban population in India in 2011 was 377 million, while in 2001 it was 285 million which

A. Singhal (✉) · S. Goel

Civil Engineering Department, IIT Kharagpur, Kharagpur, West Bengal, India
e-mail: sudhagoel@civil.iitkgp.ac.in

© Springer Nature Switzerland AG 2021

P. K. Shit et al. (eds.), *Spatial Modeling and Assessment of Environmental Contaminants*, Environmental Challenges and Solutions,
https://doi.org/10.1007/978-3-030-63422-3_9

137

represents a 2.8% annual exponential increase in urban population in the last census decade. With an increasing population, India is also a growing economy with an annual economic growth rate that is more than 5% (OGD Platform India). Increasing resource consumption and growing population implies that more waste is being generated by the increasing population. Thus, India's one of the biggest challenges today is management of the exponentially increasing quantities of municipal solid waste (MSW) generated.

As population is increasingly exponentially and per capita resource consumption is also increasing, solid waste management (SWM) services are not able to keep up with the increasing quantities of waste being generated (Goel 2008). The current SWM practices are inefficient, require heavy expenditure and are a potential threat to public health and the environment (Biswas et al. 2010). Most countries are still struggling to deal with their problems related to growing waste (Agamuthu et al. 2009). In large India cities, collection efficiency is around 70–90% of MSW generated, whereas in smaller cities and towns it is less than 50% of total waste generated (Sharholy et al. 2008). This uncollected waste is either burned or dumped illegally on open land causing health problems and environmental degradation (Annepu 2012; Sharholy et al. 2008; Kumar 2010). Exposure to pollutants like carbon monoxide (CO), carcinogenic hydrocarbons (HC) (includes dioxins and furans), particulate matter (PM), nitrogen oxides (NO_x) and sulphur dioxide (SO₂) can occur due to uncontrolled burning of garbage as shown in a detailed study in Mumbai (NEERI and CPCB 2010).

The problem of unsanitary landfilling is directly related to the lack of financial resources of the urban local bodies (ULBs). ULBs spend about \$10–\$30 (INR 500–1500) per ton on SWM (Department of Economic Affairs 2009). Despite large financial inputs, only about 60–70% of this amount is spent on collection, 20–30% on transportation and no funds are allocated for proper disposal of waste (Kumar 2010; Department of Economic Affairs 2009). India is still creating infrastructure for SWM which is a very heavy financial burden and is often done by borrowing money from international lending agencies like the World Bank or from market and private sources.

Based on annual reports provided by State Pollution Control Boards to the Central Pollution Control Board for the period April 2013 to Dec 2016, the amount of MSW generated in India in urban local bodies (ULBs) was 135,198 tons/day, while the amount collected was 111,028 tons/day (82% of generated waste). Only 25,572 tons/day was the amount treated (18.9% of the generated MSW), while some of the waste was disposed in landfills and is estimated to be 47416 tons/day (35%) (CPCB 2017). The remaining waste remains in the open dumpsites increasing environmental burden in the urban areas (Peter et al. 2019).

As mentioned above, a large fraction of the MSW collected in India is disposed on open land or in unsanitary landfills. In most large metropolitans, existing landfill sites are exhausted and the responsible urban local bodies do not have resources to acquire new land (Annepu 2012). As the area provided for landfills is completely occupied, the only remaining option is to increase the height of the dumps. In many cities like Mumbai, Delhi, Ahmedabad and Kolkata, the dumping sites now have

man-made mountains of garbage. The dumping site in Dhapa, Kolkata is 17 m high, three open dumping sites in Delhi have heights of more than 40 m and Deonar dumping ground in Mumbai has an area of 144 hectares and height of roughly 55 m (Saldanha and Lukose 2014). Leachate generated from unsanitary landfills contaminates soil, surface and groundwater resources (Sharholly et al. 2008; Biswas et al. 2010). Using water contaminated by solid waste for bathing, food processing, irrigation and drinking exposes individuals to disease organisms and other contaminants (Hoorweg and Bhada-Tata 2012). MSW dumped in landfills also generates greenhouse gases like methane which has 21 times more global warming potential than carbon dioxide. According to International Energy Agency, improper dumping of SWM contributes to 6% of India's methane emissions and is the third largest source of methane in India. This is much higher than the global average of 3% methane emissions from solid waste. Solid waste currently produces 16 million tons of CO₂ equivalents per year and this number is expected to rise to 20 million tons of CO₂ equivalents by 2020 (International Energy Agency 2009).

Geospatial and remote sensing (RS) technologies now become widely available, readily accessible and more apparent in our daily lives than ever before (Bodzin et al. 2014). Together, RS and GIS have been widely used in various stages of MSWM like waste collection and transportation, route optimization, calculating size of dumping sites and identifying landfill fires (Brimicombe 2003; Dutta and Goel 2017; Khan and Samadder 2016; O'Connor 2013). However, some preliminary knowledge is required to use RS and GIS tools. Learning to use satellite imagery data and software like ArcGIS, Q-GIS and ERDAS takes time, experience and effort to use them efficiently and precisely. Simple tools and software like Google Maps, Bing Maps, Google Earth and Google Earth Pro can also be effectively used for climate and environmental studies due to the availability of high-resolution satellite images. Google Earth software is a virtual globe that contains and integrates a wide arrangement of remotely sensed and modelled images created with various satellite and aircraft data at different points in time. In Google Earth, available images can be zoomed in to where the resolution is about 1–15 m/pixel enabling users to identify physical features such as river catchments, canyons, agricultural fields and mountains along with their elevations (Bodzin et al. 2014). Currently, researchers have been using Google Earth to visualize data for studying various environmental issues and phenomenon including LULC change impacts on river basin, to study flow and dispersion of pollutants, forest conservation, mapping mining areas and its impacts assessment, etc. (Gorelick et al. 2017; Kumar and Mutanga 2018; Liu and Kenjeres 2017; Tsai et al. 2018; Zurqani et al. 2018). Google Earth can be a very effective tool to generate data for the areas where good quality RS-GIS data is unavailable. Google Earth can be used to identify various dumping locations in and around cities and to evaluate changes in the shape and size of these dumpsites with respect to time.

The objective of this study was to analyse changes in the shape and size of the open dumping sites over a period of time and to evaluate problems related to unsystematic dumping practices using Google Earth. The area selected for the study was Kharagpur city situated in the state of West Bengal, India. Changes in land use/land cover (LULC) are routinely monitored using Google Earth Pro and the

same concept was applied for delineation of open solid waste dumping sites in Kharagpur from 2010 to 2017. The approach used in the study was quite simple and Google Earth is an easily accessible software due to which anyone with a basic idea about online satellite maps (like Google Maps, Bing Maps) and MSWM can use this approach. Besides the simplicity of the approach, the present study can provide valuable information to planners and decision-makers regarding land use/land cover changes over time. This methodology can also be adopted for regular monitoring of solid waste dumping sites in any city or town.

9.2 Study Area and Current Scenario of MSW Management in Kharagpur

Kharagpur is in West Bengal, India and is about 120 km away from Kolkata, one of the largest cities in India. Kharagpur has one of the largest railway workshops in India and the third longest railway platform (1.0725 km long) in the world. Kharagpur is located at Latitude 22.33°N and Longitude 87.32°E with an average elevation of 29 m (95 ft.) above mean sea level. Kharagpur municipal area has a population of 2,89,129 (according to the 2011 Census) spread over 91 km² area and is divided into 35 wards as shown in Fig. 9.1a. The Indian Air Force has two airbases close to Kharagpur city: Kalaikunda and Salua.

Major sources of MSW in the Kharagpur area are residential areas, commercial/market areas, government offices, hotels/restaurants and institutions. Kharagpur Municipality is responsible for the collection, treatment and disposal of solid waste. The estimated population of Kharagpur in 2017 is 314,628 persons and with a per capita waste generation rate of 0.5 kg/capita-day, the total amount of solid waste generated in Kharagpur is estimated to be 158 metric tons (MT)/day. Of this 158 MT of waste, only half of the waste is collected by the municipality, while the rest of the waste is either burned or dumped illegally. Due to poor collection efficiency and lack of proper waste treatment, illegal dumping of waste is common in the city. There are several illegal dumps in city; one of them is situated near the IIT Kharagpur flyover adjacent to a state highway and in between two railway tracks.

Characterization of MSW generated in Kharagpur city was done by Kumar and Goel (2009), which shows 19.6 % of the generated waste was recyclables (plastics, paper and textiles) and 80.4% was mixed residue (includes organic material, soil, mud and other inert materials). This mixed residue had an organic carbon content of 8.92 (± 5.92)% and fixed solids content of 80.35 (± 9.54)%. Due to hot and humid environmental conditions, organic matter degrades rapidly in the city resulting in foul smell when openly dumped.

Currently Kharagpur Municipality has two official dumping grounds where waste is dumped without any treatment: Nimpura and Ayma. At present there is no sanitary landfill in Kharagpur and location of all the present dumpsites are also not according to Indian regulations. According to Indian regulations, a landfill should be located at

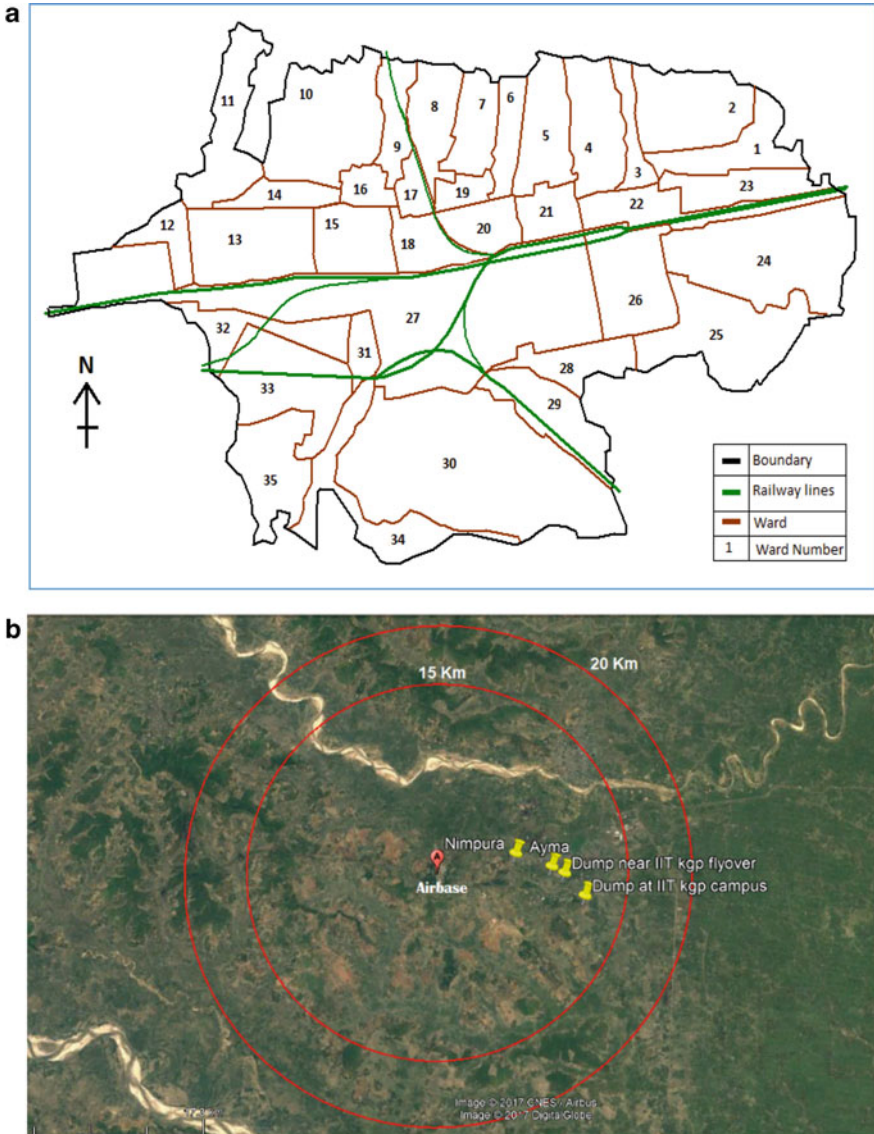


Fig. 9.1 (a) Cities of Kharagpur and Kolkata (Google Maps). (b) Location of dumping sites with respect to local airbase

least 500 m away from any residential settlement and State/National Highway and at least 20 km away from the airbase runway (SWM Rules 2016). Both Nimpura and Ayma are in contravention of these rules. The disposal site at Nimpura is less than 5 km away, whereas the site in Ayma is around 8 km away from the Kalaikunda Airbase (Fig. 9.1b).

Table 9.1 Location of dumpsites studied and time period of time-series analysis study

Dumpsite	Latitude	Longitude	Time-series analysis period
OT road	22°21'43.38"N	87°20'17.26"E	Jan-2010 to Nov-2015
Ayama	22°19'56.22"N	87°17'58.42"E	Jan-2011 to Oct-2016
Nimpura	22°20'30.17"N	87°16'18.89"E	Jan-2011 to Oct-2016
Near IIT Kgp flyover	22°19'38.40"N	87°18'34.36"E	Nov-2014 to Oct-2016
Inside IIT Kharagpur	22°18'42.45"N	87°19'30.12"E	May-2012 to Jan-2017

9.3 Material and Methodology

A time-series analysis was done by comparing satellite images of the same dumpsite location at different times. Historical satellite images were obtained by using historical imagery in Google Earth Pro software (version 7.3.1.4507(64-bit)). A total of five dumpsites were studied in the present study. Location of five dumpsites and study period of the time-series analysis are shown in Table 9.1. Area and perimeter of each dump were calculated by drawing the outline of the dumps in the mapping software. Time-based comparison of dumps was done on the basis of the area rather than perimeter. Since area and perimeter were not always directly proportionate to each other, area was found to be a better estimate of the size of a dump rather than the perimeter. Satellite images before 2010 are not used for time-series analysis due to their poor resolution which may lead to a false conclusion. Also, many satellite images after 2010 were also not very clear due to cloud cover or poor resolution or darkness, so only clear and good resolution satellite images were used in the study for accurate results.

After completing the time-series analysis, possible reasons were sought for change in size of dumps by visiting the sites and conducting a ground survey. Personal interviews and meetings with authorities responsible for waste management (Kharagpur Municipality and IIT Kharagpur Sanitation department), nearby residents and ragpickers also provided some reasons for changes in dump areas. Further, to check locations of the dumpsite as per Indian regulations, distance of dumpsites was calculated from the airbase runway, nearby railway line and nearby roads using the ruler tool in Google Earth Pro.

9.4 Results and Discussion

9.4.1 Site Near OT Road (Dumpsite 1)

Kharagpur municipality was using the site on Orissa Trunk (OT) road from 2007 to 2015 for dumping solid waste. This dumpsite was cleaned in 2015 for widening of OT road and now there are several big business establishments along this road and others are planned as well. Prior to 2015, it was one of the major dumping grounds

for municipal waste and fly ash from a neighbouring thermal power plant (Kumar and Goel 2009). Comparison of satellite images from 20-January-2010 to 22-November-2015 is shown in Table 9.2. The size of the dump increased from 20-January-2010 to 30-March-2014 and started declining after that because municipality cleaned the site and transferred waste to another site (Fig. 9.2 shows the result of time-series study of OT road dumpsite). By the end of 2015, the site was cleaned up completely and currently, there is a residential complex at the dumping site.

9.4.2 Site Near Railway Workshop in Ayma (Dumpsite 2)

Kharagpur Municipality has been using the site in Ayma since 2006. This site is situated near the railway workshop and waste is dumped near the workshop building and the railway lines. There is a huge vacant area at the back of the workshop where waste is dumped at three different locations around 160–170 m apart from each other (Fig. 9.3). Ayma is located 8 km away from the Kalaikunda Airbase of the Indian Air Force which is not in accordance with Indian regulations.

Comparison of satellite images from 13-January-2011 to 30-Oct-2016 is shown in Table 9.2. The size of this dump increased from 2011 to 2013, but after 2013, the size of the dump started fluctuating. Comparing images from 2013 and 2016, it is clear that the size of the dump has reduced significantly (Fig. 9.3). Reason behind the reduction in the dump size was frequent burning of the waste at the dumping site. Waste is burned frequently at the other dumping sites in the city by the municipality or local people to reduce the size of the garbage pile. Currently, Ayma dumping site occupies an area of 0.65 hectares of the land and its leachate flows directly to an open drain. The soil in Ayma is laterite soil which is highly permeable due to which chances of groundwater contamination are very high in the area.

9.4.3 Dumping Site in Nimpura (Dumpsite 3)

The waste dumping site at Nimpura is amidst a densely populated area, and the nearest settlement is not more than 10 m away from the site. Problems of foul smell and pests (especially mosquito and flies) are quite common in the area and in the rainy season it gets worse. Nimpura is also located in the proximity of the Kalaikunda Airbase of the Indian Air Force just like the disposal site at Ayma. The disposal site at Nimpura is less than 5 km away from the airbase due to which risks of scavenger bird hits are greater at Nimpura compared to all other sites.

Currently, the Nimpura dumping site covers 0.66 hectares of land. Comparison of satellite images from 13-January-2011 to 30-Oct-2016 is shown in Table 9.2. The size of this dumping site increased from 2011 to 2013, but after 2013 the size of the dump start decreasing till 2015 after which it has been increasing continuously. Reasons for size reduction include cleaning of a part of the site when garbage is

Table 9.2 Results of time-series analysis on all five dumpsites

Dates	OT Road dumpsite			Ayma dumpsite			Nimpura dumpsite			Kgp flyover dump			ITT Kgp dumpsite	
	Area (in m ²)	Perimeter (in m)		Area (in m ²)	Perimeter (in m)		Area (in m ²)	Perimeter (in m)		Area (in m ²)	Perimeter (in m)		Area (in m ²)	Perimeter (in m)
20 Jan 2010	472	90		–	–		–	–		–	–		–	–
18 Dec 2010	1201	133		–	–		–	–		–	–		–	–
13 Jan 2011	–	–		4937	586		3137	345		–	–		–	–
20 May 2012	2718	222		9135	1168		–	–		–	–		0	0
19 Apr 2013	–	–		13,256	1318		–	–		–	–		–	–
20 May 2013	–	–		–	–		6363	355		–	–		34,998	1154
30 Mar 2014	3673	491		11,259	1461		5815	344		–	–		52,022	1807
17 Jun 2014	3439	501		–	–		–	–		–	–		–	–
6 Nov 2014	–	–		–	–		–	–		0	0		–	–
22 Nov 2015	0	0		9065	1319		5244	389		3582	350		48,015	2165
29 Mar 2016	–	–		10,394	1464		6184	380		3999	393		68,034	1883
30 Oct 2016	–	–		6438	1187		6578	375		4488	415		13,653	1706
05 Jan 2017	–	–		–	–		–	–		–	–		33,978	1813

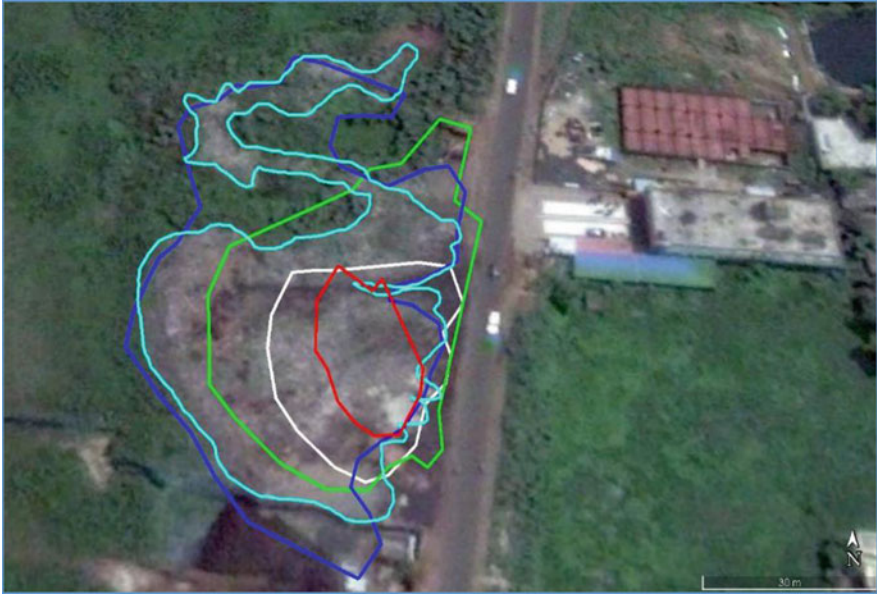


Fig. 9.2 Time-series analysis of OT road site from 20-Jan-2010 to 22-Nov-2014 (colour code: red, 20-Jan-2010; white, 18-Dec-2010; green, 20-May-2012; blue, 30-Mar-2014; cyan, 17-Jun-2014)



Fig. 9.3 Time-series analysis of Ayma dumpsite (colour code: Red, 13-Jan-2011; white, 20-May-2012; green, 19-Apr-2013; yellow, 30-Mar-2014; black, 22-Nov-2015; cyan, 29-Mar-2016; pink, 30-Oct-2016)

dumped too close to the adjacent road. Reported by the local residents and rag-pickers, the dumpsite is partially cleaned many times but never cleaned completely (Fig. 9.4).

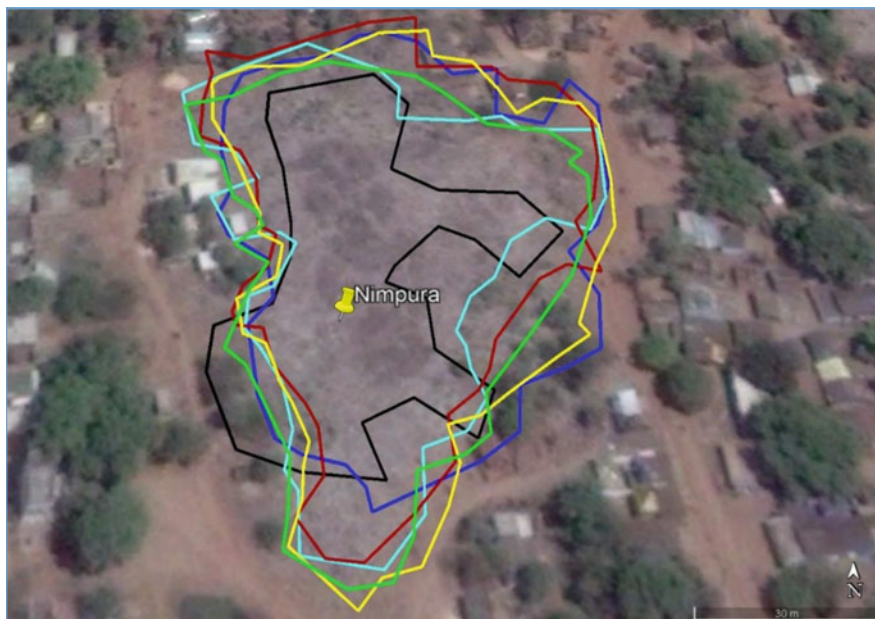


Fig. 9.4 Time-series analysis of Nimpura dumpsite (colour code: black, 13-Jan-2011; blue, 20-May-2013; green, 17-Mar-2014; cyan, 22-Nov-2015; red, 29-Mar-2016; yellow, 30-Oct-2016)

9.4.4 *Illegal Dumping Site Near IIT Kharagpur Flyover (Dumpsite 4)*

Another major waste dumping site is close to IIT Kharagpur campus and on State Highway-5 (SH-5) just at the end of the IIT Kharagpur flyover. It is an illegal dumping site used by the residents of Ward 27. This dumping site is located between two railway lines as shown in Fig. 9.5. This dumpsite is also located in the proximity of the Kalaikunda Airbase just like Ayma and Nimpura dumpsites (9.5 km away from the runway).

Initially, the site was created for dumping waste construction material from the construction of the adjacent flyover. Residents in the area started dumping their garbage illegally at this location mainly due to the absence of community bins in the ward at that time. Slowly this illegal dumping site started expanding and currently, it occupies an area of 0.45 hectare with a height varying from 0 to 2.5 m. In terms of topography, the dumping site is situated at higher ground level compared to nearby areas including the road. Due to this, leachate generated goes directly into the stormwater drains and during heavy rains, leachate enters houses adjacent to the waste dumping site (houses are <100 m away). Many street animals move over the site and scatter waste alongside the road (Fig. 9.5b). Many accidents have also occurred on the highway and railway line due to stray animals.



Fig. 9.5 (a) Time-series analysis of illegal dumpsite near Kgp flyover (colour code: blue, 22-Nov-2015; yellow, 23-Mar-2016; black, 30-Oct-2016). (b) Picture of the illegal dump where waste is scattered along the road

The earliest satellite image in which dumping is apparent is from Nov 2015; no dumping is apparent in the image from 06-Nov-2014. Therefore, dumping at the site is likely to have started in late 2014 or in early 2015. On comparing images of 22-Nov-2015 and later, it is clearly visible that within a year, the size of the dump increased significantly and continues to grow. Even though garbage at the site is burned on continuous basis but size of the dumpsite still keeps on increasing. On 30-Oct-2016, size of this illegal dump was about 0.45 hectare.

9.4.5 Dumping Site in IIT Kharagpur Campus (Dumpsite 5)

The campus of Indian Institute of Technology Kharagpur is at the southern end of the city, i.e., Ward 30 of Kharagpur city. Another waste dumping site is located inside the campus boundary near the south-west corner of the campus. Currently, the site is used for dumping of institutional waste (waste generated from hostels, campus markets, departments and laboratories) and construction and demolition (C&D) waste. The nearest settlement is within the institute boundary and 400 m away from the dumpsite. Further, the site is hardly 50 m away from the road and 55–60 m away from the railway line (Fig. 9.6a). The distance of this site from Kalaikunda airbase runway is 11.5 km which is again not in accordance with regulations. During the rainy season, leachate generated from the dump accumulates in a nearby pit having an area of approximately 500 m². This accumulated leachate is a suitable environment for breeding mosquitoes and other harmful pests resulting in health hazards for sanitary workers, ragpickers and others working in the area. Also, this accumulation of leachate increases the chances of groundwater contamination due to shallow groundwater table depth (5–10 m) and highly permeable laterite soil.

The institute sanitation department started using this site for dumping waste in late 2012. In a time-series analysis of this site, it was seen that the size of the dump increased significantly from 20-May-2013 to 30-March-2014. Most of the waste from the site was cleaned after March-2014 and the rest of the waste was burned at the site due to which the size of the dump decreased considerably. After Mar-2014, the size of the dump increased again until 29-March-2016. In April-2016, there was a fire accident in the campus, near the dumping site. The fire spread rapidly in nearby areas because of dry vegetation. A large part of the waste dump also caught fire due to which the size of the dump was reduced drastically. After 30-October-2016, the area of the dumpsite has been increasing again. Based on the 05-Jan-2017 satellite image, the dumping site occupies an area of 3.4 hectares.

Garbage is burned on a weekly basis to reduce the size of the dump (Fig. 9.6b) despite regulations against it. The smoke resulted from open burning is a health hazard for those exposed to it due to the presence of high concentrations of dioxins, sulphur oxides, nitrogen oxides, carbon oxides, arsenic and lead. In the daytime, there are many ragpickers at the site, collecting plastics, metal and other recyclables while children often play nearby. So, these ragpickers and their children are directly exposed to this hazardous smoke on a daily basis. Besides regular institutional waste, hazardous waste generated from chemical and biological labs was also dumped at the site (Fig. 9.6b). This could be a greater threat to the ragpickers, sanitary workers and nearby environment compared to regular MSW. Burning of this hazardous waste will many times increase the toxicity and exposure of the toxic smoke.

Soil near the dumping site is highly permeable laterite and the average groundwater table depth is just 5–10 m below the ground surface. Therefore, the chances of groundwater contamination are extremely high and due to hazardous waste at the site

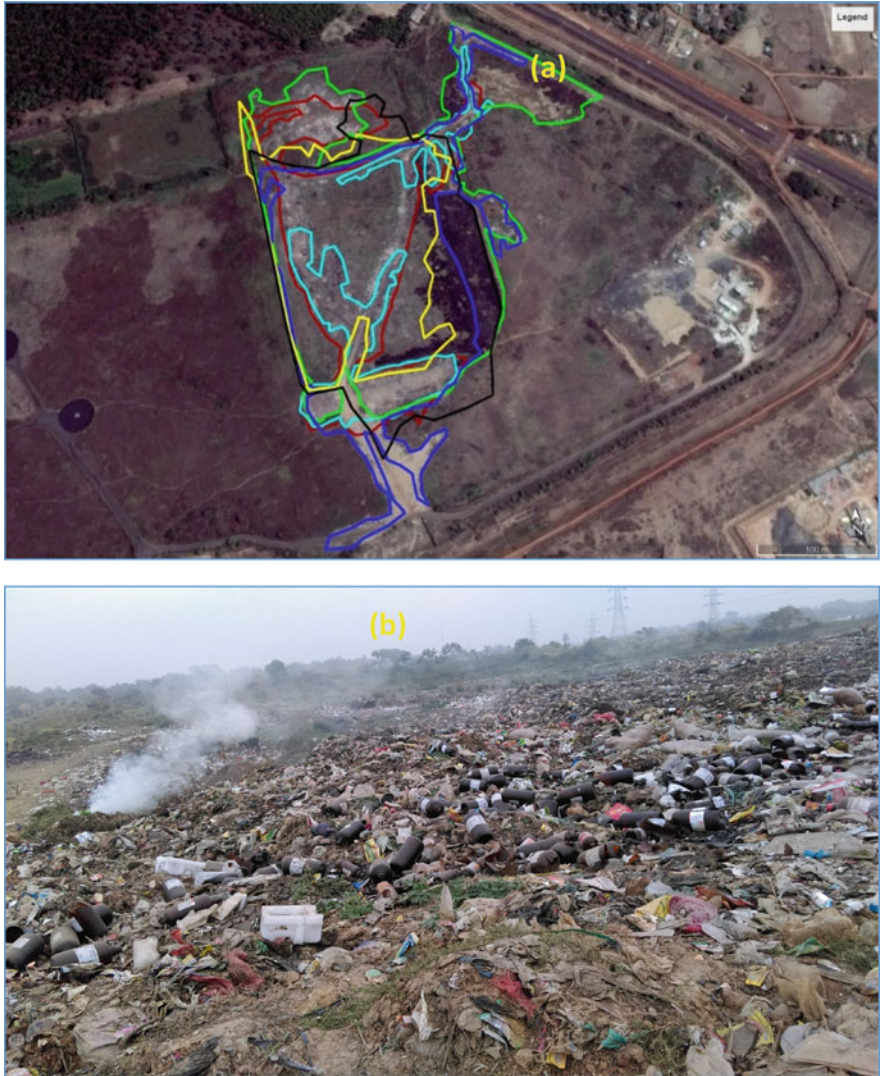


Fig. 9.6 (a) Time-series analysis of dumpsite at IIT Kharagpur (colour code: yellow, 20-May-2013; black, 30-Mar-2014; blue, 22-Nov-2015; green, 29-Mar-2016; cyan, 30-Oct-2016; red, 05-Jan-2017). (b) Current photo of the dumping site at IIT Kharagpur. (c) Open burning of garbage and empty chemical bottles/containers at the site

it could lead to a catastrophe. In the Prembazar area, which is hardly 500–700 m away from the dumping location, many people still use groundwater via hand pumps or open dug wells. So, if the groundwater gets contaminated it will directly affect the population in this area.

9.5 Conclusions

A time-series analysis of five municipal solid waste dumping sites in Kharagpur, including one that was closed in 2015, has been completed using historical satellite images from Google Earth Pro. These images along with information collected from municipality officials and local people were used to determine changes in the sizes of these dumping sites and the reasons for these changes. The results of the study show that except unofficial waste dumpsite, the area of all the dumping sites is varying significantly with the passing years. There are two major reasons behind these fluctuations in the area of the dumpsites. First is the frequent open burning of the garbage to reduce the size of the dump piles. Second is the partial cleaning of the dumpsites to reduce the dump size or due to large number of complaints by local residents. The unofficial waste dumpsite is continuously increasing from 2015. Locations of all the five dumpsites are not in accordance with the Indian regulation, all of them are located in the proximity of the nearby airbase (<12 km) and two of the sites are located around a densely populated area (<100 m). Currently all the five dumpsites are degrading nearby environmental quality, especially IIT Kharagpur dumpsite which is a much greater threat due to frequent dumping and open burning of the hazardous waste. This work shows that it is possible to use Google Earth in conjunction with ground-based information to rapidly evaluate changes in land use/land cover and quantify areas covered by waste dumping sites. The methodology used in this study can be extended to cover an entire city or even several cities within a specific time period. Cleanliness drives and other programs initiated by the government can be monitored and quantified using these tools.

Declaration of Conflicting Interests

The authors declared no potential conflicts of interest with respect to the research, authorship and/or publication of this article.

Funding The authors received no financial support for the research, authorship and/or publication of this article.

References

- Agamuthu P, Khidzir KM, Hamid FS (2009) Drivers of sustainable waste management in Asia. *Waste Manag Res* 27(7):625–633
- Annepu RK (2012) Sustainable solid waste management in India. MS Thesis, Department of Earth Environmental Engineering, Columbia University, New York
- Biswas AK, Kumar S, Babu SS, Bhattacharyya JK, Chakrabarti T (2010) Studies on environmental quality in and around municipal solid waste dumpsite. *Resour Conservat Recycl* 55(2):129–134. <https://doi.org/10.1016/j.resconrec.2010.08.003>
- Bodzin AM, Anastasio D, Kulo V (2014) Designing Google Earth activities for learning Earth and environmental science. In *Teaching science and investigating environmental issues with geospatial technology*. Springer, Dordrecht, pp 213–232

- Brimicombe AJ (2003) A variable resolution approach to cluster discovery in spatial data mining. In International conference on computational science and its applications. Springer, Berlin, pp 1–11
- CPCB (2017) Annual review report: 2015-16. Delhi. www.cpcb.nic.in
- Department of Economic Affairs (2009) Position paper on the solid waste management sector in India. Ministry of Finance, Government of India
- Dutta D, Goel S (2017) Applications of remote sensing and GIS in solid waste management—a review. In Advances in solid and hazardous waste management. Springer, pp 133–151
- Goel S (2008) MSWM in India—a critical review. *J Environ Sci Eng* 50(4):319–328
- Gorelick N, Hancher M, Dixon M, Ilyushchenko S, Thau D, Moore R (2017) Google Earth Engine: Planetary-scale geospatial analysis for everyone. *Rem Sens Environ* 202:18–27
- Hoomweg D, Bhada-Tata P (2012) What a waste: a global review of solid waste management. World Bank, Washington, DC. <https://doi.org/10.1111/febs.13058>
- International Energy Agency (2009) Turning a liability into an asset : the importance of policy in fostering landfill gas use worldwide. Paris, France
- Khan D, Samadder SR (2016) Allocation of solid waste collection bins and route optimisation using geographical information system: A case study of Dhanbad City, India. *Waste Manag Res* 34(7):666–676
- Kumar S (2010) Effective municipal solid waste management in India. Rijeka, Croatia
- Kumar KN, Goel S (2009) Characterization of municipal solid waste (MSW) and a proposed management plan for Kharagpur, West Bengal, India. *Resour Conserv Recycl* 53(3):166–174
- Kumar L, Mutanga O (2018) Google Earth Engine applications since inception: usage, trends, and potential. *Rem Sens* 10(10):1509. <https://doi.org/10.3390/rs10101509>
- Liu D, Kenjeres S (2017) Google-Earth based visualizations for environmental flows and pollutant dispersion in urban areas. *Int J Environ Res Public Health* 14(3):247. <https://doi.org/10.3390/ijerph14030247>
- NEERI & CPCB (2010) Air quality assessment, emissions inventory and source apportionment studies: Mumbai, vol 2010. Mumbai
- O'Connor DL (2013) Solid waste collection vehicle route optimization for the City of Redlands, California. Master's thesis, University of Redlands. http://inspire.redlands.edu/gis_gradproj/201
- Peter AE, Nagendra SS, Nambi IM (2019) Environmental burden by an open dumpsite in urban India. *Waste Manag* 85:151–163
- Saldanha A, Lukose A (2014) Mumbai: city of garbage hits a dead end. *Indian Express*, February
- Sharholi M, Ahmad K, Mahmood G, Trivedi RC (2008) Municipal solid waste management in Indian cities—a review. *Waste Manag* 28(2):459–467
- Tsai Y, Stow D, Chen H, Lewison R, An L, Shi L (2018) Mapping vegetation and land use types in Fanjingshan national nature reserve using Google Earth Engine. *Rem Sens* 10(6):927. <https://doi.org/10.3390/rs10060927>
- Zurqani HA, Post CJ, Mikhailova EA, Schlautman MA, Sharp JL (2018) Geospatial analysis of land use change in the Savannah River Basin using Google Earth Engine. *Int J Appl Earth Observ Geoinf* 69:175–185

Part II
Water Contaminants, Risk Assessment and
Remediation

Chapter 10

Introduction to Part II: Water Contaminants, Risk Assessment, and Remediation



Pravat Kumar Shit

Abstract Nowadays water contamination is gaining importance because of its use in every sector. Non-point source pollutants especially which are coming out from the agricultural operation are diffuse in nature and very difficult to track and curb. The integration of RS, GIS, and geostatistics techniques with knowledge of hydrogeology has effectively been used to assess groundwater potential and the groundwater pollution problem. This section analyzed and synthesized on surface water and groundwater contaminants, risk assessment, and remediation using geospatial technology.

Keywords Arsenic contamination · Spatial water quality index · Microplastic contaminant · Hydro-chemical facies · Geochemical processes

10.1 Introduction

Since the dawn of civilization water plays an important role in societal development in many folds. Groundwater is the primary source of freshwater in many parts of the world. Some regions are becoming overly dependent on it, consuming groundwater faster than it is naturally replenished and causing water tables to decline unremittingly (Bhunia et al. 2018). Despite the increasing pressure placed on water resources by population growth and economic development, the laws governing groundwater rights have not changed accordingly, even in developed nations. Nor is groundwater depletion limited to dry climates: pollution and mismanagement of surface waters can cause overreliance on groundwater in regions where annual rainfall is abundant. Not only the direct anthropogenic activities related to contamination are severe, but also the natural contamination triggered by human activities like arsenic, fluoride, microbiological contamination has severe implications to

P. K. Shit (✉)

PG Department of Geography, Raja N. L. Khan Women's College (Autonomous), Vidyasagar University, Midnapore, West Bengal, India

© Springer Nature Switzerland AG 2021

P. K. Shit et al. (eds.), *Spatial Modeling and Assessment of Environmental Contaminants*, Environmental Challenges and Solutions, https://doi.org/10.1007/978-3-030-63422-3_10

155

environmental and human health. Soil salinity and sodicity have become the twin problem for sustainable agricultural development especially in the arid and semi-arid region of the world. Recently the microplastic pollution has added a new dimension to the environmental contaminants.

Due to faulty agricultural practices and change in land uses soil erosion has become rampant in many parts of the world. Soil erosion shows its on-site and off-site impacts. With the eroded soils huge amount of plant available nutrients are being lost from the fertile soils and deposited in the aquatic systems and pollute the aquatic ecosystems. Assessment of aquatic ecotoxicity is an important issue hunting the global community. Along with the surface runoff and sediments, the agrochemicals like pesticides are also coming to the rivers, lakes, and seas and entering into the food chain. Tons of domestic waste is dumped every day. Some waste from homes, offices, and industries can be recycled or burnt in incinerators. There is still a lot of garbage, such as refrigerators and washing machines that are dumped in landfills simply because they cannot be reused in anyway nor recycled. Plastics factories, chemical plants, oil refineries, nuclear waste disposal activity, large animal farms, coal-fired power plants, metals production factories, and other heavy industries all contribute to land pollution. Therefore pesticides contamination assessment and its effects on the human and other animals are also very important.

All these activities are not only concentrated on the surface water bodies. As our ecosystems are interlinked, groundwater contamination is also a big concern. Arsenic, fluoride, and heavy metals in the groundwater have risen in such level that it is directly affecting the well-being of the human population and the country's economy. Water pollution can be defined as alteration in physical, chemical, or biological characteristics of water through natural or human activities and making it unsuitable for its designated use (Shit et al. 2019). Freshwater present on the earth surface is put to many uses. It is used for drinking, domestic and municipal uses, agricultural, irrigation, industries, navigation, and recreation. The used water becomes contaminated and is called wastewater. Most of the water contamination is man-made. It may also occur naturally by addition of soil particles through erosion of animal wastes and leaching of minerals from rocks. The major source of water pollution is the wastewater discharged from industries and commercial bodies, these industries are chemical, metallurgical, food processing, textile, and paper industries. They discharge several organic and inorganic pollutants, which proves highly toxic to living beings. Now seawater ingression into the coastal lands is also possessing great threat to the people living along the sea coast.

Nowadays water contamination is gaining importance because of its use in every sector. Non-point source pollutants especially which are coming out from the agricultural operation are diffuse in nature and very difficult to track and curb. Modeling approach will be the best solution for this. For satisfactory calibration and validation of models we need huge and good quality data of surface water quality. As there are more and more people inhabiting the earth, food is in higher demand and so forests are chopped down and turned into farmland. In addition, herbicides, pesticides, artificial fertilizers, animal manure are washed into the groundwater and pollute it.

10.2 Individual Chapters

This second section of this book aims at reviewing and expanding the current state of knowledge on surface water and groundwater contaminants, risk assessment, and remediation. This section will provide an exhaustive overview of our current understanding of the contaminants process, impact on plant and human health and as well as environments. All chapters over extensively the literature present new results and management ideas through geospatial technology for future work.

In Chap. 11, Ghosh presents the groundwater arsenic contamination zone based on geospatial technology. This study has also reviewed the reason: how arsenic is transferred from contaminated irrigation water to plant, then to crop, and finally to our food chain. She also discusses the management approaches and some remedial measures to minimize the contaminant risk on plant and human health.

In Chap. 12, Adeola and Oluseyi present the relations between surface water pollution and industrial activities. They describe in detail the heavy metallic contaminants like As, Pb, Cr, Cd, and Ni at various points along the river. In Chap. 13, Mallick et al. examine the spatial water quality index (SWQI) in freshwater aquaculture regions using GIS techniques. Chapter 14 describes an overview of the heavy metal contamination in groundwater and its impact on plant and human health.

Chapter 15 written by a group of researchers under the lead of Ghosh well describes emerging threats of microplastic contaminant in freshwater environment and consequences. This chapter also emphasizes on the various remediation and pollution management strategies based on present approach and provides a research assessment for future research and advancement. In Chap. 16, Singh examined the particle size transport variability of suspended sediments in two alpine catchments over the lesser Himalayan region in India. In Chap. 17, Verma et al. describe the groundwater salinity, hydro-chemical facies, and corrosion indices. Chapter 18 written by Bat and their co-authors presents the threats to quality in the coasts of the Black Sea in heavy metal pollution of seawater, sediment, macro-algae, and seagrass.

Chapter 19 written by a group of researchers under the lead of Chakraborty discusses the groundwater quality for drinking through water quality index using geospatial modeling. They emphasize on health risk assessment on human body due to intake of contaminated groundwater. In Chap. 20 Khan and their co-authors have discussed pharmaceuticals and personal care products (PPCPs) in the conventional water treatment process and the consequences of aquatic environment. In Chap. 21 Kaur and Paikaray have examined the geochemistry during pre- and postmonsoon seasons in groundwater. They present new insights on the complex geochemical processes responsible for arsenic (As) toxicity enrichment and its mobilization control.

References

- Bhunias GS, Keshavarzi A, Shit PK, Omran ESE, Bagherzadeh A (2018) Evaluation of groundwater quality and its suitability for drinking and irrigation using GIS and geostatistics techniques in semiarid region of Neyshabur, Iran. *Appl Water Sci* 8(6):168
- Shit PK, Bhunia GS, Bhattacharya M, Patra BC (2019) Assessment of domestic water use pattern and drinking water quality of Sikkim, North Eastern Himalaya, India: a cross-sectional study. *J Geol Soc India* 94(5):507–514

Chapter 11

Groundwater Arsenic Contamination Zone Based on Geospatial Modeling, Risk, and Remediation



Merina Ghosh

Abstract Geospatial technique is very powerful tool to model and map groundwater arsenic contamination, to quantify the risk assessment process and helps to take remedial measures to counter the effect of contamination on both human and plants. This study aims to prepare map of groundwater arsenic contamination zone of district North 24 Parganas, of West Bengal, India, through geospatial interpolation technique and also to assess contaminant risk on plant and human. The arsenic concentration value of groundwater has been spatially distributed by Thiessen polygon interpolation technique. Depending on that spatial distribution, classification into seven arsenic concentration zones has been done for the entire district. Different levels of contamination zones have been defined by taking reference of maximum arsenic concentration limit declared by WHO, i.e., 0.01 mg/L for safe zone. To observe temporal as well as annual change in groundwater arsenic for further assessment of future risk, total six seasonal (pre/post-monsoon) data from year 2006 to 2008 has been analyzed and interpreted. Through this study the main threat found is the areas which were not arsenic affected in the pre-monsoon season of year 2006, became affected by the end of year 2008. Moreover, this research elucidates how the subsurface geology, surface water, and depth of the tube wells impact groundwater arsenic contamination of the study area. This study has also reviewed the reason how arsenic is transferred from contaminated irrigation water to plant to crop and finally it comes to our food chain. In addition, this study proposes some remedial measures to minimize the contaminant risk on plant and human.

Keywords Arsenic (As) · Spatial Interpolation · Thiessen Polygon · Hydraulic Station (HS) · PMTDI (Provisional Maximum Tolerable Daily Intake) · STW (Shallow Tube Well)

M. Ghosh (✉)

Department of Geography and Environment Management, Vidyasagar University, Midnapore, West Bengal, India

Geospatial Delhi Ltd., A Govt. of NCT of Delhi Company, New Delhi, India

© Springer Nature Switzerland AG 2021

P. K. Shit et al. (eds.), *Spatial Modeling and Assessment of Environmental Contaminants*, Environmental Challenges and Solutions,

https://doi.org/10.1007/978-3-030-63422-3_11

11.1 Introduction

Subterranean water contamination by arsenic in Bengal Basin is one of the worst chemical disasters which affect millions of people. This arsenic contaminated groundwater is main source of drinking as well as irrigation of the entire region, particularly in South-East Asia where large alluvial and deltaic plain occurs (mostly Bengal Delta). The maximum permissible limit set by WHO is 0.05 mg/L. But in this region the average arsenic concentration in groundwater has been reported several times higher of that limit. Unfortunately, such a dangerously contaminated groundwater is main drinking water source and also source of irrigation water for the immense population of this vast flood plain (Ghosh et al. 2020). Nearly about eleven districts in the territory of West Bengal, India has been reported to be badly affected by this water contamination through arsenic (As). Main source of arsenic in Bengal Delta is Arsenopyrite (FeAsS), the arsenic ore mineral.

Arsenic (As) belongs to group VB in periodic table and it is a naturally occurring mineral found widely in the environment. It is a colorless, orderless element and be present in numerous oxidation states, primarily arsenite and arsenate (Kinniburgh and Smedley 2001). Arsenite is trivalent and arsenate is pentavalent. The trivalent arsenic is more toxic than pentavalent (Tareq et al. 2003). World Health Organization warned that consumption of arsenic contaminated drinking water which exceeds 0.05 mg/L on long term basis could become significant cause of cancer called arsenicosis in human health. Arsenicosis is a chronic illness which produces so many diseases like skin disorder (Melanosis Palm and Keratosis sole), gangrene and cancers of the kidneys and bladder (Fig. 11.1).

Thus, detection and zonation of groundwater arsenic contamination could prevent these diseases to widespread as treatment of these diseases is very costly. But there is no concrete information sheet or digitized map from which one can get information about arsenic prone zone or from where one can get arsenic free safe drinking water. So zonation mapping of groundwater arsenic contamination through geospatial interpolation technique on basis of limited in situ sparse sampling data can be a cost-effective method for detection of contamination at a non-sampled location (Chowdhury et al. 2010).

The main objective of this research study is to detect and map the arsenic contamination zone by spatial modeling through geospatial interpolation technique.



Fig. 11.1 Arsenical skin diseases including (a) Melanosis Palm & Keratosis Sole, (b) Gangrene, (c) Melanosis Palm & Keratosis Sole, (d) Melanosis Palm, (e) Keratosis Sole. Source: www.hindi.indiawaterportal.org

For zoning of arsenic contamination, a deterministic interpolation approach, i.e., Thiessen polygon technique, has been applied to the entire available data set and after that by incorporating field based analytical data contamination risk has been assessed by analyzing different seasonal and annual maps. The average arsenic concentration value and year/season of data collection are used as variables for graphical presentation of risk. This study also reviewed that how utilization of contaminated irrigation water on long term basis for agricultural purpose poses threat of arsenic consumption on plant species and finally it comes to food chain through crop for human dietary exposure. This research note also suggested some remedial measures to combat against this chemical environmental menace.

11.2 Materials and Methodology

11.2.1 Study Area and Data

District North 24 Parganas of West Bengal, India is the present study area for this research. This district is one of the most horrible arsenic affected districts of the state West Bengal. On the east side this district shares the international boarder of Bangladesh and on the west it is bordered by Hugli River. It is positioned in the southern part of The Bengal Delta. Latitudinal extent of the district falls between 22 °08"N and 23 °16"N and longitudinal extension is from 88 °18"E to 89 °04"E surrounding an area of near about 4049 sq. km. As per Census 2011 the district comprises 22 blocks with a very high population density, i.e., 2445 persons/sq. km. The main challenge for the administrator, decision makers, and executors is to supply arsenic free drinking water to vast rural population of the entire district.

The primary data for this study is arsenic concentration value of groundwater samples collected from various water source or aquifers of different blocks of the said district. Water samples have been collected randomly all over the district for two seasons, i.e., pre-monsoon (before rainy season) and post-monsoon (after monsoon) between the time span of year 2006 and 2008. During the field survey the depth (in meter) of the aquifers below ground level has also been noted. Most data, i.e., water samples collected in every year have been tested in chemical lab of Dept. of Environment Science, Kalyani University, West Bengal, India and also few data has been tested in SWID (State Water Investigation Directorate, provincial Govt. of West Bengal, India) lab with taking permission from authentic sources. The groundwater arsenic concentration value in mg/L of each and every water samples has been extracted from those labs. Secondary data regarding groundwater arsenic has been gathered from different research articles published from department of SOES, Jadavpur University, India. Additional data products served as reference data for this study are the Survey of India (SOI) topographical sheets, NATMO district planning map, statistical handbook of the district North 24 Parganas which published by the Govt. of West Bengal's Bureau of Applied Economics and Statistics dept. and census data, 2011.

ArcGIS 10.0 software of ESRI has been utilized for whole technical work.

11.2.2 Methodology

11.2.2.1 Data Processing

District boundary map encompasses with block boundary has been digitized from geocoded, NATMO district planning map. The information for georeferencing has been accumulated from eight topographical sheets with scale of 1:50,000 which cover the whole district. The geocoding process and after that reprojection has been performed applying UTM (Universal Transverse Mercator) projection system with referenced ellipsoid and also with Everest datum. For identification and to locate the aquifer location inside the map, three or more tube wells in every block have been randomly selected. We articulated these tube wells as “Hydraulic Station” (HS). By GPS survey, the x, y lat/lng value of these hydraulic stations was estimated. The tube well location has been encoded in the digitized block map by spatial entity of points (Fig. 11.6). For this study a sum of 80 hydraulic stations/aquifers has been surveyed and located all over the district.

The arsenic concentration value (mg/L) of water samples collected from selected Hydraulic Station from 2006 to 2008 for two seasons has been considered as main field of attribute of those hydraulic stations. Further fields of attributes were: Block Name, Tube Well Depth, Village Name of HS, Year of sample collection, Season (before or after monsoon) of sample collection, etc. Querying any hydraulic station by information tool bar in Arc GIS, one would get to know the name of block where the HS has been situated, year and season of water sample collection, arsenic concentration value of HS of corresponding year as well as season, the depth of tube well, etc. only by one click. To execute the entire process Arc GIS’s data editing module has been applied.

11.2.2.2 Preparation of Arsenic Concentration Zone Map by Applying Thiessen Polygon Spatial Interpolation Method

Spatial interpolation is a technique where the known value of a point is used to estimate the values at another points. So in GIS analysis this technique is usually applied to a raster for estimations of values for all cells. Therefore this approach is a means to generate surface data through sample points. This surface data then can be used for analysis and modeling (Chang 2017) purpose devoid of having to deal with any data gap. Key focus of this research study is to apply Thiessen polygon technique (a spatial mapping tool) to generate groundwater arsenic concentration zone map and also to predict future risk by use of temporal data.

11.2.2.3 Mechanism of Thiessen Polygon

Thiessen polygons are also designated as proximal polygon which interpolates with the logic that the value of any point inside a polygon is nearer to the value of polygons known point than value of any other known points (Chang 2017). Thiessen polygon technique can be employed for modeling the catchment area for the points (Burrough 1986; Watson 1992). Delaunay triangulation method is frequently used to prepare Thiessen polygon (Davis 1996). The mechanism of this method makes sure that each identified point is joined to its nearest neighbors, the resultant triangles are as equilateral as possible. After that, Thiessen polygons could be easily created by joining lines drawn perpendicular to the sides of each triangle at their midpoints. Thiessen polygon interpolation approach is used in various applications, mainly for analysis of service area of public facilities like drinking water source, health centers, etc. (Sibson 1981) (Fig. 11.2).

11.2.2.4 Impact of Subsurface Geology in Groundwater Arsenic of Study Area

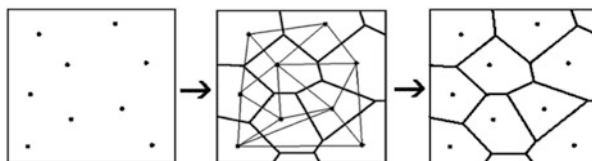
The present study area district North 24 Parganas falls in the southern region of Bengal Basin. Arsenic toxicity in human health was reported from this region before 1980s. But very minimal work on subsurface geology of the terrain in this region has been done so far.

Here we are presenting borehole lithologs showing the variation in lithology along depth for different boreholes in district North 24 Parganas. Groundwater arsenic for the associated aquifers is indicated as AF, LA, MA, and HA at the right side of the lithologs. AF—arsenic free, LA—low arsenic, MA—moderate arsenic, and HA—high arsenic (Pal and Mukherjee 2009).

The borehole lithologs showing the lithology along depth are sequentially here (Fig. 11.3a and 3b).

Pal and Mukherjee (2009) published an article in Environment Geology (2009) regarding the study of subsurface geology in locating arsenic free groundwater in Bengal Delta, West Bengal, India and they classified the aquifer types of the entire zone on the basis of variations in color and mineralogy of the aquifer sands and also on the presence or absence of overlying clay beds. Below table depicts characteristics of different aquifer types of the entire region. Basis of this subsurface geological data we could also explain the arsenic concentration zones in our present study area (Table 11.1).

Fig. 11.2 Steps in Thiessen polygon creation



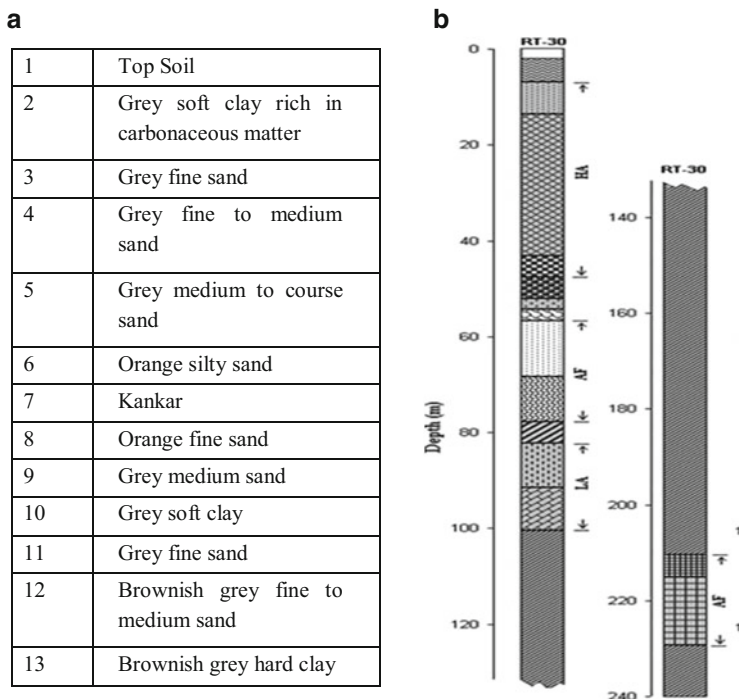


Fig. 11.3 (a) Borehole lithologs showing the variation in lithounits along depth in the study area. (b) Borehole lithologs showing the variation in lithology along depth in the study area. Source: Pal and Mukherjee (2009)

It is interpreted that high arsenic in the groundwater of Type-2 and Type-5 aquifers in the Bengal delta is due to their overlying gray soft clay. This clay contains more pore water and organic matter which is biodegradable and also favorable to generate reducing environment which facilitate to release arsenic from its ore mineral in the underlying aquifer. Thus an aquifer with overlying very dark gray and very soft clay yields groundwater arsenic as much as 0.80 mg/l (e.g., Type-2 aquifer) compared to the light gray and relatively harder clay yielding groundwater arsenic only 0.01–0.15 mg/l (e.g., Type-5 aquifer). The nature of overlying gray soft clay, therefore, determines the concentration of groundwater arsenic in the overlying aquifer and the spatial distribution of Type-2 and Type-5 aquifers with the variance of gray soft clay thus delineates the arsenic distribution pattern of a particular area.

In district North 24 Parganas the presence of Type-2 and Type-5 aquifers is abundant in the areas which fall under high arsenic zone.

Table 11.1 Characteristics of aquifer types in the Bengal Delta

Aquifer types	Fluvial setup	Stratigraphy	Nature of aquifer	Starting depth (m) bgl	Thickness (m)	Description	Characteristics minerals/ Phases	Sediment-arsenic	Groundwater-arsenic (mg/l)
Type-1	UFD	HOLOCENE	Unconfined	1-2	1-20	Gray to brownish gray, fine to medium sand	Ms, Bt, ill, Chl, FeCG	2-6	<0.01 (AF)
Type-2			Leaky confined	1-2	1-20	Gray to very dark gray, soft, organic carbon rich homogeneous clay	Ill, Kaol, Chl, OM	8-21	-
				3-20	1-60	Gray, fine to medium sand	Ms, Bt, Ill, Chl, OM	2-8	0.01-0.80 (LA, MA, HA)
Type-3	MFD	PLEISTOCENE	Unconfined	1-3	1-35	Orange, fine to coarse sand	Ill, FeCG	3-12	<0.01 (AF)
Type-4			Confined	1-30	1-10	Bluish gray to brownish yellow, hard, inhomogeneous clay	Mont, Kaol, Ill, Gt	7-11	-
Type-5			Leaky confined	20-35 30-60	1-25 1-30	Orange, fine to coarse sand Gray to very dark gray, soft, organic matter rich homogeneous clay	Ill, FeCG, Sid Kaol, Mont, Chl, OM	3-12 7-23	<0.01 (AF) -
Type-6	LFD	PLIO- PLEISTOCENE	Confined	60-70 120-150	10-80 30-50	Brownish gray to gray, fine to coarse sand Brownish gray, hard, inhomogeneous clay	Ill, FeCG, OM -	2-11 -	0.01-0.15 (LA, MA) -
				>150	-	Brownish gray, medium to coarse sand	Ill, FeCG	-	<0.01 (AF)

Source: Pal and Mukherjee (2009)

The values presented here are from parts of West Bengal, India. AF, LA, MA, HA are as described previously

Ms muscovite, Bt biotite, Ill illite, Chl chlorite, FeCG feoxyhydroxide coated grains, Kaol kaolinite, Mont montmorillonite, OM organic matter, Gt goethite, Sid siderite

11.2.2.5 Transfer Pathways of Arsenic from Irrigation Water to Crop System

In the last three decades, there has been a vigorous increase in number of Shallow Tube Wells (STWs) in the Asian region. These STWs become principle sources of irrigation water to farmers for cultivation of additional crops during dry season. Construction of these STWs is inexpensive. Prolonged use of arsenic contaminated irrigation water for agriculture purpose could result in As accumulation in the soil and then absorption of this accumulated arsenic from soil by crops will substantially add to the dietary As intake, resulting additional human health risks. By the following steps arsenic normally transfers from groundwater to soil to crop system.

Arsenic Speciation in Soil

Arsenic subsists in the environment in different inorganic and organic forms mainly arsenate (AsV) and arsenite (AsIII). Reduction and oxidation processes (redox) largely control the speciation of inorganic arsenic in soil (Halder et al. 2014; Takahashi et al. 2004).

The Role of Iron Hydroxide, Phosphate, and pH

Presence of iron hydroxide and phosphate plays an important role in speciation of arsenic in aerobic soils. These ions influence the process of absorption by plants for uptake (Chen et al. 2017; Williams et al. 2003). Absorption of AsV decreases with increasing pH, however for AsIII the opposite occurs. Maximum absorption for AsV on iron hydroxide lies around pH 4, whereas for AsIII at approximately pH 7–8.5 the absorption is maximum (Kumarathilaka et al. 2018; Mahimairaja et al. 2005).

Arsenic in Cultivated Crop

The rice plants transport oxygen from the leaves to the roots, for oxidizing rhizosphere (the microenvironment around the roots) which precipitates iron hydroxide (FeOOH) around the root, known as Fe-plaque. This Fe-plaque influence As speciation and uptake (Meharg et al. 2014; Weiss et al. 2004). But the uptake mechanism of organic arsenic is not so much clear, whereas inorganic arsenic like AsIII and AsV are taken up by different mechanisms. AsV is taken up via the high affinity phosphate uptake system (Halder et al. 2014; Meharg 2004) and AsIII is actively taken up by so-called water channels (aquaporins) in the roots (Meharg and Jardine 2003). After uptake of arsenic in the roots, translocation and accumulation of inorganic As to above ground part of plants happen (Abedin et al. 2002).

After uptake, for metabolism, AsV is reduced to AsIII rapidly, causing oxidative stress which induces the formation of certain antioxidants. It is considered as a mechanism of detoxification (Sneller et al. 1999, 2000; Meharg and Hartley-Whitaker 2002). The transfer pathways of arsenic from water to crop depicted here by a flow chart (Fig. 11.4).

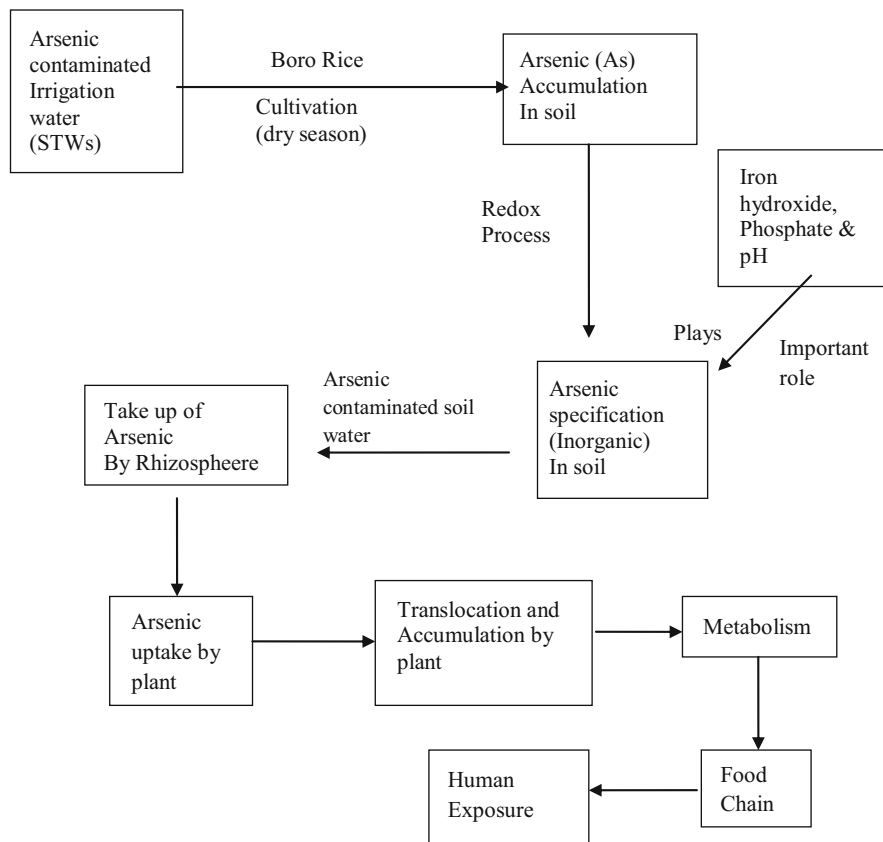


Fig. 11.4 The transfer pathways of arsenic from water to crop depicted

11.2.2.6 Arsenic in Food Chain

11.2.2.6.1 Arsenic Intake Via Rice Consumption and Vegetables

Rice accounts for one of principle food grain in India. In India out of total food grain production nearly 42.5% food grain is rice. Nearly 23% of agricultural land of India are being used for rice production and in West Bengal, only rice covers 5,900,000 ha cultivable land. Approximately 15.48% of India’s rice production yields from West Bengal. In the district North 24 Parganas, rice covers 277,100 ha and nearly 50% of total gross cropped area are used for production of rice. These data implies the importance of rice for huge population of West Bengal as well as district North 24 Parganas for their caloric intake.

Under anaerobic condition, rice is cultivated in arsenic contaminated soils when arsenic is highly available for uptake by plants. After irrigated with arsenic contaminated groundwater, concentration of arsenic in rice is supposed to be high compared

Table 11.2 Total Arsenic concentration (mg/kg dw) data in rice samples collected from West Bengal

State	Location	Rice (mg/kg)	Remarks	References
West Bengal	Jalangi & Domkal	0.569 (0.198–1.930)	Cooked rice ($n = 18$)	Roychowdhury et al. (2002)
	South 24-Parganas	0.072 ± 0.010	Precooked rice	Mandal et al. (2019)
	Jalangi & Domkal	0.239 (0.043–0.662)	Raw rice ($n = 34$)	Roychowdhury et al. (2002)

Table 11.3 Summary of Arsenic concentrations in vegetables, roots and tubers, pulses, and spices

Group	Total number of samples/group	Number of different food items/group	Min-max/group (mg/kg dw)	Range of means of different items (mg/kg dw)
Pulses	25	5	<0.04–0.20	0.03–0.10
Leafy vegetables	9	5	0.10–0.79	0.13–0.79
Fruit vegetables	64	16	0.05–1.59	0.11–0.62
Roots and tubers	21	6	<0.04–1.93	0.20–0.74
Spices	25	5	<0.04–0.98	0.04–0.49

Source: Williams et al. (2006)

to any other crops and vegetables (Kwon et al. 2017; Huang et al. 2015). As paddy rice is considered as main food items and high arsenic concentration in paddy rice becomes an important source of dietary arsenic intake (Nachman et al. 2018). Later when this rice would be cooked with arsenic polluted water; arsenic intake would be increased much more. Roychowdhury (2008) reported that cooked rice had nearly twice the arsenic level than raw rice which is likely to be because of boiling/or parboiling of rice in As-contaminated water. Besides, excess cooking water from rice used as hot gruel in rural villages of west Bengal serves as popular drink which believes to fulfill lack of nutrient content in diet of rural Bengal is also a remarkable source of arsenic for dietary intake (Mandal et al. 2019).

William et al. in 2006 collected a large number of samples (rice: 330, pulses and species: 50, vegetables: 94) from entire Bangladesh and published the first data on arsenic speciation in rice. Mandal et al. in 2019 reported a positive relationship between As levels in groundwater and As levels in rice. It has also been noticed that Boro rice contained more As than Aman rice. This may be caused, while Boro rice is irrigated with mostly arsenic contaminated groundwater supplied from Shallow tube wells, largely constructed in the study area while Aman rice is mainly rain fed (Table 11.2).

Table 11.3 presenting a summary of the results of total As from collected samples in pulses, leafy vegetables, fruit vegetables, roots and tubers, and species.

11.2.2.6.2 Drinking Water and Cooking Water Consumption

The amount of water intake by adult women and men in arsenic affected area has been studied by Watanabe et al. (2004) and as per their report, women consume 4.2 l/day and consumption by men is 4.6 l/day, respectively. Both men and women directly consume drinking water nearly 3 l/day on an average basis. Water intake via cooking purpose and food preparation added another 1 l/day (women) and 1.6 l/day (men). Kumarathilaka et al., 2019 also added valuable data for amount of arsenic content through cooking water (Fig. 11.5).

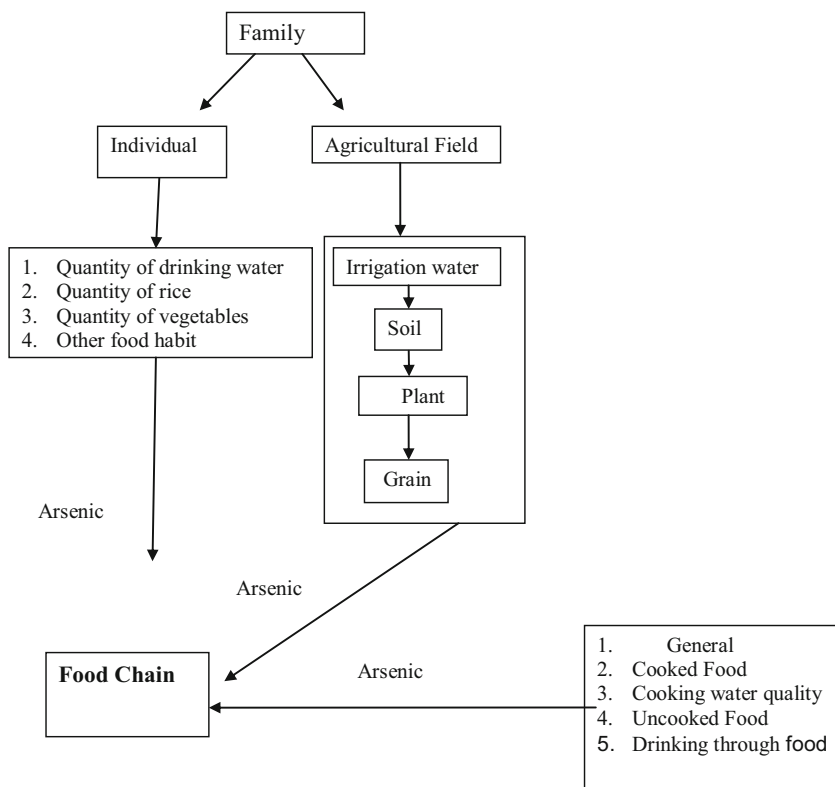


Fig. 11.5 Different sources of inorganic arsenic in Food Chain by Flow Chart

11.3 Results and Discussion

11.3.1 Preparation of Zone Maps of Groundwater Arsenic Concentration

The sampled, geo-tagged hydraulic stations (total 80), distributed homogeneously in several blocks of the entire study area, with their corresponding attribute data (the before-monsoon and after-monsoon arsenic concentration value from year 2006 to 2008 and the corresponding spatial coordinate of HS), are used as input for interpolation technique. These HSs were indicated by point shape file (vector) (Fig. 11.6) and then it has been converted to raster through Thiessen polygon interpolation technique (Fig. 11.7).

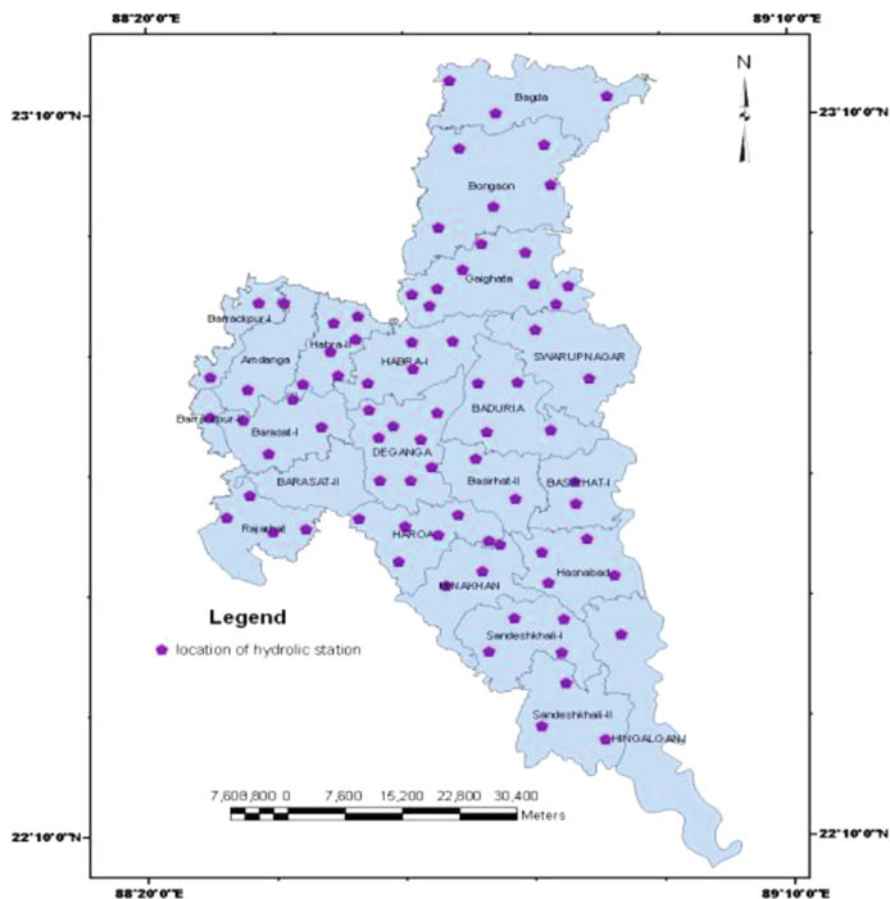


Fig. 11.6 Block wise point map of Hydraulic station of District North 24 Parganas



Fig. 11.7 Interpolation through Thiessen

From point information, arsenic concentration value distributed spatially throughout the district by Thiessen polygon (Fig. 11.7). Now the arsenic concentration value under the area of each polygon contains same value of that tube well inside it. After that, we classified arsenic concentration value into seven concentration zones (using 2006 pre-monsoon data) to prepare zone map (Fig. 11.8) by classifier tool of ArcGIS. Similarly we generated arsenic concentration zone map for every season (pre/post) of every year with available data from 2006 to 2008 (Fig. 11.9). The thematic map specifies (Fig. 11.8) arsenic concentration range (mg/L) in every defined zone:

Danger Zone—Above 0.125	Very High Arsenic Zone—(0.100–0.125)
High concentration zone—(0.075–0.100)	Moderately affected zone—(0.05–0.075)
Low concentration zone—(0.03–0.05)	Very low arsenic zone—(0.01–0.03)
Arsenic free—below 0.01	

So it is depicted from Fig. 11.7 that, for the each hydraulic station, Thiessen polygon used here acts as proximal polygon for modeling the catchment area (Ghosh

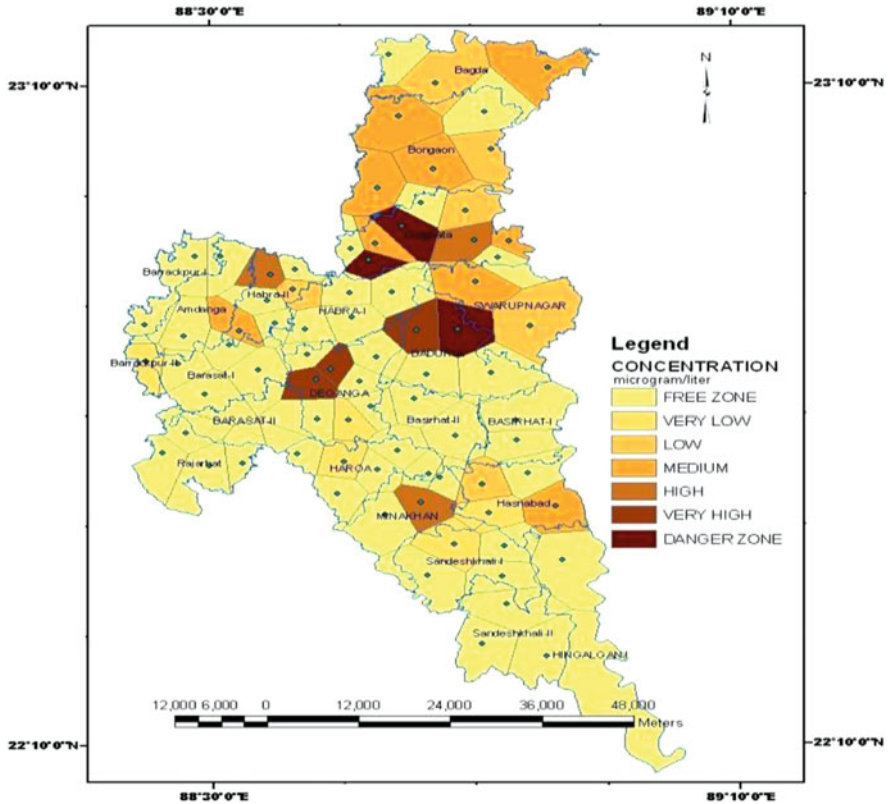


Fig. 11.8 Spatial distribution map of Arsenic concentration created from Thiessen polygon using 2006 pre-monsoon data

et al. 2020). It has been found from arsenic zone map (Fig. 11.8) overlaid on block boundary map of research area, that the blocks Baduria, Amdanga, Bagda, Hasnabad, Bongaon, Haroa, Gaighata, Part of Habra I & II have arsenic value in groundwater greater than maximum permissible limit (0.01 mg/L) set by WHO. These areas come under highly affected zone. So these blocks need more attention from administrative point of view. The blocks which are safe zone/arsenic free are—Part of Hingaljanj, Sandeshkhali I & II, and Minakhan.

11.3.2 Arsenic Total Daily Intake (Dietary Exposure to Arsenic)

In this study an attempt has been made to evaluate by considering Tables 11.2 and 11.3 data, how much As is transfer to human health through food chain.

The PMTDI (Provisional Maximum Tolerable Daily Intake) value for inorganic arsenic (As) is (0.126 mg/day for a person with 60 kg weight). As discussed earlier in Sect. 2.2.5 (Arsenic in food chain), it has been accomplished that the largest source of inorganic As from foods is rice. Assuming a person of age 60, rice consumptions are 400 g/day, vegetables consumption 130 g/day, and intake of water 3 l/day, then the daily total intake has been calculated:

Calculation:	
Different dietary sources	Amount of inorganic as (mg/kg)
Cooked Rice (400 g/day) (Indian std. 0.569 mg/kg)	0.25 mg/kg
Water (3 l/day) (as 0.050 mg/l arsenic in West Bengal, India drinking water stander)	0.15 mg/kg
^aVegetables (130 g/day)	0.03 mg/kg
Total daily intake	0.43 mg/kg

Source: Kumarathilaka et al. (2019), Meharg et al. (2014)

So total daily intake of inorganic arsenic (As) is 0.43 mg/kg for a man of age 60 years, which exceeds the PMTDI (For a 60 kg person 0.126 mg/day) by a factor ~ 3.5. Rice contributes 58% of total daily intake of As

^aVegetables have small contribution. Yet for a worst case scenario the contribution is only 0.03 mg/kg. Above data is on basis of that

After assessment of the levels of exposure, the results require to compare with a reference value like tolerable daily intake (TDI) value. Only a provisional maximum tolerable daily intake (PMTDI) data is obtainable for arsenic. In 1988, the provisional value of inorganic arsenic was established and the value is 0.0021 mg/kg body weight/day. This is used as reference to assess dietary intake of arsenic (WHO 2001). The PMTDI value has still not been ratified almost after three decades.

11.4 Risk Assessment and Remediation

Interpretation of arsenic status maps to quantify seasonal and annual fluctuation for assessment of risk with respect of time.

The spatial zone maps of study area portray spatial distribution of arsenic concentration scenario in Fig. 11.9.

Figure 11.9(a and b) reveals arsenic pollution set up in before- and after-monsoon (Pre & Post) season in year 2006, whereas Fig. 11.9(c and (d) reflects the same in year 2007 and Fig. 11.9(e and f) reveals arsenic pollution status in 2008 in both pre- and post-monsoon season, respectively. A clear trend is indicated here that despite the depth of aquifer, arsenic status is varying seasonally and as well as annually in various blocks of said districts.

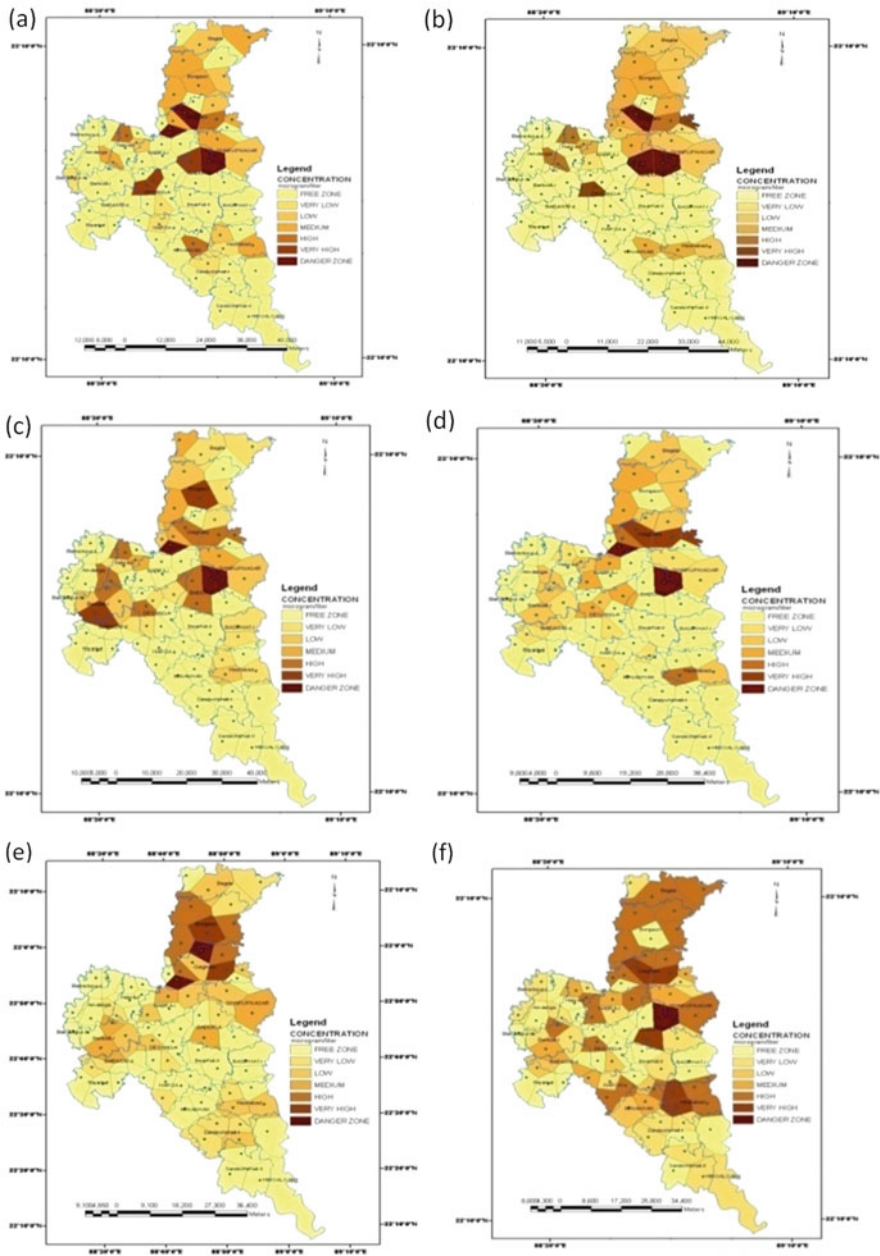


Fig. 11.9 Spatial distribution map of As concentration in different season from year 2006 to 2008 prepared through Thiessen polygon: (a) spatial distribution map of 2006-pre-monsoon data, (b) spatial distribution map of 2006-post-monsoon data, (c) spatial distribution map of 2007-pre-monsoon data, (d) spatial distribution map of 2007-post-monsoon data, (e) spatial distribution map of 2008-pre-monsoon data, and (f) spatial distribution map of 2008-post-monsoon data

Analyzing spatially distributed zone maps of arsenic from 2006 to 2008, it has been observed that some blocks those were arsenic free in pre-monsoon of 2006 in Fig. 11.9(a) became affected at the end of 2008 in Fig. 11.7f and also some blocks which were at low arsenic range in pre-monsoon of 2006 transferred to high arsenic concentration range at end of year 2008. Name of these blocks are Basirhat I, Haroa, Sandeshkhali I & II, Rajarhat and Barrackpur I. The fact signifies that, even if the depth of tube well remains same the average groundwater arsenic concentration values of aquifers of the study area maintains increasing trend. Unfortunately this research study exposes that, with passage of time, the arsenic hazard is slowly but surely spreading its tentacles spatially (Ghosh et al. 2020).

Table 11.4 shows different parameters of groundwater arsenic concentration used for this entire study of each block of the said district prepared from field survey data. From these temporal data of different season and different year we could assess the contamination risk by graphically presenting the data.

From above table a graphical presentation of arsenic status of two seasons (Pre- & Post-monsoon) from year 2006 to 2008 of the study area has been portrayed to assess the risk of increasing trend of groundwater arsenic seasonally as well as annually (Fig. 11.10).

From above graphs it has been seen that As value in year 2008 is greater in pre-monsoon season compare to post-monsoon but in year 2006 and 2007 arsenic value is higher in post-monsoon season in some blocks like Hasnabad, Gaighata, Habra, Bongaon of the study area. Again in 2008, some blocks like Baduri, Swarupnagar, etc., the arsenic value is higher in post-monsoon season than pre-monsoon and in the year 2007, the value of groundwater arsenic is greater in pre-monsoon seasons for the same blocks than post-monsoon. Noticeably in 2006, arsenic values of every blocks of the said district are higher in post-monsoon than pre-monsoon season. Also the diagram of Fig. 11.10(d) importantly points out that some blocks (like Sandeshkhali I&II, Haroa, Rajarhat, Basirhat I, Barrackpur I, etc.), those were not arsenic affected in 2006, became affected at the end of year 2008.

So from above observation, this research study reveals that, arsenic concentration value seasonally as well as annually fluctuates, in spite of the same depth of the aquifer below the ground level. The basic tendency is that in post-monsoon season, the value of arsenic in groundwater of hydraulic station is higher than pre-monsoon. The main reason may be, during post-monsoon season some portion of rain water infiltrates through soil grains. Then from lattice of the soil (where arsenical ore is present and acts as source of arsenic), this rain water acquired some arsenic and reaches to groundwater through leaching and raise the arsenic concentration value of that water. There are also some data which shows increasing arsenic values in before-monsoon (Pre) season. This could be analyzed when arsenic free rain water reached to groundwater through infiltration it dilutes the contaminated groundwater to some extent. So we get lower arsenic value in after-monsoon (post) season compared to pre-monsoon. But there is no noteworthy trend of track in fluctuation, as arsenic incidence in groundwater is ruled through a multifaceted geogenic process. In some zones arsenic values are higher in before monsoon and in some places it is higher in after monsoon. Arsenic status maps of year 2008

Table 11.4 Descriptive statistics for groundwater arsenic concentration values in various blocks of the study area (Prepared from supplementary material Table S1)

Sl. no.	Block name	Average arsenic concentration (mg/L)								Average depth of tube well (mtr)		
		2006				2007				2008		bgl
		Post-Monsoon	Pre-Monsoon	Post-Monsoon	Pre-Monsoon	Post-Monsoon	Pre-Monsoon	Post-Monsoon	Pre-Monsoon	Post-Monsoon		
1	BAGDA	0.026	0.023	0.013	0.026	0.0366	0.0166	52				
2	DEGANGA	0.018	0.0387	0.02	0.0125	0.0087	0.0075	72				
3	BONGAON	0.046	0.03	0.046	0.038	0.036	0.262	48				
4	RAJARHAT	0	0	0.0025	0	0.005	0.0025	73				
5	BARASAT-I	0	0	0	0.05	0.015	0.005	60				
6	GAIGHATA	0.08	0.07	0.12	0.075	0.0477	0.255	57				
7	HABRA-I	0.015	0.02	0.0325	0	0.035	0.05	58				
8	HABRA-II	0.041	0.026	0.016	0.04	0.016	0.0016	79				
9	BADURIA	0.2	0.1	0.067	0.1	0.127	0.02	60				
10	AMDANGA	0.015	0.02	0	0	0.005	0	56				
11	HAROA	0	0.0016	0.003	0	0.02	0.0012	105				
12	MINAKHAN	0.02	0.023	0	0	0.03	0	129				
13	HASNABAD	0.02	0.02	0.03	0.02	0.02	0.0016	165				
14	SWARUPNAGAR	0.04	0.04	0.015	0.04	0.04	0.01	53				
15	BARRACKPUR-I	0	0	0	0	0.01	0	53				
16	BARRACKPUR-II	0	0.01	0	0.01	0	0	52				
17	BASIRHAT-I	0	0	0	0	0	0	52				
18	BASIRHAT-II	0	0	0	0	0.005	0	50				
19	SANDESHKHALI-I	0	0.0025	0	0.0025	0.0075	0.0015	118				
20	SANDESHKHALI-II	0	0	0	0	0.02	0	109				

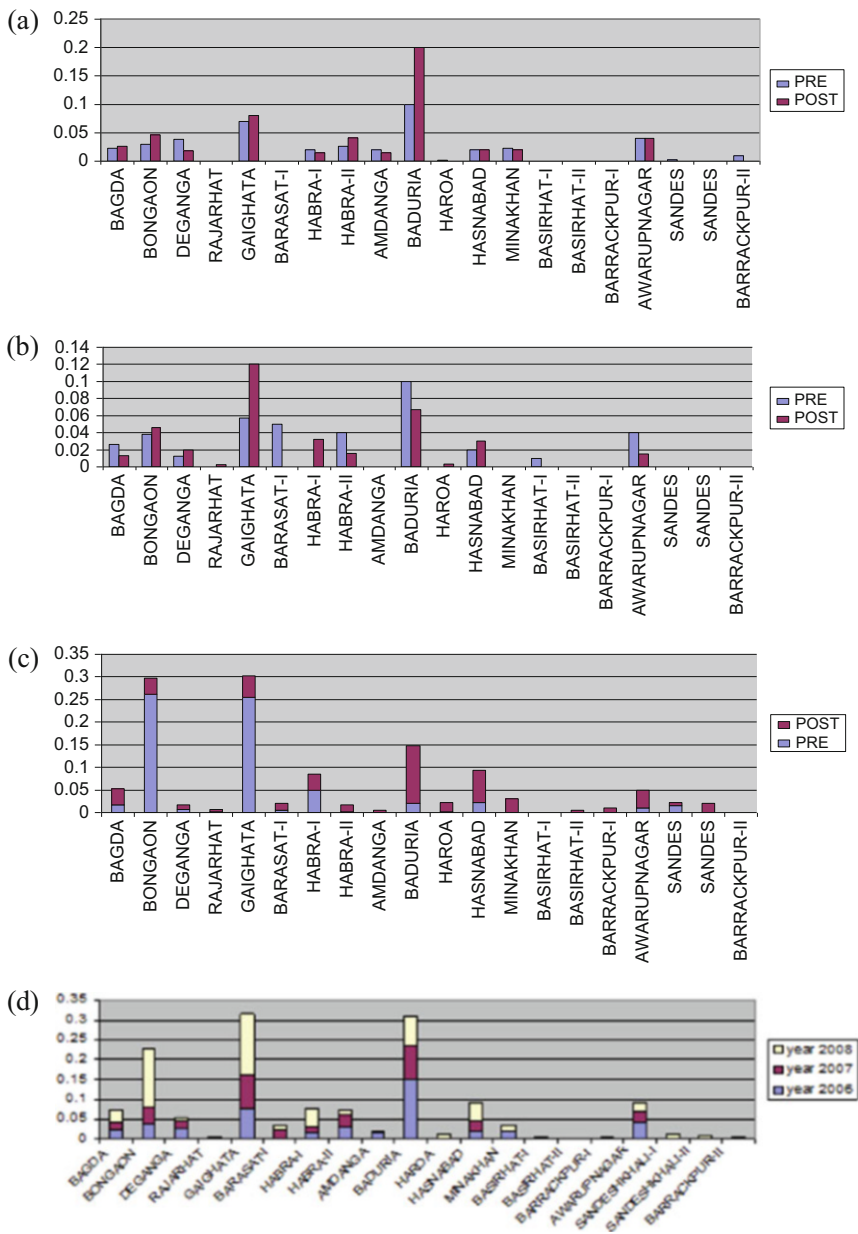


Fig. 11.10 (a) Stats of arsenic level (mg/L) in various blocks in pre- and post-monsoon period in year 2006, (b) Statistics of arsenic level (mg/L) in different blocks in pre- and post-monsoon season in year 2007, (c) Statistics of arsenic level (mg/L) in different blocks in pre- and post-monsoon season in year 2008, and (d) Subdivided bar diagram of average arsenic concentration in the blocks of the study area in three different years 2006, 2007, and 2008

Fig. 11.9{(e) and (f)} illustrate the above facts, where it shows some blocks with low or medium arsenic concentration value in pre-monsoon, moved to high range at post-monsoon of the same year. It is also clear from diagram Fig. 11.10(d) and as well as arsenic status maps of Fig. 11.9(a) and 11.9(f) that with increasing time average arsenic concentration keeps its steady increasing trend.

11.4.1 Correlation between Depth of the Tube Well and Groundwater Arsenic Concentration

In this research study a correlation has been found between average arsenic concentration of tube well water and depth of that tube well.

Statistically this relation can be calculated by the parameter “Correlation Coefficient.” If we calculate correlation coefficient between depth and concentration value from above Table 11.5, then we can relate between this two.

Table 11.5 Statistics of average depth of tube well and corresponding average arsenic concentration. (Prepared from supplementary material Table S1)

Sl. no.	Block name	Avg depth of the hydraulic station (mtr)	Average arsenic concentration (mg/L)			General average
			2006	2007	2008	
1	BAGDA	52	0.0245	0.0195	0.0266	0.0235
2	BONGAON	48	0.038	0.042	0.149	0.0763
3	DEGANGA	72	0.02835	0.01625	0.0081	0.0175
4	RAJARHAT	73	0	0.00125	0.00375	0.0016
5	GAIGHATA	57	0.075	0.0885	0.15135	0.104
6	BARASAT-I	60	0	0.025	0.01	0.0116
7	HABRA-I	58	0.0175	0.01625	0.0425	0.0254
8	HABRA-II	79	0.0335	0.028	0.0088	0.0234
9	AMDANGA	56	0.0175	0	0.0025	0.0066
10	BADURIA	60	0.15	0.0835	0.0735	0.1023
11	HAROA	105	0.0008	0.0015	0.0108	0.0043
12	HASNABAD	165	0.02	0.025	0.047	0.0306
13	MINAKHAN	129	0.0215	0	0.015	0.0121
14	BASIRHAT-I	52	0	0.005	0	0.0016
15	BASIRHAT-II	50	0	0	0.0025	0.0008
16	BARRACKPUR-I	53	0	0	0.005	0.0016
17	SWARUPNAGAR	53	0.04	0.0275	0.025	0.0308
18	SANDESHKHALI-I	118	0.00125	0	0.01125	0.0041
19	SANDESHKHALI-II	109	0	0	0.01	0.0033
20	BARRACKPUR-II	52	0.005	0	0	0.0016

$$\text{cov}(xy) = \sum xy/n - \left(\sum x/n\right) \cdot \left(\sum y/n\right) = -0.18708$$

where

- n number of sample point.
- x Depth of tube well,
- y Average arsenic concentration.

$$\delta x^2 = \sum x^2/n - \left(\sum x/n\right)^2 = 1014.148.$$

$$\text{Or, } \delta x = \sqrt{1014.148} = 31.84568.$$

$$\delta y^2 = \sum y^2/n - \left(\sum y/n\right)^2 = 0.000972.$$

$$\text{Or, } \delta y = \sqrt{0.000972} = 0.031183.$$

$$\begin{aligned} \text{Correlation Coefficient } (r) &= \text{cov}(xy)/\delta x \cdot \delta y \\ &= -0.18708/31.84568 \times 0.031183. \\ &= -0.18839. \end{aligned}$$

$$\delta x = \text{std.deviation of } x = 31.84568.$$

$$\delta y = \text{std.deviation of } y = 0.031183.$$

Negative correlation coefficient (r) indicates that there is negative correlation between arsenic concentration value and depth of tube well. If depth of tube well is greater, then concentration of arsenic in water from that tube well will be less. It implies that water in deep tube well will contain less arsenic contamination than shallow tube well. Normally groundwater below 110 mtr depth is arsenic free.

11.4.2 Role of Surface Water Body to Alleviate Arsenic Risk

To study impact of surface water and other land use/land cover on groundwater arsenic, we selected 40 hydraulic stations randomly out of total 80 throughout the study area. We classified these tube wells in four arsenic concentration zones, i.e., severely affected, high affected, low affected, and very low or arsenic free. After that we picked 10 tube wells from each zone and a ring buffer had been prepared around each tube well with radial distance of 1 km from the center of the ring. We assumed that people resides within this 1 km radius area are using the water of that particular tube well/hydraulic station for their drinking and other livelihood purpose. Now we evaluated the dominating land use/land cover class with their areal extent around

those buffer zones. The dominating land use/land cover features of the study area are arable land, surface water body, fallow land, forest cover, settlement, and marshy fallow land. The areal extent of every land use land cover features inside different buffer zone has been depicted in below tables (Tables 11.6 and 11.7).

Similarly we have calculated areal extent of different land use/land cover class around buffer zone of highly affected zone and also low affected zones.

Finally, we evaluated the mean areal extent of each and every land use/land cover class for every arsenic concentration zone. Table 11.8 depicts that statistics:

It is evident from the above table that areal coverage of surface water is very minimal or zero in severely arsenic affected zone compared to agricultural (Arable) land and settlement cover. Blocks fall under this category are: Bongaon, Gaighata, and Baduria. Where as in arsenic free zones average areal extent of surface water is 35.346 acres/sq.km. Blocks fall under this category are Hingalganj, Sandeshkhali I, Sandeshkhali II, etc. So many small river channels like Raimangal, Kalindi, Haribhanga, Vidyadhari, etc. are the main source of surface water here. Community reside here are using these river water bodies through canal system for their agriculture and other utilization purposes. This water is mostly free of arsenic. The dominant geohydrological unit also shows that in this area fresh water is overlain by saline groundwater. So shallow tube wells yield brackish water. People do not construct shallow tube well in these areas. Average depth of tube well is 110 mts. (bgl) here. Groundwater from this depth is normally arsenic free.

Table 11.6 Aerial extent of Different Land use/Land cover class and population density around buffered zone of Worststly Arsenic affected (0.20–0.70) µg/L hydraulic stations

Name of block	Name of H.S.	Land use/Land cover class (Areal extent in acres)										Population density
		Surface water	Arable land	Settlement	Fallow land	Forest cover	Vegetation	Marshy fallow	Water logged area			
Bonga on	(i)	0	312.549	301.307	38.823	38.300	53.856	24.444	23.790	1022/sq.km		
	(ii)	0	265.36	275.425	32.810	61.830	128.62	25.882	1.830			
	(iii)	0	163.922	358.693	0	29.673	239.739	0.784	0			
	(iv)	0	238.824	335.164	6.013	45.751	153.333	9.803	4.183			
Gaighata	(v)	0	248.889	227.059	28.627	9.2810	279.216	0	0.1307	1235/sq.km		
	(vi)	0	119.346	420.654	11.241	87.712	86.274	56.209	10.849			
	(vii)	0	155.948	309.673	5.620	103.791	209.02	4.444	4.836			
	(viii)	0	73.5948	318.562	1.437	106.797	209.28	57.124	24.575			
Baduria	(ix)	0	181.177	346.405	1.699	11.634	248.758	0.1307	3.267	1378/sq.km		
	(x)	0	441.046	315.425	15.032	1.830	14.902	3.790	1.307			
Mean value		0	220.365	320.836	14.130	49.659		18.261		1164/sq.km		

Source: Ghosh et al. (2012)

Name of H.S.(Hydraulic Station): (i) Chowberia, (ii) Sripally Free, (iii) Goran pota, (iv) Pella(S.H.C), (v) Gaighata BSF, (vi) Dharampur S.H.C, (vii) Hanspur, (viii) Rammagar G.P.O, (ix) Ichchapur East(F.P.S), (x) Aluria

Table 11.7 Areal extent of different Land use/Land cover class and population density around buffered zone of very low Arsenic affected or arsenic free (below 0.02) µg/L hydraulic stations

Name of block	Name of H.S.	Land use/Land cover class (Areal extent in acres)										Population density
		Surface water	Arable land	Settlement	Fallow land	Forest cover	Vegetation	Marshy fallow	Water logged area			
HabraII	(i)	0	262.353	397.909	37.9085	13.968	72.6798	4.5751	3.9215	1330		
BasirhatI	(ii)	0.5228	144.967	495.164	4.575	5.882	64.836	70.980	5.3594	1321		
BasirhatII	(iii)	0.39215	18.1699	196.863	0	9.80392	12.8105	448.366	105.49	1523		
BarrackI	(iv)	0.26143	229.412	322.353	53.856	3.790	40.2615	112.81	30.4575	1985		
BarrackII	(v)	0	257.647	418.693	11.2418	3.660	12.941	75.555	12.9412	3890		
SandeshI	(vi)	69.542	10.719	2.8758	0.6535	0.1307	3.2679	531.373	175.163	771		
	(vii)	6.7973	539.739	162.353	49.1503	1.0457	1.1764	27.843	3.7908			
SandeshII	(viii)	249.15	113.333	55.4249	81.9608	0	0.9150	289.543	2.0915	691		
	(ix)	7.32026	316.994	33.986	332.811	0	1.4379	92.549	7.0895			
Hingalganj	(x)	19.477	524.314	111.111	9.673	0	4.967	94.771	27.7124	655		
Mean value		35.346	241.764	219.673	58.182	3.829		174.836		1216,1362		

Source: Ghosh et al. (2012)

Name of H.S.(Hydraulic Station): (i) Iswarigacha, (ii) Nimberia, (iii) Raghunathpur, (iv) Babanpur, (v) Muragacha, (vi) boyarmari, (vii) Bholakhali, (viii) Dheknamari Pny School, (ix) Dheknamari D.A. School, (x) hingalganj

Table 11.8 Descriptive statistics of mean areal extent of different land use/land cover features in four classified arsenic concentration zones

Arsenic concentration class	Land use/land cover class (average areal extent in acres)						Dominant geomorphic unit	Dominant geo-hydrologic unit	Population density per sq km
	Surface water	Arable land	Settlement	Fallow land	Forest cover	Marshy fallow			
(i) Worst or severely affected hydraulic station (0.20–0.70)µg/L	0	220,365	320,83	14.13	49.65	18,261	Upper matured deltaic plain	Aquifer with primary intergranular porosity	1164
(ii) Highly affected hydraulic station (0.05–0.2) µg/L	0.566	209,644	263,07	21,481	13.73	157,95	Upper/lower matured deltaic plain		1305
(iii) Low affected hydraulic station (0.02–0.05) µg/L	9,978	315,410	310,370	25,635	0.609	69,556	Flood plain of River Basin/L. M.D.P		1237
(iii) Very low or arsenic free hydraulic station (below 0.02 µg/L)	35,346	241,764	219,673	58,182	3,829	174,836	LMDP	Fresh water overlain by saline groundwater	655

Source: Ghosh et al. (2012)

11.4.3 Remediation

From above study it is evident that arsenic concentration value of groundwater fluctuates temporally regardless the depth of hydraulic station (tube well). This fluctuation occurs in an increasing fashion with respect of time. Analyzing arsenic concentration maps of three consecutive years (2006–2008), of different seasons, it is being observed that tube well which was arsenic free in 2006 became arsenic affected by the end of year 2008. It implies that if we declare a tube well as arsenic safe today, it may become arsenic prone in future time. So it requires to monitor periodically the tube wells which are extensively used by civilian. Excessive extraction of groundwater is the main cause of this increasing trend in groundwater arsenic value. In this situation utilization of surface water is very important factor to combat against this menace. So we have to protect our surface water. Prolonged use of arsenic contaminated irrigation water plays a major role in transferring arsenic from water to crop. This research study reveals that in affected regions the main contributor to As intake is contaminated drinking water. The next largest contributor is food, especially rice, followed by vegetables. This study also calculated that nearly 40% of total arsenic (daily) intake is contributed by rice only in the study area.

Thus to mitigate groundwater arsenic contamination problem, the following aspects must be taken into accounts:

The main challenge of the Government of arsenic affected countries (Like India, Bangladesh) is to supply millions of people of arsenic affected region with arsenic safe, bacteriologically as well as chemically safe alternative source of drinking water. For achieving this goal, following action plan should be initiated.

To get an accurate picture of arsenic status of the entire region a coordinated region-wide survey of all drinking water wells is necessary. Sufficient numbers of water sample must be collected devoid of any biasness and these samples should be analyzed properly in laboratory. The mitigation of this chemical environmental disaster is purely depend on how accurately we identify the contaminated wells.

- Using reliable data collected from field survey, the cause of arsenic pollution of any region should be investigated thoroughly.
- To get the actual number of patients who are suffering from disease related to arsenic, door to door intensive survey is necessary in all over the contaminated regions.
- Proper identification of arsenic safe aquifers in arsenic affected regions must be given in priority.
- As in most blocks of the said district mostly deep aquifers are free from arsenic, so as an alternative source of water, low cost, small capacity deep tube wells could be installed. But leaching of arsenic polluted water from the upper shallow aquifers must be prohibited.
- *Development of Public Awareness:*

Local and international seminars should be organized by various government and private organizations like several NGOs, to develop public awareness about the menace of groundwater arsenic contamination. The mass media like TV and

radio could play a major role to create a large-scale public awareness by which the issue will come and remain into the limelight. During our door to door survey for this research study we found a very few percentage of people knows about this environmental disaster while surveying their tube wells but majority of those are still in the dark.

Various options could be taken into account to mitigate the arsenic contamination in both drinking water and irrigation water:

Surface Water Supply As surface water normally has very minimal arsenic value (typically $<5 \mu\text{g L}^{-1}$) so with proper treatment by removing bacteria and waterborne disease it could be used for livelihood purpose at village level. Low cost water treatment plant can serve the purpose.

Dug Wells This is the oldest method of extraction of groundwater for supplies. Dug wells water are free from arsenic/iron or water concentration is below the permissible limit. By sealing the well top and as well as the upper part of the well lining, dug wells water could be protected from bacteriological contamination. One could also seal the space between the soil and wall to protect the well water. Installation cost is also low.

Deep Tube Wells In regions where arsenic safe groundwater can be extracted from deeper aquifer safely, installation of deep tube wells could be promoted. These DTW's further could fitted with TARA pumps, suction mode hand pump for individual household supply or with motorized pumps for community based supply of piped water could be taken into consideration.

Ponds Sand Filter Pond Sand Filter (PSF) technology is one of the alternate option for arsenic free potable water supply suitable for household level at rural region. If per mouza one pond could be protected from bacterial contamination, with minimal treatment, it may be a source of drinking water. By this system surface water is stored in a small tank/reservoir which is underlain by a sand bed and through taps the filtered water is collected.

Rainwater Harvesting Out of all drinking water sources available for community, rainwater is the least to face arsenic contamination problems. The method needs a suitable roof to collect and a storage tank with proper sealing to guard it from various algal and bacterial contamination. Usually rainwater is collected after 5 min of rain starts, through a pre-fabricated jar or a container, which need no treatment (apart from filtration to separate the suspended solids, if any) before use for domestic purpose at the household level. As rainwater harvesting only could provide a seasonal water supply for drinking, so in arid region its use will be much more limited. Even it is available only for a few months still the provision of rainwater is beneficial.

Agricultural Management Options Natural resources like groundwater should be used in a sustainable manner so that the input of contaminants to the environment through these natural resources could be minimized or avoided. We should reduce

the use of irrigation water for cultivation of rice. This will decrease the input of arsenic in food chain, minimize leaching of nutrients and also reduce extraction of groundwater. Besides we should also promote those types of cropping pattern which requires less irrigation water in high arsenic regions. For example, people should replace cultivation of Boro rice with other crops like mustard seeds, maize, wheat, etc.

11.5 Conclusion

For this research study we carried out field survey for three years (from 2006 to 2008) and collected six season data pertaining to pre-monsoon and post-monsoon for each year. Using these data we prepared arsenic concentration zone map by geospatial interpolation technique and also we estimated the future trends. But this is very short term data to evolve a definitive trend. To establish a state of the art trend it is required to deal with longer term data. So the GIS database which have been prepared up to 2008 need to be updated year after year. Besides, for this study water samples from 80 hydraulic stations from different blocks of the study area have been collected and tested. But groundwater arsenic associated research of a study region needs thousands of water samples (that would not permit data extrapolation) with a particular interval of time periodically which is a money consuming as well as time consuming process. So without any assistance from government body or other non-govt. organization it is virtually impossible for a researcher to successfully continue arsenic related study. Zone map of groundwater arsenic concentration prepared using advanced geospatial interpolation technique like Thiessen polygon with data of different season and year will help planners, administrator and policy makers to make a decision based strategic planning. And as this database will be updated and enriched, query generation will be easy in GIS environment to inform people about the present arsenic scenario of any block at any time. Lithostrata of the terrain, i.e., the subsurface geology, different land use/land cover, especially surface water body also play important role in controlling groundwater arsenic contamination of the study area. It has been observed that tube well depth above 110 meter below ground level is normally arsenic free. So much more construction of deep tube well rather than shallow tube well should be encouraged and taken into consideration by the concerned planners and administrator. Considering the impending serious effects of increasing risk of As contamination in groundwater and crop systems and ultimately its toxic effect through food and water in human health, the identified gaps in understanding need to be filled. It is very essential to quantify the scale of the problem which must be based on scientific methodologies to achieve trustworthy results. To assess human health risk from arsenic contamination for Asian nations, particularly for India and Bangladesh, it is essential to evaluate the input of inorganic As from cooked rice and cooked dal (pulses), for calculation of accurate estimates of TDI (Tolerable Daily Intake), sign in spite of. As both rice and dal are cooked with a large amount of water. So in this research we have calculated the tolerable daily

intake of inorganic arsenic coming from different sources. Besides these factors, groundwater acts must be enacted by government for controlling various activities regarding sustainable exploration of groundwater, development, and management.

Acknowledgments This work was supported by Dept. of Geography and Environment Management, Vidyasagar University and Dept. of Environment Science, Kalyani University, India. We would like to express our gratitude to State Water Investigation Directorate (SWID), Govt. of West Bengal, India for providing testing facilities of data samples for this entire research study.

References

- Abedin MJ, Cotter-Howells J, Meharg AA (2002) Arsenic uptake and accumulation in rice (*Oryza sativa L.*) irrigated with contaminated water. *Plant Soil* 240:311–319
- Burrough PA (1986) Principles of geographical information systems for land resources assessment, vol 1. Oxford University Press, New York, p 54
- Chang K (2017) Introduction to geographical information systems. Tata McGraw Hill, New Delhi
- Chen Y, Han Y-H, Cao Y, Zhu Y-G, Rathinasabapathi B, Ma LQ (2017) Arsenic transport in rice and biological solutions to reduce arsenic risk from rice. *Front Plant Sci* 8:268
- Chowdhury M, Alouani A, Hossain F (2010) Comparison of ordinary kriging and artificial neural network for spatial mapping of arsenic contamination of groundwater. *Stoch Environ Res Risk Assess* 24:1–7
- Davis JC (1996) Statistics and data analysis in geology. Wiley, New York
- Ghosh M, Pal DK, Santra SC (2012) Different land use and other physical and socio-economic parameters in ground water arsenic concentration. *Int J Sci Emerg Technol* 3:89–101
- Ghosh M, Pal DK, Santra SC (2020) Spatial mapping and modeling of arsenic contamination of groundwater and risk assessment through geospatial interpolation technique. *Environ Dev Sustain* 22:2861–2880. <https://doi.org/10.1007/S10668-019-00322-7>
- Halder D, Biswas A, Šlejkovec Z, Chatterjee D, Nriagu J, Jacks G, Bhattacharya P (2014) Arsenic species in raw and cooked rice: implications for human health in rural Bengal. *Sci Total Environ* 497:200–208
- Huang Y, Wang M, Mao X, Qian Y, Chen T, Zhang Y (2015) Concentrations of inorganic arsenic in milled rice from China and associated dietary exposure assessment. *J Agri Food Chem* 63:10838–10845
- Kinniburgh DG, Smedley PL (2001) Arsenic contamination of groundwater in Bangladesh. Ministry of local government, rural government and cooperatives, government of Bangladesh, BGS Technical Report WC/00/19, vol 1
- Kumarathilaka P, Seneweera S, Meharg A, Bundschuh J (2018) Arsenic speciation dynamics in paddy rice soil–water environment: sources, physico-chemical, and biological factors—a review. *Water Res* 140:403–414
- Kumarathilaka P, Seneweera S, Meharg A, Bundschuh J (2019) Arsenic in cooked rice foods: assessing health risks and mitigation options. *Environ Int* 127:584–591. <https://doi.org/10.1016/j.envint.2019.04.004>
- Kwon JC, Nejad ZD, Jung MC (2017) Arsenic and heavy metals in paddy soil and polished rice contaminated by mining activities in Korea. *Catena* 148:92–100
- Mahimairaja S, Bolan NS, Adriano DC, Robinson B (2005) Arsenic contamination and its risk management in complex environmental settings. *Adv Agron* 86:1–82
- Mandal U, Singh P, Kundu AK, Chatterjee D, Nriagu J, Bhowmick S (2019) Arsenic retention in cooked rice: effects of rice type, cooking water, and indigenous cooking methods in West Bengal. *India Sci Total Environ* 648:720–727

- Meharg AA (2004) Arsenic in rice – understanding a new disaster for South-East Asia. *Tr Plant Sci* 9:415–417
- Meharg AA, Hartley-Whitaker J (2002) Arsenic uptake and metabolism in arsenic resistant and nonresistant plant species. *New Phytol* 154:29–43
- Meharg AA, Jardine L (2003) Arsenite transport into paddy rice (*Oryza sativa*) roots. *New Phytol* 157:39–44
- Meharg A, Williams P, Deacon C, Norton GJ, Hossain M, Louhing D, Marwa E, Lawgalwi Y, Taggart M, Cascio C (2014) Urinary excretion of arsenic following rice consumption. *Environ Pollut* 194:181–187
- Nachman KE, Punshon T, Rardin L, Signes-Pastor AJ, Murray CJ, Jackson BP, Guerinot ML, Burke TA, Chen CY, Ahsan H (2018) Opportunities and challenges for dietary arsenic intervention. *Environ Health Perspect* 126:084503
- Pal T, Mukherjee PK (2009) Study of subsurface geology in locating arsenic-free groundwater in Bengal delta, West Bengal, India. *Environ Geol* 56:1211–1225. <https://doi.org/10.1007/s00254-008-1221-4>
- Roychowdhury T (2008) Impact of sedimentary arsenic through irrigated groundwater on soil, plant, crops and human continuum from Bengal delta: special reference to raw and cooked rice. *Food Chem Toxicol* 46:2856–2864
- Roychowdhury T, Uchino T, Tokunaga H, Ando M (2002) Survey of as in food composites from an as-affected area of West Bengal. *India Food Chem Toxicol* 40:1611–1621
- Sibson R (1981) A brief description of natural neighbor interpolation. Chapter 2. In: *Interpolating multivariate data*. John Wiley & Sons, New York, pp 21–36
- Sneller FEC, Noordover ECM, Ten Bookum WM, Schat H, Bedaux JJM, Verkleij JAC (1999) Quantitative relationship between phytochelatin accumulation and growth inhibition during prolonged exposure to cadmium in *Silene vulgaris*. *Ecotoxicology* 8:167–175
- Sneller FEC, Van Heerwaarden LM, Schat H, Verkleij JAC (2000) Toxicity, metal uptake, and accumulation of phytochelatin in *Silene vulgaris* exposed to mixtures of cadmium and arsenate. *Environ Toxicol Chem* 19:2982–2986
- Takahashi Y, Minamikawa R, Hattori KH, Kurishima K, Kihou N, Yuita K (2004) Arsenic behavior in paddy fields during the cycle of flooded and non-flooded periods. *Environ Sci Technol* 38:1038–1044
- Tareq SM, Safiullah S, Anawa HM, Rahman MM, Ishizuka T (2003) Arsenic pollution in groundwater: a self-organizing complex geochemical process in the deltaic sedimentary environment, Bangladesh. *Sci Tot Environ* 313:213–226
- Watanabe C, Kawata A, Sudo N, Sekiyama M, Inaoka T, Bae M, Ohtsuka R (2004) Water intake in an Asian population living in arsenic-contaminated area. *Toxicol Appl Pharmacol* 198:272–282
- Watson D (1992) *Countouring: a guide to the analysis and display of spatial data*. Pergamon Press, London
- Weiss JV, Emerson D, Magonigal JP (2004) Geochemical control of microbial Fe(III) reduction potential in wetlands: comparison of the rhizosphere to non-rhizosphere soil. *FEMS Microbiol Ecol* 48:89–100
- WHO (2001) *Environmental health criteria*. Geneva, 224, Arsenic and Arsenic Compounds
- Williams LE, Barnett MO, Kramer TA, Melville JG (2003) Adsorption and transport of arsenic (V) in experimental subsurface systems. *J Environ Qual* 32:841–850
- Williams PN, Islam MR, Adomako EE, Roab A, Hossian SA, Zhu YG, Feldmann J, Meharg AA (2006) Increase in rice grain arsenic for regions of Bangladesh irrigating paddies with elevated arsenic in groundwater. *Environ Sci Technol* 40:4903–4908

Chapter 12

Geospatial Assessment of Surface Water Pollution and Industrial Activities in Ibadan, Nigeria



Olutoyin Adeola Fashae and Rotimi Oluseyi Obateru

Abstract Surface water pollution from industrial, agricultural, municipal, and transportation sources constitutes a serious menace to ecological functioning. In the developing countries of Africa, rapidly emerging urban centers like Lagos, Ibadan Bamako, Niamey, and Nairobi, lack of appropriate wastewater disposal, and treatment facilities feature commonly on prominent river basins. Public health and the adjoining and distal terrestrial and aquatic ecosystems are usually at the receiving end of the resultant malevolent impacts. Several mathematical models have been designed to address surface water pollution problems such as eutrophication, heavy metal toxicity, nutrient contamination, etc. Most of these models are too theoretical and do not consider the multifaceted interactions that are associated with ever increasing anthropogenic activities. This informs the need for geoinformation techniques to model the pattern of pollution along a river that drains an industrial estate with a view of identifying and analyzing risk potential. The industrial basin is found in Ibadan, southwestern Nigeria. The river was sampled around each industry for 14 physicochemical properties using standard laboratory procedures. The diffusion pattern and magnitude of the toxicity was modeled in the geospatial environment while the risk level of the industrial river basin was assessed. Considerable heavy metallic contaminants like As, Pb, Cr, Cd, and Ni were identified at various points along the river. Human settlements and ecosystems within this basin are highly exposed to pollution hazards while settlements downstream of the river are at potential environmental risk. Phytoremediation was considered the most viable method to remediate the situation.

Keywords Surface water · Contamination · Industrial activities · Heavy metals · Pollution

O. A. Fashae (✉) · R. O. Obateru
Department of Geography, University of Ibadan, Ibadan, Nigeria

12.1 Introduction

The availability of freshwater for humanity both in terms of quality and quantity has been a challenge to both the developed and the developing countries of the world (Fashae et al. 2019a, b). This challenge has so far posed severe impairments on public health, ecological well-being, and economic advancement of many nations.

Over 60% of the world's largest rivers have their natural courses modified by damming and other developmental activities causing drastic alteration of material movement to downstream reaches, devastation of water characteristics, and impaired ecological well-being (WWAP 2003). The judicious use of the available but limited water resources is beset with the problem of poor management of wastewater, which, when discharged into the environment, deteriorates surface water and groundwater quality. Globally, the annual quantity of wastewater produced has been estimated to be around 1500 km³, which is about 600% more than the water available in all rivers (WWAP 2003). Surface water bodies, which can also be connected to shallow groundwater aquifers, are largely used as sources of drinking water. They are sometimes contaminated by toxic chemicals emanating from poorly managed hazardous waste sites or from industrial areas. The United States government set up a clean-up and rehabilitation program in the 1980s to handle such instances under the Superfund Programme (USEPA 2000). Since most rivers terminate in the ocean, the marine ecosystems are adversely impacted. Persistent chemical substances like polychlorinated biphenyls (PCBs) and dioxins, even at low concentrations, pose considerable health risk to phytoplanktons and zooplanktons (Yassi et al. 2001), while the renowned instance of the fish contamination by mercury in the Minamata disease outbreak in Japan in 1956 will ever remain memorable (WHO 1976). This problem will be exacerbated in the future by climate change, which will cause increased water temperatures, thawing of glaciers, and increased incidences of flood and drought (Schwarzenbach et al. 2010). The impact of this on human health includes lack of safe drinking water, poor sanitation, and susceptibility to threats posed by chemical toxicants and pathogens. In view of the aforementioned, this study aimed at assessing the magnitude and spatial pattern of surface water contamination and the associated environmental risk in a small industrial basin in Olubadan Estate, Ibadan, Nigeria.

12.1.1 *Surface Water Contamination*

FWR (2015) defined pollutant as any contaminant that exists in the environment or could go into the environment and can be harmful due to its characteristics, or quantity or concentration. Contaminants were further characterized as agents, materials, or substances that are undesirable in the environment. Surface water contaminants can be of either natural or anthropogenic origin or a combination of both. Common natural sources include weathering and erosion of rock formations,

volcanic ash and lava, and forest fire, among others. Industries, agriculture, municipalities, and transportation are prominent anthropogenic sources of surface water contaminants. In the world today, about 80% of wastewater from municipal sources are released into surface water bodies in the untreated form, while millions of tons of heavy metals, toxic sludge, and solvents among other wastes are deposited into rivers and seas (WWAP 2017). Over two million tons of agricultural, industrial, and sewage wastes are released into water bodies globally on a daily basis and this amounts to the weight of 6.8 billion people (WWAP 2003), while in developing countries about 70% of industrial wastes are disposed into surface waters without treatment thereby polluting the available limited water supplies (UN-Water 2009). The agricultural industry contributes significantly to water pollution through the discharge of large amounts of agrochemicals, drug residues, organic materials, and sediments into the environment resulting, in the devastation of both the terrestrial and aquatic ecosystems. Rivers are used as site for the disposal of refuse, human sewage, and wastewater from kitchens, abattoirs, and industries making freshwater reservoirs the most affected of all the water bodies (Fashae et al. 2017). Moreover, Fashae and Olusola (2017) opined that the high level of urbanization within river basin, increase in human activities such as grazing along the river corridor, discharge of industrial effluents, dumping of solid wastes in the river, and construction of buildings close to the river are accountable for most surface water contamination in the many developing countries.

Surface water bodies can receive chemical contaminants from point sources and nonpoint sources (Fig. 12.1). Point source contamination includes the discharge of waste materials from a single source such as wastewater outlet from an industry. Nonsource contamination involves a number of minute sources, which combine to cause significant pollution as in the case whereby surface runoff during storm events transports pollutants in solution and suspension from industrial, agricultural, and urban areas into rivers, lakes, reservoirs, seas and oceans, and groundwater bodies (Kjellstrom et al. 2006). Runoff from agricultural locations transports sediments, which increase turbidity and nutrients like nitrates and phosphates, which contribute to eutrophication and consequently a boom of algae and plant growth in surface water bodies. Since 1990, the mean nitrate levels in global waterways have undergone 36% increment with the most drastic situation observed in the Eastern Mediterranean and Africa, where nitrate contamination level has increased in more than two folds (GEMS 2004). Example of point source contamination is discharge of large volume of liquid and solid waste into the ecosystem by paper and pulp mills. Such liquid wastes are characterized by high concentrations of suspended solids, biochemical oxygen demand, and chlorinated organic compounds (World Bank 1999). Surface waters may be contaminated during the storage and transportation of the solid wastes. As documented by the United Nations, chlorinated solvents observed in 30% of water supply from groundwater sources in 15 Japanese cities, at times, diffuse as far as 10 km from the pollution origin (UNEP 1996) (Fig. 12.1).

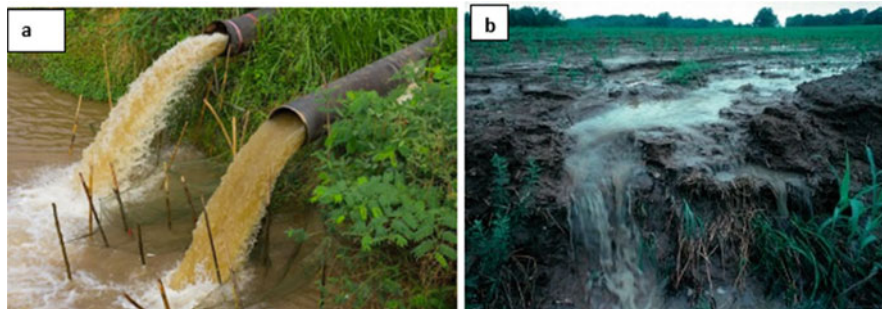


Fig. 12.1 Pollution source types: (a) point source (nationalgeographic.org); (b) nonpoint source (Source: nationalgeographic.org)

12.1.2 Industrial Activities and Surface Water Pollution

Industrialization, due to its role in economic advancement, is germane to the development of nations. But it poses inevitable environmental challenges especially through the contamination of the atmospheric and water resources (Gyawali et al. 2012) (Table 12.1). Most industries are situated near water bodies because of their wet nature in which a large amount of water is usually required for processing and disposal of wastes (Adekunle and Eniola 2008). Wastes generated from industrial and manufacturing activities are usually discharged into surface water bodies with such wastes in the range of garbage, dirt and gravel, concrete and masonry, chemicals, trash, solvents, oil, scrap metals, plant debris, scrap lumber, and wood, among others. The receiving water bodies will have their physical, chemical, and biological characteristics altered by these materials.

Industrial pollutants can exist in any of the three states of matter (solid, liquid and gas), depending on the industrial activity generating them. Irrespective of the physical state of occurrence, they can either be hazardous or nonhazardous. Hazardous pollutants are contaminants that are of significant or potential threats to humans and the ecosystem, and whose material composition exhibit one or more of ignitability, reactivity, corrosiveness, and toxicity. Nonhazardous pollutants are those that do not display any of the aforementioned properties and are not municipal waste. Prominent sources of hazardous industrial pollutants are cement production factories, mining, chemical, mechanical, and paper and pulp industries, wood processing facilities, oil and hydrocarbon contaminated materials, and spent solvents, among others. Although data on the generation, quantity, and disposal of industrial hazardous wastes are limited, it has been estimated that developing countries such as Lebanon generate 3000–15,000 tons of hazardous industrial wastes annually as a result of poor physical infrastructure and environmental monitoring strategies (El-Fadel et al. 2001). The quantity of hazardous industrial waste generated globally has increased appreciably since the period of Industrial Revolution. For instance, the estimated quantity of hazardous wastes produced annually by the manufacturing sector in the United States increased from 4.5 million tons after the World War II to

Table 12.1 Some industrial sectors and their contribution to water pollution

Industrial sector	Water pollution	Atmospheric pollution
Base metal and iron ore mining	Toxic metal sludge	PM
Cement manufacturing	Sludge	PM
Coalmining and production	Sludge	PM, coal dust
Copper smelting	Arsenic	Arsenic
Electricity generation	Hot water	PM, SO ₂
Foundries	Solvents	PM
Iron and steel smelting	Sludge	PM
Lead and zinc smelting	Lead, cadmium, arsenic	PM, SO ₂ , lead, cadmium, arsenic
Meat processing and rendering	High biological oxygen demand	Odor
Oil and gas development	Oil	SO ₂ , carcinogens
Pesticide manufacturing	Pesticides and toxic intermediates	Pesticides and toxic intermediates
Petrochemicals manufacturing	Oil	SO ₂
Petroleum refining	Sludge, hydrocarbons	SO ₂
Phosphate fertilizer plants	Nutrients	PM
Pulp and paper mills	High biological oxygen demand, mercury	Odor
Tanning and leather finishing	Chromium, acids	Odor
Textile manufacturing	Toxic dyes	Odor

Source: World Bank (1999)

about 57 million tons in 1975, and to about 265 million tons by 1990. In 1989, the USEPA estimated that over 70,000 different chemicals were being produced in the United States, with about 1000 new ones being added annually. The ecological implication of all these remains unquantifiable. Surface waters also receive contaminants through atmospheric deposition; hence, the contributions of some selected industries to water and air pollution are illustrated in Table 12.1.

12.1.3 Global Scenario of Industrial River Pollution

As reviewed by Kibria (2016), most rivers in the USA, Central Asia, the Middle East, the Indian subcontinent, and eastern China are under severe risk of pollution, emanating from various human activities. In fact, rivers in Asia, particularly in Bangladesh, China, India, and Indonesia, have been reported to be championing the league of the most polluted rivers in the world. In Bangladesh, River Buriganga, a highly polluted river, is characterized by low level of dissolved oxygen that is less



Fig. 12.2 World's most polluted rivers: (a) River Buriganga, Bangladesh (Source: burigangariverkeeper.org) (b) River Citarum River, Indonesia (Source: James Wendlinger 2019)

than 2.8 mg/l, high concentration of metals such as Cd, Cu, Cr, Ni, Pb, trace metals concentration 5–500 times higher than the permissible limit for the protection of aquatic resources (Ahmad et al. 2010). About 44% of rivers in the United States is compromised as a result of agricultural wastes, hydromodification, pathogens loadings, and organic concentration (USEPA 2004). The ecological health of the Ganges River in India has been highly impaired as fecal coliform counts (*Escherichia coli*) level has attained 900–150,000 per 100 ml coliform (Trivedi 2010). About 75% of the major lakes and about 25% of coastal waters in China are extremely contaminated from the discharge of toxic chemicals from industries into surface waters (Kibria 2016). Typically, the China's Yellow River is a receptacle of billions of tons of sewage and other industrial hazardous wastes (Kibria 2016). In Indonesia, the Citarum River earned the reputation of the world's most polluted river. This river which receives hazardous wastes containing lead, mercury, arsenic, and other toxins, from over 2000 industries in Bandung and Cimahi, supplies water to about 30 million people for domestic, municipal industrial, agricultural, and sanitary uses. Effluents like dyes, chemicals, etc., are discharged into the river by over 200 textile industries, while plastic and other municipal solid wastes have been reported in the river; the lead contamination in this river is reported to be 1000 times greater than the permissible limit recommended by the USEPA (Kibria 2016). Other notable rivers that made the list of the world's top most polluted rivers as reviewed by Kibria (2016) include Matanza-Riachuelo River (Argentina), Yamuna/Jamuna River (India), Ganges River (India), Sarno River (Italy), Marilao River (Philippines), the Mississippi River (the United States), and the Cuyahoga River (the United States), among others (Fig. 12.2).

12.1.4 The Threat of Industrial River Pollution in Nigeria

Nigeria is not immune to the global problem of water quality despite her dense river networks and abundant groundwater water reserve. Rapidly urbanizing and



Fig. 12.3 River pollution in Nigeria: (a) Oil spillage in the Niger Delta region (Source: www.stakeholderdemocracy.org); (b) River pollution in Lagos (Source: Pius Utomi 2019)

industrializing cities like Lagos, Kaduna, Kano, Port Harcourt, and Aba, where municipal and manufacturing activities rely heavily on surface water bodies, are facing decline in water quality due to the discharge of contaminants and wastewater into the environment. The indiscriminate disposal of industrial wastes in these cities has led not only to the contamination of inland and coastal water bodies, but also the presence of water quality stressors like nutrients, heavy metals, toxic chemicals, and organic chemicals, which may include polynuclear aromatic hydrocarbons (PAHs) and pesticides in the environment (Merem et al. 2017). Notable industrial sectors at the forefront of surface water contamination in Nigeria include mining, petroleum, pharmaceuticals, food, plastics, iron and steel, wood and pulp, brewing, and paint. The persistent occurrence of accidental oil spillage especially in the country's Niger Delta area renders the petroleum industry the greatest threat to fresh water resources. This predicament is further heightened by corrosion of petroleum pipelines, discharge from petroleum refineries, and the usual act of sabotage to oil facilities by rebels in the region (Fig. 12.3).

In a study of industrial activities and environmental pollution by Adekola and Eletta (2007), elevated concentration of zinc, iron, chromium, copper, and manganese in Asa River sediments in southern Nigeria was attributed to bottling, detergents, tannery, and other industrial effluents usually discharged into the river. The impact of effluents from textile industries has been reported on the Kaduna River basin, with river channels characterized by high concentration of chemical oxygen demand, biological oxygen demand, sulfur compounds, and particulate matter that exceeds the Federal Environmental Protection Agency (FEPA) permissible limits in multiple folds (Yusuff and Sonibare 2004). Similarly, Sangodoyin (1995) noted that surface waters in Ikeja, the capital of Lagos State, are characterized with ever increasing concentration of industrial effluent contaminants. River Ogun, which is also a receptacle of industrial effluents from Lagos and Abeokuta, has been observed to be impaired by significant iron, oil and grease, turbidity, and fecal coliform (Jaji et al. 2007). In Ibadan city, prominent rivers like Ona, Ogunpa, and Kudeti are largely contaminated by the combined effects of municipal and industrial waste

discharge (Fashae et al. 2017). Other industrially polluted rivers in Nigeria, whose water quality characteristics have been studied, include Rivers Niger, Benue, Imo, and Calabar, among others (Iroye and Igbozurike 2018).

Mitigation of industrial river pollution has not received so much attention in Nigeria (Olayinka and Alo 2004). Commitment to environmental protection began to acquire momentum in Nigeria in the late 1980s following the deposition of hazardous waste at Koko port in the Niger delta area by an Italian ship. This prompted the setting up of the FEPA and the publication of National Guidelines and Standards for Environmental Pollution, which basically addressed industrial pollution. The FEPA is saddled with the responsibility of ascertaining the level of compliances of industries with discharge effluent standards set by the agency. The agency also prescribes analytical methods required to determine significant properties of waters and wastewaters for industries, which follows the monitoring process used by the United States Environmental Protection Agency (USEPA). In a bid to ensuring a cleaner and safer environment for the Nigerian populace, the Federal Government of Nigeria in 2007 established the National Environmental Standards and Regulations Enforcement Agency (NESREA), an agency whose statutory role is to ensure environmental protection and to enforce environmental standards, laws, polices, and guidelines.

12.1.5 Modeling Water Pollution and Its Associated Environmental Pollution

Over time, different techniques have evolved and are still evolving in assessing surface water pollution and its associated risks. The application of nonspatial models in water quality assessment dates back to the 1920s with the renowned mathematical model of Phelps and Streeter, which illustrated dissolved oxygen balance in rivers. Subsequently, water quality modeling underwent significant transformation. Kaushik (2015) formulated a dynamical model to analyze water pollution and self-purification of River Ganges. In a mathematical modeling of river pollution, Mazaheri et al. (2015) used the inverse problem framework involving advection–dispersion contaminant transport equation to determine the distribution and magnitude antecedents of contaminating point sources. Pimpunchat et al. (2009) adopted a simple one-dimensional mathematical model to assess the impact of aeration on pollutant degradation of Tha Chin River in Thailand. The model consists of two coupled advection–dispersion equations, which assess the intensities of the pollutant and the dissolved oxygen. A novel method of computational modeling of pollutant transmission in rivers was introduced by Parsaie and Haghiabi (2017), which is associated with the use of both finite volume technique as numerical method and artificial neural network (ANN) as soft computing method together in simulation. As identified in a review by Yan et al. (2015), notable methods that have used to evaluate water quality globally include single-factor pollution index (SFPI),

complex pollution indices (CPI), fuzzy comprehensive evaluation (FCE), analytic hierarchy process (AHP), gray evaluation (GE), principal component analysis (PCA), artificial neural network (ANN), fuzzy comprehensive-quantifying assessment (FCQA), and water quality identification, among others. These techniques are beset with inability to give a spatial impression of the contaminant distribution and to identify risk prone sections of surface waters (Yan et al. 2015).

Yaghi and Salim (2017) produced thematic maps for nonpoint source pollutants like fertilizers and pesticides in Al-Abrash Syrial coastal basin using remote sensing and GIS techniques and emphasized the relevance of these techniques in land management. Yan et al. (2015) combined single-factor index, comprehensive factor index, geostatistics, and GIS to agricultural, industrial, and municipal pollution level at the China's Honghe River basin. A combination of geospatial and statistical techniques was used by Fashae et al. (2019a, b) to evaluate the effects of land use on surface water characteristics in Oshogbo, Nigeria. Yetik et al. (2009) developed a platform that integrated ArcMap and water quality model in Matlab in predicting the levels of river contamination. Meng et al. (2018) combined a heavy metal module with the SWAT (Soil and Water Assessment Tool) model to simulate the transport of metal in a mine-impacted basin in China. Other studies that have adopted geospatial technologies in monitoring surface water pollution include Oke et al. (2013), Ramaraju and Giridhar (2015), Sener et al. (2017), Ogbozige et al. (2018), Sukojo and Sianipar (2018), Allsgeer et al. (2018). GIS and Remote sensing techniques are effective decision-making tools that allows for the integration of spatial data from different sources, whose results could inform sustainable development.

12.2 Materials and Method

12.2.1 Study Site

The study site is a small river basin found in the eastern part of Ibadan, Nigeria. There are five industrial estates in Ibadan, but the choice of this industrial study site is based on the diversity of the industries and the release of varieties of industrial effluents into the river that drains the area. The study site is located between latitude $7^{\circ}23'50''$ N and $7^{\circ}24'35''$ N and longitude $3^{\circ}57'45''$ E and $3^{\circ}58'45''$ E with an area extent of about 58,096 m² (Fig. 12.4). The estate was acquired in 1978 with 8 industrial, 11 commercial, and 288 residential plots.

The climate of the estate, just like that of Ibadan, is characterized by two marked seasons: the wet season, which spans between March and October under the influence of wet tropical maritime air mass, and the dry tropical continental air mass, with the latter bringing about dry season that extends from November to February (Fashae and Olusola 2017). This estate has gently undulating topography with elevation ranging between 190 m and 210 m above sea level. It is drained by a stream that emerges at the north-eastern corner of the basin and flows in a dendritic pattern in a southwesterly direction to join a major river. The soil is formed from fine

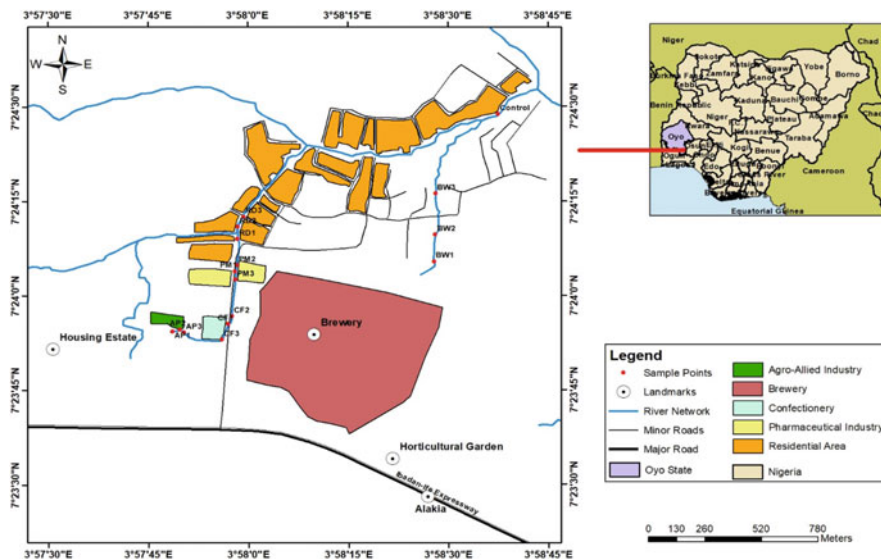


Fig. 12.4 Map of an Industrial estate within a River Catchment in Ibadan, Nigeria showing the sampling points

grained biotite gneisses and schist that weather readily with texture ranging between clayey and sandy clay. The industrial section of the estate accommodates many manufacturing industries such as pharmaceutical, confectionary, brewing, and agro-processing industries. Water processing factories are also located within the residential zone.

12.2.2 Sampling

Surface water was sampled at different points along the stream adjacent to the different industries by composite sampling technique in sterile transparent 75 cl plastic bottles (Fig. 12.4). The samples were taken to the laboratory for physico-chemical analysis. Water properties like electrical conductivity (EC) and pH were measured in situ during the field sampling. Surface water temperature was measured using the dry bulb mercury thermometer. The main tributary of the river draining this industrial basin flow through five prominent land use activity sites, namely, agro-processing industry, confectionary industry, pharmaceutical industry, brewing industry, and residential area. The residential area was sampled as well as a control point at the upstream of the basin before receiving contaminants from the industries (Fig. 12.4). In all, 16 samples were collected and immediately moved to the laboratory in an ice chest. In order to prevent contamination and/or deterioration prior analysis, the samples were kept in the refrigerator on arrival at the laboratory.

Each sample was analyzed for the following properties: nitrate (NO_3^-), arsenic (As), calcium (Ca), iron (Fe), copper (Cu), zinc (Zn), lead (Pb), chromium (Cr), cadmium (Cd), and nickel (Ni).

12.2.3 Laboratory Analysis

The JENWAY 3540 Bench was used to measure pH and electrical conductivity in situ. Nitrate (NO_3^-) was analyzed using HI83200 multispectral bench photometer at a wavelength of 525 nm. The flame atomic absorption spectrophotometer was used to analyze the metals.

12.2.4 Geospatial Analysis

The study area map was derived from Google Earth image. The geographic coordinates of the sampling points were collected with the Global Positioning System (GPS) device. They were subsequently inputted into Microsoft Excel (2007) and subsequently imported into ArcGIS 10.5 environment so to identify important features like road networks. The concentration of the physiochemical parameters at the various sampling points were imported into the ArcGIS. The values were interpolated along the stream network using the spherical semivariograms kriging technique to generate thematic maps for the various physiochemical parameters. The locations from where the samples were taken were designated as followings: brewing industry (BW), residential area (RD), pharmaceutical industry (PM), confectionery industry (CF), and agro-processing industry (AP).

12.3 Results and Discussion

12.3.1 Distribution of Selected Physiochemical Parameters

The spatial distribution of selected physiochemical properties along the industrial stream—temperature, pH, electrical conductivity, nitrate, and calcium is illustrated in Figs. 12.4 and 12.5. The mean values of these parameters at the industrial sites were used as the basis of the discussion to give a more explicit insight of the effect of the industrial discharge of the effluents into the adjoining stream. The layout of the industrial basin is such that the residential area is sandwiched in compacted manner within the industrial estate. The stream under study drains the entire length of the estate as the distributaries are fed with discharge from the industrial and domestic outlets (Fig. 12.4).



Fig. 12.5 Thick coats of Oil-Based industrial effluents discharged into the stream

The temperature along the stream channel does not exhibit considerable spatial variation as the value ranges between 25.9 °C and 26.9 °C. The lowest value was observed at the control where the water is free from industrial discharges. The minute temperature differences can partly be attributed to the slight variation in vegetation cover around the stream bank. On the basis of this, one cannot say that the basin is free from thermal pollution, as these industries have specific periods for the discharge of hot effluents into the drains. Temperature has a counter relationship with dissolve oxygen content as cold water retains more dissolved oxygen than warm water (Davie 2008). High temperature will also increase the solubility of metallic compounds in water bodies, and hence, increasing the chances of heavy metal contamination.

The effect of industrial contamination becomes evident from the pH level as the value varies from about 5.5 at the control to 5.91 at the brewing industry and 6.28 at the residential area. pH values observed from other industrial sites further downstream were lower but between 6.18 and 5.5. This suggests that the effluents from the brewing industry and the residential area have potential to raise the stream water alkalinity. In spite of this, the stream can still be characterized as slightly acidic. An increasing acidity was noticed around the pharmaceutical, confectionery, and agro-processing industries. Acidic rivers tend to encourage the dissolution of ions, especially metals. The greater the stream acidity, the more the metals that will be held in solution (Davie 2008). Based on this assertion, the alkaline nature of the industrial effluent can be relevant in minimizing the amount of associated heavy metal contaminants that will dissolve. However, fly ash from industrial activities can increase surface water alkalinity and might lead to a reduction in the uptake of essential bases and causing the death of phytoplanktons (Singh and Gupta 2017).

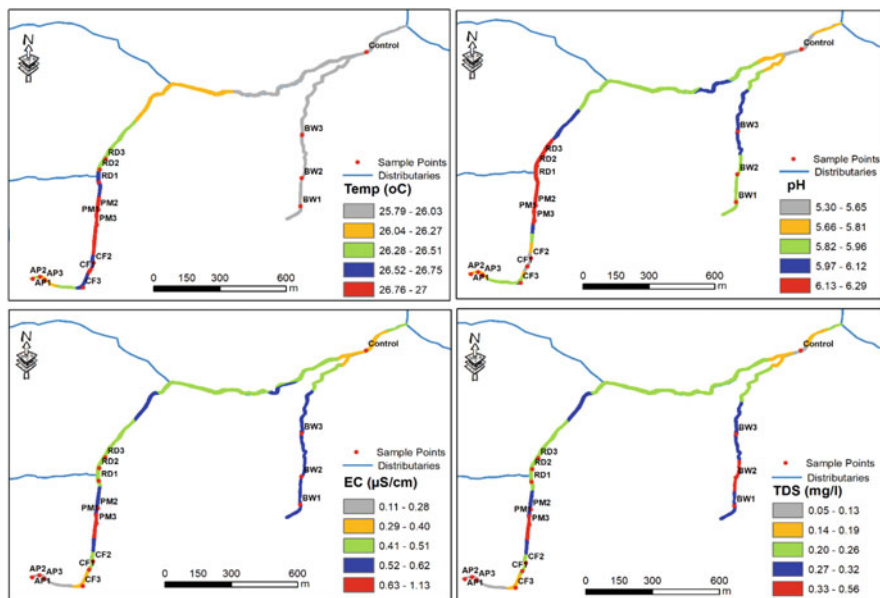


Fig. 12.6 Spatial pattern of temperature, pH, electrical conductivity (EC) and total dissolved solids (TDS)

Relatively high concentration of Total Dissolved Solids (TDS) was noticed around the brewing industry, residential area, and pharmaceutical industry with mean values of 300 mg/l, 240 mg/l, and 370 mg/l, respectively, relative to 50 mg/l at the control. A similar pattern was observed for Electrical Conductivity (EC) wherein mean concentration of 590 µS/cm was observed at the brewing industry, 470 µS/cm at the residential area, 740 µS/cm at the pharmaceutical industry, 340 µS/cm at the confectionery industry, and 110 µS/cm at the agro-processing industry, compared to 120 µS/cm at the control. The increasing magnitude of electrical conductivity can be linked to the increase in the amount of inorganic particulate materials in overland flow and the existence of nitrates from other industrial activities, which, by implication, increase the turbidity of the water body (Elbag 2006). Fly ash from industries coalesces to form thick floating cover (Fig. 12.5) on rivers and thus minimizing the degree of penetration of light Singh and Gupta (2017) (Fig. 12.6).

Nitrate concentrations were less than 50 mg/l, the permissible limit set by WHO (2003), although a downstream decrease was observed along the channel. An increase in concentration was noticed from 0.22 mg/l at the control, 0.45 mg/l at agro-processing industry, to 0.50 mg/l and 0.53 mg/l at the confectionary and pharmaceutical industries, respectively. At the residential area, a lower concentration of 0.46 mg/l was observed while the brewing industry recorded 0.51 mg/l. Even though the nitrate level is still within the recommended standard for drinking water, the increasing concentration may eventually attain this limit sooner or later. A rare

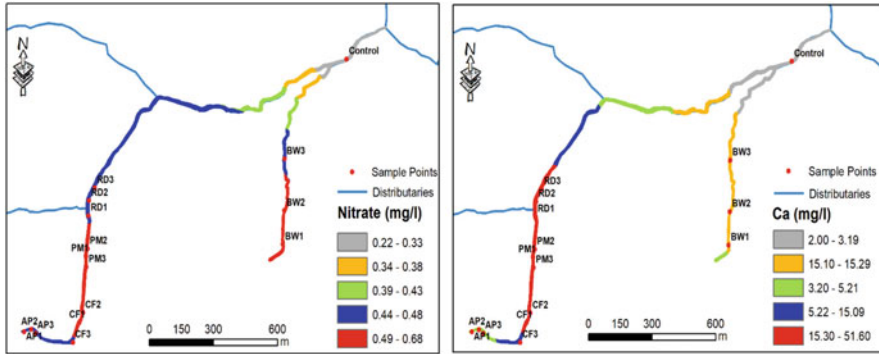


Fig. 12.7 Spatial pattern of nitrate and calcium along the Industrial Estate River

health risk associated with nitrate contamination is methemoglobinemia, also called the blue baby syndrome, which seldom features among newborn babies. As reviewed by Davie (2008), it is rare to have nitrate level higher than 50 mg/l, but a peak nitrate concentration of 21 mg/l has been recorded for River Lea in England with the norm ranging between 5 mg/l and 10 mg/l. However, the greatest challenge of nitrate pollution is eutrophication with the associated problem of over-production of plant matter in river systems. Calcium concentration generally ranges between 3.26 mg/l and 27.8 mg/l with the highest value obtained at the pharmaceutical industry, while a value of 2.14 mg/l was observed at the control (Fig. 12.7). It is therefore evident that all the industries contribute adversely to the stream water quality. But it can be inferred that the brewing industry impacts the stream more compared to other industries because there is usually a sharp contrast between the value at this point and value upstream at the control.

12.3.2 *Spatial Pattern of Heavy Metals and Their Associated Health Implications*

Industrial areas are often characterized with heavy metal pollution at different levels depending on the technological sophistication, size of the industries, and nature of manufactured products. Heavy metals like arsenic, iron, copper, zinc lead, chromium, cadmium, and nickel were observed along the industrial stream at varying level, and their concentrations were mapped and illustrated in Figs. 12.8 and 12.9. The mean concentration at each site is used in discussing the spatial pattern across the basin. The presence of arsenic (As) signifies a serious health risk. Although arsenic concentration of 0.01 mg/l was observed at the control point, its concentration increased gradually from 0.03 mg/l at the agro-processing industry through 0.03 mg/l at the confectionary industry to 0.1 mg/l at the pharmaceutical industry. The contamination level declined to 0.06 mg/l at the residential area and peaked at

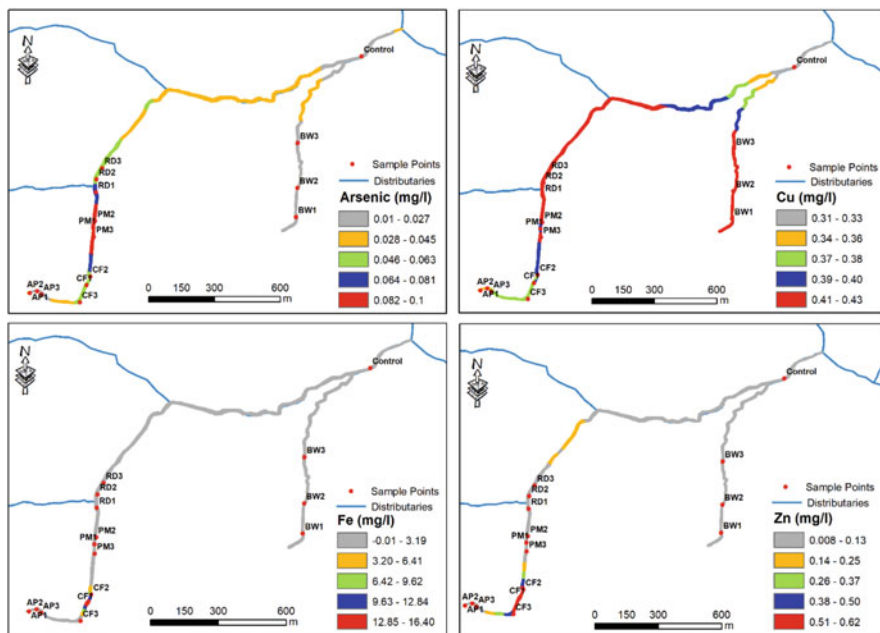


Fig. 12.8 Spatial pattern of arsenic, copper, iron, and zinc along the Industrial Estate River

0.18 mg/l at the brewing industry. It becomes evident that the risk of arsenic contamination is gradually on the increase in this basin since the concentration levels exceeded 0.01 mg/l, which is the provisional guideline for drinking water by WHO (2008). In addition, the erratic situation of power supply in the country has compelled industries to resolve to the use of generators and industrial machineries that are powered by petrol and diesel. Lubricants and other hydrocarbon materials are often washed into surface water by surface runoff during rain storm events. The ingestion of water that has been contaminated with arsenic by humans can lead to cancer of the liver, lungs, and bladder (Inyinbor Adejumo et al. 2018).

Iron (Fe) concentration was 0.11 mg/l at control, 0.46 mg/l at the brewing industry, 0.06 mg/l at the residential area, 1.0 mg/l at the pharmaceutical industry, 8.22 mg/l at the confectionary industry, and 0.12 mg/l at the agro-processing industry. WHO (2008) standard stipulates a maximum of 0.1 mg/l in drinking water. High iron concentration may occur in sources of water that are anaerobic, and this may be accompanied by high turbidity and considerable discolouration, and hence the depleting the aesthetic value of the water (Fawell and Nieuwenhuijsen 2003). Copper (Cu) exhibits a gradual increase downstream almost in a consistent manner with values ranging between 0.31 mg/l and 0.44 mg/l. These values are less than the WHO (2008) provisional guideline of 2.0 mg/l. Surface runoff from roads into streams usually possesses certain concentration of copper, derived from vehicle brake pads (Davie 2008). Vehicles and trailers that convey raw materials and manufactured goods from the industrial estate are important contributors in this

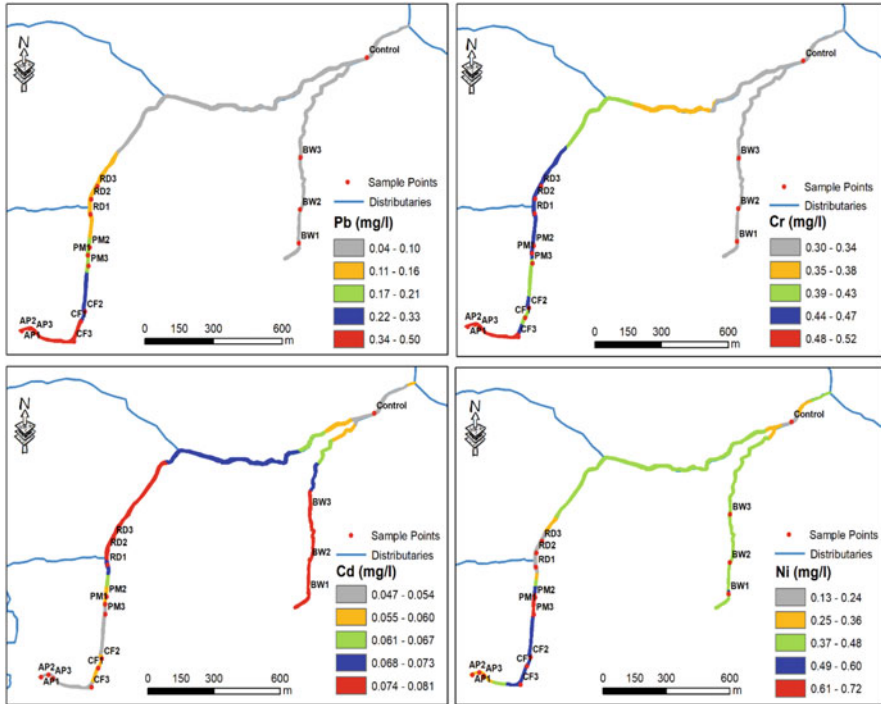


Fig. 12.9 Spatial pattern of lead, chromium, cadmium, and nickel along the Industrial Estate River

regard. Hence, there is high tendency for copper concentration in this basin to increase in the nearest future due to the rapidly urbanizing nature of the environment. The concentration of zinc (Zn) was 0.021 mg/l upstream at the control, then range between 0.013 mg/l and 0.56 mg/l among the industrial sites, while least value of 0.01 mg/l was observed at the residential area. Industries, from time to time, engage in structural repairs and construction activities. As identified by Alloway and Ayres (1997), zinc contamination can be derived from galvanized steel, especially in roofs and wire fencing.

The risk of lead (Pb) contamination is evident in this basin as its concentration ranges between 0.037 mg/l and 0.346 mg/l. Values such as 0.346 mg/l, 0.302 mg/l, 0.185 mg/l, and 0.234 mg/l, which are higher than 0.01 mg/l, the WHO (2008) permissible limit for drinking water, were observed at the agro-processing, confectionary, pharmaceutical, and brewing industries, respectively. The industries use heavy engines that require the use of petrol and diesel, which are major sources of lead. The exposure of children to lead contamination even at very low level may cause loss of memory, impede learning, cause psychological instability, and aggressiveness (Verma and Schneider 2017). High level of lead exposure in pregnant women may cause miscarriage, while in men, it adversely impacts the organs vital for sperm production (Inyinbor Adejumoke et al. 2018). The concentration of

chromium throughout the basin exceeds the WHO (2008) provisional guideline of 0.05 mg/l. The mean values are 0.33 mg/l at the control, 0.31 mg/l at the brewing industry, 0.46 mg/l at the residential area, 0.44 mg/l at the pharmaceutical industry, 0.46 mg/l at the confectionary industry, and 0.52 mg/l at the agrochemical industry. The concentration of cadmium is also higher than the WHO recommended limit of 0.003 mg/l. The values range between 0.043 mg/l and 0.081 mg/l, with the highest level recorded at the brewing industry. The ingestion of cadmium contaminated food can cause bone flimsiness as well as kidney and brain damage (Inyinbor Adejumo et al. 2018).

The level of nickel includes 0.16 mg/l at the control, 0.49 mg/l at the brewing industry, 0.14 mg/l at the residential area, 0.67 mg/l at the pharmaceutical industry, 0.56 mg/l at the confectionery industry, and 0.29 mg/l at the agro-processing industry. These values all exceed the WHO (2008) permissible limit for drinking water.

12.4 Risk Assessment

Developing countries like Nigeria are exposed to the problem of imbalance between socio-economic and environmental considerations in siting industries. Urban centers in Nigeria are characterized by the siting of residential areas around industrial zones as in the case of the estate examined in this study as well as other industrial estates in Ibadan. There are also some common industrial activities that are situated within residential areas and along major roads apart from being situated in industrial estate. Specifically, haulage parks and mechanic workshops are good examples of these activities. Fashae et al. (2019b) for instance found a positive relationship between the soil and the various heavy metals concentration of the adjoining land of a haulage park. This is an environmentally unfriendly practice that poses severe threats to public health. Industrialization, especially in Nigeria, is largely dominated by the use of crude equipment that are characterized with environmental challenges such as surface water and groundwater contamination, atmospheric pollution, improper disposal of waste effluents, and environmental degradation of terrestrial and aquatic resources.

Although the presence of certain heavy metals such as zinc, copper, cobalt, iron, vanadium, and manganese, which are referred to as essential elements, are necessary in minute quantity for normal functioning of body metabolism, others such as arsenic, cadmium, and mercury offer considerable threat to the biological system. Sewage sludge derived from industries, when release waste into sewage systems, is usually rich in heavy metals (Davie 2008). It is important to note that the surface water bodies receive contaminants not only as direct discharge of waste materials into them and surface runoff carrying pollutants but also through atmospheric deposition of pollutants, which sometimes coalesce and settle down on water surfaces.

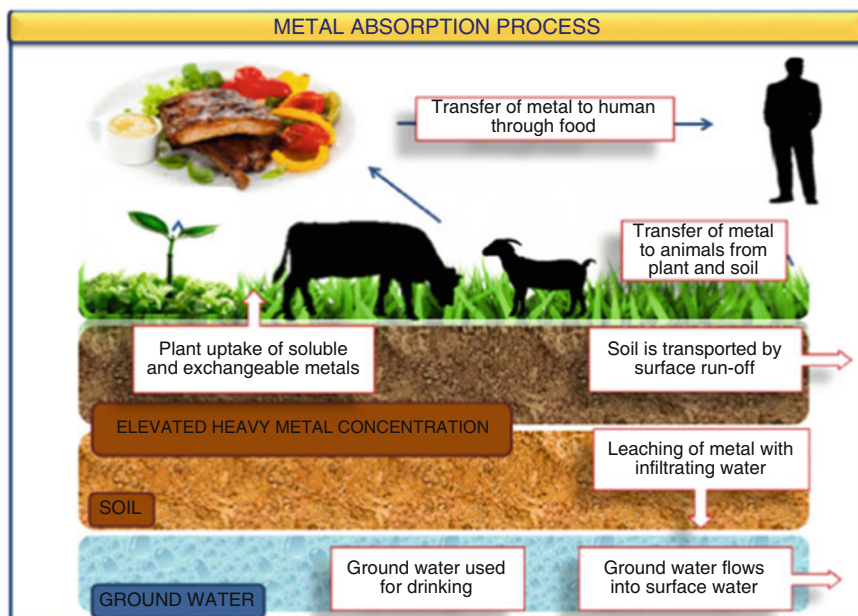


Fig. 12.10 Process of metal absorption process from the ecological food chain. (Source: Singh and Prasad 2015)

Heavy metals are important inorganic contaminants with diverse range of adverse impacts on aquatic and terrestrial organisms, and humans. Their presence in the environment can alter the metabolism and normal function of plants system. Humans and animals can be exposed to severe health hazards through the intake of water containing these contaminants. They can also bioaccumulate in plants and follow the food chain sequence to animals and humans (Inyinbor Adejumoke et al. 2018). The problem of biomagnification can also manifest where the concentration of the contaminants increases from one level in the food chain to another (Fig. 12.10).

Common health implications of heavy metal toxicity in humans include mild eye, nose, and skin irritations, stomach ache, headache, dizziness, vomiting, hematemesis, necrosis, cirrhosis, low blood pressure, hypertension, and gastrointestinal distress (Dada et al. 2016). Since industries utilize heavy hydrocarbon engines for their production and generators for power supply, it can be said that they all contribute to heavy metal contamination in the industrial basin. Even the residential zone is not exonerated as most people rely on the use of gasoline and diesel engines for electricity generation, on the one hand, and utilize automobiles for transportation on the other hand.

Even though only some physicochemical parameters and heavy metals were assessed in this study, pharmaceutical chemicals, which find their ways into the environment through discharge from the pharmaceutical industry, household waste, drainage and sewage, and leachate from landfill, among others, are renowned for

both acute and chronic toxicity on aquatic organics (Archer et al. 2017). Pharmaceuticals are members of endocrine disruptive chemicals (EDCs). EDCs are often associated with abnormal endocrine system alternation, which can range from a decrease in the production of eggs and sperm cells to feminization of female aquatics (Akanyeti et al. 2017).

Since risk is a product of the amount and/or duration of exposure of the organism and the toxicity of the contaminants, it can be said that the residential zone is the most vulnerable to hazards associated with heavy metal contamination. The residential area is at a considerable risk of contamination from industrial effluents. Residents rely on surface water if not for drinking but for other domestic activities like cooking and washing. Polluted overland flow infiltrates into the soil profile to contaminate the groundwater aquifer into which wells have been sunk and drinking water is dependent upon. During dry seasons, the stream lose water to the soil through lateral flow. The contaminants remobilize in the soil and sometimes move vertically through the soil profile under capillary action to accumulate in the top soil layer. Moreover, in the residential compounds where arable cropping and livestock rearing are also practiced, the possibility of bioaccumulation and biomagnification becomes high.

12.5 Remediation

The 2030 Sustainable Development Goals emphasized the need to consider future policies relating to water pollution mitigation as national and international priorities. For any remediation technique to be effective in the industrial basin, effluent discharge standards, polices, and guidelines as stipulated by the National Environmental Standards and Regulations Enforcement Agency (NESREA) must be strictly adhered to. Industries sites must meet permissible limits for their effluents, while enforcement must take place without political favoritism. Singh and Prasad (2015) carried out a comparative evaluation of different techniques of metal remediation in the environment. The methods identified include physical method (mechanical separation, electrokinetic remediation), chemical method (soil washing, soil flushing), soil amendments (addition of lime, chelating agents, and biological products), biological method (use if micro-organism), phytoremediation (phytostabilization, phytoextraction, phytofiltration, phytovolatilization), biotechnological approach (use of genetic tools), and nanotechnology approach. However, Zaidi and Pal (2017) have affirmed the potency of phytoremediation as an effective technique for cleaning up metal contaminated aquatic systems. Phytoremediation is considered as the most viable method to remediate the situation of heavy metal contamination in the studied industrial basin. The choice of the method takes into consideration the level of technological sophistication of the country and the mild to severe level of contamination in the basin. Plants have proven useful in removing contaminants such as organic compounds, heavy metals, trace elements, and radioactive compounds, from water, soil, and sediments by degenerating organic pollutants or by

acting as filters or traps that will stabilize metallic pollutants (Zaidi and Pal 2017). Categories of phytoremediation include: phytoextraction, phytostabilization, phytofiltration, and phytovolatilization. These techniques require the use of both terrestrial and aquatic plants in the absorption, concentration, or precipitation of metallic ions. These plants decontaminate water and soil through the activation of metals in the rhizosphere or by their translocation in the aerial parts of the plants (Singh and Prasad 2015). Relevant plant families in this regard are Brassicaceae, Asteraceae, Fabaceae, Caryophyllaceae, Lamiaceae, Euphorbiaceae, Cyperaceae, and Poaceae (Sarma 2011). In aquatic systems, phytofiltration method has been adjudged more effective for metal removal (Jing et al. 2007). Tobacco, sunflower, rye, Indian mustard, corn, and spinach are plants that are useful in remediating heavy metals in water bodies in the process of rhizofiltration (Jadia and Fulekar 2009; Singh and Prasad 2015). The long and fibrous nature of the roots of some of these plants helps in increasing their decontamination property (Raskin and Ensley 2000). Prasad and Freitas (2003) reported the effectiveness of the roots of Indian mustard in decontaminating cadmium, chromium, copper, nickel, zinc, and lead. Phytoremediation as a metal remediation method is known for its efficiency, cheapness, and eco-friendliness. However, the decontamination process is relatively slow compared to physical and chemical methods (Zaidi and Pal 2017).

12.6 Conclusion

Industrial activities are usually accompanied by a serious level of environmental pollution ranging from surface and groundwater contamination through atmospheric pollution to ecosystem degradation in general. This study assessed the magnitude and distribution of 14 physiochemical parameters in an industrial basin using a simple geospatial technique. The concentration of heavy metals such as arsenic, lead, chromium, cadmium, and nickel were observed to exceed the recommended standards. Public health and ecosystems in the basin are exposed to pollution hazards. Phytoremediation was, however, recommended as an environmentally friendly and affordable technology to remediate the basin from these metallic contaminants.

References

- Adekola FA, Eletta OAA (2007) A study of heavy metal pollution of Asa River, Ilorin, Nigeria; trace metal monitoring and geochemistry. *Environ Monit Assess* 125(1–3):157–163
- Adekunle AS, Eniola ITK (2008) Impact of industrial effluents on quality of segment of Asa river within an industrial estate in Ilorin, Nigeria. *New York Sci J* 1(1):17–21
- Ahmad MK, Islam S, Rahman S, Haque M, Islam MM (2010) Heavy metals in water, sediment and some fishes of Buriganga River, Bangladesh. *Environ Sci Pollution Res Int* 22 (20):15880–15890

- Akanyeti I, Kraft A, Ferrari MC (2017) Hybrid polystyrene nanoparticle-ultrafiltration system for hormone removal from water. *J Water Process Eng* 17:102–109
- Alloway B, Ayres DC (1997) Chemical principles of environmental pollution. CRC Press, Boca Raton, FL
- Allsgeer HMA, Gasim MB, Hanafiah MM, Abdulhadi ERA, Azid A (2018) GIS-based analysis of water quality deterioration in the Nerus River, Kuala Terengganu, Malaysia. *Desalin Water Treat* 112:334–343
- Archer E, Petrie B, Kasprzyk-Hordern B, Wolfaardt GM (2017) The fate of pharmaceuticals and personal care products (PPCPs), endocrine disrupting contaminants (EDCs), metabolites and illicit drugs in a WWTW and environmental waters. *Chemosphere* 174:437–446
- Dada OA, Adekola FA, Odebunmi EO (2016) Kinetics and equilibrium models for sorption of Cu(II) onto a novel manganese nano-adsorbent. *J Dispers Sci Technol* 37(1):119–133
- Davie T (2008) Fundamentals of hydrology. Routledge, New York
- Elbag MA (2006) Impact of surrounding landuses on surface water quality. M.Sc. Thesis in Environmental Engineering Worcester Polytechnic Institute
- El-Fadel M, Zeinati M, El-Jisr K, Jamali D (2001) Industrial-waste management in developing countries: the case of Lebanon. *J Environ Anagement* 61(4):281–300
- Fashae OA, Olusola AO (2017) Land use types within channel corridor and River Channel morphology of river Ona, Ibadan, Nigeria. *Indones J Geogr* 49(2):111–117
- Fashae OA, Ayomanor R, Orimoogunje OO (2017) Land use dynamics and surface water quality in a typical urban Centre of south-western, Nigeria. *Analele Universităţii din Oradea, Seria Geografie* 27(1):98–107
- Fashae OA, Ayorinde HA, Olusola AO, Obateru RO (2019a) Landuse and surface water quality in an emerging urban city. *Appl Water Sci* 9(2):25
- Fashae OA, Olusola AO, Orekan P (2019b) Assessing heavy metal distribution and contamination of soil in Ogere trailer terminal, Ogun state (Southwestern Nigeria). In: Boughdiri M, Bádenas B, Selden P, Jaillard E, Bengtson P, Granier B (eds) Paleobiodiversity and tectono-sedimentary records in the mediterranean tethys and related eastern areas. CAJG 2018, advances in science, technology & innovation (IEREK interdisciplinary series for sustainable development). Springer, Cham
- Fawell J, Nieuwenhuijsen MJ (2003) Contaminants in drinking water. *Environmental pollution and health. Br Med Bull* 68(1):199–208
- FWR (Foundation for Water Research) (2015) Sources of pollution information note FWR – WFD16
- GEMS (2004) State of water quality assessment reporting at the global level (R. Robarts). Presentation at the UN International Work Session on Water Statistics
- Gayawali S, Techato K, Yuangyai C (2012) Effects of industrial waste disposal on the surface water quality of U-tapao river, Thailand. In: International conference on environment science and engineering, international proceedings of chemical, (vol. 3(2), pp. 109–113), Biological and Environmental Engineering, Singapore
- Inyinbor Adejumoke A, Adebesein Babatunde O, Oluyori Abimbola P, Adelani Akande Tabitha A, Dada Adewumi O, Oreofe Toyin A (2018) Water pollution: effects, prevention, and climatic impact. *Water Challenges of an Urbanizing World*, 33
- Iroye KA, Igbozurike JC (2018) Assessment of heavy metal in urbanized Tropical River in Ibadan, Nigeria. *Int J Multidiscip Stud* 5(2):42
- Jadia CD, Fulekar MH (2009) Phytoremediation of heavy metals: recent techniques. *Afr J Biotechnol* 8(6):921–928
- Jaji MO, Bamgbose O, Odukoya OO, Arowolo TA (2007) Water quality assessment of Ogun River, south West Nigeria. *Environ Monit Assess* 133(1–3):473–482
- Jing Y, He Z, Yang X (2007) Role of soil rhizobacteria in phytoremediation of heavy metal contaminated soils. *J Zhejiang Univ Sci B* 8:192–207
- Kaushik R (2015) Mathematical modelling on water pollution and self-purification of river Ganges. *Pelagia Res Libr* 6(7):57–64

- Kibria G (2016) World Rivers in crisis: water quality and water dependent biodiversity are at risk—threats from pollution, climate change and dams development. p 12, <https://doi.org/10.13140/RG.2.1.1791.5365/2>
- Kjellstrom T, Lodh M, McMichael T, Ranmuthugala G, Shrestha R, Kingsland S (2006) Air and water pollution: burden and strategies for control. In: Disease control priorities in developing countries, 2nd edn. The International Bank for Reconstruction and Development/the World Bank, Washington, DC
- Mazaheri M, Mohammad Vali Samani J, Samani HVM (2015) Mathematical model for pollution source identification in rivers. *Environ Forensic* 16(4):310–321
- Meng Y, Zhou L, He S, Lu C, Wu G, Ye W, Ji P (2018) A heavy metal module coupled with the SWAT model and its preliminary application in a mine-impacted watershed in China. *Sci Total Environ* 613:1207–1219
- Merem EC, Twumasi Y, Wesley J, Isokpehi P, Shenge M, Fageir S, Crisler M, Romorno C, Hines A, Hirse G, Ochai S (2017) Analyzing water management issues using GIS: the case of Nigeria. *Geosciences* 7(1):20–46
- Ogbozige FJ, Adie DB, Abubakar UA (2018) Water quality assessment and mapping using inverse distance weighted interpolation: a case of river Kaduna, Nigeria. *Niger J Technol* 37(1):249–261
- Oke A, Sangodoyin A, Ogedengbe K, Omodele T (2013) Mapping of river waterquality using inverse distance weighted interpolation in Ogun-Osun river basin, Nigeria. *Acta Geogr Debrecina Landscape Environ* 7(2):48–62
- Olayinka KO, Alo BI (2004) Studies on industrial pollution in Nigeria: the effect of textile effluents on the quality of groundwater in some parts of Lagos. *Niger J Health Biomed Sci* 3(1):44–50
- Parsaie A, Haghiabi AH (2017) Computational modeling of pollution transmission in rivers. *Appl Water Sci* 7(3):1213–1222
- Pimpunchat B, Sweatman WL, Wake GC, Triampo W, Parshotam A (2009) A mathematical model for pollution in a river and its remediation by aeration. *Appl Math Lett* 22(3):304–308
- Prasad MNV, Freitas HMD (2003) Metal hyperaccumulation in plants—biodiversity prospecting for phytoremediation technology. *Electron J Biotechnol* 93(1):285–321
- Ramaraju A, Giridhar MVSS (2015) Spatial analysis of surface water bodies quality using GIS. Hydro 2015 International IIT Roorkee, India, 20th international conference on hydraulics, Water Resources and River Engineering
- Raskin I, Ensley BD (2000) Phytoremediation of toxic metals. John Wiley and Sons, New York
- Sangodoyin AY (1995) Characteristics and control of industrial effluent-generated pollution. *Environ Manag Health* 6:15
- Sarma H (2011) Metal hyperaccumulation in plants: a review focusing on phytoremediation technology. *J Environ Sci Technol* 4(2):118–138
- Schwarzenbach RP, Egli T, Hofstetter TB, Von Gunten U, Wehrli B (2010) Global water pollution and human health. *Annu Rev Environ Resour* 35:109–136
- Singh MR, Gupta A (2017) Water pollution-sources, effects and control. Centre for Biodiversity, Department of Botany, Nagaland University, Lumami
- Singh A, Prasad SM (2015) Remediation of heavy metal contaminated ecosystem: an overview on technology advancement. *Int J Environ Sci Technol* 12(1):353–366
- Sukojo BM, Sianipar RE (2018) Spatial analysis of water pollution using multitemporal satellite imagery (case study: river Lamong estuary, Surabaya). In: IOP Conference series: earth and environmental science (vol. 165(1), p. 012015). IOP Publishing, Bristol
- Trivedi RC (2010) Water quality of the Ganga River—an overview. *Aquat Ecosyst Health Manag* 13(4):347–351
- United Nations Environment Programme (UNEP) (1996) Groundwater: a threatened resource. UNEP environment library no. 15. UNEP, Nairobi, Kenya
- UN-Water (2009) World water day brochure. <http://www.unwater.org/worldwaterday/downloads/wwd09brochureenLOW.pdf>
- USEPA (2000) <https://www.epa.gov/superfund/superfund-history>

- USEPA (2004) The national water quality inventory: report to congress for the 2004 reporting cycle – A profile. (EPA 841-R-08-00) http://water.epa.gov/lawsregs/guidance/cwa/305b/2004report_index.cfm
- Utomi P (2019) Why microplastics found In Nigeria’s freshwaters raise a red flag. <https://newsproben.com/why-microplastics-found-in-nigerias-freshwaters-raise-a-red-flag/>
- Verma M, Schneider JS (2017) Strain specific effects of low level lead exposure on associative learning and memory in rats. *Neurotoxicology* 62:186–191
- Wendlinger J (2019) Polluted rivers as the major source of marine debris: a study case of Citarum River. <https://waste4change.com/blog/polluted-rivers-as-the-major-source-of-marine-debris-a-study-case-of-citarum-river/>
- WHO (2003) Guidelines for drinking-water quality, volume 1, recommendations (1st addendum to 3rd ed.). World Health Organization, Geneva
- WHO (2008) Guidelines for drinking-water quality: incorporating the first and second addenda. World Health Organization, Geneva
- WHO (World Health Organization) (1976) Mercury. Environmental health criteria 1. WHO, Geneva
- World Bank (1999) Pollution prevention and abatement handbook 1998. World Bank, Washington, DC. <http://wbln0018.worldbank.org/essd/essd.nsf/GlobalView/PPAH>
- WWAP (2003) United nations world water assessment Programme. In: The world water development report 1: water for people, water for life. UNESCO, Paris
- WWAP (2017) The United Nations world water assessment report 2017: wastewater, the untapped resource, United Nations world water assessment Programme (WWAP). United Nations Educational, Scientific and Cultural Organization, Paris
- Yaghi A, Salim H (2017) Integration of Rs/gis for surface water pollution risk modeling. Case study: Al-Abrash Syrian coastal basin. *Int Arch Photogram Remote Sens Spat Inf Sci* 42 (2/W7):949–954
- Yan CA, Zhang W, Zhang Z, Liu Y, Deng C, Nie N (2015) Assessment of water quality and identification of polluted risky regions based on field observations & GIS in the honghe river watershed, China. *PLoS One* 10(3)
- Yassi A, Kjellström T, De Kok T, Guidotti TL (2001) Basic environmental health. Oxford University Press, Oxford
- Yetik MK, Yüceer M, Berber R, Karadurmuş E (2009) River water quality model verification through a GIS based software. *IFAC Proc* 42(11):798–803
- Yusuff RO, Sonibare JA (2004) Characterization of textile industries’ effluents in Kaduna, Nigeria and pollution implications. *Global Nest Int J* 6(3):212–221
- Zaidi J, Pal A (2017) Review on heavy metal pollution in major lakes of India: remediation through plants. *Afr J Environ Sci Technol* 11(6):255–265

Chapter 13

Aquaculture-Based Water Quality Assessment and Risk Remediation along the Rasulpur River Belt, West Bengal



Suraj Kumar Mallick, Biswajit Maity, and Somnath Rudra

Abstract Over the past few decades, intensive aquaculture activity created negative consequences on the surface water quality in the developing nations. This study has given emphasis on the assessment of the use of chemicals in the aquaculture activities along the Rasulpur River belt and its impact on water quality. For that purpose, 24 samples of freshwater and saline water were collected during a field survey in post-monsoon, 2018, and pre-monsoon, 2020, and those samples are tested to analyze the physicochemical composition of aquaculture like pH, TDS, SO_4 , F^- , As, DO, BOD, NO_3 , chloride, and total hardness. The use of disinfectants, antibiotics, fertilizers, feed additives, and water-treated compounds was collected through the interviewing method to know the contamination level of aquaculture. The result of the spatial water quality index (SWQI) map depicted that the water quality of aquaculture was more contaminated along the river bank due to applying ample amount of chemical compounds for commercial shrimp culture, but in the case of freshwater, aquaculture away from the river was less contaminated for the subsistence nature of aquaculture. Although the results showed that the production of aquaculture was increasing, the practitioners were not concerned about the human health impact and quality of the water. So, there is an urgent need for proper assessment and evaluation regarding these anxieties, which have already been taken in the developed nations.

Keywords Aquaculture · Physicochemical composition · Chemical compounds · Spatial water quality index (SWQI) map

S. K. Mallick · B. Maity · S. Rudra (✉)
Department of Geography, Vidyasagar University, Midnapore, India

© Springer Nature Switzerland AG 2021
P. K. Shit et al. (eds.), *Spatial Modeling and Assessment of Environmental Contaminants*, Environmental Challenges and Solutions,
https://doi.org/10.1007/978-3-030-63422-3_13

213

13.1 Introduction

Aquaculture is one of the fastest emerging economic activities in Southeast Asia (Ali et al. 2016). In the case of India, now aquaculture has taken a significant spot in respect of economic structure (FAO 2016). By this time, aquaculture activity is divided into two categories, and one of them is marine aquaculture and another one is freshwater-based aquaculture. In respect of India, inland aquaculture produced 60% of total production and 6.3% share in the world in 2014 (Handbook on Fisheries Statistics 2014). But, in very few occasions where saline water availability is much higher in manner, we can see the development of saline water-based aquaculture or marine aquaculture. In the last decade, aquaculture has been taken a booming up activity in terms of production (FAO 1998). Moreover, this type of culture basically influences local economy and creates scopes of engagement for the rural women and marginal farmers. Moreover, this type of culture basically influences local economy and creates scopes of engagement for the rural women and marginal farmers. In West Bengal, fishes are produced from all types of water bodies like freshwater, sewage water, saline water, and marine water (Paul and Chakrabarty 2016). Although this type of aquaculture is produced for subsistence to provide the food in daily life, there has some negative impact on environment as well.

In the aquaculture system, pond dynamics have exhibited a continuous and persistent fluctuation. The pond experiences an enormous collection of physical exchanges and chemical reactions. So, it is very difficult to maintain the good quality of water for survival and constant growth of aquaculture organisms. Moreover, the surpass level of metabolites can adversely affect the growth, especially for the shrimp, prawns, or fishes.

The recent sprout of aquaculture activities has converted the agriculture land to fisheries along a vast tract of Rasulpur River at Purba Medinipur district of West Bengal. Nowadays, an ample number of local farmers are associated with both the freshwater farming and saline water farming. Moreover, most of the farmers still do not have any training or scientific bases for this kind of farming. Consequently, the quality of water has become an issue for aquaculture farming. The standard and optimum level of water quality in aquaculture has been characterized by adequate oxygen supply and quality of limited metabolism (Ali et al. 2016). Therefore, water quality assessment for sustainable aquaculture development has become a growing concern for developing nations.

Many researchers worked in this field regarding chemical and biological impacts on aquaculture (Graslund and Bengtsson 2001; Rico et al. 2012; Ali et al. 2016), environmental impacts (Santos et al. 2015; Perdikaris et al. 2016), aquaculture sustainability (Vassallo et al. 2007; Pullin et al. 2007; Valenti et al. 2011), lifecycle assessment (Medeiros et al. 2017), and future prospects of aquaculture (Folke and Kautsky 1992).

In this study, the geographical information system (GIS) has played a significant role in the analysis of the spatial water quality index (SWQI) and its dynamics over time (Saleem et al. 2016). There are many established methods for spatial water

quality assessment such as IDW interpolation method, Kriging interpolation method, etc. (Kupwade and Langade 2013). We have used the Kriging interpolation method to detect the changes in aquaculture water quality at the post-monsoon, 2018, and pre-monsoon, 2020. It helps to generate more accurate spatial data compared to other geospatial interpolation methods (Li and Heap 2014).

So, the prime objective of the study is to evaluate the water quality related to aquaculture activity and its chemical and physicochemical impacts along the Rasulpur river belt, Purba Medinipur, West Bengal.

13.2 Databases and Methodology

13.2.1 Study Area

For this study, we have selected four CD-blocks of Purba Medinipur district in West Bengal, which are Khejuri-II in the north, Contai-II in the south, and Contai-III in the west, and Rasulpur River flows across the middle of the study area. The extension of the study area is from $21^{\circ}40'22.94''\text{N}$ to $22^{\circ}02'47.24''\text{N}$ latitude and from $87^{\circ}39'4.71''\text{E}$ to $87^{\circ}58'38.45''\text{E}$ longitude with the elevation of 5–6 m from the mean sea level (MSL) covering an area of 47.72 km^2 (Fig. 13.1). Rasulpur River basin and its surrounding C.D block like Khejuri-I, Khejuri-II, Contai-II, and Contai-III are the parts of the area where the growing concern of land transformation from agricultural land to aquaculture land is noticed. Geographically, this area is situated along the Rasulpur River and is a part of flood plain of river Hugli. In general, this region occupies a monotonous low-lying tract with lesser elevation just above sea level. The construction slope of this area is from west to east.

Naturally, the entire geological structure is marked by alluvial deposits of river Hugli and Rasulpur. This area has experienced monsoon climate. During winter season, mean temperature is about 20°C , and in summer season, it is 32°C . The mean annual precipitation is 120–140 cm. The highest rainfall has been occurred during the month of July and August. The suitable physical and climatic condition allows enough dynamicity in land transformation of the region.

13.2.2 Sample Collection

In this study, we have collected 24 samples from the freshwater and saline water aquaculture ponds during a field study of post-monsoon, 2018, and pre-monsoon, 2020 (Fig. 13.2), through stratified random sampling technique, and the collected samples are tested in the laboratory to analyze the physicochemical composition of aquaculture like pH, TDS, SO_4 , F^- , As, DO, BOD, NO_3 , chloride, and total hardness. Then, the laboratory-tested results have been calculated and checked by standard water quality index values (WHO 2011) comprehensively. Moreover, some

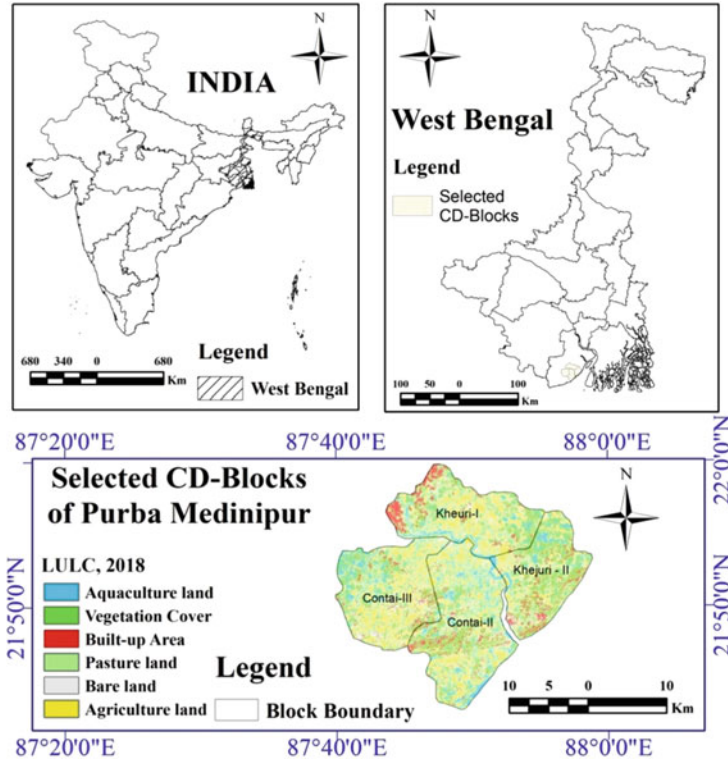


Fig. 13.1 Location map of the study area with the current land-use scenario

interview has been taken of some experts and practitioners regarding aquaculture activity to validate the collected field data.

13.2.3 Data Analysis and Spatial Water Quality Assessment

Collected data have been computerized using various statistical software for social science like SPSS and Excel software. The physicochemical components are tabulated, and the water quality index has been calculated using the standard formula (Eq. (13.1)). Then, these index values are inserted into the attributed table in ArcGIS 10.3 software. It has been classified into four categories (very good, good, poor, and very poor) on the basis of water quality index values at the standard scale (WHO 2011). Then, the spatial water quality index (SWQI) map has been prepared using the Kriging Interpolation method on ArcGIS. Kriging is defined as linear least square estimates of data (Remy et al. 2011). It has used Z-score to generate a spatial map using spatial scattered sets of data in a different time interval. It has been used for

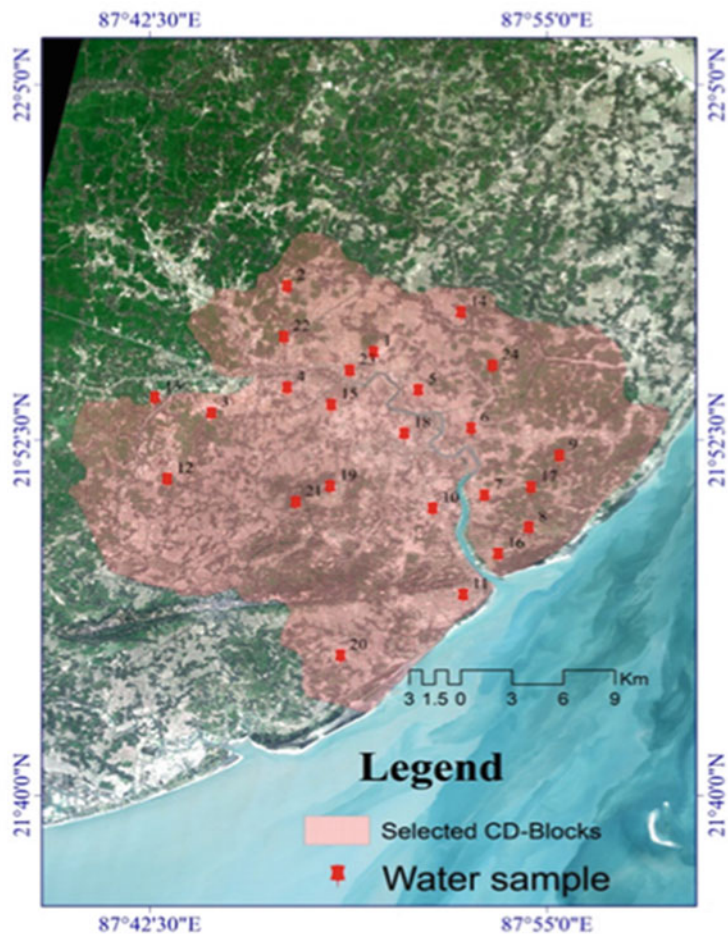


Fig. 13.2 Collected water sample sites of freshwater and saline water

sample data set rather than any kind of pre-assumed model. This interpolation has given more specific sample weight to the nearby location. Finally, for better understanding, we have used a cross-sectional profile over the interpolated map. Moreover, SQWI can be performed well to denote the different water quality during the post-monsoon and pre-monsoon period. Thereafter, chemical impacts can be validated for the water quality of aquaculture pond, and it can be cross-checked by expert opinions as well.

$$WQI = \sum q_n W_n \div \sum W_n \tag{13.1}$$

where q_n = water quality rating; W_n = unit weight of the selected parameter.

13.3 Results and Discussion

13.3.1 *Status of Physicochemical Components in the Aquaculture Pond*

The physicochemical components have been tested and then validated the given results as per national and international standard scales. The process of the calculation method is shown in the water quality index table for sample 1, and a similar calculation method is followed for the rest of the 23 samples (Tables 13.1 and 13.2).

13.3.1.1 pH

The concentration of hydrogen ions (H^+) or pH measures the alkalinity or acidity present in the pond water. This scale ranges from 0 to 14, where 0 is indicated the most acidic in nature and 14 being the utmost alkaline. In this study, the pH value of the water sample was ranged between 6.5 and 8.5 during pre-monsoon and 6.2–8.1 during post-monsoon; it can be maintained the acceptable growth of aquaculture products. The suitable range of pH for growth and production should be maintained: pH 6.8–8.7 (WHO 2011). If the pH value is increased ($pH > 9.0$), then the ammonia toxicity increases accordingly. Therefore, the pH value has to be under control for aquaculture activity for both the seasons.

13.3.1.2 Total Dissolved Solid (TDS)

Total dissolved solid (TDS) is an important physicochemical component that can be useful for the measurement of water quality. TDS is the combination of potassium, sodium, calcium, magnesium, phosphate, chloride, and other particles. The highest TDS value was found in sample number 14 (623 mg/l), while the lowest value was observed in the sample number 23 (270 mg/l) during pre-monsoon, and in post-monsoon, the highest TDS value was found in sample number 14 (642 mg/l), and the minimum value was found in sample number 24 (210 mg/l). However, the sample numbers 14, 15, and 19 were found to have more than the actual permissible limits, which have to be below 500 mg/l for aquaculture (WHO 2011). Here, the results showed that more contaminated water was present during pre-monsoon.

13.3.1.3 Sulfate (SO_4)

Sulfate has been found especially in the waste and contaminated water. This important physicochemical parameter is used to measure the quality of surface and groundwater. The highest and lowest value of SO_4 was found to be 361 mg/l and 210 mg/l during the pre-monsoon and 264 mg/l and 190 mg/l during post-monsoon,

Table 13.1 WQI table based on water quality rate and unit weight of the selected parameters during post-monsoon, 2018

Chemical parameter (Sample 1)	Standard permissible value (S_n) mg/l	$1/S_n$	K	Actual value (V_i)	Observed value (V_n)	Quality rating (Q_n)	Weightages (K/S_n)	Standard error (SE)
pH	6.5	0.167	1.23	6.5	7.5	125.25	0.19	1.15
SO ₄	250	0.004		-	242	96.80	0.00492	0.968
Fluoride	1.5	0.67		-	0.93	62.31	0.82	0.62
As	0.01	100		-	0.0019	19	0.0123	0.19
BOD	3	0.333		-	1.13	37.63	0.41	0.38
DO	8	0.125		-	5.67	70.87	0.1757	0.71
TDS	500	0.002		-	824	164.80	6.15	1.65
Total hardness	300	0.003		-	459	137.70	4.10	1.37
Chloride	250	0.004		-	221	88.40	307.5	0.88
NO ₃	45.0	0.02		-	22.4	24.80	61.50	0.28

Note: The rest of the 23 samples are calculated by the same calculation method

Table 13.2 WQI table based on water quality rate and unit weight of the selected parameters during pre-monsoon, 2020

Chemical parameter (Sample 1)	Standard permissible value (S_n) mg/l	$1/S_n$	K	Actual value (V_i)	Observed value (V_n)	Quality rating (Q_n)	Weightages (K/S_n)	Standard error (SE)
pH	6.5	0.167	1.23	6.5	8.5	141.95	0.19	1.30
SO ₄	250	0.004		–	341	136.40	0.00492	1.36
Fluoride	1.5	0.67		–	0.77	51.59	0.82	0.51
As	0.01	100		–	0.0012	12	0.0123	0.12
BOD	3	0.333		–	8.28	275.72	0.41	2.76
DO	8	0.125		–	4.47	55.88	0.1757	0.56
TDS	500	0.002		–	614	122.80	615	1.23
Total hardness	300	0.003		–	1050	315	410	3.5
Chloride	250	0.004		–	357	142.8	307.5	1.43
NO ₃	45.0	0.02		–	58.6	117.20	61.50	1.30

Note: The rest of the 23 samples are calculated by the same calculation method

respectively. The WHO (2011) prescribed that the permissible limit of sulfate is below 250 mg/l, and the water quality was contaminated more in the pre-monsoon period than post-monsoon due to intensive aquaculture activity during the pre-monsoon periods.

13.3.1.4 Fluoride (F^-)

Fluoride (F^-) deteriorates the water quality for ground and surface, and its amount surpasses the permissible limit. It has biological impacts more than chemical impacts. Although F^- is missing in most of the water samples, it has been found occasionally in a very insignificant level. The highest and lowest F^- value was found to be 0.98 mg/l and 0.05 mg/l during pre-monsoon and 0.77 mg/l and 0.00 mg/l during post-monsoon, respectively. However, the standard acceptable limit of F^- is 1.5 mg/l (BIS 2012). Although post-monsoon had less prevalence of F^- than the pre-monsoon, in all occasions the F^- value had been below the permissible limit. It is a good sign for aquaculture activity over the study area.

13.3.1.5 Arsenic (As)

Arsenic (As) is one of the most important elements for determining the surface and groundwater quality. In this study area, arsenic was observed in very little amount ranging between 0.002 and 0.0005 during post-monsoon and from 0.0018 to 0.0001 during pre-monsoon. However, the permissible limit of the As is 0.01 (WHO 2011). So, there has no such impact of As on aquaculture activity.

13.3.1.6 Dissolve Oxygen (DO)

Diffusion is the only process that helps the detection of the oxygen from air to water. Atmosphere diffuses oxygen into the pond water, and later on, it has been saturated. The dissolve oxygen (DO) concentration in water is an indicator of organic pollution (Kupwade and Langade 2013). The tested results of DO were found from 3.54 mg/l to 6.67 mg/l during the post-monsoon period, and during pre-monsoon, the value was slightly increased from 4.11 mg/l to 7.14 mg/l; however, the overall value of DO is under the permissible limit (below 8) (WHO 2011), and it has indicated well the quality of metabolism throughout the season in aquaculture due to the active aeration process.

13.3.1.7 Biological Oxygen Demand (BOD)

Biological oxygen demand (BOD) can affect animal growth (Kupwade and Langade 2013). Surface water sources should have a BOD limit below 3 mg/L (WHO 2011).

If the BOD is exceeded, then the conventional water treatment process will be poorly affected. However, BOD was found in a high concentration along the Rasulpur river belt. The BOD of Sample 1 during the pre-monsoon period is about 8.28 mg/l, and it had crossed the permissible limit at the standard scale. Because of this, this sample site quickly converted to a high mortality site. Prevention of this problem on an urgent basis will only change the total water.

13.3.1.8 Nitrate (NO₃)

Nitrate concentration in surface water is due to the leaching of nitrate into the soil. The highest nitrate found from this study area was about 58.6 mg/l and the lowest value was 11.1 mg/l during pre-monsoon. But, during post-monsoon, the highest value was 74.44 mg/l and the lowest value was 17.91 mg/l. The important source of nitrate may be the nitrogen-based fertilizer that was used more often in the agriculture field. It had percolated with river water during the rainy season. So, during post-monsoon, nitrate creates an impact on the aquaculture pond along the river site. However, the acceptable limit of nitrate in aquaculture water is 45 mg/l (WHO 2011). Overall results showed that nitrate crossed the permissible limits and affected aquaculture species greatly.

13.3.1.9 Chloride

Chloride is another dangerous toxic element found in both the ground and surface water. The concentration of chloride was observed from 185 to 257 mg/l during pre-monsoon and 172 to 425 mg/l during post-monsoon. Along the Rasulpur river site, chloride was concentrated extremely higher than the other parts of the study area due to direct industrial discharge effects. However, the permissible limit of chloride is 250 mg/l (BIS 2012), and most of the collected samples had the concentration of chloride below the permissible limits.

13.3.1.10 Total Hardness

Total hardness is also an important parameter to understand about how much water quality drinkable for human beings or suitable for aquaculture. Basically, it has been categorized into two aspects, i.e. temporary hardness that deals with the presence of calcium bicarbonate or magnesium in the surface water or groundwater and permanent hardness that deals with calcium chloride or magnesium sulfate concentration in the pond water or groundwater. Permanent hardness has more dangerous or harmful effects on aquaculture species, because it has created various diseases of kidney and stomach (WHO 2011). The total hardness value found during post-monsoon was 1050 mg/l, and during pre-monsoon, it was 675 mg/l. But, the average hardness of water was higher during pre-monsoon than during the post-monsoon period except

Samples 1 and 14. So, as per the BIS (2012) standard, the observed results are not within the permissible range except Samples 3, 4, 5, 23, and 24 in both seasons.

13.3.2 Spatial Analysis of Water Quality during Pre-monsoon and Post-monsoon

The spatial water quality index maps (Fig. 13.3) were prepared based on water quality index data (Table 13.3). The water quality data ranged from 33.45 to 169.73 during post-monsoon, 2018, and from 42.47 to 216.69 during pre-monsoon, 2020. On the basis of spatial analysis of water quality, the study area was classified into four zones, i.e., very good water quality, good water quality, poor water quality, and very poor water quality zone (Table 13.4). Most of the area (15.03 sq. km) was concentrated by very good quality of water during post-monsoon of 2018 compared to the area during pre-monsoon, 2020. But, very poor quality of water was found in a very small extent, i.e., below 5 sq. km in both the seasons. More or less, the water quality during the post-monsoon season was quite better than pre-monsoon season. The spatial water quality index profile showed the better outcomes and understanding about the spatial variations (Fig. 13.4) and level of water quality in different seasons.

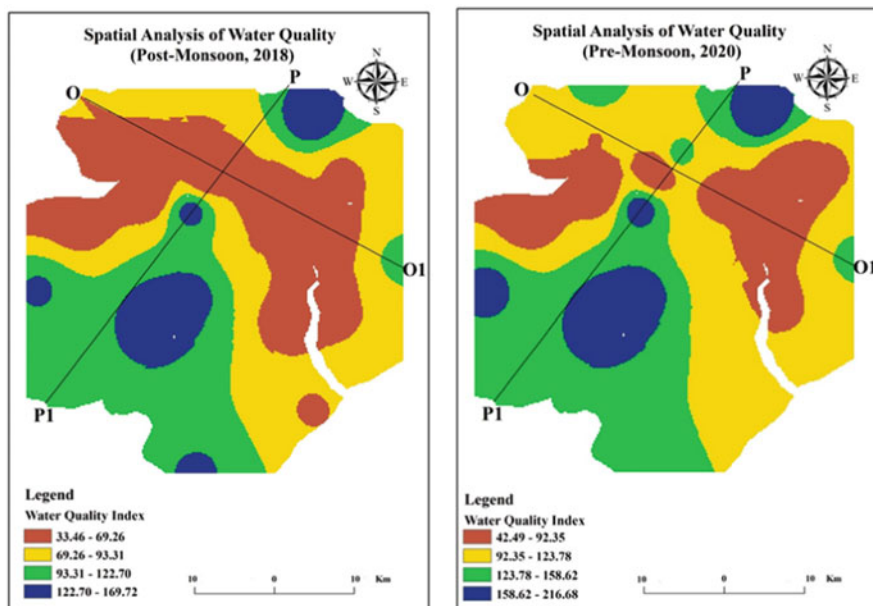


Fig. 13.3 Spatial analysis of water quality during post-monsoon, 2018 and pre-monsoon, 2020

Table 13.3 Water quality index (WQI) table of each sample for post-monsoon (2018) and pre-monsoon (2020)

Sample No.	Sample sites	WQI (post-monsoon, 2018)	WQI (pre-monsoon, 2020)
1	Saline water	80.86	137.13
2	Saline water	83.82	143.28
3	Saline water	42.76	47.34
4	Saline water	33.45	45.66
5	Saline water	39.25	68.39
6	Saline water	44.21	68.21
7	Saline water	48.34	71.43
8	Saline water	72.84	102.72
9	Fresh water	117.32	146.17
10	Saline water	54.61	95.54
11	Saline water	66.67	99.67
12	Fresh water	128.73	177.28
13	Fresh water	52.16	86.52
14	Fresh water	169.73	216.69
15	Fresh water	143.15	192.51
16	Fresh water	77.53	104.77
17	Saline water	72.48	106.84
18	Saline water	68.82	97.68
19	Fresh water	144.13	193.45
20	Fresh water	126.73	148.73
21	Fresh water	158.67	198.76
22	Saline water	60.23	91.62
23	Saline water	37.18	47.81
24	Saline water	63.27	42.47

Table 13.4 Calculated table for spatial water quality index (SWQI) zone during post-monsoon, 2018 and pre-monsoon, 2020

Class	SWQI zone (post-monsoon, 2018)	Area in Sq. Km	SWQI zone (pre-monsoon, 2020)	Area in Sq. Km	SWQI status
Class-1	33.46–69.26	15.03	42.49–92.35	9.76	Very good
Class-2	69.26–93.31	14.66	92.35–123.78	18.64	Good
Class-3	93.31–122.70	13.54	123.78–158.62	14.35	Poor
Class-4	122.7–169.72	4.49	158.62–216.68	4.97	Very poor

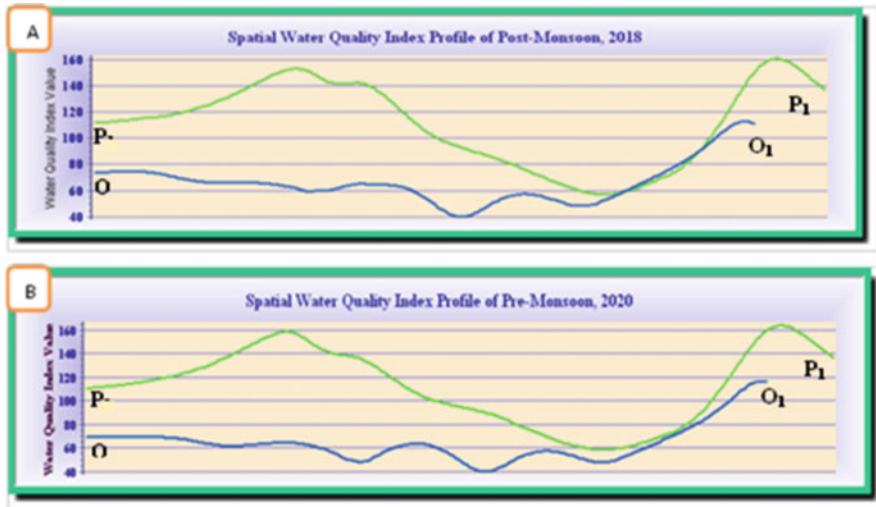


Fig. 13.4 Cross-sectional profile of spatial water quality performance level: (a) post-monsoon, 2018 (P-P₁); (b) pre-monsoon, 2020 (O-O₁)

13.3.3 Chemical Components Inside the Aquaculture Pond

The use of chemical components in the aquaculture of this area is increasing day by day to fulfill the increasing demand. That's why most of the aquaculture ponds have faced deteriorating water quality and thus high risk of diseases. Fertilizer and liming materials are mostly usable products in aquaculture to increase production and treatment of water. Meanwhile, disinfectants, probiotics, herbicides, algacides, and antibodies are also applied for increasing fish production (Boyd and Massaut 1999). Sometimes, chlorine is also used in aquaculture as a disinfectant or to regulate the pH of water. The chemical components used by farmers in this study area are listed in Table 13.5.

13.3.3.1 Soil and Water Treatment Components

Various types of chemical components are used in pond aquaculture for treatment of soil and water, such as aluminum sulfate ($\text{Al}_2[\text{SO}_4]_3 \cdot 14\text{H}_2\text{O}$) or aluminum potassium sulfate ($\text{AlK}[\text{SO}_4]_3 \cdot 14\text{H}_2\text{O}$) used at a concentration of 10–20 mg/l and calcium sulfate or gypsum [$\text{CaSO}_4 \cdot 2\text{H}_2\text{O}$] used at a concentration of 250–1000 mg/l. However, liming materials such as calcium carbonate, calcium magnesium carbonate, calcium oxide, and dolomite are used for treatment of soil and water before aquaculture (Boyd 1995; GESAMP 1997; Graslund and Bengtsson 2001). The most common soil and water treatment materials are used by farmers in the

Table 13.5 Chemical components used for fresh and saline water aquaculture in study area

Soil and water treatment components		Calcium carbonate, calcium hydroxide, calcium oxide, dolomite, potassium dichromate, sodium chloride			
Fertilizer		Pesticides		Disinfectants	References
Inorganic	Ammonium sulfate; Calcium; ammonium nitrate; NPK; Super phosphate; Triple super phosphate	Fungicide	Copper sulfate Malachite green Trifluralin	Benzalkonium chloride, calcium hypochlorite, DDAB, formaldehyde, iodine, and potassium permanganate	Pathak et al. (2000) Amaraneni (2006) Rico et al. (2012)
		Herbicide	2,4-D Dalapon Diuron Paraquat		
		Insecticides	Endosulfan Lindane Malathion Dimethoate		
Organic	Chicken manure; Cow manure	Piscicides	Oil cake Rotenone Saponin (teased cake)		

Rasulpur river belt, but these are limed materials. In the pre-monsoon season, farmers add 100–800 kg/ha to treatment of the bottom soil of the pond, but in the post-monsoon season, 10–500 kg/ha lime is used for treatment. Some farmers add zeolite at the doses of 100–500 kg/ha to eliminate hydrogen sulfide and CO₂ through adsorption in shrimp ponds.

13.3.3.2 Fertilizers

The use of organic and inorganic fertilizers for commercial aquaculture cultivation is very common in the Rasulpur River belt region. Most of the farmers of this region use chicken manure in shrimp farming. Along with organic manure, a combination of inorganic fertilizers, i.e. ammonium phosphate (N:P: K = 16:20:0) and di-ammonium phosphate (18:46–48:0) (Primavera et al. 1993), is also used. The use of chicken manure increases methane (NH₄) in the bottom soil in the pond, and the use of inorganic manure deteriorates the quality of water of the aquaculture pond (Pathak et al. 2000). That's the reason farmers used more chemical components in the water to continue the production. The utmost worrying situation is that the contaminated materials are concentrated in the human body through the biomagnification process, and it is the common biological impact for the aquaculture farmers.

13.3.3.3 Pesticides and Disinfectants

Pesticides are used in shrimp ponds to kill snails, fungi, algae, crustaceans, etc., and algicides are used to control weed growth in ponds (GESAMP 1997). Disinfectants can also be used for site and equipment disinfection, controlling phytoplankton, and sometimes treating disease. Sodium hypochlorite (NaOCl) and calcium hypochlorite [$\text{Ca}(\text{OCl})_2$] were used at a concentration level of 20–30 mg/l in the pond water before stocking, and a concentration of 10–30 mg/l was added to the pond water stocked with shrimp for viral control. In this region, farmers also use formalin (formaldehyde solution) as an antifungal agent at a concentration of 120–3200 $\mu\text{L}/\text{L}$. Moreover, potassium permanganate (KMnO_4) is used as a disinfectant to oxidize the bottom soil of the pond and to treat the water. It has still not been found as a devil for aquaculture in our study area, but it has a great threatening tendency for shrimp culture rather than freshwater aquaculture (Ali 2016).

13.3.3.4 Antibiotics

Prophylactic use of antibiotics in commercial shrimp culture has a widespread phenomenon in most of the countries in the world (GESAMP 1997). Furazolidone, nifurpirinol, and chloramphenicol are used as antibiotics for Gram-negative and Gram-positive bacteria (Rang and Dale 1987). Rifampicin is also widely used in the shrimp pond for control of mycobacteria in this region and for maintaining the production quality in the study area during both the seasons, pre-monsoon and post-monsoon.

13.3.3.5 Feed Additives

Vitamin C is used in the water as a shrimp feed, especially for tiger shrimp, and vitamin E is added to the shrimp culture for the enhancement of disease resistance of shrimp (GESAMP 1997). However, in our study area, vitamin B12 was used as a feed additive for shrimp ponds including vitamins C and E due to more enhancement of disease resistance during the pre-monsoon period rather than the post-monsoon period. Simultaneously, it was effectively used in freshwater aquaculture so far in the study area in both the seasons. Moreover, it has no side effects except producing methane. So, feed additives have no long-term impacts on aquaculture and its water quality as per FAO (2016).

13.4 Risk Assessment and Remediation

The Global Aquaculture Alliance (GAA) has developed some management recommendations on the basis of the guiding principles by the Food and Agriculture Organization (FAO) for responsible aquaculture formulation more than 20 years ago (FAO 1998). It has been established that aquaculture farming is not permanently harmful to the environment (Boyd and Clay 1998). Certainly, aquaculture farming is having various significant benefits in terms livelihood and environment. However, lack of awareness, planning, and management by practitioners, as well as weak governance, has introduced various diseases to the species. Therefore, an environmental risk assessment framework has been developed by the World Health Organization (WHO), which is derived from the guidelines for environmental risk assessment of marine fish aquaculture (Bondad-Reantaso et al. 2008). International experts across the globe are reviewed and accepted this common analytic framework, and we have cast it off with some modifications (Fig. 13.5).

In this study, aquaculture is the prime economic source of the study area without hampering the environment. A study has stated that shrimp farming is explicitly less harmful to the environment rather than other farming activities (Paez-osuna 2001). Soil and water quality are the growing concern for this kind of intensive aquaculture. If we have to maintain the quality of both the variables, then it will be effective for the production in the future. Intensive chemical compounds are used in the study area for an increase of production, and as a result of this, after 3–4 years, the pond faces the deteriorating water quality and high risk of diseases. The intensity of methane also increases day after day, and huge fishes die by this element. Consequently, BOD increases in the species. Although all the chemical and physicochemical components are validated through international as well as national scale, along the Rasulpur River belt, the ponds are deteriorating season after season. During pre-monsoon, water quality is degraded greatly and almost 50% of ponds degrade the water quality (Shit et al. 2020). So, alternative remediation measures are needed to implement into the practice. Practitioners will be more concerned about this farming along with scientific management, introduction of scientific pond treatment processes, use of adequate fertilizers with prescribed ratio, use of pesticides and disinfectants in the proper amount, and proper vaccinations. Lastly, we have to recommend that practitioners and local government or nongovernmental organizations would have more concern about the diseases and formulate step-by-step processes from the initial stage, and that will be a more comprehensive way of aquaculture management.

13.5 Conclusion

The present study highlighted aquaculture-based water quality assessment along the Rasulpur River belt, Purba Medinipur, West Bengal. Here, aquaculture farming has been identified as a substitute economic activity, which supplies fishery product and

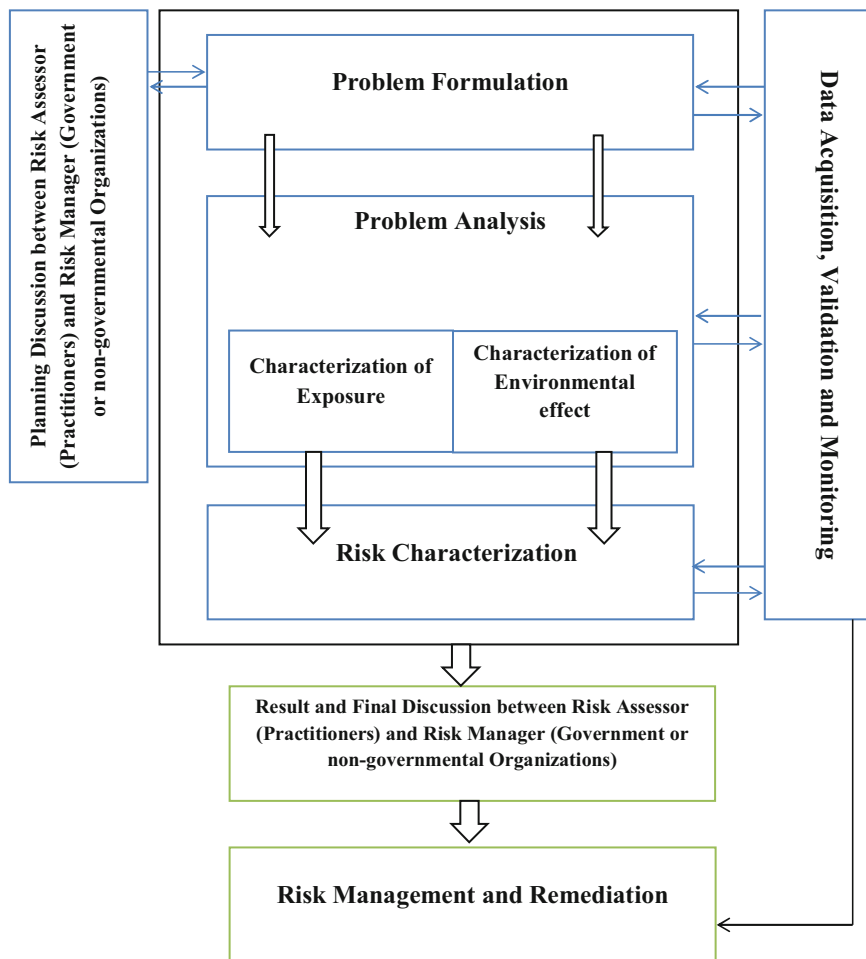


Fig. 13.5 The modified generic environmental risk assessment framework

generates various kinds of employment opportunities to the rural people. The results explicated that chemical components had a great impact on aquaculture farming to resist the diseases and to increase the production. The farmers are responsible for deteriorating the water quality of aquaculture by applying huge chemical compounds, especially in the pre-monsoon periods. However, spatially, water quality has a good nature, 62.21% during post-monsoon and 59.51% during pre-monsoon period. In the case of aquaculture pond, post-monsoon is the suitable time for upgrading and restarting the process because all the toxic and organic elements have drained out and reduced TDS along with less temporal hardness of water. Moreover, seawater influxes during tide at the monsoon season will be another option for water exchange in our study area. Sometimes, farmers are partially upset for dry summer, and aquaculture has become vulnerable to infection.

Consequently, species diseases or outbreaks have a great impact on economy. Whether it is intensive subsistence or extensive commercial, the farmers are facing the same problem so far.

However, environmental conditions often fluctuate in this study area. Moreover, overcrowding, water temperature, organic contents, high level of toxic elements, and unscientific way of management have made this practice difficult day by day, and consequently, saline water-based aquaculture has lost its quality and productivity than the freshwater aquaculture. So, it needs a scientific management, well organic element-based aquafarming, and quarterly water exchange; otherwise, the quality and production will get hampered in the near future to a broad extent.

Acknowledgment The authors Mallick and Maity are thankful to the University Grant Commission (UGC) for providing research grant and the DST-FIST sponsored laboratory of Department of Geography and Department of Aquaculture for water sample test in Vidyasagar University. The authors acknowledge the postgraduate students of Department of Geography for field study and data collection. The authors are also thankful to Giovanni (www.Giovanni.gsfc.nasa.gov) for administrative map of India and also thankful to USGS for providing Landsat data.

Declaration of Conflict of Interest The authors declared that there is no such conflict of interest regarding the results and data.

References

- Ali H, Rico A, Murshed-e-Jahan K, Belton B (2016) An assessment of chemical and biological product use in aquaculture in Bangladesh. *Aquaculture* 454:199–209. <https://doi.org/10.1016/j.aquaculture.2015.12.025>
- Amaraneni SC (2006) Distribution of pesticides, PAHs and heavy metals in prawn ponds near Kolleru lake wetland, India. *Environ Int* 32:294–302
- Bondad-Reantaso MG, Arthur JR, Subasinghe RP (eds) (2008) Understanding and applying risk analysis in aquaculture. FAO fisheries and aquaculture technical paper no. 519. FAO, Rome, pp 135–151
- Boyd CE (1995) Chemistry efficacy of amendments used to treat water and soil quality imbalance in shrimp ponds. World Aquaculture Society, Baton Rouge, Louisiana
- Boyd CE, Clay JW (1998) Shrimp aquaculture and the environment: an adviser to shrimp producers and an environmentalist present a prescription for raising shrimp responsibly. *Sci Am* 278(6):58–65. <https://doi.org/10.1038/scientificamerican0698-58>
- Boyd CE, Massaut L (1999) Risk associated with the use of chemicals in pond aquaculture. *Aquaculture Eng* 20:113–132
- Bureau of Indian Standards (BIS) (2012) Drinking water specification *IS: 10500:2012*. Bureau of Indian Standards, New Delhi
- FAO (1998) Report of the ad-hoc expert meeting on indicators and criteria of sustainable shrimp culture. Fisheries Report, no. 582. FAO, Rome, p 86
- FAO (2016) The state of world fisheries and aquaculture: contributing to food security and nutrition for all. FAO, Rome, p 200
- Folke C, Kautsky N (1992) Aquaculture with its environment: prospects for sustainability. *Ocean Coast Manage* 17:5–24
- GESAMP (IMO/FAO/UNESCO-IOC/WMO/WHO/IAEA/UN/UNEP) (1997) Joint group of experts on the scientific aspects of marine environmental protection. Towards safe and effective

- use of chemicals in coastal aquaculture. Reports and studies, GESAMP. No 65, FAO, Rome, p 40
- Graslund S, Bengtsson BE (2001) Chemicals and biological products used in south-east Asian shrimp farming and their potential impact on the environment- a review. *Sci Total Environ* 280:93–131
- Handbook on Fisheries Statistics (2014) Department of Animal Husbandry and Dairying. <https://dadf.gov.in/related-link/handbook-fisheries-satistics-2014>
- Kupwade RV, Langade AV (2013) Pre and post monsoon monitoring of ground water quality in region near Kupwad MIDC, Sangli, Maharashtra. *Int J ChemTech Res* 5(5):2291–2294
- Li J, Heap AD (2014) Spatial interpolation methods applied in the environmental sciences: a review. *Environ Model Softw* 53:173–189. <https://doi.org/10.1016/j.envsoft.2013.12.008>
- Medeiros MV, Aubin J, Camargo AFM (2017) Life cycle assessment of fish and prawn production: comparison of monoculture and polyculture freshwater systems in Brazil. *J Clean Prod* 156:528–537
- Paez-osuna F (2001) The environmental impact of shrimp aquaculture: causes, effects, and mitigating alternatives. *Environ Manag* 28(1):131–140. <https://doi.org/10.1007/s002670010212>
- Pathak SC, Ghosh SK, Palanisamy K (2000) The use of chemicals in aquaculture in India. South-east Asian Fisheries Development Centre, Tigbauan, pp 87–112
- Paul P, Chakrabarty S (2016) A focus on perspective on development, Nadia district. *Int J Fish Aquacult* 6(1):59–76
- Perdikaris C, Chrysaf IA, Ganias K (2016) Environmentally friendly practices and perceptions in aquaculture: a sectorial case-study from a Mediterranean-based industry. *Rev Fish Sci Aquacult* 24:113–125
- Primavera JH, Lavilla-Pitogo CR, Ladja JM, Dela Pena MR (1993) A survey of chemical and biological products used in intensive shrimp farms in the Philippines. *Mar Pollut Bull* 26:35–40
- Pullin R, Froese R, Pauly D (2007) Indicators for the sustainability of aquaculture. In: Bert TM (ed) Ecological and genetic implications of aquaculture activities. Springer, Dordrecht, pp 53–72
- Rang HP, Dale MM (1987) Pharmacology. Churchill Livingstone, New York, p 736
- Remy N, Boucher A, Wu J (2011) Applied geo-statistics with SGeMS: a user's guide. Cambridge University Press, New York
- Rico A, Satapornvanit K, Haque MM, Min J, Nguyen PT, Telfer TC, Brink PJ (2012) Use of chemicals and biological products in Asian aquaculture and their potential environmental risks: a critical review. *Rev Aquac* 4:75–93. <https://doi.org/10.1111/j.1753-5131.2012.01062.x>
- Saleem M, Hussain A, Mahmood G (2016) Analysis of groundwater quality using water quality index: a case study of greater Noida (region), Uttar Pradesh (U.P), India. *Cogent Eng* 3:1–11. <https://doi.org/10.1080/23311916.2016.1237927>
- Santos AAO, Aubin J, Corson MS, Valenti WC, Camargo AFM (2015) Comparing environmental impacts of native and introduced freshwater prawn farming in Brazil and the influence of better effluent management using LCA. *Aquaculture* 444:151–159
- Shit PK, Bhunia GS, Bhattacharya M, Patra BC (2020) Tidal morphology and environmental consequences of Rashulpur River in the Era of Anthropocene. Anthropogeomorphology of Bhagirathi-Hooghly River System in India. CRC Press. <https://doi.org/10.1201/9781003032373>
- Valenti WC, Kimpara JM, Preto BL (2011) Measuring aquaculture sustainability. *World Aquacult* 42(3):26–30
- Vassallo P, Bastianoni S, Beiso I, Ridolfi R, Fabiano M (2007) Energy analysis for the environmental sustainability of an inshore fish farming system. *Ecol Indic* 7:290–298
- WHO (2011) Guidelines for drinking water quality, 4th edn. WHO Press, Geneva, p 564

Chapter 14

Heavy Metal Contamination in Groundwater and Impact on Plant and Human



A. Nivetha, C. Sakthivel, and I. Prabha

Abstract Heavy metal contamination is considered as one of the major sources of environmental pollution, which affects the plant and human beings. There are natural and anthropogenic sources producing heavy metal contamination to the groundwater. Magmatic (Earth's crust which constitutes crystalline or glassy material) and metamorphic rocks, weathering, soil formation, rock cycle, and sedimentary are the natural sources that have been utilized for industrial activities, whereas landfills and synthetic agricultural inputs are the anthropogenic sources of heavy metal contamination. Heavy metal contamination has mainly been caused by the presence of cadmium (Cd), mercury (Hg), chromium (Cr), and lead (Pb). These metals have led to various problems for the survival of plants in the glorious environment. Cadmium leads to leaf chlorosis (insufficient chlorophyll) in growing plants. Excess mercury and lead have led to the reduction of root development and photosynthesis in plants. Chromium decreases the seedling dry weight seriously and is nonbiodegradable. They enter into the food chain and get accretion in different trophic stages causing undesirable effects on plant growth. Hence, effective utilization of groundwater, periodic risk assessment of heavy metal contamination, and remediation are mandatory. Hence, this chapter explores the current status of groundwater caused by heavy metal poisoning, impacts on human and plant species, and heavy metal remediation.

Keywords Assessment · Contamination · Groundwater · Heavy metals · Poisoning · Remediation

A. Nivetha · C. Sakthivel · I. Prabha (✉)
Department of Chemistry, Bharathiar University, Coimbatore, Tamilnadu, India
e-mail: prabhainbaraj@buc.edu.in

© Springer Nature Switzerland AG 2021
P. K. Shit et al. (eds.), *Spatial Modeling and Assessment of Environmental Contaminants*, Environmental Challenges and Solutions,
https://doi.org/10.1007/978-3-030-63422-3_14

233

14.1 Introduction

The earth is covered by three-fourth amounts of water, and 1% of water is utilized for drinking and other purposes. According to the WHO, 1.1 billion people are affected by the lack of drinking water. Water scarcity is caused by overpopulation, increased number of industries, and climate changes (Anjum et al. 2016). The groundwater is the major source for agriculture and drinking purposes. Approximately 60% of water is used for irrigation in farming, and 85% is for drinking water. According to the National Commission for Integrated Water Resources Development, 1180 billion cubic meter water may be used in the year 2050. In India, 253 billion cubic meter of groundwater is consumed, and it is the major consumer of groundwater. In India, 62% of groundwater is used for development and approximately 90% of groundwater is used for farming (CGWB 2017). The groundwater is polluted via both natural and anthropogenic paths. During the year 2020, 54% of India's groundwater levels are diminishing and 100 million peoples are affected (Chinchmalatpure et al. 2019). Industrialization and urbanization are the main causes for increasing world's population day by day. The utilization of sources and production of waste material is increased; the accretion of wastes in the surroundings is also increased. A large amount of released effluents pollute the environment with heavy metals, organic dyes, and agricultural wastes. The accumulation of waste materials leads to soil, water, and also air pollutions. However, the main drawback is the availability of very less water resources. Hence, there is a need to raise groundwater levels with high purity.

The important threat to the environment is the heavy metal contamination in the groundwater sources. The classification of toxic elements like metalloids, lanthanides, actinides, and transition metals belongs to heavy metals. The elements occupied in the periodic table like chromium, cobalt, copper, manganese, zinc, mercury, molybdenum, nickel, tin, cadmium, lead, and antimony are some examples of the heavy metals, which increase the toxic level to the environment. According to the recent literature survey, the represented heavy metals are found to be very toxic to the plants and living organisms present in the environment. However, they will create toxicless effects to the environment when they are consumed at an advised level. The main toxic elements like cadmium (Cd), mercury (Hg), chromium (Cr), and lead (Pb) are at the crown of the toxicity record among the assorted metal ions. Among the heavy metals in groundwater contamination, cadmium causes the Itai-Itai (cadmium poisoning from Japan), methyl mercury causes poisoning (who ingests fish and shellfish contaminated by MeHg), chromium leads to chrome ulcers and kidney disease. Figure 14.1 illustrates the sources of heavy metal pollution in the existing environment.

The Objectives of the Study are

- To explore the current status of groundwater caused by heavy metals to the environment.
- To create the impact of heavy metal poisoning and its metabolism in the human body.



Fig. 14.1 Sources of heavy metal pollution in the existing environment

- To find the effect of heavy metals on plant species and spatial modeling.
- To study the risk assessment for living beings.
- To synthesize the clay-supported eggshell charcoal.
- To investigate the pilot study for heavy metal remediation using solar light irradiation.

14.1.1 Essential and Nonessential Heavy Metals

Depending upon the consequences of heavy metals in plants and animals, there are two kinds of heavy metals such as

- Essential heavy metals.
- Nonessential heavy metals.

Table 14.1 shows the major sources and toxic effects of heavy metals at the permissible level. Iron (Fe), copper (Cu), zinc (Zn), manganese (Mn), molybdenum (Mo), cobalt (Co), and nickel (Ni) are the heavy metals essential for plants and animals. Also, they serve the major role as micronutrients; if their ingestion is surplus to the plant, it causes toxic results. Owing to their incidence in small quantity, i.e., trace 10 mg kg^{-1} , or mg L^{-1} or in ultratrace $1 \text{ } \mu\text{g kg}^{-1}$, or $\mu\text{g L}^{-1}$,

Table 14.1 Major sources and toxic effects of heavy metals

Heavy metals	Permissible level (Mg/L)	Toxic effects	Major sources
Arsenic	0.02	Hepatomegaly, bone marrow depression, dermatitis, bronchitis, and hemolysis	Pesticides, rock sedimentation, mining, and smelting
Lead	0.1	Anorexia, Anemia, loss of appetite, brain damage, mental retardation, kidney, liver, and gastrointestinal damage	Burning of coal, battery manufacturing, mining, electroplating, and pigments
Copper	0.1	Diarrhea, neurotoxicity, dizziness, and acute toxicity	Paint, copper polishing, printing operations, and plating
Nickel	0.2	Lung cancer, chronic bronchitis, and reduced lung function	Electroplating, porcelain enameling, paint formulation, and nonferrous metal
Cadmium	0.06	Bone marrow, hypertension, weight loss, Itai-Itai disease, kidney damage, and bronchitis	Pesticide, fertilizer, plastic, refining, and mining
Zinc	15	Gastrointestinal distress and short term metal fume fever	Plumping, mining, refineries, and brass manufacturing
Mercury	0.01	Dermatitis, protoplasm poisoning, damage to the kidney and nervous system, corrosive to eyes, skin, and muscles	Mining, batteries, paint, and paper industries

they are called trace elements in the ecological matrices. These metals/elements play a significant role in effective and complete physiological and biochemical functioning in both plants and animals. These are indispensable contributions in the redox reaction. Arsenic, cadmium, selenium, mercury, and lead are not used in plant and animal organisms and are called nonessential heavy metals. When the plants and animals consume a very small quantity of these, it becomes very harmful to existing organisms in the present environment.

14.1.2 Sources of Heavy Metals

The sources of heavy metals are natural, farming, industrialized sources, and household effluents. Geologic parent materials or rock outcroppings are the major vital sources of heavy metal liberation in the environment. The concentration and composition of the heavy metals depend upon the kind of rock, circumstances of surroundings, and the natural climate or weather condition. Cr, Mn, Co, Ni, Cu, Zn, Cd, Sn, Hg, and Pb are present highly in geologic parent materials. Olivine, augite, and hornblende are the igneous rocks having the substantial quantity of Mn, Ni, Cu, Co, and Zn, which provide the essential and required level or compositions

to the soils. The use of organic and inorganic fertilizers in the process of farming, pesticides, and irrigation from farming are the major reason for the discharge of heavy metals.

Phosphate and inorganic fertilizers as well as fungicides containing Cd, Cr, Ni, Pb, and Zn are liberated. Intake of Cd by plant leaves at a very high quantity and then the transfer of the element to the living organisms, which eat these plant leaves, take place. Zn, Cr, Pb, Ni, Cd, and Cu are presented in the soil by the use of animal compost. Liming enhances the heavy metal levels in the soil compared with nitrate fertilizers and manure. Heavy metals are discharged from mining, refinement, etc. Coal mines liberate As, Fe, Cd, etc., and gold mines liberate Hg. Smelting and casting at high temperature discharge Pb, Zn, Sn, Cd, Cu, and As in the form of vapor and react with water to form aerosols. These are deposited in the presence of wind or air available in the environment as a dry deposition or precipitation and occur due to rainfall. Through the movement of crude ores from erosion of mine ores, leakage of heavy metals and deterioration of metals lead to the pollution or increase the toxic level to the groundwater. This process occurring in paper industries, textiles, plastics, and wood conservation leads to the heavy metal contamination in the groundwater level. Household effluents are also the main reason for the liberation of heavy metals to the living society. The small quantity of metals such as iron, manganese, chromium, cobalt, zinc, strontium, and boron is discharged from detergents used for our domestic lives polluting the environment (Sandeep et al. 2019).

14.1.3 Photocatalytic Degradation Mechanism

The photodegradation reaction in the presence of a catalyst is photocatalysis, and the material used is photocatalyst with the support of light energy. The photocatalyst will not interfere with the reaction mixture, but it induces the rate of the photodegradation reaction fast in the presence of UV/sunlight. The catalyst is regained after the photodegradation reaction and reused for 4–5 times efficiently. The photocatalyst has coupled with UV or solar lights to oxidize the heavy metals and organic pollutants into nontoxic materials such as CO₂ and water, which disinfects certain bacteria. This method is very effective for removing heavy metal contamination. Figure 14.2 shows the mechanism of photocatalytic reaction using catalysts in the presence of UV/solar light irradiation (Nivetha et al. 2019).

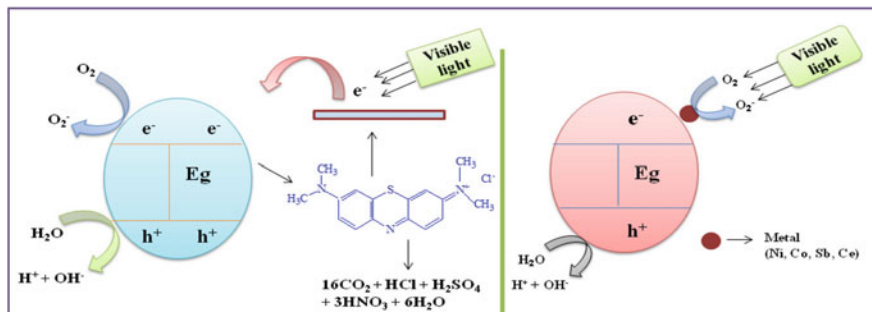


Fig. 14.2 Photocatalytic mechanism of heavy metal degradation

14.2 Materials and Methods

14.2.1 Materials Required

Ethanol, sulfuric acid, and cadmium nitrate were of analytical grade purchased from Merck, India. The raw clay was collected from the farms of Chinnaveerampatti village located near Udumalpet, Tamilnadu, India. The eggshell was collected from the kitchen waste. Double distilled water has been used throughout the preparation and photodegradation studies.

14.2.2 Preparation of Eggshell Charcoal Powder

The eggshells were collected from kitchen waste and washed several times with deionized water to eliminate the dirt particles. Then, the eggshells were dried at room temperature completely. After drying, they were incubated in hot air oven at 40 °C for 40 min. Incubated eggshells were then powdered using mortar and pestle and sieved to obtain the particle size up to 60–100 mesh. The prepared eggshells were stored in an airtight container for further purpose. Now, 20 g of shell powder was treated slowly with 15 ml of concentrated sulfuric acid. The treated powder material of shell powder was kept in a hot air oven for 48 h at 80 °C. Finally, shell powder was got converted into carbon material. The powder was washed several times with deionized water to remove the acids and impurities present in it. Finally, the charcoal was dried at 80 °C for 24 h to get fine powder for further adsorption and photodegradation studies in solar light.

14.2.3 Preparation of Clay-Supported Eggshell

A certain quantity of raw clay was taken, and it was dried completely. After drying, it was finely powdered using a pestle mortar. The powdered clay was sieved and stored separately for the experimentation work. Now, 25 g of the sieved clay powder was taken in a 500-ml beaker and 300 ml of distilled water was added. And, it was stirred on the magnetic stirrer for continuous stirring for 30 min. Next, it was allowed to stand for 90 min at room temperature without any disturbance. After the settlement, the clay solution was centrifuged. The upper solution was collected, and it was filtered. The filtered clay was washed several times with ethanol, and it was dried at 50 °C for 24 h till for its complete dryness. The dried clay particles were sieved to obtain the particle size up to 60–100 mesh. To the clay particle, prepared eggshell was mixed thoroughly and used for the removal of cadmium from the water. The BET surface area of the prepared catalyst was found to be 418 m²/g, and the total pore volume of the catalyst was found to be 0.181 cm³/g.

14.2.4 Preparation of Sample Wastewater

To prepare stock solution, accurately weighed 1000 mg of cadmium nitrate was dissolved in 1 L of deionized water completely. Thus, the stock solution was consecutively diluted with deionized water to acquire the desired test concentration of metal ions.

14.2.5 Photocatalytic Degradation of Cadmium in Wastewater

The photodegradation study of cadmium stock solution was performed in a batch reactor system under sunlight using clay-supported eggshell charcoal powder as a catalyst under sunlight. For sunlight-mediated photocatalysis, an open rectangular tray of 16 cm × 15 cm × 5 cm made from borosilicate glass was used as a reactor to contain the stock solution. The slurry of 250 ml of stock solution of known concentration mixed with a known mass of the clay-supported shell charcoal powder was stirred thoroughly with a magnetic stirrer with medium rotation and was allowed to equilibrate for adsorption before exposure to sunlight for 30 min. The photodegradation study was performed in direct sunlight under optimum conditions. Solar light intensity was measured every 30 minutes, and the average light intensity over the duration of each experiment was calculated. The residual concentration of cadmium solution was measured at 440 nm using a UV–Vis spectrophotometer. The light intensity was measured by a digital flux meter, and the intensity of the sunlight during the reaction time was in the range of 820 lux. The intensity was nearly

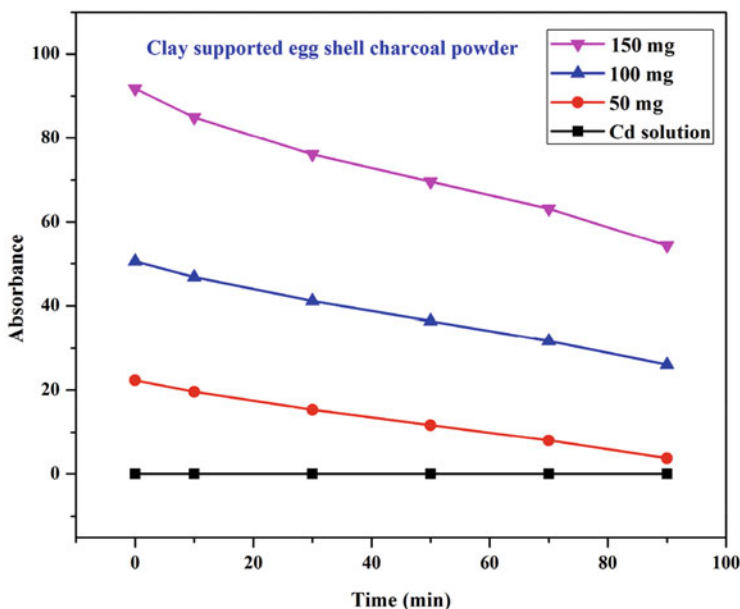


Fig. 14.3 Graphical representation of the degradation % of photocatalyst

constant during the experiments. Also, 50, 100, and 150 mg of catalyst were used for the removal of cadmium from stock solution. The pH of the solution was maintained to 7. After exposure of sunlight, the sample was collected every 20 minutes once. Then, the absorbance value was measured to calculate the degradation percentage. Finally, degradation efficiency was found to be 32.70, 43.94, and 88.07% for clay-supported eggshell as a catalyst with 50, 100, and 150 mg.

The charcoal-based materials acted as better photocatalysts in the removal of cadmium metal from stock solution due to their suitability of flat band potentials and nontoxicity. The pores present in the adsorbent were heterogeneous in nature. The higher removal of cadmium from stock solution can be increased by increasing the contact time and adsorbent dose; i.e., high cadmium removal can be accomplished at higher contact time and a higher dose of clay-supported eggshell charcoal powder (Tizo et al. 2018). The photocatalytic degradation study was performed against cadmium solution as a pollutant. Figure 14.3 shows the graphical representation of the degradation % of photocatalyst. In the presence of photocatalyst, cadmium stock solution has taken place under the solar irradiation as a light source. Table 14.2 shows the absorbance values of degradation of cadmium solution by clay-supported eggshell charcoal powder.

Table 14.2 Degradation % of Cd solution by clay-supported eggshell charcoal powder

S. No.	Time (mts)	Absorbance at respective clay-supported eggshell charcoal powder weight		
		50 mg	100 mg	150 mg
1	0	77.9	83.2	85.2
2	10	74.3	77.8	72.1
3	30	69.2	69.2	65.4
4	50	65.3	61.3	51.9
5	70	61.6	59.1	48.7
6	90	58.7	57.8	45.3
Degradation %		32.70%	43.94%	88.07%

14.3 Risk Assessment and Remediation

14.3.1 Risk Assessment on Human Health

Risk assessment is defined as the route of estimating the possibility of incidence of any given feasible scale of unfavorable health issues over a particular time period, and it is the function of the vulnerability and contact. The health hazard appraisal of every poisonous metal typically depends upon the amount of the hazard stage, and it is denoted in terms of carcinogenic or noncarcinogenic health effects. For carcinogenic and noncarcinogenic hazards analysis, slope factor and reference dose have been assessed, respectively. The peoples are affected by toxic metals available in the environment through three different ways: inhalation, straight intake, and absorption via skin. In these three categories, ingestion is the most predominant way to the heavy metals, which are affecting the human beings. Ingestion may be of drinking or eating. The United States Environmental Protection Agency (USEPA) describes the dosage obtained via the way which was determined using the following equation:

$$ADD = (C \times IR \times EF \times ED) / (BW \times AT)$$

where

- ADD Average daily dose, unit – $\mu\text{g}/\text{Kg}/\text{day}$.
 C Average concentration of toxic metals in water, unit – $\mu\text{g}/\text{L}$
 IR Ingestion rate, unit – L/day
 EF Exposure frequency, unit – days/year
 ED Exposure duration, unit – years
 BW Bodyweight, unit – Kg
 AT Averaging time in days

Risk analysis is the ultimate step in health risk evaluation. The health issues from groundwater utilization were assessed relative to its carcinogenic effects, derived from the calculation of average daily dose (ADD) estimates, and this describes the toxicity values for every potentially toxic metal consistent with the subsequent

relationships. The noncarcinogen risk was calculated as the hazard quotient as follows:

$$\text{Hazard Quotient (HQ)} = \text{ADD}/R_fD$$

If several toxic metals are present in the drinking water, a hazard index (HI) was used by totaling all the calculated hazard quotient values of metals as illustrated as follows:

$$\text{Hazard index (HI)} = \sum_{i=1}^n \text{HQ}_i$$

If $\text{HQ} < 1$, then it leads to the noncarcinogenic effect on human health. And, if the $\text{HQ} > 1$, then it leads to the carcinogenic effect on human health issues. The predictable value is the additive prospect of an individual increasing any kind of cancer above a lifetime owing to carcinogenic contact. According to the United States Environmental Protection Agency (USEPA), the bearable range is between 10^{-6} and 10^{-4} for the carcinogenic risk (Fallahzadeh et al. 2018; Shahid et al. 2018; Hu et al. 2019).

$$\text{Cancer risk} = \text{ADD} \times \text{SF} \quad \text{ADD} \times \text{SF}.$$

14.3.2 Remediation

The groundwater remediation is a significant division of site remediation. There are two different kinds that can be used for groundwater remediation as follows:

- In situ technology (on-site).
- Ex situ technology (off-site).

The in situ remediation technology engages in purifying the water wherever it is currently located before eradicating and moving it to another place. Biodegradation, air sparging, bioventing, etc. belong to the in situ technology. Ex situ remediation explains about the collection of waste water from the field areas and it should be treated at the field itself. The remediation technology can be done based on the circumstance of location like geochemistry and hydrogeology of the location. The technology is also chosen by the kind of pollutant and its concentration.

Bioremediation is an ecological and a natural method for the waste management like heavy metal contamination. Arsenic and selenide are the contaminants that can be removed by the bioremediation method. The evolutionary adjustment of microbes for the opposition of ecological pollutants facilitates them to replicate in polluted environmental circumstances and also to eliminate the pollutants owing to strong assortment force. The broad range of environmental pollutants is eliminated by the

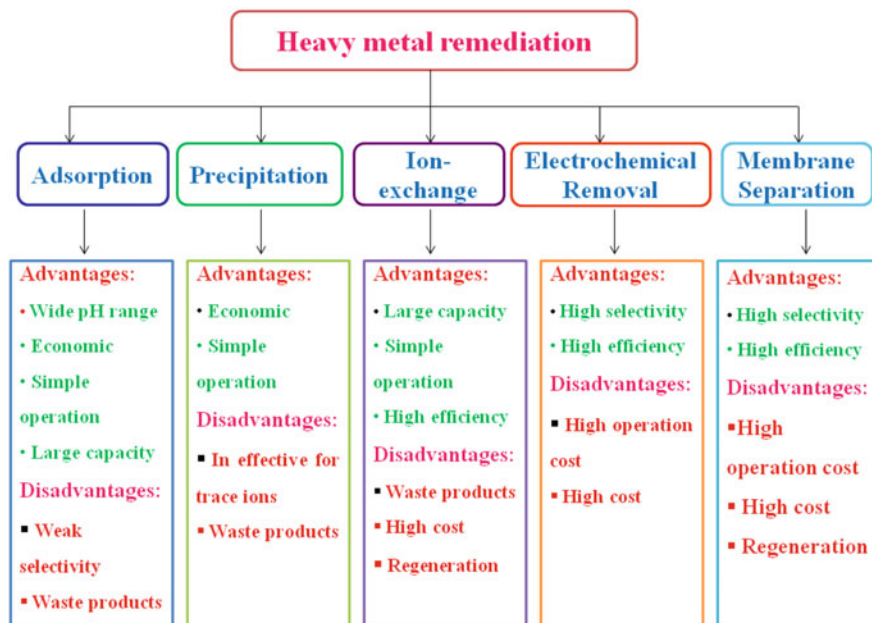


Fig. 14.4 Various processes of heavy metal remediation

microbe-supported bioremediation process completely. The lethal compounds can be converted to low lethal products by the bioremediation process. For example, As (III) gets converted to As (V). Bioremediation does not cause the main interruption to the environment, and it is the main advantage of microbe-assisted bioremediation. It is an economical method to degrade the heavy metals from the groundwater (Paul and Saha 2019). Figure 14.4 shows the various processes of heavy metal remediation.

Phytoremediation is the technique for the treatment of water, which takes more time duration. Phytoremediation technique leads to the reduction of heavy metal pollutants at shallow depths and will finally diminish the threat of discharge to groundwater. This method has no side effects on the groundwater. This is an economical method and is suggested for enduring the treatment of surface pollutants in the study area. Even after the water treatment, vegetable planting is banned and the additional treatment is advisable for the drinking purpose (Ali et al. 2020).

Nanoscience and nanotechnology play a vital role in groundwater remediation successfully. Nanomaterials such as carbon-based materials (carbon nanotubes, fullerenes, graphenes, and single-walled and multiwalled carbon nanotubes), metal nanoparticles (zero-valent iron, semiconductors, and bimetallic nanoparticles), and titanium oxide nanotubes are used for the remediation process. These materials have the capability to oxidize organic contaminants present in the wastewater into nonhazardous materials. Nanomaterials are used to demolish the pollutants as a division of neither in situ nor ex situ technology. The U.S. Environmental Protection

Agency's Office of Superfund Remediation and Technology Innovation have prepared the nanomaterials for site remediation. Photo-oxidation with semiconductors and adsorption on self-assembled monolayers on mesoporous supports (SAMMS) belong to the *ex situ* technology. Mercury, arsenate, selenite, chromate, and pertechnetate are remediated by SAMMS due to its good adsorptive properties and Cu^{2+} and Pb^{2+} eliminated by dendritic polymers (Anjum et al. 2016).

Nowadays, numerous adsorbents have been used in groundwater remediation like aluminosilicates, activated carbon, and polymeric resins. To eliminate the low-soluble metals as well as organic and inorganic materials, grainy activated carbon is used as the adsorbent material. Adsorption is merely a separation method wherein remaining pollutants are eliminated from the water; however, the pollutants are not demolished. The adsorbent can be replaced and should be reinforced. The water treatment cost might be increased because of reinforcement of adsorbent. Stabilized zero-valent iron nanoparticles have provided benefit to the heavy metals in groundwater which leads to the growth of novel *in situ* remediation through direct distribution of the nanoparticles into polluted area. *In situ* method has the potential to degrade the heavy metal contaminants in the groundwater, and it is an economical method compared to the conventional remediation techniques like pump and treat, etc. When the pollutants are situated deeply, *in situ* method can be the only probable solution to eliminate the heavy metals from the contaminants completely (Matlochova et al. 2013).

14.4 Conclusion

The study revealed that high cadmium removal can be accomplished by higher contact time and higher quantity of the catalyst. The degradation percentage was found to be 32.70, 43.94, and 88.07% for clay-supported eggshell as a catalyst with 50, 100, and 150 mg, respectively. Heavy metal contamination in groundwater is a major ecological and health concern, leading to food chain contamination and other related health challenges. In the present era, we are in need of advanced water treatment technology for getting freshwater by the removal of the various types of contaminants present in the water resources to strengthen the industrial manufacturing processes of wastewater. Nowadays, several research groups are working on the elimination of heavy metals from the contaminated sites. Nanoscience and nanotechnology play a vital role in wastewater treatment. Different kinds of nanomaterials have been synthesized for water treatment processes like nano adsorbents, photocatalysts, nanomembranes, and electrocatalysts. Every method has its individual merits and demerits with the efficiency to eliminate the contaminants. Nanoadsorbent has the efficiency to eliminate the heavy metals in the freshwater. Photocatalysts can be used to treat both heavy metals and toxic pollutants. Nanomembranes have the efficiency to diminish foulants, heavy metals, and dyes. During the treatment process of water by using nanomaterials, there is a chance for the accumulation of nanomaterials in the environment and it causes serious health

problems. Hence, photodegradation method is very effective for the treatment of metal contamination to solve the issues of economically feasible and time consuming with less effective results. Phytoremediation can be effectively used to extract and harvest large concentrations of deleterious metals as well as other inorganic and organic pollutants. Nowadays, genetic engineering approaches to develop transgenic plants with high biomass production, more metal accumulation, tolerance against metal toxicity, and well adapted to a variety of climatic conditions might be more beneficial in this respect. Further research is needed in the field to improve the methods by introducing novel advanced and functional materials to be synthesized by the waste generated from the environment to undergo the process of nanoabsorption to make more effective, time saving, and economically feasible (Sarwar et al. 2016).

References

- Ali S, Abbas Z, Rizwan M, Zaheer IE, Yavas I, Unay A, Abdel-DAIM MM, Bin-Jumah M, Hasanuzzaman M, Kalderis D (2020) Application of floating aquatic plants in phytoremediation of heavy metals polluted water: a review. *Sustainability* 12:1927–1959
- Anjum M, Miandad R, Waqas M, Gehany F, Barakat MA (2016) Remediation of wastewater using various nano-materials. *Arab J Chem* 12(8):4897–4919
- Central Ground Water Board (CGWB) (2017) Dynamic groundwater resources of India (As on 31st March 2013). Ministry of water resources, river development & ganga rejuvenation, government of India, Faridabad
- Chinchmalatpure R, Gorain B, Kumar S, Camus DD, Vibhute SD (2019) Groundwater pollution through different contaminants: Indian scenario. In: Dagar J, Yadav R, Sharma P (eds) *Research developments in saline agriculture*. Springer, Singapore
- Fallahzadeh RA, Khosravi R, Dehdashti B, Ghahramani E, Omid F, Adli A, Miri M (2018) Spatial distribution variation and probabilistic risk assessment of exposure to chromium in groundwater supplies; a case study in the east of Iran. *Food Chem Toxicol* 115:260–266
- Hu G, Bakhtavar E, Hewage K, Mohseni M, Sadiq R (2019) Heavy metals risk assessment in drinking water: an integrated probabilistic-fuzzy approach. *J Environ Manag* 250:109514–109526
- Matlochova A, Placha D, Rapantova N (2013) The application of nanoscale materials in groundwater remediation. *Pol J Environ Stud* 22(5):1401–1410
- Nivetha A, Devi SM, Prabha I (2019) Fascinating physic-chemical properties and resourceful applications of selected cadmium Nanomaterials. *J Inorg Organomet Polym Mater* 29:1423–1438
- Paul T, Saha NC (2019) Environmental arsenic and selenium contamination and approaches towards its bioremediation through the exploration of microbial adaptations: a review. *Pedosphere* 29(5):554–568
- Sandeep G, Vijayalatha KR, Anitha T (2019) Heavy metals and its impact in vegetable crops. *Int J Chem Stud* 7(1):1612–1621
- Sarwar N, Imran M, Shaheen MR, Ishaq W, Kamran A, Matloob A, Rehman A, Hussain S (2016) Phytoremediation strategies for soils contaminated with heavy metals: modifications and future perspectives. *Chemosphere* 171:710–721
- Shahid M, Khalid M, Dumat C, Khalid S, Niazi NK, Imran M, Bibi I, Ahmad I, Hammad HM, Tabassum RA (2018) Arsenic level and risk assessment of groundwater in Vehari, Punjab province, Pakistan. *Expo Health* 10:229–239

Tizo MS, Blanco LAV, Cagas ACQ, Dela Cruz BRB, Encoy JC, Gunting JV, Arazo RO, Mabayo VIF (2018) Efficiency of calcium carbonate from eggshells as an adsorbent for cadmium removal in aqueous solution. *Sustain Environ Res* 28:326–332

Chapter 15

Emerging Threats of Microplastic Contaminant in Freshwater Environment



Pratik Ghosh, Ritwik Patra, Prasanta Patra, Nabarun Chandra Das, Suprabhat Mukherjee, Bidhan Chandra Patra, Bhaskar Behera, and Manojit Bhattacharya

Abstract The development of plastic brings world-shattering changes in industrialization, commercialization, and mankind and is now the most predominant widely used essential product. The disposal and degradation of plastic leads to the generation of microplastic and is a potential and crucial pollutant in our ecosystem. The discharge of microplastic to the aquatic bodies and finally its migration to the marine ecosystem draw attention of many researchers toward its noxious effects. The primary and secondary sources of microplastic that makes its path toward the riverine ecosystem causing pollution and interference with the aquatic organism resulting in contamination and toxicity is primarily discussed in this chapter. The impacts of microplastic in aquatic organisms affect its biological ingestion process causing clogging and indigestion and in adverse condition hinder the biological processes resulting in toxicity, immune dysfunction, reproductive abnormalities, alteration of behaviors and feeding habit, and finally death. In addition to this, the absorption of microplastic results in bioaccumulation and biomagnification across the food chain, making its route to the human body. Furthermore, this chapter also emphasizes the various remediation and pollution management strategies based on the present approach and provides a research assessment for future research and advancement.

Keywords Aquatic organisms · Freshwater environments · Pollution · Microplastics

P. Ghosh · P. Patra · B. C. Patra
Department of Zoology, Vidyasagar University, Midnapore, West Bengal, India

R. Patra · N. C. Das · S. Mukherjee
Integrative Biochemistry and Immunology Laboratory, Department of Animal Science, Kazi Nazrul University, Asansol, West Bengal, India

B. Behera · M. Bhattacharya (✉)
Department of Zoology, Fakir Mohan University, Balasore, Odisha, India

© Springer Nature Switzerland AG 2021

P. K. Shit et al. (eds.), *Spatial Modeling and Assessment of Environmental Contaminants*, Environmental Challenges and Solutions,
https://doi.org/10.1007/978-3-030-63422-3_15

247

15.1 Introduction

Continuous demand and growth of plastic material across the world impose global challenges in waste management and pollution control. Characteristically, plenty of plastic is used in daily life due to its versatility, durability, and lower price. The chief constituents of plastic are commonly derived from petrochemical sources: polyethylene, polypropylene, polyvinyl chloride, polystyrene, polyethylene terephthalate, and polyurethane. They together cover over 80% of the total plastic (van Wezel et al. 2016). According to Ma et al., due to the extensive practice of plastic goods every year, an average of 5–13 million tons of plastic litter arrives in the marine ecosystem (Ma et al. 2019). Since the 1940s, the plastic production has doubled globally, and by the end of 2014, it exceeded more than 311 million metric tons, overall 4.0% growth in the year 2013. In the year 2010, out of 2.5 billion metric tons of solid contaminant formed in 198 countries, about 275 million tons was composed of plastic. Due to the insufficient solid waste management system, it has been predicted that the range of 4.8–12.7 million ton plastic pollutants piled up into the various wetlands. The major alarming situation is about the visible plastic derbies as a microplastic, growing daily due to its huge practice in the modern era.

According to Avio et al., when used plastics are thrown into the environment, those plastic materials have been degraded by several biological and chemical processes and lose their original physical stiffness (Avio et al. 2017). After that process, those plastic materials start the degradation process, and at the peak of degradation, the plastic substances fragment to powdery material called microplastics. These plastic pieces, as small as the size of an ant and a virus, now can be found in lakes and seas and in sediments of rivers and deltas, and these plastic pieces now hamper the normal water quality worldwide. Microplastic is also found within the stomach of several organisms ranging from whales to zooplankton. Barnes et al. 2009 suggested that the size of the microplastic has a microscopic range between a few micrometers to 500 μm (0.5 mm) (Barnes et al. 2009). Due to their small structure variants, microplastics are easily mistaken for food, and they have been ingested by a wide range of marine organisms with different feeding mechanisms, including zooplankton (Desforges et al. 2015; Sun et al. 2018), filter-feeding bivalves (Van Cauwenberghe et al. 2015; Li et al. 2016), deposit-feeding lugworms, fishes, and crustaceans (Devriese et al. 2015; Welden and Cowie 2016). Researchers also estimated that 63,320 microplastic particles per square kilometer float on the water surface, with extensive regional variations like concentrations in East Asian seas being 26 times higher (Isobe et al. 2015). Moreover, chemical additives are often used during the production of plastic to create or enhance certain properties, thus making the material more durable by introducing flame-retardant, anti-microbial, rigidity, UV resistance, malleability, and waterproofing features. Such enhanced plastic products include packaging materials, bins, containers, pipes, fishing nets, bottles, furniture, etc.

The bioaccumulation process of plastics and their related persistent organic pollutants (POPs) across freshwater trophic levels is much crucial for aquatic health

management, and it is associated with human health. Given that lower trophic organisms, specifically, invertebrates, can ingest and accumulate microplastic particles, microplastics will likely be introduced to the food web.

15.2 Sources of Microplastics

Microplastics contain various types of petrochemicals and display their diversifying physiochemical belongings related to their emission sources into the aquatic body. On the basis of the diversity in size, shape, composition, and polymeric additives of microplastics, they are divided into two categories: primary microplastics and secondary microplastics (Andrady 2017).

15.2.1 Primary Microplastics

Plastics with microscopic size usually manufactured by industrial practices are called primary microplastics (Zitko and Hanlon 1991). Primary microplastics are small, micron in size (typically 2–5 mm in diameter), which are used in pharmaceuticals, textiles, and cosmetics such as facial, scrubbing agents in toiletries, shower gels, and body grinding (Boucher and Friot 2017). Those microplastics are directly released into the environment in the form of small particulates (Fig. 15.1). Additionally, those tiny plastics may originate from the scrape of large plastic objects during manufacturing, use, or maintenance such as the erosion of tires when driving, or the abrasion of synthetic textiles during washing releases microplastics.

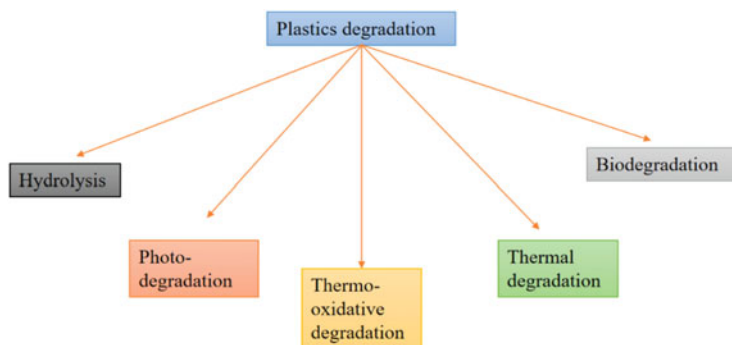


Fig. 15.1 Ways of plastic degradation in the environment

15.2.2 Secondary Microplastics

Secondary microplastics are generated due to the fragmentation of large plastic fragments found both in marine and terrestrial habitat (Thompson et al. 2004; Ryan et al. 2009). This occurs due to photodegradation and may involvement of weathering processes. The mismanaged wastes such as discarded plastic bags or from unintentional losses such as fishing nets have main sources of secondary microplastics. Growing evidence recommends that fibres from synthetic fabrics are important causes of secondary microplastics, usually found in wastewater and in the aquatic environment.

15.3 Ecotoxicological Effects on Freshwater Organisms

The toxic effects of microplastics are chiefly intensive on marine life, and toxicological effects on freshwater organisms are still unclear. Consequences of ecotoxic effects on the aquatic organisms increase their death rate and affect their reproductive capacity growth, development, food intake, and gene expression. Here, the chronic effects of microplastics on the fresh water organism and their harmful consequences are summarized. Research has exposed that both harmful and persistent substances are bioaccumulated relatively at a shorter period of time and biomagnified as predators eat prey, especially in species high in lipids. In this way, seafood can become contaminated; predominantly, higher-level predators like sea fish, mollusc, and crabs raise fear for human health.

15.3.1 Toxicity of Microplastics

The microplastic enters inside the aquatic animals, gets bioaccumulated, and acts as a toxic compound leading to toxicity. Ingestion of microplastics might disturb the aquatic life in various ways (Scherer et al. 2018). Microplastic toxicity is revealed by physical injury, blocks the gastrointestinal (GI) tract of aquatic organisms, hampers the regular absorption of nutrients, and also increases energy expenditure for digestion, consequences of which lead to starvation. These effects affect the growth and development of organisms, and also deaths have occurred (Table 15.1). Additionally, the exposure of these microplastics along with their chemical additives induces toxic effects, leading to impairment of physiological functioning, histopathological alterations, and reproductive abnormalities. Various experimental tests on freshwater animals like *Danio rerio*, *Hyalella Azteca*, *Caenorhabditis elegans*, *Hydra attenuate*, *Scenedesmus*, *Scenedesmus obliquus*, *Chlorella*, and *Gammarus pulex* reveal that they come into contact with chemical components of microplastics. Those are mainly polypropylene fiber, polyamide, polyvinyl chloride, polystyrene,

Table 15.1 The compound toxicity of microplastics on aquatic organisms

Test organism	Polymer	Concentration	Size	Time	Effect criteria
<i>Danio rerio</i>	Polyamide polyvinyl chloride; polystyrene polypropylene, polyethylene	0.001–10.0 mg/L	70 μm	10 days	Changes of survival rate; morphological and as well as histopathological changes found
<i>Hyalella azteca</i>	Polypropylene, polyethylene;	0–20,000 ind/mL	10–27 μm	10 days	Mortality rate increase
<i>Caenorhabditis elegans</i>	Polyamide polyvinyl chloride; polystyrene polypropylene, polyethylene	0.5–10.0 mg/m ²	70 μm	2 days	Changes of survival rate; morphological and as well as histopathological changes found
<i>Hydra attenuata</i>	Polyethylene	0.01–0.08 mg/L	<400 μm	30 min; 60 min	Changes of feeding rate; morphological and reproduction percentage
<i>Scenedesmus</i>	Polystyrene	0.08–0.8 mg/mL	20 nm	2 h	Adsorption number of algae by polystyrene beads; the rate of CO ₂ exhaustion
<i>Scenedesmus obliquus</i>	Polystyrene	44–1100 mg/L	70 nm	72 h	Algae growth inhibition and reproduction depleted and mass loss
Chlorella	Polystyrene	0.08–0.8 mg/mL	20 nm	2 h	Adsorption number of algae by polystyrene beads; the rate of CO ₂ exhaustion
<i>Gammarus pulex</i>	Polyethylene terephthalate	0.8–4000 ind/mL	10–150 μm	24 h; 48 h	Changes of rates of survival; development; metabolism and feeding activity

H hours

polyethylene, and polyethylene terephthalate particles of microplastics exposed to the aquatic organisms, which affect the normal digestive function of organisms, reducing their growth and reproduction. However, the accumulation of microplastic components in *Danio rerio* (zebrafish) and *Caenorhabditis elegans* (nematode) causes intestinal damage and splitting of enterocytes, as well as cracking of villi, so those cause great impacts on food absorption by GI tract, and the ultimate fate is

death. Evidence also proved that high exposure of microplastic particles to nematodes had the highest mortality shown. *Hydra attenuata* and *Hyalella azteca* exposure to microplastics can significantly reduce the feeding rate; morphological and reproduction percentage is found to be negatively significantly correlated with the microplastic concentration. This reveals the chemical effect of microplastics on freshwater invertebrate *Gammarus pulex*, higher in juvenile *Gammarus pulex* (average length: 6–9 mm) than the mature *Gammarus pulex* (average length: 13–18 mm). The bioaccumulation of high-density polyethylene and polystyrene microplastics within the tissue of *Danio rerio* triggers various transcriptional changes, leading to alteration of the immune system and downregulation of genes associated with the integrity and lipid metabolism in epithelial tissues, inducing the overproduction of neutrophils within gills and intestinal epithelium that may lead to dysfunction of host defence mechanism against pathogens and also various behavioral changes (Limonta et al. 2019).

15.3.2 Harmful Effects on Human Health

The usage of microplastics has increased day by day from various sources such as scrubs, cosmetics, hand washes, and toothpaste. Besides the toxic effects of microplastics, hazardous ingredients like phthalates or PCBs within the microplastics or other chemicals adsorbed to the surface of microplastics may contribute to the dietary exposure of humans (Lassen et al. 2015). Additionally, consumption of microplastic-enriched seafoods, such as oyster, mussel crab, sea cucumber, and fish, leads to the transfer of those harmful substances to humans and hampers their health. Inappropriately, no real data are available for the particle size, chemical composition, shape, or concentration of microplastic particles in seafood (Fig. 15.2). The absolute health hazards ensue from the use of various primary microplastics such as hand cleansers, face washes, and dental care products, which contain microplastic particles. Vigorous use of microplastic ($\geq 1 \mu\text{m}$) particles in daily life and lengthy use of plastic-containing goods lead to absorption of polyethylene and polypropylene particles and ultimately result in skin damage. Toothpaste derivative microplastics and microbead particles are absorbed through the gastrointestinal tract (Lassen et al. 2015), and alternative ingestion may change the genetic arrangement and lead to obesity, cancer, and infertility (Anderson et al. 2015). Additionally, it will be dangerous in women's body, and breast cancers may occur in women if estrogenic hormones are mimicked by plastic-containing chemicals. In the modern era, humans take microplastics in their daily diet, and seafood makes a major hazard to human health (Van Cauwenberghe and Janssen 2014).

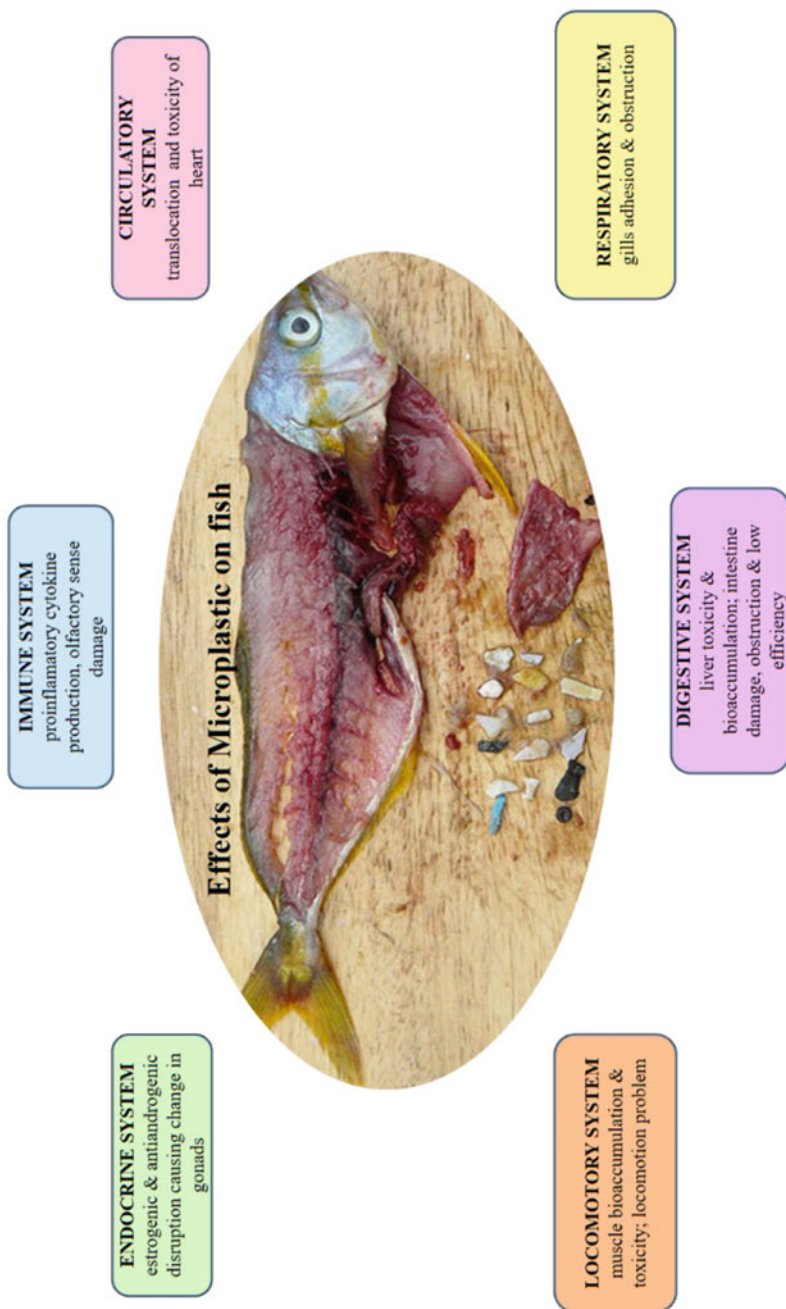


Fig. 15.2 Effects of microplastic in fish model

15.4 Remediation of Microplastic Pollution

The proper wastewater management and urban waste management are the key for regulating microplastic contaminations and pollution in the aquatic ecosystem. Regarding the microplastic pollution management, United Nations Environment Programme (UNEP) promoted clean-up programs through the engagement of over 40 million peoples across 120 countries worldwide to educate and encourage the reduction and reuse of plastic items and facilitate proper disposal (Caruso 2015). Moreover, various strategies for bioremediation using microorganisms are being used for the degradation and remediation of microplastic. The extracellular enzymes released from *Rhodococcus ruber*, fungus like *Penicillium simplicissimum*, and the bacterium *Brevibacillus borstelensis* have the ability to degrade polyethylene (Yamada-Onodera et al. 2001; Orr et al. 2004). Other microbes like *Alcaligenes faecalis*, *Clostridium botulinum*, *Bacillus brevis*, *Penicillium roqueforti*, etc. have the ability to degrade polycaprolactone (PCL) and polylactic acid (PLA)-associated microplastics; however, the process of degradation of PLA is slow and susceptible to microbial pathogenesis. The use of biofilm technology is very much effective and efficient for the biodegradation of microplastic.

15.5 Discussion

According to Andrady (2011), plastics will fragment into micro and nano pieces; additionally, there was no evidence to clarify the real time of this process (Andrady 2011; Roy et al. 2011; Hidalgo-Ruz et al. 2012). Furthermore, within the short range of time, if those microplastics have not been degraded, then their hazardous effects affect marine as well as freshwater ecosystems (Figs. 15.3 and 15.4). Microplastics are the reservoirs of toxic chemicals in the environment and are biomagnified through the food chain. Different types of polymers like polyethylene, polypropylene, and colored plastics may be adsorbed by POPs (persistent organic pollutants) from the environment differently. According to Zarfl and Matthies 2010, Microplastics carry pollutants over huge oceanic areas and pollute the aquatic biota when ingested (Teuten et al. 2009; Zarfl and Matthies 2010; Tanaka et al. 2013). Physical damage occurred by the eating of plastic debris; those were disposed due to physical damage and doses of pollutants were not earlier accessible. Aquatic organisms of every level of the food chain consume microplastics according to different biological food intake mechanisms, but those are dwelling in industrialized areas are bare to high quantities and might be extra polluted. However, the hazardous quantities of pollutants vary suggestively among fragments within the same area; accordingly, the toxicity of pollutants and integration into physical tissues vary for each biological species. Some groups (e.g., holothurians) speciously ingest microplastics with specific colors and shapes. If those groups adsorb higher quantities of pollutants, the consequences are most likely greater. Here, primary

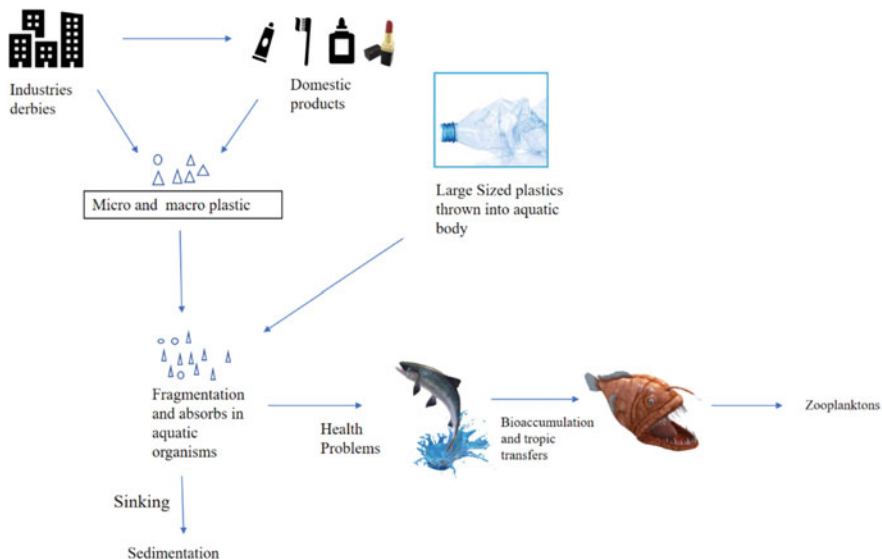


Fig. 15.3 Sources of microplastics and their absorption in aquatic organisms

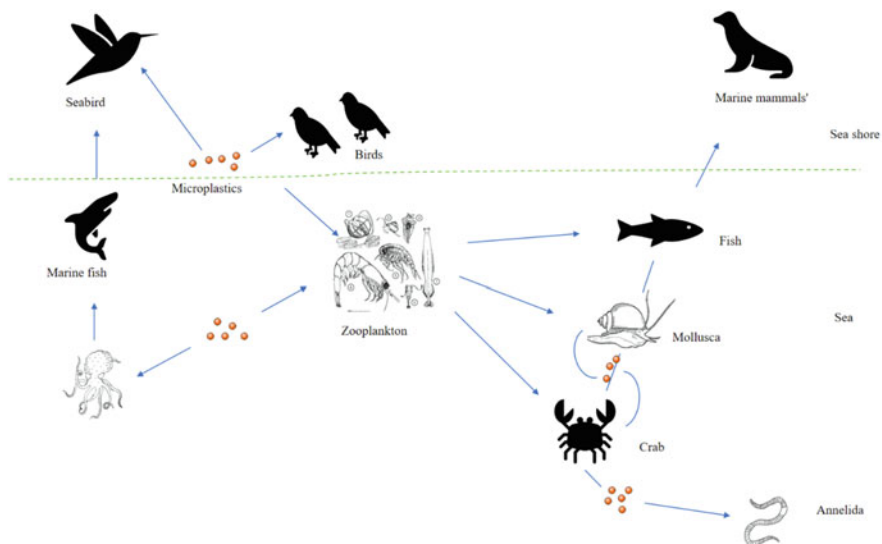


Fig. 15.4 Microplastics in different trophic levels of the aquatic environment

producers are known to incorporate microplastics and organic pollutants (Oliveira et al. 2012); then, those microplastics are bioaccumulated to top predators (Fig. 15.4) (Farrell and Nelson 2013). Hypothetically, microplastics with low and high densities are consumed; when present in the marine and freshwater environment, they tend to

float on the water surface, and a wide range of aquatic organisms consume microplastics passively or actively at a large number and consequently damage their physical health. According to Lattin et al. 2004, if the polymer is denser than the seawater, then it will sink or becomes neutrally buoyant. Higher quantities of buoyant microplastics were stated in the North Pacific Ocean, particularly the NPCG, than in additional ocean basins. This section is presently mentioned as the “eastern garbage path”(Moore et al. 2001, 2002; Lattin et al. 2004; Rios et al. 2010). Microplastics were also related to fishing in the gyre and inland releases at highly industrialized low latitudes.

15.6 Conclusions and Future Directions

Microplastic contamination in the freshwater ecosystem is an alarming situation for modern civilization. It shows a harmful effect on aquatic biota and transfer its effect along the food web. Developing countries like India, Bangladesh, Pakistan, Sri Lanka, Vietnam, Indonesia, Thailand, Korea, Philippines, and China are the main contributors of microplastic contamination in freshwater as well as marine ecosystem. Lack of rules and regulation for microplastic pollution is a serious problem in developed countries. The active participation of governments should introduce strong legislative rules and focus on the long-term effects of plastics particles. Additionally, active roles regarding microplastics played by normal people are important; this will reduce the plastic consumption. The effectiveness of plastic pollution is still unrecognizable by the overall population. Arrangement of social programs and awareness campaigns should be adopted for public health awareness to counter the long-lasting and chronic effects of plastic pollution. Furthermore, global awareness of plastic pollution led by socially active international organisations, such as International Maritime Organisation (IMO) and United Nations Environment Programme (UNEP), is arranged for various social campaigning to diminish microplastic pollution. Lastly, the plastics industry should take the liability of their products recycling and eco-friendly contact with water and soil. The local government should pass “zero tolerance” for industries or factories to custom biodegradable resources for easy recycling with environments. As the microorganisms play a role to degrade or decompose this biodegradable material, finally reducing the life period of those plastics in the environment, the proper recycling or upgrading of plastic debris should diminish the pollutions globally. The tertiary recycling practices of plastic appear as one of the advance technique where plastic materials are converted into smaller rubbishes, which can further be used for manufacturing petrochemical goods.

Conflict of Interest All of the authors declare that there is no competing interest in this work.

References

- Anderson A, Andrady A, Arthur C, Baker J, Bouwman H, Gall S, Hidalgo-Ruz V, Köhler A, Lavender Law K, Leslie H (2015) Sources, fate and effects of microplastics in the environment: a global assessment. GESAMP reports & studies series 90. International Maritime Organization, London, UK
- Andrady AL (2011) Microplastics in the marine environment. *Mar Pollut Bull* 62(8):1596–1605
- Andrady AL (2017) The plastic in microplastics: a review. *Mar Pollut Bull* 119(1):12–22
- Avio CG, Gorbi S, Regoli F (2017) Plastics and microplastics in the oceans: from emerging pollutants to emerged threat. *Mar Environ Res* 128:2–11
- Barnes DK, Galgani F, Thompson RC, Barlaz M (2009) Accumulation and fragmentation of plastic debris in global environments. *Philos Trans Royal Soc B: Biol Sci* 364(1526):1985–1998
- Boucher J, Friot D (2017) Primary microplastics in the oceans: a global evaluation of sources. IUCN, Gland, Switzerland
- Caruso G (2015) Plastic degrading microorganisms as a tool for bioremediation of plastic contamination in aquatic environments. *J Pollut Eff Cont* 3(3):1–2
- Desforges J-PW, Galbraith M, Ross PS (2015) Ingestion of microplastics by zooplankton in the Northeast Pacific Ocean. *Arch Environ Contam Toxicol* 69(3):320–330
- Devriese LI, Van der Meulen MD, Maes T, Bekaert K, Paul-Pont I, Frère L, Robbens J, Vethaak AD (2015) Microplastic contamination in brown shrimp (*Crangon crangon*, Linnaeus 1758) from coastal waters of the southern North Sea and channel area. *Mar Pollut Bull* 98(1–2):179–187
- Farrell P, Nelson K (2013) Trophic level transfer of microplastic: *Mytilus edulis* (L.) to *Carcinus maenas* (L.). *Environ Pollut* 177:1–3
- Hidalgo-Ruz V, Gutow L, Thompson RC, Thiel M (2012) Microplastics in the marine environment: a review of the methods used for identification and quantification. *Environ Sci Technol* 46(6):3060–3075
- Isobe A, Uchida K, Tokai T, M SJ, Iwasaki PB (2015) East Asian seas: a hot spot of pelagic microplastics. *Mar Pollut Bull* 101(2):618–623
- Lassen C, Hansen SF, Magnusson K, Hartmann NB, Jensen PR, Nielsen TG, Brinch A (2015) Microplastics: occurrence, effects and sources of releases to the environment in Denmark
- Lattin GL, Moore CJ, Zellers AF, Moore SL, Weisberg SB (2004) A comparison of neustonic plastic and zooplankton at different depths near the southern California shore. *Mar Pollut Bull* 49(4):291–294
- Li J, Qu X, Su L, Zhang W, Yang D, Kolandhasamy P, Li D, Shi H (2016) Microplastics in mussels along the coastal waters of China. *Environ Pollut* 214:177–184
- Limonta G, Mancia A, Benkhalqui A, Bertolucci C, Abelli L, Fossi MC, Panti C (2019) Microplastics induce transcriptional changes, immune response and behavioral alterations in adult zebrafish. *Sci Rep* 9(1):1–11
- Ma P, Wang m W, Liu H, Chen y F, Xia J (2019) Research on ecotoxicology of microplastics on freshwater aquatic organisms. *Environ Pollut Bioavailab* 31(1):131–137
- Moore CJ, Moore SL, Leecaster MK, Weisberg SB (2001) A comparison of plastic and plankton in the North Pacific central gyre. *Mar Pollut Bull* 42(12):1297–1300
- Moore CJ, Moore SL, Weisberg SB, Lattin GL, Zellers AF (2002) A comparison of neustonic plastic and zooplankton abundance in southern California's coastal waters. *Mar Pollut Bull* 44(10):1035–1038
- Oliveira M, Ribeiro A, Guilhermino L (2012) Effects of exposure to microplastics and PAHs on microalgae *Rhodomonas baltica* and *Tetraselmis chuii*. *Comp Biochem Physiol Part A* 163: S19–S20
- Orr IG, Hadar Y, Sivan A (2004) Colonization, biofilm formation and biodegradation of polyethylene by a strain of *Rhodococcus ruber*. *Appl Microbiol Biotechnol* 65(1):97–104

- Rios LM, Jones PR, Moore C, Narayan UV (2010) Quantitation of persistent organic pollutants adsorbed on plastic debris from the northern Pacific Gyre's "eastern garbage patch". *J Environ Monit* 12(12):2226–2236
- Roy PK, Hakkarainen M, Varma IK, Albertsson A-C (2011) Degradable polyethylene: fantasy or reality. *Environ Sci Technol* 45(10):4217–4227
- Ryan PG, Moore CJ, van Franeker JA, Moloney CL (2009) Monitoring the abundance of plastic debris in the marine environment. *Philos Trans R Soc Lond B Biol Sci* 364(1526):1999–2012
- Scherer C, Weber A, Lambert S, Wagner M (2018) Interactions of microplastics with freshwater biota. In: *Freshwater microplastics*. Springer, Cham, pp 153–180
- Sun X, Liang J, Zhu M, Zhao Y, Zhang B (2018) Microplastics in seawater and zooplankton from the Yellow Sea. *Environ Pollut* 242:585–595
- Tanaka K, Takada H, Yamashita R, Mizukawa K, Fukuwaka M-a, Watanuki Y (2013) Accumulation of plastic-derived chemicals in tissues of seabirds ingesting marine plastics. *Mar Pollut Bull* 69(1–2):219–222
- Teuten EL, Saquing JM, Knappe DR, Barlaz MA, Jonsson S, Björn A, Rowland SJ, Thompson RC, Galloway TS, Yamashita R (2009) Transport and release of chemicals from plastics to the environment and to wildlife. *Philos Trans R Soc B: Biol Sci* 364(1526):2027–2045
- Thompson RC, Olsen Y, Mitchell RP, Davis A, Rowland SJ, John AW, McGonigle D, Russell AEJS (2004) Lost at sea: where is all the plastic? *Science* 304(5672):838
- Van Cauwenbergh L, Janssen CR (2014) Microplastics in bivalves cultured for human consumption. *Environ Pollut* 193:65–70
- Van Cauwenbergh L, Claessens M, Vandegehuchte MB, Janssen CR (2015) Microplastics are taken up by mussels (*Mytilus edulis*) and lugworms (*Arenicola marina*) living in natural habitats. *Environ Pollut* 199:10–17
- van Wezel A, Caris I, Kools SA (2016) Release of primary microplastics from consumer products to wastewater in the Netherlands. *Environ Toxicol Chem* 35(7):1627–1631
- Welden NA, Cowie PR (2016) Environment and gut morphology influence microplastic retention in langoustine, *Nephrops norvegicus*. *Environ Pollut* 214:859–865
- Yamada-Onodera K, Mukumoto H, Katsuyaya Y, Saiganji A, Tani Y (2001) Degradation of polyethylene by a fungus, *Penicillium simplicissimum* YK. *Polym Degrad Stab* 72(2):323–327
- Zarfl C, Matthies M (2010) Are marine plastic particles transport vectors for organic pollutants to the Arctic? *Mar Pollut Bull* 60(10):1810–1814
- Zitko V, Hanlon MJMPB (1991) Another source of pollution by plastics: skin cleaners with plastic scrubbers. *Mar Pollut Bull* 22(1):41–42

Chapter 16

Exploring Particle Size Transport Variability of Suspended Sediments in Two Alpine Catchments Over the Lesser Himalayan Region, India



Omvir Singh

Abstract Sediments discharged from mountain rivers show different emptying patterns and transport behavior due to rainfall erosivity, human actions, and types of surface materials. Despite the long history of geoscience studies in the Himalayan region, little is known about particle size transport variability and patterns of suspended sediments. Therefore, to know the sediment emptying patterns and transport behavior in the region, this study presents information on particle size variability of the suspended sediments discharged by the Lesser Himalayan catchments (Sainj and Tirthan) of Himachal Pradesh, India. The examination has revealed the prevalence of fine >coarse >medium-sized particles in the Sainj catchment, whereas it has been found in the order of fine >medium >coarse in the Tirthan. The evacuation of medium-sized sediments has been observed more in quantity than coarse sediments but less than the fine sediments. The concentration of fine-, medium-, and coarse-sized particles fraction in the total suspended sediment concentration does not change much from October to April (lean flow period) months. Apart from this, the fine fraction sized particle load has exhibited the lowest variations among all seasons. Overall, the study has indicated that the maximum erosion, transportation, and vacation of suspended sediments take place through the monsoon season from the two catchments. The results of the study will be beneficial for hydropower generation and reservoir sedimentation management in the Himalayan region.

Keywords Suspended sediments · Particle size · Transport · Reservoir · Lesser Himalaya

O. Singh (✉)

Department of Geography, Kurukshetra University, Kurukshetra, Haryana, India

© Springer Nature Switzerland AG 2021

P. K. Shit et al. (eds.), *Spatial Modeling and Assessment of Environmental Contaminants*, Environmental Challenges and Solutions,

https://doi.org/10.1007/978-3-030-63422-3_16

259

16.1 Introduction

In fluvial systems, transportation of suspended sediments via streams is a major process, which is generally controlled by lithology, soil type, sediment delivery dynamics, seasonal alterations of winds, rainstorm events, runoff, human actions, and type of surface materials (Milliman and Meade 1983; Xu 1999, 2002; Singh et al. 2010; Xu et al. 2012). The particle size transport characteristics of suspended sediments from fluvial systems is one of the important subjects for a long time among hydrologists, fluvial geomorphologists, geochemists, hydraulic engineers, and an extended community of researchers. These research endeavors have been justified by several implications of particle dynamic forces, which are closely associated with the geological and geographical background of the streams (Phillips and Walling 1999; Xu 1999, 2002; Grangeon et al. 2012). Indeed, an excess of different particle size transport in streams has exhibited a variety of environmental effects (Owens et al. 2005; Accornero et al. 2008). For example, a rise in turbidity has led to a reduction in light penetration depth, affecting algae, macrophytes, and fish habitation (Kemp et al. 2011). From a functional point of view, especially in hilly catchments, an increased transport of different types of particles has been problematic for hydropower plants through reservoir siltation. Temporal change in particle size of stream-suspended sediments has been expected to reflect sedimentary processes of erosion, transportation, and deposition both in catchments and channels (Xu 1999). Moreover, it has also influenced the composition of land surface materials, energy budget, and the shape of channels (Xu 2002). Furthermore, particle size transportation behavior from watershed systems affects the planetary biogeochemical phasing of elements, continental landscapes, and several other sedimentary processes (Milliman and Meade 1983; Raymo and Ruddiman 1992; Syvitski et al. 2003).

Particle size composition and load studies of suspended sediments in lowland rivers (below 300 m altitude) have been found in abundance spatially and temporally (Walling and Moorehead 1989; Xu 1996, 2002, 2007; Slattery and Burt 1997; Stone and Walling 1997; Phillips and Walling 1999; Walling et al. 2000; Woodward and Walling 2007; Williams et al. 2007). However, hilly catchments have been acknowledged as great suppliers of different particle size load to larger systems (Milliman and Syvitski 1992). The nature of the absolute size distribution is strongly controlled by catchment altitude. More the average altitude of a catchment, coarser are the particles and vice-versa. A limited number of studies regarding particle size composition and their transport from hilly catchments have been documented due to technical difficulties (Lenzi and Marchi 2000; Woodward et al. 2002; Peticrew 2005; Haritashya et al. 2010). Another likely clarification for this deficiency is the requirement to compute the actual particle size in situ (Phillips and Walling 1995). Till date, the instruments that have been applied for the measurement of particle size in hilly catchments have proved unfit due to larger size of grains, greater slope, and higher velocities of streamflow. Therefore, much research so far in abroad and India has been done with reference to water discharge, suspended sediment concentration (SSC), and suspended sediment load (Sarma 2005; Singh et al. 2008; Haritashya

et al. 2010), but suspended sediment particle size concentration and load studies are, however, somewhat limited. Therefore, to bridge this gap, an attempt in this study has been made to explore the particle size transport variability of suspended sediments with respect to Sainj and Tirthan catchments in the Lesser Himalayan region of Himachal Pradesh, India. Knowledge regarding particle size transport behavior of suspended sediments from these rivers will be beneficial for hydropower generation, reservoir sedimentation, and land management across the Himalayan region. Additionally, results of this study will improve our awareness about sediment transport dynamic forces, which may have been of significant use in sediment transport models.

16.2 Materials and Methods

16.2.1 Geographic Setting

The study area comprises two different catchments named Sainj (741 km²) and Tirthan (687 km²). Both are left bank tributaries of Beas river system in the Lesser Himalayan region. The catchments spread between 31°30'28"N to 31°55'02"N latitudes and 77°13'02"E to 77°45'57" east longitudes as shown in Fig. 16.1. The

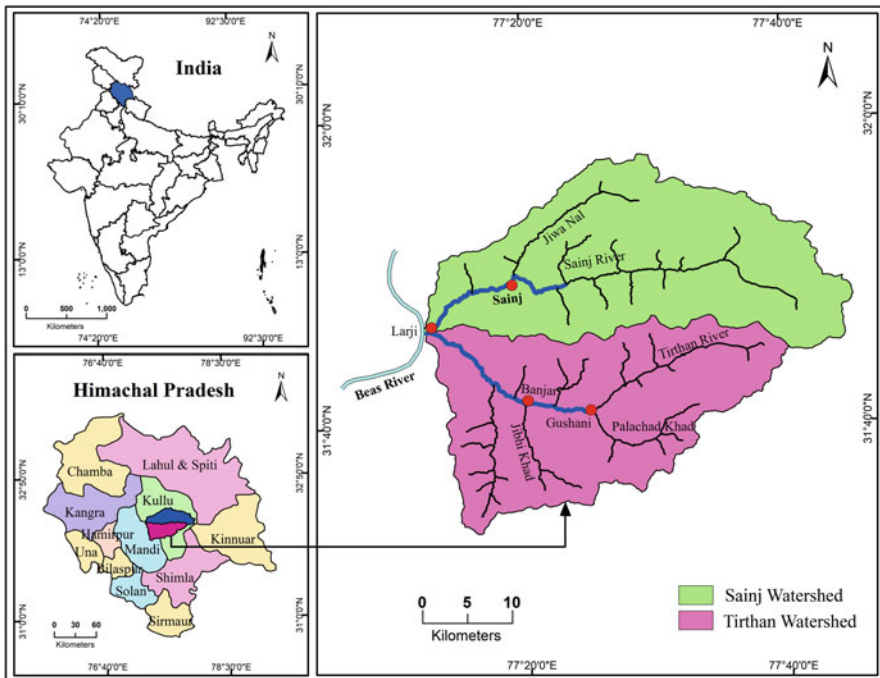


Fig. 16.1 Location of the Sainj and Tirthan catchments in the state of Himachal Pradesh

study area is a representative of moderate to high rugged topography with several peaks over 4000 m. The normal slope of the two catchments is 38.12° and 40.04° , whereas mean elevations are 3510 and 2826 m, respectively. The direction of slope for both the catchments is from east to west (Singh 2007). The major rock types are alluvium, colluvium, glacial deposits, slate, phyllite, dolomites, quartzites, schist, sandstone, and granites. The soil texture ranges from loam to sandy loam, while organic matter content is around 70%. In terms of land use and land cover, the two catchments have maximum area under forests followed by rocky outcrops, snow cover, cultivated lands, and glaciers.

The Sainj and Tirthan catchments have a typical warm temperate climate. The catchments receive about 1000 mm of average annual rainfall, of which more than 50% is received from June to September months. Snowfall is confined to upper reaches and during winter season only. The mean monthly temperature varies from a minimum of 8.7°C during January to the maximum of 26.3°C during June. The maximum and minimum relative humidity has been recorded to the tune of 78.7% (August) and 63.3% (May), respectively. Minimum evaporation has been recorded in the month of January (coldest month), while the maximum has been observed in the month of June (warmest month).

16.2.2 Acquisition of Discharge and Suspended Sediment Concentration Data

Data on sediment flux for the Lesser Himalayan region are minimal due to unevenness, remoteness, and inaccessibility. In this study, sediment flux data gauged at the outlet points of the Sainj and Tirthan rivers along with standardized sections at the Larji gauging station have been acquired from the Bhakra Beas Management Board (BBMB). The acquired data have been for a period of 24 years from 1981 to 2004. Suspended sediment samples have been collected every day from three transects across the two rivers with depth integrating samplers. The samples have been then filtered one by one through a 100-mesh sieve; the fraction detained has been dried up and weighed. It denotes the coarse fraction (>0.20 mm). The sieved samples have been again stirred and permitted to stand for the time needed for settling down of the medium fraction (0.075–0.20 mm) relying upon the temperature of water. A 25 ml sample of the left-out material has been dried up and weighed to describe the fine fraction (<0.075 mm) and dissolved salts. Another 25 ml has been refined, dried up, and weighed to denote the dissolved salts. The weight of the fine fraction has been ascertained by removing the weight of the dissolved salts from the mix of fine fractions and dissolved salts. Apart from this, the average sediment concentration in 1 liter of water has been computed. The sediment load in the water of two catchments has been computed by multiplying the average sediment concentration with the equivalent discharge. This has been converted to cubic meter unit by distributing the

load in tones by 1.4, accepting that the sediment density was 1.4 t m^{-3} (Sharma et al. 1991; Jain et al. 2003).

Furthermore, to compute seasonal variability, the year has been broadly classified into four seasons, namely winter (December–March), summer (April–June), monsoon (July–September), post-monsoon (October–November), the criterion commonly adopted by researchers in the Himalayan region (Singh et al. 1995, 1997; Singh 2007; Kumar and Jain 2010).

16.3 Results and Discussion

16.3.1 *Suspended Sediment Concentration and Particle Size Distribution*

During the study period, the distribution of different particle size fractions (coarse, medium, and fine) concentration in the water of Sainj catchment has been in the order of fine > coarse > medium, while for Tirthan it has been in the order of fine > medium > coarse (Table 16.1). The average content of fine fractions concentration has constituted more than two and half times of coarse and medium combined fractions for Tirthan catchment. In the context of percentage particle size distribution, the results from Sainj and Tirthan rivers are in close agreement with the results communicated by Sharma et al. (1991) for Sutlej River, which forms the southwestern boundary of the two catchments. To sum up, suspended sediment transport from the two catchments has been mainly controlled by fine-grained materials, which may be associated with the deep chemical weathering and clay enriched soils. Apart from this, the transport behavior of nutrients within a fluvial system depends more on the fine fractions of the sediments than on the coarse fractions of sediments.

16.3.2 *Temporal Variability of Suspended Sediment Concentration and Particle Size Distribution*

A variation in particle size distribution on a monthly basis for the entire 24-year period has been given in Table 16.2. Monthly and average monthly distribution of different size fractions in suspended sediment concentration has been observed in the

Table 16.1 Distribution of suspended sediment concentration under different particle sizes in the Sainj and Tirthan catchments

Catchments	Fine (<0.075 mm)	Medium (0.075–0.20 mm)	Coarse (> 0.20 mm)
	Sediment fraction (%)		
Sainj	60.9	19.5	19.6
Tirthan	71.8	17.2	11.0

Table 16.2 Monthly percentage distribution of suspended sediment particles of different sizes in the Sainj and Tirthan catchments

Months	Sainj catchment			Tirthan catchment		
	Coarse (>0.20 mm)	Medium (0.075–0.20 mm)	Fine (<0.075 mm)	Coarse (>0.20 mm)	Medium (0.075–0.20 mm)	Fine (<0.075 mm)
	%					
January	5.0	7.5	87.5	4.8	7.3	87.2
February	5.2	7.7	87.2	5.0	7.6	87.5
March	5.1	8.2	86.7	5.3	8.5	86.3
April	6.0	9.5	84.6	5.7	9.2	85.1
May	11.6	14.2	74.2	6.3	10.2	83.7
June	18.0	19.8	62.2	7.7	12.7	79.2
July	22.7	22.5	54.8	13.0	19.5	67.5
August	20.2	24.0	55.7	12.7	20.1	67.4
September	15.9	19.0	65.3	9.9	15.5	74.6
October	6.8	10.3	82.5	5.5	8.2	85.4
November	5.6	8.8	86.4	4.9	7.7	87.3
December	5.1	7.8	87.1	4.7	7.5	87.3
Average	10.6	13.2	76.2	7.1	11.2	81.5

order of fine > medium > coarse. A marginal exception has been observed only in the month of July in the Sainj catchment. The table highlights that fine, medium, and coarse particle fractions in the total suspended sediment concentration do not change much during the lean period (October–April) in both catchments, whereas the percentage share has varied marginally from month to month. Moreover, May and June months also show the similar trend as that of the October–April period in the Tirthan catchment.

This is attributed to the large glaciated and snow-covered areas in the Sainj catchment, and melting starts in early summers, which results in a higher, suspended sediment concentration during May and June months as well. This variation in suspended sediment concentration has been well witnessed in the months of May and June at the outlet of two catchments. Furthermore, the coarse and medium-sized fraction has been found to be at its optimum level in July, August, and September months, which can be better explained both by the high rainfall intensity and higher melt water runoff in the streams. This phenomenon leads to removal of sediments from larger surface areas of the two catchments and a greater degree of contact with its bottom and bed sediments through high streamflow periods as well.

Significant variations have been observed in fine, medium, and coarse contents of sediment fraction percentage during different years in both the catchments, recommending that the sediment production and transfer processes in the catchments have changed significantly during the study period (Fig. 16.2). The seasonal concentration of different grain-size particles has almost followed the similar pattern as that of the suspended sediment.

16.3.3 Suspended Sediment Load and Particle Size Distribution

Suspended sediment load has long been recognized as an important contaminant affecting water resources in catchments. In this study, suspended sediment load has been employed as an index of particle accessibility. A comprehensive understanding of sediment load and transport is considered essential to the design and implementation of effective plans for sediment management in reservoirs and hydropower projects (Osterkamp et al. 1998). Similar to suspended sediment load, the quantity of different types of sediments (coarse, medium, fine) transported has varied annually. The large grain-size particles will be less in quantity than the fine ones. Annually, the minimum load transported by a river will be coarse because it needs more kinetic energy. On an average, 152.9×10^3 and 50.6×10^3 tons of coarse sediments have been transported annually from the Sainj and Tirthan catchments during the study period. It has accounted for about 23.0% in the Sainj and 13.7% in the Tirthan catchment of the average annual total sediment load. The coarse sediment has a very high annual variation of 152.2% and 148.9% (Table 16.3). The quantity of coarse sediment in the Sainj River has varied from 17.4×10^3 t in 1984 to 908.0×10^3 tons

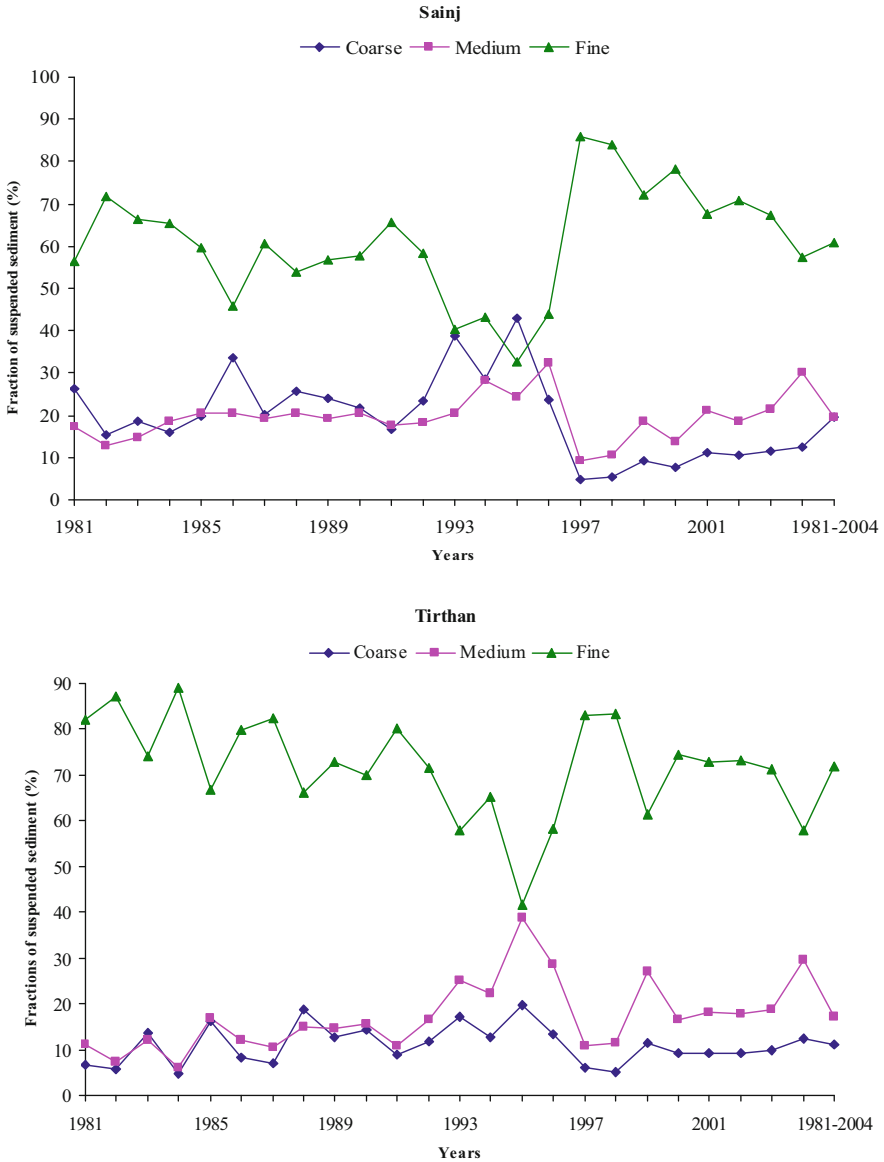


Fig. 16.2 Fractions of coarse, medium, and fine suspended sediments in the Sainj and Tirthan catchments

in 1995. Similarly, the Tirthan catchment has transported a quantity of 3.4×10^3 tons in 1981 to 244.9×10^3 tons of coarse sediment in 1993 (Fig. 16.3). However, the runoff has not been high and low, respectively, during these years (Fig. 16.4).

Table 16.3 Distribution of suspended sediment load from the Sainj and Tirthan catchments

Units	Sainj catchment				Tirthan catchment			
	Fine (<0.075 mm)	Medium (0.075–0.20 mm)	Coarse (>0.20 mm)	Total	Fine (<0.075 mm)	Medium (0.075–0.20 mm)	Coarse (>0.20 mm)	Total
10 ³ (t)	265.5	115.4	152.9	533.8	185.7	755.8	506.3	312.0
%	55.9	21.1	23.0	100.0	66.1	20.2	13.7	100.0
C.V.	59.5	86.0	152.2	79.4	97.3	151.3	148.9	109.4

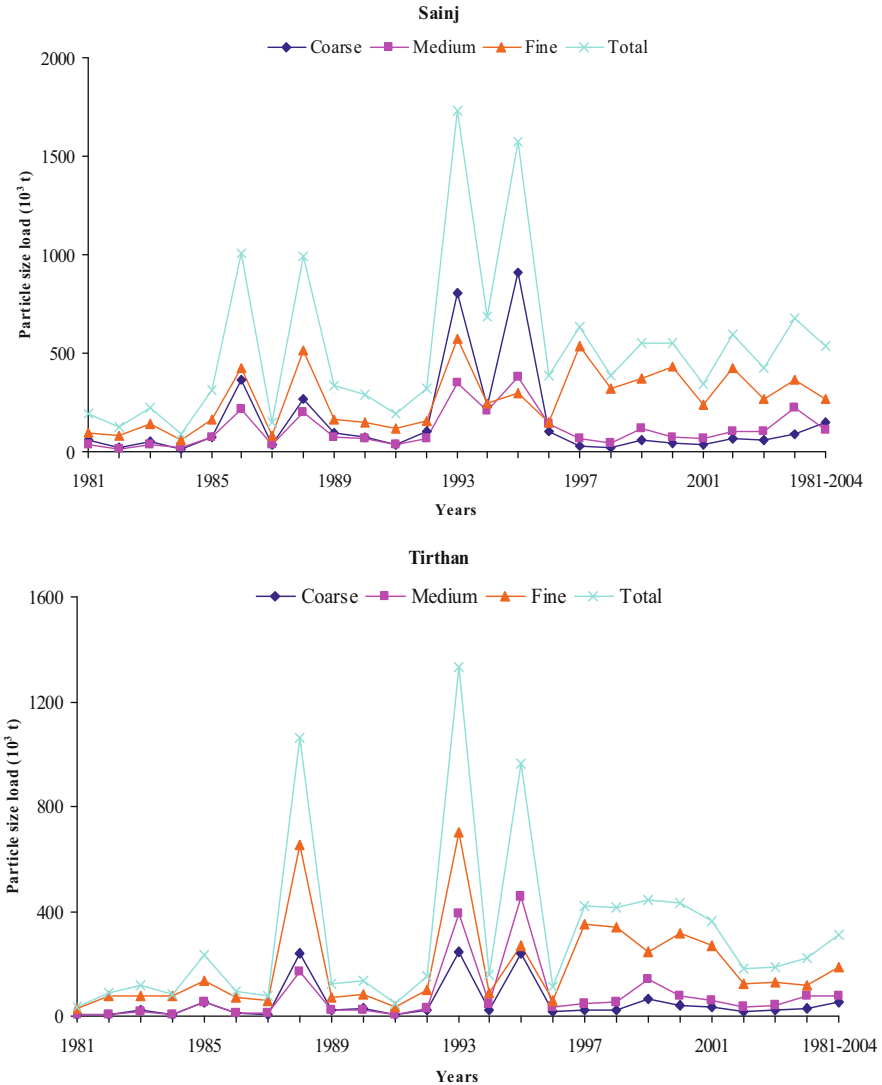


Fig. 16.3 Distribution of particle size load in the Sainj and Tirthan catchments

This phenomenon has indicated that it is not only the amount of rainfall but also its intensity and spell characteristics that determine the quantity of sediment transport.

The medium-sized sediments have been transported in more quantity than coarse sediments but less than the fine sediments. The Sainj and Tirthan catchments on an average have transported 115.4×10^3 and 75.6×10^3 tons of sediments, which forms 21.1% and 20.2% of the total sediment load annually. It has varied from 183.3×10^3 tons in 1982 to 377.9×10^3 tons in the year 1995 in the Sainj River and 6.1×10^3 tons in 1981 to 453.9×10^3 tons during 1995 in the Tirthan, showing a

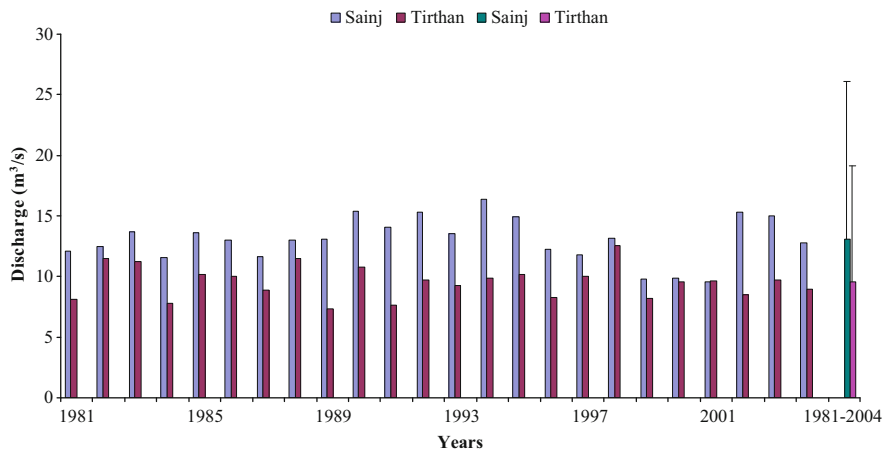


Fig. 16.4 Annual total and annual mean discharge in the Sainj and Tirthan catchments

coefficient of variation of 86% and 151.3% in respective rivers. Again, the medium sediments transported by two catchments have not been in tune with the runoff volumes.

The maximum amount of load has been transported in the form of fine sediment particle fraction in both the catchments. On an average, 265.5×10^3 and 185.7×10^3 tons of fine sediments have been transported annually, which accounts for 55.9% and 66.1% in the Sainj and Tirthan catchments during the 1981–2004 period, respectively. Fine sediments have the lowest variability among the three types of sediments analyzed (Table 16.3). Quantity of fine sediments has varied from 56.3×10^3 tons in 1984 to 578.2×10^3 tons in 1993 in the Sainj catchment and 27.4×10^3 tons in 1981 to 701.5×10^3 tons during 1993 in the Tirthan (Fig. 16.3).

Of the different fraction size load described above, the Tirthan catchment has high coefficient of variability than the Sainj. Furthermore, the above analysis has also revealed the hypothesis that the larger particles transport less in quantity than the small ones stand negated in the Sainj catchment because the percentage and total quantity of different particle size fraction are in the order of fine load > coarse load > medium load (Table 16.3). High quantity of coarse load transportation in the Sainj catchment may be due to high gradient, and 32% area is glacierized. It produces high-density waters with more kinetic energy causing coarse load. Additionally, the characteristics of rainfall, whether heavy or sparse, determine the distribution of different size fraction sediment load.

16.3.4 Temporal Variability of Suspended Sediment Load and Particle Size Distribution

Since the runoff is highest during the monsoon, sediment load is also high for that season. Nearly 95% coarse and medium sediment and more than 85% of the fine sediments have been transported during the monsoon period in both catchments. The season has a mean coarse sediment value of 37.6×10^3 tons and 12.3×10^3 tons with a coefficient of variability 252.4 and 192.4% in the Sainj and Tirthan rivers, respectively. This variability has been very high when compared with other two sediment types through the monsoon season, except medium sediments in the Tirthan catchment (Table 16.4). The medium fraction sediments have a mean value of 27.9×10^3 tons with a variation of 184.3% in the Sainj River while in Tirthan the mean value stands at 18.3×10^3 tons with a variability of 226.1%. The fine sediments have the lowest variation, that is, 141.1% (Sainj) and 169.8% (Tirthan), when compared with other size fractions during the monsoon season (rainy). Fine sediments have a mean value of 60.7×10^3 tons in the Sainj and 41.8×10^3 tons in the Tirthan catchment for the entire study period. On an average, 126.1×10^3 tons and 72.4×10^3 tons sediments have been transported through the monsoon season, which accounts for higher than 85% of the total annual load from the Sainj and Tirthan catchments. During monsoon season, rain spell-oriented runoff has carried all fine materials to the stream, which makes the suspended sediment load finer. Apart from this, soils on the hillslopes during this season may be removed by surface runoff created by rainstorms and then finally transported into the stream. The suspended sediments thus have become somewhat fine. The total sediments have 187% and 181% variability in the season in respective catchments.

The post-monsoon season has low sediment loads as the runoff volume starts decreasing after the monsoon rainfall. During this season, the fine sediments have formed a major part of the sediment load. It has accounted for about 81% and 84% of the total sediment load in the season in two catchments, respectively. The rest 7% and 12%, respectively, account for coarse and medium sediment load in the Sainj while 6% and 10% in the Tirthan catchment. This season has very low contribution to annual sediment load. The fine sediments have accounted for only 5% and 8% of the annual sediment load, whereas the coarse and medium sediments have formed approximately 3% and 5% of the annual load, respectively, in the two catchments. The coarse and medium sediment load has less coefficient of variability during post-monsoon than monsoon season, even though the post-monsoon season has higher runoff variability in both the rivers. The fine sediments have higher variation than the monsoon season in respective catchments.

The winter season has the lowest load in the Sainj and Tirthan rivers. This season also have the lowest runoff means. The fine sediments have constituted the major chunk of the total sediment transported. It has nearly come to 85% and 81% of the total sediment load in Sainj and Tirthan catchments, respectively. In this season, the coarse sediments are 6% and 8% and medium sediments are 9% and 11% in the respective catchments. The coarse and medium sediment load has higher coefficient

Table 16.4 Discharge and sediment transport under different particle sizes from the Sainj and Tirthan rivers

Season	Discharge (m ³ /s)		Coarse sediment (t)		Medium sediment (t)		Fine sediment (t)		Total suspended sediment (t)	
	Average	CV	Average	CV	Average	CV	Average	CV	Average	CV
Sainj catchment										
Summer	975.6	28.8	867.2	88.3	1109.2	81.3	6069.5	70.2	8044.9	67.1
Monsoon	2105.9	21.8	37578.8	252.4	27947.9	184.3	60650.9	141.1	126097.0	186.7
Post-monsoon	592.1	25.3	292.8	134.9	537.2	150.5	3680.8	168.6	4548.0	157.6
Winter	375.6	23.2	54.1	78.8	91.4	97.2	860.6	53.3	1006.2	89.9
Annual total	4049.2	—	38792.8	—	29685.7	—	71261.8	—	139696.0	—
Tirthan catchment										
Summer	853.7	35.3	257.3	67.9	434.9	77.0	3725.0	82.9	4417.1	79.2
Monsoon	1433.5	32.4	12327.8	192.4	18338.9	226.1	41758.2	169.8	72384.9	181.0
Post-monsoon	431.7	37.1	276.1	179.2	498.5	225.7	4241.9	221.9	5042.9	216.0
Winter	313.9	22.6	63.7	122.4	90.0	117.9	695.1	64.1	849.1	71.7
Annual total	3032.9	—	12924.9	—	19362.2	—	50420.2	—	82694.0	—

of variability during the season in the Tirthan catchment than Sainj. Fine fraction size particle load has displayed the lowest variations among all seasons during winter in both the catchments (Table 16.4). This season has contributed negligible amounts of sediment load to the annual sediment load. The total sediment during the season has only 90% and 72% variation, lowest of all the seasons in Tirthan and second lowest in the Sainj catchment.

The summer season fraction size sediment load contributions have been found second highest after monsoon in the Sainj catchment, whereas in Tirthan it has been observed higher only than the winter season. But their contribution toward the annual sediment load has been only 5% in both catchments. The variability of summer runoff has been found highest among all the seasons in the Sainj catchment and second highest in the Tirthan. In the summer season, coarse and medium fraction sediments have recorded the lowest variability in the Tirthan catchment and fine fractions with annual load in the Sainj (Table 16.4). Fluctuations in runoff have not led to fluctuations in sediment load; therefore, the highest variability in runoff and lowest fluctuations in total suspended sediment load are beyond understanding in the Sainj catchment.

In general, about 50% and 60% of the total sediment load carried away by the two catchments are fine, about 20% and 22% medium, and the remaining are coarse sediment load from respective rivers. Among the seasons, the monsoon season has transported optimum sediment load. It has accounted for more than 85% of the total annual sediment load. The monsoon season has the highest coefficient of variability in the Sainj catchment and post-monsoon season in the Tirthan. The total sediment load during winters has been very low. The high sediment load during monsoons can be attributed to high intensity of rainfall storms and simultaneous snow melting at the higher reaches of the two catchments. Seasonal load under different grain-size particles has also followed the analogous trend, which has been found in tune with the total suspended sediment load.

16.4 Conclusions

The study of particle size distribution of suspended sediments is important because it affects the agricultural productivity, macrophytes, algal growth, and fish habitat in watershed systems. The present study has revealed significant information regarding concentration and load of different particle sizes of suspended sediments, which has previously been lacking in the Himalayas. The major conclusions drawn from the study are as follows:

- A significant variation exists in the transport of fine, medium, and coarse sediment fraction percentages for different years in Sainj and Tirthan catchments, which suggests that the sediment production and transfer processes have changed significantly during the study period.

- More than 75% of suspended sediment load from the two catchments is principally composed of fine size particles, indicating toward low streamflow and kinetic energy.
- Enormous quantities of fine sediments have been transported from these catchments during peak flow periods on account of heavy intensity rainstorms and surface runoff erosion.
- Most of the coarse and medium suspended sediments have been derived through bottom polishing and bank erosion.
- Higher percentage transfer of fine size particles from the two catchments is attributed to various anthropogenic activities such as sand and slate mining, road construction, construction of hydropower projects, deforestation, and agricultural practices. Recently, both catchments witnessed about 5% growth in area under agriculture, whereas forest area decreased by 2% and 5% in Sainj and Tirthan catchments, respectively, between 1977 and 1999.
- The percentage particle size distribution of the two catchments is in close agreement with the upper parts of Sutlej catchment, which forms the southwestern boundary of the Sainj and Tirthan catchments.

References

- Accornero A, Gnerre R, Manfra L (2008) Sediment concentrations of trace metals in the Berre lagoon (France): An assessment of contamination. *Arch Environ Contam Toxicol* 54:372–385
- Grangeon T, Legout C, Esteves M, Gratiot N, Navratil O (2012) Variability of suspended particles size during highly concentrated flood events in a small mountainous catchment. *J Soils Sediments* 12:1549–1558
- Haritashya UK, Kumar A, Singh P (2010) Particle size characteristics of suspended sediments transported in meltwater from Gangotri Glacier, central Himalaya—an indicator of subglacial sediment evacuation. *Geomorphology* 122:140–152
- Jain SK, Singh P, Saraf AK, Seth SM (2003) Estimation of sediment yield for a rain, snow and glacier fed river in the Western Himalayan region. *Water Resour Manag* 17:377–393
- Kemp P, Sear D, Collins A, Naden P, Jones I (2011) The impacts of fine sediment on riverine fish. *Hydro Process* 25:1800–1821
- Kumar V, Jain SK (2010) Trends in seasonal and annual rainfall and rainy days in Kashmir valley in the last century. *Quat Int* 212:64–69
- Lenzi MA, Marchi L (2000) Suspended sediment load during floods in a small stream of the Dolomites (north-eastern Italy). *Catena* 39:267–282
- Milliman JD, Meade RH (1983) Worldwide delivery of river sediment to the oceans. *J Geol* 91(1):1–21
- Milliman JD, Syvitski PM (1992) Geomorphic and tectonic control of sediment discharge to the ocean: the importance of small mountain rivers. *J Geol* 100:525–544
- Osterkamp WR, Heilman P, Lane LJ (1998) Economic considerations of a continental sediment monitoring program. *Int J Sediment Res* 13(4):12–24
- Owens PN, Batalla RJ, Collins AJ, Gomez B, Hicks DM, Horowitz AJ, Kondolf GM, Marden M, Page MJ, Peacock DH, Petticrew EL, Salomons W, Trustrum NA (2005) Fine-grained sediment in river systems: environmental significance and management issues. *River Res Appl* 21:693–717

- Petticrew EL (2005) The composite nature of suspended and gravel stored fine sediment in streams: a case study of O'Ne-eil Creek, British Columbia, Canada. In: Droppo IG, Leppard GG, Liss SN, Milligan TM (eds) Flocculation in natural and engineered environmental systems. CRC Press, Boca Raton, FL, pp 71–93
- Phillips JM, Walling DE (1995) Measurement in situ of the effective particle-size characteristics of fluvial suspended sediment by means of a field-portable laser backscatter probe: some preliminary results. *Mar Freshw Res* 46:349–357
- Phillips JM, Walling DE (1999) The particle size characteristics of fine-grained channel deposits in the River Exe Basin, Devon, UK. *Hydrol Process* 13:1–19
- Raymo ME, Ruddiman WF (1992) Tectonic forcing of late Cenozoic climate. *Nature* 359:117–122
- Sarma JN (2005) Fluvial processes and morphology of the Brahmaputra River in Assam, India. *Geomorphology* 70:226–256
- Sharma PD, Goel AK, Minhas RS (1991) Water and sediment yields into the Sutlej river from the High Himalaya. *Mt Res Dev* 11:87–100
- Singh O (2007) Geomorphological evaluation, soil erosion assessment and management in Himalayan catchment, Himachal Pradesh. Ph.D. thesis submitted to Jawaharlal Nehru University, New Delhi
- Singh P, Ramasastri KS, Kumar N (1995) Topographical influence on precipitation distribution in different ranges of western Himalayas. *Nord Hydrol* 26:259–284
- Singh P, Jain SK, Kumar N (1997) Estimation of snow and glacier-melt contribution to the Chenab River, Western Himalaya. *Mt Res Dev* 17:49–56
- Singh O, Sharma MC, Sarangi A, Singh P (2008) Spatial and temporal variability of sediment and dissolved loads from two alpine catchments of the Lesser Himalayas. *Catena* 76:27–35
- Singh O, Singh P, Sarangi A, Sharma MC, Kumar S (2010) Anthropogenic impacts on the sediment flux in two alpine catchments of the Lesser Himalayas. *Curr Sci* 99:608–618
- Slattery MC, Burt TP (1997) Particle size characteristics of suspended sediment in hillslope runoff and stream flow. *Earth Surf Process Landf* 22:705–719
- Stone PM, Walling DE (1997) Particle size selectivity considerations in suspended sediment budget investigations. *Water Air Soil Pollut* 99:63–70
- Syvitski JP, Peckham SD, Hilberman R, Mulder T (2003) Predicting the terrestrial flux of sediment to the global ocean: a planetary perspective. *Sediment Geol* 162(1):5–24
- Walling DE, Moorehead PW (1989) The particle size characteristics of fluvial suspended sediment: an overview. *Hydrobiologia* 176/177(1):125–149
- Walling DE, Owens PN, Waterfall BD, Leeks GJL, Wass PD (2000) The particle size characteristics of fluvial suspended sediment in the Humber and Tweed catchments, UK. *Sci Total Environ* 251(252):205–222
- Williams ND, Walling DE, Leeks GJL (2007) High temporal resolution in situ measurement of the effective particle size characteristics of fluvial suspended sediment. *Water Res* 41:1081–1093
- Woodward JC, Walling DE (2007) Composite suspended sediment particles in river systems: their incidence, dynamics and physical characteristics. *Hydrol Process* 21:3601–3614
- Woodward JC, Porter PR, Lowe AT, Walling DE, Evans AJ (2002) Composite suspended sediment particles and flocculation in glacial meltwaters: preliminary evidence from Alpine and Himalayan catchments. *Hydrol Process* 16(9):1735–1744
- Xu J (1996) Complex behaviour of suspended sediment grain size downstream from a reservoir: an example from the Hanjiang River, China. *Hydrol Sci J* 41(6):837–849
- Xu J (1999) Grain-size characteristics of suspended sediment in the yellow river, China. *Catena* 38:243–263
- Xu J (2002) Implications of relationships among suspended sediment size, water discharge and suspended sediment concentration: the yellow river basin, China. *Catena* 49:289–307
- Xu J (2007) Trends in suspended sediment grain size in the upper Yangtze River and its tributaries, as influenced by human activities. *Hydrol Sci J* 52(4):37–41

Xu Y, Song J, Duan L, Li X, Yuan H, Li N, Zhang P, Zhang Y, Xu S, Zhang M, Wu X, Yin X (2012) Fraction characteristics of rare earth elements in the surface sediment of Bohai Bay, North China. *Environ Monit Assess* 184:7275–7292

Chapter 17

Salinity and Corrosion Potential of Groundwater in Mewat District of Haryana, India



Gaurav Verma, Smita Sood, Priyanka Sharma, and Shakir Ali

Abstract Groundwater salinity is a major problem in India and is mainly confined to arid and semiarid areas. The present study was conducted to assess the groundwater salinity, hydrochemical facies, and corrosion indices in the Mewat district of Haryana, India. This study is based on the groundwater samples collected during intervals of field campaigns conducted in the year 2018 from three blocks, namely, Nuh, Nagina, and Ferozpur Jhirka of Mewat. It was found that the electrical conductivity (EC) of the water in the regions varies from 353–10,181 $\mu\text{S}/\text{cm}$ and the majority of the samples belong to Mg-Cl hydrochemical facies. Various corrosion indices such as Langelier Saturation Index (LSI), Puckorius Scaling Index (PSI), Ryznar Scaling Index (RSI), and Aggressive Index (AI) were evaluated based on the analyzed physicochemical parameters. It was observed that the water is slightly noncorrosive to LSI and corrosive to intensely corrosive to RSI, while AI values indicate the nonaggressive nature of water. This study suggests that the aquifers are highly saline, but a few freshwater pockets do exist in the aquifers of Mewat. Thus, a judicious approach toward the usage of saline water must be inducted and a regular supply of safe drinking water should be provided to villagers in the area for their sustenance in daily life and agriculture.

Keywords Salinity · Mewat · Groundwater · Corrosion indices · Southern Haryana · India

G. Verma (✉) · S. Sood · P. Sharma
School of Basics and Applied Sciences, G.D. Goenka University, Gurugram, India

S. Ali
Department of Geology, University of Delhi, Delhi, India

17.1 Introduction

Groundwater is depleting at a higher rate in the developing world, particularly through industrialization (Rodell et al. 2009). The research in the field of groundwater has taken a huge rise since the concern for the conservation of groundwater has intensified (Singh and Kumar 2014; Nagaraju et al. 2014; Saha et al. 2016; Singh 2017; Ali et al. 2016, 2018; Saha et al. 2020). The problem of saline groundwater is affecting livelihood in Mewat, as the major source of earning of the locals is through agriculture. Thus, this study was conducted to evaluate the saline aquifers and observed that the groundwater is highly saline but there are some freshwater pockets present in these aquifers. Major ions analysis of the water samples suggests the dominance of Mg-Cl water facies. Furthermore, various corrosion indices such as Langelier Saturation Index (LSI), Puckorius Scaling Index (PSI), Ryznar Scaling Index (RSI), and Aggressive Index (AI) were evaluated for corrosion potential of water for portability. LSI values suggest that the water is slightly noncorrosive and corrosive to intensely corrosive to RSI. The AI values indicate the nonaggressive nature of water. This study suggests the rejuvenation of ponds and canal systems present in the area, which are to be maintained and managed wisely for the daily usage and effective groundwater recharge.

17.2 Study Area

Mewat district is situated in the southern part of the Haryana state and can be located between 26 °39'00"N and 28 °32'25"N latitude and between 76 °39'30"E and 77 °20'45"E longitudes. The geographical area of Mewat is approximately 1859.61 square kilometers, accounting for 1441.71 square kilometers of rural area, and the district comprises 95.23% rural, 3.51% urban, 1.31% wasteland, and 1.99% forest area out of a total geographical area of 1859.61 square kilometers (Table 17.1). The district shares its boundary with two other districts of Haryana viz. Gurgaon from the north and Palwal from the east and also with the Alwar district of Rajasthan in the west (District Census Book, Mewat 2011) (Fig. 17.1). The climate of the region is tropical steppe, hot, and semiarid during summers (April to June) and extreme cold in the winters (December and January). The months of July to early

Table 17.1 Land use land cover of Mewat district (District Disaster Management Plan, Mewat 2016–2017 and Central Ground Water Board 2012)

Geographical area (km ²)	1859.61
Land use area (km ²)	
Cultivable area	1361
Net sown area	1740
Forest area	30
Land cover area (km ²)	
Irrigated area	880
Gross irrigated area	2364.34

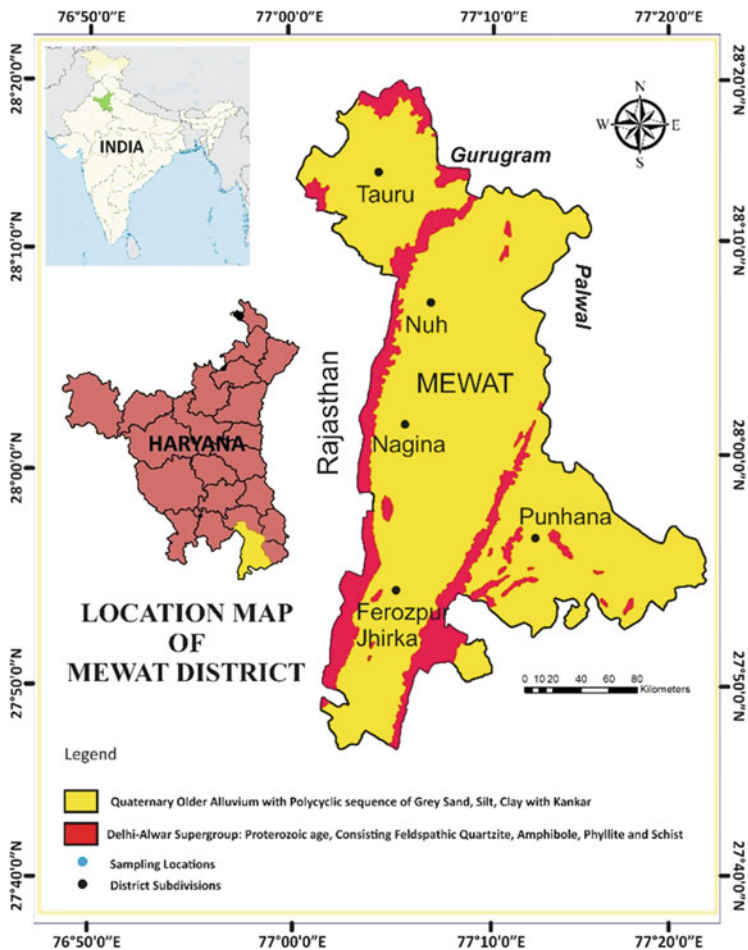


Fig. 17.1 Location and geological map of Mewat district of Haryana, India

September consist of monsoon (CGWB 2012). The Mewat district consists of limited freshwater bodies and receives scanty rainfall throughout the year (District Census Book, Mewat 2011; CGWB 2012, District Disaster Management Plan, Mewat 2016–2017).

17.3 Material and Methods

17.3.1 Groundwater Sampling

Groundwater samples were collected from the Mewat district, covering three administrative blocks Nuh, Nagina, and Ferozpur Jhirka (Fig. 17.1). The sampling sources

were identified using the groundwater well data of the Public Health Department, Nuh, and with the help of the software Google Earth. The types of groundwater wells present in the area are mostly dug wells, shallow handpumps, and tube wells with an average depth of 45 meters. Each groundwater sample was collected in two separate polypropylene bottles (Polylab), for the analysis of major anions and cations. The EC and pH were recorded at the field with the help of handheld EC and pH meters (Wasser Professional EC-TDS and HM Digital pH-80, respectively). The EC and pH meters were calibrated before taking them to the field with the help of standard buffer solutions of pH 7.01 (Hanna HI 70007) and TDS 1000 ppm NaCl solution (Hanna). The samplings were carried out during April–June and October–December months in the year 2018. The GPS latitude and longitude of sampling sites were recorded using mobile GPS during sampling for spatial reference records and creating a database for the preparation of spatial distribution maps for various ions. The groundwater samples were brought to the laboratory within 3 h of sampling and refrigerated at 3 °C until the completion of chemical analysis.

17.3.2 Physicochemical Analysis

The groundwater samples were analyzed in the laboratory of Civil and Environmental Engineering at G.D. Goenka University in Gurugram, Haryana. The processes and instruments suggested by the Bureau of Indian Standards (2012) (BIS, IS 10500), WHO (2017) and APHA (1992) were used for performing the chemical analysis of calcium (Ca^{2+}), magnesium (Mg^{2+}), total alkalinity (TA), chloride (Cl^-), and sulfate (SO_4^{2-}).

The carbonate (CO_3^{2-}) and bicarbonate (HCO_3^-) or total alkalinity for each sample was analyzed with the help of titrimetric methods, using standard H_2SO_4 (0.02 N) solution with indicators, phenolphthalein for CO_3^{2-} , and methyl orange for HCO_3^- .

For determining the total hardness (TH), samples were titrated with the ethylene diamine tetra acidic acid (EDT Eriochrome Black T) as an indicator. For calcium concentrations, the buffer solution of diethylamine and SBT (Solochrome Black T) was used as an indicator. The concentration of Mg^{2+} is calculated by subtracting the concentration of Ca^{2+} from total hardness.

Chloride (Cl^-) concentration was calculated using the argentometric titration method, in which the samples were titrated with 0.0141 N silver nitrate (AgNO_3) standard solution with potassium dichromate ($\text{K}_2\text{Cr}_2\text{O}_7$) as an indicator.

The concentrations of Na^+ and K^+ were measured with the help of a flame photometer. Sulfate (SO_4^{2-}) concentrations were determined using the digital spectrophotometer, the samples were prepared using the conditioning reagent (glycerol + HCL+ isopropyl alcohol) and barium chloride (BaCl_2), and a standard curve plot between absorbance and standard concentrations at 442 nm wavelength was prepared. The absorbance of the unknown samples was recorded, and with the help of the standard curve plot, the concentration of sulfates was calculated.

17.3.3 Water Stability Indices

The chemical analysis results were first checked for the ion-balance error, and only 12 samples were found to be within $\pm 15\%$ error and used for this study. The selected samples were further examined for various water stability indices and explained in the following.

Langelier Saturation Index (LSI)

LSI is an indication of instability of water in relation to CaCO_3 for interpreting the corrosive or incrusting ability. This is calculated by the difference between the measured pH and the calculated pH (pH_s) (Subba Rao 2016).

$$\text{LSI} = \text{pH} - \text{pH}_s \dots \quad (17.1)$$

where pH = saturation or calculated pH at which water is in equilibrium with solid CaCO_3 , without changing the total alkalinity and calcium content of the water.

pH_s is the difference among the TDS, water temperature, and the total hardness and alkalinity.

$$\text{pH}_s = 9.3 + (\text{A} + \text{B}) - (\text{C} + \text{D}) \dots \quad (17.2)$$

where

- A factor of TDS;
- B factor of water temperature;
- C CaCO_3 content in mg/L or two-thirds of the TH (mg/L); and
- D methyl orange alkalinity expressed as CaCO_3 (mg/L).

A value of LSI near zero is an indication of chemical balance in the water, while a positive value shows a tendency to deposit CaCO_3 and a negative value indicates a tendency to dissolve CaCO_3 (Tables 17.2 and 17.3).

Ryznar Stability Index (RSI)

RSI was calculated for assessing the scaling or corrosive tendencies of water, and with LSI, it gives the accurate prediction (Table 17.4; Subba Rao 2016) and it is calculated using the following formula:

Table 17.2 Carrier index for Langelier saturation index (LSI)

Sl. no.	Langelier saturation index (Carrier)	Indication
1.	$-2.0 < -0.5$	Highly corrosive
2.	$-0.5 < 0.0$	Slightly corrosive but nonscale forming
3.	$= 0.0$	Balanced but pitting corrosion possible
4.	$0.0 < 0.5$	Slightly scale forming but corrosive
5.	$0.5 < 2$	Only scale forming but noncorrosive

Table 17.3 Water stability indices

Index	Index value	Water condition
Langelier saturation index (LSI)	LSI > 0	Supersaturated and tend to precipitate CaCO ₃
	LSI = 0	Saturated with equilibrium CaCO ₃
	LSI < 0	Undersaturated and tend to dissolve solid CaCO ₃

Table 17.4 Carrier index for Ryznar stability index

Sl. no.	Ryznar index	Indication (Carrier 1965)	
1.	4.0–5.0	Heavy scale	Supersaturated, tend to precipitate CaCO ₃
2.	5.0–6.0	Light scale	
3.	6.0–7.0	Light scale or corrosion	Saturated, CaCO ₃ is in equilibrium
4.	7.0–7.5	Corrosion significant	Undersaturated, tend to dissolve solid CaCO ₃
5.	7.5–9.0	Heavy corrosion	
6.	> 9.0	Corrosion intolerable	

$$RSI = 2pH_s - pH$$

Puckorius Scaling Index (PSI)

PSI is also one of the corrosive indices developed for predicting CaCO₃ scaling, especially in the cooling tower systems. It is also known as practical scale index and calculated based on the total alkalinity (TA) value, and the difference between pH (pH_s) of saturation of CaCO₃ and the equilibrium pH (pH_{eq}) as

$$PSI = 2pH_s - pH_{eq}$$

The equilibrium pH (pH_{eq}) was a result of a detailed study of actual case histories by Puckorius and Brooke; afterward, they developed a mathematical formula for calculating the equilibrium pH (pH_e) and the formula used is

$$pH_{eq} = 1.485 \log TA + 4.54$$

where TA = total alkalinity as CaCO₃.

Puckorius scaling index (PSI)	PSI < 6	Scaling is unlikely to occur
	PSI > 7	Likely to dissolve scale

Aggressive Index (AI)

For the corrosive nature of water, AI can be calculated by using the following formula:

$$AI = pH + \log (AH)$$

where

A total alkalinity, mg/L as CaCO₃;

B calcium hardness, mg/L as CaCO₃.

Aggressive index (AI)	AI > 12	Nonaggressive
	10 < AI < 12	Moderately aggressive
	AI < 10	Highly aggressive

17.4 Results and Discussion**17.4.1 Water Quality Assessment**

The major ions of groundwater of Mewat were analyzed and correlated with various permissibility standards provided by the BIS 2012 and WHO 2017. The pH of groundwater is the area ranging from 7.6 to 9.2, while EC was found to be higher than the permissible limits and varies from 353 to 10,181 μS/cm, and the EC of 45% of the samples was found to be exceeding 5 times the permissible limits (Table 17.5).

The other parameters such as Na⁺ and K⁺ are found to be in a range of 48–3492 ppm and 1–86 ppm, respectively. The Ca²⁺ values were ranging from 40 to 800 ppm, and Mg²⁺ was in the range of 30–750 ppm. Other ions like Cl⁻ and SO₄²⁻ were in the range of 20–5233 and 487 to 887 ppm, respectively (Fig. 17.2).

17.4.2 Hydrochemical Facies

The water type of all the groundwater samples was evaluated based on the major ion analysis. It was found that the water type of the area is highly variable in terms of facies and suggests diverse rock–water interactions. The major ions of the groundwater samples are plotted in Piper trilinear diagram, and it was found that the majority of the samples belong to Mg-Cl hydrochemical facies (Fig. 17.3).

Table 17.5 The mean, median, and mode of the physicochemical parameters of the groundwater in Mewat district, Haryana

Parameters major ions	Min	Max	Mean	Median	Mode	Std. deviation	WHO (2011)	BIS (2012) IS: 10500	
								Desirable	Permissible
pH	7.60	9.20	8.40	8.40	8.20	0.45	7.0–8.5	6.5–8.5	–
EC ($\mu\text{S}/\text{cm}$)	353.18	10181.75	4370.16	3642.45	–	3498.87	750	750	–
Na ⁺	48	3492	453	122	49	976.60	200	–	–
K ⁺	1.00	86.00	35.92	32.50	–	30.65	–	–	–
Ca ²⁺	40.00	800.00	347.50	270.00	500.00	236.57	75	75	200
Mg ²⁺	30.00	750.00	185.83	120.00	200.00	195.28	30	30	100
Cl ⁻	20.00	5233.00	1193.58	598.00	598.00	1680.03	250	250	1000
HCO ₃ ⁻	40.00	120.00	63.33	60.00	60.00	26.05	200	200	600
SO ₄ ²⁻	487.00	887.00	573.67	516.50	520.00	138.56	200	200	400

Note: All major ions in the table are in mg/L, and pH has no unit

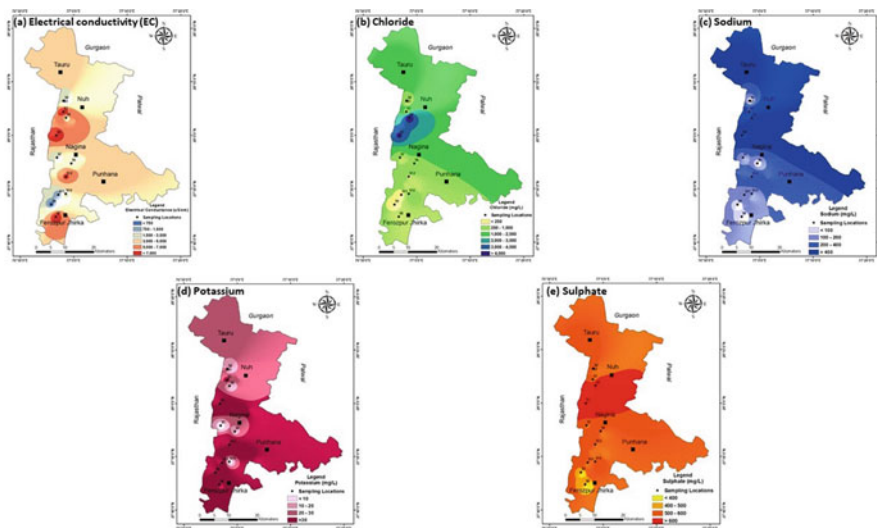


Fig. 17.2 Spatial distribution maps of various groundwater parameters in Mewat district of Haryana, India based on Table 17.5. (a) Electrical conductivity, (b) chloride, (c) sodium, (d) potassium, and (e) sulfate

17.4.3 Corrosion Indices

In the present study, various corrosion indices such as LSI, PSI, RSI, and AI were evaluated for groundwater portability (Table 17.6). In this regard, various corrosion indices such as Langelier Saturation Index (LSI), Puckorius Scaling Index (PSI), Ryznar Scaling Index (RSI), and Aggressive Index (AI) were evaluated for corrosion potential of groundwater in the Mewat area. LSI values suggest that the water is slightly noncorrosive and corrosive to intensely corrosive to RSI (Fig. 17.4), whereas the AI values indicate the nonaggressive nature of water.

17.5 Conclusion

The high salinity of groundwater in the area seems to be affecting the life of inhabitants in the Mewat district of Haryana. Thus, this study was conducted to evaluate the saline aquifers, and it was observed that the groundwater is highly saline in general, but a few pockets of freshwater zones in these aquifers also exist. The major ions of the groundwater samples suggest the dominance of Mg-Cl hydrochemical facies. In this study, various corrosion indices such as LSI, PSI, RSI, and AI for corrosion potential of water were evaluated for potability. This study suggests that the LSI values of water are slightly noncorrosive and corrosive to intensely corrosive to RSI. Further, the AI values of all samples indicate the

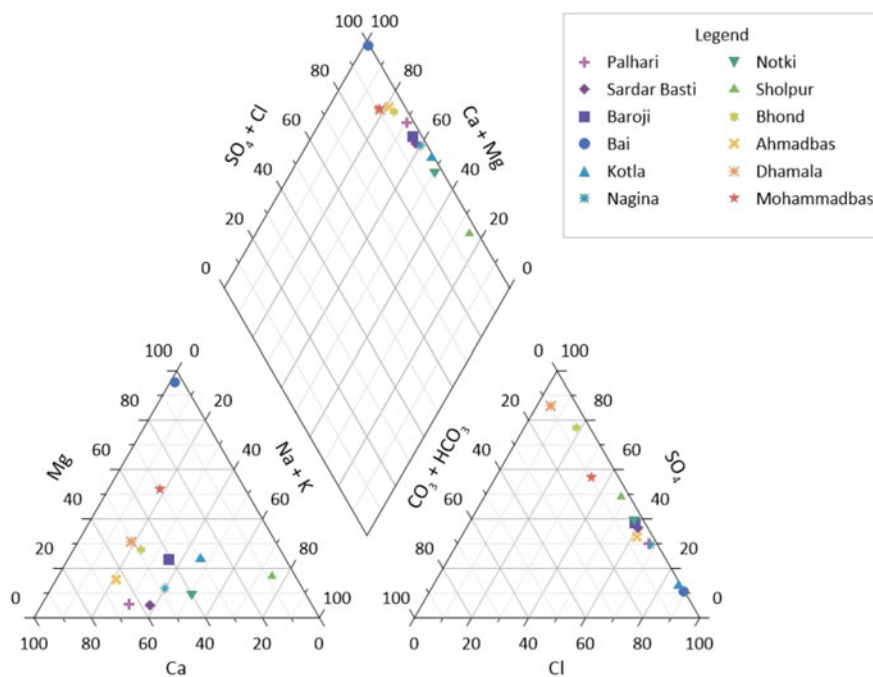


Fig. 17.3 Piper trilinear diagram showing the hydrochemical facies of groundwater. Majority of the samples belong to Mg-Cl hydrochemical facies

Table 17.6 Corrosion potential of groundwater in the Mewat district of Haryana

Sample code	Location name	LSI +ve = scale -ve = no scale	PSI >6 = no scale <6 = scale	RSI >6 = no scale <6 = scale	AI >12 = not aggressive <12 = aggressive
S1	Palhari	0.65	7.09	6.60	12.63
S2	Sardar Basti	0.88	6.99	6.40	12.82
S3	Baroji	-0.54	6.19	8.70	11.99
S4	Bai	-0.50	5.27	9.00	11.72
S5	Kotla	0.50	6.36	7.20	13.09
S6	Nagina	1.10	5.96	7.00	13.38
S7	Notki	1.30	6.89	6.10	13.42
S8	Sholpur	-0.49	4.67	9.60	12.62
S9	Bhond	1.10	6.07	6.60	12.74
S10	Ahmadb	1.30	7.97	5.90	13.36
S11	Dhamala	1.30	7.09	6.10	13.06
S12	Mohammadbas	0.43	7.16	7.50	12.82

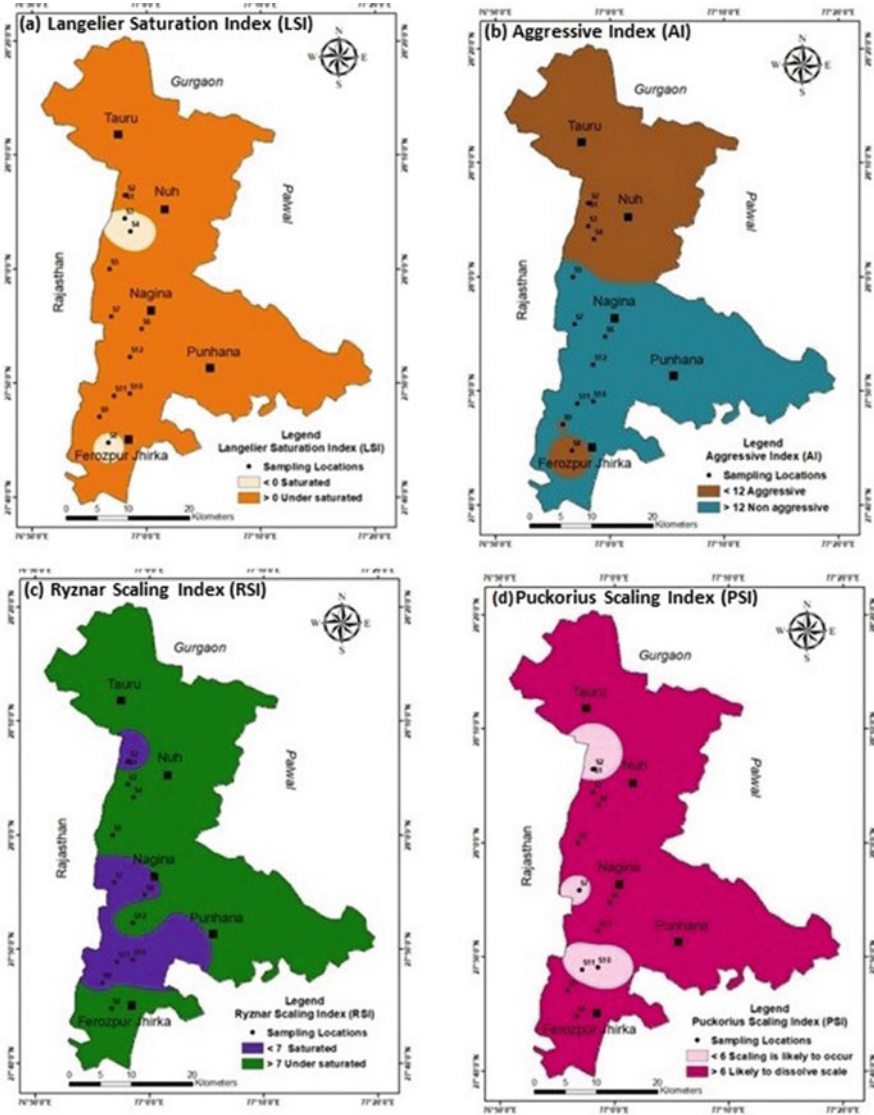


Fig. 17.4 Contour maps showing corrosion potential of groundwater in the Mewat district of Haryana based on Table 17.6

nonaggressive nature of water. This study is helpful for the portability of the groundwater in the area. It is recommended that the rejuvenation of extinct water bodies and canal systems should be revitalized for effective recharge of groundwater in the Mewat district of Haryana. Construction of canal systems in the area may improve groundwater quality and further help in improving the irrigation practices.

References

- Ali S, Thakur SK, Sarkar A, Shekhar S (2016) Worldwide contamination of water by fluoride. *Environ Chem Lett* 14:291–315. <https://doi.org/10.1007/s10311-016-0563-5>
- Ali S, Shekhar S, Bhattacharya P, Verma G, Gurav T, Chandrashekhar AK (2018) Elevated fluoride in groundwater of Siwani block, Western Haryana, India: a potential concern for sustainable water supplies for drinking and irrigation. *Groundw Sustain Dev* 7:410–420. <https://doi.org/10.1016/j.gsd.2018.05.008>
- APHA (1992) Standard methods for the examination of water and wastewater, 18th edn. American Public Health Association (APHA), Washington DC
- Bureau of Indian Standards (2012) Drinking water specification (IS 10500), Indian Standard. <https://www.niti.gov.in/writereaddata/files/tenders/tenderwatercolor-new.pdf>
- CGWB (2012) Ground Water Year Book - India. <http://cgwb.gov.in/documents/Ground%20Water%20Year%20Book%20-%20202011-12.pdf>
- District Census Book, Mewat (2011) Directorate of Census Operations, Haryana. http://censusindia.gov.in/2011census/dchb/0619_PART_B_DCHB_MEWAT.pdf
- District Disaster Management Plan, Mewat (2016–2017) Haryana Institute of Public Administration, department of revenue and disaster management, Government of Haryana <http://www.cdmhipa.in/admin/admin2/plans/upload/Final%20DDMP%20Mewat%202016-17.pdf>
- Ground Water information booklet, Mewat district (2012) Central ground water board, Ministry of water resources, Government of India, North-Western India, Chandigarh. http://cgwb.gov.in/District_Profile/Haryana/Mewat.pdf
- Nagaraju A, Kumar KS, Thejaswi A (2014) Assessment of groundwater quality for irrigation: a case study from Bandalamottu lead mining area, Guntur District, Andhra Pradesh, South India. *Appl Water Sci* 4:385–396. <https://doi.org/10.1007/s13201-014-0154-1>
- Rodell M, Velicogna I, Famiglietti JS (2009) Satellite-based estimates of groundwater depletion in India. *Nature* 460(7258):999–1002
- Saha D, Shekhar S, Ali S, Vittala SS, Raju NJ (2016) Recent hydrogeological research in India. *Proc Indian Natl Sci Acad* 82:787–803. <https://doi.org/10.16943/ptinsa/2016/48485>
- Saha D, Shekhar S, Ali S, Elango L, Vittala S (2020) Recent scientific perspectives on the Indian hydrogeology. *Proc Indian NatSci Acad* 86(1):459–478. <https://doi.org/10.16943/ptinsa/2020/49790>
- Singh A (2017) Managing the environmental problems of irrigated agriculture through the appraisal of groundwater recharge. *Ecol Indic* 92:388. <https://doi.org/10.1016/j.ecolind.2017.11.065>
- Singh AK, Kumar SR (2014) Quality assessment of groundwater for drinking and irrigation use in the semi-urban area of Tripura, India. *Eco Env Cons* 21(1):97–108. (2015) Copyright@ EM International ISSN 0971–765X
- Subba Rao N (2016) Hydrogeology: problems with solutions, 1st edn. PHI, Delhi. isbn:978-81-203-5278-0
- World Health Organization (2017) Guidelines for drinking-water quality, 4th ed. World Health Organization, Geneva. isbn: 9789241548151. <https://apps.who.int/iris/bitstream/handle/10665/254637/9789241549950-eng.pdf?sequence=1>

Chapter 18

Threats to Quality in the Coasts of the Black Sea: Heavy Metal Pollution of Seawater, Sediment, Macro-Algae and Seagrass



Levent Bat , Elif Arici , and Aysah Öztekin 

Abstract Marine zones are facing threats due to ever increasing levels of contaminants that affect an organism's functions and ecological services. In particular, heavy metal pollution is a global issue of public health concern due to bio-magnification effects in marine ecosystems. Macro-algae constitute the basis of the marine food chain. The Black Sea is Turkey's most productive seas. Most of the fishing is done in this sea. Unfortunately, it has undergone significant radical changes in the last few decades. The Black Sea is a natural semi-closed water basin situated among Europe and Asia. The Black Sea which is almost isolated from the Atlantic Ocean has a connection to the Mediterranean by the Turkish Straits System. It goes to the Sea of Marmara and from there to the Aegean Sea through the Dardanelles. Due to this complicated natural system, the renewal of seawater in the Black Sea is desperately tardy. Turkey, Bulgaria, Romania, Russia, Ukraine and Georgia located on the Black Sea coast. Ukraine is the longest coast in the Black Sea countries are followed by Turkey. The population of the coastal regions of these countries is nearly 20 million. Although the Black Sea is mostly affected by the human activities of these countries, it is also affected by the wastes of seventeen countries through the large rivers spilling into the sea. The Danube, Dnieper, Don, Dniester, Kuban, Rioni, Kamchia, Kızılırmak, Yeşilirmak and Sakarya rivers are among the biggest rivers flowing into the Black Sea. Contaminants reach the Black Sea through these major rivers and one of the most critical of these is heavy metals. When heavy metals reach the sea, they either dissolve in water, adhere to suspended particles, settle down to the bottom and bind to organic substances or are taken up by living organisms. However, they eventually accumulate at the bottom and benthic organisms are directly exposed to heavy metals. Although mobile organisms have a chance to escape from contaminated areas, sessile organisms do not have this possibility. Especially algae are the most affected organisms. Accumulation of

L. Bat (✉) · A. Öztekin

Department of Hydrobiology, Fisheries Faculty, University of Sinop, Sinop, Turkey

E. Arici

Vocational School of Health Services, University of Sinop, Sinop, Turkey

© Springer Nature Switzerland AG 2021

P. K. Shit et al. (eds.), *Spatial Modeling and Assessment of Environmental Contaminants*, Environmental Challenges and Solutions,

https://doi.org/10.1007/978-3-030-63422-3_18

289

elements in macro-algae is considered as notable risk in Asian countries for many years with official settings. In Europe, a specific regulation for edible seaweeds was established in 1990, but still lacks approved protocols. The European Parliament issued in the area of Marine Environment Policy Marine Strategy Framework Directive (MSFD), sea environmental standard, the nearshore and offshore systems, has been build up to save and re-establish. MSFD is predicated on the policy of ecosystem-based management considers all oppressions of the seas and attempts to the sea regionally. The objective of the MSFD is to maintain Good Environmental Status (GES) by 2020, and seagrasses are used as bio-indicators to assess ecosystem quality in GES. In Turkey, there is no legislative regulation for macro-algae, but seaweeds are proposed as biological quality elements under EU-MSFD. By the reasons of macro-algae have a sedentary lifestyle, accumulate heavy metals in their bodies, have enough tissue for metal measurement, are common on the coast, are easy to collect from the field and, have the ability to accumulate metals from sediment and water column, are used as biological indicator species in bio-monitoring studies. Bio-monitoring of the levels of heavy metal contamination in macro-algae is important to assess and control the environment. Metal contents in macro-algae vary between species and locations. This review compares the accumulation of metals in seawater and sediments, metal uptake capacities of macro-algae divisions and seagrass and sets up a data base for the Black Sea coasts.

Keywords Black Sea · Heavy metals · Accumulation · Toxic · Seawater · Sediment · Algae · Seagrass

18.1 Introduction

Marine pollution is defined as the introduction of impurities into the sea, and includes the dumping of domestic, agricultural, industrial and chemical wastes, oil spills from ships and discharges from mining. The results of marine pollution range from short-term economic losses due to the unsightly fouling of beaches by litter, oil spills and other floatable substances to less visible but longer-term effects on the whole ecosystem. Marine coasts have been considered as the most altered areas because of different anthropogenic repression forms, which contain domestic wastes, sewage or municipal discharge, terrestrial runoff, fisheries and touristic activities. Millions of tons of toxic waste are dumped into the Black Sea annually. It is clear that the compounds of this and other sources of contamination are inducing the sea to become loaded beyond their capacity to cleanse themselves of these toxic materials. This issue may eventually have large-scale ecological and economic problems. In this context, the dumping of wastes into the sea has become an important topic. The Black Sea dumping can be addressed in a total system framework that includes contaminant fate, its ecological effects and economic impacts, and resulting governmental policy actions. In this context, an important issue is to ensure that the amounts of toxic substances accumulated in biota remain below the level that causes unacceptable ecological or economic consequences. The fast

development of coastal locations in the Black Sea coasts, together with a lack of funds for right urban progress is also very important issue which should be solved (Bakan and Büyükgüngör 2000; Altaş and Büyükgüngör 2007; Bakan and Böke Özkoç 2007; Bat et al. 2009). It has proven difficult to apply to specific problems because of the lack of data on contaminants in coasts of the Black Sea, difficulty in measuring concentration levels and the unsolved problem of estimating the cumulative effects of multiple contaminants.

There is increasing interest in general over the determining levels of contaminants in the marine coastal component, and their results on the environment. Macro-algae and seagrass species act as useful bio-indicators as they have no mobility and are unable to avoid contaminants and also their abundance and distribution can reflect the health of the marine coastal environment. In addition, easy sampling of macro-algae and seagrass makes them the suitable species in pollution studies. Therefore, they are used extensively in bio-monitoring studies. This review will provide insights in lighting the distribution heavy metals in macro-alga and seagrass in a stressful coastal environment of the Black Sea.

18.2 Brief General Features of the Black Sea

Tons of water is poured into the Black Sea through many rivers and it takes more freshwater than it loses from evaporation, so the mean salinity is very low (17‰). The less salty waters of the Black Sea flow from the Marmara Sea to the Aegean Sea and the salty waters of the Mediterranean Sea pass deeper into the Black Sea in the same way but the volume is roughly twice smaller. These two different concentrations of water are very difficult to mix with each other, and dense water will sink to the bottom. Waters with a depth of approximately one hundred metres from the surface have less salinity. The replacement of the Black Sea deep waters with new seawater from the Mediterranean for hundreds of years. This very slow rate of replacement and the great input of freshwater of the Black Sea have caused to stratification. This situation does not supply sufficient oxygen for the decomposition process and the bacteria in the lower layers use it completely. That is why the Black Sea is nearly lifeless under a depth of around 155 m. In addition, the metabolism of some bacteria produces H_2SO_4 which is a soluble toxic gas. This express that 87% of its volume is almost lacking of marine life (Zaitsev and Mamaev 1997; Zaitsev 2008), except for some forms of bacteria and meiobenthos (Ürkmez et al. 2014, 2015, 2016). Consequently, the Black Sea is the biggest natural anoxic water form in the world, but, the Black Sea is even now in proportion to rich in living resources (Zaitsev and Mamaev 1997; Zaitsev 2008).

The Black Sea is also linked to the Sea of Azov by the Strait of Kerch from the north. Major cities along the coast are Batumi, Burgas, Constanta, İstanbul, Novorossiysk, Odessa, Samsun, Sevastopol, Sochi, Trabzon and Varna. The Black Sea is bordered by Turkey, Bulgaria, Romania, Russia, Ukraine and Georgia. Environmental problems and the protection of the Black Sea are of major issues for the coastal ecosystem (Bat et al. 2018). Figure 18.1 shows the Black Sea

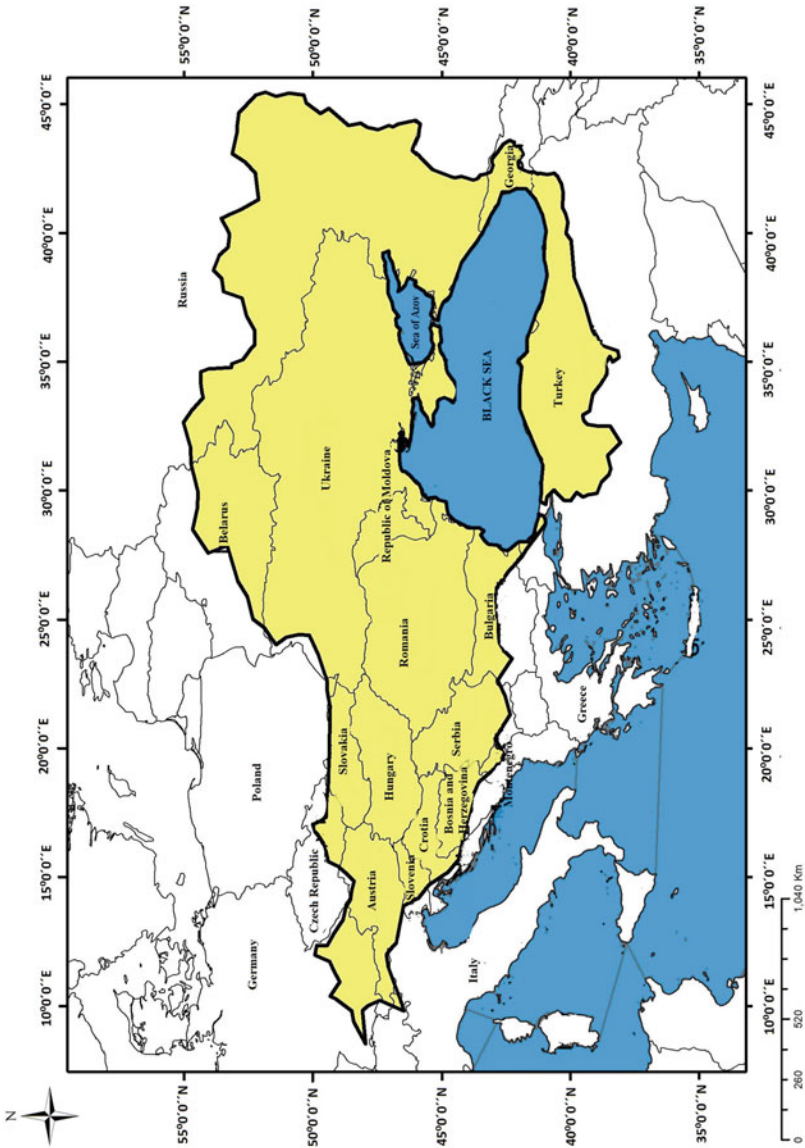


Fig. 18.1 The Black Sea basin (from Bat et al. 2018)

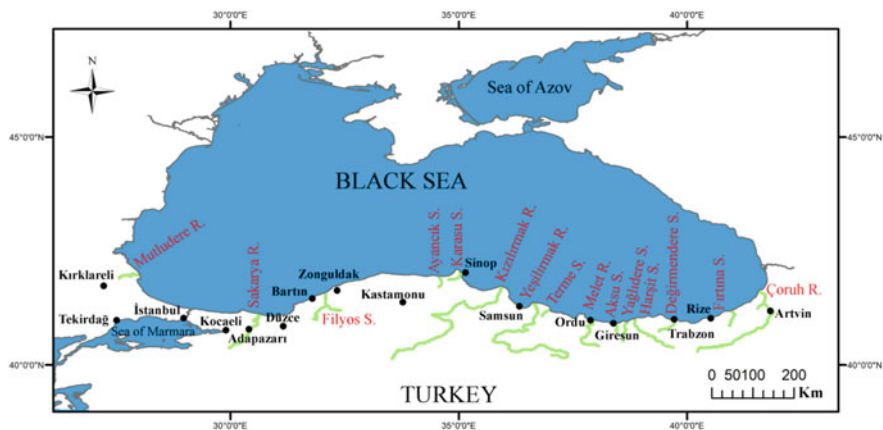


Fig. 18.2 The Black Sea coastal towns and major rivers (from Bat et al. 2018)

catchment under countless contaminants. The major rivers and locations in the Black Sea coasts of Turkey were also demonstrated in Fig. 18.2.

18.3 Pollution Problems in the Black Sea

The most notable course leading to deterioration of the Black Sea in terms of pollution is related has been the huge over-fertilization by nitrogen and phosphorus compounds, occurring mostly from industrial, agricultural and domestic sources. This situation named as eutrophication has altered the whole Black Sea ecosystem. The contaminants get the Black Sea from sources in the seventeen countries in its cleaning out area, mostly via the Danube River (Mee 1992). Other important problems can be listed as follows.

Oil compounds get in the Black Sea as a consequence of operational discharges of ships and accidents, and owing to land-derived sources. Radioactive contents have been entered the sea in trace amounts from nuclear power generation and after the Chernobyl accident in 1986. Solid wastes and litter are dumped into the Black Sea from vessels and coastal cities (Öztekin and Bat 2017a; Bat et al. 2017a; Öztekin et al. 2020). One of the today's biggest problems is plastics for the sea (Öztekin and Bat 2017b). Contamination sources and contaminants of the Black Sea have been discussed in many new reviews (Bat 2014, 2017; Bat et al. 2018). Furthermore, many non-native species entered the Black Sea via the ballast waters of the ships and changed the ecosystem. Some of these species have increased rapidly, being predators to the native species thus collapsing the Black Sea environment (Finenko et al. 2003; Svetlichny et al. 2004; Anninsky et al. 2005; Finenko et al. 2006).

The most important contaminants that threaten the Black Sea are heavy metals. Their presence in marine environments, their long stay intact and their widespread

use have made heavy metals important. Because it can accumulate in every element of the marine ecosystem and through food it can harm human health and even cause death.

18.4 Importance of Heavy Metals

Among the most important contaminants in marine systems are heavy metals. Although heavy metals are in traces in the marine environment, their natural levels and accumulations in the organism are different. The term heavy metal includes all metals and metalloids in nature. It has been found that heavy metals are present in natural waters in forms absorbed into free ions, inorganic or organic compounds and particulate matter. Even if they are collapsed or absorbed in the sediment, they can be converted back into ionic form by some physical and chemical events and show their toxic effects. These metals are of great importance in the marine ecosystem as they cause environmental pollution and have a toxic effect on marine organisms and human via consumption even at very low concentrations. Some of the heavy metals, e.g. iron, zinc, copper, manganese are essential at low amounts, but they are toxic at high amounts for living organisms. Other heavy metals, e.g. mercury, lead and cadmium show toxic effects, even at very trace amounts are present. Toxic metals accumulate in internal organs and cause various diseases such digestive system disorders, nervous diseases and cancer and, even deaths. Thus, it is very important to determine the amount of heavy metals in water, sediment and biota in marine ecosystem.

The determination of heavy metal levels in water, sediment and indicator species has been carried out for years in order to reveal the existing heavy metal pollution in marine environments. However, since the levels of heavy metals in the waters are very low, their determination is not only economical but also difficult. When the metals reach the sea, they eventually sink into sediment and accumulate there. Benthic species are exposed to these metals in sediment.

Researchers determine the amount of heavy metals in the consumed seafood and evaluate how they have negative effects on the people who consume them (Bat and Arıcı 2018). However, especially seagrass and macro-algae are frequently used in heavy metal studies. Since macro algae and sea-grasses are sessile organisms, they cannot escape contaminants. These organisms absorb heavy metals from both water and sediment. Many researchers have used these organisms as metal pollution indicator species and are still using them. Heavy metal levels in seagrass and macro-algae vary depending on seasons, localities and species. This review will provide a comparative study of heavy metal studies on water, sediment, macro-algae and seagrass collected from the Black Sea coast.

18.5 Importance of Macro-Algae and Seagrass

Marine plants and animal life of the Black Sea is richest near the coastal area. Sunlight can reach the bottom of the shallow waters, so that marine flora grow up with dissolved minerals and energy of the sunlight. The flora provide food, a haven for breeding and habitats for a variety of animals. The macro-algae and seagrass are found in the Black Sea and play important roles in food web. They generate oxygen through photosynthesis. Herbivores consume these organisms and themselves fall prey to other organisms. The higher link in the food web comprises fish, turtles, birds and mammals. But as this substance utilize the food web, decreasingly is directly consumed as food. The remain is altered back into minerals, somewhat by scavengers and the continuous process of excretion along the chain. Any threat to the macro-algae and seagrass will have considerable knock-on effects through the food web. Contaminants especially heavy metals are readily absorbed with food, but they cannot be destroyed and can only be converted from one chemical compound to another. They tend to build up in water, sediment and living organisms. Some plants can accumulate higher levels of heavy metals from the water and sediment in which they grow.

18.6 Amounts of Metals in Water in the Black Sea Coasts

Since the 1990s heavy metal concentrations in the Black Sea waters have started to be determined. In most of these studies, heavy metal analyses in sea water, sediment and biota especially in macro-algae were determined in coastal pollution monitoring studies. For the purpose of comparison, the heavy metal levels in the Black Sea seawater are given in Table 18.1. The 11 elements were detected in waters of the Black Sea, namely As, Cd, Cr, Co, Fe, Cu, Hg, Mn, Pb, Ni and Zn.

According to the results of the available studies, generally Hg was found to be least followed by non-essential metals Cd, As and Pb. As can be understood from the literature, these toxic elements have not been studied sufficiently. These toxic elements are very toxic even at very low levels for marine life. For example, although Hg levels were sometimes found high in polluted coastal areas, the average values were low (Arıcı and Bat 2017). High Cd levels were detected in Romanian coasts of the Black Sea (NIMRD 2011), followed by Trabzon coast of Turkey (Çevik et al. 2008). High Pb levels in seawater were found on the coasts of Hopa, Artvin (Çevik et al. 2008). Sea water samples where heavy metal measurements are taken are mostly surface waters. Since the waters of the Black Sea have a static structure, circulating or regeneration takes quite a long time. It is normal that these heavy metal values are high in enclosed bays or gulfs and where water circulation is low. These high values given in Table 18.1 may be due to the pollutants carried by the Danube on the Romanian coast. Likewise, it may be caused by contaminants transported by many streams to the shores of Trabzon and Artvin. The reason for the

Table 18.1 The metal concentrations in waters of the Black Sea

Station	unit	As	Cd	Cr	Co	Cu	Fe	Hg	Mn	Ni	Pb	Zn	References
Black Sea	µg/L	0.01–2.8				0.1–86	0.8–32					0.6–14	Andreev and Simeonov (1990)
Artvin	mg/L					ND-2.9	ND-0.28						Ataç et al. (1997)
Artvin	ppm					ND-0.1	0.05–0.72					ND-0.02	Ataç et al. (1997)
Rize	ppm					ND-0.02	0.06–0.79					ND-0.03	Ataç et al. (1997)
Trabzon	mg/L					0.03–3.46	0.01–0.47						Ataç et al. (1997)
Trabzon	ppm					ND-0.02	0.05–0.73					ND-0.03	Ataç et al. (1997)
Giresun	ppm					ND	0.04–0.78					ND-0.03	Ataç et al. (1997)
Ordu	ppm					ND	0.04–0.72					ND	Ataç et al. (1997)
Samsun	mg/L					0.01–3.61	0.01–3.4						Ataç et al. (1997)
Kastamonu	mg/L					0.01–0.52	0.02–0.85						Ataç et al. (1997)
Zonguldak	mg/L					ND-0.04	ND-1.4						Ataç et al. (1997)
Bolu	mg/L					0.01–0.03	0.03–0.7						Ataç et al. (1997)
Sakarya	mg/L					ND-0.04	0.02–1.34						Ataç et al. (1997)

Kocaeli	mg/L								0.01–0.06							Ataç et al. (1997)
Istanbul	mg/L								ND-0.24							Ataç et al. (1997)
Sakarya	ng/L									2.40						Ünsal et al. (1998)
Bartın	ng/L									1.40						Ünsal et al. (1998)
Istanbul	ng/L									<ng/L						Ünsal et al. (1998)
Black Sea-Aegean Sea	nM	0.36–13.7									nd-29.1					Zeri et al. (2000)
Black Sea	nM	0.003–0.161			0.003–1.80				0.79–7		0.69–29	0.018–17.5	0.010–1.4	0.135–8.33		Tankere et al. (2001)
Ukraine	µg/L	<1–2.2							<50	<0.01–0.012			<1–9.3	0.5–11.3		BSC (2008)
Trabzon	µg/L								680.00				ND	6.50		Çevik et al. (2008)
Rize	µg/L								130–290				ND-29	12–207.5		Çevik et al. (2008)
Artvin	µg/L								340.00				ND	81.50		Çevik et al. (2008)
Romania	µg/L												12.49–27.13	4.75–12.10		Oros (2008)
Zonguldak	ppb												1.12–39.34	5.19–8.02	11.35–54.22	Çoban et al. (2009)
Black Sea	ng/L								0.83–1780				0.09–7600	5.3–350	1.7–910	Yığırhan et al. (2011)
Romania	µg/L													0.35–9.24	0.13–15.91	NIMRD (2011)

(continued)

Table 18.1 (continued)

Station	unit	As	Cd	Cr	Co	Cu	Fe	Hg	Mn	Ni	Pb	Zn	References
Romania	µg/L		0.41– 2.72	0.67– 2.19		3.06–20.26				2.50– 2.70	4.03– 8.05		Jitar et al. (2015)
Romania-Turkey-Bulgaria	µg/L		0.20 (0.05– 0.76)	2.54 (1.14–6.06)		0.65 (0.10–2.99)				0.14– 12.38	1.16–3.70		Oros et al. (2016)
Sinop	ppb	1.50– 1.82	0.32– 0.64		1.31–2.14	1.39–17.56	151.19– 1557.78	0.03– 0.27	7.33– 64.76	3.22– 6.84	1.23– 6.61	181.20– 508.71	Arci and Bat (2017)
Sinop	µg/L		0.28			1.43		0.04			1.28	174	Bat et al. (2019)
Romania	µg/L		0.551– 0.568			11.24 ± 0.93					12.78– 12.93	20.12– 21.17	Cadar et al. (2019)

relatively high amounts of some heavy metals reported in the sea waters along the coasts of Sinop (Table 18.1) may be partly due to the effect of the dominant winds, locally called “karayel” and “gündogusu”. As these winds are harsh and increase the flow of surface water, contaminants can reach the coastal areas from far away. The lack of industry in the Sinop region supports this conclusion (Bat et al. 2018). Differentiations in metal concentrations in seawaters found in different studies (Table 18.1) in the same areas can be explained by different measurement methods, differences in sensitivity of instruments and differences in sampling times or seasons.

18.7 Amounts of Metals in Sediment in the Black Sea Coasts

In the Black Sea contaminants from rivers were carried into surrounding coastal waters in dissolved and suspended form and in sediment even in the biota. Heavy metals tend to attach to particles suspended in the water column, which then settle to the sea bottom. The average sedimentation rate in the Black Sea is 30 cm per 1000 years (Kocataş, 2005). Metals attached to organic material and silt, thus it is very important to determine the amount of metal in the sediments. Heavy metal levels in surface sediments can also give data information on the metal intakes at that region (Bat et al. 2015a). The detection of heavy metal content in sediments of the Black Sea coast has been carried out for more than 30 years. Table 18.2 shows the achievable studies of heavy metal contamination in sediments of the Black Sea coasts. When the comparison of the results of the studies in the Black Sea sediments is examined, there are large differences. The existence of different results in the Black Sea ecosystem with such stagnant and slow sedimentation complicates the interpretation, therefore, main conclusions cannot be drawn because of the complex nature of the local environment conditions.

Maximum Cu, Cd and Pb levels were found in south-eastern part of the Black Sea (Ünsal et al. 1998). Similarly, high Mn, Fe, Hg and Cr levels were determined from large rivers such as Kızılırmak and Yeşilirmak (Ünsal et al. 1995; Balkıs et al. 2007; Yiğiterhan and Murray 2008). Most metals were found to be minimal on the coast of Sinop Peninsula except Al and As (Karakum) (Bat et al. 2017b), Zn (Tersane) (Arıcı and Bat 2019a).

Balkıs et al. (2007) measured Cd, Cu, Co, Pb, Cr, Ni, Mn, Fe and Zn levels in sediments in the major river mouths of the southern Black Sea (Yeşilirmak, Kızılırmak and Sakarya). Pb and Cd levels were lower than the detection limit (0.01 µg/L) in samples, while Co, Cr, Ni, Mn, Fe and Zn contents were higher than the shale average.

Ergül et al. (2008) determined Cd, Cr, Cu, Co, Mn, Ni, Zn, As, Fe, Sb and Pb levels in sediment on the Turkish Black Sea coasts as seasonal, with bottom sediment samplers and sediment trap. Cd, Mn and Pb levels were found to be maximal in the sediment trap samples except summer, whereas Zn, Fe, Co and Ni concentrations were much lower than surface sediments. However, Cr, Cu, Sb and

Table 18.2 The metal concentrations in sediments of the Black Sea

Station	Al	As	Cd	Cr	Co	Cu	Fe	Hg	Mn	Ni	Pb	Zn	References
Black Sea				13–224	<20	15–87	2000–49,000		112–1064	11–202	12–66	24–138	Yücesoy Eryılmaz and Ergin (1992)
Sinop						0.08–0.42		0.05–0.40			3.06–3.77		Ünsal et al. (1995)
Kızılırmak						12–357		0.86–4			6.22–11.32		Ünsal et al. (1995)
Yeşilirmak						528		0.29–2.02			38.74		Ünsal et al. (1995)
Black Sea				32–171	7–37	29–68	13,000–43,000		355–751	38–130	14–35	50–108	Kıratlı and Ergin (1996)
Black Sea			0.001–19.5			2–8580					5–2920	12–345	Ünsal et al. (1998)
Sinop				218.1									Topçuoğlu et al. (1998)
Black Sea			0.6–0.9	22–122	5.2–17.2	23–75	26,000–49,000		354–902	2.2–69.1	11–30	57–127	Topçuoğlu (2000)
Black Sea											2.9–617.8		Ünsal (2001)
Kırklareli-İğneada			<0.02	74.7	21.45	13.57	29,000		519.1	31.57	<0.05	119.3	Topçuoğlu et al. (2002)
İstanbul-Kilyos			<0.02	10.8	<0.05	4	5000		206.6	13.55	<0.05	33.9	Topçuoğlu et al. (2002)
Amasra			0.73	58.5	8.28	27.6	27,000		338.2	33.5	21.4	92.6	Topçuoğlu et al. (2002)
Sinop			0.89	115.5	13.4	37.3	35,000		424.3	65.2	15.1	91.5	Topçuoğlu et al. (2002)

Ordu-Perşembe		0.93	21.8	16.8	69.9	44,000		514.1	18.5	31.1	82.9	Topçuoğlu et al. (2002)
Rize		<0.02	38.88	36.44	95.5	54,000		870.3	37.26	<0.05	267.4	Topçuoğlu et al. (2002)
Black Sea			51–135	9–19	20–47	19,000–39,000		312–995	34–88	19–51	50–111	Ergin et al. (2003), Ergin (2005)
Rize-Pazar		<0.02			15.5–506.5			414.4–647.5		<0.5–39.2	50.1–484.2	Topçuoğlu et al. (2003a)
Samsun		<0.02	53.05–99.3		32.9–64.85			441.55–668.75	7.9–49.25	12.13–223.7	109.55–261.65	Bakan and Özkoç Böke (2007)
Yeşilirmak		<0.02	370.8–1276.5	33.6–63.7	43.7–59.9	47,000–85,000		864–2915	128.1–129.9	<0.01	119.8–325.3	Balkis et al. (2007)
Kızılırmak		<0.02	231.9–720.6	22.7–27.4	23–27.6	49,000–78,000		989–1206	104.6–120	<0.01	91.4–119.5	Balkis et al. (2007)
Trabzon-Yomra	12.60–13.10	<0.02	70.02–74.24	22.60–23.90	52.03–56.86	5680–6050		651.9–672.8	23.61–26.53	<0.1	169–182	Ergül et al. (2008)
Black Sea-rivers		0.38	135	23	66	47,200		3140		26	146	Yığiterhan and Murray (2008)
Zonguldak		0.13–0.81			21–39					28–50	66–103	Çoban et al. (2009)
Trabzon					13.68–315.99				10.6–29.2	7.8–83.78	47.6–286.3	Özşeker and Erüz (2011)
Black Sea		0.18–0.53	54–147	12.9–28.9	39.8–72.46	33,800–50,100	0.03–0.13	383–763	49.5–140.6	18.13–44.33	82.8–183.9	Özkan and Büyüksık (2012)
Black Sea		0.03–1.04			2.87–407.93		0.47–2.86			2.51–79.78		Sur et al. (2012)
Rize		0.1–1.4			34–279		0.01–0.07			16–33	82–383	Gedik and Boran (2013)
Sakarya		1.4–5.8			5.1–18					5.1–25	43–286	Yalçın et al. (2013)

(continued)

Table 18.2 (continued)

Station	Al	As	Cd	Cr	Co	Cu	Fe	Hg	Mn	Ni	Pb	Zn	References
Trabzon					17.2– 18.9	56.8– 88				20.9– 26.6	35.6– 49.8	106.6– 123.1	Özşeker et al. (2014)
Sinop			0.03– 0.07			6.9– 7.6		0.06– 0.08			5.8– 6.9	15–23	Bat et al. (2015a)
Trakya			0.07– 0.35					bd– 0.06			0.86– 16		Mülayim and Balkis (2015)
Rize			0.2– 0.5			33–67					14–31	78–130	Alkan et al. (2015)
Trabzon			0.2– 2.1			22– 2334					17– 158	50– 1828	Alkan et al. (2015)
Black Sea							12223.5						Engin et al. (2015)
Giresun			0.09– 0.23			11–51					9.6–21		Uncumusaoglu et al. (2016)
Sinop	1780– 8110	4.9– 17.5	0.05– 0.17	22– 254	5.3– 30.9	5.21– 52.42	1240– 5400	<0.01– 0.15	328– 1031	13.1– 34.1	5.08– 27.61	18.6– 66.7	Bat et al. (2017b)
Sinop	400– 5724	0.42– 7.4	0.02– 0.08		0.22– 4.5	0.54–9	613.7– 10,617	0.005– 0.03	12.2– 516	0.33– 18.2	0.19– 39.3	0.79– 21.1	Ancı and Bat (2017)
Sinop	3528.8	4.23	0.05		2.72	4.85	6251.7	0.02	236.4	10.03	2.92	12.8	Ancı et al. (2019)
Sinop			0.006			3.03		0.008			0.28	8.14	Bat et al. (2019)
Sinop	164.0– 1117.7	1.5– 3.56	0.32– 0.64		1.31– 2.14	1.39– 17.56	151.19– 1557.78	0.03– 0.27	7.33– 64.76	3.22– 6.84	1.23– 6.61	181.2– 508.71	Ancı and Bat (2019a)

As levels displayed no specific trend with sediment type. High Cd, Co, Cu, Sb, Zn and Fe amounts in particles were found in winter and it was suggested that raised fossil fuel combustion, which arises over this season in adjacent industrial and urban areas acts a major role in the metal content of falling particles in the coastal area. Ergül et al. (2008) also pointed out that the downward vertical transportation of grain heavy metals in Trabzon coasts was associated with the high amount of the resultant particulate flux dynamics and land erosion.

Yiğiterhan and Murray (2008) were determined Ti, Al, V, Fe, Mn, Cr, Cu, Zn, Co, Ag, Cd, Mo, Pb, U and Ba levels in suspended matter and sediments in the Danube River draining from Europe and from Turkish rivers, namely Kizilirmak, Sakarya, Yesilirmak and Filyos. It was found that the compositions of the surface sediment from Danube River and the particulate matter from Turkish rivers were similar. Both samples had a little higher amount than global mean crust. High levels of Pb, Zn, Cu, Cd, Mn and Ag levels because of anthropogenic contamination indicated the presence of some hot spots on the Danube River. It was stated that the optimum selection for extract the terrigenous part from the Black Sea sediment and particulate samples is the mean of the rivers in Turkey suspended material and Danube River sediment samples (Yiğiterhan and Murray 2008).

Özşeker and Erüz (2011) determined Ni, Cu, Pb and Zn levels in surface sediment of Trabzon coasts which is most populated and industrialized city in the south-eastern of the Black Sea. It was suggested that the evaluation of sediment enrichment factor and pollution load index reveal the existence of the metals which were indicative of contamination in that area.

Gedik and Boran (2013) evaluated metal pollution and ecological risk in the sediments of Rize Harbour and found that six sites were heavily contaminated with Cu.

Özşeker et al. (2014) studied heavy metal contamination in sediment near Trabzon coasts of the south-eastern Black Sea. They found that sediments were influenced by Degirmendere, Yanbolu and Solakli rivers. The maximum metal concentrations were determined in sediment influenced by Solakli and the minimum levels were found in sediment affected by Yanbolu. Sampling region were severely contaminated by Pb, Cu and Zn.

Alkan et al. (2015) evaluated metal pollution in core sediments from south-eastern Black Sea coast and found that Sürmene coasts of Trabzon have been contaminated by mining activities.

Bat et al. (2015a) evaluated metal pollution in sediment from the Sinop coasts of the Black Sea in 2013. The distribution of the metals shows a variable pattern. In terms of metal pollution, the quality of sediment in Sinop coasts was determined by the enrichment factor technique (EF). The lowest EF amounts were between 0–5 in Cu, Zn, Fe, Ni, Pb, Cd, Co and Mn. These results showed no statistically significant differences. Comparatively higher enrichment values were found for As, Cr and Hg levels than other the metals.

Bat et al. (2017b) studied the spatial distribution and transportation of heavy metals in sediments up to a depth of 10 cm along Sinop coasts of the southern Black Sea. The influences of anthropogenic metals contamination in surface sediments of

Sinop coasts were analysed by using I_{geo} . Metal concentrations were importantly correlated each other and represented an important relationship with Fe content, whereas most heavy metals were not enriched. Although some metals were found high levels in some sampling points, the most metal levels at Sinop coasts were lower than the contents pointed out by the sediment quality. It was concluded that the most of metals were not extraordinarily contaminated in surface sediments and did not indicate a significant threat to the local biota.

Bat and Şahin (2019) assessed the current Cd, Pb, Hg, Cu, Fe and Zn levels in surface sediments of Sinop shores of the Black Sea in 2017. Heavy metal levels were compared to the Sediment Quality Criteria and the metal amounts were quite below the levels recommended the sediment quality guideline values (SQGV). Mostly the EF values for heavy metals were less than 1 which indicated no enrichment. However, some EF values were between 1 and 2.21 indicate minor enrichment. These values have not been considered significant. The I_{geo} values showed that surface sediments in Sinop shores of the Black Sea was uncontaminated.

All these studies show that there is no evidence indicating heavy metal pollution in the Black Sea. The fact that the current studies are carried out independently and that both sampling methods and metal analyses are performed with different methods makes it difficult to compare the results. The lack of data will get it unlikely to predict future trends in contamination or to adequately save the Black Sea ecosystem and even public health. This situation requires both serious precautions and close cooperation between all the Black Sea countries. Regular pollution studies, especially in coastal areas, ports, reference zones and river mouths affected by industrial zones, provide better data for decision-makers to protect the ecosystem.

18.8 Concentrations of Metals in Macro-Algae and Seagrass of the Black Sea

The protection of public health and ecosystem is the first precedence in scientific studies of metal pollution in marine biota. Marine organisms, especially algae, have the potential to accumulate heavy metals in their bodies. Data from studies on heavy metal contamination in algae show differences depending on contaminant sources, metals and species. Heavy metal monitoring investigations should be conducted regularly because they play a critical role in metabolism and their low or high levels can equally harm living organisms.

Passive bio-monitoring with macro-algae was firstly introduced in the early 1950s (Phillips and Rainbow 1994) and still have been used widely to determine heavy metal pollution in marine ecosystems (Olivares et al. 2016).

Considering the long period (1992–2019) noted, the number of existing studies on metal amounts in the Black Sea algae is relatively scarce. In this review, 20 species of macro-algae and 2 species of seagrasses were assessed in the Turkish coasts of the Black Sea. The divisions included Chlorophyta (*Chaetomorpha* spp.,

Table 18.3 The taxonomic groups and functional form groups of the seaweed species collected from the Black Sea coasts of Turkish

Taxonomic group	Species	Functional form group
Chlorophyta	<i>Chaetomorpha</i> spp.	Filamentous
	<i>Cladophora sericea</i>	Filamentous
	<i>Ulva flexuosa</i>	Filamentous
	<i>Ulva intestinalis</i>	Sheet
	<i>Ulva lactuca</i>	Sheet
	<i>Ulva linza</i>	Sheet
	<i>Ulva rigida</i>	Sheet
Ochrophyta	<i>Cystoseira barbata</i>	Thick-leathery
	<i>Cystoseira crinita</i>	Thick-leathery
	<i>Ectocarpus</i> spp.	Filamentous
	<i>Padina pavonica</i>	Thick-leathery
	<i>Scytosiphon lomentaria</i>	Sheet
Rhodophyta	<i>Antithamnion cruciatum</i>	Filamentous
	<i>Ceramium virgatum</i>	Filamentous
	<i>Corallina officinalis</i>	Coarsely-branched
	<i>Corallina panizzoi</i>	Coarsely-branched
	<i>Ellisolandia elongata</i>	Coarsely-branched
	<i>Gelidium crinale</i>	Coarsely-branched
	<i>Gelidium spinosum</i>	Coarsely-branched
	<i>Haliptilon virgatum</i>	Coarsely-branched
	<i>Laurencia obtusa</i>	Coarsely-branched
	<i>Phyllophora crispa</i>	Thick-leathery
	<i>Pterocladia capillacea</i>	Coarsely-branched
	<i>Vertebrata fucoides</i>	Filamentous

Cladophora spp., *Ulva* spp.), Ochrophyta (*Cystoseira* spp., *Ectocarpus* spp., *Padina pavonica*, *Scytosiphon lomentaria*) and Rhodophyta (*Antithamnion cruciatum*, *Ceramium* spp., *Corallina* spp., *Ellisolandia elongata*, *Gelidium* spp., *Haliptilon virgatum*, *Laurencia obtusa*, *Phyllophora crispa*, *Porphyra umbilicalis*, *Pterocladia capillacea* and *Vertebrata fucoides*). The taxonomic and functional forms of groups are shown in Table 18.3.

The algal species with the highest number of studies were *Ulvalactuca*, *U. intestinalis* and *U. linza* belong to Chlorophyta; *Padina pavonica* and *Cystoseirabarbata* belong to Ochrophyta; *Ceramium virgatum*, *Corallina officinalis*, *Gelidium crinale*, *Phyllophora crispa*, *Porphyra umbilicalis* belong to Rhodophyta. Bonanno and Orlando-Bonaca (2018) emphasized that it was impossible to claim that a given macro-algae group has a higher capacity for metal accumulation.

Heavy metals levels of the macro-algae from the Turkish Black Sea coast are presented in Tables 18.4, 18.5 and 18.6. Metal concentrations in all studied green, brown and red algae decrease in the order: Fe > Al > Zn > Mn > Ni > Cu > Co > Pb > As > Cr > Cd > Hg,

Table 18.4 Heavy metal content in phylum Chlorophyta along the Turkish Black Sea macro-algae (mg/kg dry wt.)

Species	Station	Al	As	Cd	Cr	Co	Cu	Fe	Hg	Mn	Ni	Pb	Zn	References
<i>Chaetomorpha linum</i>	Sinop			0.03	2.10	0.37	3.40			17.20	12.30	2.10	7.70	Topcuoglu et al. (2003b)
<i>Chaetomorpha</i> spp.	Sinop			0.60–2.10		1.00–3.30	2.20–4.80	751–2328		21–57	1.25–1.30	1.40–5.00	12–25.70	Bat and Arıcı (2016)
<i>Cladophora sericea</i>	Sinop					2.09	2.09	1190.00			1.09	0.01	63.11	Türk Çulha et al. (2010)
<i>Cladophora</i> spp.	Sinop			0.02			4.60	392.00				0.01	34.00	Altuğ et al. (2005)
<i>Cladophora</i> spp.	Sinop			0.09–0.90		0.90–1.80	1.10–3.40	98–328		1.78–8.00	2.20	0.40–0.90	8–37	Bat and Arıcı (2016)
<i>Cladophora</i> spp.	Sinop	2202.08	5.60	1.20		0.74	7.36	1788.46	0.02	31.74	5.18	2.44	291.24	Arıcı and Bat (2017)
<i>Ulva flexuosa</i>	Sinop	1150.53	1.50	0.04		0.73	3.75	1093.78	0.02	246.43	2.90	6.05	67.95	Arıcı and Bat (2017)
<i>Ulva intestinalis</i>	Rize			0.03	1.49	6.63	9.08	2747.00		48.10	3.16	1.01	12.40	Tüzen et al. (2009)
<i>Ulva intestinalis</i>	Trabzon			0.01	2.48	1.56	7.14	343.00		60.60	4.62	0.60	9.50	Tüzen et al. (2009)
<i>Ulva intestinalis</i>	Sinop				2.07	6.25	1.70	585.00		37.60	2.75	0.07	3.64	Tüzen et al. (2009)
<i>Ulva intestinalis</i>	Sinop					0.03–1.83	3.17–7.44	352–1744			2.16–4.00	0.01	0.19–45.4	Türk Çulha et al. (2010)
<i>Ulva intestinalis</i>	Samsun			0.01		0.01	22.73	1505.64			9.91	0.01	24.15	Türk Çulha et al. (2013)
<i>Ulva intestinalis</i>	Ordu			0.01		2.16	9.46	753.18			2.01	0.01	0.01	Türk Çulha et al. (2013)
<i>Ulva intestinalis</i>	Trabzon			0.01		0.01	13.26	1137.30			2.80	0.01	7.89	Türk Çulha et al. (2013)

<i>Ulva intestinalis</i>	Istanbul		0.01		1.73	7.60	1051.94			3.86	0.01	0.01	Türk Çulha et al. (2013)
<i>Ulva intestinalis</i>	Sinop		0.07–2.00		0.70–1.20	2.80–6.20	655–1512	23–67		1.34–3.20	3.60–8.00	13–36	Bat and Arıcı (2016)
<i>Ulva intestinalis</i>	Sinop	1114.6	0.12	2.18	0.48	3.08	1379.24	0.02	37.36	3.16	1.18	78.46	Arıcı and Bat (2017)
<i>Ulva lactuca</i>	Istanbul		0.50		0.65–0.90	5.90–24.1	147.30–501.5	12.80–49.7		3.85–8.1	0.10–23.50	24.10–35.20	Topçuoğlu et al. (2001)
<i>Ulva lactuca</i>	Istanbul		0.02		0.05	3.87–13.8	550–778	21.80–45.1		0.10–9.70	0.10	9.60–21.2	Topçuoğlu et al. (2003b)
<i>Ulva lactuca</i>	Sinop		0.02		0.05	7.70–11.3		12.50–41.1		0.10–9.00	0.10	13.5–394.40	Topçuoğlu et al. (2003b)
<i>Ulva lactuca</i>	Rize		0.01		2.91	9.52	425.00	17.20	2.16	1.35	15.60		Tüzen et al. (2009)
<i>Ulva lactuca</i>	Trabzon				0.50	4.95	277.00	9.98	2.06			6.50	Tüzen et al. (2009)
<i>Ulva lactuca</i>	Sinop		0.02		32.20	6.78	306.00	11.70	2.72		0.02	19.10	Tüzen et al. (2009)
<i>Ulva lactuca</i>	Istanbul						1570.00						Apaydın et al. (2010)
<i>Ulva lactuca</i>	Sinop				0.06–1.01	3.61–8.30	117–567			2.78–4.70	0.01	20.37–40.62	Türk Çulha et al. (2010)
<i>Ulva lactuca</i>	Ordu		0.01		2.66	11.23	1053.36			3.69	0.01	0.01	Türk Çulha et al. (2013)
<i>Ulva lactuca</i>	Trabzon		0.01		0.01	10.91	550.72			2.30	0.01	4.58	Türk Çulha et al. (2013)
<i>Ulva lactuca</i>	Istanbul		0.01		0.80	44.87	1621.73			2.97	0.01	66.00	Türk Çulha et al. (2013)
<i>Ulva lactuca</i>	Inebolu		0.66				1754.00	64.00	2.40				Arıcı and Bat (2016a)

(continued)

Table 18.4 (continued)

Species	Station	Al	As	Cd	Cr	Co	Cu	Fe	Hg	Mn	Ni	Pb	Zn	References
<i>Ulva lactuca</i>	Sinop			0.09								0.08		Ancı and Bat (2016a)
<i>Ulva lactuca</i>	Samsun											1.90		Ancı and Bat (2016a)
<i>Ulva lactuca</i>	Sinop			0.11–1.30		0.20–1.40	5.50–10.00	117–1375		8.20–15.4	2.11–2.70	4.00–5.60	12.00–39.00	Bat and Arıcı (2016)
<i>Ulva lactuca</i>	Sinop	213.4	0.60	0.04		0.50	2.45	283.50	0.01	23.70	1.85	0.50	32.50	Ancı and Bat (2017)
<i>Ulva linza</i>	Sinop			0.32–0.46			22.08–33.70	452.5–561.5		100.5–134.00	57.68–70.83		37.43–47.15	Öztürk and Bat (1994)
<i>Ulva linza</i>	Istanbul			0.85		0.05	7.63	440.70		49.66	6.95	3.40	8.98	Topçuoğlu et al. (2001)
<i>Ulva linza</i>	Sinop			0.02–0.06	0.06–2.30	0.85–4.49	2.60–18.2			50.10–192.4	7.7–24.40	0.1–9.10	7.10–43.2	Topçuoğlu et al. (2003b)
<i>Ulva linza</i>	Sinop					2.34	4.05	944.00			8.38	0.01	24.92	Türk Çulha et al. (2010)
<i>Ulva linza</i>	Samsun			0.01		0.01	26.69	1099.92			34.89	0.01	28.88	Türk Çulha et al. (2013)
<i>Ulva linza</i>	Ordu			0.01		2.40	14.20	2577.87			3.03	0.01	13.21	Türk Çulha et al. (2013)
<i>Ulva linza</i>	Trabzon			0.01		2.63	8.89	511.16			1.33	0.01	12.01	Türk Çulha et al. (2013)
<i>Ulva linza</i>	Sinop									2.00			7.00	Ancı and Bat (2016a)
<i>Ulva linza</i>	Sinop			0.04–0.06		0.32–1.40	1.50–14.00	681–1342		3.00–31.00	1.20–18.4	5.20–6.00	4.10–19.00	Bat and Arıcı (2016)
<i>Ulva linza</i>	Sinop	1085.75	14.08	0.54		0.46	2.42	1181.78	0.03	35.38	2.32	1.18	52.72	Ancı and Bat (2017)

<i>Ulva rigida</i>	Istanbul		0.10	1.10	0.32	2.53	235.00		9.50	31.00	1.30	3.90	Topcuoglu et al. (2003b)
<i>Ulva rigida</i>	Sinop		1.50– 2.30		1.00– 2.60	2.60– 9.00	1112– 2002		10.00– 21.00	1.20– 2.4	4.00– 5.9	3.00	Bat and Arici (2016)
<i>Ulva rigida</i>	Sinop	279.88	1.15		0.15	3.82	335.85	0.01	13.53	1.92	1.12	83.58	Arıcı and Bat (2017)

Table 18.5 Heavy metal content in phylum Ochrophyta along the Turkish Black Sea macro-algae (mg/kg dry wt.)

Species	Station	Al	As	Cd	Cr	Co	Cu	Fe	Hg	Mn	Ni	Pb	Zn	References
<i>Cystoseira barbata</i>	Istanbul			1.00–2.20			3.20–11.80	124–474		14.40–81.60	35.00	5.30–8.70	18.10–69.10	Güven et al. (1992)
<i>Cystoseira barbata</i>	Kırklareli							100.00		21.45			7.00	Güven et al. (1992)
<i>Cystoseira barbata</i>	Sinop			1.30–2.4			4.20–7.9	446–3414		21.70–73.3	25.00	5.30–12.8	12.10–85.8	Güven et al. (1992)
<i>Cystoseira barbata</i>	Istanbul							164.00					49.10	Topçuoğlu et al. (1998)
<i>Cystoseira barbata</i>	Istanbul			0.35–0.75	0.6–0.95	0.60–0.95	4.80–6.85	166.6–1066		21.45–24.85	2.20–6.2	1.00–14.00	50.40–97.2	Topçuoğlu et al. (2001)
<i>Cystoseira barbata</i>	Istanbul			0.02–0.78	0.06	0.05	2.20–5.7	130–427		6.70–32.1	0.10–9.1	0.1–1.40	13.90–35.1	Topçuoğlu et al. (2003b)
<i>Cystoseira barbata</i>	Sinop			0.02–0.20	0.06–1.20	0.05–1.78	1.70–6.00			22.7–33.5	4.70–7.2	0.1–3.50	6.5–191.50	Topçuoğlu et al. (2003b)
<i>Cystoseira barbata</i>	Sinop			1.02			16.40	560.00				2.10	48.00	Altuğ et al. (2005)
<i>Cystoseira barbata</i>	Kırklareli			0.13	2.50		6.90			57.20		0.20	8.30	Güven et al. (2007)
<i>Cystoseira barbata</i>	Sinop				0.99	9.05	2.47	242.00		14.90	2.05		6.62	Tüzen et al. (2009)
<i>Cystoseira barbata</i>	Sinop					0.01–2.72	2.01–6.03	81–991			0.79–9.26	0.01	0.08–20.47	Türk Çulha et al. (2010)
<i>Cystoseira barbata</i>	Kastamonu			0.01		0.01	16.33	283.67			14.30	0.01	15.30	Türk Çulha et al. (2013)
<i>Cystoseira barbata</i>	Ordu			0.01		1.28	5.06	632.55			3.37	0.01	5.83	Türk Çulha et al. (2013)
<i>Cystoseira barbata</i>	Samsun			0.01		0.38	6.53	534.43			4.60	0.01	0.20	Türk Çulha et al. (2013)

<i>Cystoseira barbata</i>	Sinop									4.02	536.00				5.03	0.01	10.28	Türk Çulha et al. (2013)
<i>Cystoseira barbata</i>	Inebolu					1.50												Arıcı and Bat (2016a)
<i>Cystoseira barbata</i>	Kastamonu									37.00	1151.00			55.00	2.10	1.40	58.00	Arıcı and Bat (2016a)
<i>Cystoseira barbata</i>	Kırklareli									10.00	878.00			33.00	1.00	1.20	21.00	Arıcı and Bat (2016a)
<i>Cystoseira barbata</i>	Samsun									25.00	1250.00			43.00	0.90	1.30	65.00	Arıcı and Bat (2016a)
<i>Cystoseira barbata</i>	Sinop									5.00	327.00			11.00	0.80	1.00	44.00	Arıcı and Bat (2016a)
<i>Cystoseira barbata</i>	Sinop									1.30–7.00	261–2143			2.40–64	1.74–15.00	5.00–10.00	5.00–76.00	Bat and Arıcı (2016)
<i>Cystoseira barbata</i>	Sinop									10.20	481.40			0.01	21.30	4.44	59.50	Arıcı et al. (2019)
<i>Cystoseira crinita</i>	Sinop									5.70	540.00					2.30	46.00	Altuğ et al. (2005)
<i>Cystoseira crinita</i>	Sinop									4.43	305.34			0.01	34.33	4.16	47.40	Arıcı (2017)
<i>Cystoseira crinita</i>	Sinop									4.27	322.50			0.01	32.80	4.11	47.89	Arıcı et al. (2019)
<i>Ectocarpus</i> spp.	Sinop									9.30	1248.55			0.03	24.85	8.05	54.55	Arıcı (2017)
<i>Padina pavonica</i>	Sinop									5.40	410.00					0.01	32.00	Altuğ et al. (2005)
<i>Padina pavonica</i>	Sinop									3.35	591.00			156.00	5.20	2.86	15.70	Tüzün et al. (2009)
<i>Padina pavonica</i>	Sinop									3.73	1909.30			111.00	4.03	2.77	48.87	Arıcı (2017)
<i>Scytosiphon lomentaria</i>	Sinop									6.05	1761.20			16.80	4.80	1.35	284.50	Arıcı (2017)

Fe > Al > Zn > Mn > Cu > Ni > Co > As > Pb > Cr > Cd > Hg and Fe > Al > Mn > Zn > Ni > Co > Cu > Pb > Cr > Cd > As > Hg, respectively. The results showed that depending on macroalgal species, the general heavy metal uptake was the order of Rhodophyta > Chlorophyta > Ochrophyta.

Previous studies along the Black Sea coasts were also indicated that red algae species accumulate more heavy metals than the other phylum (Strezov and Nonova 2009).

In case of macro-algae, the highest Cd, Al, Cr, Co, Mn, Ni, Fe and Zn levels were determined in Rhodophyta species, whereas high Cu and Pb levels were found in Chlorophyta species and high As levels were found in Ochrophyta species. The highest Hg levels (0.02 mg kg⁻¹ dry wt.) were found in both in Rhodophyta and Chlorophyta species.

Heavy metal accumulation capacity of red algae is higher than brown and green algae, depending on phylogeny. Especially, filamentous seaweeds indicate a higher metal uptake than sheet and thick-leathery algae (Trifan et al. 2015). The filamentous seaweeds *Ceramium rubrum*, *Cladophora* spp. and *Ectocarpus* sp. are strong accumulators that could be used as bio-indicators for evaluation of metal contamination along the Black Sea coasts.

Corallina sp. deposits calcareous within the cell walls and shows a lower metal amounts comparison with non-calcified algae (Wallentinus 1984). The corallina accumulate higher amount of Cd than in the sediment (Fowler and Knauer 1986; Altuğ et al. 2005; Arıcı 2017).

Algal polysaccharides are employed as determinative for algal taxonomy. Chlorophyta are a resource of ulvans and other glycans; Rhodophyta make carrageenan, agars and variants; and Ochrophyta also make alginates, fucoidans and laminarins. These polysaccharides of cell wall of the marine algae supply amino, carboxyl, phosphate and sulphate groups for metal binding. Algae and sea grasses are in control of the most of the primary productivity of coastal ecosystems. The metals when found in large concentrations in coastal waters, impact the algal divisions in different amounts.

Generally, the genera *Ulva* are accepted as suitable bio-indicators of metal contaminations in marine coastal waters (Villares et al. 2002; Üstünada et al. 2011).

The Black Sea has various macro-algae species and one of the common brown species is the genus *Cystoseira*. *Cystoseira* sp. live in contact with sediment or coastal rocky bottom, so that it accumulates heavy metals both from surrounding water and from sediment. As is indicator for *Cystoseira* sp. (Phillips 1990). Large amounts of arsenic accumulation in brown seaweeds have been associated with big phosphate levels in those species (Phillips 1990). Farias et al. (2007) stated that these seaweeds absorb and bio-accumulate arsenate from water column as a phosphorus analogue. It was also pointed out that seaweeds can bio transform inorganic As take up from seawater into lesser harmful organic arsenical species (Farias et al. 2007); indications for excretion of arsenite and methylated arsenic species to clean up intra cellular As amounts has been also supported by in vitro investigates with micro-algae (Foster 2008). *Padina pavonica*, living a life member of the thick-leathery group, showed in some degree large levels of many elements such as Mn, Cr and Ni,

Table 18.6 Heavy metal content in phylum Rhodophyta along the Turkish Black Sea macro-algae (mg/kg dry wt.)

Species	City	Al	As	Cd	Cr	Co	Cu	Fe	Hg	Mn	Ni	Pb	Zn	References
<i>Antithamnion cruciatum</i>	Rize			0.02	4.13	27.60	6.83	1524.00		43.50	2.45	2.77	16.20	Tüzen et al. (2009)
<i>Antithamnion cruciatum</i>	Sinop			0.04	11.60	81.90	17.10	3949.00		285.00	10.30	3.97	48.90	Tüzen et al. (2009)
<i>Antithamnion cruciatum</i>	Trabzon				3.00	4.42	7.74	2873.00		78.10	2.80	0.15	11.60	Tüzen et al. (2009)
<i>Antithamnion cruciatum</i>	Samsun			0.04		0.60		1714.00		11.00		0.05	18.00	Ancı and Bat (2016b)
<i>Ceramium</i> spp.	Sinop			1.05			20.00	1970.00				1.80	60.00	Altuğ et al. (2005)
<i>Ceramium</i> spp.	Sinop			0.08–2.2		0.09	1.22–8.00	311–968		12.00–29	0.18–2.9	0.50–2	1.60–50	Bat and Ancı (2016)
<i>Ceramium</i> spp.	Sinop	3076.0	2.89	0.38		1.34	8.69	2792.75	0.03	83.15	6.84	3.08	89.39	Ancı and Bat (2019a)
<i>Ceramium virgatum</i>	Istanbul			0.45–0.81	1.45	0.55–1.35	6.05–15.9	664–709.5		23.75–58.64	1.90–4.32	10.00–10.8	41.70–61.6	Topçuoğlu et al. (2001)
<i>Ceramium virgatum</i>	Sinop			1.62	0.06	4.36	16.80			249.50	11.20	0.10	58.00	Topçuoğlu et al. (2003b)
<i>Ceramium virgatum</i>	Rize			0.01	1.99	7.20	7.17	1479.00		31.20	3.53	0.01	16.90	Tüzen et al. (2009)
<i>Ceramium virgatum</i>	Sinop				3.29	10.30	6.55	996.00		92.50	2.72	0.08	41.60	Tüzen et al. (2009)
<i>Ceramium virgatum</i>	Trabzon			1.95	1.95	5.42	7.28	1953.00		74.30	3.10	0.53	12.50	Tüzen et al. (2009)
<i>Ceramium virgatum</i>	Sinop					0.01	2.65	691.00			0.28	0.01	0.28	Türk Çulha et al. (2010)
<i>Ceramium virgatum</i>	Istanbul			0.01		1.86	32.57	2717.82			6.06	0.01	41.94	Türk Çulha et al. (2013)

(continued)

Table 18.6 (continued)

Species	City	Al	As	Cd	Cr	Co	Cu	Fe	Hg	Mn	Ni	Pb	Zn	References
<i>Ceranium virgatum</i>	Ordu			0.01		0.01	17.19	3178.92			2.34	0.01	12.12	Türk Çulha et al. (2013)
<i>Ceranium virgatum</i>	Samsun			0.01		2.86	13.20	1470.40			10.81	0.01	13.56	Türk Çulha et al. (2013)
<i>Ceranium virgatum</i>	Trabzon			0.01		0.01	11.65	1898.88			3.31	0.01	20.80	Türk Çulha et al. (2013)
<i>Ceranium virgatum</i>	Samsun			0.02		0.10						0.05		Ancı and Bat (2016b)
<i>Corallina officinalis</i>	Istanbul			1.10		1.30	2.78	520.00				5.80	21.90	Güven et al. (1998)
<i>Corallina officinalis</i>	Istanbul			0.49		3.16	3.36	475.00				3.85	17.20	Kut et al. (2000)
<i>Corallina officinalis</i>	Sinop			1.07			18.20	1221.00				2.50	62.20	Altuğ et al. (2005)
<i>Corallina officinalis</i>	Sinop					0.01	1.77	139.00			2.02	1.39	20.79	Türk Çulha et al. (2010)
<i>Corallina officinalis</i>	Ordu			0.01		1.26	7.55	1483.68			2.88	0.01	14.04	Türk Çulha et al. (2013)
<i>Corallina officinalis</i>	Sinop					0.01–0.10	0.06–1.77	139–326			2.02–3.76	1.39–4.84	20.79–55.78	Türk Çulha et al. (2013)
<i>Corallina officinalis</i>	Samsun			0.03		0.30	10.00	675.00		31.00	1.7–3.00	0.05	41.00	Ancı and Bat (2016b)
<i>Corallina officinalis</i>	Sinop	404.30	1.80	0.20		0.30	3.40	466.20	0.01	72.90	5.10	1.40	34.80	Ancı and Bat (2019a)
<i>Corallina panizzoi</i>	Sinop			1.10–3.10		0.10–1.10	1.78–3.00	402–805		7.00–38.00	3.00–5.00	11.00–28.00	26.00–33.00	Bat and Ancı (2016)
<i>Corallina</i> spp.	Sinop					0.10	0.06	326.00			3.76	4.84	55.78	Türk Çulha et al. (2010)

<i>Ellisolandia elongata</i>	Istanbul			0.02	0.06	0.05	0.03–3.1	173–595	22.20–64.7	0.10	0.10	22.50–43.4	Topçuoğlu et al. (2003b)
<i>Ellisolandia elongata</i>	Sinop			0.02	0.06	0.05	3.90–4	626–1508	48.5–56.70	0.10	0.10	19.10–39.3	Topçuoğlu et al. (2003b)
<i>Ellisolandia elongata</i>	Sinop				4.48	7.52	3.84	99.00	27.70	8.29	1.07	26.40	Tüzen et al. (2009)
<i>Gelidium crinale</i>	Sinop					0.01	16.80	421.00		9.53	0.01	0.28	Türk Çulha et al. (2010)
<i>Gelidium crinale</i>	Sinop	985.50	3.08	0.10		1.78	10.08	834.53	164.45	10.80	1.88	101.55	Arci and Bat (2019a)
<i>Gelidium spinosum</i>	Sinop			0.01	1.95	16.70	6.84	618.00	77.60	1.73	1.45	64.80	Tüzen et al. (2009)
<i>Halipiton virgatum</i>	Istanbul			5.90–6.50		1.30–2.60	3.3–4.00	206–1395	16.6–71.5	0.28–8.29	20.8–22.60	33.2–59.30	Güven et al. (1992)
<i>Halipiton virgatum</i>	Sinop			1.00–6.1		1.40–3.10	3.30–8	592–2203	42–69		4.80–24.6	25.50–43.2	Güven et al. (1992)
<i>Halipiton virgatum</i>	Istanbul			0.5–0.65	1.05–5.50	0.40–1.3	1.95–10.4	122.30–771.9	17.20–85.85	0.15–2.3	0.50–7.5	42.20–89.2	Topçuoğlu et al. (2001)
<i>Halipiton virgatum</i>	Istanbul			0.08	0.90	1.92	0.77	231.00	17.90	4.10	2.20	8.90	Topçuoğlu et al. (2003b)
<i>Laurencia obtusa</i>	Sinop	346.70	1.60	0.20		0.10	5.80	402.40	11.00	2.90	0.90	41.10	Arci and Bat (2019a)
<i>Phyllophora crisa</i>	Istanbul			0.50	0.90–1.20	3.35–6.3	10.9–16.50	324.1–481.80	95.35–296.4	64.9–83.80	3.00–20	81.90–107.6	Topçuoğlu et al. (2001)
<i>Phyllophora crisa</i>	Istanbul			0.02–0.12	0.06–1.10	0.05–3.12	5.46–11.9	359–743	75.80–88.3	47.4–70.00	0.1–1.90	24.00–71.8	Topçuoğlu et al. (2003b)
<i>Phyllophora crisa</i>	Sinop			0.02	0.06	9.08	20.10		364.60	70.60	0.10	54.40	Topçuoğlu et al. (2003b)
<i>Phyllophora crisa</i>	Sinop				3.10	49.90	14.10	1559.00	261.00	36.20	2.22	48.60	Tüzen et al. (2009)

(continued)

Table 18.6 (continued)

Species	City	Al	As	Cd	Cr	Co	Cu	Fe	Hg	Mn	Ni	Pb	Zn	References
<i>Porphyra umbilicalis</i>	Rize			0.02	0.50	42.60	3.93	784.00		19.10	4.04	0.65	22.40	Tüzen et al. (2009)
<i>Porphyra umbilicalis</i>	Sinop				0.84	7.98	4.19	114.00		13.30	2.24	0.28	19.40	Tüzen et al. (2009)
<i>Porphyra umbilicalis</i>	Trabzon			0.01	1.48	6.59	4.92	330.00		22.30	0.27	0.01	22.80	Tüzen et al. (2009)
<i>Porphyra umbilicalis</i>	Samsun			0.02			5.00	280.00			0.40	0.06		Ancı and Bat (2016b)
<i>Pterocladia capillacea</i>	Istanbul			0.90–2	1.05–1.15	0.80–1.60	5.4–8.70	258.5–403.30		46.65–72.10	3.60–5.25	3.00–9.50	75.70–107.9	Topçuoğlu et al. (2001)
<i>Pterocladia capillacea</i>	Istanbul			1.36–1.53	0.06	0.05	5.30–10.3	158–288		52.10–91.1	0.10–10.8	0.10	86.20–119.8	Topçuoğlu et al. (2003b)
<i>Pterocladia capillacea</i>	Sinop			0.02	0.06	0.05	0.03			10.80	0.10	0.10	176.80	Topçuoğlu et al. (2003b)
<i>Pterocladia capillacea</i>	Kırklareli			0.03	2.50		8.80			41.70		14.00	18.00	Güven et al. (2007)
<i>Vertebrata fucoides</i>	Sinop	2363.50	2.63	0.53		0.87	7.53	1633.50	0.02	98.43	5.70	3.00	129.63	Ancı and Bat (2019a)

could be mayhap imputed to the probability that this species, get in touch with sediments, accumulate metals either from water column or from sediments or suspended inorganic particulates, likely concluding in large element amounts contrast to macro-algae living far from sediments; seaweed tissues contacting surface sediments and suspended particulates may scavenge metals whose strength of binding to seaweed tissues is greater than those in particles (Luoma 1983). *Cystoseira barbata* have shown a clear selectivity for some metals (see Table 18.5, section Ochrophyta), which may be encouraged their use as bio-monitor organism for clean seawaters. However, generalizations cannot be made.

Recent review of Bonanno and Orlando-Bonaca (2018) stated that red algae have a larger metal accumulation capacity than ambient sediments and waters, then by green and brown algae in the Mediterranean Sea. In this review we made for the Black Sea, the results are the same. Many species belong to Rhodophyta, Chlorophyta and Ochrophyta species were analysed for metal concentrations. Tables 18.4, 18.5 and 18.6 show that fluctuations in the consequences from an area as for the time factor were originated from differences in local inputs that changed from time to time. These differences depend on the living environment of the species. Factors influencing the metal amounts in algal species listed and discussed by Bonanno and Orlando-Bonaca (2018). They are; (1) biological such as growth strategy, age, phylogeny thallus, morphology; and (2) environmental such as temperature, salinity, pH, season, organic and inorganic compounds, oxygen content, light intensity, geology, nutrient, metal amounts in water, interactions among metals.

There are still questions to be answered. Bonanno and Orlando-Bonaca (2018) expressed that the rate of metal accumulation or the correlation between metal levels in sediments or/and surrounding water and algal tissues are less studied, and advance investigations are required to make clear metal intake mechanisms.

Seagrass are marine angiosperms that inhabit shallow, soft bottoms of most coastal areas. They are regarded as an important part of coastal ecosystems due to the identification of varied ecological functions, sources and services. Seagrass rich in species diversity are cornerstone and highly productive ecosystems which fulfil a key role in the marine ecosystem. Seagrass can supply source managers with further signs of degrading ecological circumstances arose by poor water quality and pollution (Ondiviela et al. 2014). Seagrass increase habitat diversity and have role water quality since they deed as filters by trapping suspended matter in the water column and by absorbing dissolved inorganic nutrients. They also have a role as regulators of coastal sediment dynamics owing to the fact that they reduce sediment resuspension. The leaf canopy and the network of rhizomes and roots stabilize the sediment, and may accumulate contaminants from water column and sediment.

Metals display different translocation movements in seagrass tissues related to exposure time to contamination in surrounding water and sediments where they live. Zn, Cd and Mn accumulate in sediments over time depending on anthropogenic impacts and metals translocate to upward (Faraday and Churchill 1979; Penello and Brinkhuis 1980; Arici and Bat 2019b). These basipetally movements (below to

Table 18.7 Concentrations of metals in tissues of seagrasses (mg/kg dry wt.) in the Black Sea coasts

Species	Tissues	Station	Al	As	Cd	Cr	Co	Cu	Fe	Hg	Mn	Ni	Pb	Zn	References
<i>Z. marina</i>	Leaves	Trabzon			1.05	1.52	3.04	0.84	9370		138.4	4.80	1.17	3.63	Tuncer and Yaramaz (1992)
<i>Z. marina</i>	Shoots	Trabzon			1.05	2.20	3.14	0.60	510		91.6	3.56	3.14	23.22	Tuncer and Yaramaz (1992)
<i>Z. marina</i>	Leaves	Sinop	1847.4	2.00	0.10		2.00	13.6	1719.7	0.02	761.8	7.30	1.90	114.8	Ancı and Bat (2019b)
<i>Z. marina</i>	Shoots +Rhizomes	Sinop	4957.4	3.70	0.10		2.00	14.	4151	0.03	444	11.50	3.70	115.2	Ancı and Bat (2019b)
<i>Z. noltei</i>		Sinop			0.18			1.70	521.7		174.5		0.90	14.50	Bat et al. (2015b)
<i>Z. noltei</i>	Leaves	Sinop	3266.9	1.60	0.50		1.70	5.20	2237.3	0.01	459.5	4.60	3.20	78.00	Ancı and Bat (2019b)
<i>Z. noltei</i>	Shoots+ Rhizomes	Sinop	2055	2.20	0.30		1.70	5.20	3214	0.01	339.3	4.20	4.00	85.80	Ancı and Bat (2019b)

above) are minimal for Co and Cu (Carter and Eriksen 1992; Arıcı and Bat 2019b). Although the data of translocation is inadequate, intake of Pb present acropetally (above to below) translocation (Lyngby and Brix 1982; Bond et al. 1985; Arıcı and Bat 2019b). In addition to them, Hg and Ni exhibit bi-directional movement capabilities (Arıcı and Bat 2019b).

For these, determination of metal amounts in seagrass is very important. Interestingly, there are few studies on metal pollution related to seagrass on the Black Sea coast (Table 18.7).

18.9 Environmental Risk and Remediation

High accumulation abilities of sedentary organisms' threat plant, animal and human health in the aquatic ecosystems. To estimate metal exposure of bio-indicators matters for sustainability. Thus, remediation of metals is necessary for keeping under control of water quality and for removal of pollutants.

There is some clean-up (or remediation) technologies available for reducing harmful effects of metals include chemical, physical and microbial processes such as precipitation, adsorption, biosorption, ion-exchange, filtration, coagulation and cementation. Bioremediation is in demand treatment method by using seaweeds that reduce pollution impact on the marine environment.

All remediation methods are preferred for eco-friendly approach and cost-effective properties; offer public health and environmental benefits.

18.10 Conclusion

The Marine Strategy Framework Directive (MSFD) (2008/56/EC) demands that European Member States get the necessary acts to reach Good Environmental Status (GES) by 2020. The intent of the MSFD with attention to Descriptor 8 and 9 is to make sure that amounts of contaminants including metals are at levels not giving increase to contamination effects. The appraisal of accomplishment of GES should be principled upon observing programmes including the MSFD indicators. The MSFD Descriptor 8 "Concentrations of contaminants are at levels not giving rise to pollution effects" and Descriptor 9 "Contaminants in fish and other seafood for human consumption do not exceed levels established by Community legislation or other relevant standards" are both aiming at the subject of marine contamination. Contaminant monitoring under the Marine Strategy Framework Directive descriptor D8 is associated to evaluation of environmental pollution done within the Water Framework Directive (2000/60/EC). The use of marine organisms in bio-monitoring studies is highly promoted by both the Water Framework Directive and the MSFD.

It should not be forgotten that macro-algae and sea meadows are the first producers in the seas, they create habitats for many benthic organisms, they are an

important food source for many species, they cannot escape from the habitats they live in and are exposed to contaminants in seawater and sediment.

In this review, studies on water, sediment, macro-algae and sea grasses of the Black Sea, especially Turkish waters in a period of approximately 27 years are examined. Current literature shows us that macro-algae are used as bio-indicator species in monitoring studies. Macro-algae species appear to accumulate much higher amounts of heavy metals than the waters they inhabit. This shows us that macro-algae accumulate metals even at very low concentrations. It should be noted that macro-algae can also uptake metals from sediments. It is possible to transfer heavy metals from sediment or particles into water. Along with macro-algae, seagrass has also been used in metal pollution studies on the Black Sea coasts. Seagrasses can absorb metals from water with their roots from sediment with roots. It is very difficult to reach a clear result with the available data. For this purpose, monitoring of metal pollution in both macro-algae, seagrasses and sediments and waters should be carried out with the same method in coordination between the Black Sea countries. MISIS (MSFD Guiding Improvements in the Black Sea Integrated Monitoring System) project with Bulgaria, Turkey and Romania are among these objectives had been achieved (MISIS 2015), it is necessary to also include other Black Sea countries.

Conflict of Interest Statement We declare that we have no conflict of interest.

References

- Alkan N, Alkan A, Akbaş U, Fisher A (2015) Metal pollution assessment in sediments of the southeastern Black Sea coast of Turkey. *Soil Sediment Contam Int J* 24(3):290–305
- Altaş L, Büyükgüngör H (2007) Heavy metal pollution in the Black Sea shore and offshore of Turkey. *Environ Geol* 52(3):469–476. <https://doi.org/10.1007/s00254-006-0480-1>
- Altuğ G, Yardımcı C, Aydoğan M (2005) Levels of some toxic metals in marine algae from the Turkish coast of the Black Sea, Turkey. *The 1st Biannual Scientific Conference: The Black Sea Ecosystem* pp 244–249
- Andreev G, Simeonov V (1990) Distribution and correlation of elements in waters, suspensions, sediments and marine organisms from the Black Sea. *Toxicol Environ Chem* 28(1):1–9
- Anninsky BE, Finenko GA, Abolmasova GI, Hubareva ES, Svetlichny LS, Bat L, Kideys AE (2005) Effect of starvation on the biochemical compositions and respiration rates of ctenophores *Mnemiopsis leidyi* and *Beroe ovata* in the Black Sea. *J Mar Biol Ass U K* 85:549–561
- Apaydın G, Aylıkçı V, Cengiz E, Saydam M, Küp N, Tıraşoğlu E (2010) Analysis of metal contents of seaweed (*Ulva lactuca*) from Istanbul, Turkey by EDXRF. *Turk J Fish Aquat Sci* 10:215–220
- Arıcı E (2017) Using dominant macroalgae and seagrass in Sinop coastline of the Black Sea as biomonitor for determination of heavy metal pollution. Sinop University, PhD thesis, p 161
- Arıcı E, Bat L (2016a) Using marine macroalgae as biomonitors: Heavy metal pollution along the Turkish west coasts of the Black Sea. 41st CIESM Congress, 12–16 September, Kiel-Germany. *Rapp Comm Int Mer Medit* 41:238
- Arıcı E, Bat L (2016b) Red algae as bioindicators of heavy metal pollution from Samsun coasts of Turkey. 41st CIESM Congress, 12–16 September, Kiel-Germany. *Rapp Comm Int Mer Medit* 41:239
- Arıcı E, Bat L (2017) Assessment of elemental uptakes by *Ulva* (Chlorophyta) species collected from Sinop coasts of the Black Sea. *Pakistan J Mar Sci* 26(1–2):1–13

- Arıcı E, Bat L (2019a) Environmental monitoring of heavy metals by common Rhodophyta species in Sinop coastal ecosystem. International Congress on Engineering and Life Science, 11–14 April, Kastamonu, Turkey, pp 699–705
- Arıcı E, Bat L (2019b) Sediment-water interactions with eelgrass (*Zostera* spp.) from Sinop shores of the Black Sea. CJES (in press)
- Arıcı E, Bat L, Yıldız G (2019) Comparison of metal uptake capacities of the brown algae *Cystoseira barbata* and *Cystoseira crinita* (Phaeophyceae) collected in Sinop, Turkey. Pakistan J Mar Sci 28(1):5–17
- Ataç U, Aktas M, Alemdag N, Zengin B, Alkan A (1997) Determination of factors causing water pollution in the Black Sea region and investigation of the effects on fisheries. Project no: TAGEM/IV/96/12/02/001 (in Turkish)
- Bakan G, Büyükgüngör H (2000) The Black Sea. Mar Pollut Bull 41(1–6):24–43
- Bakan G, Böke Özkoç H (2007) An ecological risk assessment of the impact of heavy metals in surface sediments on biota from the mid-Black Sea coast of Turkey. Int J Environ Stud 64 (1):45–57
- Balkis N, Topcuoğlu S, Güven KC, Öztürk B, Topaloğlu B, Kirbaşoğlu Ç, Aksu A (2007) Heavy metals in shallow sediments from the Black Sea, Marmara Sea and Aegean Sea regions of Turkey. J Black Sea/Mediterr Environ 13(2):147–153
- Bat L (2014) Heavy metal pollution in the Black Sea. In: Düzgüneş E, Öztürk B, Zengin M (eds) Turkish fisheries in the Black Sea. Turkish Marine Research Foundation (TUDAV), Istanbul, pp 71–107
- Bat L (2017) The contamination status of heavy metals in fish from the Black Sea, Turkey and potential risks to human health. In: Sezgin M, Bat L, Ürkmez D, Arıcı E, Öztürk B (eds) Black sea marine environment: the turkish shelf. Turkish Marine Research Foundation (TUDAV), Istanbul, pp 322–418
- Bat L, Arıcı E (2016) Heavy metal concentrations in macroalgae species from Sinop coasts of the Southern Black Sea. J Coast Life Med 4(11):841–845
- Bat L, Arıcı E (2018) Chapter 5. Heavy metal levels in fish, molluscs, and crustacea from turkish seas and potential risk of human health. In: Holban AM, Grumezescu AM (eds) Handbook of food bioengineering, volume 13, food quality: balancing health and disease. Elsevier, Academic Press, London, pp 159–196. <https://doi.org/10.1016/B978-0-12-811442-1.00005-5>
- Bat L, Şahin F (2019, April) Assessment of heavy metal pollution and potential ecological risk in sediments of Sinop shores of the Black Sea. ICELIS 11–14:734–739
- Bat L, Gökkurt O, Sezgin M, Üstün F, Sahin F (2009) Evaluation of the Black Sea land based sources of pollution the coastal region of Turkey. Open Mar Biol J 3:112–124
- Bat L, Özkan EY, Öztekin HC (2015a) The contamination status of trace metals in Sinop coast of the Black Sea, Turkey. Caspian J Environ Sci 13(1):1–10
- Bat L, Öztekin HC, Arıcı E, Vişne A (2015b) A preliminary study on the heavy metal levels of dwarf eelgrass *Zostera noltii* Homermann in the Black Sea. J Aquac Mar Biol 4(1):1–5
- Bat L, Öztekin A, Arıcı E (2017a) Marine litter pollution in the black sea: assessment of the current situation in light of the marine strategy framework directive. In: Sezgin M, Bat L, Ürkmez D, Arıcı E, Öztürk B (eds) Black sea marine environment: the turkish shelf. Turkish Marine Research Foundation (TUDAV), Istanbul, pp 476–494
- Bat L, Özkan EY, Büyükkisik HB, Öztekin HC (2017b) Assessment of metal pollution in sediments along Sinop peninsula of the Black Sea. Int J Mar Sci 7(22):205–213
- Bat L, Öztekin A, Şahin F, Arıcı E, Öz sandıkcı U (2018) An overview of the Black Sea pollution in Turkey. MedFAR 1(2):67–86
- Bat L, Şahin F, Öztekin A (2019) Assessment of heavy metals pollution in water and sediments and Polychaetes in Sinop shores of the Black Sea. KSU J Agric Nat 22(5):806–816. <https://doi.org/10.18016/ksutarimdogu.v22i45606.535882>
- Bonanno G, Orlando-Bonaca M (2018) Chemical elements in Mediterranean macroalgae. A review. Ecotoxicol Environ Saf 148:44–71

- Bond AM, Broasbury JR, Hudson A, Garnham JS, Hanna PJ, Strother S (1985) Kinetic studies of lead uptake by the seagrass *Zostera muelleri* in water by radiotracing, AAS and electrochemical techniques. *Mar Chem* 24:253–263
- BSC (2008) State of the environment of the Black Sea (2001–2006/7). In: Oguz T (ed) Publications of the commission on the protection of the black sea against pollution (BSC) 2008–3. BSC, Istanbul, p 448
- Cadar E, Sirbu R, Pirjol BSN, Ionescu AM, Pirjol TN (2019) Heavy metals bioaccumulation capacity on marine algae biomass from Romanian Black Sea Coast. *Rev Chim (Bucharest)* 70 (8):3065–3072
- Carter RJ, Eriksen RS (1992) Investigation into the use of *Zostera muelleri* (Irmisch ex Aschers) as a sentinel accumulator for copper. *Sci Tot Environ* 125:185–192
- Çevik U, Damla N, Kobya AI, Bulut VN, Duran C, Dalgıç G, Bozacı R (2008) Assessment of metal element concentrations in mussel (*M. galloprovincialis*) in Eastern Black Sea Turkey. *J Hazard Mater* 160(2–3):396–401
- Çoban B, Balkıs N, Aksu A (2009) Heavy metal levels in sea water and sediments of Zonguldak, Turkey. *J Black Sea/Mediterr Environ* 15(1):23–32
- Engin MS, Uyanık A, Cay S, Kir I (2015) Evaluation of trace metals in sediment, water, and fish (*Mugil cephalus*) of the central Black Sea coast of Turkey. *Hum Ecol Risk Assess Int J* 22 (1):241–250
- Ergin M (2005) Metal pollution at sea, Jeologic and anthropologic heavy metal pollution in the Black Sea, Aegean Sea and Mediterranean Sea sediments. In: Güven KC, Öztürk B (eds) Marine pollution. Turkish Marine Research Foundation (TUDAV), Istanbul, Turkey, pp 161–176. (in Turkish)
- Ergin M, Keskin Ş, Algan O, Alpar B, Ongan D, Kırıcı E, Bayhan E, Temel A (2003) Güneybatı Karadeniz kıta sahanlığının geç Kuvaterner jeolojisi: sedimantolojik, sığ sismik stratigrafik, mineralojik ve jeokimyasal arařtırmalar. Technical Report, TÜBİTAK Project no:198Y083, p 175
- Ergül HA, Topcuođlu S, Ölmez E, Kırbařođlu Ç (2008) Heavy metals in sinking particles and bottom sediments from the eastern Turkish coast of the Black Sea. *Estuar Coast Shelf Sci* 78 (2):396–402
- Faraday WE, Churchill AC (1979) Uptake of cadmium by the eelgrass *Z. marina*. *Mar Biol* 53:293–298
- Farias S, Smichowski P, Velez D, Montoro R, Curtosi A, Vodopivec C (2007) Total and inorganic arsenic in Antarctic macroalgae. *Chemosphere* 69(7):1017–1024
- Finenko GA, Romanova ZA, Abolmasova GI, Anninsky BE, Svetlichny LS, Hubareva ES, Bat L, Kideys AE (2003) Population dynamics, ingestion, growth and reproduction rates of the invader *Beroe ovata* and its impact on plankton community in Sevastopol Bay, the Black Sea. *J Plankton Res* 25(5):539–549
- Finenko GA, Romanova ZA, Abolmasova GI, Anninsky BE, Pavlovskaya TV, Bat L, Kideys AE (2006) Ctenophores invaders and their role in the trophic dynamics of the planktonic community in the coastal regions off the Crimean coasts of the Black Sea (Sevastopol Bay). *Oceanology* 46 (4):472–482
- Foster JW (2008) *Irish Novels 1890–1940: New Bearings in Culture and Fiction*. United Kingdom, Oxford
- Fowler SW, Knauer GA (1986) Concentrations of Hg, Cd, Cu, Zn, Fe and Mn in deep sea benthic fauna: a case study on southeastern area. *Environmental Monitoring and Assessment* 7:59–78
- Gedik K, Boran M (2013) Assessment of metal accumulation and ecological risk around Rize harbor, Turkey (Southeast Black Sea) affected by copper ore loading operations by using different sediment indexes. *Bull Environ Contam Toxicol* 90(2):176–181
- Güven KC, Topcuođlu S, Kut D, Esen N, Erentürk N, Saygı N, Cevher E, Öztürk B (1992) Metal uptake by Black Sea algae. *Bot Mar* 35(4):337–340

- Güven KC, Okuş E, Topcuoğlu S, Esen N, Küçükcezzar R, Seddigh E, Kut D (1998) Heavy metal accumulation in algae and sediments of the Black Sea coast of Turkey. *Toxicol Environ Chem* 67(3–4):435–440
- Güven KC, Topcuoğlu S, Balkıs N, Ergül H, Aksu A (2007) Heavy metal concentrations in marine algae from the Turkish coast of the Black Sea. *Rapp Comm Int Mer Mediterr* 38:266
- Jitar O, Teodosiu C, Oros A, Plavan G, Nicoara M (2015) Bioaccumulation of heavy metals in marine organisms from the Romanian sector of the Black Sea. *New Biotechnol* 32(3):369–378
- Kıratlı N, Ergin M (1996) Partitioning of heavy metals in surface Black Sea sediments. *Appl Geochem* 11(6):775–788
- Kocataş A (2005) Oseanoloji Deniz Bilimlerine Giriş. Ege Üniversitesi Yayınları Su Ürünleri Fakültesi, Ege Üniversitesi Basımevi, Bornova İzmir (in Turkish), p 562
- Kut D, Topcuoğlu S, Esen N, Küçükcezzar R, Güven KC (2000) Trace metals in marine algae and sediment samples from the Bosphorus. *Water Air Soil Pollut* 118(1–2):27–33
- Luoma SN (1983) Bioavailability of trace metals to aquatic organisms – a review. *Sci Total Environ* 28(1–3):1–22. [https://doi.org/10.1016/S0048-9697\(83\)80004-7](https://doi.org/10.1016/S0048-9697(83)80004-7)
- Lynby JF, Brix H (1982) Seasonal and environmental variation in the Cd, Cu, Pb and Zn concentrations in eelgrass in the Limfjord, Denmark. *Aquat Bot* 14:59–74
- Marine Strategy Framework Directive (2008) Directive 2008/56/EC of the European Parliament and of the Council of 17 June 2008 establishing a framework for community action in the field of marine environmental policy
- Mee LD (1992) The Black Sea in crisis: a need for concerted international action. *Ambio* 21(4):278–286
- MISIS (2015) MSFD (Marine Strategy Framework Directive) guiding improvements in the Black Sea integrated monitoring system (2012–2015) in response to the call for proposals under the EU Program ‘Preparatory action – Environmental monitoring of the Black Sea Basin and a common European framework Programme for development of the Black Sea region’, Ref. Black Sea and Mediterranean 2011. Agreement number: 07.020400/20 12/616044/SUB/D2
- Mülayim A, Balkıs H (2015) Toxic metal (Pb, Cd, Cr, and Hg) levels in *Rapana venosa* (Valenciennes, 1846), *Eriphia verrucosa* (Forskål, 1775), and sediment samples from the Black Sea littoral (Thrace, Turkey). *Mar Pollut Bull* 95(1):215–222
- NIMRD (2011) Report on the state of the marine and coastal environment in 2010. NIMRD, Constanta, Romania, p 55
- Olivares HG, Lagos NM, Gutierrez CJ, Kittelsen RC, Valenzuela GL, Lillo MEH (2016) Assessment oxidative stress biomarkers and metal bioaccumulation in macroalgae from coastal areas with mining activities in Chile. *Environ Monit Assess* 188:25
- Ondiviela B, Losada IJ, Lara JL, Maza M, Galvan C, Bouma TJ, Belzen J (2014) The role of seagrasses in coastal protection in a changing climate. *Coast Eng* 87:158–168
- Oros A (2008) Trace metals concentrations in the Romanian Black Sea coastal waters between 1997–2007
- Oros A, Coatu V, Secieru D, Tiganus D, Vasiliu D, Atabay H, Beken C, Tolun L, Moncheva S, Bat L (2016) Results of the assessment of the western Black Sea contamination status in the frame of the MISIS Joint Cruise. *Cercetări Mar* 46:61–81
- Özkan EY, Büyüksık B (2012) Geochemical and statistical approach for assessing heavy metal accumulation in the southern Black Sea sediments. *Ekoloji* 21(83):11–24
- Özşeker K, Erüz C (2011) Heavy metal (Ni, Cu, Pb, Zn) distribution in sediments from the coast of Trabzon in the Black Sea. *Indian J Geo-Marine Sci* 40(1):48–54
- Özşeker K, Erüz C, Ciliz S, Mani F (2014) Assessment of heavy metal contribution and associated ecological risk in the coastal zone sediments of the Black Sea: Trabzon. *Clean-Soil Air Water* 42(10):1477–1482
- Öztekin A, Bat L (2017a) Seafloor Litter in the Sinop Inceburun coast in the Southern Black Sea. *Int J Environ Geoinformatics (IJEGEO)* 4(3):173–181

- Öztekin A, Bat L (2017b) Microlitter pollution in sea water: a preliminary study from Sinop Sarikum coast of the southern Black Sea. *J Fish Aquat Sci* 17:1431–1440. https://doi.org/10.4194/1303-2712-v17_6_37
- Öztekin A, Bat L, Gökkuurt-Baki O (2020) Beach litter pollution in Sinop Sarikum Lagoon coast of the southern Black Sea. *J Fish Aquat Sci* 20(3):197–205. https://doi.org/10.4194/1303-2712-v20_3_04
- Öztürk M, Bat L (1994) Heavy metal levels in bioindicator organisms collected from Sinop bay and harbor. *Trakya University Faculty of Science and Letters XII. National Biology Congress*, p 20–25
- Penello WF, Brinkhuis BH (1980) Cadmium and manganese flux in the eelgrass *Z. marina* modelling dynamics of metal release from labelled tissues. *Mar Biology* 58:181–186
- Phillips DJH (1990) Arsenic in aquatic organisms: a review, emphasizing chemical speciation. *Aquat Toxicol* 16:151–186
- Phillips DJH, Rainbow PS (1994) In: Cairns J, Harrison RM (eds) *Biomonitoring of trace aquatic contaminants*. Chapman and Hall, New York, p 371
- Strezov A, Nonova T (2009) Influence of macroalgal diversity on accumulation of radionuclides and heavy metals in Bulgarian Black Sea ecosystems. *J Environ Radioact* 100:144–150
- Sur M, Sur Hİ, Apak R, Erçağ E (2012) The pollution status of bottom surface sediments along the Turkish coast of the Black Sea. *Turk J Fish Aquat Sci* 12(5):453–460
- Svetlichny LS, Abolmasova GI, Hubareva ES, Finenko GA, Bat L, Kideys AE (2004) Respiration rates of *Beroe ovata* in the Black Sea. *Mar Biol* 145:585–593
- Tankere SPC, Muller FLL, Burton JD, Statham PJ, Guieu C, Martin JM (2001) Trace metal distributions in shelf waters of the Northwestern Black Sea. *Cont Shelf Res* 21 (13–14):1501–1532
- Topçuoğlu S (2000) Black Sea ecology. Pollution research in Turkey of the marine environment. *IAEA Bull* 42(4):12–14
- Topçuoğlu S, Güven KC, Okus E, Esen N, Güngör N, Ünlü S (1998) Metal contents of algae and sediments of Turkish coasts in the Black Sea (1979–1989 and 1991–1993) the Proceedings of the First International Symposium on Fisheries and Ecology Proceedings, pp 437–438
- Topçuoğlu S, Güven KC, Kırbasoğlu Ç, Güngör N, Ünlü S, Yılmaz YZ (2001) Heavy metals in marine algae from Şile in the Black Sea, 1994–1997. *Bull Environ Contam Toxicol* 67 (2):288–294
- Topçuoğlu S, Kırbasoğlu Ç, Güngör N (2002) Heavy metals in organisms and sediments from Turkish coast of the Black Sea, 1997–1998. *Environ Int* 27(7):521–526
- Topçuoğlu S, Ergül HA, Baysal A, Ölmez E, Kut D (2003a) Determination of radionuclide and heavy metal concentrations in biota and sediment samples from Pazar and Rize stations in the eastern Black Sea. *Fresenius Environ Bull* 12(7):695–699
- Topçuoğlu S, Güven KC, Balkis N, Kırbasoğlu C (2003b) Heavy metal monitoring of marine algae from the Turkish coast of the Black Sea, 1998–2000. *Chemosphere* 52(10):1683–1688
- Trifan A, Breaban IG, Sava D, Bucur L, Toma C-C, Miron A (2015) Heavy metal content in macroalgae from Roumanian Black Sea. *Rev Roum Chim* 60(9):915–920
- Tuncer S, Yaramaz Ö (1992) Heavy metals and other elements in *Zostera marina* L. on the Trabzon Coast Line (Black Sea-Turkey). *Rapp Comm Int Mer Médit* 33:186
- Türk Çulha S, Koçbaş F, Gündoğdu A, Topçuoğlu S, Çulha M (2010) Heavy metal levels in macroalgae from Sinop in the Black Sea. *Rapp Comm Int Mer Méditerr* 39:239
- Türk Çulha S, Koçbaş F, Gündoğdu A, Çulha M (2013) Heavy metal levels in marine algae from the Black Sea, Marmara Sea and Mediterranean Sea. *Rapp Comm Int Mer Méditerr* 40:827
- Tüzen M, Verep B, Öğretmen AO, Soylak M (2009) Trace element content in marine algae species from the Black Sea, Turkey. *Environ Monit Assess* 151(1–4):363–368
- Uncumusaoglu AA, Sengul U, Akkan T (2016) Environmental contamination of heavy metals in the Yaglidere Stream (Giresun), southeastern Black Sea. *Fresenius Environ Bull* 25 (12):5492–5498

- Ünsal M (2001) Lead pollution and its sources along the Turkish coast of the Black Sea. *Mediterr Mar Sci* 2(2):33–44
- Ünsal M, Bekiroğlu Y, Beşiktepe (Akdoğan) Ş, Kayıkcı Y, Alemdağ Y, Aktaş M, Yıldırım C (1995) Determination of the land-based sources of heavy pollution in the middle and eastern Black Sea Coast. Tarım ve Köyişleri Bakanlığı Trabzon Su Ürünleri Araştırma Enstitüsü. Project No: DEBAG–121/G; p 59 (in Turkish)
- Ünsal M, Çağatay N, Bekiroğlu Y, Kıratlı N, Alemdağ N, Aktaş M, Sarı E (1998) Karadeniz’de Ağır Metal Kirliliği. Project no: YDEBÇAG-456/G-457/G (in Turkish)
- Ürkmez D, Sezgin M, Bat L (2014) Use of nematode maturity index for the determination of ecological quality status: a case study from the Black Sea. *J Black Sea/Mediterr Environ* 20 (2):96–107
- Ürkmez D, Brennan ML, Sezgin M, Bat L (2015) A brief look at the free-living nematoda of the oxic/anoxic interface with a new genus record (*Trefusia*) for the Black Sea. *Oceanol Hydrobiol Stud* 44(4):539–551. <https://doi.org/10.1515/ohs-2015-0051>
- Ürkmez D, Sezgin M, Karaçuha ME, Öksüz İ, Kayağan T, Bat L, Dağlı E, Şahin F (2016) Within-year spatio-temporal variation in meiofaunal abundance and community structure, Sinop Bay, the Southern Black Sea. *Oceanol Hydrobiol Stud* 45(1):55–65. <https://doi.org/10.1515/ohs-2016-0006>
- Üstünada M, Erduğan H, Yılmaz S, Akgül R, Aysel V (2011) Seasonal concentrations of some heavy metals (Cd, Pb, Zn and Cu) in *Ulva rigida* J. Agardh (Chlorophyta) from Dardanelles (Çanakkale, Turkey). *Envi Monit Ass* 177:337–342
- Villares R, Puente X, Carballeira A (2002) Seasonal variation and background levels of heavy metals in two green seaweeds. *Environ Pollut* 119:79–90
- Wallentinus I (1984) Partitioning of nutrient uptake between annual and perennial seaweeds in a Baltic archipelago area. *Hydrobiologica* 116(117):363–370
- Water Framework Directive (2000) Directive 2000/60/EC of the European Parliament and of the Council of 23 October 2000 establishing a framework for Community action in the field of water policy
- Yalçın MG, Şimşek G, Ocak SB, Yalçın F, Kalaycı Y, Karaman ME (2013) Multivariate statistics and heavy metals contamination in beach sediments from the Sakarya Canyon, Turkey. *Asian J Chem* 25(4):2059–2066
- Yiğiterhan O, Murray JW (2008) Trace metal composition of particulate matter of the Danube River and Turkish rivers draining into the Black Sea. *Mar Chem* 111(1–2):63–76
- Yiğiterhan O, Murray JW, Tuğrul S (2011) Trace metal composition of suspended particulate matter in the water column of the Black Sea. *Mar Chem* 126(1–4):207–228
- Yücesoy Eryılmaz F, Ergin M (1992) Heavy-metal geochemistry of surface sediments from the southern Black Sea shelf and upper slope. *Chem Geol* 99(4):265–287
- Zaitsev Y (2008) An introduction to the Black Sea ecology. Smil Editing and Publishing Agency, Odessa, p 228
- Zaitsev Y, Mamaev V (1997) Marine biological diversity in the Black Sea. A study of change and decline. *GEF Black Sea Environ Ser* 3:208
- Zeri C, Voutsinou-Taliadouri F, Romanov AS, Ovsjany EI, Moriki A (2000) A comparative approach of dissolved trace element exchange in two interconnected basins: Black Sea and Aegean Sea. *Mar Pollut Bull* 40(8):666–673

Chapter 19

Geospatial Assessment of Groundwater Quality for Drinking through Water Quality Index and Human Health Risk Index in an Upland Area of Chota Nagpur Plateau of West Bengal, India



**Baisakhi Chakraborty, Sambhunath Roy, Amit Bera,
Partha Pratim Adhikary, Biswajit Bera, Debashish Sengupta,
Gouri Sankar Bhunia, and Pravat Kumar Shit**

Abstract Groundwater quality is directly related to human health. Therefore, analysis of groundwater quality and its effect on human health in any area on a spatial scale are very important. It is even more important in an undulating area where topography, land use, human settlement and aquifer parameters vary on a short distance. Such an area is the Nituria block of Purulia district where an investigation on groundwater quality for drinking purpose has been carried. 52 groundwater samples were collected during pre-monsoon and post-monsoon seasons to estimate hydro-chemical characteristics and its suitability to human health. Drinking water suitability is analysed by a composite Water Quality Index based on standard limit of

B. Chakraborty (✉) · S. Roy · P. K. Shit
PG Department of Geography, Raja N. L. Khan Women's College (Autonomous),
Vidyasagar University, Midnapore, West Bengal, India

A. Bera
Department of Earth Sciences, Indian Institute of Engineering Science and Technology,
Shibpur, West Bengal, India
e-mail: amit.rs2017@geology.iiests.ac.in

P. P. Adhikary
ICAR-Indian Institute of Water Management, Bhubaneswar, Odisha, India

B. Bera
Department of Geography, Sidho Kanho Birsha University, Purulia, India

D. Sengupta
Department of Geology and Geophysics, Indian Institute of Technology (IIT), Kharagpur,
West Bengal, India
e-mail: dsgg@gg.iitkgp.ac.in

G. S. Bhunia
Seacom Skill University, Birbhum, West Bengal, India

© Springer Nature Switzerland AG 2021

P. K. Shit et al. (eds.), *Spatial Modeling and Assessment of Environmental Contaminants*, Environmental Challenges and Solutions,
https://doi.org/10.1007/978-3-030-63422-3_19

each parameter for drinking purpose set by Bureau of Indian Standard. Groundwater of this area is partially contaminated and the origin of contamination is geogenic. Different multivariate analysis of groundwater as well as piper trilinear diagram shows active cations and anions are the determinant factors to control groundwater quality. It suggests interaction of minerals with groundwater is the principal cause of water quality changes along with secondary anthropogenic contribution. The overall Water Quality Index ranges from 59.40 to 171.43. 'Sabari' (171.43) and 'Purana Panchakot' (168.21) village indicates highest Water Quality Index value during pre- and post-monsoon seasons, respectively. GIS analysis shows most of the area falls under 'good' to 'moderate' water quality zone. Human health risk due to intake of Fe and F^- was assessed by following the USEPA method. Health Hazard Index during pre-monsoon period indicates that 88.46% and 94.23% groundwater samples are at noncarcinogenic health risk zone for male and female, respectively. During post-monsoon season, 69.23% and 78.84% samples were under noncarcinogenic health risk for male and female, respectively. This study identified the hot spots of groundwater contamination where remedial measures as suggested in this work can be undertaken.

Keywords Chota Nagpur plateau · Groundwater quality · Hazard Index · Health risk · Hydro-chemical characteristics

19.1 Introduction

The safest source of water resource is situated under the earth surface, called as groundwater. It is naturally colourless, odour free and lucid which occupies only one fifth of the total water resource of the world (Saatsaz et al. 2011). Groundwater contributes a lot to sustain life and socio-economic development of the people and it has been considered as the purest form of drinking water. The majority of the population in urban and rural India directly depend on groundwater resource for their drinking purpose. This valuable and precious natural resource is now facing continuous deterioration of its quality by various natural and anthropogenic pollution or contamination which changes its quality to hazardous for health. Rising number of population and socio-economic activities like agriculture, industry, domestic waste, etc. terribly affects the quality of groundwater in twenty-first century (Nagaraju et al. 2018; Shaji et al. 2018). Continuous drinking of contaminated groundwater often causes various chronic diseases to the human body and sometimes becomes responsible for death. Therefore, assessment of groundwater quality and its degree of pollution is very relevant to make awareness of the people for health consciousness and suitable management of water resources for remediation.

Many researches have been conducted in various parts of the world to analyse groundwater quality for drinking purpose (Rao et al. 1997; Umar et al. 2006; Pandian and Sankar 2007; Raju 2007). Groundwater suitability is based on

hydro-chemical characteristics which are generally combined with various chemical components and therefore a large amount of data is required for its assessment (Naseem et al. 2011; Hossein 2004; Afzali et al. 2014). The source of groundwater, process of ion exchange and aquifer media plays very important role to govern the hydro-chemical characteristics of groundwater (Kundu and Nag 2018). Any changes in the concentration of components in groundwater can bring many health related problems to the human body and thus standard limit of various chemical components in drinking water has been prescribed by WHO, BIS and many other agencies in various countries for public health. Many studies on groundwater have been carried out by researchers for health purpose (Jalali 2006; Al-Futaisi et al. 2007; Pritchard et al. 2008; Ishaku 2011). In India, many researchers have been conducted with standard geostatistical method for groundwater suitability (Subba Rao 2002; Kumar and Ahmed 2003; Ramakrishnaiah et al. 2009; Tiwari 2011; Singh et al. 2012; Nag and Ghosh 2013; Nag and Das 2017; Priyanka et al. 2017; Nishi et al. 2018). Water Quality Index (WQI) is very useful to determine groundwater suitability (Batabyal and Chakraborty 2015; Kundu and Nag 2018). It is a mathematical model where a large complex data has been processed to integrate in a single score using standard limit of parameters for drinking water suitability.

Many researches have been proved that excess concentration of fluoride in drinking water affects people of many region especially in South India (Subba Rao et al. 2012; Adimalla and Li 2018; Narsimha and Sudarshan 2017). In India, about 66 million people seriously suffer from 'fluorosis' disease through high intake of F^- with drinking water (Adimalla et al. 2018a, b). Multivariate data analyses such as Hierarchical Cluster Analysis (HCA) and Principal Component Analysis (PCA) have been performed by many researchers for assessment of hydro-chemical characteristics of groundwater (Singh et al. 2004; Zhang et al. 2012). Advance GIS based groundwater modelling and mapping have popularly followed by many researchers in their study for spatial analysis of water quality (Brindha and Elango 2012; Shanmugasundharam et al. 2015).

Development of industries and settlement in mining areas leads to pollution on the groundwater and thus its quality goes down very drastically. Nituria block of Purulia district is highly enriched with minerals like coal and iron in Damodar river basin with fertile soils. Therefore, this block is developing its mining sector as well as agriculture. In this socio-economic condition where industry and agriculture both have been spread equally, the quality of groundwater and its risk potentiality to human health have never been analysed. Thus, the objective of the present study is to assess the groundwater quality using WQI and various statistical methods and to identify human health risk (HHR) by applying GIS technology for adoption of suitable management strategies.

19.2 Study Area

Nituria block is situated under the catchment of river Damodar in the northern part of Purulia district. The geographical extent of this block is $23^{\circ}41'51''N$ to $23^{\circ}34'19''N$ and $86^{\circ}36'25''E$ to $86^{\circ}51'19''E$ with an area of 203.65 km^2 . This block consists of 124 mouzas with 110 villages and 3 census towns (Fig. 19.1). River Damodar separates Nituria block from Paschim Bardhaman district of West Bengal in the north and Dhanbad district of Jharkhand in north-west. The entire block is situated on the Damodar Dwaraka upland of chota Nagpur plateau with undulating surface and scattered monadnocks. Geological structure of this block consists of granite-gneiss, mica-schist, phyllite and coal bearing sandstone, shale of Gondwana series,

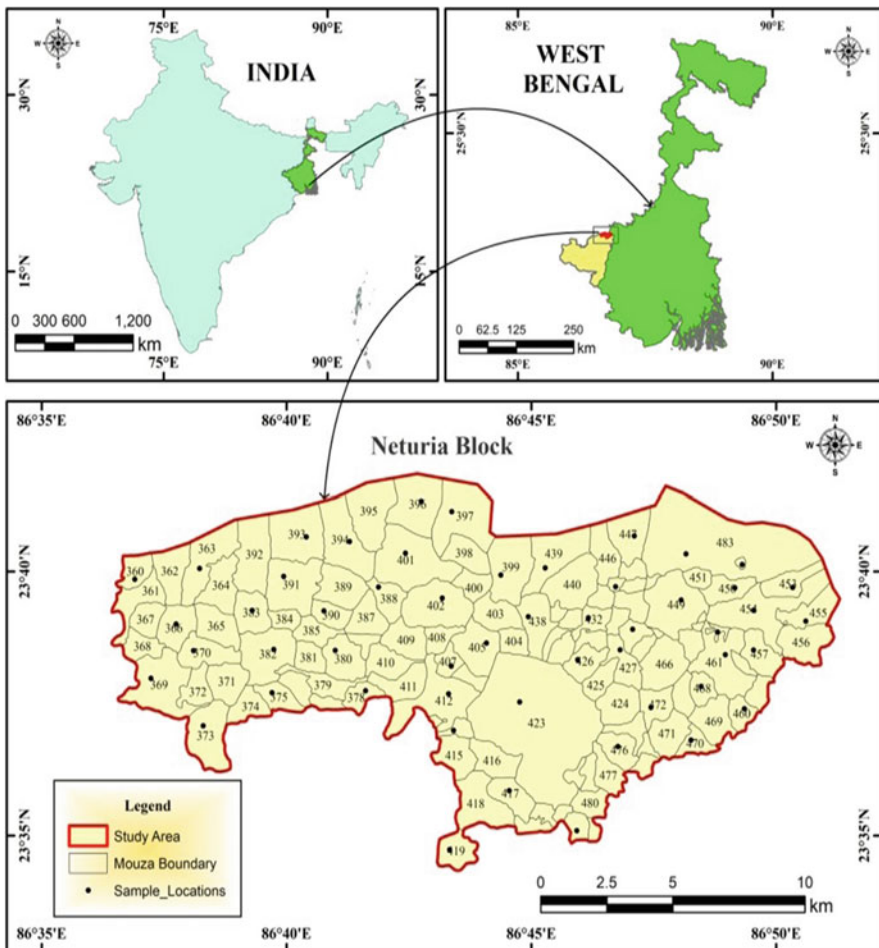


Fig. 19.1 Location map of the study area

etc. Groundwater appears generally as unconfined and semi-confined conditions and it recharges mainly by precipitation. Dug well, bore well are commonly used by the local people for extraction of groundwater. Climatically, this block faces scorching heat in summer season (March to May). In winter season (November to February), this block experiences dry and cold weather. Average temperature recorded as 5–6 °C in cold season and 45–50 °C in summer season. Rainfall occurs in monsoon period from June to October with 1300–1400 mm average rainfall. The soil of this block is made of laterite and covered with alluvial deposition of river Damodar. Dry deciduous forest with sal, palms, dates, palash like principal species mainly found in this region.

19.3 Materials and Methods

Methodological flow chart of the present study has been given in Fig. 19.2.

19.3.1 Sample Collection and Measurement

Groundwater samples were obtained from 52 different locations in pre-monsoon (March–May) and post-monsoon (November–February) period of 2019 by field observations. All sample locations were recorded by Global Positioning System

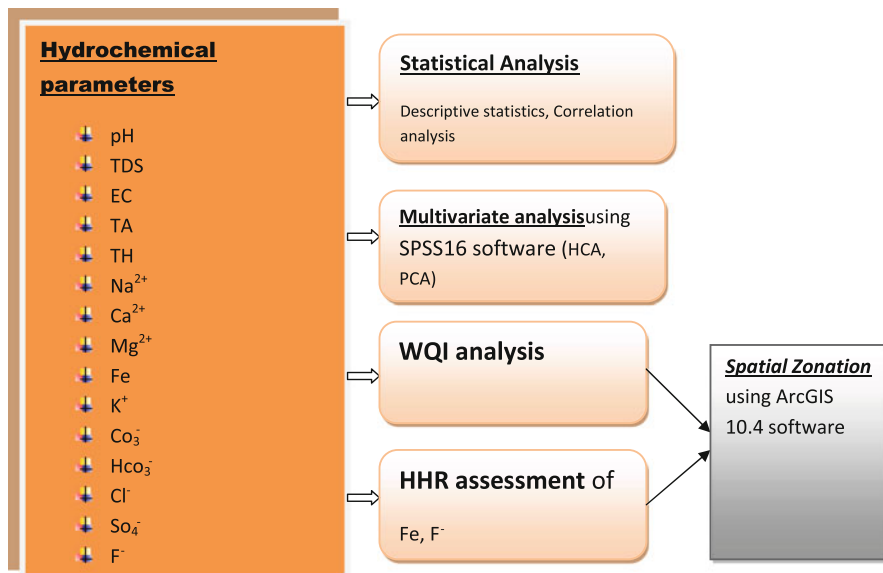


Fig. 19.2 Methodological flow chart of the groundwater quality assessment

instrument (GARMINGPSmap 78 s). Collecting bottles were pre-washed by 1:1 hydrochloric acid and cleaned with distilled water. Each bottle contained 500 ml sample water from 52 tube wells of different villages. All samples were analysed by standard method of APHA (2012). Portable water quality meter was used to measure the pH and electronic conductivity (EC) of the sample water at the site immediately. TDS was measured by multiplying EC with a factor of 0.64. Total Hardness (TH) and Ca^{2+} were measured by EDTA titration method. Difference of TH and Ca^{2+} values indicates the concentration of Mg^{2+} in each sample. Values of Na^{2+} and K^{+} were measured from flame photometer. Anions such as HCO_3^{-} and CO_3^{-} were measured by HCL volumetric method. Spectrophotometric techniques were used to determine SO_4^{2-} and F^{-} . Cl^{-} was estimated by titration method of AgNO_3 . Concentrations of all the parameters were expressed in mg/l except pH and EC.

19.3.2 Statistical Analysis

Hierarchical cluster analysis (HCA) is one of the popular types of multivariate analysis which has been used to classify various sample of groundwater into different groups or cluster based on their similarity (Zhang et al. 2012). Principal component analysis (PCA) is also an effective tool for groundwater chemical analysis by reduction of large number of variables or chemical parameters of groundwater (Keshavarzi et al. 2011). Both HCA and PCA analyses were computed by using SPSS16 software.

19.3.3 Piper's Diagram

Piper trilinear diagram (Piper 1944) is used to determine drinking water suitability by graphically representing the distribution of anions and cations on two separate ternary plots. These plots are extrapolated onto a diamond diagram. This method is helpful to generating idea about chemical intensity of groundwater for health purpose.

19.3.4 Water Quality Index (WQI)

Water quality index is a reliable technique to analyse the quality of groundwater. The weightage system of each physio-chemical parameter indicates different influence on groundwater quality (Batabyal and Chakraborty 2015).

First of all, weight (wi) has been given to all of the groundwater quality parameters. Highest weight (5) has been given to pH, TDS, SO_4^{-} and F^{-} because of its major influence and minimum weight (1) has been given to K^{+} for its less

significance on overall groundwater quality. EC, TA, TH, Na^{2+} , Ca^{2+} , Mg^{2+} , Fe^{-} , CO_3^{2-} , HCO_3^{2-} , Cl^{-} have got their weight as relative importance on water quality.

Secondly, relative weight (W_i) of each parameter is calculated by using the following formula (Mukherjee et al. 2012):

$$W_i = w_i / \sum w_i \quad (19.1)$$

where W_i is relative weight of each parameter and w_i is weight of each parameter.

Thirdly, the quality rating scale (q_i) is computed according to the guidelines by BIS for drinking water standards (BIS 2012). For computing q_i , concentration of each chemical parameter in every sample is divided by its respective standards laid by BIS (2012) and the output is multiplied by 100.

$$q_i = (c_i \times s_i) \times 100 \quad (19.2)$$

where q_i denotes quality rating, c_i denotes concentration of each chemical parameter in each sample (mg/l), s_i denotes drinking water standard for each parameter (mg/l).

Next, the sub-index (SI) is computed for measuring the WQI of each sample by using the following formula:

$$\text{SI} = (q_i \times w_i) \quad (19.3)$$

And finally, WQI is calculated from summation of each SI of every sample:

$$\text{WQI} = \sum \text{SI} \quad (19.4)$$

where Si is the sub-index of each parameter and q_i is the quality of each parameter.

The WQI is classified into four groups according to its suitability for drinking water as 'very poor', 'poor', 'moderate' and 'good'. ArcGIS 10.4 software has been used to generate map of WQI on the basis of pre- and post-monsoon data. All the data of WQI were interpolated by using inverse distance weighted (IDW) method for generating WQI distribution map. IDW has been chosen for its accuracy on mapping because on this method the weight of each pixel gradually decreased from its output pixel. The values of WQI are divided into four groups and spatial distribution of WQI maps on pre-monsoon and post-monsoon periods was generated.

19.3.5 Human Health Risk Assessment (HHR)

Health risk assessment on human body due to intake of contaminated water is a very vital work to evaluate the probable adverse effects of a particular chemical component on human body over a certain time period (Li et al. 2014; Adimalla 2018a, b; Wu and Sun 2016). Higher concentration of ferrous and fluoride in drinking water

gives harmful impact on human body after long term consumption. Therefore, in this study the noncarcinogenic health risk has been assessed for Fe and F^- in the study region over male and female adult residents. The United States Environment Protection Agency (USEPA 1989) introduced a standard method for HHR assessment and has been widely accepted (Adimalla and Rajitha 2018; Li et al. 2016). Risk assessment has been calculated by the following formula (Adimalla 2018a, b).

$$CDI = \frac{CPW \times IR \times ED \times EF}{ABW \times AET} \quad (19.5)$$

$$HQ = \frac{CDI}{RfD} \quad (19.6)$$

$$\Sigma HI = \sum (HI_{Fe} + HI_F) \quad (19.7)$$

where CDI indicates chronic daily intake of chemical (mg/kg/day). CPW indicates concentration of Fe and F^- in drinking water. IR is ingestion rate for adults (male and female), i.e. 2.5 l/day. ED indicates exposure duration as 64 years for adults. EF is exposure frequency which is 365 days because all residents are depending on groundwater for drinking on the whole year. Average body weight (ABW) is 65 kg for male and 55 kg for female. Average time (AET) is 10,950 for adults. HQ is Hazard Quotient and RfD is reference dose. Reference dose of Fe is 0.70 mg/kg/day and F^- is 0.06 mg/kg/day (USEPA 2014). The value of HQ and HI greater than 1 (>1) indicates health risk for human body.

19.4 Results and Discussion

19.4.1 Hydro-chemical Analysis

Groundwater hydrochemistry is shown in descriptive statistics for clear observation of their characteristics in pre-monsoon (Table 19.1) and post-monsoon (Table 19.2) periods. The pH in groundwater samples ranged from 6.02 to 7.06 with an average of 6.75 ± 0.54 in pre-monsoon season appears as slightly neutral in nature. In the post-monsoon season, the pH value ranged from 6 to 7.67 with an average of 6.84 ± 0.43 , also neutral in nature. Concentrations of TDS and EC ranged from 140 to 1070 ml/l and 240 to 1400 $\mu\text{S/cm}$ with an average value of 511.15 ± 249.04 ml/l and 884.80 ± 293.43 $\mu\text{S/cm}$, respectively, in pre-monsoon period. In post-monsoon season TDS ranged from 270 to 1300 mg/l with an average of 862.84 ± 242.36 mg/l and EC ranged from 340 to 2400 $\mu\text{S/cm}$ with an average value of 947.69 ± 431.78 $\mu\text{S/cm}$. This value of TDS and EC shows that mixing of minerals in groundwater has been increased in post-monsoon season. In pre-monsoon season TA and TH show their ranges from 110 to 420 mg/l and 134 to 1401 mg/l with an average value of 202.53 ± 79.47 mg/l and 591.05 ± 320.87 mg/l, respectively. In post-monsoon season, concentration of TA

Table 19.1 Descriptive statistics of hydro-chemical parameters (pre-monsoon season)

Parameters	Mean	Std. Dev	Kurtosis	Skewness	Range	Minimum	Maximum	Sum	Count
pH	6.75	0.54	-1.13	0.45	1.94	6.02	7.96	351.15	52.00
TDS	511.15	249.04	-0.81	0.44	930.00	140.00	1070.00	26580.00	52.00
EC	884.81	293.43	-0.38	-0.19	1160.00	240.00	1400.00	46010.00	52.00
TA	202.54	79.48	-0.22	0.95	310.00	110.00	420.00	10532.00	52.00
TH	591.06	320.88	-0.62	0.46	1267.00	134.00	1401.00	30735.00	52.00
Na ²⁺	30.54	12.46	-0.62	0.10	49.00	8.00	57.00	1588.00	52.00
Ca ²⁺	139.04	97.34	-1.04	0.80	312.00	28.00	340.00	7230.00	52.00
Mg ²⁺	51.94	36.88	0.54	0.88	161.00	3.00	164.00	2701.00	52.00
Fe	7.70	5.12	-1.43	0.46	15.33	1.21	16.54	400.19	52.00
K ⁺	41.21	18.19	-0.96	0.07	74.00	10.00	84.00	2143.00	52.00
CO ₃ ⁻	63.19	27.01	-0.12	0.42	122.00	20.00	142.00	3286.00	52.00
HCO ₃ ⁻	247.06	69.53	-0.76	-0.06	283.00	104.00	387.00	12847.00	52.00
Cl ⁻	128.40	87.62	0.53	1.30	302.00	45.00	347.00	6677.00	52.00
SO ₄ ⁻	59.15	19.82	-0.07	-0.43	83.00	14.00	97.00	3076.00	52.00
F ⁻	0.76	0.36	-1.08	0.30	1.22	0.14	1.36	39.56	52.00

Table 19.2 Descriptive statistics of hydro-chemical parameters (post-monsoon season)

Parameters	Mean	Std. Dev	Kurtosis	Skewness	Range	Minimum	Maximum	Sum	Count
pH	6.84	0.44	-1.00	0.20	1.67	6	7.67	355.92	52
TDS	862.85	242.37	0.15	-0.61	1030	270	1300.00	44,868	52
EC	947.69	431.79	2.56	1.46	2060	340	2400.00	49,280	52
TA	513.06	166.60	0.37	0.64	730	240	970.00	26,679	52
TH	425.08	264.81	-0.57	0.80	884	101	985.00	22,104	52
Na ²⁺	57.79	24.70	-1.13	0.05	90	14	104.00	3005	52
Ca ²⁺	71.17	44.82	4.77	2.00	228	17	245.00	3701	52
Mg ²⁺	78.12	37.70	0.04	1.07	131	35	166.00	4062	52
Fe	6.32	5.19	-1.36	0.56	15.31	0.14	15.45	328.74	52
K ⁺	2.40	1.03	-0.18	0.30	4.74	0.38	5.12	124.95	52
CO ₃ ⁻	91.88	38.58	1.12	1.04	170	34	204.00	4778	52
HCO ₃ ⁻	163.71	77.37	-0.35	0.73	281	64	345.00	8513	52
Cl ⁻	81.25	29.10	-0.65	0.34	108	34	142.00	4225	52
SO ₄ ⁻	69.10	24.13	-0.11	0.62	103	27	130.00	3593	52
F ⁻	0.75	0.41	-1.51	0.33	1.2	0.24	1.44	38.99	52

and TH ranged from 240 to 970 mg/l and 101 to 985 mg/l with average value of 513.05 ± 166.6 mg/l and 425.07 ± 264.81 mg/l, respectively.

The cation concentration such as Na^{2+} , Ca^{2+} , Mg^{2+} , K^{+} are ranged from 8 to 57 mg/l, 28 to 340 mg/l, 3 to 164 mg/l and 10 to 84 mg/l with average values of 30.53 ± 12.45 mg/l, 139.03 ± 97.34 mg/l, 51.94 ± 36.88 mg/l and 41.21 ± 18.18 mg/l, respectively. The mean value of these cations shows the order of average concentration as $\text{Ca}^{2+} > \text{Mg}^{2+} > \text{K}^{+} > \text{Na}^{2+}$ in pre-monsoon. In the post-monsoon season the presence of Na^{2+} , Ca^{2+} , Mg^{2+} and K^{+} ranged from 14 to 104 mg/l, 17 to 245 mg/l, 35 to 166 mg/l and 0.38 to 5.12 mg/l with average values of 57.78 ± 24.70 mg/l, 71.17 ± 44.81 mg/l, 78.11 ± 37.70 mg/l, 2.40 ± 1.02 mg/l, respectively. The order of average concentration may be arranged as $\text{Mg}^{2+} > \text{Ca}^{2+} > \text{Na}^{2+} > \text{K}^{+}$. The anion distribution of groundwater in study area reveals the value of CO_3^{2-} , HCO_3^{-} , Cl^{-} and SO_4^{-} are ranged from 20 to 142 mg/l, 104 to 387 mg/l, 45 to 347 mg/l and 14 to 97 mg/l with average values of 63.19 ± 27.01 mg/l, 247.05 ± 69.53 mg/l, 128.40 ± 87.61 mg/l and 59.15 ± 19.81 mg/l in pre-monsoon season. In this season the order of mean values of anions may be arranged as $\text{HCO}_3^{-} > \text{Cl}^{-} > \text{CO}_3^{-} > \text{SO}_4^{-}$. In post-monsoon season CO_3^{-} , HCO_3^{-} , Cl^{-} and SO_4^{-} are ranged from 34 to 204 mg/l, 64 to 345 mg/l, 34 to 142 mg/l, and 27 to 130 mg/l with averages of 91.88 ± 38.57 mg/l, 163.71 ± 77.36 mg/l, 81.25 ± 29.09 mg/l and 69.09 ± 24.12 mg/l, respectively. The major anion concentration order may be arranged as $\text{HCO}_3^{-} > \text{CO}_3^{-} > \text{Cl}^{-} > \text{SO}_4^{-}$ in post-monsoon season.

Two very important parameters, Fe and F^{-} give significant impacts on quality of groundwater. The values of Fe and F^{-} ranged from 1.21 to 16.54 mg/l and 0.14 to 1.36 mg/l with average values of 7.69 ± 5.12 mg/l and 0.76 ± 0.35 mg/l, respectively, in pre-monsoon period. On the other hand, the values of Fe ranged from 0.14 to 15.45 mg/l with average value of 6.32 ± 5.18 mg/l and values of F^{-} is ranged from 0.24 to 1.44 mg/l with an average value of 0.74 ± 0.40 mg/l in post-monsoon.

19.4.2 Correlation Analysis

Correlation analysis is a powerful tool of statistics which explains the interrelation between two parameters and indicates the dependency of each parameter to others to control water quality (Chapman 1996; Zeng and Rasmussen 2005; Box et al. 1978). In the present study correlation matrix is shown for pre-monsoon (Table 19.3) and post-monsoon seasons (Table 19.4). In the pre-monsoon period correlation coefficient result shows that there was a moderately high positive correlation in pH with TH ($r = 0.53$) and Fe ($r = 0.73$). TH is also highly related with Ca^{2+} and Cl^{-} . Cl^{-} is highly related with TA, Na^{2+} , Fe and CO_3^{-} . Fe is highly related with TDS, EC, TA, TH, Na^{2+} , Ca^{2+} , Mg^{2+} . Fe indicates the most dominant parameter of water quality in pre-monsoon season. In post-monsoon period high positive correlation was found between TH and Mg^{2+} ($r = 0.60$), TH and CO_3^{-} ($r = 0.62$), and TH with Fe ($r = 0.71$). CO_3^{-} has high positive relation with Na^{2+} , HCO_3^{-} and Fe in this season.

Table 19.3 Correlation analysis of groundwater quality parameters in pre-monsoon

Parameters	pH	TDS	EC	TA	TH	Na ²⁺	Ca ²⁺	Mg ²⁺	Fe	K ⁺	CO ₃ ⁻	HCO ₃ ⁻	Cl ⁻	SO ₄ ⁻	F ⁻
pH	1														
TDS	0.46	1													
EC	0.40	0.37	1												
TA	0.45	0.29	0.37	1											
TH	0.53 *	0.47	0.41	0.44	1										
Na ²⁺	0.41	0.31	0.45	0.40	0.47	1									
Ca ²⁺	0.31	0.29	0.35	0.37	0.51 *	0.48	1								
Mg ²⁺	0.42	0.26	0.45	0.29	0.38	0.50 *	0.26	1							
Fe	0.73 *	0.52 *	0.55 *	0.59 *	0.68 *	0.60 *	0.57 *	0.57 *	1						
K ⁺	0.16	-0.02	0.09	0.23	0.07	0.13	0.18	0.02	0.10	1					
CO ₃ ⁻	0.29	0.41	0.30	0.32	0.38	0.45	0.47	0.54 *	0.55 *	-0.06	1				
HCO ₃ ⁻	0.32	0.11	0.02	0.19	0.13	0.06	0.05	0.12	0.21	0.04	0.09	1			
Cl ⁻	0.40	0.36	0.44	0.57 *	0.54 *	0.56 *	0.48	0.41	0.58 *	0.14	0.52 *	0.03	1		
SO ₄ ⁻	0.25	0.15	0.11	0.21	0.20	0.20	0.12	0.18	0.12	0.06	0.14	0.17	0.26	1	
F ⁻	0.45	0.43	0.38	0.25	0.49	0.39	0.29	0.20	0.53	0.12	0.29	0.20	0.22	0.29	1

Bold values indicate correlation greater than 0.50%

Table 19.4 Correlation analysis of groundwater quality parameters in post-monsoon season

Parameters	pH	TDS	EC	TA	TH	Na ²⁺	Ca ²⁺	Mg ²⁺	Fe	K ⁺	CO ₃ ⁻	HCO ₃ ⁻	Cl ⁻	SO ₄ ⁻	F ⁻
pH	1.00														
TDS	0.33	1.00													
EC	0.28	0.37	1.00												
TA	0.20	0.20	0.06	1											
TH	0.16	0.43	0.33	0.13	1										
Na ²⁺	0.12	0.12	0.37	0.23	0.43	1									
Ca ²⁺	0.35	0.47	0.24	0.09	0.37	0.24	1								
Mg ²⁺	0.31	0.28	0.20	0.11	0.60*	0.21	0.10	1							
Fe	0.32	0.44	0.58*	0.29	0.71*	0.57*	0.49	0.54*	1						
K ⁺	0.11	0.10	0.35	0.10	0.31	0.25	0.25	0.24	0.36	1					
CO ₃ ⁻	0.33	0.34	0.31	0.33	0.62*	0.50*	0.19	0.49	0.60*	0.37	1				
HCO ₃ ⁻	0.34	0.39	0.33	0.20	0.35	0.38	0.36	0.32	0.52*	0.30	0.51*	1			
Cl ⁻	0.38	0.41	0.49	0.06	0.47	0.47	0.29	0.44	0.51*	0.27	0.48	0.44	1		
SO ₄ ⁻	0.44	0.36	0.36	0.36	0.38	0.18	0.39	0.21	0.45	0.23	0.34	0.50*	0.33	1	
F ⁻	0.31	0.32	0.38	0.23	0.39	0.20	0.27	0.30	0.43	0.24	0.20	0.14	0.28	0.41	1

Bold values indicate correlation greater than 0.50%

HCO_3^- indicates moderate positive correlation with Fe and SO_4^- in post-monsoon season. All positive values of correlation (r) greater than 0.5 have been marked by an asterisk in the correlation matrix.

19.4.3 *Multivariate Statistical Analysis*

19.4.3.1 **Hierarchical Cluster Analysis**

In many hydro-chemical studies multivariate analysis has been used to determine water quality (Das and Nag 2017). Hierarchical cluster analysis is one of the best multivariate analyses where multiple parameters or samples were arranged as cluster based on their similarity (Routroy et al. 2013; Singh et al. 2005). In the present study, 52 groundwater samples were classified into 4 subgroups and 2 groups and plotted in dendrogram by using HCA analysis in SPSS 16 software for pre-monsoon (Fig. 19.3) and post-monsoon (Fig. 19.4). Average linkage (between groups) was used for clustering among the samples and Squared Euclidean distance method was used for measuring distance of linkage. In the pre-monsoon season, a large number of samples are clustered in first group. In this group very close similarity has found among sample number 23, 25, 6, 41, 12, 14, 33, 31, 44, 24, 27, 34, 7, 26, 19, 5, 21 and 22 (subgroup 1). Group 1 comprise mainly with HCO_3^- - Cl^- - SO_4^- type of water. High values of EC, TA, TH, HCO_3^- and Cl^- indicates high cation exchange between groundwater and sediment of aquifer at those sampling point in this season. Another close similarity has been found among sample number 9, 10, 2, 8, 35, 39, 48, 49, 4, 13 (subgroup 2). Third subgroup has been found among sample number 43, 46, 20, 42, 17, 32, 15, 16, 50, 3, 45, 1 and 11. In dendrogram second group is showing strong similarity of water quality among sample number 18, 30, 29, 47, 51, 36, 37, 38, 52, 40 and 28 (subgroup 4). Second group comprise with mainly Ca^{2+} - CO_3^- - Cl^- type with high value of TH, Cl^- and Fe in groundwater of pre-monsoon season.

In post-monsoon season all of the groundwater samples out of 52 are clustered in the first group except sample number 36 and 37. Samples of group 1 is characterised with low concentration of cation and anion in water. This indicates lower presence of values of EC and TDS in groundwater samples. Sample no. 36 and 37 are comprised with high EC, TDS, Fe, Na^{2+} and Cl^- , indicates activity of chemical parameters that led to groundwater pollution.

19.4.3.2 **Principal Component Analysis**

Factor analysis is a very useful statistical tool for managing a large amount of data to reduce its variation. Principal component analysis (PCA) is a best model for factor analysis of multivariate data. Thereby, PCA is popularly used to groundwater

Dendrogram using Average Linkage (Between Groups)

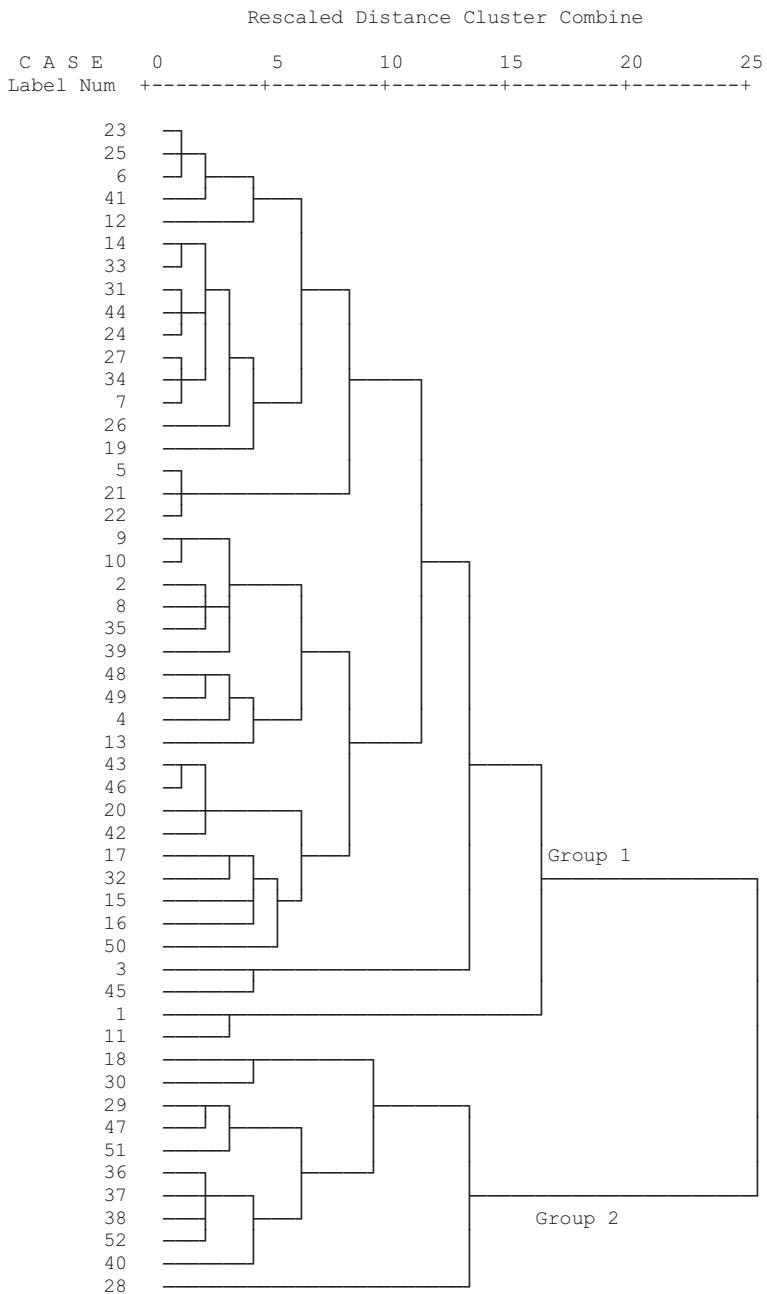


Fig. 19.3 Dendrogram using HCA of groundwater quality parameters for pre-monsoon season

Dendrogram using Average Linkage (Between Groups)

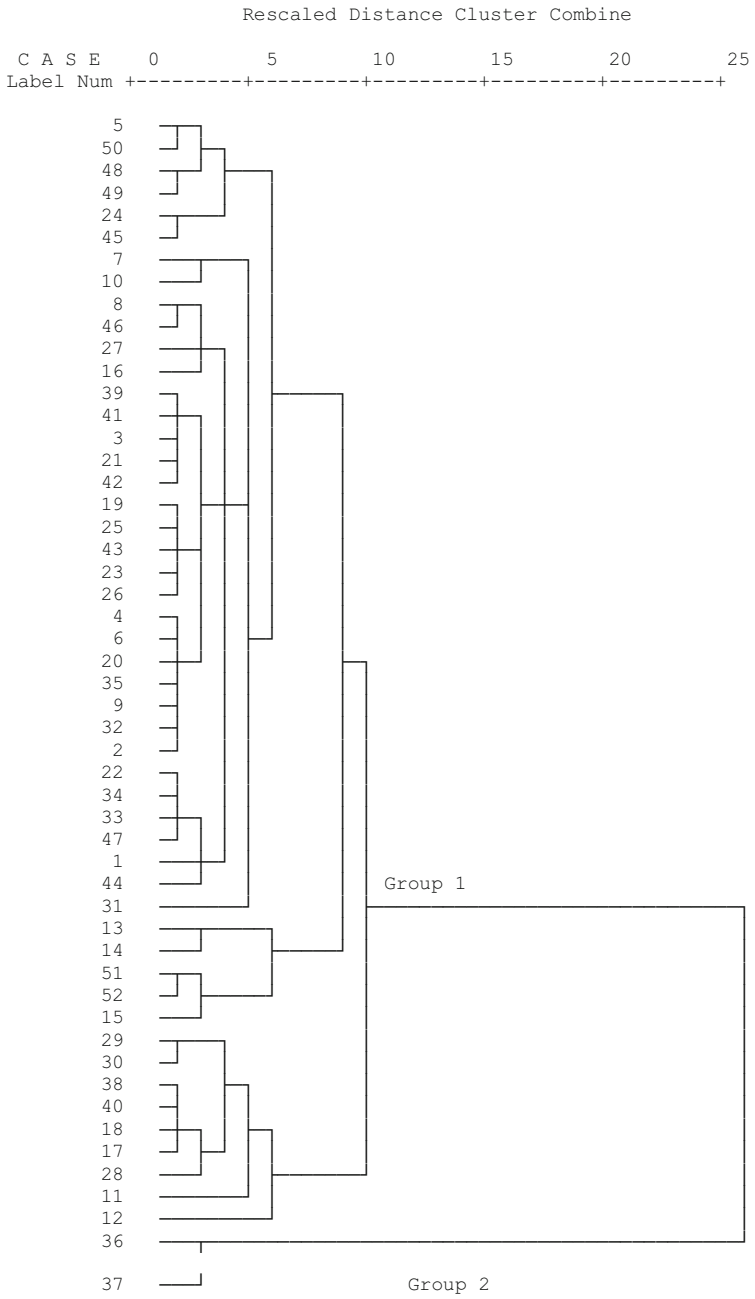


Fig. 19.4 Dendrogram using HCA of groundwater quality parameters for post-monsoon season

Table 19.5 Varimax rotation and factor loadings of pre-monsoon season

Variable	Factor1	Factor 2	Factor 3	Factor 4
pH	0.291	0.556	0.289	0.383
TDS	0.189	0.801	-0.045	0.032
EC	0.470	0.460	0.153	-0.080
TA	0.528	0.166	0.464	0.241
TH	0.534	0.532	0.114	0.152
Na ²⁺	0.702	0.285	0.177	0.016
Ca ²⁺	0.435	0.426	0.393	-0.224
Mg ²⁺	0.620	0.254	0.001	0.046
Fe	0.757	-0.120	-0.244	0.345
K ⁺	0.005	-0.086	0.837	0.066
CO ₃ ⁻	0.626	0.374	-0.078	-0.103
HCO ₃ ⁻	0.029	0.081	0.009	0.841
Cl ⁻	0.801	0.170	0.252	0.029
SO ₄ ⁻	0.032	0.294	0.259	0.379
F ⁻	0.181	0.629	-0.080	0.275
Eigen value	5.344	1.280	1.192	1.055
% variance	35.626	8.532	7.949	7.032
Cumulative % variance	35.626	44.158	52.107	59.140

analysis especially for identifying the leading cause of quality changes in water (Helena et al. 2000; Yidana 2010; Reghunath et al. 2002).

In the present study, PCA was performed by varimax rotation and Kaiser normalisation for both pre- and post-monsoon period using SPSS 16 software. In the pre-monsoon period varimax rotation of factor loadings has been shown in Table 19.5. Eigen values of four factors have been found greater than one in the PCA of pre-monsoon which were rotated in seven iteration. Factor 1 with 35.62% of the total variance shows high positive loadings of chloride, carbonate, iron, sodium, magnesium to the groundwater and very low contribution of bicarbonate, sulphate and potassium. This indicates active geogenic influence to the groundwater in pre-monsoon period. Factor 2 with 8.53% of total variance indicates high positive loadings of TDS, pH, fluoride, TH and negative loading of Fe and potassium. Factor 3 of 7.94% total variance indicates high positive loadings of potassium occurred by interaction of alkaline type feldspar to the groundwater. Negative loadings of TDS, Fe, CO₃⁻ indicate low presence of anion in the groundwater. Factor loading 4 with 7.03% of total variance shows high positive loading of bicarbonate and negative loading of EC, Ca²⁺, CO₃⁻ in the groundwater. The correlation analysis shows that there has negative relation among K⁺, Fe, CO₃⁻ and TDS in pre-monsoon season. Scree plot of pre-monsoon has been shown in Fig. 19.5.

In the post-monsoon season varimax rotation of factor loadings has been given in Table 19.6. Four components with Eigen value greater than one have been generated and rotations were converged in 7 iterations. Factor 1 with 38.79% of total variance shows high positive loadings of pH, TDS, Ca²⁺, SO₄⁻ and negative loading of Na⁺

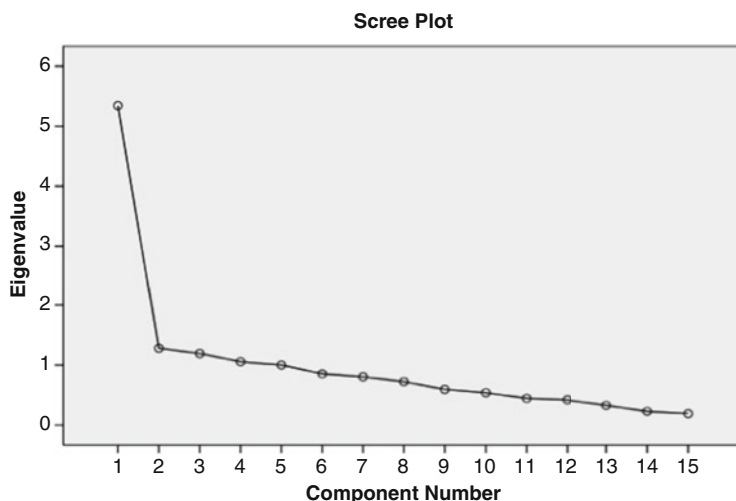


Fig. 19.5 Scree plot for pre-monsoon season

Table 19.6 Varimax rotation and factor loadings of post-monsoon season

Variable	Factor1	Factor 2	Factor 3	Factor 4
pH	0.664	-0.048	0.207	0.200
TDS	0.695	0.066	0.298	-0.023
EC	0.443	0.620	0.080	-0.156
TA	0.150	0.071	0.046	0.891
TH	0.266	0.358	0.720	0.023
Na ²⁺	-0.035	0.747	0.256	0.209
Ca ²⁺	0.682	0.314	-0.038	-0.056
Mg ²⁺	0.162	0.033	0.887	0.028
Fe	0.406	0.579	0.500	0.146
K ⁺	0.089	0.650	0.082	0.040
CO ₃ ⁻	0.110	0.442	0.626	0.378
HCO ₃ ⁻	0.385	0.449	0.243	0.266
Cl ⁻	0.372	0.448	0.476	-0.119
SO ₄ ⁻	0.660	0.203	0.068	0.421
F ⁻	0.540	0.145	0.208	0.107
Eigen value	5.819	1.381	1.114	1.029
% variance	38.794	9.204	7.426	6.858
Cumulative % variance	38.794	47.998	55.425	62.283

in this season. Factor 2 with 9.20% of total variance indicates negative loading of pH and high positive loading of potassium, TDS, Na⁺ in groundwater. Moderate loading of TH, Ca²⁺, Fe, CO₃⁻, HCO₃⁻, Cl⁻ indicates decrease of ion concentration and improvement of groundwater quality. Factor 3 explains 7.42% of total variance that indicates negative loading of Ca²⁺ and high positive loading of TH, Mg²⁺ and CO₃⁻

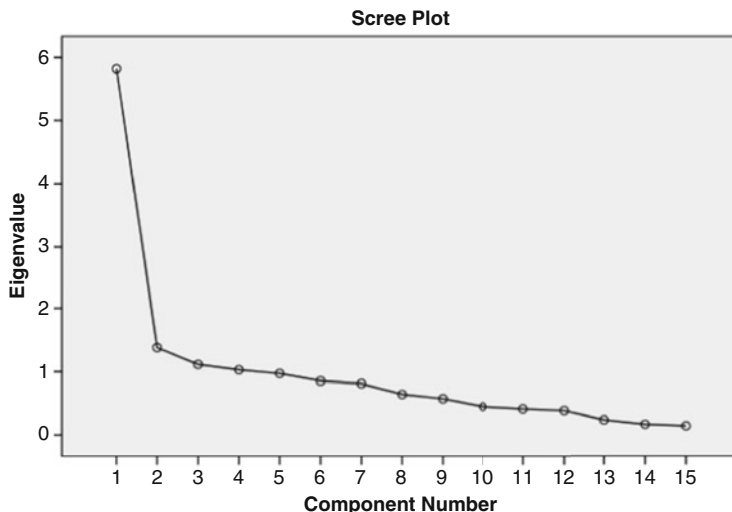


Fig. 19.6 Scree plot of post-monsoon season

in groundwater. Factor 4 with 6.85% of total variance shows negative loading of TDS, EC, Ca^{2+} and Cl^{-} in groundwater. High positive loading of TA indicates increase of alkaline ion in groundwater on this season. Scree plot of post-monsoon season has been shown in Fig. 19.6.

19.4.4 Piper Diagram

Concentration of cation and anion indicates the type of groundwater for its suitability to use. Piper trilinear diagram (Piper 1944) was used to analyse chemical concentration of the groundwater in present study area. Piper diagram of pre-monsoon season (Fig. 19.7a) shows that almost 85% of samples are magnesium bicarbonate type of water (weak acids exceed strong acids) which is considered for drinking water suitability. 15% of samples are mixed type of water (strong acid exceeds weak acid) which is generally not suitable for healthy drinking water. In the post-monsoon season piper diagram (Fig. 19.7b) indicates most of water samples (96%) are bicarbonate type or fresh water type and only 5% of samples are mixed type for drinking purpose.

19.4.5 Water Quality Index (WQI) Assessment

WQI of pre- and post-monsoon period has been analysed by using standard limit of chemical concentration of each parameter prescribed by BIS (2012). The weights

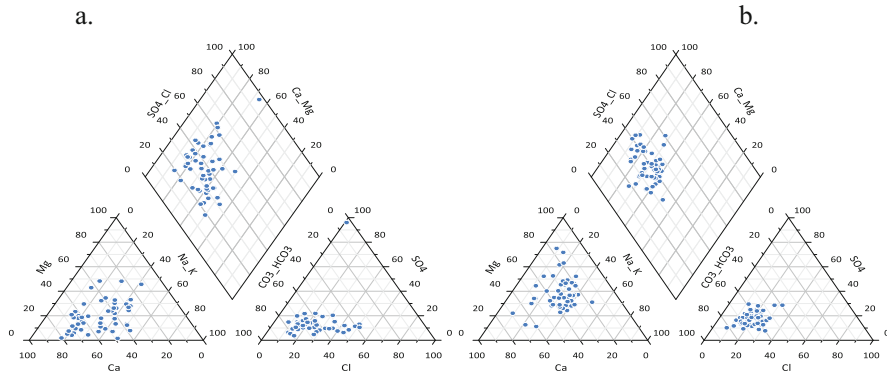


Fig. 19.7 Piper diagram of groundwater parameters for (a) pre-monsoon (b) and post-monsoon

Table 19.7 Standard value of parameters and their relative weight

Parameters	Drinking water standards (BIS 2012)	Weight (w_i)	Relative weight (W_i)
pH	7.5	5	0.104167
TDS	500 mg/l	5	0.104167
EC	730 μ S/cm	2	0.041667
TA	200 mg/l	2	0.041667
TH	200 mg/l	2	0.041667
Na ²⁺	200 mg/l	4	0.083333
Ca ²⁺	75 mg/l	2	0.041667
Mg ²⁺	30 mg/l	2	0.041667
Fe	3 mg/l	3	0.062500
K ⁺	10 mg/l	1	0.020833
CO ₃ ⁻	100 mg/l	3	0.062500
HCO ₃ ⁻	300 mg/l	3	0.062500
Cl ⁻	250 mg/l	4	0.083333
SO ₄ ⁻	150 mg/l	5	0.104167
F ⁻	1.5 mg/l	5	0.104167

used for this study to calculate WQI are presented in Table 19.7. According to BIS, parameter which exceeds its perishable limit in groundwater samples has been presented in Table 19.8. In the post-monsoon season, the concentration of TA and Mg²⁺ was above the safe limit in all samples and Cl⁻ was within its safe limit in all samples of groundwater of Nituria block.

The overall WQI analysis of pre-and post-monsoon shows its ranges from 59.40 to 171.43 and it has been classified into four types of water as ‘good’ (59.40–87.40), ‘moderate’ (87.40–115.40), ‘poor’ (115.40–143.40) and ‘very poor’ (143.40–171.43) (Table 19.9). WQI value of each groundwater sample is presented in Table 19.10. The highest value of WQI in pre-monsoon season has been found in ‘Sabari’ village (171.43) because of high concentration of pH, TDS, Fe, F⁻ and HCO₃⁻ in groundwater. In post-monsoon season highest WQI has been found in

Table 19.8 Parameters exceeds its concentration in groundwater samples

Parameters	Pre-monsoon (%)	Post-monsoon (%)
pH	11.53	9.61
TDS	44.23	92.30
EC	44.23	92.30
TA	36.53	100
TH	92.30	75
Na ²⁺	7.69	9.61
Ca ²⁺	59.61	33.34
Mg ²⁺	65.38	100
Fe	76.92	55.76
K ⁺	9.61	13.46
CO ₃ ⁻	7.69	30.76
HCO ₃ ⁻	21.15	5.76
Cl ⁻	17.30	0
SO ₄ ⁻	19.23	7.69
F ⁻	15.38	7.70

Table 19.9 Groundwater samples under different water quality types

Water quality	Ranges	Pre-monsoon (%)	Post-monsoon (%)
Good	59.40–87.40	42.30	40.38
Moderate	87.40–115.4	26.92	28.85
Poor	115.4–143.4	9.62	15.39
Very poor	143.4–171.43	21.16	15.38

‘Purana Panchakot’ village (168.21). It is due to high presence of Fe, TDS, pH, Cl⁻ and Mg²⁺ in its groundwater sample. Various previous researches on groundwater quality assessment have been documented that concentrations of Fe, Mg²⁺, bicarbonates are very important factors to control the quality of groundwater (Batabyal and Chakraborty 2015; Kundu and Nag 2018; Nag and Das 2017; Das and Nag 2017). Our present study also proves that high values of WQI are highly determined by presence of those ions in groundwater. Interpolation technique using IDW (Inverse Distance Weighted) in ArcGIS software for spatial distribution of WQI has been presented for pre-monsoon (Fig 19.8a) and post-monsoon season (Fig 19.8b). GIS analysis clearly indicates spatially decreasing ‘good’ quality of groundwater and increasing ‘moderate’ quality groundwater in post-monsoon season.

19.4.6 Human Health Risk (HHR) Analysis

Health risk assessment of human body of the present study area has been followed by USEPA (United States Environment Protection Agency) for noncarcinogenic risk of male and female residence especially by oral intake of Fe and F⁻ with drinking water. Hydro-chemical assessment of groundwater quality has been already shown

Table 19.10 WQI values of each sample point in Nituria block

Location code (source: Census report, 2011)	Sample no.	Location name	WQI (Pre-monsoon)	WQI (Post-monsoon)
360	1	Bharatpur	130.87	146.37
363	2	Naynakuri	79.90	95.88
366	3	Jorberya	82.29	76.44
369	4	Achkoda	99.80	91.68
370	5	Dumarhir	74.57	83.99
373	6	Naragarya	80.04	80.86
375	7	Asta	75.38	93.35
378	8	Paharudi	93.33	90.38
380	9	Gunyara	79.71	85.86
382	10	Ray band	97.22	99.12
383	11	Sulanga	128.03	145.33
388	12	Birbaldi	88.92	93.31
390	13	Alkusha	127.41	138.07
391	14	Simuliya	85.29	117.33
393	15	Bhiringi	132.59	161.36
394	16	Kalipathar	93.86	112.02
396	17	Ghatkul	151.48	141.51
397	18	Tantloi	166.53	131.04
399	19	Mahishnadi	91.55	93.50
401	20	Bhurkunrabari	99.90	89.43
402	21	Bathanbari	65.82	79.67
405	22	Shihulibari	74.27	94.72
407	23	Lakshanpur	79.49	86.78
412	24	Rampur	62.03	67.13
414	25	Pahargora	65.57	81.87
417	26	Gobag	79.36	77.18
419	27	Maharajnagar	72.95	81.63
423	28	Garh panchkot	153.18	159.72
426	29	Natundi	166.84	164.79
427	30	Digha	167.45	143.83
430	31	Nabagram	74.51	108.28
432	32	Pochhyara	96.32	84.56
438	33	Puapur	88.56	104.42
439	34	Kelyasota	69.92	100.65
445	35	Mahukura	103.56	87.28
447	36	Deilya	158.92	139.13
449	37	Sarbari	171.43	164.31
450	38	Nituria	162.37	150.44
452	39	Gosaindi	81.39	78.58
453	40	Hirakhun	137.40	127.14
454	41	Bhamaria	94.36	69.08

(continued)

Table 19.10 (continued)

Location code (source: Census report, 2011)	Sample no.	Location name	WQI (Pre-monsoon)	WQI (Post-monsoon)
455	42	Asanbani	82.05	68.12
457	43	Dhangajor	84.46	77.67
460	44	Saontalmotha	70.54	87.19
461	45	Bonra	81.49	69.00
462	46	Baruipara	98.23	85.94
468	47	Goaladi	159.69	124.52
470	48	Rangdihi	84.63	69.41
472	49	Inganpur	91.13	59.40
476	50	Madandi	110.18	80.65
481	51	Purna panchakot	157.50	168.22
485	52	Par beliya (CT)	166.52	161.52

that near about 77% and 56% of samples has their concentration of iron above its perishable limit in the study region for pre- and post-monsoon season, respectively. On the other hand, concentration of fluoride exceeds their perishable limit in near about 15% and 8% of groundwater samples in pre-monsoon and post-monsoon season.

Therefore, noncarcinogenic health risk of human body was made by computation of Hazard Quotient (HQ) and integrated Hazard Index (HI) for male and female adults in pre-monsoon and post-monsoon seasons (Table 19.11). In the study region availability of iron in parent rocks supplies Fe into groundwater. Intake of excess Fe with drinking water for a long time affects chronic genetic disorder to human body (WHO 1996). HI values were calculated from summation of HQ values of iron and fluoride ($HQ_{Fe} + HQ_{F^-}$). In the pre-monsoon season HI values of male adults are ranged from 0.60 to 3.77 with a mean value of 1.94. 88.46% of groundwater samples indicate that HI values greater than 1 are noncarcinogenic health risk for male adult population. The HI values of female adults are ranged from 0.70 to 4.45 with mean value of 2.29. About 94.23% samples are indicate HI values >1 for health risk. The mean values of HI of male and female show that females are much affected by health hazard due to excess intake of Fe with drinking water. In post-monsoon season HI values of male and female are ranged from 0.56 to 3.67 with mean value of 1.76 and 0.66 to 4.33 with mean value of 2.08, respectively. Above 69.23% and 78.84% of water samples indicates noncarcinogenic risk (>1) for male and female adults, respectively. Mean value of HI shows high health risk for female than male in this season also. Assessment of human health risk of noncarcinogenic pollutants in previous researches also proves that female adults were much affected than male adults by higher intake of F^- with drinking water in different part of India (Adimalla 2018a, b; Adimalla and Rajitha 2018; Adimalla et al. 2018a, b). IDW technique has been used for spatial mapping on health hazard index (HI) on pre-and post-monsoon for male (Fig. 19.9a and b) and female (Fig. 19.10a and b) in the study area.

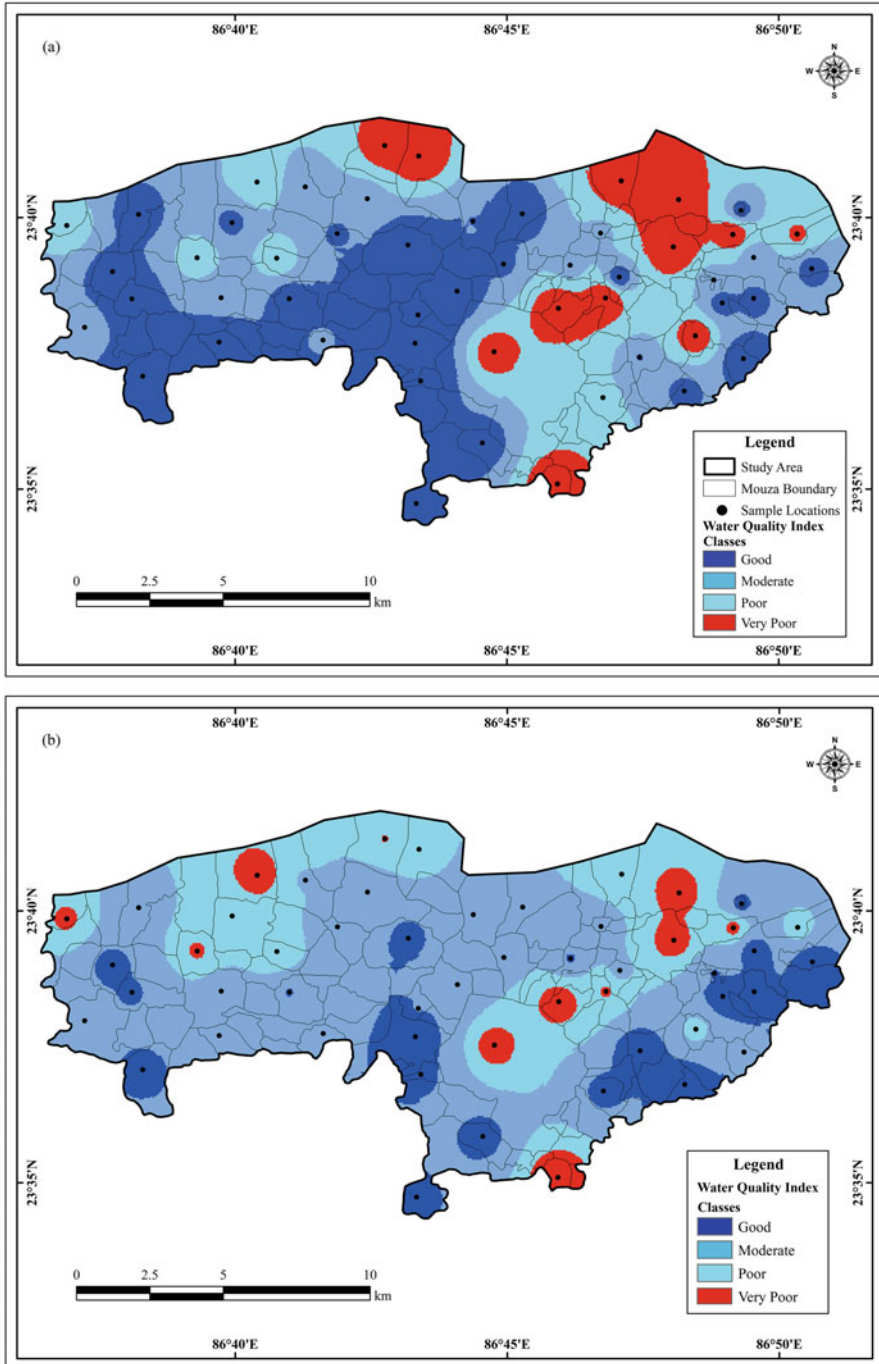


Fig. 19.8 WQI of pre-monsoon season (a) and post-monsoon season (b)

Table 19.11 Noncarcinogenic Hazard Index of Male and Female adults of Nituria block in pre-monsoon and post-monsoon period

Sample no	Location name	Hazard index (Male)		Hazard index (Female)	
		Pre-monsoon	Post-monsoon	Pre-monsoon	Post-monsoon
1	Bharatpur	3.08552	3.09255	3.64652	3.65483
2	Naynakuri	1.11238	1.24327	1.31463	1.46932
3	Jorberya	1.15770	0.69744	1.36820	0.82424
4	Achkoda	1.52654	1.86374	1.80410	2.20260
5	Dumarhir	1.23038	1.53241	1.45408	1.81102
6	Naragarya	1.18466	1.04713	1.40006	1.23752
7	Asta	0.94281	0.76503	1.11423	0.90413
8	Paharudi	1.50857	1.57617	1.78286	1.86274
9	Gunyara	1.78090	1.78911	2.10470	2.11440
10	Ray band	1.25617	1.08230	1.48456	1.27908
11	Sulanga	2.98784	3.44811	3.53108	4.07504
12	Birbaldi	1.82896	2.16342	2.16150	2.55677
13	Alkusha	2.70027	2.07629	3.19123	2.45380
14	Simuliya	1.74105	1.36244	2.05760	1.61016
15	Bhiringi	3.40396	3.19023	4.02286	3.77027
16	Kalipathar	0.86623	0.84005	1.02372	0.99278
17	Ghatkul	3.41529	2.97221	4.03625	3.51261
18	Tantloi	2.47092	1.87038	2.92017	2.21045
19	Mahishnadi	1.26281	0.86505	1.49241	1.02234
20	Bhurkunrabari	1.51053	1.32142	1.78517	1.56167
21	Bathanbari	0.75214	0.75448	0.88889	0.89166
22	Shihulibari	1.97900	1.82662	2.33882	2.15873
23	Lakshampur	0.91468	0.99204	1.08098	1.17241
24	Rampur	0.60054	0.67907	0.70973	0.80254
25	Pahargora	0.62593	0.56264	0.73974	0.66494
26	Gobag	1.49724	1.02838	1.76947	1.21535
27	Maharajnagar	1.12371	0.95023	1.32802	1.12300
28	Gar panchkot	3.53485	3.67082	4.17755	4.33824
29	Natundi	3.77123	3.61885	4.45691	4.27683
30	Digha	2.66159	2.04737	3.14551	2.41962
31	Nabagram	1.93407	2.21265	2.28571	2.61495
32	Pochhyara	1.25968	0.89162	1.48872	1.05374
33	Puapur	1.45817	1.32571	1.72329	1.56675
34	Kelyasota	1.22178	1.67072	1.44392	1.97449
35	Mahukura	2.31736	1.70549	2.73870	2.01558
36	Deilya	2.25524	2.33026	2.66528	2.75394
37	Sarbari	3.63175	3.47233	4.29206	4.10367
38	Nituria	3.66730	3.43990	4.33408	4.06534
39	Gosaindi	1.11824	0.61538	1.32156	0.72727
40	Hirakhun	3.41138	3.26720	4.03163	3.86124
41	Bhamaria	1.52733	0.89280	1.80502	1.05512

(continued)

Table 19.11 (continued)

Sample no	Location name	Hazard index (Male)		Hazard index (Female)	
		Pre-monsoon	Post-monsoon	Pre-monsoon	Post-monsoon
42	Asanbani	1.20107	0.57514	1.41945	0.67971
43	Dhangajor	1.07175	0.67399	1.26661	0.79654
44	Saontalmotha	1.84186	1.19209	2.17674	1.40883
45	Bonra	1.29211	1.80943	1.52704	2.13841
46	Baruipara	2.61822	2.13099	3.09426	2.51844
47	Goaladi	3.32581	3.20039	3.93051	3.78228
48	Rangdihi	1.27453	0.83223	1.50626	0.98355
49	Inganpur	1.19639	0.75096	1.41391	0.88750
50	Madandi	2.35370	1.40308	2.78165	1.65818
51	Purna panchakot	3.57001	3.31565	4.21911	3.91850
52	Par beliya (CT)	3.02574	3.21602	3.57587	3.80075

19.5 Summery and Conclusions

Groundwater quality analysis has been carried out in Nituria block, West Bengal during pre- and post-monsoon seasons of the year 2019. 52 samples were collected from different village and analysed various hydro-chemical parameters to understand suitability for drinking purpose and health related hazard among male and female residence of the study area.

In the study area average value of cations shows its order of concentration as $\text{Ca}^{2+} > \text{Mg}^{2+} > \text{K}^+ > \text{Na}^{2+}$ and anions as $\text{HCO}_3^- > \text{Cl}^- > \text{CO}_3^- > \text{SO}_4^-$ in pre-monsoon season. In the post-monsoon season average cation concentration arranged as $\text{Mg}^{2+} > \text{Ca}^{2+} > \text{Na}^{2+} > \text{K}^+$ and anion concentration as $\text{HCO}_3^- > \text{CO}_3^- > \text{Cl}^- > \text{SO}_4^-$.

Correlation analysis shows that Fe (iron) is most dominant parameter to control other parameters in pre-and post-monsoon season. The natural availability of iron in the study area supplies abundant Fe to the groundwater.

Hierarchical cluster analysis presents two groups of water samples in pre-monsoon as $\text{HCO}_3^- > \text{Cl}^- > \text{SO}_4^-$ (group-1) and $\text{Ca}^{2+} > \text{CO}_3^- > \text{Cl}^-$ (group-2) type in the study area. Principal component analysis also indicates that anion and cation are the principal factors of controlling water quality on both seasons.

Groundwater suitability to drinking purpose was analysed by WQI method using standard limits of parameters prescribed by BIS (2012). Concentration of TA and Mg^{2+} exceeds their permissible limit in all samples at post-monsoon season. Safe limit of Fe is crossed in 76% sample of the study area in pre-monsoon season and near about 55% samples in post-monsoon season. Concentration of F^- exceeds its permissible limit nearly 15% of samples in pre-monsoon and 7% samples in post-monsoon season.

WQI result of pre- and post-monsoon ranges from 59.40 to 171.43 and classified in four groups as 'good', 'moderate', 'poor', and 'very poor'. In pre-monsoon season

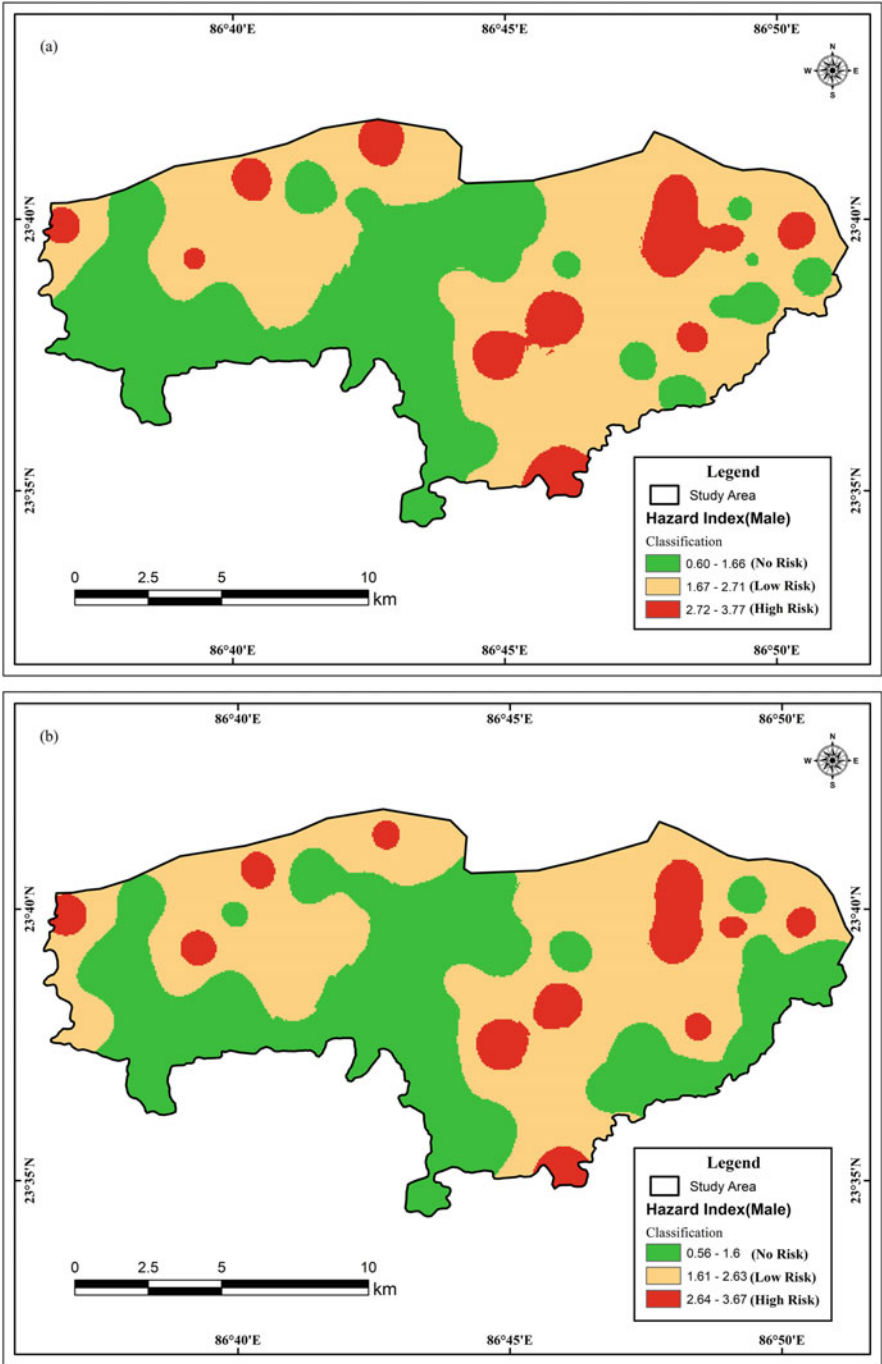


Fig. 19.9 Hazard Index of Male in pre-monsoon (a) and post-monsoon (b)

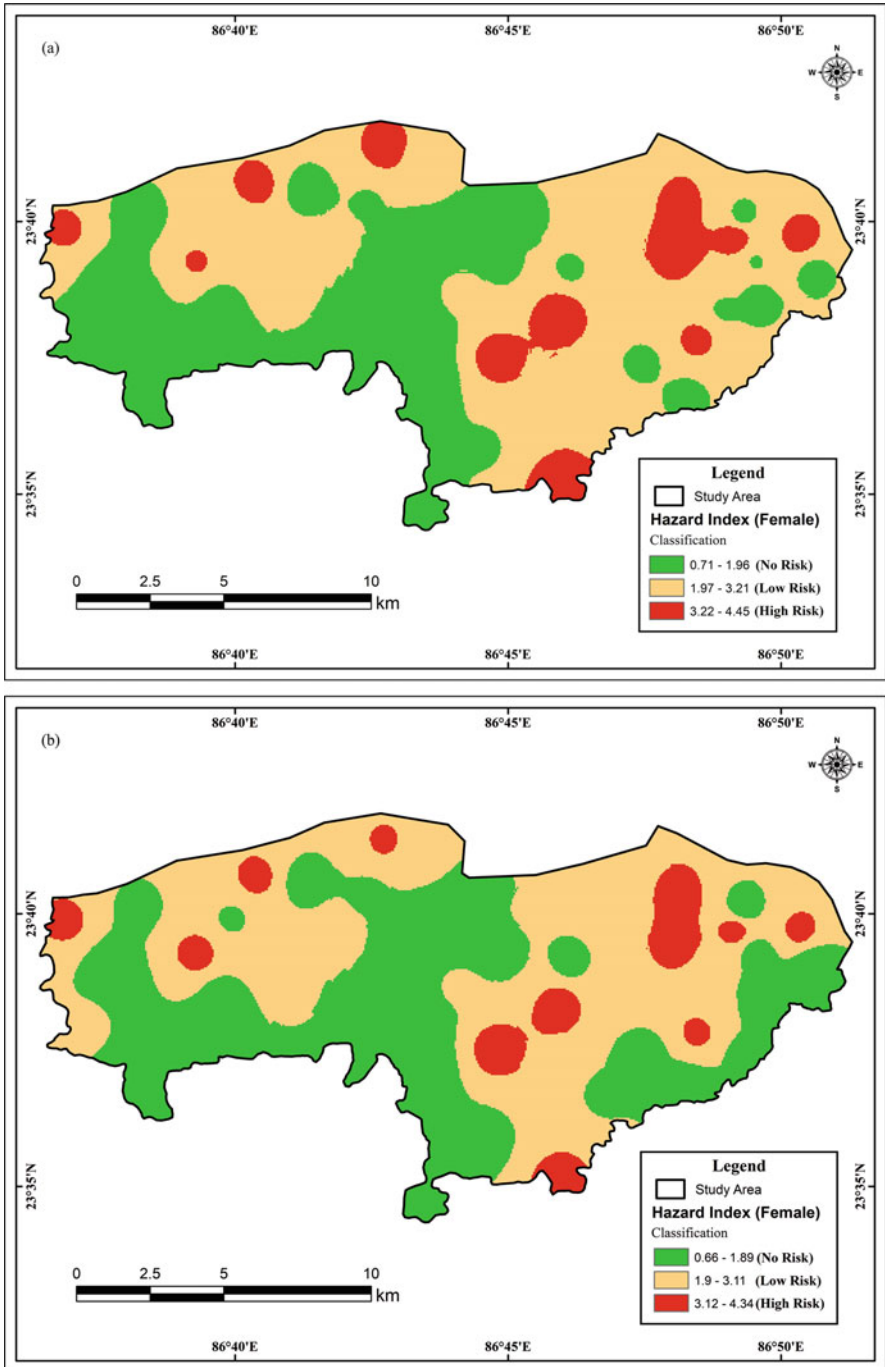


Fig. 19.10 Hazard Index of Female in pre-monsoon (a) and post-monsoon (b)

highest value of WQI has been found in 'Sabari' (171.43) village. In post-monsoon season highest WQI value has been found in 'Purana Panchakot' (168.21) village. High concentration of pH, TDS, Fe, Mg^{2+} and bicarbonate at these two locations indicates concentration of natural as well as anthropogenic activities to the groundwater. GIS mapping shows increase of 'moderate' quality groundwater and decrease of 'good' quality groundwater than pre-monsoon season.

Health risk assessment on adult male and female of noncarcinogenic disease by higher intake of Fe and F^{-} in study area was done followed by USEPA. HI values indicate that 88.46% and 94.23% of groundwater samples are prone to healthy risk (>1) for male and female, respectively, in pre-monsoon season. In post-monsoon season 69.23% and 78.84% of groundwater samples indicate HI values >1 and health risk for male and female, respectively. Mean value of HI indicates that females are more prone to health hazard than male in both the seasons.

The overall assessments of groundwater quality of Nituria block show most of the region is 'good' to 'moderate' for drinking purpose. Near about 21% and 15% samples indicate 'very poor' quality of water in pre- and post-monsoon, respectively. High mixing of Na^{2+} , Mg^{2+} , Cl^{-} , HCO_3^{-} indicates various anthropogenic activities which contaminated groundwater by leaching process. High concentration of Fe and F^{-} indicates adverse geogenic condition for health purpose.

To reduce chemical concentration on groundwater parameters, suitable land use practice should be encouraged to the practitioners by government or local agencies.

Rain water harvesting should be the best supplementary source for domestic purpose. Proper filtration process (distillation) to reduce Fe and F^{-} concentration before drinking should be very effective to prevent health hazard.

Serious monitoring to provide safe drinking water to the residence should be encouraged to the local agencies or NGOs by the government bodies.

GIS mapping on spatial zonation of health hazard related to Fe and F^{-} should be helpful to further planning on those areas which have to be taken proper management and public awareness to use groundwater for a healthy drinking purpose.

Acknowledgement The authors are deeply acknowledged to the Research Centre for Natural Science, Raja Narendra Lal Khan Women's College, Midnapore; Department of Earth Sciences, Indian Institute of Engineering Science and Technology (IEST), Shibpur, West Bengal, and Department of Geology & Geophysics, Indian Institute of Technology (IIT), Kharagpur, West Bengal, India for their laboratory facilities and kind encouragement.

References

- Adimalla N (2018a) Groundwater quality for drinking and irrigation purposes and potential health risks assessment: a case study from semi-arid region of South India. *Expo Health* 11:109. <https://doi.org/10.1007/s12403-018-0288-8>
- Adimalla N (2018b) Spatial distribution, exposure, and potential health risk assessment from nitrate in drinking water from semi-arid region of South India. *Hum Ecol Risk Assess.* <https://doi.org/10.1080/10807039.2018.1508329>

- Adimalla N, Li P (2018) Occurrence, health risks, and geochemical mechanisms of fluoride and nitrate in groundwater of the rock-dominant semi-arid region, Telangana State, India. *Hum Ecol Risk Assess.* <https://doi.org/10.1080/10807039.2018.1480353>
- Adimalla N, Rajitha S (2018) Spatial distribution and seasonal variation in fluoride enrichment in groundwater and its associated human health risk assessment in Telangana state, South India. *Hum Ecol Risk Assess* 16:752–757. <https://doi.org/10.1080/10807039.2018.1438176>
- Adimalla N, Li P, Qian H (2018a) Evaluation of groundwater contamination for fluoride and nitrate in semi-arid region of Nirmal Province, South India: a special emphasis on human health risk assessment (HHRA). *Hum Ecol Risk Assess* 25:1107–1124. <https://doi.org/10.1080/10807039.2018.1460579>
- Adimalla N, Venkatayogi S, Geeta S (2018b) Hydrogeochemical data on groundwater quality with special emphasis on fluoride enrichment in Munneru river basin (MRB), Telangana state, South India. *Data Brief* 17:339–346. <https://doi.org/10.1016/j.dib.2018.01.059>
- Afzali A, Shahedi K, Roshan MHN, Solaimani K, Vahabzadeh G (2014) Groundwater quality assessment in Haraz alluvial fan, Iran. *Int J Sci Res Environ Sci* 2(10):346–360
- Al-Futaisi A, Rajmohan N, Al-Touqi S (2007) Groundwater quality monitoring in and around Barka dumping site, Sultanate of Oman. In: Proceedings of second IASTED WRM conference, Honolulu, Hawaii, USA.
- APHA (2012) Standard methods for the examination of water and wastewater, 22nd edn. American Public Health Association, Washington, DC
- Batabyal AK, Chakraborty S (2015) Hydrogeochemistry and water quality index in the assessment of groundwater quality for drinking uses. *Water Environ Res* 87(7):607
- BIS (Bureau of Indian standards) (2012) Indian standard, drinking water—specification, second revision, IS 10500: 2012, ICS 13.060.20
- Box GFP, Hunter WG, Hunter JS (1978) Statistics for experiments. An introduction to design data analysis and model building. Wiley, Toronto, p 653
- Brindha K, Elango L (2012) Impact of tanning industries on groundwater quality near a metropolitan city in India. *Water Resour Manag* 17:47–1761
- Chapman D (1996) On the behalf of UNESCO, WHO. UXEP. Water quality assessments—a guide to use biota, sediments and water in environmental monitoring. F & F Spoil, London, Chapter 9
- Das S, Nag SK (2017) Application of multivariate statistical analysis concepts for assessment of hydrogeochemistry of groundwater—a study in Suri I and II blocks of Birbhum District, West Bengal, India. *Appl Water Sci* 7:873–888. <https://doi.org/10.1007/s13201-015-0299-6>
- Helena B, Pardo R, Vega M, Barrado E, Fernandez JM, Fernandez L (2000) Temporal evolution of groundwater composition in an alluvial aquifer (Pisuerga River, Spain) by principal component analysis. *Water Res* 34(3):807–816
- Hosseini MT (2004) Hydrochemical evaluation of groundwater in the Blue Nile Basin, eastern Sudan, using conventional and multivariate techniques. *Hydrogeol J* 12(2):144–158
- Ishaku JM (2011) Assessment of groundwater quality index for Jimeta-Yola area, northeastern Nigeria. *J Geol Mining Res* 3(9):219–231
- Jalali M (2006) Chemical characteristics of groundwater in parts of mountainous region, Alvand, Hamadan, Iran. *Environ Geol* 51:433–446
- Keshavarzi B, Moore F, Mosaferi M, Rahmani F (2011) The source of natural arsenic contamination in groundwater. *West of Iran Water Qual Expo Health* 3:135–147
- Kumar D, Ahmed S (2003) Seasonal behaviour of spatial variability of groundwater level in a granitic aquifer in monsoon climate. *Curr Sci* 84(2):188–196
- Kundu A, Nag SK (2018) Assessment of groundwater quality in Kashipur block, Purulia district. *West Bengal Appl Water Sci* 8:33. <https://doi.org/10.1007/s13201-018-0675-0>
- Li P, Wu J, Qian H, Lyu X, Liu H (2014) Origin and assessment of groundwater pollution and associated health risk: a case study in an industrial park, Northwest China. *Environ Geochem Health* 36(4):693–712. <https://doi.org/10.1007/s10653-013-9590-3>

- Li P, Li X, Meng X, Li M, Zhang Y (2016) Appraising groundwater quality and health risks from contamination in a semiarid region of Northwest China. *Expo Health* 8(3):361–379. <https://doi.org/10.1007/s12403-016-0205-y>
- Mukherjee D, Dora SL, Tiwary RK (2012) Evaluation of water quality index for drinking purposes in the case of Damodar River, Jharkhand and West Bengal region, India. *J Bioremed Biodeg* 3:9. <https://doi.org/10.4172/2155-6199.1000161>
- Nag SK, Das S (2017) Assessment of groundwater quality from Bankura I and II blocks, Bankura District, West Bengal, India. *Appl Water Sci* 7:2787–2802. <https://doi.org/10.1007/s13201-017-0530-8>
- Nag SK, Ghosh P (2013) Variation in groundwater levels and water quality in Chhatna block, Bankura district, West Bengal- a GIS approach. *J Geol Soc India* 81(2):261–280
- Nagaraju A, Balaji E, Sun LH, Thejaswi A (2018) Processes controlling groundwater chemistry from Mulakalacheruvu area, Chittoor district, Andhra Pradesh, South India: a statistical approach based on hydrochemistry. *J Geol Soc India* 91:425–430
- Narsimha A, Sudarshan V (2017) Assessment of fluoride contamination in groundwater from Basara, Adilabad district, Telangana state, India. *Appl Water Sci* 7:2717–2725. <https://doi.org/10.1007/s13201-016-0489-x>
- Naseem S, Ahmed P, Shamim SS, Bashir E (2011) Geochemistry of sulphate-bearing water of Akra Kaur dam, Gwadar, Balochistan, Pakistan and its assessment for drinking and irrigation purposes. *Environ Earth Sci* 66:1831–1838
- Nishi K, Singh PK, Kumar B (2018) Hydrogeochemical characterization and groundwater quality of Jamshedpur urban agglomeration in Precambrian terrain, eastern India. *J Geol Soc India* 92:67–75
- Pandian K, Sankar K (2007) Hydrogeochemistry and groundwater quality in the Vaippar River basin, Tamil Nadu. *J Geol Soc India* 69:970–982
- Piper AM (1944) A graphic procedure in the geochemical interpretation of water-analyses. *Trans Am GeolSurv* 475-B:186–188
- Pritchard M, Mkandawire T, O'Neill JG (2008) Assessment of groundwater quality in shallow wells within the southern districts of Malawi. *Phys Chem Earth* 33:812–823
- Priyanka S, Smita S, Gayatri D (2017) Seasonal variation of groundwater quality in rural areas of Jaipur district, Rajasthan. *Ind J Sci Technol*. <https://doi.org/10.17485/ijst/2017/v10i30/115534>
- Raju NJ (2007) Hydrogeochemical parameters for assessment of groundwater quality in the upper Gunjanaeru River basin, Cuddapah District, Andhra Pradesh, South India. *Environ Geol* 52 (2007):1067–1074
- Ramakrishnaiah CR, Sadashivaiah C, Ranganna G (2009) Assessment of water quality index for the groundwater in Tumkur Taluk, Karnataka state, India. *E-J Chem* 6(2):523–530
- Rao YS, Reddy TVK, Nayudu PT (1997) Ground-water quality in the Niva River basin, Chittoor district, Andhra Pradesh, India. *Environ Geol* 31(1):56–63
- Reghunath R, Sreedhara Murthy TR, Raghavan BR (2002) The utility of multivariate statistical techniques in hydrogeochemical studies: an example from Karnataka, India. *Water Res* 36:2437–2442
- Routroy S, Harichandran R, Mohanty JK, Panda CR (2013) A statistical appraisal to hydrogeochemistry of fluoride contaminated ground water in Nayagarh District, Odisha. *J Geol Soc India* 81:350–360
- Saatsaz M, Sulaiman WNA, Eslamian S, Mohammadi K (2011) GIS DRASTIC model for groundwater vulnerability estimation of Astaneh- Kouchesfahan plain, northern Iran. *Int J Water* 6(1):1. <https://doi.org/10.1054/IJW.2011.043313>
- Shaji E, Gomez A, Hussein S, Deepu TR, Anilkumar Y (2018) Salinization and deterioration of groundwater quality by nitrate and fluoride in the Chittur block, Palakkad, Kerala. *J Geol Soc India* 92:337–345
- Shanmugasundharam A, Kalpana G, Mahapatra SR, Sudharson ER, Jayaprakash M (2015) Assessment of groundwater quality in Krishnagiri and Vellore District in Tamil Nadu. *India Appl Water Sci* 7:1869. <https://doi.org/10.1007/s13201-015-0361-4>

- Singh K, Malik A, Mohan D, Sinha S (2004) Multivariate statistical techniques for the evaluation of spatial and temporal variations in water quality of Gomti River (India)—a case study. *Water Res* 38:3980–3992
- Singh PK, Malik A, Sinha S (2005) Water quality assessment and apportionment of pollution sources of Gomti river (India) using multivariate statistical techniques—a case study. *Anal Chim Acta* 538:355–374
- Singh VK, Bikundia DS, Sarswat A, Mohan D (2012) Groundwater quality assessment in the village of Lutfullapur Nawada, Loni, district Ghaziabad, Uttar Pradesh. *India Environ Monit Assess* 184:4473–4488
- Subba Rao N (2002) Geochemistry of groundwater in parts of Guntur District, Andhra Pradesh. *India Environ Geol* 41:552–562
- Subba Rao N, Surya Rao P, Venktram Reddy G, Nagamani M, Vidyasagar G, Satyanarayana NLVV (2012) Chemical characteristics of groundwater and assessment of groundwater quality in Varaha River basin, Visakhapatnam district, Andhra Pradesh, India. *Environ Monit Assess* 184:5189–5214
- Tiwari RN (2011) Groundwater quality assessment of Mangawa area, Rewa District, Madhya Pradesh, India. *Int J Earth Sci Eng* 04(06):1000–1009
- Umar R, Khan MMA, Absar A (2006) Groundwater hydrochemistry of a sugarcane cultivation belt in parts of Muzaffarnagar District, Uttar Pradesh, India. *Environ Geol* 49(7):999–1008
- USEPA (1989) Risk assessment guidance for superfund, vol 1, Human health evaluation manual (Part A). Office of Emergency and Remedial Response, Washington, DC
- USEPA (2014) Human health evaluation manual, supplemental guidance: update of standard default exposure factors-OSWER directive 9200.1-120. United States Environmental Protection Agency, Washington, DC, p 6
- WHO (1996) Guideline for drinking water quality, 2nd edn. World Health Organization, Geneva
- Wu J, Sun Z (2016) Evaluation of shallow groundwater contamination and associated human health risk in an alluvial plain impacted by agricultural and industrial activities, mid-West China. *Expo Health* 8(3):311–329. <https://doi.org/10.1007/s12403-015-0170-x>
- Yidana SM (2010) Groundwater classification using multivariate statistical methods: southern Ghana. *J Afr Earth Sci* 57:455–469
- Zeng X, Rasmussen TC (2005) Multivariate statistical characterization of water quality in Lake Lanier, Georgia, USA. *J Environ Qual* 34:1980–1991
- Zhang B, Song XE, Zhang YH, Han DM, Tang CY, Yu YL, Ma Y (2012) Hydrochemical characteristics and water quality assessment of surface water and groundwater in Songnen plain. *Northeast China Water Res* 46:2737–2748

Chapter 20

Existence of Pharmaceuticals and Personal Care Products (PPCPs) in the Conventional Water Treatment Process



Noor A. Khan, Kavita N. Gandhi, Vidyasagar Devtade, Kirti Nandanwar, Deep Chand, S. Kashyap, and N. P. Thacker

Abstract Pharmaceuticals and personal care products (PPCPs) are categorized as contaminants of concerns. It mainly includes regularly used personal care and cosmetic products and medicines. PPCPs have been widely detected in different water matrices. PPCPs being adversely affecting the ecological system and human health and therefore are of great concerns. Presence of PPCPs in effluents from municipal wastewater treatment plants, behaviour and biological impact have become a topical concern and important issues of water quality. PPCPs are considered as potent endocrine disruptors (EDCs). Their bioactive metabolites find its way into the aquatic environment in the form of complex combinations through a number of ways but mostly by both untreated and treated sewage.

The work was done to understand the fate of PPCPs during the conventional treatment. Four class of PPCPs, viz.; phenols, anti-microbial, oestrogen, and stimulants were targeted. One compound from each class, i.e. 4-*n*-Nonylphenol, Triclosan, 17 β -estradiol, and Caffeine was selected for method standardization in GC-MS. The samples from inlet and outlet of STP were analysed for the selected compounds. Sufficient concentration of three compounds, viz.; 4-*n*-Nonylphenol, Triclosan, and 17 β -estradiol were detected in inlet samples. Also considerable concentration of these compounds was found in outlet samples. Although much work have been done to find out different treatment methods for the deletion of PPCPs from wastewater and receiving waters. However in Indian scenario, the treatment system is designed

N. A. Khan (✉) · D. Chand · N. P. Thacker
CSIR–National Environmental Engineering Research Institute, Delhi Zonal Centre, New Delhi,
India
e-mail: na_khan@neeri.res.in

K. N. Gandhi · V. Devtade · K. Nandanwar
Pesticide Residue Laboratory, CSIR–National Environmental Engineering Research Institute,
Nagpur, India

S. Kashyap
Analytical Instrumentation Division, CSIR–National Environmental Engineering Research
Institute, Nagpur, India

© Springer Nature Switzerland AG 2021

P. K. Shit et al. (eds.), *Spatial Modeling and Assessment of Environmental Contaminants*, Environmental Challenges and Solutions,
https://doi.org/10.1007/978-3-030-63422-3_20

359

for the conventional process which is not effective in the removal of these PPCPs. This is clearly revealed in the results of study that PPCPs are highly concentrated in the inlets of STPs and their removal needs to be look-in during treatment process.

Keywords Pharmaceuticals · Personal care products · Toxicity · Treatment process

20.1 Introduction

Nowadays, occurrence of pharmaceutical and individual care items in nature is a serious concern (Daughton and Ternes 1999; Daughton 2001; Veldhoen et al. 2007; Kummerer 2008). Pharmaceuticals and Personal Care Products (PPCPs) as pollutants refers, in general, to any item utilized by people for individual well-being or for cosmetic purpose or utilized by agribusiness to upgrade development and strength of animals. PPCPs involve assortment of thousands of synthetic organic chemicals substances utilized in common items including human and veterinary medication, helpful medications, aromas, personal and beauty care products, for example, soaps, toothpaste, moisturizers, cream, etc. (USEPA 2012). These Pharmaceuticals and PCPs (PPCPs) structure a wide collection of significant “unrecognized”, “rising” pollutants in regular urban activities (Maria and Basaglia 2007). In excess, of ten thousand PPCPs are utilized all over world, many PPCPs are yet unknown (Okuda et al. 2009). Pharmaceutical and individual care items have been recognized in the environment and are also considered as strong endocrine disruptors (EDCs) (Barcelo 2003). Since conventional water treatment process is not adequate enough to remove PPCPs from sewage water. It is, therefore, become important to decide a range of PPCPs concentration level (ng/L or µg/L) in the effluents of wastewater treatment plants (WWTPs) (Ke et al. 2012; Ferguson et al. 2013; Ryu et al. 2014). Further on the basis of understanding about physico-chemical properties, viz.; acidity, lipophilicity, volatility, and sorption potential of individual compounds, a process can be designed to expel distinctive PPCPs from waste water (Sonia et al. 2008).

Due to production and utilization of a massive quantity of synthetic chemicals, mainly prescribed drugs, and personal care products (PPCPs), these compounds detected with higher rate and are persistent in all types of water sources, viz.; natural, drinking, and wastewater. In recent years, the prevalence and destiny of pharmaceutically lively compounds (PhACs) in the water environment is one of the rising issues in environmental chemistry as these have been identified in aquatic environment.

Mostly PPCPs reach environment by disposal of hazardous wastes from industries and individual households (EUROPA 2012). As per Daughton’s report there might be as 60 lakhs PPCP substances are commercially accessible universally and that the utilization of pharmaceutical is expanding at the rate of as 3–4% per year by weight (Daughton 2003). Pharmaceutical compound enters in to the environment by means of a wide variety of passages, such as wastages from industries, wrong dispose of unused/expired medicinal drugs into the trash, and via the excretion of

urine or faeces. Most of medicine found in sewage treatment plants often come from the human excretion. As majority of them are no longer absorbed in the body and are expelled through the urine or faeces. One of such example is of antibiotic amoxicillin, during the course of its metabolism, about 80–90% is excreted out unchanged from human body (Hirsch et al. 1998).

PPCPs before entering into aquatic environment are gradually converted into its disintegrated products or transformed into new more stable compounds during its path in the sewage treatment plants (STPs) (Heberer 2002). However, there are sources that attributed directly or indirectly to input of such compounds in environment. The use of drugs in aquaculture/pisciculture facilities could be a direct source, whereas the applications of fertilizer/manure in agriculture are possible indirect sources (Boxall et al. 2003). Similarly, industrial manufacturing site of such compounds and liquid waste from hospitals been other direct sources of PPCPs (Gurunadharao et al. 2001; Bendz et al. 2005; Larsson et al. 2007; Santos et al. 2010). PPCPs as environmental pollutants are pushed via various scientific and logical concerns. The main concern is of its dangerous effect on human health and environment is when these chemicals are uptake in food web and there occur the danger of exposure. A best example of such exposer are fisheries industries in arctic coastal region. Contamination of any marine species that are utilized for human consumption is a significant concern. Few of such pharmaceuticals (e.g. diclofenac) have shown alarming consequences on fish and vultures (Oaks et al. 2004). Diclofenac, an anti-inflammatory is no more used in India, due to its damaging outcomes on the population of vulture. However, for such chemical the concentration as well as frequency of detection in freshwater differs amongst person, compounds, and type of water matrices. A huge difference of concentrations and detection frequencies has broad variability in destiny of individual PPCP compounds inside aquatic ecosystems (Kolpin et al. 2002, 2004; Ashton et al. 2004; Brun et al. 2006; Focazio et al. 2008; Glassmeyer et al. 2008).

The Strategic Approach to International Chemicals Management (SAICM) pointed out the requirement to safeguard our environment including organism and human being from synthetically produced endocrine disrupting (ED) substances, classified as an emerging contaminants. During the assembly of delegates from industries and public organizations from 120 countries in SAICM 2012, the EDCs were of major concern and also a political issue throughout the world (SAICM 2012).

As far as we could possibly know, the examination of the selected PPCPs had not been done in Nagpur region. Additionally, this examination emphasizes the significance of the assurance of PPCPs in water. In India, MRL for PPCPs is not included in guidelines issued by control boards, who are related to administering the drinking water quality and its quality for human utilization. This study will provide an overall view on the existence of selected PPCPs during the treatment process.

20.1.1 Classification of PPCPs

PPCPs have been classified into two main groups such as Pharmaceutical and Personal Care Product, respectively. Thereafter, pharmaceutical is classified under subgroups such as Antibiotics, Hormones, Analgesics and anti-inflammatory drugs, Antiepileptic, Blood lipid regulators, β -blockers, Contrast media, Cytostatic drugs. Whereas, the personal care product is subgrouped under categories, viz.; Antimicrobial agents/Disinfectants, Synthetic musks/Fragrances, Insect repellants, Preservatives, Sunscreen UV filters. Representative Compounds are categorized based on application under the subgroups, as shown in Table 20.1.

20.1.2 PPCPs Production and Usage in India

Pharmaceutical industries are developing rapidly in India. The pharmaceutical enterprise produces a large group of human and veterinary drug compounds, used broadly in large portion. After America and EU, our country is the third largest manufacturer of pharmaceutical chemical compounds with annual turnover is likely to move US\$70 billion in line with per year through 2020 (CCI 2012). The pharmaceutical generation is increased by the huge demand of human medicines and veterinary medicines by the huge number of human and livestock population. About 85% demand of production are in domestic markets (IDMA 2009). Local consumption of the drugs in huge quantity causes the discharge of more such substance and related products in the environment. Generally water after use is treated and released for further usage via different populations dwelling downstream. In each such cycle, the clean water are taken up and used water is released with or with no treatment down with numerous contaminants. It critically and significantly impacts the water quality. Its management is one of the most challenging problems in the chemical world presently. These compounds were categorized in a brand new classes of pollution, referred to as emerging contaminants (EC's) (Mutiyaar and Mittal 2013). EC's include drugs, herbal and synthetic hormones, artificial sweeteners, personal care products, and so on., in which PPCPs rank better in the EC's listing.

20.2 Materials and Methods

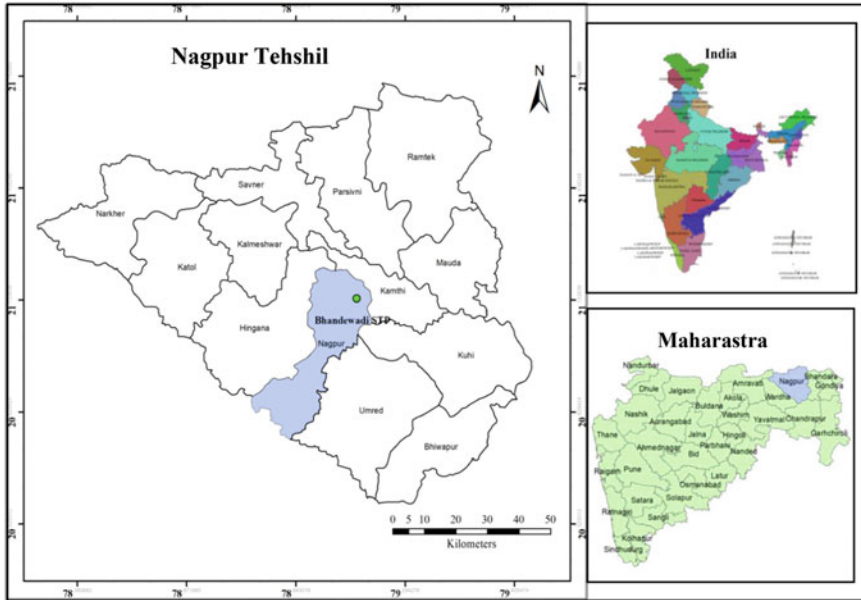
20.2.1 Area of Study

Bhandewadi sewage treatment plant (STP) is selected for the investigation of PPCP. It is located in south central Nagpur region of Maharashtra, India ($21^{\circ} 8'17.56''N$, $79^{\circ} 9'20.29''E$). This STP received waste water from the society of moderate- to

Table 20.1 Classification of PPCPs (Liu and Wong 2013)

Group	Subgroups	Representative compounds	
Pharmaceuticals	Antibiotics	Clarithromycin	
		Erythromycin	
		Sulfamethoxazole	
		Sulfadimethoxine	
		Ciprofloxacin	
		Norfloxacin	
	Hormones	Estrone (E1)	
		Estradiol (E2)	
		Ethinylestradiol (EE2)	
	Analgesics and anti-inflammatory drugs	Diclofenac	
		Ibuprofen	
		Acetaminophen	
		Acetylsalicylic acid	
		Antiepileptic	Carbamazepine
			Primidone
	Blood lipid regulators	Clofibrate	
		Gemfibrozil	
	β -Blockers	Metoprolol	
		Propranolol	
	Contrast media	Diatrizoate	
Iopromide			
Cytostatic drugs	Ifosfamide		
	Cyclophosphamide		
Personal care products	Antimicrobial agents/disinfectants	Triclosan	
		Triclocarban	
	Synthetic musks/fragrances	Galaxolide (HHCb)	
		Tonalide (AHTN)	
	Insect repellants	N,N-diethyl-m-toluamide (DEET)	
	Preservatives	Parabens (alkyl-p-hydroxybenzoates)	
	Sunscreen UV filters	2-ethyl-hexyl-4-trimethoxy cinnamate (EHMC)	
		4-methyl-benzilidene-camphor (4MBC)	

high-income group, and is operated by Nagpur Municipal Corporation, with 100 MLD installed capacity and treats 80 MLD water since the 2001. The occurrence of targeted PPCPs in sewage treatment plant of Nagpur region was studied over monthly basis. Site location show in Fig. 20.1.



a.



b.

Fig. 20.1 Study area of the Bhandewadi sewage treatment plant (STP)

20.2.2 Chemicals

Reference standards of 6 PPCPs, triclosan (TCS), 4-nonylphenol (NP), β -estradiol (ES), caffeine (CF), ibuprofen (IBU), and paraxanthine (PX) were procured from Dr. Ehrenstorfer (Augsburg, Germany). Throughout the study analytical grade (AR) solvents from Merck, Darmstadt, Germany were used. These solvents, viz.; acetone, ACN, EtCOOCH₃, hexane, DCM, and MeOH chemicals were used directly without any purification. A Milli-Q unit (Millipore, USA) used for the production of the ultrapure water. The methanol was used to prepare stock solutions of individual compounds. Finally a mix-working standard was prepared prior to each run on GC-MS by diluting the stock solutions. The volumetric flask containing stock solution is wrapped with aluminium foil and stored in refrigerator at 4 °C in dark place. Mixtures of analytes and working solutions were also stored in a similar way.

20.2.3 Sample Collection

Grab samples from raw and treated sewage were collected from influents and effluents of the STP. Regular samplings were carried out during the study period, i.e. July 2013–Feb 2014. Each time collection of samples was done in triplicated (~2000 mL of influents and 3000 mL of the others). The samples were collected in amber coloured prewashed glass bottles and were kept at low temperature during sampling. The transportation of samples to the laboratory was done within 1 h of collection. In laboratory the samples were stored in cold cabinet at 4 °C until further analysis.

20.2.4 Characterization of Water Quality

The values of water quality parameters such as pH, alkalinity, turbidity, total suspended solids (TSS), demand parameters like BOD and COD, phosphorous, and ammonia values were taken from the data of sewage treatment plant for all the samples. In addition, regularly examined parameter such as pH and alkalinity of grab samples were determined as per the standard methods (Eaton and Franson 2005), before and after filtration in the laboratory.

20.2.5 Preparation of Samples

The preparation of samples is one of the most crucial and important steps of PPCPs analysis. The water samples processing includes solid phase extraction and minimal

clean up if necessary. Solid phase extraction (SPE) is most appropriate and preferred method available for the preparation and analysis of environmental water samples. USEPA-Method 1694 is adopted for this work. All the water samples had been extracted and analyzed as per the USEPA process with slight laboratory changes, as soon as delivered to the laboratory. All the samples were filtered through glass microfiber filters (GF/F, Whatman). Solid Phase Extraction (AutoTrace 280 SPE instrument by Dionex Corporation Version 1.00 Cartridge Model) equipped with C18 cartridge used for the extraction of waste water samples. Before loading samples, the C18 cartridges were preconditioned with 10 mL type-1 water, 10 mL methanol followed by 6 mL ethyl acetate in series by gravity. All samples were passed through the SPE cartridge with the flow rate of 5–8 mL/min and maintained the flow with the aid of a vacuum. The rinsed cartridge (10 mL water) was dried out under the vacuum condition for about 15 min. Sample elution was done under gravity using 10 mL MeOH and 6 mL ACN:MeOH (1:1) mixture. The extracted samples were evaporated under moderate nitrogen gas to dryness and reconstituted with 1 mL acetonitrile. Further the extracted samples were analyzed by GC-MS technique.

20.2.6 GC-MS Detection

The gas chromatograph (Saturn, Varian) coupled directly to the mass spectrometer (240 MS) source has been used. An ion trap GC-MS equipped with Electron impact (EI) mode and MS capability was used for analysis of targeted compounds. The various conditions were set for the GC-MS and ion-trap for the GC resolution and mass spectra. The ion trap was held at 150 °C and was connected by a heated (230 °C) transfer line to GC. The GC separation of selected PPCPs was carried out on DB-5 capillary column with standard dimensions (length 30 m, 0.25 mm ID, and 0.25 micron film thickness). Column was connected to injector (Split/Splitless) on one end and its other end was directed into ion source of ion trap mass spectrometer. The temperature of injector was fixed at 270 °C. The EI mode was run at electron energy of 70 eV. The gas flow rate has been optimized at 1.0 mL/min. A 35-min temperature programmed was used to separate the mixture of compounds. The samples (1 µL) were injected and the column oven temperature programmed from 60 °C isothermal for 1.0 min, with rise of 15 °C/min to 270 °C and hold time for 20 min. The filament of the ion source was switched off during elution of the solvent. The complete mass spectra in scan mode were obtained over an appropriate m/z range. The identification of compounds was done w.r.t to reference standard compounds on the basis of their retention time on GC along with spectra of sample and match of ion-abundance ratios on MS.

20.3 Results and Discussion

20.3.1 Targeted Compounds

A set of PPCPs was selected for investigation which include an antibiotic, analgesic, surfactant, a hormone, and stimulant (Table 20.2). Numerous reports claimed the presence of antibiotic's residues in different water matrices. These varieties of matrices showing the presence of PPCPs residues include effluents from WWTPs (ETPs/STPs), wastewater coming from hospitals, and also in the raw water used for treatment for drinking purpose (Zuccato et al. 2000; Lindsey et al. 2001; Lindberg et al. 2004; Diwan et al. 2010).

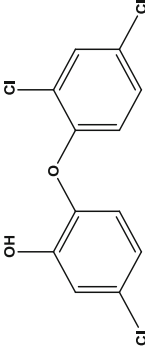
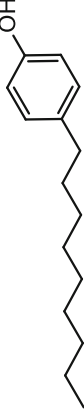
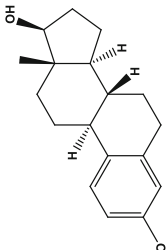
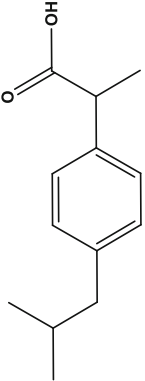
Triclosan is a polychloro **phenoxy phenol** with antibacterial and antifungal activity. It is mostly used in products (PCPs) such as soap, lotions, face ointments, hand wash, deodorants, etc. as well as in items of household usage like plastic chopping boards, sports equipments and shoes for its topical antibiotic activity. Triclosan is added in toothpastes to prevent gum disease. It acts as a xenobiotic, a persistent organic pollutant and a drug allergen.

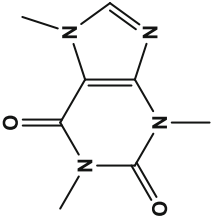
17 β -estradiol, a human secreting hormone, more often transported from individual households sewage waste to bulk waste water chosen for investigation. These oestrogenic substances are of concern when present in environment as it interferes in the male reproduction system in all organisms including human. The hormones 17 β -estradiol and estrone are excreted as per natural process in women (2–12 μ g/person/day) and female animals (3–20 μ g/person/day). Similarly estrone are excreted by men (5 μ g/person/day) naturally (Gower 1975).

Caffeine, a **methyloxanthine** alkaloid found in the seeds, nuts, or leaves of a variety of plants native to South America and East Asia that is structurally associated to **adenosine** (PubChem, NCBI). It is one of the most commonly consumed psychoactive substances throughout the globe (Higgins et al. 2007). It is a stimulant that can be easily get over-the-counter (OTC). The half-life of caffeine is about three to 4 h. It has been reported that <10% of it is expelled out unchanged through urine (Julien 2005). Further it has been found that out of total caffeine consumed, enzymatic reactions convert partly into paraxanthine (approx. 8%), a demethylated caffeine metabolite, and partly converted to theobromine and theophylline (16%) (Bolignano et al. 2007). Caffeine quickly and practically completely absorbed in the abdominal portion and small intestine, from where it is distributed in different tissues of body including brain. Excessive intake of caffeine is responsible for some physiological consequences including affect on central nervous system, high blood pressure, increased metabolic rate, and diuresis.

Study revealed that concentration of caffeine in different coffee beverages varied differently. It has been found that a normal coffee cup is accepted to give 100 mg of caffeine. Further investigations in the USA reported different quantity of caffeine in 240 mL of coffee. In brewed coffee its value ranged from 72 to 130 mg, whereas in espresso the quantity of caffeine varied from 58 to 76 mg, in a single shot.

Table 20.2 Properties of targeted PPCPs compounds

Compound	Chemical structure	Usage	log K_{ow} ^a	log K_{oc} ^b
Triclosan	 5-chloro-2-(2,4-dichlorophenoxy)phenol	Antimicrobial	4.76	4.3
4-Nonylphenol	 4-nonylphenol	Surfactant	3.80	4.7
17 β -estradiol	 (8R,9S,13S,14S,17S)-13-methyl-7,8,9,11,12,13,14,15,16,17-decahydro-6H-cyclopenta[a]phenanthrene-3,17-diol	Hormone	3.94	3.97
Ibuprofen	 2-(4-isobutylphenyl)propanoic acid	Analgesic	3.50	4.20

Caffeine	 <p data-bbox="382 931 405 1310">1,3,7-trimethyl-1<i>H</i>-purine-2,6(3<i>H</i>,7<i>H</i>)-dione</p>	Stimulant	0,09	-0,0135
----------	---	-----------	------	---------

^alog K_{ow} : octanol-water partition coefficient

^blog K_{oc} : soil adsorption coefficient

Nonylphenol polyethoxylates (NPPE) signify a group of important non-ionic surfactants. These compounds are used extensively throughout the world in a number of formulations. These formulations whether commercial or household, include detergents, cosmetic products, inks, water-based paints, and textiles (Birkett and Lester 2003). Additionally, it is used as a spermicide in contraceptives. Nonylphenol is an organic compound of the more extensive group of alkylphenols. This chemical has been synthesized in industry arrangement during the alkylation procedure of phenols, especially in the synthesis of polyethoxylate detergents (PubChem, NCBI). Nonylphenols are categorized as xenobiotics which is the man-made origin. The biodegradation of NPPE in the sewage water treatment process results in the formation of smaller compounds. In the breakdown process the hydrophilic ethoxylate chain of NPPE is broken down and resultant compounds are nonylphenol monoethoxylate (NP1EO) and diethoxylate (NP2EO). Further biodegradation of these NP1EO and NP2EO produces more lipophilic and toxic deethoxylated Nonylphenol. As compared to long chain ethoxylates which we have chosen for present study, this deethoxylated compound is resistant to biodegradation (Ahel et al. 1994).

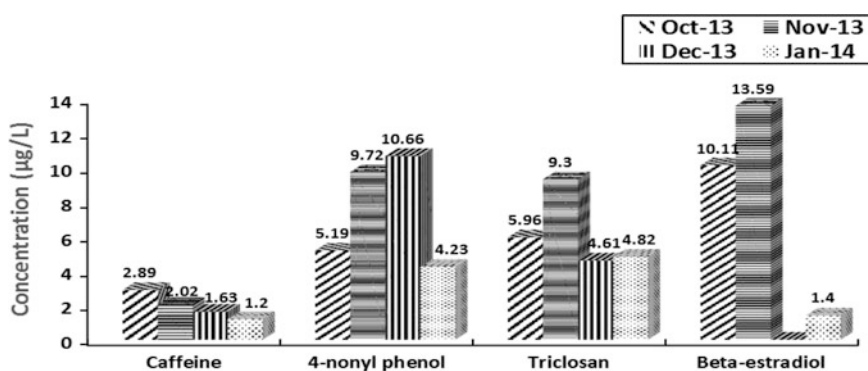
Ibuprofen is a type of non-steroidal anti-inflammatory drug (NSAID). This drug inhibits prostaglandin synthesis. Also when taken during the latter stage of pregnancy, it may cause closure of the foetal ductus arteriosus, foetal renal impairment, inhibition of platelet aggregation, and delay child birth (Goldfrank and Goldfrank 2006). Ibuprofen is well absorbed after oral administration. The $t_{1/2}$ of ibuprofen in blood plasma is about 1.9–2.2 h. As per the IBP data sheet, approximately 95% of a single dose of 500 mg is excreted via urine within 24 h. Of this 35% was excreted as metabolite A (+) 2–4-(2-hydroxy-2-methylpropylphenyl) propionic acid (15% free, 20% conjugated), 51% as metabolite B (+) 2–4-(2-carboxypropylphenyl) propionic acid (42% free, 9% conjugated), and 9% as ibuprofen (1% free, 8% conjugated) (NZ MMDSA., Ibp data sheet).

20.3.2 Concentrations of Targeted Compounds

The targeted PPCPs compounds were monitored in the field samples through GC-MS method developed for their determination. The results are given in Tables 20.2 and 20.3 which are the calibration equations and coefficients of assurance (R^2) for concentrations ranged from 0.5 to 1 μgL^{-1} of each analyte, limits of identification and evaluation. The concentrations of 17 β -estradiol and Nonylphenol were highest of all detected compounds. As oestrogen is a human secreted hormone transported from household sewage to bulk waste water. Triclosan and Nonylphenol are the most common contaminants detected in every sample due to their vast usage in the city (Fig. 20.2).

Table 20.3 Analytical parameters of GC-MS method for the identification

Compound	Calibration equation	R^2	LOD (μgL^{-1})	LOQ (μgL^{-1})
4-n-Nonylphenol	$y = 2\text{E}+07x$	0.9948	0.51	1.54
Triclosan	$y = 5\text{E}+07x - 3\text{E}+07$	0.9930	0.56	1.70
17 β -estradiol	$y = 3\text{E}+06x + 4\text{E}+06$	0.9951	0.46	1.42
Caffeine	$y = 4\text{E}+06x - 216,667$	0.9961	0.41	1.26

**Fig. 20.2** Identification of the PPCPs compounds and their concentration in inlet of STP

20.3.3 Effect of Seasonal Variation

The concentration of PPCPs in the effluent of Sewage Treatment Plant is affected by number of factors. Temperature being a very significant factor for the better elimination and it results in reducing the concentrations in the discharge water. Ambient temperature plays a significant contribution for expulsion of PPCP contaminants in open treatment plants. The monthly average temperature in the Nagpur region during the entire sample collection period was noted in the range of 22–28 °C (data taken from weather.com).

The concentrations of different compounds in inlet of STP during the sampling period are given in Fig. 20.2. The concentrations of caffeine ranged from 1.2–2.89 $\mu\text{g/L}$, 4-nonylphenol ranged from 4.2–10.66 $\mu\text{g/L}$, Triclosan from 4.61–9.3 $\mu\text{g/L}$, and beta-estradiol from 0–13.59 $\mu\text{g/L}$.

20.3.4 Effect of Treatment Process

The effect of treatment process utilized in the STP, on the concentration of selected compound is shown in Fig. 20.3(a–d). High concentration of all the selected compounds was found in the inlet samples during all the samplings, except for

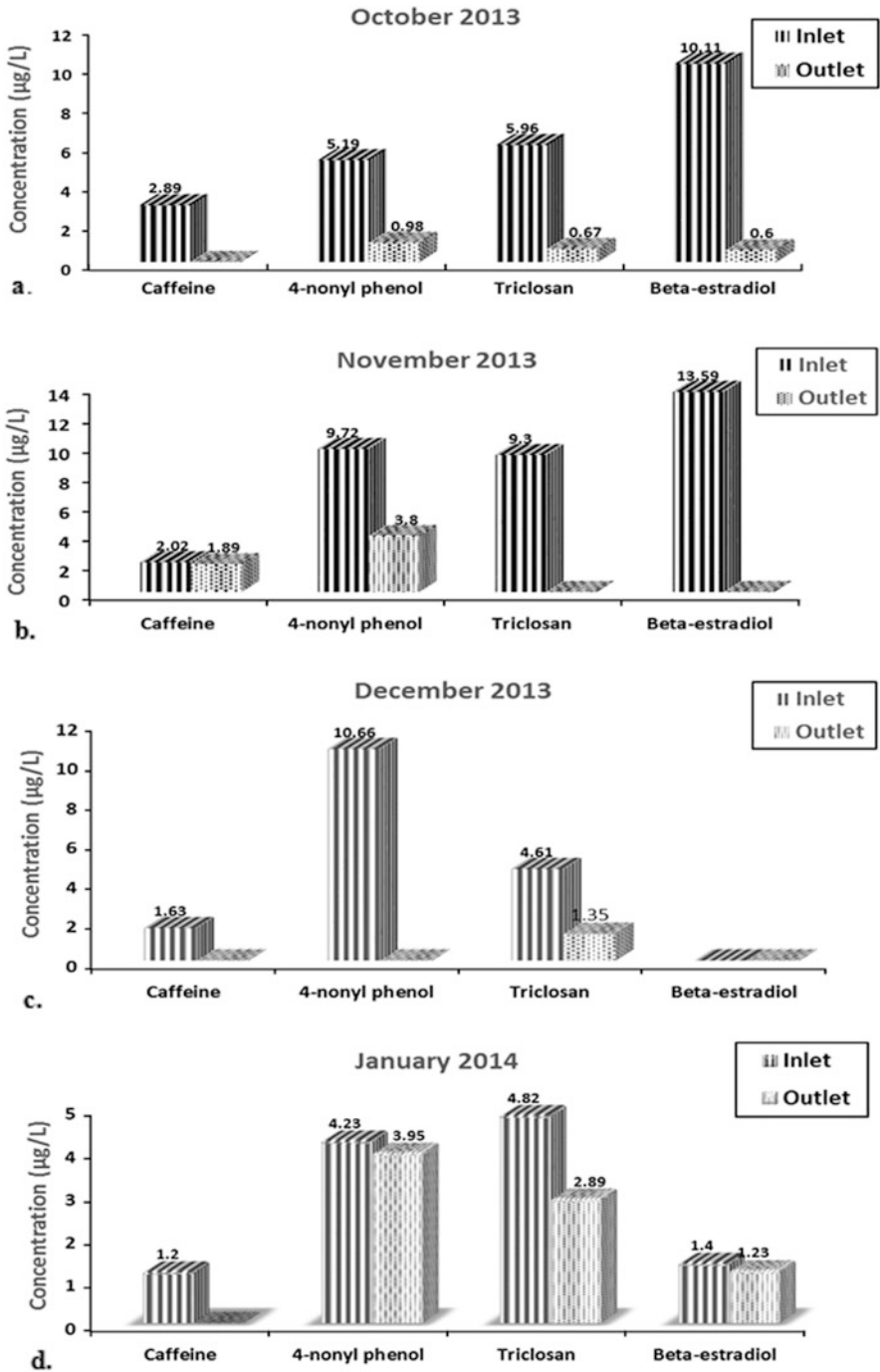


Fig. 20.3 (a-d) showing concentration of selected compounds in inlet and outlet of STP during different sampling time

beta-estradiol which was not detected in sample collected in December-13. However, there is decrease in the concentration of few compounds or some compounds are not detected in the outlet samples. In the outlet samples, caffeine was detected only in November-13 sample (1.89 $\mu\text{g/L}$). Similarly, beta-estradiol was detected only in October-13 (0.6 $\mu\text{g/L}$) and January-14 (1.2 $\mu\text{g/L}$) samples. The concentration values for 4-nonylphenol range from 0–3.95 $\mu\text{g/L}$, it was not detected only in December-13 sample. In a similar pattern the concentration of triclosan ranges from 0.67–2.89 $\mu\text{g/L}$, and it was not detected only in November-13 sample. The results revealed that the decrease in concentration of selected compounds in outlet water is not only because of treatment in STPs but might be due to cumulative factors responsible for this reduction.

20.4 Occurrence of PPCPs in Different Environmental Resources and Risk Assessment

More than 100 of pharmaceutically active compounds are detected in different classes, have been available in water, soil, sediment, sewage, manure from animals derived, bio-solids material, and also in potable water. The compounds that have been identified with a wide kind of PPCPs classes, which are including anti-microbials, antiphlogistics, antiepileptics, beta-blockers, lipid controllers, vasodilators, and sympathomimetics. The vast majority of the proof of such compounds are available in nature that are accumulated in the aquatic ecosystem (Jjemba 2019).

A few PPCPs are persisting in the surroundings, however those won't be persistent to expose their risky consequences as these are constantly being released to the environment. These compounds has been returned back to us again and again via potable water or via food chain (Fig. 20.4). Such exposure is of finest large concern, in particular for pregnant moms and youngsters. PPCPs are considered as endocrine disrupting agents who lead to unfavourable developmental outcomes in aquatic organisms even at environmentally applicable concentrations, i.e. concentrations which typically considered to be minimal and harmless. Dangerous results of PPCPs can be categorized as

- Effect of PPCPs on aquatic ecology.
- Terrestrial species.
- Human health.

Pharmaceuticals drugs are designed to be pretty active and need to produce results at very low concentrations. The pharmaceuticals drugs are constantly discharged in the river basins, so the aquatic organisms get lifelong exposures.

The pharmaceutical residues present in wastewater are threat to aquatic life (Zhang et al. 2012). Modification in expression of gene caused by way of exposure to an excessive dilution of the industrial effluent containing PPCPs, confirmed that fishes are responding to chemical exposure. The pharmaceutical industrial effluent

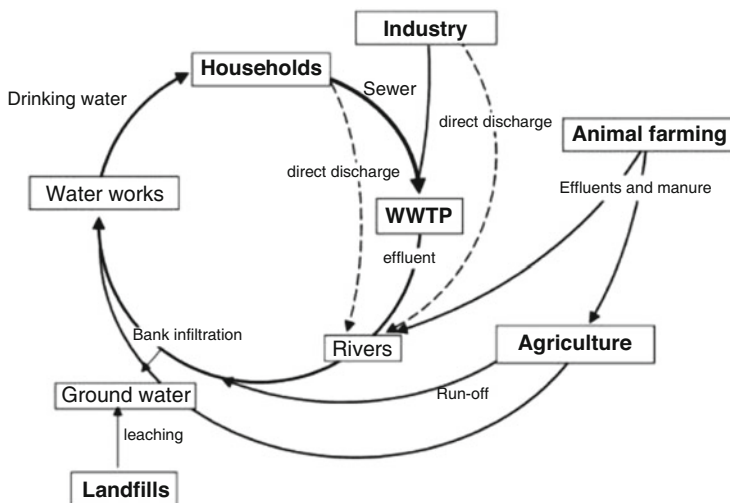


Fig. 20.4 Sources of contaminants in the Environment (Petrovic et al. 2003)

was sampled from Patancheru Pharmaceutical Industrial Cluster, Hyderabad (India) and was diluted to 1000 times earlier than exposing to fishes (Gunnarsson et al. 2009). These findings confirmed that PPCPs residues in Indian surroundings are at extraordinarily risky stages. Further, the residues of analgesic medicine have severely affected the populace of Indian vultures (Oaks et al. 2004; Taggart et al. 2009). Now, it is established that antibiotic residues (quinolone) are a threat to avian scavengers as well (Lemus et al. 2008). So, antibiotic residue's risk is not always restrained to aquatic organisms most effective, but poses critical threat to avian scavengers additionally. Microorganisms currently within the aquatic surroundings are exposed to the drug residues. Chronic exposure might also cause mutations and the improvement of latest strains. Current classification of antibiotic-resistance bacteria within the surroundings has enhanced new size to the chance created by way of the occurrence of drug residues within the environment.

20.5 Conclusion

This study targeted on the removal of PPCPs by a local sewage treatment plant. Mostly selected compounds concentration cannot be effectively removed by normal treatment process. However, it is significant to look into the slight reduction in PPCPs concentrations during the course of treatment. Although the work on the treatment and remediation of PPCPs is gaining attention worldwide, in India the research gap in this part still exist. Further research is needed to the advanced technology for proper treatment of the PPCPs compounds in treated water from STPs. Investigations are also needed on the fate and movement of PPCPs in the

environment, their uptake by crop plants when treated effluent water is used for irrigation and finally their direct or indirect influence on public health.

Acknowledgment Financial support for the study was given by Water Technology Initiative (WTI), Department of Science and Technology, Govt. of India (Project code: DST/TM/WTI/2 K12/49). The authors are thankful to Director, NEERI for providing infrastructure facility to carry out this research work.

References

- Ahel M, Giger W, Koch M (1994) Behaviour of alkylphenol polyethoxylate surfactants in the aquatic environment—I. Occurrence and transformation in sewage treatment. *Water Res* 28:1131–1142
- Ashton D, Hilton M, Thomas KV (2004) Investigating the environmental transport of human pharmaceuticals to streams in the United Kingdom. *Sci Total Environ* 333:167–184
- Barcelo D (2003) Emerging pollutants in water analysis. Special issue. *Trends Anal Chem* 22:–10
- Bendz D, Paxéus NA, Ginn TR, Loge FJ (2005) Occurrence and fate of pharmaceutically active compounds in the environment, a case study: Høje River in Sweden. *J Hazard Mater* 122 (3):195–204
- Birkett JW, Lester JN (2003) Endocrine disrupters in wastewater and sludge treatment processes. CRC Press, Boca Raton, FL
- Bolignano D, Coppolino G, Barillà A, Campo S, Criseo M, Tripodo D, Buemi M (2007) Caffeine and the kidney: what evidence right now? *J Ren Nutr* 17(4):225–234
- Boxall ABA, Kolpin DW, Halling-Sørensen B, Tolls J (2003) Peer reviewed: are veterinary medicines causing environmental risks? *Environ Sci Technol* 37:286A–294A
- Brun GL, Bernier M, Loiser R, Doe K, Jackman P, Lee HB (2006) Pharmaceutically active compounds in Atlantic Canadian sewage treatment plant effluent and receiving waters, and potential for environmental effects as measured by acute and chronic aquatic toxicity. *Environ Toxicol Chem* 25:2163–2176
- CCI (2012) A report on pharmaceutical industry in India. http://www.cci.in/pdf/surveys_reports/Pharmaceutical-Industry-in-India.pdf
- Daughton CG, Ternes TA (1999) Pharmaceuticals and personal care products in the environment: agents of subtle change? *Environ. Health Perspect* 107:907–938
- Daughton C (2001) Pharmaceuticals and personal care products in the environment; overarching issues and overview. In: Daughton CG, Jones-Lepp T (eds) Scientific and regulatory issues, ACS symposium series 791. American Chemical Society, Washington, DC, pp 2–38
- Daughton C (2003) Pollution from combined activities, actions and behaviours of the public: pharmaceuticals and personal care products. *SETAC News* 14(1):5–15
- Diwan V, Tamhankar AJ, Khandal RK, Sen S, Aggarwal M, Marothi M, Iyer RV, Tonderski KS, Lundborg CS (2010) Antibiotics and antibiotic-resistant bacteria in water associated with a hospital in Ujjain, India. *BMC Public Health* 10:414–422
- Eaton AD, Franson MAH (2005) Standard methods for the examination of water and wastewater. American Public Health Association, American Water Works Association, Water Environment Federation, Washington, Denver, Alexandria
- EUROPA (2012). http://ec.europa.eu/environment/water/index_en.html
- Ferguson PJ, Bernot MJ, Doll JC, Lauer TE (2013) Detection of pharmaceuticals and personal care products (PPCPs) in near-shore habitats of southern Lake Michigan. *Sci Total Environ* 458:187–196
- Focazio MJ, Kolpin DW, Barnes KK, Furlong ET, Meyer MT, Zaugg SD, Barber LB, Thurman ME (2008) A national reconnaissance for pharmaceuticals and other organic wastewater

- contaminants in the United States — II. Untreated drinking water sources. *Sci Total Environ* 402:201–216
- Glassmeyer ST, Kolpin DW, Furlong ET, Focazio M (2008) Environmental presence and persistence of pharmaceuticals an overview. In: Aga D (ed) *Fate of pharmaceuticals in the environment and in water treatment systems*. CRC Press, New York, pp 3–51
- Goldfrank LR, Goldfrank ED (2006) *Toxicologic emergencies*, 8th edn. McGraw Hill, New York, NY
- Gower DB (1975) Catabolism and excretion of steroids. In: Makin HLJ (ed) *Biochemistry of steroid hormones*. Blackwell, Oxford, pp 127–148
- Gunnarsson L, Kristiansson E, Rutgersso C, Sturve J, Fick J, Forlin L, Larsson DGJ (2009) Pharmaceutical industry effluent diluted 1:500 affects global gene expression, cytochrome P450 1A activity, and plasma phosphate in fish. *Environ Toxicol Chem* 28:2639–2647
- Gurunadharao VVS, Dhar RL, Subrahmanyam K (2001) Assessment of contaminant migration in groundwater from an industrial development area, Medak district, Andhra Pradesh, India. *Water, Air, Soil Pollut* 128:369–389
- Heberer T (2002) Occurrence, fate, and removal of pharmaceutical residues in the aquatic environment: a review of recent research data. *Toxicol Lett* 131:5–17
- Higgins GA, Grzelak ME, Pond AJ, Cohen-Williams ME, Hodgson RA, Varty GB (2007) The effect of caffeine to increase reaction time in the rat during a test of attention is mediated through antagonism of adenosine A2A receptors. *Behav Brain Res* 185:32–42
- Hirsch R, Ternes TA, Haberer K, Mehlich A, Ballwanz F, Kratz KL (1998) Determination of antibiotics in different water compartments via liquid chromatography-electrospray tandem mass spectrometry. *J Chromatogr A* 815(2):213–223
- IDMA (2009) *India's quality affordable generics: for global healthcare 47th Annual Publication IDMA 2009*
- Jjemba PK (2019) *Pharma-ecology. The occurrence and fate of pharmaceuticals and personal care products in the environment*, 2nd edn. John Wiley & Sons, New York, p 416
- Julien RM (2005) *A primer of drug action*, 10th edn. Worth Publishers, New York
- Ke Y, Li B, Zhang T (2012) Direct rapid analysis of multiple PPCPs in municipal wastewater using ultrahigh performance liquid chromatography–tandem mass spectrometry without SPE pre-concentration. *Anal Chim Acta* 738:59–68
- Kolpin DW, Furlong ET, Meyer MT, Thurman EM, Barber LB, Buxton HT (2002) Pharmaceuticals, hormones, and other organic wastewater contaminants in U.S. streams, 1999–2000: a national reconnaissance. *Env Sci Technol* 36:1202–1211
- Kolpin DW, Skopec M, Meyer MT, Furlong ET, Zaugg SD (2004) Urban contribution of pharmaceuticals and other organic wastewater contaminants to streams during differing flow conditions. *Sci Total Environ* 328:119–130
- Kummerer K (2008) *Pharmaceuticals in the environment: sources, fate, effects and risks*. Springer, Berlin
- Larsson DGJ, de Pedro C, Paxeus N (2007) Effluent from drug manufactures contains extremely high levels of pharmaceuticals. *J Hazard Mater* 148:751–755
- Lemus JA, Blanco G, Grande J, Arroyo B, García-Montijano M, Martínez F (2008) Antibiotics threaten wildlife: circulating quinolone residues and disease in avian scavengers. *PLoS One* 3: e1444
- Lindberg R, Jarnheimer PA, Olsen B, Johansson M, Tysklind M (2004) Determination of antibiotic substances in hospital sewage water using solid phase extraction and liquid chromatography/mass spectrometry and group analogue internal standards. *Chemosphere* 57(10):1479–1488
- Lindsey M, Meyer TM, Thurman EM (2001) Analysis of trace levels of sulfonamide and tetracycline antimicrobials in ground water and surface water using solid-phase extraction and liquid chromatography/mass spectrometry, *anal. Chem* 73(19):4640–4646
- Liu JL, Wong MH (2013) Pharmaceuticals and personal care products (PPCPs): a review on environmental contamination in China. *Env Int* 59:208–224

- Maria CP, Basaglia G (2007) GC-MS analytical methods for the determination of personal-care products in water matrices. *Trends Anal Chem* 26:1086–1094
- Mutiyar PK, Mittal AK (2013) Pharmaceuticals and personal care products (PPCPs) residues in water environment of India: a neglected but sensitive issue, 28th National Convention of environmental engineers and National Seminar on hazardous waste management and healthcare in India, Patna
- New Zealand Medicines and Medical Devices Safety Authority (NZ MMDSA) (n.d.) APO-Ibuprofen data Sheet. <http://www.medsafe.govt.nz/>
- Oaks JL, Gilbert M, Virani MZ, Watson RT, Meteyer CU, Rideout BA, Shivaprasad HL, Ahmed S, Chaudhry MJI, Mahmood AM, Ali S, Khan AA (2004) Diclofenac residues as the cause of vulture population decline in Pakistan. *Nature* 427:630–633
- Okuda T, Yamashita N, Tanaka H, Matsukawa H, Tanabe K (2009) Development of extraction method of pharmaceuticals and their occurrences found in Japanese wastewater treatment plants. *Environ Int* 35:815–820
- Petrovic M, Gonzalez S, Barcelo D (2003) Analysis and removal of emerging contaminants in wastewater and drinking water. *Trends Anal Chem* 22:685–696
- Ryu J, Oh J, Snyder SA, Yoon Y (2014) Determination of micropollutants in combined sewer overflows and their removal in a wastewater treatment plant (Seoul, South Korea). *Environ Monit Assess* 186:3239–3251
- SAICM (2012) Strategic approach to international chemicals management. <http://www.saicm.org>
- Santos LHMLM, Araújo AN, Fachini A, Pena A, Delerue-Matos C, Montenegro M (2010) Ecotoxicological aspects related to the presence of pharmaceuticals in the aquatic environment. *J Hazard Mater* 175:45–95
- Sonia S, Carballa M, Omil F, Lema JM (2008) How are pharmaceutical and personal care products (PPCPs) removed from urban wastewaters? *Rev Environ Sci Biotechnol* 7:125–138
- Taggart MA, Senacha KR, Green RE, Cuthbert R, Jhala YV, Meharg AA, Mateo R, Pain DJ (2009) Analysis of nine NSAIDs in ungulate tissues available to critically endangered vultures in India. *Environ Sci Technol* 43:4561–4566
- USEPA (2012) Pharmaceuticals and personal care products. <http://www.epa.gov/ppcp/faq.html>
- Veldhoen N, Skirrow RC, Osachoff H, Wigmore H, Clapson DJ, Gunderson MP, Van Aggelen G, Helbing CC (2007) The bactericidal agent triclosan modulates thyroid hormone-associated gene expression and disrupts postembryonic anuran development. *Aquat Toxicol* 80:217–227
- Zhang R, Zhang G, Zheng Q, Tang J, Chen Y, Xu W, Zou Y, Chen X (2012) Occurrence and risks of antibiotics in the Laizhou Bay, China: impacts of river discharge. *Ecotoxicol Environ Saf* 80:208–215
- Zuccato E, Calamari D, Natangelo M, Fanelli R (2000) Presence of therapeutic drugs in the environment. *Lancet* 355(9127):1789–1790. <https://pubchem.ncbi.nlm.nih.gov/compound/5564>

Chapter 21

Arsenic-Rich Surface and Groundwater around Eastern Parts of Rupnagar District, Punjab, India



Navjot Kaur and Susanta Paikaray

Abstract Arsenic-rich (As) groundwater is a serious concern in Punjab affecting thirteen districts along the Sutlej and Ravi River alluvial deposits including the present study site of Rupnagar district. Water samples from the Quaternary deposits along eastern part of Rupnagar have been examined for detailed geochemistry during pre- and post-monsoon seasons. Two traverses were made along the northern and southern side of a thermal power and cement plant with total of twenty surface stream, hand pump (~50–60 ft.) and bore well (~180–200 ft.) samples. Overall circum-neutral pH with relatively greater cationic and anionic contents with higher As along the southern traverse (mostly hand pumps and bore wells) compared to northern traverse (mostly stream waters) characterize the areal geochemistry and, interestingly, the groundwater flow direction is Southwest in the region. Post-monsoon samples contain more As than pre-monsoon for any particular location and As concentrations are relatively higher near to the waste dumps that slowly lowers outward. The present findings suggest that the huge coal ash wastes might be a dominant contributor of such high As, especially along the southern traverse, while not overruling geogenic As-rich alluvial deposits as evidenced along northern traverse. Greater As contents during post-monsoon season are attributed to favorable leaching by monsoonal infiltration. Arsenic correlation with PO_4^{3-} is indicative of a likely ionic exchange between PO_4^{3-} and HAsO_4^{2-} owing to their comparable ionic radius resulting higher $\text{As}_{(\text{aq})}$, whereas significant correlations of As with HCO_3^- and Si^{4+} suggests the role of bicarbonate and silicate on mobilization of As in the groundwater due to the carbonation of arsenic sulfide minerals (e.g. As_2S_3 or $\text{As}_4\text{S}_4/\text{AsS}$) and silicate weathering, respectively.

Keywords Geogenic arsenic · Quaternary aquifers · Thermal plant waste · Sutlej River valley · Monsoonal leaching

N. Kaur (✉) · S. Paikaray
Department of Geology, Panjab University, Chandigarh, India

21.1 Introduction

Arsenic (As) poisoning is severely affecting more than 100 countries worldwide with >200 million population (Chakraborti et al. 2016; Murcott 2012). India is among the severely As affected countries such as Taiwan, China, Bangladesh, Nepal, Vietnam, Hungary, Cambodia, and USA (Smedley and Kinniburgh 2002). High As contamination of groundwater, soil and dietary components are being reported from West Bengal, Uttar Pradesh, Bihar, Jharkhand, Madhya Pradesh, Chhattisgarh, Andhra Pradesh, Assam, Manipur, and Haryana (Chakraborti et al. 2016; Saurav et al. 2015; Kumar et al. 2015). Both natural and anthropogenic sources greatly contribute to As enrichment in ecosystem which include As-rich sulfides and oxides, coal burned fly ash, mining operations, industrial discharge, and agricultural use of pesticides and fertilizers, etc. (Abrahams and Thornton 1987; Ravenscroft et al. 2011; Smith et al. 1998). Arsenic enrichment in soil and water is governed by micro- and meso-scale processes such as aquifer heterogeneity, surface/groundwater-soil interaction, redox state of As, etc. that ultimately lead to variability in As toxicity in any given region. Four major mobilization mechanisms, i.e., reductive dissolution, alkali desorption, sulfide oxidation, and geothermal activity are responsible for huge flux of As from source into the water resources. Higher adsorption of inorganic As in the gastrointestinal tract of living beings make it more toxic than organic form of As (Guha Mazumder 2003). Chronic exposure of such forms of As by drinking water results in different kind of skin ailments and progressively leads to cancer and ultimate death (WHO 1993, 2006).

Indo-Gangetic alluvial belts along Sutlej and Ravi River flowing through Punjab are severely affected by As pollution that caused serious threat to ~13 districts of Punjab (Hundal et al. 2007, 2009; Shah et al. 2015; Virk 2019). Such dynamic behavior of As is best reflected in river basins for which Sutlej alluvial plain along eastern part of Punjab were investigated where both surface (SW) and groundwater (GW) serve as the main water source for domestic and agricultural purposes. Rupnagar district has been categorized under moderate to high As status category (Hundal et al. 2007) with elevated concentrations of As (Sharma et al. 2016, 2017, 2018; Singh et al. 2015; Thakur et al. 2016). Despite such high concentrations, there have been no detailed in-depth studies of such high As enrichments, mobilization, and monsoonal effects to the best of our knowledge. The present study is based on quantitative assessment, origin, and possible mobilization mechanisms of As in surface and groundwater around alluvial plains of Sutlej and Sirsa River, coal fired cement plant (CP), and Thermal power plant (TPP) during pre- and post-monsoon season in the area. In addition to understand the above processes, role of fly ash and CP/TPP wastes on As distribution around the locality serves as another important objective.

This study certainly brings out many new insights on the complex geochemical processes responsible for As enrichment, its mobilization control, and most importantly, the origin of As in the given area. Risk of As toxicity and its variability between surface and groundwater and effect of monsoon on local

hydrogeochemistry will greatly benefit the water usability for agricultural and domestic purposes. Being regions of highest storage for freshwater resources along alluvial plains overseas and prone for contamination by river laden soils, the findings from this work may greatly contribute to ongoing river basin geochemical studies.

21.2 Materials and Methods

The present study area is located along eastern part of Rupnagar district of Punjab, India. The Sutlej River meanders through this area in a NW-SE direction and then flowing out of the state by taking a steep west direction. Sirsa River, a tributary of Sutlej River enters the state from Himachal Pradesh to join into the Sutlej River. Both the rivers serve as a major surface water source for irrigation and domestic purposes in this region. The study area covers an area of ~40 km² stretch of mainly Quaternary alluvial soils between 76 °31'E and 76 °36'E longitude and 31 °01'N and 31 °04'N latitude (Fig. 21.1) with altitude of 264–287 m above MSL. The area has hot to semi-arid type climate with 7–45 °C of annual temperature and ~ 775.6 mm of average rainfall. The region experiences three major seasons, i.e., summer (March–June), winter (November–February), and monsoon (July–October) seasons.

Based on these climatic conditions, systematic sampling was carried out during the pre- (June 2019) and post-monsoon (December 2018) seasons in two traverses along the northern (sample no. I1 to I5) and southern side (sample no. II1 to II5) of a thermal power and cement plant with total of twenty surface stream, hand pump

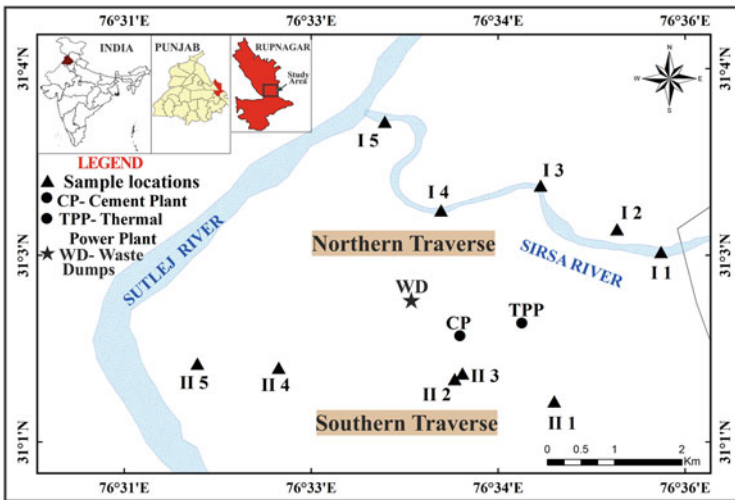


Fig. 21.1 Map showing Rupnagar district, Punjab and location of study site (inset) and sampling traverses along the northern (I1–I5) and southern (II1–II5) ends of the thermal power and cement plant

(~50–60 ft.) and bore well (~180–200 ft.) samples. The field sampling was designed in order to address the (1) effect of monsoon, (2) role of CP and TPP, and (3) aquifer depth on overall As distribution in the given region. Each sampling site was maintained ~2 km apart from each other to minimize geological similarities among them and both traverses are ~7 km long that ultimately meets with Sutlej main river flow. The northern side constitutes both SW along Sirsa River and GW from bore wells, while southern side lacks any SW because of its unavailability along this traverse (III–II5).

After carefully rinsing the polyethylene bottles with that particular water thrice, samples were filtered through Whatman no. 42 filter paper into 1 Land 100 mL bottles. All the on-site field parameters like pH, ORP, and Temperature (pH 700 meter, EUTECH instruments, Singapore) and TDS (Digital TDS-3 meter, WDS, India) were measured during sampling and immediately transported to laboratory and stored at 4 °C until analysis. The unacidified 1 L samples were used for analysis of Ca^{2+} , Mg^{2+} , Na^+ , K^+ , CO_3^{2-} , HCO_3^- , SO_4^{2-} , Cl^- , NO_3^- , PO_4^{3-} , Fe(T) , Al^{3+} , and Si^{4+} using standard methods, while the 100 mL acidified samples were analyzed for As(T). The major cations, anions, and trace elements were analyzed in laboratory by employing the standard methods (APHA 1994). UV-VIS spectrophotometer (Lasany Double beam LI-2004 UV-Vis spectrophotometer, Japan) was used for NO_3^- (Panchagnula 2018), PO_4^{3-} (USEPA 1978), Si^{4+} (Grasshoff et al. 1999), and As(T) (Dhar et al. 2004) measurements. EC was calculated from TDS ($\text{EC} = \text{TDS}/0.64$) (Sen 2014). For reproducibility, all the analysis was done in duplicates.

21.2.1 Risk Assessment

Humans are exposed to arsenic through respiratory/airborne pathways (industrial emissions, domestic fuel, etc.), dermal pathways (pesticides application, washing, bathing, phosphate detergents, etc.), and ingestion (drinking water, food, cooking water, medicines, etc.) (Ravenscroft et al. 2011). Chronic daily intake (CDIs, $\text{mg kg}^{-1} \text{ day}^{-1}$) of As from SW and GW of pre- and post-monsoon seasons by the residents was used for risk assessment. Along with CDI, non-cancer health hazard quotient (HQs), and cancer risk (CR) were estimated as per the guidelines of USEPA (1989).

$$\text{CDI} = C_M \times \frac{\text{DI}}{\text{BW}}$$

where C_M (mg L^{-1}) is the average concentration of As in GW or SW. DI is daily intake of water (2 L day^{-1}) (Bortey-Sam et al. 2015) and BW is the average body weight (70 kg) (Jan et al. 2010).

$$HQ = \frac{CDI}{R_f D}$$

where $R_f D$ is the oral reference dose of As ($0.0003 \text{ mg kg}^{-1} \text{ day}^{-1}$) (USEPA 2015). $HQ < 1$ is termed as safe and non-carcinogenic for human health, whereas $HQ > 1$ indicates major potential health concern and appearance of non-cancerous health problems (USEPA 1989).

$$CR = CDI \times SF$$

where SF is the slope factor for oral carcinogenic dose of As, i.e., $1.5 \text{ mg kg}^{-1} \text{ day}^{-1}$ (USEPA 2015). $CR \geq 1.00 \times 10^{-6}$ USEPA limit indicates higher possibilities of cancer cases with one case out of 1,000,000 individuals.

21.3 Results and Discussion

The physiochemical parameters of the studied water samples are summarized in Table 21.1. Overall circum-neutral pH with pH 6.78–7.57 in pre-monsoon and 6.89–8.03 in post-monsoon was observed. pH of all the samples were within the recommended permissible limits of 8.5 (WHO 2004) and slight alkaline nature of post-monsoon samples were noticed which may be due to excess leaching during monsoon. The ORP in the vicinity of the industrial plants was very low pointing towards reducing conditions at those locations. Electrical conductivity of around 90% of the total samples exceeds the permissible limits of $500 \mu\text{S cm}^{-1}$ as prescribed by WHO (2004). The highest EC and TDS was observed in sample closest to the CP and TPP (sample no. II3). Such high EC value indicates ion exchange, chemical weathering and solubilization in the aquifers (Ravindra and Garg 2007).

One sample of pre-monsoon and seven samples of post-monsoon season exceeds the desirable limit of 75 mg L^{-1} for Ca^{2+} . On an average GW samples contain more Ca^{2+} as compared to SW samples. Similarly, higher Fe(T) concentrations were measured in post-monsoon as compared to pre-monsoon season with 80% and 10% samples exceeding the desired limit, respectively. Al^{3+} and Si^{4+} concentrations were within the safe limits with more enrichment of Al^{3+} and Si^{4+} in post- and pre-monsoon, respectively. K^{+} contents in 20% of samples each in pre- and post-monsoon season exceed the desirable limit of 12 mg L^{-1} with average concentration greater in the southern traverse during both the seasons. On the other hand, Mg^{2+} concentrations were higher in the pre-monsoon with only 20% of samples exceeding the WHO (2004) desirable limit of 50 mg L^{-1} . Although Na^{+} contents were within the desirable limits in all the samples. Pre-monsoon and SW contain comparatively higher Na^{+} than the post-monsoon and GW samples. Cationic distributions indicate variability in their overall SW vs. GW enrichments. Cations that are more prone to chemical leaching exhibits post-monsoon enrichments, e.g., Ca^{2+} , Fe

Table 21.1 Physiochemical characteristics with minimum, maximum, mean, and standard deviation values of water samples during pre-monsoon (June 2019) and post-monsoon (December 2018) seasons in the study area; BDL—below detection limit

Parameter	Units	WHO (2004) limit in drinking water	Pre-monsoon				Post-monsoon			
			Min	Max	Mean	Std dev.	Min	Max	Mean	Std dev.
Temp	°C	–	25.30	31	28.37	2.15	1.5	26	19.90	2.15
pH	–	6.5–8.5	6.78	7.57	7.04	0.23	6.89	8.03	7.29	0.45
TDS	Mg L ⁻¹	1000	195	1250	594	333.49	293	1250	577.20	274.79
EC	µS cm ⁻¹	500	304.7	1953.1	521.08	881.25	457.81	1953.1	901.88	429.35
Ca ²⁺	Mg L ⁻¹	75	8.02	88.18	28.46	24.05	49.70	137.07	93.55	27.70
Mg ²⁺	Mg L ⁻¹	50	16.57	60.42	37.33	13.43	1.95	47.75	20.52	14.41
Na ⁺	Mg L ⁻¹	200	8.50	193	85.15	72.19	11	123	66.02	46.37
K ⁺	Mg L ⁻¹	12	2.20	141	19.68	42.80	0.7	188	22.85	58.14
Fe(T)	Mg L ⁻¹	0.1	0.02	0.13	0.08	0.04	0.15	0.65	0.28	0.17
Al ³⁺	Mg L ⁻¹	0.2	BDL	0.03	0.01	0.01	BDL	0.13	0.05	0.04
Si ⁴⁺	Mg L ⁻¹	–	11	38.02	19.82	7.57	3.34	25.75	12.80	7.06
HCO ₃ ⁻	Mg L ⁻¹	500	230	830	387	167.40	230	830	394	170.83
SO ₄ ²⁻	Mg L ⁻¹	250	32.79	149	60.14	32.20	34.18	138.42	67.99	28.44
Cl ⁻	Mg L ⁻¹	200	35.50	376.3	141.29	134.90	21.3	234.3	102.24	82.68
NO ₃ ⁻	Mg L ⁻¹	50	15.71	97.14	55.21	29.65	4.29	48.57	21.29	16.79
PO ₄ ³⁻	Mg L ⁻¹	0.1	0.01	5.55	0.67	1.72	0.01	0.67	0.17	0.21
As(T)	µg L ⁻¹	10	BDL	1446.2	192.22	443.04	87.21	780.52	309.12	199.54

(T), Al^{3+} , and K^+ , whereas decrease in Na^+ and Mg^{2+} in this season might be due to monsoonal dilution.

The average HCO_3^- contents were greater in the GW samples as compared to the SW samples with 1 and 2 samples exceeding the desirable limits of 500 mg L^{-1} in pre- and post-monsoon seasons, respectively. The SO_4^{2-} contents of all the samples were safe as per WHO (2004) with average concentrations in GW and southern traverse samples greater than that of SW and northern traverse samples, respectively. In contrast, the Cl^- contents were comparatively higher in the SW, pre-monsoon and northern traverse samples as compared to GW, post-monsoon and southern traverse samples, respectively. Likewise, ~50% of the samples exceed the desirable limit of 50 mg L^{-1} in case of NO_3^- during pre-monsoon season whereas none of the post-monsoon samples exceeds this limit; while PO_4^{3-} concentrations were higher than the WHO (2004) permissible limits of 0.1 mg L^{-1} in 40% samples each in pre- and post-monsoon season. The higher PO_4^{3-} contents were measured in SW samples and sample near to the industrial plants. Monsoonal dilution effect further reflected in case of anion distribution as well, e.g., Cl^- , NO_3^- , and PO_4^{3-} . The greater HCO_3^- and SO_4^{2-} contents along the southern traverse (GW samples) indicative of industrial inputs into the aquifers. The excess Cl^- contents in the samples imply brackish to brackish-salt water in the study site (Sen 2014).

The ionic abundances suggest the mean anionic trend in pre- and post-monsoon as $\text{HCO}_3^- > \text{Cl}^- > \text{SO}_4^{2-} > \text{NO}_3^- > \text{PO}_4^{3-}$, whereas cationic trend varies as $\text{Na}^+ > \text{Mg}^{2+} > \text{Ca}^{2+} > \text{Si}^{4+} > \text{K}^+ > \text{Fe(T)} > \text{Al}^{3+}$ and $\text{Ca}^{2+} > \text{Na}^+ > \text{K}^+ > \text{Mg}^{2+} > \text{Si}^{4+} > \text{Fe(T)} > \text{Al}^{3+}$ for pre- and post-monsoon seasons, respectively. The dramatic increase in Ca^{2+} concentrations during post-monsoon season suggests calcareous nature of soils which is further reflected in alkaline pH during this period. The significantly low Fe(T) ($\text{Fe}^{3+} + \text{Fe}^{2+}$) and Al^{3+} in the studied water samples possibly resulted by favorable precipitation of Fe-Al-oxyhydroxides around the measured pH conditions that became a part of aquifer material. Comparatively greater cationic and anionic contents were observed in most of the samples of southern traverse which are of GW samples (mostly hand pumps and bore wells) than that of northern traverses which are mostly stream waters. In general, the water type in this region is Ca-Mg- HCO_3 , Ca- HCO_3 , and Na-Cl type (Piper 1944).

21.3.1 Arsenic Distribution

The spatial distribution of As during pre- and post-monsoon season in the study area is illustrated in Fig. 21.2. Post-monsoon season is enriched with greater As contents than pre-monsoon season for any particular location (except sample no. II3) (Fig. 21.3). This is attributed to favorable leaching from As-rich soils into the stream flow and groundwater due to monsoonal infiltration (Oinam et al. 2011) as also observed for TDS, Ca^{2+} , K^+ , HCO_3^- , SO_4^{2-} , Al^{3+} , and Fe(T). The concentration of As ranged up to $1446 \text{ } \mu\text{g L}^{-1}$ in pre-monsoon with mean of $192.22 \text{ } \mu\text{g L}^{-1}$ and from 87.21 to $780.52 \text{ } \mu\text{g L}^{-1}$ with mean $309.12 \text{ } \mu\text{g L}^{-1}$ in post-monsoon season.

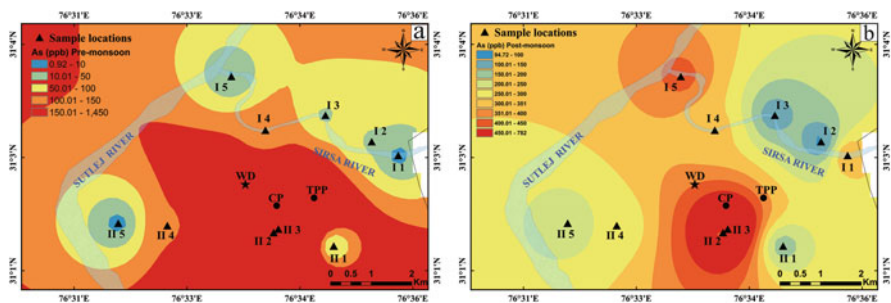


Fig. 21.2 Spatial distribution of As in the study area during pre-monsoon (a) and post-monsoon (b) season. Sample I1-I5 and II1-II5 are along the northern and southern traverses, respectively. CP and TPP represent cement and thermal power plant, respectively

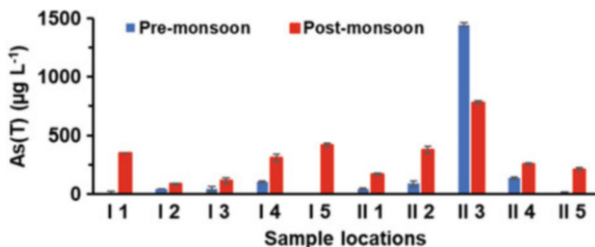


Fig. 21.3 Surface (I1, I4 and I5) and groundwater (I2, I3 and II1-II5) As concentrations ($\mu\text{g L}^{-1}$) during pre- and post-monsoon seasons

Although pre-monsoon samples exhibited relatively lower as contents, the exceptionally high As concentration (1.45 mg L^{-1}) is located close to the TPP and along the down flow direction. Further, all the water samples of the southern traverse which is the down flow side of the CP and TPP contain greater As contents than the northern traverse and groundwater flow direction in this region is south-western (CGWB 2017), i.e., towards southern traverse direction. A careful observation suggests that As concentrations are relatively higher near to the waste dumps of the TPP that slowly lowers outward as the sample distance from waste dumps increases. Both pre- ($1446 \mu\text{g L}^{-1}$) and post-monsoon ($780.52 \mu\text{g L}^{-1}$) samples exhibited the highest As concentration close to the CP and TPP. Hence, the present findings suggest that the huge coal ash wastes might be a dominant contributor of such high As, especially along the southern traverse (Jurkovič et al. 2011). Relatively low As content in sample no. II3 during post-monsoon season compared to pre-monsoon is possibly because of monsoonal dilution in contrast to other samples where monsoon fascinated leaching from soil might have contributed majorly. The surface and groundwater samples of the northern traverse also showed high As enrichments which may be due to geogenic As-rich alluvial deposits along the Sirta River. Almost 85% of samples exhibited higher concentrations than the limit of $10 \mu\text{g L}^{-1}$ in drinking water (WHO 1993).

21.3.2 Geochemical Relationship between As and Other Ions

Certain ionic concentration distribution and physical parameters such as EC, K^+ , Si^{4+} , HCO_3^- , SO_4^{2-} , NO_3^- , and PO_4^{3-} were correlated with their respective As contents in order to establish their likely control on As mobility from aquifer into the GW/SW resources. Pearson correlation analysis was adopted for this purpose. The correlation coefficient value (r) near to +1 or -1 is said to be highly correlated where r greater than 0.7 is considered a strong correlation and r value between 0.5 and 0.7 stands for a moderate correlation. The values less than 0.5 mean a weak correlation (Kumar et al. 2006). In the pre-monsoon samples, As showed a very significant positive correlation with EC ($r = 0.70$, $p \leq 0.01$; Fig. 21.4a), Mg^{2+}

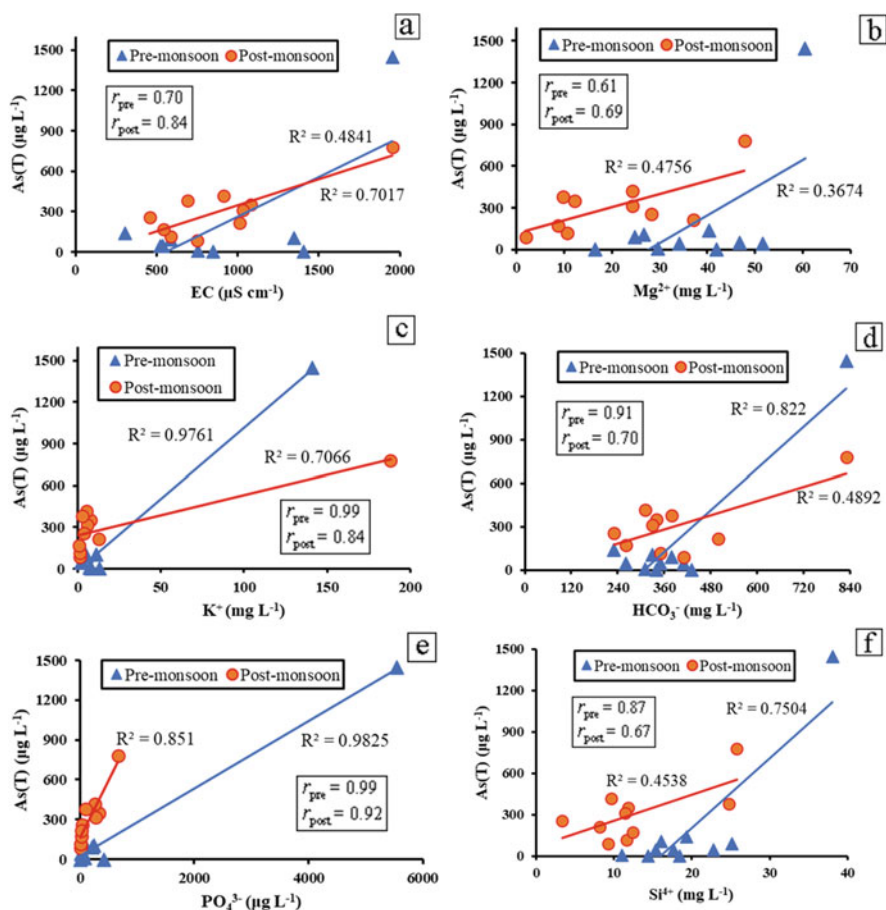
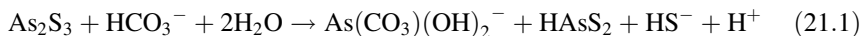


Fig. 21.4 Bivariate plots of As(T) with EC (a), Mg^{2+} (b), K^+ (c), HCO_3^- (d), PO_4^{3-} (e), and Si^{4+} (f) for pre- and post-monsoon seasons. Correlation coefficient (R^2), r_{pre} (pre-monsoon), and r_{post} (post-monsoon) are shown on each plot for convenience

($r = 0.61, p \leq 0.05$; Fig. 21.4b), K^+ ($r = 0.99, p \leq 0.01$; Fig. 21.4c), HCO_3^- ($r = 0.91, p \leq 0.01$; Fig. 21.4d), PO_4^{3-} ($r = 0.99, p \leq 0.01$; Fig. 21.4e), and Si^{4+} ($r = 0.87, p \leq 0.01$; Fig. 21.4f) and similar is the case for post-monsoon period with EC ($r = 0.84, p \leq 0.01$), Mg^{2+} ($r = 0.69, p \leq 0.01$), K^+ ($r = 0.84, p \leq 0.01$), HCO_3^- ($r = 0.70, p \leq 0.01$), PO_4^{3-} ($r = 0.92, p \leq 0.01$), and Si^{4+} ($r = 0.67, p \leq 0.01$). Role of HCO_3^- on mobilization of As in the groundwater appears to be very significant due to the carbonation of arsenic sulfide minerals such as orpiment (As_2S_3), Realgar (As_4S_4/AsS), etc. that leads to leaching of As (Eq. 21.1) (Kim et al. 2000).



Although silicate usually possess a poor affinity for As and lower exchange capacity (Swedlund and Webster 1999), the significant positive correlation between As and Si^{4+} in this study may be likely because of release of both the ions into the aqueous phase upon clay mineral dissolution (Sathe et al. 2020). Phosphate is known as a strong competitor with As for the same adsorption sites and possess an excellent exchange capability (Katsoyiannis and Katsoyiannis 2006). However, the near-neutral pH condition in the present study area where PO_4^{3-} has a relatively weak desorption ability towards As suggests excess PO_4^{3-} loading out of used fertilizers might partly enhance As release from soil through ligand exchange process (Oinam et al. 2011). Positive correlations of Mg^{2+} and As also point towards the anthropogenic activity by using the arsenical pesticides like magnesium arsenate [$Mg_3(AsO_4)_2$] (Rasool et al. 2017). Some hydrochemical processes like hydrolysis of K-feldspar might be the reason of K^+ and As positive correlation. Evaporative concentrations can also lead to high concentration of As as evident from the positive correlation of As with EC and higher values of Cl^- in this semi-arid area (Gao et al. 2013). Unlike the above correlations, poor correlation of As with Fe(T) and SO_4^{2-} indicates likely minimal role of these ions on As distribution in the given region.

21.4 Risk Assessment

In the study area, groundwater is used for both irrigation and drinking purposes, while surface water is only used for irrigation purpose. Risk assessment was done on the surface and ground water samples of pre- (summer) and post-monsoon (winter) season to find out the health risks posed on the residents by As exposure via consuming food crops and water. For this purpose, CDI, HQ, and CR were estimated and their results are summarized in Table 21.2. It was observed that the CDI and HQ of As were greater in the post-monsoon season than pre-monsoon season for both surface and groundwater which may be due to rainfall that caused leaching of As into the water bodies (Rajmohan and Elango 2005). When compared between surface water vs. groundwater, CDI and HQ of groundwater was higher as compared to that of surface water in the pre-monsoon, whereas in the post-monsoon season the

Table 21.2 Summary of risk assessment of As intake via surface (I1, I4, and I5) and groundwater (I2, I3, and II1–II5) during pre- and post-monsoon seasons

		Pre-monsoon season		Post-monsoon season	
		Surface water	Groundwater	Surface water	Groundwater
CDI (mg kg ⁻¹ day ⁻¹)	Range	8.29E-04–1.11E-03	4.31E-03–4.37E-03	1.02E-02–1.04E-02	6.55E-03–6.65E-03
	Mean ± SE	9.71E-04 ± 2.02E-04	4.34E-03 ± 4.04E-05	1.03E-02 ± 1.47E-04	6.60E-03 ± 7.01E-05
HQ	Range	2.76–3.71	14.38–14.57	34.05–34.74	21.84–22.17
	Mean ± SE	3.24 ± 0.67	14.48 ± 0.13	34.40 ± 0.49	22.00 ± 0.23
CR	Range	1.24E-03–1.67E-03	6.47E-03–6.56E-03	1.53E-02–1.56E-02	9.83E-03–9.98E-03
	Mean ± SE	1.46E-03 ± 3.03E-04	6.51E-03 ± 6.06E-05	1.55E-02 ± 2.21E-04	9.90E-03 ± 1.05E-04

**Fig. 21.5** Different skin symptoms around the study site due to As toxicity: (a) dorsal keratosis, and (b–c) diffuse melanosis (Chakraborti et al. 2016)

reverse trend was observed. The HQ values were > 1 in surface and groundwater samples of both pre- and post-season indicating higher risks of incidences of non-cancerous health issues (USEPA 1989). Surface water samples of post-monsoon season pose the highest risk of such problems. Results of cancer risk analysis (CR) indicate that the use of both surface and groundwater of pre- and post-monsoon season pose serious risk of cancer to the population of the region accepting USEPA acceptable limit of 1.00E-06. Arsenic toxicity and effects among the local residents were also encountered during the field work as seen by human skin disorders (Fig. 21.5).

21.5 Remediation

Based on the source water quality, suitable treatment options can be adopted to remove As from the water system. The concentrations and relation of iron, phosphate, silicate, bicarbonate, chloride, and dissolved organic matter with As should be pre-determined before selecting any remediation method. The remediation methods that can be adopted in the present study area are passive oxidation that lets the formation of iron precipitates which can adsorb As, coagulation by using aluminum sulfate and ferric sulfate as active coagulants that can readily remove As more effectively at pH 5.0–8.0 (EPA 2000). Use of suitable adsorbent like oxides of aluminum, iron, manganese, titanium, and cerium will be helpful. Other adsorbents like iron-modified activated alumina (AA/ γ -Al₂O₃) can also be effectively used (Ravenscroft et al. 2011; Westerhoff et al. 2006). Membrane technologies like reverse osmosis (Ning 2002) and nanofiltration (Oh et al. 2000) can also turn out well in near-neutral pH water. Hydrotalcite-like layered double hydroxides (HT-LDHs) are also very effective in controlling the migration of contaminants like As via sorption and/or in situ co-precipitation processes (Paikaray et al. 2013).

21.6 Conclusion

The study demonstrated on As distribution in the surface and groundwater around the eastern parts of Rupnagar District of Punjab, India. The water is mainly of Ca-Mg-HCO₃, Ca-HCO₃, and Na-Cl type where most cation and anions are under acceptable limits except few post-monsoonal samples. Monsoonal effect on elemental distribution is clearly observed by marginal dilution and/or chemical leaching of aquifer soils. Arsenic concentrations were found above the permissible limit of the WHO, i.e., 10 $\mu\text{g L}^{-1}$ in ~85% of the samples. Post-monsoon samples contain higher contents of arsenic as compared to pre-monsoon samples due to leaching from As-rich soils into the stream flow and groundwater. Favorable leaching due to monsoon, industrial wastes, and coal ash wastes might be contributing significantly to the groundwater As contents in the region as evidenced from its down flow side enrichment and greater As concentrations near to the huge coal ash waste dump sites. Geogenic arsenic might be the overall origin in this region as inferred from surface water of upward side of the groundwater direction. Strong correlation of As with HCO₃²⁻, PO₄³⁻, Si⁴⁺, EC, Mg²⁺, and K⁺ suggest mobilization of As by PO₄³⁻-HAsO₄²⁻ ligand exchange, carbonation of arsenic sulfide minerals and silicate weathering. Higher As enrichments are also evident from the skin disorders in the residents of the area.

Acknowledgments The authors acknowledge Department of Geology, Panjab University, Chandigarh, India for providing all the necessary technical and infrastructural facilities to carry out the research. Department of Science and Technology, Govt. of India is acknowledged for DST-INSPIRE Fellowship to Ms. Kaur. University Grants Commission, India has partly supported

financial assistance to SP through UGC Start-up grant for instrumental analysis and consumables. The authors are also thankful to Mr. Kuldeep Bist (lab assistant), Aishwarya Juneja, Piyush and Yash Bhanu for their help in the laboratory analysis and field work.

References

- Abrahams PW, Thornton I (1987) Distribution and extent of land contaminated by arsenic and associated metals in mining regions of Southwest England. *Trans Inst Min Metall Sect B Appl Earth Sci* 96:1–8
- APHA-AWWA-WPCF (1994) Standard methods for the examination of water and wastewater, 23rd edn. American Public Health Association, Washington, DC
- Bortey-Sam N, Nakayama SM, Ikenaka Y, Akoto O, Baidoo E, Mizukawa H, Ishizuka M (2015) Health risk assessment of heavy metals and metalloids in drinking water from communities near gold mines in Tarkwa, Ghana. *Environ Monit Assess* 187(7):397
- Central Groundwater Board (CGWB). (2017). Aquifer mapping and management plan, Ropar District Punjab
- Chakraborti D, Rahman MM, Chatterjee A, Das D, Das B, Nayak B et al (2016) Fate of over 480 million inhabitants living in arsenic and fluoride endemic Indian districts: magnitude, health, socio-economic effects and mitigation approaches. *J Trace Elem Med Biol* 38:33–45
- Dhar RK, Zheng Y, Rubenstone J, Van Geen A (2004) A rapid colorimetric method for measuring arsenic concentrations in groundwater. *Anal Chim Acta* 526(2):203–209
- EPA (2000) Technologies and costs for removal of arsenic from drinking water. EPA/815/R-00-028, US Environmental Protection Agency, Washington, DC
- Gao X, Su C, Wang Y, Hu Q (2013) Mobility of arsenic in aquifer sediments at Datong Basin, northern China: effect of bicarbonate and phosphate. *J Geochem Explor* 135:93–103
- Grasshoff K, Kremling K, Ehrhardt M (eds) (1999) Methods of seawater analysis. John Wiley & Sons, New York, pp 206–207.1
- Guha Mazumder DN (2003) Chronic arsenic toxicity: clinical features, epidemiology, and treatment: experience in West Bengal. *J Environ Sci Health A* 38(1):141–163
- Hundal HS, Kumar R, Singh K, Singh D (2007) Occurrence and geochemistry of arsenic in groundwater of Punjab, Northwest India. *Commun Soil Sci Plant Anal* 38(17–18):2257–2277
- Hundal HS, Singh K, Singh D (2009) Arsenic content in ground and canal waters of Punjab, north-West India. *Environ Monit Assess* 154(1–4):393
- Jan FA, Ishaq M, Khan S, Ihsanullah I, Ahmad I, Shakirullah M (2010) A comparative study of human health risks via consumption of food crops grown on wastewater irrigated soil (Peshawar) and relatively clean water irrigated soil (lower Dir). *J Hazard Mater* 179(1–3):612–621
- Jurkovič LU, Hiller E, Veselská V, Pet'ková K (2011) Arsenic concentrations in soils impacted by dam failure of coal-ash pond in ZemianskeKostolany, Slovakia. *Bull Environ Contam Toxicol* 86(4):433–437
- Katsoyiannis IA, Katsoyiannis AA (2006) Arsenic and other metal contamination of groundwaters in the industrial area of Thessaloniki, northern Greece. *Environ Monit Assess* 123(1–3):393–406
- Kim MJ, Nriagu J, Haack S (2000) Carbonate ions and arsenic dissolution by groundwater. *Environ Sci Technol* 34(15):3094–3100
- Kumar M, Ramanathan AL, Rao MS, Kumar B (2006) Identification and evaluation of hydrogeochemical processes in the groundwater environment of Delhi, India. *Environ Geol* 50(7):1025–1039
- Kumar M, Kumar M, Kumar A, Singh VB, Kumar S, Ramanathan AL, Bhattacharya P (2015) Arsenic distribution and mobilization: a case study of three districts of Uttar Pradesh and Bihar

- (India). In: Safe and sustainable use of arsenic-contaminated aquifers in the Gangetic plain. Springer, Cham, pp 111–123
- Murcott S (2012) Arsenic contamination in the world. IWA Publishing, London
- Ning RY (2002) Arsenic removal by reverse osmosis. *Desalination* 143(3):237–241
- Oh JI, Yamamoto K, Kitawaki H, Nakao S, Sugawara T, Rahman MM, Rahman MH (2000) Application of low-pressure nanofiltration coupled with a bicycle pump for the treatment of arsenic-contaminated groundwater. *Desalination* 132(1–3):307–314
- Oinam JD, Ramanathan AL, Linda A, Singh G (2011) A study of arsenic, iron and other dissolved ion variations in the groundwater of Bishnupur District, Manipur, India. *Environ Earth Sci* 62(6):1183–1195
- Paikaray S, Hendry MJ, Essilfie-Dughan J (2013) Controls on arsenate, molybdate, and selenate uptake by hydroxalite-like layered double hydroxides. *Chem Geol* 345:130–138
- Panchagnula S (2018) Spectrophotometric analysis of water for nitrate and nitrite nitrogen. *IJRAR v* (3):226–230
- Piper AM (1944) A graphic procedure in the geochemical interpretation of water-analyses. *EOS Trans Am Geophys Union* 25(6):914–928
- Rajmohan N, Elango L (2005) Nutrient chemistry of groundwater in an intensively irrigated region of southern India. *Environ Geol* 47(6):820–830
- Rasool A, Xiao T, Farooqi A, Shafeeqe M, Liu Y, Kamran MA et al (2017) Quality of tube well water intended for irrigation and human consumption with special emphasis on arsenic contamination at the area of Punjab, Pakistan. *Environ Geochem Health* 39(4):847–863
- Ravenscroft P, Brammer H, Richards K (2011) Arsenic pollution: a global synthesis, vol 94. John Wiley & Sons, West Sussex
- Ravindra K, Garg VK (2007) Hydro-chemical survey of groundwater of Hisar city and assessment of defluoridation methods used in India. *Environ Monit Assess* 132(1–3):33–43
- Sathe SS, Goswami L, Mahanta C, Devi LM (2020) Integrated factors controlling arsenic mobilization in an alluvial floodplain. *Environ Technol Innov* 17:100525
- Saurav D, Sudipta BS, Jyoti LP, Madhumita B, Yadav RNS, Mridul C (2015) Groundwater arsenic contamination in north eastern states of India. *J Environ Res Dev* 9(3):621
- Şen Z (2014) Practical and applied hydrogeology. Elsevier, New York
- Shah J, Sharma R, Sharma I (2015) Study and evaluation of Groundwater quality of Malwa region, Punjab (North India). *J Chem Environ Sci Appl* 2(1):41–58
- Sharma S, Kaur J, Nagpal AK, Kaur I (2016) Quantitative assessment of possible human health risk associated with consumption of arsenic contaminated groundwater and wheat grains from Ropar Wetland and its environs. *Environ Monit Assess* 188(9):506
- Sharma S, Kaur I, Nagpal AK (2017) Assessment of arsenic content in soil, rice grains and groundwater and associated health risks in human population from Ropar wetland, India, and its vicinity. *Environ Sci Pollut Res* 24(23):18836–18848
- Sharma S, Kaur I, Nagpal AK (2018) Estimation of arsenic, manganese and iron in mustard seeds, maize grains, groundwater and associated human health risks in Ropar wetland, Punjab, India, and its adjoining areas. *Environ Monit Assess* 190(7):385
- Singh KP, Kishore N, Tuli N, Loyal RS, Sharma M, Dhanda D, et al. (2015, March) Observations on occurrence of arsenic in groundwater especially in parts of south-West Punjab. In Workshop: Arsenic Contamination in Groundwater, CGWB (Chandigarh), Ministry of Water Resources, River Development and Ganga Rejuvenation, Govt of India, 45–52
- Smedley PL, Kinniburgh DG (2002) A review of the source, behaviour and distribution of arsenic in natural waters. *Appl Geochem* 17(5):517–568
- Smith ERG, Naidu R, Alston AM (1998) Arsenic in the soil environment. Doctoral dissertation, Academic Press
- Swedlund PJ, Webster JG (1999) Adsorption and polymerisation of silicic acid on ferrihydrite, and its effect on arsenic adsorption. *Water Res* 33(16):3413–3422
- Thakur T, Rishi MS, Herojeet RK, Renu L, Konchok D (2016) Arsenic contamination in groundwater of Punjab state: an overview. *Environ Tradit Sci Res* 1(1):1–6

- United States Environmental Protection Agency (USEPA) (2015) Risk Based Screening Table. Composite Table: Summary Tab 0615.US EPA; Available from: URL: <http://www2.epa.gov/risk/risk> based screening table generic tables
- US Environmental Protection Agency (1978) Method 365.3: phosphorous, all forms (colorimetric, ascorbic acid, two reagent)
- USEPA (U.S. Environmental Protection Agency) (1989) Development of Risk Assessment Methodology for Land Application and Distribution and Marketing of Municipal Sludge, EPA/600/6-89/001
- Virk HS (2019) A survey report on Groundwater contamination of Malwa Belt of Punjab due to heavy metal arsenic. *Int J Sci Res (IJSR)* 8(3):1721-1726
- Westerhoff P, De Haan M, Martindale A, Badruzzaman M (2006) Arsenic adsorptive media technology selection strategies. *Water Qual Res J* 41(2):171-184
- WHO (1993) Environmental health criteria 18: arsenic. World Health Organization, Geneva
- WHO (2004) Guidelines for drinking-water quality, vol 1. World Health Organization, Geneva
- World Health Organization (2006) WHO guidelines for the safe use of wastewater excreta and greywater, vol 1. World Health Organization, Geneva

Part III
Environmental Contaminants, Impacts and
Sustainable Management

Chapter 22

Introduction to Part III: Environmental Contaminants, Risk Assessment and Remediation



Debashish Sengupta

Abstract Environmental contamination can be referred to any undesirable change in physical, chemical or biological characteristics of any component of the environment, i.e. air, water, soil which can cause harmful effects on various forms of life or property (Central Pollution Control Board, Environmental standards for ambient air, automobiles, fuels, industries and noise. Pollution Control Law Series - PCLS/4/2000-2001, 2000). However, this section on Environmental Contamination, Risk and Remediation comprises eleven instructive chapters, all of which deal with state-of-art procedures for studying risk assessment and evolving appropriate remediation, as feasible.

Keywords Thorium abundance · Ultra-fine particles in indoor and outdoor environments · Environmental impact of coal mining

22.1 Introduction

Environmental contamination can be referred to any undesirable change in physical, chemical or biological characteristics of any component of the environment, i.e. air, water, soil which can cause harmful effects on various forms of life or property (CPCB 2000). These undesirable changes are caused by many substances which are of natural and anthropogenic in nature. Nature will take care to the natural undesirable changes. Our concern should mainly focus on the undesirable changes made by the human activities.

However, the present section of the book, specifically the relevant on “Environmental Contaminants Risk Assessment and Remediation” comprises 11 chapters, related to timely and significant topics especially the present day situation prevailing

D. Sengupta (✉)

Department of Geology and Geophysics, Indian Institute of Technology (IIT), Kharagpur, West Bengal, India

e-mail: dsgg@gg.iitkgp.ac.in

© Springer Nature Switzerland AG 2021

P. K. Shit et al. (eds.), *Spatial Modeling and Assessment of Environmental Contaminants*, Environmental Challenges and Solutions,
https://doi.org/10.1007/978-3-030-63422-3_22

397

world-wide. It has detailed data acquisition and analysis, modelling with suitable case histories. The important aspects highlighted in the various Chapters would facilitate a suitable bench mark/base-line for future studies and adopting robust remediation measures. The studies have been contributed by eminent Scientists and Researchers from reputed Institute, Universities and Organization.

22.2 Individual Chapters

The Section on Environmental Contamination, Risk and Remediation comprises 11 instructive chapters, all of which deal with state-of-art procedures for studying risk assessment and evolving appropriate Remediation, as feasible. First Chapter of the section deals with the rare Earth Enrichment due to geological processes and the risk assessment in a High Background Radiation Area in coastal Odisha due to elevated Thorium abundance. The next Chapter by S. Anand and co-authors discusses the dynamics of ultra-fine particles in indoor and outdoor environments and facilitates knowledge based evolution of system dynamics and assessment of effects of ultra-fine particles. Md. Ahsan Habib and Rahat Khan have provided the environmental impact of coal mining as well as burning of coal in thermal power plants and its impact, in a developing country with global relevance. Ambikapathi Ramya and co-authors have given an instructive overview of indoor air pollution and its impact on human health. The mineralogy and morphological characteristics of Technogenic magnetic particles, in industrial dust and its impact has been described by Suprya Mondal and co-workers. The wide use of pesticides and its toxic effects and strategies based on bioremediation has been described by Rujul Deollikar and co-workers. The well-known indigenous “Neem plant” has been a subject of extensive study, in terms of its ameliorating affects, by Santosh Kumar Giri and co-authors. A novel concept based on Random Forest Algorithm for particulate matter estimation has been discussed by Eeshan Basu and Chalantika Laha Salui. Bio-monitoring of a trans-boundary river based on functional roles of benthic mollusks and fungi has been delineated by Susanta Kumar Chakraborty and their co-authors. Basavaraj R. Hiremath and Sudha Goel have described their studies on aerobic biodegradable potential of leaf litter, in Municipal solid waste. Debjani Dutta and Srimanta Gupta have discussed the rising trend in air pollution over Gangetic West Bengal and its decadal consequences.

Each Chapter presents an instructive overview of the recent studies undertaken in their respective areas of expertise along with a list of exhaustive references having global ramifications. This would prove to a big boon to the readers of the present Book. The reader gets a good idea of the respective studies undertaken world-wide apart from the study areas selected by the respective authors.

Reference

Central Pollution Control Board (2000) Environmental standards for ambient air, automobiles, fuels, industries and noise. Pollution Control Law Series - PCLS/4/2000-2001

Chapter 23

Dynamics of Ultrafine Particles in Indoor and Outdoor Environments: A Modelling Approach to Study the Evolution of Particle Characteristics



S. Anand, Jayant Krishan, and Y. S. Mayya

Abstract Emission of ultrafine particles due to combustion, gas-to-particle conversion and vapour phase nucleation has been receiving increased attention in recent years because of their potential contribution to air pollution, climate change and health effects. Industrial emissions, biomass burning, material synthesis and engineered nanoparticles are some of the human activities responsible for these emissions. In general, mass and number-based metrics are used to characterize these sources in indoor as well as outdoor environments. Methodology to assess mass-based metrics is well established. However, the accuracy in estimation of number-based metrics such as concentration, emission rate, etc. is compromised due to limitations of near source monitoring techniques and dominance of coagulation process, which leads to rapid reduction of number concentration in spatial domain. It must be noted that number concentration is increasingly perceived to be an important factor for quantifying climatic and health effects. Also, aerosol dynamic equations used for modelling purposes generally require the data on number concentration. There is thus a fundamental need of models to estimate number-based metrics in order to assess their effects. In this chapter, a few aerosol modelling studies are presented that covers a spectrum of problems from contained indoor conditions to open environment. These studies highlight the tools and theory behind them which can be used to simplify the problem at hand to get a reasonable

S. Anand

Health Physics Division, Bhabha Atomic Research Centre, Mumbai, India

Homi Bhabha National Institute, Bhabha Atomic Research Centre, Mumbai, India

e-mail: sanand@barc.gov.in

J. Krishan

Health Physics Division, Bhabha Atomic Research Centre, Mumbai, India

Y. S. Mayya (✉)

Department of Chemical Engineering, Indian Institute of Technology Bombay, Mumbai, India

e-mail: ysmayya@iitb.ac.in

© Springer Nature Switzerland AG 2021

P. K. Shit et al. (eds.), *Spatial Modeling and Assessment of Environmental Contaminants*, Environmental Challenges and Solutions,

https://doi.org/10.1007/978-3-030-63422-3_23

401

knowledge about evolution of the system dynamics and assess the effects of ultrafine particles.

Keywords Ultrafine particles · Coagulation · Survival fraction · Dispersion · Indoor

23.1 Introduction

Ultrafine particles (diameter <100 nm), a subset of aerosols are observed to have severe health effects especially in case of indoor exposure scenarios like cooking, biomass burning, room heating, burning scent sticks, etc. (Schneider et al. 2011; Morawska et al. 2013). Conversely, apart from health effects, ultrafine particles (UFPs) from natural and anthropogenic sources in the outdoor environment affect the Earth's climate by contributing to the source of PM_{2.5} (particulate matter < 2.5 μm) aerosols (Mitchell 2017), nucleation processes in the atmosphere (Joshi et al. 2016), etc. Health hazards due to the fine and coarse particulate matter based on mass concentration are very well established (Venkataraman et al. 2018). However, in the case of UFPs, mass concentration cannot be used to quantify the exposure due to its poor correlation to the total mass concentration (Isaxon et al. 2015). Hence, the exposure and the corresponding risk due to these UFPs is generally represented in terms of UFP number and surface area concentrations (Oberdörster et al. 2005; Pedata et al. 2015) in addition to the conventional mass concentration. Improved understanding of these aerosol metrics is crucial for formulating several mitigation strategies such as source control, ventilation/dilution removal, exposure duration control, air cleaning technologies by filtration, etc.

UFPs released from emission sources undergo various aerosol microphysical and atmospheric processes and ultimately become a part of the background aerosols. Several measurement devices and techniques are required to understand the spatial as well as temporal evolution of particle metrics in the environment, which is a strenuous process. Also, there is a limitation in measurements due to saturation of particle counters as number concentration reaches the upper limiting value in the case of strong emission sources, which is overcome by either dilution based measurement technique (Kittelson 1998, 2001) or placement of devices far away from the sources. However, these techniques may introduce error in the estimates significantly due to undergoing microphysical process, mainly coagulation. Alternatively, these problems can be addressed through analytical and numerical models.

The role played by microphysical processes nearer to the sources is similar in case of controlled/contained environment (like indoor aerosols released during cooking, biomass fuel burning, aerosol reactors, etc.) or open atmosphere (vehicular emissions, forest fire, etc.). But different overall approaches are required to study the evolution of particle metrics depending upon the problem to be solved. Some indoor models neglect coagulation losses (Wallace et al. 2004; Wallace and Ott 2011), while few studies treat coagulation as a linear removal process (Bhangar et al. 2011) and few others do exhaustive numerical analysis of the Smoluchowski coagulation

equation with continuous source and sink terms (Anand et al. 2012). In the case of outdoor models, some reasonable approximations are made during model formulation itself, like use of uniformly mixed-volume expansion/dilution model (Nathans et al. 1970; Radke et al. 1995; Turco and Yu 1997; Fiebig et al. 2003) or diffusion-coagulation model (Anand and Mayya 2009, 2011) to study the simultaneous coagulation and dispersion in an aerosol cloud. Volume expansion models handle atmospheric dispersion processes through dilution mechanics, while Anand and Mayya (2011, 2015) use the standard diffusion equation to study the dispersion of puff and plume releases.

All these modelling studies are not only useful in explaining the complex behaviour of particle properties in the environment but their results are valuable in formulating empirical relationships for quick estimates of the particle metrics, parameterization scheme for the microphysical processes in global circulation models and guidance in the UFP toxicological studies. In this chapter, a few aerosol modelling studies are presented that cover a spectrum of problems from contained indoor conditions to open environment. These studies highlight the tools and theory behind them which can be used to simplify the problem at hand to get reasonable knowledge about the evolution of the system dynamics and assess the effects of ultrafine particles.

23.2 Materials and Methods

General dynamic equation (GDE) for the evolution of aerosols in any environment is given by

$$\begin{aligned} \frac{\partial n(u, r, t)}{\partial t} + U \frac{\partial n(u, r, t)}{\partial r} = S(u, r, t) + \nabla \cdot (D(r, t) \nabla n(u, r, t)) + \left. \frac{\partial n(u, r, t)}{\partial t} \right|_{\text{coag}} \\ + \left. \frac{\partial n(u, r, t)}{\partial t} \right|_{\text{cond/evap}} - \left. \frac{\partial n(u, r, t)}{\partial t} \right|_{\text{rem}}, \end{aligned} \quad (23.1)$$

where $n(u, r, t) du$ is the number of particles with volumes lying between u and $u + du$ per unit volume of the fluid at position r and time t , U is the advection velocity and D is the coefficient of turbulent diffusion. $S(u, r, t)$ is the term representing source, i.e. mean number of particles injected per unit volume of space per unit time per unit particle volumes around u directly or formed due to nucleation (gas/vapour to particle conversion). Fourth and last term on RHS account for condensation/evaporation and removal processes (deposition, decay, ventilation, etc.).

Coagulation, second term of Eq. (23.1), is handled by nonlinear integro-differential equation. Obtaining solution to this equation is complex compared to

other processes described in GDE. Hence, it is discussed in detail here. The coagulation term in Eq. (23.1) is given by

$$\left. \frac{\partial n(u, r, t)}{\partial t} \right|_{\text{coag}} = \frac{1}{2} \int_0^u K(u', u - u') n(u', r, t) n(u - u', r, t) du' - n(u, r, t) \int_0^\infty K(u', u) n(u', r, t) du', \quad (23.2)$$

where $K(u', u - u')$ is the coagulation kernel between particles of volumes u' and $u - u'$ due to various forces acting between these particles. This essential input comes from the Fuchs coagulation kernel ($K_{\text{Fuchs}}(u, u')$) which describes the rate at which particles of size u coagulate with particles of size u' due to kinetic + diffusion (Brownian) mechanisms and intermolecular forces.

Brownian coagulation kernel for the complete size spectrum (in the absence of inter-particle forces) is given by

$$K_{\text{Fuchs}}(u, u') = \frac{K_{\text{co}}(u, u')}{\frac{r+r_{u'}}{r_u+r_{u'}+\delta_{uu'}} + \frac{K_{\text{co}}(u, u')}{K_{\text{fm}}(u, u')}} \quad (23.3)$$

where r_u and $r_{u'}$ are the radii of the particles with volume u and u' , respectively, $K_{\text{co}}(u, u')$ and $K_{\text{fm}}(u, u')$ are the Brownian coagulation kernels in the continuum and free-molecular regime, respectively, and $\delta_{uu'}$ is the distance between the collision surface and the regime dividing surface. Fuchs (1964) proposed, for a single particle,

$$\delta_{uu'} = \frac{(d_u + \lambda_u)^3 - (d_u^2 + \lambda_u^2)^{\frac{3}{2}}}{3 d_u \lambda_u} - d_u, \quad (23.4a)$$

and for a pair of particles,

$$\delta_{uu} = \sqrt{\delta_u^2 + \delta_{u'}^2}, \quad (23.4b)$$

where d_u is the particle diameter, $\lambda_u = \frac{8D_u}{\pi \bar{v}_u}$ is the mean free path of the particle, D_u is the particle diffusion coefficient and \bar{v}_u is the mean thermal speed of a particle. The diffusion coefficient (D_u) is given by

$$D_u = \frac{k_B T_a}{6 \pi r_u \eta_a} G_u, \quad (23.5)$$

where k_B is the Boltzmann constant, T_a is the fluid (air) temperature, η_a is the viscosity of the fluid and G_u is the particle Knudsen number dependent slip-flow correction factor for a given particle size u .

Coagulation of primary solid particles may lead to formation of fractal-like agglomerates, which tend to increase the coagulation kernel value, thereby leading to enhanced rate of coagulation (Jacobson 2005). The fractal nature of the particles is initially accounted by Matsoukas and Friedlander (1991) by replacing the volume-equivalent diameter by fractal diameter as shown below

$$d_{pf} = d_{p0} \left(\frac{d_p}{d_{p0}} \right)^{3/d_f}, \quad (23.6)$$

where d_{pf} is the fractal diameter, d_p is volume-equivalent diameter, d_{p0} is diameter of the individual spherule that forms the fractal and d_f is fractal dimension. The Fuchs coagulation kernel (Eq. 23.3) is then modified to account for the fractals using the numerical recipe from Jacobson (2005).

Since the Fuchs kernel (Eq. 23.3) is a non-homogeneous function, it is analytically impossible to solve the GDE (Eqs. 23.1 and 23.2), and hence, numerical methods are employed. Since numerical methods are computationally intensive which demands good amount of resources and time, we introduce appropriate simplifications either at the level of problem formulation or at obtaining solutions based on the complexity of the problem, which are discussed below.

23.2.1 *Effective Coagulation Coefficient Method for Strong Emission Sources in the Indoor Environment*

Let us consider a large volume where UFPs are injected at a constant rate. The defined aerosol system evolves by coagulation and particle removal processes due to wall deposition and ventilation. It is assumed that the aerosols are mixed rapidly in the air space due to temperature gradients and presence of mixing elements such as natural or forced ventilation, thereby ensuring homogeneous distribution of the aerosols. This exposure scenario requires development of a detailed numerical solution for the spectral evolution of the aerosol size distribution by considering the Fuchs coagulation kernel (K_{Fuchs}) that incorporates Brownian diffusion effects over the entire particle size range.

Alternatively, the simplistic approach of constant coagulation kernel may be advantageous in the case of one time injection problems but fails to capture important aspects of aerosol dynamics in case of continuous releases. Therefore, to overcome the limitations of constant kernel, yet retaining the simplicity of the approach, concept of “effective coagulation coefficient” is introduced, without sacrificing the intricacies associated with the interplay of coagulation and ventilation for continuous emission scenario (Anand et al. 2016a; Anand and Mayya 2017). It must be emphasized that the effective coagulation coefficient method is more of a simplified procedure (rather than a systematic approximation), which cannot be rigorously justified a priori by theoretical analysis.

The main difference between constant and effective coagulation kernel is that the former is a constant throughout the history of evolution of particle size spectrum, whereas the latter captures the transformation of the particle size characteristics from the source region to exposure environment. The effective coagulation coefficient (K_{eff}) is then introduced into the constant kernel model, and the steady-state form of GDE (Eq. (23.1) in the absence of advection, turbulent diffusion and condensation/evaporation) is written as

$$S = \frac{1}{2}K_{\text{eff}}(N_0, \lambda)N_0^2 + \lambda N_0, \quad (23.7)$$

where K_{eff} turns out to be a function of a single parameter $\beta = \lambda/N_0$ (m^3s^{-1}), the ratio between prescribed effective removal rate (λ) and steady-state total number concentration (N_0). Here, constant kernel (K) in the steady-state solution is replaced by an effective coagulation coefficient (K_{eff}). The K_{eff} is obtained by integrating the K_{Fuchs} over the initial particle size emitted at the source and can be expressed as

$$K_{\text{eff}}(N_0, \lambda) = \frac{\int_{u_0}^{\infty} \int_{u_0}^{\infty} K_{\text{Fuchs}}(u, u')n(u; N_0, \lambda)n(u'; N_0, \lambda)du du'}{N_0^2}. \quad (23.8)$$

The integral in Eq. (23.8) is evaluated using the solution for the size spectrum for a steady-source under constant kernel approximation available in the literature (Hendriks and Ziff 1985):

$$n(u)du = \frac{N_0}{\gamma^{1/2}\Gamma(-0.5, \gamma)} \left(\frac{u}{u_0}\right)^{-3/2} e^{-\gamma\frac{u}{u_0}} \frac{du}{u_0} \quad (23.9)$$

u_0 is the average primary particle volume emitted by the source, and

$$\gamma = \ln \left[1 + \frac{\beta^2}{K_{\text{eff}}^2 + 2\beta K_{\text{eff}}} \right]. \quad (23.10)$$

In the present case, if we denote $x = u/u_0$, then Eq. (23.9) becomes

$$f(x; \gamma) = (n(u)u_0)/N_0 = \frac{x^{-3/2}e^{-\gamma x}}{\gamma^{1/2}\Gamma(-1/2, \gamma)}. \quad (23.11)$$

Substituting Eq. (23.11) in Eq. (23.8), we get

$$K_{\text{eff}}(u_0, \gamma) = \frac{1}{[\gamma^{1/2}\Gamma(-1/2, \gamma)]^2} \int_1^\infty \int_1^\infty K_{\text{Fuchs}}(u_0 x, u_0 y) (xy)^{-3/2} e^{-\gamma(x+y)} dx dy. \quad (23.12)$$

Equations (23.10)–(23.12) are nonlinearly coupled implicit equations which are solved for K_{eff} in an iterative manner, through an initial guess for the value of γ , until K_{eff} converges to an accurate value for a given β .

Apart from predicting number concentration from the given source emission rate and ventilation, this method can also be used in the reverse direction, i.e. estimation of source emission rate if measured values of concentration are given at some distance away from the source. In a practical context, it may not be always possible to perform complete numerical simulations including the coagulation process to estimate the source strength from the measured data. Hence, a simple recipe based on “effective coagulation coefficient” approach is developed that estimates the source strength through measured steady-state concentration and ventilation rate by the well-known constant kernel solution with ventilation (Anand et al. 2016a).

23.2.2 Nodal Method to Study Evolution of Aerosol Metrics in a Chamber/Indoor Environment

The effective coagulation coefficient approach is a good approximation to get a gross overview of aerosol number concentration as a function of ventilation rate for continuously emitting source. However, detailed numerical simulations incorporating size dependent Fuchs kernel in the coagulation equation may be required in some cases, e.g. studying the behaviour of nanoparticles released into well-mixed chamber/indoor environment (Seipenbusch et al. 2008). This system evolves due to steady injection of aerosols, coagulation and removal mechanisms. The injected aerosols are uniformly mixed in the given volume instantaneously and evolution of number concentration as a function of time can be expressed as

$$\frac{\partial n(u, t)}{\partial t} = \frac{\partial n(u, t)}{\partial t} \Big|_{\text{coag}} - \frac{\partial n(u, t)}{\partial t} \Big|_{\text{rem}} + S(u, t). \quad (23.13)$$

The source term/particle injection rate ($\text{m}^{-3} \text{s}^{-1}$) in this equation is given by $S(u, t) = \left(\frac{\dot{Q}}{V}\right)$, \dot{Q} is the number emission rate (s^{-1}), V is the chamber/indoor environment volume (m^3). At $t = 0$, $n(u, 0) = 0$.

The GDE (Eq. 23.13) with Fuchs coagulation kernel needs to be solved numerically to study the aerosol metrics as a function of time. Many numerical techniques are available in the literature to solve coagulation equation (Jacobson 2005). However, we present a relatively simple numerical technique here, called as nodal

method (Prakash et al. 2003). This approach reduces the finite size bins to discrete nodes on a logarithmic size scale given by

$$\frac{\partial n_k}{\partial t} = \frac{1}{2} \sum_{i=1} \chi_{ijk} K_{i,j} n_i n_j - n_k \sum_{i=1} K_{i,k} n_i, \quad (23.14)$$

$$j = 1$$

where $K_{i,j}$ is the coagulation coefficient for the interacting particles of size i and j , and χ_{ijk} is the size-splitting operator given by

$$\chi_{ijk} = \begin{cases} \frac{u_{k+1} - (u_i + u_j)}{u_{k+1} - u_k}; & u_k \leq u_i + u_j \leq u_{k+1} \\ \frac{(u_i + u_j) - u_{k-1}}{u_k - u_{k-1}}; & u_{k-1} \leq u_i + u_j \leq u_k \\ 0; & \text{Otherwise} \end{cases}, \quad (23.15)$$

where u_i is the particle volume at the i^{th} node. χ_{ijk} rearranges particles among the nodes after every coagulation step so as to ensure conservation of mass. This numerical method is simple to use and easy to implement in the numerical code for solving GDE (Eq. 23.13).

23.2.3 Diffusion-Coagulation Model to Estimate Atmospheric Background Particle Number Loading Factors

In general, atmospheric transport of aerosols must be integrated with their microphysical transformation processes to study the overall evolution of atmospheric aerosols. Atmospheric transport processes include advection and turbulent diffusion mechanisms, whereas aerosol microphysical processes comprise nucleation, coagulation, vapour condensation/evaporation and removal mechanisms (Friedlander 2000; Seinfeld and Pandis 2006). Of all the aerosol microphysical processes, coagulation is computationally intensive and this process dominates near the high emission sources such as forest fires, biomass burning, volcanic releases, etc. (Radke et al. 1995; Fiebig et al. 2003). Hence, coagulation needs to be accounted during transport of particles from source to atmosphere.

From Eq. (23.1), the dynamics equation in this scenario is given by

$$\frac{\partial n(u, r, t)}{\partial t} + U \frac{\partial n(u, r, t)}{\partial r} = \nabla \cdot (D(r, t) \nabla n(u, r, t)) + \left. \frac{\partial n(u, r, t)}{\partial t} \right|_{\text{coag}} + S(r, u, t). \quad (23.16)$$

For the constant coagulation kernel (K) and diffusion coefficient (D), the evolution of total number concentration in a puff from Eq. (23.16) is written as

$$\frac{\partial N(r, t)}{\partial t} = D \nabla^2 N(r, t) - \frac{K}{2} [N(r, t)]^2, \quad (23.17)$$

where $N(r, t) = \int_0^\infty n(u, r, t) du$.

In the case of steady-state plume releases, Eq. (23.16) becomes

$$U \frac{\partial N(x, r)}{\partial x} = \frac{U}{4} \frac{d\sigma^2(x)}{dx} \left[\frac{1}{r} \frac{\partial}{\partial r} \left(r \frac{\partial N(x, r)}{\partial x} \right) \right] - \frac{K}{2} [N(x, r)]^2, \quad (23.18)$$

where x and r are the axial and radial coordinates, respectively, U is the wind velocity, $\sigma^2(x)$ is the square of variance of the plume width across the radial coordinate. In these cases (Eqs. (23.17) and (23.18)), $S(u, r, t)$ is provided in the form of initial and boundary conditions. The diffusion coefficients and variance of the plume width can be expressed as $D = \frac{U}{4} \frac{d\sigma^2(x)}{dx}$, and $\sigma^2(x) = \sigma_0^2 + 4 D_0(x/U) + C \varepsilon(x/U)^3$ (Ott and Mann 2000), where σ_0^2 is the square of initial plume width, D_0 is the particle diffusion coefficient, C is a constant and ε is the rate of dissipation of turbulent kinetic energy. Initial distribution of the particle number concentration is assumed to be Gaussian in space and size spectra is monodisperse. Finally, Eqs. (23.17, 23.18) are solved using Fourier transform and the ansatz that accounts for the coagulation-induced flattening effect (Anand and Mayya 2011). Thus, a diffusion–coagulation model is developed to study the evolution of a spatially inhomogeneous aerosol puffs and plumes, and approximate analytical relations capturing the relative importance of different types of source and dispersion scenarios are obtained.

23.3 Results and Discussion

Models described above provide alternate approaches, and they are applied to the problems involving estimation of aerosol metrics in the contained and outdoor environment. Any given problem can be solved using multiple approaches and we always thrive to get the characteristics of the system using most simplistic models, yet capturing the important phenomenon involved. Apart from providing an alternate approach, it is equally important to validate these approaches and verify the applicability of the model to the problem at hand. Once applicability of the model is verified, this can further be used to study other problems depending upon the domain of applicability. This section highlights the important results and observations pertaining to a few solved problems published in the literature.

23.3.1 Effective Coagulation Coefficient Method for Strong Emission Sources in the Indoor Environment

Effective coagulation coefficient (K_{eff}) approach is a handy tool to study the behaviour of aerosol metrics without carrying out intensive numerical computation of GDE with Fuchs kernel. Let us consider a case in which UFPs are continuously emitted from the source with log-normal size distribution (count median diameter (CMD) = 10 nm and geometric standard deviation (GSD) = 1.3) in an indoor environment (Roy et al. 2009; Dhaniyala et al. 2011). An equivalent effective wall deposition rate of 0.45 h^{-1} is considered along with ventilation removal rate in this case. Using Eq. (23.12), K_{eff} values are generated as a function of β using Mathematica (Wolfram Research 2005) and the numerical results are fitted using logistic function as shown below:

$$K_{\text{eff}}(m^3 s^{-1}) = 10^{-16} \left[A_1 + \frac{A_2}{1 + (B \beta(m^3 s^{-1}) 10^{16})^C} \right], \quad (23.19)$$

where the fitting parameters (A_1, A_2, B, C) are tabulated in Table 23.1 for different values of d_f . A_1 represents the large β limit, $A_1 + A_2$ is the limit at low β (~ 0.005) and C represents steepness of transition of K_{eff} between these values. Although the values of C are similar for all the three cases, it is highest for compact particles, thereby implying a steeper fall of K_{eff} with β for this case.

Numerical values of K_{eff} vs β for different d_f values are plotted in Fig. 23.1. From Fig. 23.1, it is observed that K_{eff} values are smaller for large values of β and it increases with decreasing values of β . Larger values of β correspond to either large ventilation or weak sources and hence coagulation corrections will be negligible. In such a case, the aerosol evolution is controlled by ventilation. As β decreases, coagulation correction becomes progressively more important and dominates in the region of low β . The ratio between the maximum and minimum values of K_{eff} is about 3 for compact particles ($d_f = 3$) and it increases up to 12 (corresponding to $d_f = 2$) for fractals. These results are consistent with the well-known fact that the coagulation effects are enhanced for fractals as compared to spherical particles.

This K_{eff} approach can be used to obtain steady-state number concentration for the continuous emission case as described above. The results of a case study using K_{eff} model are presented here (Anand and Mayya 2017). Plots of normalized concentration, i.e. $N_0(\lambda)/N_0(\lambda = 0)$ with ventilation rate (λ) for fractal dimensions ($d_f = 2, 2.5$ and 3) for different emission rate (S) (low— $10^8 \text{ m}^{-3} \cdot \text{s}^{-1}$, medium— $10^{10} \text{ m}^{-3} \cdot \text{s}^{-1}$, high— $10^{12} \text{ m}^{-3} \cdot \text{s}^{-1}$) and uniform surface deposition rate ($\lambda_w = 0.45 \text{ h}^{-1}$)

Table 23.1 Parameters to estimate K_{eff} for various d_f

d_f	A_1	A_2	B	C
2	18.638	226.242	8.026	0.555
2.5	18.914	70.389	2.228	0.616
3	19.255	36.540	1.719	0.657

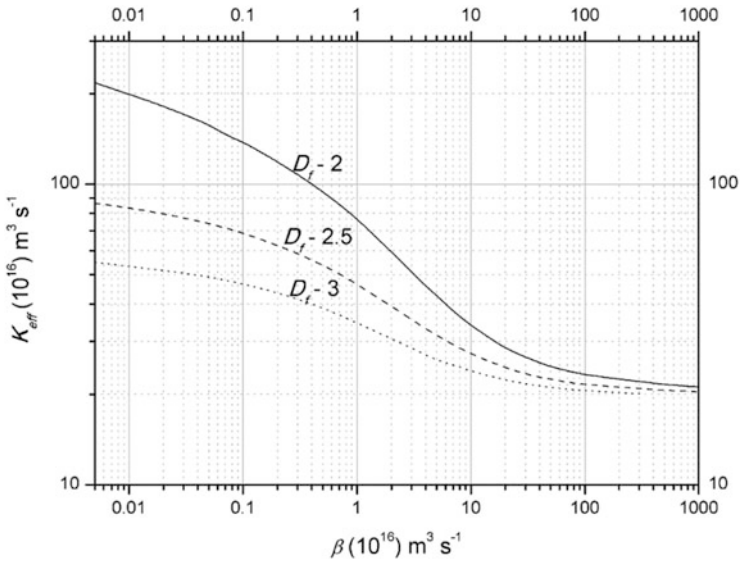


Fig. 23.1 Effective coagulation coefficient as a function of β for different fractal dimensions, initial particle diameter (d_{p0}) is 10 nm (Anand and Mayya 2017)

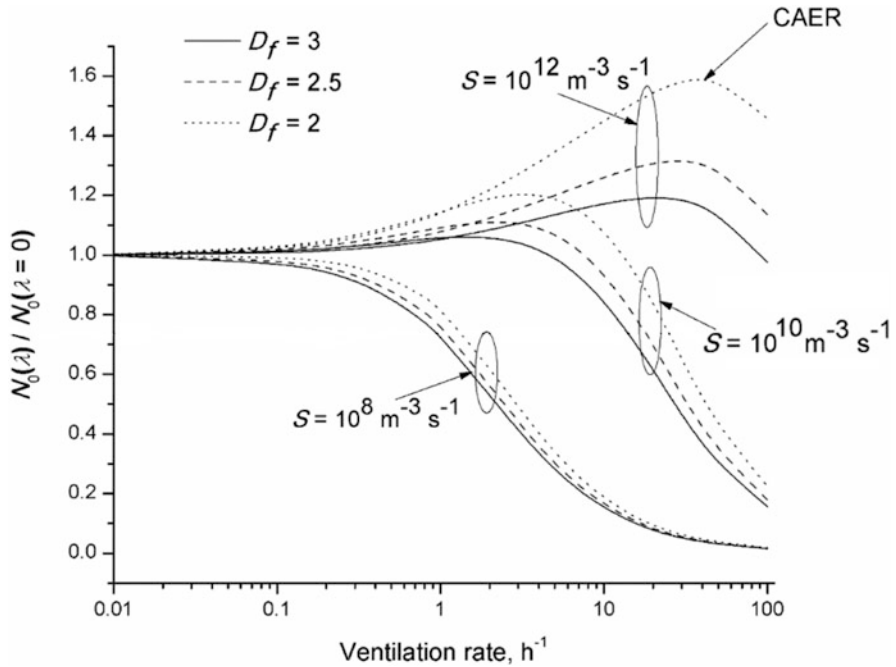


Fig. 23.2 Steady-state number concentration ratio ($N_0(\lambda)/N_0(\lambda = 0)$) as a function of ventilation rate for different fractal dimensions and source strengths. It is to be noted that $N_0(\lambda = 0)$ is different for each of the emission scenario (Anand and Mayya 2017)

are shown in Fig. 23.2. The plots show that for high emission rates, the steady-state values increase between the low λ regime and medium λ regime, reaches a peak and then decreases with ventilation rate in the high λ regime. The increase in the steady-state value between the low λ regime and medium λ regime is due to the removal of large size particles in the system by small ventilation, thereby reducing the effective coagulation rate. For low emission rates, there is no peak and the concentration tends to decrease monotonically as the ventilation rate increases, for all d_f values. The steady-state results predicted by the K_{eff} approach are validated against the numerical solution of coagulation equation (Anand et al. 2016b) involving size dependent Fuchs kernel for different set of input parameters (i.e. ventilation rate, emission rate, fractal dimension).

Here, we define critical air exchange rate (CAER), which is a point where UFP number concentration peaks amidst the competing processes of hetero-coagulation and removal due to ventilation. The CAER values are higher for fractals because of the greater dominance of coagulation as compared to that for compact particles. For strong sources, the CAERs required to break-even the concentration peaking effect are 24 h^{-1} for $d_f = 3$ and 39 h^{-1} for $d_f = 2$ (Fig. 23.2). The removal of UFP concentrations (number, surface area and mass) is governed by ventilation beyond CAER value but higher ventilation rate may be required to reduce the UFP metrics significantly. The reduction in concentration may not ineluctably follow inverse law with respect to ventilation due to simultaneous prevalence of coagulation, which has nonlinear dependence on UFP metrics. Therefore, to quantify reduction in concentration as a function of ventilation rate, a concept of half value air exchange rates (HaVAER) similar to half-lives in context of radioactivity is defined (Anand et al. 2016b; Anand and Mayya 2017). This study highlights the striking difference between the mass and number UFP metrics; total PM is inversely dependent on the ventilation rate, whereas number concentration and the size distribution are controlled by coagulation and may require much higher ventilation rate for removal. However, it must be noted that if ultrafine mass and surface area are taken into consideration along with the number concentration, these ventilation rates do not turn out to be as high as one would assume.

The K_{eff} approach can also be used to estimate the release rate from a strong emission source if measurement at some distance away from the source is given. To demonstrate this, let us consider the case of a combustion source in an uninhabited house described in Wallace et al. (2008). From the reported λ and N_0 data, the β estimate for this case turns out to be about $\sim 10^{-16} \text{ m}^3 \text{ s}^{-1}$ which corresponds to the region of dominance of coagulation over removal; K_{eff} for this β value is $\sim 3.5 \times 10^{-15} \text{ m}^3 \text{ s}^{-1}$. The source emission rate is then estimated using Eq. (23.7) as $7.3 \times 10^9 \text{ m}^{-3} \text{ s}^{-1}$. This estimate is ~ 25 times higher than the value reported by the authors. Thus, coagulation correction leads to a significant change in the estimate of number emission rate. This study clearly demonstrates usefulness of the K_{eff} method for estimating coagulation corrected number emission rate for sources using effective removal rate and steady-state number concentration obtained from the experiments.

23.3.2 Nodal Method to Study Evolution of Aerosol Metrics in a Chamber/Indoor Environment

A comprehensive numerical study based on nodal method is carried out to understand the experimental observations of aerosol metrics in a well-mixed chamber with steady injection of nanoparticles (Seipenbusch et al. 2008). It is observed that the total number concentration in the chamber reaches a peak value initially and then gradually decreases with time, while nanoparticles are continuously injected into the chamber. Also, the evolution of bimodal size distribution is noted in their experiments. Since these experimental observations cannot be explained by simplistic models using constant coagulation kernel, intricate numerical model capable of capturing size dependent dynamics must be used. That is, inclusion of realistic, size dependent coagulation kernels in the numerical simulation becomes important. Hence, numerical simulations are carried out using the nodal method described in Section 23.2.2 for different source injection rate (S), ventilation rate, size distribution and fractal dimensions to understand the complex evolution of aerosol metrics. The numerical results are presented in Figs. 23.3 and 23.4.

Figure 23.3a shows that there is a steep rise in the concentration due to continuous injection of the particles. In the initial time period, coagulation effects are insignificant since particle number concentration is small. After a certain amount of time, number concentration attains a peak value and is sufficiently high for coagulation to be significant and subsequent increase in the rate of coagulation reduces the rate at which number concentration increases. Therefore, number concentration first increases, reaches a peak value and then reduces monotonically as time progresses. It is also interesting to study the changes in fractal dimensions of the particles that result in the formation of aggregates of different sizes. Figure 23.3a shows that the maximum concentration and the time at which this peak occurs are lesser (\sim half) for fractals as compared to compact particles. Coagulation leads to formation of

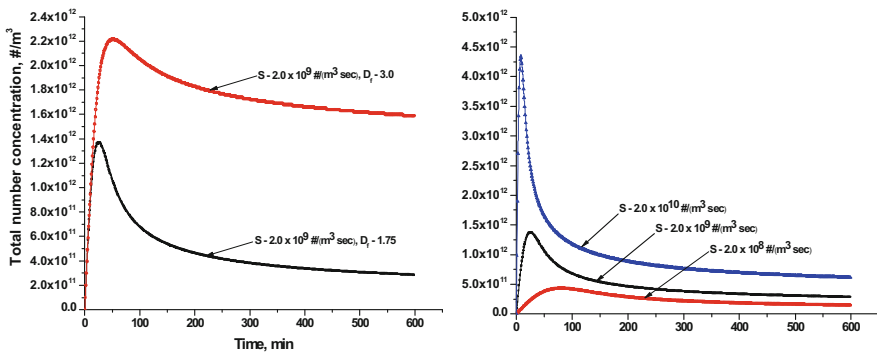


Fig. 23.3 (a) Dependence of fractal dimension on the evolution of total number concentration in the absence of ventilation; (b) Dependence of particle number concentration on source injection rate in the absence of ventilation, $d_f = 1.75$ (Anand et al. 2012)

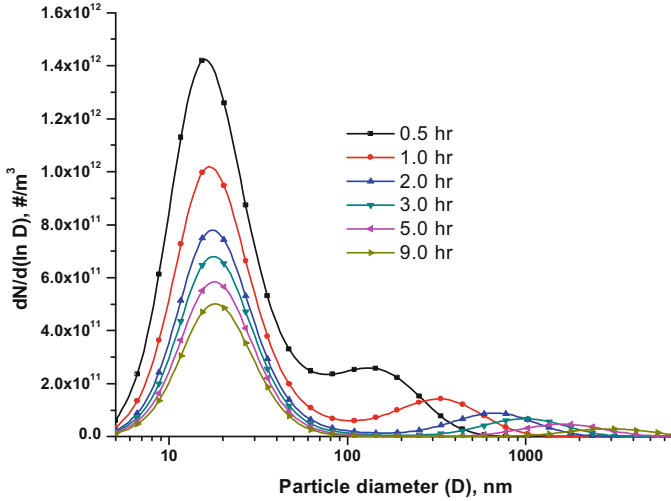


Fig. 23.4 Temporal evolution of particle size spectrum for fractal particles ($d_f = 1.75$, $CMD = 15$ nm, $S = 2 \times 10^{10} \text{m}^{-3} \text{s}^{-1}$) at a higher injection rate for zero ventilation rate (Anand et al. 2012)

secondary particles after a certain amount of time. As size of the secondary particles increases, value of coagulation kernel for the primary–secondary interactions also increased. Therefore, the primary particles are removed at an enhanced rate, proportional to the size of the secondary particles which can be visualized as an enhancement of effective coagulation kernel with time.

From this simulation as well as experimental results, it is observed that the number concentration asymptotically tends to zero, even if particles are injected continuously into the system at a steady rate. This contrasts with the results obtained using constant coagulation kernel, where the number concentration attains a steady-state value under conditions of steady injection rate and no ventilation. The difference in the number concentration behaviour suggests the importance of the size dependent kernels over constant kernel for the cases where size distribution evolves with time.

The plot of number concentration with time for different emission rates (Fig. 23.3b) suggests that higher injection rate leads to higher peak value of total number concentration and reduced time to attain the peak. If number concentration vs time is plotted in terms of scaled variables, the plots for different emission rates converge to a single curve in the absence of removal processes (Anand et al. 2012). This is an interesting result which demonstrates the applicability of scaling parameters in predicting number concentration for any source injection rate, provided removal processes in the system are negligible.

Furthermore, experimentally observed secondary size mode is captured by this numerical model which incorporates size dependent coagulation kernel. It is observed from Fig. 23.4 that early formation of secondary mode (110 nm at 0.5 h) occurs only in case of fractals ($d_f = 1.75$). As time lapses, the secondary mode

flattens and shifts towards larger size, similar to self-preserving size distribution. A distinctive secondary mode is observed for lower fractal dimensions and larger size of primary particles due to more pronounced coagulation effects. Again, these features are not observed in the case of simulations with constant coagulation kernel.

This study shows that numerical models handling size dependent kernels capture the peaking trend in the number concentration, their asymptotic behaviour and the formation of bimodal size distribution. This complex behaviour is due to the competing processes of fresh aerosol injection and removal due to coagulation or ventilation.

23.3.3 Diffusion-Coagulation Model to Estimate Atmospheric Background Particle Number Loading Factors

The analysis of contribution of aerosol sources (anthropogenic and natural) to the persistent background particle concentrations in the outdoor environment is important for health effect and climate change studies. High number concentration of particles are often encountered near the aerosol emission sources, and they would undergo significant change in the size distribution and concentration due to coagulation during their dispersion (Turco and Yu 1997; Anand and Mayya 2009). It is important to know what fraction of the particles released would survive intra-coagulation effect to persist in the atmosphere and ultimately interact with existing background aerosols. An effective way of quantifying this effect is to model their survival fraction (SF), defined as fraction of particles emitted from a source ultimately surviving intra-coagulation and dispersing as persisting background aerosols.

Analytical solutions are obtained for constant and free-molecular coagulation kernels by combining prescribed diffusion approximation (Jaffe 1940) with Laplace transforms and scaling theory, respectively (Anand and Mayya 2009). Later, these approximate formulae for the survival fraction are improved by introducing the coagulation-induced flattening of the concentration profile in the spatial domain. This is achieved by solving the moment equations governing number concentration and its spatial variance for puff/plume. The results of important analytical and numerical approaches developed in the past to solve the GDEs (Eqs. 23.16–23.18) such as expanding plume model (Turco and Yu 1999) and diffusion-coagulation model (Anand and Mayya 2011) are summarized in Table 23.2.

The comparison of results from these two models (Turco and Yu 1999; Anand and Mayya 2011, 2015) closely resembles in the case of higher survival fractions as compared to conditions with lower survival fractions. In another study related to geo-engineering problem (Stuart et al. 2013), the inherent capability of the diffusion based model to generate a similarity variable with inbuilt exponents for the parameters used in the survival factor parameterization is demonstrated (Anand and Mayya 2015). The simplicity offered by diffusion based model comes at a cost since the coagulation coefficient for an evolving aerosol system cannot be determined as

Table 23.2 Semi-analytical/numerical solutions

References	Survival fraction	Remarks
Anand and Mayya (2011)	Puff releases $F_\infty = (1 + \frac{5A}{4})^{-4/5}; A = \frac{KN_a}{4(2\pi)^{3/2}b_0D}$ N_a is the initial total number in the puff, K is the constant coagulation kernel, b_0 is the initial puff width	Rigorous diffusion-coagulation formulation; simplification at the solution stage; based on analytical approximations
	Plume releases $F_\infty = (1 + 1.32\mu)^{-0.76};$ $\mu = \frac{KS_0}{6\sqrt{3}U\sigma_0^{4/3}(C\varepsilon)^{1/3}}$ S_0 is the number source emission rate	
Turco and Yu (1999)	$N(t) = \frac{N_0N_T}{N_T+N_0}; N_T = \left[\frac{K}{2} \int_0^t \frac{1}{V(t)} dt \right]^{-1}$ N_0 and $N(t)$ are total number concentration at time $t = 0$ and at any time t , respectively, $V(t)$ is the volume expansion rate	Simplification at formulation stage; replace dispersion by uniform volume expansion

efficiently as in the case of Stuart et al. (2013). Further development of this parameterization for global aerosol transport models is in progress to account for the polydisperse aerosol size distribution and effective coagulation kernel.

23.4 Environmental Risk and Remediation

The modelling studies show the significance of number-based metrics in understanding the complexity involved in the evolution of UFPs in the indoor environment. The studies reveal that the aerosols exhibit different behaviours depending upon the source characteristics and the environment in which they are released. It also brings out the importance of proper indoor ventilation (ex. CAER, HaVAER) and its effectiveness for a given source strength. Further, the indoor modelling studies highlight an atypical behaviour of the aerosol concentration, i.e. peaking of total number concentration and formation of bimodal distribution in the clean environment. These indoor models will be useful in the inhalation toxicological studies and exposure risk assessments.

In the case of outdoor environment, aerosols have a wide spectrum of implications ranging from pollution which lead to health hazards to change in the radiation flux affecting the Earth’s climate. Study of effective contribution of emission sources to the background aerosols in the atmosphere through models is very important to assess the importance of microphysical processes that needs to be included in the large scale models. Alternatively, parameterization schemes are being developed for the long range aerosol transport models to reduce the computational cost. The quantification of the aerosol parameters such as number loading factors, concentration and size distribution is useful in the remediation studies such as geo-engineering techniques to reduce the Earth’s surface radiation flux, etc.

23.5 Conclusion

Simulations based on modelling the number concentration bring out the theoretical perspective on the complex evolution of the UFP metrics as a function of controlling source and sink parameters, in the indoor environment. Indoor study results suggest that the number concentration is one of the important metric to be considered while assessing the risk due to UFPs in addition to the mass and surface area concentration. Furthermore, the aerosol emission from intense sources shows a complex behaviour such as peaking of total number concentration and formation of bimodal size distribution. These models will help in the accurate estimation of aerosol emission factors from the households to open environment for the general circulation models that are used in studying the health and climate effects.

To quantify the contribution of various sources to background aerosol particle number loading (ex. geo-engineering problems, forest fires, volcanic releases, etc.), a simplified modelling approach is developed to estimate survival fraction for puff and plume sources. The challenge in estimating the number survival fraction is due to simultaneous existence of atmospheric diffusion and nonlinear coagulation effects. The study provides simplified, ready reckoner tools for estimation of the number survival fractions, as a function of atmospheric and aerosol parameters. These formulae are valid for wide range of applications, from highly diffusive to highly coagulating systems, and are appropriate to incorporate into global/regional scale air pollution models for predicting the contribution of localized sources to the particle number loading in the atmosphere.

Acknowledgments The authors (SA and JK) would like to acknowledge Shri Kapil Deo Singh and Dr M S Kulkarni, Health Physics Division, Bhabha Atomic Research Centre for their support and encouragement.

References

- Anand S, Mayya YS (2009) Coagulation in a diffusing Gaussian aerosol puff: comparison of analytical approximations with numerical solutions. *J Aerosol Sci* 40(4):348–361
- Anand S, Mayya YS (2011) A simplified approach for solving coagulation–diffusion equation to estimate atmospheric background particle number loading factors contributed by emissions from localized sources. *Atmos Environ* 45(26):4488–4496
- Anand S, Mayya YS (2015) Comment on “Reduced efficacy of marine cloud brightening geoengineering due to in-plume aerosol coagulation: parameterization and global implications”. *Atmos Chem Phys* 15:753–756
- Anand S, Mayya YS (2017) Modeling Critical Air Exchange Rates (CAERs) for aerosol number concentrations from nano-particle sources using an effective coagulation coefficient approach. *Aerosol Sci Technol* 51(4):421–429
- Anand S, Mayya YS, Yu M, Seipenbusch M, Kasper G (2012) A numerical study of coagulation of nanoparticle aerosols injected continuously into a large, well stirred chamber. *J Aerosol Sci* 52:18–32

- Anand S, Sreekanth B, Mayya YS (2016a) Effective coagulation coefficient approach for estimating particle number emission rates for strong emission sources. *Aerosol Air Qual Res* 16:1541–1547
- Anand S, Sreekanth B, Mayya YS (2016b) Ventilation dependence of concentration metrics of ultra-fine particles in a coagulating household smoke. *Inhalation Toxicol* 28(1):39–47
- Bhangar S, Mullen NA, Hering SV, Kreisberg NM, Nazaroff WW (2011) Ultrafine particle concentrations and exposures in seven residences in northern California. *Indoor Air* 21:132–144
- Dhaniyala S, Dubey P, Balakrishnan K (2011) Air quality in rural India: the role of ultrafine particles from cook stoves, *Air and Waste Management Association's Magazine for Environmental Managers*, pp 14–18
- Fiebig M, Stohl A, Wendisch M, Eckhardt S, Petzold A (2003) Dependence of solar radiative forcing of forest fire aerosol on ageing and state of mixture. *Atmos Chem Phys* 3:881–891
- Friedlander SK (2000) *Smoke, dust, and haze: fundamentals of aerosol dynamics*. Oxford University Press, Oxford
- Fuchs NA (1964) *Mechanics of aerosols*. Ann Arbor Press, Chelsea, MI
- Hendriks EM, Ziff RM (1985) Coagulation in a continuously stirred tank reactor. *J Colloid Interface Sci* 105(1):247–256
- Isaxon C, Gudmundsson A, Nordin EZ, Lonnblad L, Dahl A, Wieslander G, Bohgard M, Wierzbicka A (2015) Contribution of indoor-generated particles to residential exposure. *Atmos Environ* 106:458–466
- Jacobson MZ (2005) *Fundamentals of atmospheric modeling*. Cambridge University Press, Cambridge, UK
- Jaffe G (1940) The theory of recombination. *Phys Rev* 58:968–976
- Joshi M, Khan A, Anand S, Sapra BK (2016) Size evolution of ultrafine particles: differential signatures of normal and episodic events. *Environ Pollut* 208:354–360
- Kittelson DB (1998) Engines and nanoparticles: a review. *J Aerosol Sci* 29(5/6):575–588
- Kittelson DB (2001) Recent measurements of nanoparticle emissions from engines, current research on diesel exhaust particles. Japan Association of Aerosol Science and Technology, Tokyo
- Matsoukas T, Friedlander SK (1991) Dynamics of aerosol agglomerate formation. *J Colloid Interface Sci* 146(2):495–506
- Mitchell EJS (2017) Emissions from residential solid fuel combustion and implications for air quality and climate change. PhD Dissertation. University of Leeds, Leeds, UK
- Morawska L, Afshari A, Bae GN, Buonanno G, Chao CYH, Hanninen O, Hofmann W, Isaxon C, Jayaratne ER, Pasanen P, Salthammer T, Waring M, Wierzbicka A (2013) Indoor aerosols: from personal exposure to risk assessment. *Indoor Air* 23:462–487
- Nathans MW, Thews R, Holland WD, Benson PA (1970) Particle size distribution in clouds from nuclear airbursts. *J Geophys Res* 75(36):7559–7572
- Oberdörster G, Oberdörster E, Oberdörster J (2005) Nanotoxicology: an emerging discipline evolving from studies of ultrafine particles. *Environ Health Perspect* 113(7):823–839
- Ott S, Mann J (2000) An experimental investigation of the relative diffusion of particle pairs in three-dimensional turbulent flow. *J Fluid Mech* 422:207–223
- Pedata P, Stoeger T, Zimmermann R, Peters A, Oberdörster G, D'Anna A (2015) Are we forgetting the smallest, sub 10 nm combustion generated particles? *Particle Fibre Toxicol* 12(34):1–4
- Prakash A, Bapat AP, Zachariah MR (2003) A simple numerical algorithm and software for solution of nucleation, surface growth, and coagulation problems. *Aerosol Sci Technol* 37(11):892–898
- Radke LF, Hegg AS, Hobbs PV, Penner JE (1995) Effects of aging on the smoke from a large forest fire. *Atmos Res* 38:315–322
- Roy AA, Baxla SP, Gupta T, Bandyopadhyaya R, Tripathi SN (2009) Particles emitted from indoor combustion sources: size distribution measurement and chemical analysis. *Inhalation Toxicol* 21:837–848

- Schneider T, Brouwer DH, Koponen IK, Jensen KA, Fransman W, Duuren-stuurman BV, Tongeren MV, Tielmans E (2011) Conceptual model for assessment of inhalation exposure to manufactured nanoparticles. *J Expo Sci Environ Epidemiol* 21:450–463
- Seinfeld JH, Pandis SN (2006) Atmospheric chemistry and physics: from air pollution to climate change, 2nd edn. Wiley, Hoboken, NJ
- Seipenbusch M, Binder A, Kasper G (2008) Temporal distribution of nanoparticle aerosols in workplace exposure. *Ann Occup Hyg* 52(8):707–716
- Stuart GS, Stevens RG, Partanen A-I, Jenkins AKL, Korhonen H, Forster PM, Spracklen DV, Pierce JR (2013) Reduced efficacy of marine cloud brightening geoengineering due to in-plume aerosol coagulation: parameterization and global implications. *Atmos Chem Phys* 13:10385–10396
- Turco RP, Yu F (1997) Aerosol invariance in expanding coagulating plumes. *Geophys Res Lett* 24:1223–1226
- Turco RP, Yu F (1999) Particle size distributions in an expanding plume undergoing simultaneous coagulation and condensation. *J Geophys Res* 104(19):227–241
- Venkataraman C, Brauer M, Tibrewal K, Sadavarte P, Ma Q, Cohen A, Chaliyakunnel S, Frostad J, Klimont Z, Martin RV, Millet DB, Philip S, Walker K, Wang S (2018) Source influence on emission pathways and ambient PM_{2.5} pollution over India (2015–2050). *Atmos Chem Phys* 18:8017–8039
- Wallace L, Ott W (2011) Personal exposures to ultrafine particles. *J Expo Sci Environ Epidemiol* 21:20–30
- Wallace L, Emmerich SJ, Howard-Reed C (2004) Source strengths of ultrafine and fine particles due to cooking with a gas stove. *Environ Sci Technol* 38:2304–2311
- Wallace L, Wang F, Howard-Reed C, Persily A (2008) Contribution of gas and electric stoves to residential ultrafine particle concentrations between 2 and 64 nm: size distributions and emission and coagulation rates. *Environ Sci Technol* 42(23):8641–8647
- Wolfram Research Inc. (2005) Mathematica, version 5.2, Champaign, IL

Chapter 24

Environmental Impacts of Coal-Mining and Coal-Fired Power-Plant Activities in a Developing Country with Global Context



Md. Ahasan Habib and Rahat Khan

Abstract To represent a comprehensive scenario regarding the coal mining and coal-fired power plant activities in a developing country (Bangladesh) and to understand the total environmental impacts, potential coal resources of Bangladesh, environmental geochemistry and dispersion of pollutants, eco-toxicological impacts, human health risks as well as socioeconomic impacts are evaluated in this chapter. Potential coal reserves along with the future plants are estimated. Technogenic sources of environmental pollutants including environmentally toxic heavy metals, health hazardous radionuclides, persistent organic pollutants, suspended particulate matters, etc. are assessed. In doing so, scarce associated data from coal mine (Barapukuria, Bangladesh) and Barapukuria coal-fired power plant (BTTP) of Bangladesh have been reconciled by using and arguing the previous works around the globe. Immense and proper literature reviews as well as the existing data on Barapukuria coal mine and BTTP are tabulated to compare and understand the condition along with the potential prevention and remediation approaches.

Keywords Coal mine in Bangladesh · Coal-based thermoelectric power plant · Organic, inorganic, and radiogenic pollutants · Environmental impacts · Eco-toxicological and human health risks · Prevention and remediation approaches

M. A. Habib
Geological Survey of Bangladesh, Segunbaghicha, Dhaka, Bangladesh

R. Khan (✉)
Institute of Nuclear Science and Technology, Bangladesh Atomic Energy Commission, Savar,
Dhaka, Bangladesh

24.1 Introduction

Coal is a very complex sedimentary rock and is the main natural solid fuel source for power generation (Depoi et al. 2008). It is a mixture of (in) combustible compounds, an organic fraction (macerals), and an inorganic fraction (minerals) (Goodarzi 2006; Orem and Finkelman 2014; Habib et al. 2019a, b) which was usually stratified, and was originated from the physicochemical alteration of plant debris over a geologic time (Orem and Finkelman 2014). Geologically, coal carries minute amounts of NORMs (Naturally Occurring Radioactive Materials: ^{226}Ra , ^{232}Th , ^{238}U , and ^{40}K) along with small amounts of other contaminants like trace metals (e.g., As, Cd) and organic pollutants (e.g., polycyclic aromatic hydrocarbons—PAHs, persistent organic pollutants—POPs, volatile organic compounds—VOCs) contaminants (Sengupta and Agrahari 2017; Verma et al. 2015; Bragato et al. 2012; Hower et al. 2016; Khandekar et al. 1999).

Coal combustion residues (CCRs) are, the noncombustible major residuals generated by coal-fueled thermoelectric power plants (CTPs). The multistage processes of combustion causing enormous changes of (in)organic constituents in feed coal and simultaneously produce large volume of CCRs with physical-chemical-mineralogical transformation, elemental speciation, and isotopic fractionation of radionuclides in CCRs (Michalik et al. 2013; Sajwan et al. 2011; Meij and Te Winkel 2009; Ozden et al. 2018). Although CTPs arrest the most of coarse flyash, ~1–3% finest portion of total flyash escaped to the atmosphere and biosphere regardless of using filtration systems and consequently spread out over a huge area owing to the convectional process of the atmosphere (Tripathi et al. 2014; Dragović et al. 2013; Charro et al. 2013; Papastefanou 2010). Along with CCRs, coal combustion emits NO_x , CO, SO_2 , volatile organics, NH_3 , fine particulate matters (PM: PM_{10} , $\text{PM}_{2.5}$), As, and Hg.

Presently, Bangladesh suffers from a shortage of electricity production. Considering this fact, multiple approaches have been considered to resolve this deficiency where coal fuel will have an important significance (Zaman et al. 2018; Ahamad 2016). Thus, the Bangladeshi energy sector is currently emphasizing electricity production from coal. At present in Bangladesh, eight (08) coal-based power projects are under construction with a total capability of 6543 MW (Ahmed et al. 2017; Zaman et al. 2018). Thus in the upcoming years, a significant fraction of the total electric power will be generated from coal fuel source (Islam and Khan 2017). Currently installed power production capacity of Bangladesh is >12,780 MW which is intended to enhance up to 39,000 MW by the year 2030, of which ~50% will be produced from local or imported coal (Zaman et al. 2018; Islam and Khan 2017). Currently, the first and only coal-based power plant (BTTP: subcritical), with a capacity of 250 MW (2×125 MW), supplies only 3.75% of total electric power while the major fraction (~69.7%) of electricity is exclusively produced from natural gas (locally available in Bangladesh), which is being rapidly consumed (Zaman et al. 2018). The BTTP has been operated since 2005 while a third unit with 275 MW capacity has been started since 2017.

Bangladesh has five potential coalfields having reserve of about 3.33 billion tons (Bt) of highly volatile bituminous B ranked Permian Gondwana coal (except, Jamalganj coal basin) (Hossain et al. 2019, 2020; Bakr et al. 1996; HCU 2018; Islam 2002; Akhtar and Kosanke 2000; Norman 1992; Bostick et al. 1991). However, the coal mine in Barapukuria (reserve: 377Mt) is the only active commercially operational coal basin, so far (Islam and Khan 2017; Farhaduzzaman 2013; Farhaduzzaman et al. 2012; Islam 2008, 2009; Islam and Hayashi 2008). A significant portion of extracted coal from Barapukuria coal mine is combusted in BTPP which generates a huge amount of CCRs.

Fossil fuel coal is the most abundant and readily combustible solid energy source containing more than 70% carbonaceous organic constituents by volume (Zaman et al. 2018; Ozden et al. 2018). Due to price stability, cost efficiency, and intensive uses, coal is a popular and indispensable solid fuel in many countries including Bangladesh (e.g., Mishra 2004; Bhangare et al. 2014). Thus, coal fuel has become the primary non-renewable energy source which contributes more than 40% of world electric power production (IEA 2017) and this is supposed to be increased progressively (Amin et al. 2013). The coal mining, combustion, and discharging of byproducts may cause pollution risk to human health, soils, vegetables and crops, and water resources due to the higher abundances of heavy metals (HMs), rare earth elements (REEs), organic pollutants, soluble salts, radionuclides, etc. (Ram and Masto 2010). The leaching and chemical solubility of HMs and other elements in coal and combustion residues may deteriorate the environmental systems. Considering the environmental and human health hazard, it is essential to evaluate the eco-toxicological, environmental, and human health-oriented impacts of coal mining and coal-based power plant activities.

24.2 Coal Bearing Areas in Bangladesh

24.2.1 Geographical Region

Coal basins are located (Fig. 24.1) in a subtropical humid region with double/triple cropped farming area in northwestern Bangladesh. According to the Population Census of Bangladesh (2011), the population density of the study area is 770 per km². Most of the lands are mainly cultivable (about 80%) with single/double-cropped and the rest of the land is covered with settlement (15%), orchard, ponds, other fallow lands, channels, and rivers (5%). Pedologically, the study area has been named as gray Floodplain Soils and non-calcareous Floodplain Soils, Barind Tract, and mainly level Barind Terrace Soils (Brammer 1996). Physiographically the area is classified as Barind Tract and Teesta Alluvial Fan systems (Brammer 1996). Geomorphologically, the area is categorized into several types, i.e., floodplain, flood basin, channel bar, point bar, oxbow lake, Brind, and rivers. The survey reveals

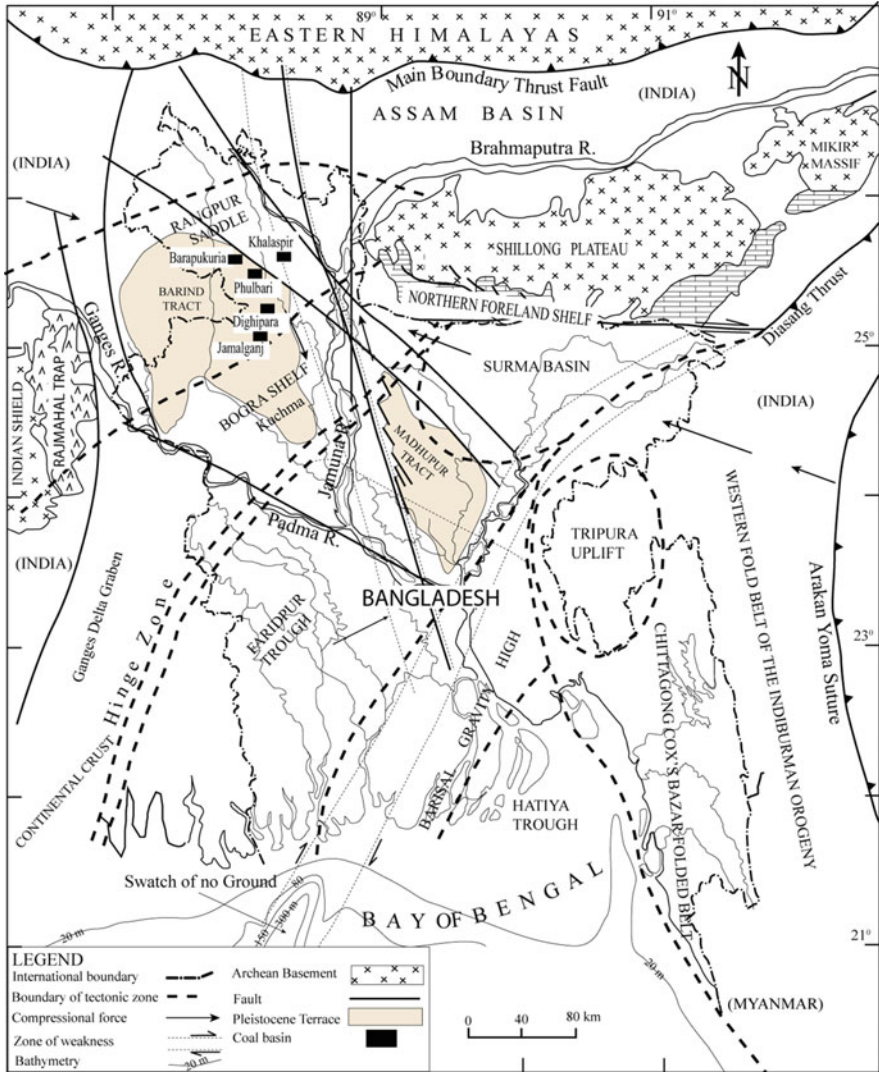


Fig. 24.1 Map showing the distribution of major coal basins with tectonic elements of Bangladesh and adjoining areas (adopted and modified from Islam and Hayashi (2008), Uddin and Islam (1992), Frielingsdorf et al. (2008), Samsuzzaman (2011), Rashid et al. (2015))

that the study area is elevated 27 to 31 m from the mean sea-level. The average yearly rainfall is 1800 to 2000 mm of which ~85% takes between May and September (BBS 2018).

24.2.2 Geology

Tectonically, the Coal basins (except Jamalganj) locate in the Rangpur Saddle and are enclosed by Indian Shield on the west, Bogra Shelf in the south, Shillong Massif on the east and Himalayan Foredeep in the north of Bengal basin (Khan 1991; Bakr et al. 1996; Frielingsdorf et al. 2008; Islam 2008, 2009; Farhaduzzaman 2013) (Fig. 24.1). In Bangladesh, five subsurface Gondwana basins have been discovered in the northern part of the country. These basins are formed within the Precambrian basement complex during Permo-carboniferous time (355–270 million years ago). Permian Coal Basins (except Jamalganj) occur in one of several north-north-west to south-south-east (NNW-SSE) extended intra-tectonic basins in Rangpur saddle which was formed when the Indian subcontinent was joined to Africa, Madagascar, Australia, and Antarctica as part of Gondwana during Permian times (Alam 1989; Akhtar and Kosanke 2000; Roy and Roser 2013). Northern Bangladesh basement has a slope of 1° – 2° towards NNW and SSE direction from the Rangpur area and the slope suddenly increased beyond south of Bogra, which formed NE-SW trending hinge zone (continental shelf break). The Gondwana rocks are present on the top of the basement complex. The upper contact is either Tertiary rocks on the northern side or Cretaceous/Jurassic rocks in the southern side. The Gondwana basins are fault-bounded asymmetric type (half-graben) basin formed on the basement complex.

Coalfields are within the Gondwana sediments that lie over the Precambrian Basement Complex. The overlying rocks of the coal-bearing sequences vary from basin to basin. In Barapukuria (Hossain et al. 2017, 2018, 2019) and Dighipara basin the overlying rock is Dupi Tila sandstone (Farhaduzzaman et al. 2013a, b, 2015), in Khalaspir coalfield the overlying rocks are the Surma Group sandstone and mudstone (Roy and Roser 2013; Islam et al. 1992) and in Jamalganj coalfield the overlying rock is the Cherra sandstone (Islam 1998; Imam et al. 2002). The Gondwana rock has consisted of carbonaceous sandstone, feldspathic sandstone, carbonaceous shale, conglomerate, and thick coal beds. The area is covered mostly with Pleistocene Barind clay and unconsolidated Holocene Teesta Alluvial fan, which were built under fluvial-alluvial and rapidly prograding-deltaic condition (Uddin et al. 2016; Hossain et al. 2002; Bakr et al. 1996; Uddin and Islam 1992; Alam et al. 1990). Plio-Pleistocene Dupi Tila formation is concealed by Barind clay residuum (Islam and Hayashi 2008). The coal-bearing sediments are composed of subordinate carbonaceous-shales, Gondwana Permian age sandstones, siltstones, and six correlated coal seams which are inconsistently overlain by Quaternary as well as Tertiary deposits, against which the coal seams are sequentially sub-cropped to the west (Farhaduzzaman et al. 2012, 2013a, b). Depending on lithology, sediments in the coal basin have been classified into four (04) lithostratigraphic groups: (1) Dupi Tila, (2) Barind Clay, (3) Alluvium having Permian age, Pleistocene, Plio-Pleistocene, and (4) Holocene (Norman 1992; Farhaduzzaman et al. 2013a, b). A comprehensive stratigraphic succession of the coal-bearing areas of northern Bangladesh is shown in Table 24.1.

Table 24.1 Stratigraphic sequences of the north-western part of the Bengal Basin (sourced from Frielingsdorf et al. 2008; Rashid et al. 2018)

	Age	Bogra Shelf/ Jamalganj	Rangpur Platform/ Barapukuria	Lithology
		Group/formation	Formation/ group	
1.	Recent to Sub-Recent	Alluvium (88 m)	Alluvium (88 m)	Sand, clay, and silt
2.	Pleistocene	Barind Clay (15 m)	Barind Clay (15 m)	Clay (sandy clay, yellowish-brown, sticky)
3.	Middle Pliocene to Late-Miocene	Dupi Tila Formation (276 m)	Dupi Tila Formation (276 m)	Shale and Sandstone with subordinate pebble bed
4.	Early-Miocene	Jamalganj Formation (Surma Gr. Undiff) (413 m)	Surma Group (413 m)	Sandstone (Fine to medium-grained), shale (sandy and silty), and siltstone interbedded with coal beds
5.	Oligocene	Bogra Formation (163 m)	x	Fine-grained sandstone, siltstone, and carbonaceous shale
6.	Late Eocene	Kopili Formation (42 m)	x	Sandstone, locally glauconitic and highly fossiliferous shale; calcareous bands
7.	Middle to Late Eocene	Sylhet Limestone formation (197 m)	x	Nummulitic-limestone with sandstone interbeds
8.	Middle Eocene	Tura Sandstone Formation (104 m)	x	White and gray sandstone with subordinate greenish-gray shale, coal
9.	Late Cretaceous	Sibganj Formation (131 m)	x	Coarse-grained yellow to brown sandstone, white clay, and volcanic materials
10.	Late-Jurassic to Middle-Cretaceous	Rajmahal Trap (305 m)	x	Amygdaloidal basalt, serpentinized shales, and agglomerates
11.	Late Permian	Paharpur formation (421 m) Kuchma formation (493 m) Gondwana group (1100 m)	Gondwana Group (815 m) Barapukuria Formation (565 m)	Shale and coal beds, feldspathic sandstone, sandstone, and grit with subordinate shale interbedded with coal
12.	Precambrian	Basement Complex	Basement Complex	Gneiss, diorite, schist, granodiorite, granite, diabase and adamellite.
	x-missing			

24.2.3 Hydrogeology

The mapped area is vehemently influenced by the Atrai-Teesta river basin. The coal mine area is drained by several rivers including Atrai, little Jamuna, Karatoya, Banglai, Jabuneswari, Kala, Kharkhari, Tillay, Chirmai, etc. (distributaries of River

Table 24.2 Hydro-stratigraphic sequences of Barapukuria coal basin (Bakr et al. 1996; Howladar 2013, 2017)

Age	Formation/ group	Lithology	Aquifer
Recent	Alluvium	Sandy and silty clay, organic matter.	
Plio-Pleistocene	Barind clay (exposed)	Light brown silty clay, massive, sticky, containing Fe and Mn nodules, yellowish-brown with mottling of red silty clay, reddish-brown silty clay, moderately sticky and plastic. The lower part is sandy.	Shallow
Pliocene	Upper DupiTila	Sandstones, pebbly sandstones, and clay/mudstone, Sandstones, claystone.	Intermediate
	Lower DupiTila	Mudstone with white clay and silica.	
Early Permian	Gondwana formation	Feldspathic sandstones, carbonaceous sandstone and shale, ferruginous sandstone, conglomerates, and coal seams.	Deep
Paleoproterozoic	Basement complex	Diorite, gabbro, microcline rich granite, granodiorite, quartz diorite, syenite, quartz monzonite, pegmatite, quartz diorite, mica schist/gneiss, quartz feldspathic gneiss with the weathered top (5–10 m).	

Teesta), flowing from north to south. There are two major aquifers: one, the Upper DupiTila (UDT) formation whose thickness varies from 102 to 136 m, and the other, the Gondwana formation with an average thickness of 360 m. The Barind Clay sediments show an aquiclude character having a thickness of 10 m with an infiltration rate of $\sim 1.5 \text{ mm.day}^{-1}$. The UDT is the major underground water reservoir (average thickness: $\sim 104 \text{ m}$; depth: 102–136 m) for irrigation and drinking which is mostly comprised of unconsolidated fine to medium-grained sandstones, clay/mudstone and pebbly sandstones and claystone compositions (Bakr et al. 1996). The UDT aquifer can be characterized in terms of hydrogeological entities including specific yield values (25–30%), permeability (0.004%), hydraulic gradients (0.0004–0.0006%), and average transmissivity ($12,000 \text{ m}^2.\text{day}^{-1}$) (Howladar 2013, 2016, 2017; Howladar et al. 2014). The Hydro-stratigraphic sequences of Barapukuria are provided in Table 24.2.

24.3 Coal Mining and Coal-Fueled Power Plant Activities in Bangladesh

24.3.1 Coal Resources of Bangladesh

In Bangladesh, 5 coal basins (Barapukuria, Phulbari, Khalashpir, Jamalganj, and Dighipara) have been discovered and their energy properties are summarized and

compared with other world coal basins (Table 24.3, 24.5, and 24.6). The results demonstrate that the coals are inertinite rich highly volatile bituminous B ranked coal. The total in-situ deposits of coal in these fields are about 3300 Mts which is comparable to 85.5 TCF (trillion cubic feet) of natural gas (HCU 2018). Among these five coalfields, coal at the Jamalganj field is too deep to be mined (Fig. 24.2). The coals in the other four fields are within the mineable depth. About 2200 Mts of in-situ coal is present in the Barapukuria, Khalaspir, Phulbari, and Dighipara coalfields. These coals are high quality, low sulfur bituminous coal and can be used for any type of thermal conversion. Among these four shallow depth coalfields, only Barapukuria coal-field is under production by underground mining method and is used in the 525 MW power plants situated at the mine mouth. Coal in the other three coalfields if mined in a scientific way could play a vital role to improve the energy scenario of Bangladesh. The quality of coal indicates that it is possible to run 500 MW power plants for every 1.80 Mts of coal. It is estimated that Phulbari has a deposit of 572 Mts, Khalaspir has a deposit of 685 Mts and Dighipara has a deposit of 600 Mts of in-situ coal. The total deposits of these three fields are 1857 Mts (Uddin and Islam 1992; HCU 2018). The mineable reserves of Dighipara and Khalaspir have not yet been determined but approximately 25% of these deposits (equivalent to 465 Mts) may be mined from these three coalfields. If 10 Mts of coal is mined annually from these coalfields then it is possible to run 3300 MW power plants for 46 years by using all the coal. This will reduce the pressure on the power demand of the country.

24.3.2 Coal Based Power Plant in Bangladesh

Barapukuria underground coal mine (BCM) and BTPP are situated in Dinajpur district, Bangladesh (Fig. 24.3). The salient features of the BTPP power plant and the BCM have appeared in Table 24.4. In Bangladesh, BTPP is the first and only coal-based subcritical power plant. Other than BTPP, eight more potential thermal power plants are proposed to be built in Rampal, Payra, Matarbari, and Moheskhali.

Approximately, 5–20% of the total mass of the feed coals are converted to CCRs during the incineration of coals in CTPs which produces fly ash (FA: 85–95%) and bottom ash (BA: 5–15%) along with few slag (Gollakota et al. 2019; Zierold and Odoh 2020; Li et al. 2018; Yao et al. 2015; Jayaranjan et al. 2014; Shaheen et al. 2014). Briefly, FA and BA are the lighter and heavier fractions of CCRs, respectively whereas slag is the melted materials and pond ash is the mixture of different type of CCRs dumped into the disposed site (Ahmaruzzaman 2010; Hower 2012; Bartoňová 2015; Hower et al. 2017a, b). CCRs are geochemically complex and highly enriched with extremely heterogeneous constituents, composed of (in)organic pollutants (Hower et al. 2017a, b; Verma et al. 2015; Liu et al. 2008). They contain potentially hazardous toxic elements, radiotoxic radionuclides (Turhan et al. 2018; Wang et al. 2016a, b; Hower et al. 2016; Sahu et al. 2009, 2014, 2017), unburned carbon, rock-fragment, amorphous glass, micron to nanoparticles/minerals

Table 24.3 In-situ coal resources and coal properties of different coalfields of Bangladesh are compared with those of literature data

Basin unit	Discovery (year)	Depth range (m)	Aggregated thickness (m)	Area (planimeter) (km ²)	Ash (wt.%)	Fixed carbon (wt.%)	Volatile matter (wt.%)	Moisture (wt.%)	Total sulfur (wt.%)	GCV (Btu.lb. ⁻¹)	Maturity (R _o)	Estimated resources (Mt)	Proved reserves (Mt)
<i>Coalfields in Bangladesh</i>													
Barapukuria	1985	118–509	51	5.16 (7.2)	6.7–25.2 (15)	44.7–58.7 (53)	27.4–31.8 (28)	3.3–4.6 (4)	0.43–0.80 (0.63)	9839–12,658 (11364)	0.55–0.84	377	303
Phulbari	1997	150–240	38	(12.4)	11.6–24.6 (15)	44.2–56.7 (51)	29.4–33.7 (31)	2.4–2.8 (2.6)	0.75–0.80 (0.77)	12,474–13,320 (12897)	0.82	572	288
Khalashpir	1989	257–483	50	12.26 (12.2)	7.6–27.3 (20)	48.6–60.4 (54)	17.4–40.4 (23)	1.2–4.1 (3.2)	0.56–0.96 (0.77)	10,436–11,580 (11264)	0.79–0.94	685	143
Dighipara	1995	328–407	61	5	5.7–28.8 (15)	47.7–60.6 (54)	22.4–33.5 (28)	2.0–4.6 (3)	0.32–1.14 (0.66)	8666–13,146 (11426)	0.7–1.1	600	150
Jamalgonj	1962	640–1158	64	6.8–41 (24.5)	10–60 (21)	33–54 (45)	30–40 (30)	(3.6)	0.54–0.65 (0.55)	7388–13,000 (12100)	0.66–0.84	1053	–
<i>Literature data</i>													
^a Greece					12.96	57.71	29.33	1.9		12541.27			
^b Turkey					3.2–44.6		45.5–61.5	8.8–36.2		1470–2786			
^c Indonesia					6.99		33.4	16.93		5733.75			

GCV gross calorific value. Data from HCU (2018), Inaam (2013), Islam and Hayashi (2008), Farhaduzzaman et al. (2012), Farhaduzzaman et al. (2013a, b), Islam et al. (1992), Bakr et al. (1996)

^aKoukouzas (2007), ^bBaba et al. (2010), ^cBelkin et al. (2009)

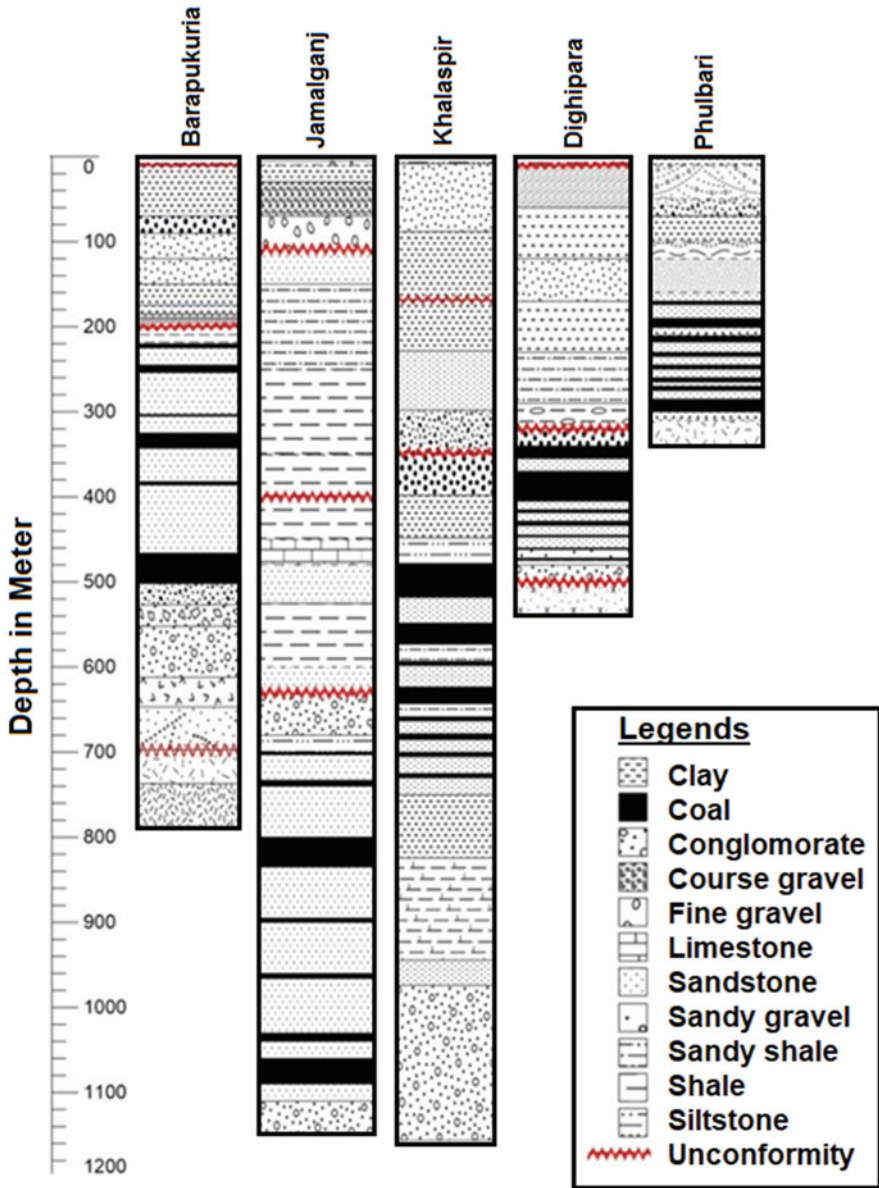


Fig. 24.2 Stratigraphic correlation among five major Coal Basins of Bangladesh. Coal basin locations are indicated in Fig. 24.1

(Jambhulkar et al. 2018; Dai et al. 2014; Zhao et al. 2017; Hower 2012). CCRs are originated mostly from the inorganic constituents of feed coal (Hower et al. 2017a, b; Fungaro et al. 2013; Hower 2012; Lu et al. 2012a, b; Islam et al. 2011; Koukouzas

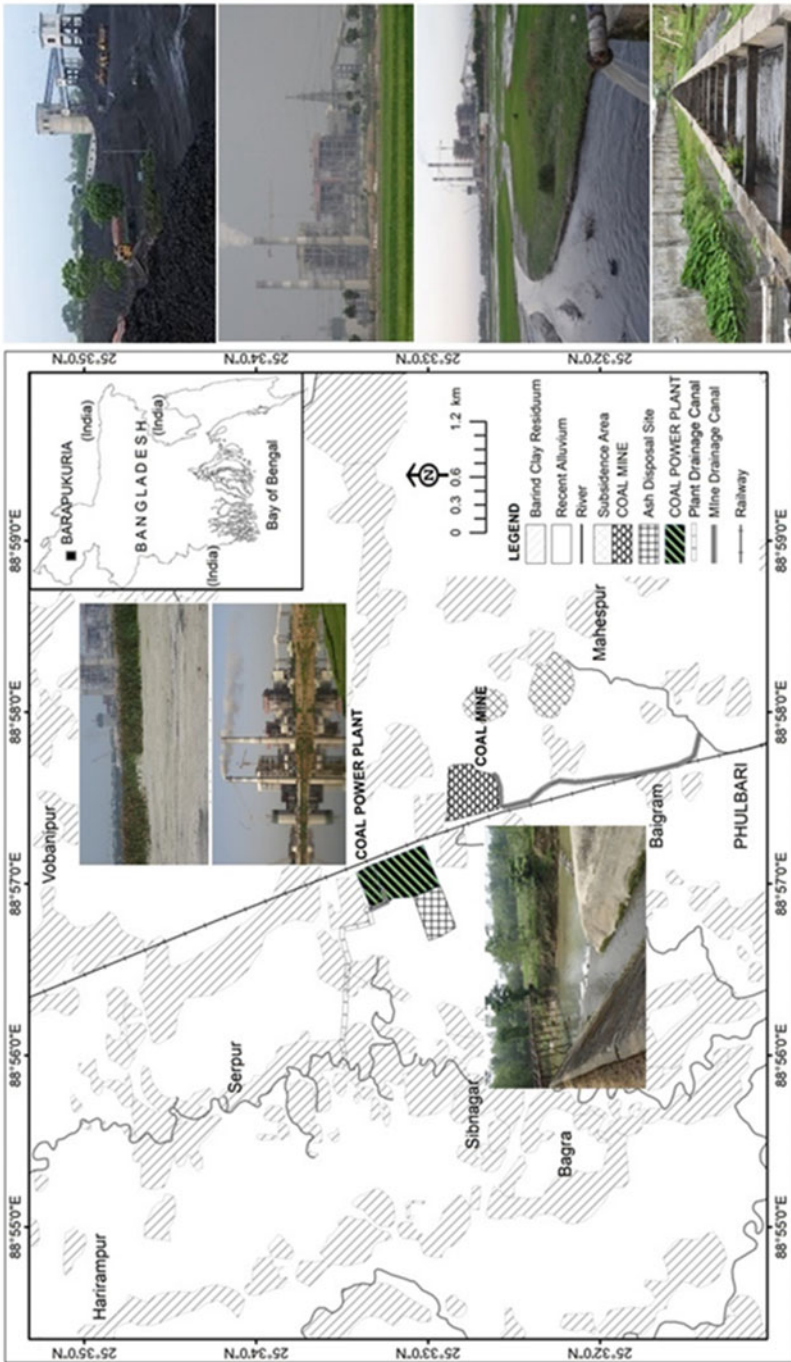


Fig. 24.3 Maps showing the Barapukuria coal mine (BCM) and Barapukuria coal-fired power plant (BTTP), Dinajpur district, Bangladesh

Table 24.4 Salient features of the Barapukuria coal mine (BCM) and Barapukuria coal-fired power plant (BTPP), Dinajpur district, Bangladesh

Type	Subcritical
<i>BTPP</i>	
Operation	2005
Stack (Chimney) height	100 m
Thermal efficiency	36%
Emission control device	Electrostatic precipitators (Efficiency \leq 99%)
Yearly coal consumption	0.72 Mts
Daily coal consumption	2400 tons
Coal consumption/kWh	0.4 kg
Water consumption/h	800–1200 tons
Yearly ash production	0.08 MT (12 to 14% ash produced of feed coal)
Unit	2 \times 125 MW
Capacity	250 MW
Year of operation	2005
Ash pond	Capacity about 0.183 Mt
Fuel source	Barapukuria underground coal mine
New unit	275 MW operated in 2018
<i>BCM</i>	
Commercial extraction	2005
Coal extraction method	Underground mining
Number of coal seams	6
Depth range of coal seams	118–518 m (below surface)
Coal resource	377 Mts
Yearly coal production	1 Mt
Thickness range of coal seam VI	21.63–42.37 m
Coal type	High-volatile bituminous B rank
Calorific value	6100 kcal/kg
Age of coal	Permian
Depositional mode	Peat swamp flood basin (terrestrial origin)
Basin area	6.68 km ²
Paleovegetation	Coniferous gymnosperms (herbaceous plants)

et al. 2006). In BTPP, about one million tons (Mt) of coal is being mined from BCM annually, of which 65% is combusted for power generation (Howladar 2013; Howladar and Hasan 2014; Howladar and Islam 2016). Approximately 4000 tons (t) of feed coal is burnt per day in the BTPP boiler which generates nearly 480 tons of solid byproducts (Zaman et al. 2018), simultaneously. Every year about 0.08 Mt. CCRs are produced, of which, 80% is approximated to be FA and the rest is BA (Hashan et al. 2013; Howladar and Islam 2016). Coal-based industrial activities generate different forms of pollutants, such as solid (coal dust, coal spoil, FA, BA, pond ash, nano-particulates), liquid (leachate, effluents, acid mine drainage), and gaseous (volatiles, CO₂, CO, SO₂, SO₃, H₂S) as well as air particulate matters.

24.3.3 *Characterization of Coals and CCRs*

To assess the contamination levels and hazards to the public health and the environmental compartments were intensively studied and reported in literature considering following parameters and observations such as organic pollutants (e.g., polycyclic aromatic hydrocarbon), toxic heavy metals, rare earth elements and radioactive elements, nanominerals/particles (e.g., nanoquartz, anatase, pyrite), etc. in the coals, CCRs, soils, water, air, river sediments, agricultural plants, human body specimen samples from CTP's surrounding area employing different approaches and modes of advanced techniques such as gamma spectrometry with HPGe detector, ICP-OES, ICP-MS, (ED)XRF, AAS, INAA, optical and transmission microscopy, XRD, XPS, FTIR, etc. (Rabha et al. 2018; Saikia et al. 2015a, 2016, 2018; Kalia and Tang 2017; Dutta et al. 2017; Finkelman and Greb 2008; Saini et al. 2016; Ribeiro et al. 2010a, b, 2014, 2016; Oliveira et al. 2014; Weng et al. 2013; Tian et al. 2008, 2013; Dai et al. 2008, 2012; Silva et al. 2011a, b, 2012; Silva and DaBoit 2011; Huggins and Goodarzi 2009; Taylor et al. 1998 and the references therein). These approaches and techniques are commonly used around the world for environmental studies.

Previously several studies on the coals from five coal basins in terms of their palynological (Akhtar and Kosanke 2000), petrological, geological, sedimentological (Hossain et al. 2014, 2019; Bostick et al. 1991; Islam et al. 1992; Bakr et al. 1996; Islam 1998; Imam et al. 2002; Farhaduzzaman et al. 2012; Farhaduzzaman et al. 2013a, b; Islam and Hayashi 2008; Uddin et al. 2016), radiological, thermal and geochemical properties (Habib et al. 2019a; Islam et al. 2011; Haider et al. 2011; Podder et al. 2004) applying HPGe gamma spectrometry, EDXRF, PIXE, LIBS, and INAA techniques and CCRs characteristics and its potential uses (Howladar and Islam 2016) have been carried out. Besides, several studies on Barapukuria soils suggested that it was intensively contaminated with trace elements released from the coal matrix owing to the coal mining activities (Hossain et al. 2015, 2019; Zakir et al. 2013, 2017; Zakir and Arafat 2020; Bhuiyan et al. 2010b, b; Halim et al. 2015, Halim et al. 2013) employing EDXRF and AAS techniques for environmental studies.

The proximate and eventual analyses as along with the geochemical studies of coals from Bangladeshi coal basins along with the literature data are presented in Table 24.5. However, the abundances of these components depend on the coal types (Orem and Finkelman 2014). Integrated compositional analytical information of coals is useful for describing the coal quality which can predict the behavior of byproducts during incineration in the boiler. In Tables 24.5, 24.6, 24.7, 24.8, and 24.9, some basic characteristics of Bangladeshi coals and CCRs from BTPP are compared to those of coals and CCRs from different countries. Table 24.7 presents major oxides contained in coal, coal ash, coal combustion residues from Barapukuria, and other coal basins and CTPs. Elemental compositions of coals from Bangladesh are compared with coals from other countries data available in the literature are summarized in Table 24.8. The reported values for La, Hf, Th, Ta

Table 24.5 Major elemental components (in %) in Bangladeshi coal are compared to those of literature data

Basin	C	H	N	O	S
<i>Bangladesh</i>					
Barapukuria	83.16 (81.83–84.58)	5.1 (4.95–5.23)	1.63 (1.59–1.76)	9.52 (8.14–10.68)	0.64
Phulbari	78	4.8	1.7	15.5	
Dighipara	66.55 (49.80–77.0)	3.94 (3.13–4.57)	1.49 (0.91–1.83)	27.34 (16.30–45.72)	0.66 (0.32–1.14)
Khalaspir	70.28	4.61	1.51	7.63	0.77
Jamalgonj	79.0	5.4	1.81	12.5	0.65
<i>Literature data</i>					
Greece ^a	68.42	3.91	1.32	12.69	0.7
Turkey ^b	56.48–80.19	4.09–5.78	0.68–1.89	0.85–20.89	7.77–26.09
Indonesia ^c	59.36	3.96	0.97		

^aKoukouzas (2007), ^bBaba et al. (2010), ^cBelkin et al. (2009)

Table 24.6 Properties of Permian bituminous coals from Barapukuria, Bangladesh (Islam and Hayashi 2008; Bakr et al. 1996)

PS	SS	OS	TS	MM
0.24 (0.07–0.41)	0.02 (0.01–0.07)	0.23 (0.04–0.42)	0.59 (0.52–0.64)	10.3 (6.7–14.5)
pH	TOC	Vitrinite	Liptinite	Inertinite
4.7	63 (50–76)	35.6 (26.4–47.6)	6.41 (3.7–8.9)	57.99 (48.7–66.7)

All values are in percentage. Average and ranges are in parenthesis

PS pyritic sulfur; OS organic sulfur; SS sulfate sulfur; TS total sulfur; TOC total organic carbon; MM mineral matter

are 2–3 times higher and slightly higher for Sc, V, Cr, Co, Ga, Ce, Sm, Eu, and Yb compared to the world hard coal averages. It is also noticeable that REEs and radioactive elements concentrations are higher compared to those of Australia and Turkey coal (Table 24.8). Elemental concentration and distribution in FA from Bangladesh are 2–4 times higher for La, Sm, Ta, Hf, W, Ce, and Th in comparison with the world hard coal ash world coal average, while bottom ash is enriched with Mn, Hf, and Ta with 2–3 order of magnitude (Table 24.9). It is also noticeable that Sc, Mn, V, Cr, Co, Fe, Cs, Sb, Ba, La, Ce, Rb, Sm, Eu, Yb, and W are 2–12 times higher as compared to China fly ash concentrations, while Sc, Ga, Sb, Hf, Ta, W, Th 2–12 times higher than Indian fly ash (Table 24.9). It is clearly seen that ash residues are elevated in concentration in comparison with feed coal (Tables 24.8 and 24.9). Most of the reported elements possess a higher concentration in FA compared to those in BA, except for Mn, Fe, Hf, and Ni.

Table 24.7 Major chemical composition (as received basis; wt.%) in coal combustion residuals (CCRs) from Barapukuria coal-fueled power plant (BTTP) and comparison with other studies

	SiO ₂	Al ₂ O ₃	Fe ₂ O ₃	TiO ₂	CaO	MgO	Na ₂ O	K ₂ O	P ₂ O ₅	SO ₃	MnO	LOI
<i>Coal</i>												
Barapukuria	8.10	2.89	3.91	0.11	2.69	0.92	0.09	0.26	0.02		0.02	
China ^a	8.47	5.98	4.85	0.33	1.23	0.22	0.16	0.19	0.09		0.015	
<i>CCRs</i>												
Barapukuria	59.06– 74.24	19.23– 33.62	1.97– 2.67	2.75– 3.48	2.14– 3.31	0.39– 0.44	0.13– 0.14	0.42– 0.49	0.30– 0.93	0.41– 1.02	0.05– 0.32	
Khalaspir	55.82– 76.13	16.6–34.69	3.52– 4.21		1.61– 3.84	0.09– 0.26		0.42– 0.55		0.56– 0.93		
BTTP FA ^b	50.2	40.10	3.32	2.38	1.29	0.2	0.06	0.93	0.66	0.45	0.05	2
China FA ^c	40.72	48.78	2.2	2.24	2.58	0.19	0.04	0.56	0.11	0.00	0.018	1.89
China BA ^c	28.9	36.24	1.1	0.93	2.19	0.24	0.28	0.33	0.00	0.10	0.00	30.05
Indian FA ^d	38–63	27–44	3.3–6.4	0.4–1.8	0.2–8	0.01–0.5	0.07– 0.43	0.04–0.9	0.00	0.00	0.1–0.5	0.2– 3.4
EU FA ^e	28.5–59.6	17.6–35.6	2.6–16	0.5–2.6	0.5–27.3	0.6–3.8	0.1–1.2	0.4–4	0.1–1.7	0.1–8.6	0.03–0.1	1.1– 8.1
Brazil ^f	1.25	0.10	0.31	n.a	47.68	0.14	n.a	0.15	0.21	49.86	n.a	
Turkey ^f	2.57	0.66	0.27	n.a	40.33	0.53	n.a		n.a	54.51	n.a	

LOI loss on ignition; CCRs flyash (FA) and bottomash (BA) collectively; n.a not available

^aDai et al. (2014a, 2015), ^bHossain et al. (2015), ^cDai et al. (2014), ^dRam and Mastro (2010), ^eMoreno et al. (2005), ^fLi et al. (2012a), ^gShreya et al. (2015), ^hMedina et al. (2010), ⁱFu et al. (2016)

Table 24.8 Elemental compositions of coals from Bangladesh are compared with coals from other countries

Origin	Barapukuria, Bangladesh	India	China	Australia	Turkey	World	Indonesia	Canada	China	Australia
[Ref.]	[a]	[b]	[c]	[d]	[e]	[f]	[h]	[h]	[j]	[k]
Na (%)	0.0145				0.034				0.12	0.095
Al (%)	2.45								3.16	3
K (%)	0.1	0.03			0.063				0.16	0.0075
Sc	6.5			4.4	2.09	2.5	2.05–8.04		4.38	0.4
Ti (%)	0.29	0.14							0.2	0.04
V	38.18		35			36	13.3–73.0	8.7–18.0	35.1	3.5
Cr	24.26	20.9	70	15	5.95	86	1.19–25.5	4.5–13.3	15.4	2.2
Mn	48.12	0.47	100	116		101	3.92–253	52.5–256	116	21
Fe (%)	0.89	0.21			0.284				3.39	0.17
Co	4.32	73	11	7.1	5.79	5.2	1.33–4.77	1.7–3.7	7.08	0.6
Ni		5.03	45			17			13.7	
Cu		17.15	20			16			17.5	
Zn		13.3	40	41	23	40	4.85–21.2	14.6–64.5	41.4	3.5
Ga	8.15	5.6		6.6		3.2			6.55	
As	0.7	1.4		3.8	1.61	275	0.43–5.23	1.6–84	3.79	0.2
Rb	8.64	5.4		9.3		22				
Cd			1.3			18				
Sb	0.38			2	0.62	2			0.25	
Cs	1.22			1.1	0.29	29	0.23–0.55	0.29	0.84	0.1
Ba	117			159	67	300	38–189	41.3–615	159	63
La	23.7			23	6	4.3			22.5	1.3
Ce	41.06			46.7	15.28	8.1			46.7	10
Sm	3.13			4.1	1.79	0.6			4.07	0.3
Eu	0.55			0.87	0.27				0.84	0.06
Yb	1.44			2.12		1			2.08	0.2

Lu	0.22			0.38			0.2												0.38	0.03
Hf	3.55			3.7	1.37		1.2												3.71	0.3
Ta	0.84			0.62		1	0.3													0.1
W	1.52			1.1	1.35		0.99													0.5
Hg													0.1							
Pb		34.3	15				9					3							15.1	
Th	9.59			5.8	2.55	1.6	3.2		1.53–2.61					1.15–5.7					5.84	0.3
U	2.05			2.4	0.81	1.9	1.9		0.38–1.26	0.49				0.39–2.7						0.4

All the elemental abundances are in ppm otherwise specified

^aIslam et al. (2011), ^bPodder et al. (2004), ^cAverage Indian coal (Mukherjee et al. 1988, Saikia et al. 2009, Khandekar et al. 1999, Basu et al. 2009), ^dDai et al. (2012), ^eMeij and Te Winkel (2009), ^fKarayigit et al. (2018), ^gWorld hard coal, Ketris and Yudovich (2009), ^hLestiani et al. (2015), ⁱBelkin et al. (2009), ^jChen et al. (2011), ^kFardy et al. (1989)

Table 24.9 Elemental compositions of ash from Bangladesh are compared with ashes from other countries

Origin [Ref.]	Fly ash (FA)											Bottom ash (BA)	
	Bangladesh [a]	EU [b]	Turkey [b]	Croatia [c]	World [d]	USA [e]	Thailand [f]	Australia (SB) [g]	Australia (B) [g]	Bangladesh [a]	Croatia [c]	HCA [h]	
Na [%]	0.53-0.7							1.64	0.4	0.56-0.6			
Al [%]	10.46-17.27							10.9	12.7	12.4-14.4			
K [%]	0.5-0.62							0.57	1.3	0.41-0.46			
Sc [ppm]	36.6-49.9	-	13		25-50	4.2		12	19	32.3-33.9		24	
Ti [%]	1.13-1.64			0.11		0.61		0.48	0.64	0.097-1.54	0.068	0.53	
V [ppm]	189-218	154-514	285	747.1			2400	120	130	122.6-151.4	379.7	170	
Cr [ppm]	90.4-193.9	47-281	114	179.8	110-2900	115	500	96	50	128.6-137.1	106.3	120	
Mn [ppm]	489.5-628.5	-	361	40.2				870	630	1153-1535	30.5	430	
Fe [%]	3.98-11.86			1.9	43,626			9.7	3.1	7.12-8.98	1.5		
Co [ppm]	11.7-24.1	20-112	15	5.7	35-55	84	8000	224	16	6.99-14.2	3.8	37	
Ni [ppm]		49-377	77	104.1		56	2000				75.2		
Cu [ppm]		39-254	58	44.6		149	2500				53.3		
Zn [ppm]		70-924	167	50.3		5000	5000	600	110		68.5	170	
Ga [ppm]	55.2-76.3	-	24						35	11.5-19.4		36	
As [ppm]	3.82-9.57	22-162	79	24.7	25,689		500	80	5.1	0.46-0.61	5.8	46	
Rb [ppm]	43.3-55.8	22-202	77				100			25.7-33.1		110	
Cd [ppm]		43,471	4	1.5		0.5					0.4		
Sb [ppm]	1.93-5.15	1-120	2	3.1				2.2	3.4	0.63-0.92	3.9	7.5	
Cs [ppm]	5.26-8.33	-	21	1.6				6.3	4.8	4.68-5.2	0.3	8	

Ba	[ppm]	608.2–667.7	311–3134	605	32.4	1000–5000		10,000	2240	520	675.7–487.5	20.7	980
La	[ppm]	41.4–171.8		21.12			12		77	62	106–126.1		76
Ce	[ppm]	269.5–343		39.24		120–460	21		140	110	210–244.5		140
Sm	[ppm]	21.3–65.3		3.18			1.7		11	11	16.39–30.91		14
Eu	[ppm]	2.98–7.06		0.76			0.4		2.4	2.2	1.89–2.94		2.6
Yb	[ppm]	8.42–9.78		1.35			0.95		5.7	7.8	8.12–8.43		6.9
Lu	[ppm]	1.18–1.73		0.21			0.14		0.7	1.1	bd-1.19		1.3
Hf	[ppm]	21.7–48.5		4.1		43,626			5	12	18.8–23.1		9
Ta	[ppm]	5.63–7.4		1.9					1.2	1.5	4.51–4.81		2
W	[ppm]	29.14–35.05							3.5	5.5	11.9–14.3		7.8
Hg	[ppm]		<0.01–1.4	–				20					
Pb	[ppm]		40–175	54	16.1		43	1000				3	
Th	[ppm]	53.9–66.4	17–65	19		15–80			9.9	24	41.8–47		23 (93.38)
U	[ppm]	10.7–17	43,614	30	109.1	43,794			3.6	7.3	7.3–12.2	47.9	15 (185.25)

^aIslam et al. (2011), ^bEU (European Union: Moreno et al. 2005; Li et al. 2012a; Shreya et al. 2015; Medina et al. 2010; Ram and Mastro 2010), ^cMedunić et al. (2016), ^dAl-Areji et al. (2008), ^eUSA (Hower et al. 1999; Finkelman and Gross 1999; Gollakota et al. 2019), ^fPhoungthong and Techato (2018), ^{SB}: sub-bituminous; B: bituminous, ^gFardy et al. (1989), ^hHCA (hard coal ash); Ketris and Yudovich (2009)

24.4 Environmental Pollutants

In many developing and developed countries, coal is the major or significant source of energy for electricity generation, although some European countries have phased out their coal-based power plants considering the environmental and health-related issues. However, considering the increasing demand for energy and the enormous recoverable deposits of coal around the world invoke the continuity of coal-based power plant. Coal-based industrial activities have caused a number of radiological, ecological, socio-environmental, and economical risks and challenges including soil, sediment, water, air, and sound pollutions.

24.4.1 Inorganic Contaminants

Barapukuria coal mining operation has been done in a very thick seam under water-abundant aquifers. Therefore, the mine management has to take a number of precautions against some of the possible hazards which may be due to water inundation, fire, gas/dust explosion, roof fall/caving, emission of harmful gases, etc. Since the commencement of mine in June 1996, the mine has witnessed a severe water inrush in April 1998, which was finally dewatered in June 1998 by pumping. The risk of inundation of the mine is mainly from the UDT aquifer above the Seam VI, which is heavily water bearing with water flowing through the fissures and faults providing a direct make-up of water in Seam VI.

Environmental concerns regarding the potential pollution of natural resources (e.g., water, soil) owing to the water-soluble HMs in the ash pond leachate is of great significance. Usually CCRs are highly enriched in potentially toxic constituents, i.e., HMs, e.g., Pb, Cu, Se, Zn, As, Ni, Cr, Cd, etc. Several factors can be influential on the HM's mobility in an aqueous system, e.g., particle size, initial concentration of HMs, leaching time, solid-liquid ratio, extracted solution's pH, etc. (Izquierdo and Querol 2012; Saikia et al. 2016; Verma et al. 2015; Xiang et al. 2012; Baba et al. 2010; Ward et al. 2009). Under favorable geochemical conditions, a significant portion of these potentially toxic HMs can easily be leached out from the CCRs particles by the interaction with water compartments (e.g., pond water). The water-soluble HMs can pollute the soil and the aquatic system (including both surface and groundwater) (Shreya et al. 2015; Yilmaz 2015; Li et al. 2012a; Medina et al. 2010; Depoi et al. 2008; Moreno et al. 2005). Metal contaminants, e.g., Pb, V, Cd, Cr, and Ni are potentially hazardous to the environmental systems even at low concentrations (Yao et al. 2015). Some physicochemical properties (e.g., pH, water temperature, etc.) significantly govern the HM's leaching, for instance at pH < 5, HM's dispersion in the aquatic phase increase (Baba et al. 2010).

Environmental and ecological concerns regarding the potential pollution of natural resources (e.g., soil and water) owing to the occurrence of soluble HMs in ash pond leachate is of great significance. If the ash mound is unlined, a major

portion of ash leachate infiltrates from the sub-ground to the saturated layer. Rain water and slurry water are treated as the main leachates, which carry the CCRs to the groundwater (Haykiri-Acma et al. 2011; Izquierdo and Querol 2012). Toxicity characteristics leaching procedure (TCLP) extracts the targeted toxic elements from ash residues at different phases and pH conditions (Jegadeesan et al. 2008). The degree of leaching of the HMs in ash residues depends on pH (acidity-alkalinity) condition and temperature variations (Xiang et al. 2012; Zhang et al. 2016; Baba et al. 2010; Ward et al. 2009; Jegadeesan et al. 2008).

Pollutants are supposed to be liberated from the CCRs during the interaction with water. pH-dependent aquatic leachability, mobility, and transportation of HMs from CCRs are well-known mechanisms that are governed by dissolution and reprecipitation of iron with coprecipitation of associated trace metals. Some HMs (which form cations in solution) are more mobile at acidic pH whereas others (which form oxy-anions) more mobile at neutral or alkaline pH (Izquierdo and Querol 2012; Ward et al. 2009). However, most of the metals possess lower mobility at a relatively short period of water-ash interaction. A monotonic release trend of Pb, As, Mn, Cr, Cu, and K can be continued over a long-term leaching (~180 days) (Dutta et al. 2009; Silva et al. 2010) where the leaching characteristics of the elements are influenced by the oxides ratio (Ward et al. 2009; Izquierdo and Querol 2012).

Combustion of coal in thermal plant produces a large amounts of CCRs and these CCRs having toxic heavy metals including B, As, Hg are sometimes improperly disposed to the nearby large ash mounds (disposal site) (Querol et al. 1996a, b; Wang et al. 2008) from which toxic metals can migrate to the soil and groundwater. It has considerable environmental impacts by occupying large land areas, and releasing leachates and dusts to pollute the aquifers (Spadoni et al. 2014; Pandey et al. 2011; Sajwan et al. 2011). Toxic elements (including As, Cd, Cr, Cu, Ni, Zn, Se, Pb, etc.) are relatively enriched in FA (Tiwari et al. 2015; Oliveira et al. 2012; Silva et al. 2010; Izquierdo and Querol 2012; Saikia et al. 2006), which can pollute different environmental compartments. Disposal of unutilized FA in landfills/lagoons can contaminant (by HMs) soil by seepage, runoff from landfills, and discharge of rainwater into the soil regimes. HMs (from the FA disposal site) entered into the soil are primarily redistributed into a variety of chemical forms by slow and fast adsorption reactions, e.g., mineral precipitation and dissolution, biological (im)-mobilization, aqueous complexation, ion exchange, plant uptake, adsorption/desorption, etc. (Medunić et al. 2018; Čujić et al. 2015, 2016, 2017; Sultana et al. 2016; Rodriguez-Iruretagoiena et al. 2015; Noli and Tsamos 2016; Halim et al. 2013, 2015; Wuana and Okieimen 2011; Dragović et al. 2013; Bhuiyan et al. 2010b). Studies (Mandal and Sengupta 2006) on the layerwise distribution of HMs (e.g., Mo, Cr, Mn, Ni, Co, As, Pb, V, Cu, Zn, Be, etc.) in soil samples around the ash ponds showed that topsoils are enriched with HMs which are also enriched in the pond ash (Table 24.14). Mandal and Sengupta (2006) invoked that the enrichment of those HMs in the topsoils was originated from the CCRs disposal site, as there were no other sources of industrial effluents. Additionally, over some threshold level, some toxic HMs in FA might become more active and obstruct microbial activities (Izquierdo and Querol 2012; Adriano et al. 1980).

Mining, processing, and coal combustion in thermoelectric power plant are the significant sources of environmental (soil and water) contamination owing to the production of the huge volume of ash residues which are discharged off to the ash ponds (disposal site) in the proximity of power plants (Querol et al. 1996a, b). CCRs are highly enriched in contaminants that are highly mobilized from CCRs that could affect associated water. It is a matter of concern about a large volume of ash residuals generation and environment pollution on global scale (Huang et al. 2016b, 2017).

Hossain et al. (2015) mentioned that concentrations of SO_4^{2-} in surface water exceed the standard limit in and around the BTTP and elements (Ca, Mg, Zn, Cu, Fe, Pb) in the soil are greatly increased in the vicinity of the power station. Hossain et al. (2015) and Howladar et al. (2014) documented those the abundances of Mn and Fe are high in surface water and soil, As and Cd are slightly higher near the BTTP (Table 24.12). Lacking of proper treatment plant of Barapukuria, mine wastewater spread out thoroughly in the adjacent area of mine that degrade the soil quality. Sultana et al. (2016) demonstrated that overall BCM area is moderately contaminated with Cu, As, and Cd (Table 24.14). Ramya et al. (2013) mentioned that F^- concentration is rich in ash but its severity is low due to the elevated concentration of Ca^{2+} and SO_4^{2-} in water. Spadoni et al. (2014) showed that the groundwater exceeds the concentration limits for Mg^{2+} , Ca^{2+} , NO_3^- , SO_4^{2-} , TDS; and As, Mo, V, B, F concentrations are also relatively high in circulating water linking to the leaching ashes around the CTP (Table 24.12).

Mandal and Sengupta (2006) showed that the elevated abundances of Mn, Cu, Ni, Zn, Pb, and As in soil around the coal-based powerplants attributing to the input from ash disposal site (Table 24.14). According to Pavlov and Chudnenko (2015) water with enriching Ca^{2+} content percolates into the groundwater system from the ash pond. The impact of ash ponds on groundwater quality in the sub-watershed surrounding the disposal sites of CTPs were assessed in India where disposal of CCRs are one of the prime sources of soil and groundwater contamination (Ramya et al. 2013) and also documented that the SO_4^{2-} is one of the critical hazardous parameters polluting the groundwater due to ash ponds and found concentration is very high (>1 ppb) close to the ash pond and in the downstream direction and the quantity of F^- in drinking water exceeds the standard.

24.4.2 Radionuclides

Inherently, coals, coal combustion residuals (CCRs), and soils commonly possess naturally occurring radioactive materials (NORMs) including Th and U actinide series and their progenies, along with other radionuclide, e.g., ^{40}K (Habib et al. 2019a, b; Chen et al. 2011, 2017a, b; Orem and Finkelman 2014; Arbizov et al. 2011) (Table 24.14). The degree of gamma radiation is directly related to the radioactivity concentrations of NORMs (Siegel and Bryan 2014). Considering the abundances of NORMs (^{226}Ra , ^{232}Th , ^{238}U , and ^{40}K), the evaluation of radiological risks owing to the environmental radioactivity is more important compared to merely

studying the hazardous radioactive wastes (Dragović et al. 2008, 2013; Vuković et al. 1996). Thus, attaining the information of the level of activity concentrations of NORMs in coal and CCRs is essential (Pak et al. 2018; Lauer et al. 2017; Sajwan et al. 2011) for assessing the radiological health risks. The presence and enrichment of NORMs can modify the radiological characteristics of geomaterials and raise the degree of natural radiation background through ionizing radiations (α , β , γ -radiations) and simultaneous release of gaseous radon (^{222}Rn ; Amin et al. 2013).

The abundances of the majority of NORMs in CCRs are enriched by several orders of magnitude due to combustion by reducing the coal volume $\sim 85\%$ (Turhan et al. 2018; Hower et al. 2016; Basu et al. 2009). These are consistently disposed to the ash ponds (disposal site) with a high environmental risk as it is highly enriched in radiotoxic radionuclides and environmentally sensitive TEs (Querol et al. 2011; Bhangare et al. 2014). Pollutants are released from CTP in different form and stages of the processing system, i.e., before (coal storage, processing), during combustion (flue gas), and after combustion processes and CCRs deposition, transportation, and utilization to the ambient environments as in the form of the gaseous phase, solid, and liquid discharges (Dai et al. 2007, 2008, 2012, 2014a, b; Dragović et al. 2013; Mahur et al. 2013; Saikia et al. 2014, 2015a, b, 2016; Karamanis et al. 2009).

Some studies working on the NORMs contamination due to the coal-burning appeal for a trivial influence of radioactivity originated from CCRs on the soil environment (e.g., Habib et al. 2019b; Charro et al. 2013; Papaefthymiou et al. 2013; Charro and Pena 2013; Rosner et al. 1984), whereas other studies (e.g., Gören et al. 2017; Parial et al. 2016; Liu et al. 2015; Mandal and Sengupta 2006; Ćujić et al. 2015, 2016; Flues et al. 2002; Amin et al. 2013; Gür and Yaprak 2010; Lu et al. 2012a, b, 2013; Dai et al. 2007; Bem et al. 2002; Papp et al. 2002) have demonstrated that a significant augmentation of NORM's content in the soil around CTP, mostly owing to the higher abundance of ^{238}U and ^{226}Ra in feed coals and associated CCRs (Table 24.10). However, it is essential to determine the level of NORMs and associated impacts on the ambient environment and on human health around CTPs. Mishra (2004) reported that the ash ponds are the source of the highest radiation dose. Several studies on soil radionuclides found that the radioactivity in the soil is higher closer to the CTP within 1 km (Dai et al. 2007).

Along with the potentially toxic HMs, fly ash also contains radionuclides including ^{40}K , ^{210}Pb , ^{220}Rn , ^{222}Rn , ^{226}Ra , ^{228}Ra , ^{232}Th , ^{238}U , etc. (Ozden et al. 2018; Hower et al. 2016; Papaefthymiou et al. 2013; Sahu et al. 2014, 2017; Amin et al. 2013; Baeza et al. 2012; Papastefanou 2010; Mandal and Sengupta 2003, 2005) (Table 24.10). During the technogenic process(es) of coal combustion, NORMs are fractionated in gaseous and solid combustion products and are released to and accumulated in the surrounding environmental compartments (Noli et al. 2017; Barescut et al. 2011; Galhardi et al. 2017a, b; Tanic et al. 2016; Liu et al. 2012a, b, 2015; Charro et al. 2013; Ćujić et al. 2015, 2017; Campaner et al. 2018).

Habib et al. (2019b) demonstrated that the average radioactivity concentrations (in Bq kg^{-1}) in BTTPP's feed coals are 67 ± 24 , 42 ± 18 , 63 ± 26 , and 232 ± 227 for ^{238}U , ^{226}Ra , ^{232}Th and ^{40}K , respectively, while in CCRs, they are 206 ± 72 , 141 ± 28 , 202 ± 45 , and 233 ± 44 , respectively (Table 24.10). With an exception

Table 24.10 Radioactivity concentrations (in Bqkg⁻¹) in coal, ash, and surrounding soils of Barapukuria, Bangladesh are compared to those of literature data

	²²⁶ Ra	²³² Th	⁴⁰ K	References
<i>Coal</i>				
Barapukuria, Bangladesh	27.6	45.5	38.2	Habib et al. (2019a, b)
India	11–67	18–93	14–445	Mishra (2004)
India	16.8	19.5	37.2	Sahu et al. (2014)
China	33	37.5	105.7	Lu et al. (2012b)
Brazil	813–1251	22–40	200–450	Flues et al. (2002)
Nigeria	8.18	6.97	27.38	Kolo et al. (2016)
USA	7.4	6.3	27.0	Coles et al. (1978)
Turkey	11.12	123.01	14.55	Cevik et al. (2007)
Poland	13–29	8–21	43–181	Bem et al. (2002)
World	20	20	50	UNSCEAR (2010)
<i>Ash</i>				
Barapukuria, Bangladesh	175.4	263.7	277.8	Habib et al. (2019a, b)
India	40–152	96–178	148–840	Mishra (2004)
India	78.8	61.7	99.1	Sahu et al. (2014)
China	69.5	79.3	233	Lu et al. (2012a, b)
Brazil	1442–2718	43–95	471–1144	Flues et al. (2002)
Turkey	242	51	493	Cevik et al. (2007)
Poland	75–120	47–92	448–759	Bem et al. (2002)
USA	85.1	62.9	299.7	Coles et al. (1978)
World	240	70	265	UNSCEAR (2010)
<i>Soil</i>				
Barapukuria, Bangladesh	63.6	103.4	494.2	Habib et al. (2019a, b)
NW Bangladesh	91	151	1958	Hamid et al. (2002)
Critical levels in soil	370	2–40	810–925	Kabata-Pendias and Pendias (1984)
World average	35	30	400	UNSCEAR (2010)
Mawan, South China	204.0	265.0	1269.0	Liu et al. (2015)
Baqiao, China	36.1	51.1	733.9	Lu et al. (2012b)
Nasik, India	37.0		396.0	Mishra (2004)
Kapar, Malaysia	86.7	74.3	297.3	Amin et al. (2013)
Figueira, Brazil	133.0	39.0	233.0	Flues et al. (2002)
Lodz, Poland	16.6	15.7	306.7	Bem et al. (2002)
Ajka, Hungary	129.0	26.9	337.0	Papp et al. (2002)
Afsin-Elbistan, Turkey	33.0	36.0	379.0	Cevik et al. (2007)
Megalopolis, Greece	45.0	32.5	337.0	Papaefthymiou et al. (2013)
Velilla, Spain	38.7	42.9	445.3	Charro et al. (2013)

NW North-West

of ^{40}K , all the studied NORMs are 3.10 to 3.37 times higher in CCRs compared to those in feed coals. Elevated concentrations of NORMs in the CCRs can be a potential source of radioactivity in the surrounding environments of BTPP which can be further revealed by the higher radioactivity in the soil around the BTPP. Although, the mean activity concentrations ($\text{Bq}\cdot\text{kg}^{-1}$) of ^{238}U , ^{226}Ra , ^{232}Th and ^{40}K in soil specimens collected from and around the BTPP are 103 ± 41 , 64 ± 7 , 103 ± 14 , and 494 ± 108 , respectively (Table 24.10) (Habib et al. 2019b) which are relatively higher compared to those in the world mean value (UNSCEAR 2010) but the X-ray diffractometer and microscopic studies invoke that the elevated levels of radioactivities are mostly governed by the occurrence of monazite, zircon, kaolinite, Illite, and rutile minerals in the soil specimens compared to that of technogenic contributions from the BTPP (Habib et al. 2019b).

24.4.3 Organic Pollutants

Other than inorganic pollutants, organic pollutants, i.e., POPs, for instance, PAHs and formaldehyde are also a major environmental concern due to their persistence, carcinogenicity, and mutagenicity (Callén et al. 2011; Ouyang et al. 2018; Khillare et al. 2012; Sahu et al. 2009; Liu et al. 2008, 2012a, b; Abdel-Shafy and Mansour 2016). There are trace levels of PAHs present in the FA, usually upto 25 mg kg^{-1} (Medunić et al. 2016). Due to the low solubility, the leachate from CCRs contains very low abundances of PAHs (Stalikas et al. 1997). However, some research (Liu et al. 2008; Bragato et al. 2012) found that coal combustion is one of the most significant sources of environmental PAHs. Emissions of organic pollutants are mostly the consequence of incomplete combustion of coal fuels and are a function of many variables, such as combustion method, the frequency, and duration of stove uses, fuel type, and air supply conditions (Wang et al. 2010; Verma et al. 2015). Anthracene and methylanthracene are more abundant in Barapukuria coals (Hossain et al. 2014). Hossain and Hossain (2019) demonstrated that the presence and distribution of PAHs in finer coal fractions from BCM. Abundances of pyrene (Pyr), benzo[a]pyrene (BaP), fluoranthene (Flu), benzo[b,j,k]fluoranthene (Bflas), and benzo[e]pyrene (BeP) were relatively high, followed by benzo[g,h,i]perylene (BghiP), phenanthrene (Phe), coronene (Cor), and indeno[1,2,3-cd]pyrene (InP). Mean abundances of carcinogenic PAHs in BCM finer coal portions follow the order as $\text{Bflas} > \text{BeP} > \text{BaP} > \text{BghiP} > \text{InP} > \text{Cor}$. The values of $\text{BeP}/(\text{BeP} + \text{BaP})$ vary from 0.61 to 0.85 (mean: 0.74) which indicates the decay of BaP owing to the prolonged exposure to the solar radiation. Elevated concentrations of land plant markers including retene (Ret) and Phe, and the ratio of BaP/BghiP ($\sim 0.10\text{--}6.16$, mean: 1.89) indicate that organic matter in the BCM area was derived from characteristic botanical origins. Furthermore, the presence of more middle- and higher molecular weight PAHs over lower molecular weight PAHs in most coal fractions from BCM indicates higher toxicity with adverse consequences on human health. Health risk evaluation factors (BaP_{eq}) vary from 0.55 to $6.51 \text{ ng}\cdot\text{g}^{-1}$ implies the

moderate to high health risk from the carcinogenic PAHs in the ambient atmosphere. Calculated incremental lifetime cancer risk (ILCR) values for children (5.56×10^{-6} – 1.12×10^{-6}) and adults (9.96×10^{-5} – 1.27×10^{-4}) were found to be greater than/equal to the range of 1.0×10^{-6} – 1.0×10^{-4} (Hossain and Hossain 2019). Pyrene (Py), fluoranthene (Fla), benzo[b]k]fluoranthene (Bfla) and benzo[e] pyrene (BePy) are abundant PAHs in the coal shales, and the ratios of low Fla./Py, benzo[a]anthracene (BaAn)/228 and indeno[1,2,3-cd]pyrene/(indeno[1,2,3-cd]pyrene + benzo[ghi]perylene) (InPy/(InPy + BghiP)) suggest that these 4–6-ring PAHs were mostly originated from small-to-medium scale wildfires during dry season. The occurrence of higher combustion-derived PAHs, for instance, Py, Fla, Bfla, and BePy in the Gondwana succession implies small-medium scale forest-fires with uneven intensity (Hossain et al. 2019).

24.4.4 Air Particulate Matters

It is obligatory for the coal mines to monitor particulate matter of 10 μm in diameter or less dust particle (PM_{10}) emitted to the ambient atmosphere (Kollipara et al. 2014; Jelic et al. 2017). Technogenic processes like crushing or grinding operations during coal mining produce dust particles which can cause health concern as they can be inhaled into and accumulated in the respiratory organs. Coal-fired power plants emit gaseous (dominate) and solid-phase (subordinate) pollutants which can move through the air and can repeatedly be deposited and re-emitted into the atmosphere (Saini et al. 2016; Suhana and Rashid 2016; Gao et al. 2016; Khan et al. 2014; Din et al. 2013; Tian et al. 2016; Higginbotham et al. 2010; Querol et al. 1996a, b). These gaseous and particulate matters (PMs) released to the air as flu-gas by the stack/chimney and some of it settle down and precipitated on rivers, lakes, and ground surface by rain and surface runoff (Gao et al. 2015, 2016; Callén et al. 2011; Wang et al. 2016a; Pandey et al. 2014;). Pollutants are released from different stages of the process and sources during the operation of the power plant, i.e., before (coal storage), during combustion (flue gas), and after combustion processes (ash pond or disposal site) (Huang et al. 2016a; Zhang et al. 2015; Medunić et al. 2016; Kurth et al. 2015; Lestiani et al. 2015; Li et al. 2012b). Kollipara et al. (2014) demonstrated that suspended particulate matter (SPM) released from the burning of coals in the power plant impacts on health. However, monitoring cannot sufficiently determine the more risky very fine dust particles that are $<2.5 \mu\text{m}$ in diameter ($\text{PM}_{2.5}$) released from coal combustion in power plants. $\text{PM}_{2.5}$ can penetrate deep into the lungs and then into the blood-stream. Fine PM and TEs emissions from coal-burning power plants are affiliated with considerable negative effects on water and air quality, and human and animal health as well as on soil and sediment health impairment (Raja et al. 2015). Some air particulate contaminants escape into the air and some find their way into the soil through deposition and subsequent infiltration and some nearby pond/stream/river/channels through surface runoff. Infiltration of pollutants occurs into the soil/sub-ground on the geological setting system, depending on its lithology,

porosity, and permeability. Moreover, it takes part in the geochemical processes and reaches the water table and subsequently, it goes to the aquifer through geological, hydrogeochemical, and hydrogeological processes and lastly mixing to the groundwater flow. If there is no aquiclude (impermeable layer like clay) beneath the surface in and around the power plant area, it might be easy for pollutants to rapidly penetrate the aquifer system through the soil. Additionally, the small particulates of TEs those liberate from the waste (e.g., ash disposal site), are circulated by the wind, landing on the soil and in the beds of water courses and slowly integrating the tissues of aquatic living organisms, such as fish.

24.5 Impacts of Coal Mining and CTP Activities

24.5.1 Environmental Impacts

24.5.1.1 Impacts on Water Resources

Unplanned release of the mine water can be toxic depending on the soil condition of the mine and can damage aquatic life (Yucel et al. 2016). As a consequence of mining operation, exposure to the acids originated from specific types of ore, mostly sulfuric acid to water and air, water generally ends up being polluted by the acid drainage and in turn reacts with other exposed minerals. Contamination from self-perpetuated dumping of acidic and toxic material can go on for hundreds of years. Mine water from Barapukuria Coal mine is discharged to the surrounding paddy fields and water courses without any treatment (Habib et al. 2020; Howladar et al. 2014; Howladar and Hasan 2014; Hossain et al. 2019, 2015; Sahoo et al. 2016; Howladar 2013, 2017; Halim et al. 2013, 2015; Bhuiyan et al. 2010b). Discharge of untreated mine water containing pyrite (FeS_2), chalcopyrite (CuFeS_2), sphalerite ($(\text{Zn}, \text{Fe})\text{S}$) and other common sulfide minerals in coal seams which form sulfuric acid threatened the environment as the water might be acidic which would ultimately contaminate the surface water and soil (Sultana et al. 2016; Zakir et al. 2013, 2017; Khan et al. 2017a, b) (Table 24.14). It may also contain a lot of dissolved HMs like Fe, Mn, some oil, suspended solids, and NH_3 resulting from the use of NH_4NO_3 based explosives. High abundances of contaminants can cause considerable ecological risks, as botanical species are very much sensitive to SO_2 even at a low abundance.

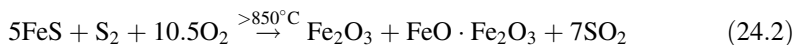
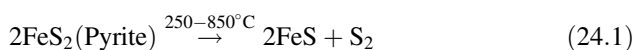
Barapukuria coals are normally banded and fractured which are filled with secondary calcite and pyrite with other unidentified minerals (Farhaduzzaman et al. 2012; Islam and Hayashi 2008) (Table 24.6). Pyrite mineral in feed coal is possibly the most interesting, important, and environmentally sensitive mineral in the run for exploitation and beneficiation of fuel coals and their produced wastes because of its tendency to oxidize during combustion, weathering, and produce acidity (Saikia et al. 2016, 2018; Kim and Chon 2001; Akcil and Koldas 2006; Spears et al. 1999; Sahoo et al. 2014; Silva et al. 2011b). Iron sulfide minerals,

especially pyrite (FeS_2) and pyrrhotite $\text{Fe}_{(1.0-0.8)}\text{S}$, govern dominantly in generating the acid mining drainage (AMD) (Pinetown et al. 2007; Silva et al. 2013; Vass et al. 2019; Valente et al. 2015; Jain et al. 2016a, b; Campaner et al. 2014). Bakr et al. (1996) reported that pyrite S, sulfate S, organic S, and total S contents are 0.24 (0.07–0.41)%, 0.02(0.01–0.07)%, 0.23 (0.04–0.42)% and 0.59 (0.52–0.64)%, respectively and fluorine (F) content is about 6.4 to 408 ppm in the Barapukuria coal (Bakr et al. 1996).

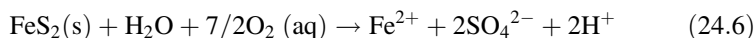
The presence of high S in feed coals could cause environmental deterioration including AMD (Spears et al. 1993; Sahoo et al. 2010, 2014; Silva et al. 2011a, b, 2013; Saikia et al. 2016; Dutta et al. 2017, 2019; Equeenuddin et al. 2010) which may cause contamination of soils, sediment, water as well as vegetation (Bhuiyan et al. 2010b; Galhardi and Bonotto 2016; Huang et al. 2016b). It is unsafe for the environment and crops as well. Higher occurrence of iron may form pyrites (along with S) which would eventually cause environmental hazards (Hower et al. 2008; Kolker 2012).

The presence of these kinds of pyrite, utilizing the coal most frequently causes acid rain (Kulshrestha 2013). It may also cause AMD, which could influence the background pH conditions of the soil, sediment, and water resources and effects on the ecosystem (Silva et al. 2011a, b, 2013; Sahoo et al. 2010, 2014; Galhardi and Bonotto 2016; Equeenuddin et al. 2010; Saikia et al. 2016; Bhuiyan et al. 2010b). Though, SO_2 is common but volumetrically minor constituent in coal. Health effects caused by exposure to its higher level include breathing and respiratory problems, deteriorate the lung's defense, and aggravating cardiovascular and respiratory diseases (Swaine 1990; Hower et al. 2008; Finkelman et al. 2018; Verma et al. 2015).

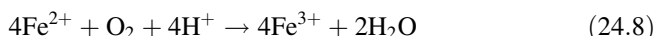
Pyrite in feed coals transformation and consequent releasing of S and SO_2 to the ambient atmosphere and aquatic system during combustion processes involve the following equations (Eqs. 24.1–24.5) (Demir et al. 2001; Koukouzas et al. 2006; Silva et al. 2011a; Jain et al. 2016a, b):



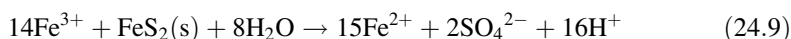
Pyrite (FeS_2) (which may form acid leachates) in coals can be dissolved into water. It may release soluble metal ions to solution as it contains hazardous TEs (Pb, As, Co, Cd, Cu, Mn, Sb, and Zn) as impurities (Jain et al. 2016a, b) and be transported into natural water sources (Silva et al. 2011a, 2013; Saikia et al. 2016; Sahoo et al. 2014; Bhuiyan et al. 2010b). Weathering of Pyrite liberates soluble ferrous iron (Fe^{2+}) and acidity (Eqs. 24.6–24.8) which can also modify the pH condition of water, sediment, and soil.



The ferrous ion can then further be oxidized to ferric iron:

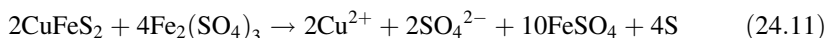
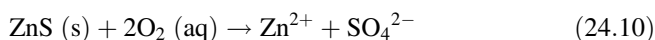


For pH values above 4, this abiotic reaction might be empowered by several types of naturally occurring bacteria in sulfide ore (Singh et al. 2013). But at low pH (<4), this abiotic oxidation of Fe^{2+} is slowed down though this microorganism-mediated oxidation possesses an important role in AMD formation (Jain et al. 2016a, b; Silva et al. 2011a, b, 2013; Spears et al. 1993; Sahoo et al. 2010, 2014; Dutta et al. 2017; Equeenuddin et al. 2010; Saikia et al. 2016). In contact with pyrite, Fe^{3+} can bring pyrites in aquatic solution to create more acid:



As an oxidizing agent, Fe^{3+} reacts with pyrite which produces Fe^{2+} (Eq. 24.9) and biological oxidation (Eq. 24.8) of Fe^{2+} brings back Fe^{3+} ion and thus a self-sustaining cyclic process being formed. The regeneration of Fe^{3+} is the key to the cyclic process (Equeenuddin et al. 2010; Sahoo et al. 2010, 2014; Silva et al. 2011a, b, 2013; Spears et al. 1993; Jain et al. 2016a, b; Dutta et al. 2017; Saikia et al. 2016). If such reaction continuously increases the acidity of the solution, more Fe^{3+} tends to be dissolved which enhance the pyrite's oxidation. The consequential increase in acidity, other metals naturally occurred in coal or in ore, including Ni, Cu, Zn, and Pb will readily be dissolved and released to the environment from coal matrix.

Metal sulfides other than pyrite may not essentially increase the acidity but may liberate soluble metal ions to the solution (Howladar et al. 2017; Bhuiyan et al. 2010b; Hower et al. 2008; Kolker 2012; Jain et al. 2016a, b; Gammons et al. 2010). For example, sphalerite (ZnS) and chalcopyrite (CuFeS_2) may release Zn and Cu, respectively, into the environment by oxidization through the reaction (Eqs. 24.6–24.9) below.

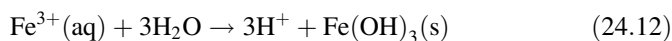


Heavy and toxic metals (for instance, Pb, Cd, Hg, Ni, etc.) which are partitioned into the sulfides can also be released into the surface and groundwater following the abovementioned equations. The solubility of Fe^{3+} depends on pH, and thus the propagation of AMD as well. At pH higher than 3, Fe^{3+} can precipitate out of solution as $\text{Fe}(\text{OH})_3$ in the form of a yellow, orange, or red deposit (known as yellow boy) in streams (Jain et al. 2016a, b):

Table 24.11 Water percolation from different coal faces and record of high water temperature in the underground roadways in BCM as of 2011

Longwall face	Quantity of water inflow from the face ($\text{m}^3 \cdot \text{h}^{-1}$)			Water temperature ($^{\circ}\text{C}$)	Relative humidity (%)	Possible cause of water inflow
	Initial	Closing	Present			
1111	305	525	525	42–45	97	Fault, fissure, fractured floor sandstone and coal seam
1109	86	549	199	47–51	96	
1104	108	121	62	33–37	97	
1112	10	63	65	41	95	

Quality of mine environment of BCM (Kabir and Imam 2013)



Integrated interactions among physical, biological, geochemical, and hydrological factors can affect the AMD potential and its generation and/or propagation rate. Owing to the small particle size and high surface area, waste rock piles and tailings possess higher potential for the AMD. However, the availability of both oxygen and water which are essential for AMD formation indicates that local weather and hydrology play a significant role in AMD generation.

Owing to the varying reaction rates and oxidation products, different sulfide minerals possess varying potentials for AMD. Minerals like pyrite, marcasite, and pyrrhotite are very reactive and oxidation of these sulfide minerals result in highly acidic water (Jain et al. 2016a, b; Pinetown et al. 2007; Campaner et al. 2014; Valente et al. 2015; Silva et al. 2013; Vass et al. 2019). Other minerals, e.g., covellite (CuS), galena (PbS), and millerite (NiS) are less reactive due to the absence of iron release during oxidation process(es), thermodynamically stable crystal structures as well as their encapsulation by less-soluble minerals (Jain et al. 2016a, b). On the other hand, cinnabar (HgS) is the least reactive and generally does not produce acidic waters (Jain et al. 2016a, b).

The water requirement for a CTP is $\sim 0.005\text{--}0.18 \text{ m}^3 \cdot \text{kWh}^{-1}$. In CTPs, the water necessity has marginally been reduced from ~ 0.18 to $0.15 \text{ m}^3 \cdot \text{kWh}^{-1}$, due to the setting up of treatment facilities for the ash pond decants. However, water necessity ($0.15 \text{ m}^3/\text{kWh} = 150 \text{ L}$) per Unit of electricity generation is still very high compared to that of domestic water requirements for a mega-city. Water percolation from different coal faces and record of high water temperature and relative humidity in the underground roadways in BCM are tabulated in Table 24.11. It reflects that mine water temperature and relative humidity of mine environment are higher than the natural environmental condition from Barapukuria. It is not suitable and healthy for aquatic lives as well as occupational mine workers. Ash pond decant includes toxic HMs (e.g., Hg, As, B) which possess a tendency of leaching out over a time-duration, can pollute the ground and surface water. At Ramagundam and Chandrapur CTPs seepage of ash pond, decants were observed to a small natural-channel which was harmful to fisheries and other aquatic biota (Jain et al. 2016a, b).

In Table 24.12, anion concentrations (SO_4^{2-} , NO_3^- , HCO_3^- , CO_3^{2-} , Cl^- and F^-), elemental abundances (Na, Mg, Ca, K, Fe, Cu, Mn, Cd, Zn, As and Pb) and

Table 24.12 Anion concentrations (in mg.L⁻¹), heavy metal abundances (in mg.L⁻¹), and physicochemical parameters of water samples around Barapukuria are compared to those literature data

	SO ₄ ²⁻	NO ₃ ⁻	HCO ₃ ⁻	Cl ⁻	F ⁻
<i>Barapukuria</i>					
SW ^a	2.4	0.4			
SW ^b	3.1	1.6			
SW ^c	2.481	1.05	120.43	11.31	
SW ^d					11.85
SW ^e					
SW ^f	22.69		128.1	25.24	
SW ^g					
GW ^h					
EU (DW) ⁱ	250	50		250	1.5
DW ^j	400	10	600	150–600	1
For wastewater ^j					
Max. desirable ^k	200	–	200	250	0.6–0.9
Highest permissible ^k	600	50	600	600	1.5
EU ^l					
USA ^m	500	10		250	4
Acceptable limit ⁿ	200	45	200	250	1
Highest permissible ⁿ	400	100	600	1000	1.5
Desirable limit ^k	200–400	50	200	200–600	1.0–1.5
China ^o	–				
India (SW) ^p	570	7	411	0.71	99
Barakar, India (MW) ^q	327.2	3.8	214.8	37.8	1.01
Raniganj, India (MW) ^q	67.4	5.7	420.8	65.7	0.76
Greece (PEW) ^r					

(continued)

Table 24.12 (continued)

	Ca	Mg	Na	K	Fe	Mn	Cd	Cu	As	Pb	Zn
<i>Barapukuria</i>											
SW ^a					0.45	0.19					
SW ^b					0.61	0.26					
SW ^c	26.82	17.79	17.35	5.35	0.45		0.05		0.0015		0.001
SW ^d			38.7	3.1	0.16		0.21		0.07	0.58	7.4
SW ^e				1.28	0.11	0.004	0.007	0.0004	0.004	0.027	7.48
SW ^f	30.8	12.8	21.8	8.2	0.97	0.78		0.07			0.07
SW ^g				2.1			0.01			0.09	7.52
GW ^h					1.58	1.18	0.00802			0.06802	0.33909
EU (DW) ⁱ			200		0.2	0.05	0.005	2	0.01	0.01	5
DW ^j	75	30–35	200	12	0.3–1.0	0.1	0.005	1	0.05	0.05	5
For wastewater ^l											
Max. desirable ^k	75	30	50	12	0.3	0.1	0.003	2	0.01	0.01	3.0
Highest permissible ^k	200	150	200	200	1	0.5					3
EU ^l	400	60	900		5	0.2	0.2	0.2	0.1	5	2
USA ^m					0.3	0.05	0.005	1.3	0.01	0.015	5
Acceptable limit ⁿ	75	30			0.3	0.1	n.r.	0.05	0.01	0.01	5
Highest permissible ⁿ	200	100			1	0.3	n.r.	1.5			15
China ^o						0.001	0.005	1	0.05		0.5
India (SW) ^p	81	307	19			0.00001–0.0033	bdl-0.06	bdl-0.00009		bdl-0.46	0.011–2.05
Barakar, India (MW) ^q	86.8	82.4	32	7.3							
Raniganj, India (MW) ^q	19.3	26.2	1535	4.2							
Greece (PEW) ^r				68.8	2.7		3.6		1	11.1	8.3

	pH	Temp. [°C]	Turbidity [NTU]	EC [$\mu\text{S cm}^{-1}$]	TSS	TDS	COD	BOD	DO	TH
<i>Barapukuria</i>										
SW ^a	7.2			342						
SW ^b	7.4			388						
SW ^c	8.37		31.74	213.07		149.03				44.6
SW ^d	7.4	35.2	273.2			247.2	18	11.3		
SW ^e	7.48									
SW ^f	7.16			304.3		445.1			1.7	129.4
SW ^g	7.52	25	360		198	273		8		
GW ^h	6.44			203.07		108.04				
EU (DW) ⁱ	6.5–9.5			2500						
DW ^j	6.5–8.5	20–30	10	1000		2000	8	0.2		200–500
Wastewater ^d	6.5–9.2	40–45		1200		2100	200	50		330
Max. desirable ^k	6.5–8.5			750		500	10	6		100
Highest permissible ^k	6.5–9.2			1500		1500				500
USA ^m				2500				5		
Acceptable limit ⁿ	6.5–8.5		1			500				300
Highest permissible ⁿ	8.5–9.2		10			2000				600
China ^o	5.5–8.5					43,467	0.2	0.08		
India (SW) ^p	7.4		1.4			1743				246
Barakar, India (MW) ^q	8			887		803				556
Raniganj, India (MW) ^q	8			949		790				156
Greece (PEW) ^r	8.3	24.6	996		847					

Units of all the measured parameters (except for pH) are in $\text{mg}\cdot\text{L}^{-1}$ otherwise specified
 SW surface water; GW groundwater; DW drinking water; MW mine water; PEW plant effluent water; n.r. no relaxation; EC electrical conductivity; TSS total suspended solids; TDS total dissolved solids; COD chemical oxygen demand; BOD biological oxygen demand; DO dissolved oxygen; TH total hardness (as HCO_3); *bdl* below detection limit; ^aHossain et al. (2015); ^bHowladar et al. (2017); ^cHowladar et al. (2014); ^dBhuiyan et al. (2010a); ^eHalim et al. (2013); ^fZakir et al. (2016); ^gFardushe et al. (2016); ^hHabib et al. (2020); ⁱEU (1998); ^jECR (1997); ^kWHO (2011) and BIS (2012); ^lFAO (2011); ^mUS EPA (2012); ⁿBIS (2012); ^oChabukdhara and Singh (2016); ^pSpadoni et al. (2014); ^qSingh et al. (2010); ^rKaramanis et al. (2009)

physicochemical parameters (pH, temperature, chemical oxygen demand, total dissolved solids, electrical conductivity, turbidity, total suspended solids, biological oxygen demand, dissolve oxygen and total hardness) of BTTP are compared to those of internationally recognized limit values as well as those of water samples from different CTPs in the world. The average abundances of HMs (e.g., Ni, Fe, Mn, Cr, Cd, and Pb) surpassed the recommended limits for drinking water quality prescribed by the WHO, DoE (Bangladesh) and BIS standards, except for Co, Cu, and Zn at several areas which implies anthropogenic contribution to the ground-water. Out of the reported TEs namely Cu, Zn, Cd, and Pb seem to be derived mainly from anthropogenic activities, whereas other metals are originated from geogenic/natural source(s), i.e., water–rock interaction (Habib et al. 2020). Elevated abundances of Fe, Mn, Cd, and Pb in groundwater are mainly owing to the rapid infiltration followed by accumulation of highly toxic mine water in the aquifer (Habib et al. 2020). Bicarbonate is the most dominant anion in the surface water as well as in the groundwater (Halim et al. 2013; Hossain et al. 2015; Zakir et al. 2013; Howladar et al. 2014, 2017; Bhuiyan et al. 2010b; Habib et al. 2020; Fardushe et al. 2016), although HCO_3^- contents are lower than the maximum recommendation limit ($200 \text{ mg}\cdot\text{L}^{-1}$), highest permissible limit ($600 \text{ mg}\cdot\text{L}^{-1}$) and acceptable limits (WHO 2011; BIS 2012) for water bodies.

24.5.2 Impacts on Air Quality and Ambient Atmosphere

Air quality impacts from coal industrial activities depend on several aspects including development and construction of surface facilities, ventilation and shaft or drift access development, removing topsoil along with vegetation for mine development, blasting and drilling, removing or replacing overburden, transporting and dumping coal/ore, crushing (coal, ore and other materials), screening, washery options, beneficiation of material, general materials handling, transporting and placing washery rejects, workshop and power plant operations, wind erosion from open pit, rehabilitation, rail transport, and ship loading activities/sources (Saini et al. 2016). Air pollutants sources are storage (of dust, volatile organic compounds-VOC's), waste storage from CTPs stack emissions (NO_x , SO_x , CO_2 , dust, F, TEs, radioactive components, VOCs) (Callén et al. 2011; Agrawal and Agrawal 1989; Din et al. 2013; Gao et al. 2016; Saini et al. 2016; Khan et al. 2014). The major anthropogenic sources of SO_2 emissions are the combustion of sulfur-rich coals and heating oils in thermoelectric power plants, followed by metal smelting and industrial boilers.

During coal combustion, a huge complex mixture of several components, e.g., toxic gases and Particulate matter (PM) (the smallest respirable particles mostly soot) are emitted. PM is concentrated on and coated with a mixture of several toxic and hazardous substances, e.g., TEs and PAHs (Liu et al. 2008, 2012a, b). It is reported that the airborne ultrafine particulates and nanominerals are responsible for the generation of tumor cells due to the particles overload in the lung clearance system

(Saikia et al. 2015a, b, 2016; Martinello et al. 2014; Ribeiro et al. 2010b, 2013; Sehn et al. 2016; Oliveira et al. 2014; Rabha et al. 2018; Silva et al. 2011a, b, 2012). Finer particulates in emitting materials from chimneys/stacks are considered to be more hazardous as they persist in the atmosphere for a longer period and travel a long distance with wind and spread further. Moreover, it may enter into deeper portions of the lungs and stick therein, and its removal/excretion can take a longer time, months, or even years (Finkelman et al. 2002; Sambandam et al. 2014).

Only a very little works have been carried out so far regarding air pollution around the BTTP. However, reviewing previous related literatures can draw an assumable air pollution scenario. In the study of Agrawal and Agrawal (1989) on vegetation around Obra CTP in Mirzapur district of Uttar Pradesh, India, contingent liabilities of power plants to the contaminants in terms of the foliar injury symptoms and changes in ascorbic acid, chlorophyll, and sulfur content of the vegetables were observed. These changes were positively correlated with ambient SO_x and SPM contents and the amount of dust settled on leaf surfaces. The SPM and SO_x concentrations were significantly high in the immediate environs of CTP. Emitted SPM from CTPs spread over 25 km radius of land and cause respiratory and related ailments to human beings and animal kingdom (Masud et al. 2014; Chabukdhara and Singh 2016). Accumulation of SPMs on the leaves can affect photosynthesis (Rizwan et al. 2013; Guttikunda and Jawahar 2014). Diffusion of contaminants inside the plant's physiology throughout the leaves and branches can imbalance the major and micro nutrients in the plants which can affect the plant's growth (Kujawski 2011; Sharma et al. 2018). However, in a lichen diversity evaluation performed around a CTP by Bajpai et al. (2010) demonstrated an augmented effect on lichen abundances.

CTP's inputs on the atmospheric electrical parameters not only cause health and environmental problems but also pose substantial adverse effects on local weather, point discharge current, the surface atmospheric electric-field and the wind in the surrounding environs of CTPs (Manohar et al. 1989).

A coal mine associated with long-term coal fire (e.g., JCF: Jharia coalfield in India) can inadvertently discharge a huge amount of greenhouse gases (Table 24.13) like CO_2 , CH_4 , oxides of nitrogen, etc. (Saini et al. 2016). Harmful gases (e.g., CO_2 and CH_4) emissions in the interior air of the coal mine in Barapukuria are appeared in Table 24.13. Quantification of greenhouse gases released in a year gives an insight into the impact they may pose on the global climate. Andrup-Henriksen (2007) reported a conservative greenhouse gases emission estimate of three potent greenhouse gases (namely CO , CO_2 and CH_4) at about $108 \text{ kg}\cdot\text{year}^{-1}$ for JCF.

24.5.3 Land Subsidence and Potential Soil Pollution

To install hydroelectric, gas, and coal-based power plants of a unit megawatt of capacity, the land requirements are 6.6, 0.26, and 0.1–4.7 hector, respectively (Pokale 2012). Gas-based power plant can be established in any suitable place

Table 24.13 Interior air sample analysis results at return junction and air return of different longwall panels in BCM

Longwall panel	Date/month	Tail gate junction closed to the face		Air return (tail gate)	
		CO (ppm)	CH ₄ (%)	CO (ppm)	CH ₄ (%)
1116	01–10 Jan, 2012	10–60	0.06–0.14	0–5	0.04–0.08
1111	14–24 Sep, 2011	30–80	0.24–0.34	5–7	0.02–0.04
1112	06–17 Apr, 2011	5–120	0.08–0.90	4–80	0.04–0.50
1108	04–15 Nov, 2010	5–180	0.06–1.34	5–20	0.04–0.14
1105	20–30 Mar, 2010	7–130	0.04–0.46	5–40	0.04–0.28

Harmful CO, CO₂, CH₄ emission in the interior air of the coal mine at Barapukuria (Quamruzzaman et al. 2014)

where the gas-pipeline can be taken economically. Land requirements for hydro-electric power plants are generally hilly landscape or valleys. However, the coal-fired power plants are generally near the area of the coal mines. Along with the land requirements for coal mining and power plants, relatively a large land area is required for discarding the CCRs, e.g., 2616 ha., 321 ha. and 74 ha. of lands were used to discharge FA from coal-fired power plants at Chandrapur, Ramagundam and Gandhinagar, respectively (Agrawal and Agrawal 1989). Thus considering the coal mining, power plant installation, and establishment of disposal site a large area is involved for a coal-fired thermoelectric power plant which can alter the natural soil properties, e.g., increased soil alkalinity due to the alkaline FA. Moreover, dispersion and atmospheric precipitation of SPM on soil disturb the soil-strata, thus farming and forest land turn less productive (Chaudhuri 1992).

The disposal of CCRs may cause contamination risks to soil, sediment, water, crops, and plants owing to the enriched levels of TEs (e.g., As, Cd, Cr, Co, U, Cu, Ni, Mo, Pb, V, Se, Zn, Th, and Cs), soluble salts, alkalinity/acidity and unstable radioisotopes (Ram and Mastro 2010). In addition to the above mentioned TEs, REEs in CCRs are also important regarding the environmental and health risks (Khan et al. 2018, 2019c, 2020, 2021; Finkelmann et al. 2018). However, as the CCRs possess alkaline pH, elements having anionic chemical forms (e.g., As, Mo, and Se) may become more mobile and cause environmental contamination. At alkaline pH, leading components including Al₂O₃, SiO₂, and SO₄²⁻ can also form different types of secondary minerals (e.g., calcium aluminosilicate hydrate, ettringite, and calcium silicate hydrate gel) which can decrease the mobility of TEs either by physically lowering the porosity/permeability of CCRs or by binding the TEs with the secondary minerals chemically (Singh et al. 2011).

Annually coal-fired power plants generate over 750 Mt. of CCRs around the globe, however, approximately 50% of world CCRs production remains unutilized (Izquierdo and Querol 2012). Larger portions of these CCRs are either temporarily stored in stockpiles or discharged in lagoons and/or landfills. CCRs are considered as the significant source of releasing potentially toxic HMs to the ambient environment. However, considering the leachability and geochemical mobility of HMs, they

(Izquierdo and Querol 2012) also demonstrated that a huge number of HMs are strongly bound with CCRs and are not easily discharged to the ambient environment disregarding the ash characteristics. The physical and chemical mode of presence of a specific HM in feed coal plays a significant role in the leaching characteristics of FA. The Ca content in the FA possesses a governing impact on the pH of the water-ash system. The alkalinity of FA hinders the discharge of a large number of HMs (e.g., Cu, Sn, Cd, Hg, Co, Ni, Pb, Zn, etc.) but simultaneously, it increases the discharge of oxoanionic chemical species (of As, B, Mo, Cr, Se, W, V, and Sb). The precipitation of secondary mineralogical phases, for instance, ettringite may capture several pollutants (e.g., B, As, Cr, Sb, Se, and V) by chemical binding (Izquierdo and Querol 2012).

Currently, many countries like India, Thailand, Indonesia, and Bangladesh are immensely concerning about the pollution of soils followed by crops with TEs for the probable adverse impacts on health and long-term sustainability of food production in the polluted areas. Kim and Chon (2001) reported that mean abundances of Cd, Pb, Cu, and Zn in topsoil (0-15 cm) of the rice paddy field were 0.11 ppm (range: 0 to 1.01), 4.84 ppm (0–66.4), 0.47 ppm (0–41.6) and 4.47 ppm (0–96.7), respectively where Cd was found to be the most mobile HM in the soil and more available to crop, with great risk of entering into the food chain. In Table 24.14, elemental abundances in the topsoil around the BCM and the thermoelectric power plant are compared to those of soil samples from different mining and/or power plant areas of the world as well as those of several internationally recognized limit values. For quantifying the contamination levels, several environmental indices for instance contamination factor, pollution load index, geo-accumulation index as well as ecological indices, for instance, element-specific potential ecological risk factor (E^i_r) and potential ecological risk index (RI) have long been used (e.g., Islam et al. 2020; Tamim et al. 2016; Khan et al. 2017a, 2019a, b). So to have an insight into the quantification of contamination and ecological risk, in Table 24.15 environmental and ecological indices from the previous works are tabulated whereas the associated classifications of those indices are mentioned in Table 24.16.

24.5.4 Socioeconomic Impact

In designing coal mining operations, it is important to consider the socioeconomic (and environmental) impacts at three different stages: (i) construction, (ii) operation and (iii) closure. The impacts are likely to vary significantly at these stages and it would be desirable to identify the impacts separately for each stage. A major element of socioeconomic impacts is the need for resettlement required due to mining activities. In particular, land subsidence and associated impacts represent the major effects of underground mining (Hossain et al. 2015). To be effective, the resettlement plans need to be fully integrated with socioeconomic mitigation measures. The major elements are:

Table 24.14 Elemental abundances of topsoil samples from Barapukuria and the world literature data and their international limit values

	Cr	Mn	Fe	Co	Ni	Cu	Zn	Se	As	Cd	Sb	Ba	Pb	Th	U
Barapukuria, Bangladesh ¹	55.79					28.43	44.83			0.19			20.94		
Barapukuria, Bangladesh ²	47.39	261.79	2.28	12.53	22.34	43.76	57.63	3.15	36.22	0.84	3.35	353.85	22.55	4.64	4.67
Barapukuria, Bangladesh ³	–	1886.0	5.98			–	296.0		17.55				433.0		
Barapukuria, Bangladesh ⁴	105.9	1041.9	2.62		98.2	28.3	160.03		21.1				187.0		
World median ⁵	70.0	1000.0	4.0	8.0	50.0	30.0	90.0	0.4	6.0	0.35	1.0	500.0	35.0	9.0	2.0
UCC ⁶	92	775	3.92	17.3	47	28	67	0.09	4.8	0.09	0.4	624	17	10.5	2.7
Non-contaminated soil ⁷	100				30	30	100		–	1			50		
Threshold limit ⁸	100	2000	5	20	50	100	200		5	1	2		60		
Permissible limit ⁸	200			100	100	50	250		50	10	10		200		
Eco-toxicological limit ⁹	230				210	190	720								
PTE-MPC ¹⁰	200				50	100	250			0.3			300		
Critical levels ¹⁰	10		0.005		50	50–125	300	5–10	20–50	3			100		
MPA ¹¹	3.8			24	2.6	3.5	16	0.11	4.5	0.76	0.53	9	55		
Netherlands ¹²	100			9	35	36	140	0.7	29	0.8	3		85		
Canada ¹³	64				50	63	200		12	1.4			70		
Australia ¹⁴	50				60	60			20	3			300		
EQS, China ¹⁵	150			–	40	50	200	–	30	0.3			250		
Grade I, China ¹⁵	90					35	100		15	0.2			35		
Grade II, China ¹⁵	250					100	250		25	0.6			300		

Table 24.14 (continued)

	Cr	Mn	Fe	Co	Ni	Cu	Zn	Se	As	Cd	Sb	Ba	Pb	Th	U
Gangreung, Korea ²⁷	35.8				42.6	41	87.3			1.1			32.9		
Spain ²⁸	63.2				28.35	120.8	465.8		191.9	6.59			881.8		

Values in ppm (except for Fe in %) on the dry weight. Average concentrations of TEs in coal industrial soils from various sources compared with global reference values

¹Zakir et al. (2017), ²Sultana et al. (2016), ³Bhuiyan et al. (2010b), ⁴Halim et al. (2015), ⁵Bowen (1979), ⁶UCC: upper continental crust) Rudnick and Gao (2014), ⁷Kabata-Pendias and Pendias (1984), ⁸Toth et al. (2016), UNEP (2013), WHO (1996), ⁹McGrath (1997), ¹⁰Wei and Yang (2010), PTE-MPC: “maximum permissible concentrations of potential toxic elements” for agricultural soils of china, ¹¹Vodyanitskii (2016), MPA: maximum permissible addition of trace elements, ¹²Department of Soil Protection, Netherlands (1994), ¹³CCME (Canadian Council of Ministers of the Environment) (1993), ¹⁴NEPC (2013), ¹⁵EQS (1995) and Jiang et al. (2017), ¹⁶Noli and Tsamos (2016), ¹⁷Medunić et al. (2016) soils from SW direction, ¹⁸Pastrana-Corral et al. (2017), ¹⁹Baba (2003), ¹⁶Keegan et al. (2006), ¹⁷Mandal and Sengupta (2006), ¹⁸Lu et al. (2013), ¹⁹Adeyi and Torto (2014), ²⁰Dragović et al. (2013), ²¹Čujić et al. (2016), ²²Liang et al. (2017), ²³Zhai et al. (2009), ²⁴George et al. (2015), ²⁵Khan et al. (2019a, b), ²⁶Sahoo et al. (2016), ²⁷Kim and Chon (2001), ²⁸Li et al. (2014)

- Land likely to be affected by the mining and supplementary land requirement for mitigation measures.
- Reclamation and compensation issues.
- Phased costs and cash flows.
- Capital investment program phased in accordance with project implementation program and mining plan.
- Operating costs linked with phased mining plan justifying operational cost phasing.

For making realistic and viable socioeconomic analysis, all relevant geological, technical, and other related data must be put in place to conduct a credible assessment. Similarly, the efficacy of financial and economic evaluation critically depends on the availability of all required data including reliable cash flow information.

Though the coal industrial activities may create employment opportunity and better livelihood with changing the life quality of local people, major influences domains around Barapukuria are on demographic profile, polarization in land ownership, employment opportunity and availability of manpower, education, occupational pattern, communication demand of electricity, population migration, communal diversity, income and expenditure, social institution, resettlement, land compensation. Displacement causes landlessness, homelessness, joblessness, food insecurity, disruption of community social and cultural networks. The coal mining and utilization activities in Barapukuria cause impacts on the socioeconomic environment, water, air, soil quality and fertility, fisheries, ecosystem, biodiversity, and landform and type, land use, and landscape. They have impacted and interrupted the local people's livelihood and lifestyles adversely. The peoples face significant problems in their daily-livelihood owing to many adverse consequences of both coal-fired power plant and coal mine such as the air, soil quality, and fertility, and water contamination, acquisition of homesteads, and agricultural land, mass eviction, loss of assets, light, noise, etc. Changes of the profession from agricultural to non-agricultural activities cause losses of farmland are another evident event. Occupational patterns and people's income level and concomitant livelihood styles have been altered unfavorably (Hossain et al. 2015).

Several square kilometers of settlements and productive farming land will need to be acquitted for mine footprint, town and village resettlement sites, and realignment of transport infrastructure. A large number of populations should be displaced for rail and road alignment and relocation villages to be displaced from mine footprint. Resettlement of local inhabitants for land acquisition, the release of solid wastes (fly and bottom ash residues), warm water, heat, and emission of flue gases with PM are the key predicted impacts. Livelihood and income-oriented impacts include those on agricultural livelihood, natural resources, and other common properties, non-agricultural livelihood, and mine employment and business development opportunities. Impacts on social, community, and cultural practices include splitting and loss of social consistency in the isolated communities and kinship; and increased social conflicts. There are several impacts including loss of productive farming land, loss of generational farming communities, loss of social cohesion in isolated

Table 24.15 Environmental indices (contamination factor, pollution load index, enrichment factor, geo-accumulation index, element-specific ecological risk factor, and sampling site specific potential ecological risk index) for the Barapukuria soil samples are compared to those of literature data

	Cr	Mn	Fe	Co	Ni	Cu	Zn	As	Cd	Pb	PLI	RI	References
<i>Contamination factor (C_f)</i>													
Barapukuria	0.77	0.47			0.7	5.22	1.09	3.82	2.04	1.07			Sultana et al. (2016)
Barapukuria		3.3					4.37	1.54		15.35	4.29		Bhuiyan et al. (2010a)
Barapukuria	1.51	1.84			5.53	1.03	2.36	1.96		6.69	2.42		Halim et al. (2015)
Gnagreung, Korea	0.5				2.39	1.45	1.29		2.24	1.17	1.29		Kim and Chon (2001)
Jaintia, India	2.02	0.41			2.16	0.81	0.79		3.12	0.82	1.16		Sahoo et al. (2012)
Makum, India	2.85	0.7			4.66	0.8	0.94		2.69	0.49	1.37		Equeenuddin et al. (2010)
Serbia	0.5	0.9	0.8	1.7	3.1	1.4	1.5		1.4	1.1			Čujić et al. (2015)
India	1.6			1.7	1.5	2.3	1.3	2.7	1.7	1.2			George et al. (2015)
Jinsha, China	0.55					1.11		1.32	0.93	1.29			Huang et al. (2017)
<i>Enrichment factor (EF)</i>													
Barapukuria		1.25–3.67					0.88–6.53	0.42–1.63		1.42–4.4			Bhuiyan et al. (2010a)
Mexico	1				0.8	1			0.2	1.5			Pastrana-Corral et al. (2017)
India	2.4	0.8	1.2		0	0	1						Das and Chakrapani (2011)
Kolaghat, India	2.6	2.1		1.8	2.4	2.5	1.8	1.9		1.1			Mandal and Sengupta (2006)
Serbia	0.7	1.2		2.2	3.9	1.8	1.4		1.8	1.3			Čujić et al. (2015)
Turkey	17.6				44.5	2.2	4.7	95.3	3.5	11.1			Özkul (2016)
Obrenovac, Serbia	1.96	1.54		1.25	2.8	3.95	2.14	0.17	11.8	1.3–7.42 (3.1)			Dragović et al. (2013)

West Macedonia, Greece	0.98–4.64	1.09–4.18			1.88–18.2	1.14–3.48	0.96–3.87	1.25–5.71	Stalikas et al. (1997)		
West Bengal, India	2.6–3.2	2.1–2.6	1.8–2.8		2.4–3.0	2.5–3.5	1.8–2.5		Mandal and Sengupta (2006)		
Kahramanmaraş, Turkey	1.12–2.74	0.51–2.03			1.85–6.89	0.91–3.01	0.64–2.51		Tumuklu et al. (2008)		
India	1.3		1.3		0.6	1.1	1.2	2	George et al. (2015)		
Jinsha, China	0.27					0.53	0.64	0.64	Huang et al. (2017)		
<i>Geo-accumulation index (Igeo)</i>											
Barapukuria		1.14					0.11	1.38	Bhuiyan et al. (2010a)		
Barapukuria	0.13	0.29		-0.23	0.24	23	0.09	1.5	Halim et al. (2015)		
Jaintia, India	0.43	-1.88			0.52	-0.89	-0.91	1.09	Sahoo et al. (2016)		
Makum, India	0.93	-1.1			1.64	-0.9	-0.68	0.87	Sahoo et al. (2016)		
Gnagreung, Korea	-1.57				0.67	-0.05	-0.21	0.61	Kim and Chon (2001)		
Mexico	0.1				-0.01	0.2		-2.3	Pastrana-Corral et al. (2017)		
India	0	0	0	0			0		Das and Chakrapani (2011)		
Serbia	-1.6	-0.8	0.1	-0.9	0.9	-0.1	-0.03	-0.4	Čujić et al. (2015)		
Turkey	0.6				1.8	-2.3	-1.3	2.7	Özkul (2016)		
India	0.3		0.6		-0.4	0.1	-0.3	1.5	George et al. (2015)		
Jinsha, China	-1.49					-0.79		-0.47	Huang et al. (2017)		
<i>Potential ecological risk factor (E_p)</i>											
Barapukuria	1.55				3.52	26.14	1.09	38.25	61.21	5.32	Sultana et al. (2016)

(continued)

Table 24.15 (continued)

	Cr	Mn	Fe	Co	Ni	Cu	Zn	As	Cd	Pb	PLI	RI	References
Barapukuria							4.37	15.35		76.77		96.49	Bhuiyan et al. (2010a)
Barapukuria	3.02					5.14	2.36	19.65		33.44		63.61	Halim et al. (2015)
Jaintia, India	4.03					4.06	0.79		93.67	4.08		106.64	Sahoo et al. (2016)
Makum, India	5.7					4.02	0.94		80.82	2.46		93.94	Sahoo et al. (2016)
Gnagreung, Korea	1.01					7.27	1.29		67.35	5.83		82.75	Kim and Chon (2001)

PLI pollution load index; *RI* potential ecological risk index

Table 24.16 Classification of environmental and ecological indices

Contamination factor (C_f^i ; Luo et al. 2007)		Pollution load index (PLI; Tomlinson et al. 1980)	
Category	Description	Category	Description
$C_f^i < 1$	Low	$PLI \leq 1$	No contamination
$1 \leq C_f^i < 3$	Moderate	$1 < PLI \leq 3$	Slight contamination
$3 \leq C_f^i < 6$	Considerable	$3 < PLI \leq 5$	Moderate contamination
$C_f^i \geq 6$	High	$PLI > 5$	Severe contamination
Enrichment factor (EF; Sezgin et al. 2004)		Geo-accumulation index (I_{geo} ; Müller 1981)	
Category	Description	Category	Class
$EF < 2$	Minor enrichment	$I_{geo} < 0$	0
$2 < EF < 5$	Moderate enrichment	$0 < I_{geo} < 1$	1
$5 < EF < 20$	Significant enrichment	$1 < I_{geo} < 2$	2
$20 < EF < 40$	Very severe enrichment	$2 < I_{geo} < 3$	3
$EF > 40$	Extremely severe enrichment	$3 < I_{geo} < 4$	4
		$4 < I_{geo} < 5$	5
		$5 < I_{geo} < 6$	6
Potential ecological risk factor (E_f^i ; Maanan et al. 2014)		Potential ecological risk index (RI; Hakanson 1980)	
Value	Pollution degree	Category	Description
$E_f^i < 40$	Low risk	$RI < 150$	Low risk
$40 \leq E_f^i < 80$	Moderate risk	$150 \leq RI < 300$	Moderate risk
$80 \leq E_f^i < 160$	Considerable risk	$300 \leq RI < 600$	Considerable risk
$160 \leq E_f^i < 320$	High risk	$RI \geq 600$	High risk
$E_f^i \geq 320$	Very high risk		

communities, and loss of water supply. The development of community facilities owing to the establishment of any power-project and the number of accidents owing to hazardous working conditions can also impact on ambient socioeconomic condition.

24.5.5 Sound Pollution

Any kind of disturbing or unwanted sounds that interfere or harm mankind or wildlife are termed as sound pollution. Unlike the soil, water, or air pollution, sound pollution draws less attention due to its abstract form. General mining activities round the clock thus contribute to sound pollution include loading and unloading, drilling and blasting, overburden removal, excavating, use of generators, crushing, and vehicular traffic.

Principal sources of sound pollution in coal-based power plants include the boilers and auxiliaries, turbine generators and auxiliaries, coal pulverizers, fans and ductwork, reciprocating engines, condensers, compressors, pumps, precipitators, piping and valves, plate vibrators, motors, circuit breakers, transformers, etc. Before the beginning of coal mine activities and establishment of power plant, the BTPP site was relatively noiseless as there were no activities, except for small business and agriculture. Ambient noise level in the process area is within the permissible limits as per standards set by ECR (1997). Table 24.17 represents that the highest sound level at the power plant area was 65 dB in the morning and 60 dB in the afternoon which was within the permissible limit.

In coal-fired power plant employees are generally exposed to a high noise levels. Furthermore, the enhanced transportation activities around the operation of power plant lead to the amplification of noise levels in nearby population/communities.

24.5.6 Eco-Toxicological Impacts

Over all water quality as well as the aquatic ecosystem can primarily be affected by the acid mine drainage (Jain et al. 2016a, b) as AMD runoff decreases the pH of stream and lake water. pH of the water reserver can reach as low as 2.0–4.5 for which several fish species are supposed to be rigorously impacted. Moreover, dissolved HMs, e.g., Zn and Cu are toxic to several aquatic species. HMs and acidic pH can also affect the downstream water resources which make the water unusable for agricultural purpose, human, and/or recreational uses without appropriate treatment. Other than human health and ecological risks, excess sulfate levels from AMD can alter the drinking water taste and may pause corrosion in water infrastructures (Bhuiyan et al. 2010b; Galhardi and Bonotto 2016; Huang et al. 2016a, b). Ground-water resources can also be contaminated by HMs and sulfate by AMD through infiltration.

Table 24.17 The noise level in decibel (dB) near Barapukuria coal industrial site

Observation time	Noise level (2005) ^a		Noise level (2014) ^a		Limit ^b
	Lowest	Highest	Lowest	Highest	
Morning (8.30 am)	30	60	30	65	60–70
Afternoon (6.30 pm)	25	60	25	60	60–70
Evening (12.45 pm)	20	55	20	60	60–70

^aHossain et al. (2015), ^bECR (1997)

Other than the AMD, potentially eco-toxic HMs and the associated chemical species from FA can cause eco-toxicological impacts. For instance, Tolle et al. (1983) demonstrated that abundances of As in Lucerne-tissue were higher than the toxic level ($3.4 \text{ mg}\cdot\text{kg}^{-1}$) in sheep in case of large application rates of FA to soil. Similarly, toxic levels of Se have also been found in herbage grown on flyash treated soils (Tolle et al. 1983; Pandey et al. 2014). Furthermore, growth depressions of plants grown in soils altered by FA (Pandey et al. 2014; Adriano et al. 2002) and toxicological impacts on livestock (Tolle et al. 1983) are observed due to the B and Mo (originated from FA), respectively. Howladar et al. (2017) demonstrated that elevated levels of Fe, Mn, As, and Cd near the BTTP reduce vegetative and animal growth.

The extent of pollution in BCM area reflects moderate contamination (Bhuiyan et al. 2010b). In terms of ecological risk index (E_r^i) of specific HM (order: $\text{Cd} > \text{As} > \text{Cu} > \text{Pb} > \text{Ni} > \text{Cr} > \text{Zn}$), cadmium possesses the highest risk index and causes immense damage to the soil around BCM areas. Enrichment factor (EF), geo-accumulation index (I_{geo}) and potential ecological risk indices imply those there are considerable As and Cd pollution, mostly induced by drainage water from the BCM (Halim et al. 2013; Sultana et al. 2016) (Table 24.14).

24.5.7 Biological and Thermal Impact

Impacts on both flora and fauna should be considered while discussing the environmental biosphere. Emissions of flue gas and land acquisition mostly affect the flora by leading to the loss of habitats. The disposed wastewater from power plants possessing relatively higher temperatures (Table 24.11) may cause adverse effects on the local aquatic biota (Jain et al. 2016a, b). Higher wastewater temperature causes thermal pollution which alters the dissolved oxygen level, cause direct thermal shocks. Since the specific heat capacity of water is very high it can absorb a large amount of thermal energy with only tiny alteration of water temperature. Thus even a narrow range of temperature change can harm the thermal energy-sensitive enzymatic systems of most aquatic organisms. These stenothermic species may die by the abrupt temperature alterations those are higher than the tolerance limits for their metabolic system. Furthermore, sequential heat management used for

clearing the cooling system from the fouling organisms (which are responsible for clogging the intake pipes) can result in fish mortality.

24.5.8 *Effects on Biodiversity*

Ecosystem services, e.g., regulating, provisioning, and cultural services are positively affected due to the increased biodiversity (Jain et al. 2016a, b; Mishra and Das 2017). Thus, by considering decreases in wildlife species & their populations can measure the degradation of ecological systems. Large and healthy wildlife populations possess economic, esthetic, and moral significance.

Eco-toxicological impacts cannot be separately assessed leaving the contamination impacts from the coal mining or coal-based power plant activities on the total environment including deterioration of water, sediment, soil, and air quality. Specific descriptions of ecological impacts due to environmental deterioration are provided in the preceding sections. Demolition of habitats & vegetation, deforestation, and deterioration of soil, water, and air quality are ecological impacts specific to coal mining activities, which can hamper the existence of animals, fishes, birds, plants, and invertebrates (Hossain et al. 2015).

Wildlife and the overall biodiversity can be directly and/or indirectly impacted adversely by coal mining. Some of these impacts are short-termed and confined to the mining area whereas others are long-termed which can spread over a long distance. Impacts on wildlife originate mostly from removing and redistribution of land areas. The most prominent direct impacts on the wild biodiversity are destruction and/or displacement of species and spoils piling in the excavation areas. Zoological species such as invertebrates, burrowing rodents, small mammals, and many reptiles may be directly destroyed. However, mobile wild species like birds, predators, and animals leave the mining site. Fish, amphibians, and aquatic invertebrates can be ruined, if lakes, streams, marshes/ ponds are filled with CCRs or, received coal industrial leachates. The scarcity of food supplies for predators can be occurred due to the destruction of the land and water species (Dhar and Thakur 1996; Chabukdhara and Singh 2016).

Furthermore, noise pollution from coal mining and CTP activities possess harmful impacts on wildlife species by deteriorating habitat's quality, elevating stress level & masking natural sounds. Continual exposure of noise is particularly troublesome for the chordates (e.g., owls and bats) those depend on sound-echo for hunting and/or communication (Bayne et al. 2008; Barber et al. 2010). Additionally, avian species those depend on echo-based communication (e.g., nocturnal animals) tend to avoid the mining areas due to sound pollution (Barber et al. 2010; Bayne et al. 2008). Declining of the foraging activities and the concomitant reduction of avian populations can cause negative impacts on seed dispersion, affect diversity & ecosystem services (Francis and Barber 2013).

24.5.9 Human Health Risks

Contamination of indoor-air quality (due to coal combustion) in the developing countries was noticed as a severe health risk. Other than the indoor-air, coal combustion supplies PAHs along with the altered products or derivatives of PAHs to the ambient atmosphere which are typically more toxic compared to the progenitor PAHs and cause the potential human health risk. Coal burning has been identified as a technogenic process for causing respiratory problems (e.g., emphysema, chronic bronchitis, dyspnea, and expectorative cough) (Finkelman et al. 2002; Xiao et al. 2019; Liu et al. 2008; Callén et al. 2011; Tian et al. 2008, 2011; Cheng et al. 2013; Kim et al. 2015). For example, Guttikunda and Jawahar (2014) studied the proportionate mortality and case-control in India and demonstrated that coal burning may possess prominent risks of cancers (of the lung, buccal cavity, nasopharynx, esophagus & bladder). Additionally, SO₂ from CTPs can cause several respiratory-related problems. Similar to most of the air pollutants, SO₂ can cause a greater health hazards to sensitive age groups (e.g., elderly people, chronic asthmatic patients, children & infants). Consequential acid rain from SO₂ may cause considerable impacts on surface water, plants and buildings.

Fine particulate matter and trace elements possess important negative effects on human and animal health and water quality. HMs (e.g., Cd, Zn, As, Cu, Cr, Ni & Pb) contaminated soil is considered as a major route of HM's exposure to the human (Raja et al. 2015) (Table 24.14). The fine particles not only pause visibility reduction, climate perturbations, and acid rain, but also originate severe health hazards by penetrating & delivering coated chemicals to the human respiratory system.

Dust from the coal-based thermoelectric power plant deteriorates the air quality of the surrounding area which may cause negative impacts on vegetation, and can results hazards to the health and safety of mine workers and local residents. Several authors (Oliveira et al. 2014; Dai et al. 2008; Tian et al. 2008, 2016; Jelic et al. 2017; Wang et al. 2016a, b;) reported submicron to nanoquartz in coals from China, probably related to the lung cancer. Potentially bio-reactive nature of nanoparticles and nanominerals (in coals) can increase health hazards originated from such materials inhalation (Silva et al. 2012; Dias et al. 2014). Several mine workers and local inhabitants around coal mines and CTPs in China are affected with serious lung diseases caused by inhalation of flying coal dust, finest FA, pyrite, clay, quartz, etc. (Jelic et al. 2017; Kollipara et al. 2014).

24.5.10 Radiological Risks

CTP arrest the most of coarse flyash, however, ~1%–3% finest portion of the total flyash having radionuclides escaped to the atmosphere and biosphere even with the use of filtration systems and consequently spread over a long distance due to the air convection (Papastefanou 2010; Tripathi et al. 2014; Charro et al. 2013; Dragović et al. 2013). These air particulate FA are then settle down on the earth surface and

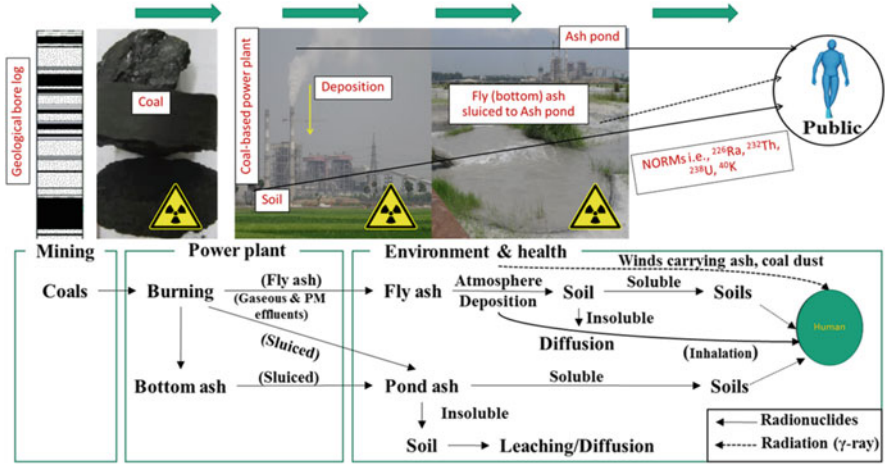


Fig. 24.4 Potential pathways of radionuclides migration through the different media from a coal power plant to soil

eventually find the way to the surface water and soil leading to contaminate through mobilization, migration processes, and finally reach the human physiology by inhalation, ingestion, and exposure to external radiation (Fig. 24.4) (e.g., Finkelman et al. 2018; Wang et al. 2016a; Querol et al. 2011; Sahu et al. 2017; Dai et al. 2012; Skoko et al. 2017). Pollutants like Ra are reported as potential hazardous radionuclide to the ambient environment and human physiology even at low levels (Blissett and Rowson 2012; Yao et al. 2015; Kalia and Tang 2017; Medunić et al. 2016; Skousen et al. 2013). Radionuclides having CCRs origin can even reach the natural drainage systems and sub-soil, and pollute the water sources with radionuclides (Noli and Tsamos 2016; Dragović et al. 2013; Charro et al. 2013; Islam et al. 2018) (Table 24.10). It may finally lead to harmful effects on human health due to their higher radiation level and pose acute and chronic diseases to public health (e.g., lung and bone cancer, respiratory illnesses, cell damage, etc.) (e.g., Fergusson 1990; Dai et al. 2008, 2012; Silva et al. 2009; Campaner et al. 2018; Oliveira et al. 2014; Munawar 2018; and the references cited therein).

Considering the negative impacts on human health and on the environment caused by NORMs from CTP, it is important to study the radiological risks of NORMs in coals, CCRs, and soils. The average values of radiological risk indices in CCRs from BTTP was $447 \pm 95 \text{ Bqkg}^{-1}$ for radium equivalent activity (Ra_{eq}), 1.2 ± 0.3 for external hazard index (H_{ex}), $201.1 \pm 42.2 \text{ nGy h}^{-1}$ for absorbed gamma dose (D), $0.25 \pm 0.05 \text{ mSv year}^{-1}$ for annual effective dose (E) and $8.6 \times 10^{-4} \pm 1.8 \times 10^{-4} \text{ Sv}^{-1}$ for excess lifetime cancer risk (ELCR), most of which are higher than the permissible limits (Habib et al. 2019a). However, in soil samples around the BTTP, the average Ra_{eq} (in $\text{Bq}\cdot\text{kg}^{-1}$), D (in nGy h^{-1}), H_{ex} , E (in $\text{mSv}\cdot\text{year}^{-1}$) and ELCR are 250 ± 22 , 114 ± 9 , 0.67 ± 0.06 , 0.20 ± 0.02 , and

$4.9 \times 10^{-4} \pm 0.4 \times 10^{-4}$, respectively, which are within the acceptable limits (Habib et al. 2019b).

24.5.11 Accidents of Coal-Mining

The coal mine faces roof collapse, water in rush, land subsidence, methane emission, etc. Several number of geo-environmental mine hazards are caused, such as (i) mining-induced fault reactivation, (ii) seam gas outburst, (iii) rockburst with major roof fall, and (vi) ground movement and water inrush/inflow, have been noticed during mining activities which cause negative impacts on exploration and underground coal mining in BCM (Islam 2009). Based on the analysis of accident statistics of BCM, it is found that the major (dead) accidents which led to the death of miners are due to collapse of the roof and sidewalls, hit by falling/rolling coal lump, coal bump, heatstroke, road-header operation, electric shock, etc. Amongst all, accidents due to the collapse of roof and side walls resulted maximum number of fatalities leading to the death of 03 miners during 2004 to 2008 (Monir and Hossain 2012). During this period, the other causes of accidents in the mine resulting in minor or serious bodily injury to the miners are due to collapse of the roof, mine cars, slushier machine, steel supports, belt conveyors, etc.

24.6 Pollution Prevention and Remediation Approaches

Coal mining is a multistage short-term activity with long-term environmental and health risk-oriented impacts (Zhengfu et al. 2010). So, for a proper pollution prevention approach for coal mining, several aspects of environmental geochemistry, mining procedures, and the potential socio-economic impacts should be considered before the commencement of mining activities (Dontala et al. 2015; Jain et al. 2016a, b). Demographically, the whole Dinajpur district (an administrative area of Bangladesh) is highly populated (population density: 823/km²) area possessing highly fertile three-cropped land where more than 75% of people are depending on agricultural activities. Open pit mining is less costly but more damaging to environment. In the coal mine areas, the primary impact would be the loss of livelihood by the majority of households who depend mostly on agriculture for their income. Along with compensation payment for the loss of economic activities and support to engage in alternative livelihood activities, social mitigation measures (including compensation and financial incentives) need to be included to ensure livelihoods for their future generations (Shamshad et al. 2012). The economic analysis should include costs of activities to offset the loss of livelihood of affected persons and their descendants such as (i) preference to affected persons for employment during mine construction and operation; (ii) construction of model villages to locate displaced families; (iii) zone areas for locating retail business activities at mine sites; and

(iv) zone areas for establishing manufacturing units based on local raw materials and mine supplies to generate alternative employment. The costs may also include investments for upgrading surrounding agriculture to create employment opportunities. The costs should include the details of reclamation and a closure plan.

The standard procedure especially for open-pit mining is to include the costs of restoration of levels and return the land to its original uses as mining proceeds. This may require a substantial volume of materials (including soil from river dredging, for example) equivalent to the volume of coal extracted over the life of the mine at least to reclaim a large part of the land. For the remaining area, the costs of developing viable alternative use for the expanse of water may be included. This may cover several options depending on physical and economic viability such as turning into amenity areas for tourists, developing large and small-scale fish farming, source of irrigation, and others. These should form components of the closure plan.

In terms of benefits, the direct benefits are obvious. But what is not so obvious is the identification and valuation of indirect benefits. For example, the associated infrastructure investments in power, communications, road, rail, port, and in developing new urban centers will create additional employment and income-generating opportunities in general and in the lagging northern region in particular which will contribute to reducing poverty and regional disparity in development. The development of coal mines will contribute to reducing dependency on firewood and saving trees. Similarly, imparting skills through training and the use of new coal mining technologies will create spillover effects benefiting other industries. New industries (e.g., based on coal co-products like gravel, glass sand, china clay, water) will diversify economic activities and provide sustainable livelihoods and create earning opportunities for all sections of the population.

The biological and chemical reactions or processes related to the AMD are geogenic procedures which are generally slow in uninterrupted mine can cause only a little ecological risk (Jain et al. 2016a, b). Conversely, in active mining site above mentioned biological and chemical processes are significantly accelerated by huge land are interruption, increased contacts of sulfide minerals with water and oxygen. Reactions involved in AMD form a cyclic process that enables the repeated generation of AMD. As a result, AMD can continue all through the lifetime of an active coal mine and can persist for a long time even after abandoning the mine. Thus, any activities those may cause the interruption of sulfide-rich materials should be considered with a complete assessment of AMD potentiality. In this sort of assessment, preventing and mitigating AMD generation should get prior consideration rather than the AMD treatment (Jain et al. 2016a, b), as AMD treatment results in high unending costs.

Soil contamination by toxic HMs, salts, PAHs, NORMs, etc., owing to the mining and coal-fired power plant can cause adverse health effects for both animal and plant. Soil is comprised of both organic (mostly the topsoil) and inorganic (sub-soil: soils below the layer of topsoil) components (Asrari 2014; Sultana et al. 2015; Su et al. 2014; Wuana and Okieimen 2011). In continuous contamination, pollutants have progressively entered the inorganic-layers of soil. Varying kinds of soil contamination (e.g., industrial, agricultural & urban) cause reduced fertility of

the soil (Yao et al. 2012; Laraia 2015; Abdel-Shafy and Mansour 2016; Sengupta and Agrahari 2017). Thus, appropriate steps should to be adopted for averting soil pollution and for preserving soil-fertility. In doing so, biofertilizers as well as biopesticides and biofungicides should get priority instead of their corresponding synthetic chemical counterpart. Simultaneously, dependable procedures should be adopted for discharging the waste (Pandey et al. 2009). Juwarkar and Jambhulkar (2008) demonstrated that introduction of biofertilizer and using farmyard manure to the agricultural soil helped in decreasing the toxicity of HMs from FA, e.g., the toxicity of Zn, Cu, Pb, Cr, Cd, and Ni can be decreased by 25, 31, 46, 47, 25, and 48%, respectively. Biofertilizer reduces the toxicity of HMs by increasing the organic component of the soil and undergoing the complexation with the HMs of CCRs.

24.7 Summary

Due to Stratification, physical and chemical alterations, burial, and compaction over a geologic time, plant debris has converted into the sedimentary rock which is known as coal. Geochemically, coal carries a minute amount of heavy metals, naturally occurring radionuclides, and persistent organic pollutants. Although Bangladesh possesses five coal basins (Barapukuria, Phulbari, Khalashpir, Jamalganj, and Dighipara) with total in-situ deposits of 3300Mts coals, only Barapukuria coal mine in north-western part of Bangladesh is in active condition. Tectonically, the Coal Basins in Bangladesh were formed in the Precambrian basement complex during the Permo-carboniferous time.

Among the several potential coal-based power plants, Barapukuria coal-fired power plant is in the operating condition so far. In coal-based power plants, multistage combustion processes result from massive change in feed coal constituents and generate large amount of coal combustion residues in which inorganic components including environmentally sensitive heavy metals and radiologically hazardous NORMs are in enriched abundances. Hence, coal-based power plants and coal mining activities can cause adverse effects on every single compartments of the environments through acid mine drainage, generation of air particulate matter, land subsidence, dispersion of HMs, NORMs, and POPs. Eco-toxicological impacts as well as human health risks are quite pronounce for an improperly managed coal-based power plants and coal mining activities. However, considering the increasing energy demand and the country's economic growth properly managed coal-based power plants and coal mining activities are anticipated with proper prevention and remediation approaches.

Acknowledgment Mr. Md. Abu Bakar Siddique of BCSIR, Bangladesh, Mr. Abdul Baquee Khan Majlis & Dr. Md. Bazlar Rashid of Geological Survey of Bangladesh, Mr. Arup Kumar Biswas of Hydrocarbon Unit, Bangladesh and Dr. Kuaanan Techato & Dr. Khamphe Phoungthong of the Prince of Songkla University (Thailand) are gratefully acknowledged for their kind cooperation during the preparation of this chapter.

References

- Abdel-Shafy HI, Mansour MS (2016) A review on polycyclic aromatic hydrocarbons: source, environmental impact, effect on human health and remediation. *Egypt J Pet* 25(1):107–123
- Adeyi AA, Torto N (2014) Profiling heavy metal distribution and contamination in soil of old power generation station in Lagos, Nigeria. *Am J Sci Technol* 1(1):1–10
- Adriano DC, Page AL, Elseewi AA, Chang AC, Straughan I (1980) Utilization and disposal of fly ash and other coal residues in terrestrial ecosystems: a review. *J Environ Qual* 9(3):333–344
- Adriano DC, Weber J, Bolan NS, Paramasivan S, Koo BJ, Sajwan KS (2002) Effects of high rates of coal fly ash on soil, turf grass, and groundwater quality. *Water Air Soil Pollut* 139:365–385
- Agrawal M, Agrawal SB (1989) Phytomonitoring of air pollution around a thermal power plant. *Atmos Environ* 23(4):763–769
- Ahamad MG (2016) Local and imported coal-mix for coal-based power plants in Bangladesh. *Energy Sources B* 11(10):936–945
- Ahmaruzzaman M (2010) A review on the utilization of fly ash. *Prog Energy Combust Science* 36(3):327–363
- Ahmed MS, Rahmatullah M, Khan MAA (2017) Hydrocarbon gas generation by biochemical process of moderately barophilic methanogens in Barapukuria coal mine gas reservoir & aquifer. *Fuel* 210:121–132
- Akcil A, Koldas S (2006) Acid Mine Drainage (AMD): causes, treatment and case studies. *J Clean Prod* 14(12):1139–1145
- Akhtar A, Kosanke RM (2000) Palynomorphs of Permian Gondwana coal from borehole GDH-38, Barapukuria Coal Basin, Bangladesh. *J Afr Earth Sci* 31(1):107–117
- Alam M (1989) Geology and depositional history of cenozoic sediments of the Bengal Basin of Bangladesh. *Palaeogeogr Palaeoclimatol Palaeoecol* 69:125–139
- Alam MK, Hasan AKMS, Khan MR, Whitney JW (1990) Geological Map of Bangladesh; Geological Survey of Bangladesh, Dhaka, Scale 1:1,000,000, (Government publication)
- Al-Areqi WM, Majid AA, Sarmani S (2008) Analysis of trace elements in power plant and industrial incinerator fly ashes by instrumental neutron activation analysis (INAA). *Malaysian J Anal Sci* 12(2):375–379
- Amin YM, Khandaker MU, Shyen AKS, Mahat RH, Nor RM, Bradley DA (2013) Radionuclide emissions from a coal-fired power plant. *Appl Radiat Isotopes* 80:109–116
- Andrup-Henriksen G (2007) Estimation of gas emissions from shallow subsurface coal fires in Jharia coalfield, India, using FLIR data and coal fire gas analysis. In: 2007 GSA Denver Annual Meeting
- Arbuzov SI, Volostnov A, Rikhvanov LP, Mezhibor AM, Ilenok SS (2011) Geochemistry of radioactive elements (U, Th) in coal and peat of northern Asia (Siberia, Russian Far East, Kazakhstan, and Mongolia). *Int J Coal Geol* 86(4):318–328. <https://doi.org/10.1016/j.coal.2011.03.005>
- Asrari E (2014) Heavy metals in contaminated soils: a review of sources, chemistry, risks and best available strategies for remediation. In: Heavy metal contamination of water and soil. Apple Academic Press, New York, pp 33–82
- Baba A (2003) Geochemical assessment of environmental effects of ash from Yatagan (Mugla-Turkey) thermal power plant. *Water Air Soil Pollut* 144(1–4):3–18
- Baba A, Gurdal G, Sengunalp F (2010) Leaching characteristics of fly ash from fluidized bed combustion thermal power plant: case study: Çan (Çanakkale-Turkey). *Fuel Process Technol* 91(9):1073–1080. <https://doi.org/10.1016/j.fuproc.2010.03.015>
- Baeza A, Corbacho JA, Guillén J, Salas A, Mora JC, Robles B, Cancio D (2012) Enhancement of natural radionuclides in the surroundings of the four largest coal-fired power plants in Spain. *J Environ Monit* 14(3):1064–1072
- Bajpai R, Upreti DK, Nayaka S, Kumari B (2010) Biodiversity, bioaccumulation and physiological changes in lichens growing in the vicinity of coal-based thermal power plant of Raebareilly district, north India. *J Hazard Mater* 174(1–3):429–436

- Bakr, M. A., Rahman, Q. M. A., Islam, M. M., Islam, M. K., Uddin, M. N., Resan, S. A., Haider, M. J., Islam, M. S., Ali, M. W., Choudhury, M. E. A., Mannan, K. M., & Anam, A. N. M. H., 1996. Geology and coal deposit of Barapukuria Basin, Dinajpur district, Bangladesh. Records of the Geological Survey of Bangladesh, 8(1). Government Publication, Dhaka
- Barber JR, Crooks KR, Fristrup KM (2010) The costs of chronic noise exposure for terrestrial organisms. *Trends Ecol Evol* 25(3):180–189
- Barescut J, Lariviere D, Stocki T, Pandit GG, Sahu SK, Puranik D (2011) Natural radionuclides from coal fired thermal power plants—estimation of atmospheric release and inhalation risk. *Radioprotection* 46(6):S173–S179
- Bartoňová L (2015) Unburned carbon from coal combustion ash: an overview. *Fuel Process Technol* 134:136–158
- Basu M, Pande M, Bhadoria PBS, Mahapatra SC (2009) Potential fly-ash utilization in agriculture: a global review. *Prog Nat Sci* 19(10):1173–1186. <https://doi.org/10.1016/j.pnsc.2008.12.006>
- Bayne EM, Habib L, Boutin S (2008) Impacts of chronic anthropogenic noise from energy-sector activity on abundance of songbirds in the boreal forest. *Conserv Biol* 22(5):1186–1193
- BBS (Bangladesh Bureau of Statistics) (2018) Dinajpur District Statistics 2018. In: Statistical Year Book of Bangladesh. Govt. of the People's Republic of Bangladesh
- Belkin HE, Tewalt SJ, Hower JC, Stucker JD, O'Keefe JMK (2009) Geochemistry and petrology of selected coal samples from Sumatra, Kalimantan, Sulawesi, and Papua, Indonesia. *Int J Coal Geol* 77(3–4):260–268. <https://doi.org/10.1016/j.coal.2008.08.001>
- Bem H, Wiczorkowski P, Budzanowski M (2002) Evaluation of technologically enhanced natural radiation near the coal-fired power plants in the Lodz region of Poland. *J Environ Radioact* 61(2):191–201
- Bhangare RC, Tiwari M, Ajmal PY, Sahu SK, Pandit GG (2014) Distribution of natural radioactivity in coal and combustion residues of thermal power plants. *J Radioanal Nucl Chem* 300(1):17–22
- Bhuiyan MA, Islam MA, Dampare SB, Parvez L, Suzuki S (2010ba) Evaluation of hazardous metal pollution in irrigation and drinking water systems in the vicinity of a coal mine area of northwestern Bangladesh. *J Hazard Mater* 179(1–3):1065–1077
- Bhuiyan MA, Parvez L, Islam MA, Dampare SB, Suzuki S (2010ab) Heavy metal pollution of coal mine-affected agricultural soils in the northern part of Bangladesh. *J Hazard Mater* 173(1–3):384–392
- BIS (Bureau of Indian Standards) (2012) Bureau of Indian Standards drinking water specifications. BIS, 10500, India
- Blissett RS, Rowson NA (2012) A review of the multi-component utilisation of coal fly ash. *Fuel* 97:1–23. <https://doi.org/10.1016/j.fuel.2012.03.024>
- Bostick NH, Betterton WJ, Gluskoter HJ, Islam MI (1991) Petrography of Permian “Gondwana” coals from boreholes in northwestern Bangladesh, based on semiautomated reflectance scanning. *Org Geochem* 17(4):399–413
- Bowen HJM (1979) Environmental chemistry of the elements. Academic Press, London; New York
- Bragato M, Joshi K, Carlson JB, Tenório JA, Levendis YA (2012) Combustion of coal, bagasse and blends thereof: part II: speciation of PAH emissions. *Fuel* 96:51–58
- Brammer H (1996) The geography of the soils of Bangladesh. In: Revised and up-dated edition of a report prepared for the Food and Agriculture Organization of United Nations. University Press, Dhaka, Bangladesh, p 287
- Callén MS, De la Cruz MT, López JM, Mastral AM (2011) PAH in airborne particulate matter.: carcinogenic character of PM₁₀ samples and assessment of the energy generation impact. *Fuel Process Technol* 92(2):176–182
- Campaner P, Luiz-Silva W, Machado W (2014) Geochemistry of acid mine drainage from a coal mining area and processes controlling metal attenuation in stream waters, southern Brazil. *An Acad Bras Cienc* 86(2):539–554
- Campaner P, Luiz-Silva W, Smoak JM, Sanders CJ (2018) Radionuclide enrichment near coal processing in Southern Brazil. *Radiochemistry* 60:215–220

- CCME (Canadian Council of Ministers of the Environment) Proposed compost standards for Canada (1993) Cited in the composting Council of Canada, composting. Canadian environmental quality guidelines
- Cevik U, Damla N, Koz B, Kaya S (2007) Radiological characterization around the Afsin-Elbistan coal-fired power plant in Turkey. *Energy Fuel* 22(1):428–432
- Chabukdhara M, Singh OP (2016) Coal mining in northeast India: an overview of environmental issues and treatment approaches. *Int J Coal Sci Technol* 3(2):87–96
- Charro E, Pardo R, Peña V (2013) Chemometric interpretation of vertical profiles of radionuclides in soils near a Spanish coal-fired power plant. *Chemosphere* 90(2):488–496
- Charro E, Peña V (2013) Environmental impact of natural radionuclides from a coal-fired power plant in Spain. *Radiat Prot Dosim* 153(4):485–495
- Chaudhuri AB (1992) Mine environment and management: an Indian scenario. APH Publishing, New Delhi
- Chen J, Chen P, Yao D, Huang W, Tang S, Wang K, Liu W, Hu Y, Zhang B, Sha J (2017a) Abundance, distribution, and modes of occurrence of uranium in Chinese coals. *Fortschr Mineral* 7(12):1–13
- Chen J, Chen P, Yao D, Huang W, Tang S, Wang K, Liu W, Hu Y, Li Q, Wang R (2017b) Geochemistry of uranium in Chinese coals and the emission inventory of coal-fired power plants in China. *Int Geol Rev* 60(5–6):621–637
- Chen J, Liu G, Jiang M, Chou CL, Li H, Wu B, Zheng L, Jiang D (2011) Geochemistry of environmentally sensitive trace elements in Permian coals from the Huainan coalfield, Anhui, China. *Int J Coal Geol* 88(1):41–54. <https://doi.org/10.1016/j.coal.2011.08.002>
- Cheng Z, Jiang J, Fajardo O, Wang S, Hao J (2013) Characteristics and health impacts of particulate matter pollution in China (2001–2011). *Atmos Environ* 65:186–194
- Coles DG, Ragaini RC, Ondov JM (1978) Behavior of natural radionuclides in western coal-fired power plants. *Environ Sci Technol* 12(4):442–446
- Ćujić M, Dragović S, Đorđević M, Dragović R, Gajić B, Miljanić Š (2015) Radionuclides in the soil around the largest coal-fired power plant in Serbia: radiological hazard, relationship with soil characteristics and spatial distribution. *Environ Sci Pollut Res* 22(13):10317–10330
- Ćujić M, Dragović S, Đorđević M, Dragović R, Gajić B (2016) Environmental assessment of heavy metals around the largest coal fired power plant in Serbia. *Catena* 139:44–52
- Ćujić M, Dragović S, Đorđević M, Dragović R, Gajić B (2017) Reprint of “Environmental assessment of heavy metals around the largest coal fired power plant in Serbia.”. *CATENA* 148(Part 1):26–34. <https://doi.org/10.1016/j.catena.2015.12.018>
- Dai L, Wei H, Wang L (2007) Spatial distribution and risk assessment of radionuclides in soils around a coal-fired power plant: a case study from the city of Baoji, China. *Environ Res* 104(2):201–208. <https://doi.org/10.1016/j.envres.2006.11.005>
- Dai S, Tian L, Chou CL, Zhou Y, Zhang M, Zhao L, Wang J, Yang Z, Cao H, Ren D (2008) Mineralogical and compositional characteristics of Late Permian coals from an area of high lung cancer rate in Xuan Wei, Yunnan, China: occurrence and origin of quartz and chamosite. *Int J Coal Geol* 76(4):318–327. <https://doi.org/10.1016/j.coal.2008.09.001>
- Dai S, Ren D, Chou CL, Finkelman RB, Seredin VV, Zhou Y (2012) Geochemistry of trace elements in Chinese coals: a review of abundances, genetic types, impacts on human health, and industrial utilization. *Int J Coal Geol* 94:3–21. <https://doi.org/10.1016/j.coal.2011.02.003>
- Dai S, Seredin VV, Ward CR, Jiang J, Hower JC, Song X, Jiang Y, Wang X, Gornostaeva T, Li X, Liu H (2014a) Composition and modes of occurrence of minerals and elements in coal combustion products derived from high-Ge coals. *Int J Coal Geol* 121:79–97
- Dai S, Zhao L, Hower JC, Johnston MN, Song W, Wang P, Zhang S (2014) Petrology, mineralogy, and chemistry of size-fractionated fly ash from the Jungar power plant, Inner Mongolia, China, with emphasis on the distribution of rare earth elements. *Energy Fuel* 28(2):1502–1514
- Dai S, Li T, Jiang Y, Ward CR, Hower JC, Sun J, Liu J, Song H, Wei J, Li Q, Xie P (2015) Mineralogical and geochemical compositions of the Pennsylvanian coal in the Hailiushu Mine,

- Daqingshan Coalfield, Inner Mongolia, China: Implications of sediment-source region and acid hydrothermal solutions. *Int J Coal Geol* 137:92–110
- Das SK, Chakrapani GJ (2011) Assessment of trace metal toxicity in soils of Raniganj Coalfield, India. *Environ Monit Assess* 177:63–71. <https://doi.org/10.1007/s10661-010-1618-x>
- Demir I, Hughes RE, DeMaris PJ (2001) Formation and use of coal combustion residues from three types of power plants burning illinois coals. *Fuel* 80(11):1659–1773. [https://doi.org/10.1016/S0016-2361\(01\)00028-X](https://doi.org/10.1016/S0016-2361(01)00028-X)
- Department of Soil Protection (1994) The Netherlands Soil Contamination Guidelines; Target and Intervention Values for Soil Remediation, Reference #DBO/07494013. Ministry of Housing, Spatial Planning and Environment, Netherlands
- Depoi FS, Pozebon D, Kalkreuth WD (2008) Chemical characterization of feed coals and combustion-by-products from Brazilian power plants. *Int J Coal Geol* 76(3):227–236
- Dhar BB, Thakur DN (1996) Mining environment. CRC Press, Boca Raton, FL
- Dias CL, Oliveira MLS, Hower JC, Taffarel SR, Kautzmann RM, Silva LFO (2014) Nanominerals and ultrafine particles from coal fires from Santa Catarina, South Brazil. *Int J Coal Geol* 122:50–60. <https://doi.org/10.1016/j.coal.2013.12.011>
- Din SAM, Yahya NN-HN, Abdullah A (2013) Fine particulates matter (PM_{2.5}) from coal-fired power plant in Manjung and its health impacts. *Procedia Soc Behav Sci* 85:92–99. <https://doi.org/10.1016/j.sbspro.2013.08.341>
- Dontala SP, Reddy TB, Vadde R (2015) Environmental aspects and impacts its mitigation measures of corporate coal mining. *Procedia Earth Planet Sci* 11:2–7. <https://doi.org/10.1016/j.proeps.2015.06.002>
- Dragović S, Mihailović N, Gajić B (2008) Heavy metals in soils: distribution, relationship with soil characteristics and radionuclides and multivariate assessment of contamination sources. *Chemosphere* 72(3):491–495
- Dragović S, Čujić M, Slavković-Beškoski L, Gajić B, Bajat B, Kilibarda M, Onjia A (2013) Trace element distribution in surface soils from a coal burning power production area: a case study from the largest power plant site in Serbia. *Catena* 104:288–296
- Dutta BK, Khanra S, Mallick D (2009) Leaching of elements from coal fly ash: assessment of its potential for use in filling abandoned coal mines. *Fuel* 88:1314–1323. <https://doi.org/10.1016/j.fuel.2009.01.005>
- Dutta M, Saikia J, Taffarel SR, Waanders FB, de Medeiros D, Cutruneo CM, Silva LF, Saikia BK (2017) Environmental assessment and nano-mineralogical characterization of coal, overburden and sediment from Indian coal mining acid drainage. *Geosci Front* 8(6):1285–1297
- Dutta M, Islam N, Rabha S, Narzary B, Bordoloi M, Saikia D, Silva LF, Saikia BK (2019) Acid mine drainage in an Indian high-sulphur coal mining area: cytotoxicity assay and remediation study. *J Hazard Mater* 389:121851
- ECR (The Environment Conservation Rules) (1997) Department of Environment, Ministry of Environment and Forest, Government of the People's Republic of Bangladesh. Poribesh Bhaban E-16, Agargaon, Shere Bangla Nagar Dhaka 1207, Bangladesh, pp 179–226
- EQS (Soil environmental quality) (1995) Chinese Environmental Quality of Standard (EQS) mainly for agricultural soils. In: Chinese Environmental Protection Administration of China (CEPA). China Environmental Science Press, Beijing. (in Chinese)
- Equeenuddin SM, Tripathy S, Sahoo PK, Panigrahi MK (2010) Hydrogeochemical characteristics of acid mine drainage and water pollution at Makum Coalfield, India. *J Geochem Explor* 105(3):75–82
- EU Directive 1998/83/EC (1998) Council Directive 98/83/EC of 3 November 1998 on the quality of water intended for human consumption. *Off J Eur Communities L* 330(32)
- FAO (2011) The State of the World's h Land and Water Resources for Food and Agriculture, (SOLAW) – Managing Systems at Risk. In: Food and Agriculture, Organization of the United Nations. Rome and Earthscan, London
- Fardushe RS, Hoque MM, Roy S (2016) Assessment of soil and water quality of Barapukuria coal mining site, Dinajpur, Bangladesh. *Bangladesh J Sci Res* 27(1):63–73

- Fardy J, McOrist G, Farrar Y (1989) Neutron activation analysis and radioactivity measurements of Australian coals and fly ashes. *J Radioanal Nucl Chem* 133(2):217–226
- Farhaduzzaman M (2013) Characterization of selected petroleum source rocks and reservoir rocks of Bengal Basin (Bangladesh) based on geochemical, petrographical and petrophysical methods. 308p. Ph.D. dissertation, University of Malaya, Malaysia
- Farhaduzzaman M, Abdullah WH, Islam MA, Islam A (2012) Depositional environment and hydrocarbon source potential of the Permian Gondwana coals from the Barapukuria Basin, northwest Bangladesh. *Int J Coal Geol* 90–91:162–179
- Farhaduzzaman M, Abdullah WH, Islam MA, Pearson MJ (2013a) Organic facies variations and hydrocarbon generation potential of Permian Gondwana group coals and associated sediments, Barapukuria and Dighipara basins, NW Bangladesh. *J Petrol Geol* 36:117–137. <https://doi.org/10.1111/jpg.12547>
- Farhaduzzaman M, Abdullah WH, Islam MA (2013b) Petrographic characteristics and palaeoenvironment of the Permian coal resources of the Barapukuria and Dighipara Basins, Bangladesh. *J Asian Earth Sci* 64:272–287
- Farhaduzzaman M, Abdullah WH, Islam MA, Sia SG (2015) Quality Assessment of the permian coals from Dighipara Basin, Bangladesh based on proximate, ultimate and microscopic analyses. *J Bangladesh Acad Sci* 39:177. <https://doi.org/10.3329/jbas.v39i2.25951>
- Fergusson JE (1990) The heavy elements: chemistry, environmental impact and health effects, Civilization of the American Indian series, 1st edn. Pergamon Press, Oxford, p 123
- Finkelman RB, Greb SF (2008) Environmental and health impacts, Chapter 10. In: Suarez-Ruiz I, Crelling JC (eds) Applied coal petrology: the role of petrology in coal utilization. Elsevier/Academic Press, Amsterdam, pp 263–287
- Finkelman RB, Gross PMK (1999) The types of data needed for assessing the environmental and human health impacts of coal. *Int J Coal Geol* 40(2–3):91–101
- Finkelman RB, Orem W, Castranova TCA, Belkin HE, Zheng B, Lerh HE, Maharaj S, Bates AL (2002) Health impacts of coal and coal use: possible solutions. *Int J Coal Geol* 50(1):425–443
- Finkelman RB, Orem WH, Plumlee GS, Selinus O (2018) Applications of geochemistry to medical geology (chapter 17). In: De Vivo B, Blkin HE, Lima A (eds) Environmental geochemistry, 2nd edn. Elsevier, Amsterdam, pp 435–465
- Flues M, Moraes V, Mazzilli BP (2002) The influence of a coal-fired power plant operation on radionuclide concentrations in soil. *J Environ Radioact* 63(3):285–294
- Francis CD, Barber JR (2013) A framework for understanding noise impacts on wildlife: an urgent conservation priority. *Front Ecol Environ* 11(6):305–313
- Frielingsdorf J, Islam SA, Block M, Rahman MM, Rabbani MG (2008) Tectonic subsidence modelling and Gondwana source rock hydrocarbon potential, Northwest Bangladesh Modelling of Kuchma, Singra and Hazipur wells. *Mar Pet Geol* 25(6):553–564
- Fu B, Liu G, Liu Y, Cheng S, Qi C, Sun R (2016) Coal quality characterization and its relationship with geological process of the Early Permian Huainan coal deposits, southern North China. *J Geochem Explor* 166:33–44
- Fungaro D, Izidoro J, Santos F, Wang S (2013) Coal fly ash from Brazilian power plants: chemical and physical properties and leaching characteristics, chapter 5. In: Sarker PK (ed) Fly ash: sources, applications and potential environmental impacts. Environmental science, engineering and technology series. Nova Science Publishers, Hauppauge, New York, pp 145–164
- Galhardi JA, Bonotto DM (2016) Hydrogeochemical features of surface water and groundwater contaminated with acid mine drainage (AMD) in coal mining areas: a case study in southern Brazil. *Environ Sci Pollut Res* 23(18):18911–18927
- Galhardi JA, García-Tenorio R, Bonotto DM, Díaz Francés I, Motta JGJG, García-Tenorio R, Bonotto DM, Díaz Francés I, Motta JGJG (2017a) Natural radionuclides in plants, soils and sediments affected by U-rich coal mining activities in Brazil. *J Environ Radioactivity* 177:37–47. <https://doi.org/10.1016/j.jenvrad.2017.06.001>
- Galhardi JA, García-Tenorio R, Díaz Francés I, Bonotto DM, Marcelli MP (2017b) Natural radionuclides in lichens, mosses and ferns in a thermal power plant and in an adjacent coal

- mine area in southern Brazil. *J Environ Radioactivity* 167:43–53. <https://doi.org/10.1016/j.jenvrad.2016.11.009>
- Gammons CH, Duaiame TE, Parker SR, Poulson SR, Kennelly P (2010) Geochemistry and stable isotope investigation of acid mine drainage associated with abandoned coal mines in central Montana, USA. *Chem Geol* 269:100–112. <https://doi.org/10.1016/j.chemgeo.2009.05.026>
- Gao Q, Li S, Yuan Y, Zhang Y, Yao Q (2015) Ultrafine particulate matter formation in the early stage of pulverized coal combustion of high-sodium lignite. *Fuel* 158:224–231. <https://doi.org/10.1016/j.fuel.2015.05.028>
- Gao J, Wang H, Cai W, Wu J, He Y (2016) Pollution characteristics of atmospheric particulate mercury near a coal-fired power plant on the southeast coast of China. *Atmos Pollut Res* 7 (6):1119–1127
- George J, Masto RE, Ram LC, Das TB, Rout TK, Mohan M (2015) Human exposure risks for metals in soil near a coal-fired power-generating plant. *Arch Environ Contam Toxicol* 68 (3):451–461
- Gollakota AR, Volli V, Shu CM (2019) Progressive utilisation prospects of coal fly ash: a review. *Sci Total Environ* 672:951–989
- Goodarzi F (2006) Assessment of elemental content of milled coal, combustion residues, and stack emitted materials: possible environmental effects for a Canadian pulverized coal-fired power plant. *Int J Coal Geol* 65(1–2):17–25
- Gören E, Turhan Ş, Kurnaz A, Garad AMK, Duran C, Uğur FA, Yeğingil Z (2017) Environmental evaluation of natural radioactivity in soil near a lignite-burning power plant in Turkey. *Appl Radiat Isotopes* 129:13–18. <https://doi.org/10.1016/j.apradiso.2017.07.059>
- Gür F, Yaprak G (2010) Natural radionuclide emission from coal-fired power plants in the southwestern of Turkey and the population exposure to external radiation in their vicinity. *J Environ Sci Health Part A* 45(14):1900–1908
- Guttikunda SK, Jawahar P (2014) Atmospheric emissions and pollution from the coal-fired thermal power plants in India. *Atmos Environ* 92:449–460. <https://doi.org/10.1016/j.atmosen.2014.04.057>
- Habib MA, Basuki T, Miyashita S, Bekelesi W, Nakashima S, Techato K, Khan R, Majlis ABK, Phoungthong K (2019a) Assessment of natural radioactivity in coals and coal combustion residues from a coal-based thermoelectric plant in Bangladesh: implications for radiological health hazards. *Environ Mon Assess*. <https://doi.org/10.1007/s10661-018-7160-y>
- Habib MA, Basuki T, Miyashita S, Bekelesi W, Nakashima S, Phoungthong K, Khan R, Rashid MB, Islam ARMT, Techato K (2019b) Distribution of naturally occurring radionuclides in soil around a coal-based power plant and their potential radiological risk assessment. *Radiochim Acta*. <https://doi.org/10.1515/ract-2018-3044>
- Habib MA, Islam ARMT, Bodrud-Doza M, Mukta FA, Khan R, Siddique MAB, Phoungthong K, Techato K (2020) Simultaneous appraisals of pathway and probable health risk associated with trace metals contamination in groundwater from Barapukuria coal basin, Bangladesh. *Chemosphere* 242:125183 <https://doi.org/10.1016/j.chemosphere.2019.125183>
- Haider AFMY, Rony MA, Lubna RS, Abedin KM (2011) Detection of multiple elements in coal samples from Bangladesh by laser-induced breakdown spectrometer. *Opt Laser Technol* 43 (8):1405–1410
- Hakanson L (1980) An ecological risk index for aquatic pollution control. A sedimentological approach. *Wat Res* 14(8):975–1001
- Halim MA, Majumder RK, Zaman MN, Hossain S, Rasul MG, Sasaki K (2013) Mobility and impact of trace metals in Barapukuria coal mining area, Northwest Bangladesh. *Arab J Geosci* 6 (12):4593–4605
- Halim MA, Majumder RK, Zaman MN (2015) Paddy soil heavy metal contamination and uptake in rice plants from the adjacent area of Barapukuria coal mine, northwest Bangladesh. *Arab J Geosci* 8(6):3391–3401

- Hamid BN, Alam MN, Chowdhury MI, Islam MN (2002) Study of natural radionuclide concentrations in an area of elevated radiation background in the northern districts of Bangladesh. *Radiat Prot Dosim* 98(2):227–230
- Hashan M, Howladar MF, Jahan LN, Deb PK (2013) Ash content and its relevance with the coal grade and environment in Bangladesh. *Int J Sci Eng Res* 4(4):669–676
- Haykiri-Acma H, Yaman S, Ozbek N, Kucukbayrak S (2011) Mobilization of some trace elements from ashes of Turkish lignites in rain water. *Fuel* 90:3447–3455. <https://doi.org/10.1016/j.fuel.2011.06.069>
- HCU (Hydrocarbon Unit) (2018) Report on Energy Scenario of Bangladesh 2017–2018, 2016–17, 2015–16. A glossary of power, energy & mineral resources. Energy and Mineral Resources Division, Government of the Peoples Republic of Bangladesh. <http://hcu.org.bd/site/view/publications/>
- Higginbotham N, Freeman S, Connor L, Albrecht G (2010) Environmental injustice and air pollution in coal affected communities, Hunter Valley, Australia. *Health Place* 16(2):259–266
- Hossain HMZ, Hossain QH (2019) Polycyclic aromatic hydrocarbons (PAHs) in fine fractions of Barapukuria coal in Bangladesh. *Bangladesh J Sci Ind Res* 54(3):203–214
- Hossain HZ, Sultan-Ul-Islam M, Ahmed SS, Hossain I (2002) Analysis of sedimentary facies and depositional environments of the Permian Gondwana sequence in borehole GDH-45, Khalaspir Basin, Bangladesh. *Geosci J* 6(3):227–236
- Hossain HZ, Sampei Y, Hossain QH, Roser BP, Islam MS (2014) Characterization of alkyl phenanthrene distributions in Permian Gondwana coals and coaly shales from the Barapukuria Basin, NW Bangladesh. *Res Org Geochem* 29:17–28
- Hossain MN, Paul SK, Hasan MM (2015) Environmental impacts of coal mine and thermal power plant to the surroundings of Barapukuria, Dinajpur, Bangladesh. *Environ Monit Assess* 187(4):202
- Hossain I, Tsunogae T, Sultan-Ul-Islam M, Roy RR, Talukder S (2017) Mineralogy of Gondwana Sequence in Barapukuria formation, Bangladesh. *Earth Evol Sci* 11:3–22
- Hossain I, Tsunogae T, Tsutsumi Y, Takahashi K (2018) Petrology, geochemistry and LA-ICP-MS U-Pb geochronology of Paleoproterozoic basement rocks in Bangladesh: an evaluation of calc-alkaline magmatism and implication for Columbia supercontinent amalgamation. *J Asian Earth Sci* 157:22–39
- Hossain HZ, Sampei Y, Hossain QH, Yamanaka T, Roser BP, Sultan-Ul-Islam M (2019) Origin of organic matter and hydrocarbon potential of Permian Gondwana coaly shales intercalated in coals/sands of the Barapukuria basin, Bangladesh. *Int J Coal Geol*. <https://doi.org/10.1016/j.coal.2019.05.008>
- Hossain HZ, Hossain QH, Kamei A, Araoka D, Sultan-Ul-Islam M (2020) Geochemical characteristics of Gondwana shales from the Barapukuria basin, Bangladesh: implications for source-area weathering and provenance. *Arab J Geosci* 13(3):111
- Hower JC (2012) Petrographic examination of coal-combustion fly ash. *Int J Coal Geol* 92:90–97
- Hower JC, Rathbone RF, Robertson JD, Peterson G, Trimble AS (1999) Petrology, mineralogy, and chemistry of magnetically-separated sized fly ash. *Fuel* 78(2):197–203
- Hower JC, Campbell JI, Teesdale WJ, Nejedly Z, Robertson JD (2008) Scanning proton microprobe analysis of mercury and other trace elements in Fe-sulfides from a Kentucky coal. *Int J Coal Geol* 75(2):88–92
- Hower JC, Dai S, Eskenazy G (2016) Distribution of uranium and other radionuclides in coal and coal combustion products, with discussion of occurrences of combustion products in Kentucky power plants. *Coal Combust Gasification Prod* 8:44–53
- Hower JC, Groppo JG, Graham UM, Ward CR, Kostova IJ, Maroto-Valer MM, Dai S (2017a) Coal-derived unburned carbons in fly ash: a review. *Int J Coal Geol* 179:11–27
- Hower JC, Henke KR, Dai S, Ward CR, French D, Liu S, Graham UM (2017b) Generation and nature of coal fly ash and bottom ash, chapter 2. In: Robl T, Oberlink A, Jones R (eds) *Coal combustion products (CCPs): characteristics, utilization and beneficiation*. Woodhead Publishing, Duxford, UK, pp 21–65

- Howladar MF (2013) Coal mining impacts on water environs around the Barapukuria coal mining area, Dinajpur, Bangladesh. *Environ Earth Sci* 70(1):215–226
- Howladar MF (2016) Environmental impacts of subsidence around the Barapukuria Coal Mining area in Bangladesh. *Energy Ecol Environ* 1(6):370–385
- Howladar MF (2017) An assessment of surface water chemistry with its possible sources of pollution around the Barapukuria Thermal Power Plant Impacted Area, Dinajpur, Bangladesh. *Groundwater Sustain Dev* 5:38–48. <https://doi.org/10.1016/j.gsd.2017.03.004>
- Howladar F, Hasan MK (2014) A study on the development of subsidence due to the extraction of 1203 slice with its associated factors around Barapukuria underground coal mining industrial area, Dinajpur, Bangladesh. *Environ Earth Sci* 72:3699–3713
- Howladar MF, Islam MR (2016) A study on physico-chemical properties and uses of coal ash of Barapukuria coal fired thermal power plant, Dinajpur, for environmental sustainability. *Energy Ecol Environ* 1(4):233–247
- Howladar MF, Deb PK, Muzemder ASH, Ahmed M (2014) Evaluation of water resources around Barapukuria coal mining industrial area, Dinajpur, Bangladesh. *Appl Water Sci* 4(3):203–222
- Howladar MF, Deb P, Muzemder ASH (2017) Monitoring the underground roadway water quantity and quality for irrigation use around the Barapukuria coal mining industry, Dinajpur, Bangladesh. *Groundwater Sustain Dev* 4:23–34. <https://doi.org/10.1016/j.gsd.2016.11.002>
- Huang Q, Li S, Li G, Zhao Y, Yao Q (2016a) Reduction of fine particulate matter by blending lignite with semi-char in a down-fired pulverized coal combustor. *Fuel* 181:1162–1169. <https://doi.org/10.1016/j.fuel.2016.04.026>
- Huang X, Li N, Wu Q, Long J, Luo D, Zhang P, Yao Y, Huang X, Li D, Lu Y, Liang J (2016b) Risk assessment and vertical distribution of thallium in paddy soils and uptake in rice plants irrigated with acid mine drainage. *Environ Sci Pollut Res* 23(24):24912–24921
- Huang X, Hu J, Qin F, Quan W, Cao R, Fan M, Wu X (2017) Heavy metal pollution and ecological assessment around the Jinsha Coal-Fired Power Plant (China). *Int J Environ Res Public Health* 14(12):1589
- Huggins F, Goodarzi F (2009) Environmental assessment of elements and polyaromatic hydrocarbons emitted from a Canadian coal-fired power plant. *Int J Coal Geol* 77(3–4):282–288. <https://doi.org/10.1016/j.coal.2008.07.009>
- IEA (International Energy Agency) (2017) World energy outlook report 2017. Paris, France
- Imam B (2013) Energy resources of Bangladesh. University Grants Commission, Dhaka, Bangladesh
- Imam B, Rahman M, Akhter SH (2002) Coalbed methane prospect of Jamalganj coalfield, Bangladesh. *Arab J Sci Eng* 27:17–27
- Islam MS (1998) Origin of thick coal seam in the Gondwana Sequence of the Jamalganj basin, Bangladesh. *J Nepal Geol Soc* 18:289–298
- Islam MS (2002) Stratigraphy and Sedimentology of Gondwana rocks in the Barapukuria basin, Dinajpur District, Bangladesh. Ph.D. thesis, Jahangirnagar University, Bangladesh
- Islam MA (2008) A study on the distribution of trace elements in Barapukuria coal by neutron activation analysis and its impact on the environment. M.Phil. thesis. 118p. Bangladesh University of Engineering and Technology, Bangladesh
- Islam MR (2009) Geo-environmental hazards associated with multi-slice longwall mining of the Gondwana Barapukuria coal basin, NW Bangladesh: Constraints from numerical simulation. Ph.D. dissertation. 208p. University of the Ryukyus, Japan
- Islam MR, Hayashi D (2008) Geology and coal bed methane resource potential of the Gondwana Barapukuria Coal Basin, Dinajpur, Bangladesh. *Int J Coal Geol* 75(3):127–143
- Islam S, Khan MZR (2017) A review of energy sector of Bangladesh. *Energy Procedia* 110:611–618
- Islam MN, Uddin MN, Resan SA, Islam MS, Ali MW (1992) Geology of the Khalaspir Coal Basin, Rangpur, Bangladesh, Records of the Geological Survey of Bangladesh. Government Publication, Dhaka, Bangladesh, 6(5).

- Islam MA, Latif SA, Hossain SM, Uddin MS, Podder J (2011) The concentration and distribution of trace elements in coals and ashes of the Barapukuria thermal power plant, Bangladesh. *Energy Sources Part A* 33(9):898–898
- Islam MA, Romić D, Akber MA, Romić M (2018) Trace metals accumulation in soil irrigated with polluted water and assessment of human health risk from vegetable consumption in Bangladesh. *Environ Geochem Health* 40(1):59–85. <https://doi.org/10.1007/s10653-017-9907-8>
- Islam ARMT, Hasanuzzaman M, Islam HMT, Mia MU, Khan R, Habib MA, Rahman MM, Siddique MAB, Moniruzzaman M, Rashid MB (2020) Quantifying source apportionment, co-occurrence and ecotoxicological risk of metals from up-mid-downstream river segments, Bangladesh. *Environ Toxicol Chem.* <https://doi.org/10.1002/etc.4814>
- Izquierdo M, Querol X (2012) Leaching behaviour of elements from coal combustion fly ash: an overview. *Int J Coal Geol* 94:54–66. <https://doi.org/10.1016/j.coal.2011.10.006>
- Jain RK, Cui ZC, Domen JK (2016a) Environmental impacts of mining. In: *Environmental impact of mining and mineral processing*, Chapter 4. Butterworth-Heinemann, Boston, pp 53–157
- Jain RK, Cui ZC, Domen JK (2016b) Mitigation measures and control technology for environmental and human impacts. In: *Environmental impact of mining and mineral processing*, Chapter 7. Butterworth-Heinemann, Boston, pp 53–157
- Jambhulkar HP, Shaikh SMS, Kumar MS (2018) Fly ash toxicity, emerging issues and possible implications for its exploitation in agriculture; Indian scenario: a review. *Chemosphere* 213:333–344
- Jayaranjan MLD, Van Hullebusch ED, Annachhatre AP (2014) Reuse options for coal fired power plant bottom ash and fly ash. *Rev Environ Sci Biotechnol* 13(4):467–486
- Jegadeesan G, Al-Abed SR, Pinto P (2008) Influence of trace metal distribution on its leachability from coal fly ash. *Fuel* 87(10–11):1887–1893. <https://doi.org/10.1016/j.fuel.2007.12.007>
- Jelic TM, Estalilla OC, Sawyer-Kaplan PR, Plata MJ, Powers JT, Emmett M, Kuenstner JT (2017) Coal mine dust desquamative chronic interstitial pneumonia: a precursor of dust-related diffuse fibrosis and of emphysema. *Int J Occup Environ Med* 8(3):153–165
- Jiang Y, Chao S, Liu J, Yang Y, Chen Y, Zhang A, Cao H (2017) Source apportionment and health risk assessment of heavy metals in soil for a township in Jiangsu Province, China. *Chemosphere* 168:1658–1668
- Juwarakar AA, Jambhulkar HP (2008) Restoration of fly ash dump through biological interventions. *Environ Monit Assess* 139(1–3):355–365
- Kabata-Pendias A, Pendias H (1984) *Trace elements in soils and plants*. CRC Press, Boca Raton, FL
- Kabir SM, Imam B (2013) Geological factors contributing to high-heat in part of Barapukuria underground coal mine. *Bangladesh J Geol* 31(32):70–83
- Kalia PF, Tang D (2017) Environmental pollutants and neurodevelopment: review of benefits from closure of a coal-burning power plant in Tongliang, China. *Global Pediatric Health* 4. <https://doi.org/10.1177/2333794X17721609>
- Karamanis D, Ioannides K, Stamoulis K (2009) Environmental assessment of natural radionuclides and heavy metals in waters discharged from a lignite-fired power plant. *Fuel* 88(10):2046–2052. <https://doi.org/10.1016/j.fuel.2009.02.032>
- Karayığit Aİ, Mastalerz M, Oskay RG, Gayer RA (2018) Coal petrography, mineralogy, elemental compositions and palaeoenvironmental interpretation of Late Carboniferous coal seams in three wells from the Kozlu coalfield (Zonguldak Basin, NW Turkey). *Int J Coal Geol* 187:54–70
- Keegan TJ, Farago ME, Thornton I, Hong B, Colvile RN, Pesch B, Jakubis P, Nieuwenhuijsen MJ (2006) Dispersion of As and selected heavy metals around a coal-burning power station in central Slovakia. *Sci Total Environ* 358(1–3):61–71. <https://doi.org/10.1016/j.scitoten.2005.03.020>
- Ketris MP, Yudovich YE (2009) Estimations of clarkes for carbonaceous biolithes: world averages for trace element contents in black shales and coals. *Int J Coal Geol* 78(2):135–148. <https://doi.org/10.1016/j.coal.2009.01.002>
- Khan AA (1991) Tectonics of the Bengal Basin. *J Himalayan Geol* 2(1):91–101

- Khan M, Tuli NN, Ahmed SIU (2014) Impact of particulate matter emission from Barapukuria coal-fired thermal power plant on premature human mortality. Unpublished B.Sc. project, East West University, Bangladesh
- Khan R, Rouf MA, Das S, Tamim U, Naher K, Podder J, Hossain SM (2017a) Spatial and multi-layered assessment of heavy metals in the sand of Cox's-Bazar beach of Bangladesh. *Reg Stud Mar Sci* 16:171–180. <https://doi.org/10.1016/j.rsma.2017.09.003>
- Khan MHR, Seddique AA, Rahman A, Shimizu Y (2017b) Heavy metals contamination assessment of water and soils in and around Barapukuria coal mine area, Bangladesh. *Am J Environ Prot* 6 (4):80
- Khan R, Parvez MS, Tamim U, Das S, Islam MA, Naher K, Khan MHR, Nahid F, Hossain SM (2018) Assessment of rare earth elements, Th and U profile of a site for a potential coal based power plant by instrumental neutron activation analysis. *Radiochim Acta* 106:515–524. <https://doi.org/10.1515/ract-2017-2867>
- Khan R, Das S, Kabir S, Habib MA, Naher K, Islam MA, Tamim U, Rahman AR, Deb AK, Hossain SM (2019a) Evaluation of the elemental distribution in soil samples collected from ship-breaking areas and an adjacent island. *J Environ Chem Eng* 7. <https://doi.org/10.1016/j.jece.2019.103189>
- Khan R, Parvez MS, Jolly YN, Haydar MA, Alam MF, Khatun MA, Sarker MMR, Habib MA, Tamim U, Das S, Sultana S (2019b) Elemental abundances, natural radioactivity and physico-chemical records of a southern part of Bangladesh: implication for assessing the environmental geochemistry. *Environ Nanotechnol Monit Manag* 12:100225. <https://doi.org/10.1016/j.enmm.2019.100225>
- Khan R, Ghosal S, Sengupta D, Tamim U, Hossain SM, Agrahari S (2019c) Studies on heavy mineral placers from eastern coast of Odisha, India by instrumental neutron activation analysis. *J Radioanal Nucl Chem* 319(1):471–484. <https://doi.org/10.1007/s10967-018-6250-1>
- Khan R, Islam MS, Tareq ARM, Naher K, Islam ARMT, Habib MA, Siddique MAB, Islam MA, Das S, Rashid MB, Ullah AKMA, Miah MMH, Masrura SU, Bodrud-Doza M, Sarker MR, Badruzzaman ABM (2020) Elemental and polycyclic aromatic hydrocarbons distributions in the sediments of an urban river: influence of anthropogenic runoffs. *Environ Nanotechnol Monit Manag* 14. <https://doi.org/10.1016/j.enmm.2020.100318>
- Khan R, Islam HMT, Islam ARMT (2021) Mechanism of elevated radioactivity in Teesta river basin from Bangladesh: radiochemical characterization, provenance and associated hazards. *Chemosphere* 264(1):128459. <https://doi.org/10.1016/j.chemosphere.2020.128459>
- Khandekar MP, Bhide AD, Sajwan KS (1999) Trace elements in Indian coal and coal fly ash (chapter 6). In: Sajwan KS, Alva AK, Keefer RF (eds) *Biogeochemistry of trace elements in coal and coal combustion byproducts*. Springer, Boston, MA, pp 99–113
- Khillare PS, Jyethi DS, Sarkar S (2012) Health risk assessment of polycyclic aromatic hydrocarbons and heavy metal via dietary intake of vegetables grown in the vicinity of thermal power plants. *Food Chem Toxicol* 50(5):1642–1652
- Kim JY, Chon HT (2001) Pollution of a water course impacted by acid mine drainage in the Imgok creek of the Gangreung coal field, Korea. *Appl Geochem* 16(11–12):1387–1396
- Kim KH, Kabir E, Kabir S (2015) A review on the human health impact of airborne particulate matter. *Environ Int* 74:136–143
- Kolker A (2012) Minor element distribution in iron disulfides in coal: a geochemical review. *Int J Coal Geol* 94:32–43. <https://doi.org/10.1016/j.coal.2011.10.011>
- Kollipara K, Chugh YP, Mondal K (2014) Physical, mineralogical and wetting characteristics of dusts from Interior Basin coal mines. *Int J Coal Geol* 127:75–87
- Kolo MT, Khandaker MU, Amin YM, Hasiah W, Abdullah WHB (2016) Quantification and radiological risk estimation due to the presence of natural radionuclides in Maiganga coal, Nigeria. *PLoS One* 11(6):1–13
- Koukouzas N (2007) Mineralogy and geochemistry of diatomite associated with lignite seams in the Komnina Lignite Basin, Ptolemais, Northern Greece. *Int J Coal Geol* 71:276–286. <https://doi.org/10.1016/j.coal.2006.09.002>

- Koukouzas NK, Zeng R, Perdikatsis XW, Kakaras EK (2006) Mineralogy and geochemistry of Greek and Chinese coal fly ash. *Fuel* 85(16):2301–2309. <https://doi.org/10.1016/j.fuel.2006.02.019>
- Kujawski R (2011) Long-term drought effects on trees and shrubs. The Center for Agriculture, Food and the Environment
- Kulshrestha U (2013) Acid rain. In: *Encyclopedia of environmental management*, vol 1. Taylor & Francis, New York, pp 8–22
- Kurth L, Kolker A, Engle M, Geboy N, Hendryx M, Orem W, McCawley M, Crosby L, Tatu C, Varonka M, DeVera C (2015) Atmospheric particulate matter in proximity to mountaintop coal mines: sources and potential environmental and human health impacts. *Environ Geochem Health* 37(3):529–544
- Laraia M (2015) Radioactive contamination and other environmental impacts of waste from nuclear and conventional power plants, medical and other industrial sources (chapter 2). In: Velzen L (ed) *Environmental remediation and restoration of contaminated nuclear and norm sites*. Woodhead Publishing, Cambridge, UK, pp 35–56
- Lauer N, Vengosh A, Dai S (2017) Naturally occurring radioactive materials in uranium-rich coals and associated coal combustion residues from China. *Environ Sci Technol* 51(22):13487–13493
- Lestiani DD, Santoso M, Kurniawati S, Adventini N, Prakoso DD (2015) Characteristics of feed coal and particulate matter in the vicinity of coal-fired Power Plant in Cilacap, Central Java, Indonesia. *Procedia Chem* 16:216–221. <https://doi.org/10.1016/j.proche.2015.12.044>
- Li J, Zhuang X, Querol X, Font O, Moreno N, Zhou J (2012a) Environmental geochemistry of the feed coals and their combustion by-products from two coal-fired power plants in Xinjiang Province, Northwest China. *Fuel* 95:446–456. <https://doi.org/10.1016/j.fuel.2011.10.025>
- Li Y, Guo Y, Li P, Ding QW, Cao Z (2012b) Air pollutant emissions from coal fired power plants. *Open J Air Pollut* 1:37–41
- Li Z, Ma Z, van der Kuijp TJ, Yuan Z, Huang L (2014) A review of soil heavy metal pollution from mines in China: pollution and health risk assessment. *Sci Total Environ* 468:843–853
- Li J, Zhuang X, Querol X, Font O, Moreno N (2018) A review on the applications of coal combustion products in China. *Int Geol Rev* 60(5–6):671–716
- Liang J, Feng C, Zeng G, Gao X, Zhong M, Li X, Li X, He X, Fang Y (2017) Spatial distribution and source identification of heavy metals in surface soils in a typical coal mine city, Lianyuan, China. *Environ Pollut* 225:681–690
- Liu G, Niu Z, Van Niekerk D, Xue J, Zheng L (2008) Polycyclic aromatic hydrocarbons (PAHs) from coal combustion: emissions, analysis, and toxicology. In: *Reviews of environmental contamination and toxicology*. Springer, New York, pp 1–28
- Liu J, Liu G, Zhang J, Yin H, Wang R (2012a) Occurrence and risk assessment of polycyclic aromatic hydrocarbons in soil from the Tiefsa coal mine district, Liaoning, China. *J Environ Monit* 14(10):2634–2642
- Liu F, Luo HB, Zhu J, Yuan J (2012b) Mobility of metals from fly ashes and its potential impact on surface water quality in Guizhou Province, southwestern China. In: *Applied mechanics and materials*, vol 178. Trans Tech Publications, New York, pp 503–506
- Liu G, Luo Q, Ding M, Feng J (2015) Natural radionuclides in soil near a coal-fired power plant in the high background radiation area, South China. *Environ Monit Assess* 187(6):356
- Lu X, Li LY, Wang F, Wang L, Zhang X (2012a) Radiological hazards of coal and ash samples collected from Xi'an coal-fired power plants of China. *Environ Earth Sci* 66(7):1925–1932
- Lu X, Zhao C, Chen C, Liu W (2012b) Radioactivity level of soil around Baqiao coal-fired power plant in China. *Radiat Phys Chem* 81(12):1827–1832
- Lu X, Liu W, Zhao C, Chen C (2013) Environmental assessment of heavy metal and natural radioactivity in soil around a coal-fired power plant in China. *J Radioanal Nucl Chem* 295(3):1845–1854
- Luo W, Lu Y, Giesy JP, Wang T, Shi Y, Wang G, Xing Y (2007) Effects of land use on concentrations of metals in surface soils and ecological risk around Guanting Reservoir, China. *Environ Geochem Health* 29(6):459–471

- Maanan M, Saddik M, Maanan M, Chaibi M, Assobhei O, Zourarah B (2014) Environmental and ecological risk assessment of heavy metals in sediments of Nador lagoon, Morocco. *Ecol Indic* 48:616–626
- Mahur AK, Gupta M, Varshney R, Sonkawade RG, Verma KD, Prasad R (2013) Radon exhalation and gamma radioactivity levels in soil and radiation hazard assessment in the surrounding area of National Thermal Power Corporation, Dadri (UP), India. *Radiat Meas* 50:130–135
- Mandal A, Sengupta D (2003) Radioelemental study of Kolaghat thermal power plant, West Bengal, India: possible environmental hazards. *Environ Geol* 44:180–186. <https://doi.org/10.1007/s00254-002-0744-3>
- Mandal A, Sengupta D (2005) Radionuclide and trace element contamination around Kolaghat Thermal Power Station, West Bengal—environmental implications. *Curr Sci* 88(4):617–624
- Mandal A, Sengupta D (2006) An assessment of soil contamination due to heavy metal around a coal-fired thermal power plant in India. *Environ Geol* 51(3):409–420. <https://doi.org/10.1007/s00254-006-0336-8>
- Manohar GK, Kandalgaonkar SS, Sholapurkar SM (1989) Effects of thermal power plant emissions on atmospheric electrical parameters. *Atmos Environ* 23(4):843–850
- Martinello K, Oliveira MLS, Molossi FA, Ramos CG, Teixeira EC, Kautzmann RM, Oliveira MLS, Ward CR (2014) Direct identification of hazardous elements in ultra-fine and nanominerals from coal fly ash produced during diesel co-firing. *Sci Total Environ* 470–471:444–452. <https://doi.org/10.1016/j.scitotenv.2013.10.007>
- Masud MH, Shakib MN, Rokonzaman M (2014) Study of environmental impacts of the Barapukuria Thermal Power Plant of Bangladesh. *Global J Res Eng*
- McGrath SP (1997) Behaviour of trace elements in terrestrial ecosystems. In: Prost R (ed) *Contaminated soils*. INRA, Paris, pp 35–54
- Medina A, Gamero P, Querol X, Moreno N, De León B, Almanza M, Vargas G, Izquierdo M, Font O (2010) Fly ash from a Mexican mineral coal I: mineralogical and chemical characterization. *J Hazard Mater* 181(1–3):82–90
- Medunić G, Ahel M, Mihalić IB, Srček G, Kopjar N, Fiket Ž, Bituh T, Mikac I (2016) Toxic airborne S, PAH, and trace element legacy of the superhigh-organic-sulphur Raša coal combustion: cytotoxicity and genotoxicity assessment of soil and ash. *Sci Total Environ* 566:306–319
- Medunić G, Kuharić Ž, Fiket Ž, Bajramović M, Singh AL, Krivohlavek A, Kniewald G, Dujmović L (2018) Selenium and other potentially toxic elements in vegetables and tissues of three non-migratory birds exposed to soil, water, and aquatic sediment contaminated with seleniferous Raša coal. *Rudarsko-geološko-naftni zbornik* 33(3):53–62
- Meij R, Te Winkel BH (2009) Trace elements in world steam coal and their behavior in Dutch coal-fired power stations: a review. *Int J Coal Geol* 77(3–4):289–293
- Michalik B, Brown J, Krajewski P (2013) The fate and behaviour of enhanced natural radioactivity with respect to environmental protection. *Environ Impact Assess Rev* 38:163–171
- Mishra UC (2004) Environmental impact of coal industry and thermal power plants in India. *J Environ Radioact* 72(1–2):35–40
- Mishra N, Das N (2017) Coal mining and local environment: A study in Talcher coalfield of India. *Air Soil Water Res* 10:1178622117728913
- Monir MMU, Hossain HZ (2012) Coal mine accidents in Bangladesh: its causes and remedial measures. *Int J Econ Environ Geol* 3(2):33–40
- Moreno N, Querol X, Andrés JM, Stanton K, Towler M, Nugteren H, Janssen-Jurkovicová M, Jones R (2005) Physico-chemical characteristics of European pulverized coal combustion fly ashes. *Fuel* 84(11):1351–1363. <https://doi.org/10.1016/j.fuel.2004.06.038>
- Mukherjee KN, Dutta NR, Chandra D, Pandalai HS, Singh MP (1988) A statistical approach to the study of the distribution of trace elements and their organic/inorganic affinity in Lower Gondwana coals of India. *Int J Coal Geol* 10(1):99–108. [https://doi.org/10.1016/0166-5162\(88\)90007-9](https://doi.org/10.1016/0166-5162(88)90007-9)

- Müller G (1981) Die schwermetallbelastung der sedimente des neckars und seiner nebenflüsse: eine bestandsaufnahme. *Chemiker-Zeitung* 105:157–164
- Munawer ME (2018) Human health and environmental impacts of coal combustion and post-combustion wastes. *J Sustain Mining* 17(2):87–96
- NEPC (National Environmental Protection Council) (2013) National Environment Protection Measures. Assessment of Site Contamination – Guideline on Investigation Levels for Soil and Groundwater 2013. Canberra, Australia, National Environmental Protection Council
- Noli F, Tsamos P (2016) Concentration of heavy metals and trace elements in soils, waters and vegetables and assessment of health risk in the vicinity of a lignite-fired power plant. *Sci Total Environ* 563:377–385
- Noli F, Tsamos P, Stoulos S (2017) Spatial and seasonal variation of radionuclides in soils and waters near a coal-fired power plant of Northern Greece: environmental dose assessment. *J Radioanal Nucl Chem* 311(1):331–338
- Norman PS (1992) Evaluation of the Barapukuria coal deposit NW Bangladesh. *Geol Soc Lond Spec Publ* 63(1):107–120
- Oliveira ML, Ward CR, French D, Hower JC, Querol X, Silva LF (2012) Mineralogy and leaching characteristics of beneficiated coal products from Santa Catarina, Brazil. *Int J Coal Geol* 94:314–325
- Oliveira MLS, Marostega F, Taffarel SR, Saikia BK, Waanders FB, DaBoit K, Baruah BP, Silva LFO (2014) Nano-mineralogical investigation of coal and fly ashes from coal-based captive power plant (India): An introduction of occupational health hazards. *Sci Total Environ* 468–469:1128–1137. <https://doi.org/10.1016/j.scitotenv.2013.09.040>
- Orem WH, Finkelman RB (2014) Coal formation and geochemistry (chapter 9.8). In: Holland IHD, Turekian KK (eds) *Treatise on geochemistry*, 2nd edn. Elsevier, Oxford, pp 207–232
- Ouyang ZZ, Gao LM, Yang C (2018) Distribution, sources and influence factors of polycyclic aromatic hydrocarbon at different depths of the soil and sediments of two typical coal mining subsidence areas in Huainan, China. *Ecotoxicol Environ Saf* 163:255–265
- Ozden B, Guler E, Vaasma T, Horvath M, Kiisk M, Kovacs T (2018) Enrichment of naturally occurring radionuclides and trace elements in Yatagan and Yenikoy coal-fired thermal power plants, Turkey. *J Environ Radioact* 188:100–107
- Özkul C (2016) Heavy metal contamination in soils around the Tunçbilek thermal power plant (Kütahya, Turkey). *Environ Monit Assess* 188(5):284
- Pak YN, Pak DY, Ponomaryova M, Baizbayev MB, Zhelayeva N (2018) Radioactivity of coal and its combustion wastes. *Coke Chem* 61(5):188–192
- Pandey VC, Abhilash PC, Singh N (2009) The Indian perspective of utilizing fly ash in phytoremediation, phytomanagement and biomass production. *J Environ Manag* 90:2943–2958. <https://doi.org/10.1016/j.jenvman.2009.05.001>
- Pandey C, Singh JS, Singh RP, Singh N, Yunus M (2011) Arsenic hazards in coal fly ash and its fate in Indian scenario. *Resour Conserv Recycl* 55(9–10):819–835. <https://doi.org/10.1016/j.resconrec.2011.04.005>
- Pandey B, Agrawal M, Singh S (2014) Coal mining activities change plant community structure due to air pollution and soil degradation. *Ecotoxicology* 23(8):1474–1483
- Papaefthymiou H, Manousakas M, Fouskas A, Siavalas G (2013) Spatial and vertical distribution and risk assessment of natural radionuclides in soils surrounding the lignite-fired power plants in Megalopolis basin, Greece. *Radiat Prot Dosim* 156(1):49–58
- Papastefanou C (2010) Escaping radioactivity from coal-fired power plants (CPPs) due to coal burning and the associated hazards: a review. *J Environ Radioact* 101(3):191–200
- Papp Z, Dezső Z, Daroczy S (2002) Significant radioactive contamination of soil around a coal-fired thermal power plant. *J Environ Radioact* 59(2):191–205
- Parial K, Guin R, Agrahari S, Sengupta D (2016) Monitoring of radionuclide migration around Kolaghat thermal power plant, West Bengal, India. *J Radioanal Nucl Chem* 307(1):533–539. <https://doi.org/10.1007/s10967-015-4152-z>

- Pastrana-Corral MA, Wakida FT, Temores-Peña J, Rodríguez-Mendivil DD, García-Flores E, Piñon-Colin TDJ, Quiñonez-Plaza A (2017) Heavy metal pollution in the soil surrounding a thermal power plant in Playas de Rosarito, Mexico. *Environ Earth Sci* 76(16):583. <https://doi.org/10.1007/s12665-017-6928-7>
- Pavlov SK, Chudnenko KV (2015) Hydrogeochemical processes of wastewater leakage purification from a thermal power plant. *J Environ Sci Health A* 50(7):719–727
- Phoungthong K, Techato K (2018) Evaluating the potential reutilizing of fly ash and bottom ash in Thailand. *Iran J Public Health* 47(6):917
- Pinetown KL, Ward CR, Van der Westhuizen WA (2007) Quantitative evaluation of minerals in coal deposits in the Witbank and Highveld Coalfields, and the potential impact on acid mine drainage. *Int J Coal Geol* 70(1–3):166–183
- Podder J, Tarek SA, Hossain T (2004) Trace elemental analysis of Permian Gondana coals in Bangladesh by PIXE technique. *Int J PIXE* 14(3 & 4):89–97
- Pokale WK (2012) Effects of thermal power plant on environment. *Sci Rev Chem Commun* 2(3):212–215
- Quamruzzaman C, Murshed S, Ferdous JA, Khan P, Sharmeen S (2014) An expedient reckoning of miners hygiene in Barapukuria coal mine and Maddhapara granite mine, Dinajpur, Bangladesh. *Int J Emerg Technol Adv Eng* 4(3):489–498
- Querol X, Alastuey A, Lopez-Soler A, Mantilla E, Plana F (1996a) Mineral composition of atmospheric particulates around a large coal-fired power station. *Atmos Environ* 30:3557–3572
- Querol X, Juan R, Lopez-Soler A, Fernandez-Turiel J, Ruiz CR (1996b) Mobility of trace elements from coal and combustion wastes. *Fuel* 75(7):821–838
- Querol X, Zhuang X, Font O, Izquierdo M, Alastuey A, Castro I, Drooge BL, Moreno T, Grimalt JO, Elvira J, Cabañas M, Bartroli R, Hower JC, Ayora C, Plana F, Cab López-Soler A (2011) Influence of soil cover on reducing the environmental impact of spontaneous coal combustion in coal waste gobs: a review and new experimental data. *Int J Coal Geol* 85(1):2–22. <https://doi.org/10.1016/j.coal.2010.09.002>
- Rabha S, Saikia J, Subramanyam KS, Hower JC, Hood MM, Khare P, Saikia BK (2018) Geochemistry and nanomineralogy of feed coals and their coal combustion residues from two different coal-based industries in northeast India. *Energy Fuel* 32(3):3697–3708
- Raja R, Nayak AK, Shukla AK, Rao KS, Gautam P, Lal B, Patra DK (2015) Impairment of soil health due to fly ash-fugitive dust deposition from coal-fired thermal power plants. *Environ Monit Assess* 187(11). <https://doi.org/10.1007/s10661-015-4902-y>
- Ram LC, Masto RE (2010) An appraisal of the potential use of fly ash for reclaiming coal mine spoil. *J Environ Manag* 91(3):603–617
- Ramya SS, Deshmukh U, Khandekar J, Padmakar C, SuriNaidu L, Mahore PK, Pujari PR, Panaskar D, Labhasetwar PK, Rao SG (2013) Assessment of impact of ash ponds on groundwater quality: a case study from Koradi in Central India. *Environ Earth Sci* 69(7):2437–2450. <https://doi.org/10.1007/s12665-012-2071-7>
- Rashid B, Islam SU, Badrul I (2018) Structure and lineaments of the Northwestern Part of Bangladesh and evolution of the Barind Tract. *Am J Earth Sci* 5(3):26–36
- Rashid MB, Islam MS, Badrul I (2015) Evidences of neotectonic activities as reflected by drainage characteristics of the Mahananda River floodplain and its adjoining areas, Bangladesh. *Am J Earth Sci* 2(4):61–70. <http://www.openscienceonline.com/journal/ajes>
- Ribeiro J, da Silva EF, Li Z, Ward C, Flores D (2010a) Petrographic, mineralogical and geochemical characterization of the Serrinha coal waste pile (Douro Coalfield, Portugal) and the potential environmental impacts on soil, sediments and surface waters. *Int J Coal Geol* 83(4):456–466. <https://doi.org/10.1016/j.coal.2010.06.006>
- Ribeiro J, Flores D, Ward CR, Silva LF (2010b) Identification of nanominerals and nanoparticles in burning coal waste piles from Portugal. *Sci Total Environ* 408(23):6032–6041
- Ribeiro J, DaBoit K, Flores D, Kronbauer MA, Silva LFO (2013) Extensive FE-SEM/EDS, HR-TEM/EDS and ToF-SIMS studies of micron- to nano-particles in anthracite fly ash. *Sci Total Environ* 452:98–107

- Ribeiro J, Silva TF, Mendonça Filho JG, Flores D (2014) Fly ash from coal combustion: an environmental source of organic compounds. *Appl Geochem* 44:103–110
- Ribeiro J, Suárez-Ruiz I, Flores D (2016) Geochemistry of self-burning coal mining residues from El Bierzo Coalfield (NW Spain): environmental implications. *Int J Coal Geol* 159:155–168. <https://doi.org/10.1016/j.coal.2016.04.006>
- Rizwan SA, Nongkynrih B, Gupta SK (2013) Air pollution in Delhi: its magnitude and effects on health. *Indian J Community Med* 38(1):4
- Rodriguez-Irretagoiena A, de Vallejuelo SF-O, Gredilla A, Ramos CG, Oliveira MLS, Arana G, de Diego A, Madariaga JM, Silva LFO (2015) Fate of hazardous elements in agricultural soils surrounding a coal power plant complex from Santa Catarina (Brazil). *Sci Total Environ* 508:374–382. <https://doi.org/10.1016/j.scitotenv.2014.12.015>
- Rosner G, Bunzl K, Hötzl H, Winkler R (1984) Low level measurements of natural radionuclides in soil samples around a coal-fired power plant. *Nucl Instrum Methods Phys Res* 223 (2–3):585–589
- Roy DK, Roser BP (2013) Climatic control on the composition of Carboniferous–Permian Gondwana sediments, Khalaspir basin, Bangladesh. *Gondwana Res* 23(3):1163–1171
- Rudnick RL, Gao S (2014) Composition of the continental crust. In: *Treatise on geochemistry*, 2nd edn. Elsevier, San Diego, pp 1–64
- Sahoo PK, Bhattacharyya P, Tripathy S, Equeenuddin SM, Panigrahi MK (2010) Influence of different forms of acidities on soil microbiological properties and enzyme activities at an acid mine drainage contaminated site. *J Hazard Mater* 179(1–3):966–975
- Sahoo PK, Tripathy S, Equeenuddin SM, Panigrahi MK (2012) Geochemical characteristics of coal mine discharge vis-à-vis behavior of rare earth elements at Jaintia Hills coalfield, northeastern India. *J Geochem Explor* 112:235–243
- Sahoo PK, Tripathy S, Panigrahi MK, Equeenuddin SM (2014) Geochemical characterization of coal and waste rocks from a high sulfur bearing coalfield, India: implication for acid and metal generation. *J Geochem Explor* 145:135–147. <https://doi.org/10.1016/j.gexplo.2014.05.024>
- Sahoo PK, Equeenuddin SM, Powell MA (2016) Trace elements in soils around coal mines: current scenario, impact and available techniques for management. *Curr Pollut Rep* 2:1–14. <https://doi.org/10.1007/s40726-016-0025-5>
- Sahu SK, Bhangare RC, Ajmal PY, Sharma S, Pandit GG, Puranik VD (2009) Characterization and quantification of persistent organic pollutants in fly ash from coal fueled thermal power stations in India. *Microchem J* 92(1):92–96
- Sahu SK, Tiwari M, Bhangare RC, Pandit GG (2014) Enrichment and particle size dependence of polonium and other naturally occurring radionuclides in coal ash. *J Environ Radioactivity* 138:421–426
- Sahu SK, Tiwari M, Bhangare RC, Ajmal PY, Pandit GG (2017) Partitioning behavior of natural radionuclides during combustion of coal in thermal power plants. *Environ Forensic* 18(1):36–43
- Saikia N, Kato S, Kojima T (2006) Compositions and leaching behaviours of combustion residues. *Fuel* 85(2):264–271
- Saikia BK, Goswamee RL, Baruah BP, Baruah RK (2009) Occurrence of some HTEs in Indian coals. *Coke Chem* 52(2):54–59
- Saikia BK, Ward CR, Oliveira ML, Hower JC, Baruah BP, Braga M, Silva LF (2014) Geochemistry and nano-mineralogy of two medium-sulfur northeast Indian coals. *Int J Coal Geol* 121:26–34
- Saikia BK, Ward CR, Oliveira MLS, Hower JC, De Leao F, Johnston MN, O'Bryan A, Sharma A, Baruah BP, Silva LFO (2015a) Geochemistry and nano-mineralogy of feed coals, mine overburden, and coal-derived fly ashes from Assam (North-east India): a multi-faceted analytical approach. *Int J Coal Geol* 137:19–37
- Saikia BK, Hower JC, Hood MM, Baruah R, Dekaboruah HP, Boruah R, Sharma A, Baruah BP (2015b) Petrological and biological studies on some fly and bottom ashes collected at different times from an Indian coal-based captive power plant. *Fuel* 158:572–581. <https://doi.org/10.1016/j.fuel.2015.06.007>

- Saikia J, Narzary B, Roy S, Bordoloi M, Saikia P, Saikia BK (2016) Nanominerals, fullerene aggregates, and hazardous elements in coal and coal combustion-generated aerosols: an environmental and toxicological assessment. *Chemosphere* 164:84–91. <https://doi.org/10.1016/j.chemosphere.2016.08.086>
- Saikia BK, Saikia J, Rabha S, Silva LF, Finkelman R (2018) Ambient nanoparticles/nanominerals and hazardous elements from coal combustion activity: implications on energy challenges and health hazards. *Geosci Front* 9(3):863–875
- Saini V, Gupta RP, Arora MK (2016) Environmental impact studies in coalfields in India: a case study from Jharia coal-field. *Renew Sust Energy Rev* 53:1222–1239. <https://doi.org/10.1016/j.rser.2015.09.072>
- Sajwan KS, Alva AK, Punshon T, Twardowska I (eds) (2011) *Coal combustion byproducts and environmental issues*. Springer, New York
- Sambandam B, Palanisami E, Abbugounder R, Prakhya B, Thiyagarajan D (2014) Characterizations of coal fly ash nanoparticles and induced in vitro toxicity in cell lines. *J Nanoparticle Res* 16(2):2217
- Samsuzzaman M (2011) *Landform evolution and geo-environmental assesment of the Jamuna Valley, Bangladesh*, Unpublished Ph.D. Thesis. Rajshahi University, Rajshahi
- Sehn JL, de Leão FB, da Boit K, Oliveira ML, Hidalgo GE, Sampaio CH, Silva LF (2016) Nanomineralogy in the real world: a perspective on nanoparticles in the environmental impacts of coal fire. *Chemosphere* 147:439–443. <https://doi.org/10.1016/j.chemosphere.2015.12.065>
- Sengupta D, Agrahari S (2017) Heavy metal and radionuclide contaminant migration in the vicinity of thermal power plants: monitoring, remediation, and utilization. In: *Modelling trends in solid and hazardous waste management*. Springer, Singapore, pp 15–33
- Sezgin N, Ozcan HK, Demir G, Nemlioglu S, Bayat C (2004) Determination of heavy metal concentrations in street dusts in Istanbul E-5 highway. *Environ Int* 29(7):979–985
- Shaheen SM, Hooda PS, Tsadilas CD (2014) Opportunities and challenges in the use of coal fly ash for soil improvements: a review. *J Environ Manag* 145:249–267
- Shamshad A, Fulekar MH, Bhawana P (2012) Impact of coal based thermal power plant on environment and its mitigation measure. *Int Res J Environ Sci* 1(4):60–64
- Sharma AK, Baliyan P, Kumar P (2018) Air pollution and public health: the challenges for Delhi, India. *Rev Environ Health* 33(1):77–86
- Shreya N, Valentim B, Paul B, Guedes A, Pinho S, Ribeiro J, Ward CR, Flores D (2015) Multi-technique study of fly ash from the Bokaro and Jharia coalfields (Jharkhand state, India): a contribution to its use as a geoliner. *Int J Coal Geol* 152:25–38
- Siegel MD, Bryan CR (2014) Radioactivity, geochemistry, and health (chapter 11.6). In: Holland HD, Turekian KK (eds) *Treatise on geochemistry*, 2nd edn. Elsevier, Amsterdam, Netherlands, pp 191–256
- Silva LFO, DaBoit KM (2011) Nanominerals and nanoparticles in feed coal and bottom ash: implications for human health effects. *Environ Monit Assess* 174(1–4):187–197
- Silva LFO, Oliveira MLS, Da Boit KM, Finkelman RB (2009) Characterization of Santa Catarina (Brazil) coal with respect to human health and environmental concerns. *Environ Geochem Health* 31(4):475–485
- Silva LF, Ward CR, Hower JC, Izquierdo M, Waanders F, Oliveira MLS, Li Z, Hatch RS, Querol X (2010) Mineralogy and leaching characteristics of coal ash from a major Brazilian power plant. *Coal Combust Gasification Prod* 2(1):51–65
- Silva LF, Wollenschlager M, Oliveira ML (2011a) A preliminary study of coal mining drainage and environmental health in the Santa Catarina region, Brazil. *Environ Geochem Health* 33(1):55–65
- Silva LFO, Da Boit K, Sampaio CH, Jasper A, Andrade ML, Kostova IJ, Waanders FB, Henke KR, Hower JC (2011b) The occurrence of hazardous volatile elements and nanoparticles in Bulgarian coal fly ashes and the effect on human health exposure. *Sci Total Environ* 416:513–526

- Silva LF, Jasper A, Andrade ML, Sampaio CH, Dai S, Li X, Li T, Chen W, Wang X, Liu H, Zhao L (2012) Applied investigation on the interaction of hazardous elements binding on ultrafine and nanoparticles in Chinese anthracite-derived fly ash. *Sci Total Environ* 419:250–264. <https://doi.org/10.1016/j.scitoten.2011.12.069>
- Silva LF, de Vallejuelo SFO, Martínez-Arkarazo I, Castro K, Oliveira ML, Sampaio CH, de Brum IA, de Leão FB, Taffarel SR, Madariaga JM (2013) Study of environmental pollution and mineralogical characterization of sediment rivers from Brazilian coal mining acid drainage. *Sci Total Environ* 447:169–178
- Singh AK, Mahato MK, Neogi B, Singh KK (2010) Quality assessment of mine water in the Raniganj coalfield area, India. *Mine Water Environ* 29:248–262
- Singh S, Ram LC, Masto RE, Verma SK (2011) A comparative evaluation of minerals and trace elements in the ashes from lignite, coal refuse, and biomass fired power plants. *Int J Coal Geol* 87(2):112–120
- Singh PK, Singh AL, Kumar A, Singh MP (2013) Control of different pyrite forms on desulfurization of coal with bacteria. *Fuel* 106:876–879
- Skoko B, Marović G, Babić D, Šoštarić M, Jukić M (2017) Plant uptake of ^{238}U , ^{235}U , ^{232}Th , ^{226}Ra , ^{210}Pb and ^{40}K from a coal ash and slag disposal site and control soil under field conditions: a preliminary study. *J Environ Radioact* 172:113–121
- Skousen J, Yang JE, Lee JS, Ziemkiewicz P (2013) Review of fly ash as a soil amendment. *Geosyst Eng* 16(3):249–256
- Spadoni M, Voltaggio M, Sacchi E, Sanam R, Pujari PR, Padmakar C, Labhasetwar PK, Wate SR (2014) Impact of the disposal and re-use of fly ash on water quality: the case of the Koradi and Khaperkheda thermal power plants (Maharashtra, India). *Sci Total Environ* 479:159–170. <https://doi.org/10.1016/j.scitoten.2014.01.111>
- Spears DA, Martínez-Tarazona MR, Lee S (1993) Some environmental implications of pyrite in coal. *Fuel* 72(5):698. [https://doi.org/10.1016/0016-2361\(93\)90598-](https://doi.org/10.1016/0016-2361(93)90598-)
- Spears DA, Manzanares-Papayanopoulos LI, Booth CA (1999) The distribution and origin of trace elements in a UK coal: the importance of pyrite. *Fuel* 78(14):1671–1677
- Stalikas CD, Chaidou CI, Pilidis GA (1997) Enrichment of PAHs and heavy metals in soils in the vicinity of the lignite-fired power plants of West Macedonia (Greece). *Sci Total Environ* 204(2):135–146
- Su C, Jiang L, Zhang W (2014) A review on heavy metal contamination in the soil worldwide: Situation, impact and remediation techniques. *Environ Skeptics Critics* 3(2):24–38. <https://doi.org/10.1037/a0036071>
- Suhana J, Rashid M (2016) Naturally occurring radionuclides in particulate emission from a coal fired power plant: a potential contamination? *J Environ Chem Eng*. <https://doi.org/10.1016/j.jece.2016.07.015>
- Sultana MS, Jolly YN, Yeasmin S, Islam A, Satter S, Tareq SM (2015) Transfer of heavy metal and radionuclides from soil to vegetables and plants in Bangladesh. In: Hakeem K, Sabir M, Ozturk M, Mermut AR (eds) *Soil remediation and plants: prospects and challenges*. Elsevier/Academic Press, London, pp 331–366
- Sultana S, Biswas PK, Rahman A, Sultana S, Zaman MN (2016) Risk factor assessment of coal mine drainage water on surrounding agricultural soil: a case study at Barapukuria in Bangladesh. *J Geosci Environ Prot* 4:7–17. <https://doi.org/10.4236/gep.2016.42002>
- Swaine DJ (1990) *Trace elements in coal*. Elsevier Science, Burlington
- Tamim U, Khan R, Jolly YN, Fatema K, Das S, Naher K, Islam MA, Islam SA, Hossain SM (2016) Elemental distribution of metals in urban river sediments near an industrial effluent source. *Chemosphere* 155:509–518. <https://doi.org/10.1016/j.chemosphere.2016.04.099>
- Tanic M, Jankovic-Mandic L, Gajic B, Dakovic M, Dragovic S, Bacic G (2016) Natural radionuclides in soil profiles surrounding the largest coal-fired power plant in Serbia. *Nucl Technol Radiat Prot* 31(3):247–259
- Taylor GH, Teichmüller M, Davis ACFK, Diessel CFK, Littke R, Robert P (eds) (1998) *Organic petrology: Stach's textbook of coal petrology*. Gebrüder Borntraeger, Berlin

- Tian L, Dai S, Wang J, Huang Y, Ho SC, Zhou Y, Lucas D, Koshland CP (2008) Nanoquartz in Late Permian C1 coal and the high incidence of female lung cancer in the Pearl River Origin area: a retrospective cohort study. *BMC Public Health* 8(1):398
- Tian H, Wang Y, Xue Z, Qu Y, Chai F, Hao J (2011) Atmospheric emissions estimation of Hg, As, and Se from coal-fired power plants in China, 2007. *Sci Total Environ* 409(16):3078–3081
- Tian HZ, Lu L, Hao JM, Gao JJ, Cheng K, Liu KY, Qiu PP, Zhu CY (2013) A review of key hazardous trace elements in Chinese coals: abundance, occurrence, behavior during coal combustion and their environmental impacts. *Energy Fuels* 27(2):601–614. <https://doi.org/10.1021/ef3017305>
- Tian C, Lu Q, Liu Y, Zeng H, Zhao Y, Zhang J, Gupta R (2016) Understanding of physicochemical properties and formation mechanisms of fine particular matter generated from Canadian coal combustion. *Fuel* 165:224–234. <https://doi.org/10.1016/j.fuel.2015.10.037>
- Tiwari MK, Bajpai S, Dewangan UK, Tamrakar RK (2015) Suitability of leaching test methods for fly ash and slag: a review. *J Radiat Res Appl Sci* 8(4):523–537
- Tolle DA, Arthur MF, Van Voris P (1983) Microcosm/field comparison of trace element uptake in crops grown in fly ash-amended soil. *Sci Total Environ* 31(3):243–261
- Tomlinson DC, Wilson DJ, Harris CR, Jeffrey DW (1980) Problem in heavy metals in estuaries and the formation of pollution index. *Helgol Wiss Meeresunler* 33(1–4):566–575
- Tóth G, Hermann T, Da Silva MR, Montanarella L (2016) Heavy metal in agricultural soils of the European Union with implications for food safety. *Environ Int* 88:299–309. <https://doi.org/10.1016/j.envint.2015.12.017>
- Tripathi RC, Jha SK, Ram LC, Vijayan B (2014) Effect of radionuclides present in lignite fly ash on soil and crop produce. *J Hazard Toxic Radioactive Waste* 18(4):04014019
- Tumuklu A, Ciflikli M, Ozgur FZ (2008) Determination of heavy metals in soils around Afsin-Elbistan thermal power plant. Kahramanmaraş, Turkey
- Turhan Ş, Gören E, Garad AM, Altıkulaç A, Kurnaz A, Duran C, Hançerlioğulları A, Altunal V, Güçkan V, Özdemir A (2018) Radiometric measurement of lignite coal and its by-products and assessment of the usability of fly ash as raw materials in Turkey. *Radiochim Acta* 106(7):611–621
- Uddin MN, Islam MSU (1992) Depositional environments of the Gondwana rocks in the Khalashpir basin, Rangpur District, Bangladesh. *Bangladesh J Geol* 11:31–40
- Uddin, M. N., Ahmed, M. U., Akbar, M. A., Rahman, M. M., Kamal, M. A., Faisal, A. S. M., Sarker, M. N., Hassan, M., Hussain, S., Ahsan, K., Ali, R M. E., 2016. Geology of Dighipara Coal Basin, Nawabganj Upazila, Dinajpur District, Bangladesh. Records of the geological Survey of Bangladesh, 13(5). Government Publication, Dhaka, Bangladesh
- UNEP (United Nations Environment Programme) (2013) Environmental risks and challenges of anthropogenic metals flows and cycles. In: van der Voet E, Salminen R, Eckelman M, Mudd G, Norgate T, Hirschier R (eds) A report of the working group on the global metal flows to the international resource panel. UNEP, Nairobi, p 231
- UNSCEAR (2010) Sources, and effects of ionizing radiations, Annex B: exposures of the public and workers from various sources of radiation
- US EPA (U.S. Environmental Protection Agency) (2012) edition of the drinking water standards and health advisories. U.S. EPA, Washington, DC. <http://water.epa.gov/action/advisories/drinking/upload/dwstandards2012.pdf>. Accessed March 2013
- Valente T, Grande JA, de la Torre ML, Gomes P, Santisteban M, Borrego J, Braga MS (2015) Mineralogy and geochemistry of a clogged mining reservoir affected by historical acid mine drainage in an abandoned mining area. *J Geochem Explor* 157:66–76
- Vass CR, Noble A, Ziemkiewicz PF (2019) The occurrence and concentration of rare earth elements in acid mine drainage and treatment by-products: part 1—initial survey of the Northern Appalachian Coal Basin. *Mining Metall Explor* 36:903–916
- Verma SK, Masto RE, Gautam S, Choudhury DP, Ram LC, Maiti SK, Maity S (2015) Investigations on PAHs and trace elements in coal and its combustion residues from a power plant. *Fuel* 162:138–147. <https://doi.org/10.1016/j.fuel.2015.09.005>

- Vodyanitskii YN (2016) Standards for the contents of heavy metals in soils of some states. *Ann Agrarian Sci* 14(3):257–263
- Vuković Ž, Mandić M, Vuković D (1996) Natural radioactivity of ground waters and soil in the vicinity of the ash repository of the coal-fired power plant “Nikola Tesla” A—Obrenovac (Yugoslavia). *J Environ Radioact* 33(1):41–48
- Wang W, Qin Y, Song D, Wang K (2008) Column leaching of coal and its combustion residues, Shizuishan, China. *Int J Coal Geol* 75:81–87
- Wang R, Liu G, Chou CL, Liu J, Zhang J (2010) Environmental assessment of PAHs in soils around the Anhui Coal District, China. *Arch Environ Contam Toxicol* 59(1):62–70
- Wang R, Yousaf B, Sun R, Zhang H, Zhang J, Liu G (2016a) Emission characterization and $\delta^{13}C$ values of parent PAHs and nitro-PAHs in size-segregated particulate matters from coal-fired power plants. *J Hazard Mater* 318:487–496. <https://doi.org/10.1016/j.jhazmat.2016.07.030>
- Wang S, Zhang Y, Gu Y, Wang J, Zhang Y, Cao Y, Romero CE, Pan WP (2016b) Using modified fly ash for mercury emissions control for coal-fired power plant applications in China. *Fuel* 181:1230–1237. <https://doi.org/10.1016/j.fuel.2016.02.043>
- Ward CR, French D, Jankowski J, Dubikova M, Li Z, Riley KW (2009) Element mobility from fresh and long-stored acidic fly ashes associated with an Australian power station. *Int J Coal Geol* 80(3–4):224–236. <https://doi.org/10.1016/j.coal.2009.09.001>
- Wei B, Yang L (2010) A review of heavy metal contaminations in urban soils, urban road dusts and agricultural soils from China. *Microchem J* 94(2):99–107
- Weng ZH, Jowitt SM, Mudd GM, Haque N (2013) Assessing rare earth element mineral deposit types and links to environmental impacts. *Appl Earth Sci* 122(2):83–96
- WHO (World Health Organization) (1996) Permissible limits of heavy metals in soil and plants. WHO, Geneva
- WHO (World Health Organization) (2011) Guidelines for drinking-water quality., 4th edn. World Health Organization, Geneva, Switzerland
- Wuana RA, Okieimen FE (2011) Heavy metals in contaminated soils: a review of sources, chemistry, risks and best available strategies for remediation. *Ecology*. <https://doi.org/10.5402/2011/402647>
- Xiang W, Han B, Zhou D, Nzihou A (2012) Physicochemical properties and heavy metals leachability of fly ash from coal-fired power plant. *Int J Min Sci Technol* 22(3):405–409. <https://doi.org/10.1016/j.ijmst.2011.12.002>
- Xiao X, Zhang J, Wang H, Han X, Ma J, Ma Y, Luan H (2019) Distribution and health risk assessment of potentially toxic elements in soils around coal industrial areas: a global meta-analysis, vol 713. *Sci Total Environ*, p 135292
- Yao Z, Li J, Xie H, Yu C (2012) Review on remediation technologies of soil contaminated by heavy metals. *Procedia Environ Sci* 16:722–729
- Yao ZT, Ji XS, Sarker PK, Tang JH, Ge LQ, Xia MS, Xi YQ (2015) A comprehensive review on the applications of coal fly ash. *Earth Sci Rev* 141:105–121
- Yilmaz H (2015) Characterization and comparison of leaching behaviors of fly ash samples from three different power plants in Turkey. *Fuel Process Technol* 137:240–249
- Yucel DS, Balci N, Baba A (2016) Generation of acid mine lakes associated with abandoned coal mines in Northwest Turkey. *Arch Environ Contam Toxicol* 70(4):757–782
- Zakir HM, Arafat MY (2020) Contamination level of different chemical elements in top soils of Barapukuria coal mine area in Dinajpur, Bangladesh. *Asian J Water Environ Pollut* 17(1):59–73
- Zakir HM, Islam MM, Arafat MY, Sharmin S (2013) Hydrogeochemistry and quality assessment of waters of an open coal mine area in a developing country: a case study from Barapukuria, Bangladesh. *Int J Geosci Res* 1(1):20–44
- Zakir HM, Arafat MY, Islam MM (2017) Assessment of metallic pollution along with geochemical baseline of soils at Barapukuria open coal mine area in Dinajpur, Bangladesh. *Asian J Water Environ Pollut* 14(4):77–88
- Zaman R, Bruderemann T, Kumar S, Islam N (2018) A multi-criteria analysis of coal-based power generation in Bangladesh. *Energy Policy* 116:182–192

- Zhai M, Totolo O, Modisi MP, Finkelman RB, Kelesitse SM, Menyatso M (2009) Heavy metal distribution in soils near Palapye, Botswana: an evaluation of the environmental impact of coal mining and combustion on soils in a semi-arid region. *Environ Geochem Health* 31(6):759
- Zhang H, Zhang B, Bi J (2015) More efforts, more benefits: air pollutant control of coal-fired power plants in China. *Energy* 80:1–9. <https://doi.org/10.1016/j.energy.2014.11.029>
- Zhang Y, Cetin B, Likos WJ, Edil TB (2016) Impacts of pH on leaching potential of elements from MSW incineration fly ash. *Fuel* 184:815–825
- Zhao S, Duan Y, Chen L, Li Y, Yao T, Liu S, Liu M, Lu J (2017) Study on emission of hazardous trace elements in a 350 MW coal-fired power plant. Part 2. Arsenic, chromium, barium, manganese, lead. *Environ Pollut* 226:404–411
- Zhengfu BIAN, Inyang HI, Daniels JL, Frank OTTO, Struthers S (2010) Environmental issues from coal mining and their solutions. *Mining Sci Technol* 20(2):215–223
- Zierold KM, Odoh C (2020) A review on fly ash from coal-fired power plants: chemical composition, regulations, and health evidence. *Rev Environ Health*, 20190039, eISSN 2191-0308, ISSN 0048-7554, DOI: <https://doi.org/10.1515/reveh-2019-0039>.

Chapter 25

Overview of Indoor Air Pollution: A Human Health Perspective



Ambikapathi Ramya, Ambikapathi Nivetha, and Periyasamy Dhevagi

Abstract In the modern world, humans spend more than 80 percent of their routine lives in indoors rather than outdoors. In recent decades, the improved living standards in indoor environments like houses, commercial offices, and similar places with decorations, refurbishment activities, remodeling, and new furniture emits toxic gases. Indoor Air Pollutants (IAP) comprises carbon monoxide and dioxide, nitrogen oxides, particulate matters, volatile organic compounds (formaldehyde, benzene, ethylene, etc.), and polycyclic aromatic hydrocarbons (biphenyl, benzo[a]pyrene, benzo[ghi]perylene, benzo[c]fluorine, etc.). Inhalation of these pollutants are likely to cause mortalities and morbidities illness attributed to respiratory diseases, cardiovascular diseases, pulmonary, and lung cancer diseases in human. According to World Health Organization, around 3.8 million populations die in a year prematurely from illness attributable to indoor pollution, i.e., pneumonia (27%), ischemic heart disease (27%), chronic obstructive pulmonary disease (20%), stroke (18%) and lung cancer (8%). Under these circumstances, mitigation measures are essential to seal off pollutants from the indoor environment for the protection of occupants from exposure accounting for advanced airflow distribution, photocatalytic oxidation techniques, and green system within indoor includes phytoremediation and biofiltration techniques. Hence, this chapter aimed to provide a comprehensive overview of current information regarding the characterization of indoor air pollutants, its concentration levels, health risk assessment, mitigation strategies, and sustainable remediation intended to reduce the impact of indoor air pollution on human health.

Keywords Indoor air pollutants · Pollution monitoring · Human health · Risk assessment · Remediation

A. Ramya · P. Dhevagi (✉)

Department of Environmental Sciences, Tamil Nadu Agricultural University, Coimbatore, Tamil Nadu, India

A. Nivetha

Department of Chemistry, Bharathiar University, Coimbatore, Tamil Nadu, India

© Springer Nature Switzerland AG 2021

P. K. Shit et al. (eds.), *Spatial Modeling and Assessment of Environmental Contaminants*, Environmental Challenges and Solutions,

https://doi.org/10.1007/978-3-030-63422-3_25

25.1 Introduction

Individuals living in indoors, i.e., homes, schools, workplaces, and public places typically exposed to a variety of air pollutants. The building materials, household products including furniture, cleaning supplies, electronic affluence, copiers and printers, cooking styles and fuels, and cigarettes smoking are the main sources of indoor air pollution (Azuma et al. 2020). Primarily, indoor pollutants comprise oxides of carbon, nitrogen and sulfur, particulate matters, organic compounds, and aromatic hydrocarbons (Sharma and Jain 2020).

Among the different sources of IAP, the open firing of biomass for cooking and poorly maintained cooking stoves emits a wide range of harmful pollutants in indoors (Saini et al. 2020). Nowadays, 50% population around the world and 90% rural population in developing countries make use of biomass for cooking poses high levels of exposure to particulate matters (PM10, PM2.5, and PM1), polycyclic organic matter, formaldehyde, and oxides of carbon (CO), nitrogen (NO₂) and sulfur (SO₂) (Gautam et al. 2019). Among the indoor pollutants, the respirable PMs are important pollutants; especially PM2.5 could resident long in the atmosphere (Bai et al. 2020).

Polycyclic aromatic hydrocarbons (PAHs) are benzene rings containing aromatic compounds. In indoors PAHs released from heating sources and 70% ~ 90% of which attached on the surface of respirable particles (Jorundsdottir et al. 2014; Xu and Liu 2018). Besides indoor dust is the main pollutant acts a sink for various organic pollutants at residents (Cao et al. 2017). Ether groups containing polychlorinated biphenyls and polybrominated diphenyls emitted from electrical and electronic products and construction items are also an indoor pollutant having an average half-life of 20 years (Megson et al. 2013; Yadav et al. 2020). Moreover, cigarette smoke contributes to around 7000 toxic and carcinogenic compounds including particulate matter and benzene and formaldehyde (WHO 2018).

Globally, 3.8 million populations experiencing premature death related to indoor air pollution every year (WHO 2018). In India, about 1.24 million death cases were reported due to air pollution wherein 0.67 million were attributed to ambient air pollution and 0.48 million to household air pollution (Balakrishnan et al. 2019). The household air pollution (HAP) related issues were most comment for women and children accounting for 60% of premature deaths (WHO 2018). In households, the use of solid biomass and kerosene as cooking fuels emits 12% of global fine particulate matter (Martins and da Graça 2018). For example, in India, around 50% of the population resides in regions with particulate matter (PM2.5) concentrations exceeding the National Ambient Air Quality Standard (NAAQS) of 40 $\mu\text{g m}^{-3}$. Only less than 0.01% of the population resides in regions that meet WHO standards of 10 $\mu\text{g m}^{-3}$ for PM2.5 (Pant et al. 2016). In addition, over seven million death cases were recorded globally due to smoking habits and around a million people died just exposure to cigarette smoke (WHO 2018).

Further, exposure even at a lower concentration in indoors compared to the industrial environment, pollutants have adverse health effects on humans including

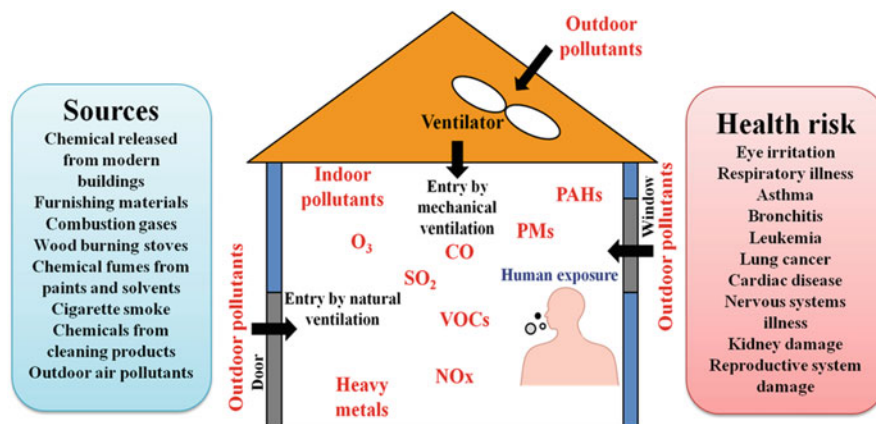


Fig. 25.1 Sources of indoor air pollutants and associated health risk

respiratory, neurological, reproductive, dermatologic, and cardiovascular diseases (WHO 2010). The possible sources of indoor air pollutants associated with health effects were depicted in Fig. 25.1. Short-term effect to indoor pollution includes suffocation, eyes irritation, fatigue and headaches, and long-term effect includes chronic disease and premature death (Maharana et al. 2018). Some of the indoor pollutants classified as carcinogens by the International Agency for Research on Cancer (IARC), Environmental Protection Agency of United States (USEPA), and World Health Organization (WHO) (Akif et al. 2020).

Consequently, continuous monitoring of indoor air quality (IAQ) is an important determinant to assess human health risk. Government authorities, for example, Occupational Safety and Health Administration (OSHA), WHO Regional Office for Europe (WHO/Europe), Office of Environmental Health Hazard Assessment of California (OEHHA), United States Environmental Protection Agency (USEPA), American Conference of Governmental Industrial Hygienists (ACGHH), Japanese National Institute of Health Sciences (NIHS) and Central Pollution Control Board, Government of India (CPCB) suggested air quality guidelines for potent health risk chemicals to protect human health.

To deal with increased health risk due to poor IAQ, numerous mitigation measures have been developed. In this view, the first step is to eliminate indoor air pollution by reducing emissions and the second step is to remediate existing indoor pollutants. Various technologies have been developed for eliminating indoor pollutants, for instance, catalytic oxidization (Grabchenko et al. 2018), photocatalytic nano-based activated carbon filters (Suarez et al. 2019), chemical sorbents (Er et al. 2016), building materials as adsorbent (Thevenet et al. 2018) and phytoremediation by green wall bio-filters (Pettit et al. 2019) were popular in terms of sustainable remediation. Hence, a critical review based on available information regarding indoor air pollution, this chapter discussed with highlights of indoor air

pollutants, potential monitoring methods, health risks assessment, and remediation technologies to guide upcoming researchers to focus on new developments.

25.2 Materials and Methods

There are several physical, chemical, and continuous online methods available in the literatures for sampling, monitoring, analyzing, and reporting indoor air pollutants to meet the NAAQS requirement. Besides, more sophisticated methods are in practice to measure indoor air quality. For instance, the high volume air sampling method is a commonly used technique for monitoring pollutants in ambient air which requires power for operation. A passive air sampling method is also used for air sampling in indoors due to its lightweight, low-cost, and non-necessity of electricity for operation (Chaemfa et al. 2009).

A light-scattering laser photometer was used to collect the PM₁₀ and PM_{2.5} and portable condensation particle counters used for real-time ultrafine particle measurements (Madureira et al. 2020). PM_{2.5} in indoors can also estimate by dust monitor (Bai et al. 2020) and quartz filters used for PM collection. Also, a real-time PM sampler with nephelometric based measurements followed for PM_{2.5} monitoring (Akther et al. 2019; Elf et al. 2019).

For volatile organic compounds (VOCs) analysis, gaseous samples can be collected using stainless steel thermal desorption tubes as a passive sampler and analyzed by gas chromatography/mass spectrometry (GC-MS) (Akif et al. 2020). Polycyclic aromatic hydrocarbons (PAHs) concentration is estimated through GC-MS and it can be extracted from PM_{2.5} collected on filters using dichloromethane (Sharma and Jain 2020; Bai et al. 2020). Airborne chlorinated, brominated, and organophosphate esters can be captured using polyurethane foam disk (PUF) passive air sampler (PAS) and extracted by solid-phase extraction method using dichloromethane and hexane mixture (Yadav et al. 2020) which can be analyzed through GC-MS. Heavy metal concentrations can be assessed using Atomic Absorption Spectrometry (AAS).

Some other gaseous pollutants like CO can be analyzed by Non-dispersive infrared (NDIR) spectroscopy, SO_x by improved West and Gaek and ultraviolet fluorescence, NO_x by modified Jacob and Hochheiser method and chemiluminescence method, O₃ by UV photometric and chemiluminescence method (CPCB 2011). In addition to the above, some of the analysis methods for IAP are described in Table 25.1.

25.2.1 Risk Assessment

The health risk assessment was performed through inhalation of pollutant, i.e., inhalation pathways, ingestion pathways, and dermal-contact pathways.

Table 25.1 Recommended methods for analyzing and monitoring indoor air pollutants (CPCB 2011; WHO 2010)

Pollutants	Manual methods	Automatic monitoring methods
Particulate matter-PM10	Gravimetric method	Tapered element oscillating microbalance (TEOM), Beta attenuation
Particulate matter-PM2.5	Gravimetric method	Tapered element oscillating microbalance (TEOM), Beta attenuation
Sulfur dioxide	Improved West and Gaeke method	Ultraviolet fluorescence
Nitrogen dioxide	Modified Jacob andHochheiser (NaOH-NaAsO ₂) method	Gas phase Chemiluminescence
Ozone	Chemical method	Ultraviolet photometric, Chemiluminescence
Ammonia	Indophenol blue method	Chemiluminescence
Carbon monoxide	–	Non-dispersive infrared (NDIR) spectroscopy
Benzene	Adsorption and desorption followed by GC analysis	Gas chromatography (GC) based continuous analyzer
Heavy metals	AAS/ICP method	–
Benzo (a)Pyrene	Solvent extraction followed by HPLC/GC analysis	Gas chromatography (GC) based continuous analyzer
PAH	HPLC/gas chromatography mass spectrometry	Gas chromatography (GC) based continuous analyzer
Radon	Alpha-track detectors, activated charcoal adsorption detectors	Continuous radon monitors using sensors including scintillation cells, solid-state silicon detectors, and current or pulse ionization chambers

The inhalation health risk was calculated using the following formula (USEPA 2009),

$$EC_i = \frac{C_i \times ET \times EF \times ED}{AT}, \quad (25.1)$$

where EC_i : exposure concentration; C_i : indoor concentration of target compound; ET: exposure time; EF: exposure frequency; ED: exposure duration and AT: averaging time (h).

The total toxic equivalent concentration (Bai et al. 2020),

$$TEQ = \sum_{i=1}^n C_i \times TEF_i, \quad (25.2)$$

where TEQ: total toxicity equivalent concentration (ng m^{-3}), C_i : concentration of individual pollutant (ng m^{-3}), and TEF $_i$: toxic equivalency factor of individual pollutant.

The carcinogenic risk is evaluated by estimating Lifetime cancer risk (LCR).

$$\text{LCR}_i = \text{EC}_i \times \text{IUR}, \quad (25.3)$$

where IUR is inhalation unit risk.

According to Bai et al. (2020), the lifetime lung carcinogenic risks (ILCR) of indoor pollutants are broadly exposed by three pathways, i.e., ingestion (ILCR_{ing}), inhalation (ILCR_{inh}), and dermal-contact pathways (ILCR_{der}).

$$\text{ILCR}_{\text{ing}} = \frac{\text{TEQ} \times \text{CSF}_{\text{ing}} \sqrt[3]{\frac{\text{BW}}{70}} \times \text{IR}_{\text{ing}} \times \text{EF} \times \text{ED}}{\text{BW} \times \text{AT} \times 10^6}, \quad (25.4)$$

$$\text{ILCR}_{\text{inh}} = \frac{\text{TEQ} \times \text{CSF}_{\text{inh}} \sqrt[3]{\frac{\text{BW}}{70}} \times \text{IR}_{\text{inh}} \times \text{EF} \times \text{ED}}{\text{BW} \times \text{AT} \times \text{PEF}}, \quad (25.5)$$

$$\text{ILCR}_{\text{der}} = \frac{\text{TEQ} \times \text{CSF}_{\text{der}} \sqrt[3]{\frac{\text{BW}}{70}} \times \text{SA} \times \text{SL} \times \text{ABS} \times \text{EF} \times \text{ED}}{\text{BW} \times \text{AT} \times 10^6}, \quad (25.6)$$

where CSF_{ing} , CSF_{inh} , and CSF_{der} : carcinogenic slope coefficients ($(\text{kg}\cdot\text{d})\cdot\text{mg}^{-1}$); EF: exposure duration; ED: exposure period; AT: average exposure time; BW: body weight; IR_{ing} : ingestion intake; IR_{inh} : inhalation intake; PEF: particulate emission factor; SA: skin exposed surface area; SL: skin adhesion; ABS: skin absorption factor.

In Eqs. (25.3), (25.4), (25.5) and (25.6), LCR and ILCR values $>10^{-4}$ indicates serious cancer risk, the value between 10^{-4} and 10^{-6} indicates as potential cancer risk, and values $<10^{-6}$ indicates that the risk could be negligible or no carcinogenic risks.

25.2.2 Potential Inhalation Dose

The measure of the quantity of pollutant inhaled through mouth or nose (USEPA 2011).

Average Daily Dose (ADD)

It is denoted as mass of pollutant per unit body weight daily over a period of time (USEPA 2011).

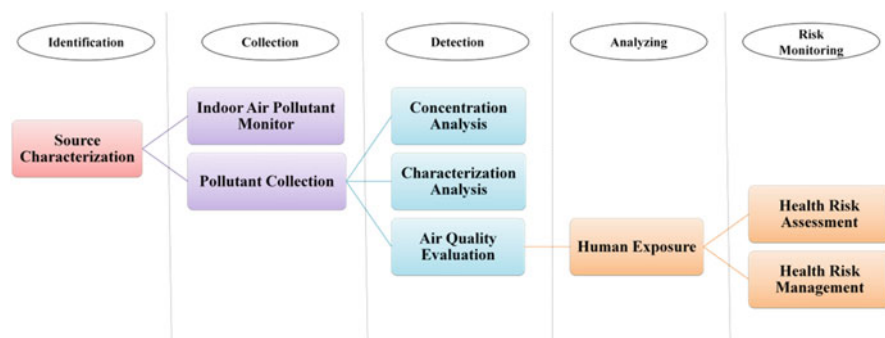


Fig. 25.2 General framework used to analyze indoor pollution from source to human health risk

$$ADD = \frac{C \times \text{InhR} \times \text{ET} \times \text{EF} \times \text{ED}}{\text{BW} \times \text{AT}}, \quad (25.7)$$

where C : pollutant concentration, InhR : inhalation rate, ET : exposure time, EF : exposure frequency, ED : exposure duration, BW : body weight and AT : averaging time.

The general structure used to identify pollutant sources, pollution monitoring and characterization, human exposure, and risk assessment followed were described in Fig. 25.2.

25.3 Results and Discussion

In worldwide, a number of studies have been reported for indoor air pollution in various indoor environments are discussed in this section. Studies revealed that the pollutant concentrations in indoors were exceeding the guidelines described by various national and international organizations. For example, $\text{PM}_{2.5}$ and PM_{10} concentrations were found to be highest in traditional cookstoves based enclosed kitchen (818 and $756 \mu\text{g m}^{-3}$) compared with open kitchen (161 and $118 \mu\text{g m}^{-3}$) in Uttar Pradesh, India (Sharma and Jain 2020). Deepthi et al. (2019) were also recorded that the highest indoor $\text{PM}_{2.5}$ and PM_{10} levels in the closed kitchen (278 and $176 \mu\text{g m}^{-3}$) compared with outdoor kitchen (65 and $49 \mu\text{g m}^{-3}$) of Telangana state. Akther et al. (2019) recorded the mean PM_{10} , $\text{PM}_{2.5}$ and PM_{1} concentrations were 203.9 ± 44.8 , 76.0 ± 16.2 and $46.1 \pm 13.4 \mu\text{g m}^{-3}$, respectively, NO_2 (0.076 ± 0.007 ppm) and total volatile organic compounds (90.0 ± 46.0 ppm) were found in residents of Dhaka, Bangladesh. The correlation of $\text{PM}_{2.5}$ concentrations in indoor was relatively weak with outdoor $\text{PM}_{2.5}$ concentrations. And, indoor activities like dusting, cooking activities, and usage of detergents are responsible for increased levels of PMs in indoor environment (Akther et al. 2019).

According to Gautam et al. (2019), exposure to CO in rural houses of Haryana, India varied from 4.81 to 7.01 and 0.20 to 1.81 mg m^{-3} for biomass and LPG-based cooking, respectively. It was noticed that only biomass-based households recorded higher CO concentration (78%) than in only-LPG using houses (14%). Also an exposure in closed kitchens has reported two times higher CO compared to open kitchens.

The indoor NH_3 in rural houses had higher concentrations with the average of 0.018, 0.065, and 0.341 ppm in summer, rainy, and winter seasons, respectively in Lucknow, India. During the rainy season the H_2S concentration reached to 0.2 ppm, CO_2 concentration recorded to be 366 ppm, SO_2 and NO_2 concentrations were less within in the permissible limit (Lawrence et al. 2020). In rural households, livestock rearing is a common source for NH_3 production and people keep livestock inside the house premises during the rainy and winter season. In the winter season, calmer climatic conditions and greater atmospheric stability with temperature inversion and low mixing heights led to less dispersion, and dilution of pollutants increases the risk (Masih et al. 2016).

Jan et al. (2016) reported that the indoor pollutant concentrations in the school environment Pune, India found to be O_3 ($83.3 \mu\text{g m}^{-3}$), CO ($268.4 \mu\text{g m}^{-3}$), NO_2 ($46.7 \mu\text{g m}^{-3}$), SO_2 ($46.7 \mu\text{g m}^{-3}$), and CO_2 (1249.11 ppm). Higher the pollutant concentration in school indoor was attributed to the location of the school in high traffic density area and insufficient ventilation. Moreover, playground, soil dust, and chalk (CaSO_4) were source for calcium, magnesium, sodium, and potassium bound with PM in indoor school environment (Jan et al. 2016).

Cooking emissions involve carcinogenic pollutants such as fine ($<2.5 \mu\text{m}$) and ultrafine ($<0.1 \mu\text{m}$) particulate matters, VOCs, PAHs, aldehydes, black carbon, and some toxic compounds (Azuma et al. 2020). Occupational exposure to VOC in commercial barbecue restaurant recorded the median concentration of $6.11 \mu\text{g m}^{-3}$ for benzene, $3.51 \mu\text{g m}^{-3}$ for chloroform, $1.58 \mu\text{g m}^{-3}$ for styrene, $1.12 \mu\text{g m}^{-3}$ for ethylbenzene, $0.11 \mu\text{g m}^{-3}$ for tetrachloromethane, and $0.06 \mu\text{g m}^{-3}$ for 1,2-dichloroethane (Akif et al. 2020). The annual mean benzene, toluene, and xylene concentration recorded to be 52.35, 8.85 and $7.23 \mu\text{g m}^{-3}$, respectively in solid biofuel burning kitchens in West Bengal, India (Nayek and Padhy 2020).

The average concentrations of PAHs from enclosed and open kitchens containing traditional cookstoves were found to be 55,371 and $17,239 \mu\text{g m}^{-3}$, respectively. In the case of improved cookstoves, the PAHs were recorded as 13,599 and 1764ng m^{-3} , respectively (Sharma and Jain 2020). The most common particulate matter bound PAHs were benzo[a]pyrene, benzo[ghi]perylene and benzo[b]fluoranthene (Sharma and Jain 2020), and benzo[a]pyrene in semi-enclosed kitchen with traditional cookstoves and improved cookstoves were 425 and 31ng m^{-3} , respectively.

In Indian state Bihar households, on averaged over all organophosphate ester flame retardant ($\Sigma_8\text{OPFRs}$) recorded the median of 351pg m^{-3} was most prominent, whereas brominated flame retardants ($\Sigma_6\text{NBFRs}$) found to be 278pg m^{-3} , polybrominated diphenyl ether ($\Sigma_9\text{PBDE}$) was 5.05pg m^{-3} and dechlorane plus ($\Sigma_2\text{DPs}$) was 2.52pg m^{-3} in indoor air (Yadav et al. 2020). Indoor dust from the

rural area of Nepal analyzed for organochlorine compounds depicted the average median concentrations of organochlorine pesticides (Σ_{26} OCPs) was 87 ng g^{-1} and polychlorinated biphenyls (Σ_{30} PCBs) was 10.5 ng g^{-1} (Yadav et al. 2020). Among the OCPs and PCBs, DDT (dichloro-diphenyl-trichloroethane) and dioxin-like-PCBs were the most abundant. Similarly, median concentrations of 1050 ng g^{-1} OCPs reported in Romania (Dirtu and Covaci 2010), 310 ng g^{-1} in Germany, and 54.7 ng g^{-1} in Pakistan (Ali et al. 2012).

Moreover, the sum DDT levels observed in dust from Pakistan (53.2 ng g^{-1}), Canada (46 ng g^{-1}) and Czech Republic (42 ng g^{-1}) were slightly lower than in Romania (1130 ng g^{-1}) and Denmark (1250 ng g^{-1}) (Audy et al. 2018; Bräuner et al. 2011; Dirtu et al. 2012). The median concentrations of sum Hexa chlorocyclohexane (Σ HCCH) in Nepal recorded to be 5.69 ng g^{-1} , Denmark (11 ng g^{-1}), China (8.2 ng g^{-1}), Canada (7 ng g^{-1}) while considerably less Σ HCCH found in Pakistan (1.4 ng g^{-1}) (Audy et al. 2018; Bräuner et al. 2011; Yadav et al. 2020a; Zhang et al. 2010). The Endosulfan concentration (Σ_2 Endos) in the dust with a median of 3.61 ng g^{-1} was recorded in Nepal and 3.1 ng g^{-1} in Portugal while 15 ng g^{-1} was in USA household dust samples (Arnold et al. 2018; Yadav et al. 2020a).

In addition to the above discussion, the list of indoor air pollutants in various indoor environments and its adverse effect on human health were presented in Tables 25.2 and 25.3. Most of the studies revealed that IAPs concentrations were higher than the guidelines of the World Health Organization (WHO) (Table 25.4).

According to Hystad et al. (2019), studies from a large group of communities showed an association between indoor air pollution and cardiovascular disease (CVD) mortality. A studied 91,350 adults with an age group from 35–70 years from 467 urban and rural population of 11 countries including Bangladesh, Brazil, Chile, China, Colombia, India, Pakistan, Philippines, South Africa, Tanzania, and Zimbabwe recorded that 6595 death cases during 9.1 years follow-up period. It was attributed to 41.8% of participant lived in solid fuel using households associated with a hazard ratio (HR) of 1.12 for all cause mortality, 1.08 for fatal or nonfatal CVD, and 1.14 for fatal or nonfatal respiratory diseases. Similarly, study within China Kadoorie Biobank (271,217 participants, 15,468 deaths, and 7.5 years period) showed a use of solid fuels for cooking compared to improved cooking fuel was associated with hazard ratio of 1.11 for all cause mortality and 1.20 for CVD mortality (Yu et al. 2018).

Due to increasing risk factor against solid fuel use, the effort to replace solid fuel use with cleaner alternative usage will reduce premature mortality and cardiovascular disease (Hystad et al. 2019). A model study by Maji and Kandlikar (2020) predicted that the adoption of LPG by 2030 in India reduces PM_{2.5} exposures to below WHO guidelines across both urban and rural households. Further, clean fuel use can reduce indoor emission and exposure by 75–86%.

Table 25.2 Indoor air pollutant concentration in various indoor environments

Location	Place	Pollutants	Concentrations	References
Taigu, Northern China	Rural residence	Total suspended particle	Non-heating period: 470 ± 256 µg m ⁻³ Heating period: 691 ± 287 µg m ⁻³	Du et al. (2020)
Chitwan, Nepal	Rural kitchen	PM2.5	98.43 ± 47.17 µg m ⁻³	Adhikari et al. (2020)
		CO	78 ppm	
Telangana, India	Rural kitchen—bio-mass based	Pb	32 mg kg ⁻¹	Yaparla et al. (2019)
		Ni	20 mg kg ⁻¹	
	Rural kitchen—LPG based	Pb	50 mg kg ⁻¹	
		Ni	8 mg kg ⁻¹	
Beijing, China	Urban residence	B[a]P	1.67 ng m ⁻³	Chang et al. (2019)
Agra, India	Urban residence	PM2.5	121.01 ± 30.42 µg m ⁻³	Rohra et al. (2018)
Hong Kong, China	Urban residence	PM2.5	7.0–8.7 ng m ⁻³	Chen et al. (2019)
Gonabad, Iran	Urban residence	Formaldehyde	21 to 360 µg m ⁻³	Dehghani et al. (2020)
Ethiopia, Africa	Urban residence	Total volatile organic compounds	350–812 µg m ⁻³	Embiale et al. (2019)
Turkey	Urban residence	CO	2.65–3.40 mg m ⁻³	Taştan and Gökozan (2019)
		NO ₂	42.8–47.9 µg m ⁻³	
		PM10	28.8–31.1 µg m ⁻³	
Tehran, Iran,	Urban residence	Benzene	53.2 µg m ⁻³	Hadei et al. (2018)
		Toluene	21.5 µg m ⁻³	
		Ethylbenzene	14.4 µg m ⁻³	
		Xylene	21.1 µg m ⁻³	
		Formaldehyde	17.9 µg m ⁻³	
Tirupur, India	Urban residence	PM2.5	0.04 to 83.84 mg m ⁻³	Rumchev et al. (2017)
		CO	2.47–50 mg m ⁻³	
Dharavi, Mumbai, India	Slums	PM2.5	150–300 µg m ⁻³	Lueker et al. (2019)
Northern China	Office building	PAH	48.6 ng m ⁻³	Bai et al. (2020)
Jeddah, Saudi Arabia	School	Pb	121.2 µg g ⁻¹	Alghamdi et al. (2019)
		Ni	35.7 µg g ⁻¹	
		Cd	2.09 µg g ⁻¹	
		As	8.0 µg g ⁻¹	
Pune, India	School	PM2.5	263.9 to 135.8 µg m ⁻³	Jan et al. (2016)

(continued)

Table 25.2 (continued)

Location	Place	Pollutants	Concentrations	References
Chennai, India	School	PM2.5	$36 \pm 15 \mu\text{g m}^{-3}$	Chithra and Nagendra (2014)
		PM10	$136 \pm 60 \mu\text{g m}^{-3}$	
Rome, Italy	School	PAH	$1.8 \sim 8.3 \mu\text{g m}^{-3}$	Romagnoli et al. (2014)
Uttarakhand, India	Library	Total volatile organic compounds	$51.7 \pm 30 \text{ ppb}$	Sahu and Gurjar (2019)
Kolkata, India	Library	Fungal loads	761 CFU m^{-3}	Chaudhuri et al. (2019)
	Computer room	Fungal loads	571 CFU m^{-3}	
	Beauty salon	Fungal loads	161 CFU m^{-3}	

25.4 Risk Assessment and Remediation

25.4.1 Risk Assessment

Currently, indoor air pollutants induced health issues are essential matter for discussion with the increasing unhealthy indoor environment. Sharma and Jain (2020) reported that the average daily dose in kitchens with traditional cookstoves was estimated to be 3.40×10^{-2} and 3.15×10^{-2} mg/kg-day (enclosed kitchen) and 5.52×10^{-3} and 3.99×10^{-3} mg/kg-day (open kitchen) for PM2.5 and PM1, respectively. Also, the inhalation dose was $\sim 3\text{--}4$ times higher than improved cookstoves. According to Madureira et al. (2020), newborns exposed fourfold higher dose of pollutants than mothers and 1.3 times less exposure in bedrooms compared to living rooms. The mean inhaled doses of PM10, PM2.5, and ultrafine particles for newborns found to be $73.9 \mu\text{g kg}^{-1}$, $69.8 \mu\text{g kg}^{-1}$, and 18×10^9 particle kg^{-1} and for mothers $17.7 \mu\text{g kg}^{-1}$, $16.7 \mu\text{g kg}^{-1}$ and 4.3×10^9 particle kg^{-1} , respectively (Madureira et al. 2020).

In the office building of Changchun city, China, the toxic equivalent concentration of indoors PAHs for heating and non-heating seasons were 4.67 and 4.47 ng m^{-3} , respectively (Bai et al. 2020). Akif et al. (2020) reported that the indoor VOC exposure and its carcinogenic potential recorded between 3.4×10^{-8} and 1.1×10^{-5} showed the possible risk of lung cancer. Nayek and Padhy (2020) observed that the average daily dose (ADD) analysis for benzene explained the median value of 1.439×10^{-3} mg/kg-day and indicated the probable cancer risk by exceeding the acceptable level.

The inhalation exposure risk to indoor pollutants was higher in children than the adult populations due to lower body weight and differentiation in inhalation rate. The median daily inhalation exposure (DIE) to polybrominated diphenyl ethers (PBDEs) in urban air recorded $3.79 \text{ pg}\cdot\text{kg}^{-1}$ for children and $0.99 \text{ pg}\cdot\text{kg}^{-1}$ for

Table 25.3 Adverse impact of indoor air pollutants on human health (WHO 2010; Lawrence et al. 2020; Akif et al. 2020)

Indoor air pollutants	Adverse impact on human health
Particulate matter	Respiratory illness, heart and lung cancer, nervous systems illness
NO ₂	Respiratory infections, airway obstruction, asthmatic bronchitis
SO ₂	Respiratory tract illness, mucus secretion, cardiac disease, asthma and chronic bronchitis, eye irritation
CO	Headache, dizziness, neuropsychological impairment, fetal damage, myocardial ischemia
CO ₂	Headache, fatigue, nausea, dizziness, vomiting
Ozone	Breathing illness, reduction in lung function, asthma
Polycyclic aromatic hydrocarbons	Lung cancer
Volatile organic compounds	Headache, drowsiness, asthma, nocturnal breathlessness, sensitization reactions, mucous membrane irritation, Central nervous system illness,
Formaldehyde	Minor eye irritation, sneezing, coughing, irritant of the skin, nasopharyngeal cancer
Radon	Acute lymphoblastic leukemia, lung cancer
Tobacco smoke	Irritation of eye, nose, and throat, lung cancer, pneumonia, bronchitis, lower respiratory tract illness illnesses, and tuberculosis
Asbestos	Lung cancer, skin irritation, Mesothelioma, asbestosis
Lead	Kidney damage, reproductive system damage, nervous system illness,
Pesticides	Eye, nose, throat irritation, Central nervous system illness, kidneys damage, Cancer risk
Biological contaminants: Pollens, bacteria, fungal spores	Allergic diseases, Neumonitis, asthma

Table 25.4 Guidelines for air pollutants by various national and international organizations (WHO 2010)

Indoor pollutants	WHO indoor air quality standards	Indoor pollutants	WHO indoor air quality standards
Carbon monoxide (CO)	10 mg m ⁻³ (8 h)	Sulfur dioxide (SO ₂)	20 µg m ⁻³ (24 h)
	7 mg m ⁻³ (24 h)		500 µg m ⁻³ (10 min)
Nitrogen dioxide (NO ₂)	40 µg m ⁻³ (annual)	Ozone (O ₃)	100 µg m ⁻³ (8 h)
	200 µg m ⁻³ (1 h)		
Particulate matter (PM _{2.5})	10 µg m ⁻³ (annual)	Benzene (C ₆ H ₆)	1 µg m ⁻³
	25 µg m ⁻³ (24 h)		
Particulate matter (PM ₁₀)	20 µg m ⁻³ (annual)	Formaldehyde	0.1 mg m ⁻³ (30 min)
	50 µg m ⁻³ (24 h)		

adult, the concentration expressed in body weight (BW) per day (Yadav et al. 2020). Similarly, DIE to PBDEs reported in Nepal ($3.6\text{--}6.6\text{ pg}\cdot\text{kg}^{-1}\cdot\text{BW}\cdot\text{day}^{-1}$) but much higher DIE revealed in Japan ($176\text{ pg}\cdot\text{kg}^{-1}\cdot\text{BW}\cdot\text{day}^{-1}$) and United Kingdom ($120\text{ pg}\cdot\text{kg}^{-1}\cdot\text{BW}\cdot\text{day}^{-1}$) (Harrad et al. 2004; Takigami et al. 2009; Yadav et al. 2017). The estimated daily exposure risk of polychlorinated biphenyls (PCBs) by ingestion and dermal contact for children were $0.5046\text{ ng}\cdot\text{kg}^{-1}\cdot\text{BW}\cdot\text{day}^{-1}$ and $0.7106\text{ ng}\cdot\text{kg}^{-1}\cdot\text{BW}\cdot\text{day}^{-1}$, respectively (Yadav et al. 2020a). Hamid et al. (2018) reported that PAHs caused health risk to adults who were 4.83 times higher compared to children due to extended exposure time and larger body weight. The health risks to females were maximum through ingestion and minimum through inhalation and dermal-contact pathway compared to males (Pongpiachan 2016). Hence, health risks associated by indoor pollutants varied with different genders and age groups, which were correlated with the inhalation rate, exposure to the skin surface, body weight and life span, etc. According to Bai et al. (2020), ingestion and dermal-contact pathways of indoor pollutants to different carcinogenic risk populations were in the order of female > male > children and through the inhalation pathway was male > female > children.

Elf et al. (2019) reported that the use of kerosene was significantly interlinked with tuberculosis (TB) in women and children in Pune, India while fuelwood was not associated. In Taiwan, $10\text{ }\mu\text{g m}^{-3}$ increases in annual PM_{2.5} exposure correlated with 40% increase in TB (Lai et al. 2016). In Nepal, kerosene was used as cooking fuel found to be significantly associated with TB which was three times higher TB occurrence compared with LPG (Pokhrel et al. 2010). Whereas in California, no association was found with 24 month PM_{2.5} and TB, but CO and NO₂ concentrations were positively associated (Smith et al. 2016). In this regard, WHO recommended against the use of kerosene which may produce NO_x, SO₂, and PAHs associated to human health risk (WHO 2018).

25.4.2 Remediation

There is a need to enhance indoor air quality and retain it at permissible levels through various remediation technologies that are discussed hereby to provide a clear idea for future researches. The first step is reducing emissions in the indoor and the second step is to remediate indoor pollutants. In this view, researchers found that improperly built living and kitchen spaces, without sufficient ventilation space entraps pollutants inside the household. Ventilation disperses and dilutes indoor pollution (WHO 2018; Nayek and Padhy 2020). Downward et al. (2014) recorded that the particulate-bound PAH concentrations were 4–10 times less in more ventilated households than unventilated households. It is also noticed that improved cookstoves significantly reduced a total PAHs concentrations by 75% and 90% in enclosed and open kitchens, respectively (Sharma and Jain 2020). Though ventilation is effective in several circumstances, which may not provide improved IAQ for areas with higher outdoor pollution and common ventilation system do not filter

gaseous air pollutants. Liao et al. (2019) recorded that the use of high-efficiency particle air (HEPA) filter significantly reduced the PM_{2.5} exposure from 103 and 137 $\mu\text{g}/\text{m}^3$ to 29 and 30 $\mu\text{g}/\text{m}^3$ for households without and with a presence of smoker, respectively. Also, the use of air filter reduced 8–37% personal mortality attributed to PM_{2.5} in Delhi.

There are numerous technologies explored for indoor air pollutant remediation including the use of plasma discharges (Zhang et al. 2016), photocatalytic degradation (Chen et al. 2017), adsorption/catalytic oxidation (Grabchenko et al. 2018), and phytoremediation (Pettit et al. 2019), etc.

Er et al. (2016) reported that the mean airborne fungal concentrations at educational buildings, Malaysia reduced by 88.2% on malt extract agar treated with potassium sorbate than control. Potassium sorbate (biocide) inhibits the cell transport processes of fungi and it can be applied at the entrances of primary airways thereby outdoor air could be treated prior to entry into the buildings. Building materials in the form of board products or ceiling tiles has been documented for indoor pollutant sorptive properties through physical or chemical process (Seo et al. 2009). A 36 m² physisorptive gypsum board (PGB) showed a maximum sorption capacity of 19.5 mmol of formaldehyde at 50% relative humidity. The equilibrium state was obtained after 102 days while chemisorptive gypsum board (CGB), equilibrium uptake was reached after 119 days (Thevenet et al. 2018). In the case of toluene, chemisorptive gypsum board was effective in lowering indoor toluene concentration (Thevenet et al. 2018).

The photocatalytic oxidation using solar light or low consumption light-emitting devices has become one of the most efficient alternatives. A metallic catalysts such as TiO₂ (Ao et al. 2004), MnOx on PAN-ACNF (Miyawaki et al. 2012), and Pd/CeO₂ (Tan et al. 2015) has been studied for formaldehyde oxidation. Suarez et al. (2019) developed a silver-copper oxide (Ag-CuO) hetero-nanostructure that achieved total photo-oxidation of n-hexane in the visible-near infrared (NIR) range. The polyacrylonitrile based activated carbon nanofibers containing pyridinic, pyrrolic, and quaternary nitrogen groups exhibited a maximum formaldehyde removal capacity (Yang et al. 2000). Ryu et al. (2019) studied formaldehyde removal capability using urea/nitric acid co-impregnated in activated carbon fiber showed 110 fold improvements.

Plants act as a biofilters in the indoor environment and are proposed as a useful technology for indoor pollutant remediation (Irga et al. 2019). A CAM plant, *Sansevieria trifasciata*, and C₃ plant, *Chlorophytum comosum* effectively removed formaldehyde, acetone, benzene xylene, and reduced CO₂ emission from cigarette smoke at a light intensity of 50 $\mu\text{mole PAR m}^{-2} \text{ s}^{-1}$ (Siswanto et al. 2020). In addition, these plant biofilters reduced PM_{2.5} within 1–2 h. According to Mo et al. (2015), the physical structure of the leaf was an essential plant parameter in the selection of species for biofiltration. Also, plant leaves with the highest ratios of trichomes and grooves reduced PM_{2.5} more efficiently compared to other plants (Chen et al. 2017). For example, PM_{2.5} reduced about 0.09–1.32 $\mu\text{g m}^{-3} \text{ h}^{-1}$ by *Pittosporum tobira*, *Lavandula angustifolia*, *Sedum album* and *Sedum reflexum* and *Syringa meyeri* accumulated 32 mg cm⁻² (Popek et al. 2013; Viecco et al. 2018).

Furthermore, common indoor houseplants, viz., spider plant (*C. comosum*), golden pothos (*Epipremnum aureum*) and snake plant (*Sansevieria trifasciata*) effectively reduce indoor O₃, NO₂, and CO. Similarly, peppermint (*Mentha piperita*) plant reduced indoor nicotine concentration in a sustainable way (Agarwal et al. 2019).

The active green walls biofilters, *Spathiphyllum wallisii* and *Syngonium podophyllum* have potential to decay at the rates of 0.021 and 0.023 for NO₂ and 0.012 and 0.031 for NO, respectively (Pettit et al. 2019). Biodegradation of VOCs by green wall rhizospheric bacteria considered as the primary sinks (Pettit et al. 2018). Moreover, Pettit et al. (2018) reported that green walls bioremediation of PM and VOCs in Australia and China resulted in reduction of about 28% within 20 min, compared without green walls. In indoors, green walls potentially reduced PM_{0.3–0.5} by 45.78% and PM_{5–10} by 92.46% (Pettit et al. 2017). The phyllosphere of *Azalea indica* supplemented with a culture of *Pseudomonas putida* TVA8 removed 95% of toluene (initial toluene concentration, 339 mg m⁻³) in indoor air (De Kempeneer et al. 2004). Apart from living green plants, vetiver root materials based mats, carpets, rugs, etc. were used to clean, purify, and humidify air in indoor environments (Shah et al. 2013).

25.5 Conclusion

This chapter presented an overview of indoor air pollutant concentration in different indoor environment and its evidence on human health. Indoor air quality is a significant factor to attain people's health and happiness index. It is revealed that considerable variation in indoor pollutants in various indoor environments exceeded the WHO guideline causing respiratory, cardiovascular, and carcinogenic illness. The studies on combined effects of all indoor pollutants with risk assessments are so far limited. In addition, the nature of cause and effect, relationships between building factors and indoor environmental quality has not been established. More researches are needed to understand how building environmental factors like site conditions, building design, occupancy, and building operations affecting indoor pollutant concentrations and human health. Evaluating principle source emission from tobacco smoke, combustion gases, building materials, furniture, and use of household products is necessary to reduce risk. Understanding the harmful effect of indoor pollutants and the protection of sensitive populations by reducing exposure is a feasible way to diminish health risk. Developing health-associated guidelines for key indoor pollutants would help in risk management. Among the remediation technologies, growing selective indoor plants gain more advantage through its effective biofiltration potential on indoor pollutants as well as it improves the esthetic indoor environment. Hence, improving indoor air quality by source control, ventilation, and remediation were the most effective ways to eliminate pollutant concentration.

References

- Adhikari S, Mahapatra PS, Pokheral CP, Puppala SP (2020) Cookstove smoke impact on ambient air quality and probable consequences for human health in rural locations of southern Nepal. *Int J Environ Res Public Health* 17(2):550
- Agarwal P, Sarkar M, Chakraborty B, Banerjee T (2019) Phytoremediation of air pollutants: prospects and challenges. In: Pandey VC, Baudh K (eds) *Phytomanagement of polluted sites*. Elsevier, Amsterdam, Netherlands, pp 221–241
- Akif ARI, ARI PE, Yenisooy-Karakaş, S. (2020) Source characterization and risk assessment of occupational exposure to volatile organic compounds (VOCs) in a barbecue restaurant. *Build Environ* 174:106791
- Akther T, Ahmed M, Shohel M, Ferdousi FK, Salam A (2019) Particulate matters and gaseous pollutants in indoor environment and association of ultra-fine particulate matters (PM 1) with lung function. *Environ Sci Pollut Res* 26(6):5475–5484
- Alghamdi MA, Hassan SK, Alzahrani NA, Almeahmadi FM, Khoder MI (2019) Risk assessment and implications of schoolchildren exposure to classroom heavy metals particles in Jeddah, Saudi Arabia. *Int J Environ Res Public Health* 16(24):5017
- Ali N, Van den Eede N, Dirtu AC, Neels H, Covaci A (2012) Assessment of human exposure to indoor organic contaminants via dust ingestion in Pakistan. *Indoor Air* 22(3):200–211
- Ao CH, Lee SC, Yu JZ, Xu JH (2004) Photodegradation of formaldehyde by photocatalyst TiO₂: effects on the presences of NO, SO₂ and VOCs. *Appl Catal B Environ* 54(1):41–50
- Arnold K, Teixeira JP, Mendes A, Costa S, Salamova A (2018) A pilot study on semivolatile organic compounds in senior care facilities: implications for older adult exposures. *Environ Pollut* 240:908–915
- Audy O, Melymuk L, Venier M, Vojta S, Becanova J, Romanak K, Vykoukalova M, Proles R, Kukucka P, Diamond M, Klanova J (2018) PCBs and organochlorine pesticides in indoor environments: a comparison of indoor contamination in Canada and Czech Republic. *Chemosphere* 206:622–631
- Azuma K, Jinno H, Tanaka-Kagawa T, Sakai S (2020) Risk assessment concepts and approaches for indoor air chemicals in Japan. *Int J Hyg Environ Health* 225:113470
- Bai L, Chen W, He Z, Sun S, Qin J (2020) Pollution characteristics, sources and health risk assessment of polycyclic aromatic hydrocarbons in PM_{2.5} in an office building in northern areas, China. *Sustain Cities Soc* 53:101891
- Balakrishnan K, Dey S, Gupta T, Dhaliwal RS, Brauer M, Cohen AJ et al (2019) The impact of air pollution on deaths, disease burden, and life expectancy across the states of India: the Global Burden of Disease Study 2017. *Lancet Planetary Health* 3(1):e26–e39
- Bräuner EV, Mayer P, Gunnarsen L, Vorkamp K, Raaschou-Nielsen O (2011) Occurrence of organochlorine pesticides in indoor dust. *J Environ Monit* 13(3):522–526
- Cao SJ, Cen D, Zhang W, Feng Z (2017) Study on the impacts of human walking on indoor particles dispersion using momentum theory method. *Build Environ* 126:195–206
- Central Pollution Control Board (CPCB) (2011) Guidelines for the measurement of ambient air pollutants, NAAQS Monitoring & Analysis Guidelines, Volume-I
- Chaemfa C, Barber JL, Kim KS, Harner T, Jones KC (2009) Further studies on the uptake of persistent organic pollutants (POPs) by polyurethane foam disk passive air samplers. *Atmos Environ* 43(25):3843–3849
- Chang J, Shen J, Tao J, Li N, Xu C, Li Y, Liu Z, Wang Q (2019) The impact of heating season factors on eight PM_{2.5}-bound polycyclic aromatic hydrocarbon (PAH) concentrations and cancer risk in Beijing. *Sci Total Environ* 688:1413–1421
- Chaudhuri A, Basu C, Bhattacharyya S, Chaudhuri P (2019) Development of health risk rating scale for indoor airborne fungal exposure. *Arch Environ Occup Health* 75:375–383
- Chen L, Liu C, Zhang L, Zou R, Zhang Z (2017) Variation in tree species ability to capture and retain airborne fine particulate matter (PM 2.5). *Sci Rep* 7(1):1–11

- Chen XC, Ward TJ, Cao JJ, Lee SC, Lau NC, Yim SH, Ho KF (2019) Source identification of personal exposure to fine particulate matter (PM_{2.5}) among adult residents of Hong Kong. *Atmos Environ* 218:116999
- Chithra VS, Nagendra SS (2014) Characterizing and predicting coarse and fine particulates in classrooms located close to an urban roadway. *J Air Waste Manage Assoc* 64(8):945–956
- De Kempeneer L, Sercu B, Vanbrabant W, Van Langenhove H, Verstraete W (2004) Bioaugmentation of the phyllosphere for the removal of toluene from indoor air. *Appl Microbiol Biotechnol* 64(2):284–288
- Deepthi Y, Nagendra SS, Gummadi SN (2019) Characteristics of indoor air pollution and estimation of respiratory dosage under varied fuel-type and kitchen-type in the rural areas of Telangana state in India. *Sci Total Environ* 650:616–625
- Dehghani MH, Zarei A, Farhang M, Kumar P, Yousefi M, Kim KH (2020) Levels of formaldehyde in residential indoor air of Gonabad, Iran. *Hum Ecol Risk Assess Int J* 26(2):483–494
- Dirtu AC, Covaci A (2010) Estimation of daily intake of organohalogenated contaminants from food consumption and indoor dust ingestion in Romania. *Environ Sci Technol* 44(16):6297–6304
- Dirtu AC, Ali N, Van den Eede N, Neels H, Covaci A (2012) Country specific comparison for profile of chlorinated, brominated and phosphate organic contaminants in indoor dust. Case study for eastern Romania, 2010. *Environ Int* 49:1–8
- Downward GS, Hu W, Rothman N, Reiss B, Wu G, Wei F, Chapman RS, Portengen L, Qing L, Vermeulen R (2014) Polycyclic aromatic hydrocarbon exposure in household air pollution from solid fuel combustion among the female population of Xuanwei and Fuyuan counties, China. *Environ Sci Technol* 48(24):14632–14641
- Du W, Yun X, Fu N, Qi M, Wang W, Wang L et al (2020) Variation of indoor and outdoor carbonaceous aerosols in rural homes with strong internal solid fuel combustion sources. *Atmos Pollut Res*. <https://doi.org/10.1016/j.apr.2020.02.013>
- Elf JL, Kinikar A, Khadse S, Mave V, Suryavanshi N, Gupte N et al (2019) The association of household fine particulate matter and kerosene with tuberculosis in women and children in Pune, India. *Occup Environ Med* 76(1):40–47
- Embiale A, Zewge F, Chandravanshi BS, Sahle-Demessie E (2019) Short-term exposure assessment to particulate matter and total volatile organic compounds in indoor air during cooking Ethiopian sauces (Wot) using electricity, kerosene and charcoal fuels. *Indoor Built Environ* 28(8):1140–1154
- Er CM, Sunar NM, Leman AM, Othman N, Kalthsom U, Jamal NA, Ideris NA (2016) The biocidal effect of potassium sorbate for indoor airborne fungi remediation. *Desalin Water Treat* 57(1):288–293
- Gautam S, Pillarisetti A, Yadav A, Singh D, Arora N, Smith K (2019) Daily average exposures to carbon monoxide from combustion of biomass fuels in rural households of Haryana, India. *Environ Dev Sustain* 21(5):2567–2575
- Grabchenko M, Mikheeva NN, Mamontov GV, Salaev MA, Liotta LF, Vodyankina OV (2018) Ag/CeO₂ composites for catalytic abatement of CO, soot and VOCs. *Catalysts* 8(7):285
- Hadei M, Hopke PK, Rafiee M, Rastkari N, Yarahmadi M, Kermani M, Shahsavani A (2018) Indoor and outdoor concentrations of BTEX and formaldehyde in Tehran, Iran: effects of building characteristics and health risk assessment. *Environ Sci Pollut Res* 25(27):27423–27437
- Hamid N, Syed JH, Junaid M, Mahmood A, Li J, Zhang G, Malik RN (2018) Elucidating the urban levels, sources and health risks of polycyclic aromatic hydrocarbons (PAHs) in Pakistan: implications for changing energy demand. *Sci Total Environ* 619:165–175
- Harrad S, Wijesekera R, Hunter S, Halliwell C, Baker R (2004) Preliminary assessment of UK human dietary and inhalation exposure to polybrominated diphenyl ethers. *Environ Sci Technol* 38(8):2345–2350
- Hystad P, Duong M, Brauer M, Larkin A, Arku R, Kurmi OP et al (2019) Health effects of household solid fuel use: findings from 11 countries within the prospective urban and rural epidemiology study. *Environ Health Perspect* 127(5):057003

- Irga PJ, Pettit T, Irga RF, Paull NJ, Douglas AN, Torpy FR (2019) Does plant species selection in functional active green walls influence VOC phytoremediation efficiency? *Environ Sci Pollut Res* 26(13):12851–12858
- Jan R, Roy R, Yadav S, Satsangi PG (2016) Exposure assessment of children to particulate matter and gaseous species in school environments of Pune, India. *Build Environ* 111:207–217
- Jorundsdottir HO, Jensen S, Hylland K (2014) Pristine Arctic: background mapping of PAHs, PAH metabolites and inorganic trace elements in the North-Atlantic Arctic and sub-Arctic coastal environment. *Sci Total Environ* 20:719–728
- Lai TC, Chiang CY, Wu CF, Yang SL, Liu DP, Chan CC, Lin HH (2016) Ambient air pollution and risk of tuberculosis: a cohort study. *Occup Environ Med* 73(1):56–61
- Lawrence AJ, Khan T, Azad I (2020) Indoor air quality assessment and its impact on health in context to the household conditions in Lucknow. *Global NEST J* 22(1):28–41
- Liao J, Ye W, Pillarisetti A, Clasen TF (2019) Modeling the impact of an indoor air filter on air pollution exposure reduction and associated mortality in urban Delhi household. *Int J Environ Res Public Health* 16(8):1391
- Lueker J, Bardhan R, Sarkar A, Norford L (2019) Indoor air quality among Mumbai's resettled populations: comparing Dharavi slum to nearby rehabilitation sites. *Build Environ* 167:106419
- Madureira J, Slezakova K, Silva AI, Lage B, Mendes A, Aguiar L, Pereira MC, Teixeira JP, Costa C (2020) Assessment of indoor air exposure at residential homes: inhalation dose and lung deposition of PM10, PM2.5 and ultrafine particles among newborn children and their mothers. *Sci Total Environ* 717:137293
- Maharana SP, Paul B, Garg S, Dasgupta A, Bandyopadhyay L (2018) Exposure to indoor air pollution and its perceived impact on health of women and their children: a household survey in a slum of Kolkata, India. *Indian J Public Health* 62(3):182
- Maji P, Kandlikar M (2020) Quantifying the air quality, climate and equity implications of India's household energy transition. *Energy Sustain Dev* 55:37–47
- Martins NR, da Graça GC (2018) Impact of PM2.5 in indoor urban environments: a review. *Sustain Cities Soc* 42:259–275
- Masih A, Lall AS, Taneja A, Singhvi R (2016) Inhalation exposure and related health risks of BTEX in ambient air at different microenvironments of a terai zone in North India. *Atmos Environ* 147:55–66
- Megson D, O'Sullivan G, Comber S, Worsfold PJ, Lohan MC, Edwards MR, Shields WJ, Sandau CD, Patterson DG Jr (2013) Elucidating the structural properties that influence the persistence of PCBs in humans using the National Health and Nutrition Examination Survey (NHANES) dataset. *Sci Total Environ* 461:99–107
- Miyawaki J, Lee GH, Yeh J, Shiratori N, Shimohara T, Mochida I, Yoon SH (2012) Development of carbon-supported hybrid catalyst for clean removal of formaldehyde indoors. *Catal Today* 185(1):278–283
- Mo YY, Tang YK, Wang SY, Lin JM, Zhang HB, Luo DY (2015) Green synthesis of silver nanoparticles using eucalyptus leaf extract. *Mater Lett* 144:165–167
- Nayek S, Padhy PK (2020) Personal exposure to VOCs (BTX) and women health risk assessment in rural kitchen from solid biofuel burning during cooking in West Bengal, India. *Chemosphere* 244:125447
- Pant P, Guttikunda SK, Peltier RE (2016) Exposure to particulate matter in India: a synthesis of findings and future directions. *Environ Res* 147:480–496
- Pettit T, Irga PJ, Abdo P, Torpy FR (2017) Do the plants in functional green walls contribute to their ability to filter particulate matter? *Build Environ* 125:299–307
- Pettit T, Irga PJ, Torpy FR (2018) Functional green wall development for increasing air pollutant phytoremediation: substrate development with coconut coir and activated carbon. *J Hazard Mater* 360:594–603
- Pettit T, Irga PJ, Surawski NC, Torpy FR (2019) An assessment of the suitability of active green walls for NO₂ reduction in green buildings using a closed-loop flow reactor. *Atmosphere* 10(12):801

- Pokhrel AK, Bates MN, Verma SC, Joshi HS, Sreeramareddy CT, Smith KR (2010) Tuberculosis and indoor biomass and kerosene use in Nepal: a case-control study. *Environ Health Perspect* 118(4):558–564
- Pongpiachan S (2016) Incremental lifetime cancer risk of PM_{2.5} bound polycyclic aromatic hydrocarbons (PAHs) before and after the wildland fire episode. *Aerosol Air Qual Res* 16 (11):2907–2919
- Popek R, Gawrońska H, Wrochna M, Gawroński SW, Sæbø A (2013) Particulate matter on foliage of 13 woody species: deposition on surfaces and phytostabilisation in waxes: a 3-year study. *Int J Phytoremediation* 15(3):245–256
- Rohra H, Tiwari R, Khandelwal N, Taneja A (2018) Mass distribution and health risk assessment of size segregated particulate in varied indoor microenvironments of Agra, India: a case study. *Urban Clim* 24:139–152
- Romagnoli P, Balducci C, Perilli M, Gherardi M, Gordiani A, Gariazzo C, Gatto MP, Cecinato A (2014) Indoor PAHs at schools, homes and offices in Rome, Italy. *Atmos Environ* 92:51–59
- Rumchev K, Zhao Y, Spickett J (2017) Health risk assessment of indoor air quality, socioeconomic and house characteristics on respiratory health among women and children of Tirupur, South India. *Int J Environ Res Public Health* 14(4):429
- Ryu DY, Shimohara T, Nakabayashi K, Miyawaki J, Park JI, Yoon SH (2019) Urea/nitric acid co-impregnated pitch-based activated carbon fiber for the effective removal of formaldehyde. *J Ind Eng Chem* 80:98–105
- Sahu V, Gurjar BR (2019) Spatio-temporal variations of indoor air quality in a university library. *Int J Environ Health Res*. <https://doi.org/10.1080/09603123.2019.1668916>
- Saini J, Dutta M, Marques G (2020) A comprehensive review on indoor air quality monitoring systems for enhanced public health. *Sustain Environ Res* 30:6
- Seo J, Kato S, Ataka Y, Chino S (2009) Performance test for evaluating the reduction of VOCs in rooms and evaluating the lifetime of sorptive building materials. *Build Environ* 44(1):207–215
- Shah V, Shah M, Shah P (2013) Use of Vetiver material to provide shades, cooling, humidification and air filtration for residential, commercial, indoor and outdoor facilities. U.S. Patent Application 13/214700
- Sharma D, Jain S (2020) Carcinogenic risk from exposure to PM_{2.5} bound polycyclic aromatic hydrocarbons in rural settings. *Ecotoxicol Environ Saf* 190:110135
- Siswanto D, Permana BH, Treesubuntorn C, Thiravetyan P (2020) *Sansevieria trifasciata* and *Chlorophytum comosum* botanical biofilter for cigarette smoke phytoremediation in a pilot-scale experiment-evaluation of multi-pollutant removal efficiency and CO₂ emission. *Air Qual Atmos Health* 13(1):109–117
- Smith GS, Van Den Eeden SK, Garcia C, Shan J, Baxter R, Herring AH, Richardson DB, Rie AV, Emch M, Gammon MD (2016) Air pollution and pulmonary tuberculosis: a nested case-control study among members of a northern California health plan. *Environ Health Perspect* 124 (6):761–768
- Suarez H, Ramirez A, Bueno-Alejo CJ, Hueso JL (2019) Silver-copper oxide Heteronanostructures for the plasmonic-enhanced photocatalytic oxidation of N-hexane in the visible-NIR range. *Materials* 12(23):3858
- Takigami H, Suzuki G, Hirai Y, Sakai SI (2009) Brominated flame retardants and other polyhalogenated compounds in indoor air and dust from two houses in Japan. *Chemosphere* 76(2):270–277
- Tan H, Wang J, Yu S, Zhou K (2015) Support morphology-dependent catalytic activity of Pd/CeO₂ for formaldehyde oxidation. *Environ Sci Technol* 49(14):8675–8682
- Taştan M, Göközan H (2019) Real-time monitoring of indoor air quality with internet of things-based E-nose. *Appl Sci* 9(16):3435
- Thevenet F, Debono O, Rizk M, Caron F, Verrielle M, Locoge N (2018) VOC uptakes on gypsum boards: sorption performances and impact on indoor air quality. *Build Environ* 137:138–146
- United States Environmental Protection Agency (USEPA) (2009) Risk assessment guidance for superfund, vol 1: Human health evaluation manual (Part F, supplemental guidance for inhalation

- risk assessment). EPA/540/R-070/002. USEPA Office of Superfund Remediation and Technology Innovation Environmental Protection Agency, Washington, DC
- United States Environmental Protection Agency (USEPA) (2011) Exposure factors handbook 2011 edition (final). U.S. Environmental Protection Agency, Washington, DC
- Viecco M, Vera S, Jorquera H, Bustamante W, Gironás J, Dobbs C, Leiva E (2018) Potential of particle matter dry deposition on green roofs and living walls vegetation for mitigating urban atmospheric pollution in semiarid climates. *Sustainability* 10(7):2431
- World Health Organisation (WHO) (2018) Household air pollution and health. Fact sheets. <https://www.who.int/news-room/fact-sheets/detail/household-air-pollution-and-health>
- World Health Organization (WHO) (2010) WHO guidelines for indoor air quality: selected pollutants, the WHO European Centre for Environment and Health, Bonn Office. http://www.euro.who.int/data/assets/pdf_file/0009/128169/e94535.pdf
- Xu C, Liu L (2018) Personalized ventilation: one possible solution for airborne infection control in highly occupied space? *Indoor Built Environ* 27:873–876
- Yadav IC, Devi NL, Li J, Zhang G (2017) Occurrence and source apportionment of halogenated flame retardants in the indoor air of Nepalese cities: implication on human health. *Atmos Environ* 161:122–131
- Yadav IC, Devi NL, Kumar A, Li J, Zhang G (2020) Airborne brominated, chlorinated and organophosphate ester flame retardants inside the buildings of the Indian state of Bihar: exploration of source and human exposure. *Ecotoxicol Environ Saf* 191:110212
- Yadav IC, Devi NL, Li J, Zhang G (2020a) Polychlorinated biphenyls and organochlorines pesticides in indoor dust: an exploration of sources and health exposure risk in a rural area (Kopawa) of Nepal. *Ecotoxicol Environ Saf* 195:110376
- Yang J, Li D, Zhang Z, Li Q, Wang H (2000) A study of the photocatalytic oxidation of formaldehyde on Pt/Fe₂O₃/TiO₂. *J Photochem Photobiol A Chem* 137(2–3):197–202
- Yaparla D, Nagendra SS, Gummadi SN (2019) Characterization and health risk assessment of indoor dust in biomass and LPG-based households of rural Telangana, India. *J Air Waste Manage Assoc* 69(12):1438–1451
- Yu K, Qiu G, Chan KH, Lam KBH, Kurmi OP, Bennett DA et al (2018) Association of solid fuel use with risk of cardiovascular and all-cause mortality in rural China. *JAMA* 319(13):1351–1361
- Zhang W, Ye Y, Hu D, Ou L, Wang X (2010) Characteristics and transport of organochlorine pesticides in urban environment: air, dust, rain, canopy throughfall, and runoff. *J Environ Monit* 12(11):2153–2160
- Zhang X, Xiao H, Hu X, Gui Y (2016) Effects of background gas on sulfur hexafluoride removal by atmospheric dielectric barrier discharge plasma. *AIP Adv* 6(11):115005

Chapter 26

Mineralogy and Morphological Characterization of Technogenic Magnetic Particles (TMP) from Industrial Dust: Insights into Environmental Implications



Supriya Mondal, Saurodeep Chatterjee, and Debesh Gain

Abstract Magnetic measurements are notable among the recent developments to encounter the spatial distribution and grades of heavy metal pollution and to determine the anthropogenic sources of such pollution. The present investigation aims towards characterizing the magnetic properties, microstructures, and mineral phase of the Technogenic Magnetic Particles (TMP) in the urban soils and to enlighten their potential environmental implications. The TMP considered for the present study are collected from Farakka area (in and around Farakka Super Thermal Power Station, FSTPS), W.B., India. The magnetic susceptibility, morphology and microstructures of the TMPs are studied using Bartington MS-2 Susceptibility Meter, Scanning Electron Microscopy (SEM) equipped with energy-dispersive X-ray spectroscopy (EDS) and X-ray diffraction (XRD). The weight percentage of TMP in the concerned topsoil ranges from 0.05% to 0.5% (on an average). The magnetic susceptibility of the samples ranges within $263.4 \times 10^{-8} \text{ m}^3/\text{kg}$ to $3.9 \times 10^{-8} \text{ m}^3/\text{kg}$. The collected samples displayed huge diversity of susceptibility values which was inevitably identified as a function of concentration and mineral composition. According to the XRD analysis, it is evident that the technogenic iron mainly occurs within the structures of silicates and other oxides. The TMP in general includes three dominant morphological forms: spherical, irregular shaped and aggregate particles. The spherical TMP belongs to a size range of 10–200 μm with a modal value of about 50 μm . EDAX studies indicating that the TMP are enriched in iron, magnesium etc. which are interpreted to have been incorporated within the lattice of major minerals present on account of their large lattice size. The concentration of the TMP bears a positive correlation with that of the heavy metal concentration within

S. Mondal · D. Gain

Department of Geological Sciences, Jadavpur University, Kolkata, India

S. Chatterjee (✉)

Department of Geological Sciences, Jadavpur University, Kolkata, India

Department of Applied Geology, Indian Institute of Technology (Indian Institute of Mines), Dhanbad, Jharkhand, India

© Springer Nature Switzerland AG 2021

P. K. Shit et al. (eds.), *Spatial Modeling and Assessment of Environmental Contaminants*, Environmental Challenges and Solutions,

https://doi.org/10.1007/978-3-030-63422-3_26

515

urban soils. Thus, in a nutshell magnetic properties, microstructures and mineral phases of Titano-magnetite can serve as the identification of pollution sources in the urban soils.

Keywords Technogenic Magnetic Particles (TMP) · Urban soils · Heavy metals · SEM-EDS · X-ray diffraction

26.1 Introduction

Magnetic particles that generally occur within the urban and industrial road dusts are generally classified under the heading of technogenic origin. Besides, heavy metal concentration within the soils is growing to be an important issue in terms of public health and ecological concerns in the urban environment. By the term, Technogenic Magnetic Particles (TMP), the iron mineral that is produced during the various technological process (including methodology, fuel consumption, ceramics, cement production, coke production etc.) are meant (Catinon et al. 2014; Magiera et al. 2011). Most of such particles expelled into the atmosphere are ferromagnetic to anti-ferromagnetic in nature (Thompson and Oldfield 1986). This ferromagnetic to anti-ferromagnetic nature basically makes it possible to use them as pathfinder minerals for heavy and toxic minerals and can be determined by magnetic measurements which are basically physical properties of such particles. Such physical (or more precisely magnetic properties) of the TMPs are used to separate the urban and the industrial dust or fly ash from the original topsoil from where they have been collected and this basically defines the basic concept of application of magnetic studies in environmental assessment (Blundell et al. 2009; Gautam et al. 2004; LeGalley and Krekeler 2013; Lu et al. 2007; Xia et al. 2014; Zhou et al. 2013). Such fast, non-destructive, and cost-efficient magnetic techniques have reached a level of importance in environmental assessment (Lu et al. 2007). Studies indicate that the TMPs are important sources of heavy metals and therefore identification of TMP particles will definitely demarcate the locations of heavy metal pollution (Lu et al. 2016; Zawadzki et al. 2015a, b). The basic properties that enable us to apply magnetic measurements in the heavy toxic metals have an affinity towards iron-oxide (mainly magnetite) rather than other silicate phases (Hullet et al. 1980; Kukier et al. 2003). The crystal lattice of magnetite and other ferrites accommodates such heavy metals in their structure and thereby threaten plants, animals, and human being (Jablonska and Smolka-Danielowska 2008; Wójcik and Smolka-Danielowska 2008; Giere and Querol 2010; Grobety et al. 2010). Thus, if we can trace the magnetic oxides (mainly iron-oxide) primarily through the magnetic susceptibility measurements, the amount of heavy metal will be proxied.

Researchers in the past decade have well documented that burning of coal, smelting of iron, recycling of solid waste produces a huge amount of dust and fine solid waste that are released into the environment which ubiquitously contains high amount of magnetic particles (Jordanova et al. 2006; Lu et al. 2009; Rachwal et al. 2015; Magiera et al. 2011; Szuszkiewicz et al. 2015). Once the magnetic particles are

deposited into the soils, there occurs magnetic enrichment of the soils, specially towards the vicinity of the industrial sites. This industrial effect is sometimes enhanced by the automobile emission which also releases highly magnetic iron-containing particles (Bučko et al. 2011; Hoffmann et al. 1999; Kim et al. 2009; Matzka and Maher 1999; Yang et al. 2010). Magnetic properties, morphology, mineralogy and chemical composition of the TMPs generally differ based on their sources: industrial fly ash or vehicle derived (Bhattacharjee et al. 2011; Magiera et al. 2013; Sokol et al. 2002; Wang 2014; Yang et al. 2014; Zhao et al. 2006). Based on this study it is reported that the magnetic particle expelled during the combustion of fossil fuels at high temperatures (i.e., industrially derived contaminants) are characteristically spherical in shape and those emitted from automobiles are non-spherical to irregular in shape (Magiera et al. 2016). Thus, the urban topsoils are basically sinks for various environmental contaminants and therefor magnetic measurements can be used as tracers to derive pollution degrees (Gautam et al. 2004; Lu et al. 2007; Xia et al. 2014; Zhang et al. 2011; Zhu et al. 2013). However, more detailed morphological and mineralogical forms need to be explored. A great deal of work has been made regarding the magnetic properties of urban soils and dusts, detailed characterization of TMPs from the topsoil of locations surrounding Thermal Power Plants is required in the next course of research.

In the present study a cumulative approach of magnetic susceptibility, scanning electron microscopy equipped with energy-dispersive X-ray spectroscopy (SEM-EDS) and X-ray diffraction has been used to establish the following:

- (a) To develop the relationship between magnetic susceptibility and heavy metal pollution.
- (b) To unravel the detailed morphology of the TMP in the urban soils.
- (c) To identify the possible source and suggest remediation.

26.2 Materials and Methods

26.2.1 Sample Collection

Topsoils (road dust at places) were collected from urban and industrial areas of Farakkaarea (in and around FSTPS). A total number of 120 samples were collected among which includes the roadside samples from the vicinity of FSTPS, residential areas, and commercial places within the studied area. The rest of the samples includes dust and soil from the rim of national and state highways in the city. Samples belonging to the industrial areas were collected from sites in and around the thermal power plant (FSTPS, NTPC) and other small-scale industries (viz. cement factory). For better and unbiased sampling, the samples were collected using a grid sampling model. After the initial demarcation of the industrial zone was fixed to be a rectangular one. The rectangular area was then divided into squared grids and four samples were collected each from the four edges of the squares. A detailed map of the study area is provided in Fig. 26.1.

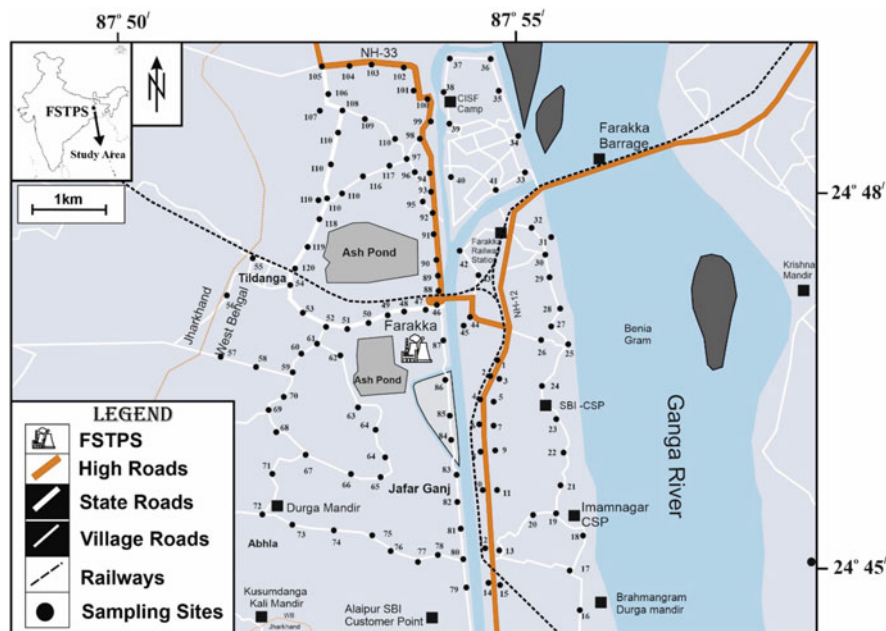


Fig. 26.1 Generalized location map of the study area. Black dots denote sampling sites

26.2.2 Sample Preparation

The collected dust and soil samples were dried to minimum amount of moisture content (removal of moisture from these types of samples are necessary because the presence of moisture ubiquitously decreases the value of magnetic susceptibility and impinges errors). Samples are initially dried by exposure sunlight and strict removal of moistures are done by automated driers. After the drying procedure is done, samples were crushed to the finest size using mortar-pestle (made of non-magnetic material, agate) and the fine samples were put into cylindrical sample holders of 2.54 cm in diameter and 2.2 cm in height (six for each site). This particular dimension is chosen because this perfectly fits the Bartington MS-2 Susceptibility Meter. The unit which possesses the highest value of susceptibility for particular sites was coated with Carbon in stubs for SEM-EDS studies and representative samples were also used for XRD analysis.

26.2.3 Magnetic Properties and XRD Analysis

Magnetic Susceptibility of the samples was measured using the Bartington MS-2B dual-frequency susceptibility meter (Bartington Ltd., UK). X-ray diffraction analysis

of the samples was carried out from the non-oriented fine powdered samples using 40 kV and 30 mA radiation using a PANalytical X-ray diffractometer (Philips, India). The diffraction patterns were recorded from 5 to 60 degrees 2θ .

26.2.4 Morphology Observation of the TMPs (SEM-EDS)

Scanning Electron Microscopy (SEM) is used to identify the morphology of the magnetic particles. First of all, the samples were mounted on SEM stub and coated with carbon using SPI-MODULE coater. The SEM were analyzed using Carl Zeiss EVO-18 Scanning Electron Microscope (Germany) housed at the Department of Geological Sciences (Jadavpur University). The machine is fixed with a 25 kV and 750 μA EDS microanalyzer. The energy-dispersive X-ray spectrograph from the samples was collected between 0 and 13 keV. Elemental analysis was done in area mode where the beam remains localized to certain particles in fixed view. The semi-quantitative analysis was done using the synchronous operation of the EDAX software (Team, Germany).

26.3 Results

26.3.1 Magnetic Susceptibility Characteristics

The distribution pattern of magnetic susceptibility values of the studied samples is represented in the Fig. 26.2. The magnetic susceptibility of the TMP ranges from $263.4 \times 10^{-8} \text{ m}^3/\text{kg}$ and $3.9 \times 10^{-8} \text{ m}^3/\text{kg}$ with an average of $134 \times 10^{-8} \text{ m}^3/\text{kg}$. Such enhanced values for the urban topsoils are due to the abundance of TMPs in them. However, the value of magnetic susceptibility for pure magnetite is much higher, the presence of iron and enhanced value of magnetic susceptibility can be

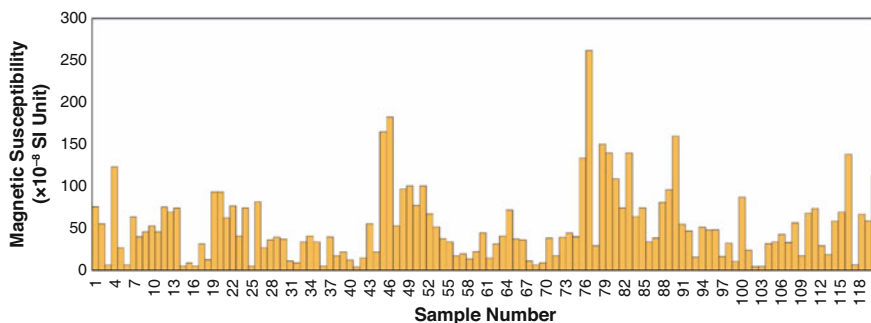


Fig. 26.2 Distribution of magnetic susceptibility in the studied samples

assumed to be due to the presence of Fe in host minerals (viz. silicates) or magnetite that have incorporated a considerable number of foreign elements.

26.3.2 Magnetic Minerals of TMP (X-Ray Diffraction Analysis)

The results of X-ray diffraction analysis of the bulk TMP samples, exhibit some important heavy metal-bearing minerals such as Tetradyomite (Bismuth-Tellurium Sulfide) and free Tellurium metal also. The Fe, that are present within the samples mainly occurs within the lattice structures of Feldspars, Pyroxenes, and other oxides with rare cases of pure magnetite or haematite. Although the samples were magnetically concentrated, they display high amount of silica which is due to the incrustation of silica. The other minerals that are identified by XRD analysis are Albite, Diopside, Anorthite, Quartz etc. Pure iron-bearing mineral phases are difficult to identify by XRD analysis because of overlapping peaks in the XRD patterns. This sort of diversity of minerals where technogenic Fe occurs, is indicative of some multiple sources of origin of TMPs (Fig. 26.3).

26.3.3 SEM-EDS Analysis

The SEM and EDS studies were used for obtaining the information regarding the morphology and surface texture of the TMPs as well as to reveal the elemental composition of the same. According to the observation in the SEM, it is revealed that the particles are largely heterogeneous in size and shape (Fig. 26.4). Based on the SEM observations chiefly three shapes of TMPs are observed: spherical (Fig. 26.5), irregular shaped (Fig. 26.6) and aggregate of particles. This sort of morphologies observed here have a close association with the magnetosphere from the fly ashes (Hower et al. 1999; Iordanidis et al. 2008; Jordanova et al. 2004; Sokol et al. 2002; Wang 2014; Yang et al. 2014; Zhao et al. 2006). As discussed earlier, this spherule shaped morphology of the TMPs are typical for those collected from industrial sites as in the present case. The sizes of such particles range from 10-100 micrometers in diameter. Both smooth and corrugated-surface variety of such spherical particles are observed (Fig. 26.7).

EDS studies depict that the concentration of Fe in such aspherical samples is as high as 22% (Fig. 26.5). The spherical shaped TMP possesses a diameter of about 50 μm with the EDS spectrum as provided corresponding to each figure. These samples have a specific chemical composition consisting of oxides of Silicon, Iron, Aluminum and Magnesium as the carrier of heavy metals. The weight percentage of different elements are as follows: Fe (11.96%), Ca (1.29%), Si (7.99 %), Al (4.94%), Mg (0.91%) and O (36.4%). The presence of Magnesium in fly ashes depicts the

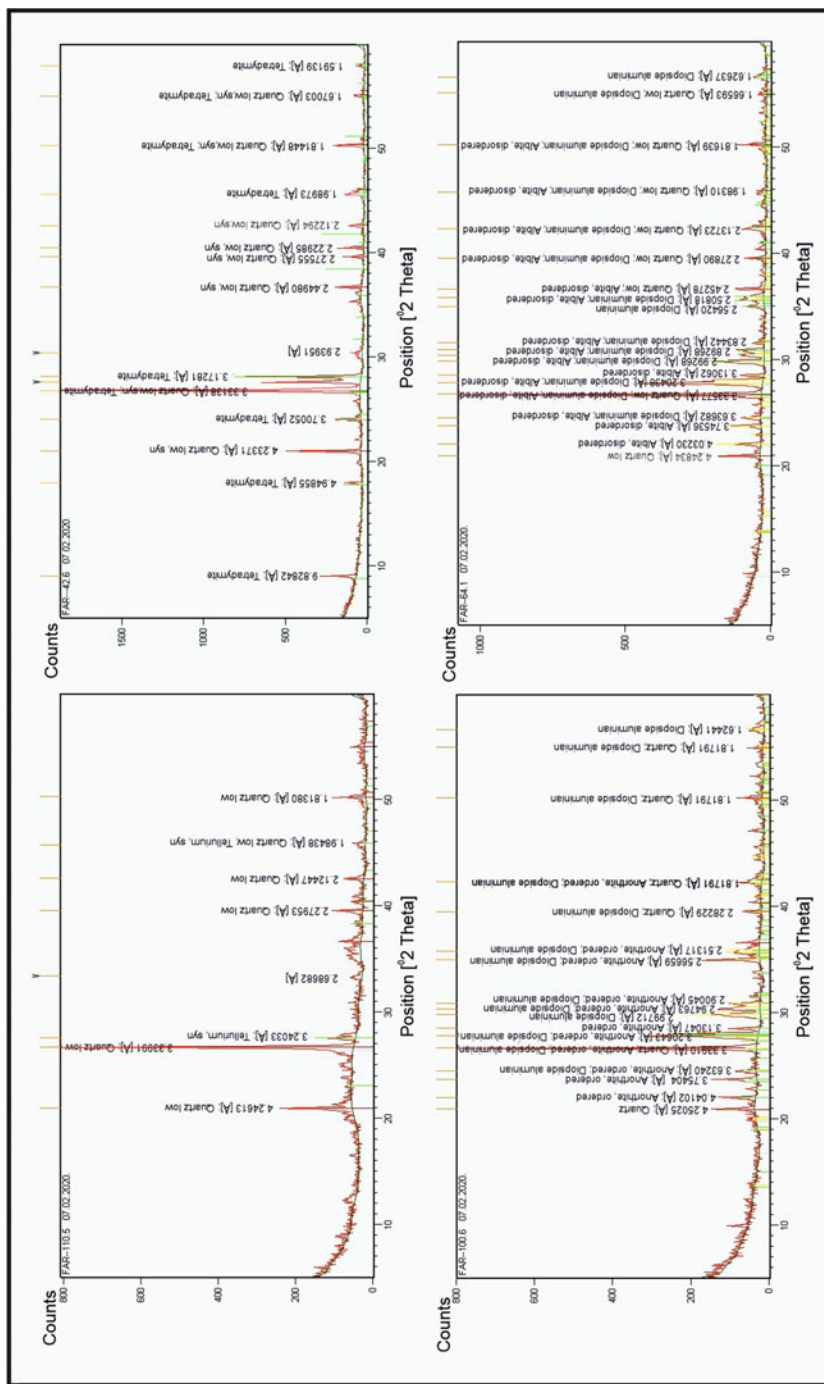


Fig. 26.3 Results from XRD analysis of representative samples

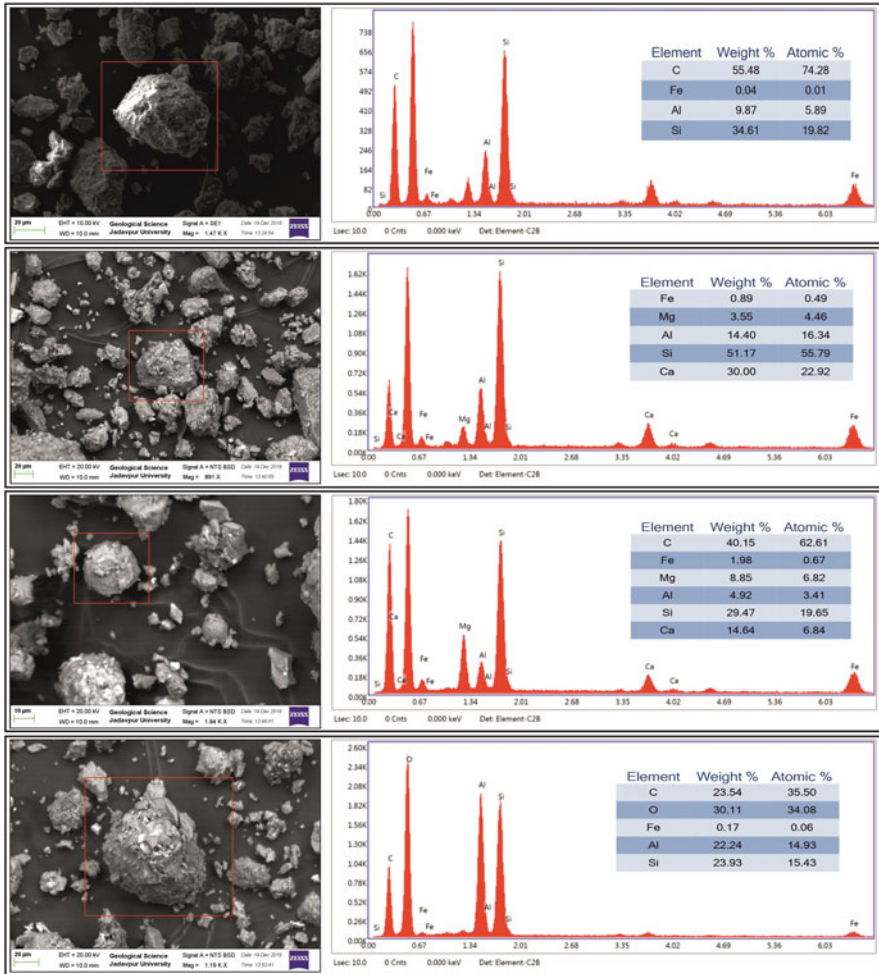


Fig. 26.4 Variation of the morphology of TMPs in urban soils and corresponding EDS spectra

presence of magnesioferrite crystals which are very commonly associated with coke dust. Considerable amount of Calcium basically points towards considerable amount of Calcium admixtures which are generally Calcium-ferrites rather than stoichiometric magnetite. High amount of Silica in some samples reveals the occurrence of iron oxides as incrustation of the surface of silicate minerals like Quartz or silica.

This typical spherical shaped TMPs detected are almost typical for the same produced during coal burning in powerplants mainly (as the samples were also collected in and around the thermal power plant). Therefore, it is evident that the spherical TMPs are formed during combustion of coal during power generation in the FSTPS.

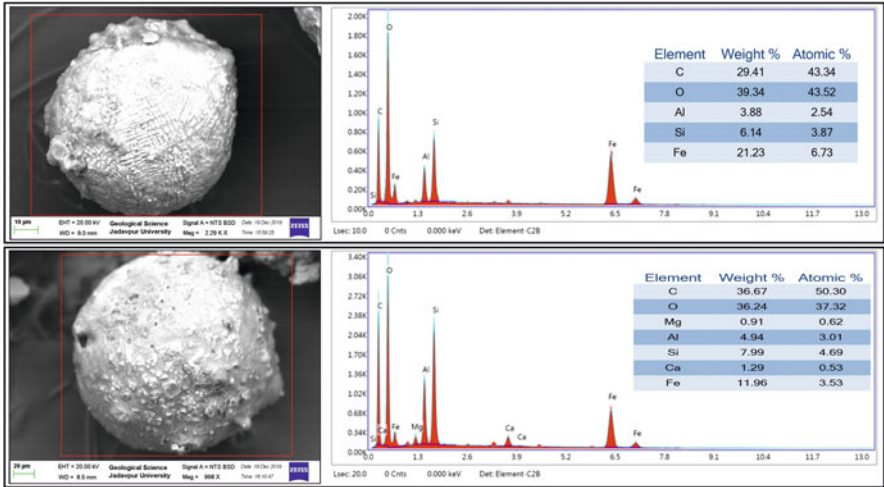


Fig. 26.5 Typical spherical TMP was released from industrial ash and corresponding EDS spectra

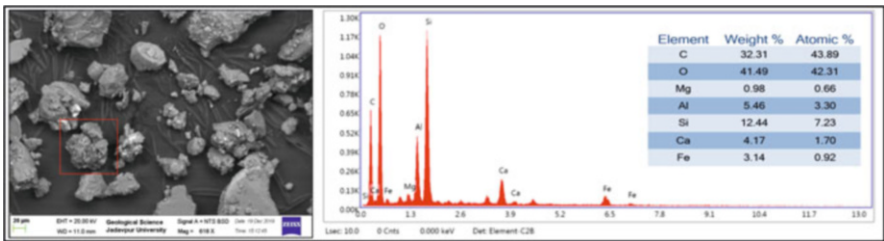


Fig. 26.6 Irregular shaped TMP was released from industrial ash and corresponding EDS spectra

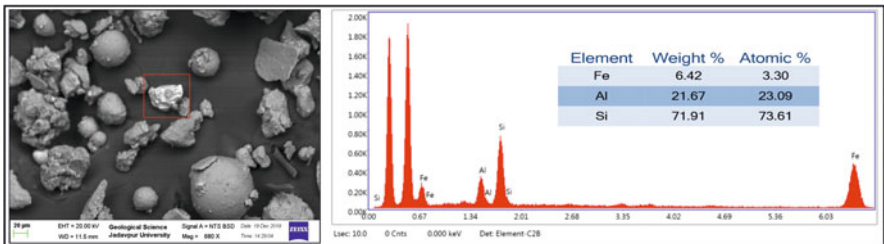


Fig. 26.7 Variation of smooth and corrugated-surface TMPs associated with industrial dusts

26.4 Discussion

Identifying and characterizing the TMP are capable of providing vivid information regarding soil and environment pollution that is caused due to the deposition of toxic wastes from industries and other sources. From the results, it is well understood that the TMP from different sources have different morphological and chemical composition. However, it is quite evident that the TMP that are originating from the coal combustion process (thermal power plant as in the present case) have a distinct spherical or near-spherical shape. Magnetic particles that are formed as wastes at the coal-burning plants are typically spherical in nature and they have a size variation from few micrometers to several hundreds of micrometers. The magnetic properties of TMP are generally found to be stable and are unalterable for a long period of time (Heller et al. 1998; Kapicka et al. 1999). From the present study, it is quite evident that the magnetic particles that are reported in the urban topsoils under the present study are spherical and they vary in sizes from few microns to hundreds of microns. Their ubiquitousness in the samples undoubtedly points towards the combustion process in the thermal power plant as a source or urban pollution. Also, it is evident that automobile emission as a source of pollution cannot be neglected. Some previous studies find that particular source to be the most important sources in their respective study areas (Bućko et al. 2011; Hoffmann et al. 1999; Kim et al. 2009; Matzka and Maher 1999).

Basically, the irregular shaped and aggregate particles are possibly associated with emissions during the metal smelting process or primary erosion of traffic parts. The presence of some irregular/aggregate is strongly reported by some earlier workers sites near to iron-smelting plants, old steel plants and waste recycling plants (Zhang et al. 2011; Zhu et al. 2013). The TMP originated from vehicular emission includes the metal parts, abrasion from brake linings, tires and road surfaces. These TMPs have a character to occur as highly packed aggregates or in well-developed crystal forms. Combining all the results it can be assured that magnetic iron phases and various morphological phases of TMP are the primary representation of pollution sources due to industrial and other anthropogenic activities.

As iron is known to be chemically active and has capability to act as scavengers for heavy metals, i.e., by replacing the Fe^{2+} and/or Fe^{3+} ions in pure or non-stoichiometric magnetite or haematite. Earlier Lu et al. (2009, 2016) established that highly magnetic iron oxides have a tendency to hold heavy metals rather than non-magnetic phases (Lu et al. 2009, 2016).

The application of the presence of magnetic minerals to extrapolate the amount of heavy metal contamination is based on the degrees of correlation of PLI and the amount of magnetic particles in a particular samples. The correlation of the Tomlinson's PLI for any particular element increases with the increase of magnetic susceptibility for any particular sample. However, it is to be noted that such correlation is more effective and stronger when the sources of pollution are single. However, in cases of multiple pollution sources, the results may vary (Lu et al. 2016).

It is very evident from the results that the industrial constraint and the traffic emission are the major causes of atmospheric and/or soil pollution in Indian industrial cities. Considering the significance of the correlation between the magnetic and morphological properties of the TMP of the urban soil, the TMP evidently reflect the accumulation and deposition of anthropogenic dust particles.

26.5 Risk Assessment and Remediation

Application of magnetic susceptibility and morphological studies on TMP obtained from Indian industrial sites are gaining importance in serving as proxies for pollution (Goddu et al. 2004; Mondal et al. 2017). The present study in the Farakka area also proved to be useful and bears significance. The distribution of the magnetic susceptibility very clearly indicates that the reason for the degradation of the environmental quality is simply due to anthropogenic causes, especially, emissions from industries like thermal power plants, cement factories, vehicular releases in dense traffic prone areas etc. This needs to be taken care off.

The first and foremost criterion for this boom in environmental pollution is lack of environmental legislation, or rather, following the available legislation. The poor maintenance of the machineries used in such industries stands first among all. The state and central governments have introduced several rules of upgradation of machineries to ensure controlled pollutant emission. However, industrial authorities are hardly concerned about the environment and thus do not take care of upgradation of machineries to modern versions and decrease environmental concerns. The major industrial controlling authorities in the studied area and other localities of the state are NTPC Limited, West Bengal Power Development Corporation Limited (WBPDC) etc. These organizations under which mainly the thermal power plants are operated needs to be more efficient and stricter in case of reducing obvious causes of environmental pollution. However, in recent times, the government is taking steps to reduce these. As per reports, considerable numbers of machineries with the old model are being replaced by modern imported models. However, still more needs to be done and for that, the common population needs to develop awareness. Simple steps can serve the purpose. These include turning the engines off during red traffic signals, usage of modern eco-friendly modes of transport such as pool cars, battery-operated cars should be strongly entertained, maintenance of both public and private vehicles regularly to avoid wear and tear of machineries etc. Moreover, motor vehicle rules should be made stricter and transparent, so that any duplicity is not entertained in pollution control documents.

Thus, the magnetic susceptibility studies once again proved to be a relatively low-cost potential measure to determine detrimental effects to our environment caused by anthropogenic activities. It is also strongly recommended that a magnetic susceptibility mapping should be carried out prior to detailed chemical analysis as it can demarcate the regions which are endangered by environmental contamination

and thereby can save money for further usage. The frequency-dependent magnetic susceptibility, on the other hand, provided a threshold value of susceptibility and thus series of measurement from any particular area can precisely define the condition of the environment in that particular locality in the long run and necessary steps can be executed therein.

26.6 Conclusion

The results drawn from the present study contain ample amount of TMP which are present in the urban topsoils. The content of TMP has a positive or at least intermediate correlation with the PLI of the urban topsoils and thus magnetic analysis can serve as strong proxies for environmental analysis. Magnetic particles detected in the urban dusts and soils may be due to various technological and anthropogenic processes like the burning of coal, dusts derived from industries, vehicular emissions etc. The morphology of the TMPs as observed are basically signatures of their origin. Thus, in a nutshell, analysis of the TMPs from the urban topsoils brings out the following conclusions:

1. Technical attributes from various industrial branches have their typical characterization of magnetic particles. Basically, their morphology and mineralogy determine their origin. These TMPs are characteristic for pollution source identification and are also pathfinders for tracing soil pollution.
2. Magnetic particles released from coal-burning units (or coal combustion as in the present case where the samples are collected from localities near thermal power plant) are typically spherical in nature. In many cases, such magnetite spherules are coated with thin films of silicate or aluminosilicate.
3. A certain type of TMP is rich in Calcium which are remnants of the additive used during the cement production process. The high calcium in the TMPs is typical signature for the dusts from the cement factories.
4. Apart from the typical spherical dust, some aggregates of irregular particles are also encountered in the study which is also results of coking processes.
5. Simple steps of public awareness and implementation of modern legislations may work out as remediation measures for industrial pollution in India.

However, there are some drawbacks or rather constraints that should be taken care off while applying this method of environmental assessment. First of all, it should be taken care that this method primarily provides the pollution affected areas, however, for determination of the three main characters of magnetic pollutants (composition, concentration and grain size) detailed rock magnetic studies need to be carried out, however, the study becomes narrow as Susceptibility analysis helps to demarcate the prone areas. Secondly, this method is risky while applying in areas in the vicinity of iron-rich area (for example, in localities close to iron ores) and may led to erroneous results. However, this issue can be handled when one determines the threshold value for magnetic particles in soil (or dust) and sets a mark for delineation

of pollution-prone areas. However, when thought in a holistic way, this method of pollution assessment remains cost-effective and can be applied at industrial level before detailed chemical studies in order to target only prone areas, which in turn again saves time and man-power.

Acknowledgments The authors deeply acknowledge Jadavpur University—R.U.S.A (2.0) Scheme for providing financial supports in all respect. SM and SC acknowledge the Department of Geological Sciences, Jadavpur University for providing all sorts of Laboratory facilities in the department.

References

- Bhattacharjee A, Mandal H, Roy M, Kusz J, Hofmeister W (2011) Microstructural and magnetic characterization of fly ash from Kolaghat thermal power Plant in West Bengal, India. *J Magn Mater* 323:3007–3012
- Blundell A, Hannam JA, Dearing JA, Boyle JF (2009) Detecting atmospheric pollution in surface soils using magnetic measurements: a reappraisal using an England and Wales database. *Environ Pollut* 57:2878–2890
- Bučko MS, Magiera T, Johanson B, Petrovský E, Pesonen LJ (2011) Identification of magnetic particulates in road dust accumulated on roadside snow using magnetic, geochemical and micro-morphological analyses. *Environ Pollut* 159:1266–1276
- Catinon M, Ayrault S, Boudouma O, Bordier L, Agnello G, Reynaud S, Tissot M (2014) Isolation of technogenic magnetic particles. *Sci Total Environ* 475:39–47
- Gautam P, Blaha U, Appel E, Neupane G (2004) Environmental magnetic approach towards the quantification of pollution in Kathmandu urban area, Nepal. *Phys Chem Earth* 29:973–984
- Giere R, Querol X (2010) Solid particulate matter in the atmosphere. *Elements* 6(4):215–222
- Goddu SR, Appel E, Jordanova D, Wehland R (2004) Magnetic properties of road dust from Visakhapatnam (India)—relationship to industrial pollution and road traffic. *Phys Chem Earth* 29(13, 14):985–995
- Grobety B, Giere R, Dietze V, Stille P (2010) Airborne particles in the urban environment. *Elements* 6(4):229–234
- Heller F, Strzyszcz Z, Magiera T (1998) Magnetic record of industrial pollution in forest soils of Upper Silesia, Poland. *J Geophys Res* 103:17767–17774
- Hoffmann V, Knab M, Appel E (1999) Magnetic susceptibility mapping of roadside pollution. *J Geochem Explor* 66:313–326
- Hower JC, Rathbone RF, Robertson JD, Peterson G, Trimble AS (1999) Petrology, mineralogy, and chemistry of magnetically-separated sized fly ash. *Fuel* 78:197–203
- Hullet LD, Weinberger AJ, Northcutt KJ, Ferguson M (1980) Chemical species in fly ash from coal-burning power plant. *Science* 210:1356–1358
- Jordanidis A, Buckman J, Triantafyllou AG, Asvesta A (2008) ESEM–EDX characterisation of airborne particles from an industrialised area of northern Greece. *Environ Geochem Health* 30:391–405
- Jablonska M, Smolka-Danielowska D (2008) Iron oxides particles in the air and fly ash, and their influence on the environment (preliminary studies), 24. Polish geological institute. *Special Papers* 93–98
- Jordanova D, Hoffmann V, Fehr KT (2004) Mineral magnetic characterization of anthropogenic magnetic phases in the Danube river sediments (Bulgarian part). *Earth Planet Sci Lett* 221:71–89

- Jordanova D, Jordanova N, Hoffmann V (2006) Magnetic mineralogy and grain-size dependence of hysteresis parameters of single spherules from industrial waste products. *Phys Earth Planet Inter* 154:255–265
- Kapicka A, Petrovský E, Ustjak S, Machackova K (1999) Proxy mapping of fly-ash pollution of soils around a coal-burning power plant: a case study in the Czech Republic. *J Geochem Explor* 66:291–297
- Kim W, Doh SJ, Yu Y (2009) Anthropogenic contribution of magnetic particulates in urban roadside dust. *Atmos Environ* 43:3137–3144
- Kukier U, Ishak CF, Sumner ME, Miller WP (2003) Composition and element solubility of magnetic and non-magnetic fly ash fractions. *Environ Pollut* 123(2):255–266
- LeGalley E, Krekeler MPS (2013) A mineralogical and geochemical investigation of street sediment near a coal-fired power plant in Hamilton, Ohio: an example of complex pollution and cause for community health concerns. *Environ Pollut* 176:26–35
- Lu SG, Bai SQ, Xue QF (2007) Magnetic properties as indicators of heavy metals pollution in urban topsoils: a case study from the city of Luoyang, China. *Geophys J Int* 171:568–580
- Lu SG, Chen YY, Shan HD, Bai SQ (2009) Mineralogy and heavy metal leachability of magnetic fractions separated from some Chinese coal fly ashes. *J Hazard Mater* 169:246–255
- Lu S, Yu X, Chen Y (2016) Magnetic properties, microstructure and mineralogical phases of technogenic magnetic particles (TMPs) in urban soils: their source identification and environmental implications. *Sci Total Environ* 543:239–247
- Magiera T, Jablonska M, Strzyszc Z, Rachwal M (2011) Morphological and mineralogical forms of technogenic magnetic particles in industrial dusts. *Atmos Environ* 45:4281–4290
- Magiera T, Gołuchowska B, Jabłońska M (2013) Technogenic magnetic particles in alkaline dusts from power and cement plants. *Water Air Soil Pollut* 224:1389–1406
- Magiera T, Mendakiewicz M, Szuszkiewicz M, Chróst L (2016) Technogenic magnetic particles in soils as evidence of historical mining and smelting activity: a case of the Brynica river valley Poland. *Sci Total Environ* 566–567:536–551. <https://doi.org/10.1016/j.scitotenv.2016.05.126>
- Matzka J, Maher BA (1999) Magnetic biomonitoring of roadside tree leaves: identification of spatial and temporal variations in vehicle-derived particulates. *Atmos Environ* 33:4565–4569
- Mondal S, Chatterje S, Maity R, Gain D, Das A, Sinha S (2017) Magnetic susceptibility as a proxy for pollution in Triveni-Bandel area, Hooghly district, West Bengal, India. *Curr Sci* 112 (11):2306–2311
- Rachwal M, Magiera T, Wawer M (2015) Coke industry and steel metallurgy as the source of soil contamination by technogenic magnetic particles, heavy metals and polycyclic aromatic hydrocarbons. *Chemosphere*. <https://doi.org/10.1016/j.chemosphere.2014.11.077>
- Sokol EV, Kalugin VM, Nigmatulina EN, Volkova NI, Frenkel AE, Maksimova NV (2002) Ferrospheres from fly ashes of Chelyabinsk coals: chemical composition, morphology and formation conditions. *Fuel* 81:867–876
- Szuszkiewicz M, Magiera T, Kapicka A, Petrovský E (2015) Magnetic characteristics of industrial dust from different sources of emission: a case study of Poland. *J Appl Geophys* 116:84–92
- Thompson R, Oldfield F (1986) *Environmental magnetism*. Allen and Unwin, Winchester, Mass. <https://doi.org/10.1007/9788036-8>
- Wang XS (2014) Mineralogical and chemical composition of magnetic fly ash fraction. *Environ Earth Sci* 71:1673–1681
- Wójcik M, Smolka-Danielowska D (2008) Phase minerals composition of wastes formed in bituminous coal combustion from individual domestic furnace in the Piekary Śląskie town (Poland). *Pol J Environ Stud* 17(5):817–821
- Xia DS, Wang B, Yu Y, Jia J, Nie Y, Wang X, Xu SJ (2014) Combination of magnetic parameters and heavy metals to discriminate soil-contamination sources in Yinchuan—a typical oasis city of northwestern China. *Sci Total Environ* 485–496:83–92
- Yang T, Liu Q, Li H, Zeng Q, Chan L (2010) Anthropogenic magnetic particles and heavy metals in the road dust: magnetic identification and its implications. *Atmos Environ* 44:1175–1185

- Yang JP, Zhao YC, Zyryanov V, Zhang JY, Zheng CG (2014) Physical–chemical characteristics and elements enrichment of magnetospheres from coal fly ashes. *Fuel* 135:15–26
- Zawadzki J, Fabijańczyk P, Magiera T, Rachwał M (2015a) Micro-scale spatial correlation of magnetic susceptibility in soil profile in forest located in an industrial area. *Geoderma* 249:61–68
- Zawadzki J, Fabijańczyk P, Magiera T, Rachwał M (2015b) Geostatistical microscale study of magnetic susceptibility in soil profile and magnetic indicators of potential soil pollution. *Water Air Soil Pollut* 226:142
- Zhang W, Jiang H, Dong C, Yan Q, Yu L, Yu Y (2011) Magnetic and geochemical characterization of iron pollution in subway dusts in Shanghai, China. *Geochem Geophys Geosyst* 12: Q06Z25. <https://doi.org/10.1029/2011GC003524>
- Zhao Y, Zhang J, Sun J, Bai X, Zheng C (2006) Mineralogy, chemical composition, and micro-structure of ferrospheres in fly ashes from coal combustion. *Energy Fuel* 20:1490–1497
- Zhou Y, Su Q, Wang Z, Deng H, Zu X (2013) Controlling magnetism of MoS₂ sheets by embedding transition-metal atoms and applying strain. *Phys Chem Chem Phys* 15:18464–18470
- Zhu Z, Li Z, Bi X, Han Z, Yu G (2013) Response of magnetic properties to heavy metal pollution in dust from three industrial cities in China. *J Hazard Mater* 246–247:189–198

Chapter 27

Pesticides: Types, Toxicity and Recent Updates on Bioremediation Strategies



Rujul Deolikar, Soumya Pandit, Jyoti Jadhav, Govind Vyavahare, Ranjit Gurav, Neetin Desai, and Ravishankar Patil

Abstract Pesticides are common agricultural chemicals widely used in farming practices to protect plants and animals from foreign pathogenic attacks and to control the rodent population. Pesticide covers different chemical agents such as herbicide, fungicide, nematicide, animal and insect repellent, etc. Besides their beneficial usage, pesticides are known to adversely affect nervous, gastrointestinal, reproductive, respiratory, and endocrine system as well as proved to be carcinogenic agents. The present chapter discusses the major pesticide classes which are being used in the agriculture sector and other purposes and these have been reviewed with common examples. Further emphasis is given to the acute and chronic health effects after exposure to these hazardous chemicals. Recent advances in the bioremedial strategies of pesticides from the field and surface water using plant and microorganisms are systematically discussed.

Keywords Bioremediation · Consortium · Environmental pollutant · Pesticides · Risk assessment · Toxicity

R. Deolikar · N. Desai · R. Patil (✉)
Amity Institute of Biotechnology, Amity University, Mumbai, Maharashtra, India

S. Pandit
Department of Life Sciences, School of Basic Sciences and Research, Sharda University,
Greater Noida, India

J. Jadhav · G. Vyavahare
Department of Biotechnology, Shivaji University, Kolhapur, Maharashtra, India

R. Gurav
Department of Biological Engineering, College of Engineering, Konkuk University, Seoul,
South Korea

© Springer Nature Switzerland AG 2021

P. K. Shit et al. (eds.), *Spatial Modeling and Assessment of Environmental Contaminants*, Environmental Challenges and Solutions,
https://doi.org/10.1007/978-3-030-63422-3_27

531

27.1 Introduction

Pesticide is a class of biological or chemical agents that are used extensively in agricultural practices that either inhibit the growth or directly kill pests by restricting their reproductive cycle (Mladenović et al. 2018). They protect plants from pests and weeds, and also provide defense to humans against vector-borne diseases. Pesticides are generally classified into various groups like insecticides, fungicides, rodenticides, weedicides, viricides, herbicides, and larvicides (Nicolopoulou-Stamati et al. 2016). Judicious use of pesticides could provide many social, economic, and environmental advantages such as affordable and edible high-quality food, proper management of land, water, and other natural resources, etc. (Popp et al. 2013). For the ever-increasing population of the world, pesticides made it possible to fight against food scarcity and hunger. Pesticides are also beneficial to control various vector-borne diseases like dengue and malaria (Townson et al. 2005; Ross 2005).

Though the initial objective of pesticide use was to target harmful or unwanted organisms without affecting nontarget organisms, over the years, they have been known to cause many health and environmental problems (WHO 1990; Nicolopoulou-Stamati et al. 2016). Heavy use of pesticides resulted in its accumulation in water bodies, soil, and finally into organisms through the food chain causing disastrous effects to the ecosystem. For example, a high concentration of toxic organochlorine pesticides like dichlorodiphenyltrichloroethane, hexachlorocyclohexane, and endosulfan have been reported in the groundwater in Karnataka, a state in India (Jayashree and Vasudevan 2007). About 1 million deaths per year are recorded due to pesticide poisoning and agricultural workers are under high threat (Environews Forum 1999; Aktar et al. 2009). Pesticides remain in the environment and can also percolate into the soil, water, and air (Lefrancq et al. 2013; Ozkara et al. 2016), making its easy exposure to susceptible organism. Pesticide accumulation in humans occurs through the ingestion of food like vegetables and fruits and during direct work in the field. This has led to the abandonment of certain pesticides in the farming sector (Alewu and Nosiri 2011; Nicolopoulou-Stamati et al. 2016).

The North American Free Trade Agreement (NAFTA), European Union, and the Codex have fixed certain “safe levels” of Maximum Residue Limits (MRLs) to enhance agricultural productivity with no adverse effect on the consumer’s health (Handford et al. 2015). However, due to farmers’ illiteracy and lack of ecological awareness, there is a tremendous use of toxic chemicals including pesticides and fertilizers than the actual requirement which is a major reason for pesticide toxicity. Moreover, the synergistic effect of pesticides is highly dangerous and known to cause endocrine-disrupting effect resulting in the suppression of the immune and endocrine systems, which leads to symptoms like dementia, reproductive disorders, and cancer (Hurley et al. 1998; Crisp et al. 1998; Brouwer et al. 1999). Hence, the removal of pesticides that are commonly released into the environment is very important for the sustainable growth of the ecosystem.

In the present chapter, the major pesticides being used in agriculture and their further adverse effects on ecosystem and health have been discussed. Further, a comprehensive emphasis is given to the recent advances in the bioremediation of pesticides from the field and surface water.

27.2 Types of Pesticides

Pesticides can be segregated into numerous categories according to the kinds of pest they target and mode of action. Apart from this, pesticides can be classified on the basis of chemical composition, for example, organochlorines, organophosphates, neonicotinoids, triazines, carbamates, etc. This kind of classification sheds light on the chemical and physical characteristics of the pesticides and further assists in determining the mode and rate of administration (Yadav and Devi 2017). WHO has categorized pesticides into I (highly toxic) to IV (slightly toxic) based on their median lethal dose (LD_{50}) (WHO 2004).

In Section 27.2 and Table 27.1, different commonly used pesticides, their nature, chemical structure, and target organisms are described and special concern is given to the adverse effects on ecosystem and human health.

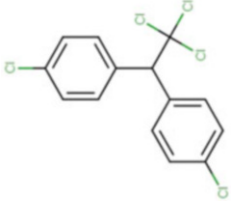
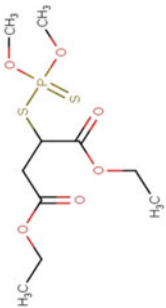
27.2.1 Insecticides

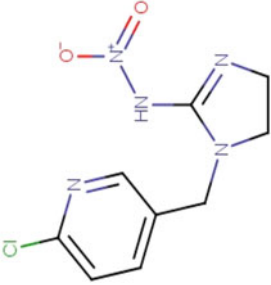
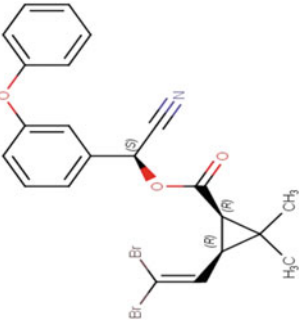
The pesticides which are used for killing insect pests on crops are known as insecticides. Due to the evolution of insecticide-resistant pest species, the composition of these substances constantly needs to be renewed or altered (Oberemok et al. 2015).

27.2.1.1 Dichlorodiphenyltrichloroethane (DDT)

Dichlorodiphenyltrichloroethane (DDT) or 1-chloro-4-[2,2,2-trichloro-1-(4-chlorophenyl)ethyl]benzene is one of the most widely used insecticides, belonging to the class of organochlorines. The molecular formula of DDT is $C_{14}H_9Cl_5$. It is a broad-spectrum insecticide, acting upon orders such as Lepidoptera, Hymenoptera, Diptera, and Orthoptera (Oberemok et al. 2015) and has important application against mosquito-borne diseases like malaria. There are several toxic effects of DDT, and hence, it is proscribed in a number of countries. DDT has a high persistence in the environment (Turusov et al. 2002; Oberemok et al. 2015). It is lipophilic in nature and remains in the human adipose and neural tissue for a longer time (Karami-Mohajeri and Abdollahi 2011). Repetitive exposure to DDT even in lower concentrations may result in its considerable accumulation in the body, which is responsible for several lethal consequences (Turusov et al. 2002). Over the years,

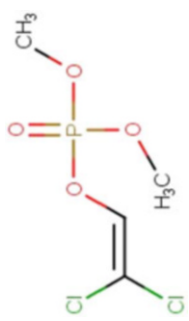
Table 27.1 Different types and classes of pesticides with target organism and adverse health effects

Type of pesticide	Examples	Biochemical class	Target organisms	Toxic health effects	References
Insecticide (kills insects and arthropods)	Dichlorodiphenyltrichloroethane (DDT) 	Organochlorine	Broad-spectrum insecticide for Lepidoptera, Hymenoptera, Diptera, and Orthoptera	Endocrine disruption, carcinogenic, affects embryo development, hematological alterations, Lipid metabolism dysfunction, reduction in bone mineral density	Tunusov et al. (2002), Tiemann (2008), Mnif et al. 2011, Freire et al. (2015), Karami-Mohajeri and Abdollahi (2011)
	Malathion 	Organophosphate	Wide range of insects, particularly ants, aphids, fleas, ticks, wasps, moths, spiders, mosquitoes, Mediterranean fruit flies, cotton boll weevils, head lice	Disruption of cholinesterase activity, genotoxicity, cellular oxidative stress because of mitochondrial dysfunction, deterioration of nervous system, non-Hodgkin's lymphoma, prenatal births, hepatotoxicity, immunotoxicity, disruption of metabolic function, dizziness, headache, vomiting, and bradycardia	Tchounwou et al. (2015), Frankowski (2004), Jensen and Whaling (2010), Uygun et al. (2005), Kalender et al. (2010), Lasram et al. (2009), Nain et al. (2011)

<p>Imidacloprid</p> 	Neonicotinoid	<p>Ricehoppers, thrips, termites, turf and soil insects, beetle species, ectoparasites on canines and felines.</p>	<p>Mutagenesis, immunotoxicity, neurotoxicity, reproductive toxicity (lower sperm count, irregular sperm morphology, lower ovarian weight, irregular ovarian shape), and endocrine disruption of androgens and estrogens</p>	<p>Iyer and Makris (2010), Bagri et al. (2016), Duzguner and Erdogan (2010a, b), Lonare et al. (2014), Gawade et al. (2013), Badgujar et al. (2013), Mikolić and Brčić Karačonji (2018), Bal et al. (2012), Kapoor et al. (2011), Memon et al. (2014)</p>
<p>Deltamethrin</p> 	Pyrethroid	<p>Mites, mosquitoes, flies, lice, cockroaches, <i>Aedes aegyptii</i> and <i>Anopheles gambiae</i> (malaria control)</p>	<p>Immunotoxicity, induction of apoptosis of thymic cells, plaque formations in the spleen and decreased activity of lymphocytes in the blood, hepatotoxicity and nephrotoxicity in rats, reproductive disabilities in rats such as decrease in sperm count, motility and disorders of epididymis and testes, algal blooms resulting in fish gills clogging, increase in BOD; neurotoxicity and Parkinson's disease through disruption of dopamine transportation, disorders of</p>	<p>Kumar et al. (2011), Shrivastava et al. (2011), Chrustek et al. (2018), Bradberry et al. (2005), Soderlund (2012), Kumar et al. (2018), Gündiz et al. (2015), Oda and El-Maddawy (2012), Barlow et al. (2001), Viel et al. (2015), Elwan et al. (2006)</p>

(continued)

Table 27.1 (continued)

Type of pesticide	Examples	Biochemical class	Target organisms	Toxic health effects	References
	Dichlorvos 	Organophosphate	Lepidopterans, dipterans, aphids, crustacean ectoparasites on fish, anthelmintic agent on dogs, pigs, and horses	the central nervous system—poor memory, sleep disorders, poor speech, low intelligence	Wang et al. (2004), Binukumar and Gill (2010), Okoroiwu and Iwara (2018), Zhao et al. (2015), Mathur et al. (2000)
		Carbamate	Moths, beetles, mosquitoes, cockroaches, ants, human head lice, mammalian ectoparasites	Neurotoxicity, affecting central and parasympathetic nervous systems along with increased neuroeffector activity, increased parasympathetic functions like salivation, lacrimation, sweating, nausea, vomiting, mental confusion, tiredness, convulsions and coma, depression, anxiety, irritability, hallucinations, reduced male reproductive activity, hepatotoxicity, irritation in respiration, hyperactivity of skeletal muscles leading to muscle cramps, weakness, and tetany	Yang et al. (2008), Mahajan et al. (2007), Gunasekara et al. (2008), Hamada

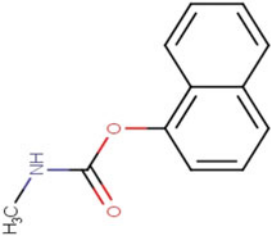
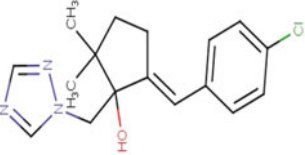

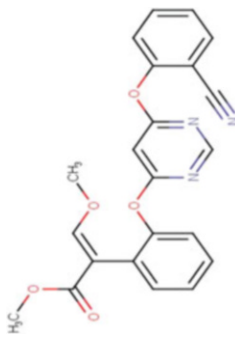
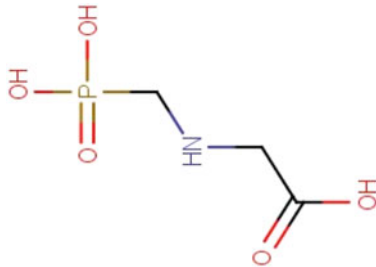
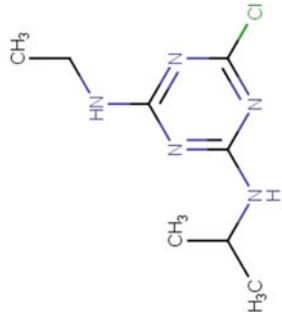
	<p>Carbaryl</p> 		<p>activity; affected acetylcholine levels in the brain and erythrocytes, increased rate of carcinomas; adenomas and sarcomas; cataracts; bladder intracytoplasmic droplets and pigmentation of the spleen; twitching; lack of motor control; low systolic blood pressure; elevated heartbeat; overall delayed polyneuropathic functions</p>	<p>(1993), Dickoff et al. (1987), Xia et al. (2005)</p>
<p>Fungicides (kills fungi and blights, mildews, mold, rusts)</p>	<p>Triticonazole</p> 	<p>Triazole</p> <p><i>Ustilago, Fusarium, Erysiphe, Puccinia, Pythium, Rhynchosporium, Cladosporium</i></p>	<p>Reduction of sterol and gibberellins biosynthesis, decrease in transpiration; delay in removal of primary leaf; long-term inhibitory effects on the soil microbiota and bacterial community</p>	<p>Baibakova et al. (2019), Yen et al. (2009), Yang et al. (2011), Niewiadomska et al. (2011), Pereyra et al. (2009)</p>
	<p>Phenylpyrrole</p>	<p><i>Fusarium, Aspergillus, Ascochyta, Helminthosporium</i></p>	<p>Stunt in plant growth; disruption of reproductive organs development;</p>	<p>Kilani and Fillingner (2016), Baibakova et al. (2019), Leroux (continued)</p>

Table 27.1 (continued)

Type of pesticide	Examples	Biochemical class	Target organisms	Toxic health effects	References
	Fludioxonil 			changes in nitrogen and/or carbon metabolism; limitation of photosynthetic activity; decreased CO ₂ assimilation; decreased transpiration rate and conductance of gases through stomata; signal transduction disruptor in prokaryotes	(1996), Petit et al. (2008), Saladin et al. (2003), Verdisson et al. (2001)
	Azoxystrobin 	Strobilurins	<i>Puccinia, Alternaria, Cladosporium, Ustilago, Erysiphe, Rhizoctonia, Rhynchosporium, Botrytis</i>	Affects aquatic organisms due to high lipophilicity; causes decreased CO ₂ assimilation; transpiration and stomatal conductance in drought-affected plants	Bartlett et al. (2002), Nason et al. (2007), Baibakova et al. (2019)

Herbicides (kills weeds and unwanted plants)	<p data-bbox="144 1296 168 1402">Glyphosate</p> 	Mixture of salts	Broad-spectrum pesticide for perennial weeds	Decrease in hepatic cytochrome P ₄₅₀ and monoxygenase activity in rats; endocrine disruption; carcinogenicity in mouse skin; disruption of human gut bacterial function; apoptosis and necrosis in testicular cells of rats; possible link to development of diabetes, Parkinson's, Alzheimer's and cancer, gluten intolerance.	Bradberry et al. (2004), Swanson et al. (2014), Samsel and Seneff (2013), Gillezeau et al. (2019), Nicolopoulou-Stamati et al. (2016), Thongprakaisang et al. (2013), de Liz Oliveira Cavalli et al. (2013)
	<p data-bbox="585 1323 609 1402">Atrazine</p> 	Triazine	Grassy and broad-leaved weeds in sugarcane, wheat, sorghum, conifers, nuts, and corn crops	Interference with lipid peroxidation; oxidative stress; reduction of chlorophyll content; inhibition of photophosphorylation; cell division and lipid synthesis in algae; effect on antioxidant enzymatic activity in freshwater fish; histopathological changes in the liver tissues of fish including vacuolization of hepatocytes; interference with osomoregulation; and	Singh et al. (2017), Kumar and Singh (2016), Akbulut and Yigit (2010), Li et al. (2012), Gao et al. (2011b), Baxter et al. (2015, 2016), Solomon et al. (2013), Nwani et al. (2010), Mela et al. (2013), Biahova et al. (2013), Khan et al. (2016), Lee et al. (2017), Zadeh et al. (2016), Silveyra et al. (2017), Simpkins et al. (2011), Schroeder et al.

(continued)

Table 27.1 (continued)

Type of pesticide	Examples	Biochemical class	Target organisms	Toxic health effects	References
				<p>changes in gill cells; effect on detoxifying enzymes in zebrafish; decrease in protein and serum albumin in grass carp; effect on digestive glands of Pacific oyster; hematological effects and decrease in glycogen content in crab; neuro-endocrine disruption in vertebrates and invertebrates; mammary adenocarcinoma; non-Hodgkin's lymphomas; reproductive disabilities due to endocrine disruption; irregular cardiac functioning; and hepatic toxicity.</p>	<p>(2001), Gely-Pernot et al. (2015), Cosselman et al. (2015), Campos-Pereira et al. (2012)</p>

DDT has been reported as an endocrine disruptor, carcinogen, and neurotoxin (summarized in Table 27.1).

Unfortunately, DDT is still manufactured in North Korea, India, and China in order to treat vector-borne diseases, the leading producer being India. In Africa, the countries of Zambia, Mozambique, and Zimbabwe have recently resumed the usage of DDT, while in North and South America, pesticide use in Mexico, Ecuador, and Venezuela is discontinued since 2000 (van den Berg et al. 2017).

27.2.1.2 Malathion

Malathion or diethyl 2-dimethoxyphosphinothioylsulfanylbutanedioate is an organophosphate insecticide, with a molecular formula $C_{10}H_{19}O_6PS_2$. It is the most commonly used insecticide in the USA for mosquito and Mediterranean fruit fly eradication and also used as an ointment for head lice (Frankowski 2004). Vector-borne diseases such as West Nile virus and malaria are controlled using malathion (Jensen and Whatling 2010). In agriculture, it has been popularly used for the protection of a large variety of fruits and vegetables from insects, such as the boll weevil that infests cotton. Unlike DDT, this compound is degraded quite quickly, having a half-life of merely 1 week.

Malathion acts as an inhibitor to acetylcholinesterase activity causing neurotoxic effects (Jensen and Whatling 2010). Apart from that, it is known to cause non-Hodgkin's lymphoma (McDuffie et al. 2001; Cantor et al. 1992), hepatotoxicity (Kalender et al. 2010), and immunotoxicity in Japanese quail (Nain et al. 2011) (Table 27.1).

27.2.1.3 Imidacloprid

Imidacloprid, or *N*-[1-[(6-chloropyridin-3-yl)methyl]-4,4,5,5-tetrahydroimidazol-2-yl]nitramide is a neonicotinoid insecticide with a molecular formula $C_9H_{10}ClN_5O_2$. Imidacloprid is an excellent broad-spectrum insecticide used on many food crops for controlling beetle and termite infestations and ectoparasites like fleas on canines (Iyer and Makris 2010). It acts against the nicotinic acetylcholine receptors (nAChRs) of the insect ultimately resulting in paralysis and demise of the insect (Tan et al. 2007; Lin et al. 2013; Mikolić and Brčić Karačonji 2018).

There are several reports indicating the toxic effects of imidacloprid on mammals, such as mutagenicity (Bagri et al. 2016), neurotoxicity (Duzguner and Erdogan 2010a, 2010b; Lonare et al. 2014; Mikolić and Brčić Karačonji 2018), immunotoxicity (Gawade et al. 2013; Badgujar et al. 2013), reproductive toxicant (Kapoor et al. 2011), and endocrine disruptor (Memon et al. 2014; Mikolić and Brčić Karačonji 2018). Moreover, the use of imidacloprid has been associated with the reduction in populations of one of the most significant pollinators in the environment, the honeybee (Oberemok et al. 2015; Raymann et al. 2018).

27.2.1.4 Dichlorvos

Dichlorvos or 2, 2-dichloroethenyl dimethyl phosphate is an organophosphate insecticide with a molecular formula $C_4H_7Cl_2O_4P$. It is being used as an effective insecticide against lepidopterans, aphids, and dipterans (Oberemok et al. 2015) and against helminths which cause diseases to dogs, pigs, and horses (USEPA 1994; Okoroiwu and Iwara 2018).

It has wide applications in pisciculture to exterminate crustaceans (Varo et al. 2003). It acts as an acetylcholinesterase inhibitor and can act on the insect either after ingestion or absorption by spiracles or integument (Binukumar and Gill 2010).

Like other organophosphates, it results in the increase of acetylcholine in the synaptic junctions, leading to deterioration of neurological function (Wang et al. 2004). It can also affect the activity of the central nervous system (IARC 1991; Binukumar and Gill 2010). Reproductive toxicity (Wang et al. 2013) and disruption in the respiratory functions have also been studied in humans (Mathur et al. 2000).

27.2.1.5 Deltamethrin

Deltamethrin or [(*S*)-cyano-(3-phenoxyphenyl) methyl] (1*R*, 3*R*)-3-(2, 2-dibromoethenyl)-2, 2 dimethylcyclopropane-1-carboxylate is from pyrethroid class of insecticide with molecular formula $C_{22}H_{19}Br_2NO_3$. It is effective against a wide variety of insects including mites, mosquitoes, flies, lice, and cockroaches (Davies et al. 2007). It has been widely used in the control of malaria vectors such as *Aedes aegypti* and *Anopheles gambiae* (Kumar et al. 2011). Deltamethrin alters the functioning of calcium and chloride ion pumps in the neurons (Bradberry et al. 2005; Soderlund 2012; Chrustek et al. 2018). The pesticide attacks the central nervous system of insects and it enters the pest's body through cuticle or oral intake (Shrivastava et al. 2011).

Despite several uses, deltamethrin has numerous lethal effects such as hepatotoxicity and nephrotoxicity (Gündüz et al. 2015), reproductive disabilities (Oda and El-Maddawy 2012), immunotoxicity and increases oxidative stress leading to apoptosis of functional cell (Kumar et al. 2018; Chrustek et al. 2018).

27.2.1.6 Carbaryl

Carbaryl or naphthalen-1-yl *N*-methlycarbamate is a carbamate insecticide with molecular formula $C_{12}H_{11}NO_2$. It is effective against moths, beetles, mosquitoes, ants, and cockroaches (Yang et al. 2008). It is also used for the maintenance of lawns and gardens, flea treatment of pets and mammalian ectoparasites (Mahajan et al. 2007; Gunasekara et al. 2008). Its activity is founded on the inhibition of the enzyme acetylcholinesterase, which causes the acetylcholine to accumulate, leading to further neurotoxicity in the pest (Hamada 1993; Gunasekara et al. 2008). Carbaryl

shows neurotoxicity in mammals through reproductive defects and decreased acetylcholinesterase levels in the brain (Dickoff et al. 1987).

27.2.2 Fungicides

Fungicides are used to restrict the growth of fungal organisms on plants and other subjects. They are cost-effective, easy to use, and efficient for controlling unwanted fungal growth and infections (Baibakova et al. 2019). There are three major classes of fungicides—triazoles, phenylpyrroles, and strobilurins as discussed below.

27.2.2.1 Triazoles

Triazoles are a class of organic compounds with a five-membered ring including two carbon and three nitrogen atoms. This class of fungicides has been used on a number of fruits and vegetables and is the most widely used class of fungicides in agriculture (Baibakova et al. 2019). The mode of action is the inhibition of ergosterol biosynthesis, the main membrane sterols in the fungi. Unfortunately, the rise of fungicide-resistant fungal strains is arising, for example, *Puccinia* strains are not completely inhibited by triadimefon (Baibakova et al. 2019). Moreover, Triazoles are phytotoxic to plants and adversely affect gibberellins and important sterols synthesis and moreover reduces the rate of transpiration in plants (Baibakova et al. 2019). Triazoles like triadimefon and triticonazole have long-term inhibitory effects on the soil microbiota and bacterial community (Yen et al. 2009; Yang et al. 2011; Niewiadomska et al. 2011).

27.2.2.2 Phenylpyrroles

Phenylpyrroles are fungicides which are chemical analogs of the natural antifungal substance called pyrrolnitrin (Kilani and Fillingner 2016; Baibakova et al. 2019). Fenpiclonil and fludioxonil are the most phyto-stable and widely used phenylpyrroles. Fludioxonil is used for preharvest and postharvest prophylactic treatment against ascomycetes and basidiomycetes fungi like *Fusarium*, *Aspergillus*, *Ascochyta*, and *Helminthosporium* on leaves, fruits, and seeds. It works by inhibiting the stages of fungal development like germination of spores, elongation of the germ tube, and growth of the mycelium (Leroux 1996).

However, applying these fungicides to the plants (Ex: *Vitis vinifera*) led to stunting in plant growth; reproductive organ disruptions; changes in nitrogen and carbon metabolism; reduction in photosynthetic activity; CO₂ assimilation; rate of transpiration; and conductance of gases by stomata of the plants (Petit et al. 2008; Saladin et al. 2003; Baibakova et al. 2019).

27.2.2.3 Strobilurins

Strobilurins are a class of fungicides that resemble the natural antifungal toxins Strobilurins A and B, which are obtained from the organism *Strobilurus tenacellus* (Balba 2007; Baibakova et al. 2019). The mode of action is to prevent the electron transfer to cytochrome c, which limits NADH oxidation and synthesis of ATP, eventually leading to fungal death (Balba 2007). Strobilurins are used in the agricultural fields to protect the crops from powdery mildew, brown rust, and other fungal diseases that affect plants. They are easily degradable in plants, animals, and soil and water (Joseph 2000) and hence are of generally low toxicity to nontarget organisms like birds, mammals, and bees.

27.2.3 Herbicides

Herbicides are the pesticides used to kill undesired and unwanted weeds or other plants. Here we address the two most commonly used herbicides—Glyphosate and Atrazine.

27.2.3.1 Glyphosate

Glyphosate is a widely used nonselective herbicide in agricultural practices. Glyphosate is an organic compound containing phosphorus and is available in various forms, like salts of ammonium, diammonium, dimethylammonium, and potassium. It also consists of surfactants in the form of an isopropylamine salt (Bradberry et al. 2004; Benbrook 2016; Gillezeau et al. 2019). Glyphosate acts through inhibition of enzyme 5-enolpyruvyl-shikimic acid-3-phosphate synthase, a critical enzyme for the shikimate pathway (found in plants), and is very essential for the synthesis of phenylalanine, tryptophan, and tyrosine plus numerous secondary products like lignin, flavonoids, and tannins (Steinrücken and Amrhein 1980).

Glyphosate causes a decrease in hepatic cytochrome P450 and monooxygenase activity and the activity of aryl hydrocarbon hydroxylase in the intestines (Bradberry et al. 2004). It is reported as endocrine disrupter, causing death of testicular cells, carcinogenic in nature, could be linked to the development of diseases like diabetes, Parkinson's disease, Alzheimer's diseases, cancer, and gluten intolerance (Thongprakaisang et al. 2013; de Liz Oliveira Cavalli et al. 2013; Swanson et al. 2014; Samsel and Seneff 2013).

27.2.3.2 Atrazine

Atrazine is a triazine herbicide manufactured synthetically with a chemical name of 6-chloro-*N*-ethyl-*N'*-(1-methylethyl)-1, 3, 5-triazine-2, 4-diamine. It is used to control grassy weeds in wheat, sugarcane, sorghum, conifers, corn, and nuts (Singh et al. 2017; Kumar and Singh 2016). It has the potential to contaminate groundwater and surface water along with agricultural fields (Kumar et al. 2013); therefore, it is proscribed in the European Union and many other countries (Vonberg et al. 2014; White 2016). The United States Environmental Protection Agency has confirmed atrazine as an endocrine-disrupting chemical (Morales-Perez et al. 2016) and the IARC has confirmed it as a potent carcinogen (Mahler et al. 2017).

Atrazine has numerous ill-effects on nontarget organisms including plants, microbes, aquatic life, terrestrial animals, and humans. Atrazine acts as a postemergence and preemergence herbicide for weeds but also has a negative impact on the peroxidase, ascorbate peroxidase, and lipid peroxidation in target and nontarget organisms (Akbulut and Yigit 2010). The generation of reactive oxygen species causes the nontarget plants to suffer from oxidative stress (Li et al. 2012). The presence of atrazine residues in water bodies exerts unfavorable effects on freshwater algae such as *Oophila ambylostomatis* (Baxter et al. 2015), *Raphidocelis subcapitata* (Baxter et al. 2016), and *Chlamydomonas mexicana* (Kabra et al. 2014).

Atrazine is proved to affect aquatic species like leopard frog (*Rana pipiens*), rainbow trout (*Onchorhynchus mykiss*), American toad (*Bufo americanus*) (Orton et al. 2006), and zebrafish (Blahova et al. 2013). Atrazine is a severe neuroendocrine disrupter that changes the pituitary hormones like follicle-stimulating hormone and luteinizing hormone, leading to prolonged secretion of prolactin and higher incidences of mammary adenocarcinomas (Yang et al. 2014; Simpkins et al. 2011). Reduced sperm motility and count in male rats (Gely-Pernot et al. 2015), development of non-Hodgkin's lymphomas in human (Schroeder et al. 2001), irregular cardiac functioning (Cosselman et al. 2015), and hepatic toxicity (Campos-Pereira et al. 2012) are some major harmful effects of atrazine.

27.3 Bioremediation of Pesticides

According to Odukkathil and Vasudevan (2013), natural degradation of pesticides does not occur properly as they are poorly soluble in water and highly stable compounds in nature. Hence, it is very essential to develop new methods and technologies to eliminate such accumulated compounds from nature. Different chemical and physical methods are being employed for the remediation of pesticides; however, higher cost, generation of toxic intermediate, and final metabolites are the major disadvantages (Debarati et al. 2005).

Parallel to this, a line of research which has proven most eco-friendly, cost-effective, and versatile is pesticide degradation using living organism, popularly

known as “bioremediation.” This technique uses the potential of microorganisms (e.g., bacteria, fungi, and microalgae) and plants (phytoremediation) to remove or degrade toxic substances like pesticide, heavy metal, hazardous synthetic dyes, hydrocarbons, antibiotics, etc. from the environment (Uqab et al. 2016). The inbuilt capacity of living organisms to detoxify the environmental pollutants through enzymatic metabolism with simple nontoxic or less toxic metabolites from harmful pollutants have been successfully exploited (Odukkathil and Vasudevan 2013). The bioremediation is said to be successful if it can utilize an efficient strain of bacteria to degrade the largest pollutant to the minimum level. The rate of bioremediation depends on four factors (Singh 2008), viz., (1) Bioavailability of the compound to the microorganisms, (2) Physiological condition of the microbes, (3) The survival of the microbes at the contaminated site, and (4) Sustainable population of the microbes.

During bioremediation, pesticides are degraded to less complex compounds by the microorganisms in situ and ultimately result in the liberation of water, CO₂, oxides, and/or mineral salts of other elements present in the pesticide (Odukkathil and Vasudevan 2013). In addition, pH, water potential, temperature, nutrients concentration, and amount of toxic pesticide or metabolite affect the biodegradation rate (Chawla et al. 2013; Uqab et al. 2016). The transformed pesticide after bioremediation can be used as a source of carbon, nitrogen, or other minerals, or a final electron acceptor in the electron transport chain (Odukkathil and Vasudevan 2013). Some microbes commonly used for pesticide remediation are *Pseudomonas* sp. (Hay and Focht 2000; Thabit and El-Naggar (2013), *Klebsiella* sp., *Bacillus* sp. (Kamal et al. 2008; Thabit and El-Naggar 2013), etc.

The degradation of the pesticide follows different pathways, based on its nature, environmental factors, the type of the microbial strain (Odukkathil and Vasudevan 2013), and its enzymatic system (Uqab et al. 2016). Bioremediation of pesticides can be done using bacteria, fungi, and plants alone or in consortium which is presented in Table 27.2 and discussed below.

27.3.1 DDT Bioremediation

Bioremediation of DDT is important because of long-term persistence in the environment including its metabolites DDE and DDD (collectively called DDTr) (Foght et al. 2010). Microbes that degrade DDT residues have been isolated from many sources, such as animals, sewage, activated sludge, soil, and plant material like wood. DDT degradation does not provide the microbes with any nutrients or energy for growth and hence needs to offer a separate source of carbon for growth and development (Bollag and Liu 1990). Commonly, pathways for the remediation of DDT comprise reductive dechlorination of DDT to DDD under reducing conditions (Sudharshan et al. 2012; Gao et al. 2011a). Aerobic degradation of DDT residues has been reported involving aromatic-degrading bacteria (Foght et al. 2010).

Table 27.2 Bioremediation of pesticides using monoculture and consortium

Pesticides	Type of bioremediation	Species	References
DDT	Bacterial remediation	<i>Proteus vulgaris</i>	Barker et al. (1965)
		<i>Alcaligenes eutrophus</i>	Nadeau et al. (1994)
		<i>Pseudomonas</i> sp.	Kamanavalli and Ninnekar (2004)
		<i>Alcaligenes denitrificans</i>	Ahuja et al. (2001)
		<i>Ralstonia eutropha</i>	Hay and Focht (2000)
		<i>Pseudoxanthomonas jiangsuensis</i>	Wang et al. (2011)
		<i>Pseudomonas</i> strain 12-3	Niu et al. (2012)
		A consortium containing 138 bacterial species and 11 uncultured bacterial species, mainly <i>Taylorella asinigenitalis</i>	Saghee and Bidlan (2018)
	Mycoremediation	<i>Phanerochaete chrysosporium</i> species	Fernando et al. (1989), Katayama et al. (1992)
		<i>Fomitopsis pinicola</i> , <i>Gloeophyllum trabeum</i> and <i>Daedalea dickinsii</i>	Purnomo et al. (2011)
Malathion	Bacterial remediation	Consortium of <i>Flavibacterium meningosepticum</i> , <i>Comamonas terrigeri</i> , <i>Xanthomonas</i> sp., and <i>Pseudomonas cepacia</i>	Paris et al. (1975)
		<i>Pseudomonas aeruginosa</i> AA112	Gibson and Burns (1977)
		<i>Bacillus thuringiensis</i> MOS-5 (Bt)	Kamal et al. (2008)
		<i>Acinetobacter johnsonii</i> MA19	Xie et al. (2009)
		<i>Pseudomonas aeruginosa</i> , <i>Bacillus pseudomycooides</i> , and <i>Bacillus licheniformis</i>	Thabit and El-Naggar (2013)
		<i>Aspergillus flavus</i>	Derbalah et al. (2020)
	Microalgae and cyanobacteria	<i>Chlorella vulgaris</i> , <i>Spirulina platensis</i> and <i>Scenedesmus quadricuda</i>	Abdel-Razek et al. (2019)
Imidacloprid	Bacterial remediation	<i>Stenotrophomonas maltophilia</i> CGMCC 1.1788	Dai et al. (2006)
		<i>Bacillus alkalinitrilicus</i> and <i>Bacillus thuringiensis</i>	Sharma et al. (2014a)
		<i>Hymenobacter latericoloratus</i> CGMCC 16346	Guo et al. (2020)
	Bacterial consortia	Consortium of <i>Bacillus aerophilus</i> and <i>Bacillus alkalinitrilicus</i>	Sharma et al. (2014b)

(continued)

Table 27.2 (continued)

Pesticides	Type of bioremediation	Species	References
		Consortium of <i>Ochrobactrum thiophenivorans</i> and <i>Sphingomonas melonis</i>	Erguven and Demirci (2019)
	Mycoremediation	<i>Trichoderma atroviride</i> strain T23	He et al. (2014)
		<i>Aspergillus terreus</i> strain YESM3	Mohammed and Badawy (2017)
Dichlorvos	Bacterial remediation	<i>Flavobacterium</i> sp. strain YD4	Ning et al. (2012)
		<i>Pseudomonas aeruginosa</i> and <i>Taonella mepensis</i>	Gaonkar et al. (2019)
	Bacterial consortia	Consortium of <i>Serratia</i> sp., <i>Proteus vulgaris</i> , <i>Acinetobacter</i> and <i>Vibrio</i> sp.	Agarry et al. (2013)
	Mycoremediation	<i>Trichoderma atroviride</i> T23	Tang et al. (2008)
	Plant-fungal consortia	Consortia of fungi <i>Cunninghamella elegans</i> , <i>Fusarium solani</i> , <i>Aspergillus oryzae</i> , <i>Penicillium</i> sp., and <i>Talaromyces atroroseus</i> coupled with the spent mushroom compost (SMC) of <i>Pleurotus ostreatus</i> and a plant <i>Panicum maximum</i>	Asemoloye et al. (2019)
Carbaryl	Bacterial remediation	<i>Pseudomonas</i> sp., <i>Rhodococcus</i> spp., <i>Micrococcus</i> spp. and <i>Rhizobium</i> sp. AC100	Li et al. (2019), Hashimoto et al. (2002), Swetha and Phale (2005)
		<i>Rhodopseudomonas capsulata</i>	Wu et al. (2019)
	Mycoremediation	<i>Aspergillus niger</i> PY168	Zhang et al. (2003)
		<i>Xylaria</i> sp. BNL1	Li et al. (2019)
	Phytoremediation	<i>Lupinus angustifolius</i>	Garcinuño et al. (2006)
Deltamethrin	Bacterial remediation	<i>Micrococcus</i> sp. strain CPN1	Tallur et al. (2008)
		<i>Streptomyces aureus</i> , HP-S-01	Chen et al. (2011)
		<i>Serratia marcescens</i> , DeI-1 and DeI-2	Cycoñ et al. (2014)
		<i>Bacillus cereus</i> strain Y1	Zhang et al. (2016)
		<i>Acinetobacter junii</i> LH-1-1 and <i>Klebsiella pneumoniae</i> BPBA052	Tang et al. (2020)
Glyphosate	Bacterial remediation	<i>Arthrobacter</i> sp. strain GLP-1	Pipke et al. (1987)
		<i>Flavobacterium</i> sp. strain GD1	Balthazor and Hallas (1986)
		<i>Pseudomonas pseudomallei</i> strain 22	Peñaloza-Vazquez et al. (1995)
		<i>Comamonas odontotermitis</i> P2	Firdous et al. (2017)

(continued)

Table 27.2 (continued)

Pesticides	Type of bioremediation	Species	References
		<i>Streptomyces</i> sp. StC	Obojska et al. (1999)
		<i>Bacillus subtilis</i> Bs-15	Yu et al. (2015)
		<i>Bacillus aryabhatai</i> FACU3	Elarabi et al. (2020)
	Bacterial consortium	<i>Ochrobactrum</i> sp. DGG-1-3, <i>Ochrobactrum</i> sp. B18, <i>Ochrobactrum</i> sp. Ge-14, <i>Pseudomonas citronellosis</i> strain ADA-23B	Góngora-Echeverría et al. (2020)
	Mycoremediation	<i>Aspergillus oryzae</i> A-F02	Fu et al. (2017)
		<i>Mucor</i> IIR & <i>Penicillium</i> IIR	Krzyśko-Łupicka and Orlik (1997)
		<i>Penicillium chrysogenum</i>	Klimek et al. (2001)
	Plant-bacteria consortia	Consortium of <i>Amaranthus caudate</i> and two bacterial isolations, <i>Pseudomonas aeruginosa</i> and <i>Bacillus megaterium</i>	Abdel-Megeed et al. (2013)
	Phytoremediation	An assemblage of indigenous wetland plant species of Renosterveld land of South Africa including <i>Cynodon dactylon</i> , <i>Juncus kraussii</i> , and <i>Isolepis prolifera</i>	Jacklin et al. (2020)
		<i>Salvinia biloba</i>	da Silva et al. (2020)
Atrazine	Bacterial remediation	<i>Pseudomonas</i> sp. strain ADP	Yamada et al. (2002)
		<i>Rhodobacter sphaeroides</i> W16 and <i>Acinetobacter lwoffii</i> DNS32	Zhang et al. (2012)
	Bacterial consortia	Consortium of <i>Pseudomonas putida</i> , <i>Pseudomonas alcaligenes</i> , <i>Acidovorax</i> sp., <i>Erwinia tracheiphila</i> , <i>Ralstonia eutrophus</i> , <i>Pseudomonas syringae</i> and <i>Enterobacter agglomerans</i> and <i>Micrococcus varians</i>	Dehghani et al. (2007)
		Consortium of <i>Rhodococcus</i> sp. BCH2, <i>Bacillus</i> sp. PDK1 and <i>Bacillus</i> sp. PDK2	Kolekar et al. (2019)
	Mycoremediation	<i>Aspergillus fumigatus</i> , <i>Rhizopus stolonifera</i> , <i>Fusarium moniliforme</i> , <i>Penicillium decumbens</i> , and <i>Trichoderma viride</i>	Kaufman and Blake (1970)
		<i>Trametes versicolor</i>	Bastos and Magan (2009)
		<i>Phanerochaete chrysosporium</i>	Mougin et al. (1994)
	Phytoremediation	<i>Populus maximowiczii</i> , <i>P. euramericana</i> and <i>P. glandulosa</i>	Chang et al. (2005)

(continued)

Table 27.2 (continued)

Pesticides	Type of bioremediation	Species	References
		<i>Iris pseudacorus</i> , <i>Acorus calamus</i> and <i>Lythrum salicaria</i>	Wang et al. (2012)
Tebuconazole	Bacterial remediation	<i>Serratia marcescens</i> B1	Wang et al. (2018)
Propiconazole		<i>Pseudomonas putida</i> MPR 4 and MPR 12	Sarkar et al. (2009)
		<i>Burkholderia</i> sp. strain BBK_9	Satapute and Kaliwal (2016)
Pyraclostrobin		<i>Klebsiella</i> strain 1805	Lopes et al. (2010)
Azoxystrobin		<i>Cupriavidus</i> sp. CCH2 and <i>Rhodanobacter</i> sp. CCH1	Howell et al. (2014)
Trifloxystrobin	Bacterial consortium	<i>Bacillus amyloliquefaciens</i> , <i>Bacillus flexus</i> , <i>Stenotrophomonas maltophilia</i> and <i>Arthrobacter oxydans</i>	Clinton et al. (2011)

DDT degradation occurs through the breakage of the carbon–chlorine bond. Thus, bioremediation of DDT requires biological species which can cleave that bond specifically through enzymatic action (Hägglom and Bossert 2003). One of the first pure bacterial cultures used for the reduction of DDT to DDD was *Proteus vulgaris*, a bacterial strain isolated from mouse intestine (Barker et al. 1965). Under anaerobic conditions, DDD can further be degraded by pure bacterial cultures of *Enterobacter aerogenes* and *Escherichia coli* (Foght et al. 2010). Aerobic degradation of DDT results in the production of chlorinated aromatic acids and loss of carbon atoms whereas; anaerobic attack may result in dechlorinated aromatic metabolites (Foght et al. 2010).

Removal of DDT was published in 1994 by Nadeau et al. using *Alcaligenes eutrophus*, which oxidizes DDT into 4-chlorobenzoic acid (4-CBA) through enzymatic action of dioxygenase under aerobic condition. Later on, Kamanavalli and Ninnekar (2004) conducted research on *Pseudomonas* sp. grown on biphenyl along with 0.05% w/v DDT and degradation was achieved with 4-CBA as a final product. Ahuja et al. (2001) used *Alcaligenes denitrificans* to metabolize DDE but they did not obtain 1-chloro-2,2-bis(4-chlorophenyl)ethylene and 4-CBA as reported previously.

Hay and Focht (2000) used *Ralstonia eutropha* enriched with mineral salts and biphenyl, thus demonstrating a DDD degradation pathway using deoxygenation and meta-fission. The result was monohydroxy–DDD intermediates formation. *Pseudoxanthomonas jiangsuensis* has been reported to degrade DDT with the use of polar lipids like diphosphatidylglycerol (Wang et al. 2011). *Pseudomonas* strain 12-3 was able to remediate about 51% DDT within 8 days (Niu et al. 2012). This strain was isolated from a DDT-polluted area in Guangzhou, China.

Saghee and Bidlan (2018) used a consortium containing 138 bacterial species and 11 uncultured bacterial species to degrade a mixture of DDT and lindane. The maximum population of the microbial sample was constituted by *Taylorella asinigenitalis*. The consortium was capable of degrading 57.8% DDT (5 ppm) within 72 h, from the mixture along with lindane.

The fungal potential for degradation of DDT has been studied by researchers. Fungi produce lignin-degrading enzymes and it has been found that the ligninolytic activity is proportional to the degradation rate of the pesticide (Sudharshan et al. 2012; Chung et al. 2009). The *Phanerochaete chrysosporium* species of fungus is investigated for the potential of DDT degradation (Fernando et al. 1989; Katayama et al. 1992). A linear correlation was obtained among the DDT mineralization and the activity of lignin peroxidase of fungi (Foght et al. 2010). Brown-rot fungi, namely *Fomitopsis pinicola*, *Gloeophyllum trabeum*, and *Daedalea dickinsii*, have shown the potential to degrade DDT in soil, by 9, 41, and 15%, respectively (Purnomo et al. 2011).

27.3.2 Malathion Bioremediation

Malathion can be degrading using the carboxylesterase enzyme which is mostly present in fungi like *Aspergillus* sp. and *Penicillium* sp. (Adhikari 2010; Mostafa et al. 1972). However, many bacterial strains are also able to detoxify malathion. A heterogeneous population of bacteria containing *Flavibacterium meningosepticum*, *Comamonas terrigeri*, *Xanthomonas* sp., and *Pseudomonas cepacia* was revealed to degrade malathion (Paris et al. 1975). *Pseudomonas aeruginosa* AA112 was studied to use malathion as the only source of carbon, forming diethylsuccinate and succinate metabolites (Gibson and Burns 1977). Kamal et al. (2008) used *Bacillus thuringiensis* MOS-5 (Bt) obtained from agricultural fields' waste water. This *Bacillus* strain was capable of degrading malathion co-metabolically with malathion monocarboxylic acid and malathion dicarboxylic acid as the major degradation products (Kamal et al. 2008; Adhikari 2010). Xie et al. (2009) found a malathion degrading bacterium, *Acinetobacter johnsonii* MA19 which could degrade malathion when it is provided an external carbon source. *Pseudomonas aeruginosa*, *Bacillus pseudomycolides*, and *Bacillus licheniformis* are similarly studied to degrade the malathion in vitro (Thabit and El-Naggar 2013). Derbalah et al. (2020) showed that *Aspergillus flavus* have the capability of 100% malathion degradation at 7 pH, 30 °C temperature, and 5 mg/L initial concentration of malathion.

Furthermore, consortia of microalgae and cyanobacteria (*Chlorella vulgaris*, *Spirulina platensis*, and *Scenedesmus quadricuda*) have been used to remove the malathion from the samples of wastewater and agricultural drainage in Egypt. It was successful in bringing about 99% degradation of malathion within 28 days (Abdel-Razek et al. 2019).

27.3.3 Imidacloprid Bioremediation

Stenotrophomonas maltophilia CGMCC 1.1788 aerobically transformed imidacloprid into 5-hydroxyl imidacloprid (Dai et al. 2006). Parallely, Ge et al. (2006) reported that imidacloprid converts into polar metabolites due to the enzymatic action of isolated bacteria *S. maltophilia*. Sharma et al. (2014a) carried out research by using five different species of bacteria belonging to *Bacillus*, *Pseudomonas*, and two other unmentioned genera. It was found that *Bacillus alkalinitrilicus* and *Bacillus thuringiensis* had the capacity of degrading imidacloprid by 36.38% and 33.70%, respectively. Later in the same year, the same researcher group published an article on the use of *Bacillus aerophilus* and *Bacillus alkalinitrilicus* consortium to effectively degrade imidacloprid (Sharma et al. 2014b). Erguven and Demirci (2019) testified a consortium of *Ochrotrichum thiophenivorans* and *Sphingomonas melonis* to remediate imidacloprid. Guo et al. (2020) showed that *Hymenobacter latericoloratus* CGMCC 16346 is capable of imidacloprid degradation in surface water, by the process of hydroxylation by co-metabolism in pure culture. The resting cells of the bacterium were able to degrade 64.4% of 100 mg/L imidacloprid in 6 days, in the presence of a co-substrate maltose.

In fungal bioremediation strategies, *Trichoderma atroviride* strain T23 produced by restriction enzyme-mediated integration method (He et al. 2014) and YESM3 strain of *Aspergillus terreus* was found to be capable of degrading imidacloprid in liquid media (Mohammed and Badawy 2017).

27.3.4 Dichlorvos Bioremediation

In 2012, a strain of *Flavobacterium* sp., YD4 which was isolated from the rape phyllosphere, exhibited efficient in situ dichlorvos degrading potential (Ning et al. 2012). Further, Agarry et al. (2013) showed that a consortium of *Serratia* sp., *Proteus vulgaris*, *Acinetobacter*, and *Vibrio* sp. could efficiently bring about degradation of dichlorvos in the presence of NPK fertilizer. Similarly, degradation of dichlorvos using cultures of *Micrococcus*, *Bordetella*, *Staphylococcus*, *Pseudomonas*, *Klebsiella*, and *Enterobacter* was studied and it was found that remediation activity is enhanced when sucrose is added to the medium (Yadav et al. 2015). Gaonkar et al. (2019) conducted a study with enriched cultures of *Pseudomonas aeruginosa* and *Taonella mepensis*, which showed a rapid degradation of dichlorvos as the sole carbon source at concentrations up to 1000 mg/L.

Fungal remediation of dichlorvos has also been carried out. Fu (2005) had isolated a strain of *Trichoderma* from soil contaminated with dichlorvos. The strain was able to degrade dichlorvos. A genetically engineered strain of *Trichoderma atroviride* T23 was also constructed using restriction enzyme-mediated integration (REMI), and apart from the higher potential of degradation (96%), it also reduced pathogenic population from the soil (Tang et al. 2008). A recent study involved the

use of fungal strains *Aspergillus oryzae*, *Fusarium solani*, *Cunninghamella elegans*, *Penicillium* sp., and *Talaromyces atrovirens* coupled with the Spent Mushroom Compost (SMC) of *Pleurotus ostreatus* and a plant Guinea grass (*Panicum maximum*). This is an example of synergistic interaction between the plant and fungal species for efficient remediation of dichlorvos (Asemoloye et al. 2019).

27.3.5 Carbaryl Bioremediation

Carbaryl degradation is pivoted in the presence of carbaryl hydrolase enzyme, which catalyzes carbaryl to 1-naphthol which is further degraded to ventilate or catechol (Hashimoto et al. 2002; Swetha and Phale 2005; Li et al. 2019). A number of bacterial species have been shown to possess carbaryl-degrading capacity, for instance, *Pseudomonas* sp., *Rhodococcus* spp., *Micrococcus* spp., and *Rhizobium* sp. AC100 (Li et al. 2019; Hashimoto et al. 2002; Swetha and Phale 2005). *Rhodopseudomonas capsulata* isolated from wastewater effluent was able to degrade carbaryl efficiently (Wu et al. 2019).

In 2003, a fungal strain of *Aspergillus niger* PY168 was used to degrade a number of carbamates, and they were found to produce a new carbaryl hydrolase, which demonstrates the possibility of fungi to be used in carbamate bioremediation (Zhang et al. 2003). Garcinuño et al. (2006) studied phytoremediation by *Lupinus angustifolius* seeds and plants under hydroponic culture, to remove carbaryl, linuron, and permethrin from contaminated wastewater. In this study, 55% removal of carbaryl from the mixture was obtained. Li et al. (2019) studied the potential of a fungus belonging to Ascomycetes, *Xylaria* sp. BNL1 against the degradation of the compound by a commonly used fungus *Pleurotus ostreatus* HAUCC 162. In the presence of active cytochrome P450 and laccase in liquid media, 99% degradation was achieved.

27.3.6 Deltamethrin Bioremediation

Deltamethrin is decomposable by bacteria which results in cleavage of the carboxyl ester bond present in the compound to form α -hydroxy-3-phenoxybenzenecetonitrile and 3-phenoxybenzaldehyde. On oxidation, the latter compound forms 2-hydroxy-4-methoxybenzophenone (Chen et al. 2011). These metabolites have more mobility and accumulate less in the soil. Under an anaerobic environment, deltamethrin is converted into carboxylic acids which further undergoes degradation (Cycoń et al. 2014). A co-culture of *Acinetobacter junii* LH-1-1 and *Klebsiella pneumoniae* BPBA052 was employed for the efficient degradation of deltamethrin, and the highest obtained degradation was 94.25% (Tang et al. 2020). *Micrococcus* sp. strain CPN1 showed the capability of degrading deltamethrin and other pyrethroids as a main carbon source (Tallur et al. 2008). Later Chen et al.

(2011) showed that *Streptomyces aureus*, HP-S-01, could degrade deltamethrin completely, along with its hydrolysis metabolite 3-phenoxybenzaldehyde. In 2014, strains of *Serratia marcescens*, DeI-1 and DeI-2, were reported to remediate deltamethrin (Cycoń et al. 2014). Zhang et al. (2016) showed that *Bacillus cereus* strain Y1 is capable to degrade deltamethrin up to 74.9% in 25 days.

27.3.7 Glyphosate Bioremediation

The key enzyme significant for the degradation of glyphosate is glyphosate oxidoreductase which acts by cleavage of the carbon–nitrogen bond. Glyphosate degradation has been widely studied using the most efficient bacterial and fungal species (Zhan et al. 2018). Most of these microbes utilize glyphosate as their key source of phosphorus, e.g., *Arthrobacter* sp. strain GLP-1 (Pipke et al. 1987), *Flavobacterium* sp. strain GD1 (Balthazor and Hallas 1986), *Pseudomonas pseudomallei* strain 22 (Peñalosa-Vazquez et al. 1995), *Mucor* IIR and *Penicillium* IIR (Krzyśko-Lupicka and Orlik 1997), and *Penicillium chrysogenum* (Klimek et al. 2001), *Aspergillus oryzae* A-F02 (Fu et al. 2017). A bacterial consortium consisting of *Ochrobactrum* sp. DGG-1-3, *Ochrobactrum* sp. B18, *Ochrobactrum* sp. Ge-14, and *Pseudomonas citronellolis* strain ADA-23B was shown to bring about more than 90% degradation of glyphosate (Góngora-Echeverría et al. 2020). Another species of bacteria, *Bacillus aryabhatai* FACU3, presented a high capacity for glyphosate-contaminated soil remediation (Elarabi et al. 2020).

Streptomyces sp. StC utilizes glyphosate as a key source of phosphorus and nitrogen (Obojska et al. 1999) while *Comamonas odontotermitis* P2 uses the main phosphorus and carbon source (Firdous et al. 2017). Although many glyphosate-degrading microbes have been isolated, it is still a dilemma to find microbes that are efficient in degrading the compound in situ. The strain of *Bacillus subtilis* Bs-15 degraded glyphosate (conc. 5000 mg/L) up to 66.97% in sterile soil and 71.57% in unsterilized soil (Yu et al. 2015). There are three main intermediate metabolites of glyphosate degradation viz., aminomethylphosphonic acid (AMPA), sarcosine, and acetylglyphosate, and different pathways are investigated for their further metabolism (Zhan et al. 2018).

In 2013, a laboratory study by Abdel-Megeed et al. in the Riyadh region of Saudi Arabia showed that amaranth plant (*Amaranthus caudate*) and two bacterial isolates *Pseudomonas aeruginosa* and *Bacillus megaterium* degrades glyphosate within 5 days. It indicated that phytoremediation could lead to the acceleration of the remediation process of glyphosate in the rhizospheric region of soil. Recently, wetland plant species from South Africa were studied for phytoremediation capacity using two different concentrations of glyphosate (Jacklin et al. 2020). The selected varieties of indigenous plants included *Cynodon dactylon*, *Cyperus textilis*, *Phragmites australis*, *Juncus effuses*, *Typha capensis*, *Arctotis acaulis*, *Zantedeschia aethiopica*, *Carpobrotus edulis*, *Aristea capitata*, *Juncus lomatophyllus*, *Bolboschoenus maritimus*, *Isolepis prolifera*, *Juncus kraussii*, and *Eleocharis*

limosa. Other alien varieties—*Arundo donax*, *Canna indica*, *Pennisetum clandestinum*, and *Prionium serratum*—were selected due to their prevalent use in the treatment of wastewater. The three most effective species for bioremediation of 0.7 mg/L glyphosate were *Cynodon dactylon*, *Juncus kraussii*, and *Isolepis prolifera* (percentage removal being 92.84–99.39%), while the most effective for 225 mg/L glyphosate were *Aristea capitate*, *Bolboschoenus maritimus*, and *Typha capensis* and they exhibited removal capacity of 88.34–99.86%. Another study by da Silva et al. (2020) showed that the aquatic macrophyte *Salvinia biloba* was able to show complete removal of glyphosate from water.

27.3.8 Atrazine Bioremediation

Bioremediation of atrazine is conventionally done by microbial species grown on minimal salt medium that contains atrazine (nitrogen source) and glucose (carbon source) (Fan and Song 2014). The first bacterial strain isolated for catabolism of atrazine was *Pseudomonas* sp. strain ADP (Yamada et al. 2002). In Iran, a consortium of bacteria consisting of seven Gram-negative bacteria, viz. *Pseudomonas putida*, *Pseudomonas alcaligenes*, *Acidovorax* sp., *Erwinia tracheiphila*, *Ralstonia eutrophus*, *Pseudomonas syringe*, and *Enterobacter agglomerans* along with a Gram-positive bacterium viz. *Micrococcus varians*, was found to catabolize atrazine for nitrogen source (Dehghani et al. 2007). Two strains namely *Rhodobacter sphaeroides* W16 and *Acinetobacter lwoffii* DNS32 were isolated from atrazine-exposed soil in China (Zhang et al. 2012). From the study, it was concluded that bacterial cells exposed to atrazine undergo lower oxidative damage. Another bacterial consortium was prepared using three bacteria viz. *Rhodococcus* sp. BCH2, *Bacillus* sp. PDK1, and *Bacillus* sp. PDK2, which showed the ability to reduce the toxicity of atrazine through catabolism (Kolekar et al. 2019).

Mycoremediation of atrazine has proved successful using numerous fungi like *Aspergillus fumigatus*, *Rhizopus stolonifera*, *Fusarium moniliforme*, *Penicillium decumbens*, and *Trichoderma viride*, among others, by N-dealkylation of alkyl or amino groups (Kaufman and Blake 1970). Lignicolous (wood-decaying) basidiomycetes are the major atrazine-degrading fungi, e.g., *Phanerochaete chrysosporium* (Mougin et al. 1994) and *Trametes versicolor* (Bastos and Magan 2009).

Phytoremediation attempts on atrazine have also been accomplished. Cutting parts of three poplar species viz., *Populus maximowiczii*, *P. euramericana*, and *P. glandulosa* showed uptake, hydrolyzation, and dealkylation of atrazine to less toxic metabolites (Chang et al. 2005). Later, Wang et al. (2012) performed an experiment on three emergent hydrophytes—*Iris pseudacorus*, *Acorus calamus*, and *Lythrum salicaria* to create a hydroponic system for remediation of atrazine. The degradation contribution of each plant was 75.6%, 61.8%, and 65.5%, respectively.

27.3.9 *Fungicides Bioremediation*

A study on the bioremediation of tebuconazole, a triazole fungicide, was carried out by Wang et al. (2018), wherein *Serratia marcescens* B1 was shown to degrade tebuconazole by 96.46%. Sarkar et al. (2009) demonstrated the bioremediation of propiconazole using the rhizospheric strain of *Pseudomonas putida* from the tea plant. The most effective strains were the MPR 4 and MPR 12 strains, which gave degradation percentages of 72.8% and 67.8%, respectively. Also, Satapute and Kaliwal (2016) showed bioremediation of propiconazole using *Burkholderia* sp. strain BBK_9 and degraded propiconazole by 88.87%.

Degradation of Strobilurin has been studied and many species of bacteria showed strobilurin-degrading ability (Feng et al. 2020). *Klebsiella* strain 1805 was able to successfully degrade strobilurin pyraclostrobin (Lopes et al. 2010) while Clinton et al. (2011) described four bacterial species viz., *Bacillus flexus*, *Bacillus amyloliquefaciens*, *Stenotrophomonas maltophilia*, and *Arthrobacter oxydans*. These species were capable of trifloxystrobin degradation as a carbon source. Azoxystrobin was shown to be degraded by *Rhodanobacter* sp. CCH1 and *Cupriavidus* sp. CCH2 for their carbon and nitrogen requirements (Howell et al. 2014).

27.4 Conclusion with Future Prospectives

A scientific literature survey on health and environment risk of particular toxicants improves knowledge and provides a better understanding of future management strategy. In the present chapter, we have included benefits obtaining from pesticides and their further complications due to prolonged and overuse. Though pesticides have a proven milestone in the growth of the agriculture sector and prevention of vector-borne diseases, these hazardous complex chemicals are detrimental to the environment and human beings. Most pesticides are disturbing the natural ecosystem and are potent neurotoxic, hepatotoxic, carcinogenic, endocrine, and reproductive system disruptors. Unfortunately, despite their harmful effects, a number of pesticides are being aggressively used in different parts of the world. Hence, an extreme decrease in the use of pesticides to a human and environmentally safer level is an urgent need.

Bioremediation is a promising eco-friendly strategy for the management of environmental pollutants. We extended our efforts to systematically review articles for the remediation of various pesticides using biological monoculture and consortium. It is apparent that considerable progress has been achieved in the pesticide degradation using bacteria, fungi, and plant systems. However, though several researchers have attempted successful pesticide degradation, in most studies the concentration used for the experiment was very less. Therefore, future focus can be given to the use of consortium, wetland system, and in situ performance of

reported and/or novel organisms with higher pesticide concentration (single and/or mixture) for the imminent development of successful bioremediation technology.

References

- Abdel-Megeed A, Sadik M, Ho AS (2013) Phyto-microbial degradation of glyphosate in Riyadh area. *Int J Microbiol Res* 5:458–466. <https://doi.org/10.9735/0975-5276.5.5.458-466>
- Abdel-Razek MA, Abozeid AM, Eltholth MM, Abouelenien FA, El-Midany SA, Moustafa NY, Mohamed RA (2019) Bioremediation of a pesticide and selected heavy metals in wastewater from various sources using a consortium of microalgae and cyanobacteria. *J Slovenian Vet Res* 56(22):61–74
- Adhikari S (2010) Bioremediation of Malathion from environment for pollution control. *Res J Environ Toxicol* 4:147–150
- Agarry SE, Olu-arotiowa OA, Aremu MO, Jimoda LA (2013) Biodegradation of Dichlorovos (organophosphate pesticide) in soil by bacterial isolates. *J Nat Sci Res* 3(8):12–16
- Ahuja R, Awasthi N, Manickam N, Kumar A (2001) Metabolism of 1,1-dichloro-2,2-bis (4-chlorophenyl) ethylene by *Alcaligenes denitrificans*. *Biotechnol Lett* 23:423–426
- Akbulut GB, Yigit E (2010) The changes in some biochemical parameters in *Zea mays* cv. “Martha F1” treated with atrazine. *Ecotoxicol Environ Saf* 73:1429–1432. <https://doi.org/10.1016/j.ecoenv.2010.05.023>
- Aktar MW, Sengupta D, Chowdhury A (2009) Impact of pesticides use in agriculture: their benefits and hazards. *Interdiscip Toxicol* 2(1):1–12. <https://doi.org/10.2478/v10102-009-0001-7>
- Alewu B, Nosiri C (2011) Pesticides and human health. In: Stoytcheva M (ed) *Pesticides in the modern world – effects of pesticides exposure*. InTech
- Asemoloye MD, Gbolagade J, Rafiq A (2019) Degradation of 2,2-dichlorovinyl dimethylphosphate (dichlorvos) through the rhizosphere interaction between *Panicum maximum* Jacq and some selected fungi. *Chemosphere* 221. <https://doi.org/10.1016/j.chemosphere.2019.01.058>
- Badgajar PC, Jain SK, Singh A, Punia JS, Gupta RP, Chandratre GA (2013) Immunotoxic effects of imidacloprid following 28 days of oral exposure in BALB/c mice. *Environ Toxicol Phar* 35:408–418. <https://doi.org/10.1016/j.etap.2013.01.012>
- Bagri P, Kumar V, Sikka AK (2016) Assessment of imidacloprid-induced mutagenic effects in somatic cells of Swiss albino male mice. *Drug Chem Toxicol* 39:412–417. <https://doi.org/10.3109/01480545.2015.1137301>
- Baibakova E, Nefedjeva E, Suska-Malawska M, Wilk M, Sevriukova G, Zheltobriukhov V (2019) Modern fungicides: mechanisms of action, fungal resistance and phytotoxic effects. *Annu Res Rev Biol*. <https://doi.org/10.9734/arrb/2019/v32i330083>
- Bal R, Türk G, Tuzcu M, Yilmaz O, Kuloglu T, Gundogdu R, Gür S, Agca A, Ulas M, Cambay Z, Tuzcu Z, Gencoglu H, Güvenç M, Ozsahin A, Kocaman N, Aslan A, Etem E (2012) Assessment of imidacloprid toxicity on reproductive organ system of adult male rats. *J Environ Sci Health B* 47:434–444. <https://doi.org/10.1080/03601234.2012.663311>
- Balba H (2007) Review of strobilurin fungicide chemicals. *J Environ Sci Health B* 42(4):441–451. <https://doi.org/10.1080/03601230701316465>
- Balthazor TM, Hallas LE (1986) Glyphosate-degrading microorganisms from industrial activated sludge. *Appl Environ Microbiol* 51(2):432–434
- Barker PS, Morrison FO, Whitaker RS (1965) Conversion of DDT to DDD by *Proteus vulgaris*, a bacterium isolated from the intestinal flora of a mouse. *Nature* 205:621–622
- Barlow SM, Sullivan FM, Lines J (2001) Risk assessment of the use of deltamethrin on bednets for the prevention of malaria. *Food Chem Toxicol* 39:407–422
- Bartlett DW, Clough JM, Godwin JR, Hall AA, Hamer M, Parr-Dobrzanski B (2002) The strobilurin fungicides. *Pest Manag Sci* 58:649–662. <https://doi.org/10.1002/ps.520>

- Bastos AC, Magan N (2009) *Trametes versicolor*: potential for atrazine bioremediation in calcareous clay soil, under low water availability conditions. *Int Biodeterior Biodegrad* 63:389–394
- Baxter L, Brain RA, Hosmer AJ, Nema M, Müller KM, Solomon KR, Hanson ML (2015) Effects of atrazine on egg masses of the yellow-spotted salamander (*Ambystoma maculatum*) and its endosymbiotic alga (*Oophila amblystomatis*). *Environ Pollut* 206:324–331. <https://doi.org/10.1016/j.envpol.2015.07.017>
- Baxter L, Brain RA, Lissemore L, Solomon KR, Hanson ML, Prosser RS (2016) Influence of light, nutrients, and temperature on the toxicity of atrazine to the algal species *Raphidocelis subcapitata*: implications for the risk assessment of herbicides. *Ecotoxicol Environ Saf* 132:250–259. <https://doi.org/10.1016/j.ecoenv.2016.06.022>
- Benbrook CM (2016) Trends in glyphosate herbicide use in the United States and globally. *Environ Sci Eur* 28(1):3
- Binukumar BK, Gill K (2010) Cellular and molecular mechanisms of dichlorvos neurotoxicity: cholinergic, noncholinergic, cell signaling, gene expression and therapeutic aspects. *Indian J Exp Biol* 48:697–709
- Blahova J, Plhalova L, Hostovsky M, Divisova L, Dobsikova R, Mikulikova I, Svobodova Z (2013) Oxidative stress responses in zebrafish *Danio rerio* after subchronic exposure to atrazine. *Food Chem Toxicol* 61:82–85. <https://doi.org/10.1016/j.fct.2013.02.041>
- Bollag JM, Liu SY (1990) Biological transformation processes of pesticides. In: Cheng HH (ed) *Pesticides in the soil environment: processes, impacts and modelling*. Soil Science Society of America, Madison, WI, pp 169–211
- Bradberry SM, Proudfoot AT, Vale JA (2004) Glyphosate poisoning. *Toxicol Rev* 23(3):159–167. <https://doi.org/10.2165/00139709-200423030-00003>
- Bradberry SM, Cage SA, Proudfoot AT, Vale JA (2005) Poisoning due to pyrethroids. *Toxicol Rev* 24:93–106
- Brouwer A, Longnecker MP, Birnbaum LS, Coglianò J, Kostyniak P, Moore J, Schantz S, Winneke G (1999) Characterization of potential endocrine related health effects at low dose levels of exposure to PCBs. *Environ Health Perspect*. <https://doi.org/10.1289/ehp.99107s4639>
- Campos-Pereira FD, Oliveira CA, Pigoso AA, Silva-Zacarin EC, Barbieri R, Spatti EF, Marin-Morales MA, Severi-Aguiar GD (2012) Early cytotoxic and genotoxic effects of atrazine on Wistar rat liver: a morphological, immunohistochemical, biochemical, and molecular study. *Ecotoxicol Environ Saf* 78:170–177. <https://doi.org/10.1016/j.ecoenv.2011.11.020>
- Cantor K, Blair A, Everett G, Gibson R, Burmeister LF, Brown LM, Schuma LM, Dick F (1992) Pesticides and other agricultural risk factors for non-Hodgkin's lymphoma among men in Iowa and Minnesota. *Cancer Res* 52:2447–2455
- Chang SW, Lee SJ, Je CH (2005) Phytoremediation of atrazine by poplar trees: toxicity, uptake, and transformation. *J Environ Sci Health B* 40:801–811. <https://doi.org/10.1080/03601230500227483>
- Chawla N, Sunita S, Kamlesh K, Kumar R (2013) Bioremediation: an emerging technology for remediation of pesticides. *Res J Chem Environ* 17:88–105
- Chen S, Lai K, Li Y, Hu M, Zhang Y, Zeng Y (2011) Biodegradation of deltamethrin and its hydrolysis product 3-phenoxybenzaldehyde by a newly isolated *Streptomyces aureus* strain HP-S-01. *Appl Microbiol Biotechnol* 90:1471–1483
- Chrutek A, Hołyńska-Iwan I, Dziembowska I, Bogusiewicz J, Wróblewski M, Cwynar A, Olszewska-Słonina D (2018) Current research on the safety of pyrethroids used as insecticides. *Medicina (Kaunas, Lithuania)* 54:61. <https://doi.org/10.3390/medicina54040061>
- Chung TV, Khue DN, Minh DB, Cheng F (2009) Use of fungal humus for 1,1,1-trichloro-2,2-bis(4-chlorophenyl) ethane (DDT) polluted soil treatment. *Asian J Chem* 2:5967–5972
- Clinton B, Warden A, Haboury S, Easton C, Kotsonis S, Taylor M, Oakeshott J, Russell R, Scott C (2011) Bacterial degradation of strobilurin fungicides: a role for a promiscuous methyl esterase activity of the subtilisin proteases? *Biocatal Biotransform* 29:119–129. <https://doi.org/10.3109/10242422.2011.578740>

- Cosselman KE, Navas-Acien A, Kaufman JD (2015) Environmental factors in cardiovascular disease. *Nat Rev Cardiol* 12(11):627–642. <https://doi.org/10.1038/nrcardio.2015.152>
- Crisp TM, Clegg ED, Cooper RL, Wood WP, Anderson DG, Baeteke KP, Hoffmann JL, Morrow MS, Rodier DJ, Schaeffer JE, Touart LW, Zeeman MG, Patel YM (1998) Environmental endocrine disruption: An effects assessment and analysis. *Environ Health Perspect* 106:11–56
- Cycoń M, Żmijowska A, Piotrowska-Seget Z (2014) Enhancement of deltamethrin degradation by soil bioaugmentation with two different strains of *Serratia marcescens*. *Int J Environ Sci Technol* 11:1305–1316
- da Silva SJ, da Silva PM, Grillo R, Fiorucci AR, José de Arruda G, Santiago EF (2020) Physiological mechanisms and phytoremediation potential of the macrophyte *Salvinia biloba* towards a commercial formulation and an analytical standard of glyphosate. *Chemosphere*. <https://doi.org/10.1016/j.chemosphere.2020.127417>
- Dai YJ, Yuan S, Ge F, Chen T, Xu SC, Ni JP (2006) Microbial hydroxylation of imidacloprid for the synthesis of highly insecticidal olefin imidacloprid. *Appl Microbiol Biotechnol* 71:927–934
- Davies TG, Field LM, Usherwood PN, Williamson MS (2007) DDT, pyrethrins, pyrethroids and insect sodium channels. *IUBMB Life* 59(3):151–162
- de Liz Oliveira Cavalli VL, Cattani D, Heinz Rieg CE et al (2013) Roundup disrupts male reproductive functions by triggering calcium-mediated cell death in rat testis and Sertoli cells. *Free Radic Biol Med* 65:335–346. <https://doi.org/10.1016/j.freeradbiomed.2013.06.043>
- Debarati P, Gunjan P, Janmejy P, Rakesh VJK (2005) Accessing microbial diversity for bioremediation and environmental restoration. *Trends Biotechnol* 23:135–142
- Dehghani M, Nasserli S, Amin S, Naddafee K, Taghavi M, Yunesian M, Maleky N (2007) Isolation and identification of atrazine-degrading bacteria from corn field soil in Fars province of Iran. *Pak J Biol Sci* 10:84–89
- Derbalah A, Khattab I, Saad AM (2020) Isolation and molecular identification of *Aspergillus flavus* and the study of its potential for malathion biodegradation in water. *World J Microbiol Biotechnol* 36(7). <https://doi.org/10.1007/s11274-020-02869-4>
- Dickoff DJ, Gerber O, Turovsky Z (1987) Delayed neurotoxicity after ingestion of carbamate pesticide. *Neurology* 37:1229–1231
- Duzguner V, Erdogan S (2010a) Acute oxidant and inflammatory effects of imidacloprid on the mammalian central nervous system and liver in rats. *Pest Biochem Phys* 97:13–18. <https://doi.org/10.1016/j.pestbp.2009.11.008>
- Duzguner V, Erdogan S (2010b) Chronic exposure to imidacloprid induces inflammation and oxidative stress in the liver & central nervous system of rats. *Pestic Biochem Phys* 104:58–64. <https://doi.org/10.1016/j.pestbp.2012.06.011>
- Elarabi N, Abdelhadi A, Ahmed R, Saleh I, Arif I, Osman G, Ahmed D (2020) *Bacillus aryabhatai* FACU: a promising bacterial strain capable of manipulate the glyphosate herbicide residues. *Saudi J Biol Sci*. <https://doi.org/10.1016/j.sjbs.2020.06.050>
- Elwan MA, Richardson JR, Guillot TS, Caudle WM, Miller GW (2006) Pyrethroid pesticide-induced alterations in dopamine transporter function. *Toxicol Appl Pharmacol* 211:188–197
- Environews Forum (1999) Killer environment. *Environ Health Perspect*. <https://doi.org/10.1289/ehp.107-1566330>
- Erguen GO, Demirci U (2019) Statistical evaluation of the bioremediation performance of *Ochrobactrum thiophenivorans* and *Sphingomonas melonis* bacteria on Imidacloprid insecticide in artificial agricultural field. *J Environ Health Sci Eng*. <https://doi.org/10.1007/s40201-019-00391-w>
- Fan X, Song F (2014) Bioremediation of atrazine: recent advances and promises. *J Soils Sediments* 14:1727–1737. <https://doi.org/10.1007/s11368-014-0921-5>
- Feng Y, Huang Y, Zhan H, Bhatt P, Chen S (2020) An overview of Strobilurin fungicide degradation: current status and future perspective. *Front Microbiol*. <https://doi.org/10.3389/fmicb.2020.00389>

- Fernando T, Aust SD, Bumpus JA (1989) Effects of culture parameters on DDT [1,1,1-trichloro-2,2-bis(4-chlorophenyl)ethane] biodegradation by *Phanerochaete chrysosporium*. *Chemosphere* 19:1387–1398
- Firdous S, Iqbal S, Anwar S (2017) Optimization and modeling of glyphosate biodegradation by a novel *Comamonas odontotermitis* P2 through response surface methodology. *Pedosphere*. [https://doi.org/10.1016/S1002-0160\(17\)60381-3](https://doi.org/10.1016/S1002-0160(17)60381-3)
- Foght J, April T, Biggar K, Aislabie J (2010) Bioremediation of DDT-contaminated soils: a review. *Bioremediation J* 5:225–246. <https://doi.org/10.1080/20018891079302>
- Frankowski BL (2004) American Academy of Pediatrics guidelines for the prevention and treatment of head lice infestation. *Am J Manag Care* 10:S269–S272
- Freire C, Koifman RJ, Koifman S (2015) Hematological and hepatic alterations in Brazilian population heavily exposed to organochlorine pesticides. *J Toxicol Environ Health A* 78:534–548. <https://doi.org/10.1080/15287394.2014.999396>
- Fu WX (2005) Research on the growth condition of organophosphate pesticides degrading strain – *Trichoderma* sp. FM10. *Biomagnetism* 5:29–31
- Fu GM, Chen Y, Li RY, Yuan XQ, Liu CM, Li B, Wan Y (2017) Pathway and rate-limiting step of glyphosate degradation by *Aspergillus oryzae* A-F02. *Prep Biochem Biotechnol* 47(8):782–788
- Gao B, Liu WB, Jia LY, Xu L, Xie J (2011a) Isolation and characterization of an *Alcaligenes* sp. strain DG-5 capable of degrading DDTs under aerobic conditions. *J Environ Sci Health B* 46:257–263
- Gao Y, Fang J, Zhang J, Ren L, Mao Y, Li B, Zhang M, Liu D, Du M (2011b) The impact of the herbicide atrazine on growth and photosynthesis of seagrass, *Zostera marina* (L.), seedlings. *Mar Pollut Bull* 62(8):1628–1631. <https://doi.org/10.1016/j.marpolbul.2011.06.014>
- Gaonkar O, Nambi IM, Suresh KG (2019) Biodegradation kinetics of dichlorvos and chlorpyrifos by enriched bacterial cultures from an agricultural soil. *Bioremediation J*. <https://doi.org/10.1080/10889868.2019.1671791>
- Garcinuño R, Hernando P, Cámara C (2006) Removal of Carbaryl, Linuron, and Permethrin by *Lupinus angustifolius* under hydroponic conditions. *J Agric Food Chem* 54:5034–5039. <https://doi.org/10.1021/jf060850j>
- Gawade L, Dadarkar SS, Husain R, Gatne M (2013) A detailed study of developmental immunotoxicity of imidacloprid in Wistar rats. *Food Chem Toxicol* 51:61–70. <https://doi.org/10.1016/j.fct.2012.09.009>
- Ge F, Dai YJ, Chen T (2006) Identification of a strain NJ2 hydroxylating imidacloprid and the transformed product. *Wei Sheng Wu Xue Bao* 46:557–560
- Gely-Perrot A, Hao C, Becker E, Stuparevic I, Kervarrec C, Chalmel F, Primig M, Jégou B, Smagulova F (2015) The epigenetic processes of meiosis in male mice are broadly affected by the widely used herbicide atrazine. *BMC Genomics* 16(1):885. <https://doi.org/10.6084/m9.figshare.c.3623711>
- Gibson WP, Burns RG (1977) The breakdown of malathion in soil and soil components. *Microb Ecol* 3:219–230. <https://doi.org/10.1007/BF02010619>
- Gillezeau C, van Gerwen M, Shaffer RM et al (2019) The evidence of human exposure to glyphosate: a review. *Environ Health* 18:2. <https://doi.org/10.1186/s12940-018-0435-5>
- Góngora-Echeverría VR, García-Escalante R, Rafael R, Giacoman-Vallejos G, Ponce-Caballero M (2020) Pesticide bioremediation in liquid media using a microbial consortium and bacteria-pure strains isolated from a biomixture used in agricultural areas. *Ecotoxicol Environ Saf*. <https://doi.org/10.1016/j.ecoenv.2020.110734>
- Gunasekara AS, Rubin AL, Goh KS, Spurlock FC, Tjeerdema RS (2008) Environmental fate and toxicology of carbaryl. In: Whitacre D (ed) *Reviews of environmental contamination and toxicology (continuation of residue reviews)*, vol 196. Springer, New York, NY
- Gündüz E, Ülger BV, İbiloğlu İ, Ekinci A, Dursun R, Zengin Y, İçer M, Uslukaya Ö, Ekinci C, Güloğlu C (2015) Glutamine provides effective protection against deltamethrin-induced acute hepatotoxicity in rats but not against nephrotoxicity. *Med Sci Monitor* 21:1107–1114. <https://doi.org/10.12659/MSM.893180>

- Guo L, Dai Z, Guo J, Yang W, Ge F, Dai Y (2020) Oligotrophic bacterium *Hymenobacter latericoloratus* CGMCC 16346 degrades the neonicotinoid imidacloprid in surface water. *AMB Exp* 10(1):7. <https://doi.org/10.1186/s13568-019-0942-y>
- Hägglom MM, Bossert ID (2003) Halogenated organic compounds—a global perspective. Microbial processes and environmental applications. Kluwer, Boston
- Hamada NH (1993) Oncogenicity study with carbaryl technical in CD-1 mice. Hazleton Laboratories America. Lab Project No. 656-138, DPR vol no. 169–267, rec. no. 123769
- Handford CE, Elliott CT, Campbell K (2015) A review of the global pesticide legislation and the scale of challenge in reaching the global harmonization of food safety standards. *Integr Environ Assess Manag* 11:525–536. <https://doi.org/10.1002/ieam.1635>
- Hashimoto M, Fukui M, Hayano K, Hayatsu M (2002) Nucleotide sequence and genetic structure of a novel carbaryl hydrolase gene (*cehA*) from *Rhizobium* sp. Strain AC100. *Appl Environ Microb* 68:1220–1227. <https://doi.org/10.1128/AEM.68.3.1220-1227.2002>
- Hay AG, Focht DD (2000) Transformation of 1,1-dichloro-2,2-(4-chlorophenyl) ethane (DDD) by *Ralstonia eutropha* strain A5. *FEMS Microbiol Ecol* 31:249–253
- He X, Wubie A, Diao Q, Li W, Xue F, Guo Z, Zhou T, Xu S (2014) Biodegradation of neonicotinoid insecticide, imidacloprid by restriction enzyme mediated integration (REMI) generated *Trichoderma* mutants. *Chemosphere* 112. <https://doi.org/10.1016/j.chemosphere.2014.01.023>
- Howell CC, Semple KT, Bending GD (2014) Isolation and characterisation of azoxystrobin degrading bacteria from soil. *Chemosphere* 95:370–378. <https://doi.org/10.1016/j.chemosphere.2013.09.048>
- Hurley PM, Hill RN, Whiting RJ (1998) Mode of carcinogenic action of pesticides inducing thyroid follicular cell tumours in rodents. *Environ Health Perspect*
- IARC (1991) Occupational exposures in insecticide application, and some pesticides; Dichlorvos. In: IARC monographs on the evaluation of carcinogenic risks to humans. IARC, World Health Organization, Lyon, France, p 267
- Iyer JP, Makris S (2010) Developmental and reproductive toxicology of pesticides. In: Krieger R (ed) Hayes' handbook of pesticide toxicology, 3rd edn. Academic Press, London, pp 381–440
- Jacklin D, Brink I, de Waal J (2020) The potential use of plant species within a Renosterveld landscape for the phytoremediation of glyphosate and fertiliser. *Water SA* 46. <https://doi.org/10.17159/wsa/2020.v46.i1.7889>
- Jayashree R, Vasudevan N (2007) Organochlorine pesticide residues in ground water of Thiruvallur district, India. *Environ Monit Assess* 128:209–215. <https://doi.org/10.1007/s10661-006-9306-6>
- Jensen IM, Whatling P (2010) Malathion: a review of toxicology. In: Kreiger R (ed) Hayes' handbook of pesticide toxicology, 3rd edn. Academic Press (Elsevier), London, Burlington, and San Diego, pp 1527–1542
- Joseph RSI (2000, March 26–30) Metabolism and degradation of the fungicide azoxystrobin. In Book of abstracts of 219th ACS National Meeting, ACS American Chemical Society National Meeting, San Francisco, CA
- Kabra AN, Ji MK, Choi J, Kim JR, Govindwar SP, Jeon BH (2014) Toxicity of atrazine and its bioaccumulation and biodegradation in a green microalga *Chlamydomonas mexicana*. *Environ Sci Pollut Res* 21(21):12270–12278. <https://doi.org/10.1007/s11356-014-3157-4>
- Kalender S, Uzun FG, Durak D, Demir F, Kalender Y (2010) Malathion-induced hepatotoxicity in rats: the effects of vitamins C and E. *Food Chem Toxicol* 48(2):633–638. <https://doi.org/10.1016/j.fct.2009.11.044>
- Kamal MZ, Nashwa AH, Fetyan A, Ibrahim AM, Sherif EN (2008) Biodegradation and detoxification of malathion by of *Bacillus thuringiensis* MOS-5. *Austr J Basic Appl Sci* 2:724–732
- Kamanavalli CM, Ninnekar HZ (2004) Biodegradation of DDT by a *Pseudomonas* sp. *Curr Microbiol* 48:10–13
- Kapoor U, Srivastava MK, Srivastava LP (2011) Toxicological impact of technical imidacloprid on ovarian morphology, hormones and antioxidant enzymes in female rats. *Food Chem Toxicol* 49:3086–3089. <https://doi.org/10.1016/j.fct.2011.09.009>

- Karami-Mohajeri S, Abdollahi M (2011) Toxic influence of organophosphate, carbamate, and organochlorine pesticides on cellular metabolism of lipids, proteins, and carbohydrates: a systematic review. *Hum Exp Toxicol* 30(9):1119–1140. <https://doi.org/10.1177/0960327110388959>
- Katayama A, Uchida S, Kuwatsuka S (1992) Degradation of white-rot fungi under nutrient-rich conditions. *J Pest Sci* 17:279–281
- Kaufman DD, Blake J (1970) Degradation of atrazine by soil fungi. *Soil Biol Biochem* 2:73–80
- Khan A, Yousafzai AM, Shah N, Ahmad MS, Farooq M, Aziz F, Adnan M, Rizwan M, Jawad SM (2016) Enzymatic profile a activity of grass carp (*Ctenopharyngodon idella*) after exposure to the pollutant named atrazine (herbicide). *Pol J Environ Stud* 25(5):2003–2008. <https://doi.org/10.15244/pjoes/62821>
- Kilani J, Fillinger S (2016) Phenylpyrroles: 30 years, two molecules and (nearly) no resistance. *Front Microbiol* 7:2014. <https://doi.org/10.3389/fmicb.2016.02014>
- Klimek M, Lejczak B, Kafarski P, Forlani G (2001) Metabolism of the phosphonate herbicide glyphosate by a non-nitrate-utilizing strain of *Penicillium chrysogenum*. *Pest Manag Sci* 57(9):815–821
- Kolekar P, Patil S, Suryavanshi M, Suryawanshi S, Khandare R, Govindwar S, Jadhav J (2019) Microcosm study of atrazine bioremediation by indigenous microorganisms and cytotoxicity of biodegraded metabolites. *J Hazard Mater*. <https://doi.org/10.1016/j.jhazmat.2019.01.023>
- Krzyško-Lupicka T, Orlik A (1997) The use of glyphosate as the sole source of phosphorus or carbon for the selection of soil-borne fungal strains capable to degrade this herbicide. *Chemosphere* 34(12):2601–2605
- Kumar A, Singh N (2016) Atrazine and its metabolites degradation in mineral salts medium and soil using an enrichment culture. *Environ Monit Assess* 188(3):1–12. <https://doi.org/10.1007/s10661-0165144-3>
- Kumar S, Thomas A, Pillai M (2011) Deltamethrin: Promisinü mosquito control agent against adult stage of *Aedes aegypti* L. *Asian Pac J Trop Med* 4:430–435
- Kumar V, Upadhyay N, Singh S, Singh J, Kaur P (2013) Thin-layer chromatography: comparative estimation of soil's atrazine. *Curr World Environ* 8(3):469–472. <https://doi.org/10.12944/CWE.8.3.17>
- Kumar A, Sasmal D, Sharma N (2018) Mechanism of deltamethrin induced thymic and splenic toxicity in mice and its protection by piperine and curcumin: in vivo study. *Drug Chem Toxicol* 41:33–41
- Lasram MM, Annabi AB, El Elj N et al (2009) Metabolic disorders of acute exposure to malathion in adult Wistar rats. *J Hazard Mater* 163(2–3):1052–1055. <https://doi.org/10.1016/j.jhazmat.2008.07.059>
- Lee DH, Rhee YJ, Choi KS, Nam SE, Eom HJ, Rhee JS (2017) Sublethal concentrations of atrazine promote molecular and biochemical changes in the digestive gland of the Pacific oyster *Crassostrea gigas*. *Toxicol Environ Health Sci* 9(1):50–58. <https://doi.org/10.1007/s13530-017-0303-7>
- Lefranq M, Imfeld G, Payraudeau S, Millet M (2013) Kresoxim methyl deposition, drift and runoff in a vineyard catchment. *Sci Total Environ* 442:503–508. <https://doi.org/10.1016/j.scitotenv.2012.09.082>
- Leroux P (1996) Recent developments in the mode of action of fungicides. *Pestic Sci* 47(2):191–197. [https://doi.org/10.1002/\(SICI\)10969063\(199606\)47:2<191::AIDPS415>3.0.CO;2-I](https://doi.org/10.1002/(SICI)10969063(199606)47:2<191::AIDPS415>3.0.CO;2-I)
- Li X, Wu T, Huang H, Zhang S (2012) Atrazine accumulation and toxic responses in maize (*Zea mays*). *J Environ Sci* 24(2):203–208. [https://doi.org/10.1016/S1001-0742\(11\)60718-3](https://doi.org/10.1016/S1001-0742(11)60718-3)
- Li F, Di L, Liu Y, Xiao Q, Zhang X, Ma F, Yu H (2019) Carbaryl biodegradation by *Xylaria* sp. BNL1 and its metabolic pathway. *Ecotoxicol Environ Saf* 167:331–337. <https://doi.org/10.1016/j.ecoenv.2018.10.051>

- Lin PC, Lin HJ, Liao YY, Guo HR, Chen KT (2013) Acute poisoning with neonicotinoid insecticides: a case report and literature review. *Basic Clin Pharmacol Toxicol* 112:282–286. <https://doi.org/10.1111/bcpt.12027>
- Lonare M, Kumar M, Raut S, Badgujar P, Doltade S, Telang A (2014) Evaluation of imidacloprid-induced neurotoxicity in male rats: a protective effect of curcumin. *Neurochem Int* 78:122–129. <https://doi.org/10.1016/j.neuint.2014.09.004>
- Lopes FM, Batista KA, Batista GL, Mitidieri S, Bataus LA, Fernandes KF (2010) Biodegradation of epoxyconazole and piraclostrobin fungicides by *Klebsiella* sp. from soil. *World J Microbiol Biotechnol* 26:1155–1161. <https://doi.org/10.1007/s11274-009-0283-0>
- Mahajan R, Blair A, Coble J, Lynch CF, Hoppin JA, Sandler DP, Alavanja MC (2007) Carbaryl exposure and incident cancer in the agricultural health study. *Int J Cancer* 121:1799–1805. <https://doi.org/10.1002/ijc.22836>
- Mahler BJ, Van Metre PC, Burley TE, Loftin KA, Meyer MT, Nowell LH (2017) Similarities and differences in occurrence and temporal fluctuations in glyphosate and atrazine in small Mid-western streams (USA) during the 2013 growing season. *Sci Total Environ* 579:149–158. <https://doi.org/10.1016/j.scitotenv.2016.10.236>
- Mathur ML, Yadav SP, Tyagi BK (2000) A study of an epidemic of acute respiratory disease in Jaipur town. *J Postgrad Med* 46(2):88–90
- McDuffie HH, Pahwa P, JR ML et al (2001) Non-Hodgkin's lymphoma and specific pesticide exposures in men: cross-Canada study of pesticides and health. *Cancer Epidemiol Biomarkers Prev* 10:1155–1163
- Mela M, Guiloski IC, Doria HB, Randi MAF, de Oliveira Ribeiro CA, Pereira L, de Assis HS (2013) Effects of the herbicide atrazine in neotropical catfish (*Rhamdia quelen*). *Ecotoxicol Environ Saf* 93:13–21. <https://doi.org/10.1016/j.ecoenv.2013.03.026>
- Memon SA, Memon N, Mal B, Shaikh S, Shah MA (2014) Histopathological changes in the gonads of male rabbits (*Oryctolagus cuniculus*) on exposure to imidacloprid insecticide. *J Entomol Zool Stud*
- Mikolić A, Brčić Karačonji I (2018) Imidacloprid reproductive toxicity and endocrine disruption in lab animals. *Arh Hig Rada Toksikol* 69:103–108
- Mladenović M, Arsić BB, Stanković N et al (2018) The targeted pesticides as Acetylcholinesterase inhibitors: comprehensive cross-organism molecular Modelling studies performed to anticipate the pharmacology of harmfulness to humans in vitro. *Molecules* 23(9):2192. <https://doi.org/10.3390/molecules23092192>
- Mnif W, Hassine AIH, Bouaziz A, Bartegi A, Thomas O, Roig B (2011) Effect of endocrine disruptor pesticides: a review. *Int J Environ Res Public Health* 8:2265–2203. <https://doi.org/10.3390/ijerph8062265>
- Mohammed YMM, Badawy MEI (2017) Biodegradation of imidacloprid in liquid media by an isolated wastewater fungus *Aspergillus terreus* YESM3. *J Environ Sci Health B* 52 (10):752–761. <https://doi.org/10.1080/03601234.2017.1356666>
- Morales-Perez AA, Arias C, Ramirez-Zamora RM (2016) Removal of atrazine from water using an iron photo catalyst supported on activated carbon. *Adsorption* 22(1):49–58. <https://doi.org/10.1007/s10450015-9739-8>
- Mostafa IY, Fakhri IMI, Bahig MRE, El-Zawahry YA (1972) Metabolism of organophosphorus insecticides. XIII Degradation of malathion by *Rhizobium* spp. *Arch Microbiol* 86:221–224
- Mougin C, Laugero C, Asther M, Dubroca J, Frasse P, Asther M (1994) Biotransformation of the herbicide atrazine by the white rot fungus *Phanerochaete chrysosporium*. *Appl Environ Microbiol* 60:705–708
- Nadeau LJ, Menn FM, Breen A, Sayler GS (1994) Aerobic degradation of 1,1,1-trichloro-2,2-bis (4-chlorophenyl)ethane (DDT) by *Alcaligenes eutrophus* A5. *Appl Environ Microbiol* 60:51–55
- Nain S, Bour A, Chalmers C, Smits JE (2011) Immunotoxicity and disease resistance in Japanese quail (*Coturnix coturnix japonica*) exposed to malathion. *Ecotoxicology* 20(4):892–900. <https://doi.org/10.1007/s10646-011-0657-6>

- Nason MA, Farrar J, Bartlett D (2007) Strobilurin fungicides induce changes in photosynthetic gas exchange that do not improve water use efficiency of plants grown under conditions of water stress. *Pest Manag Sci* 63:1191–1200. <https://doi.org/10.1002/ps.1443>
- Nicolopoulou-Stamati P, Maipas S, Kotampasi C, Stamatis P, Hens L (2016) Chemical pesticides and human health: the urgent need for a new concept in agriculture. *Front Public Health* 4:148. <https://doi.org/10.3389/fpubh.2016.00148>
- Niewiadomska A, Sawinska Z, Wolna-Maruwka A (2011) Impact of selected seed dressings on soil microbiological activity in spring barley cultivation. *Fresenius Environ Bull* 20:1252–1261
- Ning J, Gang G, Bai Z et al (2012) In situ enhanced bioremediation of dichlorvos by a phyllosphere Flavobacterium strain. *Front Environ Sci Eng* 6:231–237. <https://doi.org/10.1007/s11783-011-0316-4>
- Niu J, Wang J, Cui D, Liu X, Guang H (2012) Study on the isolation, identification and degradation characterisation of a DDT-degrading bacteria. *Adv Mater Res* 518–523:2030–2033
- Nwani CD, Lakra WS, Nagpure NS, Kumar R, Kushwaha B, Srivastava SK (2010) Toxicity of the herbicide atrazine: effects on lipid peroxidation and activities of antioxidant enzymes in the freshwater fish *Channa punctatus* (Bloch). *Int J Environ Res Public Health* 7(8):3298–3312. <https://doi.org/10.3390/ijerph7083298>
- Oberemok V, Aleksei Z, Levchenko N, Nyadar P (2015) A brief review of most widely used modern insecticides and prospects for the creation of DNA insecticides. *Entomol Rev* 97:507–518. <https://doi.org/10.1134/S0013873815070027>
- Obojska A, Lejczak B, Kubrak M (1999) Degradation of phosphonates by Streptomycete isolates. *Appl Microbiol Biotechnol* 51(6):872–876
- Oda SS, El-Maddawy Z (2012) Protective effect of vitamin E and selenium combination on deltamethrin-induced reproductive toxicity in male rats. *Exp Toxicol Pathol* 64:813–819
- Odukkathil G, Vasudevan N (2013) Toxicity and bioremediation of pesticides in agricultural soil. *Rev Environ Sci Biotechnol* 12. <https://doi.org/10.1007/s11157-013-9320-4>
- Okoroiwu H, Iwara I (2018) Dichlorvos toxicity: a public health perspective. *Interdiscip Toxicol* 11 (2):129–137. <https://doi.org/10.2478/intox-2018-0009>
- Orton F, Carr JA, Handy RD (2006) Effects of nitrate and atrazine on larval development and sexual differentiation in the northern leopard frog *Rana pipiens*. *Environ Toxicol Chem* 25(1):65–71. <https://doi.org/10.1897/05-136R.1>
- Ozkara A, Akyl D, Konuk M (2016) Pesticides. *Environ Pollut Health*. <https://doi.org/10.5772/63094>
- Paris DF, Lewis DL, Wolfe NL (1975) Rates of degradation of malathion by bacteria isolated from aquatic systems. *Environ Sci Technol* 9:135–138. <https://doi.org/10.1021/es60100a011>
- Peñaloza-Vazquez A, Mena GL, Herrera-Estrella L, Bailey AM (1995) Cloning and sequencing of the genes involved in glyphosate utilization by *Pseudomonas pseudomallei*. *Appl Environ Microbiol* 61(2):538–543
- Pereyra MA, Ballesteros FM, Creus CM, Sueldo RJ, Barassi CA (2009) Seedlings growth promotion by *Azospirillum brasilense* under normal and drought conditions remains unaltered in Tebuconazole-treated wheat seeds. *Eur J Soil Biol* 45(1):20–27
- Petit AN, Fontaine F, Clement C, Vaillant-Gaveau N (2008) Photosynthesis limitations of grapevine after treatment with the fungicide fludioxonil. *Agric Food Chem* 56:6761–6767. <https://doi.org/10.1021/jf800919u>
- Pipke R, Amrhein N, Jacob GS, Schaefer J, Kishore GM (1987) Metabolism of glyphosate in an *Arthrobacter* sp. GLP-1. *FEBS J* 165(2):267–273
- Popp J, Pető K, Nagy J (2013) Pesticide productivity and food security. A review. *Agron Sustain Dev* 33:243–255. <https://doi.org/10.1007/s13593-012-0105-x>
- Purnomo AS, Mori T, Takagi K, Kondo R (2011) Bioremediation of DDT contaminated soil using brown-rot fungi. *Int Biodeterior Biodegradation* 65(5):691–695
- Raymann K, Motta EVS, Girard C, Riddington IM, Dinser JA, Moran NA (2018) Imidacloprid decreases honey bee survival rates but does not affect the gut microbiome. *Appl Environ Microbiol* 84(13). <https://doi.org/10.1128/aem.00545-18>

- Ross G (2005) Risks and benefits of DDT. *Lancet* 366(9499):1771
- Saghee MR, Bidlan R (2018) Simultaneous degradation of organochlorine pesticides by microbial consortium. *Biosci Biotechnol Res Commun* 11:49–54. <https://doi.org/10.21786/bbr/11.1/7>
- Saladin G, Magné Christian CC, Clément C (2003) Effects of fludioxonil and pyrimethanil, two fungicides used against *Botrytis cinerea*, on carbohydrate physiology in *Vitis vinifera* L. *Pest Manag Sci* 59(10):1083–1092. <https://doi.org/10.1002/ps.733>
- Samsel A, Seneff S (2013) Glyphosate, pathways to modern diseases II: celiac sprue and gluten intolerance. *Interdiscip Toxicol* 6(4):159–184. <https://doi.org/10.2478/intox-2013-0026>
- Sarkar S, Subbiah S, Premkumar R (2009) Biodegradation of propiconazole by *Pseudomonas putida* isolated from tea rhizosphere. *Plant Soil Environ* 55:196–201. <https://doi.org/10.17221/2184-PSE>
- Satapute P, Kaliwal B (2016) Biodegradation of propiconazole by newly isolated *Burkholderia* sp. strain BBK_9. *3 Biotech* 6:110. <https://doi.org/10.1007/s13205-016-0429-3>
- Schroeder JC, Olshan AF, Baric R, Dent GA, Weinberg CR, Yount B, Rothman N (2001) Agricultural risk factors for t (14;18) subtypes of non-Hodgkin's lymphoma. *Epidemiology* 12(6):701–709. <https://doi.org/10.1097/00001648-200111000-00020>
- Sharma S, Singh B, Gupta VK (2014a) Assessment of imidacloprid degradation by soil-isolated *Bacillus alkalinitrilicus*. *Environ Monit Assess* 186:7183–7193. <https://doi.org/10.1007/s10661-014-3919-y>
- Sharma S, Singh B, Gupta VK (2014b) Biodegradation of imidacloprid by consortium of two soil isolated *Bacillus* sp. *Bull Environ Contam Toxicol* 93:637–642. <https://doi.org/10.1007/s00128-014-1386-3>
- Shrivastava B et al (2011) Impact of deltamethrin on environment, use as an insecticide and its bacterial degradation – a preliminary study. *Int J Environ Sci* 1:984–992
- Silveyra GR, Canosa IS, Rodriguez EM, Medesani DA (2017) Effects of atrazine on ovarian growth, in the estuarine crab *Neohelice granulata*. *Comp Biochem Physiol C Toxicol Pharmacol* 192:1–6. <https://doi.org/10.1016/j.cbpc.2016.10.011>
- Simpkins JW, Swenberg JS, Weiss N, Brusick D, Eldridge JC, Stevens JT, Handa RJ, Hovey RC, Plant TM, Pastoor TP, Breckenridge CB (2011) Atrazine and breast cancer: a framework assessment of the toxicological and epidemiological evidence. *Toxicol Sci* 123(2):441–459. <https://doi.org/10.1093/toxsci/kfr176>
- Singh D (2008) Biodegradation and bioremediation of pesticide in soil: concept, method and recent developments. *Indian J Microbiol* 48:35–40. <https://doi.org/10.1007/s12088-008-0004-7>
- Singh S, Kumar V, Chauhan A, Datta S, Wani A, Singh N, Singh J (2017) Toxicity, degradation and analysis of the herbicide atrazine. *Environ Chem Lett*. <https://doi.org/10.1007/s10311-017-0665-8>
- Soderlund DM (2012) Molecular mechanisms of pyrethroid insecticide neurotoxicity. *Recent Adv Arch Toxicol* 6:165–181
- Solomon KR, Giesy JP, LaPoint TW, Giddings JM, Richards RP (2013) Ecological risk assessment of atrazine in North American surface waters. *Environ Toxicol Chem* 32(1):10–11. <https://doi.org/10.1002/etc.5620150105>
- Steinrücken HC, Amrhein N (1980) The herbicide glyphosate is a potent inhibitor of 5-enolpyruvyl-shikimic acid-3-phosphate synthase. *Biochem Biophys Res Commun* 94(4):1207–1212. [https://doi.org/10.1016/0006-291x\(80\)90547-1](https://doi.org/10.1016/0006-291x(80)90547-1)
- Sudharshan S, Naidu R, Mallavarapu M, Bolan N (2012) DDT remediation in contaminated soils: a review of recent studies. *Biodegradation* 23:851–863. <https://doi.org/10.1007/s10532-012-9575-4>
- Swanson N, Leu A, Abrahamson J, Wallet B (2014) Genetically engineered crops, glyphosate and the deterioration of health in the United States of America. *J Organ Syst* 9:6–37
- Swetha VP, Phale PS (2005) Metabolism of carbaryl via 1,2-dihydroxynaphthalene by soil isolates *Pseudomonas* sp. strains C4, C5, and C6. *Appl Environ Microb* 71:5951–5956. <https://doi.org/10.1128/AEM.71.10.5951-5956.2005>

- Tallur PN, Megadi VB, Ninnekar HZ (2008) Biodegradation of Cypermethrin by *Micrococcus* sp. strain CPN 1. *Biodegradation* 19:77–82. <https://doi.org/10.1007/s10532-007-9116-8>
- Tan J, Galligan JJ, Hollingworth RM (2007) Agonist actions of neonicotinoids on nicotinic acetylcholine receptors expressed by cockroach neurons. *Neurotoxicology* 28(4):829–842. <https://doi.org/10.1016/j.neuro.2007.04.002>
- Tang J, Liu L, Hu S, Chen Y, Chen J (2008) Improved degradation of organophosphate dichlorvos by *Trichoderma atroviride* transformants generated by restriction enzyme-mediated integration (REMI). *Bioresour Technol* 100:480–483. <https://doi.org/10.1016/j.biortech.2008.05.022>
- Tang J, Hu Q, Lei D, Wu M, Zeng C, Zhang Q (2020) Characterization of deltamethrin degradation and metabolic pathway by co-culture of *Acinetobacter junii* LH-1-1 and *Klebsiella pneumoniae* BPBA052. *AMB Exp*. <https://doi.org/10.1186/s13568-020-01043-1>
- Tchounwou P, Patlolla A, Yedjou C, Moore P (2015) Environmental exposure and health effects associated with Malathion toxicity. Open Access. <https://doi.org/10.5772/60911>
- Thabit T, El-Naggar M (2013) Malathion degradation by soil isolated bacteria and detection of degradation products by GC-MS. *Int J Environ Sci*. <https://doi.org/10.6088/ijes.20130305000177>
- Thongprakaisang S, Thiantanawat A, Rangkadilok N, Suriyo T, Satayavivad J (2013) Glyphosate induces human breast cancer cells growth via estrogen receptors. *Food Chem Toxicol* 59:129–136. <https://doi.org/10.1016/j.fct.2013.05.057>
- Tiemann U (2008) In vivo and in vitro effects of the organochlorine pesticides DDT, TCPM, methoxychlor, and lindane on the female reproductive tract of mammals: a review. *Reprod Toxicol* 25:316–326. <https://doi.org/10.1016/j.reprotox.2008.03.002>
- Townson H, Nathan MB, Zaim M, Guillet P, Manga L, Bos R et al (2005) Exploiting the potential of vector control for disease prevention. *Bull World Health Organ* 83:942–947/16462987
- Turusov V, Rakitsky V, Tomatis L (2002) Dichlorodiphenyltrichloroethane (DDT): ubiquity, persistence, and risks. *Environ Health Perspect* 110:125–128. <https://doi.org/10.1289/ehp.02110125>
- Uqab B, Mudasir S, Nazir R (2016) Review on bioremediation of pesticides. *J Bioremed Biodegr* 7:343. <https://doi.org/10.4172/2155-6199.1000343>
- USEPA: Unites States Environmental Protection Agency (1994) Integrated Risk Information System (IRS) on Dichlorvos. Environmental criteria and assessment office, office of Health and Environmental Assessment, Office of Research and Development Cincinnati, OH
- Uygun U, Koksel H, Atli A (2005) Residue levels of malathion and its metabolites and fenitrothion in post-harvest treated wheat during storage, milling and baking. *Food Chem* 92:643–647. <https://doi.org/10.1016/j.foodchem.2004.08.045>
- van den Berg H, Manuweera G, Konradsen F (2017) Global trends in the production and use of DDT for control of malaria and other vector-borne diseases. *Malar J* 16:401. <https://doi.org/10.1186/s12936-017-2050-2>
- Varo I, Navarro JC, Amat F, Guilhermino L (2003) Effects of dichlorvos on cholinesterase activity of the European sea bass (*Dicentrarchus labrax*). *Pestic Biochem Physiol* 75:61–72
- Verdisson S, Couderchet M, Vernet G (2001) Effects of procymidone, fludioxonil and pyrimethanil on two non-target aquatic plants. *Chemosphere* 44(3):467–474
- Viel JF, Warembourg C, Le Mauer-Idrissi G, Lacroix A, Limon G, Rouget F, Monfort C, Durand G, Cordier S, Cherier C (2015) Pyrethroid insecticide exposure and cognitive developmental disabilities in children: the PELAGIE mother-child cohort. *Environ Int* 82:69–75
- Vonberg D, Vanderborght J, Cremer N, Putz T, Herbst M, Vereecken H (2014) 20 years of long-term atrazine monitoring in a shallow aquifer in western Germany. *Water Res* 50:294–306. <https://doi.org/10.1016/j.watres.2013.10.032>
- Wang HH, Chou YC, Liao JF, Chen CF (2004) The effect of the insecticide dichlorvos on esterase activity extracted from the psocids, *Liposcelis bostrychophila* and *L. entomophila*. *J Insect Sci* 4:1–5

- Wang GL, Bi M, Liang JD, Li SP (2011) *Pseudoxanthomonas jiangsuensis* sp. nov., a DDT-degrading bacterium isolated from a long-term DDT-polluted soil. *Curr Microbiol* 62:1760–1766
- Wang Q, Zhang W, Li C, Xiao B (2012) Phytoremediation of atrazine by three emergent hydrophytes in a hydroponic system. *Water Sci Technol* 66:1282–1288. <https://doi.org/10.2166/wst.2012.320>
- Wang Q, Zhang Y, Zhou C, Zhang J, Dou Y, Li Q (2013) Risk assessment of mouse gastric tissue cancer induced by Dichlorvos and dimethoate. *Oncol Lett* 5:1385–1389
- Wang X, Hou X, Liang S, Lu Z, Hou Z, Zhao X, Sun F, Zhang H (2018) Biodegradation of fungicide Tebuconazole by *Serratia marcescens* strain B1 and its application in bioremediation of contaminated soil. *Int Biodeterioration Biodegradation* 127:185–191. <https://doi.org/10.1016/j.ibiod.2017.12.001>
- White A (2016) Atrazine—a case of discrediting science. *Sci Educ News* 65(1):22
- World Health Organization (1990) Public health impact of pesticides used in agriculture. World Health Organization, London
- World Health Organization & International Programme on Chemical Safety (2004)
- Wu P, Xie L, Mo W, Wang B, Ge H, Sun X, Wang Y (2019) The biodegradation of carbaryl in soil with *Rhodospseudomonas capsulata* in wastewater treatment effluent. *J Environ Manag* 249:109226. <https://doi.org/10.1016/j.jenvman.2019.06.127>
- Xia Y, Cheng S, Bian Q, Xu L, Collins MD, Chang HC, Song L, Liu J, Wang S, Wang X (2005) Genotoxic effects on spermatozoa of carbaryl-exposed workers. *Toxicol Sci* 85:615–623
- Xie S, Liu J, Li L, Qiao C (2009) Biodegradation of malathion by *Acinetobacter johnsonii* MA19 and optimization of cometabolism substrates. *J Environ Sci* 21:76–82
- Yadav I, Devi N (2017) Pesticides classification and its impact on human and environment. In: *Environmental science and engineering*, Chapter 7, vol 6. Studium Press, New York
- Yadav S, Verma SK, Chaudhary HS (2015) Isolation and characterization of organophosphate pesticides degrading bacteria from contaminated agricultural soil. *J Biol Sci* 15(1):113–125
- Yamada T, Ishige T, Shiota N, Inui H, Ohkawa H, Ohkawa Y (2002) Enhancement of metabolizing herbicides in young tubers of transgenic potato plants with the rat CYP1A1 gene. *Theor Appl Genet* 105:515–520
- Yang M, Zhang J, Zhu KY et al (2008) Increased activity and reduced sensitivity of acetylcholinesterase associated with malathion resistance in a field population of the oriental migratory locust, *Locusta migratoria manilensis* (Meyen). *Pesticide Biochem Physiol* 91(1):32–38
- Yang C, Hamel C, Vujanovic V, Gan Y (2011) Fungicide: modes of action and possible impact on nontarget microorganisms. *ISRN Ecol*. <https://doi.org/10.5402/2011/130289>
- Yang S, Jia ZC, Chen JY, Hu JX, Zhang LS (2014) Toxic effects of atrazine on reproductive system of male rats. *Biomed Environ Sci* 27(4):281–288. <https://doi.org/10.3967/bes2014.050>
- Yen JH, Chang JS, Huang PJ, Wang YS (2009) Effects of fungicides triadimefon and propiconazole on soil bacterial communities. *J Environ Sci Health B* 44(7):681–689
- Yu XM, Yu T, Yin GH, Dong QL, An M, Wang HR, Ai CX (2015) Glyphosate biodegradation and potential soil bioremediation by *Bacillus subtilis* strain Bs-15. *Genet Mol Res* 14(4):14717–14730
- Zadeh AK, Sohrab AD, Alishahi M, Khazaei SH, Asgari HM (2016) Evaluation of acute and sub-lethal toxicity of herbicide, atrazine, on hematological parameters of *Tor grypus*. *J Vet Res* 71(3):295–301
- Zhan H, Feng Y, Fan X et al (2018) Recent advances in glyphosate biodegradation. *Appl Microbiol Biotechnol* 102:5033–5043. <https://doi.org/10.1007/s00253-018-9035-0>
- Zhang Q, Liu Y, Liu YH (2003) Purification and characterization of a novel carbaryl hydrolase from *Aspergillus niger* PY168. *FEMS Microbiol Lett* 228:39–44
- Zhang Y, Meng D, Wang Z, Guo H, Wang Y, Wang X, Dong X (2012) Oxidative stress response in atrazine-degrading bacteria exposed to atrazine. *J Hazard Mater* 229–230:434–438

- Zhang H, Zhang Y, Hou Z, Wang X, Wang J, Lu Z, Zhao X, Sun F, Pan H (2016) Biodegradation potential of deltamethrin by the *Bacillus cereus* strain Y1 in both culture and contaminated soil. *Int Biodeterioration Biodegradation* 106:53–59. <https://doi.org/10.1016/j.ibiod.2015.10.005>
- Zhao SX, Zhang QS, Kong L, Zong YG, Wang RQ, Nan YM et al (2015) Dichlorvos induced autoimmune hepatitis: a case report and review of literature. *Hepat Mon* 15(4):e25469

Chapter 28

Commonly Available Plant Neem (*Azadirachta indica* A. Juss) Ameliorates Dimethoate Induced Toxicity in Climbing Perch *Anabas testudineus*



Santosh Kumar Giri, Sanjib Gorain, Monoj Patra, Dinesh Gope, Nimai Chandra Saha, and Surjyo Jyoti Biswas

Abstract Organophosphorus compounds such as dimethoate (DM) widely used as pesticides due their less persistence in the environment, causes harmful effects in fish and other aquatic organisms. Alcoholic leaf extracts of *Azadirachta indica* (*A. indica*) were verified for their possible modulatory changes in fish (*Anabas testudineus*) by taking into consideration a few haematological, enzymological, histological, and behavioural parameters for 7, 15, and 45 days. Different sets of fish were segregated into the following groups, namely, Group I: normal control without any treatment, Group II: Pesticide treatment at a dose of 13.14 ppm ($\mu\text{g L}^{-1}$) which is 1/3 of LC50 value (DM), Group III: Pesticide treatment as in group II along with *A. indica* extract at a dose of 10.32 ($\mu\text{g L}^{-1}$) which is also 1/3rd of inhibitory concentration of *A. indica* used to reduce the toxicity burden of dimethoate during the determination of its LC50 bioassay, Group IV: Only plant extract treated at a dose of 10.32 ($\mu\text{g L}^{-1}$) which is 1/3rd of inhibitory concentration of *A. indica* used during acute toxicity bioassay. The haematological study reveals that there was a significant decrease of RBC, WBC, MCV, MCHC, and MCH and sudden increase in HCT, PLT in fish treated with DM in comparison to fish treated with DM+ *A. indica* extract and treated only with *A. indica* extract at all the three exposure times (7, 15, and 45 days). Similarly, ALP, ACP, GGT, the content of urea and total cholesterol increased at all three exposure times in DM treated fish group when compared to DM

S. K. Giri · S. Gorain · M. Patra · S. J. Biswas (✉)

Genetics and Cell Biology Laboratory, Department of Zoology, Sidho-Kanho-Birsha University, Purulia, West Bengal, India

D. Gope

Department of Zoology, Ghatal Rabindra Satabarsiki Mahavidyalaya, Ghatal, Paschim Medinipur, West Bengal, India

N. C. Saha

Ecotoxicology Laboratory, Department of Zoology, The University of Burdwan, Burdwan, West Bengal, India

© Springer Nature Switzerland AG 2021

P. K. Shit et al. (eds.), *Spatial Modeling and Assessment of Environmental Contaminants*, Environmental Challenges and Solutions,

https://doi.org/10.1007/978-3-030-63422-3_28

+ *A. indica* extract-treated group. Histopathological observations of gill and liver revealed marked changes in DM treated group which was remarkably modulated in DM+ *A. indica* extract-treated group. Phytochemical analysis of the leaves reveals the presence of many phytoconstituents. *A. indica* was used for the first time to protect *Anabas testudineus* against dimethoate induced toxicity and the present investigation revealed that *A. indica* had potent protective potential against dimethoate toxicity.

Keywords Dimethoate · *Anabas testudineus* · Haematology · Histopathology · GC-MS · *Azadirachta indica* · Inhibitory effect

28.1 Introduction

Agriculture is the most important sector of the Indian economy providing livelihood to nearly 70.1% of the nation's total population (Yadav and Dutta 2019). It was reported that India supported 7.84% of the world's population with 2.4% and 4% of land and water resources respectively (Indira Devi et al. 2017). The importance of pesticides rose quite appreciably over the last few decades due to the demand for increased agronomic production and to safeguard food accessibility for the countries continuously growing population. The increasing demand against declining agricultural area and lower yields led to the use of fertilizers and pesticides. In such a scenario organophosphate were the preferred pesticides due to their efficiency, biodegradability, low persistent in the nature, and their ability to hinder acetylcholinesterase activity in fish, amphibians, and invertebrates (Rhee et al. 2004; Rao et al. 2005; Agrahari et al. 2006). Organophosphates are used rampantly as an insecticide in West Bengal and other parts of India.

These pesticides reach the aquatic ecosystem by direct application and cause undesirable effects on non-target organisms as well (Islam et al. 2019; Das 2013; Nwani et al. 2017). The mutagenic potential of dimethoate was studied by several workers in fish and other aquatic organisms (Dogan et al. 2011; Ali et al. 2008).

Botanical extracts gained much attention in aquaculture to mitigate parasites and predators and slowly became a substitute for pesticides and piscicides. Botanicals are considered promising agents because of their easy availability, less cost, rapid biodegradability, and causes less or no toxicity in animal population (Senthil-Nathan 2020). Numerous works were carried out by various investigators on the efficacy of plant products on pesticidal and piscicidal activities (Tiwari and Singh 2004; Obomanu et al. 2007; Ramanujam and Dominic 2012). Plants biosynthesize a variety of chemicals of various structures that exhibited diverse biological functions and, in this regard, *Azadirachta indica* (*A. indica*, Family: Meliaceae) became popular. *A. indica* is known to have various pharmacological characteristics such as antimicrobial, anti-inflammatory, insect repellent, antifertility, antifeedant, antiparasitic, anti-cancerous, and antidiabetic properties (Lowery and Isman 1993; Purohit 1999; Gbotolorun et al. 2008; Chattopadhyay 2003; Saifullah et al. 2013;

Satyanarayana et al. 2015; Yan et al. 2015; Patel et al. 2016; Akihisa et al. 2017; Nile et al. 2018; Blum et al. 2019; Habluetzelet et al. 2019; Lu et al. 2019; Macchioni et al. 2019). *Anabas testudineus* belonging to family Anabantidae is an important fish species in the Indian subcontinent, found in all types of freshwater aquatic bodies. The fish is often recommended for its nutritional value. Also known as 'climbing perch' it is reported to be used as a fish model in toxicological studies. Hence the present investigation was carried out to find whether *A. indica* can modulate favourably against dimethoate induced toxicity in fish considering several enzymological, haematological, histological, and behavioural parameters.

28.2 Material and Methods

28.2.1 Collection and Acclimatization of Fish Samples

Healthy adult freshwater climbing perch (*Anabas testudineus*) weighing (12.05 ± 0.85 g) were collected from local ponds and acclimated for 15 days in glass aquarium containing 5 litres of dechlorinated tap water under laboratory conditions (temperature $27 \text{ }^\circ\text{C} \pm 1.32 \text{ }^\circ\text{C}$, pH 7.3 ± 0.08 , DO 5.24 ± 0.18 mg/L, Hardness 215.0 ± 5.32 mg/L, Total alkalinity 176.12 ± 4.32) with constant aeration and in natural photoperiod conditions. Water was renewed every third day. Fish were fed with rice cake twice daily and feeding was discontinued 24 h preceding the sacrifice of the test animals.

28.2.2 Preparation of the Leaf Extract

The plant was gathered from the nearby villages of West Midnapore district, West Bengal and identified. A voucher specimen was deposited with Botany Department (V-1244 MDC/2015) for the record. Sundried leaves of *A. indica* (200 g) were extracted in 50% alcohol (the ratio of dried leaves to solvent was 1:10 m/v). Constant stirring for 24 h at $50 \text{ }^\circ\text{C}$ was maintained during the extraction process. The extract so obtained was then dried by evaporation with the help of the Soxhlet apparatus and preserved at $4 \text{ }^\circ\text{C}$ until further analysis. The yield of the extract was 12.04%, which was calculated using the equation: Yield (g/100 g of dry (leaf material)) = $W_1 \times 100 / W_2$, (W_1 represents the mass of the extract after drying of solvent) and W_2 (weight of the dry leaf material).

28.2.3 *Qualitative Phytochemical Screening*

Qualitative phytochemical screening for flavonoids, alkaloids, tannins, carbohydrates, reducing sugars, glycosides, and steroids was undertaken through routine procedures.

28.2.4 *Total Antioxidant Assay and Total Phenol Content*

The antioxidant activity of the plant extracts and their standard was assessed based on the radical scavenging effect of the stable 1, 1-diphenyl-2-picrylhydrazyl (DPPH)-free radical activity by the modified method of Nooman et al. (2008). In brief, various working solutions of test extracts were made in methanol and butylated hydroxytoluene (BHT) was used as standard/reference in a 1–100 µg/ml solution, and also 0.002% of DPPH was made (dissolved in methanol). To 1 ml of sample and standard solution, 1 ml of 0.002% DPPH solution was mixed and thoroughly shaken and kept in darkness for 30 min. Then O.D. (optical density) was taken at 517 nm using (UV-1800 Shimadzu) spectrophotometer. Optical density was documented and the % inhibition calculated using the formula. % age inhibition = $A - B/A \times 100$ where A is the OD of the blank and B is the OD of the sample.

Total phenolics of the extracts were determined following the method of Sadasivam and Manickam (2008) with slight modifications.

28.2.5 *UV-Vis Analysis of Leaf Extract*

One g of *A. indica* leaf powder was kept overnight with 30 ml of 50% alcohol stirred constantly and then filtered. About 1 mL of the filtered sample was scanned using Shimadzu, UV-1800, the scanning range varied from 190 to 450 nm (scanning speed-medium, and slit width 1), to distinguish the leaf extracts distinctive wavelength.

28.2.6 *GC/MS Analysis of Aerial Parts*

GC/MS analysis of *A. indica* leaf extract was conducted as described elsewhere (Biswas et al. 2019). The Gas chromatograph was coupled to a mass spectrophotometer which was equipped with a fused capillary column, Model No: Agilent 190915-433 (HP-5MS, 0.25 mm × 30 m × 0.25 µm). For GC/MS detection the carrier gas was helium with a persistent flow rate of the sample at 1 mL/min with ionization energy of 69.9 eV being utilized. The sample volume injected was 5 µl in

GC grade ethanol at an average velocity of 37 cm/sec. The temperature of the column was initially set to 5 min at 50 °C then it was programmed to 280 °C. The total GC running time was 28 min.

28.2.7 Toxicity Tests of Dimethoate and Determination of Sublethal Concentration

Acute toxicity bioassay procedure was conducted based on earlier methods (APHA et al. 2005). LC_{50} of dimethoate to *Anabas testudineus* was estimated by exposing six groups of fish (5 per group) to differing concentrations of dimethoate with the experiment being repeated twice to obtain the $LC_{50-96-h}$ value of the pesticide. The LC_{50} value at 96 h obtained was 39.44 ppm ($\mu\text{g L}^{-1}$) for *Anabas testudineus* following the Probit analysis method and as previously reported by Finney's (1971). Similarly, LC_{50} value of AI which was 30.96 ppm ($\mu\text{g L}^{-1}$) was also obtained.

The fish specimens were now exposed to one concentration of dimethoate and neem extract in a semi-static system. The exposure was carried out for 7, 15, and 45 days respectively. They were divided into the following sets.

Group I: normal control without any treatment, Group II: Pesticide treatment at a dose of 13.14 ppm ($\mu\text{g L}^{-1}$) which was 1/3 of LC_{50} value (DM), Group III: Pesticide treatment as in group II along with *A. indica* extract at a dose of 10.32 ($\mu\text{g L}^{-1}$) which was also 1/3rd of IC_{50} value (DM+ *A. indica*), Group IV: Only plant extract treated at a dose of 10.32 ($\mu\text{g L}^{-1}$), 1/3rd IC_{50} value (*A. indica*).

Treatment and control were conducted in triplicate and on the sampling day, i.e., 7, 15, and 45 days. To collect blood, the specimen's caudal vein was punctured with heparinized syringe and the blood was collected. Whole blood was utilized for the analysis of the haematological profiles and the serum isolated was used for the analysis of the biomarkers of toxicity like ALP (alkaline phosphatase), ACP (acid phosphatase), GGT (Gama glutamyl transferase), urea, total cholesterol, and HDL cholesterol. Further, tissues including liver and gills were quickly isolated fixed in Bouin's fixative and a routine histology analysis was conducted.

28.2.8 Haematological Analysis

Whole blood with anticoagulant trisodium citrate was subjected to Haematoanalyzer (SB22Plus VET, India) for analysis of WBC, RBC, Haemoglobin, HCT, PLT, MCV, MCH, and MCHC while a part of whole blood was centrifuged at 4000 rpm to collect the serum which was used to assay different enzymes.

28.2.9 Biochemical Analysis

For the alkaline phosphatase (ALP) analysis, Kind and King (1954) technique was followed. Briefly, 50 μl of serum was added to 1500 μl of substrate consisting of phenyl phosphate, phenol, and 4 amino-antipyrine. The orange-red colour complex so formed was read at 510 nm against a suitable blank.

The Szasz (1976) method was followed for analysis of the gamma-glutamyl transferase (GGT). In brief 1000 μl of working reagent consisting of gamma-glutamyl-p-nitroanilide (GPNA) and glycylglycine was mixed with 100 μl of serum and the rate of increase in absorbance being noted at 405 nm against a suitable blank. Estimation of urea, total cholesterol, and HDL cholesterol were undertaken according to the manufacturer's instructions (Span diagnostics Ltd.).

28.2.10 Histology and Behavioural Studies

For the preparation of histological slides, the routine technique of paraffin sectioning of gill and liver (which are the major target organs of dimethoate) was followed with haematoxylin–eosin staining at day 45 only. Serial sections (5 μm) were stained and 10 sections for each animal were examined under the light microscope (E200, Nikon Eclipse).

Behavioural bioassay was carried out on a static type experimental design following the US-EPA-660/3-75-009 protocol. The fish were introduced into the aquaria and allowed to acclimatize for 72 h after which the toxicant was added to the water. Fishes of the treated and control sets were noted for immobilization, excess mucous secretion, opercular movement, scale loss, and changes in colouration of the body. Deceased fish were periodically removed from the aquaria.

28.2.11 Statistical Analysis

At least three experiments were conducted and the data expressed as mean ($\pm\text{SE}$) and analysed by ANOVA (one-way analysis of variance) with p -value less than 0.001 being considered statistically significant.

28.3 Results

Concentration of dissolved oxygen altered between 7.2 and 7.8 mgL⁻¹, water temperature varied from 24.3 °C to 27.8 °C, and the pH from 7.4 to 8.1 during the experimental period. Conductivity varied between 250 and 286 μm cm⁻¹ and the total alkalinity between 150.08 and 176.12 mgL⁻¹.

28.3.1 Phytochemical Screening, Antioxidant Assay and Total Phenolic Content

Preliminary phytochemical screening of the alcoholic leaf extract revealed the occurrence of flavonoids, alkaloids, tannins, carbohydrate, reducing sugars, glycosides, and steroids (Table 28.1). The intensity of the amount present is denoted by + symbol.

Antioxidant properties of the ethanolic leaf extract are provided in Table 28.2, where antioxidant activity (total) of the extract was significantly more compared to the BHT standard at 10 to 30 mg. Total phenolics of the alcoholic leaf extract were 87.83 mg/100 g.

UV absorption of the extract revealed 11 peaks at various wavelengths. Few notable peaks range between 450 nm to 490 nm indicated the presence of carotenoids, the peak at the 250–280 nm region indicated the presence of tannin, flavones, and flavanol resulted in a peak at the region of 300 to 380 nm (Fig. 28.1).

Table 28.1 Preliminary phytochemical screening of *A. indica* leaf extracts

Chemical compounds	Alcoholic leaf extracts of AI
Flavonoids	+++
Alkaloids	++
Tannin	++
Carbohydrate	++
Reducing sugars	++
Glycosides	++
Steroids	++
Saponins	++++

A. indica-*Azadirachta indica*, + minute, ++ less abundant, +++ and ++++ much abundant

Table 28.2 Total antioxidant activity of leaf extract of *A. indica* (**p<0.01, ***p<0.001)

Sample name	% free radical activity (IC ₅₀ values)		
	10 mg	20 mg	30 mg
Standard (BHT)	50.88 ± 0.78***	52.14 ± 0.98**	55.16 ± 0.75**
<i>A. indica</i>	80.66 ± 1.25	82.98 ± 1.11	84.68 ± 0.02

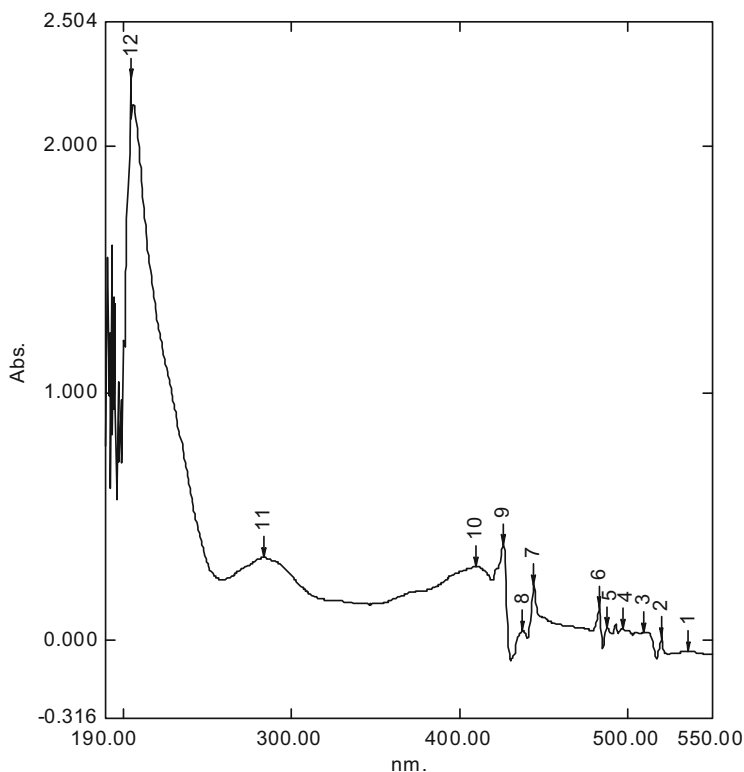


Fig. 28.1 Total antioxidant activity of leaf extract

GC-MS analysis of the alcoholic extract exhibited 12 peaks, of which phytol was a predominant compound having a percentage peak area of 65.85. Other important phytoconstituents present in the extracts were heptacosane, Coumatetralyl-isomer, 3,7,11,15 tetramethyl-2-hexadecen-1-ol (Table 28.3).

The present findings on various haematological parameters revealed that the WBC count was lower in fish treated with DM only at 7- and 15-days of exposure in comparison to DM+ *A. indica* extract-treated group. On the other hand, the RBC count of fish was higher in the DM treated group at 7, 15-, and 45-days exposure in comparison to DM+ *A. indica* group, only *A. indica* extract-treated group and control group. However, the increase was not statistically significant at all the exposure times. The haemoglobin content of fish treated with DM was significantly higher than the control group and only *A. indica* extract-treated group. The haemoglobin content fish treated with DM+ *A. indica* group after 7 days exposure was more when compared to only DM treated fish (Table 28.4). The haematocrit percentage (HCT %) was significantly higher in the DM and DM+ *A. indica* treated group in comparison to only *A. indica* treated group and control at all the exposure times (7, 15, and 45 days) ($p < 0.05$). The haematocrit value was significantly low in fish

Table 28.3 Compounds identified in the ethanolic leaf extract of *Azadirachta indica* by GC-MS study

No	RT	Name of the compound	Mol formula	Mol. wt	Peak area %
1	8.56	2-Hexadecanol	C ₁₆ H ₃₄ O	242	0.52
2	8.99	α D-glucopyranoside	C ₁₈ H ₃₂ O ₁₆	504	0.18
3	11.04	Diethyl phthalate	C ₁₂ H ₁₄ O ₄	222	6.16
4	11.36	E-9-Tetradecenoic acid	C ₁₄ H ₂₆ O ₂	226	0.48
5	13.98	3,7,11,15-Tetramethyl-2-hexadecen-1-ol	C ₂₀ H ₄₀ O	296	3.12
6	14.52	Ethanol, 2-(9-octadecenyloxy)-,(Z)-	C ₂₀ H ₄₀ O ₂	312	0.74
7	15.59	n-Hexadecanoic acid	C ₁₆ H ₃₂ O ₂	256	3.37
8	16.04	Coumatetralyl isomer-2ME	C ₂₀ H ₁₈ O ₃	306	1.72
9	16.80	4-Oxazolecarboxylic acid	C ₁₃ H ₁₅ NO ₃	233	7.08
10	17.64	Phytol	C ₂₀ H ₄₀ O	296	65.85
11	23.81	Diisooctyl phthalate	C ₂₄ H ₃₈ O ₄	390	1.43
12	28.97	Heptacosane	C ₂₇ H ₅₆	380	9.36

RT retention time

treated with DM+ *A. indica* at 7 and 15-days exposure as compared to DM treated group (Table 28.4). The platelet count (PLT) increased significantly at a steady state at 7 and 15 day exposure in the DM treated and DM+ *A. indica* treated group when compared to control and only *A. indica* treated group ($p < 0.001$). However, it dropped significantly at 45 day in DM treated fish as compared to DM+ *A. indica* treated group ($p < 0.05$). The MCV was significantly reduced in all treated groups of fish when compared to control ($p < 0.05$). It was found that the MCV value in DM treated group was significantly lower when compared to DM+ *A. indica* treated group and only *A. indica* treated group ($p < 0.001$, Table 28.4). The mean corpuscular haemoglobin was significantly lower in DM treated group as compared to control, DM+ *A. indica* treated group and only *A. indica* treated group at all the exposure times. A similar trend was also recorded in the changes of MCH and MCHC parameters (Table 28.4).

The alkaline phosphatase (ALP) and acid phosphatase (ACP) activity in serum and liver of fish in all treated groups were significantly higher ($p < 0.05$) than control at all the exposure times (7, 15, and 45 days). However, the ALP and ACP activities were comparatively higher in the DM treated group than DM+ *A. indica* and only *A. indica* treated group ($p < 0.05$) (Table 28.5). The changes in all the haematological parameters of fish treated with *A. indica* were not significant when compared to control ($p > 0.05$) except in MCH and MCHC parameters at 7 days of exposure. The GGT activity in the blood serum and liver was significantly higher in the fish treated with dimethoate in comparison to other groups ($p < 0.001$, Table 28.5). On the other hand, the activity of GGT was significantly lower in DM + *A. indica* treated group at all the exposure times (7, 15, and 45 days) ($p < 0.05$ to $p < 0.001$).

The urea content in the blood serum was significantly higher in the DM treated group as compared to control and other treated groups ($p < 0.001$) at 7, 15, and

Table 28.4 The variation in blood parameters at 7, 15, and 45 days fixation intervals between various groups of fish (DM = dimethoate, *A. indica* = *Azadirachta indica*, * $p < 0.05$, ** $p < 0.01$, *** $p < 0.001$, n=non significant)

	Group I (normal)	Group II DM treated	Group III DM+ <i>A. indica</i>	Group IV <i>A. indica</i> treated
<i>7 days</i>				
WBC ($10^9/L$)	0.25 ± 0.04	0.07 ± 0.001	0.23 ± 0.002*	0.19 ± 0.04
RBC ($10^{12}/L$)	0.01 ± 0.001	0.05 ± 0.11	0.05 ± 0.009 ⁿ	0.04 ± 0.12
HB (g/L)	13.11 ± 0.02	24.12 ± 0.08	26.88 ± 0.14 ⁿ	12.58 ± 0.25
HCT (%)	0.18 ± 0.05	0.32 ± 0.02	0.42 ± 0.14*	0.20 ± 0.02
PLT ($10^9/L$)	180.02 ± 1.11	433.09 ± 0.15	316.48 ± 0.26***	300.01 ± 1.05
MCV (fL)	100.02 ± 0.45	60.05 ± 0.14	80.11 ± 0.15*	50.25 ± 0.86
MCH (pg)	13000.48 ± 5.04	4800.41 ± 1.08	5200.48 ± 2.07***	3000.18 ± 0.51
MCHC (g/dL)	13000.21 ± 2.01	8000.71 ± 0.08	6500.78 ± 0.36***	6000.01 ± 0.14
<i>15 days</i>				
WBC ($10^9/L$)	0.27 ± 0.03	0.19 ± 0.05	0.24 ± 0.002 ⁿ	0.24 ± 0.014
RBC ($10^{12}/L$)	0.11 ± 0.006	0.15 ± 0.02	0.08 ± 0.002 ⁿ	0.07 ± 0.011
HB (g/L)	13.78 ± 0.45	25.63 ± 0.012	22.62 ± 0.11*	13.57 ± 0.86
HCT (%)	0.19 ± 0.03	0.52 ± 0.004	0.47 ± 0.001	0.21 ± 0.01
PLT ($10^9/L$)	179.07 ± 2.35	461.78 ± 4.14	374.98 ± 1.11***	280.16 ± 0.58
MCV (fL)	102.78 ± 0.22	59.47 ± 0.42	91.48 ± 3.04***	96.78 ± 1.02
MCH (pg)	13145.12 ± 4.06	5600.17 ± 1.02	6870.75 ± 1.11*	11721.54 ± 5.03
MCHC (g/dL)	13025.66 ± 1.44	9760.04 ± 4.44	12000.04 ± 3.02	12041.22 ± 4.02
<i>45 days</i>				
WBC ($10^9/L$)	0.27 ± 0.03	0.16 ± 0.001	0.22 ± 0.02*	0.18 ± 0.004
RBC ($10^{12}/L$)	0.03 ± 0.003	0.028 ± 0.001	0.07 ± 0.001	0.02 ± 0.003
HB (g/L)	19.12 ± 0.25	21.022 ± 0.013	20.05 ± 0.45 ⁿ	13.02 ± 1.22
HCT (%)	0.10 ± 0.002	0.40 ± 0.002	0.04 ± 0.01 ⁿ	0.12 ± 0.001
PLT ($10^9/L$)	180.02 ± 3.54	401.25 ± 2.25	295.03 ± 1.66****	115.33 ± 3.08
MCV (fL)	107.22 ± 0.75	50.78 ± 1.02	57.14 ± 1.08*	50.25 ± 1.11
MCH (pg)	6333.33 ± 4.33	4050.02 ± 5.28	4857.22 ± 6.35***	6500.21 ± 1.33
MCHC (g/dL)	19000.45 ± 2.33	5000.20 ± 1.25	4706.11 ± 1.03*	13001.01 ± 0.66

Table 28.6 Concentration of urea and total cholesterol in serum in different dimethoate treated and control groups at different fixation intervals (* $p < 0.05$, ** $p < 0.01$, *** $p < 0.001$)

Fixation intervals in days	Serum urea (mg/100 mL)			Total cholesterol in serum (mg/dL)		
	7	15	45	7	15	45
Group I (normal)	15.11 \pm 1.63	13.26 \pm 1.18	12.42 \pm 0.78	127.28 \pm 1.54	182.33 \pm 1.58	206.38 \pm 1.65
Group II DM treated	40.32 \pm 1.33	34.25 \pm 0.78	23.44 \pm 1.53	214.30 \pm 1.62	201.88 \pm 4.01	292.86 \pm 1.62
Group III DM+ <i>A. indica</i>	23.43 \pm 1.66*	19.56 \pm 4.08	18.29 \pm 1.45*	178.48 \pm 1.61*	195.66 \pm 0.36*	225.34 \pm 1.13**
Group IV <i>A. indica</i> treated	19.34 \pm 0.81	18.11 \pm 0.55	15.17 \pm 0.99	169.34 \pm 1.56	173.58 \pm 2.98	217.34 \pm 1.57

Table 28.7 Concentration of HDL cholesterol in dimethoate treated and control groups at the three fixation intervals (* $p < 0.05$, ** $p < 0.01$, *** $p < 0.001$)

Fixation intervals in days	Serum HDL cholesterol (mg/dL)		
	7	15	45
Group I (normal)	630.30 \pm 1.52	540.22 \pm 2.01	543.55 \pm 1.08
Group II DM treated	596.35 \pm 1.69	423.06 \pm 3.05	314.39 \pm 2.12
Group III DM+ <i>A. indica</i>	683.49 \pm 1.65**	721.22 \pm 6.08***	826.42 \pm 1.53**
Group IV <i>A. indica</i> treated	646.38 \pm 1.68	600.02 \pm 0.38	613.37 \pm 1.38

45 days of exposure. No significant change was recorded in GGT activity and urea content in *A. indica* treated group (Table 28.6). The study on the total cholesterol of blood serum revealed that it was significantly higher ($p < 0.05$) in the DM treated group as compared to other groups at all the exposure times. No significant change of total cholesterol was noted in *A. indica* treated group (Table 28.6). The HDL content of fish treated with DM was significantly lower in comparison to all other groups ($p < 0.001$, Table 28.7).

Histological sections of the gills of the fish revealed that the control group, i.e., Group I showed normal architecture such as filament, the gill lamellae, and the water channels throughout the experiment. But the notable changes such as degeneration of the gill lamellae, hyperplasia, and vacuolar degeneration were found in fish treated with DM for 45 days exposure. The intensity of damage was considerably less in DM+ *A. indica* (Fig. 28.2a–e).

The DM treated fish showed more or less rounded form of hepatocytes, nuclear degeneration, nuclear vacuolation, irregular shaped nuclei, nuclear hypertrophy at 45-day exposure time. The liver of fish treated with DM+ *A. indica* showed reduced rate of nuclear hypertrophy without any nuclear degeneration, a few numbers of irregular shaped nucleus, and vacuolations at all exposure times (Fig. 28.3a–d). No such alterations in the liver histology were recorded in control throughout the experiment at 45 days of exposure. The chord like arrangement of hepatocytes with rounded nucleus and a few vacuolations were also observed in *A. indica* treated fish at 45 days of exposure only.

The hyperexcitability followed by vertical hanging tendency was observed in fish treated with dimethoate at all the exposure times (7, 15, and 45 days). The rate of hyperexcitability gradually decreased with the progress of time of exposure. The hyperexcitability and vertical hanging tendency were also recorded in fish treated with DM+ *A. indica* but the intensity of excitability was comparatively low when compared to DM treated group. No such hyperexcitability and vertical hanging tendency were noted in control and *A. indica* treated fish at all the exposure time.

The rate of the opercular movement of fish treated with DM and DM+ *A. indica* increased significantly over control and *A. indica* treated fish. The intensity of the opercular movement was much higher in DM treated fish and the rate of opercular movement also gradually increased with the progress of time of exposure (Table 28.8). However, the movement of fish was slowed down along with uncoordinated movement noticeable at 45 days exposure period. Noticeable mucus

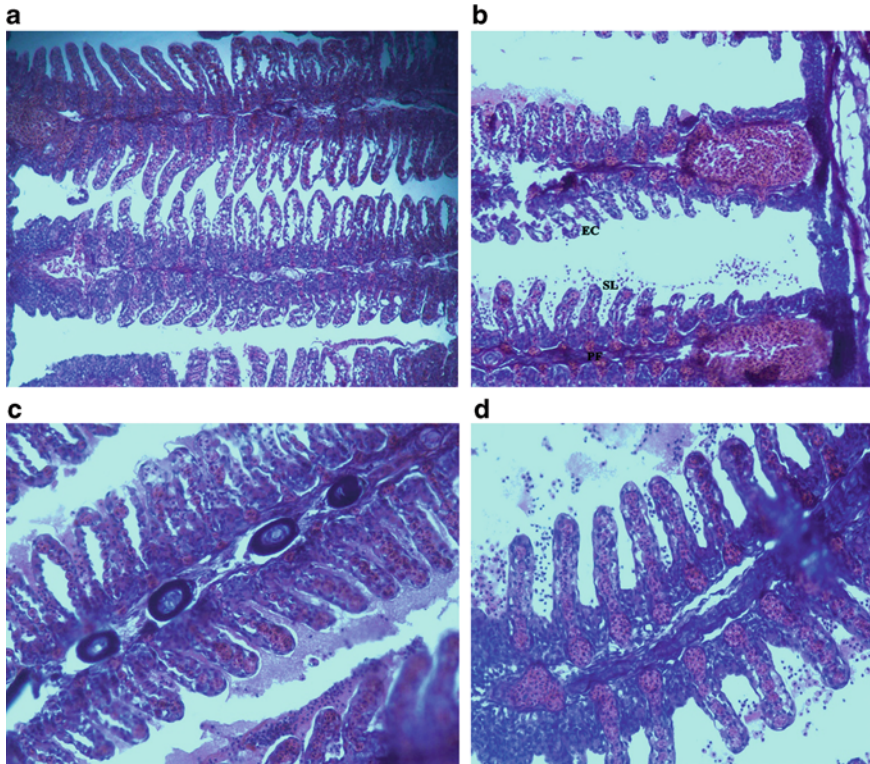


Fig. 28.2 (a) The Gills of normal control fish showed normal tissue architecture, prominent mucous cells, secondary lamellae, epithelial cells, and primary filaments at 45 days. (b) 20 \times . The Gills of DM treated fish showed haemorrhage, degeneration of primary and secondary gill lamellae, vacuolar degeneration, lifting, and proliferation of epithelial cells. 20 \times . (c) The Gills of DM+ *A. indica* treated fish showed less haemorrhage, less degeneration of primary and secondary gill lamellae, few vacuolar degeneration, and proliferation of epithelial cells. 40 \times . (d) The Gills of only *A. indica* treated fish showed no few vacuolar degeneration, almost no degeneration of primary and secondary gill lamellae though few proliferation of cells were present. 20 \times

secretion, scale loss, and the onset of black colouration was observed in fish treated with DM at 45 days of exposure when compared to control and *A. indica* treated groups. In fish that was treated with DM+ *A. indica* through mucus secretion, scale loss, and onset of black colouration was noticed their intensity was less when compared to only DM treated group at 45-day exposure time (Table 28.8).

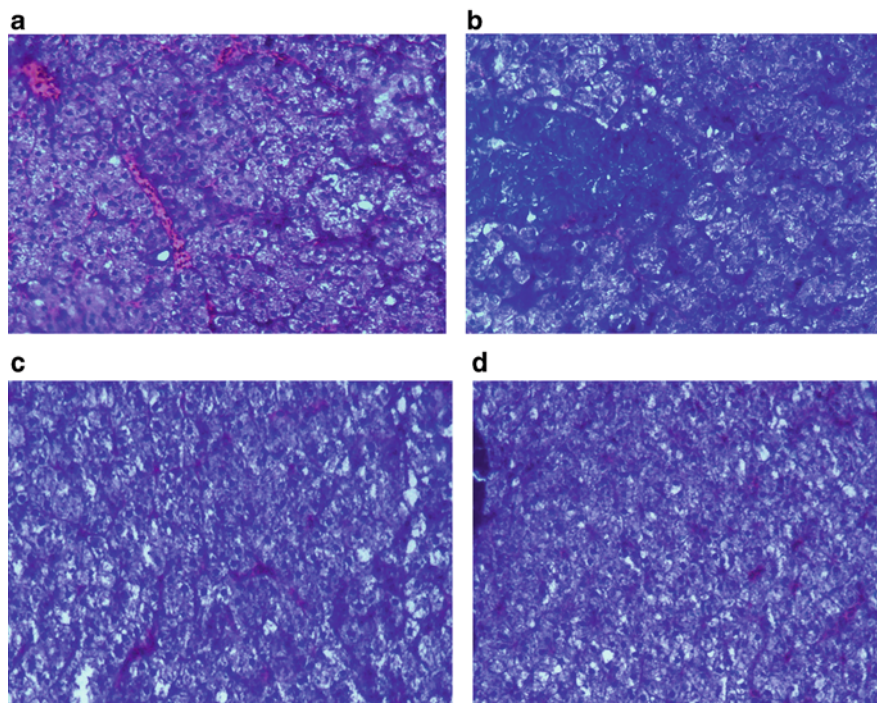


Fig. 28.3 (a) The liver of control fish showed hepatocytes which are polyhedral in shape more or less round nuclei. 20 \times . (b) The liver of DM treated fish showed nuclear hypertrophy, irregular shaped nucleus, noted eosinophilic granules in the cytoplasm, and hepatic necrosis. 20 \times . (c) The liver of DM+ *A. indica* showed somewhat reduction in nuclear hypertrophy, no hepatic necrosis was evident, less number of irregular shaped nucleus and vacuolation. 20 \times . (d) The liver of only *A. indica* treated fish showed hepatocytes arranged as chords, nucleus more or less rounded in appearances and some vacuolation was also evident. 20 \times

Table 28.8 Behavioural changes as observed in the different groups of treated and control fish

Fixation intervals (days)	7			15			45		
	MS	HE	VHP	MS	HE	VHP	MS	HE	VHP
Group I (normal)	+	+	+	+	+	+	+	+	+
Group II (DM treated)	+++	++	++	+++	+	+++	+++	+++	+++
Group III (DM+ <i>A. indica</i>)	+	++	+	+	++	++	++	++	++
Group IV (<i>A. indica</i>)	+	+	+	+	+	+	++	+	+

MS mucous secretion, HE hyperexcitability, VHP vertical hanging posture

28.4 Discussion

Fish are excellent indicators of environmental pollutants (Pacheco and Santos 2002; Scott and Sloman 2004; Obiakor et al. 2014) as they metabolize and assimilate pollutants. The entry of xenobiotics into the body increases the production of ROS

which in turn reacts with the biological molecules and causes an increase in several toxicity biomarkers viz. ALP, ACP, GGT. This was evident in the present investigation in fish treated with DM. A similar trend was also reported by other investigators (Monteiro et al. 2007; Ali et al. 2014).

The effect of dimethoate on the haematology of freshwater fish *Anabas testudineus* was studied. RBCs, haemoglobin, and haematocrit values showed a remarkable increase while MCV, MCH, and MCHC showed a declining pattern in fish treated with DM compared to the normal control, DM+ *A. indica* and only *A. indica* treated groups at all three fixation intervals. As reported by other investigators decrease of the MCHC level indicated a swelling in RBCs which produces macrocytic anaemia (Kavitha et al. 2012). In the present investigation, MCHC values in the normal group and only *A. indica* treated group were more compared to the DM treated group. WBC count increased in the DM treated fish compared to the control, DM+ *A. indica*, and *A. indica* treated groups at all three fixation intervals. Thus, it can be said that an increase in WBC count in response to a toxic condition might be due to the stimulation of lymphopoiesis or due to the release of lymphocytes from lymphoid tissues as a self defence mechanism (Harabawy and Ibrahim 2014; Maurya et al. 2019). Haematological parameters serve as an early indicator of subtle changes in fish health status and have proven to be an indispensable approach to monitor the effects of habitat changes on fish physiology and biology (Sheikh and Ahmed 2016; Abd El-Rahman et al. 2019; Fazio 2019). Gills participate in the respiration and osmoregulation process in fish. They remain in close interaction with the external aquatic environment, sensitive to minor variations in water quality parameters, and are targets of pollutants (Fernandes and Mazon 2003; Camargo and Martinez 2007; Sirimongkolvorakul et al. 2012; Ogbeide et al. 2019). In the present study, we noticed several notable changes in the histology of gills of fish that was treated with the only DM. The changes reverted to by the *A. indica* treatment of fish as found in the present investigation may be due to the conjoint effects of the phytoconstituents present in the extracts. As the liver is the organ for biotransformation it is one of the primary organs affected by contaminants. Several notable degenerative changes were encountered in the livers of fish exposed to DM; however, the intensity of the degenerative changes was favourably modulated by the *A. indica* extract administration. Several other workers have reported changes in hepatocytes due to the toxicants. Dimethoate induces oxidative stress through the generation of ROS which reacts with lipids and proteins causing oxidation (Shi et al. 2005). This could lead to the induction of micronuclei (unpublished data). In the present study, a decrease in MCHC in the DM and DM + *A. indica* treated groups could be attributed to the release of newly formed RBCs into the body circulation of fish which was in line with similar findings by other investigators (Jawale and Dama 2010). A reduction of some activities of enzymes due to *A. indica* treatment may be due to the free radical scavenging activity of the phytoconstituents in the extract which agrees with the findings of other investigators (Sirimongkolvorakul et al. 2012). During the last decade, there is a surge in the search for natural remedies to mitigate the side effects of chemicals and drugs in the aquaculture industry which included bioactive compounds of plant origin. Herbal

biomedicine is a hopeful substitute to synthetic chemicals and the application of these herbal constituents is a probable way to lessen the application of chemical substances and to overcome the ill-effects, residual issues, and drug resistivity (Balasubramanian et al. 2007; Citarasu 2010; Reverter et al. 2014; Jindal et al. 2019). In the present study countering the negative effects of DM by extract of *A. indica* might show a way to reduce the load of xenobiotics and may be helpful in the aquaculture industry. Medicinal plants contain a variety of compounds such as terpenes, and phytol, a diterpene is a product of chlorophyll metabolism. In the present investigation, GC-MS analysis showed a considerable amount of phytol (65.85% peak area), and hence it is suggested that the phytol present in the extract might be responsible for decreasing the toxic effects of dimethoate by scavenging the free radicals.

28.5 Risk and Remediation

Dimethoate is a broad-spectrum contact and systemic insecticide and acaricide which inhibits acetylcholinesterase enzymes and thus causes defective central nervous system. It was introduced in 1956 and still used in many countries. Dimethoate is absorbed readily in the intestine and since it is hydrophilic in nature it does not bioaccumulate in the body and readily excreted. However, it shows potential toxic effects not only in fish but also in other vertebrates. Birds (*Parus major*, *Coturnix coturnix japonica*) when exposed to DM showed inhibition of acetylcholine esterase and cholinesterase activity (Cordi et al. 1997; Westlake et al. 1981). When pregnant rats were treated with different doses of DM it showed various signs of toxicity such as tremors, weakness, and cholinesterase activity were drastically reduced in foetal and maternal brain tissue. The mean foetal weight and the number of living foetus also decreased when compared to controls (Farag et al. 2006). There was a decrease in plasma cholinesterase activity of sprayers who were exposed to 40% concentration of DM (Al-Jaghbir et al. 1992). All these results suggest that aquatic organisms (both target and non-target species) are likely to be more susceptible to DM since they are exposed directly (coming in contact with water). Also considering the disadvantages of synthetic drugs and chemicals there is a need to develop bioremediation strategies that are eco-friendly and sustainable in aquaculture industry. Several plants possess phytoconstituents which are used in aquaculture as chemotherapeutics, additives, growth promoters, to reduce microbial growth and to control stress (Citarasu 2010). About 60 different plants species have been reported for improvement of health status and disease management of fish (Bulfon et al. 2015). Antioxidant activities of putative phytoconstituents involve five primary mechanisms (i) radical scavenging, (ii) breakdown of peroxides, (iii) binding to transition metal ion, (iv) inhibition of chain initiation reaction, and (v) prevention of hydrogen abstraction. Hence, the free radical scavenging capacity of an extract may serve as a significant indicator of potential antioxidant activity. Intensive aquaculture practices led to substantial increase in stress in the fish population which also alters the normal

physiology of these aquatic vertebrates. Treatment of fish with antioxidants, derived from plants, has been reported to increase the efficiency of vitamins. It might be the synergistic action of the antioxidants obtained from plants such as flavonoids, polyphenols, saponins, polyphenols, epigenin, anthocyanin, etc. might counter stress in an effective way in aquatic vertebrates.

28.6 Conclusion

The results of the present investigation suggest and confirm the modulatory role of *A. indica* in restoring the biochemical, histological, and haematological variables induced by DM toxicity. This inexpensive and commonly obtainable natural resource represents a worthwhile substitute to counter pesticide toxicity in aquaculture. More in-depth studies are warranted to understand the underlying mechanism of action. We urge other investigators to confirm or refute these findings.

Acknowledgements The authors sincerely acknowledge with gratitude the Department of Science and Technology, Govt. of West Bengal for providing financial support to carry out the present work (No. 1265(Sanc.)/ST/P/S&T/5G-3/13). SKG acknowledges the support received as JRF from DST-WB. Grateful acknowledgements are also due to the DBT-BOOST No.118/14/BT(Estt)/IP-4/2013 and the DST-FIST (SR/FST/LS-I/2018/173) for infrastructural support.

References

- Abd El-Rahman GI, Ahmed SAA, Khalil AA, Abd-Elhakim YM (2019) Assessment of hematological, hepato-renal, antioxidant, and hormonal responses of *Clarias gariepinus* exposed to sub-lethal concentrations of oxyfluorfen. *Aquat Toxicol* 217:105329. <https://doi.org/10.1016/j.aquatox.2019.105329>
- Agrahari S, Gopal K, Pandey KC (2006) Biomarkers of monocrotophos in a freshwater fish *Channa punctatus* (Bloch). *J Environ Biol* 27(2):453–457
- Akihisa T, Nishimoto Y, Ogihara E, Matsumoto M, Zhang J, Abe M (2017) Nitric oxide production-inhibitory activity of limonoids from *Azadirachta indica* and *Melia azedarach*. *Chem Biodivers* 14(6). <https://doi.org/10.1002/cbdv.201600468>
- Ali D, Nagpure NS, Kumar S, Kumar R, Kushwaha B (2008) Genotoxicity assessment of acute exposure of chlorpyrifos to fresh water fish *Channa punctatus* (Bloch) using micronucleus assay and alkaline single-cell gel electrophoresis. *Chemosphere* 71:1823–1831
- Ali AO, Hohn C, Allen PJ, Ford L, Dail MB, Pruett S, Petrie-Hanson L (2014) The effects of oil exposure on peripheral blood leukocytes and splenicmelano-macrophage centers of Gulf of Mexico fishes. *Mar Pollut Bull* 79(1–2):87–93
- Al-Jaghbir MT, Salhab AS, Hamarshah FA (1992) Dermal and inhalation exposure to dimethoate. *Arch Environ Contamin Toxicol* 22:358–361
- APHA, AWWA, WPCF (2005) Standard methods for the examination of water and waste water, 21st edn. American Public Health Association, Washington, DC
- Balasubramanian G, Sarathi M, Rajesh Kumar S, Sahul Hameed AS (2007) Screening the antiviral activity of Indian medicinal plants against white spot syndrome virus in shrimp. *Aquaculture* 263:15–19

- Biswas SJ, Ghosh G, Dubey VP (2019) Modulation of sodium arsenite-induced toxicity in mice by ethanolic seed extract of *Trigonella foenum graecum*. Phcog Mag 15(S3):386–395
- Blum FC, Singh J, Merrell DS (2019) *In vitro* activity of neem (*Azadirachta indica*) oil extract against helicobacter pylori. J Ethnopharmacol 232:236–243
- Bulfon C, Volpatti D, Galeotti M (2015) Current research on the use of plant derived products in farmed fish. Aquac Res 46:513–551
- Camargo MMP, Martinez CBR (2007) Histopathology of gills, kidney and liver of a neotropical fish caged in an urban stream. Neotrop Ichthyol 5(3):327–336
- Chattopadhyay RR (2003) Possible mechanism of hepatoprotective activity of *Azadirachta indica* leaf extract: part II. J Ethnopharmacol 89:217–219
- Citarasu T (2010) Herbal biomedicines: a new opportunity for aquaculture industry. Aquac Int 18:403–414
- Cordi B, Fossi C, Depledge M (1997) Temporal biomarker responses in wild passerine birds exposed to pesticide spray drift. Environ Toxicol Chem 16(10):2118–2124
- Das S (2013) A review of dichlorvos toxicity in fish. Curr World Environ 8(1):143–149
- Dogan D, Can C, Kocyigit A, Dikilitas M, Taskin A, Bilinc H (2011) Dimethoate-induced oxidative stress and DNA damage in *Oncorhynchus mykiss*. Chemosphere 84(1):39–46
- Farag AT, Karkour TAZ, El Okazy A (2006) Developmental toxicity of orally administered technical dimethoate in rats. Birth Defects Res B 77:40–46
- Fazio F (2019) Fish haematology analysis as an important tool of aquaculture: a review. Aquaculture 500:237–242
- Fernandes MN, Mazon AF (2003) Environmental pollution and fish gill morphology. In: Val AL, Kapoor BG (eds) Fish adaptations. Science Publishers, Enfield, pp 203–231
- Finney DJ (1971) Probit analysis. Cambridge University Press, London
- Gbotolorun SC, Osinubi AA, Noronha CC, Okanlawon AO (2008) Antifertility potential of neem flower extract on adult female Sprague-Dawley rats. Afr Health Sci 8(3):168–173
- Hablutzelet A, Pinto B, Tapanelli S, Nkouangang J, Saviozzi M, Chianese G, Lopatriello A, Tenoh AR, Yerbanga RS, Taglialatela-Scafati O, Esposito F, Bruschi F (2019) Effects of *Azadirachta indica* seed kernel extracts on early erythrocytic schizogony of *Plasmodium berghei* and pro-inflammatory response in inbred mice. Malar J 18(1):35
- Harabawy AS, Ibrahim AT (2014) Sublethal toxicity of carbofuran pesticide on the African catfish *Clarias gariepinus* (Burchell, 1822): hematological, biochemical and cytogenetic response. Ecotoxicol Environ Saf 103:61–67
- Indira Devi P, Thomas J, Raju RK (2017) Pesticide consumption in India: a spatiotemporal analysis. Agric Econ Res Rev 30(1):163–172
- Islam SMM, Rahman MA, Nahar S, Uddin MH, Haque MM, Shahjahan M (2019) Acute toxicity of an organophosphate insecticide Sumithion to striped catfish *Pangasianodon hypophthalmus*. Toxicol Rep 6:957–962
- Jawale CS, Dama LB (2010) Haematological changes in fresh water fish, *Cyprinus carpio* exposed to sub-lethal concentration of piscicidal compounds from cestrum species (Fam: Solanaceae). Natl J Life Sci 7(1):81–84
- Jindal R, Sinha R, Brar P (2019) Evaluating the protective efficacy of *Silybum marianum* against deltamethrin induced hepatotoxicity in piscine model. Environ Toxicol Pharmacol 66:62–68
- Kavitha C, Ramesh M, Kumaran SS, Lakshmi SA (2012) Toxicity of *Moringa oleifera* seed extract on some hematological and biochemical profiles in a freshwater fish, *Cyprinus carpio*. Exp Toxicol Pathol 64(7–8):681–687
- Kind PR, King EJ (1954) Estimation of plasma phosphatase by determination of hydrolysed phenol with amino-antipyrine. J Clin Pathol 7(4):322–326
- Lowery DT, Isman MB (1993) Antifeedant activity of extracts from neem, *Azadirachta indica*, to strawberry aphid, *Chaetosiphonfragaefolii*. J Chem Ecol 19(8):1761–1773
- Lu XF, Lin PC, Zi JC, Fan XN (2019) Limonoids from seeds of *Azadirachta indica* and their antibacterial activity. Zhongguo Zhong Yao Za Zhi 44(22):4864–4873

- Macchioni F, Sfingi M, Chiavacci D, Cecchi F (2019) *Azadirachta indica* (Sapindales: Meliaceae) Neem oil as a repellent against *Aedes albopictus* (Diptera: Culicidae) mosquitoes. *J Insect Sci* 19 (6):12
- Maurya PK, Malik DS, Yadav KK, Kumar A, Kumar S, Kamyab H (2019) Bioaccumulation and potential sources of heavy metal contamination in fish species in river Gangabasin: possible human health risks evaluation. *Toxicol Rep* 6:472–481
- Monteiro M, Quintaneiro C, Nogueira AJ, Morgado F, Soares AM, Guilhermino L (2007) Impact of chemical exposure on the fish *Pomatoschistus microps* Krøyer (1838) in estuaries of the Portuguese northwest coast. *Chemosphere* 66(3):514–522
- Nile AS, Nile SH, Keum YS, Kim DH, Venkidasamy B, Ramalingam S (2018) Nematicidal potential and specific enzyme activity enhancement potential of neem (*Azadirachta indica* A. Juss.) aerial parts. *Environ Sci Pollut Res Int* 25(5):4204–4213
- Nooman AK, Shakya AK, Al-Othman A, El-Agbar Z, Farah H (2008) Antioxidant activity of some common plants. *Turk J Biol* 32:51–55
- Nwani CD, Somdare PO, Ogueji EO, Nwani JC, Ukonze JA, Nwadinigwe AO (2017) Genotoxicity assessment and oxidative stress responses in freshwater African catfish *Clarias garipinus* exposed to fenthion formulations. *Drug Chem Toxicol* 40(3):273–280
- Obiakor MO, Okonkwo JC, Ezeonyejiaku CD (2014) Genotoxicity of freshwater ecosystem shows DNA damage in preponderant fish as validated by in vivo micronucleus induction in gill and kidney erythrocytes. *Mutation Res Genetic Toxicol Environ Mutagen* 775–776:20–30
- Obomanu FG, Ogbalu OK, Gabriel UU, Fekarurhobo SGK, Abadi SU (2007) Piscicidal effects of *Lepidagathis alopecuroides* on mudskipper, *Periophthalmus papillio* from the Niger delta. *Res J Appl Sci* 2(4):382–387
- Ogbeide O, Uhunamure G, Uwagboe L, Osakpamwan T, Glory M, Chukwuka A (2019) Comparative gill and liver pathology of *Tilapia zilli*, *Clarias gariepinus* and *Neochanna diversus* in owan river (Nigeria): relative ecological risks of species in a pesticide-impacted river. *Chemosphere* 234:1–13
- Pacheco M, Santos MA (2002) Biotransformation, genotoxic, and histopathological effects of environmental contaminants in European eel (*Anguilla anguilla* L.). *Ecotoxicol Environ Saf* 53(3):331–347
- Patel SM, Nagulapalli Venkata KC, Bhattacharyya P, Sethi G, Bishayee A (2016) Potential of neem (*Azadirachta indica* L.) for prevention and treatment of oncologic diseases. *Semin Cancer Biol* 40–41:100–115
- Purohit A (1999) Antifertility efficacy of neem bark (*Azadirachta indica* A. Juss.) in male rats. *Anc Sci Life* 19(1–2):21–24
- Ramanujam SN, Dominic R (2012) Median lethal concentration (LC50) of piscicidal plants and their utilization in aquaculture. *J Appl Aquac* 24(4):326–333
- Rao JV, Begum G, Pallela R, Usman PK, Rao RN (2005) Changes in behaviour and brain acetylcholinesterase activity in mosquito fish, *Gambusia affinis* in response to the sub-lethal exposure to chlorpyrifos. *Int J Environ Res Public Health* 2(3–4):478–483
- Reverter M, Bontemps N, Lecchini D, Banaigs B, Sasal P (2014) Use of medicinal plant extracts in fish aquaculture as an alternative to chemotherapy: current status and future perspectives. *Aquaculture* 433:50–61
- Rhee IK, Appels N, Hofte B, Karabatak B, Erkelens C, Stark LM, Flippin LA, Verpoorte R (2004) Isolation of the acetylcholinesterase inhibitor ungeremine from *Nerine bowdenii* by preparative HPLC coupled on-line to a flow assay system. *Biol Pharm Bull* 27(11):1804–1809
- Sadasivam S, Manickam A (2008) Biochemical methods for agricultural sciences. New Age International Publication (Pvt) Ltd, Chennai, India, pp 203–211
- Saifullah KS, Azizuddin HSA, Kashif M, Jabeen A, Asif M, Mesaik MA, Ul-Haq Z, Dar A, Choudhary MI (2013) In-vitro immunomodulatory and anti-cancerous activities of bio-transformed products of dianabol through *Azadirachta indica* and its molecular docking studies. *Chem Centr J* 7:163

- Satyanarayana K, Sravanthi K, Shaker IA, Ponnulakshmi R (2015) Molecular approach to identify antidiabetic potential of *Azadirachta indica*. *J Ayurveda Integr Med* 6(3):165–174
- Scott GR, Sloman KA (2004) The effects of environmental pollutants on complex fish behaviour: integrating behavioural and physiological indicators of toxicity. *Aquat Toxicol* 68(4):369–392
- Senthil-Nathan S (2020) A review of resistance mechanisms of synthetic insecticides and botanicals, phytochemicals, and essential oils as alternative larvicidal agents against mosquitoes. *Front Physiol* 10:1591
- Sheikh ZA, Ahmed I (2016) Seasonal changes in hematological parameters of snow trout *Schizothorax plagiostomus* (Heckel 1838). *Int J Fauna Biol Stud* 3:33–38
- Shi S, Wang G, Wang Y, Zhang L, Zhang L (2005) Protective effect of nitric oxide against oxidative stress under ultraviolet-B radiation. *Nitric Oxide* 13(1):1–9
- Sirimongkolvorakul S, Tansatit T, Preyavichyapugdee N, Kosai P, Jiraungkoorskul K, Jiraungkoorskul W (2012) Efficiency of *Moringa oleifera* dietary supplement reducing lead toxicity in *Puntius altus*. *J Med Plants Res* 6(2):187–194
- Szasz G (1976) Reaction-rate method for gamma-glutamyltransferase activity in serum. *Clin Chem* 22(12):2051–2055
- Tiwari S, Singh A (2004) Toxic and sub-lethal effects of olendrin on biochemical parameters of freshwater air breathing murrel, *Channa punctatus* (Bloch). *Indian J Exp Biol* 42:413–418
- Westlake GE, Bunyan PJ, Martin AD, Stanley PI, Steed LC (1981) Organophosphate poisoning. Effects of elected organophosphate pesticides on plasma enzymes and brain esterases of Japanese quail (*Coturnix coturnix japonica*). *J Agric Food Chem* 29:772–778
- Yadav S, Dutta S (2019) A study of pesticide consumption pattern and farmer's perceptions towards pesticides: a case of Tijara Tehsil, Alwar (Rajasthan). *Int J Curr Microbiol Appl Sci* 8(4):96–104
- Yan YX, Liu JQ, Wang HW, Chen JX, Chen JC, Chen L, Zhou L, Qiu MH (2015) Identification and antifeedant activities of limonoids from *Azadirachta indica*. *Chem Biodivers* 12(7):1040–1046

Chapter 29

Estimating Particulate Matter Concentrations from MODIS AOD Considering Meteorological Parameters Using Random Forest Algorithm



Eeshan Basu and Chalantika Laha Salui

Abstract Air pollution is a major issue in urban areas. The concentration of suspended particulate matters causes a steep degradation of the air quality. Kolkata is a highly sensitive area in this respect due to its concentration of residential areas, growing population stimulating urbanization, and industrial setups. The weather of Kolkata has been changing rapidly over the last decade. Researches have proved that the increase in pollution over the last decade has a significant contribution to influencing the change in weather pattern all across the globe. The present chapter tries to analyze the inter-dependability of different meteorological parameters with the particulate matter concentration in Kolkata for a period from 2015 to 2017. In this chapter, multi-linear regression was performed to show a correlation between the daily aerosol optical depth obtained from MODIS and the ground concentration of particulate matters taking into consideration various meteorological parameters like temperature, relative humidity, wind speed, precipitation, and cloud fraction. For this purpose, cloud cover was derived for each pixel from the same input image, as time variation may cause discrepancies. Finally, a model was made using Random Forest Regression to find out the same inter-dependability. The validation accuracy for $PM_{2.5}$ and PM_{10} was 90% and 96%, respectively. According to the model, temperature was the most important parameter for the analysis.

Keywords MODIS AOD · Random forest regression · Machine learning · Meteorological parameters · Cloud fraction

E. Basu · C. L. Salui (✉)

Department of Mining Engineering, Indian Institute of Engineering Science and Technology, Shibpur, Howrah, India

© Springer Nature Switzerland AG 2021

P. K. Shit et al. (eds.), *Spatial Modeling and Assessment of Environmental Contaminants*, Environmental Challenges and Solutions,
https://doi.org/10.1007/978-3-030-63422-3_29

591

29.1 Introduction

The area of India is 3.287 million square kilometers. In India, different pollution-causing agents are monitored by the Central Pollution Control Board at 202 locations as of September 15, 2019. Because of this huge area, measurements become sporadic with a few number of ground monitoring stations. Apart from that, these observations include a lot of missing data. The number of ground stations is inadequate for such a vast area. Satellite observations can be used as a surrogate to the existing network of these ground monitoring stations (Chelani 2019).

The MODIS was built by Santa Barbara Remote Sensing. With the Terra (EOS AM) satellite, MODIS was launched into orbit by NASA in 1999. In 2002, the Aqua (EOS PM) satellite was added. It has a high radiometric sensitivity of 12 bit across 36 spectral bands, which ranges from 0.4 μm to 14.4 μm with its two satellites.

MODIS has great global coverage, dynamic ranging, high radiometric resolution, and accurate calibration in the visible and IR regions. It is designed for retrievals of atmospheric properties. Because of these reasons, it can provide accurate insight into the global distribution of aerosols (King et al. 1996).

A study over Taiwan from a period of 2006 to 2008, correlating the AOD obtained from MODIS Terra sensor and AERONET data showed a correlation coefficient of 0.91. When the Aqua sensor was used, the correlation coefficient of 0.83. The correlations in the warm season (March to August) was 0.78 to 0.87 while the correlation during the cold months (September to February) was 0.85 to 0.96.

Other satellites used for studies in this field are namely ASTER Image Sensor, LIDAR, SPOT, and LANDSAT ETM+.

Aerosols affect radiation both directly and indirectly. Direct effects on radiation by aerosols include absorption and scattering of longwave and solar radiation (Yang et al. 2016). Aerosols can change the macro- and micro-physical properties of clouds serving as cloud condensation nuclei or ice nuclei. These changes are referred to as indirect effects (Liu et al. 2012; Zhao and Garrett 2015).

Aerosol Optical Depth represents the total atmospheric columnar loading of aerosols. When surface measurements are unavailable, AOD derived from satellite images can be used to assess ground particulate air quality.

Retrieval of surface $\text{PM}_{2.5}$ concentration through aerosol satellite products has become a popular particulate matter monitoring method due to its extensive spatial distribution and ground coverage. Aerosol optical depth (AOD) is the most commonly used satellite product as there are no direct methods to estimate the surface concentration of particulate matter. Many researchers started retrieving surface $\text{PM}_{2.5}$ concentration from AOD for various regions and countries with different retrieving techniques (Tian and Chen 2010; Ma et al. 2014; Fang et al. 2016; Yin et al. 2016; Li et al. 2017a, b; Hu et al. 2017; De Hoogh et al. 2018; He and Huang 2018). These techniques mainly build a relation between $\text{PM}_{2.5}$ concentration and satellite-derived AOD.

When particulate matter air quality is monitored from space-borne sensors, the measurement is mainly confined to relating AOD with ground particulate matter

concentrations. However, the relationship is not linear and meteorological parameters such as wind speed, temperature, and humidity, and also the vertical distribution of aerosols impact the AOD–PM_{2.5} relationship.

The stability of the atmosphere is governed by the height of the planetary boundary layer, temperature, and precipitation which results in the vertical distribution of pollution. The physical properties and chemical composition of aerosols are affected by temperature, which in turn has an influence on the aerosol formation (Price et al. 2016). The horizontal transport of pollution is also influenced by temperature. Relative humidity affects the particle size of the pollutants and the extinction of radiation in the atmosphere.

A study using both ground and satellite observations in Beijing from 2011 to 2015 found a significant correlation when factors like aerosol type, RH, height of planetary boundary layer, wind speed, wind direction, and vertical structure of aerosol distribution were considered.

Boundary layer height, along with a lot of other important parameters are not routinely monitored in India (Yogesh Sathe et al. 2019). As a result, this chapter does not take into consideration the height of the planetary boundary layer.

29.2 Machine Learning Approach: Random Forest Regression

Other than the conventional statistical models, the machine learning approach has been used in recent days. Machine learning, which is a subdivision of AI, is one of the best ways to address the complex relationship among AOD, PM, and related variables, such as the meteorological parameters and generally achieve outstanding predictive results (Zhan et al. 2017). Different researchers have applied numerous machine learning approaches on the satellite-based PM_{2.5} concentration estimation; the ANN model (Feng et al. 2015), the back-propagation neural network, the generalized regression neural network (Li et al. 2017b), the geo-intelligent deep belief network (Li et al. 2017a), and support vector regression (Hou et al. 2014).

To simulate the PM_{2.5} concentration, Liu et al. (2019) built an RF model using top of the atmosphere reflectances, meteorological parameters, and observation angles. This was the Ref-PM_{2.5} model. For comparison, another RF model, the AOD-PM_{2.5} model, was developed using AOD and meteorological variables. When cross-validated, both the models, the Ref-PM_{2.5} model and the AOD-PM_{2.5} model had similar R^2 (RMSE, MPE) of 0.86 (17.2 $\mu\text{g m}^{-3}$, 10.3 $\mu\text{g m}^{-3}$) and 0.86 (17.3 $\mu\text{g m}^{-3}$, 10.3 $\mu\text{g m}^{-3}$), respectively.

Using data of 2011 over the USA, Hu et al. developed an RF model using AOD, meteorological parameters, land-use variables to estimate ground-level PM_{2.5} concentrations. They included temperature, relative humidity, barometric pressure, wind speed and direction, and other land-use parameters like population density, number

of highways, etc. in their study. He achieved an R^2 of 0.80 and MPE and RMSPE of 1.78 and $2.83 \mu\text{g m}^{-3}$, respectively.

29.3 Study Area

Kolkata ($22^{\circ}33'45.5''$ N $88^{\circ}21'46.9''$ E), the capital of West Bengal and the second most polluted city in India, is a major metropolis in eastern India (Fig. 29.1). Pollution levels during the monsoons are the lowest, followed by the summer months. Winters are the worst when it comes to pollution due to low wind speed and low temperature, and the city often experiences smog early in the morning.

Pollution levels have degraded over the past decade, and the government's stringent laws have been futile. Continued monitoring of air quality is required throughout the city, but the number of ground stations is faulty and limited. For this reason, satellite images can be used as a substitute as it covers a massive area at a single time.

The AQI on November 7, 2019 reached a new low for this year, 343, which falls in the "inferior" category of the AQI scale. From November 15 to 18, 2018, the AQI of Kolkata was even worse than Delhi and thus became the most polluted metropolis. On December 19, 2017, the $\text{PM}_{2.5}$ concentration of Kolkata was twice that of Delhi, thrice that of Mumbai, and four times that of Chennai. Reports suggest that this

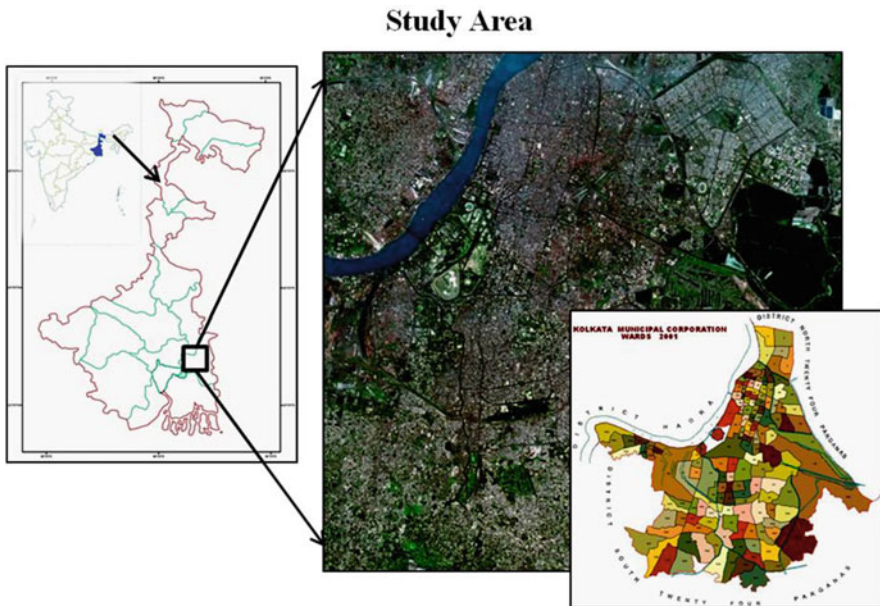


Fig. 29.1 Study area (Kolkata)

drastic decrease in air quality is mainly due to the growing number of diesel cars. Kolkata is the diesel automobile capital of India, and 65% of the vehicles plying on the road are diesel cars. For every 100,000 citizens, 18.4 of them are reported to have lung cancer in the city.

29.4 Materials and Methodology

Temporal data for each day for the years 2015–2017 was collected. The temporal data include all secondary data, namely, Satellite images—MODIS Aerosol Product MOD04_L2, PM concentrations, Rainfall, Cloud Fraction, Wind Speed, Relative Humidity, and Temperature. The images were collected from the LAADS DAAC website. The secondary data were mainly obtained from government websites, namely the Central Pollution Control Board website (<https://cpcb.nic.in/>), the West Bengal Pollution Control Board website (<http://www.wbpcb.gov.in/>). Aerosol Optical Depth for each day was obtained from the satellite images after applying image preprocessing and processing. All the other secondary data also needed to be preprocessed and processed before implementing the algorithms.

In the Random Forest algorithm, arbitrary forests were created with the whole dataset and validated for 2015–2017 by only taking the average of the dataset in which the new data falls. If the results were satisfactory, then the output was taken. If the accuracy was below par, then again, the whole process was repeated, i.e., creating random forests with the dataset and checked it with the test set (Fig. 29.2).

29.4.1 Data Collection

The collection of the data was done primarily from secondary governmental sources and later modified with the help of statistical equations.

The MODIS Aerosol Product, MOD04_L2 was used for AOD data. The website used to collect the data was <https://ladsweb.modaps.eosdis.nasa.gov/>. The sensor selected was MODIS Terra; the product chosen was MOD04_L2 (10Km). The *AOD_550_Dark_Target_Deep_Blue_Combined* algorithm was selected while retrieving the data. The site then gives the satellite images in a GeoTIFF file. In ArcGIS a scale factor of 0.001000000047497451 was multiplied with the entire raster file, using the raster calculator so that the values of all the AOD in the image fall in the range of 0 and 1.

To check whether the values collected were correct, another website <https://neo.sci.gsfc.nasa.gov/> was referred which provides tabular data at every 0.1-degree interval and a temporal resolution of 8 days.

The extraction of pollutant concentrations (PM₁₀, PM_{2.5}) was done from the website of West Bengal Pollution Control Board <http://www.wbpcb.gov.in/>. Relative humidity, rainfall, and temperature for the years 2015 to 2017 were collected

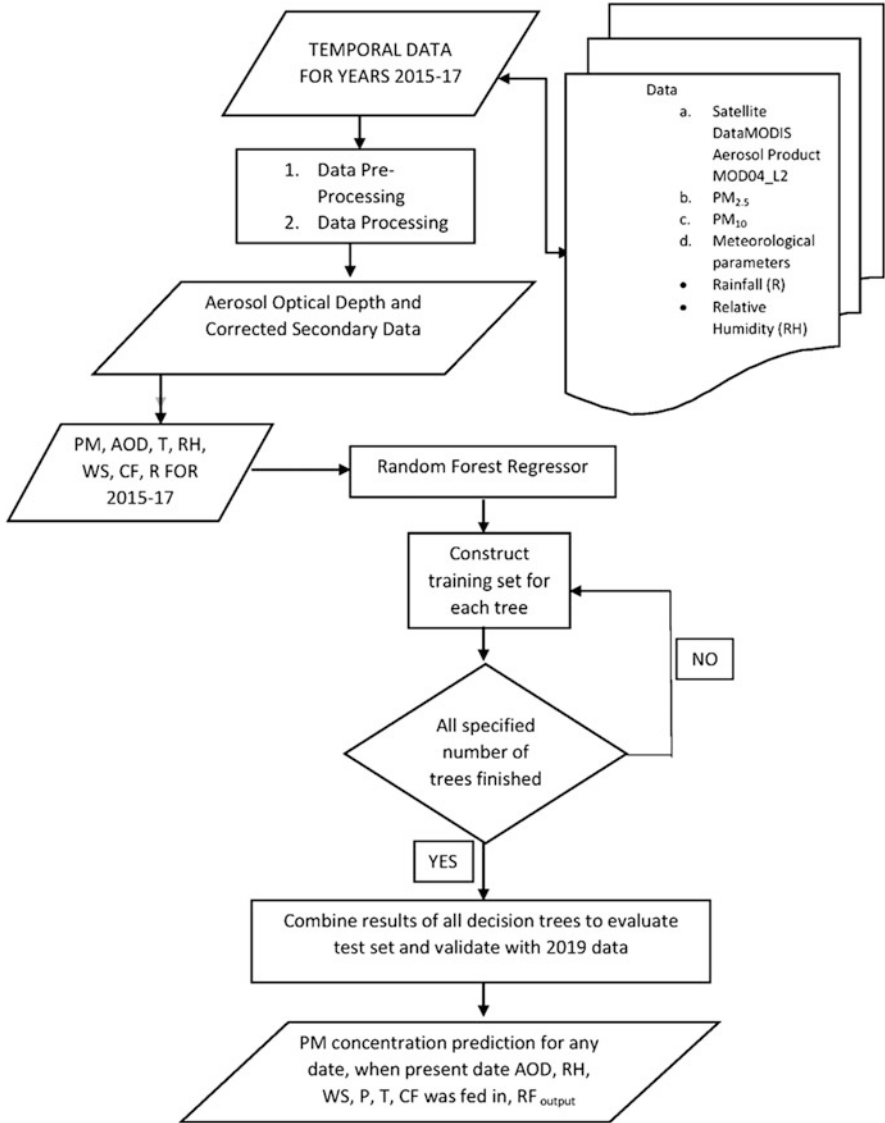


Fig. 29.2 Methodology flowchart

from the office of Regional Meteorological Centre, Kolkata located in Alipore. The data for wind speed was obtained from the website <https://www.timeanddate.com/>.

Cloud fraction, in satellite imagery, is the percentage of each pixel that is covered with clouds. A cloud fraction of unity means the pixel is completely covered with clouds, while a cloud-free pixel will have a zero value. Hence, the values of cloud fraction were between 0 and 1. Cloud Fraction data for the years 2015–2017 were

taken from https://neo.sci.gsfc.nasa.gov/view.php?datasetId=MYDAL2_M_CLD_FR.

29.4.2 Data Preprocessing

Even after taking the average of every 8 days, there were some instances in the dataset where the cells were empty. When such a situation was experienced, the entire row was deleted. After applying preprocessing on the data, the .csv file had 98 observations. This .csv file is the final dataset on which the two machine learning algorithms were implemented.

Before applying the machine learning algorithm to the data, the entire analysis was done in Microsoft Excel. This analysis was done to find the significance of each independent parameter with the dependent parameters, i.e., the concentrations of PM_{10} and $PM_{2.5}$. After doing the multi-linear regression in Excel, all the P -values (except relative humidity and cloud fraction) were well below the value of 0.01, making them significant parameters for the analysis (Table 29.1).

Still, to make the P -values even lower, the rainfall was classified into binary values of 0s and 1s. Zero was given to the cells where the average of 8 days did not receive any rain, and one was given to the cells where the average value of 8 days rainfall was not equal to zero.

Now it was seen that only the P -values of cloud fraction was around 38%, but all the other P -values were well below the 1% mark. So, this dataset, where rainfall was classified, was chosen as the file where the machine learning algorithm was run (Table 29.2).

29.4.3 Implementation

The Random Forest Regression has been implemented using Python 3.7, and the codes have been written in Spyder. The various libraries used in the codes are NumPy, pandas, Matplotlib, and Sci-Kit Learn:

Spyder: The Scientific Python Development Environment is an open-source, cross-platform IDE for scientific programming in Python.

NumPy: It is the Python library for working with arrays. It is mainly used for scientific computing. It is the numeric mathematics extension of Python.

Pandas: It is a high-level data manipulation and data analysis tool. It has been built on the NumPy package, and its data structure is called the DataFrame. Using DataFrames, data can be stored and manipulated in a tabular format in rows of observations and columns of variables.

Matplotlib: This is a plotting library used in Python and NumPy.

Sci-Kit Learn: It is a free machine learning library in Python. The models implemented in this project was run using the sci-kit learn library.

29.5 Results

29.5.1 Processing and Outcome

After importing the various libraries, the .csv file was imported using the pandas library.

```

"""Importing the libraries"""
import numpy as np
import pandas as pd
import matplotlib.pyplot as plt

"""Importing the dataset"""

dataset = pd.read_csv ("D:\project\PM2.5_rf.csv")
x = dataset.iloc[:, :-1].values
y = dataset.iloc[:, -1].values

```

All other columns except the Particulate Matter Concentrations were set as the x parameter and PM concentrations as the y parameter (Table 29.3).

Then the RandomForestRegressor class was imported from sci-kit-learn, and an object of that class was created. As the whole dataset had 98 observations, we choose ten trees per forest, i.e., $n_estimators = 10$. Then, the entire dataset was split into a training set, and test set and the $test_size$ was 0.1, i.e., 10% of the sample size.

Table 29.3 Dataset

Index	AOD	Temperature	Wind speed	Cloud fraction	Relative humidity	Rainfall	PM10
0	0.854	21.47	7.37	0.744	81.5	0	151.76
1	0.697	18.89	7.41	0.772	79.75	0	232.44
2	0.744	18.95	8.5	0.295	78.87	0	222.9
3	0.783	21.44	6.66	0.512	74.86	0	190.02
4	0.717	21.3	6.8	0.61	69.5	0	201.08
5	0.917	23.38	6.7	0.634	71.87	0	195.68
6	0.756	26.38	9.06	0.26	81.86	0	105.82
7	0.622	27.52	9.16	0.35	77.25	1	120.35
8	0.492	25.9	5.06	0.039	51.12	0	143.83
9	0.673	28.35	7.16	0.126	54.75	0	144.4


```

"""Training the Random Forest Regression model on the whole dataset"""
from sklearn.ensemble import RandomForestRegressor
regressor = RandomForestRegressor(n_estimators = 10, random_state = 0)

"""Test Train Split"""

from sklearn.model_selection import train_test_split
x_train, x_test, y_train, y_test = train_test_split(x, y, test_size = 0.1, random_state = 1)

```

After this feature scaling was applied on the x parameters except for the rainfall parameter, this was done to make the values of every parameter fall in the same range. From sklearn's preprocessing module, we imported the StandardScaler function to do the feature scaling.

```

"""Feature Scaling"""

from sklearn.preprocessing import StandardScaler
sc = StandardScaler()
x_train[:, :5] = sc.fit_transform(x_train[:, :5])
x_test[:, :5] = sc.transform(x_test[:, :5])

```

After Feature Scaling was implemented, the x_{train} and y_{train} were fit into an object of the class RandomForestRegressor, and the model was made.

```

"""Fit Model"""

regressor.fit(x_train, y_train)
y_train_pred = regressor.predict(x_train)
y_test_pred = regressor.predict(x_test)

```

While analyzing with $PM_{2.5}$, the training set accuracy was 0.961, and the test set accuracy was 0.952.

```

forest train score 0.961, forest test score: 0.952
[0.0360063 0.8156457 0.07472399 0.03482404 0.02913969 0.00966029]

```

According to this model, the most important parameter to decide the output was temperature. Using the feature importances function, it was found out that the importance of the temperature parameter was 0.815. The rainfall parameter was the least important.

The Y_{Test} vs $Y_{Predicted}$ has been plotted below (Fig. 29.3).

While modeling the Random Forest, the number of trees used were 10, but the validation accuracy was not the highest when ten trees were used for the forest. The

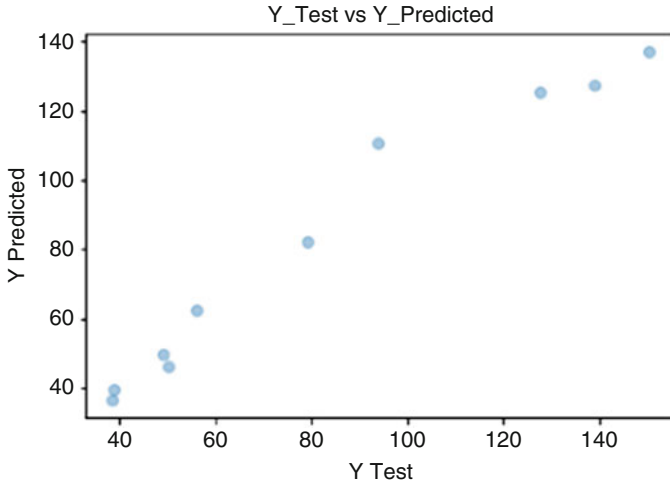


Fig. 29.3 Y_{Test} vs $Y_{Predicted}$ for $PM_{2.5}$

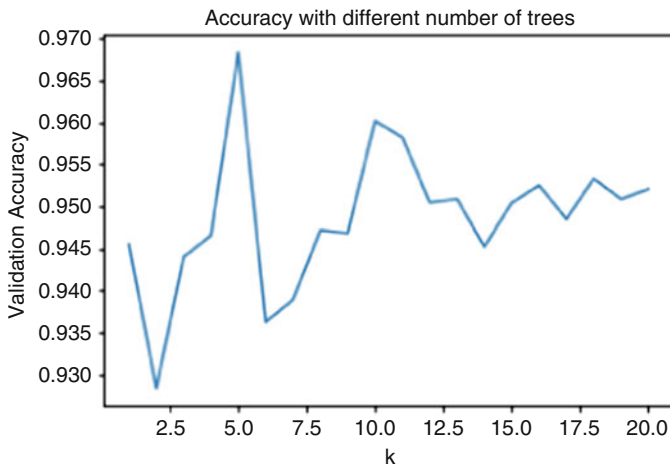


Fig. 29.4 Accuracy for different sizes of forest

below graph shows how the validation accuracy changes when the number of trees used to train the model was changed. Maximum accuracy, i.e., around 0.97, could have been achieved if five trees were used to build the forest (Fig. 29.4).

While analyzing with PM_{10} , the training set accuracy was 0.965, and the test set score was 0.932.

```
forest train score 0.965, forest test score: 0.932  
[0.03013622 0.82181312 0.05218071 0.04203503 0.04178591 0.012049 ]
```

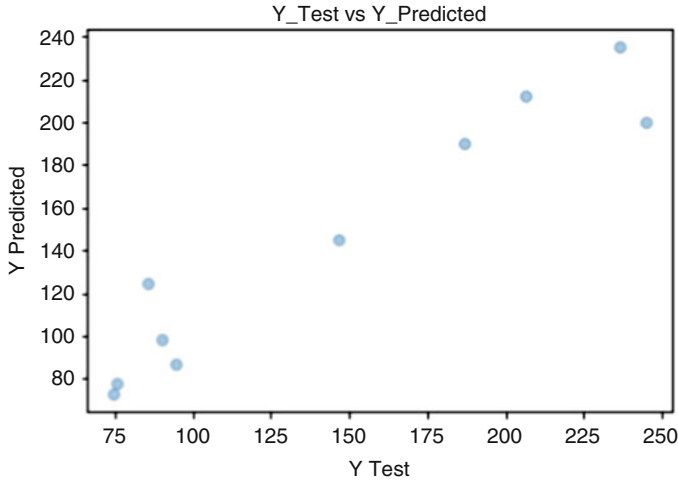


Fig. 29.5 Y_{Test} vs $Y_{Predicted}$ for PM_{10}

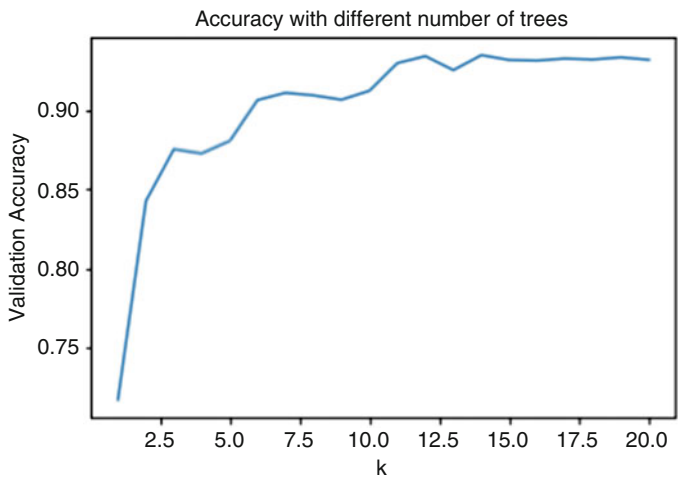


Fig. 29.6 Accuracy for different sizes of forest

For PM_{10} also, the most important parameter to decide the output was temperature. Using the feature importances function, it was found out that the importance of the temperature parameter was 0.82. The rainfall parameter was the least important. The Y_{Test} vs $Y_{Predicted}$ has been plotted below (Fig. 29.5).

In the case of PM_{10} , the maximum validation accuracy could have been achieved if >11 trees were used to build the forest (Fig. 29.6).

29.5.2 Validation

For validation, data for October 2019 was used. First, all the PM_{2.5} and PM₁₀ data were collected for all the stations of Kolkata (Fig. 29.7) namely Rabindra Bharati, Bidhannagar, Fort William, Victoria, Ballygunge, Rabindra Sarobar, and Jadavpur from October 16 to 23, 2019. Next, the AOD values were calculated using satellite images for the same period. Then the meteorological data was taken for the same time-frame for Alipore. Finally, the cloud fraction data was collected. The 8-day average was then calculated and stored in a .csv file.

Then using Kriging in ArcGIS, the PM_{2.5} and PM₁₀ concentrations were found out for Alipore, which were 132.73 and 104.11, respectively. In the .csv file, the averages of PM_{2.5} and PM₁₀ for Kolkata were 138.57 and 102.81, respectively. Then using the .csv file, the particulate matter concentrations were estimated using the

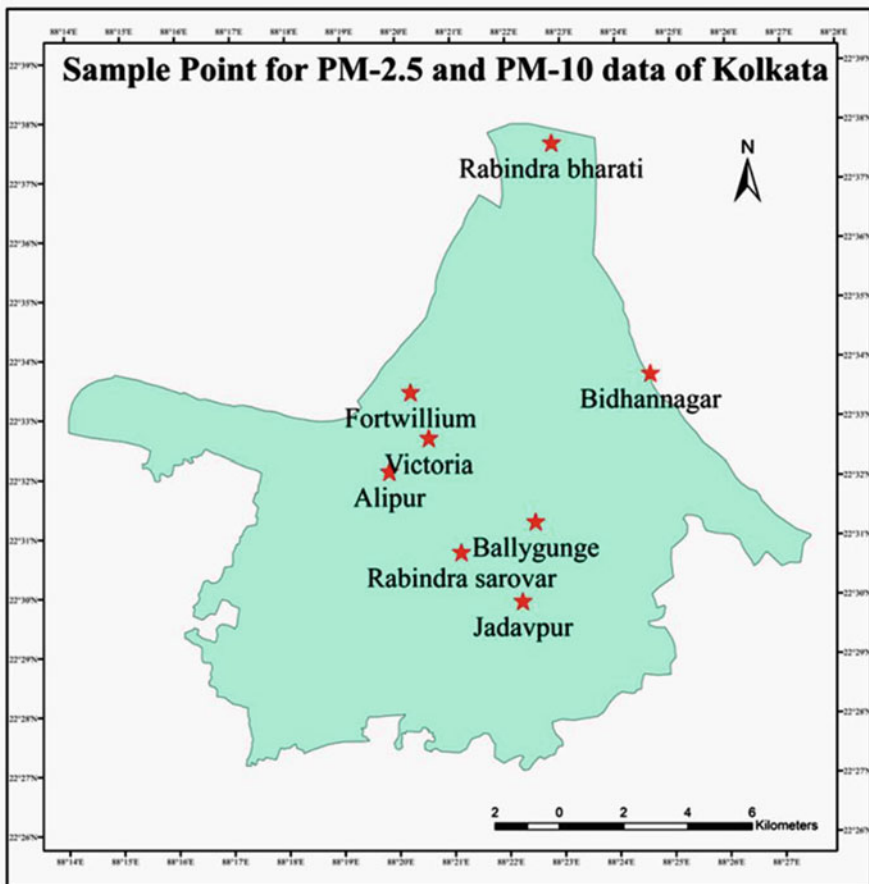


Fig. 29.7 Ground locations used for validation of the model

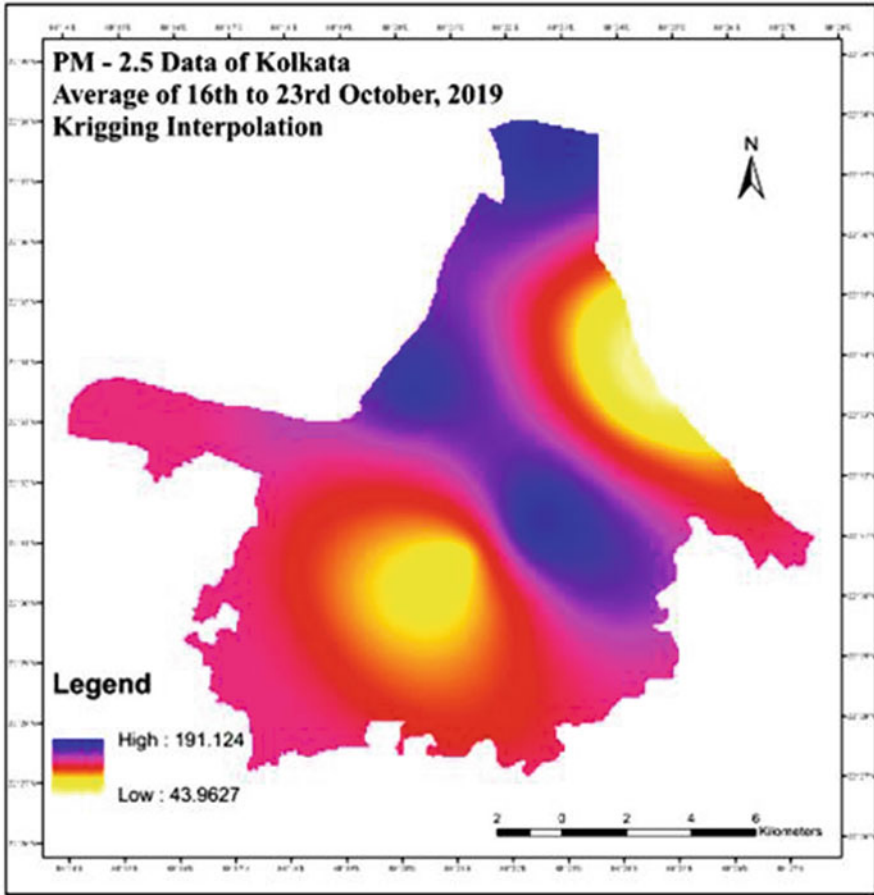


Fig. 29.8 Kriging interpolation for PM_{2.5}

Random Forest Regressor. The model predicted the PM_{2.5} level to be 124.53 and the PM₁₀ level to be 99.87, thus having an accuracy of 90% for PM_{2.5} (Fig. 29.8) and 96% for PM₁₀ (Fig. 29.9), respectively.

29.6 Risk Assessment and Remediation

There is no doubt that the weather in Kolkata has changed over the last decade. The significant factor happens to be the increased concentration of the different air pollutants residing in the atmosphere. To be specific, all these air pollutants have the inherent capacity of affecting the basic meteorological parameters (temperature, precipitation, and cloud cover), contributing to having a profound effect on the

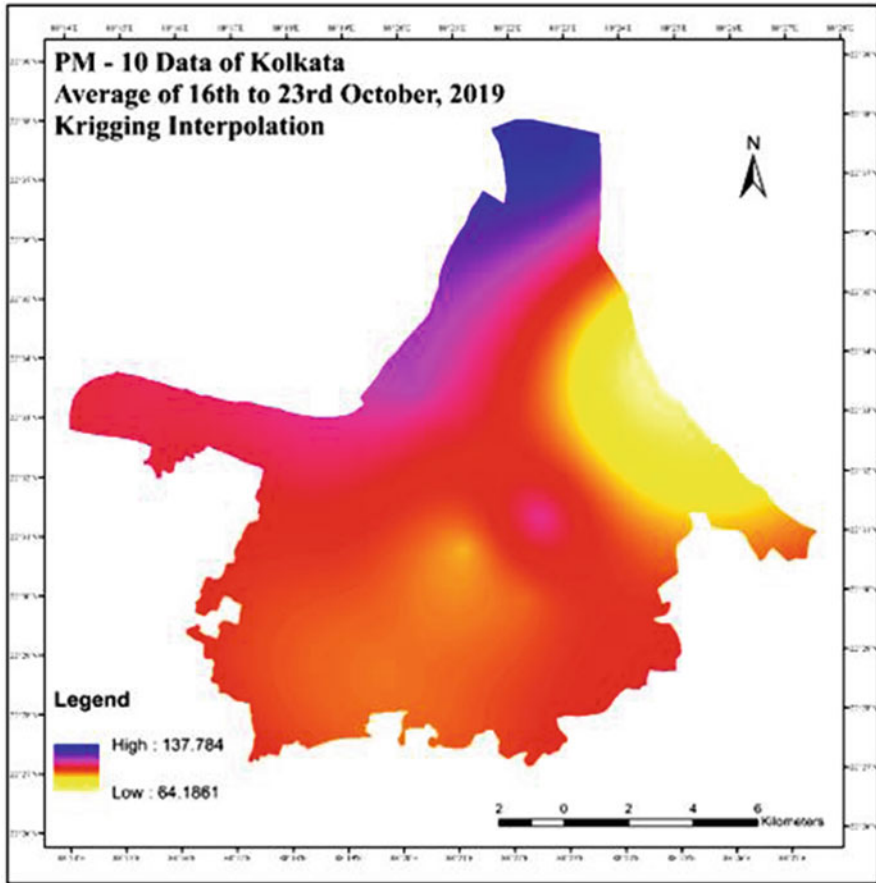


Fig. 29.9 Kriging interpolation for PM₁₀

weather. Air pollution is one of the primary reasons for concern in any urban setup in the present day. With the growing rate of population and vehicular density, air pollution needs the utmost attention. The air quality is particularly unfortunate during the cold seasons starting right after Diwali. Though stringent law has been put into effect, the citizens still lack the conscience for maintaining the air quality that is set by the authorities.

Particulate matter causes an extensive amount of destruction by affecting the respiratory system. RSPM can also affect the alveoli. The blood and lymph systems can carry the particulates to the distant organs where more hazardous effects are found to occur. Vehicular emission is the prime factor for pollution due to particulate matter. Kolkata, one of the megacities of the world, has got a diverse range of vehicles in an overwhelming quantity.

Moreover, being a commercial and economic powerhouse in Eastern India, it receives a massive influx of heavy transportations every day. The first signs of a respiratory disorder include runny or stuffy nose, which occurs due to the swollen nature of the epithelial tissue linings of the upper respiratory tract. It is also characterized by a massive amount of nose droppings, which restricts the path of the respiratory tract. One of the prime causes of this is the accumulation of particulate matters in the upper respiratory tracts. Air pollution can result in sinusitis, a typical kind of sinus infection in the upper respiratory tract due to the entry of particulate matters from the unhealthy air. Wet cough is a frequent cough and urging of mucus laden with saliva to exit from the mouth. Medical reports have detected that air pollutants congested in the nasal orifice and respiratory tract can produce wet cough or sometimes frequently dry cough. Shortness of breath is an acute inner respiratory tract disease that may cause damage in the alveoli by various air pollutants, notably particulate matter.

General signs of non-respiratory symptoms include eye irritation like redness, swollen eyes, irritating in eyes, which may be due to the presence of particulate matter or any other physical or chemical air pollutant. This irritation can lead to temporary or sometimes even permanent blindness. Nausea is another result of severe air pollution where the victim may lose self-consciousness. Loss of memory, depression, and anxiety have also been reported in individuals who are mainly exposed to long-term air pollution.

All the health issues mentioned previously make Air Pollution one of the most significant threats to humanity in the coming future, and for that constant monitoring of AQI is crucial. There are ground stations for continuous monitoring of air quality, but the numbers are meager. Due to the insufficient number of ground monitoring stations, a non-conventional approach to address the problem is using Remote Sensing. Various satellites, namely, MODIS, ASTER Image Sensor, LIDAR, SPOT, LANDSAT ETM+, are used to monitor and forecast air pollution across the world.

29.7 Conclusion

The availability of air quality data is sparse, and only four stations measure the ground concentration of various pollutants across the city. For this reason, a non-conventional approach, i.e., the use of remote sensing can be beneficial to know the particulate matter concentrations of places where there are no ground monitoring stations. It can be said that for this project, the Random Forest Regression performed pretty well, but accuracies might improve if the daily values of all the parameters are available. If the sample size increases, more observations can be put in the training set of the model, which in turn might make the model more accurate. The *P*-values of all the independent parameters chosen were low, which makes them significant for the analysis.

References

- Chelani A (2019) Estimating PM_{2.5} concentration from satellite derived aerosol optical depth and meteorological variables using a combination model
- De Hoogh K, Heritier H, Stafoggia M, Kunzli N, Kloog I (2018) Modelling daily PM_{2.5} concentrations at high spatio-temporal resolution across Switzerland. *Environ Pollut* 233:1147–1154
- Fang X, Zou B, Liu X, Sternberg T, Zhai L (2016) Satellite-based ground PM_{2.5} estimation using timely structure adaptive modeling. *Remote Sens Environ* 186:152–163
- Feng X, Li Q, Zhu Y, Hou J, Jin L, Wang J (2015) Artificial neural networks forecasting of PM_{2.5} pollution using air mass trajectory-based geographic model and wavelet transformation. *Atmos Environ* 107:118–128. <https://doi.org/10.1016/j.atmosenv.2015.02.030>
- He Q, Huang B (2018) Satellite-based mapping of daily high-resolution ground PM_{2.5} in China via space-time regression modeling. *Remote Sens Environ* 206:72–83
- Hou W, Li Z, Zhang Y, Xu H, Zhang Y, Li K, Li D, Wei P, Ma Y (2014) Using support vector regression to predict PM₁₀ and PM_{2.5}. *IOP Conf Ser Earth Environ Sci* 17(1):012268
- Hu X, Belle J, Meng X, Wildani A, Waller L, Strickland M, Liu Y (2017) Estimating PM_{2.5} concentrations in the conterminous United States using the random forest approach. *Environ Sci Technol* 51(12):6936–6944. <https://doi.org/10.1021/acs.est.7b01210>
- King MD, Menzel WP, Grant PS, Myers JS, Arnold GT, Platnick SE, Gumley LE, Tsay SC, Moeller CC, Fitzgerald M, Brown KS, Osterwisch FG (1996) Airborne scanning spectrometer for remote sensing of cloud, aerosol, water vapor and surface properties. *J Atmos Ocean Technol* 1996(13):777–794
- Li T, Shen H, Yuan Q, Zhang X, Zhang L (2017a) Estimating ground-level PM_{2.5} by fusing satellite and station observations: a geo-intelligent deep learning approach. *Geophys Res Lett* 44:11985–11993
- Li T, Shen H, Zeng C, Yuan Q, Zhang L (2017b) Point-surface fusion of station measurements and satellite observations for mapping PM_{2.5} distribution in China: methods and assessment. *Atmos Environ* 152:477–489
- Liu X, Shi X, Zhang K, Jensen EJ, Gettelman A, Barahona D, Nenes A, Lawson P (2012) Sensitivity studies of dust ice nuclei effect on cirrus clouds with the community atmosphere model CAM5. *Atmos Chem Phys* 12:12061–12079. <https://doi.org/10.5194/acp-12-12061-2012>
- Liu J, Weng F, Li Z (2019) Satellite-based PM_{2.5} estimation directly from reflectance at the top of the atmosphere using a machine learning algorithm. *Atmos Environ* 208:113–122
- Ma ZW, Hu XF, Huang L, Bi J, Liu Y (2014) Estimating ground-level PM_{2.5} in China using satellite remote sensing. *Environ Sci Technol* 48:7436–7444. <https://doi.org/10.1021/es5009399>
- Price D, Kacarab M, Cocker D, Purvis-Roberts K, Silva P (2016) Effects of temperature on the formation of secondary organic aerosol from amine precursors. *Aerosol Sci Technol* 50:1216–1226
- Sathe Y, Kulkarni S, Gupta P, Kaginalkar A (2019) Application of Moderate Resolution Imaging Spectroradiometer (MODIS) Aerosol Optical Depth (AOD) and Weather Research Forecasting (WRF) model meteorological data for assessment of fine particulate matter (PM_{2.5}) over India. *Atmos Pollut Res*. <https://doi.org/10.1016/j.apr.2018.08.016>
- Tian J, Chen D (2010) A semi-empirical model for predicting hourly ground-level fine particulate matter (PM_{2.5}) concentration in southern Ontario from satellite remote sensing and ground-based meteorological measurements. *Remote Sens Environ* 114:221–229
- Yang X, Zhao C, Zhou L, Wang Y, Liu X (2016) Distinct impact of different types of aerosols on surface solar radiation in China. *J Geophys Res Atmos* 121:6459–6471. <https://doi.org/10.1002/2016jd024938>
- Yin Q, Wang J, Hu M, Wong H (2016) Estimation of daily PM_{2.5} concentration and its relationship with meteorological conditions in Beijing. *J Environ Sci* 48:161–168

Zhan Y, Luo Y, Deng X, Chen H, Grieneisen ML, Shen X, Zhu L, Zhang M (2017) Spatiotemporal prediction of continuous daily PM_{2.5} concentrations across China using a spatially explicit machine learning algorithm. *Atmos Environ* 155:129–139. <https://doi.org/10.1016/j.atmosenv.2017.02.023>

Zhao C, Garrett TJ (2015) Effects of Arctic haze on surface cloud radiative forcing. *Geophys Res Lett* 42:557–564. <https://doi.org/10.1002/2014gl062015>

Chapter 30

Biomonitoring and Bioremediation of a Transboundary River in India: Functional Roles of Benthic Mollusks and Fungi



Susanta Kumar Chakraborty, Hirulal Pakhira, and Kishalay Paria

Abstract The increasing trend of eco-degradation of the different landscapes of the world, mostly because of human-mediated pollution has emerged as a burning environmental issue across the globe. This has necessitated to undertake sustainable eco-management in order not only to achieve proper eco-restoration of the disturbed and degraded ecosystems but also to ensure a continuous supply of ecosystem services. The embedded complexity and dynamism of the ecological problems of the riverine ecosystem require an in-depth analysis to achieve flexible, transparent, and viable environmental planning and management approaches incorporating and integrating a diversity of knowledge and values. Both the biomonitoring (an important component of eco-monitoring) and bioremediation (an integral part of any eco-restoration effort) help achieving the goal of sustainability of the functioning of the river ecosystem. This chapter of the book has dealt with the different merits and demerits of such recent developments in the arena of aquatic ecosystem management practices citing case studies emphasizing on the functional roles of benthic mollusks and fungi from a transboundary river, named as Subarnarekha, India. In dealing with such studies, meticulous and detailed analyses of the ecology of these major groups of the organisms, both from the field-based and experimental studies have been made in order to justify their contribution to the biomonitoring and bioremediation process. Deduction of Water Quality Index (WQI), Biotic Community Indices, Pollution Load Index (PLI), and Bio-Concentration Factor (BCF) based on the major prevailing water quality parameters such as Dissolved oxygen (DO), Biochemical oxygen demand (BOD), Chemical oxygen demand (COD), temperature, pH, turbidity, Total dissolved solids (TDS), conductivity, alkalinity, calcium, magnesium, chloride, total hardness, etc.; geo-chemical parameters of soils such as moisture content, pH, texture (sand, silt, and clay), organic matter, available nitrogen, and toxic substances such as heavy metals alongside documenting the diversity, distribution, and abundance of studied species across the studied stretch of the riverine flows, have been correlated with the biomonitoring and bioremediation of

S. K. Chakraborty (✉) · H. Pakhira · K. Paria
Department of Zoology, Vidyasagar University, Midnapore, West Bengal, India

© Springer Nature Switzerland AG 2021

P. K. Shit et al. (eds.), *Spatial Modeling and Assessment of Environmental Contaminants*, Environmental Challenges and Solutions,
https://doi.org/10.1007/978-3-030-63422-3_30

611

the riverine ecosystem, alongside citing an update on the recent literature concerning the strategies available for biomonitoring and bioremediation focusing mainly on the metal-contaminated water bodies using aquatic biota with a critical discussion on their main advantages and limitations.

Keywords Transboundary river · Benthic organisms · Water pollution · Heavy metals · Bio-concentration factors · Biotic indices · Biomonitoring · Bioremediation · Eco-restoration · Eco-management

30.1 Introduction

Fresh water representing 3% of the total available water is considered as the most precious life-supporting element of the globe and remains distributed mostly in the rivers, streams, floodplains, lakes, and other lentic water bodies. All these support the life form of numerous floral and faunal components in the form of phytoplankton, zooplankton, benthos, periphyton, nekton, etc. (Smith 1996; Giri et al. 2008; Guo et al. 2010; Annon 2014). Different forms of algae, fungi, angiosperms as macrophytes, insects, mollusks, crustaceans, and even larger animals like fish, amphibia, reptiles, and mammals inhabit the freshwater rivers as planktons, benthos, periphytons, and nektons (Chandra et al. 2003; Khalua et al. 2008; Karim and Panda 2014; Chakraborty 2020a, b). Rivers having freshwater environmental flows represent the lifeline of human civilization by acting as resources of drinking water, water for irrigation, other agricultural activities, energy production, ecotourism, and varied forms of industries. The intimate association of rivers with human life since the inception of human civilization mostly due to the immense benefits derived from this productive, sensitive, vulnerable, and threatened landscape of the world has necessitated a systematic study of the freshwater river ecosystem, along with eco-dynamics of biotic and abiotic factors with the prime objective of sustainable eco-management of rivers (Chakraborty and Choudhury 1992; Jonnalagadda and Mhere 2001; Harrison et al. 2008; Chakraborty 2020a, b). Knowledge bases pertaining to the ecology and behavioral manifestations of many of these life forms of rivers contribute significantly toward the eco-monitoring process and program after being determined by their specific ecological niche, habitat overlapping patterns, and heterogeneity of the riverine flows from upstream to downstream.

However, the biodiversity of the riverine ecosystem has been under the threats of decline by habitat degradation due to industrialization, urbanization, population growth, change in land use pattern, pollution, nonjudicious application of chemical fertilizers and pesticides, flow regulation by the abstraction of water, overexploitation in the fisheries, and change in the global climate, which in a synergistic manner put tremendous pressure on the freshwater bio-resources and functioning of the natural ecosystems (Suthar et al. 2009; Strayer and Dudgeon 2010; Woodward et al. 2010). Rivers as the lifeline of human society have been continuously polluted by anthropogenic activities such as urbanization, agriculture,

and industries. The scarcity of clean and healthy freshwater coupled with ongoing aquatic pollution has emerged as a major and growing concern in different corners of the world, and very little quantity of freshwater is now available in usable form (Chakraborty 2020a, b). Environmental monitoring of the aquatic system encompassing programmed estimation and recording of different pronounced water quality parameters in tune with the objectives of eco-management mostly emphasizes the need of measurement of physicochemical parameters of water. However, biological monitoring or biomonitoring deals with “the systematic use of living organisms or their responses to determine the condition or changes in the environment” (Rosenberg and Resh 1993; Rosenberg 1998; Gerhardt 1999; Oertel and Salanki 2003; Pradhan et al. 2003) and simultaneously evaluates the responses of living organisms and their constituent molecular and biochemical components (biomarkers) (Adedeji et al. 2012; Farombi et al. 2007; Dutta et al. 2014). “Biomonitoring” being a newly emerged eco-assessment tool (monitoring by biological methods) undertakes ecological exercises where several biotic components (bioindicator species) are used in ascertaining the extent of pollution of a water body (Lange and Lange 1997; Li et al. 2010;). In addition, in the process of standardizing the biomonitoring methods, major focus has been laid on the ecology of the biota especially the higher hierarchical ecological organizations, viz. populations, communities, and ecosystems. Therefore, the development of biomonitoring tools and their application in the aquatic system rely more on the usage of flora, fauna, and microbes of an ecosystem in order to understand the trend of ecological changes in an ecosystem temporarily and spatially (Pradhan et al. 2003).

Environmental monitoring with the help of direct qualitative and quantitative estimation of physical as well as chemical parameters of the water hardly reflect anything about the responses of the biotic structural components of the ecosystem against varying degrees of pollution as undesirable environmental disturbances which can also be perceived from the changes in the structure and the function of a biological system from molecular to community level (Wilhm and Dorris 1966; Foyer and Noctor 2005; Farombi et al. 2007). In order to achieve the goals of biomonitoring, i.e., the proper assessment of the changing ecological condition in the aquatic ecosystem, three sequential steps are followed:

1. Ecological survey on the selected study site having specific ecological characteristics (eco-zone) based on biotic assemblages, topography, and socioeconomic condition for biomonitoring studies (Mason 1996).
2. Surveillance as the second step which emphasizes upon collection of both qualitative and quantitative environmental data pertaining to the pollution status of the habitats based on which the subsequent eco-monitoring programs are chalked out (Chapman 1996).
3. Monitoring the programmed recording of ecological parameters for their future uses to generate research information to be used in environmental planning.

The concept of bioremediation revolves on the usage of biological agents (plants, fungi, bacteria, and even animals) to remove the toxic pollutants and contaminants from the affected aquatic or terrestrial ecosystems. It also involves the process to cause alteration of the polluted environmental condition by promoting the growth

and propagation of suitable living organisms to ensure the process of cleanliness and eco-restoration of the ecodegraded environment successfully. The toxic metals from this aquatic ecosystem can be reduced considerably by the cumulative resistance from the biotic community as evident from the changes of different biotic indices and the decreasing of the bio-concentration factor of toxic metals. Such observations indicate that toxic metals are absorbed by the biomass of the biotic community to a considerable extent from its readily available form in the aquatic medium, and such functional roles of the biota are recommended as effective eco-management agents or tools in order to ensure success in the bioremediation and eco-restoration of pollution-loaded aquatic systems. The diverse biotic community within the aquatic ecosystem experiencing a certain set of ecological variables in their own ecological niche and habitats remain very sensitive to any kind of undesirable ecological changes and resist such environmental perturbation through their resilience of functionality. The key to the successful functioning of the river ecosystem lies in the inter-linkages and interdependencies among several ecological factors leading to habitat change which in turn impose its impacts on biota and ecosystem processes. These cause–effect linkages aim at restoring watershed and river processes that drive ecosystem functions and features. The main concept pertaining to eco-restoration revolves in taking up proper measures to return the structural and functional fabrics of an eco-degraded ecosystem to its previous state (a non-degraded, unimpaired, pristine, or ecologically healthy condition), by regaining the previous ecological and biological attributes and values of the ecosystem (Bradshaw 1997; Higgs 2003).

30.2 Materials and Methods

30.2.1 *Subarnarekha River: Geomorphology and Ecology*

The name of the river “Subarnarekha” (between North latitude $21^{\circ}33'$ to $23^{\circ}32'$ and east longitude $85^{\circ}9'$ to $87^{\circ}27'$) is derived from the phrase “streak of gold” as the sand in this river basin simulate fine particles of gold (Dora and Roy 1987). The Subarnarekha River, after having its origin from Nagri village of Ranchi (eastern slopes of the tropical Chota Nagpur plateau) in the state of Jharkhand, India at an elevation of about 610 m, traverses through three states of India, namely, Jharkhand, West Bengal, and Odisha covering a distance of 395 km, before meeting the Bay of Bengal, at West Bengal, India. The river basin of the Subarnarekha River, a major transboundary river of India, has a catchment area of about 19,236 km² and experience massive mining (aluminum, iron, copper, and uranium ores) and industrial activities (iron, copper, etc.). Nonscientific and nonjudicious mining practices have exposed the earth on the river basin to suspended solids and heavy metals which in turn are washed away to the riverine flows and other water bodies especially during monsoon (Mukhopadhyay 1980; Giri et al. 2013).

The Subarnarekha River gets the water inputs through four riverine tributaries, of which three, namely the Raru, the Kanchi, and the Kharkai supply water on the right

portions of the river basin covering an approximate area of 9050 km² area whereas another tributary named as Dulung drains the river basins, having an area of 1173 km² on the left side of the river. The Kharkai, being the largest river tributary, after having its origin from forest tracts of Simlipal Biosphere Reserve in the Mayurbhanj district of the state of Odisha, India, contributes the major share of water supply (45% of the total annual flow) to the Subarnarekha River (Singh and Giri 2018). The ecological conditions of the rivers are mainly influenced by its hydrogeological properties such as water current, the velocity of flow, and discharge capacity, etc. which exhibit a wide range of fluctuation depending on the rainfall, temperature, and other meteorological parameters of the river catchment. The rhythm of the monsoon actually determines not only the flow patterns but also helps achieve the status of the perennial and non-perennial rivers and rivulets which are in turn endowed with their own ecological structural components, both living and nonliving. The Subarnarekha River is the lifeline of tribal and local human population, as they are mostly dependent on riverine resource bases, both living and nonliving, and utilize the same through their traditional age-old livelihood patterns, practices, and culture. Therefore, proper eco-monitoring of the main riverine flows of the Subarnarekha River and their associated tributaries has appeared to be an important prerequisite for undertaking effective environmental monitoring and environmental planning not only to ascertain the threat of pollution but also to combat it. A number of research investigations have been found in the literature depicting the sources, and intensity of impacts of pollution of the Subarnarekha River and its adjoining coastal belts in India (Mishra et al. 1994, 2009; Senapati and Sahu 1996; Panda et al. 2006; Chakraborty 2017, 2018).

The Subarnarekha River enters into the Purulia district in the state of West Bengal, India at Brajapur (near Muri) after flowing about 40 km over the undulating lateritic hilly forest tract. Again, it goes to the state of Jharkhand, India traversing a distance of about 135 km, and then flows through the state of West Bengal covering a distance of about stretch of 70 km and finally ends in the Bay of Bengal near Talsari, at the junction of the states of West Bengal and Odisha, India after experiencing a journey of around 55 km long way through the state of Odisha, India. The entire stretch of the Subarnarekha River from the place of its origin to the end enjoys the diversity of territorial boundaries coupled with vast diversity in valley landforms depicting the changing fluvial dynamics of the Subarnarekha River. After passing the Jamsola gorge, the width of the river strikingly increases depending on the regional slope and topographic variation. The erosion in the watershed level and vulnerability of the upper catchment area are two important aspects of the basin (Sklar and Dietrich 1998; Chatterjee et al. 2014). Those eroded materials from the upper catchment area are carried by the river course during the storm monsoonal discharge (Sklar and Dietrich 1998; Whipple and Tucker 1999). From the upstream to the lower courses of the river, the sizes of the grains of sediment gradually change from boulder, gravel, sand, silt, and clay (Chakrabarti 2005; Sharma and Singh 2015). The different landforms and geomorphic features of the river undergo changes and modifications depending on the exogenetic and endogenetic energies.

The variability of the climate of the region also acts as the key component to changing the river bed and floodplain geomorphology (Giri and Singh 2014).

30.2.2 Background and Rationality of the Selection of Study Sites

The Subarnarekha River along with its extensive river basin has been catering to the direct and indirect needs of human being in supplying drinking water and water for irrigation, local water conveyances, hydro-electric generations and acting as a repository of plenty of mineral resources [copper (Cu), Iron (Fe), Chromium (Cr), and Aluminum (Al)]. All these resource bases have had a triggering effect on the establishment and stable growth of different industries of asbestos, copper, iron, china clay, limestone, dolomite, and building stones (Giri et al. 2013). The upstream of the river passes through an industrial belt area of Jharkhand and Odisha. Eight major industrial complexes such as (i) Ranchi–Hatia industrial area; (ii) Alumina processing plant at Muri; (iii) Jaduguda–Ghatshila mining and industrial complex; (iv) Usha Martin Industries; (v) Steel Authority of India (SAIL); (vi) Tata Steel (TELCO); (vii) Hindustan Copper Limited (HCL), and (viii) Uranium Corporation of India have been developed in a full-fledged manner during the last one century. Besides these, there are large numbers of medium and small industries. The water quality parameters of the Subarnarekha River are being affected considerably by the discharge of untreated mining, domestic and industrial effluents at various sites of the river (Annon 2014).

30.2.3 Selection of Study Sites for the Long-Term Monitoring of the Ecological Status

The present study was carried out at five study sites in the stretch of Subarnarekha River mostly within the state of West Bengal, India including two at two neighboring states—the first one is in the state of Jharkhand and the last one is in the state of Odisha, India (Figs. 30.1 and 30.2). The study site I (S-I) locally named as Muri (23°22'12' N and 85°51'36' E) is located in the border of the states of Jharkhand and West Bengal, India. Both of the first study site (S-I) is characterized by the scarcity of water flow, exposed hard rocky bottom soil which is also subjected to the inflow of industrial wastewater from Aditya Birla Industry at Muri. The study site II (S-II) locally named Ghatshila (22°36'15' N and 86°28'48' E) is also situated in the state of Jharkhand and endowed with rocky bottom sediment. This study site experiences continuous discharge of pollutants and is contaminated profusely by the effluents of the Indian Copper Mining Industry at Ghatshila. The study site III (S-III) locally



Fig. 30.1 Map depicting the location of the study area

named as Gopiballavpur ($21^{\circ}57'28''$ N and $86^{\circ}44'50''$ E) is located in the western part of the Midnapore (West) district of the state of West Bengal, India and possesses sandy textured bottom sediments which also receive the contaminated water flow from the upstream. The study site IV (S-IV) locally named as Sonakonia ($21^{\circ}86'25''$ N, $87^{\circ}25'51''$ E) is located at the border of the states of Odisha and West Bengal, India, and is characterized by having a sandy river floor and basin. The study site V (S-V) locally named as Talsari ($21^{\circ}35'48''$ N and $87^{\circ}27'1''$ E) is located

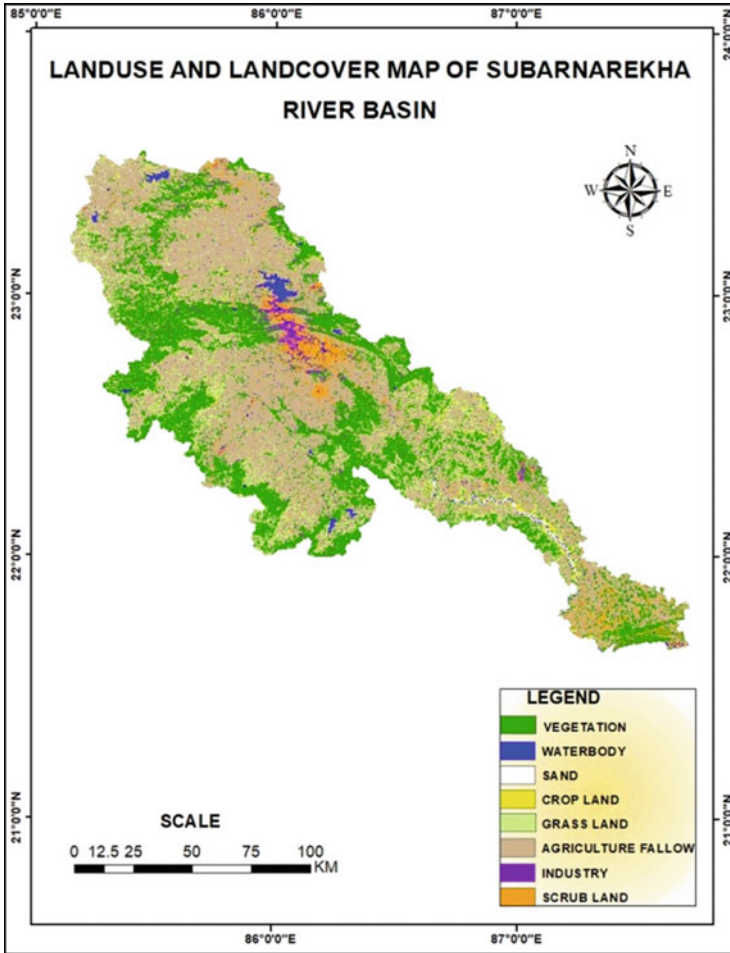


Fig. 30.2 Map highlighting the land-use patterns of the study area

in the state of Odisha, India where Subarnarekha River meets with the Bay of Bengal exhibiting brackish water environmental conditions (Figs. 30.1 and 30.2).

30.2.4 Monitoring of Different Water Quality Parameters

Standard analytical methods were followed to estimate different water quality parameters at monthly intervals (July 2012 to June 2014) from each selected study site (APHA 2005; Trivedy and Goel 1984).

30.2.5 Collection and Preservation of Benthic Mollusks

Mollusks were collected at monthly intervals (July 2012 to June 2014) from the littoral zone of either sides of the river at five ecologically contrasting study sites with the help of a metallic quadrat having an area of 0.5 m² and four such subsamples (0.5 m²) from each bank were collected randomly. Different molluscan species present within the quadrat were removed from the attached sediments manually by hand and finally by sieving with a metallic sieve with the mesh size of 0.5 mm and were preserved in 5% buffered solution. The average population density of mollusks collected from the used quadrats was expressed in No/m². Collected mollusks were identified following standard literature (Subba Rao 1989; Ramakrishna 2007). Based on the quantified information of population density and distribution of different benthic mollusks at five different study sites having contrasting ecological features through different months and seasons of two consecutive years July 2012 to June 2014, several biotic indices were deduced which were used to bio-monitor the ecological changes (Shannon and Weiner 1949; Simpson 1949; Menhinick 1964; Pielou 1966; Pakhira and Chakraborty 2016, 2018).

30.2.6 Isolation and Identification of Heavy Metal Resistance Fungi

30.2.6.1 Methods of Isolation and Identification of Aquatic Fungi

One gram soil, each taken from the five collected littoral soil samples representing different study sites (S-I to S-V) of the Subarnarekha River, India, was dissolved in sterilized distilled water and subsequently total volume was made to 100 ml. During isolation of aquatic fungi, 0.1 ml soil mixed water was spread onto sterilized potato dextrose agar (PDA) containing solid medium in aseptic condition. Thereafter, potato dextrose agar (PDA) plates containing processed samples were incubated at 28 °C temperature in an incubator. After 3–8 days of incubation, each of the developed fungal colony was isolated and pure culture was developed on several sterilized PDA containing Petri plates (Hajjaligo et al. 2006; Paria et al. 2018). The entire sequence of the isolation and identification of littoral benthic fungi can be summarized in the flowing manner:

Sampling of soil → Isolation of fungi → Development of pure culture → Selection of metal resistance strain → Storage and maintenance of pure culture.

30.2.6.2 Screening of Heavy Metal Resistance Fungi and Their Isolation and Identification

Each of the fungal colony was inoculated on separate sterilized culture plates having potato dextrose agar treated with heavy metals (Pb, Hg, and Cd) with the concentration of 50 ppm. After proper incubation, separate heavy metal tolerant fungal strains were isolated. The tolerant fungal mycelia were then cultured into separate potato dextrose broths (PDB) having 200 ppm heavy metals and incubated in BOD shaker incubator. All PDBs containing fungal samples were then subjected to shaking for a period of about 8–10 days, providing an interval of 8 h after each 16 h of observation till the formation of mature mycelia in the pure culture which are subsequently identified and confirmed by light microscope and phase contrast microscope (Paria et al. 2018).

30.2.6.3 Production of Exopolysaccharide (EPS)

F12 fungus, after being separated from about 8–10 days old culture broths by filtration and centrifugation, was preserved at 4 °C temperature with the addition of double volume of ethanol. After precipitation through centrifugation, the EPS was collected and dried by fridge drier (Paria et al. 2018).

30.2.7 Genetic Analysis of Most Active Heavy Metal Resistance Fungus

During genomic DNA isolation, specific (F12) strain of fungus was inoculated into 20 ml of potato dextrose broth (PDB) and incubated at 30 °C for 3 days. After the growth of fungi, 2 ml of culture was collected in eppendorf tubes and 10 min centrifugation were made at 16,500×g for the extraction of pellets. Extracted pellets were mixed up with 200 µl of TE buffer at the pH of 8.0, and thereafter subjected to centrifugation (16,500×g for 5 min). TE buffer was removed that added with 300 µl of extraction solution (200m MTrisHCl at pH of 8.5, 250 mM NaCl, 25 mM EDTA, 0.5% SDS). Then the mixture was added with 150 µl of sodium acetate (3 M, in the pH of 5.2) in another eppendorf tube. After this state of preparation, the mixture was homogenized for taking uniform suspension of cells. In order to avoid of RNA contamination, 20 µL of RNAase was added, and incubated at normal room temperature for 5 min. In addition, prevention of protein contamination, was done by adding 20 µL Proteinase K to isolated solution. Afterwards, the solution was centrifuged at 10000×g for 10 min adding 500 µL of phenol–chloroform in it. After proper centrifugation, the aqueous phase was separated and kept in the same amount of isopropanol containing the test tube. After incubation at 4 °C for 30 miin, the supernatant was centrifuged (16,500×g for 15 min) and the isolated DNA was

washed by 300 μl of 70% ethanol. Ultimately, the total sample was centrifuged ($16,500\times g$ for 15 min) for the removal of ethanol and DNA was dehydrated at 37°C and redissolved in TE buffer solution (50 μl). Subsequently, the DNA was prepared for the PCR and sequencing (Paria et al. 2018).

30.2.8 PCR and Sequencing

Genomic DNA of F12 fungal strain was isolated followed by the amplification of 5.8S ITS region through PCR, by using conserved primers. Using 20 pmol of each primer and genomic DNA (200 ng) were added subsequently with 50 μl reaction buffer that contained 2 mM dNTP, magnesium chloride (1.5 mM), and 5 units of Taq DNA polymerase (Bioline, USA). PCR was done in a thermocycler (ABI, USA). After completion of PCR, amplified products were analyzed by 1.0% agarose gel electrophoresis that was stained by ethidium bromide in order to visualize under UV-trans illuminator. After proper elution, products were purified by QIA quick gel extraction kit (QIAGEN) that was sequenced using Big dye terminator kit (ABI) and similar primers (used for PCR) in an automated DNA sequencer (ABI model 3100, Hitachi) (Paria et al. 2018; Paria and Chakraborty 2019).

30.2.9 Studies by Scanning Electron Microscopy (SEM) and Energy Dispersive X-Ray Analysis (EDAX)

Fungal strains were dehydrated by acetones for 20 min, and SEM images were taken at an increasing voltage of 20 kV (Paria et al. 2018). At the time of capturing SEM images, fungal samples were coated by E5200 Auto sputter coater (UK) under vacuum for a period of 15 min. On assessing the absorption patterns of the heavy metals, the fungal samples were dried up to 40°C in an oven. The dried fungal samples were then kept on graphite stub for the estimation of the X-ray dispersion patterns (Mandal et al. 2007).

30.2.10 Binding of Heavy Metals with Fungal Mycelium: Detection by FTIR Spectra

The infrared spectra (IR) were studied by thin pellets of the fungus mycelium in the form of powders in the KBr matrix. A Nexus TM 870 FTIR (Perkin Elmer) spectrophotometer equipped with a deuterated triglycine sulfate thermoelectric cool (DTGS-TEC) detector was used to collect the data over a spectral range of $200\text{--}4000\text{ cm}^{-1}$ (Paria et al. 2018).

30.2.11 Study of Antibacterial Effect of Isolated Fungus

Antibacterial activity of isolated fungi was tested by well diffusion method, where two selective Gram-positive (*Bacillus subtilis* and *Staphylococcus aureus*) and two selective Gram-negative bacteria (*Escherichia coli* and *Vibrio cholerae*) were used. About 0.2 ml of selective bacterial solutions were spread on sterilized nutrient agars containing Petri plates. Thereafter, fungal extracts (50 μ l) were poured into specific bores with control bore. After proper incubation at 37 °C for 24 h, diameters of inhibited zones were measured to understand the extent of the spread of the fungal colony (Paria and Chakraborty 2019).

30.3 Results and Discussions

30.3.1 Sources of Pollution in the Subarnarekha River

Exploitation and harvesting of both living (fishes, mollusks, etc.) and nonliving (sands, pebbles, granites, etc.) resources mostly by the traditional mining and fishing methods paying no heed to the government laid rules and regulations have imposed considerable harmful effects on the geo-hydrology and biodiversity of the natural riverine flows and river basins of the Subarnarekha River during the last one century. In addition, unregulated dumping of wastes and unplanned urbanization coupled with the development of mining and mineral processing industries mostly at the upstream (mainly Ghatsila and Muri) have led to cause considerable environmental degradation of this river during the last few decades (Singh and Giri 2018). The run-off loaded with eroded soil particles through the adjoining watersheds and wastelands (mostly developed by massive deforestation) during the monsoon seasons increased the suspended solids and heavy metal loads in the river water on reaching and mixing with riverine flows. Besides, dumping and mixing up of industrial wastes into the river water make the adversity in respect of deteriorating water quality more severe. Large-scale mining of granites, basalts, quartzite, dolerite, sandstone, limestone, dolomite, gravels, and river sands, etc. have not only posed environmental problems but also aggravated the deteriorating ecological conditions more severely (Giri and Singh 2014). The discharges from the domestic, municipal, and industrial wastewater produced by the activities of local peoples from the adjoining urban areas, along the stretch of the river pose serious pollution threats (heavy metals) to riverine flows in the river (Chakraborty et al. 2009). Lack of proper sanitation facilities coupled with age-old practices of open-air defecation, leaking of septic tanks, sewer malfunction, runoff from animal feedlots also added pathogenic bacteria into the riverine flows (Aslan-Yilmaz et al. 2004; Annon 2014).

30.3.2 Riverine Organisms (Benthic Mollusks and Microbes) Having Potential for Biomonitoring and Bioremediation

Out of the so many types of aquatic organisms, benthic mollusks and fungi have been highlighted with regard to their functional roles for biomonitoring and bioremediation in a transboundary river in India, named Subarnarekha, based on original research information derived from both the long-term field and experimental laboratory studies. Mollusks, being a major benthic biotic component influence and govern the functioning of the aquatic ecosystem by virtue of their abundance, biomass, and behavioral activities (Supian and Ikhwanuddin 2002). Realizing the ecological importance of this important aquatic animal phylum, long-term research studies on the diversity, abundance, distribution, and interaction with the surrounding aquatic systems, through different seasons and years from the contrasting eco-zones (upstream, middle stream, and downstream) of the Subarnarekha River, West Bengal, India were undertaken and research information processed toward developing biomonitoring tools and chalking bioremediation strategies. Similarly, biomonitoring potentials of microbes, both bacteria (Wilfred et al. 2004; Jan et al. 2014) and fungi (Paria et al. 2018; Paria and Chakraborty 2019), have recently been established along with proven roles as effective bioremediators. Adopting and manifesting several survival strategies such as biosorption, bioaccumulation, bio-transformation, and bio-mineralization, microorganisms have been found to cope up with deteriorating ecological conditions and thrive well in the polluted riverine water (Hamba and Tamiru 2016). The underlying scientific principles determining all these adaptive mechanisms and strategies of microorganisms can be applied to undertake ex situ or in situ bioremediation strategies (Kapoor et al. 1999; Hellawell 2012; Wuana and Okieimen 2011). Microorganisms (fungi, bacteria, and algae) serve as effective biotic agents for the bioremediation, especially for the removal of heavy metals along with dyes, and other contaminants from the polluted water through several biophysical processes such as adsorption, photocatalytic degradation, dialysis, coagulation, and filtration (Mishra et al. 2014; Geva et al. 2016; Gola et al. 2017).

The bacteria were found to considerably eliminate hydrocarbon components of crude oil through enzymatic degradation and bioremediation has been very much effective by way of cleaning residual oil in a variety of coastal environments, such as rocky shorelines (Bragg et al. 1994) and sandy intertidal belt (Venosa et al. 1996). In addition, as the oil with hydrocarbon are rich with high carbon content but low levels of other nutrients, essential for microbial growth, exogenous application or supplementation with phosphorus and nitrogen trigger higher growth and proliferation of such oil-eating (hydrocarbon-degrading) bacteria and thereby stimulate and accelerate the process of oil degradation (Atlas and Bartha 1972; Bragg et al. 1994; Swannell et al. 1995; Röling et al. 2004). The relationship between degradation with the microbial communities with similar structures are observed to be more complex and exhibit varied forms and degrees of degradation in respect of intensity

and duration, whereas heterogeneous bacterial communities accommodating different structural entities showed almost similar rates of degradation. Restoration of the bacterial community structure to a similar condition as was there prior to pollution can become more effective in determining the ecological endpoint of bioremediation. Mycoremediation (bioremediation with fungi) holds great promise as this method has not only been proven to be ecologically acceptable but also economically viable to achieve the eco-sustainability in using that uses fungi to eliminate heavy metals from water (Bhargava et al. 2012; Bharagava 2017; Paria et al. 2018). In such context, aquatic fungi in association with multi-resistant bacteria, have been observed to impart synergistic positive effects on the remediation process but also exhibit antibacterial activities (Matan et al. 2006).

30.3.3 Heavy Metals as Pollutants in Rivers: Sources, Bioavailability, and Mode of Action

Heavy metals, being a metalloid metallic element, possess high density and atomic number enjoying a higher position in the periodic table. All heavy metals [(biologically essential elements such as cobalt (Co), copper (Cu), chromium (Cr), manganese (Mn), and zinc (Zn); nonessential lighter elements such as cadmium (Cd), lead (Pb), and mercury (Hg). Arsenic (As), boron (B), and selenium (Se)] generally include elements (both metals and metalloids) having an atomic density greater than 6 g cm^3 which exhibit toxic effects on the biological world. The role of heavy metals towards causing environmental pollution is very considerable because of their toxic effect on biota. The atomic density of heavy metals exceeds five times that of water and thereby enjoys the persistence status as a chemical element (Hawkes 1997). Metals are released into the environment by several natural processes such as volcanic eruptions, weathering of rocks, etc. but major sources of metals to the riverine ecosystem are the different kinds of anthropogenic activities such as mining, industrial discharges (leather, paint, and textile industries, battery manufacturing, metal processing, petroleum refining, pesticides, electroplating, printing, and photographic industries) (Kennish 2017; Olgúin and Sánchez-Galván 2012).

Although heavy metal represents a natural constituents of earth and contribute in disperse form in the formation of rocks, but they are mostly released from the process of industrialization and urbanization in biosphere. Owing to the persistent nature, heavy metals after being released either from the natural or anthropogenic sources find their way to the riverine flows and undergo biotransformation and biomagnification (Bhattacharya and Chakraborty 2001). The uptake of metals are mainly influenced by the higher percentage of bioavailable fractions within metals coupled with the properties of solubility in water and sorption in the soils (Vamerali et al. 2010; Bhargava et al. 2012). The actual bioavailability of some abundantly available metals and their mobility in the rhizosphere are controlled by the rhizospheric microorganisms. Besides, acidification coupled with the acquisition

of micronutrients, especially phosphorus, also facilitates the enhancement of the bioavailability of certain heavy metals (Chaney et al. 2007).

Heavy metals [iron (Fe), lead (Pb), cadmium (Cd), chromium (Cr), zinc (Zn), copper (Cu), arsenic (As), mercury (Hg), nickel (Ni), silver (Ag), etc.] representing the nondegradable, persistent, and conservative chemical elements having toxic potentials occur in nature after being released from several human activities (industrial, mining, agriculture, etc.) and through the disposal of sewage. Instead of restricting their toxic effects to the lithosphere, hydrosphere, and biosphere, a relatively little proportion of heavy metals is diffused in the atmosphere as vapors or as respirable particulate matter (RSPM). Some heavy metals serving as essential elements for the aquatic organisms in low concentrations are designated as the “trace elements” or “micronutrients which are in contrast to the nonessential metals (metalloids) because of their phytotoxic and zootoxic effects and are commonly considered as ‘toxic elements’ (Verkleij and Prast 1990; Ashraf et al. 2010). However, both of these categories of metals impart their toxic effects to the living organisms at high concentrations (Adriano 2001; Rashed 2001; Park et al. 2011). Initially, most of the metals are deposited and accumulated in the soils, and therefrom they enter the land, surface, and groundwater, posing serious threats against maintaining the quality of foods and safeguarding human health (Chen et al. 2004; Lorestani et al. 2012). Owing to their persistence nature, heavy metals, after being bioaccumulated within the living world, tend to remain there for a long period in the body tissues and magnify their concentrations in the process of biotransformation from the lower trophic levels to the higher ones in the aquatic ecosystem depicting a unique ecological process, known as biomagnification (Ali et al. 2013). The heavy metals exhibit bio-concentration and biomagnification because of their bioaccumulation within the living world due to their conservative and nonbiodegradable properties. After being released from the sources, the heavy metals tend to accumulate in the bodies of several biota forming the food chain–food web networks where initiation of uptake of metals started at the primary producer level and then through eating and eaten processes at successive trophic levels (Zhang et al. 2015). Plants, especially the succulent ones, have more power of engulfing and bioaccumulating different heavy metals which cause impairment of cellular metabolism of the bioaccumulator by disrupting the normal enzymatic activity, cell division, morphogenesis, protein structure, water balance, photosynthesis, and respiration and *ATP* content (Wang et al. 2003; Foyer and Noctor 2005; Ashraf et al. 2010). The harmful effects of heavy metals on the animal world include impairment, inhibition of metabolic activity, and even the mortality of the affected faunal components (Nagajyoti et al. 2010).

On entering into the soil and water of the riverine system, most of these toxic elements cause several human health problems throughout the length and breadth of the world not only acting as cytotoxic (Mahmood et al. 2012) but also as mutagenic and even carcinogenic pollutants (Tchounwou et al. 2012). In addition, waterborne pathogen-mediated human diseases pose serious threats to human life especially in tropical developing countries mainly because of the lack of sanitation system, poor infrastructure of water supply, scarcity of water during the dry period, and unscientific methods of disposal of waste materials (Shannon et al. 2010).

In a recent studies (Annon 2014; Pakhira and Chakraborty 2018; Paria et al. 2018), different number of heavy metals on getting released from several industrial and mining activities to the Subarnarekha River tended to display variations in different seasons and registered higher concentration of Fe concentration at all study sites except S-II where Cu was estimated to be in the higher concentration (Table 30.1). The maximum values of these heavy metals were observed in pre-monsoon and the minimum values were recorded in monsoon season in both water and soil during the study period. The heavy metal Cd showed the lowest concentration at all study sites. The concentration of the heavy metal, Fe ranged from a minimum of 2.88 to 4.49 mg/l in the water, whereas, in the soil, the concentration of the same metal fluctuated from a minimum of 6.33 mg/l to a maximum of 13.95 mg/l. The concentration of the heavy metal Cu ranged from a negligible level of 0.01 mg/l to a maximum level of 0.92 mg/l in the water whereas in the soil the same metal was recorded as minimum of 0.39 mg/l to a maximum of 2.36 mg/l. The heavy metal Pb was found in minimum concentration as 0.37 mg/l and maximum of 0.48 mg/l in the water whereas in the soil the concentration of this metal fluctuated from 1.38 to 1.68 mg/l. The concentration of Zn as the heavy metal, fluctuated from a minimum of 0.25 mg/l to a maximum of 0.29 mg/l in water, but in the soil, the concentration of the same metal ranged from a minimum of 0.53 to 0.61 mg/l. Both the heavy metals Cr and Cd were recorded in almost negligible concentrations depicting a range of bdl to a maximum of 0.52 mg/l in the case of Cr (Table 30.1). The trend of heavy metal concentration in sediment and water was $Fe > Cu > Zn > Pb > Cr > Cd$ at all study sites except the study site II where it showed the trend of $Cu > Fe > Cr > Zn > Pb > Cd$. Site-wise trend of overall heavy metal concentration was higher at S-I and S-II followed by S-III, S-IV, and S-V (Annon 2010, 2014; Pakhira and Chakraborty 2018).

30.3.4 Bio-adjustment of Aquatic Organisms Against Heavy Metals

Soil subsystem of the aquatic ecosystem suffers on the deposition and accumulation of heavy metals which get transported to upper trophic levels by food chain–food web experiencing the biomagnification processes where the concentration of the persistent heavy metals are magnified in many aquatic organisms (Tiwari et al. 2007; Maiti and Chowdhury 2013; Banerjee et al. 2016). Moreover, owing to the steady and continuous interactions among bacterial communities with the pollutants of both organic and inorganic sources such as effluents and wastes from the paper, textile, leather, food processing, and pharmaceutical industries, from the sewage, from the municipal and domestic activities, leakages of the septic tanks and drains, chemical fertilizers and pesticides from agricultural runoff, and discharge of wastes from the mining activities trigger the increase of Biological Oxygen Demand (BOD) and Chemical Oxygen Demand (COD) of the contaminated and polluted water (Vesilind

Table 30.1 Range and mean (in parenthesis) of heavy metals covering six consecutive seasons of two consecutive years (2012–2014)

Heavy metals	Samples	S-I (Muri)	S-II (Ghatshila)	S-III (Gopiballavpur)	S-IV (Sonakonia)	S-V (Talsari)
Iron (Fe)	Water	3.21–5.45 (4.36)	3.65–3.84 (3.78)	4.26–4.78 (4.49)	3.09–3.39 (3.25)	2.75–3.086 (2.88)
	Soil	12.51–15.05 (13.95)	12.25–13.08 (12.62)	11.97–12.75 (12.31)	7.53–7.98 (7.75)	5.24–5.49 (5.33)
Copper (Cu)	Water	0.02–0.087 (0.061)	0.88–0.97 (0.92)	0.09–0.13 (0.11)	0.06–0.108 (0.084)	0.046–0.06 (0.053)
	Soil	0.35–0.43 (0.39)	2.19–2.54 (2.36)	0.36–0.61 (0.48)	0.45–0.51 (0.48)	0.45–0.49 (0.47)
Lead (Pb)	Water	0.33–0.51 (0.42)	0.45–0.51 (0.48)	0.37–0.52 (0.44)	0.43–0.51 (0.48)	0.33–0.41 (0.37)
	Soil	1.23–1.82 (1.53)	1.59–1.81 (1.68)	1.29–1.53 (1.38)	1.52–1.82 (1.66)	1.26–1.63 (1.43)
Zinc (Zn)	Water	0.24–0.35 (0.29)	0.21–0.301 (0.25)	0.24–0.45 (0.34)	0.23–0.31 (0.26)	0.21–0.31 (0.25)
	Soil	0.41–0.73 (0.55)	0.54–0.65 (0.59)	0.52–0.68 (0.61)	0.53–0.59 (0.57)	0.48–0.59 (0.53)
Chromium (Cr)	Water	bdl–0.024 (0.011)	0.021–0.046 (0.32)	0.014–0.036 (0.025)	0.018–0.038 (0.027)	bdl–0.032 (0.21)
	Soil	0.021–0.036 (0.027)	0.028–0.055 (0.39)	0.026–0.044 (0.034)	0.042–0.058 (0.049)	0.036–0.052 (0.052)
Cadmium (Cd)	Water	bdl–0.028 (0.019)	0.016–0.028 (0.022)	0.016–0.036 (0.024)	0.016–0.032 (0.026)	bdl–0.024 (0.018)
	Soil	0.018–0.032 (0.024)	0.024–0.036 (0.029)	0.038–0.042 (0.039)	0.016–0.032 (0.025)	0.024–0.046 (0.034)

et al. 2013). Both micro- and macroorganisms, having the power of tolerance against the deteriorating water qualities of riverine flows, have been found to display suitable adaptive strategies to cope up with deteriorating ecologically stressed condition by adopting different detoxifying mechanisms such as biosorption, bioaccumulation, biotransformation, and bio-mineralization (Hamba and Tamiru 2016). The underlying operating scientific principles behind such adaptive survival strategies of the aquatic organisms can be manipulated and exploited for bioremediation either by ex situ or in situ mechanisms (Pradhan et al. 2003; Chakraborty et al. 2009; Wuana and Okieimen 2011; Hellawell 2012; Sanyal et al. 2014, 2015).

30.3.5 Molluskan and Fungal Diversity: Potentiality as Bioindicator and Bioremediator Species

Out of the 23 different species of mollusks (15 gastropods and 8 bivalves), 9 species were found to occur at four study sites (S-I, S-II, S-III, and S-IV) within the river extending from the upstream to the upper part of midstream of the river, demonstrating their higher preference as sensitive species for freshwater-dominated eco-zones whereas the rest 14 species were observed to inhabit only at study site V (S-V), demonstrating their sensitiveness toward saline water-dominated stretch of the Subarnarekha River. Interestingly, 4 species under 3 families were recorded both from freshwater and brackish water zones, establishing their claim as tolerant bioindicator species (Table 30.2; Figs. 30.3, 30.4, and 30.5).

Out of the 112 isolated and cultured fungal isolates inhabiting in the water-sediment inter-phase of the Subarnarekha River, 16 fungi on preliminary screening demonstrated their growth against some selected heavy metals viz. lead (Pb), cadmium (Cd), and mercury (Hg) revealing different resistance patterns against the respective heavy metals (Table 30.3; Figs. 30.6, 30.7, and 30.8). The benthic fungus *Aspergillus penicillioides* after being isolated from the bottom sediment of Talsary (S-V), a confluence of Subarnarekha River with the Bay of Bengal, India showed resistance against Pb (II) and Cd (II) up to 1000 ppm and Hg (II) up to 200 ppm. Out of a number of heavy metals, which were detected from the Subarnarekha River, cadmium (Cd) has appeared to be a potentially toxic heavy metal due to its lethal toxicity in the later phase of life coupled with increasing risk after exposure (Nordberg et al. 2014). Among all isolates, *Aspergillus* sp., *Penicillium* sp., *Rhizopus* sp., *Fusarium* sp., and *Pythium* sp. have exhibited their efficiencies for scavenging heavy metals. Out of them, *Aspergillus penicillioides* has the highest heavy metals (Pb and Cd) scavenging ability in an optimum pH, temperature, and time (Paria et al. 2018). Different fungal strains were supposed to tolerate lower concentration of heavy metals as a distinct decline of the fungal diversity was noted in more heavy metals loaded eco-zones of the Subarnarekha River (Paria et al. 2018). A number of fungi have been isolated from three stretches (upstream, middle stream, and downstream) of the studied river, i.e., one (1) at upstream (S-I); two (2) at the middle

Table 30.2 Distribution and relative abundance of molluskan species in selected study sites of the Subamarekha River

Sl. no.	Family	Species	Study site I		Study site II		Study site III		Study site IV		Study site V	
			RA	Rank	RA	Rank	RA	Rank	RA	Rank	RA	Rank
1	Viviparidae	<i>Bellamyia bengalensis</i> (Lamarck, 1822)	13.06***	2	12.21***	2	33.01***	1	35.39***	1	0.88*	14
2		<i>Bellamyia dissimilis</i> (Muller, 1774)	-		-		8.05***	6	13.51***	3	-	
3	Thiaridae	<i>Tabertia granifera</i> (Lamarck, 1822)	8.67***	3	9.86***	3	9.76***	5	-		-	
4		<i>Thiara scabra</i> (Muller, 1774)	69.47***	1	51.03***	1	13.66***	2	15.39***	2	2.47*	6
5	Lymnaeidae	<i>Thiara lineate</i> (gray)	-		8.33***	6	8.03***	7	8.37***	5	-	
6		<i>Lymnaea acuminata</i> (Lamarck, 1822)	6.80***	4	8.61***	4	10.03***	3	-		-	
7		<i>Lymnaea luteola</i> (Lamarck, 1822)	-		8.39***	5	9.91***	4	12.21***	4	-	
8		Unionidae	<i>Lamellidens corrianus</i> (Lea, 1834)	-		-		3.87**	8	3.52**	8	-
9	Corbuculidae	<i>Lamellidens marginalis</i> (Lamarck, 1819)	1.98*	5	1.51*	7	3.65**	9	3.53**	7	-	
10		<i>Corbicula peninsularis</i> (Prashad 1928)	-		-		-		5.64***	6	1.65*	
11	Assimineidae	<i>Corbicula striatella</i> (Deshayes, 1854)	-		-		-		2.41*	9	1.66*	
12		<i>Assiminea brevicula</i> (Pfeiffer)	-		-		-		-		9.9***	3
13	Littorinidae	<i>Littorina (Littoraria) melanostoma</i> gray	-		-		-		-		2.87**	4
14		Potamididae	<i>Telescopium telescopium</i> (Linnaeus)	-		-		-	-		30.40***	2
15	Cerithiidae	<i>Cerithidea cingulata</i> (Gmelin)	-		-		-		-		34.47***	1
16		<i>Cerithidea abtusa</i> (Lamarck)	-		-		-		-		2.40*	7

(continued)

Table 30.2 (continued)

Sl. no.	Family	Species	Study site I		Study site II		Study site III		Study site IV		Study site V	
			RA	Rank	RA	Rank	RA	Rank	RA	Rank	RA	Rank
17	Naticidae	<i>Natica tigrina</i> (Roeding)	-		-		-		-		2.71**	5
18	Onchidiidae	<i>Onchidium tigrinum</i> (Stoliczka)	-		-		-		-		1.72*	12
19	Arcidae	<i>Anadara granosa</i> (Linnaeus)	-		-		-		-		1.79*	9
20	Mytilidae	<i>Perna viridis</i> (Linnaeus)	-		-		-		-		1.76*	10
21		<i>Modiolus undulatus</i> (Dunker)	-		-		-		-		1.75*	11
22		<i>Modiolus striatulus</i> (Hamley)	-		-		-		-		1.97*	8
23	Veneridae	<i>Meretrix Viperidae</i> (Linnaeus)	-		-		-		-		1.57*	13

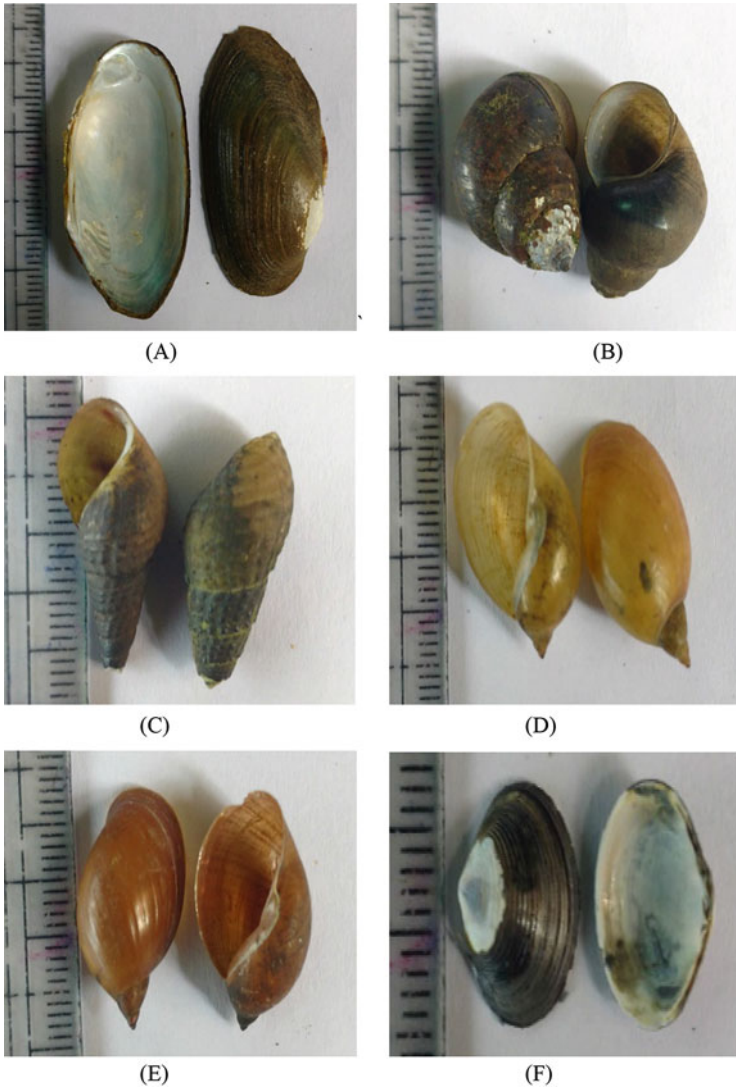


Fig. 30.3 Diversity of different molluskan species. (a) *Lamellidens marginalis*; (b) *Bellamya bengalensis*; (c) *Thiara scabra*; (d) *Lymanea acuminata*; (e) *Lymanea luteola*; (f) *Corbicula peninsularis*

stream (S-II and S-III), and three (3) at the downstream (S-IV and S-V) of the Subarnarekha River, India. During the whole survey period, a total number of 112 fungi were isolated, screened, and recorded from different sampling sites of the Subarnarekha River, India. Out of them, 16 isolates were proven to be heavy metal tolerance. Most of those recorded fungal species belong to the genus *Penicillium* (23), *Aspergillus* (27), *Pythium* (21), *Fusarium* (18), *Rhizopus*. (11), and

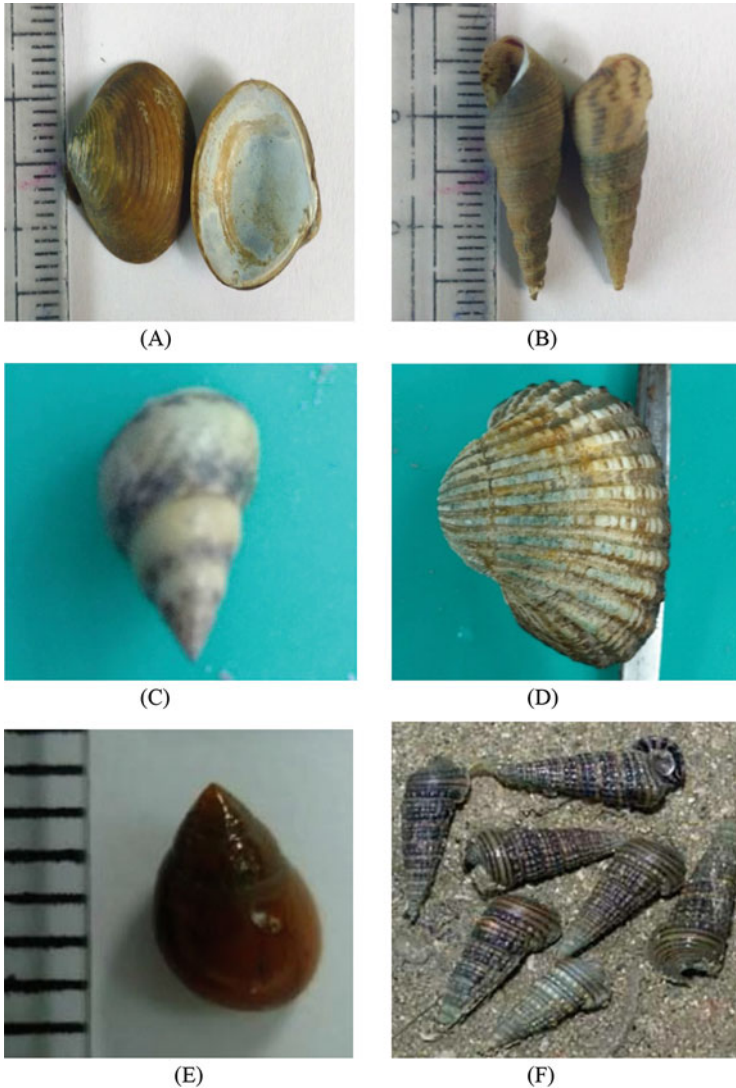


Fig. 30.4 Diversity of different molluskan species: (a) *Corbicula striatella*; (b) *Thiara lineate*; (c) *Natica tigrina*; (d) *Anadara granosa*; (e) *Assiminea breviculata*; (f) *Cerithidea cingulata*

Trichoderma (14). Out of all those species, 72%, 71%, and 76% were recorded at Muri (S-I), Sonakonia (S-II), and Talsari (S-III), respectively. In addition, a radar chart (Fig. 30.6) highlighting the distribution of fungus family have revealed that the highest fungal diversity was found at S-III followed by S-II and least at S-I. It has also been observed that *Aspergillus penicillioides* (F12) secrete a huge amount of exopolysaccharide that support and strengthen the immobilization of heavy metals and showed high adhesive activity of heavy metals. Consequently, these results

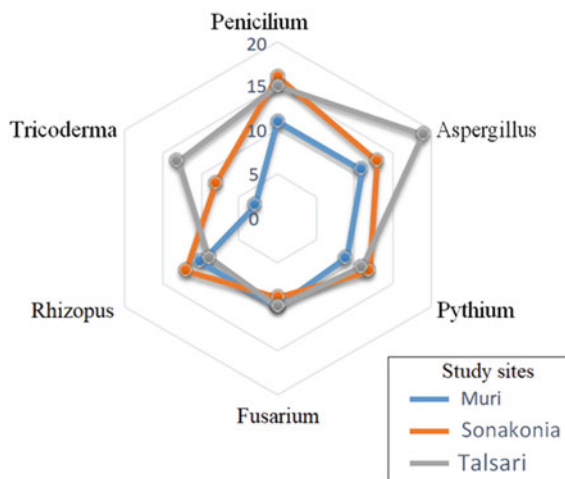
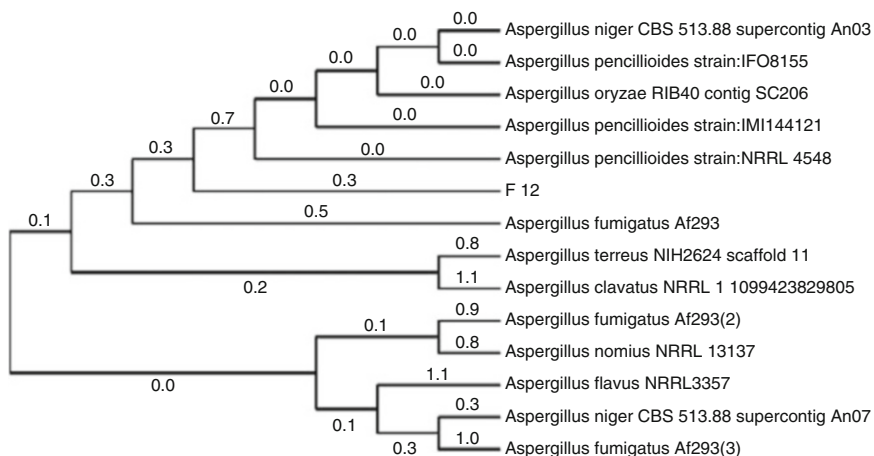


Fig. 30.5 Diversity of different molluskan species. (a) *Lamellidens corrianus*; (b) *Telescopium telescopium*; (c) *Tarebia granifer*; (d) *Meretrix meretrix*; (e) *Bellamy dissimilis*; (f) *Cerithidea abtusa*

demonstrate that both biomass and exopolysaccharides are responsible for heavy metal bioremediation from the river bank. In this respect, various species of *Aspergillus* sp. have been described as effective heavy metal reducers (Kalin et al. 2005). In addition, a recent study has also revealed the wide range of distribution patterns of fungi in the riverine ecosystems depicting their specific preferences toward ecological habitats having distinct ecological characteristics (Paria et al. 2018).

Table 30.3 Diversity of dominant types of benthic fungi found in the Subarnarekha riverine tracts at different study sites

Name of site	Dominant types of fungi
S-I	<i>Pythium</i> sp., <i>Penicillium</i> sp.
S-II	<i>Fusarium</i> sp., <i>Rizopous</i> sp., <i>Penicillium</i> sp., <i>Aspergillus</i> sp.
S-III	<i>Pythium</i> sp., <i>Rizopous</i> sp., <i>Penicillium</i> sp., <i>Fusarium</i> sp.
S-IV	<i>Aspergillus</i> sp., <i>Penicillium</i> sp.
S-V	<i>Aspergillus penicillioides</i> , <i>Aspergillus</i> sp., <i>Penicillium</i> sp.

**Fig. 30.6** Radar chart depicting diversity of the major heavy metal tolerant fungal groups**Fig. 30.7** Diversity of genetic strains of *Aspergillus penicillioides* with phylogenetic relationships

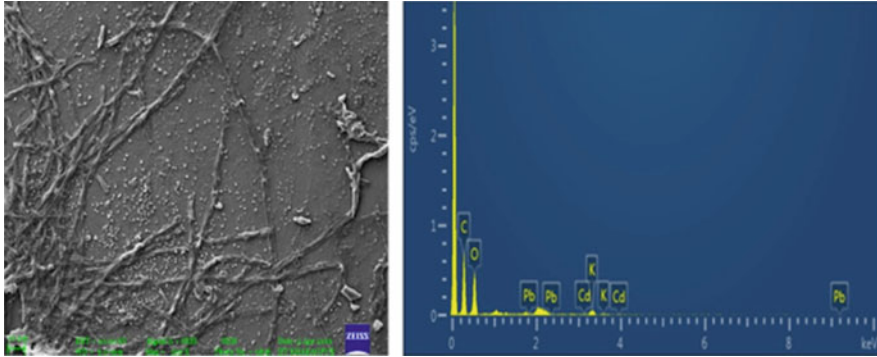


Fig. 30.8 SEM and EDEX analysis of mycelium of *Aspergillus penicillioides*

30.3.6 Molecular Identification of Highly Heavy Metal Tolerance Fungus

According to Bruns et al. (1991), a specific and distinct region conserve primer (5.8S ITS region having 500 bp DNA) was used and enlarged by PCR from isolated fungal (F12) genomic DNA and that were sequenced from its 5' end (Mandal et al. 2007). The obtained sequence showed more than 95% homology with *Aspergillus penicillioides*. The heavy metal tolerance ability of the isolated fungus strain, F12 fungal (MN210327), was found to be more similar to *Aspergillus penicillioides* (Figs. 30.6 and 30.8).

30.3.7 SEM and EDEX Analysis: Methods for the Study of Morphological Excellence of Fungi

Fungal biomass and exopolysaccharide (EPS) of the selected fungal strains were treated with 20 ppm of Pb(II) and Cd(II) metal to make them prepared for the studies under Scanning Electron Microscopy (SEM) as well as for EDEX study in order to document the morphological changes due to the bioaccumulation of heavy metals. Fungal EPS was observed to accumulate more heavy metals in comparison to other biochemical entities of the fungal biomass. It was also noted that a considerable amount of heavy metal, Pb (almost double) was removed than the heavy metal Cd when supplemented combinedly with the same concentrations (Fig. 30.8).

30.3.8 *Fourier Transforms Infrared Spectroscopy (FTIR Analysis): A Tool for the Assessment of Metal Removal Efficiency of Functional Groups*

Surface of biomaterials encompass a variety of different functional groups that mainly include thiols ($-\text{SH}$), amide ($-\text{NH}_2$), phosphate (PO_4), carboxylate ($-\text{COO}^-$), and hydroxide ($-\text{OH}$) which are responsible for the attachment of several metal ions (Wang and Chen 2009; Gupta et al. 2015). Identification of the functional group is very significant for the proper understanding of the binding mechanism of certain metal ions. The symmetric and asymmetric $\text{C}=\text{O}=\text{C}$ stretching vibrations are found to appear at the absorption band of $1000\text{--}1050\text{ cm}^{-1}$ and $1150\text{--}1250\text{ cm}^{-1}$ (Silverstein and Bassler 1991). The performed peak at the absorption band of 1036 cm^{-1} is linked to the interaction of $\text{C}-\text{O}-\text{C}$ symmetric stretching type. It is also noted that the absorption band of 1036 cm^{-1} seems occur to before vibration associates to ($-\text{CN}$) stretching free structure of carbon and the amino group nitrogen (Lal et al. 1982). FTIR spectrum on isolated mycelia biomass after being treated with heavy metal Cd(II) showed shifting of peaks from the absorption band of 1036 cm^{-1} peak to the absorption band of 1023 cm^{-1} whereas the Cd(II) treated biomass of fungal mycelia exhibited action on the $\text{C}-\text{O}-\text{C}$ bond. Besides, Pb(II) -treated fungal biomass was displaying absorption band at 965 cm^{-1} which was thought to be responsible for $\text{C}-\text{O}$ stretching vibration. The absorption band of 965 cm^{-1} is synchronized to $\text{C}-\text{O}$ stretching to the ribose sugar and phosphodiester bond of DNA (Chiriboga et al. 1998). It is confirmed that Pb(II) and Cd(II) ions directly act on DNA, that binds with $\text{C}-\text{O}$ stretching of ribose and phosphodiester bond (Bai and Abraham 2003; Elizabeth and Anuradha 2000; Ezzouhri et al. 2009; Farombi et al. 2007).

The spectrum of absorption bands with the range of $1140\text{--}1185\text{ cm}^{-1}$ is mainly responsible due to the presence of protein and carbohydrate (Parker 1971). The peak absorption band at 1163 cm^{-1} is responsible for the vibration of the $\text{C}-\text{O}$ bond of ribose sugar. In contrast, the peak at 1741 cm^{-1} indicates the vibration of $\text{C}=\text{O}$ ester that disappears with similar studies with the fungal biomass treated with metals Pb(II) and Cd(II) . Thereafter, fungal biomass-related metal removal occurs due to the vibration of $\text{C}=\text{O}$ ester and $\text{C}-\text{O}-\text{C}$ bond. The frequency of vibration at 1067 cm^{-1} points out the stretching characteristics of $\text{C}-\text{O}$ that have been moved to 965 and 985 cm^{-1} for Pb(II) and Cd(II) treated EPS, respectively (Fig. 30.9).

The biochemical properties of *Aspergillus penicillioides* as shown in Fig. 30.8 depicts that the natural cells showed two high-frequency spectra (1540 and 1656 cm^{-1}) conforming to amide II and amide I, separately. A small band (1402 cm^{-1}) as found to be responsible for symmetric stretching of COO^- groups is supposed to have been derived from the amino acids and carboxyl groups of carbohydrate. In addition, monoester phosphate and free phosphate of DNA and phospholipid functional groups were observed near 1082 and 1238 cm^{-1} , respectively (Fig. 30.9).

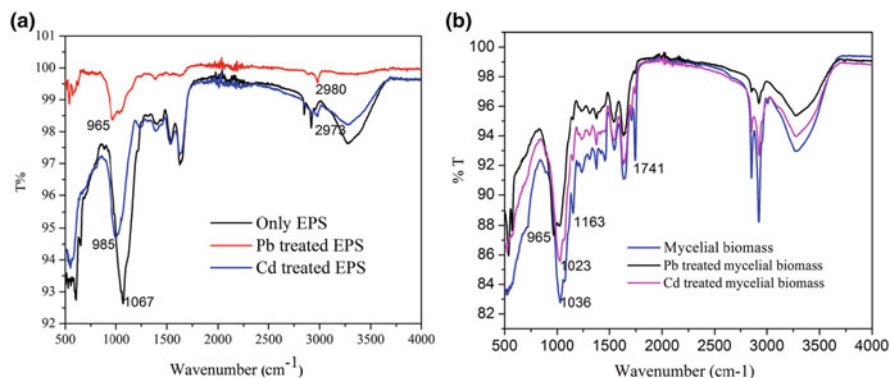


Fig. 30.9 FTIR spectrum of untreated EPS, Pb-loaded, and Cd-loaded EPS. bFTIR spectrum of untreated biomass, Pb-loaded, and Cd-loaded biomass

Table 30.4 Antibacterial activity of selected heavy metal tolerant fungus

Fungal name	<i>E. coli</i>	<i>Staphylococcus aureus</i>	<i>Bacillus subtilis</i>	<i>Vibrio cholerae</i>
<i>Aspergillus penicilloides</i>	+	++	++	++
<i>Fusarium</i> sp.	+	+	+	+
<i>Penicillium</i> sp.	+	+	+	+
<i>Rhizopus</i> sp.	+	+	+	+
<i>Pythium</i> sp.	++	+	++	++

+ zone of inhibition ranged between 7 and 12; ++ zone of inhibition ranged between 13 and 19; +++ zone of inhibition > 20; no zone of inhibition

30.3.9 Antibacterial Activities of Identified Fungus: A Prerequisite for the Maintenance of Water Quality

The fungus *Aspergillus* sp. F12 (MN210327), based on the research outcomes of in vitro antimicrobial experiment, showed prominent antibacterial activity against both Gram-positive and Gram-negative bacteria (Table 30.4). Similar experiments conducted with the fungal strains, *Pythium* sp. *Fusarium* sp. *Rhizopus* sp., and *Penicillium* sp. also showed similar results which are thought to be due to the presence of bioactive substances within the fungi and all these are supposed to be instrumental for the water purification abilities of fungi by causing massive mortality of harmful and pathogenic bacteria (Paria and Chakraborty 2019).

30.3.10 Biomonitoring of the Ecological Change: Functional Roles of Mollusks

The concept of water quality monitoring has been initiated with a view of water quality management in order to restore and maintain the natural water bodies.

Eco-monitoring is defined as the process of programmed and repeated observation measurement and recording for defined purposes of one or more parameters (physical, chemical, and biological) of an environmental setup (Jiang and Shan 2003; Kamala et al. 2015). It is usually done using physical parameters like temperature and other chemical variables like concentration of key nutrients of a significant pollutant (Maiti Dutta et al. 2014). Chemical monitoring is quite popular, being highly developed. However, it does not provide information regarding long-term effects of pollution on the ecosystem. Only mere estimation and recording of abiotic parameters in order to have an assessment of the ecological quality and health of river has several limitations and do not wholly reflect river health (Adams et al. 1993; Resh et al. 1995; Karr and Chu 1999; Dudgeon 2003; Crane et al. 2008).

The concept of biomonitoring has emerged to supplant and strengthen the already established method of eco-monitoring (programmed recording of the physicochemical parameters in order to achieve not only success in the environmental monitoring process) in order to chalk out proper environmental management strategies so that an eco-degraded ecosystem can be bio-remediated and eco-restored. In India, potential and scopes of application of biotic components such as zooplanktons (Pradhan et al. 2003; Sharma and Sharma 2010; Sanyal et al. 2015), molecular markers of benthic mollusks (Maiti Dutta et al. 2018), aquatic insects (Dalal and Gupta 2015), Benthic fauna (Sharma and Chowdhary 2011; Dutta et al. 2013), macroinvertebrates (Sharma et al. 2015), and fishes (Dutta et al. 1993) have been conducted and recommended by different researchers mostly for the aquatic ecosystem.

In view of the above discussion, recent research studies have attempted to deal with the ecology of mollusks, a significant benthic component in different eco-zones of the Subarnarekha River with a stretch of 285 km of the total length (395 km) of this river giving emphasis on diversity, distribution, seasonal dynamics of molluscan population and community in relation with seasonal fluctuation of ecological abiotic variables for a period of two consecutive years (July 2012–June 2014) and also to assess the ecological changes in respect of heavy metals' bioaccumulation and variability in temporal and spatial scales during the study period utilizing mollusk as a tool of biomonitoring through devising several biotic and heavy metal indices (Pakhira and Chakraborty 2016, 2018).

30.3.11 Monitoring of Different Water Quality Parameters

Seventeen different water quality parameters—Physical (9 parameters), organic (3 parameters), inorganic (3 parameters), and bacteriological (2 parameters)—from different study sites exhibited mostly similar trend of variation in the freshwater-dominated study sites (S-I to S-IV) whereas brackish water-dominated site (S-V) displayed different trends of fluctuation of some parameters such as chloride contents, salinity, etc. Water quality parameters exhibited different forms of fluctuations mostly under the influence of three important meteorological parameters, viz. temperature, rainfall, and wind flow which together influence the flow of water at

different study sites in different seasons [monsoon (July to October); post-monsoon (November to February); and pre-monsoon (March to June)] of two consecutive years, July 2012 to June 2014. Some pronounced water quality parameters viz. alkalinity, dissolved oxygen (DO), chloride content, total phosphate phosphorus, coliform bacteria were found to show maximum values during monsoon whereas parameters such as temperature, pH, hardness, biological oxygen demand (BOD), etc. displayed their higher results during the monsoon season. All those trends of variations have established and depicted the behavior and roles of the respective parameters in accordance with their seasonal dynamics (Pradhan et al. 2003; Jiang and Shan 2003; Giri et al. 2008; Sanyal et al. 2015) (Tables 30.5, 30.6, 30.7, 30.8, and 30.9).

30.3.12 Different Heavy Metal Indices

30.3.12.1 Contamination Factor (CF)

Contamination Factor is used to assess the pollution load of the sediments with respect to heavy metals pollution. Contamination Factor (CF) values of different heavy metals recorded at different study sites are presented in Tables 30.9 and 30.10. As per as the pollution of heavy metals and also by assessing the status of pollution in respect of contamination factor (CF), different study sites along the riverine stretches from the upstream to downstream were ranked as least polluted zone to moderately polluted zone. There are four grades of ratings on the basis of CF values (Hakanson 1980). All the study sites (S-I to S-V) displayed low CF ($CF < 1$, Class 1) to moderate CF ($1 \leq CF < 3$, Class 2) during different seasons, indicating unpolluted to moderately polluted nature of the sediments (Tables 30.10 and 30.11).

30.3.12.2 Pollution Load Index (PLI)

The pollution load index is an effective tool for assessing and comparing the sediment quality. According to Mohiuddin et al. (2010), $PLI = 0$ indicates perfection; $PLI = 1$ indicates the baseline level of pollutant; and $PLI > 1$ represents progressive deterioration of sediment. All the study sites revealed the PLI value as greater than one (Table 30.12) which reflects the polluted nature of the sediments. The maximum and the minimum PLI value as recorded from S-II and S-V, respectively, were due to the discharge of industrial effluent and anthropogenic activities carried out at the upstream region of the river.

Table 30.5 Seasonal dynamics (maximum, minimum, mean, and SD) of different physicochemical parameters at study site I during the study period July 2012–June 2014

S-I	TEM	PH	ALKA	TH	CaH	MgH	COND	TDS	TSS	DO	COD	BOD	TKN	TPP	CHL	TCOL	FCOL
MON, 12	Mini	28.4	6.9	91.6	68.5	57.7	2.64	140	59	5.2	20.1	0.7	1.34	0.05	17.6	920	540
	Max	30.5	7.3	97.2	109	72.5	8.98	156	85	6.96	35.8	1.1	1.58	0.09	20.3	2400	1600
	Mean	29.6	7.08	94.7	84.8	65.3	4.75	149	71.5	6.06	28.6	0.89	1.44	0.07	19.1	2030	1165
	Sd	0.87	0.17	2.49	17.4	6.6	2.87	26.4	6.83	11.7	0.73	6.74	0.17	0.11	0.02	1.33	740
POM, 12–13	Mini	14.5	6.5	70.7	67.2	48.3	3.05	96	49.2	6.24	34.8	1.58	1.69	0.07	24.6	540	350
	Max	20.8	7.1	78.2	76.8	54.7	6.95	108	68.9	7.1	38.5	1.96	1.98	0.09	30.8	1600	920
	Mean	17.4	6.78	74.5	71.5	51.6	4.86	102	58.3	6.68	36.4	1.75	1.82	0.08	27.6	1170	588
	Sd	3.25	0.25	3.55	4.08	2.64	1.63	9.87	5	8.96	0.39	1.55	0.16	0.12	0.01	2.6	523
PREM, 13	Mini	17.2	6.6	74.8	98.1	74.2	5.83	158	78	5.35	33.8	1.24	1.56	0.06	29.8	1600	1600
	Max	34.2	7.4	84.5	107	82.1	6.15	172	86.8	5.98	38.5	1.85	1.87	0.08	36.4	2400	2400
	Mean	29	7.08	78.5	103	78.2	5.99	165	81.7	5.62	35.9	1.55	1.7	0.07	33.2	2200	1800
	Sd	8.01	0.34	4.52	3.84	3.41	0.13	9.31	6.22	3.92	2.32	0.26	0.13	0.01	2.77	400	400
MON, 13	Mini	29.1	6.4	93.4	65.2	55.7	2.32	146	55	5.4	21.5	0.6	1.28	0.05	19.8	1600	540
	Max	30.8	6.9	98.2	106	70.3	8.66	162	82	6.85	36.7	1.2	1.56	0.09	22.2	2400	920
	Mean	30.1	6.6	95.9	87.1	64	5.64	155	70.9	6.16	29.8	0.91	1.42	0.07	20.9	2000	730
	Sd	0.73	0.22	2.05	18.7	6.33	3.07	22	6.8	11.9	0.62	6.46	0.26	0.13	0.02	1	462
POM, 13–14	Mini	15.2	6.2	74.2	63.8	47.1	4.07	102	51	6.18	32.1	1.62	1.71	0.07	26.7	920	350
	Max	20.4	6.7	81.9	73.2	52.4	5.08	112	66.8	7.2	36.8	1.88	1.94	0.09	31.3	2400	920
	Mean	17.6	6.43	77.8	68.8	49.6	4.68	107	59.3	6.71	34.7	1.75	1.84	0.08	29.1	1630	683
	Sd	2.34	0.21	3.33	3.9	2.41	0.44	10.3	4.27	7.54	0.46	2.06	0.11	0.1	0.01	1.89	605
PREM, 14	Mini	29.8	6.7	76.8	96.4	72.9	5.37	155	76	5.68	34.2	1.36	1.48	0.05	28.4	1600	1600
	Max	33.5	7.5	86.5	105	81.2	5.78	173	88	6.4	40.6	2.04	1.92	0.08	37.6	2400	2400
	Mean	31.9	7.1	81.1	100	77.3	5.59	165	81.7	6.05	36.6	1.72	1.71	0.07	33.2	2200	2200
	Sd	1.63	0.37	4.16	3.71	3.65	0.2	9.93	7.68	5.24	0.3	2.89	0.29	0.19	0.01	4.19	400

Table 30.6 Seasonal dynamics (maximum, minimum, mean, and SD) of different physicochemical parameters at study site II during the study period July 2012–June 2014

S-II	TEM	PH	ALKA	TH	CaH	MgH	COND	TDS	TSS	DO	COD	BOD	TKN	TPP	CHL	TCOL	FCOL
	Mini	29.5	6.6	85.2	68.3	56.4	2.9	264	64	4.65	29.9	0.7	1.13	0.76	16.3	540	350
	Max	31.5	7	90.5	76.9	60.2	4.07	280	92	6.95	42.9	1.1	1.5	0.94	22.9	2400	1600
MON, 12	Mean	30.5	6.83	88	73.3	58.2	3.69	273	162	80.8	36.7	0.87	1.35	0.86	19.8	1565	1118
	Sd	0.85	0.17	2.26	3.73	1.67	0.54	7.33	6.08	1	5.45	0.17	0.16	0.07	3.08	977	604
	Mini	18.6	6.88	74.4	75.6	58.7	3.83	248	98	5.8	28.6	0.01	2.01	0.32	30	540	350
	Max	20.2	7.1	78.5	89.4	65.5	5.83	260	108	6.5	30.8	1.51	2.22	0.64	34.1	2400	1600
POM, 12–13	Mean	19.4	6.97	76.5	81.9	62	4.86	255	103	6.18	29.7	1.07	2.14	0.48	32.2	1365	758
	Sd	0.73	0.1	1.76	6.74	3.18	0.91	5.29	4.16	5.97	0.3	0.71	0.09	0.13	1.74	818	569
	Mini	32.1	6.6	63.8	95.5	74.6	5.1	272	175	83	39.7	1.12	2	0.12	36.8	920	350
	Max	34.2	7.8	70.4	102	76.6	6.27	308	189	95	48.2	1.34	2.52	0.33	38.4	2400	1600
PREM, 13	Mean	33.3	7.15	67.3	99.5	75.5	5.87	290	181	89	44.3	1.24	2.35	0.23	37.6	1830	948
	Sd	0.94	0.52	3.04	3.04	0.91	0.55	14.9	6.06	4.97	3.91	0.09	0.24	0.09	0.73	714	511
	Mini	28.8	6.4	83.4	66.5	52.6	3.05	256	158	66	47.2	0.6	1.42	0.56	18.2	1600	350
	Max	31.2	6.9	87.5	74.8	58.2	4.2	278	172	90	6.84	0.96	1.52	0.86	24.4	2400	920
MON, 13	Mean	30	6.6	85.9	70.9	55.9	3.67	266	166	79.3	32.9	0.79	1.47	0.71	21.5	2200	778
	Sd	1.2	0.22	1.81	3.56	2.5	0.54	9.38	5.97	10.6	3.17	0.16	0.04	0.14	2.65	400	285
	Mini	17.9	6.8	75.2	76.2	60.4	3.86	245	92	60	26.9	1.12	1.96	0.38	29.2	540	280
	Max	20.4	7.2	79.8	90.8	66.6	6.42	265	104	78	32.4	1.62	2.31	0.58	36.8	1600	920
POM, 13–14	Mean	18.7	6.95	77.3	83.6	63.3	4.95	255	97	69.5	30	1.4	2.13	0.48	33.4	1335	570
	Sd	1.14	0.19	1.98	7.13	2.77	1.17	8.52	5.29	7.77	2.39	0.21	0.17	0.09	3.32	530	264
	Mini	31.8	6.5	62.8	93.7	73.8	4.86	274	178	85	51.8	1.21	2.01	0.18	35.1	540	280
	Max	33.9	7	86.5	105	78.2	6.49	312	188	102	56.3	1.45	2.58	0.45	39.7	2400	1600
PREM, 14	Mean	32.5	6.75	71.6	99.3	75.6	5.78	291	184	90.8	54.1	1.32	2.36	0.33	37.4	1535	835
	Sd	0.95	0.24	10.4	4.85	2.05	0.71	15.9	4.32	7.63	2.46	0.11	0.25	0.12	1.95	763	574

Table 30.7 Seasonal dynamics (maximum, minimum, mean, and SD) of different physicochemical parameters at study site III during the study period July 2012–June 2014

S-III	TEM	PH	ALKA	TH	CaH	MgH	COND	TDS	TSS	DO	COD	BOD	TKN	TPP	CHL	TCOL	FCOL
MON, 12	Mini	27.2	6.5	71.2	72.2	50.1	4.27	183	89	5.2	34.2	1.2	0.84	0.34	25.6	1600	540
	Max	29.6	6.7	83.6	76.4	58.9	5.39	253	121	7.64	53.6	1.8	1.18	0.96	34.8	2400	1600
	Mean	28.6	6.58	76.5	74.6	54.8	4.83	228	105	6.4	44.1	1.48	0.99	0.66	30.6	2000	900
	Sd	1.05	0.1	5.66	1.76	3.73	0.54	9.29	31.4	14	1	8.12	0.28	0.15	0.26	4.04	462
POM, 12–13	Mini	20.8	6.1	73.4	70.2	40.1	3.32	271	59	5.86	31.4	1.1	1.24	0.24	26.8	920	540
	Max	21.8	6.68	79.2	79.4	65.8	7.34	163	77	6.84	33	1.32	1.82	0.48	32	2400	1600
	Mean	21.3	6.37	75.9	74.6	51.3	5.69	127	66.5	6.3	32.4	1.23	1.53	0.35	29.2	1630	995
PREM, 13	Sd	0.43	0.27	2.66	3.8	10.9	1.75	33.7	7.94	0.47	0.71	0.1	0.25	0.1	2.33	605	441
	Mini	31.1	6.3	48	97.3	74.5	5.49	188	97	5.2	43.9	1.1	1.05	0.16	26.3	920	540
	Max	33	7.1	58	107	81.9	6.1	312	133	6.6	46.8	1.7	1.31	0.2	30.5	2400	1600
	Mean	32	6.75	53	102	78.4	5.67	206	114	6.02	44.9	1.38	1.18	0.18	28.4	1630	900
MON, 13	Sd	0.79	0.34	4.19	4.11	3.2	0.29	12	15.8	0.63	1.37	0.28	0.12	0.02	1.8	605	500
	Mini	26.5	6.3	68.5	73.7	52.6	5.1	268	82	5.4	32.4	1.01	0.78	0.24	23.8	1600	540
	Max	30.2	6.6	80.5	77.8	56.8	5.15	298	118	7.35	48.6	1.64	1.08	0.75	33.6	2400	1600
	Mean	28.7	6.4	75.7	75.4	54.4	5.12	282	100	6.45	40	1.43	0.91	0.53	29.3	2200	1165
POM, 13–14	Sd	1.67	0.14	5.3	1.74	1.76	0.02	26.8	15.5	0.84	7.17	0.29	0.13	0.23	4.19	400	526
	Mini	19.4	6.2	72.2	69.8	42.8	2.71	98	62	5.36	33.7	1.12	1.22	0.32	27.9	920	350
	Max	21.6	6.9	78.1	78.2	67.1	6.59	168	79	6.82	43.9	1.31	1.68	0.68	34.2	2400	1600
	Mean	20.5	6.55	74.9	74.2	54	4.92	135	69.5	6.11	39.4	1.23	1.49	0.5	30.6	1830	853
PREM, 14	Sd	0.94	0.31	2.63	3.73	10.3	1.64	29.5	7.59	0.64	4.47	0.08	0.2	0.16	3.04	714	552
	Mini	30.8	6.4	45.4	95.4	72.1	5.44	192	94	5.4	45.8	1.2	1.02	0.18	28.1	1600	540
	Max	32.8	7.2	61.6	105	81.4	5.71	322	138	6.8	52.2	1.7	1.42	0.22	31.2	2400	1600
	Mean	31.8	6.83	54.7	99.7	76.9	5.58	212	115	6.31	48.7	1.48	1.26	0.21	29.9	2000	1165
Sd	0.88	0.33	7.01	3.99	3.92	0.14	14.7	17	19.3	0.64	2.85	0.22	0.17	0.02	1.33	462	526

Table 30.8 Seasonal dynamics (maximum, minimum, mean, and SD) of different physicochemical parameters at study site IV during the study period (July 2012–June 2014)

S-IV	TEM	PH	ALKA	TH	CaH	MgH	COND	TDS	TSS	DO	COD	BOD	TKN	TPP	CHL	TCOL	FCOL
MON, 12	Mini	28.3	7.1	79.6	63.9	55.1	2.15	155	149	5.21	31.3	1.5	0.84	0.44	26.7	1600	920
	Max	30.2	7.5	86.8	68.5	59.4	2.46	201	173	7.85	48.5	2.6	1.68	0.64	36.9	2400	1600
	Mean	29.3	7.33	83.1	66.1	56.6	2.32	177	160	6.71	39.5	2.08	1.22	0.54	31.6	2200	1260
	Sd	0.79	0.17	3.27	1.89	1.91	0.16	20	11.2	1.14	7.69	0.51	0.4	0.09	4.43	400	393
POM, 12–13	Mini	18.5	6.4	63.7	76.3	44.8	7.54	104	68	4.5	26.8	1.04	1.32	0.41	28.5	920	540
	Max	20.8	7.24	75.1	91.4	53.2	9.32	142	82	5.9	30.2	1.24	1.5	0.69	31.9	2400	1600
	Mean	19.7	6.89	69.2	83	49.8	8.1	122	74	5.17	28.7	1.15	1.43	0.54	30.1	1460	900
	Sd	1.06	0.38	5.6	6.69	4.02	0.82	17.2	6.06	0.6	1.49	0.08	0.08	0.13	1.52	704	500
PREM, 13	Mini	30.8	6.8	67.9	83.6	51.8	7.73	188	145	6.13	39.8	1.3	1.45	0.33	27.5	1600	540
	Max	33.7	7.6	70.5	88.2	55.2	8.66	208	165	6.65	44.4	1.9	1.59	0.68	33.5	2400	1600
	Mean	32.1	7.23	68.9	86.1	53.1	8.05	198	156	6.38	42.3	1.56	1.52	0.5	30.5	2000	1165
	Sd	1.29	0.35	1.17	2.09	1.59	0.44	7	9.15	9.2	0.22	2.17	0.25	0.06	0.14	2.67	462
MON, 13	Mini	27.2	6.9	76.2	62.7	53.2	2.2	148	138	5.45	29.5	1.3	0.78	0.42	24.8	1600	540
	Max	30.4	7.6	86.4	68.2	57.4	2.64	205	165	7.23	45.6	2.4	1.58	0.68	38.2	2400	1600
	Mean	28.9	7.28	81.2	64.8	55.1	2.36	179	148	6.46	36.4	1.85	1.19	0.54	32	2000	900
	Sd	1.38	0.33	4.31	2.38	1.73	0.19	23.8	12.3	0.78	6.85	0.5	0.37	0.11	6.1	462	500
POM, 13–14	Mini	19.2	6.3	65.9	75.8	46.8	7.08	112	78	4.62	27.2	1.08	1.41	0.39	26.5	920	540
	Max	20.4	7.2	74.2	93.6	56.8	8.98	148	92	5.85	31.5	1.32	1.58	0.66	36.5	2400	1600
	Mean	19.8	6.73	70	84.7	51.6	8.06	130	85	5.18	29.5	1.21	1.5	0.52	30.8	1830	995
	Sd	0.49	0.4	3.4	7.79	4.48	0.81	15.5	6.22	0.54	1.87	0.1	0.07	0.12	4.42	714	441
PREM, 14	Mini	30.1	6.7	68.2	82.7	48.1	8.13	192	145	6.21	38.5	1.4	1.51	0.32	29.6	1600	540
	Max	32.9	7.6	72.4	90.2	54.9	8.61	222	162	6.71	45.2	1.85	1.62	0.71	37.2	2400	1600
	Mean	31.7	7.1	70.1	86.5	51.9	8.44	207	154	6.52	41.9	1.61	1.56	0.56	33.6	2000	1165
	Sd	1.2	0.39	1.76	3.27	2.83	0.22	12.9	7.14	0.22	3.09	0.19	0.05	0.17	3.29	462	526

Table 30.9 Seasonal dynamics (maximum, minimum, mean and SD) of different physicochemical parameters at study site V during the study period (July 2012–June 2014)

S-V	TEM	PH	ALKA	TH	CaH	MgH	COND	TDS	TSS	DO	COD	BOD	TKN	TPP	CHL	TCOL	FCOL	
MON, 12	Mini	27.5	6.4	76.6	58.2	50.9	1.78	677	255	242	5.5	43.8	1.18	1	0.21	106	1600	920
	Max	30.3	7.1	80.4	66.3	52.2	3.44	985	322	290	6.9	54.2	2.67	1.18	0.39	136	2400	1600
	Mean	28.7	6.85	78.8	62.2	51.5	2.6	765	289	271	6.13	47.9	1.8	1.07	0.31	120	2200	1260
	Sd	1.19	0.33	1.71	3.59	0.61	0.73	147	30	21.1	0.59	4.62	0.65	0.08	0.08	12.7	400	393
POM, 12–13	Mini	17.5	7	74	72.2	49.4	4.81	600	196	168	6.12	25.2	1.15	1.23	0.12	135	920	540
	Max	18.5	7.4	83.6	78.5	58.6	5.56	630	208	182	6.68	28.8	1.52	1.45	0.34	148	2400	1600
	Mean	18	7.18	78.3	75.8	54.5	5.19	616	201	175	6.39	27.5	1.37	1.32	0.22	141	1630	900
	Sd	0.5	0.17	4.12	2.83	4.43	0.42	13.2	5.29	5.74	0.23	1.57	0.16	0.09	0.09	5.56	605	500
PREM, 13	Mini	29.2	6.9	65.8	86.7	71.4	3.64	675	321	268	6.3	45.2	1.02	1.92	0.48	102	1600	540
	Max	31.2	7.5	72.6	93.5	77.6	3.88	725	330	285	6.9	54.3	1.16	2.65	0.64	132	2400	1600
	Mean	30.4	7.18	69.3	90.3	74.9	3.76	701	326	275	6.58	49.9	1.1	2.25	0.55	119	2200	1165
	Sd	0.87	0.28	2.93	2.99	2.91	0.1	21.4	3.92	7.27	0.25	3.85	0.06	0.32	0.07	12.7	400	526
MON, 13	Mini	26.8	6.1	74.8	56.2	52.1	1.04	665	254	242	5.6	41.6	1.22	1.1	0.28	112	1600	540
	Max	30.8	7.2	78.5	66.8	54.8	2.93	704	318	282	6.5	53.7	1.69	1.24	0.41	138	2400	1600
	Mean	28.6	6.7	76.6	61.2	53.3	1.94	684	287	266	6.08	47	1.88	1.18	0.35	127	2200	1165
	Sd	1.79	0.5	1.85	4.46	1.12	0.82	16.7	28.4	18.2	0.44	5.51	0.61	0.06	0.06	11	400	526
POM, 13–14	Mini	17.9	6.9	75.2	74.8	48.6	5.32	605	185	152	6.45	29.2	1.12	1.32	0.13	129	920	540
	Max	19.2	7.5	85.2	79.6	57.8	6.39	645	204	178	6.72	39.4	1.62	1.64	0.25	146	2400	1600
	Mean	18.5	7.15	80.5	76.8	53.1	5.78	630	194	167	6.58	34.8	1.43	1.48	0.2	137	1630	900
	Sd	0.59	0.26	4.73	2.23	4.02	0.46	17.4	8.1	11.4	0.12	4.47	0.22	0.13	0.05	7.14	605	500
PREM, 14	Mini	29.4	6.8	68.4	84.6	73.2	2.78	672	324	262	6.14	46.7	1.01	1.87	0.44	110	1600	540
	Max	31.8	7.6	74.8	96.5	77.9	4.54	720	336	271	6.78	54.2	1.18	2.35	0.58	131	2400	1600
	Mean	30.9	7.2	71.5	90.5	75.4	3.7	699	329	267	6.44	50.7	1.1	2.07	0.51	123	2000	995
	Sd	1.11	0.37	2.78	5.19	1.95	0.81	20.9	4.99	3.87	0.27	3.43	0.07	0.21	0.06	9.29	462	441

Table 30.10 Contamination factor of different heavy metals in the sediments of the Subarnarekha River

Heavy metals	1st year (2012–2013)					2nd year (2013–2014)				
	S-I	S-II	S-III	S-IV	S-V	S-I	S-II	S-III	S-IV	S-V
Fe	1.827	1.688	2.291	1.451	0.997	1.690	1.628	1.600	1.402	0.976
Pb	0.963	1.000	0.836	0.963	0.819	0.769	0.954	0.822	0.948	0.820
Cu	0.972	0.823	1.015	1.184	1.181	0.949	6.163	1.306	1.156	0.782
Zn	1.229	1.225	1.241	1.184	1.129	1.455	1.287	1.261	1.136	1.021
Cr	0.839	1.258	1.204	1.505	1.376	0.957	1.301	1.118	1.742	1.591
Cd	0.581	0.759	0.839	1.275	0.823	0.743	0.743	0.823	1.098	0.969

Table 30.11 Hakanson's (1980) standard table for soil quality with respect to CF

CF values (Hakanson 1980)	Class	Sediment quality
$CF < 1$	1	Low CF
$1 \leq CF < 3$	2	Moderate CF
$3 \leq CF < 6$	3	Considerable CF
$CF \geq 6$	4	Very high CF

Table 30.12 Pollution Load Index of different heavy metals of the Subarnarekha River in two consecutive years

Study site	1st year	2nd year	Mean	SE	Mini	Max
S-I	1.00413	1.041	1.022565	0.018435	1.00413	1.041
S-II	1.50231	1.511	1.506655	0.004345	1.50231	1.511
S-III	1.16009	1.121	1.140545	0.019545	1.121	1.16009
S-IV	1.24695	1.222	1.234475	0.012475	1.222	1.24695
S-V	1.03555	0.997	1.016275	0.019275	0.997	1.03555

Table 30.13 Muller's (1981) standard table for sediment quality according to geoaccumulation index

I_{geo} values (Muller 1981)	Class	Sediment quality
≤ 0	0	Unpolluted
0–1	1	Unpolluted to moderate polluted
1–2	2	Moderate polluted
2–3	3	Moderate to strongly polluted
3–4	4	Strongly polluted
4–5	5	Strongly to extremely polluted
> 5	6	Extremely polluted

30.3.12.3 Geoaccumulation Index (I_{geo})

The geoaccumulation index was introduced by Muller (1979) for determining the extent of metal accumulation in the sediments. It consists of seven-grade classification system of sediments from unpolluted to the extremely polluted nature of sediments (Tables 30.13 and 30.14). Geoaccumulation index values obtained for different metals at different study sites are presented in Table 30.14. Among the five

Table 30.14 Geoaccumulation indices for different heavy metals at different study sites from July 2012 to June 2014

Heavy metals	1st year (July 2012–June 2013)					2nd year (July 2013–June 2014)				
	S-I	S-II	S-III	S-IV	S-V	S-I	S-II	S-III	S-IV	S-V
Fe	1.841	1.806	1.799	1.460	1.297	1.807	1.791	1.783	1.445	1.288
Pb	0.279	0.296	0.217	0.279	0.208	0.181	0.275	0.210	0.272	0.209
Cu	-0.993	-0.216	-0.974	-0.908	-0.908	-1.003	-0.191	-0.865	-0.918	-1.087
Zn	-0.713	-0.715	-0.709	-0.730	-0.750	-0.640	-0.693	-0.702	-0.748	-0.794
Cr	-3.270	-3.094	-3.113	-3.016	-3.055	-3.212	-3.079	-3.145	-2.952	-2.992
Cd	-3.180	-3.064	-3.020	-2.839	-3.029	-3.073	-3.073	-3.029	-2.904	-2.958

study sites, S-I showed $1 < I_{\text{geo}} < 2$ representing the moderate polluted nature of the sediment. S-II revealed $0 < I_{\text{geo}} < 1$ reflecting the unpolluted to moderately polluted nature of the sediments; and S-III, S-IV, and S-V showed $I_{\text{geo}} < 0$ representing the unpolluted nature of the sediments (Table 30.14).

30.3.13 Seasonal Dynamics of Different Biotic Indices, Deducted from the Molluscan Diversity and Density at Different Study Sites of Subarnarekha River

30.3.13.1 Relative Abundance (RA)

Study by Pakhira and Chakraborty (2016) has shown the occurrence of 23 macrobenthic molluscan species from five selected study sites from July 2012 to June 2014. The maximum number of species (14 species) were recorded from the study site V followed by study sites III and IV (9 species), study site II (7 species), and study site I (5 species). Relative abundance and rank of different species constituting the molluscan community are shown in Table 30.1. It was found that *Thiara scabra* was the dominant species at study sites I and II and ranked one for these study sites. *Bellamya bengalensis* was the dominant species at study sites III and IV and therefore ranked one. At study site V, *Cerithidea cingulata* secured rank one and was the dominant species for this study site (Table 30.2).

30.3.13.2 Species Diversity Index (H')

Species diversity index (H') is a measurement between the number of individuals and the number of species. Species diversity tends to be high in biological ecosystems and low in physically controlled ecosystems (Odum 1971). A recent study showed that the species diversity index was highest in study site V followed by study (Pakhira and Chakraborty 2018) sites III, IV, II, and I (Table 30.15). The measures of diversity are frequently seen as indicators of well-being of the ecological system. The lower value of the diversity index is considered as an indicator of higher pollution (Wilhm and Dorris 1966). Maximum species diversity was found during

Table 30.15 Seasonal variation of Species Diversity Index of five study sites during the study period July 2012–June 2014

Study site	MON 12	POM 12–13	PREM 13	MON 13	POM 13–14	PREM 14
Study site I	0.5122	0.3697	0.4147	0.4852	0.3705	0.3977
Study site II	0.6649	0.6748	0.6577	0.6362	0.6609	0.6479
Study site III	0.8602	0.8501	0.8387	0.8835	0.8524	0.8308
Study site IV	0.7332	0.8649	0.8173	0.7759	0.8556	0.7870
Study site V	0.9076	0.8123	0.8502	0.9589	0.8200	0.8599

monsoon periods in all the five study sites and in two consecutive years followed by post-monsoon for the study sites I to IV while pre-monsoon ranked second position after monsoon at study site V. Comparatively higher species diversity index at study site V than study sites IV, III, II and I was supposed to be due to the occurrence of more dominant species as it is brackish water zone in comparison to other study sites (I–IV) having freshwater influences.

30.3.13.3 Index of Dominance

In an intra-community assemblage, species or species groups normally controlling the energy flow and strongly affecting the prevailing environment of all other species in the same community are known as ecologically dominant (Chakraborty and Choudhury 1994). The degree to which dominance concentrates on any species or species groups can be expressed by an appropriate index of dominance (Odum 1971). The dominant index value is always higher where the community is dominated by less number of species and lowers when the dominancy is shared by a large number of species (Whittaker 1965). Among the five study sites across the Subarnarekha river from the upstream to downstream, the dominance index was recorded as maximum at study site I followed by study sites II, III, IV, and V which endorses the above statement (Table 30.16). Maximum values of dominant indices were found during post-monsoon seasons for study sites I and V; pre-monsoon for study sites II and III and monsoon at study site IV whereas minimum values were recorded during monsoon season in all study sites except study sites II and IV where the minimum values were observed in post-monsoon season (Pakhira and Chakraborty 2018).

30.3.13.4 Species Richness Index

Species richness index is expressed simply by the ratio between total species and the total number of individuals in all species. Species richness index increases with increased complexity of community and decreases where simplification occurs within the community (Bhattacharya and Bhattacharya 1983). The maximum richness index was found at study site V (1.83) followed by study sites III (1.48), IV

Table 30.16 Seasonal variation of Dominance Index of five selected study sites during the study period July 2012–June 2014

Study site	MON 12	POM 12–13	PREM 13	MON 13	POM 13–14	PREM 14
Study site I	0.3956	0.5989	0.5370	0.4386	0.5915	0.5529
Study site II	0.3073	0.2842	0.3116	0.3265	0.2980	0.3200
Study site III	0.1636	0.1814	0.1913	0.1518	0.1773	0.1943
Study site IV	0.2464	0.1613	0.1969	0.2232	0.1683	0.2116
Study site V	0.1886	0.2219	0.2019	0.1609	0.2178	0.1995

Table 30.17 Seasonal variation of species richness index of five selected study sites during the study period July 2012–June 2014

Study site	MON 12	POM 12–13	PREM 13	MON 13	POM 13–14	PREM 14	Mini.	Max.
Study site I	0.663	0.556	0.613	0.675	0.542	0.593	0.542	0.675
Study site II	1.028	0.782	0.883	1.046	0.767	0.908	0.767	1.046
Study site III	1.482	1.204	1.409	1.472	1.160	1.430	1.160	1.482
Study site IV	1.272	0.984	1.237	1.249	0.979	1.283	0.979	1.283
Study site V	1.833	1.540	1.750	1.800	1.526	1.717	1.526	1.833

Table 30.18 Seasonal variation of species evenness index of five selected study sites during the study period July 2012–June 2014

Study site	MON 12	POM 12–13	PREM 13	MON 13	POM 13–14	PREM 14
Study site I	0.732	0.528	0.592	0.694	0.529	0.568
Study site II	0.786	0.798	0.778	0.753	0.781	0.766
Study site III	0.901	0.891	0.878	0.925	0.893	0.870
Study site IV	0.768	0.905	0.856	0.812	0.896	0.825
Study site V	0.753	0.674	0.706	0.796	0.681	0.713

(1.28), II (1.04), and I (0.67). Seasonal species richness fluctuated from a minimum of 0.542 to a maximum of 1.833 (Table 30.17). The maximum species richness was recorded during monsoon and minimum during pre-monsoon for all study sites.

30.3.13.5 Species Evenness Index

Species populations or individual species organisms do not exist in nature by themselves only; instead, they form a part of an assemblage of species population living together in a definite habitat enjoying the impact of certain ecological parameters of locality (Krebs 1985). Dynamic events like recruitment and mortality occurring at the population level also regulate the biotic community structure (Holland and Polgar 1976). Species evenness index is the expression of abundance, i.e., how equally the species are abundant. High evenness occurs when species are equal or virtually equal in abundance. The maximum evenness index was found at study site III (0.925) and minimum at study site I (0.592). Seasonal variation of evenness index displayed maximum during monsoon season for study sites I, III, and V and post-monsoon for study sites II and IV whereas the minimum was recorded during post-monsoon in all study sites except study sites II and IV where monsoon registered the minimum value (Table 30.18).

30.3.14 *Bioremediation: Definition, Concept, Types, and Application*

Bioremediation, defined as the ability of certain organisms or the bio-molecules or types of biomass to bind, accumulate, and concentrate selected ions or other molecules in aqueous solutions for their removal and elimination from the ecosystem. Out of the varied forms of biotic components, mostly organisms under the plant kingdom are used (both macro-sized plants and microorganisms) because of their easy availability, better scopes of cultural propagation, and higher potential for successful future development based on their environmental compatibility and possible cost-effectiveness. A wide range of microorganisms, because of their ability to at least modify toxic species, include bacteria, fungi, yeasts, and algae, and are being used as biologically active methylators. Many microbial detoxification processes include the operating scientific principles for the exclusion of metal ions from the cells, by way of reacting with biogenic ligands causing precipitation and altering their chemical properties. Plants covering the barren nonfertile soil with organic humus can restore moisture content and thereby develop conducive ecological setups for the growth and propagation of other forms of flora and fauna and also serve as a potential agent for bioaccumulating toxic substances like metals as a part of the restoring environmental health of the ecosystem.

30.3.14.1 *Phytoremediation as a New Option: Competitive and Sustainable Solution Against Heavy Metals Toxicity*

Cleaning up of the soils of the rivers contaminated with heavy metals is a very challenging and difficult task for the environmental scientists, engineers and planners due to the potential toxicity and persistent chemical properties of the heavy metals (Chaney et al. 1997; Wu et al. 2007). Alongside a number of existing ex situ and in situ techniques which have been developed to eliminate, decrease, or alter the load of heavy metals in contaminated ecosystems, phytoremediation, the application of plants and microbes for the purpose of bioremediation in different compartments of the environmental (air, soil, and water), is being recognized as an environment-friendly technology for the extraction or immobilization of metals, metalloids, and radionuclides as well as organic xenobiotics (Wu et al. 2007; Jadia and Fulekar 2009; Ali et al. 2013). Moreover, the application of this eco-friendly technique has gained very wide acceptance due to its potential, efficiency, novelty, and cost-effectiveness (Prasad and Freitas 2003; Clemens 2001; Wang et al. 2003; Willscher et al. 2013; Ali et al. 2013).

Strict adherence is required on the basic ecological principles and physical, chemical, and biological processes in devising the phytoremediation technique to remove, degrade, transform, or stabilize contaminants within air, soil, and water (McCutcheon and Schnoor 2003; Alvarez and Illman 2006). The successful outcomes on the application of the phytoremediation are dependent on several other

hydrobiological processes such as hydraulic control, bioaccumulation, biotransformation, volatilization, etc. (Alvarez and Illman 2006). The term “phytoremediation” encompasses several technological subsets, i.e., phytoextraction, phytofiltration, phytostabilization, phytovolatilization, phytodegradation, rhizodegradation, and phytodesalination (Fulekar et al. 2009; Bhargava et al. 2012; Ali et al. 2013), involving various physiological and biochemical mechanisms (Huang et al. 1997; Wu et al. 2007).

30.3.14.2 Subgroups of Phytoremediation

30.3.14.2.1 Phytoextraction

Phytoextraction, designated differently as phytoaccumulation, phytoabsorption, or phytosequestration, mainly emphasizes the modes of absorption and bioaccumulation of persistent toxic substances from the surrounding environments by the different parts of the plants, especially plant roots and their subsequent biological translocation and transfer in the aboveground biomass (Singh and Maheshwari 1993; Kapoor et al. 1999; USEPA 2001; Foyer and Noctor 2005; Wang et al. 2012; Sekara et al. 2005; Rafati et al. 2011; Bhargava et al. 2012; Ali et al. 2013). Phytoextraction of heavy metals involves two different approaches: (1) the use of hyperaccumulators, characterized in having less aboveground biomass but with the higher efficiency to accumulate more heavy metals and (2) other plants, such as *Brassica juncea* (L.) Czern. (Indian mustard) can also be used to accumulate targeted heavy metals but with less intensity and amount by the more aboveground plant biomass so that overall accumulation is almost similar to that of hyperaccumulators (Tlustos et al. 2006; Ali et al. 2013).

30.3.14.2.2 Phytofiltration

Phytofiltration, being an important component within phytoremediation processes, takes care in the removal of pollutants from aquatic ecosystems mostly by roots of aquatic or terrestrial plants and their associated rhizospheric microorganisms (rhizofiltration), making this entire process very much cost-effective (Raskin et al. 1997; Fulekar et al. 2009; Bose et al. 2011; Bhargava et al. 2012; Olguín and Sánchez-Galván 2012; Ali et al. 2013).

30.3.14.2.3 Phytostabilization

Phytostabilization involves the stabilization of contaminants through the establishment of a plant cover with the associated microbial community on contaminated sites in order to reduce the mobility of contaminants through sorption by roots, precipitation, complexation, or changes in metal valence modification of the

physicochemical conditions accumulation by roots or immobilization within the rhizosphere (Berti and Cunningham 2000; Hooda 2007; Ashraf et al. 2010; Bolan et al. 2011; Park et al. 2011).

30.3.14.2.4 Phytovolatilization

Phytovolatilization involves the volatilization of pollutants from the soil into the atmosphere by uptaking of contaminants from soil or water and their transformation into volatile compounds and transfer into the atmosphere (Banuelos et al. 1997; Ashraf et al. 2010). However, this technique involves a series of biological processes for the removal of heavy metals involving the plant community such as (1) uptake of contaminated water by roots of the plants; (2) passing of the absorbed water loaded with heavy metals from the xylem to the leaves; (3) bioconversion into volatile compounds; and (4) volatilization to the atmosphere.

30.3.14.3 Bioremediation: Roles of *Aspergillus* Fungi (F12) for the Removal of Metals

There is a need to develop technologies that can remove toxic heavy metal ions found in wastewaters. Microorganisms are known to remove heavy metal ions from the polluted water. A recent study has documented the proven role of a fungus, *Aspergillus niger* as a potential bioremediator for successfully removing heavy metals such as lead (Pb), cadmium (Cd), copper (Cu), nickel (Ni), and mercury (Hg) from the water-sediment interphase of the Subarnarekha River (Paria and Chakraborty 2019). Mycoremediation has now emerged as an economically viable and eco-sustainable in situ bioremediation technology where fungi are used to eliminate heavy metals from the wastewater (Bharagava 2017; Paria et al. 2018). Earlier studies have recorded 180 species of *Aspergillus*, many of which could exhibit antibacterial activities (Matan et al. 2006). A recent research study conducted by Paria and Chakraborty (2019) had focused on the functional roles of selected fungal strain for the successful bioremediation of selected heavy metals (Pb, Cd, and Hg) from the Subarnarekha River alongside focusing on a new idea of antibacterial roles of the same fungus against various pathogenic bacteria. The research outcomes thereby have opened up new vistas in wastewater management by ensuring bacteria-free, safe, and healthy adequate water supply to human beings. This study had also paved the way for developing a new possibility of utilizing the microbes like *Aspergillus* sp. which in turn ensure the availability and supply of clean and safe water to human beings in terms of portability, adequacy, convenience, affordability, and equity (Paria and Chakraborty 2019). The research outcomes of this study have shown direct bearings of the roles of fungus in the bioremediation process (Paria and Chakraborty 2019). In view of the above, the following research recommendations can be made:

1. The isolated *Aspergillus penicillioides* F12 (MN210327) has both antibacterial as well as heavy metal accumulation activity.
2. This F12 (MN210327) strain can tolerate up to 1000 ppm concentrations of both Cd(II) and Pb(II). Both exopolysaccharide and fungal biomass have been able to remove Hg(II), Cd(II), and Pb(II) in aqueous system.
3. More interestingly, *EPS* are appeared to be the most efficient than total fungal biomass for heavy metals bioaccumulation and their removal of the heavy metals from the aquatic ecosystem.
4. The fungal strain *F12* has been established to render an important contribution toward the simultaneous removal of *Cd(II)* and *Pb(II)* in an aqueous system particularly loaded with industrial wastes.

30.4 Conclusions and Future Perspectives

The pollution of rivers contaminating both soils and waters loaded with different forms of life, has necessitated to undertake eco-remediation and ecorestoration measures. Physical and chemical methods for cleaning up and restoration of heavy metal-contaminated aquatic ecosystem, reveals several limitations with regard to retaining water qualities within the permissible limits and also to combat the problems of the loss of biodiversity. Therefore, the development of eco-friendly methods integrating the knowledge bases of soil chemistry, molecular biology, physiology and biochemistry of plants, physiology, ecology, and microbiology as well as environmental engineering in a holistic manner has appeared to fulfill the purpose for the sustainable ecorestoration of the contaminated, polluted, and eco-degraded riverine ecosystem. Besides, several other biophysical aspects of the aquatic ecosystem such as passive adsorption, active uptake, translocation, accumulation, and chelation mechanisms are required to be taken care of alongside involving biotic agents in such ecorestoration process. It is being hoped that integration of biomonitoring tools with the recent development of bioremediation methods can address several pertinent and challenging questions relating to the future of eco-restoration of ecosystems. Recent long-term research studies by deducting Species Pollution Value (SPV) of different species and Community Pollution Value (CPV) to monitor the ecological changes of East Kolkata Wetland (a Ramsar site) based on the seasonal dynamics of zooplankton (Sanyal et al. 2015) and to assess the ecological status of the Sundarbans mangrove ecosystem (a World Heritage Site) based on the quantitative estimation macrobenthic faunal distribution (Chakraborty et al. 2009) have very effectively pointed out the prospective ways and means for ecorestoration of stressed aquatic ecosystems (Jiang and Shan 2003; Sanyal et al. 2015; Chakraborty et al. 2009; Kennish 2017).

Acknowledgments The authors are thankful to the West Bengal Pollution Control Board for financial support. Special thanks are due to Dr. Subrata Jana, Assistant Professor of Geography for helping the preparation of location maps. The library and laboratory facilities provided by the Vidyasagar University, Midnapore, West Bengal, India is thankfully acknowledged.

References

- Adams SM, Brown AM, Goede RW (1993) A quantitative health assessment index for rapid evaluation of fish condition in the field. *Trans Am Fish Soc* 122(1):63–73
- Adedeji OB, Okerentugba PO, Okonko IO (2012) Use of molecular, biochemical and cellular biomarkers in monitoring environmental and aquatic pollution. *Nat Sci* 10:83–104
- Adriano DC (2001) Trace elements in terrestrial environments: biogeochemistry, bioavailability, and risks of metals. Springer, Berlin
- Ali H, Khan E, Sajad MA (2013) Phytoremediation of heavy metals - concepts and applications. *Chemosphere* 91:869–881
- Alvarez PJJ, Illman WA (2006) Bioremediation and natural attenuation. Environmental science and technology. Process fundamentals and mathematical models. Wiley, Hoboken, NJ
- Annon (2010) Water quality monitoring of five rivers viz. Shilabati, Rupnarayan, Subarnarekha, Dwarakeshwar and Kansai sanctioned by West Bengal Pollution Control Board (Principal Investigator S.K. Chakraborty)
- Annon (2014) Hydrobiological and geomorphological studies of Subarnarekha and Kansai river basins and their interfluves (Purulia, Bankura, Purba and Paschim Midnapore districts) with special reference to environmental management (sanctioned by West Bengal West Bengal Pollution Control Board, Kolkata, India; Principal Investigator, S.K. Chakraborty)
- APHA (2005) Standard method for the examination of water and waste water, 20th edn. American Public Health Association, Washington, DC, pp 1–541
- Ashraf M, Ozturk M, Ahmad MSA (2010) Toxins and their phytoremediation. In: Ashraf M, Ozturk M, Ahmad MSA (eds) Plant adaptation and phytoremediation. Springer, New York
- Aslan-Yilmaz A, Okuş E, Övez S (2004) Bacteriological indicators of anthropogenic impact prior to and during the recovery of water quality in an extremely polluted estuary, Golden Horn, Turkey. *Mar Pollut Bull* 49(11–12):951–958
- Atlas RM, Bartha R (1972) Degradation and mineralization of petroleum in seawater: limitation by nitrogen and phosphorus. *Biotechnol Bioeng* 14:309–318
- Bai SR, Abraham TE (2003) Studies on chromium (VI) adsorption–desorption using immobilized fungal biomass. *Bioresour Technol* 87:17–26
- Banerjee S, Kumar A, Maiti SK, Chowdhury A (2016) Seasonal variation in heavy metal contaminations in water and sediments of Jamshedpur stretch of Subarnarekha river, India. *Environ Earth Sci* 75(3):265
- Banuelos GS, Ajwa HA, Terry N, Zayed A (1997) Phytoremediation of selenium laden soils: a new technology. *J Soil Water Conserv* 52(6):426–430
- Berti WR, Cunningham SD (2000) Phytostabilization of metals: phytoremediation of toxic metals using plants to clean up the environment. In: Raskin I, Ensley BD (eds) Phytoremediation of toxic metals: using plants to clean up the environment. Wiley, New York
- Bhargava RN (2017) Environmental pollutants and their bioremediation approaches. CRC Press, Boca Raton
- Bhargava A, Carmona FF, Bhargava M, Srivastava S (2012) Approaches for enhanced phytoextraction of heavy metals. *J Environ Manag* 105:103–120
- Bhattacharya T, Bhattacharya J (1983) Community structure of soil oribatida as influenced by industrial water. *Entom* 8(4):337–347
- Bhattacharya N, Chakraborty SK (2001) Distributional pattern of some heavy metals in the structural components of two contrasting wetlands in the vicinity of a iron extraction factory of Midnapore District, West Bengal, India. In: Kumar A (ed) Ecology of polluted waters. Ashish Publishing Corporation, New Delhi, pp 287–294
- Bolan N, Park JH, Robinson B, Naidu R, Huh KY (2011) Phytostabilization: a green approach to contaminant containment. *Adv Agron* 112:145–204
- Bose S, Rai V, Bhattacharya S, Chaudhuri P, Bhattacharyya AK (2011) Phytoremediation: a promising technology of bioremediation for the removal of heavy metal and organic pollutants

- from the soil. In: Golubev IA (ed) Handbook of phytoremediation. Environmental science. Engineering and technology. Nova Science, New York
- Bradshaw AD (1997) What do we mean by restoration? In: Urbanska KM, Webb NR, Edwards PJ (eds) Restoration ecology and sustainable development. Cambridge University Press, Cambridge, pp 8–14
- Bragg JR, Prince RC, Harner EJ, Atlas RM (1994) Effectiveness of bioremediation for the Exxon-Valdez oil-spill. *Nature* 368:413–418
- Bruns TD, White TJ, Taylor JW (1991) Fungal molecular systematics. *Annu Rev Ecol Syst* 22:525–564
- Chakrabarti A (2005) Sedimentary structures of tidal flats: a journey from coast to inner estuarine region of eastern India. *J Earth Syst Sci* 114(3):353–368
- Chakraborty SK (2017) Ecological services on intertidal benthic fauna and the sustenance of coastal wetlands along the Midnapore (east) coast, West Bengal, India. In: Coastal wetlands: alteration and remediation. Springer, New York, pp 777–886
- Chakraborty SK (2018) Bioinvasion and environmental perturbation: synergistic impact on coastal-mangrove ecosystems of West Bengal, India. In: Makowski C, Finkl C (eds) Impacts of invasive species on coastal environments: coast in crisis. Springer, New York, pp 171–245
- Chakraborty SK (2020a) Riverine ecology (volume 1): eco-functionality of the physical environment of the rivers. Springer, New York
- Chakraborty SK (2020b) Riverine ecology (volume 2): biodiversity conservation, conflicts and resolution. Springer, New York
- Chakraborty SK, Choudhury A (1992) Ecological studies on the zonation of brachyuran crabs in a virgin mangrove island of Sundarbans, India. *J Mar Biol Assoc India* 34(1 and 2):189–194
- Chakraborty SK, Choudhury A (1994) Community structure of macrobenthic polychaetes of intertidal region of Sagar Island, Hooghly estuary, Sundarbans, India. *Trop Ecol* 35(1):97–104
- Chakraborty SK, Giri S, Chakravarty G, Bhattacharya N (2009) Impact of eco-restoration on the biodiversity of Sundarbans mangrove ecosystem, India. *Water Air Soil Pollut* 9(3–4):303–320
- Chandra AK, Chakravarty G, Chakraborty SK (2003) Polychaete diversity of Midnapore Coastal Belt, West Bengal, India. *J Nat Conserv* 15(2):95–108
- Chaney RL, Malik M, Li YM, Brown SL, Brewer EP, Angle JS, Baker AJM (1997) Phytoremediation of soil metals. *Curr Opin Biotechnol* 8:279–284
- Chaney RL, Angle JS, Broadhurst CL, Peters CA, Tappero RV, Sparks DL (2007) Improved understanding of hyperaccumulation yields commercial phytoextraction and phytomining technologies. *J Environ Qual* 36:1429–1443
- Chapman D (1996) Water quality assessments—a guide to use of biota, sediments and water in environmental monitoring, 2nd edn. UNESCO, WHO and UNEP by E and FN Spon, London, pp 1–626
- Chatterjee S, Krishna AP, Sharma AP (2014) Geospatial assessment of soil erosion vulnerability at watershed level in some sections of the Upper Subarnarekha river basin, Jharkhand, India. *Environ Earth Sci* 71(1):357–374
- Chen Y, Li XD, Shen ZG (2004) Leaching and uptake of heavy metals by ten different species of plants during an EDTA-assisted phytoextraction process. *Chemosphere* 57(3):187–196
- Chiriboga L, Xie P, Yee H, Vigorita V, Zarou D, Zakim D, Diem M (1998) Infrared spectroscopy of human tissue. I. Differentiation and maturation of epithelial cells in the human cervix. *Biospectroscopy* 4(1):47–53
- Clemens S (2001) Developing tools for phytoremediation: towards a molecular understanding of plant metal tolerance and accumulation. *Int J Occup Med Environ Health* 14:235–216
- Crane M, Handy RD, Garrod J, Owen R (2008) Ecotoxicity test methods and environmental hazard assessment for engineered nanoparticles. *Ecotoxicology* 17(5):421
- Dalal A, Gupta S (2015) Rapid bio-assessment of Magura haor (floodplain wetland), Cachar District, Assam, India using aquatic insects. *Curr World Environ* 10(1):296
- Dora MM, Roy NN (1987) Investigation of water quality of Subarnarekha river for irrigation. *Indian J Environ Health* 29(4):292–298

- Dudgeon D (2003) The contribution of scientific information to the conservation and management of freshwater biodiversity in tropical Asia. In: Aquatic biodiversity. Springer, Dordrecht, pp 295–314
- Dutta HM, Adhikari S, Singh NK, Roy PK, Munshi JSD (1993) Histopathological changes induced by malathion in the liver of a freshwater catfish, *Heteropneustes fossilis* (Bloch). Bull Environ Contam Toxicol 51(6):895–900
- Dutta B, Baruah D, Biswas SP (2013) Biomonitoring of benthic macroinvertebrates of the tail race of Dikhow River, Assam, India. Dibrugarh University, Dibrugarh
- Dutta SM, Mustafi SB, Raha S, Chakraborty SK (2014) Assessment of thermal stress adaptation by monitoring Hsp70 and MnSOD in freshwater gastropod, *Bellamya bengalensis* (Lamarck 1882). Environ Monit Assess 186:8961–8967
- Elizabeth KM, Anuradha TVR (2000) Biosorption of hexavalent chromium by non-pathogenic bacterial cell preparations. Indian J Microbiol 40:263–265
- Ezzouhri L, Castro E, Moya M, Espinola F, Lairini K (2009) Heavy metal tolerance of filamentous fungi isolated from polluted sites in Tangier, Morocco. Afr J Microbiol Res 3(2):35–48
- Farombi EO, Adelowo OA, Ajimoko YR (2007) Biomarkers of oxidative stress and heavy metal levels as indicators of environmental pollution in African cat fish (*Clarias gariepinus*) from Nigeria Ogun river. Int J Environ Res Publ Health 4(2):158–165
- Foyer CH, Noctor G (2005) Redox homeostasis and antioxidant signaling: a metabolic interface between stress perception and physiological responses. Plant Cell 17:1866–1875
- Fulekar M, Singh A, Bhaduri AM (2009) Genetic engineering strategies for enhancing phytoremediation of heavy metals. Afr J Biotechnol 8:529–535. <http://www.academicjournals.org/AJB>
- Gerhardt A (1999) Recent trends in online biomonitoring for water quality control. In: Biomonitoring of polluted water: reviews on actual topics. Environmental research forum, vol 9. TTP Switzerland, Trasadingen, pp 95–118
- Geva P, Kahta R, Nakonechny F, Aronov S, Nisnevitch M (2016) Increased copper bioremediation ability of new transgenic and adapted *Saccharomyces cerevisiae* strains. Environ Sci Pollut Res 23(19):19613–19625
- Giri S, Singh AK (2014) Risk assessment, statistical source identification and seasonal fluctuation of dissolved metals in the Subarnarekha River, India. J Hazard Mater 265:305–314
- Giri S, Pradhan P, Chakraborty SK (2008) Studies on hydrobiological status of Kansai and Dwarakeswar river in West Bengal, India. J Indian Fish Soc India 40(1):59–64
- Giri S, Singh AK, Tewary BK (2013) Source and distribution of metals in bed sediments of Subarnarekha River, India. Environ Earth Sci 70(7):3381–3392
- Gola D, Chauhan N, Malik A, Shaikh ZA, Sreekrishnan TR (2017) Bioremediation approach for handling multiple metal contamination. Handbook of metal-microbe interactions and bioremediation. CRC Press, Boca Raton, FL, pp 471–491
- Guo Q, Ma K, Yang L, Cai Q, He K (2010) A comparative study of the impact of species composition on a freshwater phytoplankton community using two contrasting biotic indices. Ecol Indic 10:296–302
- Gupta K, Nandy A, Banerjee K, Talapatra SN (2015) Biomonitoring of river Ganga bank by identifying mollusc species as an indicator. Int Lett Nat Sci 37:71
- Hajjaligo S, Taher MA, Malekpour A (2006) A new method for the selective removal of cadmium and zinc ions from aqueous solution by modified clinoptilolite. Adv Sci Technol 24:487–496
- Hakanson L (1980) Ecological risk index for aquatic pollution control: a sedimentological approach. Water Res 14:975–1001
- Hamba Y, Tamiru M (2016) Mycoremediation of heavy metals and hydrocarbons contaminated environment. Asian J Nat Appl Sci 5:2
- Harrison ET, Norris RH, Wilkinson SN (2008) Can an indicator of river health be related to assessments from a catchment-scale sediment model? Hydrobiologia 600(1):49–64
- Hawkes JS (1997) Heavy metals. J Chem Educ 74:1369–1374

- Hellawell JM (ed) (2012) Biological indicators of freshwater pollution and environmental management. Springer, Berlin
- Higgs E (2003) Nature by design: people, natural process, and ecological restoration. MIT Press, Cambridge
- Holland AF, Polgar TT (1976) Seasonal changes in the structure of an intertidal community. *Mar Boil* 37:341–346
- Hooda V (2007) Phytoremediation of toxic metals from soil and waste water. *J Environ Biol* 28:367–376
- Huang JW, Chen J, Berti WR, Cunningham SD (1997) Phytoremediation of lead-contaminated soils: role of synthetic chelating in lead phytoextraction. *Environ Sci Technol* 31:800–805. <https://doi.org/10.1021/es9604828>
- Jadia CD, Fulekar MH (2009) Phytoremediation of heavy metals: recent techniques. *Afr J Biotechnol* 8:921–928
- Jan AT, Azam M, Ali A, Haq QMR (2014) Prospects for exploiting bacteria for bioremediation of metal pollution. *Crit Rev Environ Sci Technol* 44:519–560. Taylor and Francis Publication
- Jiang JG (2006) Development of a new biotic index to assess freshwater pollution. *Environ Pollut* 139:306–317
- Jiang JG, Shan YF (2003) Development of biotic index using the correlation of protozoan communities with chemical water quality. *J Mar Freshw Res* 37:777–792
- Jonnalagadda SB, Mhere G (2001) Water quality of the Odzi River in the eastern highlands of Zimbabwe. *Water Res* 35(10):2371–2376
- Kamala CT, Balaram V, Satyanarayanan M, Kumar AK, Subramanyam KSV (2015) Biomonitoring of airborne platinum group elements in urban traffic police officers. *Arch Environ Contam Toxicol* 68(3):421–431
- Kapoor A, Viraraghavan T, Cullimore DR (1999) Removal of heavy metals using the fungus *Aspergillus niger*. *Bioresour Technol* 70:95–104
- Karim AA, Panda RB (2014) Assessment of water quality of Subarnarekha river in Balasore region, Odisha, India. *Curr World Environ* 9(2):437
- Karr JR, Chu EW (1999) Restoring life in running waters: better biological monitoring. Island Press, Washington, DC
- Kennish MJ (2017) Practical handbook of estuarine and marine pollution. CRC Press, Boca Raton, FL
- Khalua RK, Chakravorty GC, Chakraborty SK (2008) Community structure of macrobenthic molluscs of three contrasting intertidal belts of Midnapore coast, West Bengal, India. *Zool Res Hum Welf* 6:75–82
- Krebs CJ (1985) Ecology: the experimental analysis of distribution and abundance. Harper and Row, New York
- Lal BB, Diem M, Polavarapu PL, Oboodi M, Freedman TB, Nafie LA (1982) Vibrational circular dichroism in amino acids and peptides. 5. Carbon-hydrogen, stretching vibrational circular dichroism and fixed partial charge calculations for deuterated isotopomers of alanine. *J Am Chem Soc* 104(12):3336–3342
- Lange CR, Lange SR (1997) Biomonitoring. *Water Environ Res* 69:900–915
- Li L, Zheng B, Liu L (2010) Biomonitoring and bioindicators used for river ecosystems: definitions, approaches and trends. *Procedia Environ Sci* 2:1510–1524
- Lorestani B, Cheraghi M, Yousefi N (2012) The potential of phytoremediation using hyperaccumulator plants: a case study at a lead- zinc mine site. *Int J Phytoremediation* 14:786–795
- Mahmood Q, Rashid A, Ahmad SS, Azim MR, Bilal M (2012) Current status of toxic metals addition to environment and its consequences. In: The plant family Brassicaceae. Springer, Dordrecht, pp 35–69
- Maiti SK, Chowdhury A (2013) Effects of anthropogenic pollution on mangrove biodiversity: a review. *J Environ Prot* 4(12):1428

- Maiti Dutta S, Banerjee Mustafi S, Raha S, Chakraborty SK (2014) Assessment of thermal stress adaptation by monitoring Hsp70 and MnSOD in the freshwater gastropod, *Bellamya bengalensis* (Lamarck, 1882). *Environ Monit Assess* 186(12):8961–8967
- Maiti Dutta S, Banerjee S, Mustafi RS, Chakraborty SK (2018) Biomonitoring role of some cellular markers during heat stress-induced changes in highly representative fresh water mollusc, *Bellamya bengalensis*: implication in climate change and biological adaptation. *Ecotoxicol Environ Saf* 157:482–490
- Mandal SM, Mondal KC, Dey S, Pati BR (2007) Arsenic biosorption by mucilaginous seeds of *Hyptissuaveolens* (L.) Poit. *J Sci Ind Res* 66:577–581
- Mason CF (1996) *Biology of freshwater pollution*, 3rd edn. Longman, London
- Matan N, Rimkeeree H, Mawson AJ, Chompreeda P, Haruthaithanasan V, Parker M (2006) Antimicrobial activity of cinnamon and clove oils under modified atmosphere conditions. *Int J Food Microbiol* 107(2):180–185
- McCutcheon SC, Schnoor JL (2003) *Phytoremediation. Transformation and control of contaminants*. Wiley, Hoboken, NJ
- Mehinick EF (1964) A composition of some species individuals' diversity indices applied to samples of field insects. *Ecology* 45:859–861
- Mishra A, Dutta Munshi JS, Singh M (1994) Heavy metal pollution of river Subarnarekha in Bihar, part I: industrial effluents. *J Fresh Water Bio* 6(3):197–199
- Mishra SS, Acharjee SK, Chakraborty SK (2009) Development of tools for assessing conservation categories of silurid fishes of fresh water and brackish water wetlands of South West Bengal, India. *Environ Biol Fish* 84(4):395–407
- Mishra S, Singh SN, Pande V (2014) Bacteria induced degradation of fluoranthene in minimal salt medium mediated by catabolic enzymes in vitro condition. *Bioresour Technol* 164:299–308
- Mohiuddin KM, Zakir HM, Otomo K, Sharmin S, Shikazono N (2010) Geochemical distribution of trace metal pollutants in water and sediments of downstream of an urban river. *Int J Environ Sci Technol* 79:778–783
- Mukhopadhyay SC (1980) *Geomorphology of the Subarnarekha Basin: the Chota Nagpur plateau, Eastern India*. University of Burdwan, Bardhaman
- Muller G (1979) Schwermetalle in den sediments des Rheins-Veranderugen seitt 1971. *Ther Umsch* 79:778–783
- Nagajyoti PC, Lee KD, Sreekanth TVM (2010) Heavy metals, occurrence and toxicity for plants: A review. *Environ Chem Lett* 8(3):199–216
- Nordberg GF, Fowler BA, Nordberg M (2014) *Handbook on the toxicology of metals*, 4th edn. Academic Press, Edinburgh
- Odum EP (1971) *Fundamentals of ecology*. W.B. Sundarbans, Philadelphia and Landan
- Oertel N, Salanki J (2003) Biomonitoring and bioindicators in aquatic ecosystems. In: Ambasht NK (ed) *Modern trends in applied aquatic ecology*. Kluwer Academic/Plenum Publishers, New York, pp 219–246
- Olguín EJ, Sánchez-Galván G (2012) Heavy metal removal in phytofiltration and phycoremediation: the need to differentiate between bioadsorption and bioaccumulation. *New Biotechnol* 30:3–8
- Pakhira H, Chakraborty SK (2016) Diversity and distribution of Molluscs in Subarnarekha River, India with emphasis on identifying indicator species. *Int J Curr Res* 8(11):42162–42164
- Pakhira H, Chakraborty SK (2018) Community structure of benthic mollusks in contrasting ecozones of a transboundary river in India: an ecological interpretation. *Int J Life Sci Res* 6(3):233–238
- Panda UC, Rath P, Sahu KC, Majumdar S, Sundaray SK (2006) Environmental quantification of heavy metals in the Subarnarekha, estuary and near-shore environment, East Coast of India. *Asian J Water Environ Pollut* 3(2):85–92
- Paria K, Chakraborty SK (2019) Eco-potential of *Aspergillus penicillioides* (F12): bioremediation and antibacterial activity. *SN Appl Sci* 1(11):1515

- Paria K, Mandal SM, Chakraborty SK (2018) Simultaneous removal of cd (II) and Pb (II) using a fungal isolate, *Aspergillus penicillioides* (F12) from Subarnarekha estuary. *Int J Environ Res* 12 (1):77–86
- Park JH, Lamb D, Paneerselvam P, Choppala G, Bolan N, Chung JW (2011) Role of organic amendments on enhanced bioremediation of heavy metal(loid) contaminated soils. *J Hazard Mater* 185:549–574
- Parker FS (1971) *Application of infrared spectroscopy in biochemistry, biology and medicine*. Plenum, New York
- Pielou EG (1966) The Measurement of diversity in different types of biological collection. *J Theor Biol* 13:131–144
- Pradhan P, Mishra SS, Majumder R, Chakraborty SK (2003) Environmental monitoring with special emphasis on bio-monitoring: a prerequisite for sustainable environmental management: a case study in Darwakeswar river of South West Bengal, India. In: Kumar A, Bhora C, Sing LK (eds) *Environment pollution and management*. Ashish Publishing Corporation, New Delhi, pp 87–103
- Prasad MNV, Freitas H (2003) Metal hyperaccumulation in plants and biodiversity prospecting for phytoremediation technology. *Electron J Biotechnol* 6:275–321
- Rafati M, Khorasani N, Moattar F, Shirvany A, Moraghebi F, Hosseinzadeh S (2011) Phytoremediation potential of *Populus alba* and *Morus alba* for cadmium, chromium and nickel absorption from polluted soil. *Int J Environ Res* 5:961–970
- Ramakrishna DA (2007) *Handbook on Indian freshwater molluscs*. Zoological Survey of India, Kolkata, pp 1–399
- Rashed MN (2001) Cadmium and lead levels in fish (*Tilapia niloticus*) tissues as biological indicator for lake water pollution. *Environ Monit Assess* 68:75–89
- Raskin I, Smith RD, Salt DE (1997) Phytoremediation of metals: using plants to remove pollutants from the environment. *Curr Opin Biotechnol* 8:221–226
- Resh VH, Norris RH, Barbour MT (1995) Design and implementation of rapid assessment approaches for water resource monitoring using benthic macroinvertebrates. *Aust J Ecol* 20 (1):108–121
- Röling WFM, Milner MG, Jones DM, Fratepietro F, Swannell RPJ, Daniel F, Head IM (2004) Bacterial community dynamics and hydrocarbon degradation during a field-scale evaluation of bioremediation on a mudflat beach contaminated with buried oil. *Appl Environ Microbiol* 70 (5):2603–2613
- Rosenberg DM (1993) In: Resh VH (ed) *Freshwater biomonitoring and benthic macroinvertebrates*. Chapman and Hall, New York
- Rosenberg DM (1998) A national aquatic ecosystem health program for Canada: we should go against the flow. *Bull Entomol Soc Can* 30(4):144–152
- Sanyal P, Bhattacharya N, Chakraborty SK (2015) Biomonitoring of four contrasting wetlands of Kolkata, West Bengal based on zooplankton eco-dynamics and biotic indices. *J Environ Prot* 6 (7):683–699
- Sanyal P, Chakraborty SK, Ghosh PB (2014) Phytoremediation of sewage-fed wetlands of East-Kolkata, India: a case study. *Int Res J Environ Sci* 4(1):80–89
- Sekara A, Poniedzialek M, Ciura J, Jedrszczyk E (2005) Cadmium and lead accumulation and distribution in the organs of nine crops: implications for phytoremediation. *Pol J Environ Stud* 14:509–516
- Senapati NK, Sahu KC (1996) Heavy metal distribution in Subarnarekha River East Coast of India. *Indian J Mar Sci* 25:109–114
- Shannon CE, Weaver W (1949) *The mathematical theory of communications*. Illinois University Press, Urbana
- Shannon MA, Bohn PW, Elimelech M, Georgiadis JG, Marinas BJ, Mayes AM (2010) Science and technology for water purification in the coming decades. In: *Nanoscience and technology: a collection of reviews from nature journals*. World Scientific, Singapore, pp 337–346

- Sharma KK, Chowdhary S (2011) Macroinvertebrate assemblages as biological indicators of pollution in a central Himalayan River, Tawi (JK). *Int J Biodivers Conserv* 3(5):167–174
- Sharma S, Sharma P (2010) Biomonitoring of aquatic ecosystem with concept and procedures particular reference to aquatic macro invertebrates. *J Am Sci* 6:1246–1255
- Sharma S, Singh DN (2015) Characterization of sediments for sustainable development: state of the art. *Mar Georesour Geotechnol* 33(5):447–465
- Sharma KK, Kour S, Antal N (2015) Diversity of zooplankton and macrobenthic invertebrates of two perennial ponds in Jammu region. *J Glob Biosci* 4(2):1382–1392
- Silverstein RM, Bassler GC, Morrill TC (1991) Spectrometric identification of organic compounds. John Wiley & Sons, Oxford
- Simpson EH (1949) Measurement of biodiversity. *Nature* 163:688
- Singh AK, Giri S (2018) Subarnarekha river: the gold streak of India. In: *The Indian rivers*. Springer, Singapore, pp 273–285
- Singh H, Maheshwari JK (1993) Phytotherapy for diphtheria by the Bhoxas of Nainital district, Uttar Pradesh, India. *Ethnobotany* 5:63–65
- Sklar L, Dietrich WE (1998) River longitudinal profiles and bedrock incision models: stream power and the influence of sediment supply. In: *Rivers over rock: fluvial processes in bedrock channels*, vol 107, Boca Raton, FL, pp 237–260
- Smith RL (1996) *Ecology and field biology*, 5th edn. Addison-Wesley Educational Publishers, New York, p 740
- Strayer DL, Dudgeon D (2010) Freshwater biodiversity conservation: recent progress and future challenges. *J N Am Benthol Soc* 29(1):344–358
- Subba Rao NB (1989) *Freshwater Molluscs of India*, vol XXIII. Handbook Zoological Survey of India, Calcutta, pp 1–289
- Supian Z, Ikhwanuddin AM (2002) Population dynamics of freshwater molluscs (gastropod: *Melanooides tuberculata*) in Crocker Range Park, Sabah. *ASEAN Rev Biodivers Environ Conserv (ARBEC)* 11:1–9
- Suthar S, Nema AK, Chabukdhara M, Gupta SK (2009) Assessment of metals in water and sediments of Hindon River, India: impact of industrial and urban discharges. *J Hazard Mater* 171(1–3):1088–1095
- Swannell RPJ, Croft BC, Grant AL, Lee K (1995) Evaluation of bioremediation agents in beach microcosms. *Spill Sci Technol Bull* 2:151–159
- Tchounwou PB, Yedjou CG, Patlolla AK, Sutton DJ (2012) Heavy metal toxicity and the environment. In: *Molecular, clinical and environmental toxicology*. Springer, Basel, pp 133–164
- Tiwari S, Dixit S, Verma N (2007) An effective means of biofiltration of heavy metal contaminated water bodies using aquatic weed *Eichhornia crassipes*. *Environ Monit Assess* 129(1–3):253–256
- Tlustos P, Szakova J, Hruby J, Hartman I, Najmanova J, Nedelnik J, Pavlikova D, Batysta M (2006) Removal of As, Cd, Pb, and Zn from contaminated soil by high biomass producing plants. *Plants Soil Environ* 52:413–423
- Trivedy RK, Goel PK (1984) *Chemical and biological methods for water pollution studies*. Environmental Publications, Karad, pp 1–215
- USEPA (2001) Best management practices for lead at outdoor shooting ranges. EPA-902-B01-001. USEPA, Washington, DC
- Vamerali T, Bandiera M, Mosca G (2010) Field crops for phytoremediation of metal-contaminated land. A review. *Environ Chem Lett* 8:1–17
- Venosa AD, Suidan M, Wrenn T, Strohmeier BA, Haines KL, Eberhart JR, King BL, Holder E (1996) Bioremediation of an experimental oil spill on the shoreline of Delaware Bay. *Environ Sci Technol* 30:1764–1775
- Verkleij JAC, Prast JE (1990) Cadmium tolerance and co-tolerance in *Silene vulgaris*. *New Phytol* 111:637–645

- Vesilind PA, Peirce JJ, Weiner RF (2013) Environmental pollution and control. Elsevier, Amsterdam
- Wang J, Chen C (2009) Biosorbents for heavy metals removal and their future. *Biotechnol Adv* 27 (2):195–226
- Wang WS, Shan XQ, Wen B, Zhang SZ (2003) Relationship between the extractable metals from soils and metals taken up by maize roots and shoots. *Chemosphere* 53:523–530. [https://doi.org/10.1016/S0045-6535\(03\)00518-6](https://doi.org/10.1016/S0045-6535(03)00518-6)
- Wang J, Feng X, Anderson CWN, Xing Y, Shang L (2012) Remediation of mercury contaminated sites – a review. *J Hazard Mater* 221–222:1–18
- Whipple KX, Tucker GE (1999) Dynamics of the stream power river incision model: implications for height limits of mountain ranges, landscape response timescales, and research needs. *J Geophys Res Solid Earth* 104(B8):17661–17674
- Whittaker RH (1965) Dominance and diversity in land plant communities. *Science* 147:250–260
- Wilhm JL, Dorris TC (1966) Species diversity of benthic macroinvertebrates in a stream receiving domestic and oil refinery effluents. *Am Midland Nat* 76:427–449
- Wilfred F. M. Röling, Michael G. Milner, D. Martin Jones, Francesco Fratepietro, Richard P. J. Swannell, Fabien Daniel, and Ian M. Head 2004 Bacterial community dynamics and hydrocarbon degradation during a field-scale evaluation of bioremediation on a mudflat beach contaminated with buried oil. *Applied and Environmental Microbiology* 70(5):2603–2613
- Willscher S, Mirgorodsky D, Jablonski L, Ollivier D, Merten D, Büchel G, Wittig J, Werner P (2013) Field scale phytoremediation experiments on a heavy metal and uranium contaminated site, and further utilization of the plant residues. *Hydrometallurgy* 131–132:46–53
- Woodward G, Perkins DM, Brown LE (2010) Climate change and freshwater ecosystems: impacts across multiple levels of organization. *Philos Trans R Soc Lond B Biol Sci* 365 (1549):2093–2106
- Wu LH, Luo Y, Song J (2007) Manipulating soil metal availability using EDTA and low-molecular-weight organic acids. In: Willey N (ed) *Methods in biotechnology: phytoremediation. Methods and reviews*. Humana, Mahwah, NJ
- Wuana RA, Okieimen FE (2011) Heavy metals in contaminated soils: a review of sources, chemistry, risks and best available strategies for remediation. *Ecology*
- Zhang Y, Sillanpää M, Li C, Qu B, Kang S (2015) River water quality across the Himalayan region: element concentrations in headwaters of Yarlung Tsangpo, Indus and Ganges River. *Environ Earth Sci* 73:4151–4163

Chapter 31

Assessing the Maximum Aerobic Biodegradation Potential of Leaf Litter, an Organic Fraction of Municipal Solid Waste, Under Optimum Nutrient Conditions



Basavaraj R. Hiremath and Sudha Goel

Abstract Biological processes for the treatment of municipal solid waste (MSW) require knowledge of the rate and extent to which each Organic Fraction of MSW (OFMSW) can be biodegraded. A new, rigorous, and controlled laboratory method for determining the maximum biodegradation potential of any OFMSW under aerobic conditions is described here. A batch biodegradation study was conducted in the laboratory with soil inoculum under carbon-limiting aerobic conditions. Leaf litter was used in this study since it is a major organic fraction of MSW in India. Leaf litter samples were incubated at 35 °C in the dark for 180 days. Three sets of samples were evaluated: biotic samples (S), biocide control using sodium azide (SAC), and autoclaved Controls (C). Samples were sacrificed at different time intervals during the incubation period and analyzed for dissolved oxygen, tannin–lignin, pH, conductivity, temperature, Heterotrophic Plate Counts (HPC), Scanning Electron Microscopy (SEM), and Energy Dispersive X-ray (EDX) analysis.

The rates of biodegradation were estimated based on a decrease in Total Suspended Solids (TSS) or Volatile Suspended Solids (VSS). It was observed that TSS removals for biotic, SAC control, and autoclaved control samples were 70.65%, 22.47%, and 17.65%, while removal of VSS were 72.62%, 24.69%, and 21.52%, respectively. Biodegradation kinetics were fit to different reaction orders and the mixed-order model was found to be the best-fit based on R^2 values. This study showed that the rates of biodegradation in biotic samples were much higher compared to SAC and Control samples. The addition of 100 mg/L of sodium azide successfully inhibited the biodegradation of TSS and VSS.

Keywords Tannin · Lignin · Sodium azide · Autoclaved · Abiotic · Heterotrophic plate counts (HPC)

B. R. Hiremath · S. Goel (✉)

Civil Engineering Department, IIT Kharagpur, Kharagpur, India

e-mail: sudhagoel@civil.iitkgp.ac.in

© Springer Nature Switzerland AG 2021

P. K. Shit et al. (eds.), *Spatial Modeling and Assessment of Environmental Contaminants*, Environmental Challenges and Solutions,

https://doi.org/10.1007/978-3-030-63422-3_31

663

31.1 Introduction

Municipal solid waste (MSW) generation rates are increasing exponentially all over the world for two major reasons: increasing population growth and increasing per capita resource consumption (Bundela et al. 2010; Hoornweg and Bhada-Tata 2012; IBRD 1999). Per capita resource consumption is directly related to per capita waste generation (Daskalopoulos et al. 1998; Goel 2008). In the year 2002, MSW generated globally was approximately 0.68 billion tons/year and increased to 1.3 billion tons/year in 2012 (Hoornweg and Bhada-Tata 2012). It is expected to increase to 2.2 billion tons/year by 2025. This represents a significant increase in average per capita waste generation rates from 0.64 (in 2002) to 1.42 (in 2025) kg per capita per day.

Management of MSW is a major challenge not only due to the exponentially increasing quantities of waste but also due to the lack of suitable facilities for its treatment and disposal. Nowadays, landfilling is considered the least preferred option after various other treatment options like composting, incineration, and energy recovery methods like anaerobic digestion. Segregation of organic fractions of MSW is necessary for subsequent treatment by waste-to-energy (WTE) and composting (Goel 2017). In India, the market share of various MSW management technologies is estimated to be composting (50%), anaerobic digestion (30%), pelletization (10%), and sanitary landfilling (10%) (Singh et al. 2011).

Composting has proved to be popular in India both in the public and private sectors making it one of the most cost-effective MSW treatment options. Composting is defined as the conversion of organic waste to stable compost which is rich in inorganic nutrients like N and P. Compost can be used as a nutrient source for plants and as a soil conditioner, making it a valuable end-product. Composting is a biological process that is initially aerobic and can become anaerobic over time depending on the mixing frequency. Composting can be done in windrows with or without turning, in static piles with passive aeration or no aeration, and in reactors. The degree of mixing or turning and its frequency determines the level of aeration in these processes and is a major factor in the efficiency of composting.

Various factors that affect composting include the nature and chemical composition of the waste components, their moisture content, pH, temperature, and nutrient concentrations. MSW contains different organic fractions like leaf litter, newspaper, kitchen or food waste, plastics, rubber, and several other materials. Most of the organic fractions like paper, rubber, and plastic are recyclable and the bulk of these materials are removed prior to disposal in India. Leaf litter and street sweepings in residential areas contribute significant amounts of MSW around the year (Hazra and Goel 2009; Sathiskumar et al. 2001).

The main objective of this study was to measure the maximum possible rate and extent of biodegradability of leaf litter, an organic component of MSW, under optimum conditions by providing more than adequate amounts of oxygen and inorganic nutrients. This information is important for the design of reactor-based composting processes. All essential nutrients required by microorganisms were provided in excess so that carbon could serve as the only growth- and rate-limiting

substrate. Dried leaves of Sal (*Shorearobusta*) were used as the representative organic fraction for leaf litter. Various parameters like dissolved oxygen, pH, total solids, volatile solids, tannin–lignin, conductivity, temperature, and heterotrophic plate counts (HPC) were monitored during an incubation period of 180 days.

31.2 Materials and Methods

31.2.1 Sample Collection and Characterization

Leaf litter from a single species *Shorearobusta* (common name Sal, family *Dipterocarpaceae*) was collected from the vehicle parking area of Civil Engineering Department, IIT Kharagpur, Kharagpur, West Bengal. The sample was dried, ground, and sieved through 300 μ sieves and the powder was used as a sample in the batch biodegradation study. Grinding and sieving the sample ensured that the sample particles were small and relatively uniform in size. The biodegradability of any particle is inversely proportional to its size; therefore, grinding and sieving enhanced the biodegradability of the leaf litter samples. The samples were characterized according to Standard methods for water and wastewater analysis (APHA et al. 2005) where possible and are described in brief in Sect. 31.2.3.

31.2.2 Batch Biodegradation Study with Dried Leaf Litter

Batch biodegradation studies were conducted to determine the extent and rate of aerobic biodegradation of leaf litter in this study.

31.2.2.1 Glassware

All glassware and other materials used in this study were acid-washed and rinsed with distilled water and then autoclaved. Five sets of 15 test tubes were used in this study: three sets of biotic test tubes which were inoculated with soil media, one set of Sodium Azide control (SAC) test tubes were inoculated, and another set of autoclaved Control test tubes which were not inoculated.

31.2.2.2 Mineral Media

Mineral media was added to sample tubes to make sure that carbon from the solid waste sample was the only limiting nutrient and to provide a buffer during incubation (Kandakatla et al. 2013). Concentrations of essential nutrients to be added are based on an estimate of the organic content/gram of sample and the standard BOD

dilution water composition. Five liters of autoclaved double-distilled water were taken in a large glass bottle for each study and mineral media was prepared with the following concentrations (Kandakatla et al. 2013):

Potassium dihydrogen phosphate (KH_2PO_4)—0.08 g/L
Dipotassium hydrogen phosphate (K_2HPO_4)—0.22 g/L
Disodium hydrogen orthophosphate ($\text{Na}_2\text{HPO}_4 \cdot 7\text{H}_2\text{O}$)—0.33 g/L
Ammonium chloride (NH_4Cl)—0.18 g/L
Magnesium sulfate ($\text{MgSO}_4 \cdot 7\text{H}_2\text{O}$)—0.40 g/L
Calcium chloride (CaCl_2)—0.03 g/L
Ferric chloride solution ($\text{FeCl}_3 \cdot 6\text{H}_2\text{O}$)—0.004 g/L
Peptone—0.24 g/L (for providing trace nutrients)

The initial DO of the mineral media was 7.4 mg/L and the initial pH was around 7.28. The mineral media was autoclaved prior to adding it to the autoclaved test tubes.

31.2.2.3 Soil Microbial Seed for Inocula

For microbial seed preparation, 2 g of soil was mixed with 20 mL phosphate buffer (0.008 M) and was made to 200 mL. Soil microbes were added to the buffer solution to create an isotonic media for microbes. This sample was shaken for 1 h and then allowed to settle for half an hour. One milliliter of the supernatant solution was then added to each bioactive (biotic) tube and sodium azide control tubes to provide microbial seed for biodegradation.

31.2.2.4 Procedure for Batch Biodegradation Experiments

A schematic of the procedure followed for these experiments is provided in Fig. 31.1.

1. 50 mg of the dried leaf litter was added to each of 49 ($14 \times 3 = 42 + \text{Extra } 7 = 49$) test tubes along with mineral media and soil bacterial seed and sealed with vented plastic autoclaved caps. These plastic caps were used to ensure aerobic conditions during incubation while avoiding contamination by airborne bacteria. These test tubes were biologically active and are designated “Biotic” (S in figures).
2. For the Control set, 50 mg of sample along with mineral media was added to 21 test tubes and then autoclaved to ensure that there were no bacteria (unseeded) in these tubes. Degradation of leaf litter in the control was indicative of abiotic degradation of the sample.
3. For Biocide Control—Sodium Azide Control (SAC) samples, 50 mg of sample along with mineral media and 1 g/L of Sodium Azide (NaN_3) were added to

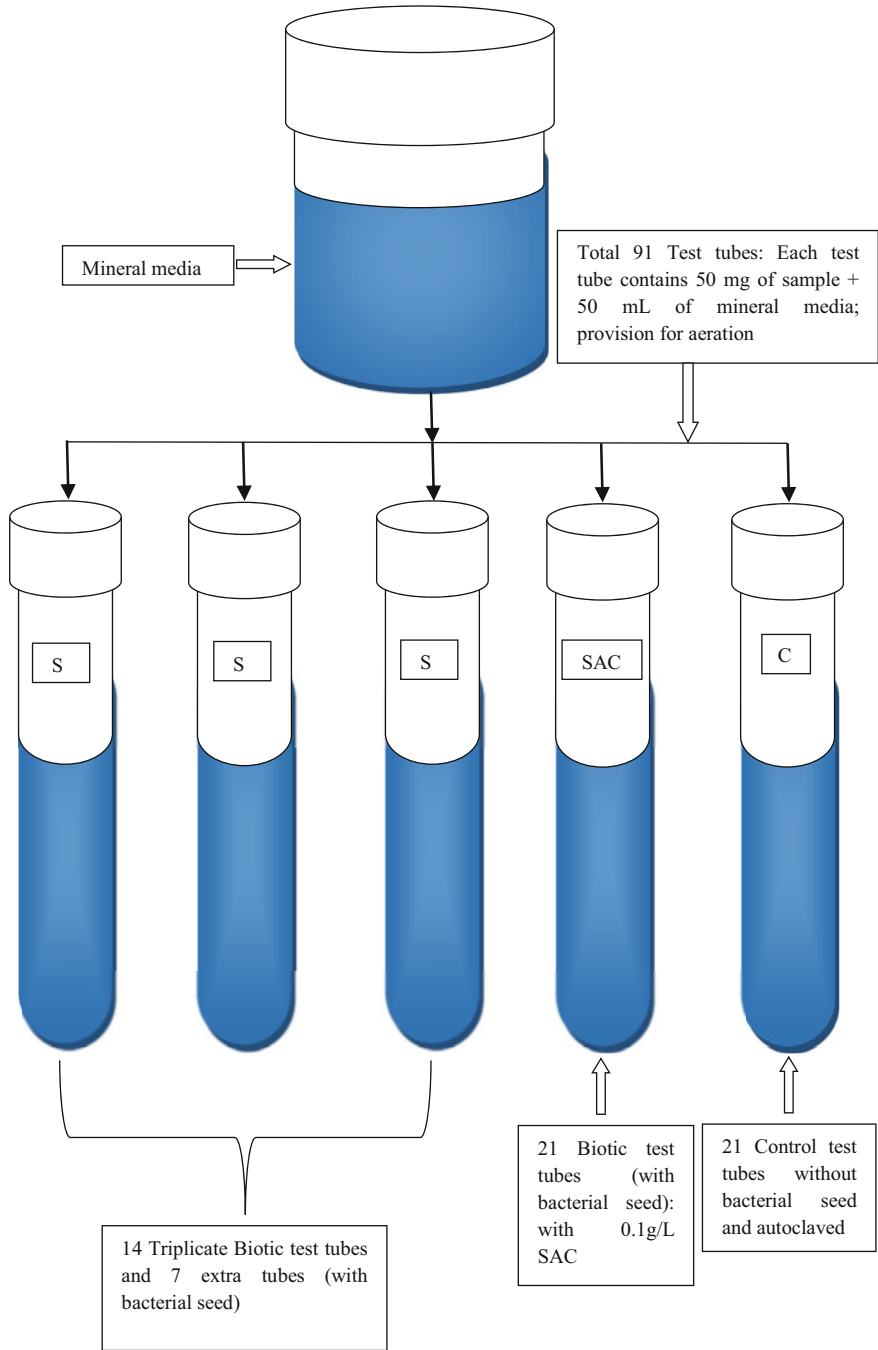


Fig. 31.1 Test tubes used in the batch aerobic biodegradation study with leaf litter

21 test tubes to evaluate the degradation of the organic fraction in the presence of a biocide.

4. For autoclaved control (C in figures)—50 mL of autoclaved mineral media solution that did not contain microbial seed was then added to all tubes. All tubes were sealed with a little headspace for circulation of air.
5. A total of 91 autoclaved test tubes of 50 mL capacity each [Biotic ($14 \times 3 = 42 + 7 \text{ Extra} = 49$) and seeded SAC (21), and unseeded Control samples (21)] were used in the batch biodegradation study. Triplicate sets of bioactive (or “biotic”) tubes (S_1 , S_2 , and S_3), one SAC and one control set were prepared in each study.
6. The sealed tubes were placed in stands and the stands were fixed in a shaker-incubator. This ensured that the tubes were shaken continuously at 120 rpm and incubated in the dark at 35 °C. Dark conditions were necessary to ensure that photosynthesis does not occur in the test tubes.
7. Triplicate biotic tubes were sacrificed along with the two control test tubes and analyzed on each of the following days: 0, 1, 2, 3, 5, 8, 13, 21, 34, 55, 89, 120, 150, and 180 days. Each of the sacrificed tubes was analyzed for the following parameters: DO, pH, TSS, VSS, conductivity, temperature, tannin–lignin, and HPC.
8. Only 2 to 4 samples from each set were sacrificed for SEM and EDX tests.

31.2.3 Analytical Methods

31.2.3.1 Moisture Content (MC)

Each sample of 25 g was taken in a separate crucible dish, and dried to a constant weight in a hot air oven at 105 °C, cooled in a desiccator and the difference in weight recorded. Percentage weight loss of samples after drying gives the moisture content of that sample (Worrell and Vesilind 2012).

31.2.3.2 Solids Characterization

For characterization of solid samples, Total Solids (TS), Volatile Solids (VS), and Fixed Solids (FS) were measured whereas in the case of batch biodegradation study, the liquid samples were filtered and Total Suspended Solids (TSS), Volatile Suspended Solids (VSS), and Fixed Suspended Solids (FSS) were analyzed.

31.2.3.2.1 TS, VS, and FS Analysis

TS was measured by taking 25 g of leaf litter in a crucible and dried overnight at 105 °C in the hot air oven (Bhattacharya and Co., range: 0 °C to 300 °C). Then VS

and FS were measured by burning the samples in a muffle furnace at 550 °C for 1 h (Reico Equipment & Instrument Pvt. Ltd) based on Method 2540 G (APHA et al. 2005).

31.2.3.2.2 TSS, VSS, and FSS Analysis

TSS, VSS, and FSS in the waste samples were analyzed after filtering the sample through Whatman Glass Microfiber Filters, Grade 934-AH having diameter 47 mm and pore size 1.5 µm based on Method 2540 D and 2540 E (APHA et al. 2005). The filter papers with residues of samples were dried overnight at 105 °C in the hot air oven (Bhattacharya and Co., range: 0 °C to 300 °C) and TSS was determined. Then VSS and FSS were measured by burning the samples in a muffle furnace at 550 °C for 1 h (Reico Equipment & Instrument Pvt. Ltd.).

31.2.3.3 Phosphate

Phosphate was determined in the laboratory using a spectrophotometric method, Method 4500-P: D (APHA et al. 2005). One gram of oven-dried sample was digested with 50 mL of HCl acid for 12 hours and samples were filtered through Whatman filter paper (Grade 1, pore size 11 µm) and made to 100 mL with double-distilled water. The absorbance of each sample was measured at 690 nm (Thermo Scientific, Orion Aquamate 7000 VIS Spectrophotometer).

31.2.3.4 Total Kjeldahl Nitrogen (TKN)

TKN was determined using the Kjeldahl distillation apparatus based on Method 4500 B (APHA et al. 2005). One gram of oven-dried sample was mixed with 200 mL of ammonia-free water and poured into a Kjeldahl flask and was subjected to ammonia/ammonium nitrogen and organic nitrogen determination, respectively.

31.2.3.5 Calorific Value

Calorific value was determined in the laboratory using a bomb calorimeter which provides the gross calorific value at constant volume (Worrell and Vesilind 2012).

31.2.3.6 Tannin–Lignin

Tannin–lignin was determined in the lab by using a spectrophotometric method based on Method 5550 B (APHA et al. 2005). One gram of oven-dried sample was digested with 50 mL of HCl acid for 12 hours and samples were filtered through

Whatman filter paper (Grade 1, pore size of 11 μm) and made to 100 mL with double-distilled water. One milliliter Folin phenol reagent and 10 mL carbonate tartrate reagents were added to standard solutions as well as samples. The absorbance of each sample was measured at 700 nm (Thermo Scientific, Orion Aquamate 7000 VIS Spectrophotometer).

31.2.3.7 Chemical Oxygen Demand (COD)

COD is a measure of the oxygen required to oxidize soluble and particulate organic matter present in water. One gram of oven-dried sample was taken and digested with 50 ml HCl acid overnight at room temperature. The sample was then filtered through Whatman filter paper (Grade 1, pore size of 20 μ) and made to 100 mL with double-distilled water. 2.5 mL of the filtered sample was then subjected to the standard COD test based on Method 5220 D (APHA et al. 2005).

31.2.3.8 Total Organic Carbon (TOC)

TOC was measured using Aurora 1030 W TOC Analyser (O.I. Analytical model 1020A USA) which uses the USEPA-approved combustion method for analyzing samples containing 2 ppb to 30,000 ppm of organic carbon. One gram of oven-dried samples were digested with 50 mL HCl acid, filtered through Whatman filter paper (Grade 1, pore size of 11 μm) and made to 100 mL with double-distilled water. Aqueous samples were injected into the TOC Analyser where it was heated to 680 $^{\circ}\text{C}$ in an oxygen-rich environment. Water vapor is removed from the system, and the total carbon content of the sample is oxidized to form carbon dioxide. The carbon dioxide generated by oxidation is detected using a non-dispersive infrared gas analyzer (NDIR) which is directly proportional to the amount of organic carbon in the sample (O.I. Analytical 2002).

31.2.3.9 CHN Analysis

The samples were analyzed in PE 2400 CHNS/O Elemental Analyser which is a combustion technique that provides weight percent of carbon, hydrogen, nitrogen, sulfur, and oxygen.

31.2.3.10 Dissolved Oxygen (DO)

Initially, the DO meter was calibrated as per the manufacturer's instructions based on oxygen in the air. DO concentration in liquid samples was analyzed by placing the probe of the DO meter in the samples (Lutron's Digital Instruments, Model: PDO - 519).

31.2.3.11 Conductivity and Temperature

Conductivity and temperature were measured by using Lab Quest 2 (Vernier Instruments, USA) instrument by placing specific electrodes in the samples after calibration.

31.2.3.12 pH

It was analyzed by using a pH meter (Toshcon Industries Pvt. Ltd., Haridwar, Model: CL 46+) by placing the electrode of the instrument in the samples after calibration.

31.2.3.13 Heterotrophic Plate Counts (HPC)

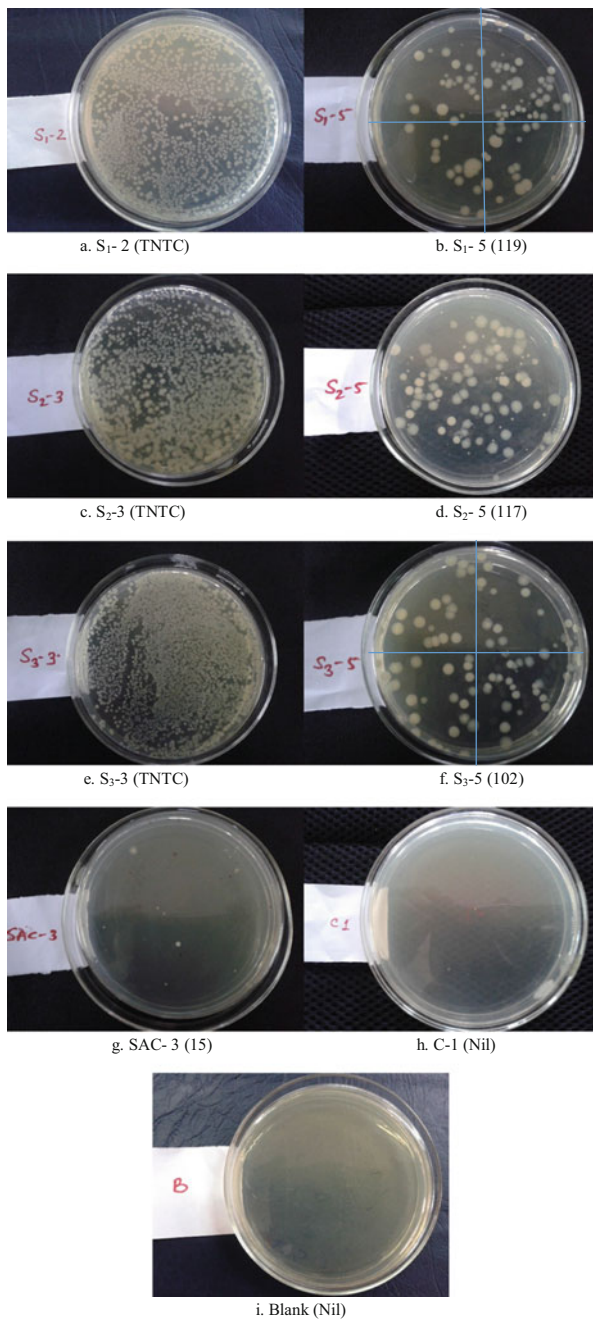
Heterotrophic microbes are broadly defined as microbes that require organic carbon for growth. A variety of simple culture-based tests that are intended to recover a wide range of microorganisms from water are collectively referred to as “heterotrophic plate count” or “HPC test” (Bartram et al. 2004). To determine viable microorganisms, samples from each of the sacrificed test tubes were diluted in sterilized double-distilled water. The numbers of colony-forming units (CFU) were determined by plating 0.1 mL from tenfold serial dilutions on nutrient agar plates (APHA et al. 2005). Plates were incubated at 35 °C for 24–48 h. In HPC tests, a statistically significant number of colonies range from 30–300 colonies; only plates with a statistically significant number of colonies are reported here. The bacterial count per milliliter was computed by the following equation (APHA et al. 2005):

$$\text{CFU/mL} = (\text{Colonies counted}) / (\text{Actual volume of sample added to dish, mL}).$$

Examples of how plate counts were converted to microbial concentrations are explained in detail here.

Some Petri plates with colonies of heterotrophic bacteria are shown in Fig. 31.2a–i for triplicate biotic (S_1 , S_2 , and S_3), SAC (Sodium Azide Control), Control (C), and blank samples, respectively. Dilutions that gave useful results are shown along with results that were Too Numerous To Count (TNTC). Here, S_1 -2 indicates the second dilution of the S_1 sample and S_1 -5 means fifth dilution of the S_1 sample. Similarly, SAC, Control (C), and Blank Petri plates are shown. The values in brackets represent the numbers of bacterial colonies on the plate. These values also represent the number of cells present in 0.1 mL of the respective samples. For example, S_1 -5 (119) indicates that the fifth dilution of S_1 sample, i.e., 10^5 , contained 119 CFU/0.1 mL which is equivalent to 1.19×10^8 CFU/mL. Similarly, S_2 -5 (117) and S_3 -5 (102) result in an average microbial concentration of $1.13 \times 10^8 \pm 9.29 \times 10^6$ CFU/mL in biotic samples and 1.50×10^5 CFU/mL in SAC samples. The control samples

Fig. 31.2 (a–i) Plate counts for S_1 , S_2 , S_3 , SAC, C, and Blank samples in Petri dishes on Day 0 of incubation. (a) S_1 -2 (TNTC), (b) S_1 -5 (119), (c) S_2 -3 (TNTC), (d) S_2 -5 (117), (e) S_3 -3 (TNTC), (f) S_3 -5 (102), (g) SAC-3 (15), (h) C-1 (Nil), (i) Blank (Nil)



were autoclaved and no colonies were detected. In case the numbers of colonies were high, four quadrants were marked on the bottom side of the Petri dish as shown in Fig. 31.2b, f. Colonies in each quadrant were then counted separately and the total numbers of colonies were counted by adding all the colonies present in all four quadrants.

Since a single colony can be detected on a plate, the lower detection limit for HPC in this study was 10 CFU/mL for any plate while it was difficult to count more than 200 colonies so the upper detection limit for each plate was 2000 CFU/mL.

31.2.3.14 Energy Dispersive X-Ray Analysis (EDX) and Scanning Electron Microscope (SEM)

EDX is an X-ray technique used to identify the elemental composition of the surfaces of different materials; depth of sampling is about 1 micron with EDX. For quantitative measurements with EDX using beam energy $E_0 = 5$ keV, the minimum possible detection limit is 0.01 mass fraction or 0.1%. All elements of the Periodic Table can be detected at this beam energy except H, He, and Li (Newbury 2002). EDX and SEM systems were combined in this case and the specimen was characterized by both. EDX analysis shows the spectra of peaks of each elemental constituent of the sample. SEM scans the surface of the sample using a focused beam of electrons and produces images of the sample surface. Thus, the interaction of electrons with the sample atoms produces many signals which contain details of the sample's composition and topography.

31.3 Results and Discussion

31.3.1 Sample Characterization

Leaf litter was characterized for various physicochemical parameters since the rate and extent of biodegradation are related to these characteristics. Three samples of leaf litter were collected and characterized in the laboratory and the results are summarized in Table 31.1 along with typical values for yard wastes as mentioned in Tchobanoglous et al. (1993) or other publications. Values for these leaf litter samples fall within the range noted in these publications.

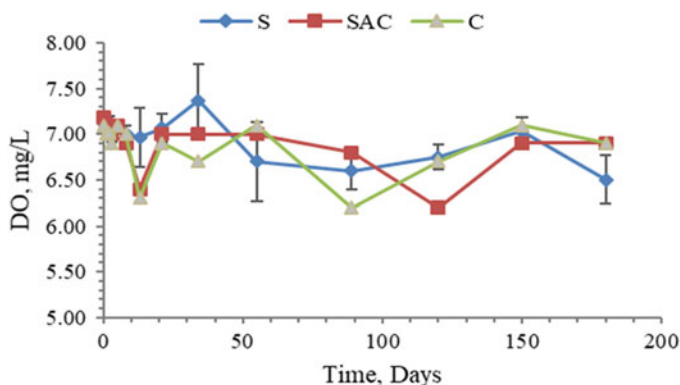
31.3.2 Batch Biodegradation Study

Various parameters were measured for each test tube that was sacrificed and the results are discussed in the following sections.

Table 31.1 Characterization of leaf litter

Parameter	Present study	Typical values
Moisture content (%)	41.28 ± 0.79	30–80% ^a ; 35 ^b ; 40.4 ^c
Calorific value (kJ/kg)	18,129 ± 851	2326–18,600 ^a ; 15,873 ^b ; 16416 ^c
Phosphate (mg P/g waste)	0.54 ± 0.12	0.49 ± 0.03 ^d ; 0.7 ^c
TKN (mg N/g waste)	0.67 ± 0.14	0.336 ^c
TS (%)	77.93 ± 0.56	59.96 ^c
VS (% of TS)	71.35 ± 0.33	50–90 ^a ; 87.5 ± 0.67 ^b ; 69.21 ^c
FS (% of TS)	28.79 ± 0.33	2–6 ^a ; 30.79 ^c
Tannin–lignin (mg/g waste)	12.77 ± 0.54	13.00 ^c
TOC (% C, dry sample waste)	40.43 ± 0.87	41.2 ± 0.23 ^b ; 39.55 ^c
Carbon (%)	43.89 ± 0.65	47.8 ^a ; 41.1 ± 3.00 ^b ; 43.8 ± 0.10 ^d
Hydrogen (%)	06.33 ± 0.38	6 ^a ; 6.70 ± 16 ^b
Nitrogen (%)	01.09 ± 0.15	3.4 ^a ; 1.03 ± 15 ^b ; 1.09 ± 0.08 ^d ; 0.72 ± 0.025 ^c
Oxygen (%)	43.20 ± 1.18	38 ^a ; 38.3 ± 1.7 ^b
C:N ratio	40.27	40.5 ± 10 ^b

Adapted from ^aTchobanoglous et al. (1993); ^bKomilis et al. (2012); ^cKandakatla et al. (2013); ^dSingh et al. (1999); ^eHossain et al. (2013)

**Fig. 31.3** Change in DO concentration in test tubes during incubation of leaf litter samples

31.3.2.1 Dissolved Oxygen

DO concentrations in each set of test tubes are shown in Fig. 31.3 and no significant decrease in DO was observed throughout the experiment. The initial DO concentration of the biotic samples was 7.12 ± 0.10 mg/L and it fluctuated between 6.5 and 7.37 mg/L during the incubation period of 180 days. It was 6.5 ± 0.26 mg/L on the last day of incubation as the availability of air was constant throughout the experiment. Similarly, the initial DO concentration of SAC samples was 7.18 mg/L and it was 6.9 mg/L on the last day of incubation. DO concentration in the Control samples was 7.1 mg/L in the beginning and 6.9 mg/L on the 180th day. The test tubes were

sealed with vented caps which allowed air to enter and maintain aerobic conditions in tubes while preventing the entry of airborne microbes.

31.3.2.2 pH

During the experiment, pH fluctuated between 7.2 and 5.89. The initial pH for biotic samples was 6.85 ± 0.056 (Fig. 31.4) which gradually decreased to 5.89 ± 0.082 after 55 days. Thereafter, it increased to 7.12 ± 0.076 on the 180th day of incubation. Similarly, in SAC control samples, the initial pH was 6.88 which decreased to 6.36 on the 180th day of incubation. In the case of autoclaved Control samples, pH decreased from 6.71 from the first day to 6.47 on the 55th day, and then slightly increased to 6.51 by the 180th day of incubation. These results indicate adequate buffering of the test tube solutions of mineral media used in these experiments.

31.3.2.3 Conductivity and Temperature

Significant changes in conductivity versus time were observed in the biotic, SAC, and control tubes and are shown in Fig. 31.5. Initial conductivity in the biotic tubes was 1.42 ± 0.006 mS/cm and then it fluctuated between 1.39 ± 0.044 mS/cm and 1.45 ± 0.046 mS/cm until day 34. There was a steady increase in conductivity from day 34 until the 180th day and the final value was 2.03 ± 0.043 mS/cm. Similarly, initial conductivity in Sodium Azide Control (SAC) tubes was 1.51 mS/cm and then it fluctuated between 1.44 mS/cm and 1.57 mS/cm until the 21st day. It increased steadily until the 180th day and was recorded as 2.10 ± 0.043 mS/cm. The same trend was followed by autoclaved control (C) samples; the initial conductivity was 1.40 mS/cm and then it fluctuated between 1.35 mS/cm and 1.41 mS/cm up to the 21st day. After that, it increased to 2.13 mS/cm on the 180th day.

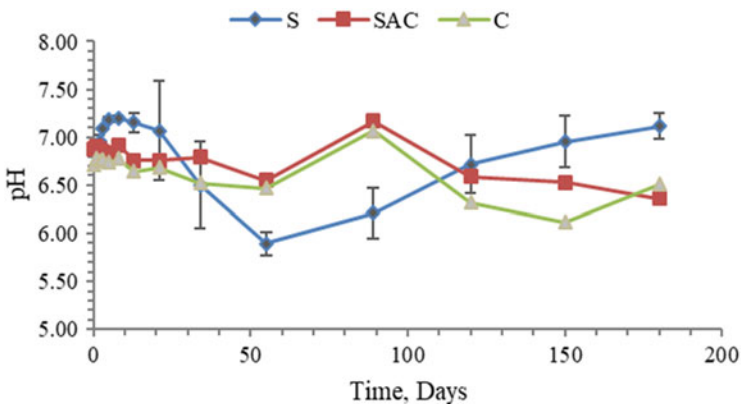


Fig. 31.4 Change in pH in test tubes during incubation of leaf litter samples

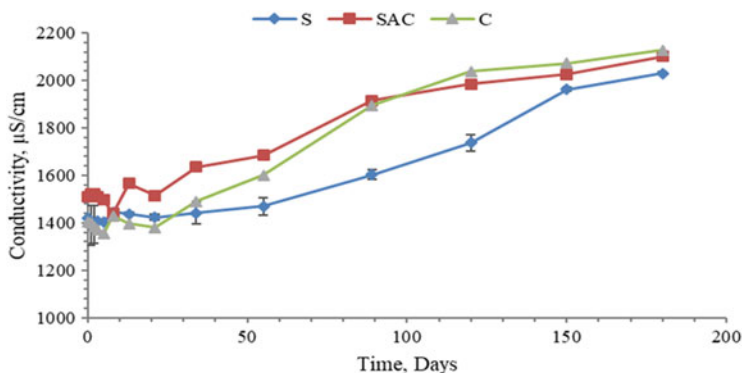


Fig. 31.5 Change in conductivity in test tubes during incubation of leaf litter samples

An increase in conductivity indicates an increase in ionic strength of the solution which may be attributed to the solubilization of suspended solids. There was no significant difference in the increase in conductivity of biotic versus control samples after 180 days while solubilization was slower in the biotic samples compared to the Controls. Slower increase in the biotic samples may be due to the uptake of ions by biomass along with the solubilization of solid waste. Since there is no significant difference between biotic and control samples after 180 days, it suggests that the solubilization process was primarily abiotic.

The temperature of the test tube solutions was found to be approximately equal to the incubator temperature setting of 35 °C throughout the study period.

31.3.2.4 Tannin–Lignin

All tubes were monitored for tannin–lignin content during the incubation period. Initial average tannin–lignin concentration in biotic tubes (S_1 , S_2 , and S_3) was 12.01 ± 0.040 mg/L, which decreased to 2.08 ± 0.018 mg/L in 180 days (Fig. 31.6). For SAC samples, initial tannin–lignin was 12.25 mg/L and decreased to 8.94 mg/L, a small decrease in 180 days. A similar path was followed by sodium azide control (SAC) samples from 13.12 to 10.15 mg/L.

31.3.2.5 HPC

HPC measurements in terms of colony-forming units (CFU/mL) are a measure of the viable microbial cell population. HPC was measured for each of the sacrificed test tubes and converted to microbial cell concentrations as described in Sect. 31.2.3.13. Microbial cell concentrations over the period of incubation in biotic (S) and SAC; and C samples are shown in log-linear graphs in Fig. 31.7.

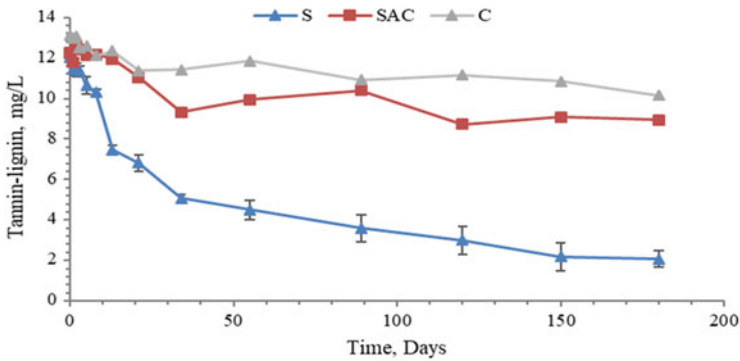


Fig. 31.6 Change in tannin–lignin concentration in test tubes during incubation of leaf litter samples

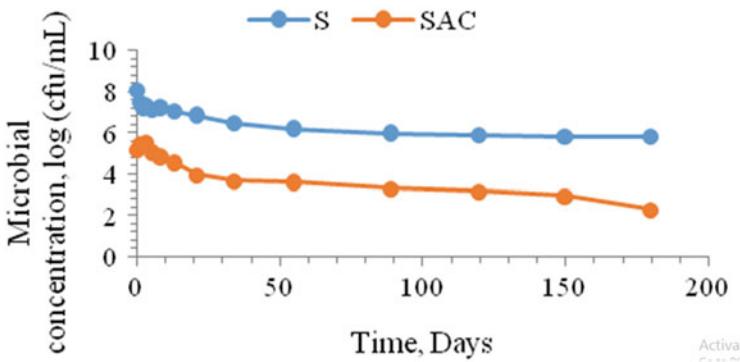


Fig. 31.7 Microbial growth in S and SAC samples

Plate Counts on the 0th Day of Incubation

The average initial microbial concentration in the biotic S tubes was $1.13 \times 10^8 \pm 9.29 \times 10^6$ CFU/mL and decreased rapidly to $1.53 \times 10^6 \pm 1.04 \times 10^5$ CFU/mL by the 55th day of incubation. On the 89th day of incubation, it was $9.47 \times 10^5 \pm 2.52 \times 10^4$ CFU/mL and then remained constant till the end of the incubation period, i.e., $6.27 \times 10^5 \pm 6.03 \times 10^4$ CFU/mL. The constant microbial concentrations of S samples that were observed after 55 days suggest that the growth of microbes was sustainable in these cultures only up to this concentration and the inocula concentrations were too high to increase any further.

Initial microbial concentrations in SAC tubes were 1.5×10^5 CFU/mL; this concentration is 2.824 logs less than the initial concentration in the Biotic tubes and can be attributed to the instantaneous impact of the biocide–sodium azide on microbial concentrations. Final microbial concentrations for S (average) and SAC samples were $6.27 \times 10^5 \pm 6.03 \times 10^4$ CFU/mL and 20 CFU/mL, respectively, after 180 days of incubation and the photographs of the Petri plates are shown in Appendix. Here, S₁₋₃ (62) indicates the third dilution of S₁ sample which contains

62 CFU/0.1 mL. That means S_1 sample contains 6.20×10^5 CFU/mL microbes, similarly S_2 -3 and S_3 -3 Petri dishes contain 6.90×10^5 and 5.70×10^5 CFU/mL microbes, respectively. The sodium azide control sample showed very low concentrations of microbes, 2.0×10^2 CFU/mL, while the autoclaved Control and blank samples remained nil, i.e., no microbes were detected in these samples.

31.3.2.6 Total Suspended Solids (TSS)

TSS concentrations over 180 days are shown in Fig. 31.8. It is apparent that there are three phases in this study: 0 to 55 days, 55 to 120 days, and 120 to 180 days. The initial average TSS concentration in biotic tubes (S_1 , S_2 , and S_3) was 0.92 ± 0.02 g/L which decreased to 0.51 ± 0.02 g/L in 55 days and is a 44.57% decrease in TSS concentration. After 120 days, TSS had decreased to 0.39 ± 0.04 g/L which is a 57.61% decrease in TSS compared to the initial concentration. After 180 days of incubation, the final TSS concentration was 0.27 ± 0.03 g/L, i.e., a 70.65% decrease in TSS concentrations as shown in Fig. 31.8. TSS includes organic and inorganic solids and a decrease in TSS can be attributed to the solubilization of the waste sample and biodegradation of organic matter.

For Sodium Azide Control samples (SAC), initial TSS was 0.89 g/L which decreased to 0.80 g/L in 55 days, 0.76 g/L in 120 days, and 0.69 g/L in 180 days of incubation. The percentage decrease in TSS concentration was 10.11%, 14.61%, and 22.47%, respectively.

Similarly, for the autoclaved Control samples (C), initial TSS was 0.85 g/L which decreased to 0.75 g/L in 55 days and 0.72 g/L in 120 days, and 0.70 g/L in 180 days of incubation. The percentage decrease in TSS concentration was 11.76%, 15.29%, and 17.67%, respectively.

These results indicate that this decrease in TSS may be due to biotic or abiotic factors. The decrease in TSS in both SAC and C samples was very similar. The decrease in TSS in C samples was due to abiotic factors only since no microbes were present in these samples while the decrease in TSS in SAC samples was mainly due

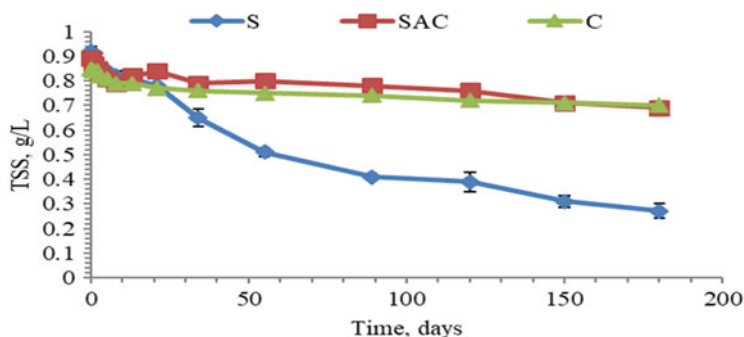


Fig. 31.8 Change in TSS concentrations in test tubes during incubation of leaf litter samples

Table 31.2 Change in biodegradation with respect to time

Sample/day	dC/dt		
	0–55	55–120	120–180
S ₁	0.0073	0.0023	0.0018
S ₂	0.0082	0.0009	0.0031
S ₃	0.0068	0.0022	0.0013
Average (S)	0.0075	0.0018	0.0020
Standard deviation	0.0007	0.0008	0.0009
SAC	0.0016	0.0006	0.0012
C	0.0018	0.0005	0.0003

to abiotic factors with minimal levels of microbial activity; most likely these microbes were from the samples. The inhibitory effect of a biocide–sodium azide on microbial concentrations was observed in SAC samples since TSS reduction in SAC samples was much less than in biotic tubes and almost the same as the control samples.

TSS reduction in the biotic test tubes is mainly due to microbial activity since the microbial concentrations ranged from an average initial concentration of $1.13 \times 10^8 \pm 9.29 \times 10^6$ CFU/mL to $6.27 \times 10^5 \pm 6.03 \times 10^4$ CFU/mL and is much greater than TSS reduction in the SAC and autoclaved Control samples.

The rate of change in TSS concentration was faster in the initial stage, i.e., up to 55 days; for the S sample it was 0.0075 ± 0.0007 and then it became slower from 55 to 120 days (0.0018 ± 0.0008) and from 120 days to 180 days (0.0020 ± 0.0009). Similar trends with much less change in TSS concentration were observed in SAC and C samples as shown in Table 31.2.

31.3.2.7 Volatile Suspended Solids (VSS)

Changes in VSS concentrations during incubation are shown in Fig. 31.9. Initial average VSS concentrations in biotic tubes (S₁, S₂, and S₃) was 0.84 ± 0.02 g/L which decreased to 0.46 ± 0.01 g/L in 55 days, i.e., 45.24% decrease was observed. After 120 days, VSS was 0.32 ± 0.02 g/L which amounts to a 61.90% reduction in VSS. After 180 days of incubation, VSS was found to be 0.23 ± 0.03 g/L, i.e., a 72.62% decrease in VSS concentrations as shown in Fig. 31.9. For Sodium Azide Control samples (SAC), initial VSS was 0.81 g/L which decreased to 0.72 g/L in 55 days and 0.68 g/L in 120 days and 0.61 g/L on the 180th day of incubation, the percentage of decrease in VSS concentration was 11.11%, 16.05%, and 24.69%, respectively. Similarly, for Control samples (C), initial VSS was 0.79 g/L which decreased to 0.68 g/L in 55 days and 0.64 g/L in 120 days and 0.62 g/L on the 180th day of incubation, the percentage decrease in VSS concentration was 13.79%, 18.99%, and 21.52%, respectively.

Significant differences in biodegradation of samples in the biotic and control tubes demonstrate that soil microbes in the biotic tubes were capable of degrading leaf litter. Microbes detected in plate counts included bacteria and fungi.

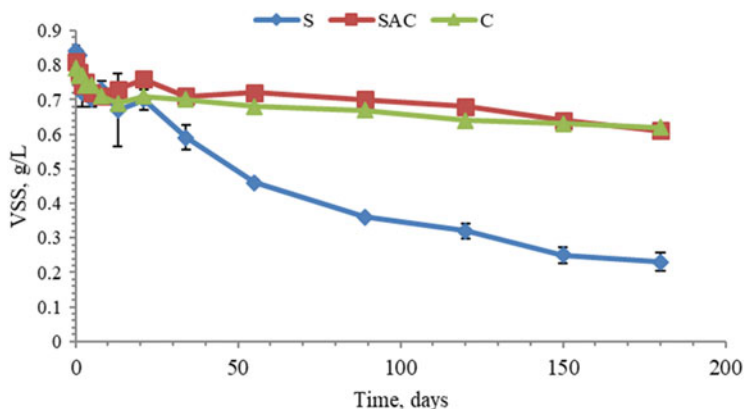


Fig. 31.9 Change in VSS concentration in test tubes during incubation of leaf litter samples

31.3.2.8 EDX Analysis

Elemental analyses of leaf litter, before and after biodegradation, were done by energy-dispersive X-ray spectroscopy (EDX).

Before Biodegradation

Four leaf litter (LL) samples were taken for EDX initially and the % concentration of various elements, their average (Avg.) and standard deviations (SD) values are tabulated in Table 31.3. Some elements were not detected (ND) in some samples.

The initial average concentrations of carbon, nitrogen, and oxygen in leaf litter were $60.00 \pm 4.29\%$, $4.73 \pm 3.64\%$, and $33.60 \pm 1.03\%$, respectively. All other elements were present in lesser amounts. From a composting perspective, C/N ratio is one of the most important parameters and the average was 12.15 in the initial sample.

After Degradation

Elemental analysis was done by selecting four spots in each sample and their averages and standard deviations were determined and are shown in Table 31.3. Since Biotic samples were in triplicate, the total number of Biotic samples was 12. Similarly, four spots were identified in SAC and C samples and the results are tabulated in Table 31.4 along with their average and standard deviations.

All elements were enriched in Biotic (S) samples after degradation except carbon and sulfur indicating their loss from TSS after degradation. The C/N ratio in the S samples was the lowest in comparison to SAC and C samples indicating preferential loss of carbon and enrichment of all other elements due to microbial activity. All other nutrients except carbon were added as part of the mineral media. Al, Si, and Ca were $>1\%$ after degradation of the samples. Inert alumino-silicates are abundant in soil or earth materials and their relative percentage increased due to loss of carbon

Table 31.3 Elemental analysis (% weight) of S, SAC, and C samples before and after biodegradation

Sample/ element	Avg— initial (<i>n</i> = 4)	SD— initial	Avg—S (<i>n</i> = 12)	SD	Avg—SAC (<i>n</i> = 4)	SD	Avg—C (<i>n</i> = 4)	SD
C (K)	60.00	4.29	47.27	3.73	50.31	5.39	58.40	5.19
N (K)	4.73	3.64	10.07	0.91	5.45	3.51	3.14	3.14
O (K)	33.60	1.03	37.14	2.59	41.37	3.80	36.44	5.48
Na (K)	0.04	0.01	ND	—	0.06	0.02	0.05	0.02
Mg (K)	0.16	0.06	0.53	0.27	0.31	0.10	0.26	0.06
Al (K)	0.1	0.08	1.24	0.62	0.46	0.16	0.15	0.05
Si (K)	0.22	0.08	1.41	0.44	0.68	0.28	0.22	0.14
S (K)	0.15	0.07	0.10	0.00	0.07	—	0.03	0.02
P (K)	0.21	0.11	0.50	0.53	0.09	0.01	ND	—
K (K)	0.05	0.04	0.11	0.08	0.11	0.04	0.10	0.03
Ca (K)	0.54	0.16	1.00	0.52	0.70	0.34	0.82	0.13
Mn (K)	0.10	0.05	0.26	0.13	0.12	0.10	0.17	0.14
Fe (K)	0.10	0.06	0.37	0.27	0.27	0.13	0.22	0.04
C/N ratio	12.69		4.73		9.32		18.8	

ND not detected

from the samples by degradation. All other elements were also enriched in Biotic samples for the same reason.

In the case of SAC samples, average carbon, nitrogen, and oxygen contents were $50.31 \pm 5.39\%$, $5.45 \pm 3.51\%$, and 41.37 ± 3.80 , respectively; similarly, for autoclaved control samples, average carbon, nitrogen, and oxygen contents were $58.40 \pm 5.19\%$, $3.14 \pm 3.14\%$, and $36.44 \pm 5.48\%$, respectively. This clearly indicates that the carbon content in biotic samples was utilized to a greater extent compared to SAC and control samples.

31.3.2.9 Scanning Electron Microscopy (SEM)

Leaf Litter Before Biodegradation

SEM images of leaf litter samples before biodegradation shows the solid structure of leaf litter (Fig. 31.10).

Leaf Litter After Biodegradation (After 180th Day)

SEM images of S₁, S₂, and S₃, SAC, and C samples after incubation for 180 days are shown in Fig. 31.11a–e. The obvious change in the character of the samples after incubation is attributed to the loss of the degradable fraction during incubation. The fraction remaining in Biotic samples (S₁, S₂, and S₃) after 180 days is highly filamentous in nature and is likely to be lignocellulose residues. Based on a comparison with images available on the Internet, these images seem to be a combination of lignin and cellulose with an average diameter of less than 3 μm and most of them

Table 31.4 R^2 values and reaction rate constants for different reaction orders and TSS removal

Sample	R^2 values (k values)			Mixed-order rate constant (k) (mg/L-day)	Velocity constant (K) (g/L)
	Zero-order	First-order	Second-order		
S	0.9266 (0.0037)	0.9754 (0.0069)	0.9910 (0.0141)	2.39×10^{-3}	0.81
SAC	0.8138 (0.0011)	0.8319 (0.0008)	0.8467 (0.0014)	8.7×10^{-5}	0.78
C	0.8142 (0.0007)	0.8343 (0.001)	0.8535 (0.0013)	8.4×10^{-5}	0.78

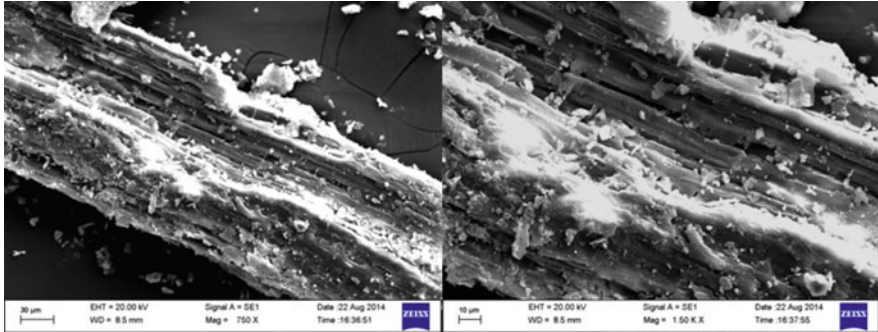


Fig. 31.10 SEM images of leaf litter before biodegradation

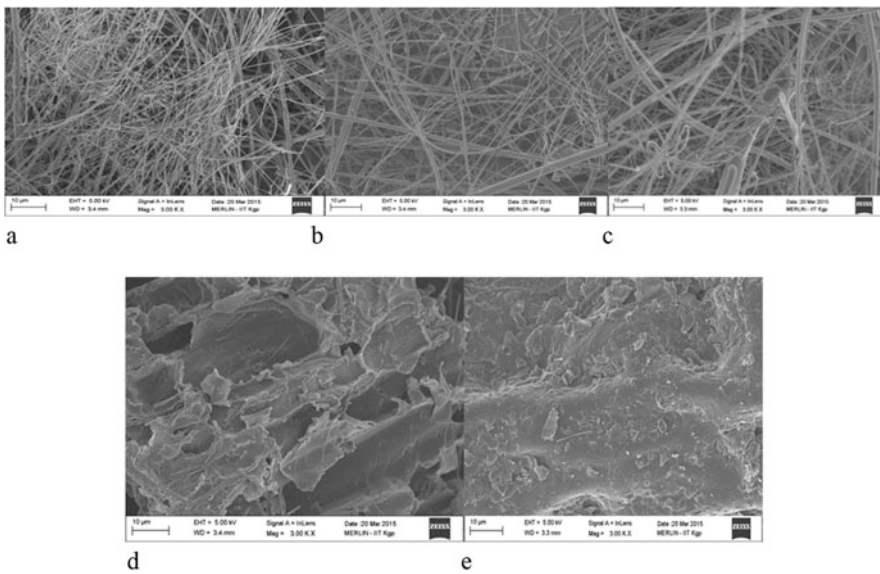


Fig. 31.11 (a–e) SEM images of leaf litter samples S₁, S₂, S₃, SAC, and C samples after 180 days of incubation. (a) SEM image for S₁ sample. (b) SEM image for S₂ sample. (c) SEM image for S₃ sample. (d) SEM image for SAC sample. (e) SEM image for C sample

are about 1 µm. Images of the Control and SAC samples are completely different in nature after incubation and maybe due to the formation of a chemical layer on the sample. The addition of mineral media salts and their precipitation on the solid materials may have resulted in this chemical layer thus preventing microbial growth and degradation of samples.

31.3.3 Reaction Kinetics

Microbial reaction rates are usually considered to be macroscopic explanations of overall reactions for organic matter decomposition based on the order of reaction that best fits the experimental data (Kabbashi and Suraj 2014).

The biodegradation reaction rate constants were determined on the basis of TSS and VSS concentrations during the incubation period. The coefficient of determination (R^2) values were used to determine goodness-of-fit for zero-order, first-order, and second-order reaction kinetics. These reaction rate constants are needed in composter design and can be used to compare the biodegradability of different organic fractions of MSW.

31.3.3.1 Total Suspended Solids

Results for all three sets of test tubes were tested for different models and the graphs for TSS removals from biotic samples S (average of S_1 , S_2 , and S_3) for zero-order (S), first-order (ln S), and second-order (1/S) are shown in Fig. 31.12. Curve-fitting for mixed-order kinetics is shown for the same data set in Fig. 31.13. Similarly,

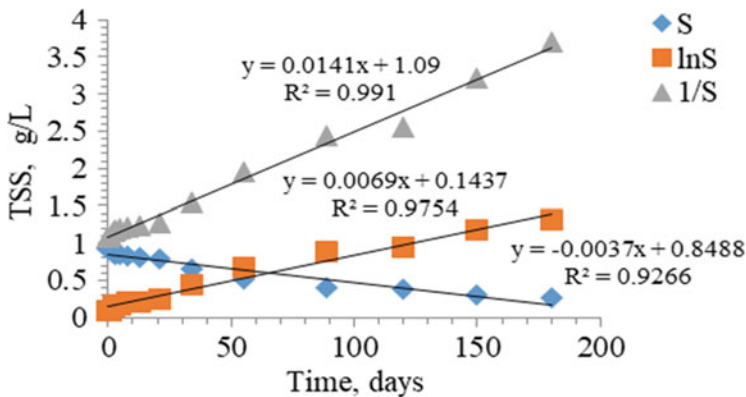


Fig. 31.12 Reaction kinetics (zero-, first-, second-order) for TSS removal from Biotic (S) sample

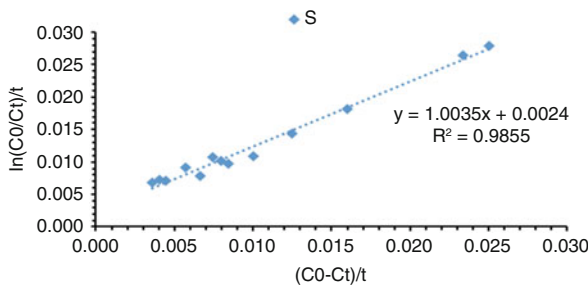


Fig. 31.13 Mixed-order reaction kinetics for TSS removal from biotic (S) sample

model results for TSS removals for SAC (with seed) and Control samples (without seed) were calculated and the corresponding R^2 values and reaction rate constants (k) in parenthesis and mixed-order (saturation) R^2 and k values are summarized in Table 31.4.

From the above graphs and tables, it is clear that TSS values for all the three samples, i.e., S, SAC, and C samples were best-fit by the mixed-order reaction kinetic model. The k value for the biotic samples was much higher (0.00239 mg/L-day) than for SAC and Control. The k value of S samples is slightly higher than reported by Singh et al. (1999) (1.8×10^{-3}).

31.3.3.2 Volatile Suspended Solids

The coefficients of determination (R^2) values and reaction rate constants (k) of the three biotic samples S (average of S_1 , S_2 , and S_3), SAC, and C for VSS, for zero-order (S), first-order (ln S), second-order (1/S), and mixed-order were determined for VSS data. The corresponding R^2 values and order reaction rate constants (k) are summarized in Table 31.5.

From the preceding graphs and tables, it is clear that the VSS values of all three samples, i.e., S, SAC, and C samples were best-fit for mixed-order reaction kinetics.

The k values for TSS and VSS of S samples were 0.00239 and 0.00137 mg/L-day, respectively. The higher k value for TSS as compared to VSS is due to a combination of solubilization and biodegradation while the k values for SAC and Control are mainly due to solubilization of leaf litter sample. Biotic samples had much higher k values than SAC and Control samples, whereas there was very little difference between the k values for SAC and Control samples. This indicates that the reaction rate in biotic samples is much faster than the SAC and Control samples and can be attributed to the mineralization of organic material by microbes. In the case of sodium azide (a biocide) samples, the growth of bacteria was inhibited while the rate of reaction of Control samples was naturally reduced as they were autoclaved and had no microbial seed.

Table 31.5 Comparison of R^2 values (goodness-of-fit) and mixed-order rate constants (k) of VSS values for the three samples

Samples	R^2 values				Mixed-order rate constants (k) (mg/L-day)
	Zero-order	First-order	Second-order	Mixed-order	
S	0.9205 (0.0034)	0.9762 (0.0072)	0.9905 (0.0173)	0.9965	1.37×10^{-3}
SAC	0.7759 (0.0007)	0.7986 (0.0011)	0.8170 (0.0016)	0.9996	7.824×10^{-5}
C	0.7934 (0.0008)	0.8196 (0.0011)	0.8840 (0.0016)	0.9998	1.6×10^{-4}

31.4 Conclusions

- A batch aerobic biodegradation study was conducted with leaf litter, a major organic fraction of municipal solid waste (OFMSW) to determine its maximum biodegradation potential under controlled laboratory conditions. The method used here can be applied to any OFMSW to determine its biodegradable fraction.
- TSS removals for biotic, sodium azide control, and autoclaved control samples were 70.65%, 22.47%, and 17.67%, respectively. Removals of VSS for biotic, sodium azide control, and autoclaved control samples were 72.62%, 24.69%, and 21.52%, respectively. These results indicate that biodegradation was least in the autoclaved control samples compared to the biotic samples and demonstrates that abiotic factors caused a small but measurable decrease in VSS.
- The addition of 100 mg/L of sodium azide inhibited but did not prevent biodegradation of TSS and VSS. However, there was more degradation in SAC compared to the autoclaved Control due to the addition of microbial seed in SAC. This suggests that biodegradation of the sodium azide control samples was mainly due to abiotic factors as evidenced by low microbial counts. The differences in biodegradation of the samples in the biotic, SAC, and control tubes demonstrate that soil seed was capable of degrading leaf litter. Also, autoclaving was more effective in preventing microbial growth as compared to sodium azide. Microbes detected in plate counts included bacteria and fungi.
- Based on EDX analysis, only C was significantly reduced in these samples after biodegradation resulting in a lower C:N ratio. All other elements were enriched in the sample.
- Mixed-order or saturation kinetics were the best-fit for the biodegradation data in this study.

Acknowledgments This research was funded by the Ministry of Human Resources Development, Government of India under the Future of Cities project. The authors are grateful to Central Research Facility, IIT Kharagpur for performing EDX and SEM analysis; Department of Chemistry, IIT Kharagpur for CHNOS analysis; Geology Department, IIT Kharagpur for ICPMS analysis; and SESE Department, IIT Kharagpur, for TOC analysis. The first author is grateful to the Chairman BVVS and Principal of Basaveshwar Engineering College, Bagalkot; DTE Karnataka State, for deputation under QIP quota. The authors would like to thank Rajesh K for his help with laboratory analysis.

Appendix

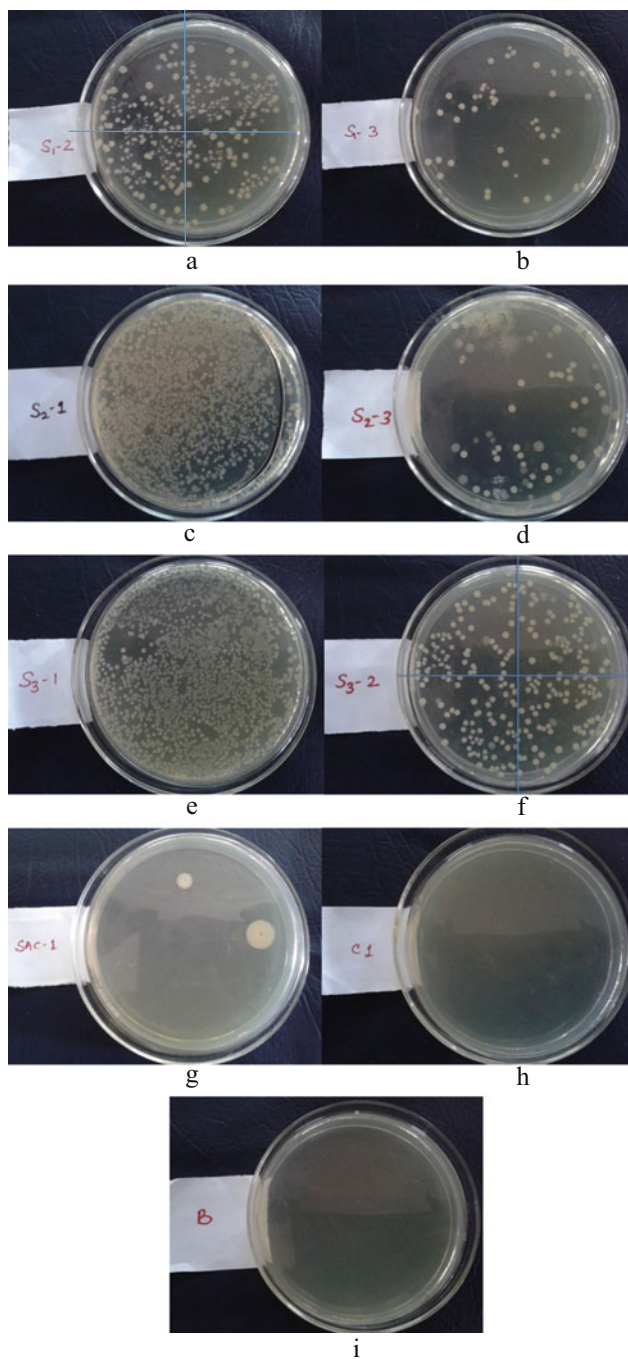


Fig. 31.14 (a–i) HPC for S, SAC, C, and Blank samples on 180th day of incubation. (a) S₁-2 (TNTC), (b) S₁-3 (62), (c) S₂-1 (TNTC), (d) S₂-3 (69), (e) S₃-1 (TNTC), (f) S₃-2 (TNTC), (g) SAC-1 (02), (h) C-1 (NIL), (i) Blank (Nil)

References

- APHA, AWWA, WEF (2005) Standard methods for Examination of Water and Wastewater, 21st ed. American Public Health Association
- Bartram J, Cotruvo J, Exner M, Fricker, C, Glasmacher A (2004) Heterotrophic plate Count measurement in drinking water safety management. *Int J Food Microbiol* 92(3):241–247
- Bundela PS, Gautam SP, Pandey AK, Awasthi MK, Sarsaiya S (2010) Municipal solid waste management in Indian cities - a review. *Int J Environ Sci* 28:459–467
- Daskalopoulos E, Badr O, Probert SD (1998) Municipal solid waste: a prediction methodology for the generation rate and composition in the European Union countries and the United States of America. *Resour Conserv Recycl* 24:155–166. [https://doi.org/10.1016/S0921-3449\(98\)00032-9](https://doi.org/10.1016/S0921-3449(98)00032-9)
- Goel S (2008) Municipal solid waste management (MSWM) in India: a critical review. *J Environ Sci Eng* 50:319–328
- Goel S (2017) Solid and hazardous waste management: an introduction. In: Goel S (ed) *Advances in solid and hazardous waste management*. Springer and Capital Books, Delhi, pp 1–370
- Hazra T, Goel S (2009) Solid waste management in Kolkata, India: practices and challenges. *Waste Manag* 29:470–478. <https://doi.org/10.1016/j.wasman.2008.01.023>
- Hoornweg D, Bhada-Tata P (2012) What a waste: a global review of solid waste management. Urban Development Series Knowledge Papers, Washington, DC. <https://doi.org/10.1111/febs.13058>
- Hossain Z, Ahmed A, Hoque S (2013) Decomposition and nutrient release of Sal leaf litter as influenced by legume leaf litter of the Sal forests. *Dhaka Univ J Biol Sci* 22(2):183–186
- IBRD WB (1999) What a waste: solid waste management in Asia. World Bank, Washington, DC
- Kabbashi N, Suraj O (2014) Kinetic study for compost production by isolated fungal strains. *Int J Waste Resour* 04:1–6. <https://doi.org/10.4172/2252-5211.1000169>
- Kandakatla P, Mahto B, Goel S (2013) Extent and rate of biodegradation of different organic components in municipal solid waste. *Int J Environ Waste Manag* 11:350–364
- Komilis D, Evangelou A, Giannakis G, Lymperis C (2012) Revisiting the elemental composition and the calorific value of the organic fraction of municipal solid wastes. *Waste Manag* 32:372–381. <https://doi.org/10.1016/j.wasman.2011.10.034>
- Newbury DE (2002) Barriers to quantitative electron probe x-ray microanalysis for low voltage scanning electron microscopy. *J Res Natl Inst Stand Technol* 107:605–619
- Sathiskumar R, Chanakya HN, Ramachandra TV (2001) CES technical report 85:60
- Singh KP, Singh PK, Tripathi SK (1999) Litter fall, litter decomposition and nutrient release patterns in four native tree species raised on coal mine spoil at Singrauli, India. *Biol Fertil Soils* 29:371–378
- Singh RP, Tyagi VV, Allen T, Ibrahim, MH, Kothari R (2011) An overview for exploring the possibilities of energy generation from municipal solid waste (MSW) in Indian scenario. *Renew Sust Energ Rev* 15(9):4797–4808
- Tchobanoglous G, Theisen H, Vigil S (1993) *Integrated solid waste management: engineering principles and management issues*. McGraw Hill, Singapore
- Worrell WA, Vesilind PA (2012) *Solid waste Engineering*, 2nd edn. Cengage Learning, Stamford. <https://doi.org/10.1017/CBO9781107415324.004>

Chapter 32

Rising Trend of Air Pollution and Its Decadal Consequences on Meteorology and Thermal Comfort Over Gangetic West Bengal, India



Debjeni Dutta and Srimanta Gupta

Abstract Indo-Gangetic Plain is a renowned hotspot of high-level air pollution for the last few decades. Beginning with the northern urban–industrial development, now the pollution sources have spread over its lower catchment at an alarming rate, covering the south of the state West Bengal. Subsiding winds have further escalated the pollution level over this state by carrying pollutants from the upper catchment. Responding to those two factors, the aerosol optical depth over the lower Gangetic plain in West Bengal often crosses a value of 0.6, with an emission of more than 130 metric tons of carbon dioxide annually. This region is mainly dominated by eight distinct land use classes and has diverse pollution sources from industrial emissions, vehicular emissions, domestic pollution to biomass burning. With the rapid urban–industrial progress, the pollution emission is at its high peak in recent history, but not enough remediation policies are taken till date with a poor pollution monitoring status. Outcomes of the WRF-CHEM model indicate an increase of 0.8 °C to 1.2 °C air temperature with 1.5 to 1.8 W/m² increase of sensible heat flux due to rising air pollution in the lower Gangetic plain of West Bengal. Vertical pressure–temperature profile as well as the boundary layer temperature and surface humidity are found to be affected by certain high pollution periods over the year. The altered atmospheric chemistry by anthropogenic pollution is often found to push the temperature–humidity index level from “mild stress” to “severe stress” category in pre-monsoon seasons, compelling the residents to feel an irritating level of thermal discomfort.

Keywords Air pollution · WRF-CHEM · Thermal discomfort · Lower gangetic plain · West Bengal

D. Dutta · S. Gupta (✉)

Department of Environmental Science, The University of Burdwan, Bardhaman, India

© Springer Nature Switzerland AG 2021

P. K. Shit et al. (eds.), *Spatial Modeling and Assessment of Environmental Contaminants*, Environmental Challenges and Solutions,

https://doi.org/10.1007/978-3-030-63422-3_32

689

32.1 Introduction

Anthropogenic emissions, including aerosols and greenhouse gases, are identified as the major sources of pollution in contemporary times. It not only has a direct impact on human health but also secures an indirect way to affect healthy living by influencing the weather conditions from time to time (Seinfeld and Pandis 1998; Rosenfield et al. 2008). Many of the urban heat islands face a suffocating condition in the high pollution period because of increased heat and humidity levels in the cities (Wang et al. 2019). The increase of greenhouse gases is considered as the reason for a 0.8 °C increase in global temperature since the industrial revolution (Allen et al. 2009). Apart from the gases, 20–40% of the global aerosol optical depth and one-fourth to two-third of cloud condensation nuclei formation are found to occur as anthropogenic contribution (Boucher et al. 2013). Though the warming potential of greenhouse gases majorly has brought a serious concern on policymakers, making the global political powers to sign in various treaties of controlling the pollution, the aerosols are not much behind in this case. The sulfate and carbonaceous aerosols are found to have a direct impact on cloud formations, rainfall, and radiative forcing in the past few decades (Rosenfield 2000; Luan et al. 2019).

The rising pollution has been pointed out as one of the causes of the rising number of respiratory diseases (Ghude et al. 2016), and sometimes is surmised of causing some lung cancer cases also (Cohen 2003; Bhargava et al. 2018). In its indirect affecting method, the asphyxiate atmosphere created by the changed meteorological conditions by various human activities decreases the working ability of people (Yildizel et al. 2015), and in some cases, can lead to a sunstroke. The increase of temperature may not be enough for creating a serious effect on health, but associating with humidity and other weather parameters, it can cross the critical level of thermal comfort (Armstrong 1994).

The sources of pollution in India are mainly confined to the energy sector, then industries and transportation sectors (www.ghgplatform-india.org accessed on 12.02.2020). Studies found that a good number of aerosols are also being transported from the Middle East (Das et al. 2013) in pre-monsoon times. The subsiding zone of this out-country pollution is mainly the Indo-Gangetic plain (Kumar et al. 2018), and in India itself, this Indo-Gangetic plain (IGP) is recognized as the major area emitting air pollutants (Sapkota et al. 2015; Ojha et al. 2020). The industries along the Ganga river tract, the biomass burnings in upper IGP, the pollution emitted from urban activities in the major cities, all contribute to this process. The IGP region experiences different weather and climatic patterns in its different parts, as it covers a 2.5 million km² area, where the uppermost part goes through a dry and quite extreme hot and cold weather, the lowermost part consists of hot and humid atmospheric conditions with mild winter. There are many studies on the pollution aspect in IGP and its interaction with climate in the upper catchment of Ganga (Badarinath et al. 2009; Ghosh and Tripathi 2014; Jethva et al. 2019), whereas fewer numbers are available on its lower catchment (Kar et al. 2010; ParthSarathi et al. 2019; Talukdar

and Maitra 2020), particularly concentrating over Kolkata, the capital of West Bengal. The climate of the lower part of the Gangetic plain may have a different interaction pattern with the atmospheric chemistry in different seasons, and maybe, therefore, the pollution-reducing policies also ought to be different for this portion, if needed, as sometimes the micro-region's results look different than a regional area (Ehret et al. 2012). Another interesting fact regarding the importance of weather-chemistry simulation studies is that very limited research till date has been able to establish the perfect set of relationships between meteorology and chemical variables portraying exactly the same scenario like the real conditions, particularly in the Indian subcontinent. Because of the presence of too many interdependent phenomena among the interacting variables, the use of computerized simulations by numerical models like WRF-CHEM, CHEMIRE, CAM-CHEM, WRF-CMAQ has gained popularity at present time (Kong et al. 2015; Forkel et al. 2016). The outcome of these models too bears a distinct range of bias between the real and modeled outputs of variables. Studies conclude that improvements are needed in the simulation processes as well as in the emission inventories to get a better result (Makar et al. 2014; Saikia et al. 2019).

The present research aims to figure out the interaction between the weather and pollution in the lower part of Gangetic plain, i.e., the southern part of the state West Bengal in India, over the last decade (2010–2019). Another objective of this research is to estimate the thermal comfort level in the study area in different seasons, particularly in peak pollution periods. This can help to understand the effect of anthropogenic pollution on healthy living with respect to heat regime, besides the direct effect of pollution on human health.

32.2 Study Area

The lowermost part of the IGP catchment, i.e., the region near the mouth of river Ganga in the Bay of Bengal, is selected as the study area for this research. It is the southern part of the state West Bengal in India, with a 69,945 square kilometer area, covering 15 districts of the state, namely, Murshidabad, Birbhum, Nadia, Purba Bardhaman, Paschim Bardhaman, Purulia, Bankura,

Hooghly, Howrah, Kolkata, North 24 Parganas, South 24 Parganas, Purba Medinipur, Paschim Medinipur, and Jhargram (Fig. 32.1). In general, the climate of this portion is of tropical savanna type, but the western portion, which is a part of highland, is comparatively dry than the humid eastern and southern part. This humid nature reduces a bit in winter upon the influence of cold and dry northern winds, with an average temperature of 15 °C. In summer, the temperature often reaches to maximum 40 °C with humidity more than 80% in monsoon seasons in some areas (Sarkar et al. 2013).

Throughout the last few decades, with an increasing population (according to the census, 2011 study area population is 71 million with a decadal growth of 13.93%), the anthropogenic emissions also increase in this area. The rising pollution in

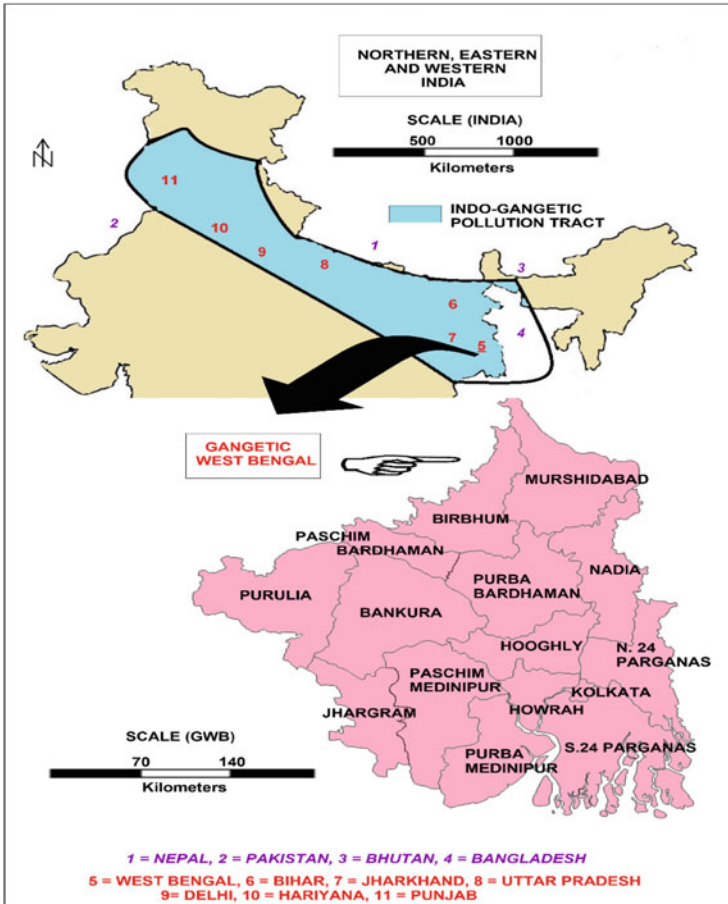


Fig. 32.1 Study area

Kolkata metropolitan area is a headache for the last 15 years, and in 2019, six more cities, namely, Asansol, Durgapur, Raniganj, Howrah, and Haldia belonging to the Gangetic West Bengal (GWB) are listed as non-attainment cities by CPCB. All of the cities are from industrial sectors. In the north-western part of GWB, there are 107 active coal mines in the Paschim Bardhaman district, followed by a large number of industries, including cement and iron and steel industries, sometimes denoted as “ADDA” or Asansol Durgapur Development Authority’s region (MSME 2019). The Haldia Petrochemical industries belong to the Haldia industrial cluster from the 1960s in the Purba Medinipur district. Since long back Kolkata and Howrah remain as a big hub of urban–industrial activities (Fig. 32.2). There are numerous small clusters of industries having air pollution potential in Murshidabad, Nadia, Bagnan–Kolaghat area, and Barasat. Among them in 72 air quality monitoring stations are located on or near those urban-industrial areas in Gangetic West Bengal

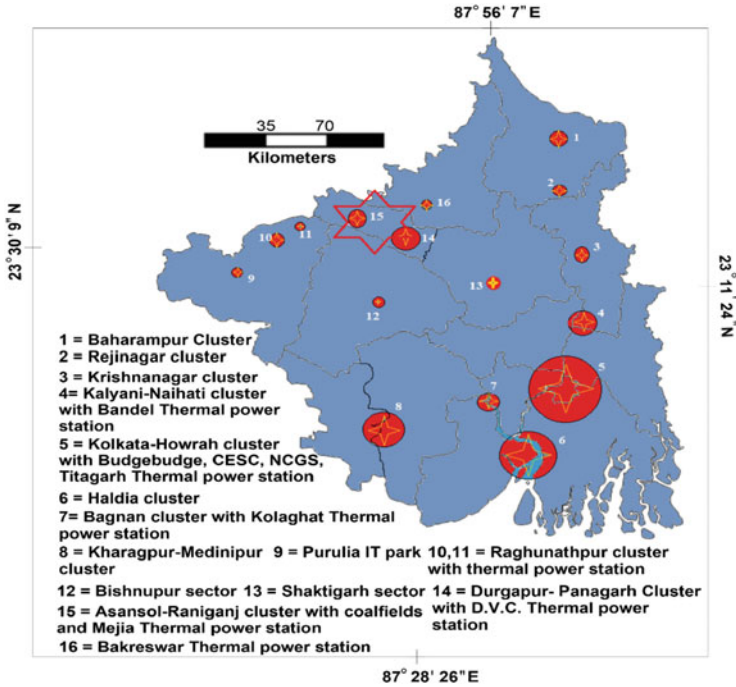


Fig. 32.2 Major urban–industrial and thermal power clusters in Gangetic West Bengal

operating since 2016. GWB also has 12 coal-based and three gas-based thermal power plants spreading all over the area. West Bengal state government has a plan to create mega industrial clusters in Kolkata, Moyna (Purba Medinipur), Habra, South 24 Parganas, and Jhargram (www.msmewb.org accessed on 10.01.2020), which have the potentiality to raise the pollution to a critical level, if any suitable pollution reduction plan or technology is not adopted.

32.3 Materials and Methods

Being a vast area, Gangetic West Bengal experiences diversity in local weather and in the emission of pollutants. The areas adjacent to the major rivers including Ganga and the areas nearest to the seashore consist of higher humidity than the western part of Gangetic Bengal, an extension of Chhotanagpur plateau. The urban–industrial clusters like the ADDA zone, Howrah–Kolkata zone can also be assumed to create more pollution than the rural areas. Studies in urban areas such as Kolkata (Khan and Chatterjee 2016; Bajani and Das 2020) and Durgapur (Dutta et al. 2018; Choudhury et al. 2019) show a higher temperature in comparison to their adjacent areas. The different degrees of meteorological and pollution parameters are most likely to

interact differently with each other, and therefore, the end result may also differ in those different areas, at least slightly. So, in this study, the whole area is divided into some smaller parts according to their specific characteristics, and small-scale studies are executed over them at first, and thereafter, they are blended together in order to get a holistic picture in a regional way.

The entire lower Gangetic West Bengal is divided into four parts: the Northern Gangetic Bengal Plain (NGP), Southern Gangetic Bengal Plain (SGP), Eastern Gangetic Bengal Plain (EGP), and Western Gangetic Bengal Plain (WGP). NGP consists of Murshidabad and Birbhum districts; SGP contains Kolkata, Howrah, North 24 Parganas (south portion), South 24 Parganas, Purba Medinipur, and Paschim Medinipur district; EGP contains Purba Bardhaman, Hooghly, Nadia, and the northern parts of North 24 Pargana district; and WGP contains Paschim Bardhaman, Bankura, Purulia, and Jhargram (Fig. 32.1).

The present study is bounded to 10 years, i.e., from 2010 to 2019, covering the last decade. Monsoon season is not taken into account, as the majority of the air pollutants become washed out in this season. The air pollution, mainly the status of PM_{10} , carbon dioxide (CO_2), carbon monoxide (CO), sulfur dioxide (SO_2), and nitrogen dioxide (NO_2) are analyzed over 10 years in respect of three seasons, i.e., winter (January and February), pre-monsoon (March to May), and post-monsoon (October to December) seasons. As the emission level of the pollutants is not uniform over the year because of seasonal effects, this seasonal study is expected to portray the weather–chemistry interaction more accurately than an annual study. Because the emission level also not remains the same throughout a season, some specific periods from the seasons having a maximum level of pollution are selected with associating meteorological conditions.

In this analysis, the transported pollution fraction is also taken into account with the total pollution amount of the study area. This is because this study aims to portray the original situation of the meteorological condition in Gangetic West Bengal affected by the pollution which not only contains the in situ pollutants but the ex situ also, as the intrusion of wind in one area from another area is inevitable. In spite of this transportation of pollutants from one place to another, a study by Tripathi et al. (2005) and Fosu et al. (2017) found that most of the anthropogenic pollutants present in these areas are generated locally.

32.3.1 Data Collection

For the analysis of pollutants, the ground station data from West Bengal Pollution Control Board (WBPCB) is used along with the field-based observation data. The emission of carbon dioxide is assessed from the selling data of diesel and petrol, statistics from thermal power plants and vehicular statistics. Besides that, for fitting in the WRF-CHEM model, the global EDGAR data of anthropogenic emission ($0.1^\circ \times 0.1^\circ$ resolution) for each time period studied is used along with MEGAN (for biogenic emissions) data of the same spatial resolution.

Ground station data of the Indian Meteorological Department (IMD), field observation data of authors, NCEP operational global forecast system data (0.25° resolution), NCEP/NCAR reanalysis 209 km data (with 28 vertical sigma level), and ERA interim 1.125° data are used for the meteorological analysis in this study.

Besides that, several land use (LUDCP 2025 Report 2015; District Industrial Profile 2019; MSME 2011), energy (Energy Statistics 2018), transport (www.statista.com accessed on 10.02.2020), and pollution (www.ghgplatform-india.org accessed on 12.02.2020, www.wbpcb.com accessed on 14.12.2019) reports by the Government of West Bengal are used to account for the anthropogenic activities in those years.

32.3.2 Analysis of Air Pollutants

Many of the pollution monitoring stations among the 72 stations of WBPCB produce continuous data only after 2016. Before that, there are some discrete data for some regions, and some are totally blank. To interpolate the missing data, multiple regression analysis is applied. First, the correlation is established between the various pollutant and meteorological data, and then a back prediction is done using that relationship. For particulate matter interpolation, relative humidity (RH), near-surface air temperature (T), planetary boundary layer height (PBLH), surface pressure (P), vertical mixing coefficient (V_{MIX}), horizontal mixing coefficient (U_{MIX}), and wind speed are used from the meteorological parameters, and aerosol optical depth (AOD) is used as an alternative measure for pollution besides SPM, as the AOD data is continuously available from 2010.

The trends and status of the pollutants are then analyzed for the specified time periods, along with the effect of transportation of air pollutants by wind.

32.3.3 Analysis of the Effect of Air Pollutants on Meteorology

The most dynamic thing in atmospheric studies is the weather. It changes with seasons, with land use, land cover, with influences from oceans, and with celestial influences. It has a major role in the distribution and concentration of pollutants. In this process, the air pollutants also affect the meteorological parameters known as the “feedback effect.” But, before analyzing the trend of meteorological parameters influenced by pollutants, it is important to analyze the normal trend of them, extracting out the weather extremities influenced by factors other than pollution. So, at first, the time periods without weather extremes are identified and the general range of weather parameters is accounted for after wiping out the seasonal influences.

A numerical weather simulation model (WRF) version 3.8 with a chemistry attachment (CHEM), together named WRF-CHEM, is then used to analyze the

effect of pollution on meteorology. This is a non-hydrostatic model developed by NCAR, using Arakawa C-grid, and Runge–Kutta time-split integration scheme for meteorological simulations (Skamarock and Klemp 2008). In a weather research and forecasting model (WRF) coupled with a chemistry module, all meteorological and chemical parameters have a scope to fully interact in between them, and the feedback effect between chemistry and climate can be analyzed.

In this study, the model is run with a Morrison double moment microphysics scheme (Morrison et al. 2009), rapid radiative transfer model (RRTMG), longwave radiation scheme, Goddard shortwave radiation scheme (Chapman et al. 2008), and Yonsei University planetary boundary layer scheme (Hu et al. 2013) to create the model meteorological conditions. In the chemistry input, MOZART gas-phase chemistry with GOCART aerosol scheme (Pfister et al. 2011) is used. The coupling of aerosols and radiations, therefore, projects the direct effects of aerosols on meteorology.

All the gridded meteorological and emission inputs are then downscaled for studying the effect of pollution on weather conditions in the selected subparts of the study region. The initial chemistry and boundary conditions are set following the MOZART database (Emmons et al. 2010). The use of WRF-CHEM in atmospheric chemistry simulation has been proven quite efficient over the Indian region (Michael et al. 2013).

To extract the effect of anthropogenic emissions, at first, the WRF-CHEM model is run without the chemistry option, only with the meteorology. In the second step, the model is run again with the addition of chemistry input, complying with the same atmospheric physics schemes and data outcome from the previous run. The difference in meteorological outputs in two different simulations reveals the aim of this research.

After the outputs are originated, they are validated with the observed data at the ground.

32.3.4 Analysis of Thermal Comfort

The level of thermal comfort can be estimated by various processes for various perspectives; it may be calculated to reach physical, behavioral, or psychological expectations. All those perspectives are interconnected, but the ultimate result depends on the degree of the variables. Another important parameter that comes in this discussion is the adaptation capability of the living beings (Dear et al. 2013), which differs from region to region. Being in a high-humidity region, many places in West Bengal frequently show discomfort with respect to temperature in summer and monsoon seasons (Bhattacharya et al. 2013; Sansaniwal et al. 2020).

The thermal comfort level over Gangetic West Bengal is calculated using Thom's temperature–humidity index (THI). According to Thom (1959),

$$\text{THI} = 0.4 \times (T + T_w) + 15, \quad (32.1)$$

where T = air temperature in Fahrenheit and T_w is the dew point temperature in Fahrenheit. THI value of 70 makes the environment thermally uncomfortable for humans.

Besides the THI index, the status of apparent temperature (A_T) is also analyzed to study the discomfort level of local residents due to meteorological changes driven by pollution. Apparent temperature is the temperature humans feel which may not be the same as the temperature measured by a thermometer. This feeling is caused by humidity, wind, and other weather elements affecting the sensory organs of the human body.

The equation for apparent temperature is as follows (Steadman 1984):

$$A_T (^{\circ}\text{C}) = -1.3 + 0.92T + 2.2e, \quad (32.2)$$

where T is the temperature ($^{\circ}\text{C}$) and e is water vapor pressure (kpa).

The apparent temperatures are classified using Steadman's table of heat index (Steadman 1984).

32.4 Results and Discussion

The total area of lower Gangetic plain falling in the state of West Bengal encompasses eight distinct land use patterns having different anthropogenic activities e.g. agricultural farming, coal mining, heavy metal industries, brick-kiln industries and thermal power stations. Besides that, there are dense forests and wide barren lands where human activity is minimal. The rate of air pollution in this lower Gangetic plain of West Bengal is mainly dictated by these anthropogenic activities along with meteorological factors. Apart from the local sources, studies show that (Tripathi et al. 2007; Srivastava et al. 2012) there is a submerging region of wind in this lower catchment of Indo-Gangetic plain, later identified to be caused by negative vorticity over this region (ParthSarathi et al. 2019). Through this corridor, polluted air mass of northern Gangetic plain is often transported to its lower reaches in West Bengal in winter, which in turn increases the total pollutant loads of this area. In this study, both the in situ and transported pollution are taken into account, as the actual scenario of pollution contains them both. Because the transported pollutant amount fluctuates both seasonally and annually, the trend of total pollutant load of lower Gangetic West Bengal (GWB) sometimes does not match with the trend of its indigenous production of pollution, but, other than some extreme atmospheric event periods, this transportation remains more or less same. In this study, the time periods of extreme weather events like sandstorms, western disturbances are not considered to avoid the abnormality in atmospheric chemistry and physics in those times which may affect the regular trend, if included. The monsoon periods are also

not taken into account, as, in this season, pollution load is minimal due to the pollutant washout mechanism.

32.4.1 Fact Findings of Particulate Matter Pollution

With an increasing range of various human activities, the amount of particulate matter in the southern Gangetic plain is found to increase as well. The common anthropogenic sources are coal mining, industrial activities, vehicular emissions, and constructional works.

The southern part of lower Gangetic plain (SGP), particularly in the adjacent regions of Howrah and Kolkata, has had an increase of total number of active industries from 114 to 147 between 2010 and 2019, which ultimately led to an increase in PM_{10} concentration from 172 to 241 $\mu\text{g}/\text{m}^3$. This increase in particulate matter is partially contributed by vehicular emission as well. In Kolkata city, the annual average traffic rate is increased by 15% in the last decade (Roy Chowdhury 2015, www.statista.com accessed on 10.02.2020), with an increase of 7.3% in $PM_{2.5}$ concentration. At present, more than 60,000 vehicles are active in Kolkata and its adjacent areas. During office hours in Kolkata, it is not possible for any vehicle to move at a speed more than 25 km/hour, and at that speed, the PM_{10} emission rate from large vehicles like buses is 284 $\mu\text{g}/\text{m}^3$ and from small vehicles like auto, it is 379 $\mu\text{g}/\text{m}^3$ as per the vehicle emission guidelines of WBPCB (www.wbpcb.com accessed on 18.12.2019, Pollution Control law CPCB). That is why the SPM level is always high in every busy traffic point in the southern part of Gangetic West Bengal. Even in the outskirts of the cities, there are enough buses (42% of all transport mediums) used as transport mediums, which increase the SPM level in rural and semi-urban areas along the highways. The emission rate may be a bit less as the speed of the vehicles are much higher than inside the cities. It is reported that at a speed of 75 km/hour, the emission rate of PM_{10} is 154 $\mu\text{g}/\text{m}^3$ (Roy Chowdhury 2015).

The transport of particulate matter over this southern part of Gangetic West Bengal is mainly contributed by the wind coming from north-east direction in winter (Fig. 32.3) and in some times of pre-monsoon season. The source region is most of the time located in Punjab, Uttar Pradesh, and Bihar, and after reaching West Bengal, it blows through the mining and industrial region of the northern portion of WGP, where the Asansol Durgapur Development Authority (ADDA) industrial zone is located. ADDA industrial zone is marked among the 22 critical pollution zone of India by CPCB.

The western part of Gangetic West Bengal (WGP) consists of a wide barren plateau in the north and land covered with forest in the south. The barren lands of this plateau region are the sources of dust generation but this dust-generating period is somehow limited in the pre-monsoon and late winter period. The southern portion of WGP has a distinct number of industrial clusters sparsely distributed over the region, which often crosses the critical limit of PM_{10} in ambient air (as defined by NAAQS,

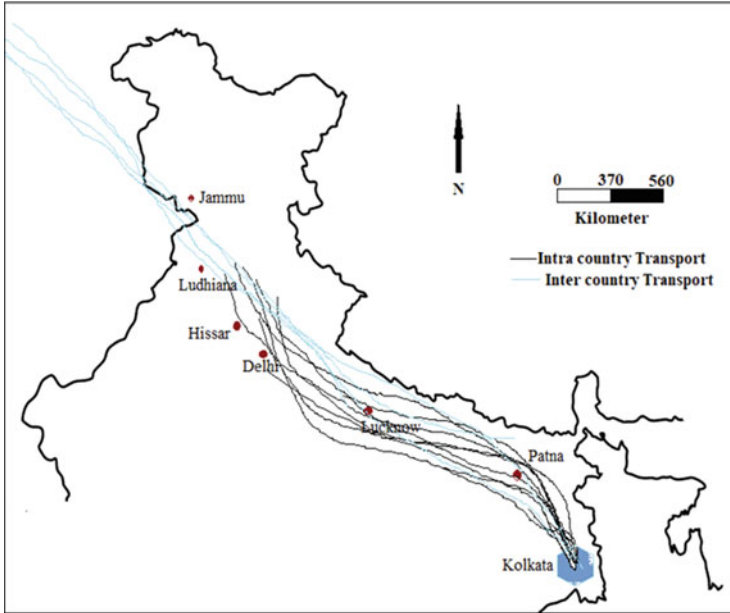


Fig. 32.3 Direction of transport of air pollutants according to backward wind trajectory

100 $\mu\text{g}/\text{m}^3$ in 24 h) in winter. In the pre-monsoon and post-monsoon period, the PM_{10} level remains in a range of 40–110 $\mu\text{g}/\text{m}^3$, but in winter, its range increases from 90 to 130 $\mu\text{g}/\text{m}^3$ on an average. Between 2016 and 2019, the amount of PM_{10} in the southern part of WGP is found to be increased by 3.8%. The vehicles registered in between those years also have increased by 7.3% with an average trip length of 2.5 km/day. There were more than 25 state buses operating through the area with distance coverage of 50–100 km on an average per day in 2019. They take near about one and half to 2 hours covering a distance of 60–100 km (www.sbstconline.com website accessed on February 2020) which makes an average speed of 40–60 km/h. If a bus travels at a speed of 50 km/hours, it will emit 282 $\mu\text{g}/\text{m}^3$ of PM_{10} per kilometer along the road (Roy Chowdhury 2015). This makes the roadside areas more polluted than the inside villages, and with the association of moderate to high winds, these pollutants spread over a large area within and outside of western Gangetic Bengal.

In the north of WGP, there is a wide region of coal mines and different types of industries including ferro-alloy, cements, brick kiln, and six thermal power stations. In the year 2013–2014, two major industries of Durgapur urban–industrial region along with a few more small-scale industries in Paschim Bardhaman district (then Burdwan) had shut down which pulled down the particulate matter and gaseous emissions a little bit, but from 2016, it again started to rise till 2019 with a decrease in 2018. The increase from 2016 despite the closing of cement and heavy metal industries may be caused by the increase of construction works (5% of the total

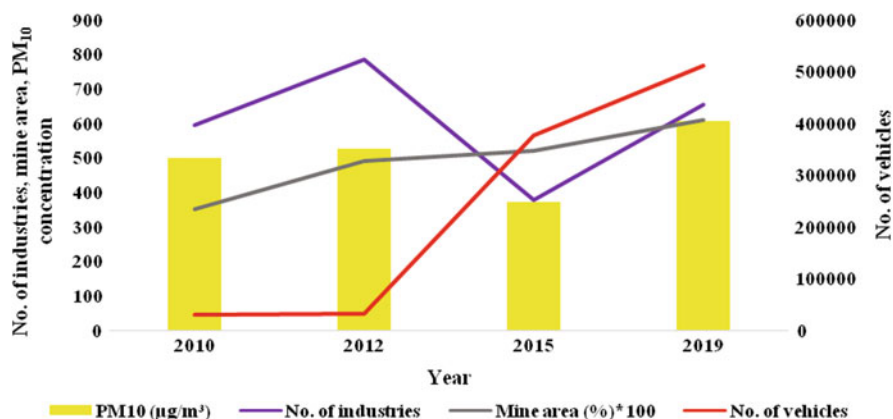


Fig. 32.4 Trend of PM_{10} in air and its contributing factors over 10 years in the urban-industrial and mining WGP

land is changed to paved land during 2015–2016), increase in vehicle numbers (11.38% compounded annual average growth rate of vehicles), and small-scale industries (6.5%). In the past 10 years, the number of coal mines in this region has increased and so the transportation rate, but the trend of pollution level does not follow their increasing trend that much, rather it is more associated with industrial emissions (Fig. 32.4).

The northern part of Gangetic West Bengal is mostly occupied with agricultural activities, some rice mills, brick-kiln industries, and a few food-processing industries. Though the number of large- and medium-scale industries is very less here, traffic load is quite the same like in the other parts of the study area. The concentration of annual PM_{10} remains under $50 \mu\text{g}/\text{m}^3$ in most of the areas with some exception in the roadside places where sometimes concentration reaches up to $90\text{--}101 \mu\text{g}/\text{m}^3$. From 2016 to 2019, the concentration of PM_{10} increased at a rate of 1.1% per year with an increase of 0.2% pollutants transported by wind from outside of the study region. The average traffic also increased by 8.5% in the last 5 years, which shows a correlation coefficient value of 0.62 with the increase of PM_{10} concentration.

The eastern part of Gangetic West Bengal, composed of a large area of agricultural field, also consists of industrial clusters in Nadia, Purba Bardhaman, Hooghly, and in eastern parts of North 24 Parganas. These industries grow over the decade at a rate of 5.8% with an increased PM_{10} emission of 7.6% over the last 5 years on an average. According to the analysis of HYSPLIT dispersion modeling using Lagrangian transport, a part, near about 0.12% of the total amount of particulate matter in the eastern Gangetic West Bengal, is contributed by the wind transport from upper Gangetic plain of Uttar Pradesh and Bihar, and from the industrial-mining zone of north-western portion of Gangetic West Bengal.

The overall scenario of industries in West Bengal indicates an increase from 8230 manufacturing factories to 8422 manufacturing factories including large, medium,

and small industries. The annual average daily traffic has increased from 2.75 million to 7.45 million over the decade. The overall outsourcing of particulate matter via wind flow increased from 0.156% to 0.2% of the total amount of particulate matter on an average in the last decade.

There are 120 state buses operating throughout the whole Gangetic West Bengal from 2015 on an average standard speed of 50 km/hr. At this pace, PM_{10} emission by all of the state buses every hour is 0.34 g/m^3 per km at a rate of $282 \text{ } \mu\text{g/m}^3/\text{km}$ whereas the permissible limit of PM_{10} by NAAQS standard is $80 \text{ } \mu\text{g/m}^3$. As the vehicles are moving, the pollution exerted by them spread over a large area along their moving path. This is only the contribution from a very little part of vehicle transport to the total particulate matter; linking all industrial emissions and total vehicle unit emission will enhance this amount twice or thrice more.

The average amount of particulate matter is largest in the north-western and south portion of Gangetic West Bengal in the winter season from 2015 to 2019, mostly in the industrial clusters of ADDA and 24 Pargana–Kolkata–Howrah regions (Fig. 32.5). The north portion covering the northern Murshidabad remains satisfactory under the permissible limit of PM_{10} other than the winter season. The east and west portions move from moderate to high pollution levels in between the seasons.

This analysis is not full proof because of the scarcity of PM_{10} data in 55 pollution monitoring stations before 2015, and therefore, interpolation has been made to fill up the data gap. In the case of spatial interpolation also, the analysis is done on the basis of data from industrial, mining, and roadside areas mostly. But the error margin of this interpolation shows $a + 1.25$ standard error when compared with some discrete data set before 2015 for 30 stations among the specific 55 stations, making this analysis acceptable (www.blog.minitab.com accessed on 14.01.2020).

Following the multiple regression equation, the backward interpolation of PM_{10} shows a standard error of 13.05 between the observed and estimated value of PM_{10} in the WGP over 35 selected dates based on the observed data availability.

The Gangetic plain of West Bengal shows a positive increase of particulate matter with an R^2 value of 0.5714 (Fig. 32.6) after adding the interpolated values from 2010 to 2014 with the observed values of 2015–2019.

32.4.2 Analysis of Gaseous Pollutants

In the last decade, the level of carbon monoxide has increased from $2.3 \text{ } \mu\text{g/m}^3$ to $5.2 \text{ } \mu\text{g/m}^3$ in the winter season over the Kolkata–Howrah cluster of the southern part of Gangetic West Bengal. It often crosses the critical limit ($2 \text{ } \mu\text{g/m}^3$) on some of the winter days in these cities. In the ADDA zone, the level of carbon monoxide has a gross increase of $2.5 \text{ } \mu\text{g/m}^3$ every year. It is found to cross the critical limit in a few pollution periods of the winter season. The increase of carbon monoxide in the other major urban–industrial clusters of West Bengal, like the Bagnan–Amta industrial zone, Salboni–Midnapore industrial zone, industrial areas of Bankura, has barely crossed the critical level to date. The cause of this increment may be due to the

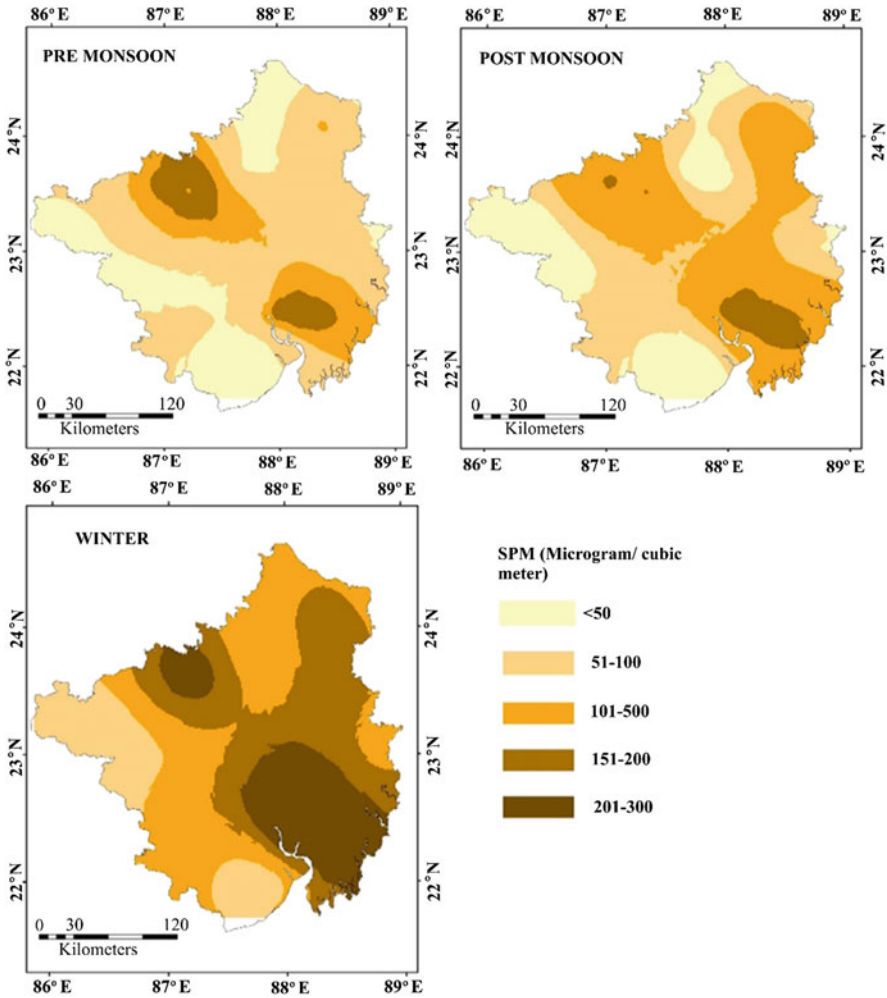


Fig. 32.5 Average PM₁₀ level in Gangetic West Bengal over seasons (2015–2019)

increased number of vehicles and iron and steel industries. The increased rate of vehicle density is 11.38% annually (www.statista.com accessed on 12.02.2020), which is increasing vehicular contribution to total pollution load every year, associating with industrial emissions (40% increase throughout the decade). The increase of CO concentration (15% in 10 years), therefore, may be the result of the aforesaid contributions. In the case of the Kolkata–Howrah cluster, the increase is mostly contributed by vehicular pollution.

The level of sulfur dioxide in Gangetic West Bengal generally remains under the critical level (80 µg/m³) specified by NAAQS. In a few episodes of winter, it is found to cross the limit in the ADDA region, because of an increased industrial emission. On the other hand, the level of nitrogen dioxide often becomes vulnerable in the

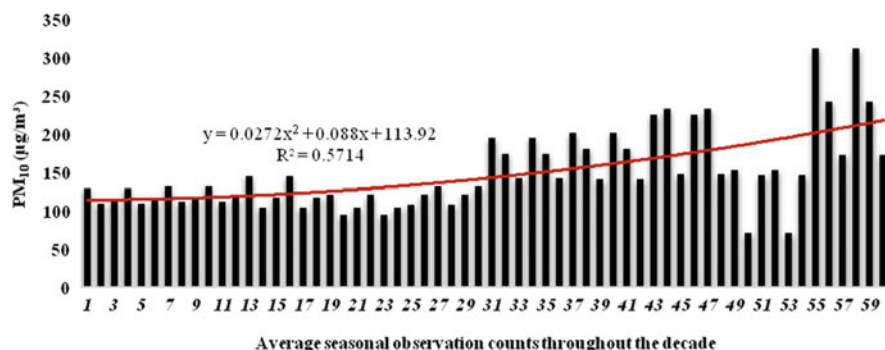


Fig. 32.6 Trend of PM₁₀ over middle portion of Gangetic West Bengal (2010–2019)

urban–industrial clusters of the study area. The level of NO₂ is found to be more than 90 µg/m³ on average over the industrial zones. At times, it crossed 120 µg/m³ and exceeds 150 µg/m³ in the ADDA region. The level of NO₂ is found to be more than 130 µg/m³ in the Barasat–Kolkata–Howrah area in pre- and post-monsoon seasons also.

The level of SO₂ and NO₂ in rural areas of Gangetic West Bengal remains far lower than the critical level, other than the areas closer to the industries.

The emission level of carbon dioxide seems to increase over the decade as well. With the increase of automobile emission, industrial emissions, and thermal power production with an increase of population, the carbon dioxide emission has reached its highest peak in 2019 in the last few decades.

CO₂ emission from thermal power plants of Gangetic West Bengal has increased from 76 million tons in 2010–2011 to 87 million tons in 2018–2019, with a slight decrease in 2013–2014. It is found that CO₂ emission from the manufacturing sector has increased from 18 million tons in 2010–2011 to 24 million tons in 2018–2019, whereas, emission from the residential, commercial, agricultural, and fisheries sector has increased from 11 million tons to 14.2 million tons over the last 10 years in Gangetic West Bengal. The fugitive emissions from the coalfields of Paschim Bardhaman district show an increase from 1.7 million tons to 2.89 million tons of CO₂ in the last decade. Considering the vehicular CO₂ emissions with the above-mentioned sectors, the total emission of CO₂ in Gangetic West Bengal is found to increase from 117 million tons to 150 million tons in the last decade.

These amounts of GHG productions are, therefore, making the pollution scenario of West Bengal worse day by day affecting the health of the residents as well as the meteorological conditions.

32.4.3 Effect of Pollution on Meteorological Phenomenon

The alteration of atmospheric chemistry by meteorological variables is well known. The dispersion of pollutants cannot be analyzed without including the wind factor. Air pollution concentration levels in the atmosphere, duration of concentration, all are highly affected and controlled by the meteorological variables, and, on the other hand, these pollutants also have a role to alter the atmospheric chemistry. The feedback process between atmospheric chemistry and physics can change the atmospheric conditions simultaneously.

According to global warming researches, an increase to 3.67 trillion metric tons of CO₂ emission will lead to an increase of 2 °C more to the global temperature (Allen et al. 2009).

Globally, the CO₂ emission in 2019 was 33 gigatons. In Gangetic West Bengal, the level of emission that year was nearly 0.2 gigatons. According to EPA (www.archive.epa.gov accessed on 12.02.2020), 1 ton of CO₂ emitted anywhere can melt 3 m³ ice of a glacier. Following that, the total CO₂ emission of West Bengal has the potential to melt down 4.5×10^8 m³ of ice.

The average annual temperature of Gangetic West Bengal showed an overall increase of 0.23 degrees in the past 10 years (Fig. 32.7), without the influence of the seasonal extreme. It also shows a positive relationship with the increasing gaseous and particulate matter pollutants over the decade, which might support the influence of pollutants on the temperature.

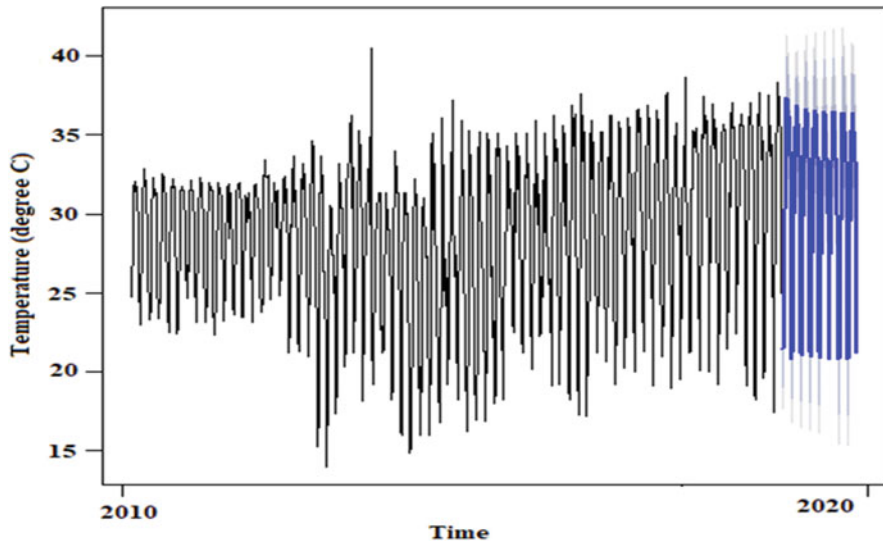


Fig. 32.7 Autoregressive moving average of temperature trend in Gangetic West Bengal (2010–2019)

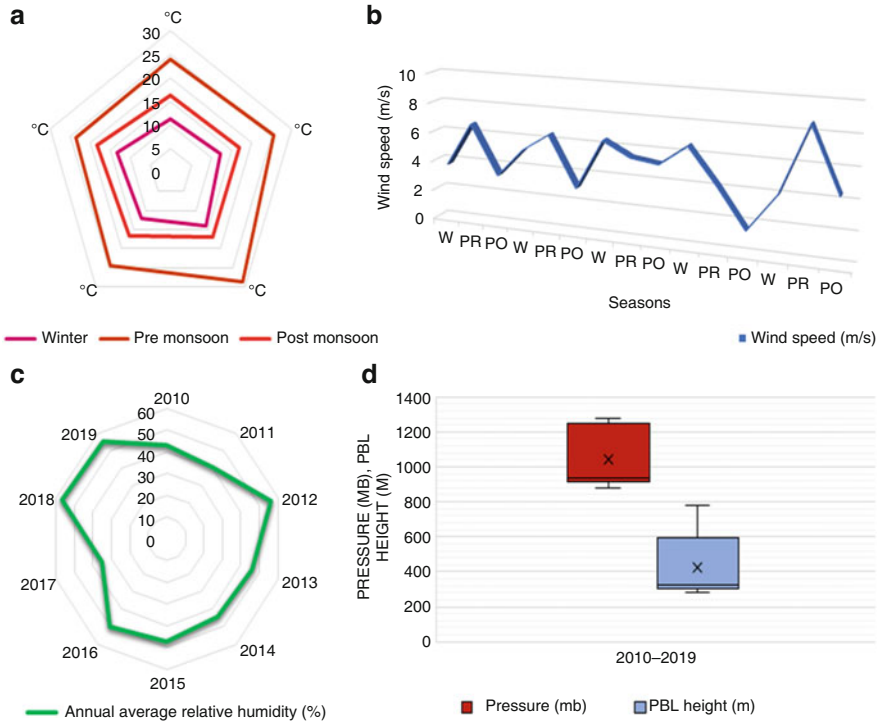


Fig. 32.8 Average meteorological conditions in Gangetic West Bengal (2010–2019); (a) annual average temperature, (b) annual average wind speed (*W* winter; *PR* pre-monsoon; *PO* post-monsoon), (c) annual average relative humidity, (d) average surface pressure and planetary boundary layer height

In comparison to the 0.05 °C increase in global temperature trend during 2010–2018, the increase of more than 0.1°C temperature in Gangetic West Bengal points toward indigenous effect in terms of anthropogenic activities behind the increase. Other than that, the downward solar radiation flux also increased a bit in that time span (0.02–0.05 W/m²).

The temperature and humidity are found to be highest in pre-monsoon and monsoon seasons, and lowest in the winter seasons, other than certain depression episodes in some years. The wind speed and PBL height also seem to be low in the winter season. This gives the pollutants the perfect condition to concentrate and in turn affect the previous atmospheric condition. The average annual relative humidity of Gangetic West Bengal remains between 32% and 66%, temperature 9 °C and 30 °C and sometimes as high as 45 °C in summer (Fig. 32.8).

To identify the effect of particulate matters and gaseous pollutants on meteorological variables, the simulation model is run once without atmospheric chemistry and then with the atmospheric chemistry, in different high pollution episodes in different seasons at different regions specified below.

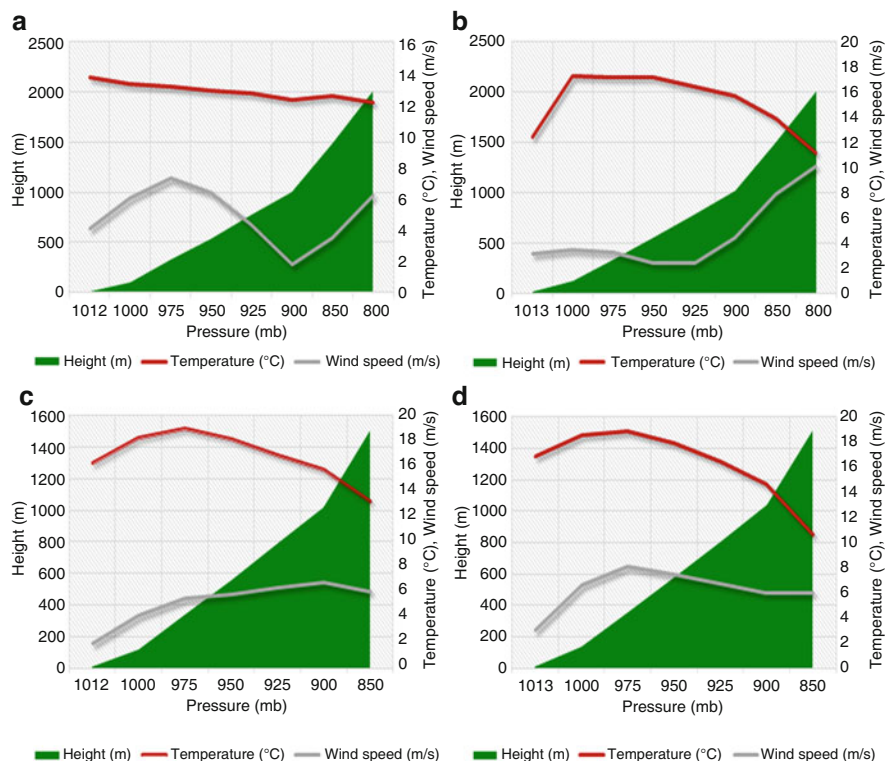


Fig. 32.9 Atmospheric conditions of SGP in winter season without chemistry [(a) 2011, (c) 2019] and with chemistry [(b) 2011, (d) 2019] simulation

Kolkata–Howrah–24 Parganas’ industrial region with a high vehicle loading is considered as one of the highly polluted regions of the southern part of Gangetic West Bengal (SGP) and is considered as “region 1” for this study. The northern part of WGP, with the urban, industrial, and coal mining pollutions is considered as “region 2.” Altogether eight high pollution periods encompassing different seasons such as winter, pre- and post-monsoon are selected from 2010–2011 and 2018–2019; 2015–2016 and 2017–2018, respectively.

In winter 2011, the atmospheric conditions without simulating the chemistry show calm weather with temperature following the environmental lapse rate indicating no instability. With an addition of the chemistry, however, the condition is found to be a little changed (Fig. 32.9). The temperature profile turns to create an inversion layer at 50 m height and temperature increases to 16.2 °C from 13.03 °C at that height. The pressure gradient also shows a change simultaneously affecting the wind speed. These changed meteorological conditions, therefore, may have prolonged the pollution period staging a suitable condition for pollutant concentration at surface level. On the other hand, winter 2019 pollution period shows an already forming inversion layer which becomes intense after adding the chemistry of

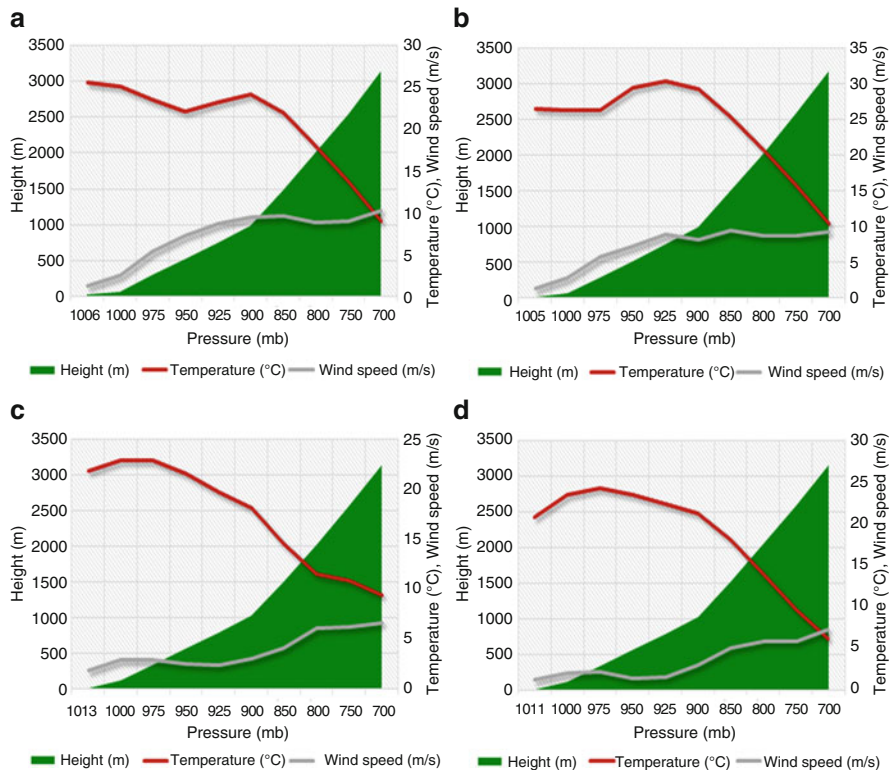


Fig. 32.10 Atmospheric conditions without (a, c) and with (b, d) chemistry coupled simulation for pre-monsoon 2015–2016 (a, b) and post-monsoon 2017–2018 (c, d) in SGP

this pollution period (Fig. 32.9). It increases the temperature profile from 0.5 °C at 50 m height to 0.4 °C at 120 m height. This surface warming resulted in upper air cooling at 1517 m height, where the temperature dropped from 13.2 °C to 10.6 °C after chemistry coupling. In both periods, change in vertical temperature gradient and fluctuations in wind direction leads the condition to a more stable position, shifting to Pasquill stability class “G” from “E” (Chapman 2017).

The pre-monsoon sequence of chemistry coupling of “region 1” shows a little bit different scenario.

In pre-monsoon 2015, the temperature first decreases up to 500 m followed by the abrupt increase of 1.1 °C at 1050 m and then again decreases following the natural relationship of height and temperature (Fig. 32.10a). After including the chemistry, the near-surface temperature decreases over 1 °C and becomes constant till 300 m height, then increases and forms an inversion layer there up to 2100 m. In post-monsoon 2017, this area observed a decrease in near-surface temperature by 1 °C and at upper air over 2 °C after the inclusion of the chemistry module in the model. The inclusion of chemistry also has smoothed the temperature graph in post-monsoon 2017–2018 pollution periods. This temperature drop may be associated

with the presence of greater number of non-carbonaceous aerosols in atmosphere, which leads to increase the albedo. In the layers where environmental lapse rate shows a positive value, a Pasquill stability class “D” or “E” is found to prevail, which supports the intensification of pollution concentration underneath.

Temperature inversion at PBL height is well known for increasing the pollutant concentration at ground level, but the scenarios from region 1 shows the reverse process as well. This may be caused by the type and sizes of aerosols in different layers which radiate or absorb heat differently. The specific types of pollutants which created an inversion layer at a certain height by trapping the heat by their absorbing nature were not present in the “without chemistry” case maybe. In winter 2019, there was an addition of 35% of carbonaceous aerosols in the “with chemistry” case. This inclusion whenever changes the condition in one layer on one meteorological parameter, the other parameters, and the condition in other layers also change, as they are intensely correlated with each other. So, all the meteorological parameters like temperature, surface pressure, and wind speed are found to change simultaneously. Similar results of change in boundary layer temperature were found by the study of Talukdar et al. (2017).

The case study over region 2 also shows the alteration of meteorological parameters after the inclusion of atmospheric chemistry in the weather simulation model. Model outcome in the winter season of 2010–2011 shows a temperature inversion after 1000 m and decrease in the overall temperature value (Fig. 32.11b). In the winter pollution period of 2019, the temperature gradient remains more or less constant but the value decreases by 2 °C at 90 m to 0.8 °C at 2010 m height (Fig. 32.11d), after the chemistry inclusion. In both the selected regions from SGP and WGP, the temperature is found to increase in 2018–2019 winter than 2010–2011 winter. That indicates a decadal increase in temperature. In 2015–2016 pre-monsoon season, the “without chemistry” condition showed an inversion of temperature layer at 700 m height, which came down at 300 m when the chemistry option is included. Unlike the post-monsoon pollution case in SGP, WGP shows an overall increase in temperature after chemistry inclusion in post-monsoon, following the “without chemistry” gradient.

This increase may be caused by a greater number of absorbing aerosols and greenhouse gases released at that time period. The stable condition of the environment, analyzed by the vertical temperature gradient and fluctuations in wind direction, supports the possibility of a high concentration of air pollutants.

The observed ground temperature at the surface (2 m) is, however, different from the modeled outputs. This discrepancy may have been caused by the input data products. Air temperature at 10 m from NCEP operational global forecast system data (at 27.5 km resolution) shows a standard deviation of 2.05 with the ground data at same level without CHEM coupling. After coupling CHEM, the standard deviation reduces to 1.64 (Fig. 32.12).

Saikia et al. (2019) also found an underestimation of temperature by the WRF-CHEM model run over Eastern India. However, in spite of this data discrepancy, the correlation between the ground data and modeled temperature output in

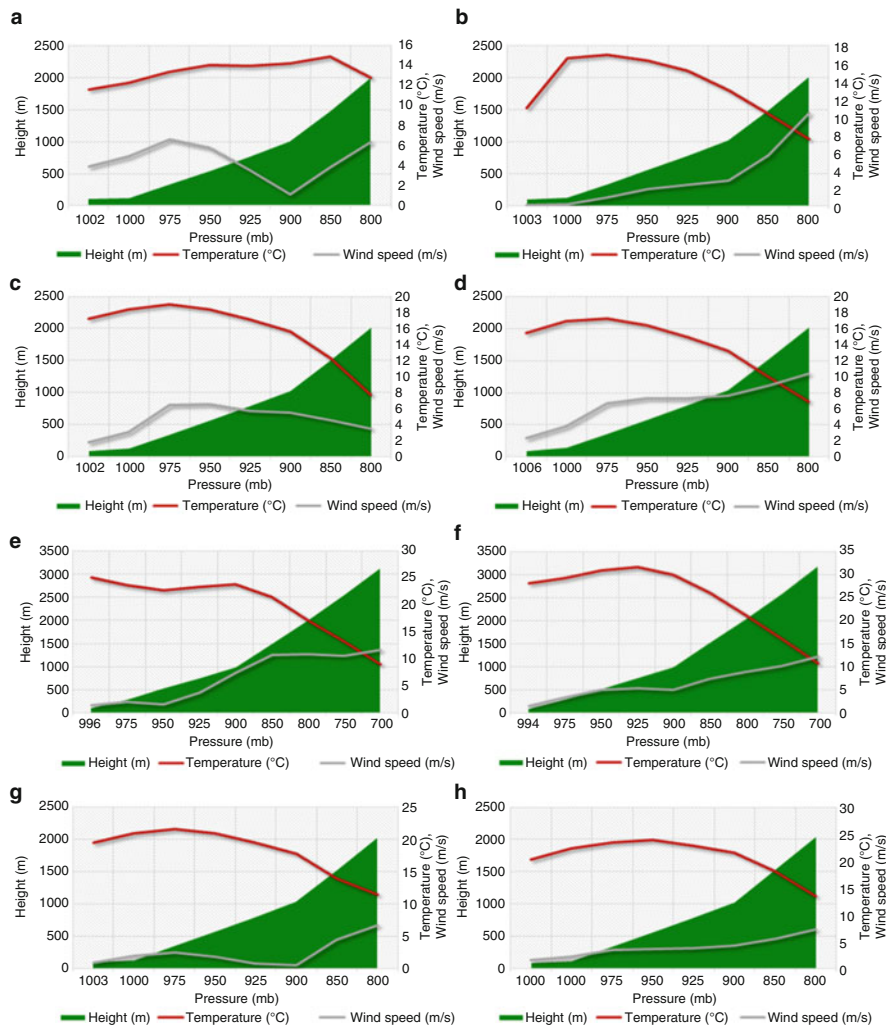


Fig. 32.11 Atmospheric conditions with and without chemistry coupling over MGP; (a, c, e, g) without chemistry coupling in 2011 winter, 2019 winter, 2015 pre-monsoon, and 2017 post-monsoon simultaneously; (b, d, f, h) with chemistry coupling in 2011 winter, 2019 winter, 2015 pre-monsoon, and 2017 post-monsoon simultaneously

“with CHEM” mode shows a correlation coefficient of 0.7472, slightly better than the coefficient with “without CHEM” mode, which is 0.7392 (Fig. 32.13).

In the pre-monsoon seasons of the last half of the last decade, cloud forcing was generally negative most of the times other than unstable atmospheric conditions (Fig. 32.14) in Gangetic West Bengal.

The cloud radiative forcing is mostly negative in the time periods studied in pre-monsoon, post-monsoon, and winter seasons, but decreases its negative value

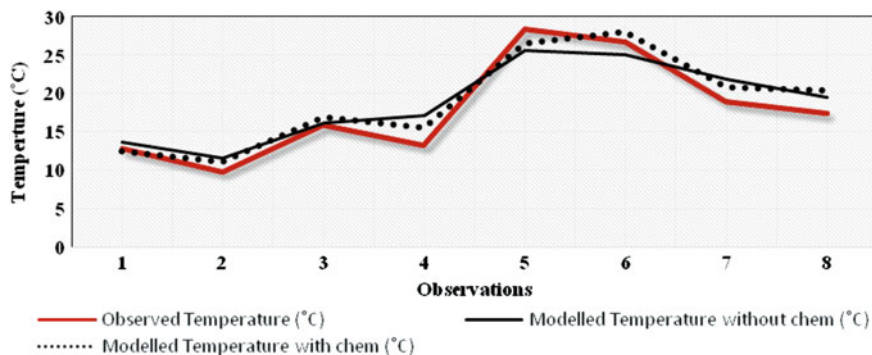


Fig. 32.12 Association of modeled temperature outputs with observed data at ground

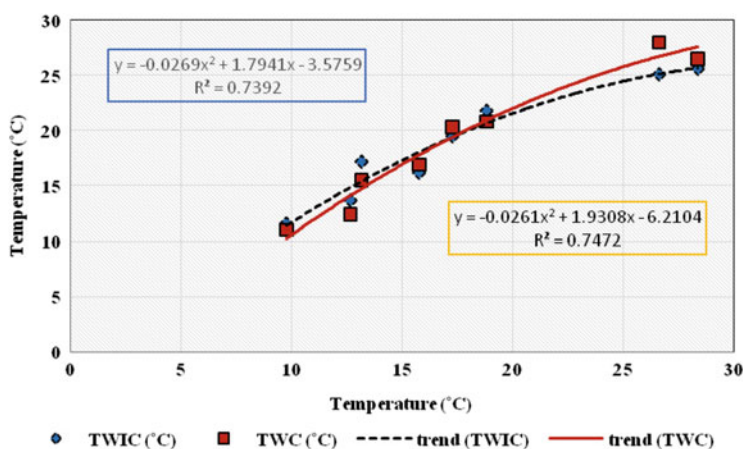


Fig. 32.13 Correlation between observed and modeled temperature data. *TWIC* temperature without CHEM coupling, *TWC* temperature with CHEM coupling

when the chemistry module is added. The negative cloud forcing may be one of the causes of decreasing the solar radiation flux at the surface than the TOA. When included in the chemistry module, the weather simulation results in an increase in sensible heat net flux and a decrease in latent heat net flux (Fig. 32.14c). This indicates that less transformation between the states of water may be caused by the addition of non-hygroscopic nuclei and alteration in temperature, which interrupts the evaporation and condensation process.

Though the analyses are based on the urban–industrial clusters, where prolonged and intense episodes of pollution are available, the near-surface temperature of their adjacent areas is also found to be affected by this pollution level, but in a smaller amount than the centers. In SGP, Kolkata–Howrah–24 Pargana and Bagan–Kolaghat regions are dominant in air pollution. In the winter pollution episode of 2019, the “with CHEM” mode hourly simulations show how the pollutants spread

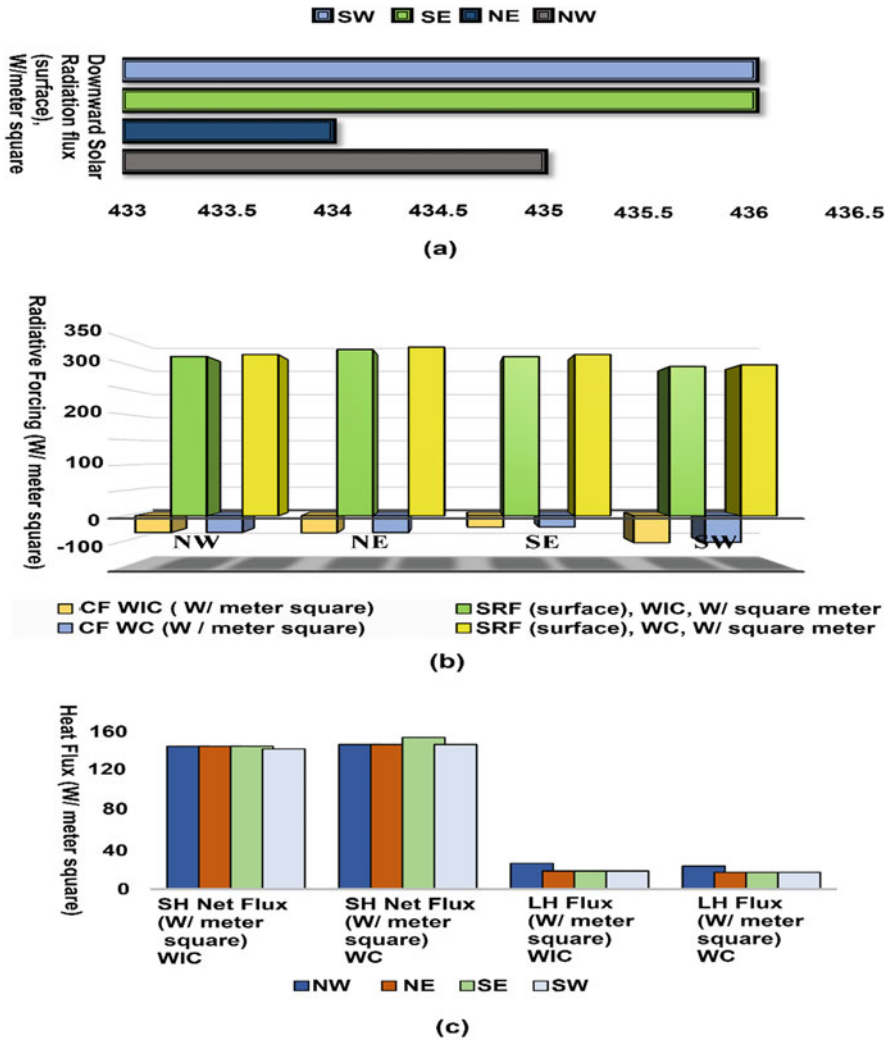


Fig. 32.14 (a) Average downward solar radiation flux at top of the atmosphere in pre-monsoon seasons (2016–2019) in four parts of Gangetic West Bengal, SW, SE, NE, and NW; (b) cloud forcing (CF) and solar radiation flux (SRF) at the surface of the subsequent area (pre-monsoonal average of 2016–2019) in without CHEM (WIC) and with CHEM (WC) condition; (c) Average Sensible (SH) and latent (LH) heat fluxes (2016–2019 pre-monsoon) in different region of Gangetic West Bengal, in without CHEM (WIC) and with CHEM (WC) condition

along the time and space and alter the spatial distribution of near-surface air temperature. The PM_{10} level is found high in both the clusters (Fig. 32.15a) whereas the level of carbon monoxide concentration is high in and around cluster 2 (Fig. 32.15c). With time, the pollutants are found to disperse all over the area

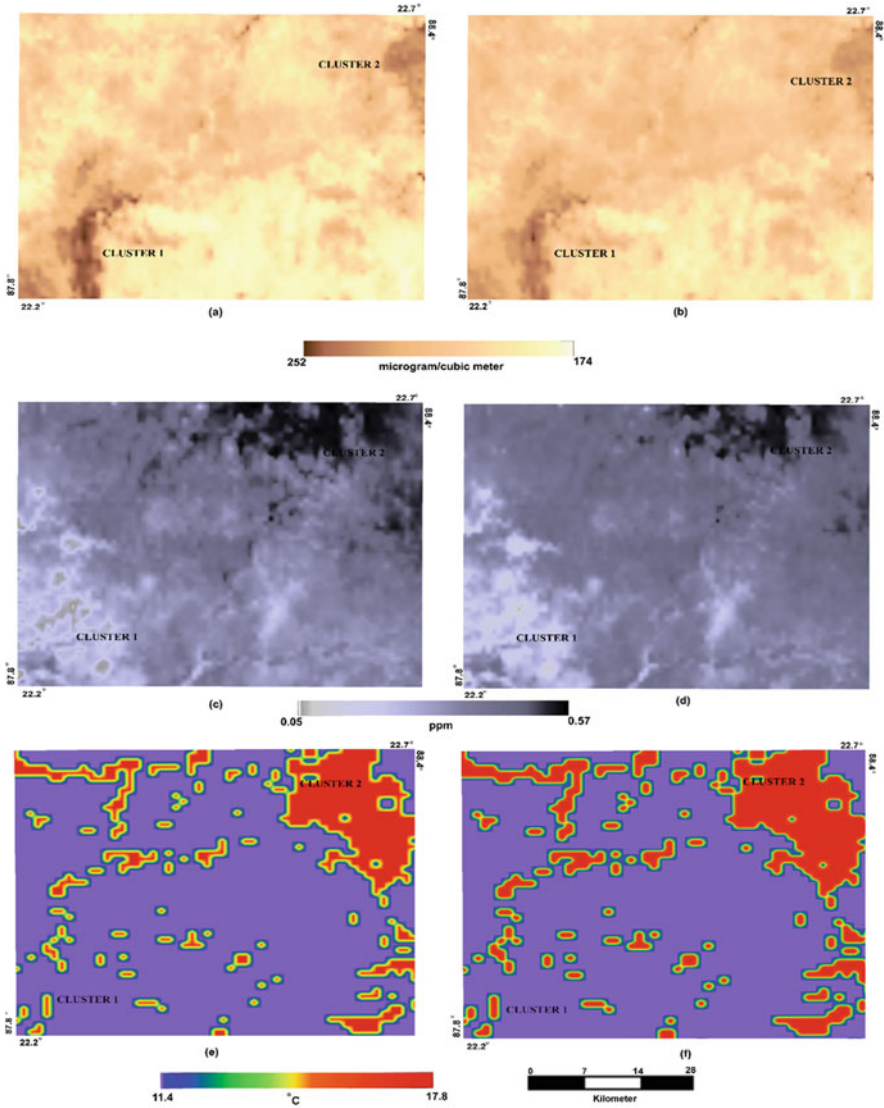


Fig. 32.15 Cluster 1—Bagnan–Kolaghat pollution zone, Cluster 2—Kolkata–Howrah pollution zone; (a, c, e) SPM, CO, temperature, respectively, in 01 h of simulation in “with CHEM” mode; (b, d, f) SPM, CO, temperature, respectively, in 119th h of simulation in “with CHEM” mode

but not in a uniform manner, and rather it shows variation in dispersion style. The urban–industrial areas, which can clearly be identified from Fig. 15e and 15f, show intensification of temperature after the pollution period. In spite of the dispersion of pollutants over the whole region from the clusters, there was not much transfer of heat from the heat islands to the village areas; rather each area perceived a slight

increase in temperature. Most probably this is because of the high amount of GHGs trapped in urban areas because of the temperature inversion layer created over them with a low PBL height and low wind speed, resulting in a much higher concentration of pollution on those areas eventually making them heat islands.

Thus, it is very clear from the analysis that the relationship between air pollution and meteorology is never binary; rather it shows numerous variations with different sets of atmospheric conditions in Gangetic West Bengal. But, at the same time, it is also found that the rapidly increasing rate of carbonaceous aerosols and GHGs is playing an important role in the overall warming of the area. The increase of temperature and GHGs over the decade has always maintained a positive correlation coefficient near about 0.5 in Gangetic West Bengal.

32.4.4 Analysis of Thermal Comfort in Altered Meteorological Condition

Gangetic West Bengal is naturally dominated by high temperatures and humidity because of its location in the tropical region near the seashore. But, as per the adaptation rules, the residents of this area are habituated with this climate. However, in the past few decades, the increase of temperature and change of land-use pattern has changed the anthropogenic activity and thereby modified the atmospheric chemistry (Sect. 32.4.1 and 32.4.2) in this area. The feedback effect of their interconnected activities, therefore, is found to change the meteorological conditions as well (Sect. 32.4.3).

In between the 12 case studies (Sect. 32.4.3), 11 pollution periods over the Gangetic West Bengal result in increasing thermal discomfort (Fig. 32.16).

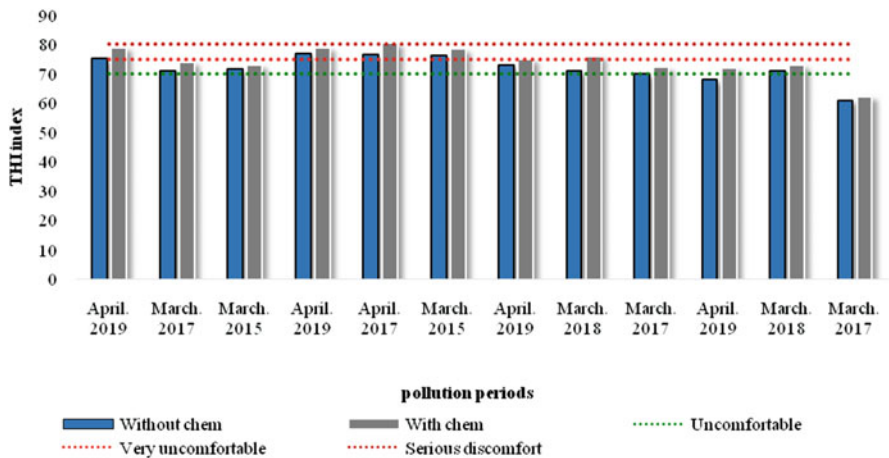


Fig. 32.16 THI index in different pollution periods over different pollution clusters over Gangetic West Bengal

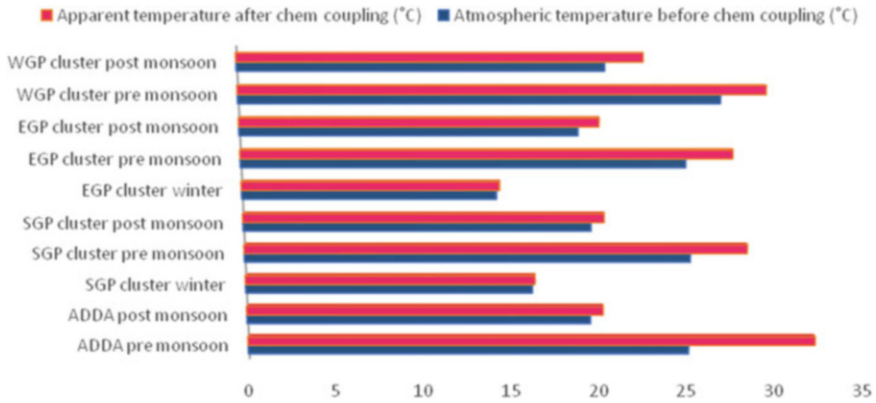


Fig. 32.17 Apparent temperature in different pollution periods over different parts of GWB

According to Thom (1959) and Armstrong (1994), a thermal heat index (THI) value of 70 indicates the starting of an uncomfortable zone in response to temperature. Stepping on a 75 THI value indicates a very uncomfortable condition and crossing 80 indicates a severe discomfort. Mostly in pre-monsoon pollution episodes, thermal discomfort was experienced. Other than the summer, some episodes in post-monsoon also lead to the thermal discomfort level, in a percentage of 35 out of the nine model runs in this season.

Though the pollution more or less spread all over the southern part of West Bengal from the urban, industrial, and mining clusters, most of the pollution concentration still remains over the clusters themselves, and increases the apparent temperature much more than the adjacent areas.

The high humidity in West Bengal works as a catalyst, increasing the apparent temperature much more than it is recorded in instruments. In January 2018, the apparent temperature resulted from the pollution is 0.02 °C higher in the whole of Gangetic West Bengal, whereas, it remains alone 0.4 °C high in Kolkata. In the pre-monsoon pollution period of 2018, the whole study area has experienced 0.34 °C increase in apparent temperature after the atmospheric chemistry initiated to react with the physical atmosphere. In the ADDA urban–industrial cluster, the apparent temperature becomes 32 °C in a pre-monsoon pollution episode in 2019, whereas the barometer temperature shows a value of 25.1 °C before the chemistry module is initiated (Fig. 32.17). In winter seasons, the apparent temperature is found to increase 0.05 °C on an average over the whole study area and in some places like ADDA industrial area, Kolkata–Howrah cluster, Bagnan–Kolaghat cluster, Kalyani cluster, it is found to increase over 1.2 °C. This increase in temperature may not look like a huge increase, but coping with the global temperature rise or rapid change in temperature, these values also indicate the need to be seriously concerned about the sequential change in heat regimes, and, eventually about the pollution growth also.

32.5 Environmental Risk and Remediation

With the progress of time, the land use–land cover patterns are gradually changing in Gangetic West Bengal, with the change in human activities. The barren lands, grasslands, even forests are being transformed into built-up areas and industries. Cities are expanding at a faster rate. Road network has increased more than a thousand kilometers in the last decade. Eventually, the pollution level is growing high day by day, with the increasing amount of vehicular exhaust, industrial emissions, and household emission. At present, the AQI level of all industrial areas in Gangetic West Bengal falls in “moderate” to “very poor” category most of the time in a year. This bad air quality can lead to many respiratory diseases of the permanent residents of these areas. According to NAAQS, exposure to more than $150 \mu\text{g}/\text{m}^3$ SPM for 24 hours can cause serious heart disease.

The spatial projection of air quality indicates that in the next 5 years, more than 20 lakh populations in a 7000 km^2 area will be exposed to poor air quality over the year except the monsoon season, if the present rate of increment in urban expansion and air pollution remains constant.

To minimize this impact, at the very first, continuous monitoring of air pollutants is needed regardless of urban and peri-urban areas. According to the pollution report audited by the Government of West Bengal (2018), only 20% of industries have submitted the SEEIA or environmental impact assessment report till 2018, in spite of being notified in early 2012. WBPCB planned to monitor 12 air pollutants in 72 stations all over West Bengal, but only four pollutants are being measured in most of the stations. So, the exact measurement of pollutants is the first and foremost need which can eradicate the errors of interpolation. Secondly, the industrial risk assessments should be completed as soon as possible to select suitable controlling measures.

There are two types of concepts in controlling air pollution. One is the assimilative capacity concept, which prohibits emissions after a critical level, and another is the principle of control concept, which emphasizes controlling the rate of emission based on specific time and type of environment and application of various measurement tools like electrostatic precipitators for heavy metal processing industries or baghouse filters for industrial particulate matter emission control (Spiegel and Maystre 1998). Though the second one has less strict rules, this requires continuous real-time monitoring in high spatial resolution and both of the processes end up suggesting the limitation of demands of civilized society which can reduce the production and use of luxury gadgets a bit.

In Gangetic West Bengal (GWB), there are a variety of sources of air pollution, including both mobile and stationary sources with the transportation of pollutants from Northern Gangetic Plains. The stationary sources also have varieties from thermal power plants to heavy metal industries to food-processing industries and brick-kiln industries with a portion of fugitive emission from coal mines. These wide varieties of pollutant sources denote the better application of the “control concept” method in Gangetic West Bengal. Guided by some similar ideas, the Central

Pollution Control Board (CPCB) of India has also set up different critical value of air pollutants for different types of environment (CPCB 2011). To apply different measures for different air pollution sources of different regions, a detailed monitoring project should be run over the whole area over different seasons of the year first. Then only the case-specific and effective measurement policies can be made. This method was proved successful for Nigeria (Yakubu 2017) and in parts of Europe (www.eea.europa.eu retrieved on 20.05.2020) and the USA (www.epa.gov retrieved on 20.05.2020). It is very hopeful that CPCB has already implemented some new techniques to monitor the heavily polluted industrial areas to check the vulnerability of pollutants in GWB.

For the iron and steel and most of the manufacturing industries, the electrostatic precipitator, scrubbers, condensers, cyclone separators, and baghouse filters can be used to filter the emissions. The substitution of raw materials, i.e., the use of cleaner fuels and materials which produce air pollutants in a lesser amount, can also reduce the vulnerability of the emissions. There are a number of thermal power plants in Gangetic West Bengal (GWB) over which a large amount of electrical power supply of West Bengal is dependent. If solar and some more hydropower plants can be built in suitable regions to share the load of thermal plants, the air pollution generated by the latter can be reduced.

For the vehicular emission reduction, the type of engines in the vehicles should be monitored more frequently as many people use old engines in the villages and town area of West Bengal till date. Mostly in the villages, the vans and “toto” run by a mixture of diesel, kerosene, and methane exert a lot of pollution. Though prohibited by the Motor Vehicles Department (Dutta and Jash 2014), the use of this fuel is still very common in rural Bengal. To recover from it, green technology should be appreciated. Other than this, keeping car-engines running in the traffic signals increases the pollution at those points at a high rate; therefore, the engines must be kept power off at the signals to reduce air pollution. Transport of the coal and sand uncovered is a common practice in GWB, mostly in the mining and industrial regions, which nonetheless increases the air pollution along the vehicles’ tract. Specifically, for coal regions, a greater number of sprinklers should be used in the sites of open cast coal mines, which will reduce the air pollutants exerted by mining activities.

There is another cause of rising air pollution in GWB, which is the transport of pollutants from the upper Ganga Basin. Only controlling the in situ emission will not work till this transportation problem is not solved. For this, the pollution eradication planning should contain a larger area than GWB, i.e., including the source areas like Punjab, Haryana, Uttar Pradesh, and Chhotanagpur Plateau, from where air pollutants are transported to GWB following the wind direction. As the speed and directions of wind change along the seasons, the planning should be season-specific, and better to be analyzed by numerical simulation model at first, which analyze pollution dispersion taking atmospheric condition into consideration. The state Pollution Control Board of West Bengal can form a policy after discussing with the authorities of those neighbor states for regulating their emissions.

The rising temperature is also found to affect the thermal comfort of residents of GWB, mostly the residents of urban areas (Sect. 4.4). As a solution, the use of air conditioners is the common practice in urban and semi-urban areas, which in turns increases pollution as well. The use of green roof technology and the plantation of more trees in the neighborhood can solve the problem better without increasing the pollution level.

Furthermore, another important step to eradicate this problem is to develop social awareness. Awareness can reduce the air pollution level emitted from households to industries in a big amount. The progression of civilization must need industrialization and technical advancements, but ignoring the environment in this process will only put the future of humankind at stake.

32.6 Conclusions

The material-indicators of civilization consist mostly of the development of communication through sufficient vehicles and well-built road, presence of modern gadgets like air conditioners and refrigerators, and skyscrapers covering most of the big cities in one face of the coin, whereas the other shows the use of modern technologies in agriculture, cattle rearing, horticulture, etc. All these developments are the results of urbanization and industrialization, which became necessary in the present context. Being the major source of air pollution, the expansion of those two sectors is escalating the risk of health issues due to air pollution at a critical level and altering the atmospheric chemistry, which in turn affects atmospheric physics. The only way to reduce air pollution in this situation is to use region-specific air pollution management policies including the use of green technology, air purifiers, and several other air pollution control devices. In the Gangetic Plain of West Bengal, there are plenty of villages that are not converted into urban places till date. The application of a suitable management plan for future conversions can help the level of air pollution to reduce in the near future. But for that, a detailed evaluation and report should be made on the present situation of this region in response to air pollutants, and for reducing the present level of air pollution in the cities, steps should be taken as soon as possible.

Acknowledgments The authors are thankful to ISRO for funding the project numbered ISRO/RES/4/625/2015-16 and to Dr. C. M. Kistawal, senior scientist and head, Atmospheric Science Division, ISRO SAC, Ahmedabad, India for his guidance and support as this project's focal person.

References

- Allen MR, Frame DJ, Huntingford C, Jones CD, Lowe JA, Meinshausen M, Meinshausen N (2009) Warming caused by cumulative carbon emissions towards the trillionth tonne. *Nature* 458. <https://doi.org/10.1038/nature08019>
- Armstrong DV (1994) Heat stress interaction with shade and cooling. *J Dairy Sci* 77(7):2044–2050. [https://doi.org/10.3168/jds.S0022.0302\(94\)77149-6](https://doi.org/10.3168/jds.S0022.0302(94)77149-6)
- Asansol Durgapur Development Authority (2015) Land use and development control plan – 2025 for Asansol sub-division. Government of West Bengal
- Badarinath KVS, Kharol SK, Sharma AR (2009) Long-range transport of aerosols from agricultural crop residue burning in indo-Gangetic Plains – a study using LIDAR, ground measurements and satellite data. *J Atmos Sol Terr Phys* 71(1):112–120. <https://doi.org/10.1016/j.jastp.2008.09.035>
- Bajani S, Das D (2020) Sustainable planning interventions in tropical climate for urban heat island mitigation - case study of Kolkata. In: Ghosh M (ed) Perception, design and ecology of the built environment. Springer, Cham. https://doi.org/10.1007/978-3-030-25879-5_10
- Bhargava A, Bunkar N, Aglawe A, Pandey K, Tiwari R, Chaudhury K, Goryacheva IY, Mishra PK (2018) Epigenetic biomarkers for risk assessment of particulate matter associated lung cancer. *Curr Drug Targets* 19(10):1127–1147. <https://doi.org/10.2174/1389450118666170911114342>
- Bhattacharya R, Pal S, Biswas G, Karmakar S, Saha G (2013) Seasonal distribution of comfortability: a regional based study over Kalyani, West Bengal India. *Int J Innov Res Sci Technol* 2:2856–2862
- Boucher O et al. (2013) Clouds and aerosols. *Climate change 2013: the physical science basis; contribution of working group 1 to the fifth assessment report of the intergovernmental panel on climate change*. Cambridge University Press, Cambridge, pp 571–657
- Central Pollution Control Board (2011) Guidelines for the measurement of ambient air pollutants. NAAQS monitoring and analysis guidelines volume 1. Ministry of Environment and Forests, Government of India
- Central Statistics Office (2018) Energy statistics 2018. Ministry of Statistics and Programme Implementation, Government of India
- Chapman HL (2017) Performance test of the Pasquill stability classification scheme. Thesis and Dissertations 1453, University of Wisconsin Milwaukee. UWM Digital Commons
- Chapman EG, Gustafson WI, Easter RC, Barnard JC, Ghan SJ, Pekour MS, Fast JD (2008) Coupling aerosol-cloud-radiative processes in the WRF-Chem model: investigating the radiative impact of elevated point sources. *Atmos Chem Phys* 9:945–964
- Choudhury D, Das K, Das A (2019) Assessment of land use land cover changes and its impact on variations of land surface temperature in Asansol-Durgapur development region. *Egy J Remote Sensing Space Sci* 22(2019):203–218. <https://doi.org/10.1016/j.ejrs.2018.05.004>
- Cohen AJ. 1995(2003) Air pollution and lung cancer: what more do we need to know? *Thorax* 58:1010–1012. <https://doi.org/10.1136/thorax.58.12.1010>
- Das S, Dey S, Dash SK, Basil G (2013) Examining mineral dust transport over the Indian subcontinent using the regional climate model, RegCM4.1. *Atmos Res* 134(2013):64–76. <https://doi.org/10.1016/j.atmosres.2013.07.019>
- Dear RJd, Akimoto T, Arens EA et al (2013) Progress in thermal comfort research over the last twenty years. *Indoor Air* 23(6):442–461. <https://doi.org/10.1111/ina.12046>
- Dutta A, Jash T (2014) Studies on energy consumption pattern in mechanized van rickshaws in West Bengal and the problem associated with these vehicles. *Energy Procedia* 54 (2014):111–115. <https://doi.org/10.1016/j.egypro.2014.07.253>
- Dutta D, Gupta S, Kistawal CM (2018) Linking LULC change with urban heat islands over 25 years: a case study of the urban-industrial city Durgapur, Eastern India. *J Spat Sci*. <https://doi.org/10.1080/14498596.2018.1537198>
- Ehret U, Zehe E, Wulfmeyer V, Warrach-Sagi K, Liebert J (2012) Should we apply bias correction to global and regional climate model data? *Hydrol Earth Syst Sci Discuss* 9:5355–5387. <https://doi.org/10.5194/hessd-9-5355-2012>.

- Emmons LK, Walters S, Hess PG (2010) Description and evaluation of the model for ozone and related chemical tracers, version 4 (MOZART 4). *Geosci Model Dev* 3:43–67. <https://doi.org/10.5194/gmd-3-43-2010>
- Forkel R, Brunner D, Baklanov A et al (2016) A multi model case study on aerosol feedbacks in online coupled chemistry meteorology models within the COST action ES1004 EuMetChem. *Air Pollut Model Appl XXIV*. https://doi.org/10.1007/978-3-319-24478-5_4
- Fosu BO, Wang S-YS, Wang S-H, Gillies RR, Zhao L (2017) Greenhouse gases stabilizing winter atmosphere in the Indo-Gangetic plains may increase aerosol loading. *Atmos Sci Lett* 18:168–174. <https://doi.org/10.1002/asl.739>
- Ghosh S, Tripathi SN (2014) Chemical characterization of summertime dust events in Kanpur: insight into the sources and level of mixing with anthropogenic emissions. *Aerosol Air Qual Res* 14:879–891
- Ghude SD, Chate DM, Jena C, Beig G, Kumar R, Barth MC, Pfister GG, Fadnavis S, Pithani P (2016) Premature mortality in India due to PM_{2.5} and ozone exposure. *Geophys Res Lett* 43:4650–4658. <https://doi.org/10.1002/2016GL068949>
- Government of West Bengal (2018) Report of the controller and auditor general of India on performance audit of pollution in industries of West Bengal (economic sector). Report no. 5
- Hu X-M, Klein PM, Xue M (2013) Evaluation of the updated YSU planetary boundary layer scheme within WRF for wind resource and air quality assessments. *J Geophys Res Atmos* 118 (10):490–505
- Jethva H, Torres O, Field RD, Lyapustin A, Gautam R, Kayetha V (2019) Connecting crop productivity, residue fires, and air quality over Northern India. *Sci Rep* 2019(9):16594. <https://doi.org/10.1038/s41598-019-52799-x>
- Kar J, Deeter MN, Fishman J et al (2010) Wintertime pollution over the Eastern Indo-Gangetic Plains as observed from MOPITT, CALIPSO and tropospheric ozone residual data. *Atmos Chem Phys* 10(2010):12273–12283. <https://doi.org/10.5194/acp-10-12273-2010>
- Khan A, Chatterjee S (2016) Numerical simulation of urban heat island intensity under urban-suburban surface and reference site in Kolkata, India. *Model Earth Syst Environ* 2:71. <https://doi.org/10.1007/s40808-016-0119-5>
- Kong X, Forkel R, Sokhi RS (2015) Analysis of meteorology-chemistry interactions during air pollution episodes using online coupled models within AQMEII phase-2. *Atmos Environ* 115 (2015):527–540. <https://doi.org/10.1016/j.atmosenv.2014.09.020>
- Kumar M, Parmar KS, Kumar DB, Mhawish A, Broday DM, Mall RK, Banerjee T (2018) Long-term aerosol climatology over Indo-Gangetic plain: trend, prediction and potential source fields. *Atmos Environ*. <https://doi.org/10.1016/j.atmosenv.2018.02.027>
- Luan T, Guo X, Zhang T (2019) Below cloud aerosol scavenging by different intensity rains in Beijing city. *J Meteorol Res* 33:126–137
- Makar PA, Gong W, Milbrandt J, et al. (2014, August) A study of feedbacks between weather and air pollution using GEM-MACH (and several other models!). WWSOC Presentation 18
- Michael M, Yadav A, Tripathi SN et al (2013) Simulation of trace gases and aerosols over the Indian domain: evaluation of the WRF-CHEM model. *Atmos Chem Phys* 13:12287–12336. <https://doi.org/10.5194/acpd-13-12287-2013>
- Morrison H, McCoy RB, Klein SA et al (2009) Intercomparison of model simulations of mixed-phase clouds observed during the ARM mixed-phase arctic cloud experiment II: multilayer cloud. *Q J R Meteorol Soc* 135:1003–1019. <https://doi.org/10.1002/qj.415>
- MSME Development Institute, Kolkata (2011) District industrial profile 2010-11. Ministry of MSME, Government of India
- MSME Development Institute, Kolkata (2019) District industrial profile 2018-19. Ministry of MSME, Government of India
- Ojha N, Sharma A, Kumar M et al (2020) On the widespread enhancement in fine particulate matter across the Indo-Gangetic plain towards winter. *Sci Rep* 10:5862. <https://doi.org/10.1038/s41598-020-62710-8>
- ParthSarathi P, Kumar S, Barat A, Kumar P, Sinha AK, Goswami V (2019) Linkage of aerosol optical depth with rainfall and circulation parameters over the Eastern Gangetic plain of India. *J Earth Syst Sci* 2019:128–171. <https://doi.org/10.1007/s12040-019-1204-8>

- Pfister GG, Avise J, Wiedinmyer C (2011) CO source contribution analysis for California during ARCTAS-CARB. *Atmos Chem Phys* 11:7515–7532. <https://doi.org/10.5194/acp-11-7515-2011>.
- Rosenfield D (2000) Suppression of rain and snow by urban and industrial air pollution. *Science* 287(5459):1793–1796
- Rosenfield D, Lohman U, Raga GB, O'Dowd CD, Kulmala M, Fuzzi S, Reissell a, Andreae MO (2008) Flood or draught: how do aerosols affect precipitation? *Science* 321(5894):1309–1313
- Roy Chowdhury I (2015) Traffic congestion and environmental quality: a case study of Kolkata city. *Int J Hum Soc Sci Invent* 4(7):20–28
- Saikia A, Pathak B, Singh P, Bhuyan PK, Adhikary B (2019) Multi-model evaluation of meteorological drivers, air pollutants and quantification of emission sources over the upper Brahmaputra basin. *Atmosphere* 10(703):1–28. <https://doi.org/10.3390/atmos10110703>.
- Sansaniwal SK, Mathur J, Garg V, Gupta J (2020) Review of studies on thermal comfort in Indian residential building. *Sci Technol Built Environ*. <https://doi.org/10.1080/23744731.2020.1724734>
- Sapkota TB, Jat ML, Aryal JP, Jat RK, Khatri-Chhetri A (2015) Climate change adaptation, greenhouse gas mitigation and economic profitability of conservation agriculture: some examples from cereal systems of Indo-Gangetic Plains. *J Integr Agric* 14(8):1524–1533. [https://doi.org/10.1016/S2095-3119\(15\)61093-0](https://doi.org/10.1016/S2095-3119(15)61093-0)
- Sarkar R, Maity P, Roy D (2013) Trends in climate of West Bengal. *PARIPEX Indian J Res* 2(7). <https://doi.org/10.36106/PARIPEX>
- Seinfeld JH, Pandis SN (1998) *Atmospheric chemistry and physics: from air pollution to climate change*. Wiley, New York
- Skamarock WC, Klemp JB (2008) A time-split non hydrostatic atmospheric model for weather research and forecasting applications. *J Comput Phys* 227(7):3465–3485. <https://doi.org/10.1016/j.jcp.2007.01.037>
- Spiegel J, Maystre LY (1998) Environmental pollution control. In: Stellman JM (ed) *Encyclopedia of occupational health and safety*, vol 4. International Labor Office, Geneva, Switzerland
- Srivastava AK, Dey S, Tripathi SN (2012) Aerosol characteristics over the Indo-Gangetic basin: implication to regional climate. In: Abdul-Razzak H (ed) *Atmospheric aerosols – regional characteristics – chemistry and physics*
- Steadman RG (1984) A universal scale of apparent temperature. *J Clim Appl Meteorol* 23:1674–1687
- Talukdar S, Maitra A (2020) Analysis of an aerosol environment in an urban region and its impact on regional meteorology. *Meas Anal Remediation Environ Pollut Energy Environ Sustain*. https://doi.org/10.1007/978-981-15-0540-9_7
- Talukdar S, Jana S, Maitra A (2017) Dominance of pollutant aerosols over an urban region and its impact on boundary layer temperature profile. *J Geophys Res* 122:1001–1014
- Thom EC (1959) The discomfort index. *Weatherwise* 12(2):57–60
- Tripathi SN, Dey S, Tare V, Satheesh SK (2005) Aerosol black carbon radiative forcing at an industrial city in northern India. *Geophys Res Lett* 32. <https://doi.org/10.1029/2005g1022515>.
- Tripathi SN, Pattnaik A, Dey S (2007) Aerosol indirect effect over Indo-Gangetic plain. *Atmos Environ* 41(2007):7037–7047
- Wang K, Aktas YD, Malki-Epshtein L (2019) Urban heat island modelling of a tropical city: case of Kuala Lumpur. *Geosci Lett* 6(4):2019
- Yakubu OH (2017) Addressing environmental health problems in Ogoniland through implementation of United Nations Environment Program recommendations: environmental management strategies
- Yildizel SA, Kaplan G, Arslan Y, Yildirim MS, Ozturk AU (2015) A study on the effect of weather conditions on the worker health and performance in a construction site. *J Eng Res Appl Sci* 4(1):291–295